

The Journal of

# PHARMACOLOGY

And Experimental Therapeutics

2023 ANNUAL MEETING ABSTRACTS



A Publication of the American Society for  
Pharmacology and Experimental Therapeutics

# The Journal of PHARMACOLOGY

## And Experimental Therapeutics

A Publication of the American Society for Pharmacology and Experimental Therapeutics

June 2023

Vol. 385, No. S3

### ASPET 2023 Annual Meeting Abstracts

#### Contents

Poster Number

#### CANCER PHARMACOLOGY

Sotorasib, a KRAS-G12C Inhibitor, Induces Chemoresistance by Activating Human Pregnane Xenobiotic Receptor <i>Julia Salamat, Kodye L. Abbott, Elizabeth L. Ledbetter, Chuanling Xu, and Satyanarayana R. Pondugula</i>	33
Identification and Testing of a Novel HUNK Inhibitor <i>Tinslee Dilday, Melissa Abt, Herman Sintim, George Sandusky, and Elizabeth S. Yeh</i>	34
Ethanollic Extract of <i>Origanum syriacum</i> L. Leaves Exhibits Potent Anti-Breast Cancer Potential and Robust Antioxidant Properties <i>Elias Baydoun, Joelle Mesmar, Rola Abdallah, and Kamar Hamade</i>	35
Aberrantly upregulated Drp1 induces mitochondrial fission and promotes colorectal cancer cell migration <i>Tianzhou Xing, Yan Xie, Peter Abel, and Yaping Tu</i>	36
Designing Tailored Thiosemicarbazones with Bespoke Properties: The Styrene Moiety Imparts Potent and Selective Anti-Tumor Activity <i>Des Richardson, mahendiran Dharmasivam, and Busra Kaya</i>	37
Histone Deacetylase Inhibitor Belinostat Regulates Metabolic Reprogramming in Killing Kras-Mutant Human Lung Cancer Cells <i>Rebecca Peter, Md. Shahid Sarwar, Yujue Wang, Xiaoyang Su, and Ah-Ng Kong</i>	38
Scaffold protein Scribble is a potent modulator of Sonic Hedgehog signaling <i>Jingwen Zhu, Sabina Ranjit, Yao Wang, Frederique Zindy, Martine Roussel, and John Schuetz</i>	39
Understanding How Cellular Metabolism Affects Clofarabine Treatment in Acute Myeloid Leukemia <i>Ashley Gray, Yu Fukuda, Lauren Brakefield, Amit Budhraj, Joseph T. Opferman, and John Schuetz</i>	40
Direct Targeting of Menin-MLL1 Interaction Inhibits Cancer Stem Cells to Inhibit Neuroblastoma Growth <i>Rameswari Chilamakuri and Saurabh Agarwal</i>	41
MCL1 Small Molecule Inhibitor S63845 Synergizes with Cisplatin in Basal-like Triple Negative Breast Cancer <i>Alexus Acton and William Placzek</i>	42
The Paracrine Action of Mutant P53 In Breast Cancer <i>Abie Williams-Villalobo, Yun Zhang, B Liu, S Xiong, G Chau, and G Lozano</i>	43
The Synergistic Antitumor Effect of Irinotecan and Flavonoids on Human Colon Cancer Xenograft Mice <i>Jyotsna Devi Godavathi, Abie Williams-Villalobo, Imoh Etim, Du Ting, Song Gao, and Yun Zhang</i>	44
Epigenetic Regulation of Medulloblastoma Proliferation by Finasteride-Induced Modulation of BTG2 and CD244 Gene Methylation <i>Anika Patel, Churchill Ihentuge, and Antonei B. Csoka</i>	45
Targeting mitochondrial protein NIX mediates resistance to sorafenib in hepatocellular carcinoma through autophagy <i>QiongRong Zeng, ZeFeng Liu, XianWen Guo, WenJuan Wang, XueLian Huang, FuJian LI, and Guo Zhang</i>	46
Evaluating the Anticancer Activity of Novel Norethindrone Analogs in Glioblastoma Cells <i>Katelyn A. Harris, Courtney A. Hollenbacher, Eric T. Doyle, Samantha T. Szoradi, Nicholas A. Reid, Laura R. Inbody, Richard W. Dudley, and Ryan A. Schneider</i>	47

Lipin-1 Silencing Alters the Phospholipid Profiles of Castration-Resistant Prostate Cancer Cells <i>Morgan C. Finnerty and Brian Cummings</i>	48
Targeting the Cell Cycle Checkpoints CHK1 and CHK2 is a Novel Therapeutic Approach for Pediatric Neuroblastoma <i>Ben Morrison, Rameswari Chilamakuri, and Saurabh Agarwal</i>	49
Impact of Microglial RGS10 Regulation of Inflammatory Mediators in the Glioblastoma Tumor Microenvironment <i>Phillip Dean and Shelley Hooks</i>	50
Characterization of a Mouse Model of Neuropathic Pain Induced by Calcaneus Implantation of NCTC 2472 Mouse Sarcoma Cells <i>Yuma Ortiz, Sushobhan Mukhopadhyay, Christopher R. McCurdy, Lance R. McMahon, and Jenny L. Wilkerson</i>	233
Troglitazone Induced Apoptosis in a Human Colon Cancer Cell Line <i>Solomon A. Ocran, David Strom, Mackenzie M. Budd, Zachary L. Lutz, Nicole J. Kang, and Nolan A. Wengert</i>	234
Structural and Mechanistic Basis for Gbetagamma-mediated Activation of Phosphoinositide 3-kinase-gamma <i>Chun-Liang Chen, Sandeep Ravala, Yu-Chen Yen, Thomas Klose, Ramizah Syahirah, John JG. Tesmer, and Qing Deng</i>	235
In Silico Analysis of DNA Methylation Status of T-Cell Inflamed Signature Reveals a Therapeutic Strategy to Improve Immune Checkpoint Inhibitors Efficacy in Wilms Tumor <i>Sarah A. Albasha, Manar Z. Almotawa, Abdulmonem A. Alsaleh, Noura N. Alibrahim, Zaheda H. Radwan, Yousef N. Alhashem, Jenan Almatouq, and Mariam K. Alamoudi</i>	236
Endocrine Disrupting Chemicals as "structural cues" for the development of drugs for the treatment of Prostate Cancer (Castration Resistant Prostate Cancer) and PCOS <i>Katayani Sharma, Angelo Lanzilotto, Søren Therkelsen, Therina du Toit, Flemming S. Jørgensen, and Amit Pandey</i>	238
Cell Free Targeted Therapy for T-cell Acute Lymphoblastic Leukemia <i>Jacob Neethling and Kostandin Pajcini</i>	239
Sanggenon G, a Diels-Alder Adduct Screened from Mori Cortex, Attenuated Irinotecan-induced Late-onset Diarrhea in Mice via a Dual Inhibition Mechanism <i>Ru YAN, Panpan Wang, Zhiqiang Chen, Rongrong Wu, and Yifei Jia</i>	240
Efficacy of Imidazole Antifungal Agents in the Treatment of Nras and Braf Mutant Human Melanoma Cells <i>David Koh, Lukas R. Jira, Hattie M. Foster, McKenzie N. Carle, Hannah K. Hall, and Maxwell A. Sutherland</i>	241
Immunoproteasome Inhibitors for the treatment of ALL driven by the t(4:11) Translocation <i>Tyler Jenkins, Alexei Kisselev, Andrey V. Maksimenko, Amit Mitra, Peter Panizzi, Jennifer L. Fields, Steven Fiering, and Jacquelyn E. Fitzgerald</i>	242
Direct Targeting of the Cell cycle Regulator <i>WEE1</i> is a Novel Therapeutic Approach for Neuroblastoma <i>Parul Suri, Rameswari Chilamakuri, and Saurabh Agarwal</i>	243
Production of TNF- $\alpha$ and IL-10 by HepG2 and THP-1 cells differs depending on whether ethanol conditioned media is derived from 3D vs. 2D cultured HepG2 cells. <i>Joshua Hood, Alexander Southern, and Luke Schroeder</i>	244
Recombinant miR-7-5p Effectively Inhibits NSCLC Cell Viability through Regulating Mitochondrial Function <i>Gavin M. Traber, Meijuan Tu, Neelu Batra, Colleen Yi, and Aiming Yu</i>	245
Defining the landscape of cancer vulnerabilities that are engendered by germline genetic variation <i>Sean Misek, Aaron Fultineer, Jeremie Kalfon, Javad Noorbakhsh, Isabella Boyle, Joshua Dempster, Lia Petronio, Katherine Huang, Thomas Green, Adam Brown, John Doench, David Root, James McFarland, Rameen Beroukhim, and Jesse Boehm</i>	246
Metformin Alleviates Chemotherapy-Induced Toxicities in Non-Diabetic Breast Cancer Patients: A Randomized Controlled Study <i>Mahmoud El-Mas, Amira B. Kassem, Noha A. El-Bassiouny, Maged W. Helmy, Yasser El-Kerm, and Manar A. Serageldin</i>	247
Targeting Adenylyl Cyclase Type 8, Orai1, and Stromal Interaction Molecule 1 in Triple-Negative Breast Cancer <i>Moana Hala'ufia and Dave Roman</i>	248
Significance of topical chemotherapy application on human and murine skin <i>Anita Thyagarajan, Krishna Awasthi, Christine Rapp, Kelly Miller, R. Michael Johnson, Yanfang Chen, Jeffrey Travers, and Ravi P. Sahu</i>	249
Characterization of microenvironmental-mediated gilteritinib resistance in Acute Myeloid Leukemia using a Bmx knockout mouse model <i>Jack C. Stromatt, Daelynn R. Buelow, Shelly J. Orwick, Eric Eisenmann, Navjot S. Pabla, Bradly W. Blaser, and Sharyn D. Baker</i>	250

Strategies to Circumvent Topoisomerase II $\alpha$ Intron 19 Intronic Polyadenylation (IPA) in Acquired Etoposide Resistance Human Leukemia K562 Cells	251
<i>Xinyi Wang, Jessika Carvajal-Moreno, Jack C. Yalowich, and Terry Elton</i>	
Enhanced Cholinergic Action of Myenteric Neurons During Chemotherapy Induced Diarrhea	432
<i>Stanley Cheatham, Karan H. Muchhala, and Hamid I. Akbarali</i>	
Mechanistic Investigation of a Combination of a Cell Cycle Inhibitor and an HDAC Inhibitor in Pancreatic Cancer Cells	433
<i>Shraddha Bhutkar, Anjali Yadav, and Vikas Dukhande</i>	
Overcoming Cetuximab Resistance in Colorectal Cancer through Inhibition of HGF Processing	434
<i>Vivian Jones, Ramona Graves-Deal, Galina Bogatcheva, Zheng Cao, James Higginbotham, Sarah Harmych, Marisol Ramirez, Qi Liu, Gregory Ayers, James Janetka, and Bhuminder Singh</i>	
Targeting Epigenetic Modification of T-Cell Inflamed Signature to Enhance Immune Checkpoint Inhibitors Response in Small Cell Lung Cancer	435
<i>Manar Z. Almotawa, Sarah A. Albasha, Abdulmonem A. Alsaleh, Noura N. Alibrahim, Zaheda H. Radwan, Yousef N. Alhashem, Jenan Almatouq, and Mariam K. Alamoudi</i>	
Critical Role of OGT-mediated Novel NF- $\kappa$ B O-GlcNAcylation in Pancreatic Cancer	436
<i>Aishat Motolani, Matthew Martin, Benlian Wang, Guanglong Jiang, Yunlong Liu, and Tao Lu</i>	
Inhibition of Autophagy and MEK Promotes Ferroptosis in Lkb1-Deficient Kras-Driven Lung Tumors	437
<i>Vrushank Bhatt, Taijin Lan, Wenping Wang, Jerry Kong, Eduardo Cararo Lopes, Khoosheh Khayati, Jianming Wang, Akash Raju, Michael Rangel, Enrique Lopez, Zhixian Sherrie Hu, Xuefei Luo, Xiaoyang Su, Eileen White, and Jessie Yanxiang Guo</i>	
Examining the DNA Methylation Profile of Childhood Solid Tumors to Identify Novel Therapeutically Targeted Sites	438
<i>Sarah A. Albasha, Manar Z. Almotawa, Abdulmonem A. Alsaleh, Noura N. Alibrahim, Mariam K. Alamoudi, Zahiah F. Al Mohsen, Yahya Aldawood, Hayyan A. Al-Taweil, Fatimah J. Al Shaikh, and Jenan Almatouq</i>	
ERO1a Expression is Required for Secretion of Extracellular Matrix and Promotes Lung Cancer Progression	439
<i>Maria Voronkova, Brennan D. Johnson, Wei-Chih Chen, Gangqing Hu, Lori Hazlehurst, and John Koomen</i>	
Metabolic Rewiring and Mechanism of Action of an Antiepileptic Drug Repurposed for its Potential in Glioblastoma	440
<i>Anjali Yadav, Shraddha Bhutkar, and Vikas Dukhande</i>	
A Novel Fluoropyrimidine Drug to Treat Recalcitrant Colorectal Cancer	441
<i>Naresh Sah, Pamela Luna, Chinnadurai Mani, William Gmeiner, and Komaraiah Palle</i>	
Use of CRISPR/Cas9 with Homology-Directed Repair (HDR) to Gene-Edit Topoisomerase II $\beta$ in Human Leukemia K562 Cells: Generation of a Resistance Phenotype	442
<i>Jessika Carvajal-Moreno, Xinyi Wang, Victor A. Hernandez, Jack C. Yalowich, and Terry Elton</i>	
Amphotericin A21 reduces cell proliferation and modulates anti- and pro-apoptotic proteins in MCF-7 cells.	443
<i>Lourdes Rodriguez-Fragoso, Rubi Escobar-Resendiz, Ivan Ortega-Blake, and Arturo Galvan-Hernandez</i>	
Synthesis And Anticancer Properties of Polyrhodanine Copper Nanocomposites	444
<i>Sarbani Ghoshal, Nickayla Spence, Moni Chauhan, Qiaxian Johnson, and Bhanu P. Chauhan</i>	
Defining the Role of Mitochondrial Dynamics in Regulating PDAC Cell Sensitivity to KRAS and ERK Inhibition	445
<i>Amber Amparo, Kristina Drizyte-Miller, Claire Gates, Adrienne D. Cox, Kirsten L. Bryant, and Channing J. Der</i>	
Prognostic and Therapeutic Implications of Genes Associated with Apoptosis and Protein-Protein Interactions in Triple-Negative Breast Cancer	446
<i>Getinent M. Adinew, Samia S. Messeha, Equar Taka, Shade Ahmed, and Karam F. Soliman</i>	
Calcium Channel Blockers as Novel Therapeutic Agents for Triple-Negative Breast Cancer	447
<i>Destiny Lawler and Robert L. Copeland</i>	
Adaptive Changes in Tumor Cells in Response to Reductive Stress	448
<i>Leilei Zhang, Jie Zhang, Zhiwei Ye, Aslam Muhammad, John Culpepper, Danyelle M. Townsend, and Kenneth Tew</i>	
Elucidating the Function of ABCA13 in SHH-Medulloblastoma	449
<i>Joseph Miller, Juwina Wijaya, Giles W. Robinson, Vikas Daggubati, David R. Raleigh, and John Schuetz</i>	
HUNK regulation of IL-4 promotes polarization of tumor-associated macrophages in TNBC tumor microenvironment	450
<i>Nicole Ramos Solis, Elizabeth S. Yeh, Mark H. Kaplan, and Anthony M. Cannon</i>	

## CARDIOVASCULAR PHARMACOLOGY

A Convolutional Neural Network Model classifies Beat-to-Beat Arterial Pressure Time-Series: Sex Stratification and Cardiovascular Risk Prediction	99
<i>Nour Mounira Bakkar, Abdalrhman Mostafa, Mohamed Abdelhack, and Ahmed F. El-Yazbi</i>	

Propofol and salvianolic acid A synergistically attenuated hypoxia/reoxygenation induced H92 cells injury under high-glucose and high-fat condition via modulating CD36	100
<i>Jiaqi Zhou, Ronghui Han, Anyuan Zhang, Jiajia Chen, Yuxin Jiang, Dongcheng Zhou, Danyong Liu, Liangqing Zhang, Weiyi Xia, Youhua Xu, and Zhengyuan Xia</i>	
Acid Sphingomyelinase Inhibitor Protects Against the Nicotine-Induced Podocyte Injury	101
<i>Atiqur Rahman, Saisudha Koka, and Krishna M. Boini</i>	
Old Dog, New Tricks: Oral Dosing Hypertensive Rats with Anti-Inflammatory Agent Colchicine Gives Vascular Remodeling and Function Recovery	102
<i>Samuel Baldwin, Jennifer van der Horst, Joakim Bastrup, Anthony M. Mozzicato, Salomé Rognant, Johs Dannesboe, and Thomas A. Jepps</i>	
Sex-dependent Differences in Pressure Overload Hypertrophy in NT-GRK2 Mice	103
<i>Kamila Bledzka, Iyad H. Manaserh, Madison Bohacek, Jessica Grondolsky, Jessica Pflieger, Julie Rennison, David Van Wagoner, and Sarah Schumacher</i>	
Therapeutic Efficacy of a Novel Pharmacologic GRK2 Inhibitor in Mice Models of Heart Failure	104
<i>Rajika Roy, Sarah Schumacher, Haley C. Murphy, Jessica Grondolsky, Kurt Chuprun, Helen V. Waldschmidt, Erhe Gao, Huaqing Zhao, Larisa Avramova, John JG. Tesmer, and Walter Koch</i>	
Role of cyclophilin A overexpression in angiotensin II/mechanical stretch-induced vascular remodeling: Protective effect of adiponectin	105
<i>Zeina Radwan, Crystal Ghantous, and Asad Zeidan</i>	
Physiological effects of fentanyl analogs found in recreational drug markets	106
<i>Charles W. Schindler, Shelby A. McGriff, Eric B. Thorndike, Li Chen, Donna Walther, Kenner Rice, Lei Shi, and Michael H. Baumann</i>	
Cardiomyocyte-specific Adhesion G Protein-Coupled Receptor F5 (ADGRF5) participates in cardiac homeostasis	107
<i>Jeanette Einspahr, Viren Patwa, Rajika Roy, and Douglas G. Tilley</i>	
ANGPTL4 attenuates hypoxia/reoxygenation-induced cardiomyocyte apoptosis via activation of Akt signaling	108
<i>Weiyi Xia, Dengwen Zhang, Weiguang Li, Zhengyuan Xia, and Yin Cai</i>	
Opposing effects of $\beta$ 2-ARs on $\beta$ 1-ARs on phospholipase C-mediated cardiac hypertrophic signaling	109
<i>Wenhui Wei and Alan V. Smrcka</i>	
Oral administration of BAF312, a selective sphingosine-1-phosphate receptor agonist, attenuates sodium retention and hypertension in DOCA-salt-treated mice	110
<i>Weili Wang, Gaizun Hu, Chaoling Chen, Joseph Ritter, Pin-Lan Li, and Ningjun Li</i>	
Mitochondrial CaMKII as a Novel Regulator of Cardiometabolic Dysfunction	155
<i>Kimberly Ferrero, Jonathan Granger, Robert Cole, Brian Foster, David Kass, Elizabeth Luczak, and Mark Anderson</i>	
Beta-catenin C-terminus inhibition reduces vascular remodeling by precluding the expression of sphingosine-1-phosphate receptor-1	156
<i>Gustavo Oliveira de Paula, Gaia Ressa, Vanessa Almonte, Dippal Parikh, Tomas Valenta, Konrad Basler, Timothy Hla, Dario Riascos-Bernal, and Nicholas Sibinga</i>	
$\beta$ 3AR-dependent BDNF generation limits chronic post-ischemic heart failure	157
<i>Seungho Jun, Alessandro Cannavo, Giuseppe Rengo, Federica Marzano, Jacopo Agrimi, Gizem Keceli, Andrea Elia, Daniela Liccardo, Giovanna G. Altobelli, Erhe Gao, Ning Feng, Walter Koch, and Nazareno Paolucci</i>	
Development of the first vascular-specific KATP channel inhibitor for the treatment of patent ductus arteriosus in newborns	158
<i>Kangjun Li, Samantha J. McClenahan, Elaine L. Shelton, Craig W. Lindsley, and Jerod Denton</i>	
Characterizing the Role of Ser670 Phosphorylation in Non-canonical Mechanisms of GRK2 Inhibition in Heart Failure	159
<i>Heidi Cho, Kimberly Ferrero, John K. Chuprun, Erhe Gao, and Walter Koch</i>	
Low-Dose Metformin Treatment Offers Modest Nephroprotection in a Mouse Model of Diabetic Kidney Disease	160
<i>Kayla Olstinske, James LeFevre, Christopher Karch, Ronald Frantz, Kevin Carvendale, and Shankar Munusamy</i>	
Resolving Unchecked Inflammation in Atrial Fibrillation	301
<i>Deanna Sosnowski, Roddy Hiram, Xiao Yan Qi, Kyla Bourque, Patrice Naud, Sandro Ninni, Darlaine Pétrin, Terry Hebert, and Stanley Nattel</i>	
SERCA Inhibition by Drugs - A Potential Therapeutic Strategy in Ischemia	302
<i>Jesika Colomer-Saucedo, Yuanzhao L. Darcy, Valeria A. Copello, Paula Diaz-Sylvester, Melanie Loulousis, and Julio A. Copello</i>	
$\beta$ -caryophyllene, a CB2 Receptor Agonist Alleviates Diabetic Cardiomyopathy via Inhibiting AGE/RAGE-Induced Oxidative Stress, Fibrosis, and Inflammasome Activation	303
<i>HEBAALLAH M. HASHIESH, Mohamed FN. Meeran, Sheikh SA. Azimullah, Ernest Adeghate, Dhanya Saraswathamma, Saeeda Almarzooqi, and Shreesh K. Ojha</i>	

Propofol and salvianolic acid A synergistically ameliorates LPS-induced H92 cells injury under hyperglycemia via enhancing SIRT1 to inhibit NLRP3 dependent-pyroptosis	304
<i>Anyuan Zhang, Ronghui Han, Jiaqi Zhou, Kaijia Han, Jiajia Chen, Yuhui Yang, Xihe Zhang, Wangning Shangguan, Liangqing Zhang, Jing Tang, and Zhengyuan Xia</i>	
HuR-dependent expression of Wisp1 is necessary for TGF $\beta$ -induced cardiac myofibroblast activity	305
<i>Sharon Parkins, Michael Tranter, Adrienne Guarnieri, Lisa Green, Sarah Anthony, and Onur Kanisicak</i>	
Cardiomyocyte Signaling Factors are Responsible for Heart-Fat Communication and Mediate the Development of Cardiometabolic Disease	306
<i>Stephanie Kereliuk, Kenneth Gresham, Jessica Ibeti, and Walter Koch</i>	
Changes of ACE-2 related-miR-200b-3p expression over time are a predictive factor of long hospitalization for COVID-19: in silico, machine learning and validation analysis	307
<i>Disha Keswani, Mikolaj Marszalek, Zofia Wicik, Ceren Eyiletten, Anna Nowak, Sérgio Simões, David Martins, Krzysztof Klos, Wojciech Wlodarczyk, Alice Assinger, Dariusz Soldacki, Andrzej Chcialowski, Jolanta Siller-Matula, and Marek Postula</i>	
Downregulation in Connexin43 expression is associated with reduced ferroptosis and enhanced tolerance to myocardial ischemia-reperfusion injury in type 1 diabetic mice	308
<i>Jiajia Chen, Danyong Liu, Jiaqi Zhou, Dongcheng Zhou, Anyuan Zhang, Yuxing Jiang, Jiefu Lin, Liangqing Zhang, Ronghui Han, Yuhui Yang, and Zhengyuan Xia</i>	
Heart-rate Corrected QT Interval and Statin use in the general population. The Polish Norwegian Study (PONS)	309
<i>Georgeta Vaidean, Sandeep Vansal, and Marta Manczuk</i>	
Osteopontin promotes G protein-coupled receptor kinase (GRK)-2-dependent desensitization of cardiac $\beta_2$ -adrenergic receptor anti-fibrotic signaling	310
<i>Anastasios Lympopoulos</i>	
$\beta$ -adrenoceptor-mediated vasodilation is enhanced by acute colchicine-treatment in men with essential hypertension	311
<i>Thomas A. Jepps, Ylva Hellsten, Jennifer van der Horst, Thomas Ehlers, Christian Aalkjaer, Lasse A. Gliemann, and Sophie A. Moller</i>	
Ovariectomy Promotes Angiotensin II-induced Renal Dysfunction and Vasopressin Excretion via 12/15-Lipoxygenase	312
<i>Shubha R. Dutta, Purnima Singh, and Kafait U. Malik</i>	
Metformin Protects Against Liposaccharide (LPS)-induced Hyperinflammation in Doxorubicin-induced Senescent Endothelial Cells	357
<i>Ibrahim Abdelgawad, Kevin Agostinucci, Bushra Sadaf, and Beshay Zordoky</i>	
Sexual Dimorphism of the Fasting Adipose: Mitigation of Metabolic and Cardiovascular Dysfunction in a Non-Obese Prediabetic Rat Model	358
<i>Haneen Dwaib, Omar Obeid, Ahmed F. El-Yazbi, and Haneen Dwaib</i>	
Alterations in pyroptotic signaling mediated by phosphorylation of GRK2 and mitochondria functional alterations	359
<i>Ruxu Zhai, Yuzhen Tian, Ole Mortensen, Priscila Sato, Emad Alnemri, and Hsin-Yao Tang</i>	
Investigating High Salt Diet Effects on Stress Responding and Microglial Activation	360
<i>Jasmin N. Beaver, Matthew T. Ford, Anna E. Anello, Lee Gilman, and Allianna K. Hite</i>	
Inhibition of Cardiac GCH1 O-GlcNAc Modification promotes cardiac BH4/eNOS signaling after myocardial ischemia-reperfusion in mice with Type-2 Diabetes	361
<i>Yuhui Yang, Dongcheng Zhou, Jiajia Chen, Weiyi Xia, Danyong Liu, Liangqing Zhang, Yin Cai, Zhidong Ge, and Zhengyuan Xia</i>	
Modulation of Mitochondrial Bioenergetics in Human Brain Microvascular Endothelial Cells by Telomerase Reverse Transcriptase	362
<i>Jesmin Jahan, Madeline Stroud, Anil Sakamuri, and Yagna Jarajapu</i>	
Angiotensin-(1-7) and Gut-Bone Marrow Axis in Aging	363
<i>Kishore Chittimalli, Jesmin Jahan, Aaron Ericsson, and Yagna Jarajapu</i>	
Dexametomidine Preconditioning Attenuates Myocardial Ischemia/Reperfusion Injury by Increasing SIRT1 Expression to Inhibit Autophagy Overactivation in Mice	500
<i>Jianfeng He, Danyong Liu, Jiajia Chen, Hanlin Ding, Dongcheng Zhou, Yuhui Yang, Weicai Yang, Ronghui Han, Sheng Wang, and Zhengyuan Xia</i>	
5-HT1F Agonist Lasmiditan Induces Mitochondrial Biogenesis And Alters Successful And Failed Repair Genes In A Mouse Model Of Acute Kidney Injury	501
<i>Paul Victor Santiago Raj, Kevin Hurtado, Jaroslav Janda, and Rick Schnellmann</i>	

Delivery of Human ACE2 Across the Blood Brain Barrier Attenuated Development of Neurogenic Hypertension Using An Engineered Liposome-Based Delivery System <i>Yue Shen, Richard Lamptey, Jagdish Singh, and Chengwen Sun</i>	502
Doxorubicin induced cardiotoxicity via inhibiting PKC- $\epsilon$ /SIRT1 pathway <i>Danyong Liu, Jianfeng He, Hanlin Ding, Chunyan Wang, Yao Chen, Junmin He, Chun Chen, Yuantao Li, and Zhengyuan Xia</i>	503
Expanding the GRK5 Interactome <i>Morgan Pantuck, Sudarsan Rajan, Eric Barr, Jessica Ibeti, Joanne Garbincius, Ryan Coleman, Kurt Chuprun, and Walter Koch</i>	504
Effects of Dapagliflozin as an Adjunct Therapy to Insulin in Streptozotocin-induced Diabetic Rats <i>Abdul-Azeez A. Lanihun, Rupesh C. Panta, and Guim Kwon</i>	505
Paradoxical Effect of Nitric Oxide on GRK2 in the Kidney and Heart: Implications for Sepsis-Associated Kidney Injury <i>Thiele Oswaldt Rosales, Jamil Assreuy, and Walter Koch</i>	506
Mitochondrial GRK2 Dependent Regulation of the Cellular and Transcriptional Composition after Myocardial Infarction <i>Samuel Slone, Kurt Chuprun, Gizem Kayki-Mutlu, Rajika Roy, Jessica Ibeti, Erhe Gao, Nathan Tucker, and Michelle Hulke</i>	507
G Protein-coupled Estrogen Receptor 1 and Pregnancy Confer Protection against Hypertension in Aged Female Mice <i>Eman Gohar, Ravneet Singh, Rawan Almutlaq, and Victoria Nasci</i>	508
Tubulin acetylation attenuates vasorelaxation in a smooth muscle-dependent manner and contributes to hypertension <i>Anthony Mozzicato, Joakim Bastrup, and Thomas A. Jepps</i>	509
The FDA Approved Therapeutic Lasmiditan, Enhances Primary Murine Renal Peritubular Endothelial Cells Wound Healing Capacity. <i>Austin D. Thompson, Jaroslav Janda, and Rick Schnellmann</i>	510
Platelet Function and Gene Expression in E-cigarette In Utero Exposed Mice <i>Ahmed Alarabi</i>	511
Using the Caprini Risk Score to increase awareness of Venous Thromboembolism Awareness in the Community: Know Your Score II <i>Chunping Huang, Joseph Tariman, Shannon Simonovich, Arav Bongirwar, Divya Honavar, Mala Niverthi, Rashi Modey, Joseph Caprini, and Atul Laddu</i>	556
Renin-Angiotensin System Components and Arachidonic Acid Metabolites as Biomarkers of COVID-19 <i>Biwash Ghimire, Sana Khajehpour, Nasser Jalili Jahani, Elizabeth A. Middleton, Robert Campbell, Mary Nies, and Ali Aghazadeh-Habashi</i>	557
Dexmedetomidine Attenuates Ischemia and Reperfusion-Induced Cardiomyocyte Injury through SIRT1/FOXO3a Signaling <i>Han-lin Ding, Danyang Liu, Jianfeng He, Jiajia Chen, Dongcheng Zhou, Chan Wang, Changming Yang, Zhengyuan Xia, and Zhongyuan Xia</i>	558
Location Biased G Protein-Coupled Receptor Signaling Modulates Distinct Spatial Conformations of $\beta$ -arrestins <i>Anand Chundi, Uyen Pham, and Sudarshan Rajagopal</i>	559
A novel combination of an AKT activator with an AKT inhibitor exacerbates hydrogen peroxide-induced death of human cardiac microvascular endothelial cells <i>Zhu-qiu Jin and Austin Qiu</i>	560
Clopidogrel Induces More Bleeding in P2Y <sub>12</sub> -deficient Mice: Optimization of Murine Tail Bleeding Assay <i>Taylor Rabanus, Adam Lauver, and Dawn Kuszynski</i>	561
Role of ferroptosis in increased vulnerability to myocardial ischemia-reperfusion injury in type 1 diabetic mice and the treatment effects of N-acetylcysteine <i>Dongcheng Zhou, Yuhui Yang, Jiajia Chen, Jiaqi Zhou, Jianfeng He, Danyong Liu, Anyuan Zhang, Bixian Yuan, Yuxin Jiang, Ronghui Han, Weiyi Xia, and Zhengyuan Xia</i>	562
Propofol and salvianolic acid A synergistically attenuated hypoxia/reoxygenation induced H92 cells injury under high-glucose and high-fat condition via modulating CD36 <i>Jiaqi Zhou, Ronghui Han, Anyuan Zhang, Jiajia Chen, Yuxin Jiang, Dongcheng Zhou, Danyong Liu, Liangqing Zhang, Weiyi Xia, Youhua Xu, and Zhengyuan Xia</i>	100

## CELLULAR AND MOLECULAR PHARMACOLOGY

G $\alpha$ protein signaling bias at 5-HT <sub>1A</sub> receptor <i>Rana Alabdali, Luca Franchini, and Cesare Orlandi</i>	77
--	----

Quantitative phosphoproteomic analysis defines distinct cAMP signaling networks emanating from AC2 and AC6 in human airway smooth muscle cells	78
<i>Isabella Cattani-Cavaliere, Yue Li, Jordyn Margolis, Amy Bogard, Moom Roosan, and Rennolds Ostrom</i>	
Lysophosphatidic Acid (LPA) Salivary Species Detection and In Situ LPAR Localization in the Intact Mouse Salivary Gland	79
<i>D. Roselyn Cerutis, Devendra Kumar, Michael G. Nichols, Gabrielle Roemer, Maxwell Fluent, Laken Beller, Takanari Miyamoto, and Yazen Alnouti</i>	
Targeting HDAC6 in the Dorsal Root Ganglia for the Management of Mechanical Allodynia in Models of Peripheral Nerve Injury	80
<i>Ilinca Giosan, Randal Serafini, Jeffrey Zimering, Aarthi Ramakrishnan, Madden Tuffy, Li Shen, and Venetia Zachariou</i>	
Structural Basis of Arrestin and Membrane Interaction	81
<i>Kyle W. Miller, Qiuyan Chen, and Shuaitong Zhao</i>	
Without a Trace: The Pirin and NF- $\kappa$ B Interaction	82
<i>Melissa Meschkewitz, Erika M. Lisabeth, and Richard Neubig</i>	
Structural and Functional Characterization of Phospholipase C $\beta$ 3	83
<i>Kennedy Outlaw, Isaac J. Fisher, Kaushik Muralidharan, and Angeline Lyon</i>	
Examining the mu-opioid receptor bias of fentanyl and 2-benzylbenzimidazole opioids in clandestine drug markets	84
<i>Meng-Hua M. Tsai, Li Chen, Michael H. Baumann, and Lei Shi</i>	
Structural Insights into Phospholipase Ce	85
<i>Elisabeth Garland-Kuntz, Kadidia Samassekou, Isaac J. Fisher, Kaushik Muralidharan, Abigail Gick, Morgan Laskowski, Emmanuel Oluwarotimi, Taiwo Ademoye, Satchal Erramilli, Anthony Kossiakoff, and Angeline Lyon</i>	
ACAT-1 Inhibition Limits iNOS in an <i>In Vitro</i> Model of Macrophage Activation	86
<i>Sung Jae Lee, Emily Stevenson, and Andrew Gow</i>	
A novel UVA-labile $\beta$ -adrenergic agonist allows for optical control of subcellular signaling	87
<i>Waruna Thotamune, Sithurand Ubeyasinghe, Ajith Karunarathne, Kendra K. Shrestha, Michael C. Young, and Mithila Tennakoon</i>	
Mechanistic insights into Rap1A-dependent regulation of phospholipase C epsilon in the heart	88
<i>Kadidia Samassekou, Elisabeth Garland-Kuntz, Isaac J. Fisher, Vaani Ohri, Livia M. Bogdan, Satchal Erramilli, Angeline Lyon, and Anthony Kossiakoff</i>	
Discovery and Validation of RGS2-FBXO44 Protein-Protein Interaction Inhibitors	121
<i>Sadikshya Aryal, Harrison J. McNabb, and Benita Sjogren</i>	
Sigma Ligand-mediated Cytosolic Calcium Modulation in BV2 Microglia Cells	122
<i>Joseph M Schober, Eric Lodholz, Faria Simin, Michael Crider, and Ken Witt</i>	
Structure-guided approach to modulate small molecule binding to the promiscuous pregnane X receptor	123
<i>Andrew D. Huber, Wenwei Lin, Shyaron Poudel, Yongtao Li, Jayaraman Seetharaman, Darcie J. Miller, and Taosheng Chen</i>	
Subcellular Localization Analysis of Sigma 1 Receptor (S1R) and Binding Immunoglobulin Protein (BiP) for Identification of Antagonists versus Agonists	124
<i>Faria Anjum Simin and Joseph Schober</i>	
Trafficking pathway of T-cell receptor mimic antibodies (TCRm) RL6A in human brain-derived endothelial cells	125
<i>Yeseul Ahn, Ehsan Nozohouri, Sumaih Zoubi, and Ulrich Bickel</i>	
Quantifying Acid Adaptivity of Normal and Cancer Cells Using a Next Generation Genetically Encoded pH Biosensor	126
<i>Daniel Isom, Sam Taylor, Kyutae Lee, and Jacob Rowe</i>	
Urothelial Knock-in of the Engineered Chloride Channel EG3RF as a Potential Treatment for Cystitis-Induced Bladder Inflammation	127
<i>Grace Ward, Jonathan Beckel, Yan Xu, Keara Healy, and Stephanie Daugherty</i>	
GPCR cargo modifies lipid order in clathrin-coated pits	128
<i>G. Aditya Kumar and Manoj A. Puthenveedu</i>	
Insurmountable Antagonism by Buprenorphine at Human Mu Opioid Receptors	129
<i>Michael Wedemeyer, Kelly Berg, and William Clarke</i>	
Amyloid Beta Protein (A $\beta$ <sub>1-42</sub> ) induced Endolysosome Iron Dyshomeostasis caused increases in Reactive Oxygen Species, Mitochondrial Depolarization, and Neurotoxicity	130
<i>Darius NK. Quansah, Peter W. Halcrow, Nirmal Kumar, Braelyn Liang, and Jonathan D. Geiger</i>	



PTBPI Contains a Novel Regulatory Sequence, the rBH3, that Binds the Pro-Survival Protein MCL1 <i>Christine Christine, Jia Cui, Alexis Acton, and William Placzek</i>	131
$\beta$ -arrestin1 Directs Substrate Lysine Selection and Linkage Type Specificity by E3 Ubiquitin Ligases <i>Chandler McElrath, Ya Zhuo, Sara Benzow, and Adriano Marchese</i>	132
GRK2 Enhances $\beta$ -arrestin Recruitment to the D2 Dopamine Receptor Through a Mechanism that is Independent From Receptor Phosphorylation or G Protein Activation <i>Noelia Boldizsar, Marta Sanchez-Soto, Julia Drube, Raphael Haider, R Benjamin Free, Carsten Hoffman, and David R. Sibley</i>	148
Molecular Determinants of Ligand-Induced Allosteric Coupling to Gq and Gi at the Angiotensin II Type 1 Receptor <i>Akua Acheampong, Laura M. Wingler, Andrew Feld, Matthew Collins, and Brandi Small</i>	149
Multimomics approach to interrogate translational regulation to GPCR signaling and its spatial bias <i>Matt J. Klauer, Caitlin Jagla, and Nikoleta Tsvetanova</i>	150
MiR-146b inhibits lung fibroblast proliferation and differentiation by targeting EGFR and TGF $\beta$ R signaling pathways <i>Venkatlaxmi Chettiar, Yan Xie, Yapei Huang, Steven K. Huang, Bethany B. Moore, Myron Toews, Peter Abel, and Yaping Tu</i>	163
Molecular mechanisms of G $\beta\gamma$ -stimulated activation of PLC $\beta$ <i>Isaac J. Fisher, Kennedy Outlaw, Kaushik Muralidharan, and Angeline Lyon</i>	164
Visualizing the chaperone-mediated folding trajectory of the G protein $\beta 5$ $\beta$ -propeller by high resolution cryo-EM <i>Mikaila Sass, Shuxin Wang, William G. Ludlam, Yujin Kwon, Ethan Carter, Peter S. Shen, and Barry M. Willardson</i>	279
Treatment of Osteoarthritis via Stem Cell Therapy <i>Gabrielle Thomas</i>	280
Structure–Activity Relationships of a Brain-Penetrant D3 Dopamine Receptor Negative Allosteric Modulator and Investigation of its Binding Site <i>Amy E. Moritz, Nora S. Madaras, Laura R. Inbody, Amber M. Kelley, Disha M. Gandhi, Emmanuel O. Akano, Kuo H. Lee, R. Benjamin Free, Xin Hu, Noel T. Southall, Marc Ferrer, Lei Shi, Kevin J. Frankowski, and David R. Sibley</i>	281
Filming the DNA Damaging Mechanisms of AuNP by the Four Dimensions Atomic Force Microscopy (4DAFM) in Molecular Environment <i>Hosam G. Abdelhady, Fadilah Aleanizy, and Arun Iyer</i>	282
Transcriptional Analysis of RGS10 Function in Microglia <i>Shwetal Talele, Stephanie Gonzalez, Violeta Saldarriaga, Shelley Hooks, and Benita Sjogren</i>	283
Curcumin ameliorates experimental colitis by suppressing PERK-UPR-signaling pathway <i>Islam I. Khan, Zahraa Baydoun, and Muddanna Rao</i>	284
Calcium-dependent regulation of G protein-coupled receptor kinases <i>Konstantin Komolov, Daniela K. Laurinavichyute, Anshul Bhardwaj, and Jeffrey L. Benovic</i>	285
Effect of Ecdysterone on Dry Eye Syndrome In Vitro and In Vivo <i>Bongkyun Park</i>	286
Development of Transgenic Mouse Platform for the Detection of Endogenous G protein Activity <i>Remi Janicot, Marcin Maziarz, Jong-Chan Park, and Mikel Garcia-Marcos</i>	287
Identification and pharmacological characterization of a novel $\beta$ -arrestin-biased negative allosteric modulator of the $\beta$ adrenergic receptor <i>Francesco F. De Pascali, Michael Ippolito, Nathan Hopfinger, Konstantin E. Komolov, Daniela K. Laurinavichyute, Leon A. Sakkal, Ajay P. Nayak, Poli AN. Reddy, Preston S. Donover, Melvin Reichman, Joseph M. Salvino, Raymond B. Penn, Roger S. Armen, Charles P. Scott, and Jeffrey L. Benovic</i>	289
Location-Biased Activation of the Proton-Sensor GPR65 is Uncoupled from Receptor Trafficking <i>Loyda M. Marie Morales-Rodriguez and Manoj A. Puthenveedu</i>	290
Identifying Novel Regulators of Adrenergic Signaling from Endosomes <i>Ian Chronis and Manoj A. Puthenveedu</i>	323
Molecular regulation of G protein prenylation under sub-optimal conditions <i>Ajith Karunarathne, Mithila Tennakoon, Waruna Thotamune, and John L. Payton</i>	324
Novel G $\alpha$ GTP Sensors to probe Subcellular signaling of Endogenous heterotrimeric G proteins <i>Dhanushan Wijayarathna and Ajith Karunarathne</i>	325
Structure-activity relationship of G protein-coupled receptor kinase 5 (GRK5) and its mutants	326

<i>Priyanka Naik, Qiuyan Chen, and John JG. Tesmer</i>	
Enhanced cAMP-based assay for GPCR deorphanization <i>Luca Franchini, Lindsay R. Watkins, and Cesare Orlandi</i>	327
Identification of a sequence of the activity-dependent neuroprotective protein (ADNP) that is necessary for its interaction with G <sub>q</sub> <i>Nathalie Momplaisir, Naincy R. Chandan, and Alan V. Smrcka</i>	328
Insights into Affinity Improvement of an Engineered Tissue Inhibitor of Metalloproteinases from Molecular Dynamics Simulations <i>Matt Coban, Thomas R. Caulfield, and Evette S. Radisky</i>	329
Spatial Compartmentalization of mTORC1 to the Nucleus to Regulate Transcription and Impact Nuclear Erk Signaling <i>Ayse Sahan, Yanghao Zhong, Consuelo Saucedo, David J. Gonzalez, and Jin Zhang</i>	330
Glial Cell Development is Changed by Genetic Overexpression of MeCP2 in a Pitt-Hopkins Syndrome Mouse Model <i>Geanne A. Freitas, Sheryl Anne D. Vermudez, Vaishnavi M. Bavadekar, Rocco Gogliotti, and Colleen M. Niswender</i>	331
Pharmacological Modulation of Hsp70 to Selectively Remove Misfolded Neuronal Nitric Oxide Synthase <i>Anthony Garcia, Emily Xu, Miranda Lau, Andrew Alt, Andrew Lieberman, and Yoichi Osawa</i>	332
Intracellular metabotropic glutamate receptor 5 (mGlu <sub>5</sub> ) triggers ER calcium release distinct from cell surface counterparts in striatal neurons <i>Yuh-Jiin I. Jong, Steven K. Harmon, and Karen O'Malley</i>	333
Agonist concentration-dependent conformational changes of formyl peptide receptor 1 contribute to biased signaling in phagocytes <i>Richard Ye and Junlin Wang</i>	334
Fluorescence Resonance Energy Transfer (FRET) Spatiotemporal Mapping of Atypical P38 Reveals an Endosomal and Cytosolic Spatial Bias <i>Jeremy J. Burton, Jennifer J. Okalova, and Neil Grimsey</i>	349
Cargo-selectivity of Vesicle-associated Membrane Proteins in GPCR Exocytosis <i>Hao Chen, Zara Weinberg, G. Aditya Kumar, and Manoj A. Puthenveedu</i>	350
Delineation of the G Protein-Coupled Receptor Kinase Phosphorylation Sites Within the D1 Dopamine Receptor and Their Role in Regulating Receptor Function <i>Nora S. Madaras, Michele L. Rankin, R. Benjamin Free, Raphael Haider, Julia Drube, Arun K. Ghosh, John JG. Tesmer, Carsten Hoffmann, David R. Sibley, and Amy E. Moritz</i>	351
Protective Effects of Ozanimod in Cisplatin-induced Neuropathic Pain in Mice: Insights from Single-cell Transcriptomic Profiling in Spinal Cord Tissues <i>Ying Li, Silvia Squillace, Luigino Giancotti, Terrance Egan, Stella Hoft, Richard DiPaolo, and Daniela Salvemini</i>	352
Design and Development of Novel Barbiturates of Pharmacological Interest <i>Dimosthenis Koinas, Bo Wu, Anthony Pajak, Zhou Xiaojuan, Keith Miller, and Karol Bruzik</i>	366
Dopamine may increase Akt through D1-like receptor activation of PI3 Kinase in Macrophages <i>Dayna Robinson, Breana Channer, and Peter Gaskill</i>	367
The Adhesion GPCR GPR114/ADGRG5 is Activated by its Tethered-Peptide-Agonist Following Receptor Fragment Dissociation <i>Tyler Bernadyn, Rashmi Adhikari, Alexander Vizurraga, Frank Kwarcinski, and Gregory Tall</i>	478
A positive allosteric modulator of M1 Acetylcholine receptors improves cognitive deficits in male and female APP <sup>swe</sup> /PSEN1 <sup>ΔE9</sup> mice via divergent mechanisms <i>Khaled Abd-Elrahman, Tash-Lynn L. Colson, and Stephen S. Ferguson</i>	479
Investigating the Intertwine Effect of Insulin Resistance and Lipocalin Prostaglandin D2 Synthase in Non-alcoholic Fatty Liver Disease using HepG2 Cells <i>Rhema Khairnar, Md Asrarul Islam, and Sunil Kumar</i>	480
Designer Autocrine Signaling Networks for Discovering GPCR-modulating Nanobodies <i>Jacob Rowe, Kyutae Lee, Sam Taylor, and Daniel Isom</i>	481
Morphological effects of caffeine and creatine on <i>Caenorhabditis elegans</i> <i>Lance Kuo-Esser, Tommy Scandura, Ramon Chen, Nijah Simmons, Kylie Lawson, Mauricio Dominguez, Kennedy Kuchinski, Steven Le, Lauren Bennett, Wilber Escorcía, and Hanna Wetzel</i>	482
Proximity Labeling-Based Network Analysis to Probe Molecular Functions of Adenylyl Cyclase-Containing Macromolecular Complexes in Cardiomyocytes <i>Taeyeop Park, Yong Li, and Carmen Dessauer</i>	483
SMARCD3: A Link Between G <sub>q</sub> and Chromatin Remodeling?	484

<i>Joseph Loomis, Naincy R. Chandan, and Alan V. Smrcka</i>	
Early-stage Development of an <i>in vitro</i> Screening Assay to Characterize the Activation of Human Adhesion Receptor ADGRE5	485
<i>Arturo Mancini, Samya Aouad, Herthana Kandasamy, Robert Cerone, Stephan Schann, and Laurent Sabbagh</i>	
Zyflamend, a novel approach for the treatment of acute pancreatitis	486
<i>Ahmed Elshaarrawi, Ahmed Bettaieb, and Presley Dowker-Key</i>	
Elucidating Signaling Mechanisms and Pharmacology for the Brain Orphan Receptor GPR37	487
<i>Andrew Frazier and John A. Allen</i>	
Heat shock protein 90 inhibition in the spinal cord upregulates Src kinase in microglia to enhance opioid antinociception in acute pain	489
<i>Jessica Bowden and John M. Streicher</i>	
Local Knockout of the Gb5-R7 Complex (Gnb5 Gene) in the Hypothalamus Causes Obesity in Mice	522
<i>Qiang Wang, Taylor Henry, and Vladlen Slepak</i>	
Podocyte injury triggers the formation of intercellular bridges	523
<i>Nina Cintron Pregosin and Sandeep K. Mallipattu</i>	
Subcellular Optogenetic Inhibition of PLC $\beta$ -G $\alpha$ qGTP Interaction Sheds Light on the Molecular Regulation of G $\alpha$ q-Governed Directional Cell Migration	524
<i>Sithurand Ubeyasinghe, Dinesh Kankanamge, and Ajith Karunarathne</i>	
Regulation of Lysophosphatidic acid receptor 3	525
<i>Karina Helivier Solís, Ma. Teresa Romero, and J. Adolfo Garcia-Sainz</i>	
Revisiting Pirin: Evidence for a Role in Translation but not in Transcriptional Control	526
<i>Anna Denaly Cab Gomez, Richard Neubig, and Erika M. Lisabeth</i>	
Effects of RS17053 at Subtypes of alpha1-Adrenergic Receptors in Rat Vas Deferens and Aorta	527
<i>James Docherty and Hadeel A. Alsufyani</i>	
Biomolecular condensates defined by Activator of G protein Signaling 3 exhibit distinct properties and regulation	528
<i>Ali Vural and Stephen Lanier</i>	
Regulation of GPCR Signaling by Sorting Nexins	529
<i>Valeria Robleto, Ya Zhuo, Joseph Crecelius, and Adriano Marchese</i>	
Mechanisms and Consequences of Compartmentalized GPCR Signaling in Neurons	530
<i>Katherine Hall</i>	
Molecular Dynamics Studies for Nirmatrelvir and the Main Protease from Variants of the Severe Acute Respiratory Syndrome Coronavirus-2 (SARS-CoV-2)	531
<i>Kathleen Frey, Ongshu Dutta, Lilian Tran, Brandon Yin, Andrew Makarus, Raymond Marmol, and Youssef Dawood</i>	
Differential Regulation of Formyl Peptide Receptor 2 Protein in Non-alcoholic Fatty Liver Disease on High Fructose and High Fat Fed Male and Female C57BL/6 Mice	532
<i>Md Asrarul Islam, Rhema Khairnar, and Sunil Kumar</i>	
Role of orphan G Protein-Coupled Receptor GPRC5B in retinoic acid induced depressive-like behaviors	533
<i>Wenqi Fu, Luca Franchini, Cesare Orlandi, and Nina Wettschureck</i>	
Development of a Genetically Encodable Fluorescent Biosensor to Examine the Spatiotemporal Regulation of NEK Kinases in Living Cells	548
<i>Brandon M. Baker, Henry Uchenna, Andrew L. White, Janetta Janetta Edwards, Kayla M. Jamison, Yasseen Abdellaoui, J. Shane Henderson, Stephanie Goodrich, Robert H. Newman, and David H. Drewery</i>	
HIV-1 gp120- and Morphine-Induced Endolysosome Iron Release Triggers Disruption of the Reactive Species Interactome and Cell Death	549
<i>Nirmal Kumar, Peter W. Halcrow, Darius NK. Quansah, Braelyn Liang, and Jonathan D. Geiger</i>	
ABCC4 Impacts Megakaryopoiesis by Regulating Intracellular cAMP levels	550
<i>Sabina Ranjit, Yao Wang, Satish B. Cheepala, Jingwen Zhu, Woo Jung Cho, Cam Robinson, Scott Olsen, and John Schuetz</i>	
Comparison of $\Delta$ 9-tetrahydrocannabinolic acid A (THCA-A) and Delta-9-tetrahydrocannabinol (THC) in neuronal cell functions	551
<i>Khalil Eldeeb, Sandra Leone-Kabler, and Allyn Howlett</i>	
Optimization of a Novel D2 Dopamine Receptor-Selective Antagonist into Lead Candidates for the Treatment of Neuropsychiatric Disorders	566
<i>Ashley Nilson, John Hanson, Andres E. Dulcey, Xin Wen, R. Benjamin Free, Raul R. Calvo, Juan J. Marugan,</i>	

and David R. Sibley

- N-cadherin Signaling via PI3K $\beta$ -Akt3 Stabilizes Occludin Tight Junctions in the Blood-Brain Barrier 567  
*Quinn Lee, Kevin Kruse, Shuangping Zhao, Leon Tai, and Yulia Komarova*
- Cannabinoid Receptor Interacting Protein 1a (CRIP1a) Associates with G $\alpha$ i in a GTP $\gamma$ S or Agonist Dependent Manner 568  
*Erin K. Hughes, Audrey Chrisman, Sandra Leone-Kabler, Glen S. Marrs, W. Todd Lowther, and Allyn Howlett*

## CENTRAL NERVOUS SYSTEM PHARMACOLOGY - BEHAVIORAL

- Early Life Adversity Disrupts Social Preference and Opioid Reward Mechanisms in Adolescent Mice 1  
*Malabika Maulik, Madison Michels, Kayla DeSchepper, Angela Henderson-Redmond, Daniel Morgan, and Swarup Mitra*
- Nicotinamide Adenine Dinucleotide (NAD) Attenuates the Rate-Decreasing Effects of Oxycodone Withdrawal in Rats with No Apparent Abuse Liability 2  
*Sarah Melton, Tamara Morris, Ashley Henderson, Aslan Abdurrahman, Will Smith, Ashton Friend, Richard Mestayer, and Peter J. Winsauer*
- R-(-)-2,5-dimethoxy-4-iodoamphetamine [(-)-DOI] decreases cocaine demand in a 5-HT $_2A$ R-mediated manner 3  
*Leah Salinsky, Christina R. Merritt, Noelle C. Anastasio, and Kathryn A. Cunningham*
- Opioid-related discriminative stimulus, antinociceptive and respiratory depressant effects of substituted 3-hydroxy-N-phenethyl-5-phenylmorphans 4  
*Carol Paronis, Tyler J. Lee, Mauricio Ruiz Soler, Dana R. Chambers, Joshua Lutz, Dan Luo, Thomas Prinszano, Agnieszka Sulima, Arthur Jacobson, Kenner Rice, and Jack Bergman*
- Behavioral and Neurochemical Effects of Extended Access to Stimulant Self-Administration in Rats 5  
*Robert Seaman, Kariann Lamon, Nicholas Whitton, Agnieszka Sulima, Kenner Rice, Kevin Murnane, and Gregory T. Collins*
- Eating a High Fat/High Carbohydrate or Ketogenic Diet Does Not Impact Sensitivity to Morphine-induced Antinociception in Rats with Hindpaw Inflammation 6  
*Katherine M. Serafine, Madeline K. Elsey, Nina M. Beltran, and Vanessa Minervini*
- GPR183 Activation in the Peripheral Nervous System Induces Behavioral Hypersensitivities in Rats 7  
*Kyle Oberkrom, Kathryn Braden, Zhoumou Chen, Luigi A. Giancotti, Christopher K. Arnatt, and Daniela Salvemini*
- KATP channel produgs reduce hypersensitivity in neuropathic and inflammatory pain models, morphine-induced hypersensitivity, and reduce withdrawal behaviors in mice 8  
*Amanda Klein, Alexis Doucette, Kayla Johnson, Shelby Hulke, Sunna Mujteba, Elena Miller, and Peter I. Dosa*
- Differential effects of kappa opioid receptor activation and blockade on the development of methamphetamine-induced sensitization in adult male and female rats 9  
*Manoranjan D'Souza, Madison Snyder, and Sarah Seeley*
- Inhibition of ACAT as a Therapeutic Target for Alzheimer's Disease is Independent of ApoE4-lipidation 10  
*Ana Valencia, Deebika Balu, Naomi Faulk, Jason York, and Mary Jo LaDu*
- Characterizing a Mesolimbic Circuit for Opioid Reward 11  
*Ruben A. Garcia-Reyes and Daniel Castro*
- Characterizing How Lesioning of Cocaine Activated Ensembles in the Nucleus Accumbens Affects Cocaine Related Behaviors 13  
*Rishik Bethi, Kim Thibeault, and Erin Calipari*
- Social Isolation Stress Leads to Synaptic Changes in Locus Coeruleus Noradrenergic Neurons 14  
*Jenny Kim*
- Genetic Brain Serotonin Deficiency Significantly Impacts a Subset of Behavioral and Molecular Responses to Psychostimulants in Mice 15  
*Benjamin Sachs, Madeline Wujek, Michelle M. Karth, Melinda D. Karth, Gianna M. Perez, and Davis J. Van Dyk*
- Mitochondria as key mediators of behavioral and metabolic effects of stress 16  
*Erin Gorman-Sandler, Breanna Robertson, Jesseca Crawford, Gabrielle Wood, Noelle Frambes, Marnie McLean, Jewel Scott, Michael J. Ryan, Susan Wood, Abbi Lane, and Fiona Hollis*
- Methamphetamine Route of Administration has a Disproportionate Impact on Females than Males 17  
*Mary F. Vest, Alexandru M. Demitrescu, Christina Ledbetter, Vinita Batra, Elliott Thompson, Nicholas Goeders, James C. Patterson, and Kevin Murnane*
- Reversal of a Scopolamine-Induced Cognitive Deficit in Group-Housed Monkeys Who Drink Ethanol 18

<i>Lindsey Galbo-Thomma, Phillip Epperly, and Paul Czoty</i>	
Microglia-Oligo Cross-Talk: PLX5622 Rescues Susceptibility to Stress, Decreases Inflammatory Markers, and Reduces Numbers of ImOL Present in mPFC	63
<i>Miguel Madeira, Zachary Hage, Styliani-Anna (Stella) E. Tsirka, and Alexandros Kokkosis</i>	
Modifying the Conditioned Reinforcing Properties of Cocaine in the New Response Acquisition Procedure	64
<i>Lauren Rysztak and Emily M. M Jutkiewicz</i>	
Aged mice exhibit more rapid acquisition of remifentanyl self-administration and an up-shifted dose-response curve	65
<i>Darius Donohue, Kelsey Carter, Patricia Vangeneugden, Kylie Handa, Sofia Weaver, Amanda L. Sharpe, and Michael J. Beckstead</i>	
GPR55 Antagonist KLS-13019 Reverses Chemotherapy-Induced Peripheral Neuropathy (CIPN) in Rats	66
<i>Michael Ippolito</i>	
Effects of a highly G Protein-Biased Mu Opioid Receptor Agonist, SR-17018, in Non-human Primates	67
<i>Mei Chuan Ko, Huiping Ding, Norikazu Kiguchi, Dehui Zhang, and Yanan Zhang</i>	
Ventilatory Effects of Mu Opioid Receptor Agonist Mixtures	68
<i>Shawn Flynn and Charles P. France</i>	
Behavioral effects of fentanyl in presence or absence of chronic neuropathic pain in male and female rats	201
<i>Gwendolyn Burgess, Hailey Y. Rizk, Shane M. Sanghvi, Melanie R. Vocelle, and Emily M. M Jutkiewicz</i>	
Genetic deletion of atypical VGLUT3 rescues Huntington's disease phenotype and neurodegeneration in zQ175 mice	202
<i>Karim Ibrahim, Khaled Abd-Elrahman, and Stephen S. Ferguson</i>	
The serotonergic psychedelic <i>N,N</i> -Dipropyltryptamine prevents seizures in a mouse model of fragile X syndrome via an apparent non-serotonergic mechanism	203
<i>Richa Tyagi, Tanishka S. Saraf, and Clinton E. Canal</i>	
Mitochondrial SIRT3 and morphine induced hyperalgesia and tolerance: the effect of polyphenol fraction of bergamot	204
<i>Sara S. Ilari, Filomena A. Lauro, Luigino Giancotti, Concetta Dagostino, Valentina Malafoglia, Lucia C. Passacatini, Cinzia Garofalo, Marco Tafani, Ernesto Palma, Carlo Tomino, Daniela Salvemini, Vincenzo Mollace, and Carolina Muscoli</i>	
Effects of Cannabinoids on Fentanyl Antinociception	205
<i>Dalal Alkhelb, Christos Iliopoulos-Tsoutsouva, Spyridon P. Nikas, Michael S. Malamas, Alexandros Makriyannis, and Rajeev I. I. Desai</i>	
Clozapine, but Not Ziprasidone, Decreases the Discriminative Stimulus Effects of 22 Hours Deprivation in Sprague-Dawley Rats	206
<i>Simon Tangen, Sydney K. Wenzel, Erika K. Cedarbloom, Giulia Lelli, and David Jewett</i>	
Fentanyl-Targeting Monoclonal Antibodies Block Fentanyl-Induced Respiratory Depression in Non-Human Primates	207
<i>Emily Burke, Paul T. Bremer, and Rajeev Desai</i>	
Dramatic increase in lever pressing activity in rats following cocaine self-administration on high fixed ratio schedules	208
<i>Jhanvi N. Desai, Abigail Muccilli, Luis Tron Esqueda, Andrew Norman, and Jeffrey A. Welge</i>	
Role of Opioid Analgesic Efficacy in the Treatment of Pain-Related Disruption of Behavior in Male and Female Mice	209
<i>Laurence Miller, Jamani Garner, Kelly Roen, and Gabrielle Pollard</i>	
Positive Allosteric Modulation of the Mu Opioid Receptor Does Not Potentiate Opioid-Mediated Side Effects	210
<i>Kelsey Kochan, Thomas Prince, and John Traynor</i>	
Allosteric Dopamine transporter modulator inhibits cocaine-induced behaviors	211
<i>Yibin Xu, Stacia Lewandowski, Christina Besada, and Ole Mortensen</i>	
Commonalities of Ginseng Extract ( <i>P. quinquefolius</i> ) and Exercise Mimetic $\beta$ -GPA for Reducing Age-related Cognitive Deficits and Modulating the Autophagy-Lysosomal Pathway	212
<i>Ben Bahr, Michael Almeida, and Stephen Kinsey</i>	
Evaluating Serotonin 2C and Dopamine D3 Receptor Ligands, Alone and in Mixtures, as Candidate Medications for Substance Use Disorders	213
<i>Briana Mason, Anona Thomas, Yonggong Shi, Christina George, Jianjing Cao, Amy Newman, and Gregory T. Collins</i>	
Novel Sigma Receptor Dual Modulator Enhances Memory Behavior in the Senescence-Accelerated Prone Mouse (SAMP8) Model of Age-Related Cognitive Decline	214
<i>Ariel Magee, Susan A. Farr, Mike Niehoff, Ivonne Larrea, Yoan Ganev, Ken Witt, and Justin Samanta</i>	
Effects of a two-hit model of early life adversity on oral ethanol self-administration and adrenergic receptor expression in adolescent rats	215
<i>Brian Parks, Paloma Salazar, Madison McGraw, Lindsey Morrison, Julia Tobacyk, Lisa Brents,</i>	

<i>and Michael Berquist</i>	
Pentobarbital More Potently Disrupts Learning in Females Than Males Compared to Other Allosteric Modulators of the GABA <sub>A</sub> Receptor Complex	216
<i>Ashley Henderson, Tamara Morris, Sarah Melton, and Peter J. Winsauer</i>	
The ascending limb of the dose-response curve for cocaine self-administration is an experimental artifact	217
<i>Luis Tron Esqueda, Jhanvi N. Desai, and Andrew Norman</i>	
Organic Cation Transporter 3 is a Crucial Modulator of Serotonin Clearance in Basolateral Amygdala and Sex-Dependently Modulates Fear Behaviors	265
<i>Nikki Clauss, Lauren Honan, William A. Owens, Rebecca Horton, Glenn Toney, and Lynette C. Daws</i>	
Ethanol Vapor Self-administration Reveals that Female Wistar Rats are More Likely to Become High Intensity Binge Users than Male Rats	266
<i>Alicia Avelar, Kareena Narula, Kalie A. Quon-adams, Stephanie Krause, Amanda Roberts, Giordano de Guglielmo, and Olivier George</i>	
Effects of Cannabinoids and a Cannabinoid Extract on Thermal Nociception and Conditioned Behavior	267
<i>Tamara Morris, Peter J. Winsauer, Scott Edwards, and Jessica Cucinello-Ragland</i>	
Hypothalamic nociceptin neurons modulate stress-induced binge eating behaviors	268
<i>Kyle Parker, Vincent Duong, Wenxi Yang, and Lamley Lawson</i>	
Role of Neuromedin S-expressing Ventral Tegmental Area Neurons in Morphine Behavior	269
<i>Cristina Rivera Quiles, Milagros Alday, Olivia Dodson, and Michelle Mazei-Robison</i>	
Self-administration of G-protein biased mu opioid agonists in nonhuman primates	270
<i>Carol Paronis, Kristen E. George, Eric W. Bow, Eugene S. Gutman, Agnieszka Sulima, Kenner Rice, Arthur Jacobson, and Jack Bergman</i>	
Targeting A3 Adenosine Receptor (A3AR) Attenuates Paclitaxel-induced Cognitive Impairment	400
<i>Silvia Squillace, Timothy Doyle, Michael Niehoff, Kenneth Jacobson, Susan A. Farr, and Daniela Salvemini</i>	
Dynorphin release in the dorsal nucleus accumbens drives decreased feeding and consummatory reward behavior in mice	401
<i>Nathanyal Ross, Sineadh Conway, and Ream Al-Hasani</i>	
A Role of NOD2 in CARTp-mediated Behavioral Hypersensitivities	402
<i>Rachel Schafer, Luigi A. Giancotti, Zhoumou Chen, Timothy Doyle, Jinsong Zhang, and Daniela Salvemini</i>	
Effect of Methylphenidate on Motor Skill Learning and Consolidation	403
<i>Cecilia Lee, Kaitlin R. Van Alstyne, and Stephan G. Anagnostaras</i>	
Nicotine Withdrawal During Contextual Fear Extinction Causes Sex Specific Impacts in the Murine Dorsal and Ventral Hippocampus	404
<i>Jack Keady and Jill Turner</i>	
Widening the Opioid Analgesia Therapeutic Window with a Dual Pharmacology Strategy	405
<i>Indu Mithra Madhuranthakam, Sarah Uribe, Danya Aldaghma, Drew Kwitchoff, Jonathan Philip, Aela A. Williams, Rohit A. Nambiar, Dishary Sharmin, James Cook, Bradford Fischer, and Thomas Keck</i>	
Blockade of selective Gβγ signaling pathway by gallein decreases development of opioid tolerance	406
<i>Alan V. Smrcka, Gissell Sanchez, and Emily M. M Jutkiewicz</i>	
M1 Positive Allosteric Modulators Enhance Domains of Cognitive Function by Activation of ssT-expressing Interneurons in the Prefrontal Cortex	407
<i>Jerri Rook, Zixiu Xiang, Jonathan Dickerson, Shalini Dogra, Kendall Jensen, Insung Kim, Megan Ohler, Kelly Weiss, and P. Jeffrey Conn</i>	
Behavioral Performance Characterization of the Putative Neuroinflammation Inhibitor 1-Methyl-Tryptophan Following Acute Traumatic Stress in Rats	408
<i>Rachel M. Taylor, Fred L. Johnson, Emily M. Scott, Aurian Naderi, Kacie M. McKinney, Kilana D. Coachman, Laurence P. Simmons, James C. DeMar, Peethambaran Arun, Joseph B. Long, Liana M. Matson, and Emily G. Lowery-Gionta</i>	
Investigation of the Contribution of Glucose Transport to Detection of Glucose Taste by Human Subjects in a Rapid Throughput Taste Discrimination Assay	409
<i>R. Kyle Palmer and Anna K. Nechiporenko</i>	
Discriminative Stimulus Properties of Lorcaserin in C57BL/6 mice	410
<i>Fan Zhang, Katherine Nicholson, Keith L. Shelton, Todd M. Hillhouse, Herbert Y. Meltzer, and Joseph Porter</i>	
Antinociceptive Effects of Fentanyl and Non-opioid Drugs in Methocinnamox-treated Rats	411
<i>Saba Ghodrati, Lawrence Carey, and Charles P. France</i>	

Microglia in the Locus Coeruleus Mediate the Behavioral and Neuronal Consequences of Social Stress in Females <i>Cora Smiley, Samantha Bouknight, Brittany Pate, Alexandria Nowicki, Evelyn Harrington, and Susan Wood</i>	412
Role of ventral tegmental area SGK1 phosphorylation and activity in drug-associated behaviors <i>Samantha Caico</i>	413
Veterinary anesthetic xylazine produces synergistic antinociceptive effects with the opioid fentanyl in mice <i>Ellen Walker, Jumar Etkins, Karen Gonzalez, and Gabriel Vivas</i>	414
Sprague Dawley Rats from Different Vendors Vary in the Modulation of Prepulse Inhibition of Startle (PPI) by Dopamine, Acetylcholine, and Glutamate Drugs <i>S. Barak Caine and Morgane Thomsen</i>	415
Discriminative Stimulus Effects of 30.0 and 300.0 mg/kg Gabapentin in Rats: Substitution Testing with Morphine and Fentanyl <i>Alexia G. Dalton, Madeline T. Van Fossen, Alexandria Iannucci, Joshua Prete, Taylor Galaszewski, Dillon S. Shekoski, Bethany E. Beavers, and Adam J. Prus</i>	416
The Effects of Eating a Traditional High Fat or a Ketogenic Diet on Sensitivity of Female Rats to Morphine-Induced Antinociception, Tolerance and Withdrawal <i>Nina M. Beltran, Alyssa N. Parra, Isabella M. Castro, Madeline K. Elsey, Ana Paulina Serrano, Jazmin R. Castillo, Vanessa Minervini, and Katherine M. Serafine</i>	417
The compulsion zone theory of cocaine self-administration behavior in rats explains the effects of fixed ratio magnitude on inter-injection intervals <i>Abigail Muccilli, Jhanvi Desai, and Andrew Norman</i>	464
A Behavioral Economic Analysis of Polysubstance Use: Studies with Cocaine, Fentanyl, and Cocaine–Fentanyl Mixtures in Sprague-Dawley Rats <i>Harmony Risca and Gregory T. Collins</i>	465
A Reinforcer Worth its Salt? <i>Lee Gilman, Marissa M. Nicodemus, Allianna K. Hite, Cameron N. Russell, Lauren R. Scrimshaw, Jasmin N. Beaver, and Brady L. Weber</i>	466
Opposing Roles of Enkephalin and Dynorphin in the Amygdala on Resilience to Social Stress in Females <i>Alexandria Nowicki, Cora Smiley, Brittany Pate, Samantha Bouknight, and Susan Wood</i>	467
The Synthetic Psychedelic 2,5-methoxy-4-iodoamphetamine (DOI) Attenuates the Positive Appetitive and Reinforcing Effects of Methamphetamine <i>Bo J. Wood and Kevin Murnane</i>	468
Corticotropin-releasing factor pathways facilitate hypervigilant behavioral and physiological responses to social stress in female rats <i>Brittany Pope, Sarah Mott, Evelyn Harrington, Cora Smiley, Jim Fadel, and Susan Wood</i>	469

## CENTRAL NERVOUS SYSTEM PHARMACOLOGY - NEUROPHARMACOLOGY

Bidirectional ERK1/2 Modulation in Dopaminergic Neurons Regulates DAT Expression and Function <i>Christina Besada, Stacia I. Lewandowski, and Ole Mortensen</i>	69
Pharmacology of Memory Dysfunction in Alzheimer’s Disease (AD) <i>Marcia Ratner and David H. Farb</i>	70
Unconventional Mechanisms of Novel Positive Allosteric Modulators of NMDA Receptors <i>Elijah Ullman, Riley Perszyk, Jing Zhang, Nick Akins, Russell Fritzemeier, Srinu Paladugu, Dennis Liotta, and Stephen Traynelis</i>	71
Agmatine inhibits NMDA Receptor-mediated Calcium Transients in Spinal Cord Dorsal Horn <i>Tongzhen Xie, Rachel E. Schorn, Cristina D. Peterson, Lucy Vulchanova, George L. Wilcox, and Carolyn A. Fairbanks</i>	72
Real-time pharmacokinetic measurements of vancomycin in the brain of mice via electrochemical aptamer-based sensors <i>Karen KS. Scida, Miguel A. Pellitero, Netzahualcoyotl Arroyo-Curras, and Gregory Carr</i>	73
Role of Glucagon-like peptide-1 Expressing Ventral Tegmental Area Neurons in Morphine Behavior <i>Olivia Dodson, Cristina Rivera Quiles, and Michelle Mazei-Robison</i>	74
Regulated Trafficking of GABA Transporters, GAT1 and GAT3, in Response to Methamphetamine <i>Hannah R. Grote, Susan G. Amara, and Suzanne M. Underhill</i>	75
Characterizing Glutamate Stimulated Noradrenaline Release in Rat Cerebral Cortex Brain Slices: Release Mediating Receptors and their Subunits Composition <i>Yousef ALJOHANI, Ghazaul Dezfuli, and Kenneth J. Kellar</i>	76

Redox-dependent Activation of Protein Kinase C and Neurotransmitter Transporter Trafficking <i>Saranya Radhakrishnan and Susan G. Amara</i>	133
Intrinsic Alterations of Dopaminergic Neurons in the 3xTg-Alzheimer's Disease Mouse <i>Harris E. Blankenship, Kylie Handa, Willard M. Freeman, and Michael J. Beckstead</i>	134
Alternatively Spliced Variants of the Mu Opioid Receptor Gene, <i>Oprm1</i> , Differentially Mediate Opioid-Induced Respiratory Depression in Rats <i>Ayma F. Malik</i>	135
Dopamine Dysregulation and Beyond: Exploring Methamphetamine-Induced Neuropathology <i>Nicole Hall, Kariann Lamon, Nicholas Whitton, and Kevin Murnane</i>	136
Novel Somatostatin Receptor Subtype-4 Agonist Enhances Memory and Neprilysin Enzyme Activity in Senescence Accelerated Mouse-Prone 8 Model of Cognitive Decline <i>Kuber Bajgain, Karin Sandoval, Ariel Magee, Susan A. Farr, Michael Niehoff, and Ken Witt</i>	137
$\beta$ -Arrestins Mediate Rapid 5-HT <sub>2A</sub> Receptor Endocytosis to Control the Efficacy and Kinetics of Serotonin and Psychedelic Hallucinogen Signaling <i>Hudson Smith, Daniel E. Felsing, Ashley Nilson, and John A. Allen</i>	138
Gain Modulation by Mouse Prefrontal Cortex Diminishes Fentanyl-Induced Respiratory Depression <i>Daniel P. Woods, Ryan S. Herzog, Qiwei W. Sun, Zachary T. Glovak, Helen A. Baghdoyan, and Ralph Lydic</i>	139
Ethanol Effects on Synaptic Transmission: Implications for Motor Learning and Memory <i>Grace Nelson, Armando Salinas, Charles Levy, and Logan Slade</i>	140
Metabotropic glutamate receptor 3 activation modulates thalamic inputs to the nucleus accumbens and rescues schizophrenia-like physiological and behavioral deficits <i>Shalini Dogra and P. Jeffrey Conn</i>	141
Characterization of Novel Tryptamines' Anxiolytic and Anti-Inflammatory Effects in Relation to their Psychoactive Effects <i>Catharine Carfagno, M. F. Vest, Kevin Murnane, Kariann Lamon, and Bo J. Wood</i>	142
Role and Regulation of BNST GluN2D-containing NMDARs in a Continuous Access Ethanol Task <i>Marie A. Doyle, Megan E. Altemus, Gregory J. Salimando, Justin K. Badt, Michelle N. Bedenbaugh, Anika S. Park, Danielle N. Adank, Richard B. Simerly, and Danny G. Winder</i>	143
Uncovering the release dynamics of enkephalins following acute stress and opioid exposure <i>Marwa Mikati, Petra Erdmann-Gilmore, Rose Connors, Sineadh Conway, Justin Woods, Robert Sprung, Reid Townsend, and Ream Al-Hasani</i>	144
TRPA1 Receptor Expressed by the Edinger-Westphal Nucleus (EWcp) is Involved in Stress Adaptation <i>Dr. Erika Pinter, Viktória Kormos, Dóra Zelena, János Konkoly, Balázs Gaszner, and Miklós Kecskés</i>	145
Diurnal Variation in Acetylcholine Modulation of Dopamine Dynamics Following Chronic Cocaine Intake <i>Melody Iacino and Mark Ferris</i>	146
Concomitant Mild Traumatic Brain and Burn Injury Elicits a Unique Gene Expression Profile within the Brain <i>Christopher O'Connell, Evan Reeder, Ryan Brown, Matthew Robson, and Jason Gardner</i>	165
Delta Opioid Receptor Activation Blocks Allodynia in a Model of PACAP-induced Headache <i>Elizaveta Mangutov, Isaac Dripps, Kendra Siegersma, Rebecca Bocian, Sarah Asif, Wiktor Witkowski, and Aymnah Pradhan</i>	166
Antisense oligonucleotides targeting microRNA binding sites in the GRN mRNA increase progranulin translation: potential therapeutic strategy for frontotemporal dementia <i>Spencer Jones, Geetika Aggarwal, Yousri Benchaar, Jasmine Bélanger, Myriam Sévigny, Denise Smith, Michael Niehoff, Ian Mitchell de Vera, Terri Petkau, Blair Leavitt, Karen Ling, Paymaan Jafar-Nejad, Frank Rigo, John Morley, and Andrew Nguyen</i>	167
A Novel Clinical-stage Small Molecule Targeting the 'Dark Side' of Opioid Addiction <i>Rhianne Scicluna, Tylah Ms. Doolan, Erin Lynch, Nicholas Everett, and Michael Bowen</i>	168
Multiplexed pharmacological calcium imaging reveals distinct GPCR-mediated response profiles of locus coeruleus neurons <i>Chao-Cheng Kuo and Jordan McCall</i>	169
Fatty Acid Binding Protein 5 Modulates Brain Endocannabinoid Tone and Retrograde Signaling in the Striatum and Hippocampus <i>Mohammad Fauzan, Saida Oubraim, Mei Yu, Sherrye T. Glaser, Martin Kaczocha, and Samir Haj-Dahmane</i>	170



Antidepressants and Dopamine Levels Induced by Substance Misuse Regulate Inflammation and HIV in Myeloid Cells <i>Stephanie Matt, Rachel Nolan, Breana Channer, Joanna Canagarajah, Samyuktha Manikandan, Yash Agarwal, Krisna Mompho, Oluwatofunmi Oteju, Kaitlyn Runner, Alexis Brantly, Emily Nickoloff-Bybel, and Peter Gaskill</i>	271
Is Ketamine a rapid acting antidepressant in juvenile rats? <i>David Middlemas, Brianna Stanley, and Alexis Klinner</i>	272
Impact of Maternal Overnutrition in Central Nervous System Circuits that Regulate Feeding <i>Sai Shilpa Kommaraju, Ming Gao, Elaine Cabrales, Chelsea Faber, and Zaman Mirzadeh</i>	273
Effects of Cannabinoid CB <sub>1</sub> agonists on extracellular levels of dopamine in the nucleus accumbens shell of male mice <i>Evan Smith, Dalal Alkheib, Christos Iliopoulos-Tsoutsouvas, Spyros Nikas, Rajeev Desai, and Alexandros Makriyannis</i>	274
Dopaminergic Immunomodulation May Amplify Macrophage Inflammation in the Context of HIV Infection <i>Breana Channer, Dayna Robinson, Oluwatofunmi Oteju, Stephanie Matt, and Peter Gaskill</i>	275
Prenatal Stress Alters Transcription of NMDA Receptors in the Frontal Cortex and Hippocampus <i>Tristram Buck and Monsheel Sodhi</i>	276
Spinal Aha1 inhibition improves morphine therapy for pain management <i>Wei Lei, Valentin M. Kliebe, Katherin Gabriel, Christopher S. Campbell, John M. Streicher, Brian S.J. Blagg, and Lauren Ball</i>	277
Nucleus Accumbens Single Nucleus RNA Sequencing Identifies Cell Subtype-Specific Maladaptations after Prolonged Spared Nerve Injury <i>Randal Serafini, Aarthi Ramakrishnan, Molly Estill, Vishwendra Patel, John Fullard, Robert Blitzer, Shahram Akbarian, Panos Roussos, Venetia Zachariou, and Li Shen</i>	278
The Ventral Tegmental Area and Medial Habenula Differentially Control Reward, Reinforcement, and Intake of Nicotine <i>Brandon Henderson, Nathan A. Olszewski, and Samuel J. Tetteh-Quarshie</i>	335
Alkoxy Chain Length Governs the <i>In Vitro</i> and <i>In Vivo</i> Potency of 2-Benzylbenzimidazole Opioids Implicated in Human Overdose Deaths <i>Michael Baumann, Donna Walther, Marthe M. Vandeputte, Meng-Hua M. Tsai, Li Chen, Christophe P. Stove, and Grant Glatfelter</i>	336
Coronaridine Congeners Attenuate Fentanyl Seeking During Prolonged Abstinence, Possibly Through Inhibiting Dopamine Release in the Nucleus Accumbens <i>Jacob D. Layne, Mason J. Hochstetler, Brandon M. Curry, Benjamin M. Williams, Christina A. Small, Scott C. Steffensen, Hugo R. Arias, and Craig T. Werner</i>	337
Effects of Aripiprazole on Nicotine Withdrawal-Like Behaviors and Murine Neuregulin 3-ErbB4 Signaling <i>Emily Prantzalos and Jill Turner</i>	338
Effect of Inhibition of Xenobiotic Transporter MRP5/ABCC5 on Neurite Elongation: Screening for MRP5 Inhibitors among Clinically Used Drugs <i>Takahiro Ishimoto, Hirofumi Yagi, Yusuke Masuo, and Yukio Kato</i>	339
Deferiprone Decreases Labile Iron in Brain and Ameliorates Abnormal Emotional Behavior in Mice with Brain Iron Accumulation <i>Ruiying Cheng, Yingfang Fan, Rajitha Gadde, Swati Betharia, and Jonghan Kim</i>	340
High-throughput, microplate reader detection of the ASP <sup>+</sup> fluorescent substrate to identify novel inhibitors of organic cation transporter-3 <i>Rheaclare Fraser-Spears, Ann Decker, Bruce Blough, and Lynette C. Daws</i>	341
Therapeutic Efficacy of Macamides on Fragile X Tremor/Ataxia Syndrome (FXT/AS) <i>Collis Brown, Sonya Sobrian, and Tamaro Hudson</i>	342
Ethanol-induced suppression of GIRK-dependent signaling in the basal amygdala <i>Ezequiel Marron, Megan E. Tipps, Bushra Haider, Tim R. Rose, Baovi N. Vo, Margot C. DeBaker, and Kevin Wickman</i>	343
Identification of Small Molecule Therapeutics and Neuroprotective Gene Targets via High Throughput Screening and RNA Interference in <i>C. elegans</i> Parkinson's Disease Models <i>Carl T. Ash, Emily E. Anderson, Amy E. Moritz, Patricia K. Dranchak, R. Benjamin Free, James Inglese, Joseph P. Steiner, David R. Sibley, and Emmanuel O. Akano</i>	344
The Cannabinoid 1 Receptor Allosteric Modulator GAT211 Impacts Behavior in a Sex-Dependent Manner <i>Alyssa Lauer and Erin Bobeck</i>	345
Dynamic Role of Intra-Locus Coeruleus Mu Opioid Receptors in Nociception <i>Makenzie Norris, Chao-Cheng Kuo, Jenny Kim, Samantha Dunn, Gustavo Borges, and Jordan McCall</i>	346

Effectiveness of GPR171 Agonist with Morphine and Identification of GPR171 Signaling Profile <i>Callie Porter and Erin Bobeck</i>	347
Presynaptic Regulation of Monoamine Release in the Dorsal Raphe Nucleus by Alpha2-adrenergic Receptors <i>Aleisha Gugel and Stephanie C. Gantz</i>	348
Chronic Morphine and Fentanyl Induce Intestinal Dysbiosis by Decreasing the Antimicrobial Activity of the Ileum <i>Karan Hitesh Muchhala, Grace K. Mahon, Eda Koseli, Jaelen Bethea, Minh Kang, and Hamid I. Akbarali</i>	368
Cellular Mechanisms of Amyloid $\beta$ Oligomers Suppressing GABAB-GIRK Signaling <i>Haichang Luo, Kevin Wickman, and Ezequiel Marron Fernandez de Velasco</i>	369
Dopamine transporter activity regulates neuroimmune communication <i>Adithya Gopinath, Phillip M. Mackie, Emily Miller, Leah T. Phan, Stephen Franks, Tabish Riaz, Aidan R. Smith, Michael Okun, and Habibeh Khoshbouei</i>	370
Chronic intermittent ethanol exposure induces spatial changes in lipid raft localization of G-proteins and their interacting proteins in rat prefrontal cortex <i>Anna Neel, James D. Miller, Shiyu Wang, Minghao Li, Jonathan C. Mayer, Haiguo Sun, Brian McCool, and Rong Chen</i>	371
Cyclodextrins decrease TRPV1 and TRPA1 ion channel activation via lipid raft disruption <i>Éva Szóke, Andrea Nehr-Majoros, Ádám Horváth, Anita Steib, Levente Szócs, Éva Fenyvesi, and Zsuzsanna Helyes</i>	372
Estrogen Depletion Alters Cortical NMDAR Function in Ovariectomized Rats <i>Kimberly Holter, McKenna G. Klausner, Bethany Pierce, Owen Ghaphery, Ashlyn Stone, and Robert W. Gould</i>	373
TrkB-containing Serum Extracellular Vesicles as a Potential Biomarker for Cognitive Improvement <i>Reiya Yamashita, Takahiro Ishimoto, Satoshi Matsumoto, Yusuke Masuo, Makoto Suzuki, and Yukio Kato</i>	470
IRX4204 enhances gait recovery in mice subjected to experimental autoimmune encephalomyelitis <i>Gracious Kasheke, Scott P. Holman, Kaitlyn Fraser, Arul Asainayagam, Sagar Vuligonda, Martin Sanders, and George Robertson</i>	471
The synaptic protein phosphatase 1 targeting protein, spinophilin, mediates striatal neuroadaptations underlying motor function <i>Anthony J. Baucum, Darryl S. Watkins, Basant Hens, Nikhil R. Shah, and Cameron W. Morris</i>	472
Calmodulin Dependent Protein Kinase II: An Effector in the Signaling Pathway of Antidepressant-like Behavior Elicited by Ketamine in Combination with Melatonin <i>Gloria Benítez-King, Armida Miranda-Riestra, Rosa Estrada-Reyes, Citlali Trueta, Jesús Argueta, Julián Oikawa-Sala, Luis Alejandro Constantino-Jonapa, and Montserrat G. Cercós</i>	473
Sex-differences in acute $\Delta 9$ -THC-induced antinociception are strain-specific <i>Courtney Lulek, Malabika Maulik, Swarup Mitra, Daniel Morgan, and Angela N. Henderson-Redmond</i>	474
Regulation of cAMP Signaling by Endothelin-A Receptor Antagonist, BQ123 in Morphine Tolerance in SH-SY5Y Human Neuroblastoma Cells <i>Shaifali Bhalla, Margi Sheth, and Zhong Zhang</i>	475
Calcium Imaging Alongside Deep Behavior Learning in Fentanyl Vapor Self-Administration <i>Mason J. Hochstetler, Jacob D. Layne, Brandon M. Curry, and Craig T. Werner</i>	476
Engagement of Beta-Arrestin 2 at the $\mu$ -opioid receptor reduces the abuse liability of opioids in mice during operant self-administration <i>Lindsey Felth, Sarah W. Gooding, Randi Foxall, Zachary Rosa, Izabella Sall, Joshua Gipoor, Anirudh Gaur, Cheryl Whistler, and Jennifer Whistler</i>	477
Retrospective Analyses of Dementia Outcomes in Patients Prescribed Immunosuppressants <i>Jacqueline Silva, Daniel Jupiter, and Giulio Tagliatela</i>	534
Who Knew? Dopamine Transporter Activity Is Critical in Innate and Adaptive Immune Responses <i>Emily Miller, Adithya Gopinath, Phillip M. Mackie, Leah T. Phan, Rosa Mirabel, Aidan R. Smith, Stephen Franks, Ohee Syed, Tabish Riaz, Brian K. Law, Nikhil Urs, and Habibeh Khoshbouei</i>	536
Discovery of an Allosteric Agonist for Schizophrenia Risk Gene GPR52 with Antipsychotic Activity <i>Ryan E. Murphy, Daniel E. Felsing, Nolan M. Dvorak, Fernanda Laezza, Kathryn A. Cunningham, and John A. Allen</i>	537
Structure based approaches on fentanyl template to design novel $\mu$ opioid modulators <i>Rohini Ople, Haoqing Wang, Qiongyu Li, Ben Polacco, Sarah Bernhard, Kevin Appourchaux, Sashrik Srihashyam, Shainnel Eans, Ruth Huttenhain, Jay McLaughlin, Brian Kobilka, and Susruta Majumdar</i>	538
Comparative Analysis of Neuro-markers in Angiotensin II High Salt Diet Hypertensive Rats <i>Helmut Gottlieb, Cynthia Franklin, Jeffrey Angell, Nikhil Joseph, Clayton Townsend, Anita Nancherla, David Yzquierdo, and Jessica Bradley</i>	539

Protein kinase D2 confers neuroprotection by promoting AKT and CREB activation in ischemic stroke <i>Jaclyn Connelly, Xuejing Zhang, Yapeng Chao, Yejie Shi, Tija Jacob, and Qiming Wang</i>	540
Sex Differences in Stimulant Action at the Dopamine Transporter <i>Jennifer Tat, Lillian Brady, and Erin Calipari</i>	541
Mediation Analysis Reveals that Opioid-Induced Sleep Disruption is Partially Mediated by Increased Motor Activity in C57BL/6J (B6) Mice <i>Diana Zebadúa Unzaga, Xiaojuan Zhu, Joshua M. Price, Michael A. Oneil, Ralph Lydic, and Helen A. Baghdoyan</i>	542
Sex Differences in GABA Regulation of Dopamine Release in the Nucleus Accumbens and its Role in Cocaine Use Disorder <i>Brooke Christensen, Addison R. Van Namen, and Erin Calipari</i>	543
Comparison of the mu-opioid receptor antagonists methocinnamox (MCAM) and naloxone to reverse the ventilatory-depressant effects of fentanyl and heroin in male rats <i>Takato Hiranita, Nicholas P. Ho, and Charles P. France</i>	544
Regulation of Neuronal Activity by GluD1 Current in Brain Slices <i>Stephanie Gantz, Daniel Copeland, and Aleigha Gugel</i>	545
Acute and Subchronic GPR171 Agonism Affects Anxiety and Depression in Female Mice <i>Megan Raddatz and Erin Bobeck</i>	546
Involvement of the Rat Medial Prefrontal Cortex 5-HT <sub>2A</sub> Receptor in Impulsive Action <i>Juliana L. Giacomini, Christina R. Merritt, Kathryn A. Cunningham, and Noelle C. Anastasio</i>	547
Butyrate Prevents Opioid Induced Peripheral Hypersensitivity via a Gut Dependent Mechanism <i>Donald Jessup and Hamid I. Akbarali</i>	569
Metabotropic mGlu <sub>1</sub> Receptor Regulation of Cortical Inhibition and Cognitive Function: Implications in Adolescent Cocaine Exposure <i>Deborah Luessen, Isabel Gallinger, Brenna Wolfe, and P. Jeffrey Conn</i>	570
Development of a Mouse Model to Study Alcohol Withdrawal-Induced Allodynia <i>Jhoan S. Aguilar, Amy Lasek, Luana Martins de Carvalho, and Arynah Pradhan</i>	571
Interactions between Biological Sex and Hormonal Cycles in Stimulant Effects on Motor Behavior <i>Abigail Carr, Jennifer Tat, Erin Calipari, and Kristy R. Erickson</i>	572
Ligand and G Protein Selectivity in Kappa Opioid Receptor Revealed by Structural Pharmacology <i>Jianming Han, Jingying Zhang, Sarah Bernhard, Lei Zhao, Peng Yuan, Jonathan F Fay, and Tao Che</i>	573
Characterizing the Role of Nicotine on Sex-Specific Neural Circuit Mechanisms Underlying Sensory Reinforcement <i>Grace Bailey, Jennifer Tat, Janet Mariadoss, Lillian Brady, and Erin Calipari</i>	574

## DRUG DISCOVERY AND DEVELOPMENT

Structure, Function, and Pharmacology of Delta Opioid Receptor Bitopics <i>Sarah Bernhard, Balazs R. Varga, Amal El Daibani, Jordy H. Lam, Saheem Zaidi, Kevin Appourchaux, Shainnel Eans, Vsevolod Katritch, Jay McLaughlin, Susruta Majumdar, and Tao Che</i>	89
Dual sEH/FAAH Inhibitors as a Promising Therapeutic Strategy for the Treatment of Chronic Pain <i>Jeannes Angelia, Ram Kandasamy, Xiaohui Weng, and Stevan Pecic</i>	90
Preclinical Assessment of CSX-1004: A High Affinity, Humanized Monoclonal Antibody for Mitigating the Effects of Fentanyl <i>Paul T. Bremer, Nicholas T. Jacob, Bin Zhou, Lisa M. Eubanks, and Kim D. Janda</i>	91
HBW-008-A, a Novel, Potent, Selective, Safe and Bioavailable p21-Activated Kinase 4 (PAK4) Inhibitor, is an Efficacious Adjuvant Agent for PD-1 Therapy in Mice <i>Ning Lee, Yingfu Li, Guanfeng Liu, and Mao Yang</i>	92
Identification of Inhibitors of the TMPRSS2 and SPIKE Interaction Through Novel uHTS Assays and Molecular Docking <i>Danielle Cicka, Andrey A. Ivanov, Sophie West, Dacheng Fan, Qiankun Niu, Yuhong Du, and Haian Fu</i>	93
Characterization of OJT008 As a Novel Inhibitor of <i>Mycobacterium tuberculosis</i> <i>Kehinde Idowu, Collins Onyenaka, Ngan Ha, Edward A. Graviss, and Omonike Olaleye</i>	94
Antioxidant Effects of Cardamonin in BV-2 Microglial Cells Through the Modulation of Keap1/Nrf2 Signaling Pathway <i>Kimberly Barber, Patricia Mendonca, and Karam F. Soliman</i>	95
Identification of Transfer RNA Modification Enzymes That Regulate a Bacterial RNA Chaperone Known as Hfq <i>Jalisa Nurse, Karl Thompson, Joseph Aubee, and Valerie de Crecy-Legard</i>	96

Comparative LC/MS Analysis of the Extraction of Cocaine and its Metabolites Using QuEChERS and Column Extraction Methods	97
<i>Zhen-Hin E. Chan and Rose Webster</i>	
Identifying the Anticancer Properties and Mechanisms of Action of Anthocyanin-rich Extracts from the <i>Aponogeton madagascariensis</i> on Triple Negative Breast Cancer Cells	98
<i>Shanukie Embuldeniya, Kerry Goralski, and Arunika Gunawardena</i>	
Patient iPSC-based high throughput drug screening identifies drug candidates involved in reduced tauopathy associated with Alzheimer's disease	111
<i>Dhruv Gohel, Yichen Li, and Feixiong Cheng</i>	
Assessment of Dextromethorphan on Compulsive Behavior Using the Schedule-Induced Polydipsia Paradigm in Rats	112
<i>Madeline T. Van Fossen, Alexia G. Dalton, Bethany E. Beavers, Dillon S. Shekoski, Taylor Galaszewski, and Adam J. Prus</i>	
Bioisosteric Replacement of Amides Linkers with 1, 2, 3-Triazoles for Improved Pharmacokinetics Without Losing Dopamine D4 Receptor Potency or Selectivity	113
<i>Diandra Panasis, Mohammad Alkhatib, Julianna Saez, John Hanson, Ashley N. Nilson, Franziska M. Jacobs, Nitish Kasarla, Bryant Wang, Maria Ladik, Abigail Muccilli, Kaylen Hong, R. Benjamin Free, David R. Sibley, Comfort A. Boateng, and Thomas Keck</i>	
Development of GPR183 antagonists for the treatment of neuropathic pain	114
<i>Vanja Kalajdzic, Israel Olayide, Kathryn Braden, Daniela Salvemini, and Christopher K. Arnatt</i>	
Novel Axin Stabilizer YA6060 is a Promising Therapy for Liver Fibrosis	115
<i>Yan Shu, Shiwei Zhou, Yong Ai, Shaoteng Wang, Amanda Xu, and Fengtian Xue</i>	
Efficacy of HS-10382 (TERN-701) in tumor xenograft models, a new investigational allosteric ABL1 kinase inhibitor as a potential treatment for CML	116
<i>Yuanfeng Zhou, Benjamin Parsons, Danni Sun, Yunfan Li, Guoliang Chen, Mingjie Luo, Christopher Jones, Xiaogang Lian, Xiaolei Wang, Yundong Sun, Jeffrey Jasper, and Huifeng Niu</i>	
Enhancement of Muscarinic Receptor-Induced Contractions by Hydrogen Sulfide-Releasing Compounds in Bovine Isolated Irides	117
<i>Fatima Muili, Anthonia Okolie, Shervin Aghaabbasi, JD Fontenot, Reem Matti, Kalu Ngele, Catherine Opere, Sunny Ohia, and YA FATOU NJIE MBYE</i>	
High brain-blood barrier permeability highlights a new class of neurolysin activators as promising candidates for stroke treatment: a pilot pharmacokinetic study in mice	118
<i>Yong Zhang, Sejal Sharma, Shiva H. Esfahani, Shirisha Jonnalagadda, Aarfa Queen, Saeideh Nozohouri, Dhavalkumar Patel, Paul C. Trippier, Vardan T. Karamyan, and Thomas J. Abbruscato</i>	
TLR Agonist INI-4001 Improves Efficacy of Heroin Vaccine Intended for Clinical Treatment of Opioid Use Disorder	119
<i>Michael Raleigh, Karthik Siram, David Burkhart, Jennifer Vigliaturo, Carly Baehr, Ann Gebo, Scott Winston, and Marco Pravetoni</i>	
Efficacy of LSD1 Directed Agents is Enhanced with Kinase Signaling Inhibition in Glioblastoma Stem Cells	120
<i>Lea Stitzlein, Jack Adams, Matthew Luetzen, Melissa Singh, Xiaoping Su, Yue Lu, Ravesanker Ezhilarasan, Joy Gumin, Frederick F. Lang, Erik Sulman, Joya Chandra, and Michelle Monje-Deisseroth</i>	
Optimizing Tuberculosis Treatment Efficacy: comparing the Standard Regimen with Moxifloxacin-containing Regimens	151
<i>Maral Budak, Jennifer Linderman, JoAnne Flynn, and Denise Kirschner</i>	
Pharmacological evaluation of <i>N</i> -hydroxypyridinediones to support optimization as HBV ribonuclease H inhibitors	152
<i>Molly Woodson, M. Abdul Mottaleb, Grigoris Zoidis, and John Tavis</i>	
Development of highly potent and selective inhibitors for GRK5	153
<i>Yueyi Chen</i>	
Natural Products as a Source of Chemical Diversity in cyclic-AMP dependent Protein Kinase A (PKA) Inhibitor Discovery	154
<i>Brice Wilson, Ning Li, Juliana Martinez Fiesco, Masoumeh Dalilian, Dongdong Wang, Sarath Senadeera, Lin Du, Richard W. Fuller, Rohan Shah, Emily A. Smith, Ekaterina I. Goncharova, John A. Beutler, Tanja Grkovic, Ping Zhang, and Barry R. O'Keefe</i>	
Pharmacological and Genetic Preclinical Models of Ghrelin Receptor Functional Selectivity to Investigate Metabolic Disease Pathophysiology	161
<i>Joshua Gross, Lara Kohlenbach, Yang Zhou, Juan J. Marugan, and Lawrence S. Barak</i>	
Design, Synthesis and Biological Evaluation of Benzothiazole-Phenyl Analogs as Multi-Target Directed Ligands for Treating Pain	162
<i>Stevan Pecic, Jeannes Angelia, and Xiaohui Weng</i>	

Pulmonary delivery of nanochelators decreases lung iron accumulation and alleviates bleomycin-induced lung fibrosis in rats <i>Mayuri Patwardhan, Wesley Stiles, Homan Kang, Hak Soo Choi, and Jonghan Kim</i>	291
Virtual Screening for Potential Hepatitis B Virus Non-Nucleoside Reverse Transcriptase Inhibitors <i>Emma Inmon, Razia Tajwar, Qilan Li, Marvin J. Meyers, and John Tavis</i>	292
Preclinical and Phase I Clinical Development of a Novel Multi-target Drug Candidate for Neuropathic Pain <i>Zsuzsanna Helyes, Adam Horvath Horvath, Nikolett Szentés, Valeria Tekus, Szilard Pal, Tamás Kálai, and Péter Mátyus</i>	293
The Modulatory Effects of Citrus Flavonoid Hesperetin on Nrf2 Expression and NF- $\kappa$ B Signaling Pathway in LPS-Activated BV-2 Microglial Cells <i>Karam F. Soliman, Jasmine A. Evans, and Patricia Mendonca</i>	294
Effect of Topical Application of cannabis fixed Oil on Imiquimod-Induced Psoriasis-like Lesions in the Thin Skin of Adult Male Albino rabbits <i>Youness Kadil, Hasnaa Bazhar, Ibtihal Segmani, afaf Banid, Fatimaezzahra kabbali, and Houda FILALI</i>	295
Herbal microbiomes are plant-specific and rich in immune-stimulating pathogen-associated molecular pattern molecules <i>Elizabeth Mazzio, Andrew Barnes, Ramesh Badisa, Henry Williams, and Karam F. Soliman</i>	296
Targeting the TAK1/TNF signaling pathway with novel pharmacological inhibitors <i>Scott Scarneo, Timothy Haystead, Philip Hughes, and Robert Freeze</i>	297
Development and Validation of a Simple and Selective HPLC-MS/MS Method for Simultaneous Quantification of GS-441524 and its Prodrug Remdesivir <i>Su Guan, Meijuan Tu, Samantha Evans, and Aiming Yu</i>	298
Marine-Derived Pharmaceuticals in Clinical Trials in 2022 <i>Alejandro M.S. Mayer, Marsha Pierce, Maria Reji, Alex C. Wu, Karolina K. Jekielek, Henry Q. Le, Katelyn Howe, Maryam Butt, Sujin Seo, David J. Newman, and Keith B. Glaser</i>	299
An Elastin-like Polypeptide-fused Peptide Inhibits MMP-2 Activity at nM Concentrations with High Specificity <i>Adesanya A. Akinleye, Richard J. Roman, and Gene L. Bidwell</i>	300
<i>In vitro</i> antiglycation and protein cross-link breakage effects of <i>Murraya koenigii</i> leaf extracts and their phytochemical composition <i>Oluwaseyefunmi Adeniran and Sechene S. Gololo</i>	313
A Selective TRPC3 Antagonist Rescues Neuronal Loss and Facilitates Spatial Learning and Memory in Alzheimer's Model <i>Jiaxing Wang, Sicheng Zhang, Vijay K. Boda, Zhongzhi Wu, and Wei Li</i>	314
Determination of Strychnine Levels in Serum and Brain via LC-MS/MS in Mice Vaccinated Against Strychnine <i>Jennifer Vigliaturo, Carly Baehr, Andrew Kassick, Diego Luengas, Aaron khaimraj, Marco Pravetoni, Saadyah Averick, and Michael Raleigh</i>	315
Analgesic and Side Effect Profiles of Novel Alpha-2 Adrenergic Receptor Agonists <i>Cristina D. Peterson, Lukas Caye, Kelley Kitto, George L. Wilcox, Laura Stone, Swati More, and Carolyn A. Fairbanks</i>	316
How ligands achieve biased signaling at opioid receptors <i>Joseph M. Paggi, Deniz Aydin, Yianni D. Laloudakis, Carl-Mikael Suomivuori, Tao Che, and Ron O. Dror</i>	317
Development and Validation of a High-Throughput Cell-Based AlphaLISA Assay to Identify Small Molecule 20S Proteasome Modulators <i>Erika Lisabeth, Sophia Staerz, Evert Njomen, Thomas Dexheimer, Richard Neubig, and Jetze Tepe</i>	318
A Computational Approach to Identify Small Molecules Interact with Crystal Structure of Programmed Cell Death Protein 1 as Potential Therapeutics for Cancer Immunotherapy <i>Hubert Chen and Mustafa Gabr</i>	319
Venglustat Analogues with Enhanced Inhibition for Protein N-Terminal Methyltransferases 1/2 <i>Rong Huang, Youchao Deng, and Ying Meng</i>	320
Targeting human melanocortin type 2 receptor (MC2R) with small molecules and designed peptides for the treatment of congenital adrenal hyperplasia <i>Amit Pandey, Shaheena Parween, and Shripriya Singh</i>	321
Marine Carotenoid Fucoxanthin as a Promising Anticancer Therapeutic Against Triple-Negative Breast Cancer (TNBC) <i>Shade Ahmed, Patricia Mendonca, Samia S. Messeha, and Karam F. Soliman</i>	322
Multivalent Vaccination against Polydrug Use in Opioid Use Disorder <i>Daihyun Song, Bethany Crouse, Jennifer Vigliaturo, and Marco Pravetoni</i>	353

Anti-allergic and anti-Inflammatory Effects of <i>Cornus officinalis</i> using Zebrafish and IgE-chip Technology <i>Young Sook Kim, Yong Wan Cho, Hye-Won Lim, Ik Soo Lee, and Yu-Ri Lee</i>	354
Investigating Birch Bark Oil Anti-Oxidative Properties in Human Keratinocytes <i>Esther Bonitto, Kate-Lynn Smith, Matthias Bierenstiel, Rajendran Kaliaperumal, and Kerry Goralski</i>	355
Characterization of the pharmacological mechanism of OJT009 as a novel inhibitor of severe acute respiratory syndrome coronavirus 2 <i>Tolulope Adebusuyi, Manvir Kaur, Anuoluwapo O. Egbejimi, Idowu Kehinde, and Omonike A. Olaeye</i>	356
Development of GPR183 antagonists to treat neuropathic pain <i>Elise D. Stuert, Israel Olayide, Kathryn Braden, Daniela Salvemini, and Christopher K. Arnatt</i>	364
Pharmacological Rescue of Human Disease Mutations in <i>KCNJ10</i> and <i>KCNJ16</i> by Novel Kir4.1/5.1 Potentiator, VU0493206 <i>Samantha McClenahan, Dongsoo Lee, and Jerod Denton</i>	365
Schizonepeta tenuifolia extract (DKB138) enhances the muscle strength in dexametasone-induced muscle atrophy mice model <i>Young Sook Kim, Dong-Seon Kim, Heung Joo Yuk, Bongkyun Park, Kyujyung Jo, Yu-Hwa Park, Do Hoo Kim, and Seung-Hyung Kim</i>	490
Multi-Target Directed Ligands for the Treatment of Alzheimer's Disease <i>Ryan West and Stevan Pecic</i>	491
Novel Molecules and Novel Mechanisms: Prevention of Toxic $\beta$ -Amyloid <sub>42</sub> Oligomerization <i>Gary Jones, Justin C. Leavitt, and Mary C. Freesh</i>	492
The Dual Role of the Natural Compound Cardamonin in Triple Negative Breast Cancer <i>Patricia Mendonca and Karam F. Soliman</i>	493
Sustained Release of Nanochelator in Thermosensitive Hydrogel Corrects Iron Overload <i>Linguxe Zeng, Seung Hun Park, Homan Kang, and Jonghan Kim</i>	494
Consequences of pharmacological inhibition of cathepsin C using Icat <sub>CXPZ-01</sub> on maturation of granzyme zymogens in cytotoxic lymphocytes <i>Roxane Domain and Brice Korkmaz</i>	495
Platycodon Grandifloras Reduces Weight Gain and Attenuates Hepatic Steatosis in a Diet-Induced Mouse Model of Obesity <i>Vitoria Mattos Pereira, Suyasha Pradhanang, Anne Margaret Chenchar, Sydney Polson, Danielle R. Bruns, Emily E. Schmitt, Raza Bashir, Sidney A. Sawan, and Sreejayan Nair</i>	496
Small Molecule Anti-Inflammatory TYK2 Inhibitors Attenuate Inflammation and Clinical Symptoms in a Mouse Model of Imiquimod Induced Psoriasis <i>Sanchari Basu Mallik, Amol Tandon, Jissy Akkarapattikal Kuriappan, Jeevak Sopanrao Kapure, Mahesh Halle, and Abishek Iyer</i>	497
Assessing how Neurodegeneration and Cognitive Impairment can be Ameliorated through the Neuroprotective Effect of Thymoquinone <i>Chukwunonso Chukwuemeka</i>	498
Profiling Context-Dependent Activity of Allosteric Modulators at mGlu <sub>7</sub> <i>Xia Lei, Alice Rodriguez, and Colleen M. Niswender</i>	499
Effects of Simultaneous Inhibition of Fatty Acid Amide Hydrolase and Soluble Epoxide Hydrolase on Acute and Persistent Pain in Male Rats <i>Cassandra Yuan, Ashley Murray, Christopher Chin, Alyssa Fernandez, Stephanie Sanchez, Stevan Pecic, and Ram Kandasamy</i>	512
Anti-Fentanyl Monoclonal Antibodies: In Vitro Characterization and In Vivo Efficacy in Reversing Apnea in Pigs <i>Carly Baehr, Dustin Hicks, Alonso Guedes, and Marco Pravetoni</i>	513
First potent macrocyclic A <sub>3</sub> adenosine receptor agonists reveal G-protein and beta-arrestin2 signaling preferences <i>Kenneth Jacobson, Courtney Fisher, Veronica Salmaso, Tina C. Wan, Ryan G. Campbell, Eric Chen, Zhan-Guo Gao, John A. Auchampach, and Dilip K. Tosh</i>	514
Discovery of Potent Therapeutics for Treatment of Cryptosporidiosis <i>Marvin J. Meyers and Christopher D. Huston</i>	515
Sildenafil is a candidate drug for Alzheimer's disease: Real-world patient and RNA-sequencing data observations in patient-induced pluripotent stem cells-derived neurons <i>Yichen Li, Dhruv Gohel, Pengyue Zhang, Chien-Wei Chiang, Andrew A. Pieper, Jeffrey Cummings, and Feixiong Cheng</i>	516

Development of Mutant-Selective Allosteric EGFR Inhibitors for Drug-Resistant Lung Cancer <i>Tyler Beyett, Ciric To, David E. Heppner, Thomas W. Gero, Nathanael S. Gray, David A. Scott, Pasi A. Jänne, and Michael J. Eck</i>	517
Identification of Small Molecule RGS10 Modulators in a Microglial Cell Model of Neuroinflammation <i>Stephanie Gonzalez and Benita Sjogren</i>	518
CPL-01, A Novel Extended-Release Ropivacaine, Demonstrates Consistent and Predictable Systemic Exposure Compared to Liposomal Bupivacaine in Multiple Surgical Models <i>Stevie Pope, Christopher Crean, Sarah Thrasher, PJ Chen, Lee Chen, DeeDee Hu, and Erol Onel</i>	519
Development and Characterization of Third Generation MDM2 PROTACs for the Treatment of Acute Myeloid Leukemia Utilizing an Achiral Ligand for E3 Ligase Cereblon <i>Ira Tandon, Qihua Fan, Chunrong Li, Nuwan Pannilawithana, Haibo Xie, Paulina Esguerra, and Weiping Tang</i>	520
Phytochemotypic profiling and GCMS Analysis of <i>Viola patrinii</i> , a Himalayan Herb <i>Sajad Yousuf, Tahira Yousuf, Olanrewaju Morenikeji, and Naseer A. Kutchy</i>	521
Monensin and its Derivatives Exhibit Anti-Melanoma Activity <i>In Vitro</i> <i>Alicja Urbaniak, Marta Jędrzejczyk, Greta Klejborowska, Natalia Stępczyńska, Adam Huczyński, and Alan J. Tackett</i>	552
Synthesis and Structure-Activity Relationship of SAE-14 Analogs as G-Protein Coupled Receptor 183 Antagonists <i>Israel Olayide, Kathryn Braden, Daniela Salvemini, and Christopher K. Arnatt</i>	553
Discovery of New Agonists and Antagonists for Ectopically Expressed Olfactory Receptor OR51E1 <i>Taylor Henry, Qiang Wang, Alexey Pronin, Olena Zhuravel, Sergey Zozulya, and Vladlen Slepak</i>	554
Comparison of Mass-Action Law Dynamic Theory-based “Top-Down” Approach with Observation/Statistics-based “Bottom-Up” Approach in Biomedical R&D <i>Ting-chao Chou</i>	555
Evaluation of Influx and Efflux Transporters of Metformin in an <i>In Vitro</i> Blood-Brain Barrier Model During Normoxic and Ischemic Conditions <i>Sejal Sharma, Yong Zhang, Ali Ehsan Sifat, Khondker Ayesha Akter, Sabrina Rahman Archie, Saeideh Nozohouri, and Tom Abbruscato</i>	563
Directed Mutagenesis Studies Reveal Amino Acid Residues Responsible for A <sub>3</sub> Adenosine Receptor Positive Allosteric Modulator Function <i>Courtney Fisher, Veronica Salmaso, Tina C. Wan, Balaram Pradhan, Kenneth Jacobson, and John A. Auchampach</i>	564
Structure-activity Exploration of Positive Allosteric Modulators of the Mu-opioid Receptor <i>Mengchu Li, John Traynor, Sherrice Zhang, Matthew Stanczyk, Xinmin Gan, and Andrew White</i>	565

## DRUG METABOLISM AND DISPOSITION (DMD)

In Vitro Application of Hydrolase Reaction Phenotyping in Early Discovery Research <i>Guo Zhong, Julie Lade, and Armina Abbasi</i>	171
HNF4A-AS1 Alleviates Ritonavir-induced Liver Injury via HNRNPC-mediated HNF4A Degradation <i>Xiaofei Wang, Jingya Wang, Pei Wang, Yihang Yu, Yiting Wang, Mengyao Yan, Shengna Han, and Lirong Zhang</i>	172
Physiologically Based Pharmacokinetic (PBPK) Modeling to Predict the Pharmacokinetics of Irbesartan in Different CYP2C9 Genotypes <i>Seok-Yong Lee, Chang-Keun Cho, Pureum Kang, Eunvin Ko, and Chou Yen Mu</i>	173
Identification of Pazopanib as an OATP1B1 Substrate from a Competitive Counterflow Screen <i>Thomas Drabison, Mike Boeckman, Eric Eisenmann, Sharyn D. Baker, Shuiying Hu, Alex Sparreboom, and Zahra Talebi</i>	174
Unusual Metabolism of Benzethonium by Cytochrome P450 <i>Ryan P. Seguin, Libin Xu, and Ryan Nguyen</i>	175
Metabolism of (-)- $\Delta^9$ -Tetrahydrocannabinol (THC) in Chicken and Potential Exposure of THC and Its Metabolites to Humans <i>Ziteng Wang, Chock Ying Soo, Evelyn Mei Ling Goh, Hooi Yan Moy, and Eric Chun Yong Chan</i>	176
The CYP11A1 substrates vitamin D3 and cholesterol induce changes in protein conformation and protein-protein interactions with Adrenodoxin <i>Janie McGlohon and D. Fernando Estrada</i>	177
Deciphering the Zonal Distribution of Hepatic Drug Metabolizing Enzymes and Transporters in Mice by Single Cell Transcriptomics <i>Joe Jongpyo Lim, Curtis Klaassen, and Julia Yue Cui</i>	178

Non-nutritive Sweeteners Acesulfame Potassium and Sucralose Competitively Inhibit P-glycoprotein <i>Laura Danner and Stephanie Olivier-Van Stichelen</i>	179
Identification and Characterization of Palmitoylation Sites in the Organic Anion Transporting Polypeptide 1B1 (OATP1B1) <i>Cecilia Villanueva, Whitney Nolte, and Bruno Hagenbuch</i>	180
In vitro and In vivo Inhibition of Nicotine Metabolism by <i>trans</i> -2-Nitrocinnamaldehyde <i>Aiden-Hung Nguyen, Uyen-Vy Navarro, Ghina Moyeen, and John Harrelson</i>	181
High-Resolution Mass Spectrometry Coupled with XCMS Online for High-throughput Detection and Identification of Drug Metabolites <i>Dilip Singh, Vijaya S. Mettu, Aarzo Thakur, Anoud Ailabouni, and Bhagwat Prasad</i>	182
The Plasma Membrane Monoamine Transporter (PMAT) is Highly Expressed in Neuroblastoma and Functions as a Mitochondrial mIBG Transporter <i>Leticia Vieira, Yuchen Zhang, Antonio J. López Quiñones, Julie R. Park, and Joanne Wang</i>	183
Deciphering the role of fatty acid metabolizing CYP4F11 in lung cancer and its potential as drug target <i>Huiling Jia, Sutapa Ray, Bjoern Brixius, and Simone Brixius-Anderko</i>	184
Understanding the cell-dependent activation of ProTides and its implications in optimizing the nucleoside antiviral prodrug design for treating pulmonary infections <i>Jiapeng Li, Shuxin Sun, Yueting Liu, Weiwen Wang, and Hao-Jie Zhu</i>	185
PXR activation attenuates liver fibrosis by down-regulating LECT2 and disrupting $\beta$ -catenin/TCF4 interaction <i>Yue Gao, Shicheng Fan, Pengfei Zhao, Yanying Zhou, Huilin Li, Xuan Li, Chenghui Cai, Min Huang, and Huichang Bi</i>	186
Identification of Putative Novel Biomarkers of Organic Anion Transporter 1 and 3 for the Prediction of Transporter-Mediated Drug-Drug Interactions <i>Aarzo Thakur, Dilip K. Singh, Mary Paine, and Bhagwat Prasad</i>	187
Plated Hepatocyte Relay Assay for the Evaluation of the Metabolic Fates of Slowly Metabolized Compounds <i>Albert Li, Binnian Wei, and Walter Mitchell</i>	374
Fluorogenic Chemical Tools to Improve Prodrug Treatment Outcomes <i>Michael Beck</i>	375
CYP3A inhibition and induction exert limited effects on brilaroxazine pharmacokinetics <i>Laxminarayan Bhat, Seema R. Bhat, Arulprakash Ramakrishnan, and Palaniappan Kulanthaivel</i>	376
The metabolism of the 8-aminoquinolines in relation to hemolytic toxicity: exploring current understanding for future antimalarial drug discovery <i>Pius Fasinu</i>	377
Production, structure, and function analyses of a recombinant miR-1291 agent <i>Meijuan Tu, Zhenzhen Liu, Tongyi Dou, and Aiming Yu</i>	378
<i>In Vitro</i> Characterization of CYP3A4 Inhibition and Induction of Nevirapine Analogs as Substitutes in HIV Treatment <i>Emily G. Gracey, Sylvie E. Kandel, and Jed N. Lampe</i>	379
Development of a Cytochrome P450 CYP3A7 Quantitative Structure-Inhibitory Relationship (QSIR) Model to Assess Drug Safety in Neonates <i>Hannah M. Work, Sylvie E. Kandel, and Jed N. Lampe</i>	380
Identification And Functional Characterization Of Alternative Transcripts Of Lncrna Hnf1a-As1 And Their Impacts On Drug Metabolism <i>Jing Jin and Xiao-bo Zhong</i>	381
Novel Single- and Multi-Tissue Chips for Predictive Pharmacokinetic Applications <i>Murat Cirit, Shiny Rajan, Jason Sherfey, Shivam Ohri, Lauren Nichols, Tyler Smith, Paarth Parekh, and Emily Geishecker</i>	382
Tenofovir Activation in Brain and Liver is Diminished in Creatine Kinase Brain-Type Knockout Mice <i>Colten D. Eberhard, Benjamin C. Orsburn, and Namandjé N. Bumpus</i>	383
Managing Drug Interactions Involving the Over-the-Counter Opioid Loperamide through Physiologically Based Pharmacokinetic Modeling <i>Zhu Zhou, Mengyao Li, Ping Zhao, Jean Dinh, and Mary Paine</i>	384
Contribution of CNT1 and CNT3 to the intestinal transport and pharmacokinetics of decitabine <i>Nadeen Anabrawi, Thomas Drabison, Mike Boeckman, Yan Jin, Madeline Halpin, Alice A. Gibson, Alex Sparreboom, Raj Govindarajan, and Sharyn D. Baker</i>	385



Development of Novel DIA Based Proteomics Tools for Quantification of Drug-protein Adducts <i>Ellen Riddle, Alex Zelter, and Nina Isoherranen</i>	386
The hepatocyte estrogen sulfotransferase dictates female sensitivity to T cell-mediated hepatitis independent of estrogens <i>Wen Xie and Jingyuan Wang</i>	387
Regulation of Hepatic Drug Transporters by Pro-inflammatory Cytokines <i>Tianran Hao, Jashvant Unadkat, and Qingcheng Mao</i>	388
Naturally Occurring Flavonoids Attenuate Irinotecan-Induced Intestinal Toxicity Through Anti-Inflammatory and Epithelial Barrier Activities <i>Imoh Etim, Ting Du, Abasifreke Benson, and Song Gao</i>	389
Family 1 P450s Form Complexes that Effect Enzyme Function <i>J Patrick Connick, George Cawley, James R. Reed, and Wayne L. Backes</i>	390
Development and Characterization of Chemical Tools to Study Ester Drug Metabolic Enzymes in Live Cells <i>Carolyn Karns, Makenzie R. Walk, Anchal Singh, Mingze Gao, Taylor P. Spidle, and Michael Beck</i>	575
A Novel <i>In Vitro</i> Hepatocyte Culture System (icHep) for Biliary Drug Excretion Analysis Using Permeation Assay <i>Yuya Nakazono, Hiroshi Arakawa, Natsumi Matsuoka, Yoshiyuki Shirasaka, and Ikumi Tamai</i>	576
Identification of endogenous biomarkers of renal organic cation transporters in rats by global metabolomics analysis <i>Anoud Ailabouni, Vijay Mettu, Dilip K. Singh, Aarzo Thakur, and Bhagwat Prasad</i>	577
Pharmacological Effects of Ketoconazole in the Treatment of Steroidogenesis Suppression via CYP17A1 Inhibition May Involve MicroRNA Regulation <i>Baitang Ning, Dongying Li, Bridgett Knox, and Weida Tong</i>	578
Single-dose Brilaroxazine Pharmacokinetics, Metabolism, and Excretion Profile in Animals and Humans <i>Laxminarayan Bhat, Seema R. Bhat, and Palaniappan Kulanthaivel</i>	579
Characterization of a novel bifunctional cytochrome P450 enzyme CYP107 from bacterium <i>Sebekia benihana</i> <i>Layne Jensen and D. Fernando Estrada</i>	580
Identification And Functional Characterization Of Alternative Transcripts Of Lncrna Hnf4a-As1 And Their Impacts On Drug Metabolism <i>Le Tra Giang Nguyen, Jing Jin, and Xiao-bo Zhong</i>	581
Goldenseal-mediated Inhibition of Enteric Uptake Transporters Decreases Metformin Systemic Exposure in Mice <i>Victoria Oyanna, Kenisha Y. Garcia-Torres, Baron J. Bechtold, Katherine D. Lynch, Ridge M. Call, Miklos Horvath, Preston K. Manwill, Tyler N. Graf, Nadja B. Cech, Nicholas H. Oberlies, Mary Paine, and John D. Clarke</i>	582
Regulation of Human Renal Drug Transporter mRNA Expression by Proinflammatory Cytokines <i>Yik Pui Tsang, Jashvant Unadkat, and Qingcheng Mao</i>	583
Analysis of novel variants in the Cytochrome P450 Oxidoreductase gene found in the Genome Aggregation Database applying Bioinformatics Tools and Functional assays <i>Maria Natalia Rojas Velazquez, Søren Therkelsen, and Amit Pandey</i>	584
Discovery of Developmental Windows of Drug Sensitivity Using High Content Screening of Normal and Pgp-Knockout Sea Urchin Embryos <i>Evan Tjeerdema, Yoon Lee, and Amro Hamdoun</i>	585
Human Cytochrome P450 Interactions with Redox Partner Cytochrome P450 Reductase <i>Sarah Burris-Hiday, Mengqi Chai, Michael L. Gross, and Emily Scott</i>	586
Predicting a Safe, Efficacious Human Dose for a Novel Anti-Cryptosporidiosis Therapeutic <i>Vicky Sun, Ryan Choi, Matthew A. Hulverson, Wesley Van Voorhis, and Samuel Arnold</i>	587
Nucleotidases Exhibit Enzymatic Activities Toward the Pharmacologically Active Metabolites of Gemcitabine and Emtricitabine <i>Herana Seneviratne, Nav R. Phulara, Chiaki Ishida, and Peter Espenshade</i>	588
Characterization of Drug Binding to Liver Fatty Acid Binding Protein (FABP1) and Its Effect on Diclofenac Metabolism by CYP2C9 <i>King B. Yabut, Ben Zercher, Matthew F. Bush, and Nina Isoherranen</i>	589
Identification of 5-hydroxycotinine in the Plasma of Nicotine-treated Mice-Implications for Cotinine Metabolism and Disposition in vivo <i>Keiko Kanamori, Syed M. Ahmad, and Kabirullah Lutfy</i>	590
Identifying the mechanism underlying iatrogenic intravenous paracetamol-induced hypotension <i>Thomas A. Jepps, Johs Dannesboe, Joakim Bastrup, and Clare L. Hawkins</i>	591

*Cara Loomis, Sang-Choul Im, Michelle Redhair, and Emily Scott*

## PHARMACOGENOMICS AND TRANSLATIONAL PHARMACOLOGY

- Chronic Exposure to Organophosphate Pesticides and Elevated Markers of Systemic Inflammation: Possible Neuroinflammatory and Genotoxic Effects 27  
*Dina El-Gameel, Noha A. Hamdy, Amira F. El-Yazbi, Maha A. Ghanem, Labiba K. El-Khordaugi, Salwa M. Abdallah, Yehia Mechref, and Ahmed F. El-Yazbi*
- Antithrombotic Therapy Optimization in a Quaternary Care Center Anticoagulation Clinic in the Middle East 28  
*Emna Abidi, Patricia Bon, Ramzi Khaddage, Antoine Cherfan, Mohammad Kolailat, Ziad Sadik, and Bassam Atallah*
- Excessive exercise increases metabolites associated with pathophysiologic changes in ultramarathon runners 29  
*Mikolaj Marszalek, Zofia Wicik, Andrzej Ciechanowicz, Disha Keswani, Ceren Eyiletten-Postula, Szczepan Wiecha, Lukasz Malek, Magdalena Kucia, and Marek Postula*
- Social stress causes the emergence of functional Histamine H3 Receptors in urinary bladder smooth muscle 30  
*B Malique Jones, Nathan Tykocki, and Gerald Mingin*
- Finasteride Induces Epigenetic Alteration of TMPRSS2 Gene Expression: A Potential role in Severe Acute Respiratory Syndrome-Corona Virus-2 Inhibition 31  
*CHURCHILL IHENTUGE and Antonei B. Csoka*
- Compound 48/80 increases bladder wall mechanical compliance via activation of MMP-2 32  
*Pragya Saxena, Sara Roccabianca, and Nathan Tykocki*
- 3D Reconstruction Reveals Changes in Mitochondrial Morphology in Mouse Skeletal Muscle Across Aging and Upon Loss of the MICOS Complex 51  
*Kit Neikirk, Zer Vue, Larry Vang, Edgar Garza-Lopez, and Antentor Hinton*
- Beta-hydroxyphosphocarnitine modifies the inflammation in rats with non-alcoholic steatohepatitis 52  
*Lourdes Rodriguez-Fragoso and Janet Sánchez-Quevedo*
- Fecal microbial SN-38G metabolites in colorectal cancer patients are associated with irinotecan-induced delayed diarrhea 53  
*Rongrong Wu, Junru CHEN, Yifei JIA, Yijia CHEN, Yang LI, and Ru YAN*
- Acute restoration of respiratory function in mice with botulism after treatment with aminopyridines 54  
*William T. McClintic, Zachary D. Chandler, Lilitha M. Karchalla, Sean O'Brien, Celinia Ondeck, Alexis Morse, and Patrick McNutt*
- Non-alcoholic Fatty Liver Disease (NAFLD) causes Erythropoietin Hyporesponsiveness 55  
*Huixi Zou and Xiaoyu Yan*
- Safety Evaluation of p5RHH-p65 siRNA Nanoparticles in Mice with Colorectal Cancer Metastases 227  
*Jeremy Cho, Luke E. Springer, Antonina Akk, Samuel Wickline, Christine T. Pham, and Hua Pan*
- Pharmacovigilance of the COVID-19 Vaccine in Ecuador During the First and Second Doses of Vaccination Campaigns 228  
*Andrea Orellana Manzano, Fernanda B. Cordeiro, Andrea Garcia-Angulo, Diana Carvajal-Aldaz, Elizabeth Centeno, Maria J. Vizcaino, Sebastián Poveda, Ricardo Murillo, Derly Andrade-Molina, Saurabh Mehta, and Washinton Cardenas*
- Hepatic PKC $\beta$  promotes aging-induced obesity: potential treatment using a novel PKC $\beta$  inhibitor INST3399 229  
*Kamal D. Mehta*
- Vitamin D3: Clueing into the crosstalk between HIF1 $\alpha$  and macrophage polarization in NASH 230  
*Basma Alaa, Olfat Hammam, Aiman ElKhatib, and Yasmeen Attia*
- ATI-450: A Novel MK2 Pathway Inhibitor - Preclinical & Clinical Translational Studies to Predict Human Dose 231  
*Heidi R. Hope, Susan Hockerman, Matt Saabye, Loreen Stillwell, Rakesh Basavalingappa, Catherine Emanuel, Steve Mnich, Madison Bangs, Emma Huff, Aparna Kaul, Anne Hildebrand, Marco Cardillo, Ajay Aggarwal, and Joseph B. Monahan*
- Comprehensive analysis of CYP2D6 mutations in human cancers 232  
*Kennedy Kuchinski, Julia Driggers, Martin Vo, Wilber Escorcía, and Hanna Wetzel*
- Development of Humanized ACE2 Mouse and Rat Models for COVID-19 Research 252  
*Hongmei Jiang, Emma Hyddmark, Jianqiu Xiao, Sara Gordon, Angela Bartels, Yumei Wu, Joe Warren, Lauren Klaskala, Andrew Brown, Michael Garratt, Helmut Ehall, and Guojun Zhao*
- Characterization of novel genetic mutations in aldehyde dehydrogenase 2 that cause alcohol flushing in humans 253  
*Freeborn Rwere, Rafaela CR. Hell, Xuan Yu, and Eric R. Gross*

Phenylacetylglutamine causes a pathologic inflammation state through the $\beta$ 2-adrenergic receptor /cAMP/PKA/NF- $\kappa$ B pathway in diabetes <i>Lu Huang</i>	254
Deciphering immunological mechanisms underlying the efficacy of nanoparticle-based vaccines and novel adjuvants against Opioid Use Disorder (OUD) <i>Fatima FH. Hamid, Scott Schactler, Debra Walter, Hardik Amin, Minh Le, David Burkhart, Chenming Zhang, and Marco Pravetoni</i>	255
The Neuroprotective Effects of DPP-4 and SGLT2 Inhibitors in Type 2 Diabetes: Possible Mechanism for Halting Cognitive Deterioration <i>Shams T. Osman, Noha A. Hamdy, Amr Y. El Feky, Labiba K. El-Khordagui, and Ahmed F. El-Yazbi</i>	256
CYP4F2*3 (V433M) Polymorphism Impacts Benzalkonium Chloride Metabolism in an Alkyl Chain Length-Dependent Manner <i>Linxi Zhu, Ryan Seguin, Nathan Alade, Justina C. Calamia, Kenneth Thummel, and Libin Xu</i>	426
Impact of SULT1A1 Genetic Polymorphisms on the Sulfation of Clioquinol and Iodoquinol by Human SULT1A1 Allozymes <i>Mohammed Rasool and MING-CHEH LIU</i>	427
Amlodipine use in Mild Cognitive Impairment reduces the risk of incident dementia in National Alzheimer's Coordinating Center participants aged $\geq$ 55 years from 2014-2019 <i>Karin Sandoval</i>	428
PKM2 Deficiency in Brown Adipocytes Enhances Differentiation and the Expression of Mitochondrial Genes <i>Presley Dowker-Key and Ahmed Bettaieb</i>	429
Probing Adropin-Gpr19 Interactions and Signal Transduction <i>Robert N. Devine, Andrew Butler, John Chrivia, Josef Vagner, and Christopher K. Arnatt</i>	430
Investigation of MMR Vaccination Rates and its Relationship with Measles, Mumps, and Rubella Outbreaks in California <i>Brianna Negrete McGinley and Prashant Sakharkar</i>	431
Asparagine depletion by the antileukemic agent PEGylated asparaginase induces hepatic stellate cell activation and fibrosis <i>Yin Zhu, Keito Hoshitsuki, and Christian Fernandez</i>	451
Brazilian Green Propolis-Based Nanostructured System and its use in diabetic rats of <i>Staphylococcus aureus</i> resistant to methicillin (MRSA)-infected wounds <i>Fernando P. Beserra, Marcos V. de Sa Ferreira, Mariana Conceição, Débora M. Rodrigues, Stéfani T. Alves Dantas, Vera L. Moraes Rall, Priscyla D. Marcato Gaspary, Jairo K. Bastos, and Cláudia H. Pellizzon</i>	452
A Novel Charged Sodium-Channel Blocker, Ntx-1175, Is Effective In Reducing Acute Visceral Hypersensitivity In Vivo <i>Ehsan Noor-Mohammadi, Casey LIGON, Beverley Greenwood-Van Meerveld, Nan Zheng, Bridget Bridget Cole, Jim Ellis, and Anthony Johnson</i>	453
Renoprotective Effects of Empagliflozin Against Experimentally Induced Renal Fibrosis In Vitro <i>Sarah Bayne and Shankar Munusamy</i>	454
Safety Evaluations of Rapamycin Perfluorocarbon Nanoparticles in Ovarian Tumor Bearing Mice <i>Adam Mitchell, Qingyu Zhou, Antonina Akk, John Harding, Luke E. Springer, Joseph P. Gaut, Ping Fan, Ivan Spasojevic, Christine T. Pham, Samuel Wickline, Daniel Rauch, Katherine Fuh, and Hua Pan</i>	455
Diagnostic and predictive value of circulating microRNAs and their regulation of BDNF signaling pathway in stroke patients <i>Mikolaj Marszalek, Disha Keshwani, Ceren Eyiletten, Zofia Wicik, Anna Nowak, Salvatore de. Rosa, Dagmara Mirowska-Guzel, Anna Czlonkowska, Guillaume Paré, and Marek Postula</i>	456

## PHARMACOLOGY EDUCATION

Building Undergraduate Professional Identity and Persistence in the Pharmaceutical Sciences through Inquiry-Team-Based Lab Courses <i>Nicholas Denton and Amy Kulesza</i>	188
Demystifying the Concept of "Spare Receptors" in Pharmacology Education Through Novel Didactic Approaches <i>Jorge Iniguez-Lluhi</i>	189
Strategies Used to Improve Quality of Multiple-Choice Questions: A Systematic Review <i>Tanvirul Hye and Monzurul Roni</i>	190
Monitoring metacognition and well-being in a medical pharmacology course: the role of information technologies <i>Ricardo Pena Silva, Juanita Velasco Castro, Christos Matsingos, and Sandra Jaramillo Rincon</i>	191

Can Virtual Reality Improve Pharmacology Education in Medical Students? <i>Monzurul Roni, Kevin Kim, Nicholas Xie, Leslie Hammersmith, and Yerko Berrocal</i>	192
Pharmacology Education, Osteopathic Principles Integration, Osteopathic Manipulation Treatment relations: Osteopathic Graduating Seniors' Perception <i>Khalil Eldeeb</i>	193
Embedding Diversity and Equity Conversations in Cardiovascular Pharmacology: Teaching Arrhythmia Management from A Diversity Context <i>Ashim Malhotra</i>	194
Design and Delivery of Small Group Pharmacology Exercises Facilitated Synchronously to Multiple Groups <i>Jennelle Richardson</i>	391
Contributions of 15 ASPET DPE Members to the International Collaborative Core Concepts Project in Pharmacology Education: Reflections and Opportunities for ASPET <i>A. Laurel Gorman, Mark Hernandez, Kelly Karpa, Carolina Restini, Fabiana Caetano Crowley, Joseph Goldfarb, Clarie Guilding, and Paul White</i>	392
Our Approach to Updating the Cardio System Pharmacology Knowledge Objectives <i>Mark Hernandez, Youssef Soliman, Andy C. Chen, Joe B. Blumer, and Kelly Karpa</i>	393
Diversity, Equity, and Inclusive Course Design in Pharmacology Education: Strategies, Opportunities and Lessons Learned <i>Katerina Venderova</i>	394
The Pharmacology Knowledge Objectives (KOs)-Current Status <i>Robert Theobald and Joe B. Blumer</i>	395
The Notable Integration of Clinically Relevant Pharmacology in Problem-Based Learning Cases <i>Tawna Mangosh</i>	396
ASPET Academy of Pharmacology Educators: Twelve Years of Pharmacology Educators' Recognition <i>Khalil Eldeeb</i>	397
Identifying Students' Causal Mechanistic Reasoning (CMR) in Medical Pharmacology <i>Rosalyn Bloch, Carolina Restini, Nathan Bautista, and Keenan Noyes</i>	593
Addressing Healthcare Inequities Through The Medical Pharmacology Curriculum <i>Jennelle Richardson</i>	594
Successful Integration of Pharmacology Instruction From Day One of Medical School <i>Sandeep Bansal, Thomas Yorio, and Kelly Pagidas</i>	595
Student perceptions of scholarly scientific writing in pharmacology: student generation of collaborative rubrics to score literature reviews in social pharmacology <i>Hanna Wetzel, Terri Ensein, and Edward Kosack</i>	596
Longitudinal Impact of Mnemonics Use on Pharmacy Students' Exam Performance and Perceptions of Knowledge Retention and Clinical Application <i>Shankar Munusamy, Carrie Koenigsfeld, and Ron Torry</i>	597
Development and Implementation of Equitable and Inclusive Teaching Practices in Pharmacology <i>Elizabeth S. Yeh</i>	598
Evaluation of Diversity and Bias Topics in a Medical School Pain & Opioid Analgesic Curriculum <i>A. Laurel Gorman and Danny Kim</i>	599
Integration and Alignment of Pharmacological Principles and Agents in a Preclinical Problem-Based Learning Curriculum Through a Web-Based Interface <i>Megan Amber Lim, Lisan Smith, Max Ledersnaider, Diamond Coleman, Noah Nigh, Christopher Pecenka, and Noelle Kwan</i>	600

## TOXICOLOGY

A Cutaneous Nitrogen Mustard Murine Injury Model to Study the Pathophysiology of its Long-term Effects <i>Andrew Roney, Dinesh Goswami, Ebenezar Okoyeocha, Steve Lundback, Holly Wright, Omid Madadgar, Ellen Kim, Jared M. Brown, and Neera Tewari-Singh</i>	19
Impairing Cytochrome P450-mediated metabolism aggravates the hepatotoxicity of serotonin and norepinephrine reuptake inhibitor duloxetine <i>Feng Li, Xuan Qin, John M. Hakenjos, Kevin Mackenzie, and Lei Guo</i>	20
The HMGB1/MAPKs/Nrf2 Signaling Arbitrates Hepatoprotection Conferred by Celecoxib in Preeclamptic Weaning Rats <i>Mahmoud El-Mas, Salwa A. Abuiessa, Reem H. Elhamammy, Nevine M. El-Deeb, and Sherien A. Abdelhady</i>	21

Effect of Vitamin E on Doxorubicin and Paclitaxel Induced Memory Impairments in Male Rats <i>Ahmad AlTarifi, Kareem Sawali, Kareem Alzoubi, Tareq Saleh, Omar Khabour, and Malik Abu Alrub</i>	22
Evaluation of the Time- and Dose-Dependent Toxicity of Sunitinib Using a 3-D Human Hepatic Spheroid Model <i>Shalon L. Harvey, Jessica L. Beers, and Klarissa D. Jackson</i>	23
Arsenic trioxide impairs primary human NK cell responses against influenza A virus <i>Allison P. Boss, Robert Freeborn, Yining Jin, Luca Kaiser, Elizabeth Gardner, and Cheryl E. Rockwell</i>	24
Multi-Walled Carbon Nanotubes Stimulate Arachidonate 5-Lipoxygenase-dependent M1 polarization of Macrophages to Promote Proinflammatory Response <i>in vitro</i> <i>Chol Seung Lim, Michael Kashon, Dale Porter, and Qiang Ma</i>	25
The Influence of Arsenic on Selenium Uptake by Red Blood Cell Anion Exchanger 1/ <i>SLC4A1</i> Variants <i>Serena Li, Kamran Shekh, Naomi M. Potter, Emmanuelle Cordat, and Elaine M. Leslie</i>	26
Interrogating Environmental Contaminant Activity Against the Druggable GPCRome: A High Throughput Approach to Assess Interaction and Pathology <i>Joshua Wilkinson and Dave Roman</i>	56
Induction of Thioredoxin-Interacting Protein and Role in NLRP3 Activation by Carbon Nanotubes in Macrophages <i>Qiang Ma, Chol Seung Lim, Fatimah Matakah, Dale Porter, and Mackenzie Buck</i>	57
Investigation of hepatotoxicity of structurally diverse pyrrolizidine alkaloids in zebrafish model <i>Yueyang Pan, Jiang MA, and Ge Lin</i>	58
Molecular Investigation of the Ameliorative Potentials of <i>Cymbopogon citratus</i> Leaves Extract in Carbon tetrachloride- Induced Hepatotoxicity in rats <i>Olorunfemi Molehin, Olusola O. Elekofehinti, Ajibade O. Oyeyemi, and Oluwabukola O. Olubaju</i>	59
Ginsenoside Rc from <i>Panax ginseng</i> Ameliorates Palmitate-induced UB/OC-2 Cochlear Cell Injury <i>Nicholas N. Gill, Presley Dowker-Key, Katelin Hubbard, Brynn Voy, Jay N. Whelan, Mark Hedrick, and Ahmed Bettaieb</i>	60
The Homemade Russian Drug Krokodil: Is it Good or Evil? <i>Emanuele Alves</i>	61
Nrf2-dependent and independent effects of tBHQ on dendritic cell function <i>Saamera Awali, Yining Jin, and Cheryl E. Rockwell</i>	62
Elucidating the Role of Inducible Nitric Oxide Synthase in E-cigarette Toxicity using Precision Cut Lung Slices <i>Melissa Kudlak, Julia Herbert, Alyssa Bellomo, Andrew Gow, Jeffrey D. Laskin, and Debra L. Laskin</i>	219
Arsenic Hepatic Sinusoidal Export is Stimulated by Methylselenocysteine and Mediated by Multidrug Resistance Protein 4 (MRP4/ABCC4) <i>Elaine M. Leslie, Janet R. Zhou, and Gurnit Kaur</i>	220
Effects of 3,3'-Dichlorobiphenyl (PCB-11) on the expression of CYP2A, 2B, and 2F enzymes in the liver and brain of CYP2A6-humanized, CYP2B6-humanized, or wild-type mice <i>Weiguo Han, Weizhu Yang, Xueshu li, Lehmler Hans-Joachim, Qing-Yu Zhang, Pamela Lein, and Xinxin Ding</i>	221
Sacubitril/Valsartan Alleviates Type 2 Diabetes-Induced NAFLD Through Modulation of Oxidative Stress, Inflammation and Apoptosis <i>Salim Al-Rejaie, Mohammed M. Ahmed, and Mohamed Mohany</i>	222
Comparison of Mustard and Urticant Vesicating Agents' Induced Cutaneous Lesions in Wild Type and Mast Cell Deficient Mice <i>Dinesh Goswami, Andrew Roney, Omid Madadgar, Satyendra K. Singh, Steve Lundback, Jared M. Brown, and Neera Tewari-Singh</i>	223
Damage to Olfactory Organs of Adult Zebrafish Induced by Diesel Particulate Matter <i>Su Jeong Song</i>	224
The Nrf2 activator tBHQ promotes OVA-Elicited Food Allergy in Mice <i>Yining Jin, Allison P. Boss, Caitlin Wilson, and Cheryl E. Rockwell</i>	225
Hepatocyte Senescence is Initiated through a Klf6-p21 Mechanism which mediates the Production of Cxcl14, a Novel Prognostic Biomarker of Acute Liver Failure <i>David Umbaugh, Nga Nguyen, Giselle Sanchez Guerrero, Cecilia Villanueva, Bruno Hagenbuch, Anup Ramachandran, and Hartmut Jaeschke</i>	226
Eugenol Protects Against Diclofenac-Induced Hepatocellular Injury in an In Vitro Mouse Model <i>Jaiden Martin, Brendan D. Stamper, and Jon Taylor</i>	257
Determination of methylphenethylamine and Its Metabolites in Whole Blood of Rats Using MMSPE and UPLC-qTOF-MS <i>Ahmad M. Alamir, James Watterson, and Ibraheem Attafi</i>	258

Generation and Characterization of a Serum Albumin-Humanized Mouse Model For Biomarker Discovery <i>Xiangmeng Wu, Weiguo Han, Weizhu Yang, Robert J. Turesky, Laura Van Winkle, Qing-Yu Zhang, and Xinxin Ding</i>	259
Differential Induction of Microsomal and Soluble Epoxide Hydrolases by Arsenic in Drinking Water <i>Hui Li, Xiaoyu Fan, Shuang Yang, Xinxin Ding, Donna Zhang, and Qing-Yu Zhang</i>	260
Evaluation of Immunomodulators as Therapeutic Treatments for Sulfur Mustard-Induced Ocular Injury <i>Ki H. Ma, Bailey T. Chalmers, and Albert L. Ruff</i>	261
Exposure to DDX in Mice Reveals Impaired Energy Expenditure May be Mediated by DNA Methylation Changes <i>Juliann A. Jugan, Sarah Elmore, Kyle Jackson, Annalise vonderEmbse, Scott Tiscione, and Michele A. La Merrill</i>	262
Gallic acid modifies EGFR phosphorylation in rat with hepatic preneoplasia <i>Lourdes Rodríguez-Fragoso, Erick Ayala-Calvillo, and Felipe Rodríguez-López</i>	263
Mitragynine Pretreatment Prevents Morphine-Induced Respiratory Depression <i>Julio D. Zuarth Gonzalez, Alexandria K. Ragsdale, Sushobhan Mukhopadhyay, Christopher R. McCurdy, Lance McMahon, and Jenny L. Wilkerson</i>	264
Evaluating the role of rodent macrophage immunometabolism in response to endotoxin <i>Rachel Sun, Jaclynn Andres, Jordan Lee, Kinal Vayas, Changjiang Guo, Andrew Gow, and Debra L. Laskin</i>	418
Damage to Intestinal Barrier of Zebrafish Larvae by Polystyrene Nanoplastics exposure <i>Hyejin Lee</i>	419
Assessing the Impact of Benzalkonium Chlorides on Gut Microbiome and Liver Metabolism <i>Vanessa A. Lopez, Joe Jongpyo Lim, Ryan Seguin, Joseph L. Dempsey, Gabby C. Kunzman, Julia Yue Cui, and Libin Xu</i>	420
Mitochondrial Modulation of Amplified Preconditioning Influences of Remote Ischemia Plus Erythropoietin Against Skeletal Ischemia/Reperfusion Injury in Rats <i>Mahmoud El-Mas, Mennatallah A. Ali, Nahed H. El-Sokkary, Samar S. Elblehi, and Asmaa A. Khalifa</i>	421
Beta-Catenin Mediates PKM2's Role in LPS-induced Renal Injury <i>Katelin Hubbard, Mohammed Alquraishi, Samah Chahed, Dina Alani, Dexter Puckett, Presley Dowker-Key, Yi Zhao, Ji Yeon Kim, Laurentia Nodit, Huma Fatima, Dallas Donohoe, Brynn Voy, Jay N. Whelan, Winyoo Chowanadisai, and Ahmed Bettaieb</i>	422
Common Pathways in Human Proximal Tubular Cells Altered by Exposures to Diverse Environmental Agents and Nephrotoxic Therapeutic Drugs <i>Lawrence Lash, Patricia Mathieu, Rita Rosati, Paul Stemmer, Xin Hu, and Dean P. Jones</i>	423
The Kratom-Derived Alkaloid Mitragynine Upregulates the Cortisol Steroidogenic Pathway In a Human Adrenocortical Cell Line <i>Phillip Kopf and Walter Prozialeck</i>	424
Effects of the E-liquid Flavoring Agents Vanillin and Ethyl Vanillin in Human Proximal Tubule Epithelial Cells <i>Ashley Cox, Kathleen Brown, and Monica Valentovic</i>	425
Cutaneous Exposures to Nitrogen Mustard in C57BL/6 Mice Cause Hematologic Toxicity that could lead to Acute and Long-term Effects <i>Ellen Kim, Dinesh Goswami, Andrew Roney, Ebenezar Okoyeocha, Steve Lundback, Dawn Kuszynski, Adam Lauver, and Neera Tewari-Singh</i>	457
Pyrolizidine alkaloids induced obstructive pulmonary disease more than pulmonary vascular diseases <i>Zijing Song, Yisheng He, and Ge Lin</i>	458
Molecular Mechanisms of Hippocampal Neurotoxicity Across Three Generations of Brominated Flame Retardants <i>Naomi Kramer, Brian Cummings, and John Wagner</i>	459
Examining the Nephrotoxicity Induced by Benzalkonium Chlorides in 2D and 3D-Cultured Human Proximal Tubule Epithelial Cells <i>Marie Brzoska, Ryan Seguin, Jade Yang, Edward J. Kelly, and Libin Xu</i>	460
Perturbation of Space-Time Gene Expression of the Liver Lobule by 2,3,7,8-Tetrachlorodibenzo-p-dioxin <i>Daniel Marri, Omar Kana, Rance Nault, Giovan Cholico, Timothy Zacharewski, and Sudin Bhattacharya</i>	461
Development of an Extraction Method for the analysis of Synthetic Opioids in Bone Samples using the Bead Ruptor <i>Kala N. Babb, David J. Cohen, and Emanuele Alves</i>	462
Maternal Electronic Cigarette Exposure Induces Inflammation, Oxidative Stress and Alters Mitochondrial Function in Postnatal Brain <i>Sabrina Rahman Archie, Ali Sifat, David Mara, Yong Zhang, and Tom Abbruscato</i>	463

# Sotorasib, a KRAS-G12C Inhibitor, Induces Chemoresistance by Activating Human Pregnane Xenobiotic Receptor

Julia Salamat,<sup>1</sup> Kodye L. Abbott,<sup>2</sup> Elizabeth L. Ledbetter,<sup>1</sup> Chuanling Xu,<sup>1</sup> and Satyanarayana R. Pondugula<sup>1</sup>

<sup>1</sup>Auburn University; and <sup>2</sup>Yale School of Medicine

Abstract ID 23343

Poster Board 33

During multidrug combination chemotherapy, activation of the nuclear receptor, human pregnane xenobiotic receptor (hPXR), has been shown to play a role in the development chemoresistance. Mechanistically, this could occur by upregulation of agonists-induced hPXR-regulated expression of drug-metabolizing enzymes and drug-efflux pumps, such as cytochrome P450 3A4 (CYP3A4) and multidrug resistance protein 1 (MDR1). CYP3A4 & MDR1, contribute to the metabolism and disposition of over 50% of clinical drugs. Therefore, during multidrug chemotherapy, drug induction of hPXR-regulated CYP3A4 & MDR1 leads to increased drug metabolism & transport, affecting the therapeutic response of co-administered drugs, leading to chemoresistance. Sotorasib (SOT) is the first FDA approved KRAS-G12C inhibitor for the treatment of advanced non-small cell lung cancer with the KRAS-G12C mutation. It is currently unknown whether SOT can activate hPXR and upregulate hPXR target gene expression, leading to chemoresistance. We therefore sought to determine whether SOT, at its therapeutically relevant concentrations, could act as an hPXR agonist and upregulate hPXR-mediated regulation of CYP3A4 & MDR1 in human hepatocytes, HepG2 liver cancer cells & LS180 colon cancer cells, and induce chemoresistance in LS180 cells. Reporter gene assays were conducted to determine the transactivation of CYP3A4 promoter activity by the nuclear receptors. Cell viability assays were performed to assess cytotoxicity. RT-qPCR assays were conducted to study CYP3A4 & MDR1 gene expression. Rhodamine-123 intracellular accumulation assays were performed to examine MDR1 function. Competitive ligand binding assays were performed to determine the ability of SOT to bind to hPXR. SOT, at its therapeutically relevant concentrations, induced hPXR transactivation of CYP3A4 promoter activity, suggesting that SOT can induce hPXR target gene expression. Indeed, SOT induced endogenous gene expression of hPXR target genes: CYP3A4 & MDR1. SOT decreased intracellular accumulation of MDR1 substrate rhodamine-123, suggesting that SOT induces MDR1 functional expression. SOT was able to bind to the ligand-binding domain of hPXR, suggesting that SOT can directly interact with hPXR to induce hPXR target gene expression. The inductive effect of SOT on CYP3A4 promoter activity as well as endogenous CYP3A4 & MDR1 gene expression was inhibited by a specific hPXR antagonist SPA70. These findings suggest that SOT induces hPXR target genes by directly activating hPXR. Moreover, while SOT activated hPXR, it failed to activate the mouse PXR and another related nuclear receptor human constitutive androstane receptor in the reporter gene assays, indicating that the effects of SOT are both species and nuclear receptor dependent. Notably, SOT decreased the sensitivity of LS180 cells to both irinotecan and its active metabolite SN-38, suggesting that SOT can induce chemoresistance by activating hPXR. Taken together, our results suggest that SOT induces chemoresistance by activating hPXR and inducing CYP3A4 & MDR1. The inductive effects of SOT on CYP3A4 & MDR1 expression caution the use of SOT in conjunction with other medications that are metabolized and transported via CYP3A4 & MDR1, as this can lead to chemoresistance.

Acknowledgments: This study was supported by Auburn University Animal Health & Disease Research Program to S.R.P.

# Identification and Testing of a Novel HUNK Inhibitor

Tinslee Dilday,<sup>1</sup> Melissa Abt,<sup>1</sup> Herman Sintim,<sup>2</sup> George Sandusky,<sup>1</sup> and Elizabeth S. Yeh<sup>1</sup>

<sup>1</sup>Indiana University School of Medicine; and <sup>2</sup>Purdue University

Abstract ID 17471

Poster Board 34

Human epidermal growth factor receptor 2-positive (HER2+) breast cancer is one of the three clinical subtypes of breast cancer that is defined by having *HER2* gene amplification that coincides with HER2 protein overexpression. HER2 is amplified in 15-30% of breast cancers and overexpression of this gene is a predictor of survival in breast cancer patients. HER2-targeted therapies have been successful in treating HER2+ breast cancer; however, over time, HER2+ breast cancer can develop resistance to these therapies establishing an urgent need for novel targets. Hormonally Up-regulated Neu-associated Kinase (HUNK) gene expression is elevated in HER2+ breast cancer and high *HUNK* expression is associated with reduced relapse free survival. HUNK activation has been found to promote autophagy enhancing survival of HER2+ breast cancer cells, which promotes resistance to HER2-inhibitors. Prior work shows that HUNK phosphorylates an autophagy protein, Rubicon, in its N-terminal domain at Serine (S) 92, promoting autophagy. Therefore, based on these findings we investigated the role of S92 Rubicon phosphorylation in HER2+ breast cancer using cell lines developed from the MMTV-neu mouse model. MMTV-neu cells expressing HUNK WT were retrovirally transduced with vector, Rubicon WT, and a Rubicon phospho-deficient mutant (S92A). Using a mammary tumor growth assay we have determined that Rubicon S92 phosphorylation promotes tumorigenesis, defining a molecular target for HUNK activity. Ponatinib is a kinase inhibitor that binds but does not inhibit the kinase domain of HUNK. In collaboration with Dr. Herman Sintim's lab at Purdue University, we chemically modified the structure of Ponatinib and have now derived a novel inhibitor of HUNK, HSL119, that inhibits HUNK kinase activity. **Therefore, the objective of this study is to demonstrate that HSL119 is a pharmacological inhibitor of HUNK activity that inhibits tumorigenesis in HER2+ breast cancer.** We have shown using a HUNK kinase assay that HSL119 inhibits HUNK's phosphorylation of Rubicon at S92. In a HER2-inhibitor resistant cell line, JIMT-1, we show that HSL119 inhibits Rubicon S92 phosphorylation and reduces viability. Furthermore, using a HER2 PDX model that is resistant to lapatinib and neratinib, we show that HSL119 strongly inhibits tumor growth compared to placebo. Together, our observations suggest that HUNK activity is inhibited using HSL119 resulting in the desired anti-tumor effect. This establishes that HUNK activity can be inhibited using HSL119 and that pharmacological inhibition of HUNK is an applicable strategy for HER2+ breast cancer.

Support/Funding Information:

R01-CA187305

100 Voices of Hope

RSFG-Award from IUPUI



# Ethanollic Extract of *Origanum syriacum* L. Leaves Exhibits Potent Anti-Breast Cancer Potential and Robust Antioxidant Properties

Elias Baydoun,<sup>1</sup> Joelle Mesmar,<sup>1</sup> Rola Abdallah,<sup>1</sup> and Kamar Hamade<sup>2</sup>

<sup>1</sup>American University of Beirut; and <sup>2</sup>University of Picardie Jules Verne

Abstract ID 17278

Poster Board 35

**Background:** Breast cancer (BC) is the second most common cancer overall. In women, BC is the most prevalent cancer and the leading cause of cancer-related mortality. Triple negative BC (TNBC) is the most aggressive BC being resistant to hormonal and targeted therapies.

**Hypothesis/Purpose:** The medicinal plant *Origanum syriacum* is a shrubby plant rich in bioactive compounds and widely used in traditional medicine to treat various diseases. However, its therapeutic potential against BC remains poorly investigated. In the present study, we identified the bioactive compounds of the ethanollic extract of *O. syriacum* (OSEE) and investigated its anticancer effects and possible underlying mechanisms of action against the aggressive and highly metastatic human TNBC cell line MDA-MB-231.

**Methods:** Column chromatography and LC-MS were used to identify the phytochemical constituents of OSEE, MTT, trans-well migration, and scratch assays were used to assess cell viability, invasion, or migration, respectively. Antioxidant potential was evaluated *in vitro* using the DPPH radical scavenging assay and ROS levels were assessed in cells in culture using DHE staining. Aggregation assays were used to determine cell-cell adhesion. Flow cytometry was used to analyze cell cycle progression. Protein levels of markers of apoptosis (BCL-2, pro-Capase3, p53), proliferation (p21, Ki67), cell migration, invasion, or adhesion (FAK, E-cadherin), angiogenesis (iNOS), and cell signaling (STAT3, p38) were determined by immunoblotting. Chorio-allontoic Membrane (CAM) assay evaluated *in ovo* angiogenesis.

**Results:** We demonstrated that OSEE was rich in phytochemical constituents mainly carvacrol. We also found that the OSEE crude extract had potent radical scavenging activity *in vitro* and induced the generation of reactive oxygen species (ROS) in MDA-MB-231 cells, especially at higher OSEE concentrations. Non-cytotoxic concentrations of OSEE attenuated cell proliferation and induced G0/G1 cell cycle arrest, which was associated with phosphorylation of p38 MAPK, an increase in the levels of tumor suppressor protein p21, and a decrease of proliferation marker protein Ki67. Additionally, only higher concentrations of OSEE were able to attenuate inhibition of proliferation induced by the ROS scavenger N-acetyl cysteine (NAC), proposing that the anti-proliferative effects of OSEE can be ROS-dependent. OSEE stimulated apoptosis and its effector Caspase-3 in MDA-MB-231 cells, in correlation with activation of STAT3/p53 pathway. Furthermore, the extract reduced the migration and invasive properties of MDA-MB-231 cells through the deactivation of focal adhesion kinase (FAK). OSEE also reduced the production of inducible nitric oxide synthase (iNOS) and inhibited *in ovo* angiogenesis. Further studies have been carried out to assess the composition of various fractions from the OSEE crude extract, in an effort to identify the bioactive molecules. Interestingly, two fractions have shown a more potent activity against the proliferation of MDA-MB-231 cells when compared to the crude extract.

**Conclusion:** Our findings reveal that OSEE is a rich source of phytochemicals and has robust anti-breast cancer properties that significantly attenuate the malignant phenotype of MDA-MB-231 cells, suggesting that *Origanum syriacum* may act as a rich source of potential TNBC therapeutics and posing *Origanum syriacum* to offer novel avenues for the design novel TNBC drugs.

# Aberrantly upregulated Drp1 induces mitochondrial fission and promotes colorectal cancer cell migration

Tianzhou Xing,<sup>1</sup> Yan Xie,<sup>2</sup> Peter Abel,<sup>2</sup> and Yaping Tu<sup>3</sup>

<sup>1</sup>Creighton University; <sup>2</sup>Creighton Univ; and <sup>3</sup>Creighton Univ School of Medicine

**Abstract ID 52235**

**Poster Board 36**

Metastasis is the major cause of cancer death. One of the major challenges in the management of cancer is to identify cancer cells with high metastatic potential, and to confine the cancer cells to their current location for destruction once detected. Understanding the molecular mechanism that allows cancer cells to acquire migratory abilities can lead to development of novel therapies. Mitochondria exist as dynamic networks that often change size and distribution, and these dynamics are maintained by two opposing processes: fission and fusion, regulated by Drp1 and mitofusin (Mfn) proteins, respectively. The present study was to investigate the role and mechanism underlying dysregulation of mitochondrial dynamics (unbalanced fission or fusion) in colorectal cancer (CRC), the 3rd leading cause of cancer-related deaths in the United States.

We performed immunohistochemical (IHC) analysis of Drp1 protein expression in commercial microarrays of 266 human CRC specimens and adjacent normal tissues. Average Drp1 staining intensities in carcinoma were increased as compared with normal or adjacent normal tissues ( $2.34 \pm 0.05$  vs  $1.12 \pm 0.08$ ,  $P < 0.001$ ). Drp1 protein expression was further increased in lymph node metastases as compared to carcinoma ( $2.96 \pm 0.13$  vs  $2.34 \pm 0.05$ ,  $^{\#}P < 0.01$ ). These data suggest that upregulation of Drp1 mitochondrial fission protein is proportional to the degree of metastasis of these CRCs. We then characterized mitochondrial dynamics in different CRC cell lines. Mitochondria are tubular network-like structures in non-metastatic SW480 cells whereas in metastatic HCT-116 and LoVo cells, mitochondria are short tubules and spheres. Transwell migration assay showed that HCT-116 and LoVo cells have 20-50-fold higher migratory abilities than SW480 cells. Western blot showed that Drp1 was markedly increased in HCT-116 and LoVo cells as compared to SW480 cells. Silence of endogenous Drp1 expression leads mitochondrial elongation and decreases migratory abilities of HCT-116 cells in vitro by over 70% whereas overexpression of recombinant Drp1 induces mitochondrial fragment and promotes SW480 cell migration in vitro. Together, our study may provide a novel strategy to prevent metastasis via target Drp1-dependent mitochondrial fission in CRC patients.

Supported by Nebraska State LB595 grants to YT and PWA

# Designing Tailored Thiosemicarbazones with Bespoke Properties: The Styrene Moiety Imparts Potent and Selective Anti-Tumor Activity

Des Richardson,<sup>1</sup> mahendiran Dharmasivam,<sup>2</sup> and Busra Kaya<sup>2</sup>

<sup>1</sup>Griffith Univ; and <sup>2</sup>Griffith University

Abstract ID 17381

Poster Board 37

**Background:** Thiosemicarbazones of the di-2-pyridylketone thiosemicarbazone class possess potent anti-tumor activity *via* binding essential metal ions in cancer cells (e.g., iron (Fe(II)), copper (Cu(II)), and zinc (Zn(II)) to form metal complexes. These agents demonstrate activity at inhibiting the “triad-of-death” in cancer, namely **(1)** metastasis; **(2)** tumor growth; and **(3)** resistance (Richardson et al. *PNAS* 2006;103:14901-6; *FASEB J.* 2020;34:11511-28; *FASEB J.* 2021;35:e21347). However, clinical trials have indicated that some thiosemicarbazones induce deleterious oxidation of heme proteins such as oxyhemoglobin leading to hypoxia (*Invest. New Drugs.* 2010;28:91–97).

**Objective/Aim:** To design, synthesize, and characterize innovative thiosemicarbazone anti-cancer agents with marked and selective anti-tumor activity that do not induce problematic oxidation of oxy-myoglobin or oxyhemoglobin.

**Hypothesis:** That bespoke structural modifications of thiosemicarbazones derived from structure-activity relationships can lead to frontier agents with marked anti-cancer activity and selectivity.

**Design/Approach/Methodology:** Medicinal chemistry, cellular and molecular biology, biochemistry, molecular pharmacology, molecular modeling, and protein docking.

**Results:** A novel, potent, and selective anti-tumor thiosemicarbazone, PPP44mT, and its analogs were synthesized and characterized and displayed strikingly distinctive properties. This activity was mediated by the inclusion of a styrene moiety, which through steric and electrochemical mechanisms, prevented deleterious oxy-myoglobin or oxyhemoglobin oxidation relative to other thiosemicarbazones, namely di-2-pyridylketone-4-cyclohexyl-4-methyl-3-thiosemicarbazone (DpC) or di-2-pyridylketone-4,4-dimethyl-3-thiosemicarbazone (Dp44mT). This prevention of heme oxidation was due to the ability of the styrene moiety to prevent the close association of PPP44mT to the heme plane of oxy-myoglobin or oxyhemoglobin. Furthermore, structure-activity relationship analysis demonstrated that specific tuning of PPP44mT electrochemistry further inhibited oxy-myoglobin or oxyhemoglobin oxidation. Both PPP44mT and its Cu(II) complexes showed conspicuous, almost immediate cytotoxicity against SK-N-MC tumor cells (within 3 h). In contrast, the Zn(II) complex of PPP44mT (*i.e.*, [Zn(PPP44mT)<sub>2</sub>]) demonstrated a pronounced delay in activity, taking 48 h before marked anti-proliferative efficacy was apparent. As such, [Zn(PPP44mT)<sub>2</sub>] was designated as a “stealth Zn(II) complex” that overcomes the near immediate cytotoxicity of PPP44mT or its Cu(II) complexes. Examining suppression of oncogenic signaling, [Zn(PPP44mT)<sub>2</sub>] was superior to DpC or Dp44mT at inhibiting the expression of pro-oncogenic cyclin D1.

**Significance:** This research demonstrates that thiosemicarbazones can be specifically tailored to achieve bespoke activity that leads to marked anti-cancer activity and selectivity.

**Support/Funding Information:** National Health and Medical Research Council of Australia; Australian Research Council; Thrasher Foundation USA; Cancer Australia; National Breast Cancer Foundation of Australia.

# Histone Deacetylase Inhibitor Belinostat Regulates Metabolic Reprogramming in Killing Kras-Mutant Human Lung Cancer Cells

Rebecca Peter,<sup>1</sup> Md. Shahid Sarwar,<sup>1</sup> Yujue Wang,<sup>1</sup> Xiaoyang Su,<sup>1</sup> and Ah-Ng Kong<sup>1</sup>

<sup>1</sup>Rutgers University

Abstract ID 18095

Poster Board 38

**Aims:** Kirsten Rat Sarcoma virus (KRAS) oncogene, found in 20-25% of lung cancer patients, regulates metabolic reprogramming and redox status during tumorigenesis. Recently, histone deacetylase (HDAC) inhibitors are widely investigated for the treatment of KRAS-mutant lung cancer. In the current study, we investigate the effect of HDAC inhibitor (HDACi) belinostat on nuclear factor erythroid 2-related factor 2 (NRF2) and mitochondrial metabolism for the treatment of KRAS-mutant cell lung cancer.

**Main methods:** LC-MS metabolomic study of belinostat on mitochondrial metabolism was performed in KRAS-mutant non-small cell lung cancer cells. Furthermore, L-methionine (methyl-<sup>13</sup>C) isotope tracer was used to explore the effect of the belinostat in one carbon metabolism. Bioinformatic analyses were performed with the metabolomic data to identify the pattern of the significantly regulated metabolites. To study the effect of belinostat on redox signaling Are-NRF2 pathway, luciferase reporter activity assay was done in stably transfected HepG2-C8 cells (containing pARE-TI-luciferase construct), followed by qPCR analysis of NRF2 and its target gene in NSCLC cells.

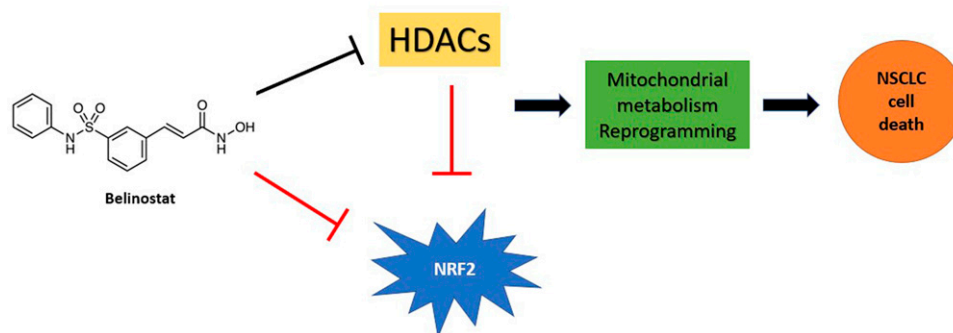
**Key findings:** Metabolomic study revealed significantly altered metabolic levels related to redox homeostasis including tricarboxylic acid (TCA) cycle metabolites (citrate, aconitate, fumarate, malate and  $\alpha$ -ketoglutarate); urea cycle metabolites (Arginine, ornithine, argino-succinate, aspartate and fumarate); and glutathione metabolism pathway (GSH/GSSG and NAD/NADH ratio) after belinostat treatment. <sup>13</sup>C stable isotope labeling data indicates potential role of belinostat in creatine biosynthesis via methylation of guanidinoacetate. Moreover, belinostat inhibited NRF2 activity and downregulated the expression of NRF2 and its target gene NAD(P)H:quinone oxidoreductase 1 (NQO1).

**Significance:** Belinostat is effective in killing KRAS-mutant lung cancer cells by regulating mitochondrial metabolism.

**Keywords:** Belinostat; HDAC inhibitor; Mitochondrial metabolism; KRAS mutation; NRF2; Lung cancer

This work was supported in part by institutional funds and and P30 ES005022 from the National Institute of Environmental Health Sciences (NIEHS).

Graphical Abstract



# Scaffold protein Scribble is a potent modulator of Sonic Hedgehog signaling

Jingwen Zhu,<sup>1</sup> Sabina Ranjit,<sup>2</sup> Yao Wang,<sup>3</sup> Frederique Zindy,<sup>3</sup> Martine Roussel,<sup>3</sup> and John Schuetz<sup>4</sup>

<sup>1</sup>St. Jude Children's Research Hospital and the University of Tennessee Health Science Center; <sup>2</sup>St Jude Children; <sup>3</sup>St. Jude Children's Research Hospital; and <sup>4</sup>St. Jude Children

Abstract ID 28302

Poster Board 39

Sonic Hedgehog (SHH) signaling plays a crucial role in cerebellum development by controlling the proliferation of granule neuron progenitors (GNP). Its aberrant expression results in SHH-Medulloblastoma (MB), which is among the most prevalent pediatric brain tumors in children younger than 3 years old. Though SHH-MB is genetically understood, current therapies are ineffective. There is an unmet need to identify new targetable regulators of SHH signaling to improve outcomes. We previously reported that the ABC transporter ABCC4 was expressed in MB and modulated the intensity of SHH pathway activity<sup>1</sup>, and have recently identified Scribble (SCRIB) as a protein that binds to the PDZ motif of ABCC4. SCRIB is a conserved scaffold protein that has known roles in cell polarity and coordinates several signaling pathways<sup>2</sup>. A recent study discussed SCRIB's association with neurodevelopmental disorders<sup>3</sup>. However, it is unknown whether SCRIB regulates the SHH pathway. In mouse cerebellum, we found that Scrib is highly expressed at postnatal day 1-7 (when SHH signaling is most active) and specifically expressed in proliferating GNPs. We hypothesized that SCRIB might regulate SHH signaling by either affecting ABCC4 or acting independently. To test if SCRIB is required for SHH signaling, *Scrib* knockdown by siRNAs was performed in NIH-3T3 cells, a model of the SHH pathway. SHH signaling was initiated by either SHH ligand or Smoothed (Smo) agonist SAG. The activation was assessed by Gli1 expression, a target gene of SHH signaling. Our results showed that suppression of *Scrib* remarkably diminished both mRNA ( $p < 0.05$ ) and protein level ( $p < 0.01$ ) of Gli1, demonstrating that SCRIB is a positive regulator of SHH signaling. We then used CRISPR-Cas9 to develop NIH-3T3 *Scrib* knockout (KO) clones that affirmed *Scrib* absence impaired SHH signaling. Because ABCC4 regulates SHH signaling by affecting cAMP transport, we excluded the possibility that SCRIB modulates the pathway by affecting ABCC4's expression, localization and function. We then investigated alternative molecular mechanisms by which SCRIB acts independently of ABCC4. The expression and localization of key elements in SHH signaling were evaluated in *Scrib*KO clones, including Smo and Gli2. There was minimal effect on the upstream SHH activator Smo, but subcellular fractionation revealed that *Scrib*'s absence dramatically reduced the SHH-induced nuclear expression of Gli2 ( $p < 0.0001$ ), a dominant downstream activator. Cycloheximide turnover studies suggested that SCRIB is required for the stability of GLI2 during SHH signaling. To understand the influence of SCRIB on the aberrant SHH signaling that drives some SHH-MBs, *Scrib* siRNAs were applied to mouse fibroblast cell lines lacking either *Ptch1* or *Sufu*. Loss of *Scrib* restrained the constitutive SHH pathway activation produced by *Ptch1* or *Sufu* absence as shown by the dramatic reduction in Gli1 ( $p < 0.01$ ). Moreover, *SCRIB* knockdown in human SHH-MB cell lines, DAOY and UW228, significantly decreased the proliferation of these tumor cells ( $p < 0.02$ ), highlighting that SCRIB suppression is a viable strategy to reduce SHH-MB tumor growth. Overall, our data demonstrates that SCRIB is a new potent modulator of SHH signaling with the potential as a novel target in SHH-MB therapy.

This work is supported by NIH and ALSAC.

## Ref:

1. Wijaya, J. *et al. Cancer Res.*2020
2. Pires, H. R. & Boxem, M. *J. Mol. Biol.*2018
3. Ezan, J. *et al. Sci. Rep.*2021.

# Understanding How Cellular Metabolism Affects Clofarabine Treatment in Acute Myeloid Leukemia

Ashley Gray,<sup>1</sup> Yu Fukuda,<sup>2</sup> Lauren Brakefield,<sup>1</sup> Amit Budhraj,<sup>3</sup> Joseph T. Opferman,<sup>3</sup> and John Schuetz<sup>2</sup>

<sup>1</sup>St. Jude Children's Research Hospital and University of Tennessee Health Sciences Center; <sup>2</sup>St. Jude Children; and <sup>3</sup>St. Jude Children's Research Hospital

Abstract ID 23291

Poster Board 40

Acute myeloid leukemia (AML) has a poor 5-year survival rate of only 40%. The poor survival rate is in part due to leukemic stem cells (LSCs) surviving traditional chemotherapeutic treatment; a high proportion of patients experience relapse because LSCs appear refractory to therapy. Previous research has indicated heterogeneous, but distinct metabolic profiles in hematopoietic stem cells (HSCs), LSCs, and AML blasts. The impact of these different metabolic pathways on therapeutic response to agents used to treat AML is not well understood. We hypothesized that the AML metabolic state could impact response to chemotherapy. We have shown that various AML cell lines of the same French American British (FAB) subtype have different metabolic states by using the Seahorse bioanalyzer. The basal metabolism of these cells can be shifted to reliance on oxidative phosphorylation (OXPHOS) by culturing cells in medium with galactose rather than glucose; cells can also be shifted to rely on glycolysis by treating cells with the complex I inhibitor, IACS-010759. Utilizing these approaches to shift metabolic state, the chemotherapeutic response based on cellular metabolism has been assessed. The current standard-of-care in AML includes a “7+3” regimen treatment with cytarabine (AraC) and an anthracycline as the backbone agents. We screened 4 M5 FAB subtype AML cell lines with various chemotherapeutic agents under “normal” glucose media culture conditions, or galactose media culture conditions. As previously reported, resistance to AraC was increased under OXPHOS conditions.<sup>1</sup> In contrast, the anthracycline Idarubicin showed no difference in response under conditions favoring neither glycolysis nor OXPHOS. In 2004, the purine nucleoside analog antimetabolite—clofarabine—was approved for use in leukemia patients with relapsed or refractory disease. While this drug is not currently the standard of care for AML treatment, clofarabine is regularly used in AML treatment regimens. Clofarabine was tested and response was different under either glycolytic or OXPHOS conditions. In the more glycolytic U937 AML cell line, we have shown that shifting the cells to rely on OXPHOS leads to increased clofarabine resistance. However, the key determinants of this change in clofarabine sensitivity (e.g., dCK, RRM1) were unchanged by the altered metabolic state of the cells. This indicates a previously unidentified mechanism of clofarabine toxicity is operative under different metabolic conditions. An unbiased approach to determine which metabolic pathways affect drug sensitivity can be conducted by a metabolic-focused CRISPR screen. The metabolic CRISPR screen includes a library containing 29,790 gRNAs which target 2,981 metabolic genes. By conducting a “drop-out” CRISPR screen, genes important to clofarabine response can be identified. Based on the results from the CRISPR screen our studies should reveal previously unidentified clofarabine mechanism of action that can be exploited to improve AML treatment with clofarabine.

## References

1 Farge T, et al. Chemotherapy-Resistant Human Acute Myeloid Leukemia Cells Are Not Enriched for Leukemic Stem Cells but Require Oxidative Metabolism. *Cancer Discov.* 2017

Funding for this project was supported by the National Institute of Health (NIH) and American Lebanese Syrian Associated Charities

# Direct Targeting of Menin-MLL1 Interaction Inhibits Cancer Stem Cells to Inhibit Neuroblastoma Growth

Rameswari Chilamakuri,<sup>1</sup> and Saurabh Agarwal<sup>2</sup>

<sup>1</sup>St Johns Univ; and <sup>2</sup>ST.JOHNS UNIVERSITY

Abstract ID 20505

Poster Board 41

Epigenetic regulators such as MLL1 play an important role in cancer progression, metastasis, and relapse. MLL1 forms a COMPASS complex with Menin and other binding partners to function as an epigenetic enzyme, an H3K4 methyltransferase. Inhibition of Menin-MLL1 interaction is known to inhibit the epigenetic enzyme functions in different cancers. We hypothesized that Menin-MLL1 inhibition will inhibit neuroblastoma cancer stem cells (NB CSCs; CD114+ cells) to inhibit overall neuroblastoma (NB) growth. NB is an extracranial solid pediatric cancer that accounts for 10-15% of all pediatric cancer-related deaths, with the long-term survival of relapsed NB patients being less than 10%. In the present study, we used a specific small molecule inhibitor, MI-503, to disrupt the Menin-MLL1 interaction in both *in vitro* and *in vivo* tumor models. *In vitro* cell proliferation studies were performed using MYCN amplified (NGP, LAN-5, IMR-32), and MYCN non-amplified (SH-SY5Y, SK-N-AS, CHLA-255) NB cell lines, patient-derived xenograft (PDX) cell lines (COG-N-415, COG-N-269, COG-N-357), and control fibroblast cell lines. We observed a dose-dependent inhibition of NB cell proliferation in both 2D cell proliferation studies and 3D spheroid tumor models, in contrast to non-cancerous fibroblasts and control treatments. Further, we observed that MI-503 significantly induces apoptosis and blocks cell cycle progression at the S phase in a dose-dependent manner in different NB cell lines tested. We further observed that MI-503 inhibits the expression of multiple oncogenic cell signaling pathways, cancer stemness-related genes such as OCT4, and Nanog, and inhibits different MLL1 fusion partner genes such as HOXA, AF9, and MEIS1. Additionally, and as expected, MI-503 significantly inhibits H3K4me3 levels, as determined by the histone immunoblot assays. Further, we determined the efficacy of MI-503 in inhibiting the NB CSCs (CD114+ cells) in NB. In our previous efforts, we have defined the CD114+ cells in NB tumors and found that these cells may drive the refractory NB relapse. Interestingly, we found that MI-503 significantly and in a dose-dependent manner inhibits the NB CSC population in comparison to control treatments in NB cells and in NB mouse models by specifically inducing apoptosis in NB CSCs, in contrast to non-CSCs (CD114- cells). Further, we determined the efficacy of MI-503 in NB mouse models and found that MI-503 significantly inhibits overall NB tumor growth and tumor burden by directly inhibiting tumor NB CSCs. Overall, our data highlights the role of the epigenetic mechanisms regulating the NB CSCs and NB growth. Our study also highlights the inhibition of Menin-MLL1 interaction by MI-503 as a novel therapeutic approach for NB. In our future efforts, we will combine epigenetic therapeutic approaches with current chemotherapies to concomitantly target both NB CSCs and bulk tumor cells to develop effective and clinically tractable therapies for NB.

# MCL1 Small Molecule Inhibitor S63845 Synergizes with Cisplatin in Basal-like Triple Negative Breast Cancer

Alexus Acton,<sup>1</sup> and William Placzek<sup>2</sup>

<sup>1</sup>Univ of Alabama at Birmingham; and <sup>2</sup>The Univ of Alabama at Birmingham

**Abstract ID 15322**

**Poster Board 42**

Triple negative breast cancer (TNBC) is an aggressive cancer that lacks specific molecular targeted therapies. Thus, current standard of care requires the use of neoadjuvant therapy with taxol, cytoxan, and platinum-based agents. There is a strong therapeutic resistance to platinum-based therapy, thus combination of multiple treatments has confirmed promising anti-tumorous effects for TNBC. The ability to avoid cell death can be attributed increased expression of the anti-apoptotic protein, myeloid cell leukemia 1 (MCL1). Multiple studies have demonstrated that MCL1 enables resistance to chemotherapy and directly correlates with increased tumor size and invasion. We recently demonstrated that MCL1 binds to the DNA damage response protein, p73, and suppresses its transcriptional activity. As p73 upregulation is a key mechanism for cisplatin induced DNA damage response and ultimately cell death, we sought to determine if coadministration of a MCL1 targeted inhibitor with cisplatin would produce a synergistic response in TNBC. This study demonstrates that the MCL1 inhibitor, S63845, combined with cisplatin synergizes in basal-like TNBC cell lines. Additionally, basal-like lines treated with this combination showed a significant increase in TAp73 mRNA expression as well as downstream targets where this observation was absent in mesenchymal TNBC. This observation provides a molecular profile for use of combined MCL1 inhibitors with cisplatin in basal-like TNBC as inhibition of MCL1 effectively initiates TAp73 anti-tumorous effect on cell cycle arrest and apoptosis.

Support/Funding Information: R01GM117391



# The Paracrine Action of Mutant P53 In Breast Cancer

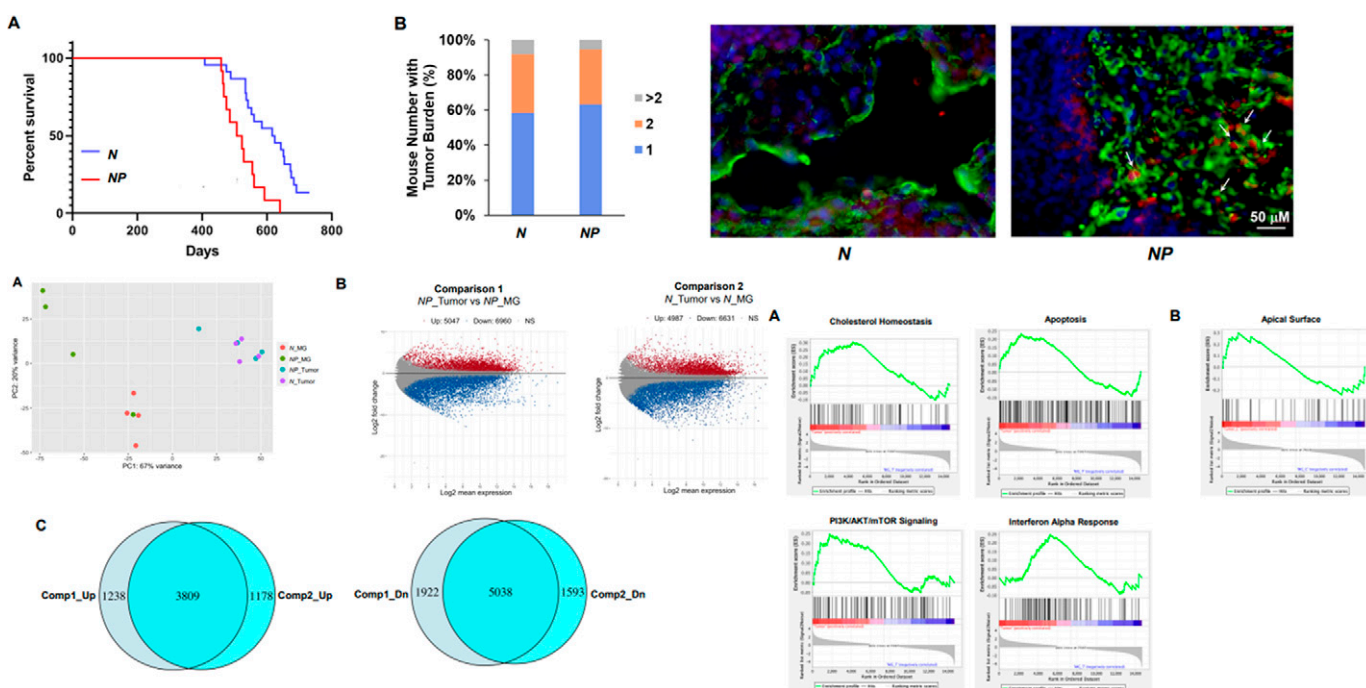
Abie Williams-Villalobo,<sup>1</sup> Yun Zhang,<sup>1</sup> B Liu,<sup>2</sup> S Xiong,<sup>2</sup> G Chau,<sup>2</sup> and G Lozano<sup>2</sup>

<sup>1</sup>Texas Southern Univ; and <sup>2</sup>MDAnderson

Abstract ID 56215

Poster Board 43

Tumor suppressor *p53* mutations have been identified in breast cancer-associated fibroblasts, correlating with a poor prognosis in patients. However, the effects of fibroblastic mutant *p53* on breast cancer remain unclear. We aim to investigate whether and how *p53*R17H mutant in stromal fibroblasts impacts breast cancer. We hypothesize that fibroblastic *p53*R172H accelerates mouse mammary tumor development via paracrine signaling(s) that alter biological pathways in the tumor. A cohort of *MMTV-neu; Fsp-Cre; p53<sup>wm-R172H/+</sup>* (*NP*) female mice was established, which develops human-epidermal-growth-factor-receptor 2 positive mammary carcinomas and contains *p53*R172H specifically in the fibroblasts. A cohort of *MMTV-neu; Fsp-Cre* (*N*) females was also established, where *p53* remains intact in the stromal fibroblasts of HER2 tumors. The *NP* female mice exhibited a significantly shorter median tumor free survival than that of the *N* females. RNA-sequencing of *NP* and *N* tumors and mammary glands revealed large number of differentially expressed genes (DEGs) between tumor and mammary glands for each genotype. The DEGs that are solely present in the *NP* tumors versus *N* tumors were subjected to the Gene Sets Enrichment Analysis. Multiple signaling pathways, including the cholesterol homeostasis, apoptosis, PI3/AKT/mTOR and interferon alpha response, were found enriched in the *NP* tumors. Our results show that fibroblastic mutant *p53* promotes mammary tumor development, potentially through a paracrine mechanism that alters gene expression profiles in the tumor.



# The Synergistic Antitumor Effect of Irinotecan and Flavonoids on Human Colon Cancer Xenograft Mice

Jyotsna Devi Godavarthi,<sup>1</sup> Abie Williams-Villalobo,<sup>2</sup> Imoh Etim,<sup>1</sup> Du Ting,<sup>1</sup> Song Gao,<sup>1</sup> and Yun Zhang<sup>2</sup>

<sup>1</sup>Texas Southern University; and <sup>2</sup>Texas Southern Univ

Abstract ID 53806

Poster Board 44

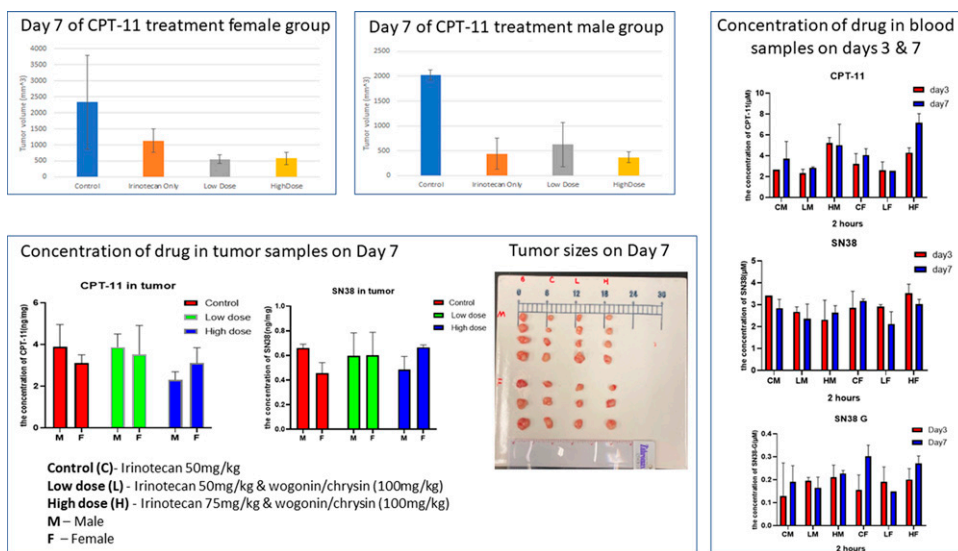
Camptothecin (CPT)-11 (irinotecan), a DNA topoisomerase I inhibitor, is one of the first-line therapeutic agents in the treatment of metastatic colorectal cancer, but its efficacy and safety can be compromised because of its severe side effects, such as gastrointestinal injury/inflammation and severe diarrhea. Previous studies reported that natural flavonoids such as wogonin and chrysin have anticancer and anti-diarrheal activities. The purpose of this study is to investigate the efficacy and safety of irinotecan when co-administered with flavonoids in the human colon cancer xenograft model.

The human colorectal adenocarcinoma cell line HT-29 was cultured, and  $2 \times 10^6$  cells/mouse were administered subcutaneously to 6 weeks old nude mice. When the tumor volume was around 500-600 mm<sup>3</sup>, the flavonoids (wogonin and chrysin mix) were administered by oral gavage at 100 mg per kg of mouse body weight (100mg/kg) per day for three days and then co-administered with CPT-11. CPT-11 was administered intraperitoneally at two different doses i.e., 50 mg/kg and 75mg/kg per day for seven consecutive days as a bolus injection. Mice that received CPT-11 monotherapy served as control.

Our study demonstrated that the combination therapy of CPT-11 co-administered with flavonoids had no major impact on mouse body weights. Furthermore, the combination therapy resulted in lower tumor volume when compared with single-agent treatment. Tumor volume decreased by 36 % with the treatment of 50 mg/kg CPT-11 plus 100mg/kg/day wogonin/chrysin and 57 % with 75 mg/kg/day CPT-11 plus 100mg/kg/day wogonin/chrysin compared to conventional irinotecan treated animals. Interestingly, female mice that received the combination therapy, either with a low dose or high dose of CPT-11, showed a 2-fold decrease in tumor volume when compared to CPT-11 only treated group. This confirms the previous reports that females mount a more robust cellular and humoral response, resulting in greater anti-tumor efficacy. Furthermore, monotherapy and combination therapy led to the same CPT-11 disposition in blood or tumor tissues, as demonstrated by the Liquid Chromatography-Tandem Mass Spectrometry (LC-MS/MS) analysis.

Taken together, our data show that CPT-11 and flavonoids (wogonin and chrysin) exhibit a synergistic anti-tumor effect and can be safely administered together for metastatic colon cancer treatment. Therefore, this combination therapy could be a promising approach in anti-tumor chemotherapy for better clinical outcomes.

Support/Funding Information: NIGMS grant award 1SC2GM135111-01, NIMHD grant award U54MD007605, CPRIT grant RP180748 and RCMI – CBMHR.



---

# Epigenetic Regulation of Medulloblastoma Proliferation by Finasteride-Induced Modulation of BTG2 and CD244 Gene Methylation

Anika Patel,<sup>1</sup> Churchill Ihentuge,<sup>1</sup> and Antonei B. Csoka<sup>2</sup>

<sup>1</sup>Texas Tech University Health Sciences Center, El Paso; and <sup>2</sup>Howard University, Washington D.C

**Abstract ID 52461**

**Poster Board 45**

Medulloblastoma is a common childhood malignant brain tumor occurring mostly in the cerebellum. B-cell translocation gene (BTG2) is a p53 transcriptional target gene that functions as a coactivator-corepressor and/or an adaptor molecule that modulates the activities of its interacting proteins. BTG2 is an inhibitor of proliferation and differentiation of medulloblastoma cells, while CD244 is an upregulator of natural killer cells in medulloblastoma. In prior work aimed at determining the epigenetic effects of finasteride, a 5-alpha reductase inhibitor, on Leydig cells, we noted the effect of finasteride on the methylation of the BTG2 and CD244 genes. Results demonstrated that finasteride upregulated BTG2 and CD244 gene expression through differential methylation. We therefore suggest that the increased expression of the BTG2 and CD244 genes by finasteride should be investigated further as a potential treatment for medulloblastoma.

# Targeting mitochondrial protein NIX mediates resistance to sorafenib in hepatocellular carcinoma through autophagy

QiongRong Zeng,<sup>1</sup> ZeFeng Liu,<sup>2</sup> XianWen Guo,<sup>3</sup> WenJuan Wang,<sup>4</sup> XueLian Huang,<sup>2</sup> FuJian LI,<sup>5</sup> and Guo Zhang<sup>2</sup>

<sup>1</sup>The People's Hospital of Guangxi Zhuang Autonomous Region, Nanning, Guangxi, P. R. China. YouJiang Medical University for Nationalities, Baise, Guangxi, P. R. China; <sup>2</sup>The People's Hospital of Guangxi Zhuang Autonomous Region, Nanning, Guangxi, P. R. China; <sup>3</sup>The People's Hospital of Guangxi Zhuang Autonomous Region, Nanning, Guangxi, P. R. China; <sup>4</sup>The People's Hospital of Guangxi Zhuang Autonomous Region, Nanning, Guangxi; and <sup>5</sup>the People's Hospital of Guangxi Zhuang Autonomous Region

Abstract ID 14447

Poster Board 46

**Aims:** Although sorafenib benefits patients with advanced hepatocellular carcinoma (HCC), its clinical efficacy is restricted by drug resistance. The pathogenesis of multisystem tumors is closely related to mitochondrial function, and anticancer drug research has also made significant progress in autophagy, but the regulatory role of mitochondria in the etiology and pharmacology of liver cancer remains unclear. To this end, we focused on the mitochondrial protein Nix (aka BNIP3L, BCL2/adenovirus E1B interacting protein 3-like), hypothesizing that induction of Nix-activated autophagy might represent a mechanism of sorafenib resistance.

**Methods:** We constructed two sorafenib-resistant HCC cell models (HepG2-SR, Huh7-SR) using the concentration-ascending method. Short hairpin RNA was used to knock down the expression of Nix in drug-resistant strains, and the consequences of autophagy signals and drug-resistant cells were observed. The correlation between Nix, autophagy and sorafenib resistance was mainly verified by western blot, IHC, qRT-PCR, CCK8 assay, and flow cytometry.

**Results:** Nix is overexpressed in liver cancer tissues and HCC lines resistant to sorafenib. In addition, the expression level of Nix was dose-dependent and positively correlated with Sorafenib resistance. Inhibiting the expression of Nix in drug-resistant strains can enhance its sensitivity to sorafenib. Furthermore, we showed that autophagy was activated in association with Nix-associated sorafenib resistance and was stopped by Nix knockdown and autophagy inhibitor.

**Conclusion:** Mitochondrial protein Nix regulated sorafenib resistance through autophagy in HCC, proving that autophagy is a cytoprotective mechanism mediating tumor drug resistance. The connection between Nix, autophagy and sorafenib resistance is first described in this study. These findings are significant as they suggest that the combination of targeting NIX therapy and autophagy provides new insights and strategies for the treatment of HCC.

This study was supported by the National Natural Science Foundation of China (NO.81860654); the Guangxi Portal Hypertension Key Laboratory Construction Project (NO. ZZH2020006); Guangxi Digestive Disease Clinical Medical Research Center Construction Project (AD17129027).

# Evaluating the Anticancer Activity of Novel Norethindrone Analogs in Glioblastoma Cells

Katelyn A. Harris,<sup>1</sup> Courtney A. Hollenbacher,<sup>1</sup> Eric T. Doyle,<sup>1</sup> Samantha T. Szoradi,<sup>1</sup>  
Nicholas A. Reid,<sup>1</sup> Laura R. Inbody,<sup>1</sup> Richard W. Dudley,<sup>1</sup> and Ryan A. Schneider<sup>1</sup>

<sup>1</sup>University of Findlay, College of Pharmacy

**Abstract ID 56141**

**Poster Board 47**

Glioblastomas are the most aggressive and fatal type of Central Nervous System cancers. Due to limited treatment options available to slow disease progression and prolong survival, glioblastoma is often associated with a poor prognosis. Given the poor prognosis and lack of effective therapies, there is a need for drug discovery efforts for glioblastoma. Previous studies have shown that outcomes are worse in glioblastoma patients with high androgen receptor activity and that silencing of the androgen receptor led to cell death in glioblastoma cell lines. As such, we investigated the use of the androgen receptor as a potential therapeutic target. We synthesized a small library of norethindrone (NE) analogs intended to inhibit androgen receptors. Previously, we reported that analogs in this library demonstrated anticancer activity in the PC3 prostate cancer cell line. We further tested these analogs in three glioblastoma cell lines to examine their anticancer activity.

To address the need for novel agents to treat glioblastoma, we synthesized a small library of analogs with different aryl and alkyl substituents at the 17-position of NE using click chemistry in a one-pot microwave-assisted reaction. This reaction took place in an Anton Parr Monowave-50 reactor that was set at 150°C and was then run for 20 minutes.

We examined the anticancer activity of analogs B and C from our library of compounds in three glioblastoma cell lines (U87, T98G, and A-172) using the XTT viability assay. Analog B demonstrated biological activity in all three glioblastoma cell lines with IC<sub>50</sub> values ranging from 85 μM to greater than 200 μM. Similar to previous results in PC3 cells, analog C demonstrated greater activity with IC<sub>50</sub> values ranging from 15 μM to 35 μM. Additional studies are ongoing to determine the mechanism(s) of anticancer activity and to further explore the structure activity relationships to determine if further chemical modifications at the 17-position of NE may enhance the observed anticancer effects.

# Lipin-1 Silencing Alters the Phospholipid Profiles of Castration-Resistant Prostate Cancer Cells

Morgan C. Finnerty,<sup>1</sup> and Brian Cummings<sup>2</sup>

<sup>1</sup>University of Georgia; and <sup>2</sup>Wayne State University

Abstract ID 23137

Poster Board 48

**PURPOSE:** The association between clinical outcomes of prostate cancer (PCa) progression and lipid remodeling is not well understood. Although it is known that increases in select circulating lipids correlate to decreased patient survival, the mechanisms mediating alterations in these lipids are not fully explained. We recently reported a correlation between the levels of phosphatidic acid (PA) and diacylglycerol (DAG) in cells representing castration-resistant prostate cancer (CRPC). We further showed correlations between PA and DAG levels with a decreased expression of a phosphatidic acid phosphatase, specifically lipin-1[MCF1]. However, the ability of lipin-1 to mediate the PCa lipidomic profile remains unknown.

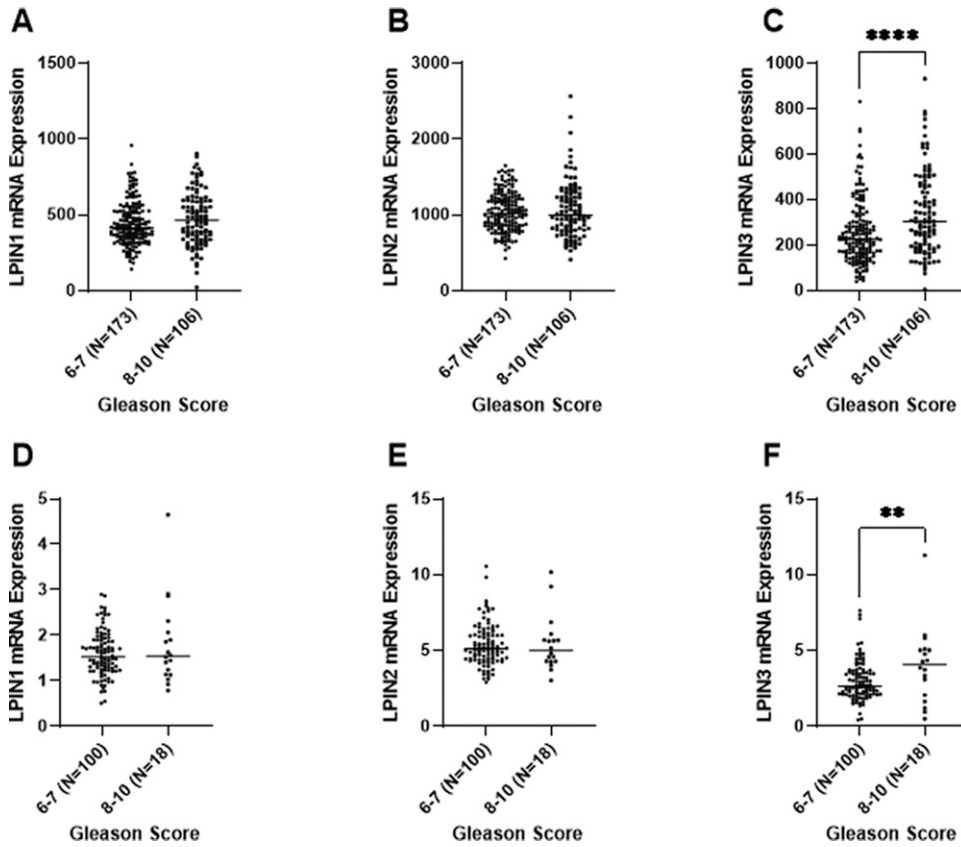
**HYPOTHESIS:** We hypothesized that the expression of lipin-1 mediates PA and DAG levels in CRPC cells and controls the overall lipidomic profile. We further hypothesized that the lipidomic profile of the *LPIN1* knockdown CRPC cells will correlate to RNA alterations.

**METHODS:** *LPIN1* silencing was established using shRNA lentiviral particles and validated with immunoblot analysis. The effect of *LPIN1* silencing on lipin-2 and lipin-3 expression was also analyzed. The cBioPortal for Cancer Genomics online database (<https://www.cbioportal.org/>) was used to analyze the expression of *LPIN1*, *LPIN2* and *LPIN3* in human prostate carcinoma patients. Gleason Scores were used to stratify patients into two cohorts (6-7 and 8-10), and changes in *LPIN1*, *LPIN2* and *LPIN3* mRNA expression were compared. Lipids were isolated using the Bligh-Dyer extraction method from control shRNA and *LPIN1* knockdown PC-3 cell lines. Lipids were analyzed using a targeted-based quantitative HPLC-ESI-Orbitrap-MS approach. RNA alterations between control shRNA and *LPIN1* knockdown PC-3 cells was analyzed by Illumina NextSeq sequencing.

**RESULTS:** Our data showed effective *LPIN1* knockdown in PC-3 cells, and the silencing of *LPIN1* increased the expression of lipin-2, but not lipin-3. Analysis of mRNA expression of *LPIN1*, *LPIN2* and *LPIN3* in PCa patients from two different clinical populations indicated that patients with higher Gleason scores (8-10) had significantly increased *LPIN3* mRNA expression than patients with lower Gleason scores (6-7). There was no correlation between Gleason Score and *LPIN1* and *LPIN2* mRNA expression.

**CONCLUSIONS:** These data suggest that *LPIN1* mediates the overall lipidomic profile of CRPC cells and *LPIN1* silencing is compensated in these cells by increased lipin-2 expression. Higher *LPIN3* expression in patients with a higher Gleason score suggest that *LPIN3* may be used as a potential prognostic biomarker for advanced PCa.

**Support/Funding Information:** Department of Defense Prostate Cancer Research Program Idea Development Award (PC150431 GRANT11996600)



Genomic data analysis shows increased *LPIN3* mRNA expression in High-Gleason score PCa tissues. (A-C) Data from the TCGA study (Taylor *et al*, Cell, 2015) showing a comparison between *LPIN1*, *LPIN2* and *LPIN3* mRNA expression in low (6–7) versus high (8–10) Gleason score (n = 279). (D-F) Data from the DKFZ study (Gerhauser *et al*, Cancer Cell, 2018) showing a comparison between *LPIN1*, *LPIN2* and *LPIN3* mRNA expression in low (6–7) versus high (8–10) Gleason score (n = 118).

# Targeting the Cell Cycle Checkpoints CHK1 and CHK2 is a Novel Therapeutic Approach for Pediatric Neuroblastoma

Ben Morrison,<sup>1</sup> Rameswari Chilamakuri,<sup>2</sup> and Saurabh Agarwal<sup>3</sup>

<sup>1</sup>Saint Johns University; <sup>2</sup>St Johns Univ; and <sup>3</sup>St. John

Abstract ID 23073

Poster Board 49

Neuroblastoma (NB) is the most common extracranial solid pediatric tumor, and the current treatments are highly toxic and lack effectiveness. In particular, high-risk NB has an extremely low survival rate and presents a major clinical challenge due to the frequent relapse of both metastatic and refractory tumors. The issues with current NB treatments warrant the development of novel therapeutic strategies that are less toxic while being more effective. We have analyzed NB patient datasets and found increased CHEK1 and CHEK2 expression (gene coding for CHK1 and CHK2) which are inversely correlated with overall patient survival. Checkpoint Kinases 1 and 2 (CHK1/CHK2) are essential cell cycle regulators that play vital roles in the progression of cell proliferation and growth. Previous studies indicate that dysregulation of CHK1 and CHK2 promotes tumor growth as well as the progression of multiple cancers including NB. In the present study, we have used a specific small molecule inhibitor of CHK1/2, AZD7762 in NB. In vitro methodologies were used to determine the efficacy of AZD7762 in multiple MYCN amplified (LAN-5, NGP, IMR-32) and MYCN non-amplified (SK-N-AS, SH-SY5Y, CHLA-255) NB cell lines. MTT assays for determining cell proliferation showed significant inhibition of NB cell proliferation in a dose-dependent manner in response to AZD7762 with IC50s of 1-2  $\mu$ M for non-amplified cell lines and 2-3  $\mu$ M for amplified cell lines. Clonogenic assays further confirmed the effects of AZD7762 by inhibiting the colony formation capacity (60-85%) of different NB cell lines. Furthermore, AZD7762 significantly induces apoptosis in SH-SY5Y and NGP cell lines in a dose-dependent manner. Inhibition of CHK1/2 by AZD7762 significantly blocked cell cycle progression at the G2/M phase compared to the control treatment in NGP and SH-SY5Y NB cell lines. Additionally, AZD7762 treatments inhibit CHEK1 and CHEK2 gene expression and phosphorylation of CHK1 in contrast to control treatment, as detected by qPCR and immunoblotting respectively. Further, we developed a 3D spheroidal assay model that mimics in vivo tumor growth patterns of NB tumors. AZD7762 treatment significantly and in a dose-dependent manner inhibits overall 3D spheroid growth and proliferation by inhibiting the live cells in the 3D spheroids. Overall, our results show that AZD7762 significantly inhibits NB proliferation and colony formation, induces apoptosis, blocks cell cycle progression, and inhibits 3D spheroid growth. These findings support that the dysregulation of CHK1/2 is vital to NB initiation and growth. Therefore, our study highlights that the inhibition of CHK1 and CHK2 using AZD7762 is an effective novel therapeutic strategy for NB treatment. In our future efforts, we will analyze the effects of AZD7762 in NB mice models and combine these strategies with current chemotherapies to develop effective targeted therapeutic approaches for NB.



# Impact of Microglial RGS10 Regulation of Inflammatory Mediators in the Glioblastoma Tumor Microenvironment

Phillip Dean,<sup>1</sup> and Shelley Hooks<sup>1</sup>

<sup>1</sup>*Univ of Georgia*

**Abstract ID 19689**

**Poster Board 50**

Glioblastoma multiforme (GBM) is the most common and aggressive form of glioma, accounting for approximately 50% of all malignant brain tumors. The GBM tumor microenvironment (TME), a dynamic ecosystem of multiple cell types and signaling mediators, plays a crucial role in development and progression of the disease. Microglia are abundant in the GBM TME, and their activation induces production of inflammatory mediators that favor tumor progression. Regulator of G protein Signaling 10 (RGS10) is highly enriched in microglia where it suppresses the expression of multiple proinflammatory genes, including the significant inflammatory enzyme cyclooxygenase 2 (COX-2) and its subsequent product, the bioactive lipid prostaglandin E2 (PGE2). COX-2/PGE2 is often upregulated in the GBM microenvironment and is associated with therapeutic resistance, immunosuppression, and poor prognosis. The anti-inflammatory role of RGS10 makes it a prime candidate for a potential therapeutic target in the GBM tumor microenvironment. Our previous work has demonstrated that RGS10 strongly suppresses lipopolysaccharide (LPS)-induced COX-2/PGE2 in microglia (this suppression is independent of its canonical G protein-targeted mechanism). Here, we sought to demonstrate the effect of microglial RGS10 inflammatory mediator regulation on the GBM tumor microenvironment. Microglia themselves being a member of the GBM microenvironment, we demonstrate that secretory mediators regulated by RGS10 suppress COX-2 in an autocrine/paracrine manner. We further demonstrate RGS10 regulated secretory mediators significantly increase COX-2 in GBM cells. We show evidence that microglial RGS10 regulation suppresses GBM cell migration in coculture and attenuates chemotherapeutic resistance in GBM cells. Collectively, these results exhibit the ability of microglial RGS10 to suppress COX-2 in the GBM tumor microenvironment and have a significant effect on multiple facets of GBM tumor progression demonstrating that RGS10 could be a viable therapeutic target in GBM.

# Characterization of a Mouse Model of Neuropathic Pain Induced by Calcaneus Implantation of NCTC 2472 Mouse Sarcoma Cells

Yuma Ortiz,<sup>1</sup> Sushobhan Mukhopadhyay,<sup>1</sup> Christopher R. McCurdy,<sup>1</sup> Lance R. McMahon,<sup>2</sup> and Jenny L. Wilkerson<sup>2</sup>

<sup>1</sup>University of Florida, College of Pharmacy; and <sup>2</sup>Texas Tech. Univ. Hlth. Sci. Ctr., Hodge Sch. of Pharmacy

Abstract ID 24304

Poster Board 233

## **Objective**

Cancer metastasis to bone is a major contributor to neuropathic pain onset in patients and affects up to 66% of those in late-stage cancer. Many preclinical cancer pain models utilize patient derived cancer cell lines and to avoid a host immune response, are implanted into immunocompromised rodents. This approach discounts the importance of a healthy and intact immune response in cancer and cancer pain therapeutic drug development. To address this, we expanded upon previous literature (Wacnik et al., 2001) and developed a host-derived cancer pain mouse model produced by implantation of murine fibrosarcoma cells into the calcaneus bone.

## **Methods**

NCTC 2472 murine fibrosarcoma cells were grown to 80% confluency, and a density of  $2 \times 10^5$  cells/10  $\mu$ L was injected into the right calcaneus bone of adult male and female C3H/HeJ mice. Injection of PBS into other mice served as a sham control. The von Frey assay was utilized to assess tumor-induced mechanical allodynia. Expulsion of acetone on the paw and recording the time spent responding was used to measure cold allodynia. Thermal hotplate latencies were used to assess thermal hyperalgesia.

## **Results**

Sarcoma implanted mice exhibited mechanical allodynia as early as 3 days post-implantation and lasted until day 13 post-implantation. Between males and females, the severity of allodynia was not different, despite a differential tumor volume increase. Despite the presence of mechanical allodynia, in both male and female mice there was no measurable onset of thermal hyperalgesia nor cold allodynia among sarcoma implanted subjects. Sham subjects did not exhibit mechanical allodynia, thermal hyperalgesia, or cold allodynia. Because tumor volume and von Frey responses were consistent from day 3 to day 8 post-implantation, these days were chosen to test analgesics. The prototypical opioid agonist morphine (1.78, 3.2, 5.6, 10 mg/kg, i.p.) dose-relatedly reversed tumor-induced mechanical allodynia. The ED<sub>50</sub> of morphine to reverse cancer pain was 3.302 (2.979 – 3.661) mg/kg. Mitragynine, the most prevalent alkaloid found in the natural product kratom, (17.8, 32, 56, 100 mg/kg, i.p.) also dose-relatedly reversed tumor-induced mechanical allodynia. The ED<sub>50</sub> of mitragynine to reverse cancer pain was 47.589 (42.833 – 52.872) mg/kg.

## **Conclusions**

Sarcoma implantation resulted in mechanical allodynia, which was dose relatedly reversed by the prototypical opioid agonist morphine as well as the kratom alkaloid mitragynine. The use of a host-derived cancer pain mouse model produced by implantation of murine fibrosarcoma cells into the calcaneus bone allows for novel pain therapeutic assessment in immune-intact animals. This approach will aid in identification of promising analgesic therapeutic options for patients experiencing cancer-induced peripheral neuropathy.

This work was supported by the National Institute on Drug Abuse DA25267 and DA48353

# Troglitazone Induced Apoptosis in a Human Colon Cancer Cell Line

Solomon A. Ocran,<sup>1</sup> David Strom,<sup>2</sup> Mackenzie M. Budd,<sup>1</sup> Zachary L. Lutz,<sup>1</sup> Nicole J. Kang,<sup>1</sup> and Nolan A. Wengert<sup>1</sup>

<sup>1</sup>Marian University; and <sup>2</sup>Marian Univ

**Abstract ID 21111**

**Poster Board 234**

Troglitazone is a member of the thiazolidinedione family which acts primarily through upregulating the peroxisome proliferator-activated receptor (PPAR) pathway. The PPARs are members of the steroid/thyroid nuclear receptor superfamily and is important in coordinating energy systems, including glucose and lipid metabolism. Binding of PPAR $\gamma$  agonists such as troglitazone and other thiazolidinediones results in increased insulin sensitivity and lower glucose levels in patients with type 2 diabetes. Treatment with troglitazone was withdrawn from its usage in type II diabetics due to hepatotoxicity. Studies have linked PPAR receptors to the development of cancer. However, the research is contradictory as to whether these pathways cause tumor genesis or assist with inhibiting cell proliferation. We have examined the effect of troglitazone on HCT116 human colon carcinoma cells. Troglitazone induced cell death was observed at 24hr by concentrations of 50uM or greater. Cell death was confirmed to be apoptosis. Using a Qiagen RT<sup>2</sup> Profiler<sup>TM</sup> PCR Array Human PPAR Targets platform, we identified numerous PPAR targets that have altered expression in HCT116 cells. We have confirmed the expression changes using RT PCR from HCT116 cells treated with troglitazone. Antagonism of PPARalpha and PPARgamma in the presence of troglitazone will be used to determine if apoptosis is being mediated through PPAR activation.

# Structural and Mechanistic Basis for Gbetagamma-mediated Activation of Phosphoinositide 3-kinase-gamma

Chun-Liang Chen,<sup>1</sup> Sandeep Ravala,<sup>1</sup> Yu-Chen Yen,<sup>2</sup> Thomas Klose,<sup>1</sup> Ramizah Syahirah,<sup>1</sup> John JG. Tesmer,<sup>2</sup> and Qing Deng<sup>1</sup>

<sup>1</sup>Purdue University; and <sup>2</sup>Purdue Univ

**Abstract ID 24273**

**Poster Board 235**

Phosphoinositide 3-kinase gamma (PI3K-gamma) converts PIP<sub>2</sub> to PIP<sub>3</sub> in a key step of chemotaxis. However, it is also highly expressed in some cancers where it contributes to metastasis, particularly in prostate, breast, and pancreatic cancer. Activation of PI3K-gamma is coordinately regulated by Gbetagamma subunits and Ras, which are activated downstream of G protein-coupled receptors (GPCRs) and receptor tyrosine kinases (RTKs), respectively. However, molecular mechanisms underlying the Gbetagamma- and Ras-mediated activation of PI3K-gamma remain unclear. In this study, we determined the cryo-EM structure of native PI3K-gamma to 3.0Å resolution and demonstrated its Gbetagamma-dependent activation. We went on to obtain various cryo-EM reconstructions of the PI3K-gamma-Gbetagamma complexes, revealing distinct Gbetagamma binding sites on the p110-gamma and the p101 subunits. Conformational changes have been observed upon Gbetagamma binding to PI3K-gamma, and key residues that were identified can be associated to allosteric activation. These findings allow for functional investigation of Gbetagamma-mediated activation mechanisms and will aid in future drug development targeting PI3K-gamma for selective cancer therapeutics. based on its unique responsiveness to Gbetagamma among PI3K isozymes.

This work was supported by American Heart Association Grant #834497/Chun-Liang Chen/2021, Purdue Center for Cancer Research (PCCR) Pilot Grant 2020-21 Cycle 2, and Shared Resource 2020-2021 Cycle 1 (Grant # 30001612).

# In Silico Analysis of DNA Methylation Status of T-Cell Inflamed Signature Reveals a Therapeutic Strategy to Improve Immune Checkpoint Inhibitors Efficacy in Wilms Tumor

Sarah A. Albasha,<sup>1</sup> Manar Z. Almotawa,<sup>2</sup> Abdulmonem A. Alsaleh,<sup>1</sup> Noura N. Alibrahim,<sup>1</sup> Zaheda H. Radwan,<sup>1</sup> Yousef N. Alhashem,<sup>1</sup> Jenan Almatouq,<sup>1</sup> and Mariam K. Alamoudi<sup>3</sup>

<sup>1</sup>Department of Medical Laboratory, Mohammed Al-Mana College for Medical Sciences; <sup>2</sup>Department of Respiratory Therapy, Mohammed Al-Mana College for Medical Sciences; and <sup>3</sup>Department of Pharmacology, College of Pharmacy, Prince Sattam bin Abdulaziz University

Abstract ID 53447

Poster Board 236

Wilms tumor, commonly known as nephroblastoma, is the most common kidney tumor in children. Despite advances in Wilms tumor care, one out of every four patients acquires negative outcomes such as metastatic or recurrent disease and has a low survival rate. Immune checkpoint inhibitors (ICIs) have shown encouraging results in adult solid tumors, opening the door for their use in pediatric solid tumors. Unfortunately, the efficacy of ICIs in pediatric solid tumors is suboptimal. The failure of ICIs in pediatric solid tumors is attributed to the fact that tumors are less immunogenic. Studies in adult tumors have demonstrated that presence of a hot immunogenic tumor, including the expression of a T-cell inflamed signature which is a group of genes indicative of T-cell and dendritic cell infiltrates within the tumor microenvironment (TME), was positively correlated with ICI response. In cold non-immunogenic tumors, aberrant epigenetic modifications have been reported which can lead to ICI failure. In our study, we aim to profile the DNA methylation status of T-cell inflamed signature genes in Wilms tumor. A 450K array data containing DNA methylation of Wilms tumors was selected and analyzed using RStudio. The TSS200 and TSS1500 annotated CpG sites that were located at gene promoter region of the T-cell inflamed genes were investigated. Differentially methylated sites were identified (defined as CpG sites with a methylation difference (delta beta) of  $\geq 5\%$ ). 36 controls and 37 cases were used for the analysis. Comparing the methylation status of T-cell inflamed signature genes between controls and cases, we found that 12 of the 37 genes, including *CCL2*, *CCL5*, *CD4*, *GZMB*, *GZMK*, *HLA-DMA*, *HLA-DOA*, *HLA-DOB*, *HLA-DQA1*, *HLA-DRB1*, *IFNG*, and *TIGIT*, were hypermethylated in Wilms tumors with methylation differences ranging from 5% to 43%, and 7 of them had at least two differentially methylated sites at promoter region. The most densely methylated gene was *CCL2* with an average methylation difference of 28.5%. Our finding that T-cell inflamed genes were hypermethylated in Wilms tumors elucidated their role in formation of cold non-immunogenic TME and subsequent development of ICI resistance. Therefore, utilizing DNA methyl transferase inhibitors (DNMTis) such as azacytidine to target DNA methylation could be a viable therapeutic method for increasing ICIs effectiveness in Wilms tumors. Further preclinical and clinical research are needed to verify our finding.

# Endocrine Disrupting Chemicals as "structural cues" for the development of drugs for the treatment of Prostate Cancer (Castration Resistant Prostate Cancer) and PCOS

Katyayani Sharma,<sup>1</sup> Angelo Lanzilotto,<sup>2</sup> Søren Therkelsen,<sup>3</sup> Therina du Toit,<sup>4</sup> Flemming S. Jørgensen,<sup>3</sup> and Amit Pandey<sup>2</sup>

<sup>1</sup>Department of Pediatric Endocrinology, University Children's Hospital; Translational Hormone Research, DBMR; Graduate School of Cellular & Biomedical Sciences, University of Bern, Bern, Switzerland; <sup>2</sup>Department of Pediatric Endocrinology, University Children's Hospital; Translational Hormone Research, DBMR, University of Bern, Bern, Switzerland; <sup>3</sup>Department of Drug Design and Pharmacology, University of Copenhagen; and <sup>4</sup>Department for BioMedical Research; University Hospital; University of Bern, Bern, Switzerland

Abstract ID 16350

Poster Board 238

**Introduction:** Endocrine-disrupting chemicals (EDCs) may influence the development of Prostate Cancer by altering the steroid metabolism. Although their exact mechanism of action in controlling tumor growth is not known, EDCs may inhibit steroidogenic enzymes such as Cytochrome P450 c17 (CYP17A1) or CYP19A1 involved in the production of Androgens or Estrogens. High levels of circulating androgens are linked to Prostate Cancer (PCa) in men and Polycystic Ovary Syndrome (PCOS) in women. Essential Oils (EOs) like lavender oil and tea tree oil are reported to act as potential EDCs and contribute towards sex steroid imbalance in case of prepubertal gynecomastia in boys and premature thelarche in girls due to regular exposure to lavender-based fragrances among the Hispanic population. We screened a range of EO metabolites to determine their effect on CYP17A1 or CYP19A1 activity that might lead to endocrine dysfunction.

**Methods:** The test compounds, found as major components in EOs had been extracted and purified from natural resources. Computational docking was performed to predict the binding of EOs with CYP17A1 using AutoDock Vina. Human adrenal NCI H295R cells were treated with 10  $\mu$ M of test compounds for 24 hours. Extracts of two medicinal plants (GP and VC) from South Asia were also tested. Enzyme activity was determined using the radiolabelled substrate for CYP17A1 or CYP19A1. Liquid Chromatography high-resolution Mass Spectrometry assays were performed for steroid profiling in adrenal cells. Cell viability assays were done in LNCaP prostate cancer cells, to study the effect of the EOs on tumor development.

**Results:** Docking studies revealed that (+)-Cedrol had the best binding with CYP17A1 and CYP19A1. Though it didn't inhibit CYP17A1 activity, it caused 30% inhibition of CYP19A1 activity. Dihydro- $\beta$ -Ionone showed 30% inhibition of both CYP17A1 and CYP19A1 activities. Eucalyptol & (-)- $\alpha$ -pinene showed 20% to 40% inhibition of CYP17A1. Many compounds bind close to the active site of CYP17A1, indicating possible inhibition of CYP17A1 activity. Compounds showed no significant impact on the whole steroid profile, except for Eucalyptol having reduced peak ionization suggesting a possible interaction with CYP17A1. GP and VC extracts showed significant inhibition in CYP17A1 activity and LNCaP viability.

**Discussion:** Due to their anti-androgenic activity, these compounds should be studied further as chemical leads for the treatment of hyperandrogenic disorders such as PCa and PCOS. Screening naturally occurring EOs provide structural cues to design better inhibitors for CYP17A1 with lesser side effect and higher efficacy. This becomes essential in the case of Castration-Resistant Prostate Cancer where the tumor develops a mechanism to escape the androgen dependency and starts recognizing androgen-like steroids as its precursors for tumor growth and development.

Support/Funding Information: Swiss Government Excellence Scholarship (2019.0385); Swiss Cancer Research (KFS-5557-02-2022) and Swiss National Science Foundation (310030M\_204518)

# Cell Free Targeted Therapy for T-cell Acute Lymphoblastic Leukemia

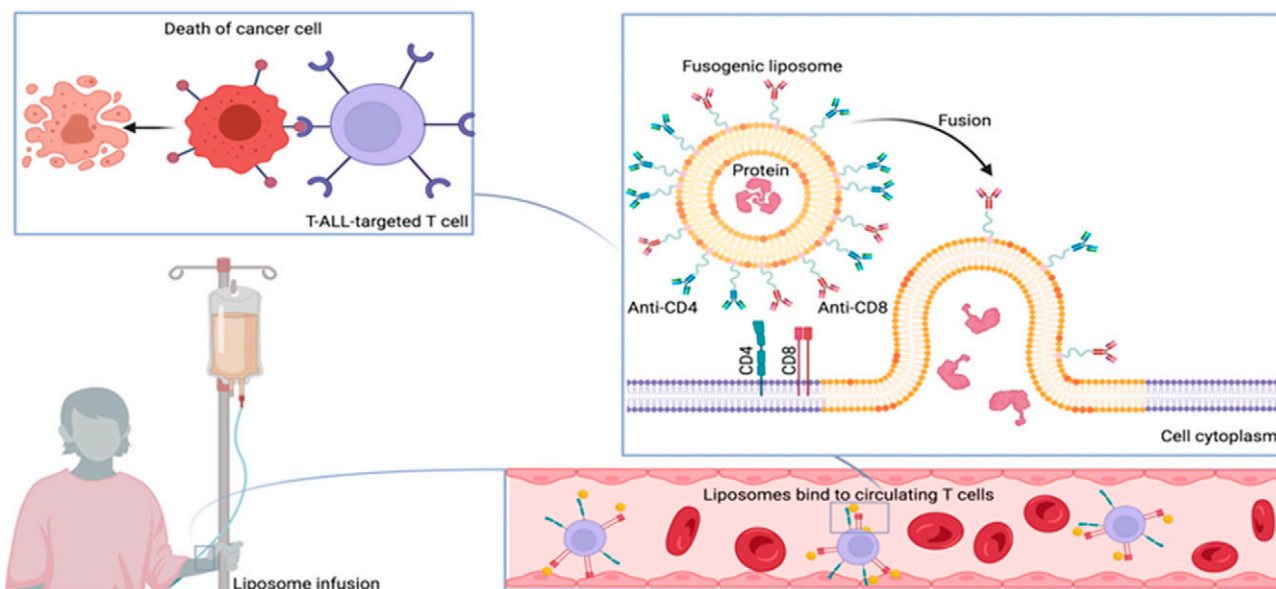
Jacob Neethling,<sup>1</sup> and Kostandin Pajcini<sup>2</sup>

<sup>1</sup>University of Illinois at Chicago College of Medicine; and <sup>2</sup>UIC

Abstract ID 21024

Poster Board 239

Notch signaling is a highly conserved signaling pathway essential for metazoan development. Sequencing of patient samples have revealed aberrant gain-of-function mutations in Notch1 leading to T-ALL in ~60% of cases. While the overall survival (OS) in children is good (~85%), the OS in adults approaches 50%; and in patients with relapsed disease, the overall survival is abysmal at ~7%. Notch inhibition can be achieved with gamma secretase inhibitors (GSIs) and anti-Notch antibodies; however, these therapies are pan Notch inhibitors and carry deleterious and toxic side effects. Therefore, non-targeted, complete abrogation of Notch signaling is not a viable therapeutic option. We have identified Deltex1 (DTX1) as a promising therapeutic target for Notch1 dependent T-ALL. Through quantitative mass spectrometry (SILAC-LCMS), our work has demonstrated that DTX1 and Notch1 physically interact at the Notch1 transcriptional activation domain. We hypothesized that Dtx1 acts as an E3 ubiquitin ligase inducing ubiquitination of Notch1 and its subsequent degradation. Utilizing a luciferase reporter assay, we have shown that Dtx1 can reduce the transcriptional activity of hyperactive patient derived Notch1 mutants in-vitro. Compelling preliminary data suggests that overexpression of Dtx1 limits Notch signaling and cell growth in multiple human T-ALL cell lines. In a collaborative effort, we are employing anti-CD4-, anti-CD8-coated fusogenic liposomal nanoparticles to specifically target T-ALL cells in-vitro and in-vivo. This will serve as a proof of principle that nanoparticles can target and deliver a Dtx1 protein specifically into double-positive leukemia cells. Following confirmed delivery of Dtx1 protein payload, we will validate Notch1 receptor degradation, a decrease in cell growth and tumor burden. Overall, our findings confirm the potential of Dtx-1 in conjunction with a cell free targeted approach as a viable therapeutic option for specific inhibition of Notch-driven T-ALL.



Targeted therapy has yet to be established for treatment of T-ALL. We will utilize a cell free model employing fusogenic liposomal nanoparticles harboring anti-CD4, -CD8 antibodies to deliver our therapeutic protein Dtx1 to leukemic lymphoblasts.

# Sanggenon G, a Diels-Alder Adduct Screened from Mori Cortex, Attenuated Irinotecan-induced Late-onset Diarrhea in Mice via a Dual Inhibition Mechanism

Ru YAN,<sup>1</sup> Panpan Wang,<sup>2</sup> Zhiqiang Chen,<sup>2</sup> Rongrong Wu,<sup>2</sup> and Yifei Jia<sup>2</sup>

<sup>1</sup>Univ of Macau; and <sup>2</sup>University of Macau

Abstract ID 22783

Poster Board 240

Irinotecan (IRT) is the first-line treatment of advanced colorectal cancer (CRC). But its dose intensification was limited by severe diarrhea resulted from regeneration of the toxic metabolite SN-38 by gut microbial  $\beta$ -glucuronidase enzymes (GUSs)<sup>1,2</sup>. The extreme structural and functional complexity of GUSs has posed big challenges to identifying GUSs involved in SN-38G deconjugation<sup>3</sup>. As a compromise, we employed a specific reaction guided broad-spectrum GUS inhibition strategy to discover inhibitors for alleviating IRT-induced late diarrhea. Specifically, inhibitors were screened *in vitro* using a 3-in-1 screening system consisting of human gut microbiota pool, representative GUS-expressing bacterial isolates and GUS proteins selected based on their metabolic profiles towards a urinary endogenous compounds pool and/or reported roles in CRC. Natural compounds of different chemical types were screened, among which flavonoid compounds, in particular the Diels-Alder (DA) adducts uniquely distributed in the plants of *Morus* genus, showed strong GUS inhibition activity towards the pool. Using activity-guided isolation with the pool combining virtual screening with *EcoGUS* from *Escherichia coli*, *SpasGUS* from *Staphylococcus pasteurii* and *SagaGUS* from *Streptococcus agalactiae*, we finally predicted GUS inhibition potentials of >40 DA compounds based on the S and RMSD values using MOE software and identified key structural factors for the protein-inhibitor interactions. Six DA compounds were isolated from Mori Cortex, all showing strong inhibition towards the GUS activity of the pool (73-94% at 100 $\mu$ M), the isolates and the proteins. Sangenon G (SGG) which showed IC<sub>50</sub> of 0.16-0.64  $\mu$ M towards purified GUSs was further assessed in mice. SGG (0.5 mg/kg, p.o. twice daily) protected mice from severe diarrhea, high mortality and intestinal injury induced by IRT (50 mg/kg/day, i.p.), agreeing well with decreased GUS activity, increased intestinal SN-38 glucuronidation and diminished colonic SN-38 accumulation. It's interesting to note that SGG also effectively suppressed OATP2B1-mediated SN-38 uptake by Caco-2 cells (IC<sub>50</sub> 4  $\mu$ M). Amoxapine (2.50 mg/kg, p.o. twice daily), a potent *EcoGUS* inhibitor, was less effective in rescuing irinotecan-induced toxicity due to weaker GUS inhibition (the pool IC<sub>50</sub> >100  $\mu$ M) and nil effect on SN-38 intestinal uptake. In conclusion, our specific reaction guided broad-spectrum GUS inhibition strategy and the 3-in-1 system were demonstrated to be feasible to cope with the extreme complexity of gut microbial GUSs. The dual inhibition mechanism makes SGG superior to other known GUS inhibitors in alleviating IRT toxicity. [Supported by the Science and Technology Development fund of Macao SAR (0091/2021/A2, 0098/2019/A2), Shenzhen-Hong Kong-Macau Science and Technology Program Category C (SGDX20210823103805038), Guangdong Natural Science Fund (2019A1515012195), and University of Macau (MYRG2018-00091-ICMS-QRCM)].

## References:

1. Fujita, D, et al (2016) *Drug Metab. Dispos* 44: 1-7.
2. Maroun JA, et. al (2007) *Curr. Oncol* 14: 13-20.
3. Wang PP, et. al (2021) *Biochem Pharmacol* 190: 114566

[Supported by the Science and Technology Development fund of Macao SAR (0091/2021/A2, 0098/2019/A2), Shenzhen-Hong Kong-Macau Science and Technology Program Category C (SGDX20210823103805038), Guangdong Natural Science Fund (2019A1515012195), and University of Macau (MYRG2018-00091-ICMS-QRCM)].

N/A



# Efficacy of Imidazole Antifungal Agents in the Treatment of Nras and Braf Mutant Human Melanoma Cells

David Koh,<sup>1</sup> Lukas R. Jira,<sup>1</sup> Hattie M. Foster,<sup>2</sup> McKenzie N. Carle,<sup>2</sup> Hannah K. Hall,<sup>2</sup> and Maxwell A. Sutherland<sup>2</sup>

<sup>1</sup>Ohio Northern Univ College of Pharmacy; and <sup>2</sup>Ohio Northern Univ. College Of Pharmacy

**Abstract ID 19624**

**Poster Board 241**

The incidence of melanoma, the most aggressive and lethal form of skin cancer, continues to rise each year in the United States. Current treatment options include conventional chemotherapy, immunotherapy, and targeted therapy. Disadvantages of these therapies, such as refractiveness and resistance, have contributed to poor outcomes in a significant number of melanoma patients. Therefore, there remains a need for new treatments. Imidazole antifungal agents potentially represent a class of new anticancer agents. Our objective here was to analyze the ability of various imidazole antifungal agents to exert anticancer effects in primary human metastatic melanoma cells, including those harboring well-known cancer mutations.

The anticancer effects investigated were the induction of cell death via flow cytometry and decreased growth and proliferation via cell growth assay. Wild-type human melanoma cells, melanoma cells possessing the BRAF V600E mutation, and melanoma cells with the NRAS Q61R mutation were analyzed. The imidazole antifungal agents, clotrimazole, econazole, and miconazole, each induced significant increases in cell death and decreases in growth and proliferation in wild-type and Braf/Nras melanoma cells with doses of 10-50  $\mu$ M. Of the antifungal agents utilized, overall clotrimazole resulted in the most efficacious effects. Interestingly, in Braf-mutant human melanoma cells, the antifungal agents led to profound decreases in cell growth but lesser effects on cell death. This may indicate an effect on cell cycle progression in Braf mutant cells. Taken together, these studies indicated that imidazole antifungal agents were effective in inducing antitumor effects in human metastatic melanoma cell lines, but with differing degrees of effects on cell death. This data suggests that melanoma tumors of each known genotype can potentially be treated with imidazole antifungal agents.

In conclusion, this study demonstrated the ability of imidazole antifungal agents to induce anticancer effects in human metastatic melanoma cells, including those harboring well-known cancer mutations. Since differing levels of effects were observed using different antifungal agents, it is possible that each agent utilized affected different molecular targets in the melanoma cells. These antifungal agents thus appear to be potential alternative treatments, as well as affordable and widely accessible therapies, for melanoma patients in the future.

# Immunoproteasome Inhibitors for the treatment of ALL driven by the t(4:11) Translocation

Tyler Jenkins,<sup>1</sup> Alexei Kisselev,<sup>2</sup> Andrey V. Maksimenko,<sup>2</sup> Amit Mitra,<sup>2</sup> Peter Panizzi,<sup>2</sup> Jennifer L. Fields,<sup>3</sup> Steven Fiering,<sup>3</sup> and Jacquelyn E. Fitzgerald<sup>2</sup>

<sup>1</sup>Auburn Univ; <sup>2</sup>Auburn University; and <sup>3</sup>Dartmouth Cancer Center

**Abstract ID 27518**

**Poster Board 242**

The t(4;11)(q21;q23) chromosomal translocation that creates the MLL-AF4 fusion protein, confers a poor prognosis in infant acute lymphoblastic leukemia (ALL). This translocation also sensitizes cells to proteasome inhibitors bortezomib and carfilzomib, which are approved by the FDA for the treatment of multiple myeloma. Clinical activity of bortezomib in combination with standard chemotherapy has been documented in several clinical trials of ALL patients, and a case of a single-agent activity against relapsed leukemia driven by the MLL-AF4 translocation has been described. However, toxicities of bortezomib and carfilzomib may be unacceptable to pediatric patients. We found that the overwhelming majority of proteasomes in this subtype of ALL are lymphoid tissue specific immunoproteasomes. Cells with MLL-AF4 translocations were sensitive to pharmacologically relevant concentrations of specific immunoproteasome inhibitors ONX-0914 and M3258. Furthermore, both compounds dramatically delayed growth of orthotopic xenograft tumors in mice. Thus, immunoproteasomes are therapeutic targets in ALL and replacing bortezomib and carfilzomib with immunoproteasome inhibitors in ALL should reduce toxicities associated with inhibition of the proteasomes in non-lymphoid tissues.

Support/Funding Information: RO1 CA213223

# Direct Targeting of the Cell cycle Regulator *WEE1* is a Novel Therapeutic Approach for Neuroblastoma

Parul Suri,<sup>1</sup> Rameswari Chilamakuri,<sup>2</sup> and Saurabh Agarwal<sup>3</sup>

<sup>1</sup>St. John's University; <sup>2</sup>St Johns Univ; and <sup>3</sup>St. John

Abstract ID 28360

Poster Board 243

High-risk neuroblastoma (NB) is a solid pediatric tumor that develops from the extracranial sympathetic nervous system. Despite recent advances in therapeutic regimens of dose-intensive chemotherapies, radiation, and surgery NB often relapses as a metastatic and drug-resistant tumor. These issues further mandate the identification and development of novel therapeutic approaches for NB treatment. Cell cycle regulators, Cdk1 in combination with cyclin B1, and Cdk2 with cyclin E regulate the G2/M checkpoint and G1/S checkpoint respectively, to obstruct the cells from proceeding into mitosis with genomic DNA damage. Wee1, a tyrosine kinase, regulates the phosphorylation of Cdk1 and Cdk2 at tyrosine residues in response to DNA damage, making them inactive. Previous studies have reported high expression of Wee1 in NB patients and associate Wee1 with an overall poor NB prognosis. Inhibition of Wee1 obstructs the Cdk1 and Cdk2 activation and is no more reliant on an intact G2/M checkpoint for survival. In the present study, we analyzed multiple NB patient datasets and found that Wee1 expression is strongly correlated with poor overall survival of NB patients. Further, we used a specific small molecule Wee1 inhibitor in NB cells and observed that Wee1 inhibition significantly and in a dose-dependent manner inhibits NB proliferation and colony formation capacity in both MYCN-amplified and MYCN non-amplified NB cells. Further, Wee1 inhibition significantly induces apoptosis up to 3-fold in different NB cells in contrast to control treatments. Additionally, we used NB 3D spheroid models that mimic *in vivo* NB tumor growth and found that Wee1 inhibition significantly and in a dose-dependent manner inhibits 3D spheroid growth and volume up to 2.3-fold in contrast to control treatments. Additionally, and as expected, inhibition of Wee1 significantly inhibits NB cell cycle progression by inhibiting cell cycle S phase and blocking G2/M checkpoint in different NB cell lines. Further, the Wee1 inhibition inhibits the gene expression levels of different cell cycle-related genes in NB cells such as CDK1, CDK2, CCNB1, CHK2, and BCL-2. Overall, our data suggest that inhibition of the cell cycle regulator Wee1 is an effective therapeutic approach for NB. Further combining Wee1 inhibitors with current therapies will pave the way for developing effective targeted therapeutic approaches for NB patients.

Support/Funding Information: Department of Pharmaceutical Sciences, College of Pharmacy and Health Sciences, St. John's University, New York

# Production of TNF- $\alpha$ and IL-10 by HepG2 and THP-1 cells differs depending on whether ethanol conditioned media is derived from 3D vs. 2D cultured HepG2 cells.

Joshua Hood,<sup>1</sup> Alexander Southern,<sup>2</sup> and Luke Schroeder<sup>2</sup>

<sup>1</sup>Univ of Louisville; and <sup>2</sup>University of Louisville

Abstract ID 16411

Poster Board 244

**Background:** One of the difficulties in cancer research is bridging the gap between human and animal tumor models. One proposed method of improving the screening of cancer-promoting toxins and novel cancer therapies is the development of pre-clinical 3D human culture models. We are currently developing 3D human hepatocellular carcinoma (HCC) culture models using the standardized HepG2 liver cancer cell line as a template. Ethanol is being used as a test agent to generate conditioned media (CM) from 2D adherent vs. 3D HepG2 suspension spheroid cultures. The conditioned media is then applied to human monocytes to determine differences in TNF- $\alpha$  (proinflammatory) and IL-10 (anti-inflammatory) cytokine induction.

**Objectives:** The experimental goals were to determine differences in the production of TNF- $\alpha$  and IL-10 between 2D and 3D cultured HepG2 cells, and by THP-1 monocytes treated with conditioned media (CM), +/- ethanol, derived from 2D and 3D HepG2 cells.

**Methods:** HepG2 cells were grown in both 2D (adherent) and 3D (suspension) cultures to produce two different patterns of cell growth (Fig. 1). The cells were then switched to fetal bovine exosome-free media and grown with and without 100 mM ethanol to produce CM. Human monocytes (THP-1 cells) were then cultured in the presence of CM. Cell viability and production of TNF- $\alpha$  and IL-10 were measured using PrestoBlue™ and Lumit™ immunoassays.

**Results:** Changes in THP-1 morphology were not observed following treatment with HepG2 CMs derived from 2D or 3D cultures with or without 100 mM ethanol. Assessment of TNF- $\alpha$  in HepG2 CM demonstrated a trending decrease in TNF- $\alpha$  production for all CMs evaluated particularly for CMs derived from ethanol treated 2D and 3D HepG2 cells. In contrast, IL-10 content tended to increase in CMs obtained from ethanol treated or untreated 3D cultured HepG2 cells. In general, induction of TNF- $\alpha$  production by THP-1s post HepG2 CM treatments hovered around baseline, while induction of IL-10 by THP-1s post HepG2 CM treatments decreased. These findings did not relate to cell viability since no significant difference in cell viability for any CM treatment was observed. Tracking the ratio of TNF- $\alpha$  to IL-10 production in THP-1s treated with HepG2 CMs revealed significant differences +/- ethanol during CM production. Baseline exofree media with ethanol increased the ratio of TNF- $\alpha$  to IL-10. In contrast, the ratio decreased for 2D and 3D CMs. CM +/- ethanol from 3D HepG2 cells produced a less dramatic increase in the ratio of proinflammatory TNF- $\alpha$  to immunosuppressive IL-10 production.

**Conclusion:** A 3D vs. 2D HepG2 model may be more suitable for pre-clinical studies requiring a better approximation of an immunosuppressive HCC microenvironment. Future investigations will explore the individual contributions of CM media components to these findings to facilitate development of new biomarkers and therapeutic targets for HCC.

Research was supported by the University of Louisville Cancer Education Program NIH/NCI (R25-CA134283), University of Louisville faculty start-up funds to J. L. Hood, and UofL Hepatobiology and Toxicology COBRE NIH NIGMS P20GM113226.

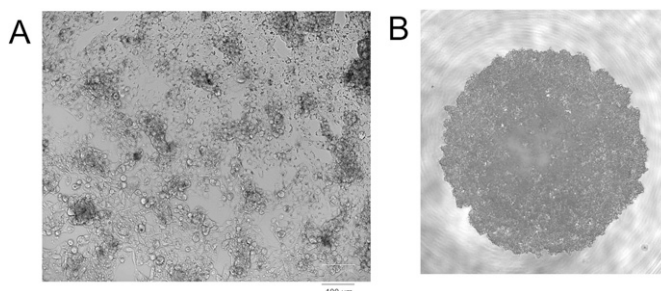


**Figure 1. A comparison of 2D vs. 3D HepG2 cell culture morphology. A)** 2D adherent cells. Image obtained of HepG2 cells growing in a T-300 culture flask. **B)** 3D suspension spheroid. Image obtained of 3D HepG2 cells in a U-shaped 96 well plate at 48 hours post incubation of 10,000 cells.

# Recombinant miR-7-5p Effectively Inhibits NSCLC Cell Viability through Regulating Mitochondrial Function

Gavin M. Traber,<sup>1</sup> Meijuan Tu,<sup>2</sup> Neelu Batra,<sup>1</sup> Colleen Yi,<sup>1</sup> and Aiming Yu<sup>3</sup>

<sup>1</sup>UC Davis School of Medicine; <sup>2</sup>Univ of California, Davis; and <sup>3</sup>Univ of California-Davis, Sch of Med

Abstract ID 15136

Poster Board 245

Non-Small Cell Lung Cancer (NSCLC) makes up 84% of all lung cancer cases and lack of effective treatment options contribute to low survival rates. RNA interfering (RNAi) microRNA (miRNA or miR) provides researchers with a versatile alternative to modulate target gene expression to combat disease. Of these, the level of tumor suppressive miR-7-5p (miR-7) is reduced in NSCLC. Notably, miR-7 downregulates many genes important in metabolism and mitochondrial function including EGFR and VDAC1, and it is a putative regulator of mitochondrial genes AGK, PPIF, and DTYMK as well as the SLC25A15 transporter. In previous studies, reintroduction of miR-7-5p has been reported to inhibit NSCLC cell growth and metastasis, however the miRNA mimics used in those studies are chemically synthesized in vitro and comprised of extensive modifications that may trigger immunogenic and off-target responses. By contrast, our laboratory has developed a novel technology to bioengineer RNAi agents (BioRNA) in vivo utilizing specific tRNA/pre-miRNA carriers to preserve the natural post-transcriptional modifications, folding, and functions of genome derived miRNAs. Using this technology, we aim to develop BioRNA/miR-7 as a novel, bio-synthesized anticancer agent that functions through endogenous RNAi mechanisms to reduce cancer cell viability through the regulation of mitochondrial function. Thus far, we have successfully cloned and overexpressed leucyl and glycyl tRNA versions of BioRNA/miR-7 in *Escherichia coli* as verified by Sanger sequencing and RNA gel electrophoresis, respectively. We have isolated leucyl and glycyl BioRNA/miR-7 from total bacterial RNA by anion exchange Fast Protein Liquid Chromatography to attain a purity of 99.5% and 98.7%, respectively, as determined by reverse phase High Performance Liquid Chromatography. Additionally, endotoxin assay showed low endotoxin levels of 0.74 and 0.68 (EU/ $\mu$ g RNA) for leucyl and glycyl BioRNA/miR-7, respectively. Moreover, we have established the effects of BioRNA/miR-7 to reduce cell viability via IncuCyte Live Cell Image Analyzer, validated the processing of glycyl tRNA-BioRNA/miR-7 to target miR-7-5p in NSCLC cells by stem-loop reverse transcription real-time qPCR assay, and assessed the functional capability of BioRNA/miR-7 to regulate known miR-7 target gene expression in comparison to a commercial miR-7 mimic by Western blot and immunofluorescent microscopy. Furthermore, we have established the effects of BioRNA/miR-7 on mitochondrial function via Seahorse Analyzer and compared treatment-induced changes in mitochondrial morphology by confocal microscopy. The success of the BioRNA technology together with previous and preliminary data on miR-7 suggests that miR-7 plays an important role in mitochondrial function, and BioRNA/miR-7 may be developed as a new therapeutic RNA for the treatment of NSCLC.

Supported by the National Institute of General Medical Sciences [R35GM140835] and National Cancer Institute [R01CA225958 and R01CA253230], National Institutes of Health. Gavin M. Traber is supported by a National Institutes of General Medical Sciences-funded Pharmacology Training Program Grant [T32GM099608 and T32GM144303].

# Defining the landscape of cancer vulnerabilities that are engendered by germline genetic variation

Sean Misek, Aaron Fultineer,<sup>1</sup> Jeremie Kalfon,<sup>1</sup> Javad Noorbakhsh,<sup>1</sup> Isabella Boyle,<sup>1</sup> Joshua Dempster,<sup>1</sup> Lia Petronio,<sup>1</sup> Katherine Huang,<sup>1</sup> Thomas Green,<sup>1</sup> Adam Brown,<sup>1</sup> John Doench,<sup>1</sup> David Root,<sup>1</sup> James McFarland,<sup>1</sup> Rameen Beroukhi,<sup>1</sup> and Jesse Boehm<sup>1</sup>

<sup>1</sup>Broad Institute

**Abstract ID 55303**

**Poster Board 246**

A range of somatic alterations in both oncogenes and tumor suppressor genes promote cancer development. Synthetic lethal relationships or collateral lethalties have emerged in the context of these genetic driver mutations, revealing new targets for therapeutic development. Most variation within cancer genomes results from germline, as opposed to somatic, mutations, but the genetic dependencies engendered by these variants have not been systematically explored. We sought to define the landscape of these interactions by leveraging the genome-scale CRISPR/Cas9 screens that were performed as part of The Cancer Dependency Map (DepMap).

In this study we systematically analyzed the associations between individual germline variants in 612 cancer cell lines and >16,000 genetic dependencies. Across all genes profiled in this analysis, we identified 121 genes whose dependency profiles are associated with the presence of specific germline variants. The top association in this analysis was between two functionally redundant Holliday junction resolvases. In this study we seek to define the nature of this synthetic lethal relationship, with a focus on how this variant impacts protein activity.

# Metformin Alleviates Chemotherapy-Induced Toxicities in Non-Diabetic Breast Cancer Patients: A Randomized Controlled Study

Mahmoud El-Mas,<sup>1</sup> Amira B. Kassem,<sup>2</sup> Noha A. El-Bassiouny,<sup>2</sup> Maged W. Helmy,<sup>3</sup> Yasser El-Kerm,<sup>4</sup> and Manar A. Serageldin<sup>5</sup>

<sup>1</sup>College of Medicine, Kuwait Univ., Kuwait; Pharmacy, Alexandria Univ., Egypt; <sup>2</sup>Faculty of Pharmacy, Damanhour University; <sup>3</sup>College of Pharmacy Arab Academy for Science, Technology and Maritime Transport; <sup>4</sup>Medical Research Institute, Alexandria University; and <sup>5</sup>Faculty of Pharmacy, Alexandria University

Abstract ID 15990

Poster Board 247

Breast cancer patients treated with adriamycin-cyclophosphamide plus paclitaxel (AC-T) are often challenged with serious adverse effects for which no effective therapies are available. Here, we investigated whether metformin, an antidiabetic drug with additional pleiotropic effects could favorably offset AC-T induced toxicities. Seventy non-diabetic breast cancer patients were randomized to receive either AC-T (adriamycin 60 mg/m<sup>2</sup> + cyclophosphamide 600 mg/m<sup>2</sup> X 4 cycles Q21 days, followed by weekly paclitaxel 80 mg/m<sup>2</sup> X 12 cycles) alone or AC-T plus metformin (1700 mg/d). Patients were interviewed regularly after each cycle to record the incidence and severity of adverse events based on the National Cancer Institute Common Terminology Criteria for Adverse Events (NCI-CTCAE), version 5.0. Moreover, baseline echocardiography and ultrasonography were done and repeated after the end of neoadjuvant therapy. The addition of metformin to AC-T resulted in significantly less incidence and severity of peripheral neuropathy, oral mucositis, and fatigue ( $p < 0.05$ ) compared to control arm. Moreover, the left ventricular ejection fraction (LVEF%) in the control arm dropped from a mean of  $66.69 \pm 4.57\%$  to  $62.2 \pm 5.22\%$  ( $p = 0.0004$ ) versus a preserved cardiac function in the metformin arm ( $64.87 \pm 4.84\%$  to  $65.94 \pm 3.44\%$ ,  $p = 0.2667$ ). Furthermore, fatty liver incidence was significantly lower in metformin compared with control arm (8.33% versus 51.85%,  $p = 0.001$ ). By contrast, hematological disturbances caused by AC-T were preserved after concurrent metformin administration ( $p > 0.05$ ). In conclusion, Metformin offers a therapeutic opportunity for controlling toxicities caused by neoadjuvant chemotherapy in non-diabetic breast cancer patients.

# Targeting Adenylyl Cyclase Type 8, Orai1, and Stromal Interaction Molecule 1 in Triple-Negative Breast Cancer

Moana Hala'ufia,<sup>1</sup> and Dave Roman<sup>2</sup>

<sup>1</sup>University of Iowa; and <sup>2</sup>Univ of Iowa

Abstract ID 16706

Poster Board 248

Triple-negative breast cancer (TNBC) is one of the most aggressive forms of breast cancer that hormonal therapies cannot treat. Current standards of care include surgical removal of the tumor and aggressive chemotherapy. Consequently, there is an urgent need for new, molecular-based therapies to treat these patients effectively<sup>1,2</sup>. On a molecular level, two proteins facilitate finely tuned calcium entry: Orai1, a pore-forming calcium channel, and stromal interaction molecule 1 (STIM1), a calcium sensor embedded in the ER membrane. Upon ER calcium store depletion, STIM1 undergoes a conformational change to bind to Orai1, which triggers extracellular calcium entry to achieve homeostasis<sup>3</sup>. Recently, it has been discovered that a third protein is implicated in this process: adenylyl cyclase type 8 (AC8)<sup>4</sup>. The N-terminus of AC8 can bind to the N-terminus of Orai1 to prolong calcium influx, which ceases upon Orai1 phosphorylation<sup>4</sup>. In normal breast epithelial cells, AC8 is expressed at a basal level and does not interfere with Orai1-STIM1 calcium entry. However, in TNBC cells, AC8 is grossly overexpressed so that all Orai1 channels become bound<sup>4,5</sup>. As AC8 binds to Orai1 on its phosphorylation site, the Orai1 channel cannot be inactivated, leading to excess calcium influx and adverse cellular effects such as proliferation and migration.

Thus, **we hypothesize** that if we inhibit the interaction between AC8 and Orai1 with a therapeutic small molecule, we will observe a decrease in proliferation in TNBC cells. We also expect that inhibiting the interaction between Orai1 and STIM1 will produce similar effects. Ultimately, we aim to screen a library of small molecules against our protein-protein interactions to find therapeutic inhibitors. We will use the NanoBIT system to study each different protein-protein interaction. Briefly, the NanoBIT system tags each protein with a split luciferase, allowing for the generation of a luminescent signal upon protein binding. Using this method, **we have found** that the interaction between STIM1 and Orai1 is strictly governed by calcium, whereas the interaction between AC8 and Orai1 is more constitutive. Interestingly, we found that forskolin, an AC8 activator, prevents AC8 binding to Orai1, as evident through loss of luminescence. This suggests that AC8 must be inactive to interact with Orai1 and that phosphorylated Orai1 cannot bind to AC8. These findings have allowed us to conduct Z-Score studies to prime for initial screening, which fall within a 0.6-0.8 range for each protein-protein interaction. To date, we have accomplished screening two libraries of small molecule compounds; NCI Diversity Set VI and NCI Approved Oncology Set X, which will be extended further to other diversity libraries. In addition, we plan to test any inhibitors in different TNBC cell lines (MDA-MB-231 and MDA-MB-157) to observe effects on cancer cell migration. **In conclusion**, understanding the unique interplay between AC8, Orai1, and STIM1 is critical to understanding how to prevent TNBC cell proliferation and migration.

## References

1. Stovgaard, et. al. Triple-negative breast cancer ... *Acta Onc.* 2018; 57:1, 74-82,
2. Bose. Triple-negative Breast Carcinoma ... *Adv. in Ana. Path.* 2015; 22: 306-313
3. Lunz, et. al. STIM1 activation of Orai1. *Cell Cal.* 2019; 77, 29-38
4. Sanchez-Collado, et al. Adenylyl Cyclase Type 8 Overexpression ... *Cancers.* 2019; 11, 1624
5. Derler, et. al. Structure, regulation and biophysics of I(CRAC), STIM/Orai1. *Adv. Exp. Med. Biol.* 2012; 740, 383-410



# Significance of topical chemotherapy application on human and murine skin

Anita Thyagarajan,<sup>1</sup> Krishna Awasthi,<sup>1</sup> Christine Rapp,<sup>1</sup> Kelly Miller,<sup>1</sup> R. Michael Johnson,<sup>1</sup> Yanfang Chen,<sup>1</sup> Jeffrey Travers,<sup>1</sup> and Ravi P. Sahu<sup>1</sup>

<sup>1</sup>Wright State University

**Abstract ID 23594**

**Poster Board 249**

Chemotherapy has remained the mainstay for the treatment of multiple types of cancers. In particular, topical use of chemotherapy has been used for skin cancers. Though effective, topical chemotherapy has been limited due to adverse effects such as local and even systemic toxicities. Our recent studies demonstrated that exposure to pro-oxidative stressors, including therapeutic agents induces the generation of extracellular vesicles known as microvesicle particles (MVP) which are dependent on activation of the Platelet-activating factor-receptor (PAFR), a G-protein coupled receptor present on various cell types, and acid sphingomyelinase (aSMase), an enzyme required for MVP biogenesis. Based upon this premise, we tested the hypothesis that topical application of gemcitabine will induce MVP generation in human and murine skin. Our *ex vivo* studies using human skin explants demonstrate that gemcitabine treatment results in MVP generation in a dose-dependent manner in a process blocked by PAFR antagonist and aSMase inhibitor. Importantly, gemcitabine-induced MVPs carry PAFR agonists. To confirm the mechanisms, we employed PAFR-expressing and deficient (*Ptafr*<sup>-/-</sup>) mouse models as well as mice deficient in aSMase enzyme (*Spm1d1*<sup>-/-</sup>). Using genetic-based approaches, our studies demonstrated that gemcitabine-induced MVP release in WT mice was blunted in *Ptafr*<sup>-/-</sup> and *Spm1d1*<sup>-/-</sup> mice. Overall, these findings indicate that pharmacological strategies to target the PAFR/aSMase pathway to block MVP release could be used as a promising approach for improving gemcitabine efficacy.

# Characterization of microenvironmental-mediated gilteritinib resistance in Acute Myeloid Leukemia using a Bmx knockout mouse model

Jack C. Stromatt,<sup>1</sup> Daelynn R. Buelow,<sup>1</sup> Shelly J. Orwick,<sup>1</sup> Eric Eisenmann,<sup>1</sup> Navjot S. Pabla,<sup>1</sup> Bradly W. Blaser,<sup>1</sup> and Sharyn D. Baker<sup>1</sup>

<sup>1</sup>The Ohio State University

Abstract ID 20840

Poster Board 250

**Introduction:** We performed single-cell RNA sequencing on samples from Acute Myeloid Leukemia (AML) patients with *FLT3* mutations (*FLT3*<sup>+</sup>) pre- and post-treatment with the FLT3 inhibitor gilteritinib and identified in unresponsive patients: (i) upregulation of bone marrow (BM)-derived inflammatory cytokines, previously shown to promote disease progression and relapse in AML; and (ii) elevated expression of bone marrow kinase on chromosome X (BMX), a non-receptor tyrosine kinase from the Tec family of kinases. In *FLT3*<sup>+</sup> cell lines and primary AML samples, we demonstrated that BMX gene knockout (KO) and inhibition reduced cytokine secretion. Mechanistic studies revealed that BMX kinase promotes AML cell-autonomous gilteritinib resistance through bypass signaling. Given the novel role of BMX in the cytokine network *in vitro*, we sought to develop a mouse model to evaluate AML cell/BM niche cell interactions *in vivo* to examine the mechanisms of BMX in promoting gilteritinib resistance.

**Methods:** Genetic engineering was utilized to create a whole-body Bmx KO mouse model. To generate a syngeneic transplant model of murine *Flt3*<sup>+</sup> AML, splenocytes (250,000 cells) from a female double mutant *Npm1<sup>cA/+</sup>/Flt3<sup>ITD</sup>* knock-in mouse (CD45.2) that produces spontaneous AML, were injected by tail vein injection (TVI) into male Bmx WT and KO mice. Starting 7 days after TVI, cohorts of mice were treated with vehicle or gilteritinib 30 mg/kg orally once daily (n=4-5 mice per cohort/per Bmx genotype). At survival endpoint, spleens were harvested and analyzed for CD45.2 cells (from vehicle-treated mice), gated for AML phenotypic markers CD11b and CD117 by flow cytometry, and murine cytokines were measured in plasma and spleen lysates by Luminex multiplex assay (from n=3-4 mice per cohort).

**Results:** In our syngeneic transplant model of murine *Flt3*<sup>+</sup> AML, gilteritinib treatment resulted in a 24-day median survival advantage over vehicle treatment (52 vs. 27.5 days) in Bmx WT mice, indicating this murine model represents a clinically relevant model of human *FLT3*<sup>+</sup> AML that responds to a FLT3 inhibitor. However, no difference in survival was observed between Bmx KO and WT mice treated with gilteritinib. This is consistent with our published data showing an AML cell-autonomous role for BMX in gilteritinib resistance and suggests co-treatment with another drug to inhibit BMX or downstream mediators will be required. At study endpoint, *Flt3*<sup>+</sup> AML cells were confirmed in spleens by expression of CD11b and CD117, compared to the normal spleen. We next sought to determine if microenvironment changes were occurring in Bmx KO vs. WT mice during gilteritinib treatment by assessing cytokine in plasma and AML cells in the spleen. We observed: (i) plasma CCLs/CXCLs and growth factors increased during gilteritinib treatment in Bmx WT mice but decreased in Bmx KO mice; and (ii) CCLs/CXCLs and other cytokines decreased in the spleens from Bmx KO vs. WT mice treated with gilteritinib.

**Conclusion:** We generated a syngeneic transplant model of murine *FLT3*<sup>+</sup> AML that mimics BMX-driven cytokine changes, which will be used to examine mechanisms underlying BMX-mediated AML cell/microenvironment niche cell interactions to promote gilteritinib resistance. This model will be used to evaluate a rational drug combination of gilteritinib + BMX inhibitor with translational potential in *FLT3*<sup>+</sup> AML.

# Strategies to Circumvent Topoisomerase II $\alpha$ Intron 19 Intronic Polyadenylation (IPA) in Acquired Etoposide Resistance Human Leukemia K562 Cells

Xinyi Wang,<sup>1</sup> Jessika Carvajal-Moreno,<sup>1</sup> Jack C. Yalowich,<sup>1</sup> and Terry Elton<sup>1</sup>

<sup>1</sup>Ohio State Univ

Abstract ID 20741

Poster Board 251

DNA topoisomerase II $\alpha$  (TOP2 $\alpha$ , 170kDa, TOP2 $\alpha$ /170) is an essential enzyme for proper chromosome dysjunction at mitosis by producing transient DNA double-stranded breaks and is a significant target for DNA damage stabilizing anti-cancer agents like etoposide. Therapeutic effects of TOP2 $\alpha$  poisons can be limited due to acquired drug resistance. We previously demonstrated decreased TOP2 $\alpha$ /170 levels in an etoposide-resistant human leukemia K562 clonal subline, designated K/VP.5, accompanied by increased expression of a C-terminal truncated TOP2 $\alpha$  isoform (90 kDa, TOP2 $\alpha$ /90). TOP2 $\alpha$ /90 is translated from TOP2 $\alpha$  mRNA due to Intron19 (I19) intronic polyadenylation (IPA). TOP2 $\alpha$ /90 heterodimerizes with TOP2 $\alpha$ /170 and is a determinant of resistance by exhibiting dominant-negative effects against etoposide activity. Previously we gene-edited/optimized the weak TOP2 $\alpha$  I19 5' splice site in K/VP.5 cells using CRISPR/Cas9 with homology-directed repair (HDR). In gene-edited cells, TOP2 $\alpha$ /90 levels were reduced, TOP2 $\alpha$ /170 levels were restored, and drug resistance was reversed.

Given that no TOP2 $\alpha$  sequence differences were identified in K562 vs K/VP.5 cells, we hypothesize that decreased TOP2 $\alpha$ /170 and increased TOP2 $\alpha$ /90 in K/VP.5 cells is related to IPA and aberrant expression of RNA cleavage/polyadenylation factor(s).

Based on 3'-Rapid Amplification of cDNA Ends (3'-RACE), polyadenylation site (PAS) #3 (out of 7 PASs found in I19) is the major site utilized in K/VP.5 which leads to IPA. Therefore, CRISPR/Cas9/HDR and anti-sense morpholinos were utilized to mutate/block the PAS #3 in TOP2 $\alpha$  I19 to eliminate/reduce IPA.

We first mutated PAS #3 from 'ATTTAA' to 'ACCCAA' in K/VP.5 cells using CRISPR/Cas9/HDR editing, and successfully obtained one, two and three-allele edited clones assessed by qPCR and Sanger sequencing [Note: three TOP2 $\alpha$  alleles are present in K/VP.5 cells]. In the PAS #3 one-allele edited clone, a ~50% decrease of TOP2 $\alpha$ /90 and a 4-fold increase of TOP2 $\alpha$ /170 mRNA/protein was detected compared to K/VP.5 cells. Growth inhibitory assays demonstrated a 5-fold reversal of etoposide resistance. CRISPR/Cas9/HDR re-transfection of the one-allele edited clone resulted in generation/isolation of PAS #3 two-allele and three-allele edited clones, validated by qPCR and Sanger sequencing. Experiments are planned to assess TOP2 $\alpha$ /170 and TOP2 $\alpha$ /90 mRNA/protein levels in the new gene-edited clones as well as to evaluate circumvention of drug resistance by etoposide-induced growth inhibition and DNA damage (Comet assay) studies.

In separate experiments, a customized anti-sense morpholino was used to hybridize and block TOP2 $\alpha$  I19 PAS #3 in K/VP.5 cells. Results showed a 50% decrease in TOP2 $\alpha$ /90 level 48 hr after transfection with the antisense morpholino compared to a control morpholino.

Taken together, results suggest that by mutating/blocking PAS #3, aberrant trans-acting factors regulating I19 IPA can no longer recognize the PAS thereby preventing TOP2 $\alpha$  I19 IPA resulting in restoration of full-length TOP2 $\alpha$ /170 levels and circumvention of chemoresistance in K/VP.5 cells. Future strategies will be directed to identify putative aberrant splicing/RNA cleavage/polyadenylation factor(s) expressed in K/VP.5 cells utilizing an unbiased MS2 (bacteriophage coat protein) tag-trap pull-down strategy and proteomics analysis.

# Enhanced Cholinergic Action of Myenteric Neurons During Chemotherapy Induced Diarrhea

Stanley Cheatham,<sup>1</sup> Karan H. Muchhala,<sup>2</sup> and Hamid I. Akbarali<sup>3</sup>

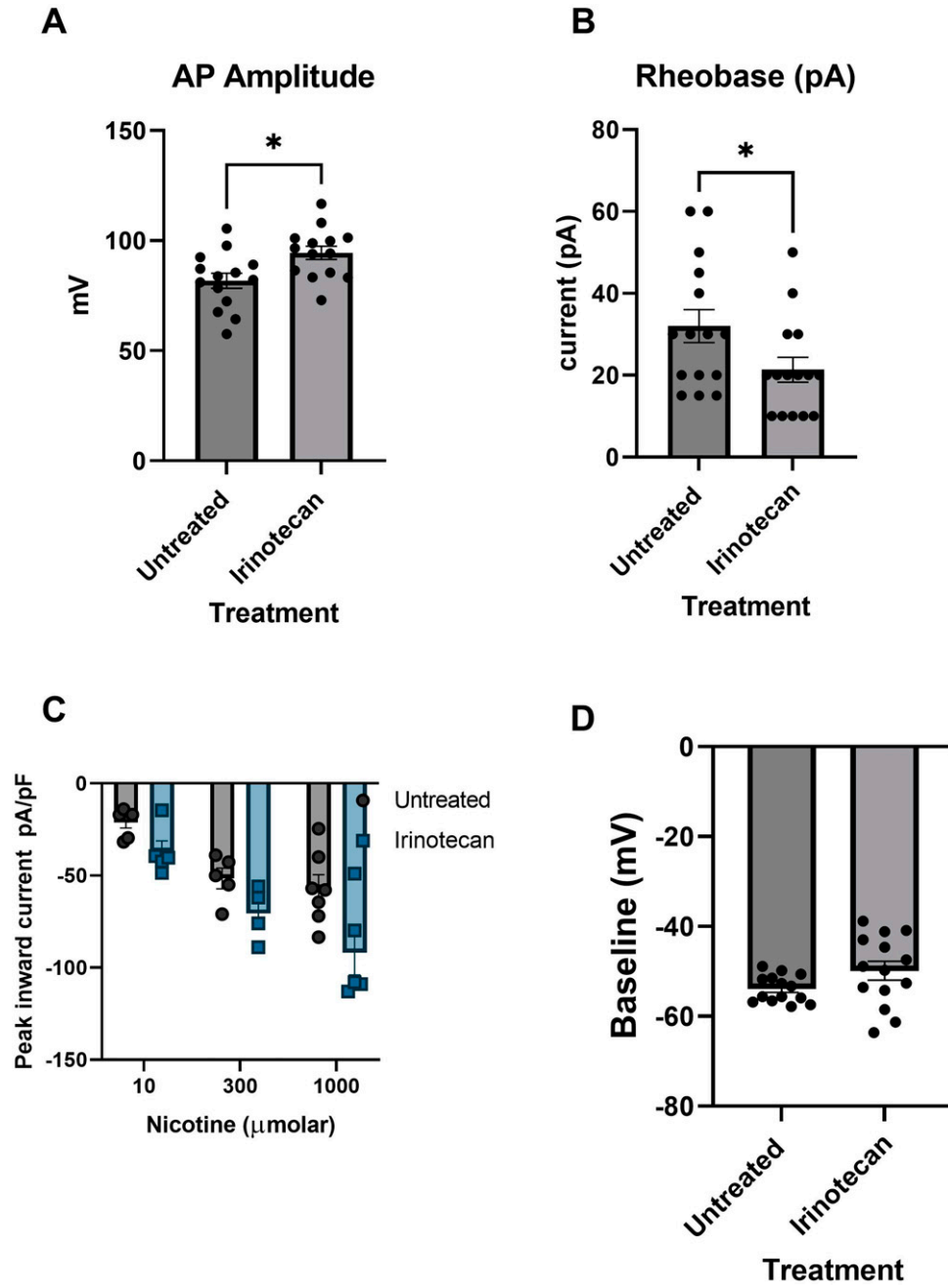
<sup>1</sup>Virginia Commonwealth University; <sup>2</sup>Virginia Commonwealth University; and <sup>3</sup>Virginia Commonwealth University

Abstract ID 14356

Poster Board 432

Diarrhea is a prevalent side effect of chemotherapeutic treatment that can result in reduction of quality of life, dose limitation, and death. Irinotecan is a widely used chemotherapeutic in the treatment of unresectable colorectal and metastatic triple-negative breast cancer. It produces both an acute cholinergic mediated diarrhea and a late onset diarrhea that has yet to be fully characterized. Treatment for the acute phase of diarrhea produced by irinotecan is treated with the muscarinic receptor antagonist atropine, however, late onset diarrhea is treated with the mu opioid receptor agonist loperamide. In a population of patients, however, diarrhea becomes refractory to treatment with loperamide. In this study we examine the role of cholinergic response in the development of tolerance to loperamide during late onset diarrhea. Previous reports have demonstrated that in a rodent model of irinotecan-induced diarrhea, choline acetyl transferase (ChAT) and vesicular acetylcholine transporter (VAChT) is increased in myenteric neurons. We hypothesize that enteric neurons become hyperexcitable following irinotecan treatment resulting in enhanced cholinergic activation precluding the efficacy of loperamide in the treatment of late onset diarrhea. In this study we measured neuronal excitability and nicotine-induced currents in isolated myenteric neurons from irinotecan-treated mice. Briefly male ICR mice were treated with 75 mg/kg irinotecan administered intra-peritoneally once daily for four consecutive days followed by monitoring and assessment of diarrhea for two additional days. On day 6 of our paradigm myenteric neurons were isolated and electrophysiological experiments were conducted to examine changes in basal properties. Animals treated with irinotecan produced a decrease in body weight over 6 days, increase in fecal water content, and time dependent increase in diarrhea scoring. We measured the electrophysiological properties of isolated myenteric neurons from irinotecan treated animals. There were no observed differences in resting membrane potentials of treated animals (fig D). Treated animals, however, produced a statistically significant increase in action potential amplitude  $94.42 \pm 3.03$  mV (n=14) when compared to their controls  $81.75 \pm 3.489$  mV (n=14) ( $P < 0.0001$  unpaired t-test) (fig A). Additionally, we found a decrease in the amount of current needed to elicit an action potential (Rheobase) in irinotecan treated animals  $21.3 \pm 3.065$  pA as compared to their control  $32 \pm 4.047$  pA ( $P < 0.05$  unpaired t-test) (fig B). In Irinotecan treated animals, nicotine inward currents were enhanced in a dose-dependent manner with maximal current at 1mM increased from  $-91.7 \pm 12.21$  pA/pF to  $-57.016 \pm 7.426$  pF/pA (n=5) ( $P < 0.01$  unpaired t-test) (fig C).

Support/Funding Information: NIH-T32DA007027-47



# Mechanistic Investigation of a Combination of a Cell Cycle Inhibitor and an HDAC Inhibitor in Pancreatic Cancer Cells

Shraddha Bhutkar,<sup>1</sup> Anjali Yadav,<sup>1</sup> and Vikas Dukhande<sup>1</sup>

<sup>1</sup>St. John's University

Abstract ID 18966

Poster Board 433

Currently, pancreatic cancer has a 5-year survival rate of about 11%, making it one of the deadliest malignancies. Better treatment strategies are required for pancreatic cancer due to late diagnosis, early metastasis, and drug resistance. Tumor growth and metastasis are facilitated by changes in the epigenetic profile caused by DNA and histone alterations. Another key feature of the cancer is the ability to elude the control of growth suppressors that monitor cell cycle. We aimed to investigate the combination of drugs that therapeutically target histone deacetylase (HDAC) and the key cell cycle regulator cyclin-dependent kinase (CDK) in pancreatic cancer. We used panobinostat, a pan-HDAC inhibitor and abemaciclib, an FDA-authorized CDK4/6 inhibitor for breast cancer. Our preliminary *in vitro* results in pancreatic cancer cells shows synergistic cytotoxicity of the combination when administered concurrently. Additionally, the proliferation and clonogenic survival of pancreatic cancer cells significantly decreased as a result of the combined therapy. Our mechanistic research on how this potent combination affects histone modifications, gene expression, and cell cycle regulation will shed light on interactions between epigenetic modifications and cell cycle in pancreatic cancer cell death. Our *in vitro* findings indicate that combining medications that pharmacologically target two crucial components of pancreatic cancer proliferation has a significant potential for treating this deadly condition and, as such, merits additional research.

The College of Pharmacy and Health Sciences at St. John's University in New York provided funding for this study together with the support from the National Institute of General Medical Sciences (Award Number R16GM145557).

# Overcoming Cetuximab Resistance in Colorectal Cancer through Inhibition of HGF Processing

Vivian Jones,<sup>1</sup> Ramona Graves-Deal,<sup>2</sup> Galina Bogatcheva,<sup>2</sup> Zheng Cao,<sup>2</sup> James Higginbotham,<sup>2</sup> Sarah Harmych,<sup>1</sup> Marisol Ramirez,<sup>2</sup> Qi Liu,<sup>2</sup> Gregory Ayers,<sup>2</sup> James Janetka,<sup>3</sup> and Bhuminder Singh<sup>2</sup>

<sup>1</sup>Vanderbilt Univ; <sup>2</sup>Vanderbilt University Medical Center; and <sup>3</sup>Washington University

**Abstract ID 55700**

**Poster Board 434**

Cetuximab is a monoclonal antibody against epidermal growth factor receptor (EGFR) and can prolong survival in metastatic colorectal cancer (CRC) patients. However, therapeutic resistance can limit its efficiency and use. Our lab has previously identified that the activation of receptor tyrosine kinases (RTKs) MET and RON contributed to cetuximab resistance. In the absence of activating mutations of MET and RON, the activity of these RTKs depends on the availability of their ligands, hepatocyte growth factor (HGF) and hepatocyte growth factor-like (HGFL), respectively. To become biologically active, the inactive precursors of HGF and HGFL must be processed by serine proteases (HGFA, matriptase, and hepsin). A survey of TCGA datasets indicated that MET and HGF were overexpressed in several CRC CMS subtypes. We found that the addition of recombinant human HGF conferred cetuximab resistance to cetuximab-sensitive cells (CC). A cetuximab-resistant phenotype was also observed in cetuximab-sensitive cells we engineered to overexpress HGF (CC-HGF). Cetuximab resistance induced by HGF addition or overexpression could be overcome by downstream inhibition with crizotinib, a multi-targeted RTK inhibitor. Our next goal was to investigate whether we could target the pathway upstream. Our TCGA analysis did not show any consistent overexpression of the serine proteases. Hepatocyte growth factor activator inhibitor type 1 and 2 (HAI-1/2) are two Kunitz-type serine protease inhibitors. HAI-1 displayed significantly reduced expression in all CMS subtypes in the TCGA datasets. We demonstrated that upstream inhibition by the addition of recombinant human HAI-1 overcomes cetuximab resistance in CC-HGF cells. ZFH7116 is a small molecule inhibitor of the serine proteases that mimics HAI-1 activity. ZFH7116 suppressed HGF cleavage and maturation in our cetuximab-resistant SC and CC-CR cell lines. We observed a cooperative effect of ZFH7116 with cetuximab to reduce SC and CC-CR cell growth in 3D collagen cultures. We are currently investigating if ZFH7116 can overcome cetuximab resistance in CC-HGF. Collectively, our findings suggest that inhibiting HGF cleavage and processing may be a unique strategy for overcoming EGFR-targeted therapy resistance in colorectal cancer.

# Targeting Epigenetic Modification of T-Cell Inflamed Signature to Enhance Immune Checkpoint Inhibitors Response in Small Cell Lung Cancer

Manar Z. Almotawa,<sup>1</sup> Sarah A. Albasha,<sup>2</sup> Abdulmonem A. Alsaleh,<sup>2</sup> Noura N. Alibrahim,<sup>2</sup> Zaheda H. Radwan,<sup>2</sup> Yousef N. Alhashem,<sup>2</sup> Jenan Almatouq,<sup>2</sup> and Mariam K. Alamoudi<sup>3</sup>

<sup>1</sup>Department of Respiratory Therapy, Mohammed Al-Mana College for Medical Sciences; <sup>2</sup>Department of Medical Laboratory, Mohammed Al-Mana College for Medical Sciences; and <sup>3</sup>Department of Pharmacology, College of Pharmacy, Prince Sattam bin Abdulaziz University

Abstract ID 53622

Poster Board 435

Small cell lung cancer (SCLC) is a more aggressive type of lung cancer with a worse prognosis. Immune checkpoint inhibitors (ICIs) showed effectiveness against SCLC, however, the response rate was low. Several studies have reported that therapeutic efficacy of ICIs was improved when the tumor microenvironment (TME) exhibited inflamed phenotype including the expression of a T-cell inflamed signature which is a set of genes associated with T-cells and dendritic cells anti-tumor response. The induction of this signature can predict ICI effectiveness. However, epigenetic modifications such as DNA methylation can switch the TME into non-inflamed phenotype and eventually lead to ICI resistance. The aim of the study was to investigate the alterations in DNA methylation levels of T-cell inflamed signature genes in SCLC. Publicly available 450K DNA methylation array data of SCLC was used for our *in silico* analysis. CpG sites at promoter region of the T-cell inflamed genes were profiled, evaluated, and differentially methylated sites with a methylation difference ( $\Delta\beta$ ) of  $\geq 5\%$  were selected. The investigation was conducted on a dataset containing 13 controls and 11 SCLC cases. The analysis revealed that 18 of the total 37 T-cell inflamed signature genes, including *CCL2*, *CCL5*, *CD27*, *CD276*, *CD4*, *CMKLR1*, *FOXP3*, *GZMB*, *GZMK*, *IDO1*, *IFNG*, *IRF1*, *LAG3*, *NKG7*, *PRF1*, *PSMB10*, *TIGIT*, and *TNF*, had at least one differentially methylated site at the promoter area and 15 of them had at least two sites. The differentially methylated genes were hypermethylated in SCLC with methylation differences ranging between 5 % and 36 %. Interestingly, *LAG3* and *PRF1* were the most densely methylated genes with eight differentially methylated sites at the promoter region (average methylation difference = 23% and 17%, respectively). Our discovery of changes in DNA methylation status of T-cell inflamed genes in SCLC can open a novel avenue for targeting this epigenetic modification to reprogram TME and promote ICI susceptibility. Moreover, our data provided support for a novel therapeutic approach of combining hypomethylating agents such as decitabine or azacytidine with ICIs to improve their outcomes in SCLC. However, additional *in vitro* and *in vivo* studies are required to validate our results.



# Critical Role of OGT-mediated Novel NF- $\kappa$ B O-GlcNAcylation in Pancreatic Cancer

Aishat Motolani,<sup>1</sup> Matthew Martin,<sup>1</sup> Benlian Wang,<sup>2</sup> Guanglong Jiang,<sup>3</sup> Yunlong Liu,<sup>3</sup> and Tao Lu<sup>4</sup>

<sup>1</sup>Pharmacology and Toxicology, Indiana School of Medicine; <sup>2</sup>Case Western Reserve University; <sup>3</sup>Medical and Molecular Genetics, Indiana University School of Medicine; and <sup>4</sup>Pharmacology and Toxicology, Indiana University School of Medicine

**Abstract ID 13965**

**Poster Board 436**

Pancreatic ductal adenocarcinoma (PDAC) has one of the highest mortalities of all malignancies, with a mere 5-year survival of ~10%. However, the current first-line treatments have poor patient outcomes, highlighting the urgent need for innovative therapeutics. The nuclear factor  $\kappa$ B (NF- $\kappa$ B) is a crucial transcription factor frequently activated constitutively in PDAC. It mediates the transcription of oncogenic and inflammatory genes that facilitate multiple PDAC phenotypes. Thus, a better understanding of the mechanistic underpinnings of NF- $\kappa$ B activation holds substantial promise in PDAC diagnosis and new therapeutics. The purpose of this study is to identify novel regulation of NF- $\kappa$ B, with the aim of providing new diagnostic and therapeutic strategies for PDAC. Here, we report protein O-GlcNAc transferase (OGT) - mediated NF- $\kappa$ B activation through novel serine O-GlcNAcylation of its p65 subunit. We show that overexpression of serine-to-alanine (S-A) mutant at the O-GlcNAcylation site impaired NF- $\kappa$ B nuclear translocation and transcriptional activity in PDAC cells. Moreover, these S-A p65 mutants downregulate NF- $\kappa$ B-target genes important to major cancer hallmarks and inhibit cellular proliferation, migration, and anchorage-independent growth of PDAC cells compared to WT-p65. Interestingly, this modification happens downstream of the inhibitor of NF- $\kappa$ B (I $\kappa$ B $\alpha$ ) degradation. Collectively, we have identified novel OGT-mediated serine O-GlcNAcylation of NF- $\kappa$ B and determined its mechanistic and cellular function in driving PDAC phenotypes. Thus, our study holds great significance as it uncovers a potential strategy for effective therapeutics development for PDAC patients.

# Inhibition of Autophagy and MEK Promotes Ferroptosis in Lkb1-Deficient Kras-Driven Lung Tumors

Vrushank Bhatt,<sup>1</sup> Taijin Lan,<sup>1</sup> Wenping Wang,<sup>1</sup> Jerry Kong,<sup>1</sup> Eduardo Cararo Lopes,<sup>1</sup> Khoosheh Khayati,<sup>1</sup> Jianming Wang,<sup>1</sup> Akash Raju,<sup>1</sup> Michael Rangel,<sup>1</sup> Enrique Lopez,<sup>1</sup> Zhixian Sherrie Hu,<sup>1</sup> Xuefei Luo,<sup>1</sup> Xiaoyang Su,<sup>1</sup> Eileen White,<sup>1</sup> and Jessie Yanxiang Guo<sup>1</sup>

<sup>1</sup>Rutgers Cancer Institute of New Jersey

Abstract ID 22421

Poster Board 437

Tumor suppressor Liver Kinase B1 (LKB1) activates 5'-adenosine monophosphate protein kinase (AMPK) and maintains energy homeostasis in response to energy crises. LKB1 and KRAS are the third most frequent co-mutations detected in non-small cell lung cancer (NSCLC), causing aggressive tumor growth and metastases. Unfortunately, standard treatment with RAS-RAF-MEK-ERK signaling pathway inhibitors has minimal therapeutic efficacy in LKB1-mutant KRAS-driven NSCLC. Thus, identifying a novel therapy for patients harboring co-mutations in LKB1 and KRAS is urgently needed. Autophagy degrades and recycles the building blocks for cancer cells to survive metabolic challenges. Using genetically engineered mouse models (GEMMs), we have previously demonstrated that autophagy compensates for Lkb1 loss for Kras-driven lung tumorigenesis; loss of an autophagy-essential gene *Atg7* dramatically impaired tumor initiation and tumor growth in *Kras*<sup>G12D/+</sup>;*Lkb1*<sup>-/-</sup> (KL) lung tumors. This is in sharp contrast to *Lkb1* wild-type (WT) (*Kras*<sup>G12D/+</sup>;*p53*<sup>-/-</sup> (KP)) tumors that are less sensitive to autophagy gene ablation. To further value our discoveries in clinical translational ability, we treated mouse lung tumor-derived cell lines (TDCLs) with FDA-approved autophagy inhibitor hydroxychloroquine (HCQ) and MEK inhibitor Trametinib and found that the combination treatment displayed synergistic anti-proliferative effects in KL TDCLs compared to KP TDCLs. To elucidate the underlying mechanism of increased sensitivity of KL TDCLs to Trametinib by autophagy ablation, we performed metabolomic profiling of KL TDCLs with Trametinib, HCQ, or combination treatment and found that several glycolytic and TCA cycle intermediates, amino acids, and ATP levels were significantly upregulated upon treatment with Trametinib, which were significantly reduced by the combination treatment. In addition, the combination treatment significantly reduced mitochondrial membrane potential, basal respiration, and ATP production in KL TDCLs. In vivo studies using tumor allografts, genetically engineered mouse models (GEMMs), and patient-derived xenografts (PDXs) showed anti-tumor activity of the combination treatment on KL tumors, but not in KP tumors. Moreover, we found increased lipid peroxidation indicative of ferroptosis in KL TDCLs and KL PDX tumors with the combination treatment compared to the single agents. Finally, treatment with a ferroptosis inhibitor rescued the reduced KL allograft tumor growth caused by the combination treatment. Taken together, our observations indicate that autophagy upregulation in KL tumors causes resistance to Trametinib treatment by maintaining energy homeostasis for cell survival and inhibiting ferroptosis. Therefore, a combination of autophagy and MEK inhibition could be a novel therapeutic strategy to specifically treat LKB1-deficient KRAS-driven NSCLC.

This research has been supported by New Jersey Commission on Cancer Research Predoctoral Fellowship, Steven Cox Scholarship, GO2 Foundation for Lung Cancer Research Award, American Cancer Society Research Scholar Award, and NIH-R01 grant.

# Examining the DNA Methylation Profile of Childhood Solid Tumors to Identify Novel Therapeutically Targeted Sites

Sarah A. Albasha,<sup>1</sup> Manar Z. Almotawa,<sup>2</sup> Abdulmonem A. Alsaleh,<sup>1</sup> Noura N. Alibrahim,<sup>1</sup> Mariam K. Alamoudi,<sup>3</sup> Zahiah F. Al Mohsen,<sup>4</sup> Yahya Aldawood,<sup>1</sup> Hayyan A. Al-Taweil,<sup>1</sup> Fatimah J. Al Shaikh,<sup>5</sup> and Jenan Almatouq<sup>1</sup>

<sup>1</sup>Department of Medical Laboratory, Mohammed Al-Mana College for Medical Sciences; <sup>2</sup>Department of Respiratory Therapy, Mohammed Al-Mana College for Medical Sciences; <sup>3</sup>Department of Pharmacology, College of Pharmacy, Prince Sattam bin Abdulaziz University; <sup>4</sup>Department of Foundation Year, Mohammed Al-Mana College for Medical Sciences; and <sup>5</sup>Department of Physical Therapy, Mohammed Al-Mana College for Medical Sciences

**Abstract ID 53598**

**Poster Board 438**

Solid tumors in children represent approximately 30% of all pediatric cancers. The most prevalent types are Wilms tumor, retinoblastoma, neuroblastoma, and Ewing's sarcoma. The literature suggested that there is a degree of similarity between these conditions (such as age of diagnosis, prognosis, etc.), indicating that they may share a similar pathogenesis. The objective of our study was to investigate the DNA methylation profile of common childhood solid tumors in order to find a common signature that can be used to understand the underlying common molecular mechanism and to identify new pharmacological targets. This was an in silico study which used publicly available data from a DNA methylation array. Illumina 450K array datasets of the four conditions were downloaded from the GEO data repository and processed on RStudio. Differentially methylated sites were selected based on scoring Student's t-test  $P$ -value  $\leq 0.001$  and a methylation difference ( $\Delta\beta$ )  $\geq 20\%$ . Differentially methylated genes were defined as genes having at least two differentially methylated sites according to the human GRCh37/hg19 annotation. The study included 82 controls and 357 cases of childhood solid tumors. The analysis revealed that there were 13,472 novel differentially methylated sites that shared a common methylation profile between all the tumors. Using the hierarchical clustering method, the differentially methylated sites properly clustered all cases of childhood solid tumors. In addition, the analysis identified 17 differentially methylated genes that were involved in cell-cell communication, signal transduction and immune system pathways. The novel discovery of the common differentially methylated sites and genes among common childhood solid tumors provided an insight towards understanding their shared molecular pathogenesis. In addition, the identified candidate genes can be used as biomarkers for the clinical diagnosis and as therapeutic pharmacoepigenomic targets of childhood solid tumors.

# ERO1a Expression is Required for Secretion of Extracellular Matrix and Promotes Lung Cancer Progression

Maria Voronkova,<sup>1</sup> Brennan D. Johnson,<sup>2</sup> Wei-Chih Chen,<sup>2</sup> Gangqing Hu,<sup>2</sup> Lori Hazlehurst,<sup>1</sup> and John Koomen<sup>3</sup>

<sup>1</sup>West Virginia Univ; <sup>2</sup>West Virginia University; and <sup>3</sup>H. Lee Moffitt Cancer Center and Research Institute

**Abstract ID 27846**

**Poster Board 439**

Lung cancer is responsible for more deaths every year than breast, prostate, and colon cancers combined, yet patient treatment options are still limited. We aimed to characterize a role of a new potential therapeutic target, ERO1a, in non-small cell lung cancer (NSCLC). Physiologically, endoplasmic reticulum oxidoreductase 1 alpha (ERO1a) participates in formation of disulfide bonds crucial to protein folding in the endoplasmic reticulum (ER). However, high ERO1a expression was shown to be a poor prognostic indicator in multiple cancer types. While the contribution of high ERO1a levels to increased tumor burden and metastatic potential has been demonstrated, the downstream mechanisms are poorly understood. In this study, CRISPR strategies were utilized to knockout ERO1a in two lung cancer cell lines, PC-9 and HCC4006. The knockout variants demonstrated a significant reduction in colony and tumor sphere formation while no changes in cell proliferation and anoikis were observed. This finding correlated with increased survival and decreased tumor burden in SCID-Beige mice injected with ERO1a knockout cells compared to control cells ( $p < 0.0045$  Log Rank Test). As ERO1a is an ER resident protein, we hypothesized that ERO1a may alter the secretome produced by NSCLC. In support of our hypothesis, the reduction in colony-formation of ERO1a knockout clones can be rescued by media conditioned by control cells. Moreover, this effect is lost when conditioned media is subjected to heat denaturation. Together these data suggest that an ERO1a-dependent secreted protein is responsible for colony formation in lung cancer cells. Analysis of publicly available lung cancer proteomic data set (CPTAC) shows that high ERO1a expression correlates with enrichment in hallmarks of cancer, such as inflammatory response and epithelial-to-mesenchymal transition (EMT). Moreover, high ERO1a expression correlates with increased levels of multiple matrix proteins including Laminin 332, PLOD2, and LOXL2. These findings in primary patient specimens strongly agreed with the knockout cell line models showing that ERO1a expression is required for secretion of matrix associated proteins in both 2D and 3D systems. We are currently exploring whether the reduced expression of LOXL2 or LAMC2 is responsible for decreased colony formation observed in ERO1a-depleted cells. Taken together, our data indicate that ERO1a modifies the local tumor microenvironment and is an attractive target for therapeutic intervention in non-small cell lung cancer.

# Metabolic Rewiring and Mechanism of Action of an Antiepileptic Drug Repurposed for its Potential in Glioblastoma

Anjali Yadav,<sup>1</sup> Shraddha Bhutkar,<sup>2</sup> and Vikas Dukhande<sup>2</sup>

<sup>1</sup>St. John's Univ; and <sup>2</sup>St. John

Abstract ID 29107

Poster Board 440

Glioblastoma multiforme (GBM), a grade IV malignant astrocytoma, is a highly proliferative primary malignant brain tumor with a dismal 5-year survival rate of ~5%. Current treatment strategies including surgery, radiation, and chemotherapy have limited success due to resistance to the standard chemotherapeutic temozolomide (TMZ). Moreover, other drug therapies have difficulty permeating the blood brain barrier, and tumor invasion in brain regions makes surgical removal challenging. The dire need of a new chemotherapeutic has thus led us to repurpose an FDA-approved drug stiripentol (STP) with lactate dehydrogenase (LDH) as its putative target. LDH is a key glycolytic enzyme in the rewiring of cancer metabolism. In fact, decreased expression of an LDH isoform has been shown to reduce metastasis and increase apoptosis in GBM. Our previous study demonstrated efficacy of STP in U87, U138, LN229 and SW1088 GBM cells: STP inhibited proliferation, colony-forming potential, and 3D spheroid growth. STP also caused G2/M phase arrest of the cell cycle. We also found STP to be effective against TMZ-resistant cells and STP had a relatively high safety profile in normal human dermal fibroblast cells. Our current studies are mainly focused on elucidating the targets and mechanism of action of STP in GBM. We will study whether LDH and GABA receptors are direct or indirect targets of STP using silencing and overexpression-based strategies. A phospho-kinase array will aid us in identifying pathways implicated in STP's mechanism of action. In addition, we will study the effect of STP on the Warburg effect and other metabolic alterations in GBM cells. Seahorse assay for extracellular acidification rate (ECAR) and oxygen consumption rate (OCR), as well as mitochondrial membrane potential (MMP) and reactive oxygen species (ROS) generation assays will be used to elucidate the metabolic effects of STP in GBM cells. Additionally, we will determine the mechanism of cell death mediated by STP's actions. The results of our study can elucidate the mechanistic basis of STP's anticancer effects and help in developing novel chemotherapeutics for GBM.

This research was supported by an award from the National Institute of General Medical Sciences of the National Institutes of Health under Award Number R16GM145557 and SC2GM125550 and by funds from the College of Pharmacy and Health Sciences, St. John's University, NY

# A Novel Fluoropyrimidine Drug to Treat Recalcitrant Colorectal Cancer

Naresh Sah,<sup>1</sup> Pamela Luna,<sup>2</sup> Chinnadurai Mani,<sup>2</sup> William Gmeiner,<sup>3</sup> and Komaraiah Palle<sup>4</sup>

<sup>1</sup>Texas Tech Univ HSC; <sup>2</sup>Texas Tech University Health Sciences Center; <sup>3</sup>Wake Forest University School of Medicine; and <sup>4</sup>Texas Tech Univeristy Health Sciences Center

Abstract ID 22462

Poster Board 441

## **Purpose:**

Colorectal cancers (CRCs) are the third leading cause of cancer-related death. Most of these deaths are exclusively due to recalcitrant disease. The sensitive form of CRCs progresses to a more metastatic and resistant form mainly due to a lack of more potent and safer chemotherapeutics as chemotherapeutic agents are the mainstay treatment for CRCs. The fluoropyrimidine (FP) drug 5-fluorouracil (5-FU) is the backbone of conventional chemotherapy regimens (e.g., FOLFOX and FOLFIRI). The several serious side effects and ineffectiveness of 5-FU along with the urgency to combat these recalcitrant CRCs necessitates the need to develop safer and more potent FP. We aimed to develop a new second-generation nanoscale FP polymer (CF10) which is safer and more potent in several preclinical models. Additionally, we also aimed to identify if CF10 blocks thymidylate synthase (TS)-mediated pro-metastatic activities and overcomes 5-FU resistance in CRCs.

## **Methods:**

We performed immunoblot to identify the markers for stalled replication forks (FANCD2, pChk1-S317) and DNA double-strand breaks (pChk2-T68, Rad51, pH2AX). We used an alkaline comet assay and immunofluorescence imaging to visualize the extent of DNA damage, followed by different treatments. The organoid culture of primary colon cancer cells was used to demonstrate the attenuation of primary colon cancer organoids. We used the Tet-on system to regulate TS expression in HCT-116 cells to further study the significance of enhanced TS as a factor in CRC metastatic progression and 5-FU resistance. Finally, we performed an invasion and migration assay to demonstrate that TS promotes pro-metastatic activities.

## **Results:**

In CRCs cells, CF10 effectively inhibited thymidylate synthase (TS), increased Top1 cleavage complex formation, and induced replication stress, whereas identical dosages of 5-FU were ineffective. The CF10 induces more replication stress in rat, mouse, human-established cell lines, and primary CRC cells compared to 5-FU. In vivo, we observed that CF10 possesses significantly higher anti-tumor activity when compared with the control. Additionally, CF10 treatment improved survival (84.5 days vs 32 days;  $P < 0.0001$ ) relative to 5-FU in an orthotopic HCT-116-*Luc* colorectal cancer mice model that spontaneously metastasized to the liver. Interestingly, we saw a reduction in metastatic tumors in the CF10 treatment group. This led us to hypothesize further that CF10 could be inhibiting the TS-mediated epithelial-mesenchymal phenotype in CRCs. We noticed that TS overexpression promoted cell migration and invasion. Strikingly, we discovered that CF10 suppresses the growth of TS-expressing primary CRC organoids, as seen by the reduction of spheroid formation.

## **Conclusion:**

CF-10 compound induces more replication stress compared to a similar concentration of 5-FU. The overexpression of TS increases epithelial-mesenchymal markers, migration, and invasion. Our findings show that CF-10 may be a successful candidate for treating recalcitrant CRCs and potential to overcome 5-FU resistance.

# Use of CRISPR/Cas9 with Homology-Directed Repair (HDR) to Gene-Edit Topoisomerase II $\beta$ in Human Leukemia K562 Cells: Generation of a Resistance Phenotype

Jessika Carvajal-Moreno,<sup>1</sup> Xinyi Wang,<sup>2</sup> Victor A. Hernandez,<sup>2</sup> Jack C. Yalowich,<sup>2</sup> and Terry Elton<sup>2</sup>

<sup>1</sup>Ohio State Univ; and <sup>2</sup>THE OHIO STATE UNIVERSITY

**Abstract ID 18186**

**Poster Board 442**

DNA topoisomerase II $\beta$  (TOP2 $\beta$ /180; 180 kDa) is a nuclear enzyme that regulates DNA topology by generation of short-lived DNA double-strand breaks primarily during transcription. TOP2 $\beta$ /180 is a target for a number of DNA damage-stabilizing anticancer drugs, whose efficacy is often limited by chemoresistance. Our laboratory demonstrated reduced levels of TOP2 $\beta$ /180 in an acquired etoposide-resistant K562 clonal cell line, K/VP.5. We hypothesized that lower expression of TOP2 $\beta$  in K/VP.5 cells leads to resistance to TOP2 $\beta$  specific drugs such as XK469. To test this hypothesis, a stop codon was added at the TOP2 $\beta$  gene exon 19/intron 19 boundary (AGAA/GTAA  $\rightarrow$  ATAG/GTAA) in parental K562 cells (which contain four TOP2 $\beta$  alleles) by CRISPR/Cas9 editing with homology-directed repair (HDR) to disrupt production of full length TOP2 $\beta$ /180. Gene-edited clones were identified and verified by quantitative polymerase chain (qPCR) and Sanger sequencing, respectively. Characterization of a TOP2 $\beta$  gene-edit clone, with all four TOP2 $\beta$  alleles edited, revealed degradation of TOP2 $\beta$ /180 mRNA and the absence of TOP2 $\beta$  protein. The lack of TOP2 $\beta$ /180 protein resulted in resistance to growth inhibition induced by XK469, a TOP2 $\beta$  specific inhibitor; in addition, preliminary studies suggested partial resistance to Etoposide. Together, results support the important role of TOP2 $\beta$ /180 as determinant of sensitivity/ resistance to TOP2 $\beta$ -targeting drugs.

# Amphotericin A21 reduces cell proliferation and modulates anti- and pro-apoptotic proteins in MCF-7 cells.

Lourdes Rodriguez-Fragoso,<sup>1</sup> Rubi Escobar-Resendiz,<sup>2</sup> Ivan Ortega-Blake,<sup>3</sup> and Arturo Galvan-Hernandez<sup>3</sup>

<sup>1</sup>Univ Autonoma Del Estado de Morelos; <sup>2</sup>Universidad Autonoma del Estado de Morelos; and <sup>3</sup>Universidad Nacional Autonoma de Mexico

Abstract ID 17083

Poster Board 443

Amphotericin A21 (AmB-A21) has been developed and evaluated by our research group. It has been found that AmB-A21 induce cytotoxicity, apoptosis, and reduced lung cancer cells invasion. Therefore, our aim was to evaluate the effect of AmB-A21 on cell proliferation and apoptosis in MCF7 cells.

**Methods:** MCF-7 cells (ATCC HTB-22), from breast cancer were used. They were cultured at 37°C, with 5% CO<sub>2</sub>, in supplemented DMEM HG medium. A dose-response curve was performed for cisplatin and AmB-A21 to obtain the IC<sub>25</sub>. Then cells were treated for all experiments with cisplatin 24.38 μM or AmB-A21 103.62 μM; cells without treatment were used as negative control. For cell proliferation cells were seeded into a 96-well plate (1,000/well), incubated for 24 h and then treated with cisplatin and AmB-A21 for 3 days; after time a MTT assay was performed. For the analysis of cell death, cells were seeded into 6-well plate (250,000/well) and incubated for 24h at 5% CO<sub>2</sub> and 37°C, cell death was identifying using an acridine orange and ethidium bromide staining assay. BCL-2 and BAX expression was carried out by an immunocytochemistry assay, it was used H<sub>2</sub>O<sub>2</sub> 30% as positive control. Finally, active caspase 9 was quantified using the Caspase-Glo® 9 kit following the manufacturer's instructions.

**Results:** Our results showed that AmB-A21 reduced approximately 50% of proliferation compared to control cells, whereas cisplatin reduced about 75% of cell proliferation at 72 h (p<0.05). The analysis of cell death revealed that AmB-A21 induced death by apoptosis in MCF-7 cells. The presence of apoptosis in cells treated with antineoplastic drugs increased 40% in cells treated with AmB-A21 and 60% with cisplatin (p<0.05) as compared with negative control. It was observed presence of cells in necrosis in presence of cisplatin, but not AmB-A21. It is well known that caspase 9 and BAX are proteins that induce the progression to apoptosis, whereas BCL-2 is involved in the evasion of cell death, then we proceeded to evaluate those proteins. We found that nuclear BAX expression was increased in those cells treated with AmB-A21 (70%) as well as in those cells treated with cisplatin group (60%) as compared with positive control (p<0.05). But nuclear BCL-2 expression was reduced in cells treated with AmB-A21 (4-fold) and with cisplatin group (p<0.05) as compared with positive control. We found that AmB-A21 increased 30% caspase 9 activity whereas cisplatin induces 25% as compared with positive control (p<0.05).

**Conclusion:** Our results demonstrated that AmB-A21 has antineoplastic effects in MCF-7 cells by reducing cell proliferation and inducing apoptosis. AmB-A21 has the potential for being considered as a antineoplastic drug.



# Synthesis And Anticancer Properties of Polyrhodanine Copper Nanocomposites

Sarbani Ghoshal,<sup>1</sup> Nickayla Spence,<sup>1</sup> Moni Chauhan,<sup>1</sup> Qiaxian Johnson,<sup>2</sup> and Bhanu P. Chauhan<sup>2</sup>

<sup>1</sup>Queensborough Community College, CUNY; and <sup>2</sup>William Patterson University

**Abstract ID 53568**

**Poster Board 444**

Rhodanine (derived from thiazolidine), a heterocyclic compound, plays an essential role in the biological system of humans. Its derivatives are present in drugs used in antibiotics, antiviruses, antidiabetics, and antifungals. Rhodanine and its derivatives can prevent HIV-1 integrase, JSP-1 Phosphates, RNA polymerase, hepatitis C virus NS5B polymerase, and PMT1 mannosyl transferase. We hypothesize that the shape-controlled synthesis of Polyrhodanine will provide an exciting perspective for diagnosing and treating diseases, including cancer. In our research, we investigate the synthesis of Polyrhodanine in a single-step oxidation-reduction reaction in the presence of transition metals in the microwave. Two morphologies for Polyrhodanine have been identified depending on the metal: core-shell and nanotubular. In the first step of the reaction, the rhodamine monomer forms a one-dimensional complex with the metal ions (Copper (I) Acetate) due to coordinative interaction. In the second step, the oxidation of Rhodanine and the reduction of metal ions result in the polymerization of Rhodanine into core-shell nano-micro spheres with embedded metal nanoparticles. The product is analyzed via Infra-Red and UV-vis Spectroscopy, SEM (Scanning Electron Microscopy), EDX (Energy Dispersive X-ray spectroscopy), and TEM (Transmission Electron Microscopy). Subsequently, we tested our compound in a human lung cancer cell line, namely A549, to measure cell viability by the colorimetric MTT (3-[4,5-dimethylthiazol-2-yl]-2,5 diphenyl tetrazolium bromide) assay. The MTT assay is used to measure cellular metabolic activity as an indicator of cell viability and cytotoxicity. The underlying principle is the ability of NADPH-dependent cellular oxidoreductase enzyme secreted by the mitochondria to convert the tetrazolium dye into insoluble formazan crystals. More formazan crystal formation indicates more viable cells. In our experiment, 20,000 cells were plated in each well of a 96-well plate and treated with the compound for 48 hours to investigate the viability of lung cancer cells. Our data shows viability of A549 cells decreases in a dose dependent manner with treatment concentrations ranging from 0.01  $\mu$ M to 1  $\mu$ M in comparison to cells in the DMSO control treatment group. Our present focus is to investigate the cell signaling pathways, by real-time PCR and Western blotting, that could be altered by our compound to identify expression of key genes and protein, that are known to be dysregulated in lung cancer. Future studies will focus on investigating effect in other cancer cell lines, including triple negative breast cancer cells.

Acknowledgements: Queensborough Community College NIH Bridges to Baccalaureate Program 5R25GM065096-21 and Research Foundation, CUNY.

# Defining the Role of Mitochondrial Dynamics in Regulating PDAC Cell Sensitivity to KRAS and ERK Inhibition

Amber Amparo,<sup>1</sup> Kristina Drizyte-Miller,<sup>1</sup> Claire Gates,<sup>1</sup> Adrienne D. Cox,<sup>1</sup> Kirsten L. Bryant,<sup>1</sup> and Channing J. Der<sup>1</sup>

<sup>1</sup>UNC Lineberger Comprehensive Cancer Center

**Abstract ID 26960**

**Poster Board 445**

Pancreatic ductal adenocarcinoma (PDAC) is driven by oncogenic activation of KRAS in over 95% of patients. Recent evidence suggests that mutant KRAS activation rewires cancer cell metabolism, altering mitochondrial morphology and function. KRAS-mutant PDAC are characterized by fragmented mitochondria. This is mediated through activation of the downstream RAF-MEK-ERK effector signaling pathway, which leads to the phosphorylation of mitochondrial fission protein DRP1, driving mitochondrial fragmentation to support PDAC growth. Consistent with this role, we determined that treatment with the ERK1/2-selective inhibitor SCH772984 (ERKi) caused mitochondrial fusion and inhibited PDAC cell growth. Similarly, we found that treatment of KRASG12D-mutant PDAC cell lines with the KRASG12D-selective inhibitor MRTX1133 (KRASi) also promoted increased mitochondrial fusion and suppressed growth. However, whether fragmented mitochondria support KRAS- and ERK-dependent PDAC proliferation remains unresolved. We hypothesized that preventing mitochondrial fusion by siRNA silencing of the mitochondrial fusion proteins OPA1 and MFN1, promoting fragmented mitochondria, will drive resistance to inhibition of KRAS-ERK signaling. To test this, we used siRNA to suppress the expression of OPA1 or MFN1, which caused a hyper-fragmented mitochondrial phenotype. These cells were refractory to ERKi-stimulated mitochondrial fusion and retained highly fragmented mitochondria but retained sensitivity to growth inhibition. Thus, mitochondrial fragmentation alone cannot support ERK-dependent PDAC growth. Ongoing studies are addressing whether sustained mitochondrial fragmentation will drive resistance to direct KRAS inhibitors.

This project was supported by the Gump Family Undergraduate Research Fund administered by Honors Carolina, the American Society for Pharmacology and Experimental Therapeutics SURF Award, and Carolina Summer Fellowship Program through the UNC Department of Pharmacology.

# Prognostic and Therapeutic Implications of Genes Associated with Apoptosis and Protein-Protein Interactions in Triple-Negative Breast Cancer

Getinent M. Adinew,<sup>1</sup> Samia S. Messeha,<sup>2</sup> Equar Taka,<sup>1</sup> Shade Ahmed,<sup>1</sup> and Karam F. Soliman<sup>3</sup>

<sup>1</sup>Florida A&M University; <sup>2</sup>Florida A&M Univ; and <sup>3</sup>Florida A&M Univ College of Pharmacy

Abstract ID 54503

Poster Board 446

Triple-negative breast cancer (TNBC) has historically had fewer treatment alternatives than other breast cancer types. Therefore, it is critical to explore and pinpoint potential biomarkers that could be utilized in treating TNBC. By doing this, we will significantly enhance a patient's prognosis and quality of life. Apoptosis-controlling genes could be manipulated to increase the death of cancer cells. It is essential to comprehend how the genes involved in the apoptotic pathway interact to identify potential therapeutic targets. Therefore, the current study is aimed to evaluate the gene expression, protein-protein interaction (PPI), and transcription factor interaction of 27 apoptosis-regulated genes in TNBC using integrated bioinformatics methods to assess the gene expression, protein-protein interaction (PPI) and transcription factor interaction. Our findings demonstrated that *CASP2*, *CASP3*, *DAPK1*, *TNF*, *TRAF2*, and *TRAF3* were substantially associated with the overall survival rate (OS) difference of TNBC patients. The results also show that breast tissue gene expressions of *BNIP3*, *TNFRSF10B*, *MCL1*, and *CASP4* were downregulated compared to normal breast tissue in UALCAN. At the same time, *BIK*, *AKT1*, *BAD*, *FADD*, *DIABLO*, and *CASP9* were downregulated in bc- GeneEx-Miner v4.5 mRNA expression (BCGM) databases. Based on the GO term enrichment analysis, the Cellular process (GO:0009987), which has about 21 apoptosis-regulated genes, is the top category in the biological process (BP), followed by biological regulation (GO:0065007). We identified 29 pathways, including p53, angiogenesis, and apoptosis signaling. We examined the PPIs between the genes that regulate apoptosis; *CASP3* and *CASP9* interact with *FADD*, *MCL1*, *TNF*, *TNFRSRF10A*, and *TNFRSF10*; additionally, *CASP3* significantly forms PPIs with *CASP9*, *DFFA*, and *TP53*, while *CASP9* with *DIABLO*. In the top 10 transcription factors, the androgen receptor (AR) interacts with five apoptosis-regulated genes ( $p < 0.0001$ ;  $q < 0.01$ ), followed by *RARA* (Retinoic Acid Receptor Alpha) ( $p < 0.0001$ ;  $q < 0.01$ ) and *RNF2* (Ring Finger Protein) ( $p < 0.0001$ ;  $q < 0.01$ ). Overall, the gene expression profile, the PPIs, and the apoptosis-TF interaction findings suggested that the 27 apoptosis-regulated genes might be used as promising targets in treating and managing TNBC. Furthermore, from a total of 27 key genes, *CASP2*, *CASP3*, *DAPK1*, *TNF*, *TRAF2*, and *TRAF3* were significantly correlated with poor overall survival in TNBC ( $p$ -value  $< 0.05$ ), which could play essential roles in the progression of TNBC and provide attractive therapeutic targets that may offer new candidate molecules for targeted therapy. It was concluded from this study that genetic alterations altering apoptosis could be possible biomarkers for the prognosis and facilitate the search for alternative treatment targets for TNBC.

This research was supported by grants from the National Institute of Minority Health and Health Disparities of the National Institutes of Health through Grant Number U54 MD 007582

# Calcium Channel Blockers as Novel Therapeutic Agents for Triple-Negative Breast Cancer

Destiny Lawler,<sup>1</sup> and Robert L. Copeland<sup>2</sup>

<sup>1</sup>Howard Univ; and <sup>2</sup>Howard Univ, Coll of Med

**Abstract ID 21157**

**Poster Board 447**

Breast cancer is a prevalent disease among women in the U.S. One of the most aggressive subtypes of breast cancer is triple-negative breast cancer (TNBC) and is predominantly seen in young African American (AA) women. TNBC is characterized by the lack of three receptors: estrogen, progesterone, and human epidermal growth factor receptor 2. Current treatment includes surgery, chemotherapy, and radiation, none of which are successful against TNBC. A signature for the disease is high levels of intracellular calcium. Therefore, components that regulate calcium could be a potential target for developing novel treatment.

Calcium signaling is immensely complex and maintenance of calcium homeostasis is strictly regulated. Calcium enters the intracellular space via voltage-gated calcium channels. Intracellular calcium is regulated by the gamma-butyrobetaine hydroxylase 1 (BBOX1) 1,4,5-inositol trisphosphate receptor 3 (IP3R3) complex on the endoplasmic reticulum (ER) and the store operated calcium entry (SOCE) mechanism. Binding of BBOX1 prevents IP3R3 ubiquitination. IP3R3 is responsible for protein stabilization, calcium homeostasis, and cellular bioenergetics. IP3R3 sends calcium from the ER to the mitochondria for mitochondrial function and glycolysis, ultimately leading to cell survival. This depletion of calcium in the ER activates the ER stromal interaction molecule 1 (STIM1) sensor to signal SOCE channels for calcium restoration back to the ER.

Based on this information, this study hypothesizes that calcium channel blockers (CCBs) also exert their effects intracellularly by acting as a BBOX1 antagonist. By blocking BBOX1, this causes protease degradation of IP3R3 and blocks mitochondrial function and glycolysis, ultimately leading to cell apoptosis. TNBC cells from AA and European American (EA) women were treated with CCBs in a dose-dependent and time-dependent manner. Cell viability assessment was performed to test the efficacy of drug treatment. Western blots and RT-PCR were performed for analysis of protein and RNA expression. Reactive oxygen species assay was used to test for oxidative stress. Our data has shown that various CCBs decrease cell proliferation in TNBC cells in a dose-dependent and time-dependent manner. In addition, ethnic differences were shown to be dependent on drug treatment. Therefore, this study presents CCBs as novel therapeutic agents for TNBC.

Support/Funding Information: NIH/NCI; HU/Georgetown Collaborative Partnership in Cancer Research (5P20CA242611-03)

# Adaptive Changes in Tumor Cells in Response to Reductive Stress

Leilei Zhang,<sup>1</sup> Jie Zhang,<sup>2</sup> Zhiwei Ye,<sup>2</sup> Aslam Muhammad,<sup>2</sup> John Culpepper,<sup>2</sup> Danyelle M. Townsend,<sup>1</sup> and Kenneth Tew<sup>3</sup>

<sup>1</sup>Medical University of South Carolina College of Medicine; <sup>2</sup>MUSC; and <sup>3</sup>Medical Univ of South Carolina

Abstract ID 20639

Poster Board 448

Reductive stress is characterized by an excess of cellular electron acceptors and can be linked with a number of human pathologies including increased cytotoxicity in cancer cells. In order to characterize cellular adaptations to reductive stress, we used step-wise, incremental selection to generate melanoma cell lines with acquired resistance to rotenone (ROT<sup>R</sup>, 5-fold), n-acetyl cysteine (NAC<sup>R</sup>, 2-fold), or dithiothreitol (DTT<sup>R</sup>, 23-fold) or rotenone (ROT<sup>R</sup>, 5-fold). Cells divided more rapidly in resistant lines and intracellular homeostatic redox- couple ratios (e.g., glutathione, NADPH) were shifted towards the reduced state. Resistance caused alterations in general cell morphology, but only ROT<sup>R</sup> cells had significant changes in mitochondrial morphology (higher numbers, and more swollen; isolated and more fragmented; decrease in networks; greater membrane depolarization). These changes were accompanied by lower basal oxygen consumption and maximal respiration rates and a more marked reliance on glycolysis for energy production. Whole cell flux analyses and mitochondrial function assays showed that NAC<sup>R</sup> and DTT<sup>R</sup> preferentially utilized TCA cycle intermediates, while ROT<sup>R</sup> used ketone body substrates such as D, L, b-hydroxybutyric acid. While NAC<sup>R</sup> and DTT<sup>R</sup> Each resistant line cells had constitutively elevated decreased levels of reactive oxygen species (ROS), in ROT<sup>R</sup> these were increased. This was accompanied by and spuriously inhibited/activated Nrf2, with concomitant decreased/increased expression of downstream gene products, such as glutathione S-transferase P in ROT<sup>R</sup>/ NAC<sup>R</sup> and DTT<sup>R</sup>. Adaptations to reductive stress also included enhanced expression/alteration of protein expression of proteins controlling the unfolded protein response (UPR). These included BiP, PDI, CHOP, ATF4, ATF6 and PERK and although expression patterns of these UPR proteins were distinct between the resistant cells, there was an enhancement of expression implying that resistance to reductive stress accompanies a constitutively increased UPR phenotype in each line, but does not result in cell death. Overall, while most tumor cell lines adapt to survive conditions of high oxidative stress, they are also flexibly capable of adapting various pathways to regulate growth and survival in conditions concentrations of drugs that would cause cell death throughof reductive stress.

This work was supported by grants from the National Institutes of Health (CA08660, CA117259, NCRR P20RR024485 - COBRE in Oxidants, Redox Balance and Stress Signaling) and support from the South Carolina Centers of Excellence program and was conducted in a facility constructed with the support from the National Institutes of Health, Grant Number C06 RR015455 from the Extramural Research Facilities Program of the National Center for Research Resources.

# Elucidating the Function of ABCA13 in SHH-Medulloblastoma

Joseph Miller,<sup>1</sup> Juwina Wijaya,<sup>2</sup> Giles W. Robinson,<sup>3</sup> Vikas Daggubati,<sup>4</sup> David R. Raleigh,<sup>4</sup> and John Schuetz<sup>2</sup>

<sup>1</sup>St. Jude Children's Research Hospital and University of Tennessee Health Science Center; <sup>2</sup>St. Jude Children; <sup>3</sup>St. Jude Children's Research Hospital; and <sup>4</sup>University of California San Francisco

Abstract ID 23062

Poster Board 449

Medulloblastoma (MB) is the most common malignant pediatric brain tumor. Of the four MB subtypes, Sonic Hedgehog Medulloblastoma (SHH-MB) is the most frequent MB subtype diagnosed in infants under 3 years of age. Targeted therapies of SHH-MB have focused on inhibition of Smoothed (SMO), the key transmembrane activator of the hedgehog (Hh) pathway. Unfortunately, SHH-MBs have evolved resistance to SMO inhibitors by developing mutations in the Hh pathway. To combat therapeutic resistance and advance SHH-MB therapy, the identification of novel, targetable Hh pathway regulators is required. Recently, we have identified a preponderance of mutations in the ATP-Binding Cassette Transporter A subfamily of lipid transporters among SHH-MB. Many of these mutations were found in the orphan transporter ABCA13 suggesting ABCA13 affects the Hh pathway. Proteomic and RNAseq data revealed ABCA13 levels increased upon Hh pathway activity. CRISPR/Cas9-mediated knockout of ABCA13 in NIH 3T3 cells (a standard cell model to study Hh pathway signaling) demonstrated disrupted Hh pathway signaling when activated with either SHH ligand or Smoothed Agonist (SAG) via measurement of GLI1 and Patched 1 (PTCH) protein level by western blot or GLI1 and PTCH mRNA levels by qPCR. Immunofluorescence microscopy data showed unexpected translocation of SMO into primary cilia in ABCA13 KO cells without activation of the Hh pathway. RNAseq of ABCA13 KO 3T3 cells under SHH ligand or SAG-activated conditions also showed downregulation of both Hh pathway genes and GLI target genes. Addition of ABCA13 back into ABCA13 KO cells via transfection partially rescued Hh pathway activity. CRISPR/Cas9-mediated knock-in of ABCA13 SHH-MB mutations into 3T3 cells showed no defects in Hh pathway activity when treated with SHH ligand or SAG via measurement of GLI1 and PTCH protein levels, indicating a possible gain of function for these mutations. Taken together, these results indicate that ABCA13 is required for optimal Hh pathway activity. Further elucidation of ABCA13's role in Hh pathway regulation may lead to novel treatments for SHH-MB.

**Acknowledgements:** Funding for the project was provided by the National Institute of Health (NIH) and the American Lebanese Syrian Associated Charities (ALSAC)

# HUNK regulation of IL-4 promotes polarization of tumor-associated macrophages in TNBC tumor microenvironment

Nicole Ramos Solis,<sup>1</sup> Elizabeth S. Yeh,<sup>1</sup> Mark H. Kaplan,<sup>1</sup> and Anthony M. Cannon<sup>1</sup>

<sup>1</sup>Indiana University School of Medicine

Abstract ID 16720

Poster Board 450

Triple-negative breast cancer (TNBC) is a type of breast cancer that does not express hormone receptors (estrogen receptor (ER) or progesterone receptor (PR) or human epidermal growth factor receptor 2 (HER2). Therefore, contrary to other types of breast cancer, TNBC is not sensitive to common endocrine therapy or HER2-targeted inhibitors. Recent new FDA approved treatments for TNBC include immunotherapy targets such as immune checkpoint inhibitors (ICI). Unfortunately, inadequate anti-tumor T-cell effector function and high abundance of tumor-associated macrophages (TAMs) have limited the efficacy of immune therapy. TAMs constitute one of the most abundant immune cell populations in mammary tumors. Within the tumor, TAMs can be polarized to classically activated M1-like and alternatively active M2-like phenotypes. M2-like macrophages contribute to cancer progression by inducing tumor angiogenic responses, promoting tumor growth and metastasis. In cancer, the polarization of macrophages toward an M2 phenotype is directed by cancer-cell-derived factors such as pleiotropic cytokines like interleukin-4 (IL-4). New knowledge suggests that IL-4 expression in cancer cells is regulated by the signal transducer and activator of the transcription 3 (STAT3) transcription factor. Intriguingly, we observed that Hormonally Up-Regulated Neu-Associated Kinase (HUNK), is responsible for IL-4 production through regulation of STAT3 in the 4T1 mammary tumor cell line, which is considered a metastatic TNBC model. We engineered 4T1 cells expressing HUNK and HUNK knockdown by shRNA. Our current data shows that 4T1 cells with HUNK knockdown have reduced HUNK expression, reduced levels of STAT3 phosphorylation, IL-4 production, and secretion compared to control 4T1 cells expressing HUNK. As well, we have observed that HUNK kinase activity is required for IL-4 production in 4T1 cells by showing that 4T1 HUNK knockdown cells that re-express wildtype HUNK rescue IL-4 production compared to 4T1 HUNK knockdown cells that re-express kinase inactive HUNK. Furthermore, we show that conditioned medium from 4T1 control cells induces M2-polarization of macrophages. The loss of IL-4 secretion in 4T1 HUNK knockdown cells corresponds to a reduced ability of conditioned medium from HUNK knockdown cells to induce alternative activation of macrophages. We also observed that HUNK has a significant effect on the presence of M2-like TAMs in the tumor microenvironment. Tumors derived from HUNK knockdown 4T1 cells have reduced M2-like TAMs compared to control tumors. Additional experiments are in progress to engineer 4T1 HUNK knockdown cells to re-express IL-4 and measure the ability of these cells to rescue the loss of M2-like TAMs in the tumor microenvironment. Furthermore, we will evaluate the pharmacological inhibition of HUNK and its effect on M2-like TAMs in the tumor microenvironment. The overall goal of these studies is to evaluate HUNK as a therapeutic target for TNBC metastasis by modulating the TAM population within the tumor microenvironment. Also, we aim to identify the HUNK signaling pathway that is responsible for pro-metastatic TAM function in TNBC.

Trainee Nicole Ramos Solis was supported by the Indiana University Immunology and Infectious Disease Training Program, NIH AI060519

# A Convolutional Neural Network Model classifies Beat-to-Beat Arterial Pressure Time-Series: Sex Stratification and Cardiovascular Risk Prediction

Nour Mounira Bakkar,<sup>1</sup> Abdalrhman Mostafa,<sup>2</sup> Mohamed Abdelhack,<sup>3</sup> and Ahmed F. El-Yazbi<sup>4</sup>

<sup>1</sup>American University of Beirut; <sup>2</sup>Mansoura University Hospitals; <sup>3</sup>Centre for Addiction and Mental Health; and <sup>4</sup>Alamein International University

Abstract ID 20324

Poster Board 99

Machine learning (ML) models have demonstrated impressive applicability in classifying hemodynamic signals according to disease-specific features of overt cardiovascular (CV) conditions like myocardial infarction and hypertension. However, there remains a pressing need for identifying subtle, subclinical deviations in hemodynamic time-series associated with early disease states, to predict prognosis and prevent deteriorating processes. Our previous work indicates the predictive capacity of non-linear parameters of blood pressure variability in discriminating between healthy and prediabetic rats in a sex- and age-specific manner. Whilst pre-diabetic rats lack signs of gross CV insult, they possess blunted baroreceptor sensitivity and dysfunctional endothelial-dependent vasorelaxation only discernible upon complex, invasive hemodynamic manipulations. Our results show that female rats are relatively protected from prediabetic CV manifestations.

Here, we evaluate the capacity of a ML convolutional neural network (CNN) in segregating arterial pressure (AP) signals collected from pre-diabetic vs. healthy controls according to disease state, age, and sex. 4-week-old Sprague Dawley, male or female rats were fed a high-calorie (HC) or a normal diet for 12 or 24 weeks (wks), representing young vs. old rats, respectively. Female rats fed for 24 wks were further divided into three subcategories: a sham group, one undergoing ovariectomy at wk 12 (OVX), and another receiving estrogen treatment for 12 wks post-surgery (OVX+E2). At weeks 12 or 24, anesthetized rats were instrumented for invasive hemodynamics monitoring via a pressure transducer inserted through the carotid artery.

AP signals of length ~300 seconds were downsampled to 50Hz, sliced to 1000 data points per bin (~16.7s), and Fourier-transformed. Fourier plots were cropped to remove graph labels/axes and were then fed into the CNN. Our model consisted of 5 convolutional layers, separated by batch normalization, ReLU activation, and max pooling. The outcome of the 5th convolutional layer had 40% of data dropped out and was delivered to a fully connected layer and then to a softmax function. The model utilized cross entropy for a loss function and ADAM for an optimization function. 80% of the data was randomly allocated for training and 10% each for validation and testing. Test accuracy (TA), AUROC, and AUPRC were used to evaluate the model.

Our CNN successfully classified rats based on diet (HC vs. control, test accuracy: 97.66%, AUROC: 0.9975, AUPRC: 0.9975), sex (TA: 96.63%, AUROC: 0.9921, AUPRC: 0.9922), surgical outcome (sham vs. OVX vs. OVX+E2, TA: 96.55%, AUROC: 0.9950, AUPRC: 0.9904), and age (16 vs. 28 weeks, TA: 96.65%, AUROC: 0.9802, AUPRC: 0.9757). Upon challenging the model with a 4-way classification task on age and diet (16 wks + control diet, 16 wks + HC, 28 wks + control, and 28 wks + HC), it was able to classify the above with TA: 92.79%, AUROC: 0.9764, and AUPRC: 0.9603.

Application of a supervised ML model provides the opportunity of capturing several undefined features of hemodynamic control. Utility of a CNN overcomes the shortcomings associated with the use of other parameters of hemodynamic fluctuations which measure a single characteristic, by probing and compiling additional layers of differences and synthesizing a global appraisal of CV signals.

Categories	N-value	Test Accuracy, TA (%)	Area Under the Receiver-Operating Curve (AUROC)	Area Under Precision-Recall Curve (AUPRC)
Diet (High calorie, HC vs. normal chow, NC)	NC: 74 HC: 65	97.66	0.9975	0.9975
Sex (Males vs. Females)	Males: 70 Females: 69	96.63	0.9921	0.9922
Surgical Outcome (Sham vs. OVX vs. OVX+E2)	Sham: 32 OVX: 8 OVX+E2: 5	96.55	0.9950	0.9904
Age (16 vs. 28 weeks (wks))	16 wks: 77 28 wks: 62	96.65	0.9802	0.9757
Age x Diet (16 vs. 28 weeks, NC vs. HC)	16 wks, NC: 38 16 wks, HC: 39 28 wks, NC: 36 28 wks, HC: 26	92.79	0.9764	0.9603

**Title:** Performance of Convolutional Neural Network (CNN) on Different Comparisons



# Propofol and salvianolic acid A synergistically attenuated hypoxia/reoxygenation induced H9c2 cells injury under high-glucose and high-fat condition via modulating CD36

Jiaqi Zhou,<sup>1</sup> Ronghui Han,<sup>1</sup> Anyuan Zhang,<sup>2</sup> Jiajia Chen,<sup>1</sup> Yuxin Jiang,<sup>1</sup> Dongcheng Zhou,<sup>1</sup> Danyong Liu,<sup>1</sup> Liangqing Zhang,<sup>1</sup> Weiyi Xia,<sup>3</sup> Youhua Xu,<sup>4</sup> and Zhengyuan Xia<sup>5</sup>

<sup>1</sup>Department of Anesthesiology, Affiliated Hospital of Guangdong Medical University, Zhanjiang, China; <sup>2</sup>Department of Anesthesiology, the Second Affiliated Hospital & Yuying Children's Hospital of Wenzhou; <sup>3</sup>Department of Orthopaedics and Traumatology, The University of Hong Kong, Hong Kong, China; <sup>4</sup>Faculty of Chinese Medicine, State Key Laboratory of Quality Research in Chinese Medicine, Macau University of Science and Technology, Taipa, Macao, China; and <sup>5</sup>State Key Laboratory of Pharmaceutical Biotechnology, Department of Medicine, The University of Hong Kong, Hong Kong, China

Abstract ID 17191

Poster Board 100

## Abstract

Subjects with diabetes are more vulnerable to myocardial ischemic-reperfusion injury (MIRI) and less or not sensitive to myocardial protective interventions such as ischemic preconditioning that are otherwise effective in non-diabetic subjects, and the underlying mechanism is unclear. Propofol (PPF), a widely used intravenous anesthetics, has been reported to attenuate MIRI through its reactive oxygen species scavenging property at high doses *in vitro* and *in vivo*, while application of propofol at high doses clinically may cause hemodynamic instability. Salvianolic acid A(SAA) is a potent antioxidant that confers protection against myocardial ischemic injuries. PPF and SAA both bear phenolic moieties in their molecular structure, however, whether or not these two molecules may confer synergistic cardioprotection, in particular in the context of myocardial ischemic injury under diabetic conditions, is unknown. The aim of this study was to investigate the protective effects and its underlying mechanisms of low doses of PPF combined with SAA against hypoxia/reoxygenation(H/R)-induced cardiomyocyte injury in high glucose (HG) and palmitate-treated H9c2 cardiomyocytes. Our data showed that culture H9c2 cells under stimulated diabetic condition with HG and palmitate resulted in significant cellular injury evidenced as decreased cell viability and increased lactate dehydrogenase (LDH) leakage that was concomitant with increased levels of the lipid peroxidation product malondialdehyde(MDA) and significant increase in CD36, while levels of p-AMPK was significantly reduced. These HG and palmitate-induced cell injuries/damages were further significantly exacerbated by H/R (composed of 6 hours of hypoxia followed by 12 hours of reoxygenation) but reversed by PPF or SAA respectively in a concentration dependent manner in the dose ranges of 12.5, 25 and 50  $\mu$ M. Co-administration of low concentrations of PPF and SAA at 12.5  $\mu$ M in H9c2 cells cultured under HG and palmitate significantly reduced the production of reactive oxygen species, ferrous ion content and lipid peroxidation and reduced CD36, while significantly increased p-AMPK, as compared to the effects of PPF at the concentration of 25  $\mu$ M. Moreover, HR-induced cellular injuries and ferroptosis were significantly exacerbated by overexpression of CD36. It is concluded that combinational usage of low doses/concentrations of PPF and SAA confer superior cellular protective effects to the use of high dose of PPF alone, and that inhibition of H/R induced CD36 over-expression may represent a major mechanism by which PPF and SAA combat against cardiomyocyte H/R injuries under HG and high lipid conditions.

# Acid Sphingomyelinase Inhibitor Protects Against the Nicotine-Induced Podocyte Injury

Atiqur Rahman,<sup>1</sup> Saisudha Koka,<sup>2</sup> and Krishna M. Boini<sup>1</sup>

<sup>1</sup>Department of Pharmacological and Pharmaceutical Sciences, College of Pharmacy, University of Houston, Houston, TX; and

<sup>2</sup>Department of Pharmaceutical Sciences, Irma Lerma Rangel School of Pharmacy, Texas A & M University, Kingsville, TX and Arkansas College of Osteopathic Medicine, Fort Smith, AR

Abstract ID 28638

Poster Board 101

**Objective:** Recent in vivo and in vitro studies have established the role of nicotine in chronic kidney diseases. However, the molecular mechanisms of how nicotine induces chronic kidney disease are still unclear. The present study tested whether acid sphingomyelinase (Asm) mediates the nicotine induced NLRP3 inflammasome activation and podocyte injury.

**Methods and Results:** Confocal microscopic analysis showed that nicotine treatment increased the colocalization of NLRP3 with Asc in podocytes compared to control cells (n=6/group, p<0.05). Pretreatment with Asm inhibitor, amitriptyline abolished the nicotine-induced colocalization of NLRP3 with Asc, suggesting that Asm mediates the nicotine-induced Nlrp3 inflammasomes activation. Biochemical analysis showed that nicotine treatment significantly increased the caspase-1 activity compared to control cells. The prior treatment with amitriptyline significantly attenuated the nicotine-induced caspase-1 activity. Immunofluorescence analysis showed that nicotine treatment significantly decreased the podocin expression compared to control cells. However, prior treatment with amitriptyline attenuated the nicotine-induced podocin reduction. In addition, prior treatment with amitriptyline significantly attenuated the nicotine-induced ceramide production and Asm expression in podocytes.

**Conclusion:** Based on the above results, it is concluded that Asm is one of the important mediators of nicotine-induced inflammasome activation and podocyte injury. Asm may be a therapeutic target for treatment or prevention of glomerulosclerosis associated with smoking.

This work is supported by NIH R01HL148711 award

# Old Dog, New Tricks: Oral Dosing Hypertensive Rats with Anti-Inflammatory Agent Colchicine Gives Vascular Remodeling and Function Recovery

Samuel Baldwin,<sup>1</sup> Jennifer van der Horst,<sup>1</sup> Joakim Bastrup,<sup>1</sup> Anthony M. Mozzicato,<sup>1</sup> Salomé Rognant,<sup>1</sup> Johs Dannesboe,<sup>1</sup> and Thomas A. Jepps<sup>1</sup>

<sup>1</sup>Københavns Universitet / University of Copenhagen

Abstract ID 14432

Poster Board 102

In the USA, resistant uncontrolled hypertensive patients express an increased risk of mortality when compared to untreated hypertensive patients<sup>1</sup>. The current pharmacopeia of hypertensive medication therefore fails to ameliorate resistant hypertension and poses a risk to the health of patients, highlighting the need for new drugs and a change in approach to how we treat hypertension.

Colchicine, a microtubule polymerization disruptor, is currently in use for its anti-inflammatory properties in the treatment of gout. Recently, work from our laboratory indicates a role for colchicine in vascular function recovery within arteries from hypertensive animals by preventing retrograde trafficking of key components of vascular reactivity<sup>2,3</sup>. The long-term *in vivo* consequences of colchicine treatment within the context of animal models of hypertension remains unclear however. The aim of this project was to determine the effect of colchicine dosing on the key hallmarks of hypertension including blood pressure, vascular function and vascular remodeling.

11-16 week old Wistar Kyoto (WKY) and spontaneously hypertensive rats (SHR) were bred and purchased from Janvier Labs, France, for tandem *in vivo* and *in vitro* experiments.

*In vivo*: Under general anesthesia (isoflurane), animals were fitted with abdominal telemetric devices which allowed for continual recording of blood pressure and body temperature. Animals were orally dosed with either placebo (PBS), or Colchicine (0.05mg/kg, in PBS) once daily for 4 weeks. Differences in blood pressure were determined by recordings generated for 1hr prior to dosing. In week 1, acute changes in blood pressure were determined by a 2hr recording post dosing.

*In vitro*: changes in vascular function via isometric tension recordings of 3<sup>rd</sup> order mesenteric arteries (MAs). Concentration effect curves were generated in response to vasoconstrictors methoxamine ( $\alpha$ -1 adrenoreceptor), U46619 (TXA<sub>2</sub>), 5-HT and KCl from basal tone, and vasorelaxant isoproterenol ( $\beta$ -adrenoreceptor), sodium nitroprusside, ML213 (K<sub>v</sub>7.2-5 channel activator) and NS11021 (BK<sub>Ca</sub> channel activator) on pre-contracted arterial tone (10 $\mu$ M Methoxamine). Changes in vascular remodeling were determined via Sirius red staining of cross sections of 3<sup>rd</sup> order MAs, in addition to electron microscopy.

Our *in vivo* investigation revealed a reduction in  $\Delta$  Blood Pressure within SHRs treated with colchicine when compared to placebo controls across the 4 weeks. Further, colchicine mediated no significant acute changes in blood pressure. Our *ex vivo* investigations similarly demonstrate an enhanced response to SNP, isoproterenol and ML213 when comparing arteries from Colchicine treated SHRs to placebo controls. Finally, sirius red and electron microscopy revealed a reduction in media to lumen ratio when comparing the arteries from the same groups.

Collectively indicating that long-term treatment with colchicine has positive outcomes for BP reduction, via enhanced vascular responsiveness to vasodilators coupled with a reduction in detrimental vascular remodeling, implicating colchicine as a novel therapeutic candidate for the treatment of hypertension.

1. Zhou D, Xi B, Zhao M, Wang L, Veeranki SP. Sci Rep. 2018;8(1):1–7.
2. Lindman J, Khammy MM, Lundegaard PR, Aalkjær C, Jepps TA. Hypertension. 2018 Feb;71(2):336–45.
3. Horst J Van Der, Rognant S, Hellsten Y, Aalkjær C, Jepps TA. Hypertension. 2022;79:2214–2227.

# Sex-dependent Differences in Pressure Overload Hypertrophy in NT-GRK2 Mice

Kamila Bledzka,<sup>1</sup> Iyad H. Manaserh,<sup>1</sup> Madison Bohacek,<sup>2</sup> Jessica Grondolsky,<sup>1</sup> Jessica Pflieger,<sup>3</sup> Julie Rennison,<sup>1</sup> David Van Wagoner,<sup>1</sup> and Sarah Schumacher<sup>1</sup>

<sup>1</sup>Lerner Research Institute of the Cleveland Clinic Foundation; <sup>2</sup>John Carroll University; and <sup>3</sup>Virginia Tech

Abstract ID 24546

Poster Board 103

G protein-coupled receptor kinase 2 (GRK2) is upregulated in the injured heart, contributes to heart failure (HF) pathogenesis and has emerged as a therapeutic target for cardiac disease. One approach used to target GRK2 activity in murine HF models involves the genetic expression of peptide inhibitors via C- or N-terminal fragments of GRK2. Herein, we subjected transgenic mice with cardiac restricted expression an N-terminal fragment of GRK2 ( $\beta$ ARKnt) to pressure overload and found that these mice exhibit sexual dimorphism in HF and atrial susceptibility. This recapitulates the clinical data indicating essential differences between men and women in HF type, epidemiology and pathophysiology. Men are predisposed to the development of HF with reduced ejection fraction due to heart-related conditions. Women, meanwhile, have a higher incidence of HF with preserved ejection fraction due to comorbidities and sex-related factors. The poor inclusion of females in clinical trials and murine studies has contributed to a poor understanding of disease behavior in women. This study carefully dissects both the acute and chronic responses of non-transgenic and  $\beta$ ARKnt female mice to trans-aortic constriction (TAC) surgery, and whether they differ from our previous observance in males. Interestingly, while left ventricular (LV) posterior wall thickness during diastole and systole and cardiac ejection fraction were all significantly higher in  $\beta$ ARKnt mice prior to surgery, our data demonstrate proportional LV hypertrophic growth in both the  $\beta$ ARKnt and non-transgenic mice in response to acute cardiac stress. During chronic stress, in contrast to non-transgenic male mice that transition to heart failure from 10-14 weeks after TAC, ejection fraction was indistinguishable between non-transgenic Sham and TAC females, with elevated yet consistent levels in the  $\beta$ ARKnt TAC and more-so Sham females.  $\beta$ ARKnt female mice exhibited a robust and continual increase in asymmetric hypertrophy across the 14 week time course. This is in contrast to non-transgenic female mice that have mild, stable and symmetric hypertrophic growth. This is also in contrast to the stable hypertrophy and cardioprotection observed in  $\beta$ ARKnt male mice, and opposite to the switch from hypertrophy to wall thinning observed in non-transgenic male mice transitioning into maladaptive remodeling and dilated cardiomyopathy. Additionally, lung weight normalized to tibia length was only elevated in the  $\beta$ ARKnt TAC female mice, suggesting pulmonary congestion. Analysis of Masson's Trichrome and WGA staining demonstrated that unlike in  $\beta$ ARKnt male mice, fibrosis and cardiac hypertrophy are evident in  $\beta$ ARKnt female mice at baseline and more pronounced following acute and chronic pressure overload stress. Further, these data suggest an increase in immune cell infiltration that is under further investigation. Data in our male mice suggested enhanced metabolic flexibility as part of the mechanism of cardioprotection by  $\beta$ ARKnt; however, the opposite was observed in females. Alternatively, RNAseq data suggests dysregulation of phagosome formation and wound healing responses as possible mechanisms for the increased pathological remodeling in our  $\beta$ ARKnt female mice that will serve as a focus of ongoing and future studies. Overall, increasing our knowledge about the underlying molecular mechanisms involved in the male versus female failing heart will contribute to more effective sex-specific therapeutic strategies.

# Therapeutic Efficacy of a Novel Pharmacologic GRK2 Inhibitor in Mice Models of Heart Failure

Rajika Roy,<sup>1</sup> Sarah Schumacher,<sup>2</sup> Haley C. Murphy,<sup>1</sup> Jessica Grondolsky,<sup>3</sup> Kurt Chuprun,<sup>1</sup> Helen V. Waldschmidt,<sup>4</sup> Erhe Gao,<sup>1</sup> Huaqing Zhao,<sup>5</sup> Larisa Avramova,<sup>6</sup> John JG. Tesmer,<sup>7</sup> and Walter Koch<sup>8</sup>

<sup>1</sup>Lewis Katz School of Medicine, Temple University; <sup>2</sup>Lerner Research Institute of the Cleveland Clinic Foundation; <sup>3</sup>Lerner Research Institute, Cleveland Clinic Lerner College of Medicine; <sup>4</sup>University of Michigan; <sup>5</sup>Lewis Katz School of Medicine; <sup>6</sup>Perdue University; <sup>7</sup>Purdue Univ; and <sup>8</sup>Temple Univ School of Medicine

Abstract ID 52525

Poster Board 104

**Background:** GRK2 is an abundantly expressed GRK in the heart and plays a crucial role in the pathogenesis of heart failure. Targeting GRK2 in HF has been previously reported to be cardioprotective in mouse models of HF, genetically with  $\beta$ ARKct and with paroxetine an FDA-approved SSRI that also has potent GRK2 inhibitory properties. To enhance the GRK2 inhibitory properties of paroxetine while still retaining its selectivity a library of compounds was generated based on its scaffold. Amongst them, the 14as compound had 50-fold higher selectivity for GRK2 and increased myocyte contractile function in vitro at doses 100-fold lower than paroxetine. Such profound in vitro effects led to its evaluation in heart failure models in vivo.

**Aim:** To evaluate cardioprotective effects and an ideal dose of 14as in two different mouse injury models of heart failure.

**Methods:** 14as was first evaluated in a mouse model of myocardial infarction (MI). 2 weeks post-MI, three different doses of 14as – high 2mg/kg/day, medium 0.5mg/kg/day and low 0.1mg/kg/day were administered via osmotic pumps. Cardiac function and LV (left ventricular) chamber dimensions were measured by echocardiography. After concluding the ideal dose of 14as in an MI model, 14as was evaluated in a transverse aortic constriction (TAC) model for its cardioprotective properties. Similar to the MI model, 14as was delivered via osmotic pumps, and cardiac function was evaluated by echocardiography starting at 2 weeks up to 12 weeks post-TAC.

**Results:** From the three doses evaluated in the MI model, both the high and the medium doses were cardioprotective. Both groups had significantly higher ejection fraction (EF) and fractional shortening (FS) with the high dose being better and near identical to the effects of paroxetine. The high-dose treated hearts displayed a smaller LV lumen size, smaller LV inner diameter at systole (LVID;s), and displayed a lower heart weight/body weight ratio and lower lung weight compared to the vehicle group, 6 weeks post MI. Post TAC hearts treated with 14as also had significantly higher EF and FS compared to the control group and a lower LV mass, LVID;s, smaller LV blood volume at end systole (Vol;s), and lower heart weight/body weight ratio compared to the control group.

**Conclusion:** In two fundamentally different injury models of heart failure, high dose 14as not only arrested declining contractile function but also reversed it and attenuated adverse LV remodeling. Being structurally similar to paroxetine it will potentially exhibit a similar safety profile in humans and can be explored as a potential new drug for heart failure in clinical trials.

This research was funded by R01 HL061690 and NIH/NHLBI 5R01HL071818-18

# Role of cyclophilin A overexpression in angiotensin II/mechanical stretch-induced vascular remodeling: Protective effect of adiponectin

Zeina Radwan,<sup>1</sup> Crystal Ghantous,<sup>2</sup> and Asad Zeidan<sup>3</sup>

<sup>1</sup>American University of Beirut; <sup>2</sup>Notre Dame University-Louaize; and <sup>3</sup>Qatar University

Abstract ID 14517

Poster Board 105

Hypertension is associated with an increase in reactive oxygen species (ROS). Cyclophilin A (CyPA) is released from vascular cells in response to oxidative stress and contributes to hypertension pathophysiology. Thereby, controlling redox imbalance and CyPA secretion may prevent hypertension-associated complications. Moreover, adiponectin (APN), an adipocyte-released cytokine, exerts protective effects on the cardiovascular system. Yet, the molecular mechanisms by which CyPA induces vascular remodeling and the role of APN in preventing CyPA secretion still need to be better understood. In this study, we used three models to mimic hypertension: The *in-vivo* rat portal vein (RPV) ligation and two *ex-vivo* models (The mechanically stretched RPVs and the angiotensin II treated rat aortas). Our results revealed plasma CyPA levels significantly increased after RPV ligation for 14 and 28 days. In addition, CyPA protein and mRNA expressions significantly increased in response to mechanical stretch and Ang-II. Furthermore, CyPA increased the wet weight of RPVs while inhibiting AMPK and eNOS phosphorylation/activation. Moreover, the CyPA effects on blood vessels were attenuated by pre-treatment with APN. In conclusion, CyPA is secreted in response to high blood pressure and promotes vascular hypertrophy by inhibiting AMPK and eNOS activities and activating the RhoA/ROCK pathway. On the other hand, APN attenuates the synthesis and release of CyPA induced by Ang-II and mechanical stretch.

# Physiological effects of fentanyl analogs found in recreational drug markets

Charles W. Schindler,<sup>1</sup> Shelby A. McGriff,<sup>1</sup> Eric B. Thorndike,<sup>2</sup> Li Chen,<sup>3</sup> Donna Walther,<sup>1</sup> Kenner Rice,<sup>4</sup> Lei Shi,<sup>3</sup> and Michael H. Baumann<sup>1</sup>

<sup>1</sup>NIDA/IRP Designer Drug Unit; <sup>2</sup>NIH/NIDA Preclinical Pharmacology; <sup>3</sup>NIDA/IRP Computational and Molecular Biophysics Section; and <sup>4</sup>NIDA/IRP Drug Design and Synthesis Section

Abstract ID 17435

Poster Board 106

Structural analogs of fentanyl are increasingly associated with human overdose fatalities, yet little is known about the pharmacology of these compounds. Here we studied the physiological effects of fentanyl analogs that have appeared in recreational drug markets worldwide. Six male Sprague-Dawley rats received surgically implanted telemetry transmitters for the measurement of blood pressure (BP), heart rate (HR), locomotor activity, and body temperature. Rats in their home cages were placed onto telemetry receivers for 3 h each weekday, with subcutaneous (s.c.) drug or vehicle injections administered twice weekly. We also examined the effects of fentanyl and its analogs in assays measuring opioid receptor binding in rat brain tissue, and inhibition of cAMP accumulation in cells transfected with mu-opioid receptors (MOR). The telemetry results revealed that all fentanyl analogs produce dose-dependent increases in BP, HR, activity, and temperature, but the potency of the compounds varied substantially. The calculated ED<sub>50</sub> values for inducing hypertensive effects showed that fentanyl was most potent (0.01 mg/kg), followed closely by fentanyl (0.014 mg/kg), cyclopropylfentanyl (0.028 mg/kg), and butyrylfentanyl (0.081 mg/kg). Acetylfentanyl (0.166 mg/kg) was slightly less potent than butyrylfentanyl, but had a potency similar to the illicit opioid heroin (0.215 mg/kg). Valerylfentanyl was the least potent analog by far (2.071 mg/kg), which had potency similar to the opioid analgesic morphine (2.689 mg/kg). Radioligand binding assays demonstrated that all fentanyl analogs displayed higher affinity for mu-opioid receptors (MOR) over delta and kappa sites, and all of the drugs induced MOR-mediated inhibition of cAMP accumulation. Importantly, the rank order of potency for the fentanyl analogs to increase BP was similar to the rank order of affinity at MOR and potency for inhibiting cAMP. We also tested the ability of opioid receptor antagonists to alter the in vivo effects of fentanyl and butyrylfentanyl. The centrally active opioid antagonist, naltrexone (0.3 mg/kg, s.c.), blocked all of the effects of both drugs, whereas the peripherally restricted opioid antagonist, naloxone methiodide (2.0 mg/kg, s.c.), partially reduced only the BP and HR effects. These findings indicate that locomotor and temperature effects induced by fentanyl and its analogs are centrally mediated, while cardiovascular effects may involve peripheral mechanisms. In conclusion, we demonstrate that fentanyl analogs evoke physiological responses that are similar to fentanyl itself, and these responses are most likely mediated via agonist activity at MOR. With the exception of valerylfentanyl, which is a very low potency agonist, fentanyl analogs are much more potent than morphine, suggesting these analogs may pose serious health risks to users.

This work was supported by NIDA/NIH.

# Cardiomyocyte-specific Adhesion G Protein-Coupled Receptor F5 (ADGRF5) participates in cardiac homeostasis

Jeanette Einspahr,<sup>1</sup> Viren Patwa,<sup>2</sup> Rajika Roy,<sup>2</sup> and Douglas G. Tilley<sup>3</sup>

<sup>1</sup>Temple Univ; <sup>2</sup>Temple University; and <sup>3</sup>Temple Univ School of Medicine

Abstract ID 56061

Poster Board 107

G protein-coupled receptors (GPCRs) remain the largest family of protein targets for approved drugs due to their impact on numerous physiologic and pathologic processes, as well as the relative ease of modulating their activity at cell surface-accessible sites. Although the heart expresses hundreds GPCRs, relatively few been explored as targets to reduce remodeling and preserve contractility during heart failure (HF). Adhesion GPCRs (AGPCRs) are an understudied family of receptors containing numerous extracellular domains that interact with various extracellular proteins, including many that are known mediators of cardiac remodeling responses to pathologic stress, thus may represent novel targets for HF. RNA-sequencing analysis of left ventricle (LV) tissue isolated from healthy hearts of adult mice identified high expression of several AGPCR family members, including ADGRF5, which was subsequently shown to become downregulated in transaortic constriction (TAC)-induced HF in mice. Further, analysis of published single cell-RNA-Seq datasets confirmed ADGRF5 expression specifically in cardiomyocytes becomes decreased over time in both mouse and human HF. Thus, to investigate the impact of cardiomyocyte-expressed ADGRF5 on cardiac function and remodeling normally or during HF, we crossed floxed ADGRF5 (ADGRF5<sup>f/f</sup>) mice with  $\alpha$ MHC-Cre mice to generate cardiomyocyte-specific ADGRF5 knockout mice (CM-ADGRF5-KO), which displayed normal cardiac structure and function at 12 weeks of age versus  $\alpha$ MHC-Cre+ control mice, as assessed via echocardiography, gravimetrics and immunohistochemistry. However, CM-ADGRF5-KO mice developed cardiac dysfunction, maladaptive remodeling, and increased mortality over time, even in the absence of pathologic insult, suggesting a homeostatic function of cardiomyocyte-expressed ADGRF5. Further, following TAC surgery, CM-ADGRF5-KO mice displayed an accelerated decline in cardiac function with enhanced remodeling and increased mortality. To attain mechanistic insight into these changes, we performed RNA-sequencing on LV tissue of 12-week-old CM-ADGRF5-KO mice and subsequently validated differential gene targets in isolated left ventricular adult mouse cardiomyocytes (AMCM). We identified *Scn1b* to be differentially upregulated in CM-ADGRF5-KO AMCM, suggesting altered regulation of sodium currents, whereas overexpression of ADGRF5 in neonatal rat ventricular myocytes (NRVM) resulted in decreased *Scn1b* expression. Finally, luciferase reporter, fluorescence resonance energy transfer (FRET) and immunoblotting analyses were performed in NRVM, revealing that ADGRF5 proximally signals in a G $\alpha$ q-dependent manner. In all, these results suggest that ADGRF5 contributes to the maintenance of cardiac health normally and during the development of HF, thus may represent a novel HF therapeutic target.

**Keywords:** GPCRs; Adhesion GPCRs; Cardiomyocytes; Heart Failure



# ANGPTL4 attenuates hypoxia/reoxygenation-induced cardiomyocyte apoptosis via activation of Akt signaling

Weiyi Xia,<sup>1</sup> Dengwen Zhang,<sup>2</sup> Weiguang Li,<sup>1</sup> Zhengyuan Xia,<sup>3</sup> and Yin Cai<sup>1</sup>

<sup>1</sup>The Hong Kong Polytechnic University; <sup>2</sup>Guangdong Provincial People's Hospital, Guangdong Academy of Medical Sciences; and <sup>3</sup>State Key Laboratory of Pharmaceutical Biotechnology, The University of Hong Kong

Abstract ID 15237

Poster Board 108

Ischemic heart disease (IHD) is a leading cause for morbidity and mortality worldwide. Reperfusion therapy restores blood flow, but paradoxically exacerbates myocardial injury, known as ischemia/reperfusion injury (I/RI). Apoptotic cell death is one of the main forms of post-ischemic cell death. Thus, inhibiting apoptosis may limit the extent of I/RI and lead to better prognosis of post-ischemic myocardial recovery. ANGPTL4, a gene known to regulate lipid metabolism, has been shown to preserve vascular integrity, reduce no-reflow and thus attenuate myocardial I/RI in rabbits. However, whether ANGPTL4 directly impacts cardiomyocytes and alleviates myocardial I/RI through reducing cell apoptosis is unknown. Therefore, we explored whether ANGPTL4 protects against hypoxia/reoxygenation (H/R)-induced cardiomyocyte injury through inhibiting apoptosis.

In vivo myocardial I/R model was induced by occluding the left anterior descending (LAD) artery for 30 mins, followed by 2 h reperfusion. Sham operations were performed by passing a silk thread under the LAD without occlusion. Infarct size was determined by using Evans blue/TTC staining. The rat cardiomyocyte-derived cell line H9C2 was transfected with scramble or ANGPTL4 siRNA, followed by H/R (6 hours hypoxia followed by 12 h reoxygenation) in the absence or presence of pre-treatment with SC-79 (4  $\mu$ g/mL, 1h, selective Akt activator) or LW-6 (20  $\mu$ M, 2h, selective HIF-1 $\alpha$  inhibitor). Cell damage was assessed by measuring Lactate dehydrogenase (LDH) release and cell viability by MTT assay. Protein levels of apoptosis markers [Bcl-2, Bax, cleaved caspase 3] and proteins related to pro-survival signaling pathway [Akt and phosphorylated Akt (S473)] were determined by Western blotting.

The result showed that ANGPTL4 increased significantly in the mouse myocardium after I/RI and in H/R-stimulated H9C2 cardiomyocytes, indicating that ANGPTL4 in cardiomyocytes may be involved in the pathogenesis of myocardial I/RI. Indeed, knock-down of ANGPTL4 in H9C2 cells with ANGPTL4 siRNA significantly aggravated H/R-induced cell injury (increased LDH level and reduced cell viability) and exacerbated cell apoptosis (greater cleaved caspase 3 expression and Bax/Bcl-2 ratio). Activation of Akt is well known to protect against myocardial I/RI via inhibition of cell apoptosis. In the present study, a significant reduction in p-Akt (S473) was observed in the ANGPTL4-knockdown cells upon H/R stimulation, suggesting that inhibition of ANGPTL4 may exacerbate H/R-induced cell apoptosis via down-regulation of Akt signaling pathway. Indeed, pre-treatment with SC-79 significantly reversed H/R-induced cell apoptosis in ANGPTL4 knockdown H9C2 cardiomyocytes, as evidenced by decreased cleaved caspase 3 expression and Bax/Bcl-2 ratio. Furthermore, HIF-1 $\alpha$  is known to be the major transcription factor activated in hypoxia in ischemic conditions. The induction of ANGPTL4 was significantly reduced when H/R-stimulated H9C2 cardiomyocytes were pre-treated with LW-6, indicating that HIF-1 $\alpha$  may upregulate ANGPTL4 upon H/R stimulation.

It is concluded that upon H/R stimulation, HIF-1 $\alpha$ -mediated upregulation of ANGPTL4 may protect against H/R-induced cardiomyocyte injury through activating Akt signaling.

This study was supported by Joint Postdoc Scheme (P0038982), Guangdong Basic and Applied Basic Research Foundation (2022A1515011116, 2019A1515110063) and National Natural Science Foundation of China (82002095).

# Opposing effects of $\beta$ 2-ARs on $\beta$ 1-ARs on phospholipase C-mediated cardiac hypertrophic signaling

Wenhui Wei,<sup>1</sup> and Alan V. Smrcka<sup>2</sup>

<sup>1</sup>Univ of Michigan; and <sup>2</sup>Univ of Michigan Med Sch

Abstract ID 24004

Poster Board 109

Chronic overstimulation of Gs-coupled  $\beta$ -adrenergic receptor ( $\beta$ -AR) signaling by catecholamines, induces pathological cardiac hypertrophy and ultimately heart failure.  $\beta$ 1-ARs and  $\beta$ 2-ARs are the two major subtypes of  $\beta$ -ARs present in the human heart and mediate the activity of sympathetic nervous system. It is known that  $\beta$ 1-ARs and  $\beta$ 2-ARs elicit significantly different or even opposite effects on cardiac functions such as contractility and heart failure, though they share overall sequence and structural homology, and both stimulate cAMP production. The molecular mechanisms underlying these distinct biological effects have not been fully elucidated.

Previously, our laboratory demonstrated that a cAMP/EPAC/phospholipase C<sub>e</sub> (PLC<sub>e</sub>)-mediated signaling pathway at the Golgi apparatus is important for regulation of cardiac hypertrophy. We also showed that this pathway is selectively stimulated by activation of  $\beta$ 1-ARs localized at Golgi apparatus but not those at the plasma membrane (PM). Access to intracellular  $\beta$ 1-ARs by catecholamines was mediated by the organic cation transporters (OCTs), and blockade of OCT3 inhibited catecholamine stimulated cardiomyocyte hypertrophy.

In my current study using adult ventricular cardiac myocytes, I found that the activation of PM  $\beta$ 2-ARs opposes stimulation of the prohypertrophic EPAC/PLC<sub>e</sub> pathway at the Golgi apparatus by either Angiotensin II, or Golgi localized  $\beta$ 1-ARs.  $\beta$ 2-AR-dependent inhibition appears to be at the level of PLC<sub>e</sub> since activation of  $\beta$ 2-AR with salmeterol blocks direct activation of EPAC/PLC<sub>e</sub> by the EPAC selective cAMP analog 8-(4-chlorophenylthio)-2'-O-methyl-cAMP (CPTOMe)-AM, and blocks PLC<sub>e</sub> activation by ATII which activates PLC<sub>e</sub> through a pathway that does not rely on EPAC. Blockade of internalization of  $\beta$ 2-ARs with Dyngo-4A abolished this inhibitory signaling. Downstream of  $\beta$ 2-ARs, I found that  $\beta$ 2-AR-dependent PLC<sub>e</sub> inhibition is not mediated by PKA. Rather, blockade of Gi with PTX, or Gbg with gallein, inhibited the ability of  $\beta$ 2-ARs to block Golgi PLC<sub>e</sub> activity. Additionally, inhibition of ERK activation by PD0325901 abolished  $\beta$ 2-AR-mediated inhibition of Golgi PLC<sub>e</sub> activity. This supports a model where  $\beta$ 2ARs internalized from the plasma membrane activate Gi releasing Gbg subunits leading to ERK activation and inhibition of PI hydrolysis at the Golgi apparatus, thereby inhibiting hypertrophic signaling by PLC<sub>e</sub>. This study reveals a novel potential mechanism for  $\beta$ 2-AR antagonism of the Epac/PLC<sub>e</sub> pathway that may contribute to the known protective effects of  $\beta$ 2AR signaling on the development of heart failure. Elucidation of a mechanism for the anti-hypertrophic versus hypertrophic signaling balance from  $\beta$ 1-ARs and  $\beta$ 2-ARs gives critical insights into the development of new strategies for treatment of heart failure by targeting  $\beta$ AR subtypes.

# Oral administration of BAF312, a selective sphingosine-1-phosphate receptor agonist, attenuates sodium retention and hypertension in DOCA-salt-treated mice

Weili Wang,<sup>1</sup> Gaizun Hu,<sup>1</sup> Chaoling Chen,<sup>1</sup> Joseph Ritter,<sup>1</sup> Pin-Lan Li,<sup>1</sup> and Ningjun Li<sup>1</sup>

<sup>1</sup>Virginia Commonwealth University

Abstract ID 21314

Poster Board 110

Our previous studies have demonstrated that sphingosine-1-phosphate (S1P) agonist stimulates urinary sodium excretion via the S1P type 1 receptor (S1PR1), that deletion of S1PR1 gene in the renal collecting duct leads to increased sodium retention and enhanced salt-sensitive hypertension under the treatment of deoxycorticosterone (DOCA) and high salt (DOCA-salt), and further, that overexpression of S1PR1 transgene in the renal medulla attenuates DOCA-salt hypertension. A pharmacological intervention would bear more clinical implications. Therefore, the present study tested the hypothesis that oral administration of a selective S1PR agonist BAF312 reduces sodium retention by promoting sodium excretion and consequently attenuates DOCA-salt hypertension. Male C57BL/6J mice around 25g bodyweight received daily oral gavage of BAF312 (3 mg/Kg dissolved in PEG-400) or vehicle for one week. The mice were then implanted subcutaneously with a silicone sheet (silastic, Dow Corning Co.) impregnated with DOCA (50mg each mouse) plus 1% NaCl drinking water to induce salt-sensitive hypertension. Thereafter, the mice underwent assessments of acute sodium excretion, chronic sodium balance or chronic blood pressure measurement. There was no difference in the above assessments between vehicle- and BAF312-treated mice under basal conditions. Under DOCA-salt challenge, mice with BAF312 treatment showed increased urinary sodium excretion ( $U_{NAV}$ ) in responses to the acute sodium loading (IV of normal saline at 5% body weight in 30 min), the  $U_{NAV}$  were  $1.85 \pm 0.22$  vs.  $5.81 \pm 1.14$   $\mu\text{mol}/\text{min}/\text{gKW}$  ( $p < 0.05$ ) in vehicle- and BAF312-treated mice, respectively. The mice with BAF312 treatment also showed enhanced pressure natriuretic responses to the elevated renal perfusion pressure ( $U_{NAV}$ ,  $4.24 \pm 1.14$  vs.  $13.3 \pm 1.57$   $\mu\text{mol}/\text{min}/\text{gKW}$ , in vehicle- and BAF312-treated mice, respectively,  $p < 0.05$ ). Under the chronic DOCA-salt treatment, BAF312-treated mice showed ameliorated sodium retention as demonstrated by the less positive sodium balance ( $4.78 \pm 0.38$  vs.  $1.23 \pm 1.18$  mmol/100g BW per 24hr in vehicle- vs. BAF312-treated mice,  $p < 0.05$ ) and the attenuation of increased blood pressure after 10-day DOCA-salt treatment, the systolic blood pressure were increased from  $119 \pm 5.3$  to  $156.2 \pm 9.7$  vs.  $119 \pm 6.9$  to  $133.8 \pm 7.5$  mmHg in vehicle- and BAF312-treated mice, respectively ( $p < 0.05$ ). These results suggested that oral administration of the selective S1PR1 agonist BAF312 attenuates sodium retention and DOCA-induced salt-sensitive hypertension and that BAF312 could be a pharmacological candidate for the management of salt-sensitive hypertension.

This study was supported by NIH grant R01HL145163

# Mitochondrial CaMKII as a Novel Regulator of Cardiometabolic Dysfunction

Kimberly Ferrero,<sup>1</sup> Jonathan Granger,<sup>2</sup> Robert Cole,<sup>1</sup> Brian Foster,<sup>2</sup> David Kass,<sup>3</sup> Elizabeth Luczak,<sup>1</sup> and Mark Anderson<sup>4</sup>

<sup>1</sup>Johns Hopkins University School of Medicine; <sup>2</sup>Johns Hopkins University; <sup>3</sup>The Johns Hopkins Hospital; and <sup>4</sup>University of Chicago Pritzker School of Medicine

**Abstract ID 29057**

**Poster Board 155**

Ca<sup>2+</sup>/calmodulin-dependent protein kinase II (CaMKII) is an established negative regulator of cardiac injury. Both the expression and activity levels of CaMKII are elevated in models of heart failure such as ischemia-reperfusion (I/R) injury and myocardial infarction (MI). This is due in part to CaMKII's role in the regulation of excitation-contraction coupling, apoptosis, activation of hypertrophic programming, arrhythmias and pro-inflammatory signaling. We have recently identified a novel mitochondrial localization for CaMKII (mtCaMKII); importantly, there is an observed increase in mtCaMKII activation with left ventricular dilation following injury in a mouse model of MI. This deleterious post-MI phenotype is rescued with genetic mitochondrial CaMKII inhibition; conversely, mice with myocardial and mitochondrial CaMKII overexpression (mtCaMKII) present with severe dilated cardiomyopathy and decreased ATP production. To date, the molecular mechanisms by which mtCaMKII regulates mitochondrial energetics are not fully elucidated. We have identified changes in the activity of enzymes in the mitochondrial electron transport chain and TCA cycle in response to increased CaMKII levels or activity, indicating a novel and critical role in mitochondrial metabolism for this kinase. We are currently mapping the mtCaMKII interactome via liquid chromatography–mass spectrometry (LCMS) and proteomics analysis of both scaffolding interactions with proximity labeling utilizing TurboID technology alongside endogenous protein pulldowns. Additionally, we are identifying novel CaMKII kinase-substrate relationships using an ATP-analogue labeling, in order to identify metabolic enzymes which may be regulated via post-translational modifications by CaMKII. The identification of previously unknown mitochondrial partners for cardiac CaMKII may uncover promising pharmacological targets for cardiovascular therapeutics, particularly in treating the progression of HF.

# Beta-catenin C-terminus inhibition reduces vascular remodeling by precluding the expression of sphingosine-1-phosphate receptor-1

Gustavo Oliveira de Paula,<sup>1</sup> Gaia Ressa,<sup>1</sup> Vanessa Almonte,<sup>1</sup> Dippal Parikh,<sup>1</sup> Tomas Valenta,<sup>2</sup> Konrad Basler,<sup>2</sup> Timothy Hla,<sup>3</sup> Dario Riascos-Bernal,<sup>1</sup> and Nicholas Sibinga<sup>1</sup>

<sup>1</sup>Albert Einstein College of Medicine; <sup>2</sup>University of Zurich; and <sup>3</sup>Harvard Medical School

Abstract ID 56626

Poster Board 156

Vascular remodeling is associated with target organ damage and fatal cardiovascular events. The molecular mechanisms that control vascular remodeling are still poorly understood, limiting effective therapeutic approaches. Vascular smooth muscle cells (SMCs), in part via activation of the Wnt/ $\beta$ -catenin signaling pathway, contribute importantly to vascular remodeling. The  $\beta$ -catenin C-terminal domain is required in SMCs for artery formation during embryogenesis, but its role in vascular remodeling in adulthood is unknown. Thus, the aim of this study was to define the importance of  $\beta$ -catenin C-terminus in SMCs during vascular remodeling and the underlying mechanisms. We found that mice expressing a C-terminus-deficient  $\beta$ -catenin in SMCs show reduced vascular remodeling and decreased SMC proliferation after arterial injury. In line with these findings, we observed that treatment with E7386, a novel  $\beta$ -catenin C-terminus inhibitor, reduces cell proliferation of both human and mouse vascular SMCs. RNA-seq analysis revealed a downregulation of the sphingosine-1-phosphate receptor 1 (S1pr1) transcript in  $\beta$ -catenin C-terminus-deficient SMCs. This receptor is known to be important in vascular remodeling, but its regulation is not fully elucidated. Interestingly, we found that  $\beta$ -catenin interacts with the S1pr1 promoter and acts through its C-terminal domain to activate S1pr1 transcription and protein expression, resulting in enhanced SMC proliferation. Consistent with these observations, S1PR1 expression was markedly decreased in SMCs of arteries from mice lacking the  $\beta$ -catenin C-terminus, and re-establishing S1PR1 expression in SMCs restored vascular remodeling in those mice. Taken together, these findings identify the  $\beta$ -catenin C-terminal output as a novel upstream regulator of S1PR1 expression and define a functional interaction between the canonical Wnt and sphingosine-1-phosphate signaling pathways that drives vascular remodeling after injury. Our study suggests that targeting  $\beta$ -catenin C-terminus/S1PR1 axis could provide a therapeutic strategy to reduce vascular remodeling and cardiovascular disease.

This study was supported by the American Heart Association Postdoctoral Fellowship 874619 (G.H.O-P), a Career Development Award from the American Heart Association 19CDA34660217 (D.R-B.), and NIH grant R01HL128066 (N.S.).

## $\beta$ 3AR-dependent BDNF generation limits chronic post-ischemic heart failure

Seungho Jun, Alessandro Cannavo,<sup>1</sup> Giuseppe Rengo,<sup>1</sup> Federica Marzano,<sup>2</sup> Jacopo Agrimi,<sup>3</sup> Gizem Keceli,<sup>4</sup> Andrea Elia,<sup>1</sup> Daniela Liccardo,<sup>1</sup> Giovanna G. Altobelli,<sup>1</sup> Erhe Gao,<sup>5</sup> Ning Feng,<sup>6</sup> Walter Koch,<sup>7</sup> and Nazareno Paolocci<sup>8</sup>

<sup>1</sup>University of Naples Federico II; <sup>2</sup>Federico II Univ, Naples; <sup>3</sup>University of Padova; <sup>4</sup>Johns Hopkins University Medical Institutions; <sup>5</sup>Temple University; <sup>6</sup>University of Pittsburgh; <sup>7</sup>Temple Univ School of Medicine; and <sup>8</sup>Johns Hopkins Medical Institutions

Abstract ID 24433

Poster Board 157

**Rationale:** Lack of brain-derived neurotrophic factor (BDNF) and/or inadequate expression/activity of its associated tropomyosin kinase receptor B (TrkB) account for brain and cardiac disorder. While  $\beta$ -adrenergic receptor ( $\beta$ AR) is responsible for the local expression of BDNF in neurons, whether a similar interaction is observed and pathophysiologically relevant in the cardiovascular system is unknown, especially in the post-ischemic myocardium with adrenergic desensitization. Moreover, it is unclear whether and how TrkB agonists counter chronic post-ischemic left ventricle (LV) decompensation.

**Methods:** We conducted *in vitro* studies with neonatal rat (NRVM)/adult murine cardiomyocytes (CMs), SH-SY5Y neuronal cells, and umbilical vein endothelial cells. We assessed the degree of impact from ischemia-related injury via either *in vivo* coronary ligation (myocardial infarction, MI) or *ex vivo* isolated hearts with global ischemia-reperfusion injury (I/R) in WT, cardiomyocyte-selective BDNF KO (myoBDNF KO) or  $\beta$ 3AR KO mice.

**Results:** In WT hearts, early after MI (In vitro, the TrkB agonist, LM22A-4 promoted neurite outgrowth and neovascularization. Moreover, LM22A-4 and another agonist, TrkB, 7,8-dihydroflavone enhanced myocyte contractility. When given to *in vivo* MI mice, LM22A-4 rescued, at least in part, LV dysfunction, denervation, and hypovascularity. Of note, when given to isolated myoBDNF KO hearts, it no longer benefited post-I/R LV structure and function. Superfusing isolated murine myocyte with the  $\beta$ 3AR-agonist, BRL-37344 enriched these cells with BDNF. Moreover, BRL-37344 limited post-I/R injury in WT mice but not in myoBDNF KO ones. Finally, the  $\beta$ 1AR blocker that upregulates  $\beta$ 3AR, augmented BDNF levels in the ischemic myocardium, improving *in vivo* post-MI dysfunction.

**Conclusions:** Lack of BDNF accounts, at least in part, for chronic post-ischemic LV decompensation. By extension, by restoring intracardiac BDNF levels, TrkB agonists can limit the extent of ischemic injury, both *in vivo* and *ex-in vivo*. Direct and indirect cardiac  $\beta$ 3AR stimulation via BRL-37344 or  $\beta$ -blocker, metoprolol, respectively, show another BDNF-centered means to arrest chronic post-ischemic HF. These findings may have relevant pharmacological implications for the treatment of chronic post-ischemic LV decompensation.

# Development of the first vascular-specific KATP channel inhibitor for the treatment of patent ductus arteriosus in newborns

Kangjun Li, Samantha J. McClenahan,<sup>1</sup> Elaine L. Shelton,<sup>1</sup> Craig W. Lindsley,<sup>2</sup> and Jerod Denton<sup>3</sup>

<sup>1</sup>Vanderbilt University; <sup>2</sup>Vanderbilt Univ; and <sup>3</sup>Vanderbilt Univ - Med Ctr

**Abstract ID 27793**

**Poster Board 158**

The ductus arteriosus (DA) is an essential fetal structure that shunts blood away from the high-resistance pulmonary circulation and toward the placental circulation, where fetal-maternal gas exchange occurs. Normally after birth, the DA undergoes vasoconstriction in response to increased arterial blood oxygen tension and secondary smooth muscle cell proliferation. The failure of the DA to close, or patent DA (PDA), is one of the most common congenital heart disorders, and its pharmacotherapy options are limited to non-specific medications that target prostaglandin pathways. ATP-regulated inward rectifier potassium (Kir) channels comprising Kir6.1 and SUR2B subunits are enriched in the DA compared to other vascular beds, suggesting they may represent novel drug targets for PDA pharmacotherapy. We hypothesize that inhibitors of Kir6.1/SUR2B will induce vasoconstriction and closure of the DA. Testing this hypothesis will require the development of highly specific inhibitors that can discriminate between Kir6.1/SUR2B and Kir6.2/SUR1 channels expressed in the pancreas and brain. We therefore performed a high-throughput screen of 47,872 compounds for novel modulators of Kir6.1/SUR2B. The most potent inhibitor discovered is VU0542270, which inhibits Kir6.1/SUR2 with an IC<sub>50</sub> of approximately 100 nM and is highly selective for Kir6.1/SUR2B over Kir6.2/SUR1 and several other Kir channels. In pressure myography experiments on isolated mouse DA tissues, VU0542270 enhanced oxygen-dependent DA constriction in a dose-dependent manner. Future experiments will explore the binding site of VU0542270 on Kir6.1/SUR2B and the molecular mechanisms of its selectivity.

# Characterizing the Role of Ser670 Phosphorylation in Non-canonical Mechanisms of GRK2 Inhibition in Heart Failure

Heidi Cho, Kimberly Ferrero,<sup>1</sup> John K. Chuprun,<sup>2</sup> Erhe Gao,<sup>2</sup> and Walter Koch<sup>3</sup>

<sup>1</sup>Johns Hopkins Univ; <sup>2</sup>Temple University; and <sup>3</sup>Temple Univ School of Medicine

Abstract ID 54365

Poster Board 159

**Background and Significance:** Heart failure (HF) is characterized by aberrant cardiac beta-adrenergic receptor ( $\beta$ -AR) signaling, leading to upregulation of GPCR kinase 2 (GRK2) and subsequent phosphorylation and desensitization of  $\beta$ -ARs. A peptide inhibitor of GRK2, comprised of the last 194 carboxyl-terminal amino acids of GRK2 ( $\beta$ ARKct), has been shown to bind to the G protein beta-gamma subunits, preventing GRK2 binding and  $\beta$ -AR desensitization. Overexpression of  $\beta$ ARKct attenuates HF and improves outcomes in animal models. Emerging evidence indicates that following oxidative stress, mitogen-activated protein kinases (MAPKs) phosphorylate the Ser670 (S670) residue of GRK2, which induces GRK2 binding to Hsp90 and localization to mitochondria, where pro-death pathways are initiated. As S670 is also found in  $\beta$ ARKct it may prevent endogenous GRK2 accumulation in the mitochondria. **We hypothesize that  $\beta$ ARKct-mediated cardioprotection in HF is due primarily to mitochondrial GRK2 blockade by  $\beta$ ARKct.** To test this notion, our lab has generated a cardiac-specific mutant  $\beta$ ARKct-S670A transgenic mouse harboring a Ser-to-Ala mutation at the S670 residue that prevents Hsp90 binding and allows for endogenous GRK2 to continue to translocate to the mitochondria upon ischemic injury, while retaining  $\beta$ ARKct in the cytosol to act on  $\beta$ -AR signaling pathways.

**Methods:** *In vivo* hemodynamic analysis was performed to assess cardiac function in  $\beta$ ARKct and  $\beta$ ARKct-S670A transgenic mice and respective normal littermate controls (NLCs). Additionally, intracellular cyclic AMP (cAMP) levels in AC16 cardiomyocytes transfected with  $\beta$ ARKct or  $\beta$ ARKct-S670A, and  $\beta$ ARKct-S670D plasmids were quantified in response to increasing doses of isoproterenol.

**Results:** Early hemodynamic analysis of the  $\beta$ ARKct-S670A mice has demonstrated increased baseline contractility in  $\beta$ ARKct-S670A mice compared to NLC mice, indicating comparable cardioprotective effects to  $\beta$ ARKct mice lacking the Ser-to-Ala mutation, which are mediated by canonical pathways. *In vitro* cAMP quantification revealed AC16s transfected with  $\beta$ ARKct,  $\beta$ ARKct-S670A, and  $\beta$ ARKct-S670D plasmids increased cAMP accumulation in response to increasing doses of isoproterenol compared to control.

**Conclusion:** Studies characterizing the mitochondrial pathways involved in HF rescue following ischemic injury are ongoing. These findings will identify new mechanistic information of GRK2 inhibition for HF, and elucidate a new method for attenuating mitochondrial dysfunction during HF.

This work is supported by NIH grants R01 HL061690-22 (W.J.K.) and T32 HL091804-11 and AHA predoctoral fellowship 23PRE1019969 (H.C.).



# Low-Dose Metformin Treatment Offers Modest Nephroprotection in a Mouse Model of Diabetic Kidney Disease

Kayla Olstinske,<sup>1</sup> James LeFevre,<sup>2</sup> Christopher Karch,<sup>2</sup> Ronald Frantz,<sup>2</sup> Kevin Carvendale,<sup>3</sup> and Shankar Munusamy<sup>4</sup>

<sup>1</sup>Drake Univ; <sup>2</sup>Drake University; <sup>3</sup>Des Moines University; and <sup>4</sup>Drake Univ College of Pharmacy and Health Sciences

Abstract ID 16082

Poster Board 160

**Background:** Diabetes mellitus affects more than 30 million people in the US, and about one-third of these patients develop diabetic kidney disease (DKD). Metformin is a widely prescribed antidiabetic medication for patients with type 2 diabetes; however, its direct effects on renal function are poorly understood. This study investigates the effects of non-glucose lowering, low-dose metformin treatment against the progression of DKD using a genetic mouse model of type 2 diabetes.

**Methods:** To accelerate the progression of kidney disease, non-diabetic (control) and diabetic mice were subjected to left nephrectomy at ten weeks of age. Following two weeks of recovery, mice were divided into four treatment groups: and received vehicle or metformin (100 mg/kg/day) for four weeks in four treatment groups: 1) vehicle-treated control, 2) metformin-treated control, 3) diabetic, vehicle-treated, and 4) diabetic, metformin-treated. Mice received vehicle or metformin (100 mg/kg/day) for four weeks. Urine, plasma, and kidney tissue samples were collected at the end of the study to measure markers of renal dysfunction—elevations in urine albumin-creatinine ratio (UACR), plasma creatinine, and kidney injury molecule 1 (KIM-1)—markers of renal injury—transforming growth factor-beta (TGF- $\beta$ ), alpha-smooth muscle actin ( $\alpha$ -SMA), and NLR family pyrin domain containing 3 (NLRP3)—and markers of nephroprotection—pyruvate kinase M2 (PKM2), mitochondrially encoded cytochrome c oxidase II (MTCO2), and microtubule-associated protein 1 light chain 3 type II (LC3II).

**Results:** Low-dose metformin treatment in diabetic mice decreased UACR ( $117.5 \pm 61.6$  vs.  $205.3 \pm 112.5$  ug albumin/mg creatinine) and KIM-1 immunostaining ( $1.5 \pm 0.9$  vs.  $2.7 \pm 0.6$ ) compared to vehicle-treated diabetic mice. In contrast, low-dose metformin treatment in diabetic mice did not alter plasma creatinine levels and only marginally reduced renal injury markers (TGF- $\beta$ ,  $\alpha$ -SMA, and NLRP3) or increased nephroprotection markers (such as PKM2, MTCO2, and LC3II) compared to vehicle-treated diabetic mice.

**Conclusion:** Findings from this study indicate modest improvement of renal markers in response to low-dose metformin treatment, mitigating the need to pursue this treatment option for DKD in future studies. Future studies must use a longer-term and higher dose to investigate metformin's nephroprotective potential against DKD.

**Support or Funding Information:** This study was supported by Drake University's intramural funds - Harris Research Endowment, Kresge Research Endowment, and Provost fund.

# Resolving Unchecked Inflammation in Atrial Fibrillation

Deanna Sosnowski,<sup>1</sup> Roddy Hiram,<sup>2</sup> Xiao Yan Qi,<sup>2</sup> Kyla Bourque,<sup>3</sup> Patrice Naud,<sup>2</sup> Sandro Ninni,<sup>4</sup> Darlaine Pétrin,<sup>3</sup> Terry Hebert,<sup>3</sup> and Stanley Nattel<sup>1</sup>

<sup>1</sup>McGill University; Montréal Heart Institute (MHI), Université de Montréal; <sup>2</sup>Montréal Heart Institute (MHI), Université de Montréal; <sup>3</sup>McGill University; and <sup>4</sup>Montréal Heart Institute (MHI) Université de Montréal; Université de Lille, Institut Pasteur, France

Abstract ID 14979

Poster Board 301

**Objective:** Persistent inflammation drives the pathogenesis and progression of atrial fibrillation (AF), but pharmacological agents targeting inflammatory pathways in AF remain under-explored as therapeutics. NLRP3 inflammasome signalling is activated in atrial cardiomyocytes (CMs) from patients with AF, highlighting the importance of pro-inflammatory mechanisms in non-immune cells toward AF pathogenesis. Specialized Pro-resolving lipid Mediators (SPMs) derived from N-3 and N-6 polyunsaturated fatty acids (PUFAs) reduce inflammation by promoting non-immunosuppressive inflammatory resolution via their respective G protein-coupled receptors (GPCRs). LipoxinA<sub>4</sub> (LxA<sub>4</sub>), an N-6 PUFA-derived SPM, signals via the formyl peptide receptor-2 (FPR2). Downstream signalling mechanisms are well-established in immune cells during acute inflammatory injury. This study investigates CM-specific inflammatory signalling in AF and the role of LxA<sub>4</sub>-FPR2 signal transduction to attenuate chronic inflammation and AF pathogenesis.

**Hypothesis:** LxA<sub>4</sub> attenuates cardiac electrical and structural remodeling in AF by FPR2-mediated signalling, which targets the NLRP3 inflammasome in atrial cardiomyocytes.

**Methods:** Adult dogs underwent implantation of a pacemaker lead into the right atrial appendage and were atrial tachypaced at 600 beats per minute (cAF) or remained in sinus rhythm for 3 weeks. Hearts from a separate cohort of healthy adult dogs were enzymatically digested by Langendorff perfusion to isolate left atrial CMs. Isolated CMs were paced *in vitro* using the IonOptix C-Pace100-culture pacer at 1Hz or 3Hz for 24 hours in parallel. Assessment of NLRP3 inflammasome, inflammatory cytokine levels, and FPR2 expression was done by western blotting and qPCR. To investigate LxA<sub>4</sub>-FPR2 downstream signalling mechanisms, iPSCs were generated from healthy adult blood cells and differentiated into iPSC-CMs. GPCR transcript levels were assessed via bulk RNA sequencing. iPSC-CMs were transfected with the ExRai-AKAR2-NLS biosensor to detect nuclear PKA activity, subsequently treated with increasing concentrations of LxA<sub>4</sub>, and imaged using an Opera Phenix high content screening system.

**Results:** FPR2 expression was significantly reduced in whole atrial tissue from cAF canines, while expression was unchanged in CMs paced at 3Hz. NLRP3 inflammasome levels and the inflammatory cytokine, IL-1ss, were increased in paced CMs indicating a critical role of the inflammasome pathway in arrhythmogenesis. Transcripts for FPR2 and other SPM GPCRs were not expressed in iPSC-CMs likely due to their immature phenotype. LxA<sub>4</sub> treatment of iPSC-CMs does not influence nuclear PKA activity in the absence of FPR2, indicating a receptor-dependent activity of LxA<sub>4</sub>.

**Conclusions and Future Directions:** CM-specific NLRP3 inflammasome signaling and FPR2 expression are disrupted in models of AF. Preliminary data suggests that LxA<sub>4</sub> does not affect downstream PKA activity in iPSC-CMs in the absence of its receptor, FPR2. Attenuation of the NLRP3 inflammasome pathway via LxA<sub>4</sub>-FPR2 signalling mechanisms remains to be assessed in our AF models and iPSC-CMs.

**Funding:** Canadian Institutes of Health Research and the Courtois Foundation

# SERCA Inhibition by Drugs - A Potential Therapeutic Strategy in Ischemia

Jesika Colomer-Saucedo,<sup>1</sup> Yuanzhao L. Darcy,<sup>2</sup> Valeria A. Copello,<sup>2</sup> Paula Diaz-Sylvester,<sup>2</sup> Melanie Loulouis,<sup>2</sup> and Julio A. Copello<sup>2</sup>

<sup>1</sup>*Southern Illinois Univ School of Medicine; and* <sup>2</sup>*SIU School of Medicine*

**Abstract ID 53843**

**Poster Board 302**

Ischemia impairs the function of the heart (metabolism, mechanical and electrical). Restoration of blood flow by reperfusion will end the ischemic event but can paradoxically increase heart damage through processes where intracellular calcium ( $\text{Ca}^{2+}$ ) signaling appears to play a central role (ischemia-reperfusion injury). During ischemia, abnormal sarcoplasmic reticulum (SR) intracellular  $\text{Ca}^{2+}$  store homeostasis induces SR  $\text{Ca}^{2+}$  overload. At the onset of reperfusion, SR overload boosts massive SR  $\text{Ca}^{2+}$  release via ryanodine receptors (RyR) causing hypercontraction, excessive production of free-radicals and calpain-mediated proteolysis, as well as mitochondrial permeability transition (MPT) pore opening. All these events associate with myocyte cell death. We aim to identify drugs that could prevent or reduce overload during ischemia, by inhibiting SR  $\text{Ca}^{2+}$ -ATPase (SERCA) pumping of  $\text{Ca}^{2+}$  into the SR. The focus is on a drug that could be less toxic than Thapsigargin and cyclopiazonic acid (classic SERCA blockers). Previous work showed that compounds in the 1,4-benzothiazepine family that associate with cell protection, inhibit SERCA (CGP-37157, K201). We think that SERCA block could be: 1) A class property of CGP analogs, including novel 1,4-BZTs (PH000-995, -902) and FDA-approved benzodiazepines (BZDs) and 2) A hidden characteristic of drugs that induce cell protective action in ischemia-like conditions. Drug effects on SERCA and RyRs were tested on SR microsomes isolated from rabbit or porcine striated muscle (cardiac and skeletal) using  $\text{Ca}^{2+}$  uptake and leak photometric assays. SERCA ATPase activity was also measured at constant  $\text{Ca}^{2+}$  (0.3, 1, 100  $\mu\text{M}$ ). Conditions tested were normal pH (7.0) or acidosis (pH 6.2-6.4) as in ischemia. Bilayers were utilized to test drug effects on RyR channel activity. Novel BZTs reduced  $\text{Ca}^{2+}$  uptake in the absence and presence of ruthenium red (RyR blocker), indicating SERCA block. ATPase assays determined BZTs block of SERCA is  $\text{Ca}^{2+}$ -dependent (higher potency at low  $\text{Ca}^{2+}$ ).  $\text{Ca}^{2+}$  leak assay and RyR channel studies found PH000902 to have full agonism on RyRs. Other BZTs displayed partial or no RyR agonism (compared to N-methyl bromo-eudistomin). BZT's properties were maintained in acidosis (pH=6.2-6.4). BZDs did not inhibit SERCA, despite being homologous to CGP, suggesting a S atom in BZT ring to be crucial for activity. Some BZD displayed partial RyR agonism. Our results also show that cell protective drugs (pimozide, carvedilol, epigallocatechin gallate) also inhibit SERCA but did not affect RyR function. In summary, SERCA inhibition is a class property of 1,4-BZTs and analogs of CGP, yet is not observed in BZDs used in therapeutics. As CGP has been found to have low toxicity in experimental animals, 1,4-BZTs could have potential for developing specific SERCA blockers to improve therapy of myocardial ischemia to attenuate reperfusion injury. Our studies also suggest that prevention of SR  $\text{Ca}^{2+}$  overload via SERCA inhibition, may be a mechanism of action of various drugs associated with cell protection.

Supported by the Eskridge Bequest and W.E. McElroy Charitable Foundation

# $\beta$ -caryophyllene, a CB2 Receptor Agonist Alleviates Diabetic Cardiomyopathy via Inhibiting AGE/RAGE-Induced Oxidative Stress, Fibrosis, and Inflammasome Activation

HEBAALLAH M. HASHIESH,<sup>1</sup> Mohamed FN. Meeran,<sup>2</sup> Sheikh SA. Azimullah,<sup>3</sup> Ernest Adeghate,<sup>4</sup> Dhanya Saraswathiamma,<sup>5</sup> Saeeda Almarzooqi,<sup>6</sup> and Shreesh K. Ojha<sup>6</sup>

<sup>1</sup>PhD student at College of Medicine and Health Sciences, United Arab Emirates University; <sup>2</sup>Postdoctoral, College of Medicine and Health Sciences, United Arab Emirates University; <sup>3</sup>Medical Specialist, College of Medicine and Health Sciences, United Arab Emirates University; <sup>4</sup>Professor at College of Medicine and Health Sciences, United Arab Emirates University; <sup>5</sup>Medical Research Specialist, College of Medicine and Health Sciences, United Arab Emirates University; and <sup>6</sup>Associate Professor, College of Medicine and Health Sciences, United Arab Emirates University

Abstract ID 14617

Poster Board 303

Chronic hyperglycemia-induced advanced glycation end products-receptor for advanced glycation end products (AGE-RAGE) following activation results in the oxidative stress, inflammasome activation, and tissue fibrosis and plays important role in the development and progression of diabetic cardiomyopathy (DCM). Provided the emerging role of cannabinoid type 2 receptors (CB2) in diabetes and its complications, the present study aimed to investigate the role of CB2 receptor activation in murine model of DCM by its agonist  $\beta$ -caryophyllene (BCP), a dietary phytocannabinoid. The study also investigated underlying signaling pathways. The experimental murine model of DCM was induced by feeding high fat diet (45% fat) for four weeks in addition to single intraperitoneal injection of streptozotocin (100 mg/kg/body weight). Following the development of diabetes, animals were orally treated with BCP (50 mg/kg/body weight) for 12 weeks. In one group to demonstrate CB2 receptor specific properties of BCP, AM630 (1.5 mg/kg), a specific CB2 receptor antagonist, was given 30 min prior to BCP treatment. At the end of the experiments, metabolic, histopathological, immunohistochemical, electron microscopic and western blotting were performed to evaluate efficacy and demonstrate mechanism. The results revealed that treatment with BCP significantly improved glucose tolerance, enhanced serum insulin level along with reducing insulin resistance. BCP restored phosphorylation of cardiac contractile protein troponin I. BCP was observed to enhance PI3K/AKT phosphorylation, reduce expression of Keap1 which upregulated antioxidant enzymes (HO1, SOD2) mediated by stimulation of Nrf2 signaling. The AGE-RAGE signaling pathway in the heart of DCM mice was significantly mitigated by BCP treatment evidenced by reduced expression of AGEs, RAGE and NOX4. Additionally, NLRP3 inflammasome activation was downregulated and expression of ASC, pro-caspase1 was significantly reduced which further decreased IL-1 $\beta$  and IL-18 expression. The H&E, Masson's trichome, and transmission electron microscopy results further supported the finding that BCP mitigated cardiac hypertrophy, collagen deposition, myofilament disarrangement, mitochondrial disruption, thickened capillary basement membrane, and increased nuclear membrane invaginations. Furthermore, BCP suppressed endothelial-to-mesenchymal transition (EndMT) in DCM mice hearts revealed by decreased expression levels of fibroblast markers ( $\alpha$ -SMA, vimentin, and collagen I) and increased expression levels of endothelial markers (CD31 and VE-cadherin). Interestingly, pre-administration of AM630 abrogated the positive effects of BCP in DCM mice. Collectively, these results demonstrate that inhibition of AGE/RAGE by BCP treatment to DCM mice rescues against diabetes associated complications by reducing oxidative damage, fibrosis, and inflammasome activation attributed to upregulation of PI3K/AKT/Nrf2 signaling, repression of EndMT transition, and inhibition of NLRP3 inflammasome activation in a CB2 receptor dependent mechanism. The study results suggest that CB2 receptors activation may be a vital therapeutic avenue for diabetic cardiomyopathy and BCP could be a novel agent of natural origin with a rationale based on pharmacological and molecular mechanisms for its use as therapeutic and nutraceutical agent.

# Propofol and salvianolic acid A synergistically ameliorates LPS-induced H92 cells injury under hyperglycemia via enhancing SIRT1 to inhibit NLRP3 dependent-pyroptosis

Anyuan Zhang,<sup>1</sup> Ronghui Han,<sup>2</sup> Jiaqi Zhou,<sup>2</sup> Kaijia Han,<sup>2</sup> Jiajia Chen,<sup>2</sup> Yuhui Yang,<sup>2</sup>  
Xihe Zhang,<sup>3</sup> Wangning Shanguan,<sup>4</sup> Liangqing Zhang,<sup>2</sup> Jing Tang,<sup>2</sup> and Zhengyuan Xia<sup>5</sup>

<sup>1</sup>Department of Anesthesiology, the Second Affiliated Hospital & Yuying Children's Hospital of Wenzhou Medical University, Wenzhou, Zhejiang, China; <sup>2</sup>Department of Anesthesiology, Affiliated Hospital of Guangdong Medical University, Zhanjiang, China; <sup>3</sup>Doctoral Scientific Research Center, Lianjiang People's Hospital, Zhanjiang, Guangdong, China; <sup>4</sup>Department of Anesthesiology, the Second Affiliated Hospital & Yuying Children's Hospital of Wenzhou; and <sup>5</sup>State Key Laboratory of Pharmaceutical Biotechnology, Department of Medicine, The University of Hong Kong, Hong Kong, China

Abstract ID 17232

Poster Board 304

Cardiac involvement during sepsis frequently occurs, and considerable diabetes mellitus (DM) patients develop sepsis with concomitant cardiac complications. Propofol (PPF), one of the commonly used intravenous agents for anaesthesia and sedation, has been shown to have moderate antioxidant capacity that enables it to confer protection against cardiovascular complications that are associated with increases in oxidative stress when used at relatively high doses. However, application of propofol at high dose may cause hemodynamic instability especially in patients with pre-existing cardiovascular depressions such as sepsis and/or advanced stages of diabetes. Salvianolic acid A (SAA), a water-soluble extract of Danshen (*Salvia miltiorrhiza* Bunge), is a potent free radical scavenger that confers cardioprotection without noticeable cardiovascular side effects. PPF and SAA share partial structural similarity in terms of phenol structure. It is unknown whether or not PPF and SAA may confer synergistic cardioprotection in subjects with diabetes and sepsis. Rat heart-derived H9c2 cells were exposed to high glucose (HG) for 48 hours, then subjected to lipopolysaccharide (LPS) for 6 hours. HG+LPS significantly decreased cell viability, increased lactate dehydrogenase (LDH) leakage in H9c2 cells, all of which were significantly reversed by either PPF or SAA (respectively applied at 12.5, 25, and 50  $\mu$ M) in a concentration-dependent manner. Administration of 12.5  $\mu$ M PPF (P12.5) jointly with 12.5  $\mu$ M SAA (S12.5) conferred superior protective effects to higher concentration of PPF alone at 25  $\mu$ M (P25), manifested as significantly reduced productions of reactive oxygen species (ROS) and inflammatory mediators, including tumor necrosis factor (TNF)- $\alpha$ , interleukin (IL)-18, IL-1 $\beta$  and IL-6. Moreover, individual application of PPF or PPF and SAA in combination all significantly reduced HG+LPS-induced myocardial cell pyroptosis evidenced as reduced expression of NLRP3, ASC, caspase-1 and GSDMD (all  $P < 0.05$ , NC vs. HG; HG vs. HG+LPS; HG+LPS vs. HG+LPS+P25 or HG+LPS+P12.5+S12.5). Mechanistically, PPF and/or SAA mediated attenuation of H9c2 cells pyroptosis was associated with increased SIRT1 expression, and the protective effects were reversed by silencing SIRT1 (all  $P < 0.05$ , HG+LPS+P25 or HG+LPS+P12.5+S12.5 vs. HG+LPS+P12.5+S12.5+siRNA). Taken together, these results indicated that PPF inhibits oxidative stress response of LPS-induced cardiomyocyte injury by targeting SIRT1 to inhibit NLRP3 dependent-pyroptosis under hyperglycemia and that SAA offers synergistic effect to PPF in cardiac protection, which may represent a novel therapeutic approach to avoid clinical side effects of high dose PPF.

# HuR-dependent expression of Wisp1 is necessary for TGF $\beta$ -induced cardiac myofibroblast activity

Sharon Parkins,<sup>1</sup> Michael Tranter,<sup>2</sup> Adrienne Guarnieri,<sup>3</sup> Lisa Green,<sup>1</sup> Sarah Anthony,<sup>1</sup> and Onur Kanisicak<sup>3</sup>

<sup>1</sup>University of Cincinnati College of Medicine; <sup>2</sup>Univ of Cincinnati College of Medicine; and <sup>3</sup>University of Cincinnati

**Abstract ID 25562**

**Poster Board 305**

We have previously shown that the RNA binding protein Human antigen R (HuR) directly mediates hypertrophic signaling in cardiac myocytes (CMs), and that CM-specific genetic deletion or pharmacological inhibition of HuR reduces pathological remodeling and preserves cardiac function following transverse aortic constriction (TAC)-induced pressure overload, in part through a reduction in pro-fibrotic gene expression. More recently, our lab demonstrated that HuR expression and activity is increased in isolated primary cardiac fibroblasts (CFs) in response to TGF $\beta$  treatment. Pharmacological inhibition of HuR significantly blunts the initial TGF $\beta$ -dependent activation of CFs to a pro-fibrotic myofibroblast (MF) phenotype as marked by a decrease in extracellular matrix (ECM) remodeling genes, collagen gel contraction, and in vitro scratch closure. However, the functional role of HuR in fibroblasts during pathological cardiac remodeling in vivo remains unknown.

To determine the functional role of HuR in CFs, we created a fibroblast-specific deletion of HuR (CF-HuR<sup>-/-</sup>) using a tamoxifen-inducible cre recombinase under control of the PDGFR $\alpha$  promoter. Characterization of basal cardiac structure and function of these mice shows no significant changes compared to wild-type control littermates at 10-12 weeks old following tamoxifen treatment. However, echocardiography results show preserved cardiac function (as marked by ejection fraction) and reduced LV dilation (left ventricular end diastolic volume) in CF-HuR<sup>-/-</sup> mice at 8 weeks following TAC-induced pressure overload.

In addition, we sought to determine whether HuR inhibition in mature MFs (after their initial activation) may also induce resolution of their pro-fibrotic phenotype. To do this, primary cardiac fibroblasts were treated with TGF $\beta$  for 48 hours to induce their activation to MFs followed by HuR inhibition. Results show that treatment with a HuR inhibitor for an additional 48 hours leads to a reduction of the myofibroblast marker gene Wisp1, but not periostin, regardless of whether the cells were maintained under continued TGF $\beta$  stimulation. Similarly, HuR inhibition in MFs appears to reduce the total proteomic content of the MF-derived ECM.

In summary, our new data suggests that fibroblast-specific deletion of HuR reduces pathological cardiac remodeling and fibrosis following pressure overload. Furthermore, inhibition of HuR in mature myofibroblasts reduces the expression of some, but not all, myofibroblast marker genes and appears to initiate remodeling of established fibroblast-derived ECM.

Our primary current funding consists of an NIH R01 (HL158671) and AHA Transformational Project Award (TPA34910086), NIH-NHLBI Training Grant T32-HL125204

# Cardiomyocyte Signaling Factors are Responsible for Heart-Fat Communication and Mediate the Development of Cardiometabolic Disease

Stephanie Kereliuk,<sup>1</sup> Kenneth Gresham,<sup>1</sup> Jessica Ibeti,<sup>1</sup> and Walter Koch<sup>1</sup>

<sup>1</sup>Temple University

Abstract ID 19127

Poster Board 306

Cardiomyocytes are known to secrete signaling factors that can communicate with other organ systems, particularly in response to cardiometabolic stressors such as obesity. Under conditions of cardiometabolic stress, the expression and activity of cardiac GPCR kinase 2 (GRK2), which regulates  $\beta$ -adrenergic receptors in the heart, is upregulated. Previously we have shown that cardiac signaling factors alter adiposity in mice fed a high fat diet, and specific metabolic responses in adipose tissue are dependent on cardiac GRK2 levels and activity. However, the mechanisms responsible for this are unknown. We hypothesize that signaling factors secreted from the heart mediate adiposity and the development of cardiometabolic disease and are regulated by GRK2. To test this, conditioned media from control and GRK2 overexpressing neonatal rat ventricular myocytes (NRVM) was collected and applied to 3T3-L1 adipocytes. 3T3-L1 cells were then assessed by BODIPY fluorescent imaging, protein immunoblotting and qPCR. NRVM conditioned media was also analyzed by mass spectrometry to identify potential signaling factors. Conditioned media treated 3T3-L1 adipocytes demonstrated reduced lipid accumulation and adipogenic marker expression. Conditioned media from GRK2 overexpressing NRVMs further decreased lipid accumulation and differentiation in 3T3-L1 adipocytes. Proteomic analysis of conditioned media revealed several proteins with adipocyte regulatory roles. These findings indicate that cardiomyocyte-released signaling factors influence adipocyte differentiation that is further enhanced by GRK2 overexpression. Future work aims to identify the specific factors responsible and whether these may be from cardiac secreted exosomes. These findings will be used to elucidate novel mechanisms involved in heart-fat communication and cardiometabolic disease development.

This research was funded by NIH R01 HL061690, NIH P01 HL134608 and AHA 18MERIT33900036.

# Changes of ACE-2 related-miR-200b-3p expression over time are a predictive factor of long hospitalization for COVID-19: in silico, machine learning and validation analysis

Disha Keswani,<sup>1</sup> Mikolaj Marszalek,<sup>1</sup> Zofia Wicik,<sup>1</sup> Ceren Eyiletten,<sup>1</sup> Anna Nowak,<sup>1</sup> Sérgio Simões,<sup>2</sup> David Martins,<sup>3</sup> Krzysztof Klos,<sup>1</sup> Wojciech Wlodarczyk,<sup>1</sup> Alice Assinger,<sup>4</sup> Dariusz Soldacki,<sup>1</sup> Andrzej Chcialowski,<sup>1</sup> Jolanta Siller-Matula,<sup>4</sup> and Marek Postula<sup>1</sup>

<sup>1</sup>Medical University of Warsaw; <sup>2</sup>Instituto Federal do Espirito Santo; <sup>3</sup>Universidade Federal do ABC (UFABC); and <sup>4</sup>Medical University of Vienna

Abstract ID 19272

Poster Board 307

COVID-19 is associated with an increased risk of mortality and adverse cardiovascular (CV) occurrences. ACE2 interaction network caused by virus infection can affect the expression levels of miRNAs and influence severity of the disease. This study aimed to analyse the diagnostic/predictive utility of ACE2-related miRNAs, which were identified by in silico analysis (miR-10b-5p, miR-124-3p, miR-200b-3p, miR-26b-5p, miR-302c-5p) in patients with COVID-19, and aimed to unravel the functions of miRNAs, by using machine learning-SHAP analysis for clinical data and bioinformatic tools.

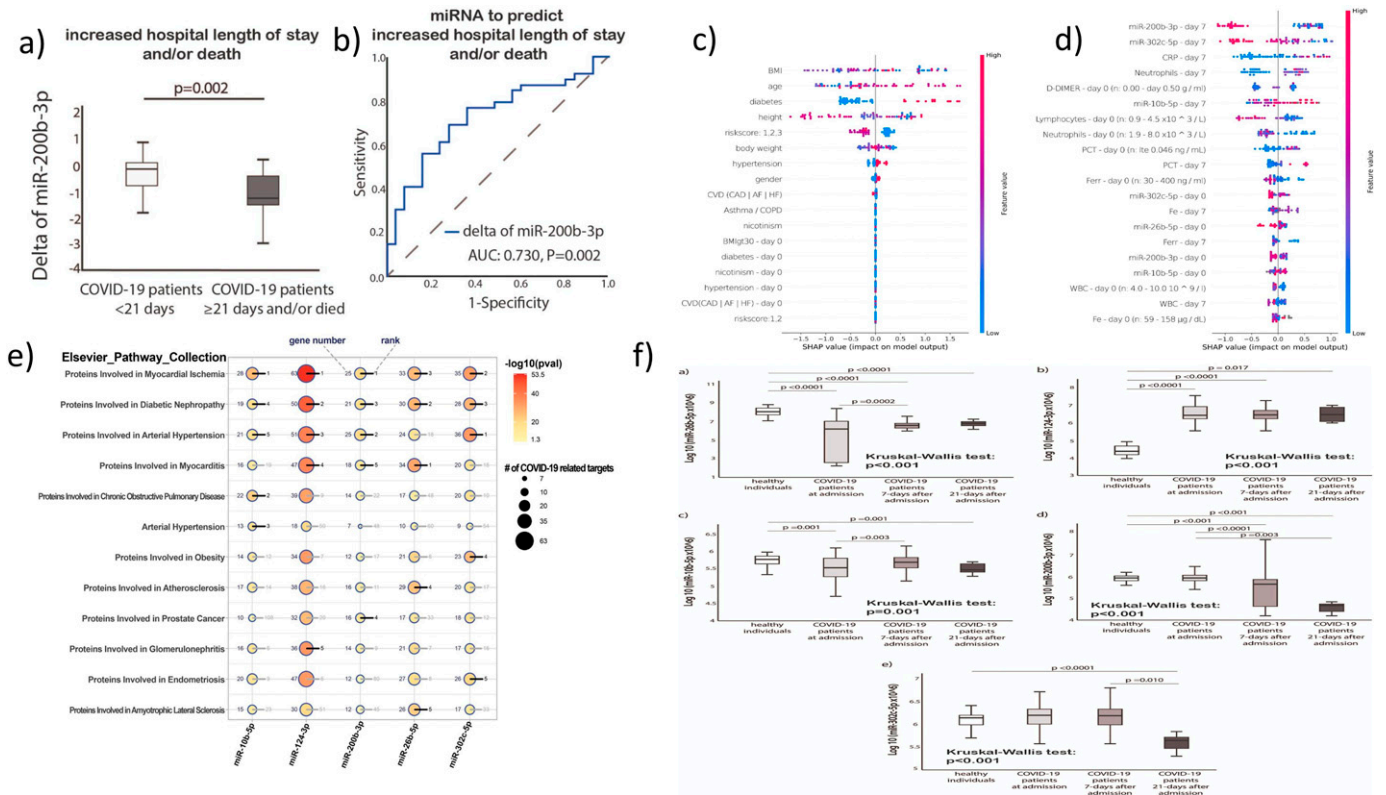
**Methods:** Blood samples and clinical data of 79 patients and 32 healthy were collected at; day of admission, 7 days in and 21 days after admission. Endpoint was hospitalisation length of stay (>21 days) and/or death in follow-up.

**Results:** Delta low miR-200b-3p expression (after 7 days of admission) presents predictive utility in assessment of the hospital length of stay and/or death in ROC curve analysis (AUC:0.730, p=0.002). Delta low miR-200b-3p expression, diabetes mellitus (DM) are independent predictors of increased hospital length of stay and/or death (OR=5.78; CI=0.57-21.21; p= 0.008, OR=4.89; CI=1- 23.86; p=0.04). MiR-26b-5p and miR-10b-5p in patients were found lower at the baseline, 7 and 21-days after admission compared to the healthy controls (p<0.0001 for all time points). SHAP analysis indicated miR-200b-3p (day 7th), miR-302c-5p (day 7th), CRP (day 7th), neutrophils (day 0), and D-Dimer (day 0) as the most promising predictors of long hospitalisation. Pathway-enrichment showed that interleukin-2 signaling pathway, and Pathways in cancer were the top pathways. MiR-200b-3p showed regulation of COVID-19-related targets associated with T cell protein tyrosine phosphatase and HIF-1 transcriptional activity in hypoxia, key pathways in COVID-19. Bioinformatics analysis pointed out the role of those miRNAs in multiple CVDs phenotypes associated with COVID-19.

**Conclusions:** In this study we validated and characterized miRNAs which could serve as novel, predictive biomarkers of the long term COVID-19 hospitalisation and can be used for early stratification of patients and prediction of severity of infection development in an individual.

**Support/Funding Information:** Grant 1M9/1/M/MGED/N/22 and the CEPT infrastructure financed by the European Union-the European Regional Development Fund within the Operational Program "Innovative economy" for 2007-2013; and CAPES, CNPq and FAPESP fundings (CNPq proc. 307145/2017-4, FAPESP proc. 2018/18560-6 and 2018/21934-5).





**Figures:**  
 a) and b) Comparison of circulating miRNAs expression between the groups, miR-200b-3p; Mann-Whitney U test and Wilcoxon test were used appropriately.  
 c) and d) SHAP values of cofactors and miRNAs  
 e) Top 5 significantly enriched disease-related pathways associated specifically with COVID19-related targets of ACE2 network related miRNAs. Red color indicates low p-values (high enrichment), and blue indicates high p-values (low enrichment).  
 f) Kruskal-Wallis test shows the difference among the four groups

# Downregulation in Connexin43 expression is associated with reduced ferroptosis and enhanced tolerance to myocardial ischemia-reperfusion injury in type 1 diabetic mice

Jiajia Chen,<sup>1</sup> Danyong Liu,<sup>1</sup> Jiaqi Zhou,<sup>1</sup> Dongcheng Zhou,<sup>1</sup> Anyuan Zhang,<sup>2</sup> Yuxing Jiang,<sup>1</sup> Jiefu Lin,<sup>1</sup> Liangqing Zhang,<sup>1</sup> Ronghui Han,<sup>1</sup> Yuhui Yang,<sup>1</sup> and Zhengyuan Xia<sup>3</sup>

<sup>1</sup>Department of Anesthesiology, Affiliated Hospital of Guangdong Medical University, Zhanjiang, China; <sup>2</sup>Department of Anesthesiology, the Second Affiliated Hospital & Yuying Children's Hospital of Wenzhou; and <sup>3</sup>State Key Laboratory of Pharmaceutical Biotechnology, Department of Medicine, The University of Hong Kong, Hong Kong, China

Abstract ID 22723

Poster Board 308

Patients with diabetes are more vulnerable to myocardial ischemia/reperfusion injury (MIRI). However, animal studies showed that short-term diabetes may have a protective effect on MIRI, but the mechanism is unclear. Studies showed that abnormal cardiac Connexin43 (Cx43) protein expression is associated with a variety of pathological conditions, such as myocardial ischemia and diabetic cardiomyopathy, while down-regulating Cx43 can alleviate acute kidney injury by inhibiting ferroptosis. However, the role of Cx43 in myocardial IRI in diabetic conditions and in particular its potential interplay with cardiac ferroptosis in this pathology is unknown. Thus, the present study aimed to explore the role and mechanism of Cx43 and ferroptosis in relation to myocardial susceptibility to IRI in diabetes. Streptozotocin (STZ)-induced diabetes mice and age-matched control mice were subjected to myocardial IRI by occluding the left coronary artery for 30 minutes followed by 2 hours of reperfusion respectively at 1,2 and 5 weeks of diabetes induction. In vitro, rat origin H9C2 cardiomyocytes (H9C2) were exposed to 35 mmol/L high glucose(HG) for 48h in the absence or presence of Cx43 gene knockdown with siRNA, followed by hypoxia for 6 hours and reoxygenation for 12 hours. Myocardial infarct size was assessed by TTC/Evan blue staining. The heart function of mice was measured by echocardiography. Myocardial mitochondrial damage was measured by transmission electron microscopy. Serum CK-MB and malondialdehyde (MDA) levels were measured by ELISA. Cell viability was detected by the CCK-8 assay, apoptosis by the TUNEL assay. BODIPY staining for ROS production. Western blot analysis was performed to assess cardiac Cx43 protein and ferroptosis-related protein expression. Compared to controls, infarct size was reduced in 1-2 weeks DM mice after I/R, but significantly increased at DM 5 weeks ( $p < 0.05$ ). Post-ischemic cardiac function was improved in 1 week mice and worsened in 5 weeks DM mice as compared to that in the non-diabetic control mice, which was associated with reduced ferroptosis in DM 1-2 weeks and significantly enhanced ferroptosis in DM 5 weeks mice (all  $p < 0.05$  vs. control). Also, cardiac Cx43 expression was significantly lower after I/R in DM 1-2 weeks mice compared to controls and significantly higher in DM 5 weeks mice. Cx43 inhibitor GAP19 significantly attenuated ferroptosis and reduced post-ischemic myocardial infarct size in 5 weeks DM mice. Application of Erastin (ferroptosis activator) reversed the cardioprotective effect of GAP19. In vitro, H9C2 cells exposed to hypoxia and reoxygenation (H/R) under high glucose environment showed a significant increase in cellular injury, as evidenced by increased LDH release, reduced cell viability, significantly increased lipid peroxidation product (MDA) and ferroptosis, which was concomitant with significantly elevated Cx43 expression. Cx43 gene knockdown in H9C2 resulted in a significant increase in glutathione peroxidase 4 (Gpx4) protein expression, reduction in MDA production and ferroptosis, and subsequently reduced post-hypoxic cell viability under high glucose (all  $p < 0.05$  vs. control). However, these beneficial effects of Cx43 gene knock-down were significantly attenuated or eliminated by Erastin. It is concluded that down-regulating the expression of Cx43 in the diabetic myocardium may subsequently inhibit ferroptosis, thereby increasing myocardial tolerance to ischemia-reperfusion injury.

# Heart-rate Corrected QT Interval and Statin use in the general population. The Polish Norwegian Study (PONS)

Georgeta Vaidean,<sup>1</sup> Sandeep Vansal,<sup>2</sup> and Marta Manczuk<sup>3</sup>

<sup>1</sup>Florida International University, Herbert Wertheim College of Medicine; <sup>2</sup>PCOM South Georgia; and <sup>3</sup>The Maria Skłodowska Curie Memorial Cancer Centre and Institute of Oncology

Abstract ID 55464

Poster Board 309

**Introduction:** Prolonged QT interval is associated with cardiac arrhythmias and sudden death. The hERG potassium channel (IKr) plays a role in cardiac repolarization. Decreased IKr may lead to QT prolongation. Due to their structural similarity to IKr blockers, statins have been suggested to prolong the QT interval in non-human models.

**Purpose:** To compare the QT interval between statin users and non-users in a large community-based population.

**Methods:** Cross-sectional data from an ongoing cohort study, following a standardized protocol. The QT intervals were obtained from digital standard 12-lead resting ECG. Heart rate correction (QTc) was performed with Bazett's formula. We excluded individuals taking medication known to influence the QT interval (anti-arrhythmics, beta blockers, digoxin, anti-psychotics), as well as other conditions (coronary heart disease, atrial fibrillation, WPW syndrome, pacemakers). Generalized linear models were used for confounding control.

**Results:** The analytic sample was 7439 participants, average age 54.92 (SD 5.4), 65.01% women, 27.11% with hypertension, 4.27% with diabetes type 2. Mean (SD) QTc were 418.18 ms (45.58) for men and 426.41 ms (44.79) for women. Mean QTc was 399.5 ms (28.32) in statin users and 393.6 ms (28.88) in non-users. Compared to those not using statins, statin users had a longer mean QT interval by 3.20 ms (95%CI 0.79 - 5.62) after adjusting for age, sex, smoking, physical activity, hypertension, diabetes, and by 3.46 ms (95% CI 1.07 - 5.84) after additional adjustment for left ventricular hypertrophy, T-wave inversion, presence of Q wave, ST segment elevation or depression and cardiac blocks. Pathologically abnormal QT prolongation (QTc > 430 ms for men, > 450 ms for women) was present in 9.61% of statin users and 9.10% of non-statin users (not statistically significant). Lipid lowering drugs other than statins were not associated with the QT interval duration.

**Conclusion:** In a population free of diagnosed heart disease, we found a modest increase in the QTc interval among statin users compared to non-users, even after ample adjustment for additional clinical and electrocardiographic characteristics.

**Implications:** While the overall cardioprotective effect of statins on cardiovascular risk is well-established, awareness of potential modest QT interval prolongation may be warranted, especially in a more complex clinical context of concomitant QT-prolonging medication.

**FINANCIAL DISCLOSURE:** The data collection was supported by a grant from the Polish-Norwegian Research Fund (PNRF-228-AI-1/07)

# Osteopontin promotes G protein-coupled receptor kinase (GRK)-2-dependent desensitization of cardiac $\beta_2$ -adrenergic receptor anti-fibrotic signaling

Anastasios Lymperopoulos<sup>1</sup>

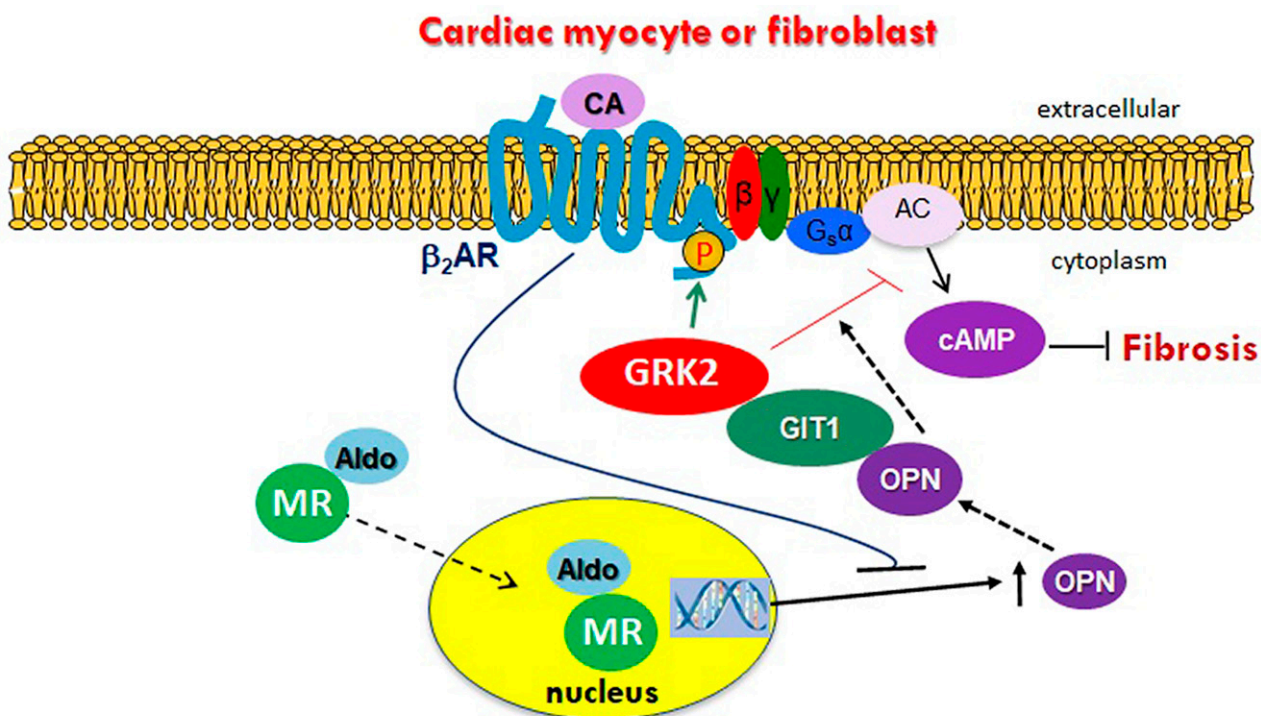
<sup>1</sup>Nova Southeastern Univ

Abstract ID 15850

Poster Board 310

Cardiac  $\beta_2$ -adrenergic receptors (ARs) are known to inhibit collagen production and fibrosis in cardiac fibroblasts and myocytes.  $\beta_2$ AR is a Gs protein-coupled receptor (GPCR) and, upon its activation, stimulates generation of cyclic 3', 5'-adenosine monophosphate (cAMP). cAMP has two effectors: protein kinase A (PKA) and the exchange protein directly activated by cAMP (Epac). Epac1 has been shown to inhibit cardiac fibroblast activation and fibrosis. Osteopontin (OPN) is a ubiquitous pro-inflammatory and pro-fibrotic cytokine, including in the heart. We report here that the cardiotoxic hormone aldosterone upregulates OPN via the mineralocorticoid receptor (MR) in H9c2 cardiomyoblasts. This is prevented by  $\beta_2$ AR-activated GPCR-kinase (GRK)-5. GRK5 directly phosphorylates and inhibits the MR in cardiomyocytes. Additionally, CRISPR-mediated OPN deletion enhances  $\beta_2$ AR-dependent cAMP generation in H9c2 cardiomyocytes and upregulates Epac1. OPN deletion also enables the  $\beta_2$ AR to completely abrogate transforming growth factor (TGF)- $\beta$ -dependent fibrosis in H9c2 cardiomyocytes. Mechanistically, OPN interacts with G $\alpha$ s subunits in H9c2 cardiomyocytes to facilitate recruitment of GRK2, the major GRK phosphorylating and desensitizing the cardiac  $\beta_2$ AR. This, in turn, augments the GRK2-dependent functional desensitization of the  $\beta_2$ AR, thereby opposing this receptor's anti-fibrotic cAMP/Epac1 signaling. In conclusion, we have uncovered a direct inhibitory effect of OPN in cardiac  $\beta_2$ AR's anti-fibrotic signaling via facilitation of GRK2-mediated receptor desensitization. Thus, OPN blockade could be of value in the treatment and/or prevention of cardiac fibrosis.

**Support/Funding Information:** 1) American Foundation for Pharmaceutical Education (AFPE) 2) NSU's President's Faculty Research & Development (PFRDG) grant



CA: Catecholamine

# **$\beta$ -adrenoceptor-mediated vasodilation is enhanced by acute colchicine-treatment in men with essential hypertension**

Thomas A. Jepps, Ylva Hellsten,<sup>1</sup> Jennifer van der Horst,<sup>1</sup> Thomas Ehlers,<sup>1</sup> Christian Aalkjaer,<sup>2</sup> Lasse A. Gliemann,<sup>1</sup> and Sophie A. Moller<sup>1</sup>

<sup>1</sup>University of Copenhagen; and <sup>2</sup>Aarhus University

**Abstract ID 17343**

**Poster Board 311**

Colchicine treatment has known beneficial effects on cardiovascular health and reduces the incidence of cardiovascular disease. Studies in isolated rodent arteries show colchicine enhances  $\beta$ -adrenoceptor-mediated vasodilation. In this translational study, we examined whether this effect of colchicine was present in humans by conducting a double-blinded, placebo controlled intervention study. Middle-aged men with essential hypertension were randomly assigned firstly to acute treatment with either 0.5 mg colchicine or placebo, and subsequently re-randomized for 3 weeks of treatment with either colchicine 0.5 mg twice daily (n=16) or placebo (n=15) followed by a washout period of 48-72 h. The vasodilator responses to isoprenaline, acetylcholine and sodium nitroprusside were determined, as well as arterial pressure, arterial compliance and plasma inflammatory markers. Acute colchicine treatment increased the isoprenaline- and SNP-mediated increase in vascular conductance, but had no effect on the response to acetylcholine. Following the washout period, three weeks of twice daily treatment of colchicine did not induce an accumulated or sustained effect on the  $\beta$ -adrenoceptor response and there was no effect on either arterial pressure, arterial compliance or on the level of measured inflammatory markers. This study provides the first translational evidence for a transient enhancement of  $\beta$ -adrenoceptor-mediated vasodilatation by colchicine in humans. The finding of an acute effect suggests that it may be clinically important to maintain an adequate bioavailability of colchicine to support the cardiovascular protective effects that have been observed with colchicine in various clinical trials.

This work was supported by a grant from Augustinusfonden (19-3644). TAJ was funded by a Lundbeck Foundation grant (R323-2018-3674). JvH was funded the European Union's Horizon 2020 research and innovation program under the Marie Skłodowska-Curie scheme (grant agreement no. 081199).

# Ovariectomy Promotes Angiotensin II-induced Renal Dysfunction and Vasopressin Excretion via 12/15-Lipoxygenase

Shubha R. Dutta,<sup>1</sup> Purnima Singh,<sup>2</sup> and Kafait U. Malik<sup>2</sup>

<sup>1</sup>Univ of Tennessee HSC; and <sup>2</sup>University of Tennessee Health Science Center

Abstract ID 51393

Poster Board 312

Hypertension is a major risk factor that contributes to kidney injury in women. While the female sex hormone 17 $\beta$ -estradiol (E2) has been shown to be cardioprotective in experimental models of cardiovascular diseases, E2 replacement therapy in postmenopausal women has been controversial. We have shown previously that ovariectomy (used as a tool to deplete endogenous E2) augments angiotensin (Ang) II-induced increase in blood pressure and plasma level of 12(S)-hydroxyeicosatetraenoic acid (HETE), a major arachidonic acid metabolite produced by 12/15-lipoxygenase (ALOX15). ALOX15 and its arachidonic acid-derived metabolite 12(S)-HETE is implicated in cardiovascular and renal diseases. This study was conducted to investigate the contribution of ALOX15 to Ang II-induced renal dysfunction in intact and ovariectomized (OVX) female mice. Ang II (700 ng/kg/min) infused subcutaneously by osmotic pumps for 2 weeks caused a marked increase in water intake (mL; 10.5 $\pm$ 0.64 vs 5.0 $\pm$ 0.40), and renal dysfunction as evidenced by increased urine output (mL; 5.06 $\pm$ 0.43 vs 1.56 $\pm$ 0.15), decreased urine osmolality (mOsm/Kg; 1.27 $\pm$ 0.04 vs 2.10 $\pm$ 0.06) and increased urinary excretion of vasopressin prosegment copeptin (pg/mL; 149.53 $\pm$ 3.47 vs 122.13 $\pm$ 1.00) measured by ELISA in OVX but not intact (with ovaries intact) wild type (WT) mice (n=4/group, p<0.05). These effects of Ang II were attenuated in intact and OVX *Alox15* knockout (ALOX15KO) female mice (water intake: 4.0 $\pm$ 0.41 and 5.25 $\pm$ 0.47; urine output: 1.18 $\pm$ 0.11 and 1.00 $\pm$ 0.10; urine osmolality: 2.56 $\pm$ 0.27 and 1.78 $\pm$ 0.07; urinary excretion of copeptin: 122.9 $\pm$ 0.56 and 118.03 $\pm$ 3.76; n=4/group, p<0.05). Moreover, in OVX-WT mice with depleted plasma E2 (pg/mL; 1.00 $\pm$ 0.26 vs 14.71 $\pm$ 1.38; n=4, p<0.05, measured by ELISA), the effects of Ang II on renal hypertrophy expressed as total kidney/body weight ratio (mg/g; 12.19 $\pm$ 0.55 vs 9.16 $\pm$ 0.22; n=6, p<0.05) and reactive oxygen species production measured by increased 2-hydroxyethidium fluorescence on staining with dihydroethidium (arbitrary unit; 16.73 $\pm$ 0.63 vs 4.33 $\pm$ 0.09, n=4, p<0.05), were also enhanced compared to intact WT mice. These effects of Ang II were attenuated in both intact and OVX-ALOX15KO mice (plasma E2: 13.96 $\pm$ 1.75 and 1.29 $\pm$ 0.44, kidney/body weight: 9.48 $\pm$ 0.18 and 10.10 $\pm$ 0.33, reactive oxygen species: 1.55 $\pm$ 0.07 and 1.82 $\pm$ 0.02). These data suggest that ovariectomy or lack of 17 $\beta$ -estradiol promotes Ang II-induced hypertension and renal dysfunction, most likely by a mechanism dependent on ALOX15/12 (S)-HETE. Therefore, the selective inhibitors of ALOX15 or 12 (S)-HETE receptor antagonists could be useful for treating hypertension and associated pathogenesis in postmenopausal, hypoestrogenic women or females with ovarian failure. Furthermore, it has been reported that two single-nucleotide polymorphisms in the *Alox12* gene, rs9904779 and rs434473 (encoding a replacement of asparagine by serine in the protein), was associated with onset of natural menopause in a small set of white women studied. Therefore, it would be important to explore ALOX15 gene polymorphism further in a larger population of diverse groups of normal aging and pre- and postmenopausal females to determine its impact on the contribution of arachidonic acid-ALOX15 derived 12(S)-HETE in hypertension and its pathogenesis.

# Metformin Protects Against Liposaccharide (LPS)-induced Hyperinflammation in Doxorubicin-induced Senescent Endothelial Cells

Ibrahim Abdelgawad,<sup>1</sup> Kevin Agostinucci,<sup>1</sup> Bushra Sadaf,<sup>1</sup> and Beshay Zordoky<sup>1</sup>

<sup>1</sup>Univ of Minnesota

Abstract ID 26880

Poster Board 357

**Introduction:** Recently, cancer survivors were shown to have a higher risk of severe infections that require hospitalization. Doxorubicin (DOX) is a widely used chemotherapeutic agent in the treatment of cancer patients. DOX has been shown to induce senescence phenotype in endothelial cells (ECs) characterized by endothelial dysfunction and secretion of pro-inflammatory cytokines termed senescence-associated secretory phenotype (SASP). Lipopolysaccharide (LPS), a bacterial component that stimulates inflammation, has been demonstrated to augment the inflammatory SASP phenotype in endothelial models of replicative senescence and irradiation-induced senescence. However, the effect of LPS in DOX-induced endothelial senescence has not been established. Therefore, in the current work, we determined the effect of LPS stimulation in DOX-induced senescent ECs in vitro. Then, we identified the effects of metformin, an anti-diabetic drug that has senomorphic properties, on LPS-induced hyperinflammation.

**Methods:** Human umbilical vein endothelial cells (HUVECs) were either treated with DOX for 24 hours followed by 72 hour-incubation without DOX to establish senescence (Sen-HUVECs) or left untreated as non-senescent proliferating cells (NS-HUVECs). The effect of LPS was determined by stimulating both Sen-HUVECs and NS-HUVECs with LPS (30 ng/ml) for an additional 24 hours. The effects of metformin on LPS stimulation were assessed in both types of cells. Culture media were collected to measure SASP factors using ELISA. Protein expression of the senescence marker, p21, was measured to confirm the induction of senescence. To delineate the molecular mechanisms, the changes in NF- $\kappa$ B, a major signaling pathway involved in inflammation, were determined using western blotting.

**Results:** DOX-induced senescence phenotype was demonstrated by upregulation of p21. A significant hyperstimulation response to LPS was observed in Sen-HUVECs compared to NS-HUVECs, demonstrated by higher secretion of SASP markers in the media including IL-6, CXCL2, and MMP3. The protein expression of ICAM-1, a marker of endothelial dysfunction, was also upregulated in Sen-HUVECs. Pretreatment with metformin blunted LPS-induced upregulation of SASP markers and normalized the expression of ICAM-1. Metformin effects were mediated by the downregulation of LPS-induced activation of NF- $\kappa$ B.

**Conclusions:** Our current work shows that DOX-induced senescent endothelial cells show hyperinflammatory response to LPS. The senomorphic drug, metformin, can be a promising strategy to ameliorate infection-induced hyperinflammation in DOX-treated cancer survivors.

Research was supported by the National Heart, Lung, and Blood Institute, grant R01HL151740. I.Y.A is supported by the Doctoral Dissertation Fellowship (DDF) offered by the University of Minnesota and the Bighley Graduate Fellowship from the College of Pharmacy.

# Sexual Dimorphism of the Fasting Adipose: Mitigation of Metabolic and Cardiovascular Dysfunction in a Non-Obese Prediabetic Rat Model

Haneen Dwaib,<sup>1</sup> Omar Obeid,<sup>2</sup> Ahmed F. El-Yazbi,<sup>3</sup> and Haneen Dwaib<sup>1</sup>

<sup>1</sup>*Palestine Ahliya Univ;* <sup>2</sup>*American university of beirut;* and <sup>3</sup>*Alexandria Univ*

Abstract ID 15333

Poster Board 358

Prediabetes is a transitional stage in the progression of Type 2 Diabetes where diabetes-related cardiovascular (CV) complications begin. Our previous work on non-obese prediabetic male rats showed that early CV and metabolic impairments were associated with confined dysfunction in the thoracic perivascular adipose tissue (PVAT) characterized by inflammation and hypoxia. There has been neither recommendations for pharmacological treatment to interrupt the hypoxic machinery in PVAT, nor clear sexual dimorphism in PVAT involvement at this stage, we therefore hypothesized that therapeutic fasting (TF) can alleviate PVAT dysfunction, metabolic and CV stress among Mild hyper-caloric (MHC)-fed rats in a sex dependent manner. Sprague-Dawley rats from both sexes (4-5weeks) were allocated into 3 groups: control diet (C), MHC diet and MHC-diet with TF, for 24 weeks. Rats were fed ad libitum in the first 12 weeks. Afterwards, the TF group were subjected to daily fasting from 7.00pm -7.00am for 12 weeks with free access to water, and to MHC-diet otherwise. Daily food intake, body weight, blood glucose, body composition (using NMR), HbA1c, serum insulin levels, echocardiographic parameters, and noninvasive blood pressure were measured. At week 24; rats were catheterized for invasive hemodynamic examination. Cardiac autonomic neuropathy was assessed by measuring baroreceptor sensitivity using the vasoactive method. After sacrifice, aortic contractility and endothelial function were measured using organ bath experiments and molecular investigation was performed on various adipose pools, in addition to cardiac and aortic tissues. To assess the role of female sex hormones 3 additional groups of females were bilaterally ovariectomized (OVX) on week 12, then the same feeding groups (C, MHC and MH-TF) were applied for the remaining 12 weeks. The same set of parameters and experiments were measured and conducted. As expected, MHC feeding induced non-obese prediabetes, signs of early cardiovascular and metabolic dysfunction with and PVAT impairment in male rats. Intact female rats resisted MHC-induced derangements, while OVX females presented an obese prediabetic phenotype, with CV and metabolic impairments and PVAT dysfunction. Moreover, on the molecular and histochemical levels, cardiac and aortic tissues as well as brainstem presented pathologies in the MHC arms presented by increased macrophage infiltration and oxidative stress in all tissues, plus an increased fibrosis in the cardiac and aortic ones. Strikingly, TF in the presence of MHC feeding and in the absence of calorie restriction, and estrogen in the case of females, seemed to substantially correct these alterations in both male and OVX rats and interrupt hypoxia in PVAT. Taken together, our work suggests a novel understanding whereby TF interferes with the hypoxia machinery in PVAT and mitigates prediabetes and related CV insults in a sex dependent manner.



# Alterations in pyroptotic signaling mediated by phosphorylation of GRK2 and mitochondria functional alterations

Ruxu Zhai, Yuzhen Tian,<sup>1</sup> Ole Mortensen,<sup>2</sup> Priscila Sato,<sup>1</sup> Emad Alnemri,<sup>3</sup> and Hsin-Yao Tang<sup>4</sup>

<sup>1</sup>Drexel University; <sup>2</sup>Drexel Univ College of Medicine; <sup>3</sup>Thomas Jefferson University; and <sup>4</sup>The Wistar Institute

**Abstract ID 17723**

**Poster Board 359**

G protein-coupled receptors (GPCRs) mediate signal transduction from the extracellular environment to the intracellular space. Receptor signaling is terminated via receptor phosphorylation mediated by GPCR-kinases (GRKs). GRK2 is one of the main isoforms in the heart and is upregulated in heart failure (HF) patients. Recently, we and others have reported a non-canonical GRK2 signaling cascade that is initiated by ERK phosphorylation of GRK2 and subsequent mitochondrial translocation of this kinase. Notably, we found that phosphorylated GRK2 at S670 post-ischemia/reperfusion decreases mitochondrial glucose oxidation and pyruvate dehydrogenase (PDH) activity. A possible link was established between GRK2 and PDH using 2D-SDS PAGE combined with phospho-proteomics. Using a novel PDH $\alpha$  KI CRISPR Cas HEK cell line, we tested the hypothesis that this phosphorylation event regulates PDH activity. Utilizing cytosolic and mitochondrially-targeted pyruvate indicators we measured pyruvate levels in WT and KI HEK cells. Moreover, using a mouse model where GRK2 cannot translocate to the mitochondria (GRK2-S670A), in the presence or absence of myocardial infarction, we are investigating the role of GRK2 mitochondrial translocation, metabolic alterations, and gasdermin signaling. Further experiments will elucidate the precise role of mitoGRK2 on cardiac metabolism, PDH activity, and mechanisms of cell survival a priori and a posteriori to cardiac ischemic events relevant to understanding cardiac metabolic remodeling in disease progression.

# Investigating High Salt Diet Effects on Stress Responding and Microglial Activation

Jasmin N. Beaver,<sup>1</sup> Matthew T. Ford,<sup>1</sup> Anna E. Anello,<sup>1</sup> Lee Gilman,<sup>1</sup> and Allianna K. Hite<sup>1</sup>

<sup>1</sup>Kent State University

Abstract ID 14239

Poster Board 360

Consuming excess salt (NaCl), the primary source of dietary sodium (Na), has become prevalent in modern society. Across species, most research on salt consumption has focused on physiology - in particular, cardiovascular function. As a result, current health guidelines advise reduced sodium intake to attenuate cardiovascular disease risk. In contrast, less research has examined how salt consumption affects brain health and function, and consequently, behavior. Much remains to be learned about how this prevalent, non-caloric component of diet impacts neurophysiology to shift basic behaviors, including responses to stressors/environmental threats. Given the challenges and ethics of manipulating salt intake in humans, we use mice to facilitate rigorous control of salt intake, environment, and stressor exposure. I hypothesized mice consuming excess salt would exhibit increased active coping strategies (e.g., more swimming/climbing, less immobility) relative to controls. Group housed adult (10-week old) male and female C57BL/6J mice had access to one or two diets for 4- or 8- weeks, with cages assigned to: 1) control (0.4% NaCl w/w) diet only; 2) high salt (4.0% NaCl) diet only; or 3) both control and high salt diets (mixed); this last allowed analyses of diet preference over time. Diet consumption, water intake, and body weight were recorded twice a week. During the final diet manipulation day, environmental threat response was assessed using a brief swim stressor. In both males and females on either a 4- and 8-week diet manipulation, swim test results indicated no significant stress responsivity differences in latency to first immobility, nor in time spent immobile, swimming, or climbing between diet conditions. Contrary to our hypothesis, our findings suggest excess salt consumption for 4-8-weeks does not augment behavioral responses to environmental stressors. Mice (8-week females and 4- and 8-week males) in the mixed diet condition initially preferred control diet, but consumed significantly more of the high salt diet after ~2 weeks. We are presently analyzing microglial activation in brain regions associated with homeostatic control, stress responses, and behavioral inhibition (medial prefrontal cortex, paraventricular nucleus of the hypothalamus, and basolateral amygdala). Overall, our behavioral findings indicate that high salt intake does not influence behaviors in either sex in response to an acute stress.

# Inhibition of Cardiac GCH1 O-GlcNAc Modification promotes cardiac BH4/eNOS signaling after myocardial ischemia-reperfusion in mice with Type-2 Diabetes

Yuhui Yang,<sup>1</sup> Dongcheng Zhou,<sup>1</sup> Jiajia Chen,<sup>1</sup> Weiyi Xia,<sup>1</sup> Danyong Liu,<sup>1</sup> Liangqing Zhang,<sup>1</sup> Yin Cai,<sup>2</sup> Zhidong Ge,<sup>3</sup> and Zhengyuan Xia<sup>1</sup>

<sup>1</sup>Affiliated Hospital of Guangdong Medical University; <sup>2</sup>GuangDong Medical University; and <sup>3</sup>Ann & Robert H. Lurie Children's Hospital of Chicago

Abstract ID 22693

Poster Board 361

Reperfusion after myocardial infarction may further increase myocardial injury, which can be exacerbated by diabetes. Strategies have been developed to ameliorate myocardial ischemia/reperfusion injuries (MIRI) yet the effectiveness of these strategies mostly diminish in diabetes largely due to diminished nitric oxide bioavailability in the cardiovascular system. GTP cyclohydrolase 1 (GCH1) and its product tetrahydrobiopterin (BH4), a co-factor of the endothelial nitric oxide synthase (eNOS), play crucial roles in cardiovascular physiology and in MIRI. O-GlcNAcylation is a ubiquitous post-translational modification that is extremely labile and plays a significant role in physiology, especially in the heart. Sustained activation of cardiac O-GlcNAcylation leads to detrimental effects on cardiovascular function. However, transient elevation of some cardiac protein O-GlcNAcylation can exert beneficial effects in the heart. When chronic diabetes meets acute ischemic injury, the role and regulation of O-GlcNAcylation and in particular its impact on cardiac GCH1 are enigmatic. Here we report that hyper-O-GlcNAc modification of GCH1 may impair its enzymatic activity and subsequently lose its cardioprotective effects against MIRI in mice with type 2 diabetes.

Male C57BL/6 mice with high-fat diet for 6 weeks received intraperitoneal injection of low dose streptozotocin to induce type-II diabetes. MIRI model was established by occluding the left coronary artery for 30 minutes, followed by restoring blood flow for 120 minutes. Results showed that post-ischemic cardiac levels of GCH1 protein expression was increased in diabetic mice but cardiac levels of BH4 and eNOS reduced as compared to non-diabetic control. However, application of the GCH1 inhibitor DAHP in diabetic mice to speed up the degradation of cardiac GCH1 proteins resulted in increased post-ischemic myocardial infarct size and dysfunction in diabetes mice, which was also concomitant with further decreases in cardiac BH4, eNOS, and increases in superoxide production. The results indicated that although the level of GCH1 was upregulated in post-ischemic cardiac tissue, its enzymatic activity was impaired and loses its cardioprotective effects by underlying factor. On the other hand, abnormal activation of cardiac GCH1 O-GlcNAcylation level after MIRI in diabetic mice was detected by proteomic mass spectrometry. After the application of OSMI-1 (a broad-spectrum inhibitor of protein O-GlcNAcylation) in diabetic mice, the cardiac GCH1 activation and protein levels of BH4 and eNOS were increased in diabetic mice at baseline and after MIRI. Surprisingly, although inhibition of O-GlcNAcylation of GCH1 restored its enzymatic activity and increased eNOS expression, the application of OSMI-1 exacerbated rather than attenuated post-ischemic myocardial infarct size in diabetes. Given that suppression of eNOS O-GlcNAcylation promotes eNOS activity, global inhibition of O-GlcNAcylation may have adversely modulated other cardiac pro-survival signaling proteins such as Akt. Findings from the current study suggest that strategies to specifically suppress the O-GlcNAcylation of cardiac GCH1 and/or eNOS in diabetes may be effective means to combat against MIRI in diabetes.

This study was supported by Guangdong Basic and Applied Basic Research Foundation (2022A1515011116, 2019A1515110063) and Natural Science Foundation of China (82270306; 81970247).

# Modulation of Mitochondrial Bioenergetics in Human Brain Microvascular Endothelial Cells by Telomerase Reverse Transcriptase

Jesmin Jahan,<sup>1</sup> Madeline Stroud,<sup>1</sup> Anil Sakamuri,<sup>1</sup> and Yagna Jarajapu<sup>1</sup>

<sup>1</sup>North Dakota State Univ

Abstract ID 22482

Poster Board 362

Human brain microvascular endothelial cells (HBMECs) play a critical role in preserving brain function by regulating blood flow and blood-brain-barrier (BBB) integrity. HBMECs use both glycolysis and oxidative phosphorylation as sources of energy. The catalytic subunit of telomerase, telomerase reverse transcriptase (TERT), is known to translocate to mitochondria during stress and regulate the generation of reactive oxygen species (ROS). This study tested the hypothesis that TERT modulates bioenergetics in HBMECs.

Cultured HBMECs were used at passage 8. Agilent Seahorse (XFp) Bioanalyzer was used for determining glycolysis and oxidative phosphorylation (OXPHOS) by analyzing extracellular acidification rate (ECAR) and oxygen consumption rate (OCR). 2-Deoxy-D-glucose (2-DG) (50 mM) and rotenone/antimycin A (R/A) (0.5  $\mu$ M), and Mito Stress Test kit (Agilent), respectively, were used to evaluate different metabolic indices that are indicators of glycolysis and OXPHOS. OCR determined basal and maximal respiration, ATP production, proton leak, spare respiratory capacity, and non-mitochondrial respiration, whereas ECAR defined basal and compensatory glycolysis, post-2-DG acidification, and glycolytic proton efflux rate (glycoPER). Pharmacological activator or inhibitor of TERT, cycloastragenol (CAG) or BIBR1532, respectively, was used to determine the role of TERT in mitochondrial bioenergetics.

BIBR1532 (1  $\mu$ M) increased basal by  $120 \pm 5\%$  ( $p < 0.05$ ) and maximal respiration (determined by FCCP (1.1  $\mu$ M) -uncoupling) by  $157 \pm 7\%$  ( $p < 0.05$ ) ( $n=5$ ). The spare respiratory capacity and nonmitochondrial respiration were unaltered by BIBR1532 ( $n=5$ ). No change was observed in the basal glycolysis by BIBR1532 ( $n=3$ ) however, the compensatory glycolysis, an indicator of the maximum glycolytic capacity, was increased ( $n=3$ ). Post-2DG acidification, an indicator of proton secretion from the non-glycolytic sources, was increased in the presence of BIBR1532 ( $n=3$ ). However, glycoPER was unaltered. CAG showed no effect on any of the parameters of OXPHOS in the concentration range of 0.3-30  $\mu$ M ( $n=3$ ).

This study shows that physiological levels of TERT negatively regulate and that acute inhibition of TERT increases OXPHOS and glycolysis.

# Angiotensin-(1-7) and Gut-Bone Marrow Axis in Aging

Kishore Chittimalli,<sup>1</sup> Jesmin Jahan,<sup>2</sup> Aaron Ericsson,<sup>3</sup> and Yagna Jarajapu<sup>1</sup>

<sup>1</sup>North Dakota State Univ; <sup>2</sup>North Dakota State University; and <sup>3</sup>University of Missouri

Abstract ID 22254

Poster Board 363

**Background:** Aging compromises the colon epithelial barrier integrity resulting in chronic systemic inflammation, which increases risk for cardiovascular diseases. Aging-associated gut microbial dysbiosis is implicated in this pathology. Metabolites derived from dysbiotic bacteria in aging are known to stimulate myelopoiesis in bone marrow, which directly contribute to the systemic inflammation. We have previously showed that the protective peptide of Renin Angiotensin System (RAS), Angiotensin-(1-7) (Ang-(1-7)), restored epithelial barrier integrity in Old mice via Mas receptor (MasR) activation. This study tested the hypothesis that Ang-(1-7) modulates gut-bone marrow axis to ameliorate systemic inflammation.

**Methods:** Young (3-4 months) and Old (20-24 months) male C57Bl/6 mice were treated with saline or Ang-(1-7) by using osmotic pumps (1 µg/Kg/min for 4 weeks). Colonic organoids were cultured and Wnt3a expression was determined. Gut microbiome was analyzed by 16S rRNA sequencing of bacterial DNA using MiSeq followed by analysis by Qiime 2.0 and Past 4.10 software. Myelopoiesis in the bone marrow cells was determined by using colony forming unit-granulocytes-macrophages (CFU-GM) assay followed by flow cytometric enumeration of monocytes (Ly6G<sup>-</sup>CD11b<sup>+</sup>Ly6C<sup>hi</sup>) and macrophages (Ly6G<sup>-</sup>CD11b<sup>+</sup>F4/80<sup>+</sup>Ly6C<sup>hi</sup>). Inflammatory cells in the colon wall were characterized by immunohistochemistry. Plasma levels of Trimethylamine Oxide (TMAO), IL-1β, IL-6, HMGB1, MCP1 and TNFα were analyzed.

**Results:** Organoid cultures showed decreased size of organoids and expression of Wnt3a in the Old group compared to the Young ( $p < 0.05$ ,  $n=6$ ), which were restored by Ang-(1-7). Aging was associated with decreased richness shown by Shannon and Chao1 diversity indices and altered beta diversity (Bray-Curtis ( $p < 0.0001$ ) or Jaccard ( $p < 0.0001$ )). Microbial dysbiosis is evident based on altered relative abundance of 222 ASVs in aging. Plasma TMAO levels ( $6.99 \pm 0.44$  µmol/L) were higher in aging compared to the Young ( $3.08 \pm 0.23$  µmol/L,  $p < 0.001$ ). Ang-(1-7) modified microbial dysbiosis, reversed changes in alpha and beta diversity in aging and decreased TMAO levels ( $3.30 \pm 0.24$  µmol/L,  $p < 0.001$  vs Old). Bone marrow cells from old mice showed increased myelopoiesis compared to young ( $p < 0.01$ ,  $n=6$ ) that were associated with increased infiltration of inflammatory cells in the colon. Ang-(1-7) decreased the number of monocytes ( $18 \pm 4/10^6$  WBC) than the old group ( $47 \pm 4/10^6$  WBC,  $p < 0.001$ ,  $n=6$ ). Pro-inflammatory macrophages were decreased by Ang-(1-7) in the bone marrow and reduced the infiltration of the colon wall. Plasma levels of IL-1β, IL-6, HMGB1, MCP1 and TNFα were higher in the old group compared to the young ( $p < 0.05$ ,  $n=5$ ), which were lowered by Ang-(1-7) ( $p < 0.05$ ,  $n=5$ ).

**Conclusion:** Ang-(1-7)/MasR pathway modulates gut-bone marrow axis by reversing microbial dysbiosis and myelopoietic bias in aging thereby ameliorates systemic inflammation.

# Dexmedetomidine Preconditioning Attenuates Myocardial Ischemia/Reperfusion Injury by Increasing SIRT1 Expression to Inhibit Autophagy Overactivation in Mice

Jianfeng He,<sup>1</sup> Danyong Liu,<sup>1</sup> Jiajia Chen,<sup>1</sup> Hanlin Ding,<sup>2</sup> Dongcheng Zhou,<sup>1</sup> Yuhui Yang,<sup>1</sup> Weicai Yang,<sup>3</sup> Ronghui Han,<sup>1</sup> Sheng Wang,<sup>4</sup> and Zhengyuan Xia<sup>1</sup>

<sup>1</sup>Department of Anesthesiology, Affiliated Hospital of Guangdong Medical University; <sup>2</sup>Xiangyang Center Hospital, Affiliated Hospital of Hubei University of Arts and Science; <sup>3</sup>Department of Anesthesia, Lianjiang People's Hospital, Zhanjiang, Guangdong, China; and <sup>4</sup>Department of Anesthesiology, Beijing Anzhen Hospital, Capital Medical University - Beijing Institut

Abstract ID 18884

Poster Board 500

Myocardial infarction (MI) is one of the primary causes of mortality in patients with coronary heart disease. Restoration of blood supply to the ischemic myocardium may cause further damage to the original ischemic myocardium, a phenomenon known as myocardial ischemia/reperfusion injury (MIRI). Dexmedetomidine (Dex) could attenuate MIRI, and Dex has been shown to activate SIRT1/mTOR signaling when applied after the onset of reperfusion. However, the role of SIRT1/mTOR signaling in Dex preconditioning cardioprotection is unclear. Thus, the present study was aimed to explore the effects of and mechanism of Dex preconditioning on MIRI. 6-8 week C57 mice were allowed to adapt to food and environment for a week and were then randomly assigned to five groups: the sham group, the MIRI group, the MIRI+Dex group, the MIRI+Dex+EX527 (SIRT1 inhibitor) group, and the MIRI+Dex+EX527+3-methyladenine (3-MA, autophagy inhibitor) group. Mice in the Dex groups were intraperitoneally injected with Dex at 20 $\mu$ g/kg one day prior to be subjected to 30 minutes coronary occlusion and 120 minutes reperfusion. EX527 (10mg/kg/day) was intraperitoneally injected for a duration of one week before inducing MIRI. 3-MA was intraperitoneally injected (30 mg/kg) 30 min before inducing MIRI. In vitro, rat-derived H9C2 cardiomyocytes (H9C2) were pretreated with 10 $\mu$ M Dex for two hours in the absence or presence of 1 $\mu$ M EX527 for two hours. In addition, cells were pretreated with 3-MA for one hour before the addition of EX527 in the group of MIRI+Dex+EX527+3-MA. After the completion of scheduled treatments above mentioned, the cells were then subjected to hypoxia/ reoxygenation (H/R) injury (composed of 12 h of hypoxia followed by 6 h of reoxygenation). Myocardial infarct size was assessed by Evan blue/TTC staining. The heart function of mice was measured by echocardiography. Levels of serum CK-MB and the lipid peroxidation product Malondialdehyde (MDA) were measured by ELISA. Cell viability was detected by the CCK-8 assay, apoptosis by the TUNEL assay. Western blot analysis was performed to assess cardiac SIRT1 protein expression and apoptosis-related proteins and autophagy-related LC3, p62 and mTOR proteins. Dex preconditioning significantly decreased post-ischemic serum CK-MB, reduced myocardial infarct size, attenuated the increase in autophagic cell death, and improved left ventricular function in mice as compared to the untreated control group (all  $P < 0.05$ , MIRI+Dex vs. MIRI), while these protective effects of Dex were significantly reversed by inhibiting SIRT1 with Ex527 (all  $P < 0.05$  MIRI+Dex vs. MIRI+Dex+Ex527). Application of 3-MA inhibited post-ischemic autophagy and reverted Ex527-mediated cancellation of Dex cardioprotective effects in mice after MIRI. In vitro, H9C2 cell viability was decreased when cells were subjected to H/R, accompanied by increased levels of LDH and MDA and autophagic cell death, and all these changes were significantly ameliorated by pre-treatment with Dex. Similar as seen in vivo, SIRT1 inhibition with EX527 cancelled Dex mediated protection in cells subjected to H/R, while application of 3-MA reverted EX527-mediated cancellation of Dex cellular protection despite SIRT1 remained inhibited in the presence of EX527. It is concluded that Dex preconditioning reduces myocardial ischemia-reperfusion injury by upregulating SIRT1 to inhibit MIRI or H/R-induced increases in autophagy.

# 5-HT<sub>1F</sub> Agonist Lasmiditan Induces Mitochondrial Biogenesis And Alters Successful And Failed Repair Genes In A Mouse Model Of Acute Kidney Injury

Paul Victor Santiago Raj,<sup>1</sup> Kevin Hurtado,<sup>1</sup> Jaroslav Janda,<sup>1</sup> and Rick Schnellmann<sup>1</sup>

<sup>1</sup>Bio5 Institute, College of Pharmacy, Department of Pharmacology & Toxicology, University of Arizona, Tucson, AZ, USA

Abstract ID 24411

Poster Board 501

**Background:** AKI is defined as an onset and progressive decline in renal function and is often accompanied by a persistent reduction in mitochondrial function, fatty acid oxidation and vascular injury. AKI is an important public health concern with no FDA-approved treatments. We have shown that FDA approved 5-HT<sub>1F</sub> receptor agonist lasmiditan stimulates mitochondrial biogenesis (MB) and accelerates renal recovery in a mouse model of AKI. *Kirita et al*, 2020 recently performed single nucleus sequencing in mouse AKI and reported conserved cellular responses and profiled successful and failed repair genes. We sought to explore the role of lasmiditan on selective successful and failed repair genes post-AKI in our AKI model system.

**Methods:** Male 8-week-old C57B/6J mice were administered 0.3mg/kg of lasmiditan or normal saline 24h after I/R and then every 24h over a 144h period (n=6/group). Kidneys were harvested and snap frozen in liquid nitrogen. Renal cortex samples were used to analyze gene expression (qRT-PCR) and protein expression (immunoblot) post AKI. One way ANOVA followed by TUKEY multiple comparison test was used to determine statistical significance between treatment groups. A p-value of p≤0.05 were used to identify statistical changes and correct for multiple comparisons.

**Results:** Serum creatinine and Kidney injury marker 1 (*KIM1*) was measured and found to be maximally elevated at 24h post I/R and lasmiditan treated groups decreased serum creatinine (~4 fold) and *KIM1* (~2.7fold) over time compared to vehicle and IR24. qRT-PCR analysis revealed increase of successful repair genes – *ACSM2a*, *LRP2*, *SLC5A12* and *HNF4A* upon lasmiditan treatment and failed repair genes – *VCAM*, *LCN2*, *RELB* and *KCNIP4* in 144h of lasmiditan treatment. At 24h and I/R vehicle, mRNA levels of successful repair genes in IR24 decreased and increased in at 144h of lasmiditan treatment. Alternatively, mRNA levels of failed repair genes were elevated at IR24 and lasmiditan treatment did not reduce the expression of failed markers to sham levels. These findings were confirmed using immunoblot analysis.

**Conclusion:** These data affirm the role of 5-HT<sub>1F</sub> agonist Lasmiditan mediating the transcriptional and translational level of successful and failed repair genes thus contributing to fatty acid metabolism, reabsorption of lactate and inflammation but the molecular mechanism is still unclear. This approach will allow us to identify and assess key genes responsible for pathophysiological changes during AKI and other kidney diseases, and the effects of drugs stimulating repair/recovery.

This work was supported by grant: BX000851 (Department of Veterans Affairs) to RGS.

# Delivery of Human ACE2 Across the Blood Brain Barrier Attenuated Development of Neurogenic Hypertension Using An Engineered Liposome-Based Delivery System

Yue Shen,<sup>1</sup> Richard Lamptey,<sup>2</sup> Jagdish Singh,<sup>3</sup> and Chengwen Sun<sup>4</sup>

<sup>1</sup>North Dakota State Univ; <sup>2</sup>North Dakota State University; <sup>3</sup>North Dakota State Univ Col of Pharm; and <sup>4</sup>North Dakota State Univ College of Pharmacy

Abstract ID 18644

Poster Board 502

The blood brain barrier (BBB) blocks therapeutic drugs access to the brain cardiovascular regulatory regions in the treatment of hypertension, which could lead to drug-resistant hypertension. To overcome this challenge, PEGylated liposomes were surface-modified with transferrin (Tf) for specific binding Tf receptor on the BBB and conjugated to a cell-penetrating peptide (CPP) to enhance their cellular uptake into the brain. Here, we evaluated the efficacy of Tf-CPP-liposome to deliver angiotensin-converting enzyme 2 (ACE2) gene or EGFP (control) gene across the BBB in Sprague Dawley (SD) rats. Systemic administration of the Tf-CPP-Liposomes carrying a lentiviral vector plasmid encoding EGFP (control) or ACE2 (150 µg/kg, I.V.) significantly increased EGFP or ACE2 expression respectively in the paraventricular nucleus (PVN) brain area and in the liver, detected using Western Blots and Real-time PCR. However, without Tf, CPP-Liposome-mediated expression of EGFP was significantly lower than Tf-CPP-Liposome in the brain. EGFP expressions in the liver are comparable between two liposomes, suggesting modification with Tf increased the specific delivery to the brain. The immunohistochemistry study demonstrated that the EGFP expression in the brain was localized on the neurons within the PVN by staining using antibodies against neuronal marker, NeuN and glial cell marker, GFAP, in the rats which received intravenous administration of Tf-CPP-Liposome EGFP. Next, we examine the effect of Tf-CPP-Liposome-mediated overexpression of ACE2 in the brain on development of hypertension. Angiotensin II (Ang II, 100ng/min) were consistently infused into left lateral ventricle (ICV) using osmotic pumps in SD rats. ICV infusion of Ang II significantly elevated mean arterial pressure (MAP, from 93.2±4.0 mmHg to 168.4±4.4 mmHg, n=5, P<0.05), reaching to the peak in 7 days (169.2±11.2 mmHg) and keeping consistent at high level for at least 3 weeks. In addition, Ang II-induced elevation in blood pressure was associated with cardiac hypertrophy and fibrosis. More interestingly, treatment with Tf-CPP-Liposome-ACE2 (150 µg/kg, I.V.) significantly attenuated Ang II-induced increases in MAP by 30%. However, Tf-CPP-Liposome-EGFP did not alter Ang II-induced pressor effect on MAP. Tf-CPP-Liposome-ACE2 also did not change the blood pressure in sham rats, which received ICV perfusion of PBS. Moreover, intravenous administration of Tf-CPP-Liposome-ACE2 significantly attenuated Ang II-induced cardiac hypertrophy and fibrosis. In summary, Tf-CPP-Liposome successfully delivered ACE2 gene across the BBB; and elevated ACE2 expression in brain cardiovascular regulatory areas. This Tf-CPP-Liposome-mediated overexpression of ACE2 dramatically attenuated neurogenetic hypertension by systemic administration.

Support/Funding Information: NIH HL143519 and NIH HL124338.



## Doxorubicin induced cardiotoxicity via inhibiting PKC- $\epsilon$ /SIRT1 pathway

Danyong Liu,<sup>1</sup> Jianfeng He,<sup>2</sup> Hanlin Ding,<sup>3</sup> Chunyan Wang,<sup>4</sup> Yao Chen,<sup>4</sup> Junmin He,<sup>5</sup> Chun Chen,<sup>6</sup> Yuantao Li,<sup>4</sup> and Zhengyuan Xia<sup>2</sup>

<sup>1</sup>Department of Anesthesiology, Affiliated Shenzhen Maternity & Child Healthcare Hospital, Southern Medical University, Shenzhen, China; <sup>2</sup>Affiliated Hospital of Guangdong Medical University; <sup>3</sup>Xiangyang Center Hospital, Affiliated Hospital of Hubei University of Arts and Science; <sup>4</sup>Affiliated Shenzhen Maternity & Child Healthcare Hospital, Southern Medical University; <sup>5</sup>The Second People's Hospital of Jingmen; and <sup>6</sup>YiChang Central People's Hospital, China Three Gorges University

Abstract ID 17200

Poster Board 503

Malignancy is a dominant cause of death globally and chemotherapy is one of the major therapeutic strategies. Doxorubicin (DOX) is widely used for the treatment of a variety of cancers. However, DOX is known to induce cardiotoxicity, characterized by increased vulnerability to heart failure and arrhythmias. The mechanism of DOX-induced cardiotoxicity remains unclear. Protein kinase C (PKC)- $\epsilon$  has been shown to promote the survival of various cell types by increasing the activation of Akt pathway and up-regulation of pro-survival factors. Moreover, PKC- $\epsilon$  overexpression is closely related to chemotherapy resistance in various cell types. However, it is unclear whether cardiomyocytes may resist DOX-induced cardiotoxicity through a PKC- $\epsilon$ -dependent mechanism. Therefore, the purpose of this study was to explore the role and mechanism of PKC- $\epsilon$  in DOX-induced cardiotoxicity. 8-10 weeks C57 / B6 mice were allowed to be adaptive to food and environment for a week before being randomly assigned to drug treatment group in which DOX (4 mg/kg once per week) was given via tail intravenous injection for a duration of 4 weeks to produce cardiotoxicity, and mice in the control group were injected with same volume of normal saline. In vitro rat derived H9C2 cardiomyocytes (H9C2) were exposed to 1  $\mu$ mol/L DOX for 24 hours in the absence or presence of the adenovirus-overexpressed PKC- $\epsilon$  gene. Echocardiography was used to measure myocardial contractile function in mice; Serum CK-MB level was detected by ELISA and cell viability detected by CCK-8 assay. Cell damage was assessed by measuring LDH release, and apoptosis was detected by TUNEL assay. Intracellular ROS production was detected by DHE staining. Western blot analysis was performed to assess cardiac PKC- $\epsilon$ , Sirt1 and apoptosis-related proteins expressions. Compared with the control group, cardiac contractile function was significantly decreased in DOX group ( $p < 0.05$ ) that was concomitant with significant increases in serum CK-MB and LDH as well as increases in Bax and Cleaved Caspase 3 proteins expression while PKC- $\epsilon$ , Sirt1, Bcl-2 proteins expression were significantly decreased, (all  $p < 0.05$  vs. control). In vitro, exposure of H9C2 cells to DOX significantly increased cell damage, manifested by increased LDH release, decreased cell viability, and significantly increased ROS production and apoptosis, along with decreased expression of PKC- $\epsilon$ , SIRT1 proteins and increased expression of pro-apoptotic proteins. Overexpression of PKC- $\epsilon$  in H9C2 cells increased SIRT1 protein expression, thereby reducing ROS production and apoptosis, leading to increased cell viability (all  $p < 0.05$ ). However, Sirt1 inhibitor Ex527 significantly attenuated or eliminated the above mentioned beneficial effects of PKC- $\epsilon$  overexpression. Inhibition of cardiac PKC- $\epsilon$  and the subsequent reduction in Sirt1 may represent a major mechanism whereby Doxorubicin induced cardiotoxicity.

**Key words:** Doxorubicin; cardiotoxicity; apoptosis; PKC- $\epsilon$ ; Sirt1.

## Expanding the GRK5 Interactome

Morgan Pantuck,<sup>1</sup> Sudarsan Rajan,<sup>1</sup> Eric Barr,<sup>1</sup> Jessica Ibeti,<sup>1</sup> Joanne Garbincius,<sup>1</sup> Ryan Coleman,<sup>1</sup> Kurt Chuprun,<sup>1</sup> and Walter Koch<sup>1</sup>

<sup>1</sup>Temple

**Abstract ID 52939**

**Poster Board 504**

Heart failure (HF) is a pathological state where the activity of the heart is insufficient to meet the metabolic needs of the body. As HF develops, the body attempts to increase the contraction force of the heart by stimulating cardiac hypertrophy. This compensatory growth is initially helpful but ultimately hinders cardiac function and drives disease progression. There is an unmet need for therapeutic interventions that can slow the development of HF by preventing cardiac hypertrophy. G Protein-Coupled Receptor Kinase 5 (GRK-5) plays a key role in driving hypertrophic growth in the heart. Although some pathological mechanisms involving GRK-5 are well understood, the full interactome of GRK-5 has yet to be determined. Therefore, we performed Biotin Proximity Labeling (BioID) followed by Mass Spectrometry (MS) in order to identify novel protein/protein interactions involving GRK-5. In this assay, the protein of interest is fused to BioID2, a promiscuous biotin ligase. When BioID2 comes within ~15 nanometers of another protein in the presence of excess biotin, it irreversibly biotinylates the target, which can be subsequently captured on streptavidin beads and analyzed via MS. In this way, many potential protein/protein interactions can be identified, including weak or transient ones. To this end, we introduced a GRK-5/BioID2 fusion protein into Neonatal Rat Ventricular Myocytes (NRVMs) using an adenoviral vector. Cells were stimulated +/- phenylephrine to activate hypertrophic signaling pathways. BioID2 expressed by itself served as a negative control. Approximately 4500 proteins were identified via MS, including many that were significantly enriched in the GRK-5/BioID conditions relative to controls. These data will support the discovery of novel mechanisms by which GRK-5 facilitates pathological hypertrophy, which may reveal new therapeutic targets for HF treatment.

This work is supported by NIH grant T32HL091804.

# Effects of Dapagliflozin as an Adjunct Therapy to Insulin in Streptozotocin-induced Diabetic Rats

Abdul-Azeez A. Lanihun,<sup>1</sup> Rupesh C. Panta,<sup>1</sup> and Guim Kwon<sup>1</sup>

<sup>1</sup>*Southern Illinois University*

**Abstract ID 17705**

**Poster Board 505**

Type 1 diabetes mellitus (T1DM) is a chronic metabolic disorder caused by the autoimmune destruction of insulin-producing beta-cells of the pancreas. Insulin, the mainstay of treatment for T1DM, is often inadequate for optimal blood glucose (BG) control with dangerous side effects such as hypoglycemia. Adjunct therapies have been proposed to provide better BG control and reduce hypoglycemic episodes. Dapagliflozin, a potent sodium-glucose co-transporter 2 (SGLT2) inhibitor, is a new class of hypoglycemic agents for type 2 diabetes, and its potential as an adjunct therapy to insulin in T1DM has been confirmed in clinical studies. However, the increased risk of diabetic ketoacidosis associated with dapagliflozin is a major concern preventing its clinical usage as an adjunct therapy for T1DM. To this end, the efficacy and safety of dapagliflozin in streptozotocin (60 mg/kg)-induced diabetic rats were evaluated using in vivo (3 weeks of baseline after diabetes induction and 8 weeks of treatment) and ex vivo studies. Male Sprague Dawley rats (300-400 g) were divided into 5 groups (n=4-6): healthy, diabetic control, diabetic treated with insulin, diabetic treated with insulin+dapagliflozin (1 mg/kg PO daily), and diabetic treated with dapagliflozin alone. Treatment with insulin or insulin+dapagliflozin caused diabetic rats to maintain body weight with reduced urination and water intake compared to diabetic control. Insulin+dapagliflozin provided better BG control with reduced total insulin injection as compared to insulin alone. Dapagliflozin, as expected, increased urine output and water intake. Lipid panel including total cholesterol, TAG, and HDL was not significantly different in rats treated with insulin+dapagliflozin vs insulin alone. Ex vivo studies indicated a trend of higher kidney weight/body weight and increased sizes of glomeruli in rats treated with insulin+dapagliflozin as compared to diabetic control or healthy rats. Moreover, a significant increase in beta-cell regeneration was observed in the rats treated with insulin alone or insulin+dapagliflozin as compared to diabetic control rats. The plasma concentration of ketones under various experimental conditions will be determined using a beta-hydroxybutyrate assay kit to assess diabetic ketoacidosis. The significance of this study is investigating the effects of dapagliflozin in a type 1 diabetic animal model, which allows ex vivo studies to assess its effects on multiple individual organs and tissues.

## Support/Funding Information:

- Southern Illinois University Edwardsville internal research grant
- Southern Illinois University Edwardsville research grants for graduate students

# Paradoxical Effect of Nitric Oxide on GRK2 in the Kidney and Heart: Implications for Sepsis-Associated Kidney Injury

Thiele Osvaldt Rosales,<sup>1</sup> Jamil Assreuy,<sup>2</sup> and Walter Koch<sup>3</sup>

<sup>1</sup>Temple Univ Health Science Center; <sup>2</sup>Universidade Federal de Santa Catarina; and <sup>3</sup>Temple Univ School of Medicine

Abstract ID 54044

Poster Board 506

**Background:** Sepsis is defined as a life-threatening organ dysfunction caused by an overwhelming immune response to infection. Sepsis clinical findings include cardiac hyporesponsiveness, vasodilatation, and decreased reactivity to vasoconstrictors leading to severe and untreatable hypotension, with nitric oxide (NO) as an important player in this dysfunction. On top of that, sepsis may lead to kidney injury, increasing sepsis mortality. Although sepsis-associated kidney injury (S-AKI) pathophysiology is not fully understood, it is known that renal vascular reactivity to catecholamines is preserved in sepsis in opposition to the systemic vasculature. G protein-coupled receptor (GPCR) kinases (GRKs) are protein kinases that recognize and phosphorylate activated GPCRs, such as adrenergic receptors, labeling them for internalization. It has been shown that NOS-2-derived NO activates GRK2 in the heart by GC/cGMP/PKG pathway, leading to decreased  $\beta_1$  adrenergic receptor density, which is associated with decreased cardiac reactivity in sepsis. Therefore, considering the distinct vascular status between the kidney and the systemic circulation during sepsis, we aimed to evaluate the role of GRK2 and  $\alpha_1$  adrenergic receptor and the putative role of NO in the renal response to sepsis.

**Methods:** Female wild-type Swiss and C57BL/6 NOS-2-KO mice were submitted to sepsis by cecal ligation and puncture (CLP). Swiss mice were treated with a NOS-2 inhibitor (1400W; 1 mg/kg), 30 min before and 6 and 12 h after CLP, with a soluble guanylate cyclase inhibitor (methylene blue; 10 mg/Kg), 6, 12 and 18 h after CLP or with a  $\alpha_1$  adrenergic receptor antagonist (prazosin; 1 mg/Kg), 12 h after CLP. *In vivo* experiments, molecular and biochemistry assays were performed 24 h after CLP. Normal Swiss mice were treated with a NO donor (SNAP, 10 mg/Kg) and analyses were carried out 4 hours later.

**Results:** Our results show that i) sepsis decreased the systemic mean arterial pressure and the vascular reactivity to phenylephrine and the basal renal blood flow; ii) treatment with prazosin rescued renal blood flow; iii) sepsis increased NOS-2 expression in the kidney, NO production, NO metabolites and plasma creatinine and urea levels; iv) GRK2 and  $\beta$ -arrestin levels were decreased, whereas  $\alpha_1$  adrenergic receptor density increased in septic kidney; v) the disappearance of renal GRK2 was prevented in NOS-2-KO mice or mice treated with 1400W but not with methylene blue treatment; vi) Guanylyl cyclase levels decreased in septic kidney; vii) GRK2 levels increased in septic heart while  $\beta_1$  adrenergic receptor density and  $\beta$ -arrestin levels were reduced; viii) treatment with a NO donor reduced GRK2 content in the kidney of non-septic mice.

**Conclusions:** Our data show that NO decreases renal GRK2 levels, leading to the maintenance of  $\alpha_1$  adrenergic receptor density, in opposition to cardiac hyporesponsiveness and increased cardiac GRK2 during sepsis. The preservation of the density and/or functionality of this receptor in the kidney, together with a higher vasoconstrictor tonus in sepsis, leads to vasoconstriction. Thus, the increased concentration of vasoconstrictor mediators together with the preservation (and even increase) of the response to them may help to explain S-AKI. Future work aims to investigate the mechanism by which NO regulates renal GRK2 and will assess the direct and indirect effects of NO via S-nitrosylation, NO/sGC/cGMP/PKG pathways.

# Mitochondrial GRK2 Dependent Regulation of the Cellular and Transcriptional Composition after Myocardial Infarction

Samuel Slone, Kurt Chuprun,<sup>1</sup> Gizem Kayki-Mutlu,<sup>1</sup> Rajika Roy,<sup>1</sup> Jessica Ibeti,<sup>1</sup> Erhe Gao,<sup>1</sup> Nathan Tucker,<sup>2</sup> and Michelle Hulke<sup>2</sup>

<sup>1</sup>Temple University; and <sup>2</sup>Masonic Medical Research Institute

Abstract ID 55232

Poster Board 507

Myocardial infarction (MI), an obstruction of coronary blood flow results in significant cardiomyocyte cell loss and subsequent pathological remodeling that leads to chronic heart failure. Although recent medical advances have provided a decline in annual death rate in cardiovascular disease, pathological remodeling post-MI remains a prevalent etiology of heart failure. GRK2 [G protein-coupled receptor (GPCR) kinase 2], essential for de-sensitization of activated GPCRs, is upregulated in human heart failure patients and is associated with poor cardiac function. Therefore, it is clinically beneficial to targeting GRK2 as a therapy for the treatment of heart failure.

Our lab has previously shown phosphorylated GRK2 at Ser670 is required for the translocation of GRK2 to the mitochondria in cardiomyocytes post-IR injury promoting cellular death, however, inducing a S670A knock-in mutation in endogenous GRK2 exhibited a reduction in cardiomyocyte cell death, myocardial infarction (MI), and a preservation of ejection fraction 24 hours post-I/R. Further *in vitro* studies using GRK2-S670A in cardiomyocytes showed improved glucose-mediated respiratory function and preserved ATP production. New data show that GRK2-S670A mice display a significant improvement of cardiac function and remodeling post-MI compared to wild-type (WT) mice out to 4 weeks then show a decline in this improvement with equal dysfunction as WT mice at 8 weeks. Therefore, the objective of this work is to delineate specific gene expression and cellular populations of GRK2-S670A mice in the acute to chronic remodeling myocardium post-MI.

GRK2-S670A and wild-type mice were subjected to permanent left anterior descending coronary ligation (MI) and hearts were collected for single nucleus RNA sequence analysis. Preliminary data from snRNA-seq at 1-week post-MI shows UMAP plot of unique cell clustering of major and minor cell types and composition analysis displayed a higher percentage of cardiomyocyte population in the GRK2-S670A mice compared to wild-type. Finally, differential expression analysis in GRK2-S670A mice post-MI show highly divergent gene regulation in major cell types including macrophages, cardiomyocytes and fibroblast compared to wild-type mice.

In conclusion, snRNA-seq suggest alternative cell types in the myocardium such as fibroblast, endothelial cells, and monocytes/macrophages contain highly divergent gene expression in the GRK2-S670A mice compared to wild-type mice which could be a contributing factor to the acute cardio-protective effect observed *in vivo* that is then lost at 8 weeks post-MI.

# G Protein-coupled Estrogen Receptor 1 and Pregnancy Confer Protection against Hypertension in Aged Female Mice

Eman Gohar,<sup>1</sup> Ravneet Singh,<sup>1</sup> Rawan Almutlaq,<sup>2</sup> and Victoria Nasci<sup>1</sup>

<sup>1</sup>Vanderbilt University Medical Center; and <sup>2</sup>University of Alabama at Birmingham

Abstract ID 14042

Poster Board 508

Hypertension, which is a leading cardiovascular risk factor impacting 40% of American women, is more frequent in aged compared to younger women. Postmenopausal women undergo a decline in the circulating level of estrogen, along with the natural aging process. It has been shown that G protein-coupled estrogen receptor 1 (GPER1) contributes to the cardiovascular protective actions of estrogen in different experimental models. Pregnancy augments GPER1-induced vasodilation in rats. However, the potential interaction between GPER1 and pregnancy in impacting the cardiovascular health later in life is not clear. We hypothesize that GPER1 signaling and pregnancy protects against hypertension in aged female mice. In our study, 16-20 months-old GPER1 knock-out (KO) and wild-type (WT) female mice with and without a history of former pregnancies were implanted with radio-telemeters for blood pressure recording. Animals were placed into metabolic cages for collection of 24h urine samples. Then, animals were euthanized and plasma was collected. To examine whether GPER1 and/or former pregnancies affects circadian blood pressure rhythm in aged female mice, blood pressure was analyzed by cosinor analysis. No significant differences in body weight were observed between groups. GPER1 deletion in virgin mice did not impact food intake or urinary Na<sup>+</sup> excretion. Assessment of plasma sex hormone levels revealed that genetic deletion of GPER1 did not alter plasma estradiol or progesterone levels in virgin mice. However, previous pregnancies increased plasma levels of estradiol ( $p=0.0063$ ), but not progesterone ( $p=0.6748$ ) in GPER1 KO mice. Of note, GPER1 deletion increased mean arterial pressure in virgin mice (KO:  $126\pm 3$ ; WT:  $107\pm 2$  mmHg;  $p<0.0001$ ). Interestingly, prior pregnancies eliminated this genotypic difference in blood pressure. Cosinor analysis revealed augmented mean arterial blood pressure amplitude in virgin GPER1 KO mice, that was attenuated in previously-pregnant GPER1 KO mice. We also measured urinary excretion of endothelin and aldosterone which are major contributors to blood pressure regulation. Previous pregnancies lowered urinary levels of endothelin-1 ( $p=0.0049$ ) and aldosterone ( $p=0.0099$ ) in GPER1 KO mice. Overall, our data demonstrate an elevated blood pressure in GPER1 KO virgin mice compared to WT virgin and previously-pregnant GPER1 KO aged mice. The current data suggest that GPER1 and former pregnancies provide protection against hypertension in aged females.

Funded by R00DK119413 to EG.

# Tubulin acetylation attenuates vasorelaxation in a smooth muscle-dependent manner and contributes to hypertension

Anthony Mozzicato,<sup>1</sup> Joakim Bastrup,<sup>1</sup> and Thomas A. Jepps<sup>1</sup>

<sup>1</sup>Copenhagen University

Abstract ID 22927

Poster Board 509

**BACKGROUND & AIMS:** Post-translational modifications (PTMs) have been known to contribute to both the onset and the severity of various diseases, due to their ability to regulate protein function, localization, and their involvement in different signaling pathways. Acetylation, a common PTM, has been linked to microtubule stabilization via its primary binding site at the Lys40 site of the  $\alpha$ -tubulin subunit, and has been shown to affect microtubule dynamics. Thus, the aim of this study was to evaluate  $\alpha$ -tubulin acetylation in spontaneously hypertensive rats (SHR), and to elucidate how this PTM might be linked to attenuated vasorelaxation via vascular smooth muscle cells (VSMCs).

**METHODS:** VSMCs isolated from mesenteric arteries of Wistar Kyoto (WKY), SHR, and control rats were assessed for acetylation by staining for  $\alpha$ -tubulin and acetylated tubulin. Acetylation of mesenteric arteries was assessed using Western Blotting (WB) to probe for  $\alpha$ -tubulin and acetylated tubulin levels. To simulate increased acetylation found in the SHR, the histone deacetylase (HDAC)-6 inhibitor, tubacin, was used to treat control arteries and isolated VSMCs. Artery contraction was assessed using wire myography to measure changes in contractile tension. Mounted arteries were treated with a microtubule network disruptor (colchicine), an eNOS inhibitor (L-NAME), and tubacin.

**RESULTS:** Isolated VSMCs from the SHR showed increased acetylation compared to WKY myocytes ( $P < 0.01$ ). VSMCs from the SHR showed no difference in acetylation when treated further with tubacin, indicating a peak acetylation state in hypertensive VSMCs. Likewise, whole artery acetylation was increased in the SHR compared to WKY vessels ( $P < 0.05$ ). Using wire myography, we showed that treatment with tubacin improved vasorelaxation when the endothelium was intact ( $P < 0.05$ ). In vessels where nitric oxide release was blocked via L-NAME treatment, tubacin severely attenuated vasorelaxation ( $P < 0.0001$ ). To investigate whether the effect of tubacin was microtubule specific, we treated mounted vessels with both tubacin and colchicine (a microtubule disruptor). When the microtubule network was disrupted via colchicine treatment, no difference in vasorelaxation was observed between control and tubacin-treated vessels, indicating that microtubule stability contributes to attenuated vasorelaxation and that the improved vasorelaxation seen in HDAC-6 intervention can be attributed to endothelial presence.

**SUMMARY:** Recently, HDAC-6 inhibitors, such as tubacin, have been suggested as therapeutics for hypertension in humans. We have shown that inhibiting HDAC-6 may improve vasorelaxation when the endothelium is intact, due to increased nitric oxide release. However, HDAC-6 inhibition increases acetylation of the VSMC microtubule network, which we have shown to be associated with attenuated vasorelaxation. Therefore, future use and consideration of HDAC-6 inhibitors in human trials must be considered and monitored, to account for the decreased endothelial function often observed in human hypertensive patients.

# The FDA Approved Therapeutic Lasmiditan, Enhances Primary Murine Renal Peritubular Endothelial Cells Wound Healing Capacity.

Austin D. Thompson,<sup>1</sup> Jaroslav Janda,<sup>1</sup> and Rick Schnellmann<sup>1</sup>

<sup>1</sup>Bio5 Institute, College of Pharmacy, Department of Pharmacology & Toxicology, University of Arizona, Tucson, AZ, USA

Abstract ID 16703

Poster Board 510

**Background:** Acute kidney injury (AKI) is defined as an episode of sudden and rapid decline in renal function and is often accompanied by a persistent reduction in mitochondrial function, renal microvasculature dysfunction/rarefaction, and tubular injury/necrosis. AKI continues to be an immense public health concern, as there remains no effective FDA-approved treatment options.

A central underlying contributor to AKI, and the subsequent development of other progressive kidney and cardiovascular related diseases, is renal microvascular endothelial cell dysfunction/rarefaction. This dysfunction/rarefaction exacerbates renal injury and increases the likelihood of AKI recurrence (~20%). Furthermore, AKI results in a persistent reduction in mitochondrial function, number, and cellular energetics. Conversely, pharmacological stimulation of mitochondrial biogenesis (MB) has been shown to restore mitochondrial function and promote renal vascular recovery post-AKI. However, **minimal** AKI research has focused on elucidating the cellular mechanisms that govern mitochondrial biogenesis (MB) and neovascularization responses post-AKI; moreover, how stimulation of MB contributes to renal peritubular endothelial cell repair mechanisms post-AKI remains **unknown**. Therefore, we conducted in-vitro wound healing assays with primary murine renal peritubular endothelial cells (MRPEC) exposed to lipopolysaccharide (LPS) in the presence/absence of the lasmiditan, a 5-HT<sub>1F</sub> receptor agonist, and a known inducer of MB within the renal cortex of mice.

**Methods:** MRPECs were isolated utilizing a refined method by Zhao et al. (2014). Briefly, renal enzymatic tissue digestion buffers were altered by replacing collagenase type 4 with collagenase type 1 and trypsin with accutase, respectively. Additionally, gentle MACS-C tubes with automated tissue dissociation were employed to reduce processing times and improve cell viability. Cells were then subjected to CD326+ magnetic microbead negative selection, to remove epithelial cells, followed by two positive selection cycles with CD146+ magnetic microbeads. Purified MRPECs were then seeded at a density of 70,000 cells/well into human plasma fibronectin precoated 35mm Ibidi wound healing chamber dishes and incubated overnight in microvascular specific media (EGM-MV2; Lonza). MRPECs were then treated with either LPS (1ug/mL) or normal saline in the presence/absence of lasmiditan (100nM) prior to the removal of chamber inserts. Wound healing dishes were then imaged at 0-, 6-, and 12- hours post treatment and subsequently analyzed by Ibidi FastTrackAI software.

**Results:** MRPECs treated with lasmiditan displayed an increase in total wound closure percentage, 1.21 and 1.44 fold compared to normal saline and LPS treated control cells, respectively. Additionally, MRPECs treated with both LPS and lasmiditan exhibited an increase in total wound closure percentage, 1.33 fold compared to LPS treated control cells. Lastly, LPS treated MRPECs displayed a decrease in total wound closure percentage compared to normal saline controls, 1.18 fold.

**Conclusion:** In conclusion, we demonstrated that lasmiditan treatment enhanced MRPEC wound healing capacity alone and following LPS induced cellular injury, in-vitro. These results suggest that lasmiditan may promote vascular recovery following kidney injury.

T32 5T32ES007091-39 (National Institutes of Health; NIEHS) to ADT.

BX000851 (Department of Veterans Affairs) to RGS.



# Platelet Function and Gene Expression in E-cigarette In Utero Exposed Mice

Ahmed Alarabi<sup>1</sup>

<sup>1</sup>Texas A&M Univ

Abstract ID 28922

Poster Board 511

Although we and others have shown that exposure to e-cigarettes (e-cigs) in adulthood is associated with a host of negative health effects, including in the context of occlusive cardiovascular diseases, whether in utero exposure exerts any effects remains ill-defined. To this end, there is growing evidence that exposure of pregnant women to e-cigs is indeed linked to harm to their offspring, which is contrary to the misperceptions regarding their safety that are currently held by the general public. Thus, to address the aforementioned issues, we performed a platelet function and a transcriptomic (mRNA & miRNA) approaches to investigate the effects and mechanism by which in utero e-cigs exposure increases the risk of thrombosis in the offspring. We used a validated protocol to expose female mice to e-cigs one week before mating and throughout the entire period of gestation. Exposure stopped at birth, and offspring the males were utilized for experimentation at 10- 12 weeks of age. Our results showed altered platelet functional responses and gene expression in the mice that were subjected to *in utero* e-cigs exposure, in comparison to those exposed to clean air. Our *in vivo* studies showed that the *in utero* e-cig exposed mice had significantly shortened bleeding time (M =156.6 sec, SD= 222.1 sec) as well as occlusion time (M = 63 sec, SD = 39.72 sec) in comparison to clean air (M = 366 sec, SD = 108.7 sec) and (M = 187.2 sec, SD = 54.13 sec) respectively. RNA sequencing demonstrated distinct changes in the gene-expression profile of circulating platelets of *in-utero* e-cig exposed mice. Gene enrichment analysis of differential expressed genes show changes in pathways associated with platelet activation, hemostasis, and inflammation. Using miRNA-seq, we found 29 differentially expressed miRNAs in *in-utero* e-cig exposed platelet compared with clean air. Using miRNA databases, interactions analysis between differential expressed miRNA and differentially expressed genes showed clear validated interactions. These findings demonstrate that *in-utero* e-cig exposure is associated with platelet enhancement, which may contribute to increasing in the risk of thrombosis in adulthood.

# Using the Caprini Risk Score to increase awareness of Venous Thromboembolism Awareness in the Community: Know Your Score II

Chunping Huang,<sup>1</sup> Joseph Tariman,<sup>2</sup> Shannon Simonovich,<sup>1</sup> Arav Bongirwar,<sup>3</sup> Divya Honavar,<sup>3</sup> Mala Niverthi,<sup>3</sup> Rashi Modey,<sup>3</sup> Joseph Caprini,<sup>4</sup> and Atul Laddu<sup>3</sup>

<sup>1</sup>DePaul University; <sup>2</sup>Rutgers University - Camden; <sup>3</sup>Global Thrombosis Forum; and <sup>4</sup>PACO Foundation

Abstract ID 56584

Poster Board 556

## Aims and objectives:

1. To assess individual participants' baseline thrombosis risk scores before injury, illness or hospitalization occur.
2. To increase awareness of VTE in the community regarding thrombosis-related risks.

**Background:** Venous thromboembolism (VTE) is a condition in which blood clots occur, resulting in a serious morbidity or mortality. A blood clot develops in the legs, arms, or abdomen and a part or the entire thrombus breaks off, traveling to the lungs resulting in Pulmonary Embolism. VTE is a worldwide public health and medical care problem due to a high rate of missed diagnosis. An estimated number of 375,000 to 425,000 cases of VTE diagnosis and treatment cost the U.S. medical system \$7 to \$10 billion a year. While majority are aware of medical conditions such as heart attack (96.1%), stroke (97.2%), diabetes (98.2%), HIV/AIDS (98.6%), cancer (97.2%) and malaria (98.2%), just a few of the participants are aware of thrombosis (41.5%) and DVT(33.8%). VTE prevention strategies must be implemented at a specific and tailored level of risk. One of methods for prevention at the level of risk is to perform a thorough risk assessment using the 40-element Caprini Risk Score (CRS). Education of the public regarding VTE and individual personal risk level are important goals for the physician. Once this information is obtained ahead of time, it can be used when a person encounters an accident or in case of emergency or even prior to a planned surgery. The approach to preventing VTE is greatly enhanced knowing the baseline information is contained in their medical record.

The purpose of this study was to know the individual CRS of the respondents so that when an illness or emergency occurs, they can be better prepared to discuss with their physician the approach to preventing a serious or fatal blood clot.

**Methods:** This quantitative study involved cross-sectional design, convenience samples. Participants tested on their own electronic devices, and the research team was blinded to the identity of the participants. The criteria for inclusion included individuals ages 18 and above who were able to follow the instructions for inclusion criteria.

**Results:** The mean CRS was 4.93+/-3.175. Participants had a CSR of 0-4 (N=460, 49.6%), 5-8 (N=394, 42.5%), and CRS of score 9 and more (N=74, 8.0%). A total 247 (26.6%) participants reported a family blood clot history. A total of 130 (52.6%) participants were less than 40 years old; 324 (34.9%) were women on birth control. Smoking history was reported in 30%, diabetes in 26%, and 17.3% of the participants reported a history of inflammatory bowel disease.

**Conclusions:** Family history of VTE is important leading to the development of VTE. Identifying the baseline risks prior to illness should lead to better selection of patients requiring thrombosis prophylaxis. The proposed strategy is expected to save several lives by having the CRS handy to the physicians at the time of emergency.

# Renin-Angiotensin System Components and Arachidonic Acid Metabolites as Biomarkers of COVID-19

Biwash Ghimire,<sup>1</sup> Sana Khajehpour,<sup>1</sup> Nasser Jalili Jahani,<sup>2</sup> Elizabeth A. Middleton,<sup>3</sup>  
Robert Campbell,<sup>3</sup> Mary Nies,<sup>2</sup> and Ali Aghazadeh-Habashi<sup>2</sup>

<sup>1</sup>Idaho State Univ; <sup>2</sup>Idaho State University; and <sup>3</sup>University of Utah

Abstract ID 26600

Poster Board 557

**Background:** COVID-19, a highly contagious infectious disease caused by SARS-CoV-2, has emerged as this century's most consequential global health crisis. It has infected over 600 million people, resulting in more than 6 million deaths. The clinical outcome of this infection varies remarkably, with most of the patients being asymptomatic or presenting mild symptoms. However, a portion of the infected population group manifests complications such as acute lung injury and acute respiratory distress syndrome, requiring hospitalization, with some patients succumbing to the disease. The virus enters the cell by binding viral spike protein (S1) to angiotensin-converting enzyme 2 (ACE2) receptors in the epithelial cells. Internalization of ACE2 receptors reduces the availability of ACE2 protein, a vital regulator of the Renin-Angiotensin System (RAS). ACE2 converts the pro-inflammatory peptide Angiotensin II (Ang II) to the anti-inflammatory peptide Angiotensin 1-7 (Ang 1-7). The resulting accumulation of Ang II activates the angiotensin 1 receptor initiating an inflammatory process that results in a so-called cytokine storm. It also upregulates phospholipase A, causing arachidonic acid (ArA) release, propagating the inflammatory cascade furthermore. Given that systemic RAS plays an essential role in the homeostasis of vital organs such as lungs, heart, liver, and kidneys, we expect that understanding these biomarkers and their association with patient demographic variables will help us predict future complications in these organs.

**Methods:** Plasma samples from 30 patients and healthy individuals were collected at the University of Utah hospital based on IRB approved by the University of Utah and Idaho State University. The plasma samples were disinfected with Triton-X and stored at -80°C until use. RAS peptides were extracted using solid phase extraction and analyzed using liquid chromatography-tandem mass spectrometry (LC-MS/MS). ArA metabolites were quantified using liquid-liquid extraction followed by LC-MS/MS analysis. Statistical correlation and ANOVA analyses were performed using SPSS, and  $p < 0.05$  was considered statistically significant.

**Results:** In COVID-19 groups, Ang 1-7 levels were significantly reduced compared to healthy controls, but there was a rise in Ang II. Higher Ang II level was also associated with high sequential organ failure assessment (SOFA) scores. The Ang 1-7/II ratio was not associated with sex; however, it was negatively correlated with age and cardiovascular comorbidities. This ratio was reduced in the patients with respiratory comorbidities, although the relationship was insignificant. Elevated levels of anti-inflammatory EETs and DiHETs were observed in infected patients.

**Conclusion:** The findings indicate that COVID-19 infection disrupts the balance of RAS, leading to increased levels of pro-inflammatory Ang II and a diminished ratio of Ang 1-7/II, which is associated with an increase in the metabolites of the ArA pathway. This observation could be explained by Ang II triggering the inflammatory cascade. The strong correlation between RAS and ArA metabolites with SOFA score suggests these biomarkers of COVID-19, which can predict the severity of the disease.

This study was supported through Small Internal Seed Grants by Idaho State University, awarded to Dr. Ali Aghazadeh-Habashi and Dr. Mary Nies.

# Dexmedetomidine Attenuates Ischemia and Reperfusion-Induced Cardiomyocyte Injury through SIRT1/FOXO3a Signaling

Han-lin Ding,<sup>1</sup> Danyang Liu,<sup>2</sup> Jianfeng He,<sup>2</sup> Jiajia Chen,<sup>2</sup> Dongcheng Zhou,<sup>2</sup> Chan Wang,<sup>3</sup> Changming Yang,<sup>3</sup> Zhengyuan Xia,<sup>2</sup> and Zhongyuan Xia<sup>4</sup>

<sup>1</sup>Xiangyang Center Hospital, Affiliated Hospital Of Hubei University Of Arts and Science; <sup>2</sup>Department of Anesthesiology, Affiliated Hospital of Guangdong Medical University; <sup>3</sup>Department of Anesthesiology, The First People's Hospital of Jingmen City; and <sup>4</sup>Department of Anesthesiology, Renmin Hospital of Wuhan University

Abstract ID 21855

Poster Board 558

Myocardial ischemia/reperfusion injury (MIRI) often occurs in patients with acute myocardial infarction undergoing reperfusion therapy. Dexmedetomidine (Dex), a sedative-analgesic, has been reported to protect against MIRI. However, the mechanism of this protective effect remains inconclusive. This study aimed to investigate the cardioprotective effects of Dex on MIRI and the role of the silent information regulator 1 (SIRT1) and forkhead box O3a (FOXO3a) signaling. 6-8 weeks C57 mice were allowed to adapt to food and environment for a week and then intraperitoneally injected with Dex at 20 $\mu$ g/kg one day prior to being subjected to 30 minutes coronary occlusion and 120 minutes reperfusion, in the absence or presence of intraperitoneal injection of the SIRT1 inhibitor EX527(10 mg/kg/day) for a duration of one week prior to inducing MIRI. In vitro, rat-derived cardiomyocytes (H9C2) were pretreated with 10 $\mu$ M Dex for two hours in the absence or presence of 1 $\mu$ M EX527. The cells were then subjected to hypoxia/reoxygenation (HR) injury (composed of 6 h of hypoxia followed by 12 h of reoxygenation). Echocardiography was used to measure myocardial contractile function in mice. Serum creatine kinase-myocardial band fraction (CK-MB) level was detected by ELISA. Myocardial infarction size was measured by Triphenyl tetrazolium chloride staining. Cell viability was assessed by CCK-8 assay. Cell damage was evaluated by LDH release using ELISA assay. Apoptotic cell death was determined by TUNEL staining. The production of reactive oxygen species (ROS) was measured using DHE staining. Protein levels of SIRT1, FOXO3a, BAX, BCL-2, and Cleaved caspase 3 were assessed by Western blot assay. The results showed that Dex pretreatment decreased serum CK-MB, reduced myocardial infarct size, alleviated histological structure damage, and improved left ventricular function following MIRI in mice, which was partially yet significantly reversed by EX527 (all  $P < 0.05$ , IR vs. IR+Dex; HR+Dex vs. HR+Dex+EX527). In vitro, HR decreased H9C2 cell viability, increased LDH leakage, and the production of ROS (all  $P < 0.05$ , CN vs. HR), all of which were significantly reversed by Dex (all  $P < 0.05$ , HR vs. HR+Dex). Moreover, we found that Dex decreased H9C2 cell apoptosis, concomitant with increased SIRT1 and FOXO3a expression, decreased BAX/BCL-2 ratio, and Cleaved caspase 3 expressions (all  $P < 0.05$ , HR vs. HR+Dex). The protective effects of Dex against HR and H/R injury were reversed by SIRT1 inhibitor EX527(all  $P < 0.05$ , HR+Dex vs. HR+Dex+EX527). It is concluded that Dex pretreatment could attenuate MIRI or HR-induced cardiomyocyte apoptosis and that upregulating SIRT1 and FOXO3a may represent a major mechanism whereby Dex confers cardioprotection.

# Location Biased G Protein-Coupled Receptor Signaling Modulates Distinct Spatial Conformations of $\beta$ -arrestins

Anand Chundi,<sup>1</sup> Uyen Pham,<sup>1</sup> and Sudarshan Rajagopal<sup>1</sup>

<sup>1</sup>Duke University

Abstract ID 53127

Poster Board 559

G Protein-Coupled receptors (GPCRs) are the largest superfamily of transmembrane receptors. They are ubiquitously expressed in the body and canonically signal through various effectors, including heterotrimeric G proteins,  $\beta$ -arrestins, and GPCR kinases (GRKs). Research has shown that the same receptor, when bound to different ligands, can selectively activate some signaling pathways over others, a concept known as 'biased agonism'. Additionally, GPCRs possess distinct signaling profiles at different subcellular locations, a phenomenon termed 'location bias'. However, the molecular mechanisms underlying the role of location bias in GPCR signaling are not well understood.

To elucidate these mechanisms, we assessed the subcellular trafficking patterns and location-specific conformations of  $\beta$ -arrestins 1 and 2 following stimulation of the Angiotensin II type 1 receptor (AT1R) with the endogenous ligand angiotensin II (AngII) and a  $\beta$ -arrestin-biased ligand TRV120023. Utilizing the NanoBiT complementation assay and bioluminescence resonance energy transfer (BRET),  $\beta$ -arrestins 1 and 2 were found to be differentially trafficked to the plasma membrane and endosomes following AT1R stimulation. Additionally, a pool of  $\beta$ -arrestins was found to localize at the plasma membrane despite receptor internalization, indicating catalytic activation of  $\beta$ -arrestins by the receptor. Using a novel conformational BRET biosensor called NanoBiT FLAsH, we revealed that  $\beta$ -arrestins 1 and 2 adopt distinct, location-dependent conformations at the plasma membrane, lipid rafts, and early endosomes. Additionally, the catalytically active pool of  $\beta$ -arrestins at the plasma membrane was found to possess different conformations from receptor-associated  $\beta$ -arrestins at the plasma membrane or endosomes. These findings suggest that location-dependent GPCR signaling modulates the conformation of  $\beta$ -arrestins, resulting in differential signaling outcomes.

# A novel combination of an AKT activator with an AKT inhibitor exacerbates hydrogen peroxide-induced death of human cardiac microvascular endothelial cells

Zhu-qiu Jin,<sup>1</sup> and Austin Qiu<sup>1</sup>

<sup>1</sup>California Northstate University

Abstract ID 28208

Poster Board 560

Ischemic heart disease is a leading cause of death worldwide. Oxidative stress-associated cell death represents a significant contributor to myocardial damage in patients with acute myocardial infarction. Cardiac microvascular endothelial cells play an essential role in cell survival and cardiac functions. Activation of AKT/protein kinase B is usually associated with cell survival. However, the combination of AKT activation with AKT inhibition on cell survival remains unknown. In the presented study, human cardiac microvascular endothelial cells (HCMECs) were cultured in endothelial cell medium supplemented with 5% fetal bovine serum and endothelial cell growth supplement in 5% CO<sub>2</sub> incubator. HCMECs from passage 4 to 7 were sub-cultured in 96-well plates coated with collagen I. Cells were pretreated with SC-79 (an AKT activator) at 4 μg/mL and MK-2206 hydrochloride (an AKT inhibitor) at 5 μM respectively or in combination for one hour followed by insult of hydrogen peroxide (H<sub>2</sub>O<sub>2</sub>, 5 mM for one hour). Cell viability was determined with measurement of MTT (3-(4,5-dimethylthiazol-2-yl)-2,5-diphenyltetrazolium bromide) assay and lactate dehydrogenase (LDH) release into medium. H<sub>2</sub>O<sub>2</sub> formation from HCMECs was measured by using fluorometric assay kit. Western blot was used to determine the protein expression of total AKT and phospho-AKT (Ser473) in HCMECs. Cell treated with H<sub>2</sub>O<sub>2</sub> reduced formation of MTT and increased release of LDH as well as formation of H<sub>2</sub>O<sub>2</sub> from HCMECs. The cell death induced by H<sub>2</sub>O<sub>2</sub> was not affected with pretreatment of either SC-79 or MK-2206 alone. Nevertheless, a combination of SC-79 and MK-2206 enhanced cell death (P<0.003 vs H<sub>2</sub>O<sub>2</sub> group) without alteration of H<sub>2</sub>O<sub>2</sub> formation from HCMECs. Our results clearly indicated that a combination of AKT activator with AKT inhibitor created a novel cell death pathway.

This study was supported by a Seed Grant Award from California Northstate University College of Pharmacy.

# Clopidogrel Induces More Bleeding in P2Y<sub>12</sub>-deficient Mice: Optimization of Murine Tail Bleeding Assay

Taylor Rabanus,<sup>1</sup> Adam Lauver,<sup>1</sup> and Dawn Kuszynski<sup>2</sup>

<sup>1</sup>Michigan State Univ; and <sup>2</sup>Therapeutic Systems Research Laboratories, Inc

**Abstract ID 17622**

**Poster Board 561**

Arterial thrombosis remains the most common cause of death in the developed world. Clopidogrel, a P2Y<sub>12</sub> antagonist, is often prescribed to inhibit platelet activation and aggregation; however, patients who take clopidogrel are known to have cerebral bleeding events. The purpose of this study was to determine if the clopidogrel bleeding effect is dependent on P2Y<sub>12</sub> receptor inhibition. Previous research from our laboratory suggests that clopidogrel possesses inhibitory effects on hemostasis independent of platelet P2Y<sub>12</sub> inhibition. We hypothesized that P2Y<sub>12</sub>-deficient mice treated with clopidogrel will bleed significantly more than the P2Y<sub>12</sub>-deficient mice treated with the vehicle. A tail-bleeding assay was used to determine clopidogrel's effect on hemostasis. P2Y<sub>12</sub> deficient mice were administered clopidogrel (10 mg/kg) or vehicle daily for five days before the procedure was performed. Bleeding was evaluated using a tail tip amputation assay. After tip amputation, the tail was quickly placed in a tube containing Drabkin's reagent. Blood loss was determined by measuring the concentration of hemoglobin in the tube using a standard curve. P2Y<sub>12</sub>-deficient animals bled more ( $5.955 \pm 1.159$  g/dl) than their wildtype littermates ( $2.491 \pm 0.962$  g/dl). Importantly, our data demonstrated that clopidogrel treatment induced more bleeding in both the P2Y<sub>12</sub>-deficient mice ( $7.921 \pm 1.015$  g/dl) and wildtype mice ( $3.898 \pm 0.324$  g/dl) compared to drug vehicle. These results suggest that clopidogrel's bleeding effect is not completely dependent on the P2Y<sub>12</sub> receptor inhibition. Other elements in the hemostatic system, such as the vessel-related factors, could be responsible for the observed clopidogrel bleeding effects.

This work was funded in part by the ASPET Summer Undergraduate Research Fellowship.

# Role of ferroptosis in increased vulnerability to myocardial ischemia-reperfusion injury in type 1 diabetic mice and the treatment effects of N-acetylcysteine

Dongcheng Zhou, Yuhui Yang,<sup>1</sup> Jiajia Chen,<sup>1</sup> Jiaqi Zhou,<sup>1</sup> Jianfeng He,<sup>1</sup> Danyong Liu,<sup>1</sup> Anyuan Zhang,<sup>2</sup> Bixian Yuan,<sup>1</sup> Yuxin Jiang,<sup>1</sup> Ronghui Han,<sup>1</sup> Weiyi Xia,<sup>1</sup> and Zhengyuan Xia<sup>1</sup>

<sup>1</sup>Affiliated Hospital of Guangdong Medical University; and <sup>2</sup>Wenzhou Medical University

Abstract ID 23318

Poster Board 562

The hearts of subjects with diabetes are vulnerable to ischemia-reperfusion injury (IRI). Interestingly, experimentally rodent hearts have been shown to be more resistant to IRI at the very early stages of diabetes induction than the heart of the non-diabetic control mice, while the specific mechanisms are still unclear. Ferroptosis, a new kind of iron-regulated cell death that differs from apoptosis and necrosis that can be induced by an oxidative stress response, has recently been shown to play an important role in myocardial IRI including that in diabetes. The present study aimed to investigate whether the antioxidant N-acetylcysteine (NAC) exerts cardioprotective effect through inhibiting ferroptosis and to explore the potential relationship between the extent of ferroptosis and the degree of myocardial vulnerability to ischemia-reperfusion injury in diabetes. Non-diabetic control (NC) and streptozotocin-induced diabetic (DM) mice were treated with 2 mmol/L of N-acetylcysteine (NAC) in drinking water for 4 weeks starting at 1 week after diabetes induction. Mice were subjected to myocardial IRI induced by occluding the coronary artery for 30 minutes followed by 2 hours of reperfusion, subsequently at 1, 2, and 5 weeks of diabetes induction. The post-ischemic myocardial infarct size in the DM group was smaller than that in NC group at 1 week of diabetes but greater than that at 5 weeks of diabetes, which were associated with a significant increase in ferroptosis at 5 weeks but not at 1 week of diabetes. NAC significantly attenuated post-ischemic ferroptosis as well as oxidative stress and reduced infarct size at 2 and 5 weeks of diabetes. Application of erastin, a ferroptosis inducer, reverses the cardioprotective effects mediated by NAC therapy. It is concluded that increased oxidative stress and ferroptosis are the major factors attributable to the increased vulnerability to myocardial IRI in diabetes and that attenuation of ferroptosis represents a mechanism whereby NAC confers cardioprotection against myocardial IRI in diabetes.

This study was supported by National Natural Science Foundation of China (82270306; 81970247).



# G $\alpha$ protein signaling bias at 5-HT<sub>1A</sub> receptor

Rana Alabdali,<sup>1</sup> Luca Franchini,<sup>1</sup> and Cesare Orlandi<sup>1</sup>

<sup>1</sup>Univ of Rochester

Abstract ID 19584

Poster Board 77

Serotonin 1A receptor (5-HT<sub>1A</sub>R) is a clinically relevant target because of its involvement in several central and peripheral functions including sleep, temperature homeostasis, processing of emotions, and response to stress. As a G Protein Coupled Receptor (GPCR) activating numerous G $\alpha_{i/o/z}$  family members, 5-HT<sub>1A</sub>R has the potential to modulate a variety of intracellular signaling pathways. This potential signaling bias in response to different therapeutics has not been thoroughly investigated. Here, we explored how ten structurally diverse 5-HT<sub>1A</sub>R agonists exert biased signaling by differentially stimulating G $\alpha_{i/o/z}$  family members. To this aim, we applied an optimized cell-based Bioluminescence Resonance Energy Transfer (BRET) assay to quantify the activation of each G $\alpha$  subtype. Our concentration-response analysis of the activation of each G $\alpha_{i/o/z}$  protein in response to the selected agonists revealed unique potency and efficacy profiles when compared to the reference 5-HT. Overall, our analysis of signaling bias identified groups of ligands sharing comparable G protein activation selectivity and also drugs with unique selectivity profiles. Considering that alternative signaling pathways are regulated downstream of each G $\alpha$  protein, our data suggest that the unique pharmacological properties of the tested agonists could result in multiple unrelated cellular outcomes. Further investigation is needed to expand on how this type of ligand bias could affect cellular responses and to shed new light onto molecular mechanisms underlying therapeutic profile and side effects of each drug.

**Support/Funding Information:** Ernest J. Del Monte Institute for Neuroscience Pilot Program, University of Rochester, to C. O.; Taif University Scholarship award to R.A.; John R. Murlin Memorial Fund to R.A.

# Quantitative phosphoproteomic analysis defines distinct cAMP signaling networks emanating from AC2 and AC6 in human airway smooth muscle cells

Isabella Cattani-Cavaliere,<sup>1</sup> Yue Li,<sup>1</sup> Jordyn Margolis,<sup>1</sup> Amy Bogard,<sup>2</sup> Moom Roosan,<sup>1</sup> and Rennolds Ostrom<sup>1</sup>

<sup>1</sup>Chapman University School of Pharmacy; and <sup>2</sup>AB Research LLC

Abstract ID 14791

Poster Board 78

Human airway smooth muscle (HASM) is the primary target of  $\text{ss}_2\text{AR}$  agonists used to control airway hypercontractility in asthma and chronic obstructive pulmonary disease (COPD).  $\text{ss}_2\text{AR}$  agonism induces the production of cyclic adenosine monophosphate (cAMP) by adenylyl cyclases (ACs), which activates PKA and leads a myriad of cellular effects including bronchodilation. Several other GPCRs expressed in HASM cells transduce extracellular signals through cAMP but these receptors elicit different cellular responses, suggesting cAMP signaling is compartmentalized. Previous work has shown these GPCR can couple to specific ACs that are localized in distinct membrane microdomains, partly explaining this compartmentation. However, little is known about the downstream steps of cAMP compartmentation. We developed a proteomic approach to define the downstream signaling networks emanating from specific AC isoforms in HASM. Stable Isotope Labeling of Amino acids in Cell culture (SILAC) was used to identify and quantify phosphorylated proteins in HASM overexpressing AC2 or AC6 after a short stimulus of AC activity by forskolin. Phosphopeptides were analyzed by LC-MS/MS and the quantitative difference between light and heavy labeled SILAC pairs represented the change in abundance of that peptide caused by forskolin treatment. Forskolin-stimulated cAMP production in control (lacZ) HASM displayed a  $\log\text{EC}_{50}$  of  $-8.14 \pm 0.04$  and an  $E_{\text{max}}$  of  $0.328 \pm 0.010$ . In AC2-overexpressing cells, forskolin potency as efficacy was moderately increased ( $\log\text{EC}_{50}$  of  $-8.79 \pm 0.02$  and an  $E_{\text{max}}$  of  $0.498 \pm 0.007$ ). AC6 overexpression led to similar increases in forskolin responses ( $\log\text{EC}_{50}$  of  $-8.67 \pm 0.12$  and an  $E_{\text{max}}$  of  $0.509 \pm 0.030$ ). Using a subtractive analysis to identify effects of just the overexpressed AC isoform (over that natively expressed in control HASM), we found 14 differentially phosphorylated proteins (DPPs) linked to AC2 signaling and 34 DPPs linked to AC6 signaling. AC2 and AC6 groups showed in common 4 up- and 3 down-regulated phosphorylated proteins (using fold change  $\geq 1.5$  or  $\leq 1/1.5$  of the light/heavy ratio with p-values  $< 0.05$ ,  $n=3$ ). The Gene Set Enrichment Analysis (GSEA) was used to identify statistically significant pathways with a p-value  $< 0.05$  reflected with enrichment scores. We identified 11 and 78 significant pathways using AC2 and AC6 differentially regulated proteins. Analysis of the phosphorylated peptides with the STRING protein interaction tool showed that AC2 signaling is more associated with modifications in RNA/DNA binding proteins and microtubule/spindle body proteins while AC6 signaling is associated with proteins regulating autophagy, calcium-calmodulin signaling, Rho GTPases and cytoskeletal regulation. One protein, OFD1, was regulated in opposite directions, with serine 899 phosphorylation increased in the AC6 condition 1.5-fold while in the AC2 condition it decreased to 0.46-fold. In conclusion, quantitative phosphoproteomics is a powerful tool for deciphering the complex signaling networks resulting from discreet signaling events that occur in cAMP compartments. Our data show key differences in the cAMP signaling networks generated by AC2 and AC6 and imply that distinct cellular responses are regulated by these two compartments.

**Funding information:** GM107094

# Lysophosphatidic Acid (LPA) Salivary Species Detection and In Situ LPAR Localization in the Intact Mouse Salivary Gland

D. Roselyn Cerutis,<sup>1</sup> Devendra Kumar,<sup>2</sup> Michael G. Nichols,<sup>3</sup> Gabrielle Roemer,<sup>3</sup> Maxwell Fluent,<sup>3</sup> Laken Beller,<sup>3</sup> Takanari Miyamoto,<sup>3</sup> and Yazen Alnouti<sup>2</sup>

<sup>1</sup>Creighton Univ - School of Dentistry; <sup>2</sup>University of Nebraska Medical Center; and <sup>3</sup>Creighton University

Abstract ID 25340

Poster Board 79

Our laboratory has pioneered studying the biology of lysophosphatidic acid (LPA) in oral homeostasis and periodontal disease. LPA is the simplest lipid mediator and plays key homeostatic and inflammatory roles. Saliva is essential for maintaining oral health, and salivary glands are thus pivotal, as they participate in regulating immunity and inflammation, especially in oral disease prevention, oral infection control (Papagerakis et al., 2014), and autoimmunity. Salivary gland secretion and function is also affected by many pharmacological agents. We (Bathena et al. 2011) and others have reported the presence of multiple LPA species in human healthy normal and in periodontal disease saliva. Therefore, we hypothesized that the same LPA species would also be present in mouse saliva, and that mouse salivary glands would also express multiple LPARs.

**Methods:** the simple, sensitive liquid chromatography/tandem mass spectrometry (LC-MS/MS) method we developed in 2011 was used to quantify LPA species (LPA 18:0, LPA 16:0, and LPA 18:1) in C57BL/6 mouse saliva. To further our work, we previously also developed whole-mount *in situ* LPA receptor (LPAR) subtype localization for various oral soft and hard tissues (Cerutis et al. 2016). Polyclonal antibodies against LPA1, LPA3, and LPA4 were used in indirect immunofluorescence for labeling normal mouse salivary glands using this whole-mount *in situ* technique.

**Results:** As we reported for humans, LPA species are also present in low, homeostatic concentrations in mouse saliva. As periodontal disease develops, paralleling what we reported in Bathena et al. (2011) for human saliva, some of the LPA species increase approximately 10-fold as well. Confocal microscopy confirmed LPA1, LPA3, and substantial LPA4 labeling; similar but different patterns of distribution were seen for each GPCR. In conclusion, this confirms LPA1 and LPA3 expression (like in NOD mice, Park et al., (2017) but is the first report of the presence of LPA4 in mouse salivary gland tissue. The presence of multiple confirmed LPARs in mouse salivary glands suggests that these receptors need to be factored into not only studies of autoimmune conditions but also for pharmacological studies of drugs affecting salivary gland biology and secretion.

**Support:** NIDCR/NIGMS 1R15DE028687-01(D.R.C).

# Targeting HDAC6 in the Dorsal Root Ganglia for the Management of Mechanical Allodynia in Models of Peripheral Nerve Injury

Ilinca Giosan,<sup>1</sup> Randal Serafini,<sup>1</sup> Jeffrey Zimering,<sup>1</sup> Aarthi Ramakrishnan,<sup>2</sup> Madden Tuffy,<sup>2</sup> Li Shen,<sup>2</sup> and Venetia Zachariou<sup>2</sup>

<sup>1</sup>Icahn School of Medicine at Mt Sinai; and <sup>2</sup>Icahn School of Medicine at Mount Sinai

Abstract ID 20519

Poster Board 80

Histone deacetylase 6 (HDAC6) is a Class IIb histone deacetylase, which is primarily located in the cytoplasm and plays an important role in cell cycle progression and transcriptional regulation. Earlier studies from our group and others have shown that HDAC6 inhibitors alleviate sensory signs of chemotherapy-induced and nerve injury-induced peripheral neuropathy. Furthermore, our recent data show that downregulation of HDAC6 in the dorsal root ganglia (DRG), achieved by injection of the sciatic nerve of adult male HDAC6<sup>fl/fl</sup> mice with AAV8-Cre-EGFP vectors, results in recovery from mechanical allodynia in paclitaxel chemotherapy induced peripheral neuropathy (CIPN) model.

We demonstrate that DRG-knockdown of HDAC6 prevents the development of mechanical allodynia after the paclitaxel CIPN model. We also use the murine spared nerve injury (SNI) model of neuropathic pain to determine the impact of the peripherally acting HDAC6 inhibitor ACY1215 (Regenacy Pharmaceuticals) on the alleviation of sensory hypersensitivity behaviors. Using the von Frey assay, we demonstrate that treatment with ACY1215 (30mg/kg) leads to recovery from mechanical allodynia developed after SNI injury in both male and female mice without affecting locomotor activity. We performed bulk tissue RNA Sequencing analysis to understand transcriptomic events and pathways in the DRG associated with the antiallodynic actions of ACY1215. We found over 800 differentially expressed genes (DEG) in the SNI condition between vehicle and ACY1215-treated animals. Most of the pathways affected by these DEGs are associated with inflammatory disorders and B-cell mechanisms, suggesting a potential impairment of circulating immune cell infiltration in to the DRG after injury, which has been shown to be necessary for the induction of sensory hypersensitivity. Furthermore, a separate bulk RNA-seq analysis of L3-6 DRGs 7 weeks after SNI highlighted a significant upregulation of several alpha- and beta-tubulin transcripts. Prior work by others suggests that this may be a compensatory response to nerve injury-induced tubulin destabilization. Therefore, we hypothesize that HDAC6 inhibition may address this molecular maladaptation by increasing acetylated tubulin levels and promoting stability and we are using Western Blot analysis to assess alpha- and beta- tubulin acetylation in the DRG following peripheral nerve injury with and without treatment with HDAC6 inhibitors. An alternative hypothesis is that HDAC6 acts as a transcription factor, and it targets several genes that are associated with hereditary neurodegenerative diseases. We hypothesize that several of these genes are regulated under SNI conditions that are rescued under the presence of ACY1215. We are testing this hypothesis by use of qPCR and Western Blot analysis.

Our findings highlight a promising therapeutic role of HDAC6 inhibitors for the alleviation of sensory hypersensitivity behaviors associated with peripheral nerve injury. Future work will define the mechanisms underlying HDAC6 action in the DRG and will test if interventions in HDAC6 activity in subjects suffering from prolonged peripheral nerve injury may reverse sensory and affective manifestations of neuropathic pain.

**Support/Funding Information:** RO1 NS086444 NINDS.

---

# Structural Basis of Arrestin and Membrane Interaction

Kyle W. Miller,<sup>1</sup> Qiuyan Chen,<sup>1</sup> and Shuaitong Zhao<sup>1</sup>

<sup>1</sup>*Indiana University School of Medicine*

**Abstract ID 56836**

**Poster Board 81**

Two non-visual arrestins selectively interact with activated and phosphorylated G protein-coupled receptors (GPCRs) and play key roles in modulating many important physiological processes. Arrestins also engage the lipid bilayer surrounding the activated receptors, which further potentiates arrestin activation and regulates GPCR trafficking. Our recent cryo-electron microscopy (cryo-EM) structures of atypical chemokine receptor 3 (ACKR3) in complex with arrestin2 and arrestin3 revealed that the arrestin finger loop directly inserts into the micelles/membrane, instead of the transmembrane core as shown in all previously reported GPCR–arrestin structures. This suggests that arrestin finger loop plays a novel role as a membrane anchor. Here, we report the cryo-EM structure of arrestin2 in complex with nanodiscs containing PI(4,5)P<sub>2</sub>. The structure reveals that the finger loop, PI(4,5)P<sub>2</sub> binding sites on C domain, and C-edge loops all contribute to nanodisc/membrane binding. Eliminating one individual site does not significantly affect arrestin2 binding to the nanodisc. In addition, arrestin2 in basal or pre-activated states show comparable binding to nanodiscs containing PI(4,5)P<sub>2</sub>. We site-specifically labelled the finger loop with monobromobimane and detected different level of fluorescence increases in the presence of nanodiscs containing various types of phospholipids. Our study provides the structural evidence that how arrestins engage the membrane via multiple contact points, which can impact arrestin-mediated signaling.

# Without a Trace: The Pirin and NF- $\kappa$ B Interaction

Melissa Meschkewitz,<sup>1</sup> Erika M. Lisabeth,<sup>2</sup> and Richard Neubig<sup>1</sup>

<sup>1</sup>Michigan State Univ; and <sup>2</sup>Michigan State University

**Abstract ID 26493**

**Poster Board 82**

Pirin is a non-heme iron binding protein and was recently identified as a protein target of the CCG-20391 series of small molecules. The CCG compounds were originally discovered in a high-throughput Rho/MRTF/SRF dependent luciferase screen and have since been shown to have anti-fibrotic and anti-metastatic properties, but the mechanism of how Pirin affects MRTF/SRF signaling has yet to be identified. Pirin has been shown to have a role in many different cellular processes, namely epithelial to mesenchymal transition, ferroptosis, senescence, and more. Interestingly, Pirin has also been thought to be a nuclear co-transcription factor to various transcription factors, one of which is the NF- $\kappa$ B family of proteins. Therefore, our hypothesis was that modulation of Pirin through the binding of the CCG compounds may modulate NF- $\kappa$ B pro-inflammatory signaling. To investigate this, we used recombinant biochemical techniques like Fluorescence Polarization, Size Exclusion Chromatography, and Gel Shift Assays to investigate the interaction between Pirin and NF- $\kappa$ B. Additionally, we developed a novel Pirin knockout (KO) mouse model to further determine the functional relationship between Pirin and NF- $\kappa$ B. Surprisingly, we are not able to detect a stable complex of Pirin and the RelA subunit of NF- $\kappa$ B nor do we observe any modulation of inflammatory genes by qPCR in a Pirin KO mouse model. Upon closer investigation of the cellular location of Pirin we found that Pirin is localized in the cytoplasm and does not translocate to the nucleus upon NF- $\kappa$ B activation. We therefore conclude that, based on our observations, Pirin has cellular functions other than a co-transcription factor. These functions may include modulation of MRTF/SRF signaling and actin polymerization, but do not affect NF- $\kappa$ B signaling.

This work is supported by NIH RO1 GM115459-07.

# Structural and Functional Characterization of Phospholipase C $\beta$ 3

Kennedy Outlaw,<sup>1</sup> Isaac J. Fisher,<sup>1</sup> Kaushik Muralidharan,<sup>2</sup> and Angeline Lyon<sup>1</sup>

<sup>1</sup>Purdue University; and <sup>2</sup>Nationwide Children's hospital

**Abstract ID 24997**

**Poster Board 83**

Phospholipase C  $\beta$  (PLC $\beta$ ) plays an important role in cardiovascular diseases and opioid analgesia. PLC $\beta$  catalyzes the hydrolysis of the inner membrane lipid into two crucial secondary messengers, phosphatidylinositol-4,5-bisphosphate (PIP<sub>2</sub>) to inositol-1,4,5-triphosphate (IP<sub>3</sub>) and diacylglycerol (DAG), which activate multiple signaling pathways to modulate cellular behavior. PLC $\beta$  is activated downstream of G-protein coupled receptors (GPCRs) by the heterotrimeric G protein subunits G $\alpha_q$  and G $\beta\gamma$ . In small-angle X-ray scattering (SAXS) experiments, the solution structure of PLC $\beta$  had additional density unaccounted for in crystal structures, suggesting that its structure was more dynamic than previously thought. To test this, we used cryo-electron microscopy (cryo-EM) single particle analysis to determine the solution structure of full-length PLC $\beta$ 3 to 4.1 Å resolution. PLC $\beta$ 3 adopted a compact, autoinhibited conformation under these conditions. This structure confirmed that the proximal C-terminal domain interacts with the core of PLC $\beta$ , but the autoinhibitory X-Y linker does not, suggesting more complex regulation of the lipase by the membrane. We are currently working to determine the structure of PLC $\beta$ 3 on a model membrane to reveal the basally active state of the lipase.

# Examining the mu-opioid receptor bias of fentanyl and 2-benzylbenzimidazole opioids in clandestine drug markets

Meng-Hua M. Tsai,<sup>1</sup> Li Chen,<sup>1</sup> Michael H. Baumann,<sup>1</sup> and Lei Shi<sup>1</sup>

<sup>1</sup>NIDA Intramural Research Program

Abstract ID 15617

Poster Board 84

Many pain medications act as agonists at the  $\mu$ -opioid receptor (MOR). Unfortunately, MOR agonists can induce severe adverse effects. The development and misuse of novel synthetic opioids (NSO), many of which are highly selective MOR agonists, have resulted in serious intoxications and fatal overdoses. The newly emerging nitazene analogs appear to be more potent than fentanyl analogs, posing significant public health risks. As a G-protein coupled receptor, MOR can activate both Gi-proteins and  $\beta$ -arrestins to trigger downstream signaling cascades. Previous studies proposed that Gi-protein biased MOR agonists are safer than  $\beta$ -arrestin biased agonists. However, other studies argue that the reduced side effects of MOR agonists could be caused by low intrinsic efficacy. In this study, to rigorously characterize the bias profiles of NSOs, we carried out *in vitro* functional measurements of both fentanyl and nitazene analogs at MOR by applying the depletion approach, which involves depletion of MOR using the irreversible antagonist methocinnamox. By fitting the data to the operational model, a general mathematical model that explicitly describes agonism, the results from the cAMP inhibition and  $\beta$ -arrestin2 recruitment assays allow us to estimate the intrinsic efficacy with tau and to measure the intrinsic affinity (i.e.,  $K_A$ ) for each compound in the Gi protein and  $\beta$ -arrestin2 pathways. Overall, fentanyls and nitazenes demonstrated noticeably different pharmacological properties. The calculation of the “bias factor” shows that fentanyl is biased toward the Gi-protein pathway, while valeryl fentanyl demonstrates some  $\beta$ -arrestin2 bias. Among the nitazene analogs, N-desethyl isotonitazene and isotonitazene are more potent than DAMGO in both the Gi protein and  $\beta$ -arrestin2 assays, but none of the nitazenes shows robust functional bias. Taken together, NSOs tested in this study show somewhat different bias profiles even within the same series of analogs, suggesting that the *in vitro* functional bias alone may not be adequate in evaluating the toxicity and abuse liability for a given opioid. Thus, a combined interpretation of the results from both *in vitro* and *in vivo* studies is required to fully understand NSOs.

Funded by the Intramural Research Program of NIDA, NIH



# Structural Insights into Phospholipase Ce

Elisabeth Garland-Kuntz,<sup>1</sup> Kadidia Samassekou,<sup>2</sup> Isaac J. Fisher,<sup>1</sup> Kaushik Muralidharan,<sup>3</sup>  
Abigail Gick,<sup>2</sup> Morgan Laskowski,<sup>2</sup> Emmanuel Oluwarotimi,<sup>2</sup> Taiwo Ademoye,<sup>2</sup> Satchal  
Erramilli,<sup>4</sup> Anthony Kossiakoff,<sup>4</sup> and Angeline Lyon<sup>1</sup>

<sup>1</sup>Purdue Univ; <sup>2</sup>Purdue University; <sup>3</sup>Nationwide Children's Hospital; and <sup>4</sup>University of Chicago

**Abstract ID 24765**

**Poster Board 85**

Cardiovascular disease remains the leading cause of death worldwide, and phospholipase Ce (PLCe) is one of the players implicated in these disease pathways. Once activated downstream of G protein-coupled receptors and receptor tyrosine kinases, PLCe hydrolyzes membrane phosphoinositide lipids to produce inositol phosphates and diacylglycerol. These secondary messengers allow release of intracellular calcium stores and activation of pro-inflammatory pathways via protein kinase C. In PLCe, the highly conserved lipase core domains are flanked by N- and C-terminal regulatory domains, including an uncharacterized N-terminal region and CDC25 domain, and two C-terminal Ras association (RA) domains. We and others have shown that many of these regulatory domains are flexibly connected to the core, but it is unclear how these regions modulate basal activity and/or regulation by small GTPases. Using new tools, including AlphaFold2 and cryo-electron microscopy with domain-specific antigen binding fragments (Fabs), we are interrogating the structure and membrane binding surface of larger PLCe variants and the full-length enzyme. In parallel, we are using cell-based activity assays to probe inter-domain interactions and to begin characterizing the membrane binding surface of the lipase. These data will further our understanding of PLCe and aid in developing small molecule allosteric modulators as potential therapies in cardiovascular disease.

# ACAT-1 Inhibition Limits iNOS in an *In Vitro* Model of Macrophage Activation

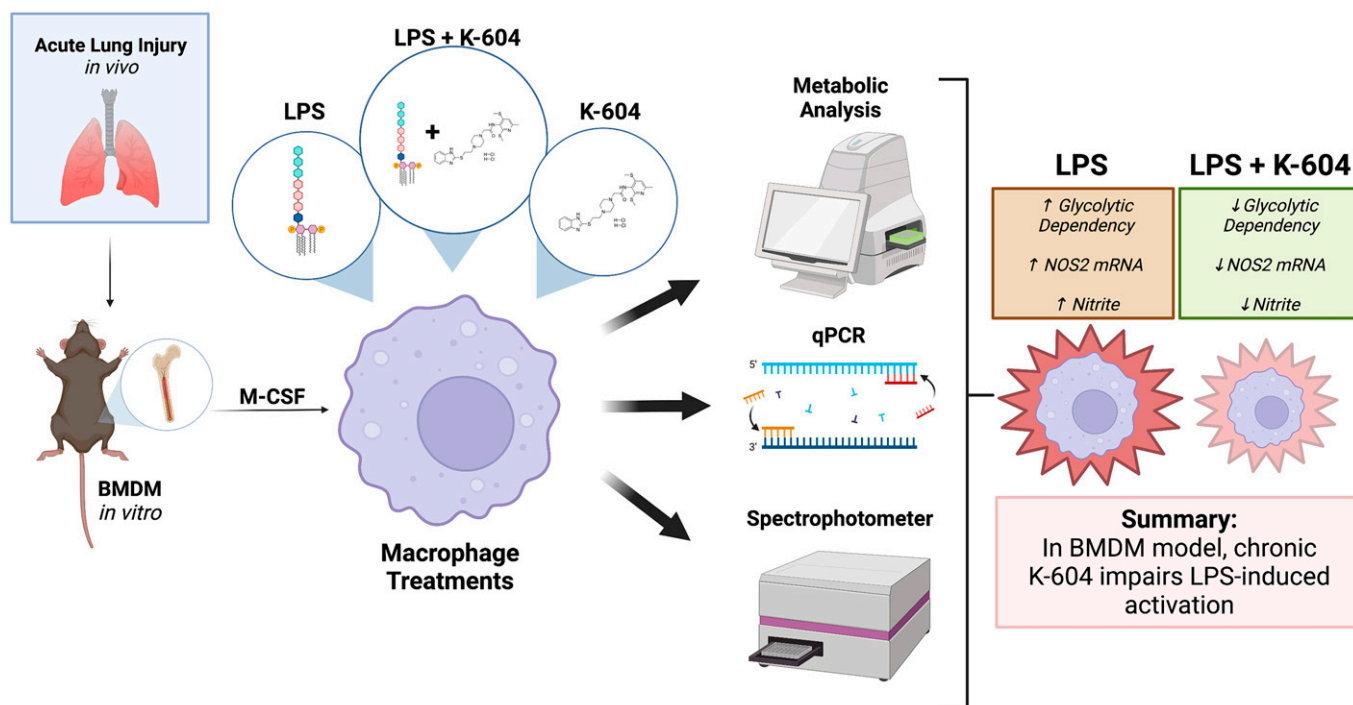
Sung Jae Lee,<sup>1</sup> Emily Stevenson,<sup>1</sup> and Andrew Gow<sup>2</sup>

<sup>1</sup>Rutgers, The State Univ of New Jersey; and <sup>2</sup>Rutgers Univ

Abstract ID 29339

Poster Board 86

Each year in the United States, there are 190,600 cases of acute lung injury (ALI), associated with over 74,000 deaths. Data shows acyl-coenzyme A acetyltransferase-1 (ACAT-1) inhibition improves pulmonary inflammation in an *in vivo* murine model of ALI. We hypothesize that ACAT-1 inhibition has anti-inflammatory effects beyond its intended use to reduce cholesterol esterification. The purpose of this study is to establish an *in vitro* bone marrow-derived macrophage (BMDM) model to investigate the effect of ACAT-1 inhibition on macrophage activation. Monocytes were harvested from the bone marrow of 6-8 week old C57BL/6J (wild-type) mice. Cells were stimulated with M-CSF on d0, 3, and 7 to induce macrophage differentiation. To examine if ACAT-1 inhibition limits macrophage activation, K-604 was co-administered with M-CSF in the wild-type derived cells. Cells were then treated with LPS on d7 and harvested after 24h. Nitrite, Nos2 expression, and iNOS protein density were determined through nitrite colorimetric measurement, RT-qPCR, and western blot, respectively. Glycolytic function and oxygen consumption rate were determined through Seahorse™ Glycolysis and Mito Stress Tests. Nitrite ( $\mu\text{M}/\text{protein}$ ) was observed to significantly increase ( $*p < 0.05$ ) in LPS-stimulated cells compared to control ( $8 \pm 1.5^* v. 0.9 \pm 0.1$ ), which was reduced with K-604 treatment ( $3.2 \pm 1.0$ ). LPS-induced Nos2 fold change ( $11,709 \pm 2,955^* v. 1.0 \pm 0.1$ ) was reduced with K-604 conjunctive treatment compared to LPS alone ( $2,235 \pm 586$ ). These data suggest that LPS-induced NO production was hindered due to a lack of the iNOS protein, which may have implications for macrophage activation. This aligns with reported *in vivo* data, where K-604 reduced pulmonary inflammation in a rodent model of ALI. Metabolic and signaling implications of ACAT-1 inhibition in this model will be discussed.



# A novel UVA-labile $\beta$ -adrenergic agonist allows for optical control of subcellular signaling

Waruna Thotamune,<sup>1</sup> Sithurand Ubeysinghe,<sup>1</sup> Ajith Karunarathne,<sup>1</sup> Kendra K. Shrestha,<sup>2</sup> Michael C. Young,<sup>2</sup> and Mithila Tennakoon<sup>1</sup>

<sup>1</sup>Saint Louis University; and <sup>2</sup>The University of Toledo

**Abstract ID 56317**

**Poster Board 87**

Adrenergic receptors are G-protein-coupled receptors (GPCRs) primarily responsible for signaling in the sympathetic nervous system, which controls numerous body functions, including increased heart rate, pupil dilation, glycogen metabolism, and adrenaline secretion. Several significant polymorphisms are found in these receptors leading to their clinical importance. Using the agonist, Isoproterenol, bound  $\beta$ 1-AR structural data, we designed and synthesized a UVA-labile, novel isoproterenol derivative (Optolso) to optically control  $\beta$ 1-AR signaling. Employing live cell confocal imaging, we examined the initiation of  $\beta$ 1-AR specific Gs-coupled cellular signaling over UVA irradiation of the cells treated with the agonist. Upon UVA exposure of cells incubated with Optolso, miniGs protein and nanobody80 (Nb-80) recruitment to the activated receptor. In addition to cyclic AMP generation, cells also showed G $\beta$ - $\gamma$  and G $\alpha$ s translocation to the cell interior. Our results demonstrated that Optolso exposed cells did not show any signaling activity before UVA irradiation, while a few pulses of UVA activated b1AR. Most importantly, by exposing Optolso incubated and subsequently washed cells to UVA, we induced endomembrane-exclusive b1-AR signaling. Given the pathological significance of deep-organelle b1-AR signaling, including cardiac hypertrophy, Optolso will be a valuable tool to the pharmacology community.

**Support/Funding Information:** R01GM140191

# Mechanistic insights into Rap1A-dependent regulation of phospholipase C epsilon in the heart

Kadidia Samassekou,<sup>1</sup> Elisabeth Garland-Kuntz,<sup>2</sup> Isaac J. Fisher,<sup>2</sup> Vaani Ohri,<sup>1</sup> Livia M. Bogdan,<sup>1</sup> Satchal Erramilli,<sup>3</sup> Angeline Lyon,<sup>2</sup> and Anthony Kossiakoff<sup>3</sup>

<sup>1</sup>Purdue University; <sup>2</sup>Purdue Univ; and <sup>3</sup>The University of Chicago

**Abstract ID 15966**

**Poster Board 88**

Phospholipase C $\epsilon$  enzymes are required for normal cardiovascular function, and their dysregulation can lead to cardiac hypertrophy and heart failure. PLC $\epsilon$  cleaves phosphatidylinositol phosphates into inositol phosphates and diacylglycerol, increasing intracellular Ca<sup>2+</sup> and activating protein kinase C. PLC $\epsilon$  activity is increased by direct binding of the Rap1A GTPase, following stimulation of  $\beta$ -adrenergic receptors. This pathway is required for maximum cardiac contractility, but sustained activation causes cardiac hypertrophy. Rap1A binds to the C-terminal Ras Association (RA) domain of PLC $\epsilon$ , and we previously showed that activation requires long-range conformational changes in the lipase. However, the residues in PLC $\epsilon$  involved in the intramolecular rearrangements are not known. As a first step, I used cryo-electron microscopy single particle analysis (cryo-EM SPA) to determine the 4 Å reconstruction of PLC $\epsilon$  PH-C in complex with an antigen binding fragment (Fab). This is the largest fragment of PLC $\epsilon$  biochemically characterized to date and is robustly activated by Rap1A. The structure defines the basal state of the enzyme and reveals a potential membrane binding surface on the PH domain. These studies set the stage for investigating the structure of the Rap1A–PLC $\epsilon$  PH-C complex and its mechanism of activation. Ultimately, this work supports long-term efforts to develop small molecule modulators of the lipase and its activated complex for treating cardiac hypertrophy.

# Discovery and Validation of RGS2-FBXO44 Protein-Protein Interaction Inhibitors

Sadikshya Aryal,<sup>1</sup> Harrison J. McNabb,<sup>2</sup> and Benita Sjogren<sup>2</sup>

<sup>1</sup>Purdue Univ; and <sup>2</sup>Purdue University

Abstract ID 16497

Poster Board 121

Regulators of G protein Signaling (RGS) proteins are negative regulators of G-protein-coupled receptors (GPCRs). They reduce the amplitude and duration of GPCR signaling by accelerating the hydrolysis of GTP to GDP through their GTPase-accelerating protein (GAP) activity. Altered RGS protein function is involved in numerous diseased states. However, the therapeutic regulation of RGS proteins is challenging as they lack binding pockets for small molecules. Therefore, identifying mechanisms that control RGS protein activity and expression could be a potential targeting strategy. A notable example where altering RGS protein activity would be beneficial is asthma, a long-term respiratory disease, characterized by inflammation of the airways, resulting in the obstruction of airflow to the lungs. Aberrant activation of  $G_{\alpha_q}$  and downstream signaling contribute to chronic symptoms of asthma. RGS2 is known to be selective for  $G_{\alpha_q}$  over other G protein subtypes and has reduced expression levels in asthmatic patients. Low RGS2 protein levels are also implicated in many other diseases such as hypertension, cancer, and heart failure. Indeed, we previously showed that pharmacologically stabilizing RGS2 protein levels inhibits  $G_{\alpha_q}$ -mediated signaling and are cardioprotective in a mouse model of cardiac injury, suggesting that enhanced RGS2 protein levels correlate with increased function. Therefore, targeting the mechanisms that regulate RGS2 protein levels would be a feasible therapeutic strategy.

RGS2 is rapidly degraded through the ubiquitin-proteasomal system (UPS). In the UPS, ubiquitin molecules are covalently linked to the substrate through the cascade of enzymatic reactions (facilitated by E1: ubiquitin-activating enzyme; E2: ubiquitin-conjugating enzyme; E3 ligase). The ubiquitinated substrate is then recognized and degraded by the 26S proteasomal complex. We recently identified the E3 ligase that recognizes RGS2. This E3 ligase complex consists of Cullin 4B (Cul4B), DNA Damage Binding Protein 1 (DDB1), and F-box Only Protein 44 (FBXO44), where FBXO44 acts as the substrate recognition site for RGS2. Therefore, we hypothesize that inhibiting the RGS2-FBXO44 interaction will lead to enhanced RGS2 levels. To identify small molecule RGS2-FBXO44 interaction inhibitors, we utilized NanoLuc® Binary Technology (NanoBiT) to detect the interaction between RGS2 and FBXO44 in a high-throughput screen (HTS). We developed a HEK-293T cell line stably expressing the RGS2-SmBit and LgBit-FBXO44 and optimized the NanoBiT assay for HTS. Using this assay, we screened 1600 compounds (Life Chemicals PPI fragment library) at the Purdue Chemicals Genomics Facility. Following hit confirmation and chemical clustering, the top 20 hits that inhibited the RGS2-FBXO44 protein-protein interaction at least 50% were selected for follow-up. The concentration-dependent activity of these 20 hits was performed to only select compounds inhibiting at least 50% of the interaction and having acceptable inhibition curves (Hill slope 0.5 – 2.0) and potencies ( $IC_{50} < 50 \mu M$ ). We are currently working to further validate these compounds as RGS2 stabilizers via inhibiting the RGS2-FBXO44 protein-protein interaction. We will also detect the effects of the selected hits on  $G_q$ -mediated signaling. These hit compounds will be optimized by applying iterative rational drug-design strategies to deliver future lead candidates to stabilize RGS2 protein levels.

# Sigma Ligand-mediated Cytosolic Calcium Modulation in BV2 Microglia Cells

Joseph M Schober,<sup>1</sup> Eric Lodholz,<sup>1</sup> Faria Simin,<sup>1</sup> Michael Crider,<sup>1</sup> and Ken Witt<sup>1</sup>

<sup>1</sup>SIUE

**Abstract ID 52385**

**Poster Board 122**

While initially protective, prolonged neuroinflammation can result in a disrupted brain microenvironment and lead to neurodegenerative diseases. With anti- and pro-inflammatory phenotypes, microglia are primary regulators of neuroinflammation. Calcium is an important regulator of the microglia phenotype and can be modulated by small, membrane bound chaperone proteins called sigma receptors. We examined the use of sigma receptor ligands to modulate cytosolic calcium in BV2 cells, a mouse microglia cell line. Immunofluorescence staining detected both sigma 1 and 2 receptors in the perinuclear region and throughout the cytoplasm. Our selection of sigma receptor ligands included both commercially available sources and compounds synthesized in our laboratories. We used the Fluo-8-AM probe to measure cytosolic calcium concentrations using flow cytometry after 15, 25 and 35-minute ligand exposure. At 1000 nM concentration, we found 9 of the 18 ligands tested significantly increased cytosolic calcium levels in BV2 cells after 15-minute exposure. We determined the location of calcium flux by pretreating cells with thapsigargin and EGTA to inhibit the endoplasmic reticulum and extracellular sources of entry. We found all four compounds tested (siramesine, PB-28, cis-8-OMe BBZI, and BN-IX-111-F1) promote calcium entry from the extracellular space, but only siramesine promotes calcium entry from both locations. We performed two-drug treatments to identify any potential antagonistic activity by low potency ligands. No antagonistic effect was observed, suggesting a potential non-receptor mediated effect facilitating the increases in calcium. We tested for a common drug-induced effect called phospholipidosis using LipidTOX phospholipid detection reagent to determine a relationship between calcium activity and a membrane-mediated effect. Only two (PB-28 and amiodarone) of five compounds tested resulted in significant phospholipid accumulation at 10  $\mu$ M treatment. Future investigations are required to target the exact mechanism of calcium flux and characterize any connection between phospholipidosis and sigma receptor-ligand binding. Nevertheless, our work emphasizes the importance of sigma ligand-modulated intracellular calcium dynamics as a potential therapy, specifically for treatment in neuroinflammation.

This work was supported by funding from SIUE RGGS and SIUE SOP.

# Structure-guided approach to modulate small molecule binding to the promiscuous pregnane X receptor

Andrew D. Huber,<sup>1</sup> Wenwei Lin,<sup>1</sup> Shyaron Poudel,<sup>1</sup> Yongtao Li,<sup>1</sup> Jayaraman Seetharaman,<sup>1</sup> Darcie J. Miller,<sup>1</sup> and Taosheng Chen<sup>1</sup>

<sup>1</sup>St. Jude Children's Research Hospital

Abstract ID 52403

Poster Board 123

Ligand-binding promiscuity in detoxification systems protects the body from toxicological harm but is a roadblock to drug development due to the difficulty in optimizing small molecules to both retain target potency and avoid metabolic events. Immense effort is invested in evaluating metabolism of molecules to develop safer, more effective treatments, but engineering specificity into or out of promiscuous proteins and their ligands is a challenging task. To better understand the promiscuous nature of detoxification networks, we have used X-ray crystallography to characterize a structural feature of pregnane X receptor (PXR), a nuclear receptor that is activated by diverse molecules (with different structures and sizes) to upregulate transcription of drug metabolism genes. We found that large ligands expand PXR's ligand binding pocket, and the ligand-induced expansion occurs through a specific unfavorable compound-protein clash that likely contributes to reduced binding affinity. Removing the clash by compound modification resulted in more favorable binding modes with significantly enhanced binding affinity. We then engineered the unfavorable ligand-protein clash into a potent, small PXR ligand, resulting in marked reduction of PXR binding and activation. Structural analysis showed that PXR is remodeled and that the modified ligands reposition in the binding pocket to avoid clashes, but the combined protein/ligand conformational changes result in less favorable binding modes. Thus, ligand-induced binding pocket expansion increases ligand-binding potential of PXR but is an unfavorable event; therefore, drug candidates can be engineered to expand PXR's ligand binding pocket and reduce their safety liability due to PXR binding.

Research reported in this publication was supported by ALSAC and National Institutes of Health National Institute of General Medical Sciences [Grant R35GM118041]. The content is solely the responsibility of the authors and does not necessarily represent the official views of the National Institutes of Health. This work utilized the FMX and AMX beamlines, which are primarily supported by the National Institutes of Health National Institute of General Medical Sciences through a Center Core P30 Grant (P30GM133893), and by the U.S. Department of Energy Office of Biological and Environmental Research (KP1607011). As part of the National Synchrotron Light Source II, a national user facility at Brookhaven National Laboratory, work performed at the Center for BioMolecular Structures is supported in part by the U.S. Department of Energy, Office of Science, Office of Basic Energy Sciences Program under contract number DE-SC0012704.

# Subcellular Localization Analysis of Sigma 1 Receptor (S1R) and Binding Immunoglobulin Protein (BiP) for Identification of Antagonists versus Agonists

Faria Anjum Simin,<sup>1</sup> and Joseph Schober<sup>2</sup>

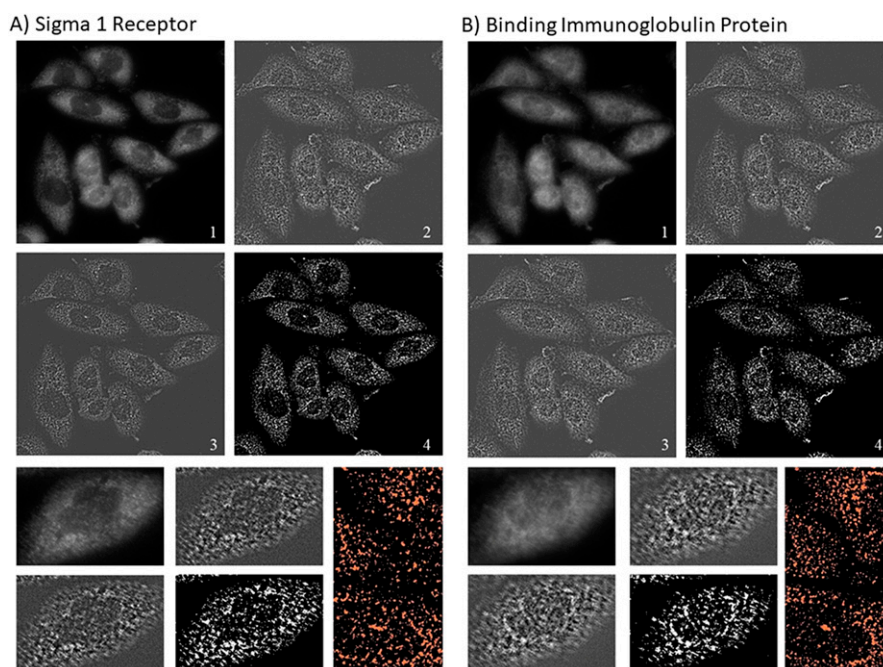
<sup>1</sup>Southern Illinois Univ; and <sup>2</sup>Southern Illinois University Edwardsville

Abstract ID 17604

Poster Board 124

Sigma receptors are attractive therapeutic targets in numerous neurological diseases and cancers. Sigma 1 receptors (S1Rs) are localized in the endoplasmic reticulum (ER) membranes associated with mitochondria where they may participate in cellular stress signaling. During ER stress or stimulation by ligands, S1Rs dissociate from binding immunoglobulin protein (BiP) and exert chaperone activity. S1R agonists promote dissociation while antagonists maintain the complex with BiP. As S1R and BiP are expressed throughout the cell, fluorescence microscopy techniques might not be sensitive to localization and co-localization changes upon ER stress and ligand binding. Therefore, this study aims to perform a quantitative image analysis of S1R and BiP subcellular localization and co-localization during ER stress, and ER stress with S1R ligand treatment. Chinese hamster ovary (CHO) cells were maintained in adherent culture and a suspension was prepared by trypsinizing and adjusting to 200 cells/ $\mu$ L. After CHO cell attachment to fibronectin-coated coverslips, one group was treated with 3  $\mu$ M thapsigargin to cause ER stress, and another group was treated with 1  $\mu$ M BD-1047 following 3  $\mu$ M thapsigargin treatment. Hoechst and phalloidin were multiplexed with secondary antibodies for S1R and BiP primary antibodies. The acquired images were subjected to multistep processing to enable analysis of S1R and BiP localization using MetaMorph software. Background and intensity unevenness were corrected with an object size estimation of 3 pixels, and then high frequencies were suppressed by replacing each pixel intensity with the local average intensity. 90% low threshold values were subtracted for each image and the resulting images were auto-scaled within 95% low and 4% high range. A sample size of 25 cells per treatment group was analyzed. All the quantifications were done at three different cellular regions: whole cell, perinuclear and nuclear. The differences among groups were analyzed by a one-way ANOVA followed by Tukey's multiple comparison test in GraphPad Prism. ER stress increased the average area of discrete objects of both S1R and BiP, increased total S1R and BiP area in whole cell measurements, and increased S1R area in nuclear and perinuclear regions. Co-localization of S1R and BiP upon ER stress is observed throughout the cell, nuclear and perinuclear regions. The co-localization is lowered by BD-1047 in perinuclear and nuclear regions where S1R and BiP participate in stress signaling activity. We conclude this image analysis approach is useful for potential classification of S1R ligands as either agonists or antagonists and predicting ligand efficiency in particular disease states.

This work was supported by SIUE School of Pharmacy and SIUE Graduate School.



Steps in processing immunofluorescence S1R and BiP images for quantitative analysis.



# Trafficking pathway of T-cell receptor mimic antibodies (TCRm) RL6A in human brain-derived endothelial cells

Yeseul Ahn,<sup>1</sup> Ehsan Nozohouri,<sup>2</sup> Sumaih Zoubi,<sup>2</sup> and Ulrich Bickel<sup>2</sup>

<sup>1</sup>Texas Tech Univ Hlth Sci Ctr; and <sup>2</sup>Texas Tech University Health Science Center

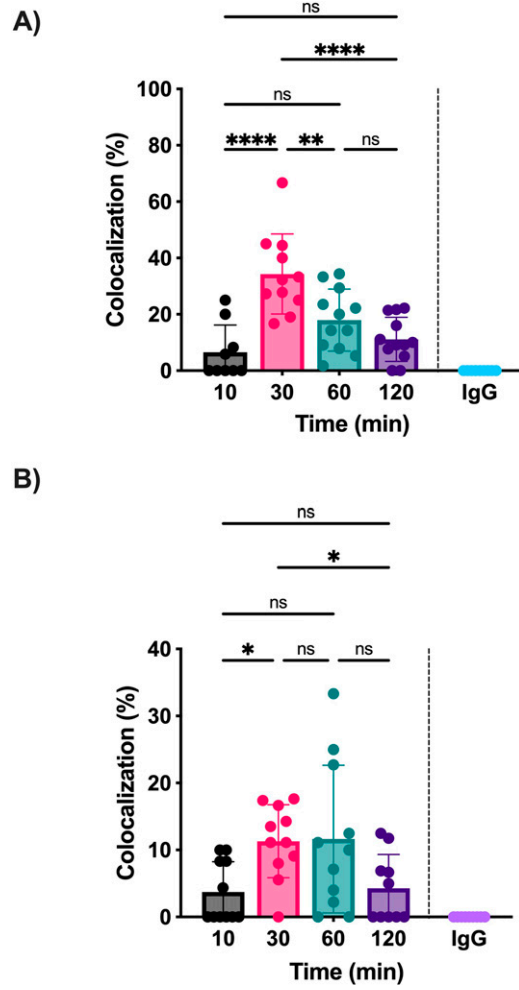
Abstract ID 18127

Poster Board 125

The Blood-Brain Barrier (BBB) protects the human brain by restricting the access of foreign substances to the brain, including even beneficial therapeutic agents with extremely low permeability. Receptor-mediated transcytosis (RMT) is a pathway to transport macromolecules such as antibodies and peptides across the BBB., which has been widely studied as a drug delivery strategy to overcome the BBB. We utilized a novel T-cell receptor mimic antibody (TCRm) to target brain endothelial cells with high affinity and specificity. The TCRm RL6A has been generated to recognize a peptide epitope derived from p68 RNA helicase (YLLPAIVHI) presented by MHC class-I subtype, HLA-A2, which is highly expressed by brain endothelial cells. Our lab previously showed the binding and internalization of RL6A in both *in-vitro* and *in vivo* brain endothelial cells. Therefore, RL6A could be a potential vector for brain drug delivery. Based on the preliminary findings, we hypothesized that the upregulated cellular peptide processing and MHC-I expression levels by Interferon gamma (IFN- $\gamma$ ) will increase the internalization of RL6A in brain endothelial cells. Additionally, we have speculated that RL6A antibodies enter the brain endothelial cells via Clathrin-Independent Endocytosis (CIE), a characteristic of MHC I endocytosis.

We studied these mechanisms on hCMEC/D3 cells, an immortalized human brain endothelial cell line, and on human induced pluripotent stem cell (iPSC) derived brain microvascular endothelial cells (hBMEC). Cells were pre-incubated with antibodies at 4°C for 30min and the internalization was initiated by adding warmed media, and then cells were incubated at 37°C at different time points up to 120 min. Then, cells were further processed for analysis by flow cytometry or confocal microscopy. Our flow cytometry data showed that RL6A internalized from the surface of hCMEC/D3 cells in a biphasic pattern with an initial rapid phase (>30% internalized within 10 min) followed by a slower phase at later time points. Furthermore, the mean fluorescence intensity (MFI) for surface-bound RL6A increased approximately two-fold for the interferon-gamma (IFN- $\gamma$ ) treated cells in both hCMEC/D3 and hBMEC cells. For the trafficking study in hCMEC/D3 cells by confocal microscopy, we used pixel-based and object-based analysis in AIVIA software to quantify the colocalization fraction between RL6A and endogenous early endosome proteins. The results showed that the fraction of RL6A colocalized with the small GTPase ARF6 increased from 6.5%  $\pm$  9.6% (mean  $\pm$  SD) at 10 min to a maximum of 34.3%  $\pm$  14.2% at 30min, and then gradually decreased at 60 min and 120 min (11.1%  $\pm$  7.8%,  $p < 0.0001$  vs 30 min). The time course for RL6A colocalization with Rab5 was similar to ARF6, but the maximum reached only 11.3% at 30 min. The colocalization of RL6A and early endosomal marker EEA1 showed slower dynamics, with a peak fraction of 5.7%  $\pm$  3.5% at 60 min. The absolute number of internalized RL6A reached a plateau after 60 min.

In conclusion, TCRm RL6A internalization occurred mainly in the first 30 min after endocytosis initiation. IFN- $\gamma$  treatment upregulated the expression level of the YLL-A2 complex and increased the RL6A binding and internalization for both hCMEC/D3 and iPSC-derived hBMEC cells. The colocalization analysis expanded on our previous results and demonstrated that RL6A undergoes CIE.



Object-based colocalization analysis between RL6A and A) ARF6 and B) Rab5

# Quantifying Acid Adaptivity of Normal and Cancer Cells Using a Next Generation Genetically Encoded pH Biosensor

Daniel Isom,<sup>1</sup> Sam Taylor,<sup>2</sup> Kyutae Lee,<sup>2</sup> and Jacob Rowe<sup>3</sup>

<sup>1</sup>Univ of Miami Miller Sch of Med; <sup>2</sup>University Of Miami Miller School Of Medicine; and <sup>3</sup>UF Scripps Biomedical Research Institute

Abstract ID 28379

Poster Board 126

Acidic pH is a threat to the viability of most cell types. As such, cells within tumor microenvironments (TMEs) must adapt to acidic conditions caused by the Warburg effect. In the extreme, this selective pressure is thought to evolve tumor cells with enhanced proliferative, survival, and metastatic characteristics. The proteins that facilitate these advantages may hold great potential as druggable vulnerabilities specific to cancer cells. However, the identity of druggable targets that initiate and sustain acid adaptivity remain largely unknown. As a first step to address this longstanding gap in knowledge, we are developing new approaches and technologies for quantifying acid tolerance in normal and cancer cell lines. Here we report a new best-in-class genetically encoded pH biosensor that uses Bioluminescent Resonance Energy Transfer (BRET) for real-time measurement of cellular pH. The characteristics of our new pH biosensor, which we have named ratiOmetRIC prOton seNsor (ORION), mark a significance advance in our ability detect and quantify pH gradients, signals, and dynamical states in mammalian cell models. Having a 20-fold dynamic range over 3.5 pH units (pH 4.25 to 7.75), ideally positioned pH midpoint of 6.0, and complete lack of autofluorescence, the signal-to-noise and applicability of ORION is unmatched. Using yeast and HEK293 cell models, we demonstrate the utility and scalability of ORION using a variety of chemical and biological stressors that alter intracellular pH. Additionally, we confirm our previous findings using another pH biosensor, pHluorin, that intracellular pH changes with extracellular pH in the widely used HEK cell model. With the advent of ORION, it is now possible to study pH (dys)regulation and acid adaptivity of normal and cancer cells at an unprecedented pace and scale. As such, we are extending our studies to a variety of cell lines and will report on our progress.

This work was supported by NIH/NIGMS 5R35GM119518 to D.G.I.

NA

# Urothelial Knock-in of the Engineered Chloride Channel EG3RF as a Potential Treatment for Cystitis-Induced Bladder Inflammation

Grace Ward,<sup>1</sup> Jonathan Beckel,<sup>2</sup> Yan Xu,<sup>3</sup> Keara Healy,<sup>3</sup> and Stephanie Daugherty<sup>3</sup>

<sup>1</sup>Emory Univ; <sup>2</sup>Univ of Pittsburgh; and <sup>3</sup>University of Pittsburgh

Abstract ID 15021

Poster Board 127

Bladder inflammation, overactivity, and pain are adverse side effects of Interstitial Cystitis/Bladder Pain Syndrome (IC/BPS), a pathological bladder condition characterized by urinary urgency, bladder pain, and inflammation that affects up to 17% of American women. IC/BPS has proven to be resistant to standard anti-inflammatory treatments and analgesics, therefore research has focused on developing new treatments for IC/BPS-associated chronic pain. One such potential avenue for treatment lies in the expression of non-native, engineered ion channels in bladder afferent nerves that can selectively reduce nerve excitability in response to inflammatory conditions or after activation with a designer ligand. To this end, we have created an engineered chloride channel, EG3RF, that is activated by both the acidic pH that is a hallmark of inflammation as well as bioactive amines, such as cysteamine or propylamine. We have previously shown that expression/activation of this channel in the bladder can inhibit bladder hyperactivity in cyclophosphamide (CYP) treated rats (a model of IC/BPS), likely by hyperpolarizing bladder afferent nerves. Surprisingly, preliminary data suggested that EG3RF activity also reduced CYP-induced bladder inflammation, suggesting secondary actions on the urothelium itself. Bladder inflammation occurs downstream of urothelial ATP release by lysosomal exocytosis, which is associated with increased lysosomal calcium release. Thus, we hypothesized that EG3RF activation may inhibit bladder inflammation by interfering with this signaling in urothelial cells. Fura-2 based calcium imaging demonstrated that EG3RF activation in urothelial cells decreases the calcium response to the TRPML1 agonist ML-SA1. Furthermore, while expression of EG3RF alone slightly decreases calcium release (-22.15%), cotreatment of EG3RF-transfected cells with ML-SA1 and a biogenic amine increases EG3RF's efficacy. Experimental results show that cysteamine is less harmful to cells and produces a greater decrease in calcium release (-52.77%) for EG3RF-transfected cells than propylamine (-21.90%). To further explore EG3RF's role in reducing bladder inflammation, next steps include identifying its intracellular location in transfected cells and confirming the effect of EG3RF activation on urothelial ATP release.

**Funding:** R01DK117884 (Beckel), R01DK117383 (Xu).

# GPCR cargo modifies lipid order in clathrin-coated pits

G. Aditya Kumar,<sup>1</sup> and Manoj A. Puthenveedu<sup>1</sup>

<sup>1</sup>Univ of Michigan

Abstract ID 15819

Poster Board 128

Endocytosis of G protein-coupled receptors (GPCRs) *via* clathrin-coated pits (CCPs) is crucial for receptor desensitization and signaling. The core protein machinery that mediate CCP initiation, maturation, and scission have been heavily studied. Although this core protein machinery is broadly distributed and shared between all CCPs, these structures are initiated at spatially non-random sites on the membrane and are restricted to specialized regions in some cell types. Whether the physical properties of the membrane itself contribute to this specialization is not well understood. Here, we use high resolution multichannel total internal reflection fluorescence microscopy (TIR-FM) to measure lipid order in the plasma membrane using a dual channel ratiometric fluorescence readout from a solvatochromic pyrene-based probe. Lipid order imaging in CCP clusters showed that CCPs represent membrane domains of a lower order relative to the rest of the plasma membrane. The lipid order in endocytic clusters exhibited time-resolved changes during CCP maturation. The prototypical GPCR,  $\beta_2$ -adrenergic receptor ( $\beta_2$ AR) clusters into a subset of CCPs in response to activation by its agonist isoproterenol. Interestingly,  $\beta_2$ AR-containing CCPs exhibited higher lipid order relative to CCPs that did not contain the receptor. However, such a difference was not observed in case of another class A GPCR, the delta opioid receptor (DOR), and the constitutively internalizing cargo, transferrin.  $\beta_2$ AR, unlike DOR, has been shown to extend CCP lifetimes and receptor residence times on the membrane via a C-terminal PDZ ligand that links the receptor to the actin cytoskeleton. We show here that the difference in lipid order between  $\beta_2$ AR-containing CCPs and CCPs that do not contain  $\beta_2$ AR was abrogated upon disruption of the  $\beta_2$ AR C-terminal PDZ ligand. Overall, our results show that CCPs represent specialized membrane domains with a distinct lipid order, and that lipid order is an important determinant of cargo-specificity in GPCR endocytosis.

# Insurmountable Antagonism by Buprenorphine at Human Mu Opioid Receptors

Michael Wedemeyer,<sup>1</sup> Kelly Berg,<sup>2</sup> and William Clarke<sup>3</sup>

<sup>1</sup>Univ of Texas Health, San Antonio; <sup>2</sup>Univ of Texas Health Science Center-San Anto; and <sup>3</sup>Univ of Texas HSC-San Antonio

**Abstract ID 16848**

**Poster Board 129**

In 2017 the US government declared a public health emergency to address the national opioid crisis. Despite this focused effort and increased awareness, opioid overdose deaths have since increased by over 50%. Individuals with opioid use disorder have increased risk of opioid related death, and medication assistance can facilitate recovery by reducing opioid cravings and withdrawal effects. One such medication is buprenorphine, an FDA approved drug for the treatment of opioid use disorder sold under the brand Suboxone®, Subutex®, and Zubsolv®. While buprenorphine is clinically described as a partial agonist of the mu opioid receptor (MOR), the literature demonstrates that its pharmacological characteristics are complex. In ongoing studies we are rigorously characterizing the pharmacological actions of buprenorphine at the human MOR.

A genetically encoded biosensor was used to monitor cAMP levels in real time in HEK293 cells expressing a low density of the human MOR. In these cells, pretreated buprenorphine acted as an antagonist, shifting the concentration response curve of the MOR agonist, DAMGO, to the right (reduced potency) in a concentration-dependent manner, similar to the action of the MOR antagonist naloxone. Unlike the effect of naloxone, buprenorphine also decreased the maximal response of DAMGO (insurmountable antagonism), an effect that saturated with increasing concentrations of buprenorphine. Similar antagonism by buprenorphine was observed when fentanyl was used as the MOR agonist. The effect of buprenorphine to decrease the potency of DAMGO was reduced by washout of buprenorphine. In contrast, the reduction in the maximal response to DAMGO was resistant to washout of buprenorphine. Both effects of buprenorphine (on DAMGO potency and efficacy) were prevented by pre-treatment with naloxone, followed by rigorous washout. This suggested that buprenorphine's effects were mediated by a naloxone-sensitive binding site, presumably the orthosteric site.

Given the slow rate of dissociation of buprenorphine binding to MOR in several published studies and the rapid time-course involved in the cAMP response, we considered the possibility that the observed insurmountable antagonism of buprenorphine was due to insufficient agonist-antagonist re-equilibration (hemi-equilibrium). Computations conducted using hemi-equilibrium equations support the hypothesis that the insurmountable antagonism of buprenorphine in this system is due to hemi-equilibrium. Indeed, the reduction of the maximal response of DAMGO by buprenorphine was abolished when measurements were taken two hours following DAMGO addition. As a frontline treatment for opioid use disorder, an understanding of the apparent insurmountable antagonism of buprenorphine may inform clinical practice in patients recovering from opioid use disorder.

This work is supported by the Institutional National Research Service Award (DA031115) Postdoctoral Training in Drug Abuse Research: Behavior & Neurobiology at UT Health San Antonio and a grant from NIH/NIDA (RO1 DA038645).

# Amyloid Beta Protein ( $A\beta_{1-42}$ ) induced Endolysosome Iron Dyshomeostasis caused increases in Reactive Oxygen Species, Mitochondrial Depolarization, and Neurotoxicity

Darius NK. Quansah,<sup>1</sup> Peter W. Halcrow,<sup>1</sup> Nirmal Kumar,<sup>1</sup> Braelyn Liang,<sup>1</sup> and Jonathan D. Geiger<sup>1</sup>

<sup>1</sup>University of North Dakota

Abstract ID 21210

Poster Board 130

Alzheimer's disease (AD) is a widely prevalent age-associated neurodegenerative disease that is characterized clinically by decreased cognitive abilities and dementia as well as pathologically by the presence of amyloid beta plaques and intraneuronal accumulations of the highly fibrillogenic amyloid beta 1-42 ( $A\beta_{1-42}$ ) protein and hyperphosphorylated tau protein. Implicated as well in the pathogenesis of AD are increased levels of reactive oxygen species (ROS) and iron dyshomeostasis. Amyloidogenesis is well known to occur in endolysosomes; acidic organelles that amongst other things contain high levels of divalent cations and these cations are released from endolysosomes when de-acidified. Endolysosomes are considered "master regulators of iron homeostasis", and neuronal cell death and neurodegenerative disorders continue to be linked to ferrous iron ( $Fe^{2+}$ ) induced ROS generation via Fenton-like chemical reactions. Because endolysosome de-acidification can induce lysosome stress responses that cause  $Fe^{2+}$  to be released from endolysosomes it was important for us to determine the extent to which and mechanisms by which  $A\beta_{1-42}$  affect endolysosomes and induce neuronal cell death. Recently, the endolysosome-specific iron chelator deferoxamine (DFO) was found to reduce the amyloid beta burden in AD but by unclear mechanisms. We reported previously that DFO is endocytosed and by chelating endolysosome stores of ferric iron ( $Fe^{3+}$ ) it prevented the efflux of the readily releasable endolysosome stores of  $Fe^{2+}$  into the cytosol and other organelles. Thus, it was important for us to determine the effects of  $A\beta_{1-42}$  on the endolysosome iron pool that might lead to an iron imbalance and increased ROS. Here, using SH-SY5Y neuroblastoma cells we show that  $A\beta_{1-42}$  de-acidified endolysosomes, decreased endolysosome  $Fe^{2+}$  levels, increased cytosolic  $Fe^{2+}$  and ROS levels, increased mitochondria  $Fe^{2+}$  and ROS levels, depolarized mitochondrial membrane potentials, and increased cell death; effects all blocked by DFO. Therefore, an increased understanding of  $A\beta_{1-42}$ -induced endolysosome iron disruption may provide novel insight into the  $A\beta_{1-42}$  burden of AD and possibly new therapeutic targets.

**Support/Funding Information:** [P20GM139759, P30GM100329, U54GM115458, R01MH100972, R01MH105329, R01MH119000, 2R01NS065957, 2R01DA032444]

# PTBP1 Contains a Novel Regulatory Sequence, the rBH3, that Binds the Pro-Survival Protein MCL1

Christine Christine, Jia Cui,<sup>1</sup> Alexis Acton,<sup>2</sup> and William Placzek<sup>3</sup>

<sup>1</sup>Harvard Medical School/Boston Children's Hospital; <sup>2</sup>Univ of Alabama at Birmingham; and <sup>3</sup>The Univ of Alabama at Birmingham

Abstract ID 15827

Poster Board 131

The maturation of RNA from its nascent transcription to ultimate translation or utilization in alternate biological processes (e.g. miR-mediated RNA silencing) is an intricately coordinated series of biochemical reactions. RNA binding proteins (RBPs) are the sites at which these biochemical reactions occur, and therefore serve as the effectors of RNA maturation and processing. Over the past several decades, there has been extensive effort to elucidate the biological factors that control the specificity and selectivity of RNA target binding and downstream function. Polypyrimidine tract binding protein 1 (PTBP1) is an RNA binding protein that is not only involved in all steps of RNA maturation but serves as a key regulator of alternative splicing of many cellular transcripts, therefore understanding its regulation is of critical biologic importance. While several mechanisms of RBP specificity have been proposed (e.g. cell- or tissue-specific expression of RBPs, secondary structure of target RNA), recently protein-protein interactions with individual domains of RBPs have been suggested to be important determinants of downstream function. Here we demonstrate a novel binding interaction between the first RNA recognition motif (RRM1) of PTBP1 and the pro-survival protein MCL1. Applying both *in silico* and *in vitro* analysis, we have demonstrated that MCL1 binds a novel regulatory sequence on RRM1 termed the rBH3. NMR spectroscopy reveals that this interaction allosterically perturbs key residues in the RNA binding interface of RRM1 and negatively impacts RRM1 association with target RNA. Pulldown of MCL1 by endogenous PTBP1 has verified that these proteins interact in an endogenous cellular environment, establishing the biological relevance of this binding event. Overall, the current study proposes a novel mechanism of regulation of PTBP1, in which a protein-protein interaction with a single RRM can impact RNA association.

This work was supported, in part, by funding from the National Institutes of Health Grants R01GM117391 (to W.J.P.) and National Institutes of Health Grants T32GM008361 (to T.Y.). The content is solely the responsibility of the authors and does not necessarily represent the official views of the National Institutes of Health.



# $\beta$ -arrestin1 Directs Substrate Lysine Selection and Linkage Type Specificity by E3 Ubiquitin Ligases

Chandler McElrath,<sup>1</sup> Ya Zhuo,<sup>1</sup> Sara Benzow,<sup>1</sup> and Adriano Marchese<sup>1</sup>

<sup>1</sup>Medical College of Wisconsin

Abstract ID 23164

Poster Board 132

$\beta$ -arrestins are multifaceted adaptor proteins that regulate the desensitization, internalization, and signaling of G protein-coupled receptors (GPCRs). Arrestins interact with many signaling molecules, including E3 ubiquitin ligases, to facilitate ubiquitination of both GPCRs and non-GPCR binding partners. However,  $\beta$ -arrestins are not required for the ubiquitination of the chemokine receptor CXCR4, although they are believed to play a role in the ubiquitination of the non-GPCR interacting partner STAM1. STAM1 is an endosomal sorting protein, and ubiquitination of STAM1 regulates CXCR4 lysosomal trafficking and thus receptor abundance and signaling, yet very little is known concerning STAM1 ubiquitination. Here, we report that  $\beta$ -arrestin1 acts as an adaptor for the ubiquitination of STAM1 and dictates lysine selection and linkage-type specificity. We developed a cell-free, reconstituted system to study *in vitro* ubiquitination of STAM1 by  $\beta$ -arrestin1 via the E3 ligase AIP4. We provide evidence that  $\beta$ -arrestin1 dose-dependently increases ubiquitination of STAM1 by AIP4. This pattern is not observed when using a  $\beta$ -arrestin1 variant that is unable to bind to STAM1, consistent with  $\beta$ -arrestin1 serving as an adaptor for STAM1 ubiquitination by AIP4. Further establishing this adaptor role downstream of CXCR4 signaling, a pre-activated version of  $\beta$ -arrestin1 mimicking the receptor-bound conformation enhanced STAM1 ubiquitination. To learn more about STAM1 ubiquitination, we set out to define the ubiquitination sites and the type of polyubiquitin chains by mass spectrometry. Mass spectrometry analysis revealed that several lysine residues on STAM1 are modified by ubiquitin with potentially multiple common ubiquitin linkage types. In addition, we identified the potential formation of M1-linked chains, a type of ubiquitin linkage previously only described for one other E3 ubiquitin ligase. Further mass spectrometry and mutagenesis studies provide evidence that  $\beta$ -arrestin1 specifies M1-linked ubiquitin chain formation by AIP4 at Lys136 on STAM1. Using a combination of wild-type and lysine-free ubiquitin, we provide evidence that  $\beta$ -arrestin1 directs STAM1 modification with an anchor ubiquitin moiety at Lys136, which is then subsequently modified with M1-linked polyubiquitin chains. These data provide evidence for the first time that  $\beta$ -arrestin1 coordinates lysine selection and specifies M1-linked polyubiquitination of a substrate by an E3 ubiquitin ligase. This is the first report describing AIP4 conjugating M1-linked ubiquitin chains, making it the second E3 ligase known to conjugate such chains. Our study expands the roles of ubiquitin into GPCR signaling and trafficking.

**Support/Funding Information:** NHLBI Ruth L. Kirschstein Individual Predoctoral Fellowship F31 Award, Medical College of Wisconsin

# GRK2 Enhances $\beta$ -arrestin Recruitment to the D2 Dopamine Receptor Through a Mechanism that is Independent From Receptor Phosphorylation or G Protein Activation

Noelia Boldizar,<sup>1</sup> Marta Sanchez-Soto,<sup>1</sup> Julia Drube,<sup>2</sup> Raphael Haider,<sup>2</sup> R Benjamin Free,<sup>1</sup> Carsten Hoffman,<sup>2</sup> and David R. Sibley<sup>1</sup>

<sup>1</sup>National Institutes of Health; and <sup>2</sup>Institute of Molecular Cell Biology, Jena University Hospital

Abstract ID 19401

Poster Board 148

The D2 dopamine receptor (D2R) interacts with and signals through both G proteins and  $\beta$ -arrestins to regulate important physiological processes, such as movement, reward circuitry, emotion, and cognition.  $\beta$ -arrestins are believed to interact with G protein-coupled receptors (GPCRs) at two interfaces: the receptor core and the phosphorylated C-terminal tail or intracellular loops. GPCR kinases (GRKs) are the primary drivers of GPCR phosphorylation, and for many receptors, this post-translational modification is indispensable for  $\beta$ -arrestin recruitment. However, GRK-mediated receptor phosphorylation is not required for  $\beta$ -arrestin recruitment to the D2R, and the role of GRKs in D2R- $\beta$ -arrestin interactions remains largely unexplored. In this study, we used GRK knockout cells engineered using CRISPR-Cas9 technology to determine if  $\beta$ -arrestin recruitment to the D2R was GRK-dependent. Genetic elimination of all GRK expression significantly decreased, but did not totally eliminate, both  $\beta$ -arrestin recruitment to the D2R and receptor internalization. However, these processes were rescued upon re-introduction of various GRK isoforms in the cells via transient transfection. Further, treatment with compound 101, a pharmacological inhibitor of GRK2/3 isoforms, dose-dependently decreased  $\beta$ -arrestin recruitment and receptor internalization, highlighting the importance of these kinases for D2R- $\beta$ -arrestin interactions. Interestingly, these results were recapitulated using a phosphorylation-deficient (PO4-null) D2R mutant, emphasizing that GRKs enhance D2R- $\beta$ -arrestin interactions independently from receptor phosphorylation. As GRK2/3 are well known to interact with the  $\beta$ - $\gamma$  subunits of G proteins following heterotrimer dissociation, we investigated the role of G proteins in GRK functionality at the D2R. Inhibition of G protein signaling with pertussis toxin modestly decreased  $\beta$ -arrestin recruitment to the D2R in cells expressing endogenous amounts of GRKs but had no effect when GRK2 was overexpressed. We also used a mutant GRK2 that is unable to bind to  $\beta$ - $\gamma$  G protein subunits (GRK2-R587Q) and found that  $\beta$ - $\gamma$  interactions were not necessary for this function of GRK2. Next, we investigated if the catalytic activity of GRK2 is required to enhance D2R- $\beta$ -arrestin interactions. Overexpression of a catalytically inactive GRK2 mutant (GRK2-K220R) did not enhance  $\beta$ -arrestin recruitment or receptor internalization in cells expressing endogenous amounts of GRKs. However, when transfected into GRK-KO cells, GRK2-K220R rescued  $\beta$ -arrestin recruitment and D2R internalization, albeit to a slightly lesser extent than WT GRK2. However, we found that GRK2-K220R is recruited to the D2R less efficiently than WT GRK2 in both parental and GRK-KO cells. Therefore, its lack of effect when overexpressed in parental cells could be due to competition from endogenous GRKs. Further, the reduced ability of GRK2-K220R to interact with the D2R could explain its reduced ability to drive  $\beta$ -arrestin recruitment compared to WT GRK2. In summary, we demonstrate that GRKs, especially GRK2/3, are necessary for maximal agonist-stimulated D2R- $\beta$ -arrestin interactions, however, their kinase activities are not required. We hypothesize that GRK2 might act through a novel non-catalytic, scaffolding mechanism to enhance  $\beta$ -arrestin recruitment to the D2R, highlighting the diversity with which GPCRs can interact with signal transduction proteins.

# Molecular Determinants of Ligand-Induced Allosteric Coupling to G<sub>q</sub> and G<sub>i</sub> at the Angiotensin II Type 1 Receptor

Akua Acheampong,<sup>1</sup> Laura M. Wingler,<sup>2</sup> Andrew Feld,<sup>3</sup> Matthew Collins,<sup>3</sup> and Brandi Small<sup>3</sup>

<sup>1</sup>Duke; <sup>2</sup>Duke Univ; and <sup>3</sup>Duke University

**Abstract ID 25473**

**Poster Board 149**

The angiotensin II type 1 receptor 1 (AT<sub>1</sub>R) is a G protein-coupled receptor that is a critical regulator of blood pressure and a validated drug target for cardiovascular disease. AT<sub>1</sub>R signaling is initiated when binding of an extracellular ligand allosterically changes the conformation of the intracellular transducer binding site to activate transducers like heterotrimeric G proteins, GRKs, and  $\beta$ -arrestins. The AT<sub>1</sub>R is known to activate several different G protein subfamilies, including G<sub>q/11</sub> and G<sub>i/o</sub>. However, these subfamilies exhibit very distinct patterns of allostery at the AT<sub>1</sub>R. G<sub>q</sub> shows strong allosteric coupling to a select few AT<sub>1</sub>R ligands, but G<sub>i</sub> shows relatively weak allosteric coupling to a much broader range of AT<sub>1</sub>R ligands. Here, we employ mini G proteins, built on a G<sub>s</sub> protein scaffold, to demonstrate that eight subtype-specific residues from the C-terminal  $\alpha 5$  helix of G<sub>q</sub> and G<sub>i</sub> are sufficient to recapitulate ligand-specific patterns of allosteric coupling to the AT<sub>1</sub>R. Within this subset of G protein residues, a few key sites disproportionately contribute to G<sub>q</sub>'s strong allosteric effects on ligand binding. These data provide insights into the specific conformational features that different transducers recognize and could ultimately contribute to the design of ligands biased towards the activation of specific G protein subtypes.

LMW is a Whitehead Scholar and a Pew Scholar in the Biomedical Sciences, supported by The Pew Charitable Trusts.

# Multomics approach to interrogate translational regulation to GPCR signaling and its spatial bias

Matt J. Klauer, Caitlin Jagla,<sup>1</sup> and Nikoleta Tsvetanova<sup>2</sup>

<sup>1</sup>Duke University; and <sup>2</sup>Duke

**Abstract ID 16887**

**Poster Board 150**

Ligand activation of G protein-coupled receptors (GPCRs) induces a plethora of cellular responses that ultimately culminate in changes in protein expression. Our lab and others have demonstrated that certain GPCR-dependent responses that feed into protein expression changes are biased by receptor localization. Specifically, we have shown that gene transcription is stimulated downstream of endosomal receptors. However, transcription represents only one layer of gene expression regulation, and therefore analysis of steady-state RNA abundance alone does not adequately capture the full breadth of changes that underlie protein expression. To address this, we apply a multomics approach to interrogate the comprehensive landscape of transcriptional and post-transcriptional changes in cellular responsiveness to receptor activation, and assess their dependence on GPCR localization. We pair RNA-seq and Ribo-seq and identify hundreds of target genes downstream of the prototypical beta-2-adrenergic receptor (B2AR) to be regulated exclusively at the transcriptional or translational level. Strikingly, none of the translational targets identified here have been previously linked to GPCR signaling. In addition, we find distinct functional categories over-represented across each set of targets (transcriptional vs translational), suggesting that unique cellular processes downstream of B2AR activation are subject to discrete regulatory mechanisms. In further studies, we show that the vast majority of these genes likely represent conserved translational targets downstream of Gas-coupled receptors. Lastly, we are probing the spatial dependence of the novel translational targets. In preliminary work, we have identified genes encoding complexes involved in iron homeostasis as exclusive translational targets, and show that at least one of these genes requires endosomal B2AR signaling for its translational regulation. These mechanisms are of broad biological relevance as they appear to be conserved in both tractable and physiologically-relevant adrenoceptor cell types such as iPSC-derive human CMs. In summary, we have successfully developed an experimental pipeline to probe gene expression regulation at multiple levels. This work is extending our understanding of the cellular processes dependent on compartmentalized receptor signaling and their underlying regulation.

# MiR-146b inhibits lung fibroblast proliferation and differentiation by targeting EGFR and TGF $\beta$ R signaling pathways

Venkatlaxmi Chettiar,<sup>1</sup> Yan Xie,<sup>1</sup> Yapei Huang,<sup>1</sup> Steven K. Huang,<sup>2</sup> Bethany B. Moore,<sup>2</sup> Myron Toews,<sup>3</sup> Peter Abel,<sup>1</sup> and Yaping Tu<sup>1</sup>

<sup>1</sup>Creighton Univ School of Medicine; <sup>2</sup>University of Michigan Medical School; and <sup>3</sup>Univ Nebraska Medical Center

Abstract ID 29836

Poster Board 163

Idiopathic pulmonary fibrosis (IPF) is the most common type of pulmonary fibrosis. It is progressive and usually fatal. Current treatments have not significantly improved survival, leaving an unmet need for novel anti-fibrotic therapies. Excess fibroblast proliferation and differentiation into myofibroblast in response to profibrotic mediators such as transforming growth factor (TGF)  $\alpha$  and  $\beta$ 1 are considered key steps in IPF progression. TGF $\alpha$  and TGF $\beta$ 1 bind and stimulate the epidermal growth factor receptor (EGFR) and TGF $\beta$  receptors (TGF $\beta$ R1/2), respectively. Upregulation of EGFR and TGF $\beta$ R and their signaling in lung fibroblasts play an important role in the pathogenesis of IPF. Thus, suppressing EGFR/TGF $\beta$ R-dependent fibroblast proliferation and differentiation are attractive targets for preventing IPF progression and death.

MicroRNAs (miRs) are important posttranscriptional gene expression regulators and several miRs are known to be dysregulated in IPF, but the mechanisms for their dysregulation and pathological effects remain largely unknown. We used both RNA sequencing and quantitative RT-PCR strategies to systematically study TGF- $\beta$ 1-induced alternations of miRNAs in human lung fibroblasts (HLF). While miR-21, miR-145, miR-424 and miR-133a were among the TGF $\beta$ 1-induced miRNAs that were previously shown to promote or inhibit pulmonary fibrosis, miR-146b is one of the most reduced miRNAs in TGF $\beta$ 1-treated cells. Quantitative RT-PCR confirmed that miR-146b expression was significantly reduced by 70% in HLFs in response to TGF- $\beta$ 1 treatment. Interestingly, normal expression of miR-146b is highest in lung fibroblasts but was markedly downregulated by about 50% in IPF patients or mice with experimental pulmonary fibrosis. Using mouse precision-cut lung slices as an *ex vivo* 3D model of fibrosis, we found that miR-146b deficiency exacerbated fibrotic pathohistological changes in response to profibrotic mediators TGF $\alpha$  and TGF $\beta$ 1. Human lung fibroblasts from IPF patients (HLF-F) also show stronger fibrotic mediator responses than non-fibrotic HLF-N. Increasing expression of miR-146b in HLF-F suppresses TGF $\alpha$ -stimulated proliferation and blocks TGF $\beta$ 1-induced myofibroblast differentiation by 60-90%, whereas deletion of miR-146b in lung fibroblasts significantly increases fibrotic responses. RNA-sequencing and KEGG pathway analysis revealed that miR-146b downregulates the cell cycle pathway and TGF $\beta$  signaling. Western blot analysis further confirmed miR-146b targets EGFR/TGF $\beta$ R-mediated proliferative and fibrogenic signaling pathways.

Together we identified miR-146b as an important endogenous anti-fibrotic factor in lung fibroblasts. It inhibits lung fibroblast proliferation and differentiation by targeting EGFR and TGF $\beta$ R signaling pathways. Importantly, TGF $\beta$ 1 repression of miR-146b provides a novel mechanism that integrates the profibrotic and hyper-proliferative aspects of human IPF.

(Supported by grants from NIH R01HL116849 to YT, R35HL144481 to BBM and SKH; Nebraska State LB595 to PWA).

# Molecular mechanisms of $G\beta\gamma$ -stimulated activation of PLC $\beta$

Isaac J. Fisher,<sup>1</sup> Kennedy Outlaw,<sup>1</sup> Kaushik Muralidharan,<sup>2</sup> and Angeline Lyon<sup>1</sup>

<sup>1</sup>Purdue Univ; and <sup>2</sup>Nationwide Children's Hospital

Abstract ID 23793

Poster Board 164

G protein-coupled receptors (GPCRs) transduce extracellular stimuli into intracellular signaling events through activation of the heterotrimeric G protein subunits,  $G\alpha$  and  $G\beta\gamma$ . G proteins in turn activate effector enzymes, such as phospholipase C  $\beta$  (PLC $\beta$ ), to produce second messengers. The four human PLC $\beta$  isoforms (PLC $\beta$ 1-4) are all potently activated by direct binding of  $G\alpha_q$ , but only PLC $\beta$ 1-3 are also directly activated by  $G\beta\gamma$ . Dysregulation of the G protein-phospholipase C signaling axis has been implicated in numerous pathologies and disease states. Direct inhibition of these pathways has shown therapeutic potential in models of inflammation, cardiac hypertrophy, opioid analgesia, and cancer. Much is known about how  $G\alpha_q$  binds to and activates PLC $\beta$ , but despite decades of research, the molecular details of  $G\beta\gamma$ -stimulated activation have been elusive. Using a protein engineering strategy and single particle cryo-electron microscopy, we have now determined high-resolution structures of functional  $G\beta\gamma$ -PLC $\beta$ 3 complexes. The structures reveal that the  $G\beta\gamma$  interacts with PLC $\beta$ 3 through multivalent interactions with the PH domain, EF hands and the C2 domains of PLC $\beta$ . The structures differ in the engagement of the  $G\beta\gamma$  subunit with the PH-EF hand interface. Intriguingly, one conformation of the  $G\beta\gamma$ -PLC $\beta$  complex is compatible with simultaneous binding of  $G\alpha_i$ , which has not been observed for any other  $G\beta\gamma$ -effector enzyme complex. Cellular activity assays suggest that this conformation is less sensitive to  $G\beta\gamma$ -dependent activation, and, in assays with purified components, that crosslinked  $G\beta\gamma$ -PLC $\beta$  complexes still sensitive to  $G\alpha_i$  inhibition. Thus,  $G\beta\gamma$  or the  $G\alpha_i\beta\gamma$  complex may also function as a scaffold for PLC $\beta$ , in which a pre-activated complex is maintained at the membrane. Current efforts in the lab include investigating the scaffolding function of these complexes and PLC $\beta$  insensitivity to  $G\beta\gamma$  activation.

# Visualizing the chaperone-mediated folding trajectory of the G protein $\beta_5$ $\beta$ -propeller by high resolution cryo-EM

Mikaila Sass,<sup>1</sup> Shuxin Wang,<sup>2</sup> William G. Ludlam,<sup>3</sup> Yujin Kwon,<sup>3</sup> Ethan Carter,<sup>3</sup> Peter S. Shen,<sup>2</sup> and Barry M. Willardson<sup>1</sup>

<sup>1</sup>Brigham Young Univ; <sup>2</sup>University of Utah School of Medicine; and <sup>3</sup>Brigham Young University

**Abstract ID 26047**

**Poster Board 279**

The cytosolic chaperonin CCT and its co-chaperone phospho-ducin-like protein 1 (PhLP1) play important roles in G protein heterotrimer assembly by folding G protein  $\beta$  subunits ( $G\beta$ ) into  $\beta$ -propeller structures. To understand this process at the molecular level, we have isolated the CCT- $G\beta_5$ -PhLP1 folding intermediate in both the open and closed CCT conformations and determined its structure by high resolution cryo-electron microscopy (cryo-EM). In the open structures,  $G\beta_5$  interacts in an unstructured state with the N- and C-termini of the CCT subunits deep inside the folding chamber between the CCT rings. Two copies of PhLP1 bind to the apical domains at the rim of the folding chamber on either end of CCT, allosterically enhancing  $G\beta_5$  binding to CCT. In the closed CCT structure,  $G\beta_5$  moves from between the CCT rings into one of the folding chambers, suggesting a path for release of  $G\beta_5$  from CCT during its ATPase cycle. The other chamber is occupied by one copy of PhLP1, which reaches across to  $G\beta_5$  in the opposite folding chamber to stabilize  $G\beta_5$  folding. 3D classification and variability analysis of the closed structure captured  $G\beta_5$  in progressively folded states that reveal its folding trajectory. CCT initiates folding on  $G\beta_5$  blade 4 and folding progresses radially around the  $\beta$ -propeller as CCT makes contacts with blades 3 and 2 in one direction and blades 5 and 6 in the opposite direction. Closing of the  $\beta$ -propeller occurs with the folding of blades 1 and 7 without making additional contacts with CCT. Unexpectedly, CCT interacts exclusively with hydrophilic surface residues of  $G\beta_5$ , which leaves the hydrophobic core free to coalesce into its  $\beta$ -sheet structures. These findings provide unprecedented molecular views of CCT-dependent folding of  $G\beta_5$  that prepares it to interact with RGS proteins and perform their essential functions in G protein signaling.

# Treatment of Osteoarthritis via Stem Cell Therapy

Gabrielle Thomas<sup>1</sup>

<sup>1</sup>Univ of Texas at Tyler

**Abstract ID 26754**

**Poster Board 280**

Osteoarthritis (OA) is a degenerative bone disease which is occur in inflammation condition of the joint cartilage. Approximately 58 million adults in the world are affected with this disease which is characterized by pain, stiffness, and a decrease in bone density. The current medication for the treatment of OA is non-steroidal anti-inflammatory drugs (NSAID), opioids, and cyclooxygenase (COX)-2-specific drugs which reduce the pain but not improving the cartilage disorder. The first approach to treatment of OA drugs have gastrointestinal problem, cardiovascular effects, and addiction ability. To overcome the limitations of knee OA drug treatment, stem-cell-based therapy is being utilized to recover the knee from the pain and regenerate the cartilage from its recent damaged state. The objective of this study is to effectively manage osteoarthritis by Human Mesenchymal Stem Cell (hMSC) delivery to bone cartilage. In our study, OA in rat knee was produced by intra-articular papain enzyme injections and was observed by pain behavior assay. Latencies in rats treated by papain enzyme was significantly decreased compared to saline. We observed that female rats was produced more arthritis by papain enzyme than male rat. The results of the hot plate test showed that paw-withdrawal threshold was significantly decreased following stem cell administration. We found 52% response by von Frey test in enzyme treated with stem cell delivery osteoarthritis rat whereas above 80% response was observed in only enzyme treated rat. In this study, we observed that stem cell delivery contributes the improvement of cartilage degradation of rat knee. Our research demonstrates that stem cell therapy could be a promising treatment in terms of combating tissue regeneration of rat knees to improve the pain state in the target area.

**Support/Funding Information:** Pilot Research and Scholarship Grant Program from Fish College of Pharmacy



# Structure–Activity Relationships of a Brain-Penetrant D3 Dopamine Receptor Negative Allosteric Modulator and Investigation of its Binding Site

Amy E. Moritz,<sup>1</sup> Nora S. Madaras,<sup>1</sup> Laura R. Inbody,<sup>1</sup> Amber M. Kelley,<sup>2</sup> Disha M. Gandhi,<sup>2</sup> Emmanuel O. Akano,<sup>1</sup> Kuo H. Lee,<sup>3</sup> R. Benjamin Free,<sup>1</sup> Xin Hu,<sup>4</sup> Noel T. Southall,<sup>4</sup> Marc Ferrer,<sup>4</sup> Lei Shi,<sup>3</sup> Kevin J. Frankowski,<sup>2</sup> and David R. Sibley<sup>1</sup>

<sup>1</sup>NINDS/NIH; <sup>2</sup>UNC Eshelman School of Pharmacy; <sup>3</sup>NIDA/NIH; and <sup>4</sup>NCATS/NIH

Abstract ID 15773

Poster Board 281

Dopamine receptors (DARs) are G-protein coupled receptors (GPCRs) that regulate diverse physiological functions including cognition, mood, movement, and reward-related behaviors, and are involved in the treatment or etiology of many neuropsychiatric disorders including schizophrenia and substance use disorder (SUD). DARs are classified as either D1-like (D1R and D5R) or D2-like (D2R, D3R, and D4R) based on structural homology and pharmacological profiles. Antagonists of D2-like DARs are currently used in the therapies for many neuropsychiatric disorders, but D3R-selective antagonists may be better therapeutics for schizophrenia or SUD as they could attenuate psychotic or drug craving symptoms without the motor side effects frequently produced by D2R-preferring antagonists due to limited distribution of the D3R in the brain. However, discovery of D3R-selective compounds is challenging due to high sequence homology of the D2R and D3R within their orthosteric binding sites, leading to the potential for off-target side effects produced by currently available compounds due to simultaneous antagonism of both subtypes or other closely related receptors. Our lab has endeavored to overcome the selectivity challenges posed by orthosteric antagonists by utilizing a D3R-mediated  $\beta$ -arrestin recruitment assay to screen the NIH Molecular Libraries Program 400,000+ small molecule library for compounds that inhibit the D3R via binding to less conserved allosteric sites. The most potent hit compound, MLS6357, was selective for the D3R versus the D2R and D4R in several functional outputs including  $\beta$ -arrestin recruitment and G-protein activation. Radioligand binding and functional assays using closely related GPCRs revealed that MLS6357 has very limited cross-reactivity with other GPCRs. Additionally, Schild-type functional assays showed that MLS6357 acts as a purely non-competitive negative allosteric modulator (NAM) of the D3R. We synthesized and characterized > 70 analogs of MLS6357 using iterative medicinal chemistry approaches which produced analogs that are 100-fold and 60-fold more potent than the parent compound in D3R-mediated  $\beta$ -arrestin recruitment and G-protein activation assays, respectively, and revealed structure–activity relationships for further optimization of the scaffold. Moreover, some analogs appear to display functional selectivity for inhibition of G-protein activation versus inhibition of  $\beta$ -arrestin recruitment, and vice versa, and some also display inverse agonist activity in G-protein signaling assays. Using *in vivo* pharmacokinetic experiments in mice via *i.p.* administration, one of the lead analogs was found to be brain penetrant and achieved sufficient concentrations to occupy the D3R *in vivo*. To identify the allosteric binding site for the MLS6357 scaffold on the D3R, we utilized various D3R/D2R chimeras, receptor mutants, and molecular modeling techniques to reveal and characterize receptor regions necessary for compound efficacy. Further refinement of the binding pocket for MLS6357 will inform future medicinal chemistry efforts. Ultimately, this novel scaffold may be of benefit as a pharmacological probe or therapeutic lead for D3R-related pathophysiology.

# Filming the DNA Damaging Mechanisms of AuNP by the Four Dimensions Atomic Force Microscopy (4DAFM) in Molecular Environment

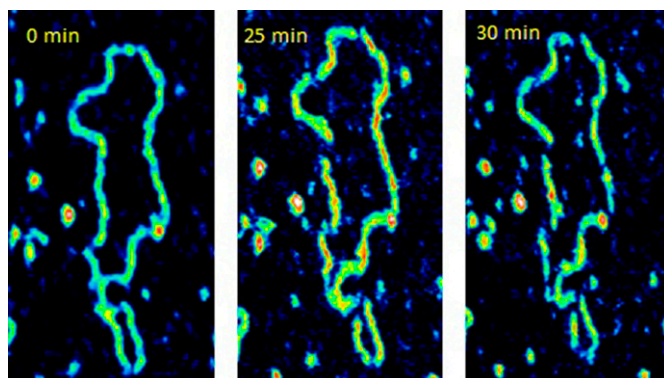
Hosam G. Abdelhady,<sup>1</sup> Fadilah Aleanizy,<sup>2</sup> and Arun Iyer<sup>3</sup>

<sup>1</sup>College of Osteopathic Medicine Sam Houston Univ; <sup>2</sup>King Saud University; and <sup>3</sup>Wayne State University

Abstract ID 25450

Poster Board 282

The unique physiochemical properties and tunable surface reactivity of gold nanoparticles made them promising materials in bionanomedicine. Although they are not themselves serious toxicants, however, they produce either direct or indirect nucleic acid (DNA and RNA) damages. Yet, the actual mechanism(s) are not fully understood. Investigating their real time damaging mechanism(s) on a single nucleic acid molecule (DNA in this study), in native environment, is essential to understand their genotoxicity. Hence, we applied the four dimensions Atomic Force Microscopy, as an imaging and nano-characterization tool, to explore their actual pathway(s) of DNA damaging, in vitro, in the absence of Particle-Induced Reactive Oxygen Species (ROS). To further examine whether the size and chemical conjugation of these AuNPs are properties that control their toxicity, we exposed the individual DNA molecules to small (~10 nm diameter) naked AuNPs, large (~22 nm diameter) naked AuNPs and large conjugated (~39 nm diameter) AuNPs. Our results provided real time molecular dynamic evidences that all AuNPs can cause fast (in minutes), direct, time-dependent DNA damages in vitro, in the absence of ROS and may help in designing efficient nanomedicines for viral treatment, cancer therapy and bio-diagnosis.



Time lapse images of the effect of AuNPs on an individual DNA plasmid in 1mM PBS, Images = 560 nm x 340 nm.

# Transcriptional Analysis of RGS10 Function in Microglia

Shwetal Talele,<sup>1</sup> Stephanie Gonzalez,<sup>1</sup> Violeta Saldarriaga,<sup>1</sup> Shelley Hooks,<sup>2</sup> and Benita Sjogren<sup>1</sup>

<sup>1</sup>Purdue Univ; and <sup>2</sup>Univ of Georgia

Abstract ID 19421

Poster Board 283

Chronic neuroinflammation characterizes Parkinson's disease, Alzheimer's disease and aging. Neuroinflammation is driven by microglia, which are CNS resident immune cells. In a healthy brain, microglia exist in a "resting" state where they regulate homeostasis. Upon an inflammatory stimulus, they polarize into the pro-inflammatory 'M1 active' state where they are highly cytotoxic, secrete cytokines, and permeabilize the blood brain barrier. In aging, microglia are primed towards this pro-inflammatory state which causes the build-up of cytotoxic factors resulting in neurodegeneration. Regulator of G protein signaling 10 (RGS10) has emerged as a prominent negative regulator of neuroinflammation. It is highly expressed in the resting state, and its levels are suppressed during neuroinflammation. RGS10 inhibits gene expression of pro-inflammatory factors in microglia, and protects neurons from degradation. However, the mechanisms that drive RGS10 suppression, regulation, and neuroprotection are unknown. To address this, we studied the transcriptomic landscape of microglia using RNA-Sequencing (RNA-Seq). We used the murine microglial cell line (BV-2; WT) and used CRISPR to generate RGS10 knockout BV-2 cells (RGS10 KO). To study the effect of RGS10 under conditions of microglial activation, we treated cells with vehicle and an endogenous inflammatory stimulus, Interferon- $\gamma$  (IFN $\gamma$ ). Thus, we had 4 conditions – BV-2 +/- IFN $\gamma$  and RGS10 KO +/- IFN $\gamma$ , with 5 replicates for each condition. 1580 genes were differentially regulated in the RGS10 KO cells when compared to the BV-2 WT cells under untreated conditions. Bioinformatic analyses revealed that genes involved in chemotaxis, immune cell migration and locomotion were the most prominent changes between the WT and RGS10 KO cells. Other changed processes between genotypes included synapse organization, hydrolase activity and trans-synaptic signaling. 3924 genes were differentially regulated in response to IFN $\gamma$  in BV-2 WT cells. Unsurprisingly, the processes associated with these genes were a part of immune and defense responses. In RGS10 KO cells, we found 4150 genes to be differentially regulated in response to IFN $\gamma$ . In addition to immune processes, as expected, cell division related processes like DNA repair and mitotic sister chromatid segregation were also significantly enriched. Canonically, RGS10 functions as a GTPase accelerating protein that inhibits G $\alpha$ i-mediated signaling; however, non-canonical RGS10 functions have been suggested as well. Our RNA-Seq data suggest that RGS10 might be playing a prominent role in regulating processes such as chemotaxis and cell division, in addition to inflammatory responses to IFN $\gamma$  stimuli. Studies validating the role of RGS10 in regulating these processes are currently underway.

# Curcumin ameliorates experimental colitis by suppressing PERK-UPR-signaling pathway

Islam I. Khan,<sup>1</sup> Zahraa Baydoun,<sup>2</sup> and Muddanna Rao<sup>2</sup>

<sup>1</sup>Kuwait University, Faculty of Medicine, Department of Biochemistry, Kuwait; and <sup>2</sup>Kuwait University, Faculty of Medicine, Kuwait

Abstract ID 16310

Poster Board 284

In this study, we investigated the underlying mechanism of the effects of curcumin on the PERK-UPR signaling pathway in experimental colitis induced in Sprague-Dawley male rats by intrarectal instillation of trinitrobenzene sulphonic acid (TNBS). Animals were treated with curcumin and 5-amino salicylate (5-ASA) daily starting 2hr prior to induction of colitis and sacrificed 2hr after the treatment on day 7 post-TNBS. Colitis was associated with an induction of the colonic expression of Grp78, ATF4, eIF2 $\alpha$  and eIF2 $\alpha$ -P PERK-pathway proteins. These changes were reversed by curcumin and 5-ASA treatments. Immunoprecipitation using anti-Grp-78 antibodies demonstrated depletion of Grp78-bound-PERK in inflamed colon suggesting activation of PERK signaling pathway. TNBS-induction of eIF2 $\alpha$ -P in inflamed colon was also supported by immunofluorescence confocal microscopy findings. However, expression of the eIF2 $\alpha$  mRNA and protein, and the yield and quality of total RNA remained unchanged in the test conditions. Therefore, the flow of eIF2 $\alpha$  into eIF2 $\alpha$ -P is independent of an enhanced transcription or translation of eIF2 $\alpha$  and is likely due to stabilization of eIF2 $\alpha$  protein in the present condition. In view of higher levels of the translational inhibitor eIF2 $\alpha$ -P, induction of PERK, Grp78 and ATF4 seems to be independent of the expression of eIF2 $\alpha$  in this case. In conclusion, we demonstrate induction of the ER-stress and its reversal by curcumin through inhibiting the PERK-signaling pathway in the present model of colitis. These findings add new insights into the disease pathogenesis and suggest that curcumin may serve as an adjunct treatment for IBD.

**Acknowledgments:** The Kuwait University Research sector for financial assistance through a grant (YM03/19) and the College of Graduate Studies. The Research Core Facility, HSC, Kuwait University.

# Calcium-dependent regulation of G protein-coupled receptor kinases

Konstantin Komolov,<sup>1</sup> Daniela K. Laurinavichyute,<sup>1</sup> Anshul Bhardwaj,<sup>1</sup> and Jeffrey L. Benovic<sup>2</sup>

<sup>1</sup>Thomas Jefferson University; and <sup>2</sup>Thomas Jefferson Univ

**Abstract ID 24257**

**Poster Board 285**

Changes in intracellular calcium regulate a variety of cellular processes including G protein-coupled receptor (GPCR) desensitization mediated by GPCR kinases (GRKs). At elevated calcium, Ca<sup>2+</sup>-binding proteins like calmodulin (CaM) and recoverin (Rec) target GRKs to terminate GRK-mediated phosphorylation of GPCRs at the plasma membrane and facilitate restoration of basal conditions in the cell. Recently, we demonstrated that calcium regulation of GRKs is more complex than merely inhibition of GPCR phosphorylation. For example, GRK5 can translocate to the cytoplasm and phosphorylate additional substrates in response to Ca<sup>2+</sup>/calmodulin binding. Strong activation of GRK5 through CaM-assisted ordering of the amphipathic  $\alpha$ N-helix of GRK5 and allosteric disruption of kinase-RH domain interaction promotes GRK5-mediated phosphorylation of cytoplasmic substrates. Here, we addressed whether other members of the GRK family can be regulated in a similar manner. Despite Rec and CaM binding to the  $\alpha$ N-helix of GRK1 and GRK6, respectively, this doesn't induce strong enzyme activation as was observed in GRK5. Both complexes also lack additional high-affinity C-terminal binding sites leading to relatively low affinity of the interaction. We found that the C-terminal binding site is critical for stable association of CaM with GRK5 and its truncation promotes dissociation of the complex. Moreover, the specific geometry of the C-terminus in GRK5 is supported by a C-terminal kink enabling close proximity of N- and C-terminal sites for bipartite interface within CaM-GRK5 complex, thereby contributing to high-affinity binding and strong activation of GRK5. We also found that CaM coupling to GRK5 is independent of its conformation since CaM binding is equally strong when GRK5 is locked in an inactive conformation or preactivated by disruption of an electrostatic contact between the RH and catalytic domains. Together, our data support evolution of calcium regulation across the GRK family from simple modulation of GPCR phosphorylation at the plasma membrane (GRK1 and GRK6) to broad effects on GRK localization, activity and substrate specificity (GRK5).

# Effect of Ecdysterone on Dry Eye Syndrome In Vitro and In Vivo

Bongkyun Park<sup>1</sup>

<sup>1</sup>Korea Institute of Oriental Medicine

**Abstract ID 53436**

**Poster Board 286**

Dry eye syndrome (DES) is caused by a lack of tear of severe evaporation of tear, also induced by various imaging devices such as mobile phone and computers. Ecdysterone (20-Hydroxyecdysone) is a naturally ecdysteroid hormone that have insect metamorphosis, antioxidant activity and anti-inflammation. Recently, in addition, ecdysterone has received the focus of attention for the role in disease prevention and health promotion. However, the exact mechanism for treatment of DES by ecdysterone is still unexploited. In the present study, we investigated whether ecdysterone has the protective effect against DES in hyperosmolar stress-stimulated human conjunctival cells and the extra-orbital lacrimal gland excised rats. In vitro, hyperosmotic media have significantly increased oxidative stress. However, antioxidant enzyme, superoxide dismutase (SOD), and antioxidant proteins, heme oxygenase-1 (HO-1), catalase (CAT), and Nuclear factor-erythroid factor 2-related factor 2 (NRF2) was considerably recovered by treatment of ecdysterone at 50 and 100  $\mu$ M. Additionally, inflammatory genes, interleukin-1beta (IL-1 $\beta$ ), tumor necrosis factor-alpha (TNF- $\alpha$ ), IL-33 and Matrix metalloproteinase 9 (MMP9), and apoptotic protein, Bcl-2-associated X protein (BAX) and activated caspase 3 were significantly inhibited by treatment of ecdysterone. In vivo, eye drops of formulated ecdysterone (FES) (0.01 %, and 0.05%) to the extra-orbital lacrimal gland excised rats were remarkably restored on tear volume. Moreover, damaged corneal condition by lacrimal gland excision was significantly attenuated by FES at 0.01 % and 0.05%. In conjunctival tissue, reduced goblet cells by DES was highly increased by eye drops of FES through inhibition on mRNA expression of inflammatory genes, IL-1 $\beta$ , TNF- $\alpha$ , interferon-gamma (IFN- $\gamma$ ) and IL-6. Taken together, these results demonstrated that ecdysterone prevents dry eye syndrome in human conjunctival cells and the extra-orbital lacrimal gland excised rats. Our study also proposes the insight to the mechanisms of ecdysterone underlying the regulation of oxidation, inflammation and apoptosis.

# Development of Transgenic Mouse Platform for the Detection of Endogenous G protein Activity

Remi Janicot,<sup>1</sup> Marcin Maziarz,<sup>1</sup> Jong-Chan Park,<sup>1</sup> and Mikel Garcia-Marcos<sup>1</sup>

<sup>1</sup>Boston University

Abstract ID 13744

Poster Board 287

G protein-coupled receptors (GPCRs) are the largest family of druggable targets in the human genome. They initiate a plethora of signaling pathways, including responses to most neurotransmitters and two-thirds of hormones, primarily by activating heterotrimeric G-proteins ( $G\alpha\beta\gamma$ ) inside the cell. Traditional approaches to measure GPCR activity rely on indirect reporters subject to amplification or cross-talk. Biosensors that directly measure G protein activity (i.e., formation of  $G\alpha$ -GTP or  $G\beta\gamma$  dissociation) are not limited by these factors, but often require overexpression of exogenous G protein, which can affect endogenous signaling, and are not suitable for implementation in physiologically relevant models. We set out to overcome all these limitations by generating transgenic mouse lines for the conditional expression of biosensors that can detect the activity of endogenous G proteins in any primary cell type compatible with *in vitro* culture. These sensors are named BERKY, for BRET biosensor with ER/K linker and YFP. We designed the mouse lines based on previously described BERKY biosensors for free  $G\beta\gamma$ ,  $G\alpha_q$ -GTP,  $G\alpha_{13}$ -GTP, or  $G\alpha_i$ -GTP, and now present progress on the development of a new BERKY biosensor for  $G\alpha_s$ -GTP, which would ensure coverage of the detection of activity of all G protein families. We currently have mouse lines for four biosensor breeding in our facilities, and have validated for some of them that endogenous G proteins activity can be detected upon conditional, Cre-dependent expression of the biosensor in primary cells. Moreover, our results also indicate that the expression of this biosensor does not interfere with endogenous G protein signaling. In summary, we are developing a platform of transgenic mice that will allow to measure the endogenous activity of any G protein subtype in physiologically relevant cell types without affecting native G protein signaling.

# Identification and pharmacological characterization of a novel $\beta$ -arrestin-biased negative allosteric modulator of the $\beta$

Francesco F. De Pascali,<sup>1</sup> Michael Ippolito,<sup>1</sup> Nathan Hopfinger,<sup>1</sup> Konstantin E. Komolov,<sup>1</sup> Daniela K. Laurinavichyute,<sup>1</sup> Leon A. Sakkal,<sup>1</sup> Ajay P. Nayak,<sup>1</sup> Poli AN. Reddy,<sup>2</sup> Preston S. Donover,<sup>3</sup> Melvin Reichman,<sup>3</sup> Joseph M. Salvino,<sup>2</sup> Raymond B. Penn,<sup>1</sup> Roger S. Armen,<sup>1</sup> Charles P. Scott,<sup>1</sup> and Jeffrey L. Benovic<sup>4</sup>

<sup>1</sup>Thomas Jefferson University; <sup>2</sup>The Wistar Institute; <sup>3</sup>Lankenau Institute for Medical Research; and <sup>4</sup>Thomas Jefferson Univ

**Abstract ID 14763**

**Poster Board 289**

The  $\beta$ 2-adrenergic receptor ( $\beta$ 2AR) is implicated in numerous physiological functions. It is activated by endogenous catecholamines and primarily signals via the canonical Gs-adenylyl cyclase-cAMP-PKA pathway. In parallel, G protein-coupled receptor kinases (GRKs) and  $\beta$ -arrestins regulate  $\beta$ 2AR signaling by promoting  $\beta$ 2AR desensitization and internalization, as well as downstream signaling often antithetical to the canonical pathway. Exogenous  $\beta$ -agonists, by targeting the  $\beta$ 2AR, are the primary therapeutic medications in the treatment of asthma. This class of drugs has shown good efficiency in relieving bronchoconstriction, but patients can also experience severe side effects, ultimately worsening asthmatic attacks. Several studies have correlated the bronchodilation effects of  $\beta$ -agonists with activation of Gs signaling, while side effects were associated with  $\beta$ -arrestin functions. Recently, we reported that Gs-biased agonists for the  $\beta$ 2AR may provide a strategy to improve the functional consequences of  $\beta$ 2AR activation in treating airway diseases. However, since these agonists were not subtype-selective, we also focused on identifying allosteric modulators for the  $\beta$ 2AR, since such molecules are often subtype-selective and can bias signaling. To this end, we screened small molecule libraries for allosteric modulators that selectively inhibit  $\beta$ -arrestin recruitment to the  $\beta$ 2AR. This screen identified several compounds with the required profile, and of these, DFPQ was found to be a selective negative allosteric modulator of  $\beta$ -arrestin recruitment to the  $\beta$ 2AR while having no effect on  $\beta$ 2AR coupling to Gs. DFPQ effectively inhibited GRK-mediated phosphorylation as well as agonist-promoted internalization of the  $\beta$ 2AR and protected against the functional desensitization of  $\beta$ -agonist-mediated regulation in cell and tissue models. The effects of DFPQ were also specific to the  $\beta$ 2AR showing minimal effects with other GPCRs, including the structurally related  $\beta$ 1AR. Molecular modeling, mutagenesis, and medicinal chemistry studies support DFPQ and DFPQ derivatives binding to an intracellular region of the  $\beta$ 2AR, including residues within transmembrane domains 3 and 4 and intracellular loop 2. Thus, DFPQ represents a novel class of biased allosteric modulators that targets an intracellular allosteric site of the  $\beta$ 2AR. The pharmacological characteristics of DFPQ can pave the way for the design of safer drugs for treating asthma and may elucidate the mechanisms behind receptor-biased signaling.



# Location-Biased Activation of the Proton-Sensor GPR65 is Uncoupled from Receptor Trafficking

Loyda M. Marie Morales-Rodriguez,<sup>1</sup> and Manoj A. Puthenveedu<sup>1</sup>

<sup>1</sup>Univ of Michigan Ann Arbor

**Abstract ID 17708**

**Poster Board 290**

The canonical view of G protein-coupled receptors (GPCR) function is that receptor trafficking is tightly coupled to signaling. GPCRs remain on the cell surface until they are activated, after which they are desensitized and internalized into endosomal compartments. This canonical view presents an interesting context for proton-sensing GPCRs because they are more likely to be activated in acidic endosomal compartments than at the cell surface. However, whether proton-sensing receptors are active in intracellular compartments, and whether trafficking is coupled to this signaling, are not known. Here we show that the trafficking of the prototypical proton-sensor GPR65 is fully uncoupled from signaling, unlike that of other known mammalian GPCRs. GPR65 internalizes and localizes to early and late endosomes, from where they signal at steady state, irrespective of extracellular pH. Acidic extracellular environments stimulate surface receptor signaling in a dose-dependent manner, although endosomal GPR65 is still required for a full cAMP response. Receptor mutants that were incapable of activating cAMP trafficked normally and were internalized and localized to endosomal compartments. Our results suggest a model where GPR65 is constitutively active in endosomes. Changes in extracellular pH reprogram the spatial pattern of receptor signaling and bias the location of signaling to the cell surface.

This material is based upon work supported by the Rackham Merit Fellowship (RMF) and the National Science Foundation Graduate Research Fellowship Program (NSF-GRFP) under Grant No. DGE 1256260. Any opinions, findings, and conclusions or recommendations expressed in this material are those of the author(s) and do not necessarily reflect the views of the National Science Foundation.

# Identifying Novel Regulators of Adrenergic Signaling from Endosomes

Ian Chronis,<sup>1</sup> and Manoj A. Puthenveedu<sup>1</sup>

<sup>1</sup>Univ of Michigan

**Abstract ID 53021**

**Poster Board 323**

Physiological responses to catecholamines in many organs, such as the heart, airways, and pancreas, rely on accurate signaling through the beta 2 adrenergic receptor (B2AR), a prototypical G protein-coupled receptor. It is becoming increasingly clear that a complete B2AR physiological response is integrated from many discrete receptor signaling events, separated in time, that originate from different subcellular locations in cells. The spatiotemporal fidelity of these discrete signaling events relies on two critical processes—those that localize receptors to specific compartments, and those that ensure that the receptors couple to the correct signaling components in these compartments. The biochemical networks that mediate these processes, however, are still not fully understood.

In this study, we focused on endosomal compartments to identify novel protein-protein interactions that ensure B2AR localization and signaling on endosomes. Using unbiased APEX proximity labeling to capture transient interactions of B2AR during endosomal localization, we identified 14-3-3 proteins—a physiologically relevant family of phosphopeptide binding proteins—as novel regulators of B2AR function. Multiple 14-3-3 protein isoforms preferentially associated with B2AR in a phosphorylation-dependent manner. 14-3-3 proteins acted as negative regulators of both global cAMP production and gene transcription downstream of B2AR activation in endosomes, without affecting ERK activation. Our results identify 14-3-3 proteins as important regulators of endosomal B2AR signaling, and suggest that B2AR interacts with discrete and regulated protein complexes at different subcellular sites to ensure spatiotemporal fidelity in signaling.

# Molecular regulation of G protein prenylation under sub-optimal conditions

Ajith Karunaratne,<sup>1</sup> Mithila Tennakoon,<sup>1</sup> Waruna Thotamune,<sup>1</sup> and John L. Payton<sup>2</sup>

<sup>1</sup>*Saint Louis University; and* <sup>2</sup>*Kenyon College*

**Abstract ID 55879**

**Poster Board 324**

Prenylation is an irreversible post-translational modification of proteins that are involved in many physiological and pathological processes. During prenylation, either a 15-C farnesyl or a 20-C geranylgeranyl isoprenyl lipid is covalently attached to the carboxy-terminal *Cysteine* residue in the CaaX motif that determines the type of prenylation. Isoprenyl Lipids are synthesized by the pathway that produces Cholesterol, the mevalonate (HMG-CoA reductase) pathway. Cholesterol-lowering medications (statins) target the rate-limiting HMG-CoA reductase enzyme. We previously showed that statins significantly disrupt the membrane localization and signaling of G protein  $\beta\gamma$  in a  $G\gamma$  subtype-dependent manner. Here we elucidate the molecular processes that regulate the efficacy of G protein  $\gamma$  prenylation using live-cell imaging, optogenetics, and pharmacological strategies. Our findings provide reasonings underlying differential prenylation sensitivities of G proteins likely to be found in pharmacologically- or genetically-induced hypolipidemic conditions.

Support/Funding Information: NIH-NIGMS: grant number R01GM140191

# Novel G $\alpha$ GTP Sensors to probe Subcellular signaling of Endogenous heterotrimeric G proteins

Dhanushan Wijayaratna,<sup>1</sup> and Ajith Karunarathne<sup>1</sup>

<sup>1</sup>Saint Louis University

Abstract ID 54893

Poster Board 325

GPCRs are the world's major drug target due to their involvement in nearly all body systems. GPCRs perceive highly spatially and temporally variable stimuli from the outer cell environment and activate G proteins. G protein heterotrimers are comprised of  $\alpha$ ,  $\beta$ , and  $\gamma$  subunits. Based on the type of G $\alpha$  subunit in the heterotrimer, G protein pathways are grouped into four families: G $\alpha_s$ , G $\alpha_q$ , G $\alpha_i$ , and G $\alpha_{12/13}$ . In the inactive GPCR form, G $\alpha$  is bound to GDP, and exchanges to GTP upon GPCR activation, which induces G $\beta\gamma$  dissociation from G $\alpha$ GTP. G $\alpha$ GTP and free G $\beta\gamma$  broadcasts the extracellular signals into the cell interior at the site of their origin as well as upon translocation to various subcellular organelles and interacting with a broad range of effectors to elicit cellular responses. Understanding the dynamics of endogenous G proteins upon subcellular GPCR activation and recapitulating *in-vivo* signaling environments can allow pathological signaling identification. Here, we show the engineering of G $\alpha$ -GTP sensors to probe endogenous G $\alpha_i$ GTP and G $\alpha_q$ GTP in cells. Compared to examination of overexpressed fluorescently-tagged G $\alpha$ , our sensors provide the extent and kinetics of endogenous G proteins with native fidelity. Here, our data with the G $\alpha_i$ -GTP sensor suggest that G protein heterotrimer dissociation (GPCR activation) and reformation (GPCR inactivation) is G $\gamma$ -subtype dependent. Further, our newly engineered sensors allow for the detection of endogenous G $\alpha$ -GTP generation with subcellular resolution. Collectively, the new G $\alpha_i$  and G $\alpha_q$  sensors shed light on the underexplored endogenous G protein signaling paradigms.

This work was funded by NIH through NIGMS grant R01 GM140191.

# Structure-activity relationship of G protein-coupled receptor kinase 5 (GRK5) and its mutants

Priyanka Naik,<sup>1</sup> Qiuyan Chen,<sup>2</sup> and John JG. Tesmer<sup>1</sup>

<sup>1</sup>Purdue University; and <sup>2</sup>Indiana University

**Abstract ID 14751**

**Poster Board 326**

G protein-coupled receptors (GPCRs) are the largest class of membrane receptors in eukaryotes. They regulate diverse functions like cardiac output, vision, and migration. GPCR kinases (GRKs) function as 'brakes' for GPCR signaling and thereby allow cells to adapt to changes in extracellular cues. Altered GRK activity is however implicated in cardiovascular diseases, diabetes, and cancer. In this study, we sought to define how GRK5 interacts with rhodopsin, a canonical model GPCR. After failing to capture the complex via chemical crosslinking, we introduced alterations into GRK5 to increase its affinity for rhodopsin such as swapping the N-terminus of GRK5 with that of GRK1, the native kinase for rhodopsin, and installing a K194R mutation to remove a crosslinking site that might compete for complex formation. We tested the mutants for kinase activity using a radiometric assay and for structural stability using a Thermofluor assay. We observed minimal changes in the kinase activity of these mutants, but deletion of the C-terminus decreased the structural stability of GRK5. We also studied the activity of GRK5 in the presence of c8-PIP<sub>2</sub>, a soluble version of the common phospholipid PIP<sub>2</sub> known to activate GRKs, and demonstrated inhibition. This inhibition is likely due to nonspecific binding of the compound to the catalytic domain of GRK5. Our findings confirmed that the mutants retain kinase activity and minimally altered structural stability, setting the stage for us to obtain a stable GRK5-rhodopsin complex for structural analysis.

# Enhanced cAMP-based assay for GPCR deorphanization

Luca Franchini,<sup>1</sup> Lindsay R. Watkins,<sup>2</sup> and Cesare Orlandi<sup>1</sup>

<sup>1</sup>University of Rochester; and <sup>2</sup>Marshfield Clinic Research Institute

Abstract ID 14850

Poster Board 327

G-protein coupled receptors (GPCRs) are the target of almost 30% of marketed drugs. However, only a small percentage of the whole GPCR repertoire is well characterized for both endogenous ligand and signaling pathways activated, with ~100 GPCRs still considered orphans (i.e. their endogenous ligand is unknown). Nonetheless, orphan GPCRs are increasingly recognized for their essential pathophysiological roles. As new pharmaceutical targets, this pool of uncharacterized GPCRs offers a lot of unrealized potential. Several methods have been exploited to discover new ligand-receptor pairs and characterize receptor-signaling coupling, for example luciferase reporter systems modulated by specific G $\alpha$  protein signaling,  $\beta$ -arrestin recruitment (PRESTO-Tango), TGF- $\alpha$  cleavage by ADAM17 in combination with G $\alpha_q$  protein chimeras (TGF- $\alpha$  shedding assay), and calcium mobilization assays with the promiscuous G $\alpha_{15}$ . However, in the last few years the number of deorphanized GPCRs has not grown as expected. According to the GPCRdb, nearly two-thirds of GPCRs are coupled to G $_{i/o/z}$  proteins, for which currently available assays display low sensitivity. To address this problem, we recently applied a set of genetic reporters in combination with G $\alpha$  protein chimeras to measure the constitutive activity of a library of orphan GPCRs expressed in a heterologous system. G $\alpha$  protein chimeras enabled to reroute the signaling of G $_{i/o/z}$ -coupled receptors to readily measurable readouts. This approach revealed G $_{i/o/z}$ -coupling for 8 out of 19 orphan GPCR tested. Later, we developed a highly sensitive assay to screen for ligands activating G $_{i/o/z}$ -coupled GPCRs by combining the use of G protein chimeras and real-time measurements of cAMP levels through the GloSensor<sup>TM</sup>. By measuring the activation of several ligand-activated G $_{i/o/z}$ -coupled receptors, we defined ideal assay conditions that take into account various system-influencing factors. Our data suggest that expression of the G $_s$ G $_z$  chimera in combination with pertussis toxin (PTX) and the phosphodiesterase inhibitor IBMX result in an extremely high sensitive assay. Finally, we further developed this cell-based assay to detect the activation of GPCRs coupled to any of the four G protein families. To this goal, we combined three G protein chimeras, G $_s$ G $_z$ , G $_s$ G $_q$  and G $_s$ G $_{13}$  (G $_s$  is endogenously expressed), in the same system and tested the activation of a subset of G $_s$ , G $_q/11$ , G $_{i/o/z}$  and G $_{12/13}$  coupled receptors. Using an innovative approach to cell transfection, we are now generating stable cell lines expressing stoichiometric ratios of each component of our enhanced cell-based assay. This universal assay is blind to the G protein-coupling profile of the examined receptor and, therefore, it will be extremely useful in high-throughput identification of endogenous and synthetic compounds activating orphan GPCRs.

The Foundation Blanceflor supported Luca Franchini in his research.

# Identification of a sequence of the activity-dependent neuroprotective protein (ADNP) that is necessary for its interaction with G<sub>i1</sub>

Nathalie Momplaisir,<sup>1</sup> Naincy R. Chandan,<sup>2</sup> and Alan V. Smrcka<sup>2</sup>

<sup>1</sup>Univ of Michigan; and <sup>2</sup>University of Michigan

Abstract ID 16245

Poster Board 328

The activity-dependent neuroprotective protein (ADNP) is crucial for the proper development and maturation of the brain. A number of reports have shown its interaction with members of the SWI/SNF complex as well as microtubule interaction partners to mediate neuroprotective functions. Recently, using an unbiased proximity-dependent labeling method coupled to mass spectrometry and immunoblotting in our laboratory, we identified ADNP as an interactor of the active subunit of the G<sub>i</sub> subfamily of G proteins. This interaction has not previously been shown in the literature.

G proteins are important transducers of signaling downstream of relevant therapeutic targets, which are G protein-coupled receptors (GPCRs). Considering the relevance of G proteins and the neuroprotective function of ADNP, the biochemical and functional characterization of its interaction with G<sub>i1</sub> is needed.

To continue characterizing this interaction, we used a nanoluciferase-based complementation assay where we fused a small fragment of nanoluc - small BiT (SmBiT) and natural peptide (NP), to the N and C termini of ADNP and assessed their interactions with G<sub>i1</sub> fused to the large fragment of nanoLuc, LgBiT. Results show a nucleotide-dependent interaction of ADNP with G<sub>i1</sub>. This nucleotide-dependent interaction was not observed with G<sub>s</sub>, or G<sub>q</sub>. We also investigated the localization of both proteins and observed a prominent nuclear localization of ADNP. In the presence of inactive and active G<sub>i1</sub>, a subset of cells showed partial membrane localization despite its prominent nuclear localization.

Further characterization of this interaction was directed at the identification of the region of ADNP important for its interaction with active G<sub>i1</sub>. We created truncation mutants of ADNP followed by the nanoluciferase-based complementation assay. We observed loss of the GTP-dependent interaction of ADNP with G<sub>i1</sub> upon truncating ADNP at residue C687 but not 733. We also found the deletion of amino acids 687-733 to abolish this interaction; this suggests that this region is necessary for the nucleotide-dependent interaction between ADNP and G<sub>i1</sub>. Ongoing work is focused on the biological relevance of this interaction, more specifically on microtubule regulation and G<sub>i</sub>-dependent regulation of genes via ADNP in PC12 cells.

Support/Funding Information:

The National Science Foundation Graduate Research Fellowship (NSF-GRFP)

T32 Pharmacological Sciences Training Program (PSTP)

The Rackham Merit Fellowship (RMF)

# Insights into Affinity Improvement of an Engineered Tissue Inhibitor of Metalloproteinases from Molecular Dynamics Simulations

Matt Coban,<sup>1</sup> Thomas R. Caulfield,<sup>1</sup> and Evette S. Radisky<sup>1</sup>

<sup>1</sup>Mayo Clinic

Abstract ID 18265

Poster Board 329

Matrix MetalloProteinases (MMPs) are a family of 23 multidomain zinc-dependent endopeptidases that primarily target extracellular matrix proteins for degradation. An array of physiological functions rely on MMP activity; dysfunction results in diseases/disorders, including cancers, cardiovascular and pulmonary disease, and arthritis. Despite considerable long-term efforts towards MMP-targeted pharmacology, most potential therapeutics fail in clinical trials due to off-target toxicity against MMPs and other zinc-dependent endopeptidases. Our group has been applying protein engineering efforts towards endogenous Tissue Inhibitors of MetalloProteinases (TIMPs) to create high-affinity and selective inhibitors for disease-associated MMPs. We previously utilized semi-random mutagenesis and yeast surface display to identify an ultrabinder variant of TIMP1 with enhanced affinity towards MMP3, a target in cancer and lung fibrotic diseases, and solved a co-crystal structure of MMP3 bound to this engineered ultrabinder TIMP variant. Here, we employ modeling and molecular dynamics simulations on unbound and MMP3-bound TIMP1 and the ultrabinder variant to investigate the biophysical etiology of MMP-TIMP molecular recognition and of mutation-induced affinity improvements. Our simulations reveal localized induced fit at the zinc-chelating portion of TIMP upon binding MMP, whereas other binding interface regions seem to rely more on innate shape complementarity and conformational selection. Inter-residue motion covariance matrices reveal that MMP binding also reorganizes motion coupling throughout TIMP globally; this suggests that allosteric regulation of the binding interface differs between the unbound and MMP-bound states. Comparisons of molecular dynamics trajectories were made between WT TIMP1 and the ultrabinder TIMP1 variant. Time-resolved analyses of ultrabinder TIMP1 shows that it possesses stable secondary structural alterations that increase TIMP interdomain interactions, as well as protein-protein interactions with MMP3. Dynamical network analyses show that the engineered TIMP1 is able to propagate internal motions with greater efficiency, which appears to suppress motions perturbing TIMP from MMP-congruent configurations. In both the unbound and the MMP-bound states, variant TIMP1 has reduced conformational variability compared to WT TIMP1, with greater representation of conformations resembling that of the bound crystal structure, and more favorable predicted binding energy to MMP3. Overall, our results show that the engineered ultrabinder TIMP1 variant possesses altered protein dynamics that promote MMP3 compatibility in multiple ways, both via preconfiguration of unbound TIMP and via maintenance of the MMP/TIMP complex. These data suggest strategies that utilize intrinsic protein dynamics to improve affinity and selectivity of TIMPs in future engineering efforts towards biopharmaceutical development.

This research is supported by NIH R01 GM132100



# Spatial Compartmentalization of mTORC1 to the Nucleus to Regulate Transcription and Impact Nuclear Erk Signaling

Ayşe Sahan,<sup>1</sup> Yanghao Zhong,<sup>1</sup> Consuelo Saucedo,<sup>1</sup> David J. Gonzalez,<sup>1</sup> and Jin Zhang<sup>1</sup>

<sup>1</sup>Univ of California, San Diego

Abstract ID 16953

Poster Board 330

Mechanistic target of Rapamycin (mTOR) complex 1 (mTORC1) integrates inputs from multiple pathways and senses diverse signals to regulate cell growth, protein translation, and proliferation. Given that signal compartmentalization can enhance signaling specificity and efficiency, spatial regulation of mTORC1 appears to be critical for this multifaceted signaling complex as it has been reported at many subcellular locations. For example, mTORC1 at the lysosome is regulated by both amino acids and growth factors and functions to promote translation and suppress autophagy. We have also previously reported a nuclear pool of mTORC1 that is regulated by nuclear Akt, by a regulatory mode distinct from the lysosomal pool of mTORC1. However, the functions of subcellular pools of mTORC1, in particular in the nucleus, are not well understood. A major limitation in the field is the availability of tools to assess the activity and function of spatially compartmentalized signaling enzymes in living cells. We have developed a genetically encodable inhibitor of mTORC1, TerminATOR, that can be spatially compartmentalized to specifically inhibit a subcellular pool of mTORC1. Using TerminATOR, we conducted a phosphoproteomics study to elucidate the role of nuclear mTORC1 in regulating transcriptional proteins. Several transcription-related proteins were differentially expressed or phosphorylated upon nuclear mTORC1 inhibition. Furthermore, the phosphoproteomics data revealed interesting crosstalk between nuclear mTORC1 and Erk activity, which we investigated more in depth by imaging and biochemical assays. Based on our findings, we hypothesize that there is a mechanism of spatially regulated crosstalk between nuclear Erk and nuclear mTORC1 that may play a role in transcription.

# Glial Cell Development is Changed by Genetic Overexpression of MeCP2 in a Pitt-Hopkins Syndrome Mouse Model

Geanne A. Freitas,<sup>1</sup> Sheryl Anne D. Vermudez,<sup>1</sup> Vaishnavi M. Bavadekar,<sup>1</sup> Rocco Gogliotti,<sup>2</sup> and Colleen M. Niswender<sup>3</sup>

<sup>1</sup>Vanderbilt University; <sup>2</sup>Loyola Univ Chicago; and <sup>3</sup>Vanderbilt Univ

Abstract ID 23944

Poster Board 331

**Introduction:** Pitt-Hopkins syndrome (PTHS) is a neurodevelopmental disorder caused by monoallelic mutations or deletions in the *Transcription Factor 4 (TCF4)* gene. PTHS symptoms include developmental delay, intellectual disability, lack of speech, and motor incoordination. Due to the established role for TCF4 in regulating the maturation of oligodendrocyte progenitors and a subpopulation of astrocytes (Phan et al., 2020; Wang et al., 2021), Kim et al. (2022) attempted to normalize Tcf4 specifically expression in oligodendrocytes; however, aberrant behavioral phenotypes were not reversed. A known phenotypic overlap between PTHS and Rett syndrome (RTT) indicates that there are possible common signaling pathways between the two neurodevelopmental disorders. We have found that increasing expression of Methyl-CpG-Binding Protein 2 (MeCP2), the causative protein in most cases of RTT, decreases hyperactivity and corrects impairments in learning and memory in a mouse model of PTHS (*Tcf4*<sup>+/-</sup>). Recent studies in our lab using *Tcf4*<sup>+/-</sup> mice have also indicated that levels of astrocytes, oligodendrocytes and microglia are changed after MeCP2 upregulation.

**Aim:** The current study sought to understand if the effects of MeCP2 overexpression on behavioral phenotypes in the *Tcf4*<sup>+/-</sup> model were due to a change in the functioning of glial cells.

**Methods/Results:** We generated four animal genotypes (WT, *MECP2*<sup>Tg1/o</sup>, *Tcf4*<sup>+/-</sup>, *MECP2*<sup>Tg1/o</sup>; *Tcf4*<sup>+/-</sup>) and performed quantitative RT-PCR from the cortex, hippocampus and striatum followed by immunohistochemistry studies using specific markers for astrocytes (Glial Fibrillary Acidic Protein; GFAP), oligodendrocytes (Oligodendrocyte Transcription Factor 2; OLIG2) and microglia (Ionized Calcium-Binding Adapter Molecule 1; IBA1) to analyze morphology and expression of these cells in our experimental groups. Both techniques revealed that some glial-associated targets are differentially expressed in *MECP2*<sup>Tg1/o</sup>; *Tcf4*<sup>+/-</sup> mice, most evidently in the cortical regions. We are currently isolating these cells in a primary culture to analyze potential functional changes after MeCP2 upregulation.

**Conclusions:** Our results support that behavioral phenotypic rescue in *MECP2*<sup>Tg1/o</sup>; *Tcf4*<sup>+/-</sup> mice may result from differential glial cell development mediated by MeCP2 overexpression.

**Funding:** The Pitt Hopkins Foundation and the International Rett Syndrome Foundation

# Pharmacological Modulation of Hsp70 to Selectively Remove Misfolded Neuronal Nitric Oxide Synthase

Anthony Garcia,<sup>1</sup> Emily Xu,<sup>2</sup> Miranda Lau,<sup>3</sup> Andrew Alt,<sup>3</sup> Andrew Lieberman,<sup>3</sup> and Yoichi Osawa<sup>3</sup>

<sup>1</sup>Univ of Michigan; <sup>2</sup>Univ of Michigan Medical School; and <sup>3</sup>University of Michigan Medical School

**Abstract ID 23589**

**Poster Board 332**

The accumulation of misfolded proteins can result in various diseases, including several neurodegenerative disorders. Critical proteins that are associated with the onset of some of these disorders are client proteins of the heat shock protein (Hsp) 90 and Hsp70 chaperone system that selectively regulates their stability and degradation. Previously, we've determined the opposing roles Hsp90 and Hsp70 have on client protein stability using neuronal nitric oxide synthase (nNOS), a well-established client protein. Hsp90 stabilizes misfolded client proteins and prevents their ubiquitination, whereas Hsp70 enhances their ubiquitination and degradation. Thus, the Hsp90/70 chaperone system is a promising target for the development of treatments for these disorders. Over 20 inhibitors of Hsp90 have been developed but all clinical trials to date have failed, in large part, due to toxicity issues. In that Hsp90 inhibition may target functional client proteins in near native states, we hypothesize that targeting Hsp70 may be more selective for misfolded proteins. In the current study, we have developed a cellular model stably expressing native nNOS or C331A mutant of nNOS, which represents a slightly misfolded but functionally active nNOS, to better test this hypothesis. We showed that Hsp70 modulators, such as YM-1 and JG-98, caused a time- and dose- dependent decrease in C331A mutant of nNOS while the native nNOS was not affected under the same conditions. The Hsp90 inhibitor, radicicol, was not as selective as loss of both C331A nNOS and wild type nNOS were observed. These results suggest that Hsp70 modulation selectively removes the misfolded client protein while sparing the natively folded or near native nNOS proteins. Future studies will focus on developing and characterizing other Hsp70 modulators to identify small molecules that may better enhance the ubiquitination and degradation of misfolded nNOS.

This was supported in whole or in part, by National Institutes of Health Grant GM077420 and the University of Michigan Medical School's Protein Folding Diseases Initiative. AMG is a trainee of the University of Michigan, Training Program in Translational Science (NIH T32-GM141840) and a Department of Pharmacology Lucchesi Fellow.

# Intracellular metabotropic glutamate receptor 5 (mGlu<sub>5</sub>) triggers ER calcium release distinct from cell surface counterparts in striatal neurons

Yuh-Jiin I. Jong,<sup>1</sup> Steven K. Harmon,<sup>1</sup> and Karen O'Malley<sup>1</sup>

<sup>1</sup>Washington University School of Medicine

Abstract ID 21099

Poster Board 333

Metabotropic glutamate receptor 5 (mGlu<sub>5</sub>) is widely expressed throughout the central nervous system and plays a fundamental role in synaptic plasticity. As such, mGlu<sub>5</sub> serves as a potential therapeutic target for various neurodevelopmental and psychiatric disorders including depression, anxiety, and autism. Recent work from our lab showed that mGlu<sub>5</sub> is one of a growing number of G protein coupled receptors (GPCRs) that can signal from intracellular membranes. Specifically, more than 90% of mGlu<sub>5</sub> is present on intracellular membranes where it can be activated by ligands that can be transported across cell membranes. Activated intracellular mGlu<sub>5</sub> leads to the upregulation of extracellular signal-regulated kinase (ERK1/2), ETS transcription factor Elk-1, and activity regulated cytoskeleton associated protein (Arc) in striatal neurons. Using cytoplasmic Ca<sup>2+</sup> indicators such as Oregon Green Bapta, previously we showed that the cell surface mGlu<sub>5</sub> agonist DHPG induced a transient Ca<sup>2+</sup> increase while the intracellular mGlu<sub>5</sub> agonist Quis mediated a sustained Ca<sup>2+</sup> elevation in striatal neurons. To determine the source of Ca<sup>2+</sup> release, here we transfected dissociated striatal neurons with a genetically encoded endoplasmic reticulum (ER)-targeted Ca<sup>2+</sup> indicator (ER-GCaMP6-150). Fluorescent changes in individual neurons were monitored in real time following application of either DHPG or Quis. As a control we used the membrane permeant Ca<sup>2+</sup> ionophore, ionomycin. One hundred seconds after ionomycin application 78% of somal ER Ca<sup>2+</sup> was reduced. In comparison to ionomycin, activation of cell surface mGlu<sub>5</sub> using DHPG led to ~18% decline in ER Ca<sup>2+</sup> whereas activation of intracellular mGlu<sub>5</sub> using Quis, resulted in a ~29% ER Ca<sup>2+</sup> decline. Quis resulted in a more rapid ER Ca<sup>2+</sup> release (T<sub>1/2</sub>=29sec) versus DHPG (T<sub>1/2</sub>= 43 sec). These results confirm and extend mGlu<sub>5</sub>-localized signaling differences which may facilitate the development of location-specific drugs.

This work was supported by National Institutes of Health Grants MH119197, NS102783, MH101874 and IDRC Grant P50 HD103525.

# Agonist concentration-dependent conformational changes of formyl peptide receptor 1 contribute to biased signaling in phagocytes

Richard Ye,<sup>1</sup> and Junlin Wang<sup>1</sup>

<sup>1</sup>The Chinese University of Hong Kong, Shenzhen

Abstract ID 19450

Poster Board 334

Phagocytes are innate immune cells that may be exposed to ligands such as inflammatory factors at sub-nanomolar to micromolar concentration range. Therefore, the G protein-coupled receptors on these cells such as formyl peptide receptor 1 (FPR1) must adapt to this concentration variation with desired physiological responses. The bacteria-derived formyl peptide fMet-Leu-Phe (fMLF) is a potent chemoattractant of phagocytes that induces chemotaxis at sub-nanomolar concentrations. At higher concentrations, fMLF inhibits chemotaxis while stimulating degranulation and superoxide production. While this switch of cellular activities in response to different concentrations of the same agonist allows effective killing of invading bacteria by the activated phagocytes, the underlying mechanism was unclear. Using a bioluminescence resonance energy transfer (BRET)-based FPR1 biosensor, we found that fMLF at sub-nanomolar and micromolar concentrations induced distinct conformational changes in FPR1. Neutrophils exposed to sub-nanomolar concentrations of fMLF polarized rapidly and migrated along a chemoattractant concentration gradient surrounding the cells. These cells also developed an intracellular  $\text{Ca}^{2+}$  concentration gradient. In comparison, higher concentrations of fMLF triggered the PLC- $\beta$ /diacyl glycerol/inositol trisphosphate pathway following activation of heterotrimeric  $\text{G}_i$  proteins, leading to  $\text{Ca}^{2+}$  mobilization from intracellular stores and  $\text{Ca}^{2+}$  influx from extracellular milieu. A robust and uniform rise in cytoplasmic  $\text{Ca}^{2+}$  level was required for degranulation and superoxide production but disrupted cytoplasmic  $\text{Ca}^{2+}$  concentration gradient and inhibited chemotaxis. In addition, elevated ERK1/2 phosphorylation and  $\beta$ -arrestin2 membrane translocation were associated with diminished chemotaxis in the presence of fMLF above 1 nM. These findings provide an example of agonist concentration-dependent biased signaling through induction of different receptor conformational changes.

Supported by funds from the National Key R&D Program of China (2019YFA0906003) and the 70th batch of General Projects from China Postdoctoral Science Foundation (2021M703092).

# Fluorescence Resonance Energy Transfer (FRET) Spatiotemporal Mapping of Atypical P38 Reveals an Endosomal and Cytosolic Spatial Bias

Jeremy J. Burton,<sup>1</sup> Jennifer J. Okalova,<sup>2</sup> and Neil Grimsey<sup>1</sup>

<sup>1</sup>Univ of Georgia Athens; and <sup>2</sup>University of Georgia

Abstract ID 29896

Poster Board 349

Mitogen-activated protein kinase (MAPK) p38 is a central regulator of intracellular signaling, driving physiological and pathological pathways. With over 150 downstream targets, it is predicted that spatial positioning and the availability of cofactors and substrates determine kinase signaling specificity. The subcellular localization of classical mitogen-activated kinase kinase 3/6 (MKK3/6) dependent p38 is highly dynamic to facilitate the selective activation of spatially restricted substrates displaying rapid nuclear translocation. In addition to classical MKK3/6-dependent p38 activation, the adaptor protein TAB1 can selectively bind to p38, inducing p38 autophosphorylation in a pathway termed atypical p38 activation. Recent studies have linked atypical p38 activity to a wide range of pathological signaling responses, including vascular inflammation and ischemic damage. However, the spatiotemporal profile of atypical p38 inflammatory signaling has not been studied and would provide valuable insight into how atypical p38-driven pathological responses.

To address this critical gap, we developed genetically encoded fluorescence resonance energy transfer (FRET) biosensors to track p38 activity with subcellular resolution. Through comparative analysis of plasma membrane, cytosolic, nuclear, and endosomal compartments, we established a characteristic profile of nuclear bias for MKK3/6-dependent p38 activation. Conversely, atypical p38 activation via thrombin-mediated G-protein coupled receptor (GPCR) protease-activated receptor 1 (PAR1) activity led to the sequestration of p38 at the endosome and cytosol, limiting nuclear translocation, a profile conserved for additional inflammatory GPCRs, including prostaglandin E2 activation of EP2. Intriguingly, perturbation of GPCR endocytosis with the dynamin inhibitor Dyngo4A led to spatiotemporal switching of atypical signaling, reducing endosomal and cytosolic p38 activation and increasing nuclear activity. Suggesting that a critical and yet unknown endosomal regulator drives the spatial bias of atypical p38 signaling. The data presented provide the first live-cell examination of the spatiotemporal dynamics for p38 activity and provide critical insight into how atypical p38 signaling drives differential signaling responses through spatial sequestration of kinase activity.

JB supported in part by the National Center for Advancing Translational Sciences of the National Institutes of Health under Award Number UL1TR002378 and TL1TR002382, and

NG, JB Supported in part by NIH NIAID R03AI171967-01

# Cargo-selectivity of Vesicle-associated Membrane Proteins in GPCR Exocytosis

Hao Chen,<sup>1</sup> Zara Weinberg,<sup>2</sup> G. Aditya Kumar,<sup>3</sup> and Manoj A. Puthenveedu<sup>3</sup>

<sup>1</sup>University of Michigan; <sup>2</sup>Carnegie Mellon Univ; and <sup>3</sup>Univ of Michigan

**Abstract ID 53076**

**Poster Board 350**

Vesicle fusion at the plasma membrane is a critical process for releasing hormones and neurotransmitters and delivering cognate GPCRs to the cell surface. Although the fusion machinery of soluble NSF-attachment receptor protein (SNARE) complex mediating neurotransmitter release is extensively studied, the SNARE complex that mediates GPCR surface delivery is largely unknown. Using multiple microscopy methods, we find subtype-dependent cargo-selectivity underlying the v-SNAREs, vesicle-associated membrane proteins (VAMPs). VAMP2 was preferentially enriched in vesicles that mediate the surface delivery of mu opioid receptor (MOR), and was required selectively for MOR recycling, but not for beta2 adrenergic receptor or transferrin receptor. Interestingly, VAMP2 was not preferentially presenting on endosomes that contained MOR, suggesting the involvement of local sorting mechanism. Together, our results identify VAMP2 as a cargo-selective v-SNARE and suggest that surface delivery of specific GPCRs is mediated by distinct SNARE complexes.

H.C. was supported by Rackham Graduate Student Research Grant under JE RGSs0666 from the University of Michigan. M.A.P. was supported by NIH grant GM117425 and DA055026, and NSF grant 1935926.

# Delineation of the G Protein-Coupled Receptor Kinase Phosphorylation Sites Within the D1 Dopamine Receptor and Their Role in Regulating Receptor Function

Nora S. Madaras,<sup>1</sup> Michele L. Rankin,<sup>1</sup> R. Benjamin Free,<sup>1</sup> Raphael Haider,<sup>2</sup> Julia Drube,<sup>2</sup> Arun K. Ghosh,<sup>3</sup> John JG. Tesmer,<sup>3</sup> Carsten Hoffmann,<sup>2</sup> David R. Sibley,<sup>1</sup> and Amy E. Moritz<sup>1</sup>

<sup>1</sup>NINDS/NIH; <sup>2</sup>University of Jena; and <sup>3</sup>Purdue University

Abstract ID 15411

Poster Board 351

Dopamine receptors (DARs) are G protein-coupled receptors (GPCRs) that regulate diverse physiological functions including movement, mood, cognition, and motivation, and are involved in the pathology and treatment of numerous neuropsychiatric disorders. The D1-like DARs (D1R and D5R) activate adenylyl cyclase and increase cAMP levels, while D2-like DARs (D2R, D3R, D4R) inhibit adenylyl cyclase and decrease cAMP levels. Additionally, all DARs recruit  $\beta$ -arrestin, leading to separate signaling cascades and the initiation of receptor desensitization and internalization.  $\beta$ -arrestin recruitment to the D1R is closely linked to receptor phosphorylation, and the D1R has been shown to be phosphorylated by various kinases including protein kinase A (PKA), protein kinase C (PKC), and G protein-coupled receptor kinases (GRKs). The D1R contains 32 intracellular serine and threonine residues within the C-terminus and third intracellular loop (ICL3) that serve as potential phosphorylation sites. Using mutational analyses, we previously identified the PKA- and PKC-mediated phosphorylation sites and showed that GRK4 constitutively phosphorylates the receptor. We have now identified the D1R residues that are phosphorylated by GRKs in response to dopamine (DA) stimulation and found that mutation of these residues severely impairs  $\beta$ -arrestin recruitment, but has little effect on G protein-mediated signaling. Our results also suggest that most of the DA-induced GRK phosphorylation of the D1R occurs at residues T360 and S362 in the proximal C-terminus, and that these residues are primarily responsible for  $\beta$ -arrestin recruitment to the receptor. We next sought to determine which GRK subtypes are involved in DA-induced  $\beta$ -arrestin recruitment to the D1R. Using CRISPR-edited HEK293 cells in which all the endogenous GRKs were knocked out, we found that DA-induced  $\beta$ -arrestin recruitment to the D1R is severely impaired in the absence of GRKs, but can be rescued by exogenous GRK overexpression. The kinase activity of the GRKs appears to be necessary for this effect, as a catalytically inactive K220R GRK2 mutant is unable to rescue DA-induced  $\beta$ -arrestin recruitment to the D1R. Using individual or combinatorial GRK KO cells, we found that GRK2 and GRK3 play little to no role in mediating DA-stimulated  $\beta$ -arrestin recruitment to the D1R, which contrasts with diminished  $\beta$ -arrestin recruitment to the D2R in GRK2 KO cells. However, we found that DA-induced  $\beta$ -arrestin recruitment to the D1R was significantly impaired in GRK5/6 and GRK6 KO cells. We found similar effects using multiple GRK2/3-selective inhibitors, in that they had no effect on  $\beta$ -arrestin recruitment to the D1R, while they severely diminished DA-induced  $\beta$ -arrestin recruitment to the D2R. We are currently using GRK5/6-selective inhibitors to determine if pharmacological inhibition of GRK5/6 imitates GRK5/6 knockout. Taken together, these results suggest that GRK6 is prominently involved in DA-induced  $\beta$ -arrestin recruitment to the D1R, and that different GRK subtypes regulate  $\beta$ -arrestin recruitment to the D1R vs. the D2R. Because GRK subtype distribution varies by tissue and brain region, it is intriguing to postulate that D1R phosphorylation by different GRKs may add layers of regulatory fine-tuning through differentially directing D1R signaling or trafficking outcomes.



# Protective Effects of Ozanimod in Cisplatin-induced Neuropathic Pain in Mice: Insights from Single-cell Transcriptomic Profiling in Spinal Cord Tissues

Ying Li,<sup>1</sup> Silvia Squillace,<sup>2</sup> Luigino Giancotti,<sup>1</sup> Terrance Egan,<sup>1</sup> Stella Hoft,<sup>1</sup> Richard DiPaolo,<sup>1</sup> and Daniela Salvemini<sup>3</sup>

<sup>1</sup>Saint Louis University; <sup>2</sup>Saint Louis Univ; and <sup>3</sup>Saint Louis Univ Sch of Medicine

Abstract ID 56337

Poster Board 352

Chemotherapy-induced peripheral neuropathy accompanied by neuropathic pain (CINP) is a major neurotoxicity of cisplatin, which is a platinum-based drug widely used for the treatment of lung, ovarian, and testicular cancer. CINP causes drug discontinuation and severely impacts quality of life; there are no FDA-approved interventions. We have reported that platinum-based drugs increase levels of the sphingolipid, sphingosine 1-phosphate (S1P) in the spinal cord and drive CINP through activation of the S1P receptor subtype 1 (S1PR1). However, the cellular and molecular mechanisms that are engaged downstream of S1PR1 remain poorly understood. Using a single-cell transcriptomic analysis of spinal cord from a mouse model of CINP, we found that cisplatin upregulated biological pathways that promote neuron death and axon myelination dysfunction. We further analyzed genes upregulated by cisplatin and reversed by the functional S1PR1 antagonist, ozanimod, in different cell types. In microglia, we discovered genes enriched in ERK1/ERK2 cascade and *Cd74*, the gene encoding the macrophage migration inhibitory factor (MIF) receptor that is known as a positive regulator of neuropathic pain. Similar analysis in astrocytes uncovered genes enriched in S1PR1 trafficking and Wnt signaling. In addition, our analyses revealed that the proportion of astrocytes with high *S1pr1* expression was increased by cisplatin and normalized by ozanimod. Overall, our results provide a comprehensive mapping of cellular/molecular changes engaged by cisplatin in CINP and deciphers novel mechanisms of action of which may facilitate the development of new therapeutics, including those targeting astrocytes and microglia.

Fundings: This study was funded by the National Institutes of Health Grant R01CA261979 (NIH) to Daniela Salvemini. All other authors claim no conflicts.

# Design and Development of Novel Barbiturates of Pharmacological Interest

Dimosthenis Koinas,<sup>1</sup> Bo Wu,<sup>2</sup> Anthony Pajak,<sup>3</sup> Zhou Xiaojuan,<sup>4</sup> Keith Miller,<sup>4</sup> and Karol Bruzik<sup>1</sup>

<sup>1</sup>University of Illinois at Chicago; <sup>2</sup>Dalian Institute of Chemical Physics; <sup>3</sup>Hospital For Special Surgery; and <sup>4</sup>Massachusetts General Hospital

Abstract ID 24095

Poster Board 366

GABA(A) receptors are ubiquitous in the CNS system where they mediate inhibitory synaptic signaling. These channels are targets of many pharmacological agents such as general anesthetics, sedatives, anticonvulsants, anxiolytics and anti-epileptics. GABA(A)Rs function is modulated by positive, negative and null allosteric modulators/ligands (PAMs, NAMs and NALs) that bind in the interfaces between the subunits. It is intuitive that these allosteric ligands influence the conformational stability and consequently the kinetic equilibria of different states of the channel during gating. Our goal is to design and develop NALs for GABA(A)Rs as reversal agents for general anesthesia and potentially non-sedative antiepileptics. These agents would attenuate the postoperative anesthesia-related complications such as, memory loss and confusion, by expediting the recovery from general anesthesia. The only clinically used NAL, flumazenil, binds to the benzodiazepine (BDZ) site in the extracellular domain's (ECD)  $\alpha+\gamma$ - interface, and is an antagonists of benzodiazepine sedatives. We embarked on a drug design campaign based on the structures of etomidate, flavanols and barbiturates, ligands that bind in the transmembrane domain sites (TMD). In the design and discovery of the new molecules, we used computational docking, structure-activity relationship studies and radioligand binding assays. We found that novel spiro-barbiturates analogs of phenobarbital bind to the GABA(A)Rs and reverse the *R*-mTFD-MPAB-induced anesthesia, while having only a marginal effect on agonist, [<sup>3</sup>H]muscimol, binding. The SAR study guided by the radioligand binding assays and the *in vivo* experiments of these novel barbiturates will be presented. The discovery of the first NALs that reverse anesthesia induced by positive allosteric modulators (PAMs) of GABA(A)Rs bound to the TMD will help understand GABAergic actions in the CNS, and potentially lead to antidotes for general anesthesia and other GABAergic CNS drugs.

Support/Funding Information: National Institute for General Medical Sciences, R01 GM135550

# Dopamine may increase Akt through D1-like receptor activation of PI3 Kinase in Macrophages

Dayna Robinson,<sup>1</sup> Breana Channer,<sup>1</sup> and Peter Gaskill<sup>2</sup>

<sup>1</sup>Drexel Univ; and <sup>2</sup>Drexel Univ College of Medicine

**Abstract ID 24972**

**Poster Board 367**

Macrophages are innate immune cells that regulate a variety of essential processes involved in the immune response. We and others have connected several of the pathways underlying these processes to dopamine receptor activation, demonstrating that dopamine drives inflammation in primary human monocyte derived macrophages (hMDMs). Our data specifically show that exposure of hMDM to elevated dopamine levels increases the activation of the transcription factor NF- $\kappa$ B and the production of inflammatory cytokines such as IL-6 and IL-1b. To examine whether these effects are mediated by dopamine driven Akt signaling, we treated hMDMs with either dopamine itself or dopamine receptor agonists or antagonists and evaluated changes in Akt phosphorylation by Western blot. Akt activation requires phosphorylation at both serine 473 and threonine 308, and our data show that dopamine significantly increases phosphorylation at both sites. Phosphorylation was also induced by the D1-like receptor agonists SKF 38389 and A68930, but not the D2-like receptor agonist Quinpirole. To further define the pathway by which dopamine receptors act on Akt, we used the phosphoinositide kinase 3 (PI3K) inhibitor, Buparlisib (BKM 120) and the protein phosphatase 2A (PP2A) inhibitor, okadaic acid (OA). BKM 120 eliminated the capacity of dopamine to phosphorylate Akt, but dopamine had no effect on OA mediated changes in Akt phosphorylation. This suggests that dopamine may act on Akt via activation of D1-like dopamine receptors that stimulate PI3K signaling. However, additional treatments with dopamine or A68930 in the presence of the pan-dopamine antagonist flupentixol show that dopamine can also increase Akt phosphorylation when dopamine receptors are blocked. This suggests that dopamine could act on Akt through both dopamine receptor dependent and independent pathways, such as adrenergic receptor activation. Future studies using receptor agonists and antagonists for dopamine and adrenergic receptors will further define and verify these processes. These data add clarity to the mechanisms by which dopamine drives macrophage immune function, potentially enabling the manipulation of dopamine-driven inflammatory activity.

# The Adhesion GPCR GPR114/ADGRG5 is Activated by its Tethered-Peptide-Agonist Following Receptor Fragment Dissociation

Tyler Bernadyn,<sup>1</sup> Rashmi Adhikari,<sup>2</sup> Alexander Vizurraga,<sup>3</sup> Frank Kwarcinski,<sup>1</sup> and Gregory Tall<sup>3</sup>

<sup>1</sup>University of Michigan; <sup>2</sup>University of Texas Health Science Center; and <sup>3</sup>Univ of Michigan

Abstract ID 17396

Poster Board 478

The second largest group of G protein coupled receptors (GPCRs) is the class B2 group or adhesion GPCRs (AGPCRs). AGPCRs are distinguished by variable extracellular regions that contain a membrane-proximal GPCR autoproteolysis-inducing (GAIN) domain that self cleaves to generate two receptor fragments, the N-terminal fragment (NTF) and the C-terminal fragment (CTF), or seven transmembrane domain (7TM). The fragments remain non-covalently bound after self-cleavage. We hypothesize that binding of the NTF to its ligand(s) that are presented by a neighboring cell or the extracellular matrix, anchors the NTF, while the AGPCR-expressing cell moves to generate force that dissociates the NTF/CTF to expose the AGPCR tethered-peptide-agonist (TA). The decrypted TA rapidly binds to its orthosteric site within the CTF to stabilize the AGPCR active state. The orphan AGPCR GPR114 was purported to be a non-cleaved, yet still capable of TA-dependent activation. This prompted confounding models of AGPCR activation, such as the TA was proposed to reside simultaneously within the GAIN domain and the CTF orthosteric site. This seems improbable as GPR114 has an identical cleavage site and TA as its closest homolog, the efficiently-cleaved AGPCR, GPR56. Here we used immunoblotting of dually epitope-tagged and untagged GPR114 to show that it is a cleaved AGPCR. Furthermore, FLAG-tagged GPR114 NTF was isolated from the culture medium of suspension cells expressing the holoreceptor, demonstrating its ability to be spontaneously shed from the cell surface. Urea treatment of AGPCR membrane homogenates is an established proxy means to induce AGPCR NTF dissociation and invoke tethered agonism. The wild type receptor, but not cleavage-defective GPR114-H225S, was activated by urea treatment to induce strong Gs activation. GPR114-H225S was activated by the AGPCR Group VI selective small molecule agonist 3-a-DOG or a synthetic peptidomimetic of its tethered agonist. Finally, engineered protease activated receptor (PAR1) / AGPCR fusion proteins of GPR114 and GPR56 were acutely stimulated with thrombin protease and shown to activate Gs and G13 respectively. Together, these results show that the GPR114 activation process typifies that of other AGPCRs and requires NTF/CTF dissociation to permit the tethered agonist to bind its CTF orthosteric site. Additional evidence demonstrating endogenous GPR114 self-cleavage mediated activation in primary cells will be presented.

# A positive allosteric modulator of M1 Acetylcholine receptors improves cognitive deficits in male and female APP<sup>swe</sup>/PSEN1 $\Delta$ E9 mice via divergent mechanisms

Khaled Abd-Elrahman,<sup>1</sup> Tash-Lynn L. Colson,<sup>2</sup> and Stephen S. Ferguson<sup>2</sup>

<sup>1</sup>Department of Anesthesiology, Pharmacology & Therapeutics, Faculty of Medicine, The University of British Columbia, Vancouver, BC, Canada; and <sup>2</sup>University of Ottawa Brain and Mind Research Institute, Department of Cellular and Molecular Medicine, University of Ottawa, Ottawa, ON, Canada

Abstract ID 13830

Poster Board 479

Alzheimer's disease (AD) is an age-related neurodegenerative disorder characterized by progressive cognitive decline with no effective treatments to slow its progression. Beta-amyloid (A $\beta$ ) protein is considered the principal neurotoxic species in AD brains that accumulates as the disease progresses. The M1 muscarinic acetylcholine receptor (mAChR) plays a key role in learning and memory and has been identified as a promising therapeutic target for AD-associated cognitive decline. Indeed, M1 mAChR agonists showed pro-cognitive activity in clinical trials but was associated with many cholinergic adverse effects that hinder their clinical utility. A newly developed M1 mAChR positive allosteric modulator (PAM), VU0486846, is devoid of direct agonist activity and adverse effects but was not tested for efficacy in AD mice. Here, we tested the efficacy of VU0486846 in AD mice by treating 9-month-old male and female APP<sup>swe</sup>/PSEN1 $\Delta$ E9 (APP<sup>swe</sup>) and wild-types with VU0486846 in drinking water (10mg/kg/day) for eight weeks. Cognitive function of all mice was assessed after treatment and brains were harvested for biochemical and immunohistochemical assessment. Eight-week treatment with VU0486846 improved cognitive function of male and female APP<sup>swe</sup> mice when tested in novel object recognition and Morris water maze. VU0486846 also improved the anxiety-like behavior of male and female APP<sup>swe</sup> mice in the open field arena. Interestingly, the improvement in cognitive function and anxiety-like behavior in APP<sup>swe</sup> mice was associated with a reduction in hippocampal soluble A $\beta$  oligomer levels in female but not male mice. Our findings also show that VU0486846 can shift the proteolytic processing of amyloid precursor protein from amylogenic to non-amyloidogenic cleavage to reduce A $\beta$  production in female but not male APP<sup>swe</sup> hippocampus. Thus, targeting M1 AChR using novel PAMs can improve cognitive deficits with minimal adverse effects in male and female AD patients via sex-specific mechanism(s).

# Investigating the Intertwine Effect of Insulin Resistance and Lipocalin Prostaglandin D2 Synthase in Non-alcoholic Fatty Liver Disease using HepG2 Cells

Rhema Khairnar,<sup>1</sup> Md Asrarul Islam,<sup>2</sup> and Sunil Kumar<sup>3</sup>

<sup>1</sup>St. John's University; <sup>2</sup>St Johns Univ; and <sup>3</sup>St. John

Abstract ID 53914

Poster Board 480

Despite non-alcoholic fatty liver disease (NAFLD) being the most common chronic liver disease worldwide, molecular mechanisms contributing to its etiology and progression are still unclear. This gap in knowledge has prevented both the understanding of its basic biology, pathogenesis, and the development of novel therapeutic agents. There are currently no FDA-approved therapies for NAFLD. A vast majority of prior studies that investigated NAFLD were performed using obese animal models since obesity and NAFLD are strongly intertwined. Therefore, the role of insulin resistance in NAFLD in non-obese has been overlooked. Interestingly, our previous study demonstrated that L-PGDS knockout mice develop insulin resistance but remain comparatively light weight despite developing fatty liver on consuming a high-fat diet. Briefly, Lipocalin Prostaglandin D2 Synthase (L-PGDS) functions as a prostaglandin synthase where it catalyzes the isomerization of PGH<sub>2</sub> to PGD<sub>2</sub>. PGD<sub>2</sub> regulates its physiological function through two individual G-protein coupled receptors named DP1 and DP2. This finding led us to delve into the role of L-PGDS, and precisely PGD<sub>2</sub>, in NAFLD. Since L-PGDS KO mice developed NAFLD and insulin resistance, it is crucial to understand this interplay of insulin and L-PGDS functioning. Therefore, we aimed to modulate the levels of L-PGDS to study its effect on glucose and fatty acid metabolism in HepG2 cells. HepG2 cells are an appropriate in-vitro model to investigate insulin signaling because HepG2 show a gluconeogenic, hepatokine and lipogenic gene-expression pattern similar to the one observed in in-vivo settings. We used a plasmid expressing myc-FLAG-tagged L-PGDS to overexpress and siRNA to silence L-PGDS expression in HepG2 cells. Our data indicates that modulation of L-PGDS expression is feasible in HepG2 cells. We will determine the level of L-PGDS mRNA and protein expression in insulin-sensitive and insulin-resistant HepG2 cells. Briefly, based on our preliminary data, we will culture HepG2 cells in presence of high glucose (30mM) alone or in combination with insulin (500nM) for 24hrs to mimic the human insulin resistance model. Further, we will identify the localization of L-PGDS in insulin sensitive and insulin-resistant HepG2 cells. Finally, we will study the function of L-PGDS on lipid accumulation in insulin-sensitive and insulin-resistant HepG2 cells. Once, we fully understand the role of L-PGDS, pharmacological agents that block hepatic lipid accumulation could be developed to treat NAFLD effectively possibly involving PGD<sub>2</sub> receptor agonist or antagonist. Collectively, our research will shed new light onto the role of L-PGDS in liver physiology and diabetes-induced NAFLD and highlight new therapeutic targets for future studies.

This research was supported by Seed Grant and Summer Support of Research internal funding award from the St. John's University, New York.

# Designer Autocrine Signaling Networks for Discovering GPCR-modulating Nanobodies

Jacob Rowe,<sup>1</sup> Kyutae Lee,<sup>2</sup> Sam Taylor,<sup>2</sup> and Daniel Isom<sup>3</sup>

<sup>1</sup>UF Scripps Biomedical Research; <sup>2</sup>University of Miami Miller School of Medicine; and <sup>3</sup>Univ of Miami Miller Sch of Med

**Abstract ID 26074**

**Poster Board 481**

Nanobodies are small antibody-derived proteins suited for recognizing structural motifs and surface facets of target proteins with high specificity. Unlike their larger antibody counterparts, nanobodies can also access protein cavities normally accessible only to ligands or unique protein interaction partners. With such abilities, nanobodies have garnered much attention in G protein-coupled receptor (GPCR) research, as these receptors contain both extracellular- and intracellular-facing cavities for accommodating ligands and G proteins, respectively. Most efforts in GPCR nanobody development have focused on identifying those that stabilize defined receptor conformations for solving GPCR structures. That said, using these same approaches for identifying nanobodies that directly modulate receptor function has been a major challenge. Here, we present a new cell-based nanobody discovery platform specially designed for identifying functionally relevant GPCR nanobodies. In the engineered system, nanobody-receptor interactions are reported only when receptor function is influenced. Additionally, the interface at which nanobody-GPCR interactions occur can be finely controlled, enabling user-defined discovery of nanobodies that interact at/near the receptor's ligand- or G protein-binding site. To date, we have demonstrated the platform's ability to identify both extracellular- and intracellular-binding nanobodies and have shown both negative and positive modes of GPCR modulation. We are currently using the designed platform to identify similar nanobodies for over 30 unique GPCRs. We anticipate these efforts will yield a large panel of nanobodies for further exploring and enhancing structural, cellular, and pharmacological studies of GPCRs, providing valuable research tools and therapeutic candidates for basic and translational research alike.

This work was supported by NIH/NIGMS R35GM119518 to D.G.I.

# Morphological effects of caffeine and creatine on *Caenorhabditis elegans*

Lance Kuo-Esser,<sup>1</sup> Tommy Scandura,<sup>2</sup> Ramon Chen,<sup>1</sup> Nijah Simmons,<sup>1</sup> Kylie Lawson,<sup>1</sup> Mauricio Dominguez,<sup>1</sup> Kennedy Kuchinski,<sup>1</sup> Steven Le,<sup>1</sup> Lauren Bennett,<sup>1</sup> Wilber Escorcía,<sup>1</sup> and Hanna Wetzel<sup>3</sup>

<sup>1</sup>Xavier University; <sup>2</sup>Xavier University; and <sup>3</sup>Xavier Univ

Abstract ID 25787

Poster Board 482

Creatine and caffeine are two supplements widely used by young adults in the U.S. Creatine is important for storing energy and to help fuel muscle contraction. Taken misguidedly as a wonder supplement to boost muscle-building, nonetheless there is promising research outcomes for creatine as a nutraceutical that improves muscle wasting linked to cancer and other chronic diseases. Caffeine is the most used psychoactive stimulant in the world. Increasingly, these supplements are taken jointly to promote fat catabolism while simultaneously increasing muscle anabolism. *Caenorhabditis elegans* (*C. elegans*) are nematode roundworms that are emerging as excellent models of drug effects, particularly those related to development, metabolism, and aging. This is due to their predictable and short lifecycle, high sequence orthology and homology to humans, and their entirely sequenced malleable genome. *C. elegans* represent an excellent model to determine impact of these commonly consumed supplements on growth and development. *C. elegans* were age matched and exposed to 8.75 mM caffeine, creatine, both caffeine and creatine, or a vehicle control for 4 hours during the L1 phase of development. The worms were then allowed to age to the L4 stage, at which point they were immobilized with sodium azide, mounted on slides and photographed using bright field microscopy. The volume of each worm was quantified using imageJ. Worms exposed to creatine had 2.0-fold larger volumes than vehicle control treated animals ( $p=0.000052$ ,  $n=149$  vehicle and 97 treated worms). However, worms treated with caffeine were not significantly different than controls ( $p=0.4$ ,  $n=25$  vehicle and 47 treated). Preliminary data suggest an epistatic interaction between caffeine and creatine, but more data is needed to confirm this interaction. Future directions include quantification of other morphology metrics, quantifying the localization and amount of various lipids, and determining the effects of caffeine and the combination of caffeine and creatine on survival rates of *C. elegans*. Given the prominence of the co-administration of caffeine and creatine it is important to understand the effects of these two compounds on the physiology of growth and development. This work will guide further research in vertebrates and humans on the effects of caffeine and creatine on these variables.

This work was supported by the Lechleiter fund for science research at Xavier University.



# Proximity Labeling-Based Network Analysis to Probe Molecular Functions of Adenylyl Cyclase-Containing Macromolecular Complexes in Cardiomyocytes

Taeyeop Park,<sup>1</sup> Yong Li,<sup>1</sup> and Carmen Dessauer<sup>1</sup>

<sup>1</sup>Department of Integrative Biology and Pharmacology, McGovern Medical School at the University of Texas Health Science Center

Abstract ID 23771

Poster Board 483

The second messenger cAMP is essential for sympathetic and parasympathetic regulation of cardiomyocytes. The spatial organization of cAMP signaling is key to the unique functional responses elicited by different hormonal inputs. This organization is achieved in part by means of scaffolding proteins that coordinate adenylyl cyclase (AC) localization in conjunction with downstream effectors of cAMP pathway, thus sensitizing the system to low levels of cAMP. However, the composition and dynamics of AC-containing macromolecular complexes in heart disease remain mostly unknown, particularly for different AC isoforms. We have carried out a comprehensive proteomic approach of AC complexes in the heart using BioID (proximity-dependent identification of near-neighbor interaction). We have fused the mini-Turbo biotin ligase with three different cardiac AC isoforms and control GFP and have expressed these fusion proteins in neonatal cardiomyocytes using adenoviruses. Neonatal cardiomyocytes were subsequently incubated with biotin for 3 hours and harvested for streptavidin pull-down and mass spectrometry. Proteins identified by BioID were incorporated into Significance Analysis of INteractome (SAINT) and high-confidence prey proteins were selected by Saint Score (0.7 and above). High-confidence prey proteins have been classified with their enriched Gene Ontology terms (GO) and cellular compartments using gProfiler, SAINT, and UniProtKB. Distribution of interactomes represented unique protein patterns for different AC isoforms, particularly with respect to GO localization terms and cellular responses to stress. To confirm our screening results, we performed Flag-pull down mass spectrometry with different AC isoforms and compared the derived interactomes with those from BioID. Proteins identified by Flag-MS overlapped with BioID-derived interactors (35-60%, depending on the AC isoform), with similar enrichment in GO terms relating to protein folding, localization, and small GTPase binding function. We further validated one specific prey protein for AC5 and AC6 that was identified by BioID and Flag-MS - an E3 ubiquitin ligase, STUB1 (also called CHIP). STUB1 interaction with AC5/6 has been assessed by IP-Western blot analysis, immunocytochemistry, and its functional consequences on AC activity verified by knock-down siRNA experiments. Our current comprehensive network analysis of complex formation is expected to provide important insights for understanding the spatial and functional significance of AC-containing macromolecular complexes in the heart.

This research was funded by National Institute of General Medical Science RO1GM060419 and the Mathers Foundation

# SMARCD3: A Link Between G $\alpha_q$ and Chromatin Remodeling?

Joseph Loomis,<sup>1</sup> Naincy R. Chandan,<sup>1</sup> and Alan V. Smrcka<sup>2</sup>

<sup>1</sup>Univ of Michigan; and <sup>2</sup>Univ of Michigan Med Sch

Abstract ID 21607

Poster Board 484

The G protein alpha subunit G $\alpha_q$  is a critical mediator of cells' response to a variety of external stimuli as a result of activation of G $\alpha_q$ -coupled GPCRs. G $\alpha_q$ -dependent signaling influences an array of physiological processes, including neurotransmission and vasoconstriction; additionally, dysregulated G $\alpha_q$ -dependent signaling has been firmly linked to several pathologies, including uveal melanoma and maladaptive cardiomyocyte hypertrophy. One established mechanism by which activated G $\alpha_q$  subunits might promote these processes involves activation of phospholipase C beta isoforms (PLC $\beta$ ), which catalyze the hydrolysis of PI(4,5)P<sub>2</sub> into inositol (1,4,5) trisphosphate (IP<sub>3</sub>) and diacylglycerol (DAG), ultimately leading to Ca<sup>2+</sup> mobilization and protein kinase C activation. However, G $\alpha_q$  subunits also signal independently of PLC $\beta$ , through p63RhoGEF and Trio, for example. Recently, our lab conducted a proximity labeling proteomic screen in HEK293 cells comparing wild-type G $\alpha_q$  and constitutively active G $\alpha_q$  Q209L each fused to TurboID, a promiscuous biotin ligase. From this, we identified numerous proteins that were selectively enriched in cells expressing G $\alpha_q$ -Q209L-TurboID compared to cells expressing G $\alpha_q$ -WT-TurboID. These enriched proteins included known G $\alpha_q$  interactors (PLC $\beta$ , Trio, and GRK2) as well as several proteins that have not been previously shown to interact with active G $\alpha_q$ , such as SMARCD3, a regulatory component of the SWI/SNF chromatin remodeling complex. Subsequently, in COS-7 cells, we found that co-transfection of SMARCD3 selectively inhibits G $\alpha_q$ -stimulated, but not G $\alpha_{12}$ -stimulated, PLC $\beta$  activity, indicating that SMARCD3 competes with PLC $\beta$  for access to active G $\alpha_q$ . Moreover, in HEK293 cells, we found that (1) SMARCD3 co-immunoprecipitates with G $\alpha_q$  and (2) preferentially interacts with active G $\alpha_q$  in a nanoluciferase fragment complementation (NanoBiT) assay. Taken together, these data indicate that SMARCD3 interacts with G $\alpha_q$  in COS-7 and HEK293 cells. Currently, we are probing for the amino acid sequences that govern SMARCD3's interaction with G $\alpha_q$ . Based on a predicted structure from AlphaFold, SMARCD3 consists of a relatively unstructured N-terminal region, a "core" region that contains  $\beta$ -sheets and a SWIB/MDM2 domain, and an extended,  $\alpha$ -helical C-terminus. Preliminary NanoBiT assay results with SMARCD3 truncation mutants suggest that deletion of either terminus does not affect SMARCD3's interaction with G $\alpha_q$ . Therefore, our ongoing studies will further define residues in SMARCD3's "core" region that coordinate interaction with G $\alpha_q$ . The SWI/SNF complex regulates gene transcription by modulating chromatin accessibility. Therefore, we are also testing whether G $\alpha_q$ 's interaction with SMARCD3 regulates transcription in mammalian cells. These endeavors may reveal a novel connection between G $\alpha_q$  signaling and chromatin remodeling and, ultimately, may inform therapeutic strategies for combatting pathologies marked by aberrant G $\alpha_q$  signaling.

This work was supported by NIH/NIGMS R35 GM127303-01 (to A.V.S), an AHA Predoctoral Fellowship (902574, to J.F.L.), and an NIH F31 Predoctoral Fellowship (1F31HL163927-01A1, to J.F.L.)

# Early-stage Development of an *in vitro* Screening Assay to Characterize the Activation of Human Adhesion Receptor ADGRE5

Arturo Mancini,<sup>1</sup> Samya Aouad,<sup>1</sup> Herthana Kandasamy,<sup>1</sup> Robert Cerone,<sup>1</sup> Stephan Schann,<sup>1</sup> and Laurent Sabbagh<sup>1</sup>

<sup>1</sup>Domain Therapeutics

Abstract ID 14943

Poster Board 485

ADGRE5 is a prototypical adhesion GPCR (aGPCR) that is expressed mainly on T lymphocytes, monocytes/macrophages, granulocytes, NK cells (especially CD56<sup>bright</sup>) and smooth muscle cells. Importantly, ADGRE5 expression is upregulated in many cancers (e.g., gastric/colorectal/pancreatic carcinomas, various leukemias, glioblastoma), whereas the corresponding normal tissues express relatively little or no ADGRE5. Previous studies indicated that ADGRE5 plays an important role in modulating cell adherence/detaching, migration, invasion, and metastasis, making ADGRE5 a potential drug target in oncology/immuno-oncology. Yet, the development of assays enabling the discovery of drugs acting on aGPCRs has been complicated by the lack of functional agonists and the complex multimodal mechanisms believed to govern receptor activation. Current methods rely on artificial methods of activation that preclude the identification of allosteric modulators acting upon ADGRE5's tractable long extracellular N-terminal fragment.

We describe a novel *in vitro* enhanced bystander (eb)BRET-based assay allowing to detect the activity of the full-length (native) form of human (h)ADGRE5 via its physiological activation mode (i.e., following mechanical stimulation (MS)). Indeed, subjecting full-length hADGRE5 isoform1- or isoform2-transfected HEK293 to vigorous orbital shaking resulted in a rapid time-dependent recruitment of ssArrestin 2 (ssArr2) to the plasma membrane. Such mechanosensitivity was not observed with a control receptor ( $\mu$  opioid receptor), despite its ability to engage ssArr2 following ligand stimulation. Interestingly, MS-induced ssArr2 engagement was absent with hADGRE5 harboring a mutated GPCR proteolysis site (GPS), which is believed to play an important role in aGPCR activation through the exposure of a tethered agonist following cleavage. Lack of activity was not related to defective cell surface expression of the GPS mutant, as both WT and GPS mutant forms of hADGRE5 displayed comparable surface expression when evaluated by flow cytometry. Similarly, MS provoked a delayed internalization of WT hADGRE5 but not that of the GPS mutant.

CD55/DAF is one of four ligands described to interact with hADGRE5's adhesive EGF-like folds and has been shown to promote MS-dependent downregulation of leukocyte ADGRE5 *in vivo*. We showed that CD55/DAF is expressed endogenously by HEK293, leading us to hypothesize that *trans*-signaling complexes between CD55/DAF and hADGRE5 could mediate the hADGRE5 activity observed in our MS assays. Indeed, addition of a neutralizing anti-CD55 antibody significantly dampened MS-induced hADGRE5 ssArr2 recruitment. Finally, the robustness of the MS ssArr2 recruitment assay was evaluated in 96-well plates and resulted in a  $Z' = 0.73$ , thus rendering this assay compatible for high-throughput screening of compound libraries.

Collectively, our ebBRET-based assay is robust and will help identify and characterize novel therapeutic agents acting on (patho)-physiologically relevant mechanisms of ADGRE5 activation through both orthosteric and allosteric receptor sites.

# Zyflamend, a novel approach for the treatment of acute pancreatitis

Ahmed Elshaarawi,<sup>1</sup> Ahmed Bettaieb,<sup>2</sup> and Presley Dowker-Key<sup>2</sup>

<sup>1</sup>The Univ of Tennessee, Knoxville; and <sup>2</sup>Univ of Tennessee, Knoxville

**Abstract ID 22963**

**Poster Board 486**

Acute pancreatitis (AP) is a frequent gastrointestinal disorder that causes significant morbidity, and its incidence has been progressively increasing in recent years. Pancreatitis starts as a local inflammation in the pancreas, leading to systemic inflammatory response and complications mediated via the NF- $\kappa$ B pathway. Approximately 25% of patients with AP develop a severe disease progression that leads to systemic inflammation and multiple organ dysfunction with mortality rates of up to 50%. AP remains without specific therapy, and understanding its pathogenesis's molecular mechanisms will aid in therapeutic intervention. A large body of evidence supports the use of phytochemicals and natural herbal extracts with anti-inflammatory properties as a potential adjuvant therapy. However, the lack of mechanistic understanding hampers the ability to refine these approaches into clinically supported treatments. Zyflamend (hereinafter referred to as PHB) is a commercially available well-defined poly-herbal blend of 10 herbal extracts, each included at a low dose relative to single-use compounds. Previous research investigated PHB for its anti-cancer properties because of its ability to activate the AMP-activated protein kinase (AMPK). Treatment of pancreatic cancer cells with human equivalent doses of PHB led to inhibition of carcinogenesis through various proposed pathways and processes, including ER stress, autophagy, and the NF- $\kappa$ B pathways. The current study aims to investigate the effects of PHB treatment on AP and characterize the underlying molecular mechanisms. To achieve this goal, complementary *in vivo* and *in vitro* approaches were employed to investigate the effects of PHB on cerulein-induced acute pancreatitis in mice and pancreatic acinar cells. Preliminary findings demonstrated that amylase and lipase activities were lower in Zyflamend-treated mice compared with controls injected with cerulein. In addition, while control mice exhibited a significant increase in local and systemic levels of inflammatory cytokines concomitant with pancreatic activation of inflammatory signaling pathways, Zyflamend treatment alleviated systemic and local inflammation. Although still preliminary, our data suggest that Zyflamend may serve a potential natural approach for the treatment and prevention of AP that is less invasive and capable of achieving long-term clinical significance.

# Elucidating Signaling Mechanisms and Pharmacology for the Brain Orphan Receptor GPR37

Andrew Frazier,<sup>1</sup> and John A. Allen<sup>1</sup>

<sup>1</sup>Univ of Texas Medical Branch

Abstract ID 55957

Poster Board 487

Andrew Frazier and John A. Allen

Center for Addiction Research, Department of Pharmacology and Toxicology, University of Texas Medical Branch, Galveston, TX USA

Corresponding author: John A. Allen, Ph.D., Department of Pharmacology and Toxicology, 301 University Blvd., University of Texas Medical Branch, Galveston, TX, Email: joaallen@utmb.edu

GPR37 is a class-A orphan G protein-coupled receptor that is most highly expressed in the human spinal cord with lesser expression in other brain regions including the amygdala, basal ganglia, hippocampus, and frontal cortex. GPR37 has been identified as a promising target for multiple conditions such as Parkinson's disease, inflammatory pain, ischemic stroke, and some forms of cancer. GPR37 is suggested to modulate cellular signaling through the activation of  $G_{i/o}$  signaling pathways; however, this has not been fully verified, and a natural ligand for GPR37 has yet to be identified. Here, we sought to elucidate GPR37 cellular signaling pathways by assessing basal or agonist-stimulated changes in cAMP levels using the Glosensor assay, release or influx of calcium using a real-time fluorescence imaging plate reader (FLIPR) assay, and  $\beta$ -arrestin2 recruitment using the Tango assay. Through these assays, we discovered that transient expression of wild-type human GPR37 in HEK293 cells significantly decreases cAMP levels in a pertussis toxin-insensitive manner, suggesting a potential signaling mechanism involving the activation of  $G_z$  but not  $G_{i/o}$ . When expressed in HEK293 cells, or in human oligodendroglioma (HOG) cells, wildtype human GPR37 and the mature N-terminally truncated form of GPR37, equally reduced cAMP levels. In addition, we determined that GPR37 expression strongly recruited  $\beta$ -arrestin2. These cellular studies also determined two previously suggested GPR37 agonists, TX14A and NPD1, fail to induce calcium signaling using the robust FLIPR assay, in opposition to previous reports. TX14A and NPD1 also failed to show a robust activation or inhibition of cAMP signaling, but both compounds decreased basal GPR37  $\beta$ -arrestin2 recruitment. The information attained from this work suggests that human GPR37 is highly constitutively active to reduce cAMP signaling and to recruit  $\beta$ -arrestin. Further research is needed to confirm additional GPR37 signaling mechanisms and to verify if TX14A and NPD1 are activators or inhibitors of this orphan receptor.

**Acknowledgments:** The UTMB Center for Addiction Research

Support/Funding Information: NIH NINDS R61NS12728

# Heat shock protein 90 inhibition in the spinal cord upregulates Src kinase in microglia to enhance opioid antinociception in acute pain

Jessica Bowden,<sup>1</sup> and John M. Streicher<sup>1</sup>

<sup>1</sup>Department of Pharmacology, College of Medicine, University of Arizona, Tucson AZ USA

Abstract ID 13722

Poster Board 489

Chronic pain remains a huge social and economic burden throughout the world and the United States. With few safe treatment options, many physicians turn to opioid analgesics; however these medications can have serious deleterious side effects including tolerance, addiction and respiratory depression. This has contributed to the opioid addiction crisis, emphasizing the need to find new ways to improve opioid therapy and decrease side effects. One such research area is the signal transduction cascades evoked by opioid receptor activation, which could be modulated to enhance their effects on pain management while decreasing negative side effects. Previously, our lab discovered that the molecular chaperone protein Heat shock protein 90 (Hsp90) when inhibited in the spinal cord through intrathecal (IT) administration of 17-N-allylamino-17-demethoxygeldanamycin (17-AAG) in mice led to a significant increase in morphine anti-nociception, which could enable an opioid dose-reduction strategy. Seeking a mechanism for this effect, we performed proteomic analysis of mouse spinal cord treated with 17-AAG, and found an upregulation of Src kinase. We thus hypothesized that Src kinase leads to enhanced opioid pain relief after Hsp90 inhibition. To test this hypothesis, CD-1 mice were treated with 17-AAG and the Src inhibitor Src-I1 intrathecally followed by morphine subcutaneously. Antinociception was measured with a thermal tail flick assay and a mechanical post-surgical paw incision model. The enhanced antinociceptive effects seen with 17-AAG were completely abolished with Src inhibition, suggesting that Hsp90 inhibition activates Src signaling to lead to enhanced opioid pain relief. CRISPR knockdown techniques confirmed the behavior seen with the inhibitor. Interestingly, the group that did not receive 17-AAG but did receive Src-I1 also showed a decrease in the anti-nociceptive effects of morphine, thus suggesting a role for Src in the opioid receptor pathway at baseline. Analysis by Western blotting showed upregulation of Src by 17-AAG treatment with the selective  $\mu$  opioid agonist DAMGO, and also showed that ERK activation was downstream of Src upregulation. Immunohistochemistry confirmed the upregulation of Src in the spinal dorsal horn and co-localized the activation to microglia cells. We used minocycline to inhibit microglial activation and were able to mimic the 17-AAG behavior effects, and using lipopolysaccharide to activate microglia we were able to mimic the Src inhibitor effects. A second CRISPR knockdown using a custom construct to target Src only in spinal microglial cells confirmed that microglial Src is essential to the enhanced opioid antinociception seen with spinal Hsp90 inhibition. This has helped elucidate a key molecular mechanism by which Hsp90 regulates opioid signaling and leads to enhanced opioid antinociception, creating potential targets for future efforts to improve opioid treatment.

This work was funded by NIH R01DA052340 to JMS. We also acknowledge shared equipment and resources from the University of Arizona Comprehensive Pain and Addiction Center. JMS is an equity holder in *Teleport Pharmaceuticals, LLC* and *Botanical Results, LLC*; however, these companies do not work in the Hsp90 space. The authors have no other relevant conflicts of interest to declare.

# Local Knockout of the Gb5-R7 Complex (Gnb5 Gene) in the Hypothalamus Causes Obesity in Mice

Qiang Wang,<sup>1</sup> Taylor Henry,<sup>1</sup> and Vladlen Slepak<sup>1</sup>

<sup>1</sup>University of Miami Miller School of Medicine

Abstract ID 16154

Poster Board 522

The *Gnb5* gene encodes a unique G protein  $\beta$  subunit. Unlike other  $G\beta$ ,  $G\beta5$  dimerizes with regulators of G protein signaling (RGS) proteins of the R7 family instead of the  $G\gamma$  subunit. The interaction between R7 and  $G\beta5$  is obligatory and is essential for stability of these complexes, so that the knockout of *Gnb5* causes proteasome degradation of the entire  $G\beta5$ -R7 family. We reported previously that the global *Gnb5* knockout (*Gnb5*<sup>-/-</sup>) mice were lean and were resistant to a high fat diet-induced body weight increase throughout their lifetime. Intriguingly, the *Gnb5* heterozygous (*Gnb5*<sup>-/+</sup>) mice exhibited an opposite phenotype: they were heavier than the *Gnb5*<sup>+/+</sup> age- and sex-matched littermates and had increased adiposity, insulin resistance, and liver steatosis. Here, we tested our hypothesis that the creation of a local knockout of *Gnb5* in the hypothalamus using Cre-lox technology may result in obesity. We generated the conditional *Gnb5* knockout using mice where the first exon of the *Gnb5* gene was flanked by lox P sites and the Cre recombinase was delivered by two alternative approaches. In the first approach, floxed *Gnb5* or wild-type mice were injected with a Cre-carrying AAV. In the second, floxed *Gnb5* mice were crossed with those carrying Cre under a hypothalamus-specific promoter. Our data show that consistent with our hypothesis, the resulting animals do have the increased body weight and adiposity, and the more detailed phenotypic analysis is ongoing. We conclude that the selective reduction of  $G\beta5$ -R7 level in hypothalamus is sufficient to perturb animal metabolism. These findings may contribute to understanding the earlier observations of genetic linkage between R7 family mutations and obesity in humans.

Supported in part by National Institutes of Health grants R56DK119262 and RO1DK126735 (to V. S.)

# Podocyte injury triggers the formation of intercellular bridges

Nina Cintron Pregosin,<sup>1</sup> and Sandeep K. Mallipattu<sup>2</sup>

<sup>1</sup>Stony Brook University; and <sup>2</sup>Stony Brook Medicine

Abstract ID 26483

Poster Board 523

**Background:** Podocytes are terminally differentiated visceral epithelial cells that are necessary for maintenance of the glomerular filtration barrier. Podocyte loss is characteristic of multiple kidney diseases, including focal segmental glomerulosclerosis (FSGS) and rapidly progressive glomerulonephritis (RPGN) which have a high risk of progression to end-stage kidney disease, requiring dialysis. In these diseases, podocyte loss triggers the activation and proliferation of neighboring parietal epithelial cells (PECs) which reside along the Bowman's capsule. Aberrant PEC proliferation leads to crescent or pseudo-crescent formation in the Bowman's space and eventual glomerular injury.

Recent evidence suggests that in the setting of injury podocytes might be capable of physically interacting with neighboring cells by forming cytoplasmic bridges from one cell to another. Similar intercellular bridges were identified in a variety of cell types including neuronal cells, epithelial cells, and immune cells, and have been established to serve as a direct mechanism of cell-cell communication. However, the role of these bridges between podocytes and PECs has not been previously characterized. The goal of this study is to investigate how podocyte-PEC bridges form, what they do, and whether they are pathological or physiological. The long-term impact of this project is to investigate intercellular bridges as potential therapeutic targets for ameliorating podocyte loss.

**Methods:** We investigated the formation of intercellular bridges in three models of podocyte injury: podocyte-specific loss of Krüppel-like factor 4 (Klf4 $\Delta$ Pod) nephrotoxic serum nephritis (NTS) and diabetic nephropathy. Immunohistochemistry, immunofluorescence staining, and electron microscopy were used to identify intercellular matrix extensions in glomeruli. Single nucleus (sn)RNA-seq was performed on each injury model.

**Results:** Periodic-acid schiff staining and electron microscopy revealed de novo bridges glomeruli of Klf4 $\Delta$ Pod mice and in mice treated with NTS. Intercellular bridge formation appeared to be correlated with the severity of injury, as few intercellular bridges were observed in mice with diabetic nephropathy. We also observed colocalization of endogenous podocyte markers (synaptopodin, nestin) and markers for activated PECs (CD44), suggesting that intercellular bridges form between podocytes and activated PECs. Enrichment analysis of differentially expressed genes between wild type and Klf4 $\Delta$ Pod mice and NTS treatment showed common upregulated pathways including focal adhesion (ACTN1, COL4a4, COL4a5, BIRC3), axon guidance (ROCK2, MYL12A, MYL21B), and actin cytoskeleton regulation (FGFR2, MYH9, MSN) in the podocyte and PEC clusters.

**Conclusions:** This is one of the first studies to demonstrate that intercellular bridges extend between injured podocytes and activated PECs.

Support/Funding Information: NIH/NIDDK, Veteran Affairs, Dr. W. Burghardt Turner Fellowship



# Subcellular Optogenetic Inhibition of PLC $\beta$ -G $\alpha$ qGTP Interaction Sheds Light on the Molecular Regulation of G $\alpha$ q-Governed Directional Cell Migration

Sithurand Ubeysinghe, Dinesh Kankanamge,<sup>1</sup> and Ajith Karunarathne<sup>2</sup>

<sup>1</sup>Washington University; and <sup>2</sup>Saint Louis University

Abstract ID 54461

Poster Board 524

Though light-sensitive G protein-coupled receptors (GPCRs), such as opsins, can activate some of the G protein signaling pathways with subcellular spatial control, the lack of approaches to control signaling of selected heterotrimeric G proteins downstream of GPCRs with a user-defined spatial and temporal control has been a limitation in understanding how such signaling regulates cell physiology and behavior. G $\alpha$ q-family G proteins primarily activate phospholipase C  $\beta$  (PLC  $\beta$ ) and hydrolyze inner membrane phosphatidylinositol 4, 5-bisphosphate (PIP<sub>2</sub>), generating inositol 1, 4, 5-triphosphate (IP<sub>3</sub>) and diacylglycerol (DAG), which mobilizes Ca<sup>2+</sup> and activates protein kinase C (PKC), respectively. PKC and Ca<sup>2+</sup> control various physiological functions, including cytoskeletal remodeling, muscle contraction, opioid-induced pain sensitivity, membrane dynamics, cell proliferation, and survival. Therefore, PLC  $\beta$  signaling involves many diseases, such as impaired platelet activation, heart diseases, cancers, and diabetes. However, the molecular basis of intricate PIP<sub>2</sub> hydrolysis regulation is poorly understood. Employing the minimum essential domain of the G $\alpha$ q-interacting helix-turn-helix (HTH) of PLC  $\beta$  as the template, we have engineered a series of optogenetic inhibitors to disrupt G $\alpha$ q-PLC  $\beta$  signaling with varying efficacies and near-zero noise. Employing subcellular spatial and millisecond temporal control of G $\alpha$ q-PLC  $\beta$  signaling, we have gained insights into G $\alpha$ q-pathway-governed directional cell migration.

This work was funded by NIH through NIGMS grant R01 GM140191.

## Regulation of Lysophosphatidic acid receptor 3

Karina Helivier Solís,<sup>1</sup> Ma. Teresa Romero,<sup>2</sup> and J. Adolfo Garcia-Sainz<sup>1</sup>

<sup>1</sup>Univ Nacional Autonoma De Mexico; and <sup>2</sup>UNAM

**Abstract ID 20533**

**Poster Board 525**

Lysophosphatidic acid receptor 3 (LPA3), is a receptor that mediates different physiological functions and pathological processes. We aimed to determine the phosphorylation pattern of LPA3 under distinct conditions such as baseline, agonist-activated and phosphorylated by protein kinase C. We hypothesize that the phosphorylation pattern of this receptor differs when activated with LPA as compared to under the action of PKC and that this might promote differential activation of distinct signaling pathways. LPA3 receptors tagged with the green fluorescent protein at the carboxyl tail were expressed in an inducible cell system (HEK293 TREx<sup>TM</sup> cells). These receptors were functional, as reflected by their ability to induce calcium signaling, ERK 1/2 phosphorylation, association with  $\beta$ -arrestin, and internalize in response to LPA; the action of PMA was also studied. LPA3 receptors were immunoprecipitated, subjected to SDS-PAGE, electrotransferred to nitrocellulose membranes, and analyzed by mass spectroscopy. The results showed that LPA3 receptors have 11 phosphorylation sites in the intracellular loop 3 and the carboxyl terminus. Interestingly, the LPA3 phosphorylation pattern of the receptor differs under the distinct conditions studied (i.e., baseline, LPA-activation, and phosphorylated in response to phorbol esters). The relationship between the phosphorylation of particular sites and the receptor's function is currently being studied.

# Revisiting Pirin: Evidence for a Role in Translation but not in Transcriptional Control

Anna Denaly Cab Gomez,<sup>1</sup> Richard Neubig,<sup>1</sup> and Erika M. Lisabeth<sup>1</sup>

<sup>1</sup>Michigan State Univ

Abstract ID 55180

Poster Board 526

Anna Denaly Cab Gomez<sup>1</sup>, Erika Mathes Lisabeth<sup>1</sup>, Richard R. Neubig<sup>1</sup>

<sup>1</sup>Department of Pharmacology and Toxicology, Michigan State University

Pirin is a 32 kDa protein that belongs to the extended cupin superfamily of plant proteins with only one human homolog. It is highly conserved across species, but its functions in mammals are very poorly understood. It is expressed ubiquitously and is over-expressed in some cancers. Pirin has been implicated in cancer, inflammation, oxidative stress, immune response, apoptosis, ferroptosis, and autophagy and has quercetinase activity. Much of the current literature, however, describes pirin as a transcriptional co-regulator for NF1, the NF $\kappa$ B subunit p65, and others. Our own studies have revealed that our series of anti-fibrotic and anti-cancer compounds (e.g. CCG-1423, CCG-257081, etc.) which inhibit the Rho/MRTF/SRF-mediated gene transcription pathway can bind to pirin though pirin's role in their mechanism is not clear.

To help define functional mechanisms of pirin, we undertook a multi-omics analysis using metabolomics and pirin-BioID-fusion-mediated biotinylation interactome analysis. A pirin-BioID fusion and a control myc-BioID fusion were transiently transfected into HEK293T cells in triplicate and treated with biotin. The biotinylated proteins were denatured, affinity-isolated using streptavidin-coupled beads, digested with trypsin and identified by Mass Spectrometry (MS) analysis. Proteins significantly enriched (FDR < 0.01) in the pirin-BioID vs myc-BioID samples included TUB4A, GSN, DNAJA2, ARF4, and RANBP2. Ingenuity Pathway Analysis (IPA) and EnrichR analysis were undertaken and implicated EIF2 signaling, EIF4/p70S6K, tRNA charging, Regulation of Actin Cytoskeleton, Amino Acid Metabolism, and Protein Processing in Endoplasmic Reticulum. Metabolomics analysis was done in NIH3T3 fibroblasts with shRNA-mediated knockdown of pirin or treatment with CCG-257081. IPA analysis showed changes in synthesis and degradation of multiple amino acids, citrulline, and ribonucleic acids as well as changes in tRNA charging. These results parallel those from the BioID analysis and implicate actions of pirin related to the Endoplasmic Reticulum (ER) and protein synthesis. Other proteins showing increased biotinylation in the pirin-BioID samples included multiple eIF proteins (EIF2B1, EIF3H, EIF3A, EIF4A2) and ribosomal proteins (RPL27A, RPL3).

Surprisingly, these studies did not result in any evidence of pirin involvement with transcription or transcription factors, as reported in the literature. Consistent with this, immunocytochemistry showed no nuclear localization of pirin but rather a perinuclear localization and co-localization with protein disulfide isomerase (PDI), a marker of the ER.

Further studies will confirm the identified interactions and explore pirin's functional effects on these pathways. However, it will be important to reconsider the literature related to pirin and gene transcription and include the ER as a likely target of pirin's role in mammalian cells and cancer.

Supported by NIH R01GM115459-07

# Effects of RS17053 at Subtypes of alpha1-Adrenergic Receptors in Rat Vas Deferens and Aorta

James Docherty,<sup>1</sup> and Hadeel A. Alsufyani<sup>2</sup>

<sup>1</sup>Royal College of Surgeons in Ireland; and <sup>2</sup>King Abdulaziz University

**Abstract ID 54729**

**Poster Board 527**

RS17053 is classed as an alpha1A-adrenergic receptor (alpha1A-AR) selective antagonist but has actions distinct from those of the commonly used alpha1A-AR antagonist RS100329. In radioligand binding studies, RS17053 shows affinities (-logM) of 8.74, 7.24 and 7.25 at alpha1A-, alpha1B- and alpha1D-ARs, respectively (mean of 3 published studies). We have examined its profile of action in functional studies at all subtypes of alpha1-AR. We have studied isometric contractions of rat aortic rings and rat vas deferens in organ bath studies of contractions to norepinephrine (NE). Isometric contractions evoked by NE in vas deferens involve alpha1D-adrenoceptors in the phasic component, and alpha1A-ARs in the tonic component to contractions. RS17053 ( $10^{-5}$ M) shifted NE potency and virtually abolished tonic contractions to NE, with little or limited effects on phasic contractions. The alpha1D-AR antagonist BMY7378 ( $3 \times 10^{-7}$ M) significantly reduced the remaining phasic component of the contractions, and the alpha1A-AR antagonist RS100329 ( $10^{-7}$ M) further blocked the residual tonic contraction. Hence, RS17053 shows high selectivity for alpha1A-ARs over alpha1D-ARs in rat vas deferens. Isometric contractions of rat aortic rings to NE involve alpha1D- and alpha1B-ARs. However, RS17053 ( $10^{-5}$ M) produced a large shift in the potency of NE in rat aorta, with a  $pK_B$  of 6.82. Large shifts of NE potency in rat aorta are consistent with actions at least partly involving block of alpha1B-ARs. In summary, results in rat vas deferens demonstrate low potency of RS17053 at alpha1D-ARs, but results from rat aorta can only be explained as demonstrating alpha1B-AR antagonism by RS17053. In conclusion, RS17053 is an alpha1A-AR antagonist with high potency at alpha1A-ARs in rat vas deferens, intermediate potency at alpha1B-ARs in rat aorta resulting in limited alpha1A-AR selectivity, but we have found surprisingly low potency at alpha1D-ARs in rat vas deferens. This differs from the ligand binding profile. This functional profile may make RS17053 a useful pharmacological tool.

# Biomolecular condensates defined by Activator of G protein Signaling 3 exhibit distinct properties and regulation

Ali Vural,<sup>1</sup> and Stephen Lanier<sup>2</sup>

<sup>1</sup>Western Michigan University Homer Stryker M.D. School of Medicine; and <sup>2</sup>Wayne State University

**Abstract ID 52172**

**Poster Board 528**

Activator of G-protein Signaling 3 (AGS3), a receptor independent activator of G-protein signaling, consists of 7 tetratricopeptide repeats (TPR) upstream from 4 G-protein regulatory motifs (GPR), each of which interact with GalphaGDP. AGS3 oscillates among different subcellular compartments in a regulated manner, which is intimately related to the functional diversity of the protein. AGS3 also exhibits an inherent and apparently regulated propensity to form biomolecular condensates (BMCs). BMCs are non-membranous, micron-scale compartments involving liquid-liquid phase separation within the cell in a regulatable manner. BMCs provide a platform to coordinate the assembly of a specific subset of molecules sequestered from the rest of the cytoplasm and are engaged in a wide range of biological and chemical events within the cell. To further address the properties and regulation of AGS3 BMCs, we asked initial questions regarding a) the distribution of AGS3 across the broader BMC landscape with and without cellular stress, and b) the core material properties of these punctate structures. Cellular stress (arsenate treatment) induced the formation of distinct stress granule BMCs and AGS3 BMCs as determined by fluorescent microscopy in two cell lines (Hela, COS7). In contrast, AGS3 colocalized with processing (P) body BMCs and this colocalization was disrupted by cellular stress with the generation of distinct AGS3 BMCs. Immunoblots of fractionated cell lysates indicated that cellular stress shifted AGS3 to the membrane pellet fraction, whereas the protein markers for stress granule and P-body BMCs remained in the supernatant. These data suggest that AGS3 BMCs may define a distinct type of BMC. To further address this hypothesis, we characterized the AGS3 BMCs by a) analysis of cell lysates under non-reducing gel electrophoresis and b) through examination of AGS3 diffusion dynamics in specific BMCs using fluorescence recovery after photobleaching (FRAP). Stress-induced AGS3 BMCs migrated as higher order structures as determined by immunoblots following non-reducing gel electrophoresis and the stress-induced properties of AGS3 BMCs were reversed by co-expression of the AGS3 binding partner Galpha3. Results from a series of FRAP experiments indicated differences in the diffusion dynamics of AGS3 in AGS3-DVL2 BMCs versus stress-induced AGS3 BMCs as well as AGS3 BMCs generated by changes in phosphorylation status. These data indicate that AGS3 BMCs, the formation of which is regulated by both cellular stress and the signaling proteins Galpha3 and DVL2, define a new type of BMC that may serve as previously unappreciated signal processing nodes.

# Regulation of GPCR Signaling by Sorting Nexins

Valeria Robleto,<sup>1</sup> Ya Zhuo,<sup>1</sup> Joseph Crecelius,<sup>1</sup> and Adriano Marchese<sup>1</sup>

<sup>1</sup>Medical College of Wisconsin

Abstract ID 27670

Poster Board 529

G protein-coupled receptor (GPCR) signaling is primarily regulated by GPCR kinases (GRKs) and  $\beta$ -arrestins. GRKs phosphorylate ligand-activated GPCRs, which promotes  $\beta$ -arrestin recruitment and binding.  $\beta$ -arrestin binding prevents G protein coupling while also targeting the GPCR for internalization via clathrin-coated pits. However, in some cases,  $\beta$ -arrestins are recruited to the receptor and promote its desensitization but fail to target it for internalization. For example, we show that ligand-stimulated internalization of the GPCR CXCR4 remains intact in HEK293 or HeLa cells that have been deleted of  $\beta$ -arrestins by CRISPR/Cas9 gene editing, despite the fact that  $\beta$ -arrestins are required for desensitization of CXCR4 signaling. Here, we report on an endocytic remodeling protein as a novel ligand-stimulated adaptor protein that mediates  $\beta$ -arrestin-independent GPCR internalization. This protein is sorting nexin 9 (SNX9), a protein that we previously showed by proximity labeling to be in the CXCR4 signaling network. We show that depletion of SNX9 by RNAi or knockout by CRISPR/Cas9 gene editing along with depletion of related protein SNX18 significantly decreased ligand-stimulated internalization of CXCR4 in HEK293 cells. In contrast, SNX9 and SNX18 depletion did not impact the internalization of GPCRs that require  $\beta$ -arrestins for internalization. Using bioluminescence resonance energy transfer (BRET) based cellular assays we show that SNX9 is recruited to CXCR4 following ligand stimulation at the plasma membrane. Through a combination of *in vitro* and cellular biophysical assays, we show that SNX9 interacts directly with the C-tail of CXCR4 in a phosphorylation-dependent manner. The determinants of this interaction do not overlap with previously identified determinants of the CXCR4/ $\beta$ -arrestin interaction. Further, we show that SNX9 is functionally relevant to CXCR4 signaling as SNX9 and SNX18 deficient cells show reduced desensitization to ligand stimulation compared with control cells. Here, we define a new internalization pathway for ligand-activated GPCRs that is dependent on the membrane remodeling protein SNX9. We provide evidence for the first time that SNX9 acts as an adaptor protein by binding directly to a phosphorylated GPCR and targeting the receptor for internalization. This represents a previously undescribed function of SNX9, which we propose is independent of its previously described role as an accessory protein during constitutive internalization. Our study expands our understanding of the mechanisms regulating GPCR signaling.

Support/Funding Information: R01 GM106727

# Mechanisms and Consequences of Compartmentalized GPCR Signaling in Neurons

Katherine Hall<sup>1</sup>

<sup>1</sup>Duke University

**Abstract ID 17816**

**Poster Board 530**

While it was canonically assumed that G protein coupled receptors (GPCRs) such as the beta-2 adrenergic receptor (B2AR), initiate signaling solely at the plasma membrane, it is now appreciated that signaling can occur from multiple intracellular compartments, such as the endosome. As a result, B2AR signaling is compartmentalized to initiate downstream phosphoproteomic and transcriptomic responses in a site-selective manner. Yet, most of this research has been done in non-physiological models, such as HEK293 and HeLa cells. Therefore, it is not clear whether compartmentalized signaling also operates in more physiological models. To address this, we seek to elucidate the mechanisms and consequences of compartmentalized B2AR signaling in neurons. We have preliminary data showing that compartmentalized signaling is occurring in both iPSC-derived neurons as well as primary hippocampal neurons. Through candidate-based approaches, we have evidence that blocking endosomal B2AR signaling affects transcription of B2AR-dependent genes and phosphorylation of B2AR targets. Therefore, we are currently extending this analysis to globally profile the impact of endosomal B2ARs on the neuronal phosphoproteomic, transcriptional, and post-transcriptional responses through unbiased approaches. In parallel, we are exploring the mechanisms that underlie these processes through unbiased approaches. B2ARs are essential for many neuronal processes such as synaptic plasticity which regulate proper learning and memory formation. Furthermore, dysregulation of B2ARs is associated with many neurological disorders. Thus, expounding upon mechanistic groundwork of B2AR signaling in the brain is essential to our understanding and treatment of such pathologies affected by dysregulated signaling.

# Molecular Dynamics Studies for Nirmatrelvir and the Main Protease from Variants of the Severe Acute Respiratory Syndrome Coronavirus-2 (SARS-CoV-2)

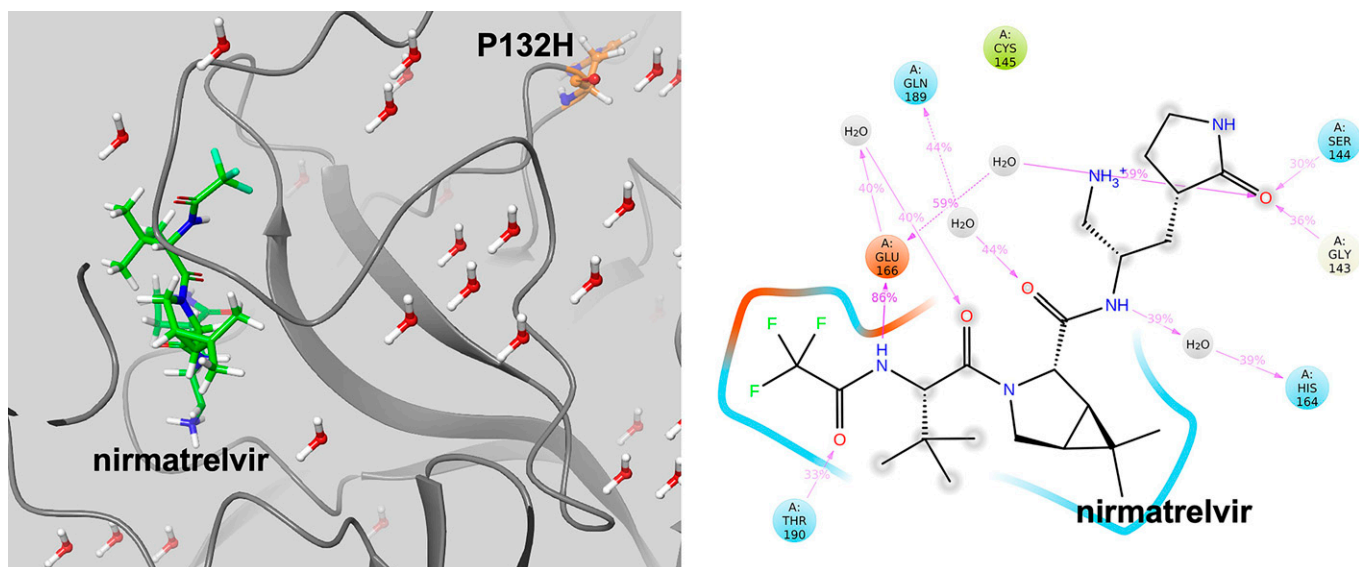
Kathleen Frey,<sup>1</sup> Ongshu Dutta,<sup>2</sup> Lilian Tran,<sup>2</sup> Brandon Yin,<sup>2</sup> Andrew Makarus,<sup>2</sup> Raymond Marmol,<sup>2</sup> and Youssef Dawood<sup>2</sup>

<sup>1</sup>Fairleigh Dickinson Univ (Pharmacy); and <sup>2</sup>Fairleigh Dickinson University

Abstract ID 19627

Poster Board 531

COVID-19 is a contagious worldwide disease that is caused by a virus called severe acute respiratory syndrome coronavirus-2 (SARS-CoV-2) and currently cases have risen to over 633 million with 6.6 million deaths cases. COVID-19 transmission is rapid and infected individuals experience diverse symptoms that include respiratory complications. Currently there are 4 vaccines available for prevention with alternative therapies including monoclonal antibodies. For small molecule drugs, there are limited treatment options that include Veklury (remdesivir), baricitinib, molnupiravir, and Paxlovid for patients with mild-to-moderate disease to reduce the risk of progression to severe disease. Paxlovid is a combination anti-viral oral drug that contains nirmatrelvir and ritonavir to combat against SARs-CoV-2. Nirmatrelvir is a viral main protease ( $M^{Pro}$ ) inhibitor that inhibits protein processing needed for viral replication. Ritonavir is co-administered as a CYP3A4 inhibitor to aid in boosting the pharmacokinetic profile of nirmatrelvir. Viruses like SARS-CoV-2 continuously evolve into variants as selective mutations occur. Variants such as omicron, lambda, and zeta have mutations in  $M^{Pro}$  that confer amino acid changes; these mutations are located remotely from the drug binding site. Previous *in vitro* studies suggest that variants remain susceptible to nirmatrelvir, but currently, there is limited data on overall efficacy of nirmatrelvir for clinically-relevant variants. Given the concern for variants, the objective of our study was to model mutations in coronavirus variants specifically in  $M^{Pro}$  and conduct molecular dynamics (MD) studies to evaluate the effects of mutations on nirmatrelvir affinity. Using programs such as Maestro and Desmond, we made *in silico* mutations representing amino acid changes from mutations observed on  $M^{Pro}$  for variants delta, omicron, zeta, and lambda. After energy minimizing the models, we conducted MD simulations using Desmond to understand the dynamic effects of the mutations. MD was conducted for 10 nanoseconds (ns) with standard temperature and pressures. Four simulations were generated for variants delta (wild-type), omicron (with Pro132His mutation in MPro), zeta (with Leu205Val mutation in  $M^{Pro}$ ), and lambda (with Gly15Ser mutation in MPro) with nirmatrelvir. In comparing the simulations for the 4 variants, we found that water networks are present in the omicron variant simulation with nirmatrelvir containing the Pro132His mutation. For variants zeta and lambda, these water networks are negligible and more direct contacts between functional groups in nirmatrelvir and amino acids in the binding site of  $M^{Pro}$  are observed. The mutations in zeta and lambda do not promote additional water networks in the binding site. As water molecules are commonly displaced during drug binding, we believe that retention of water molecules may affect the overall thermodynamics of nirmatrelvir and  $M^{Pro}$  (Pro132His) binding affinity. Results from the MD simulations suggest that these water networks may be unfavorable for binding interactions between nirmatrelvir and  $M^{Pro}$  (Pro132His) in the omicron variant. In future work, we will evaluate other  $M^{Pro}$  inhibitors and variants for this effect on binding affinity.



Molecular model of nirmatrelvir and the Main Protease from the omicron variant of Severe Acute Respiratory Syndrome Coronavirus-2 (SARS-CoV-2)



# Differential Regulation of Formyl Peptide Receptor 2 Protein in Non-alcoholic Fatty Liver Disease on High Fructose and High Fat Fed Male and Female C57BL/6 Mice

Md Asrarul Islam,<sup>1</sup> Rhema Khairnar,<sup>2</sup> and Sunil Kumar<sup>2</sup>

<sup>1</sup>St Johns Univ; and <sup>2</sup>St. John

Abstract ID 53862

Poster Board 532

Nonalcoholic fatty liver disease (NAFLD) has been a challenging health concern globally which transitions into nonalcoholic steatohepatitis (NASH) in a short span of time if remains untreated. Clinically, prevalence and severity of NAFLD/NASH are higher in men than premenopausal women which still remains a puzzle speculating possible sex specific differences in pathophysiology. But if occurs, severity and progression of fatty liver disease in post-menopausal women gets more aggressive than men. Recently, formyl peptide receptor 2 (FPR2) has caught our attention due its inflammatory responses in several organs; however, its role in the liver is unknown. Investigation of this protein became more exciting since it is more highly expressed in healthy liver of females than males possibly due to its regulation under the influence of estradiol. Obesity and fatty liver disease have a strong correlation but recently besides high fat, consumption of fructose rich western diet has been a significant contributor towards fatty liver disease development. Reason, unlike glucose, which is a ready-made source of energy, fructose is metabolized by the liver and triggers fat synthesis. Therefore, we aimed to investigate the regulation of FPR2 protein in both sexes in high fructose and high fat fed male and female C57BL/6 mice. Briefly, we divided both male and female mice into four separate groups and kept on chow, chow plus high fructose, high fat, and high fat plus high fructose diet for 22 weeks. Interestingly our preliminary hematoxylin and eosin staining data clearly showed significantly severe NAFLD in male mice compared to female mice on fructose groups. Significant body weight gain and other metabolic parameters in male mice on high fructose diet compared to female mice also strengthened the fatty liver data. Further, FPR2 protein expression was measured in liver cytoplasmic fraction but showed no significant change in male mice compared to female mice. Since protein localization of FPR2 is not fully understood yet, next we will investigate FPR2 expression using membrane as well as nuclear tissue fractions. Masson's trichrome will be performed to study a degree of fibrosis. Additionally, we will study gene expression, immunohistochemistry, and Enzyme-linked immunosorbent assay (ELISA) for FPR2 in both the sexes kept on different diets. Once regulation of FPR2 is fully understood, it can be considered as a potential future target for the treatment of fatty liver disease for pre- and post-menopausal women.

This research was supported by Seed Grant and Summer Support of Research internal funding award from the St. John's University, New York.

# Role of orphan G Protein-Coupled Receptor GPRC5B in retinoic acid induced depressive-like behaviors

Wenqi Fu, Luca Franchini,<sup>1</sup> Cesare Orlandi,<sup>1</sup> and Nina Wettschureck<sup>2</sup>

<sup>1</sup>Univ of Rochester; and <sup>2</sup>Max Planck Institute for Heart and Lung Research

Abstract ID 15567

Poster Board 533

Orphan G Protein Coupled Receptors (GPCRs) are GPCRs whose endogenous ligands are unknown or still debated. Due to the lack of pharmacological modulators, the physiological function of orphan GPCRs is understudied. However, relevant physiological roles associated with orphan GPCRs have been revealed by analysis of animal models and genome-wide association studies illuminating an untapped potential for drug discovery. G Protein-coupled Receptor class C group 5 member B (GPRC5B) is an orphan GPCR originally described as a retinoic acid-inducible gene. GPRC5B is ubiquitously expressed with an enrichment in the brain where it is one of the highest expressed GPCRs. We recently generated an exhaustive profile of *Gprc5b* mRNA transcripts in mouse brains, with a detailed dissection of excitatory versus inhibitory neurons in several brain regions. However, less is known about its physiological function. Independent transcriptomic studies have shown that GPRC5B is significantly altered in the post-mortem brain of patients diagnosed with depressive disorder. Moreover, GPRC5B protein levels have been found to be significantly increased in the hippocampus and hypothalamus in a depressive mouse model. Retinoic Acid (RA) is a fat-soluble derivative of vitamin A involved in vertebrate development, vision, and mood. Besides being a well-established regulator of embryonic development, RA is also involved in adult neurogenesis, a process tightly associated with the onset of depressive symptoms. Intriguingly, both preclinical studies and clinical reports indicate that chronic treatments with RA induce depression in humans and depressive-like behaviors in rodents. Based on this, we hypothesize that GPRC5B plays a role in RA-induced depressive-like phenotypes.

Interestingly, our detailed *in situ* hybridization study revealed enrichment of *Gprc5b* in the dentate gyrus and other brain regions involved in adult neurogenesis. Notably, our frequency distribution analysis showed a significantly higher expression of *Gprc5b* in dentate gyrus glutamatergic granule neurons than in GABAergic interneurons. To confirm *Gprc5b* as a RA inducible gene, we used quantitative RT-PCR and found an upregulation of *Gprc5b* after RA treatments in SH-SY5Y neuroblastoma cells. Then, to investigate how RA affects GPRC5B levels in the brain, we performed chronic intraperitoneal injections of RA on adult mice. We tracked the behavioral effects of RA with a sucrose preference test and confirmed RA-induced anhedonia. Additionally, using a validated custom polyclonal antibody, we analyzed how GPRC5B protein levels are modulated by RA in several mouse brain regions. Finally, to gain further insight into physiological functions of GPRC5B, we generated *GPRC5B<sup>flx/flx</sup>::Nestin-Cre* (neuronal and glial specific *Gprc5b* KO) mice. These conditional GPRC5B KO (cKO) mice will be subjected to a battery of behavioral tests to illuminate the role of GPRC5B in affective disorders including depression. Later, the same cKO mice will be tested in our model of RA-induced depression to obtain definitive evidence supporting a role for GPRC5B as a mediator of the behavioral effects of RA as suggested by our preliminary data. In the long term, we plan to expand our behavioral characterization of the different roles played by GPRC5B in the central nervous system taking advantage of the tools we developed.

# Development of a Genetically Encodable Fluorescent Biosensor to Examine the Spatiotemporal Regulation of NEK Kinases in Living Cells

Brandon M. Baker,<sup>1</sup> Henry Uchenna,<sup>2</sup> Andrew L. White,<sup>2</sup> Janetta Janetta Edwards,<sup>2</sup> Kayla M. Jamison,<sup>2</sup> Yasseen Abdellaoui,<sup>3</sup> J. Shane Henderson,<sup>2</sup> Stephanie Goodrich,<sup>2</sup> Robert H. Newman,<sup>2</sup> and David H. Drewery<sup>4</sup>

<sup>1</sup>Author; <sup>2</sup>North Carolina A&T State University; <sup>3</sup>University of North Carolina Chapel Hill.; and <sup>4</sup>University of North Carolina Eshelman School of Pharmacy

Abstract ID 26685

Poster Board 548

Never in mitosis A-related kinase (NEK) family members are an understudied, yet important, family of 11 mitotic kinases that play a critical role in cell division and the cellular response to replication stress and DNA damage. The pleiotropic relationship between this kinase family and human disease is widely recognized, yet poorly understood, particularly with respect to the spatial and temporal regulation of NEK family members within the cell. Characterizing NEK kinase activity within the endogenous cellular environment requires the development of molecular tools, such as genetically targetable fluorescent biosensors, that can track changes in the activity profiles of NEK family members in living cells with high spatiotemporal resolution. Here, we describe the development and initial characterization of a novel excitation ratiometric indicator-based NEK activity reporter (ExRai-NEKAR). ExRai-NEKAR, which was created using a generalizable molecular cloning strategy based on Gibson Assembly, exhibited a 5.5-fold increase in its 395 nm/475 nm excitation ratio in the presence of NEK1 and ATP *in vitro*. In contrast, no change in the excitation ratio was observed when the non-hydrolyzable ATP analog, AMP-PNP, was substituted for ATP in the assay, suggesting that the observed changes in ExRai-NEKAR's excitation ratio are dependent on NEK1-mediated phosphorylation and not protein-protein interactions. Interestingly, while ExRai-NEKAR was also efficiently phosphorylated by NEK5 leading to a robust response, incubation with either NEK2 or NEK9 caused only marginal changes in ExRai-NEKAR's excitation ratio, consistent with previous studies suggesting that NEK1 and NEK5 share a similar consensus motif that is distinct from those preferred by NEK2 and NEK9. Importantly, treatment of 293T cells with 200 mM H<sub>2</sub>O<sub>2</sub> led to a similar increase in ExRai-NEKAR fluorescence *in situ*, consistent with NEK1's role in the DNA damage response (DDR). We are currently using a series of novel NEK inhibitors and other pharmacological agents to further characterize ExRai-NEKAR's response in cells and to better understand the regulation of NEK family members within the endogenous cellular environment. Together, our data suggest that ExRai-NEKAR is efficiently phosphorylated by some NEK family members (e.g., NEK1 and NEK5) but not by others (e.g., NEK2 and NEK9). Likewise, live cell imaging experiments suggest that ExRai-NEKAR and its derivatives could be useful tools for monitoring real-time changes in the activity profiles of specific NEK family members with high spatiotemporal resolution under a variety of cellular conditions such as in response to pharmacological, toxicological, or pathological agents.

This research was supported by DoD Grant #78992-DD-RTL (to RHN), NIH/NCI grant 1R01CA273095 (to DHD and RHN), NSF grant #DBI-1852319 (to RHN).

# HIV-1 gp120- and Morphine-Induced Endolysosome Iron Release Triggers Disruption of the Reactive Species Interactome and Cell Death

Nirmal Kumar,<sup>1</sup> Peter W. Halcrow,<sup>1</sup> Darius NK. Quansah,<sup>1</sup> Braelyn Liang,<sup>1</sup> and Jonathan D. Geiger<sup>1</sup>

<sup>1</sup>University of North Dakota

Abstract ID 25123

Poster Board 549

Altered iron metabolism is implicated in many neurodegenerative disorders including HIV-1-associated neurocognitive disorders (HAND). Implicated in the pathogenesis of HAND is the HIV-1 coat protein gp120 as well as comorbid substance abuse, which induce iron dysregulation and the formation of reactive species that cause neuronal death. Because HIV-1 proteins and the ingestion of substances of abuse induce oxidative stress, drug-abusing patients are at a greater risk of oxidative stress-induced neuronal injury and HAND. Previous research has studied the individual effects of gp120- and morphine-induced neurotoxicity with a focus on the formation of reactive oxygen species (ROS); however, their combined neurotoxicity and effects on the newly defined reactive species interactome (RSI) remain largely unknown. Endolysosomes are subcellular acidic organelles known for their function in regulating cellular iron metabolism and redox signaling. Recently, we showed that HIV-1 gp120 and morphine cause endolysosome iron dyshomeostasis, yet the impact of impaired endolysosome iron balance on the RSI remains unknown. Here using SH-SY5Y neuroblastoma and U87MG human glioblastoma cells, we found that HIV-1 gp120 and morphine (1) de-acidified endolysosomes, (2) decreased endolysosome Fe<sup>2+</sup> levels, (3) increased cytosolic and mitochondrial Fe<sup>2+</sup> levels, (4) increased endolysosome ROS, lipid peroxidation (LPO) and nitric oxide (NO) levels and decreased endolysosome hydrogen sulfide (H<sub>2</sub>S) levels, (5) increased cytosolic ROS levels and decreased cytosolic H<sub>2</sub>S levels, (6) increased mitochondrial ROS and LPO, and NO levels and decreased mitochondrial H<sub>2</sub>S levels and (7) induced cell death; effects blocked by the endolysosome-specific iron chelator deferoxamine. Thus, an increased understanding of the endolysosome Fe<sup>2+</sup> pool that plays a critical role in regulating inter-organellar iron signaling, in RSI homeostasis, and in contributing to HIV-1 gp120 and morphine neurotoxicity may provide new insight into potential therapeutic targets for HAND progression.

Support/Funding Information: [P20GM139759, P30GM100329, U54GM115458, R01MH100972, R01MH105329, R01MH119000, 2R01NS065957, 2R01DA032444]

# ABCC4 Impacts Megakaryopoiesis by Regulating Intracellular cAMP levels

Sabina Ranjit,<sup>1</sup> Yao Wang,<sup>2</sup> Satish B. Cheepala,<sup>2</sup> Jingwen Zhu,<sup>2</sup> Woo Jung Cho,<sup>2</sup> Cam Robinson,<sup>2</sup> Scott Olsen,<sup>2</sup> and John Schuetz<sup>2</sup>

<sup>1</sup>St Jude Children's Research Hospital; and <sup>2</sup>St. Jude Children's Research Hospital

Abstract ID 17652

Poster Board 550

The role of ABC transporters in megakaryopoiesis, that is the process of platelet formation from megakaryocytes, is unknown. Recent GWAS studies<sup>1</sup> indicated ABCC4 as one of the novel genetic candidates affecting platelet number. In our study, complete blood count analysis from WT or *Abcc4*<sup>-/-</sup> mice treated with 6-mercaptopurine (6-MP), revealed a profound reduction in the platelets among the *Abcc4*<sup>-/-</sup> mice but not the lymphoid and erythroid cells. The platelets from both *Abcc4*<sup>-/-</sup> and WT mice were equally sensitive to 6-MP and displayed no enhanced apoptosis or alteration in expression of pro- or anti-apoptotic Bcl2 family members. However, the strong reduction in platelets, relative to platelet half-life, suggested 6-MP might affect platelet production. 6-MP reduced megakaryocyte number but not the megakaryocyte progenitors. ABCC4 protein expression also increased when the megakaryoblastic cell line, Meg01 was differentiated with the phorbol ester, PMA. *In vitro* differentiation with thrombopoietin of *Abcc4*<sup>-/-</sup> fetal liver-derived megakaryocytes revealed defective proplatelet formation and impaired polyploidization. To determine if ABCC4 impacted megakaryopoiesis *in vivo*, we treated WT/*Abcc4*<sup>-/-</sup> mice with 5-fluorouracil (5-FU), which destroys all cycling cells and drives quiescent hematopoietic stem cells to differentiate. 5-FU treated *Abcc4*<sup>-/-</sup> mice exhibited delayed platelet formation but not erythropoiesis, compared to WT. Because of the profound defect in platelet formation from fetal liver megakaryocytes and the small defect *in vivo*, we hypothesized that differences in gene expression might exist *in vivo* in megakaryocytes. RNA-seq analysis of megakaryocytes derived from the bone marrow of WT/*Abcc4*<sup>-/-</sup> mice revealed that several genes related to cytokines/chemokines, transcription factors and polyploidization, that regulate megakaryopoiesis, were significantly higher in WT mice compared to *Abcc4*<sup>-/-</sup>. However, only few genes associated with platelet formation were upregulated in *Abcc4*<sup>-/-</sup> mice. We extended our findings in the human megakaryoblastic Meg01 cells. Meg01 cells treated with PMA differentiated to platelets. The ABCC4 specific inhibitor, Ceefourin 2 significantly impaired polyploidization in PMA-differentiated Meg01 cells. Transmission electron microscopy of differentiated Meg01 cells revealed defective cytoplasmic maturation and abnormal platelet formation after ABCC4 inhibition. The defective megakaryopoiesis due to ABCC4 inhibition was also reflected in the gene expression of differentiated Meg01 cells. cAMP, a substrate of ABCC4, is known to inhibit megakaryopoiesis. We observed that intracellular cAMP level increased during Meg01 differentiation, which further increased after ABCC4 inhibition. Treatment with the PKA specific inhibitor (PKI-14-22) demonstrated that cAMP/PKA activity induced phosphorylation of p-38 which regulates downstream effectors involved in megakaryopoiesis. Excessive accumulation of intracellular cAMP after ABCC4 inhibition, inhibited PKA activity, as indicated by reduced phosphorylation of PKA substrates. Altogether, our results suggest that ABCC4 impacts megakaryopoiesis by regulating intracellular cAMP level and suggests it as a potential therapeutic strategy to control thrombocythemia.

1. Gieger, C. *New gene functions in megakaryopoiesis and platelet formation*. (Nature, 2011)

This work was supported by NIH and ALSAC.

# Comparison of $\Delta^9$ -tetrahydrocannabinolic acid A (THCA-A) and Delta-9-tetrahydrocannabinol (THC) in neuronal cell functions

Khalil Eldeeb,<sup>1</sup> Sandra Leone-Kabler,<sup>2</sup> and Allyn Howlett<sup>3</sup>

<sup>1</sup>Campbell Univ School of Osteopathic Medicine (CUSOM); <sup>2</sup>Wake Forest University; and <sup>3</sup>Wake Forest Univ School of Medicine

Abstract ID 55116

Poster Board 551

$\Delta^9$ -tetrahydrocannabinolic acid A (THCA-A) is a compound produced in the female cannabis plant that might serve as an endogenous tissue-protective signal. When heated, it can be converted into THC, although it is not always complete. While research on its pharmacological properties is limited, available evidence suggests that THCA-A may have therapeutic analgesic effects unrelated to its conversion to THC. This study compared the effects of THCA-A to THC on cell signaling in N18TG2 mouse neuroblastoma cells expressing the CB1 cannabinoid receptor using cAMP and ERK phosphorylation assays. We found that both THC and THCA-A induced CB1-dependent signaling in a dose-dependent manner. THC inhibited initial-rate FSK-stimulated cAMP accumulation (four minutes) in a dose-dependent fashion (1  $\mu$ M: 77  $\pm$  7.2% of FSK stimulation). Co-incubation with CB1R antagonist SR141716 1  $\mu$ M reversed the THC-mediated inhibition to (102  $\pm$  9.9% of FSK stimulation). THCA-A also inhibited FSK-stimulated cAMP accumulation in a dose-dependent fashion (1  $\mu$ M: 55  $\pm$  8.8% of FSK stimulation). This effect was reversed by co-incubation with SR141716 (1  $\mu$ M) to (99  $\pm$  5.3% of FSK stimulation). In N18TG2 cells treated with the diacylglycerol lipase inhibitor, tetrahydrolipstatin (THL, Orlistat; 1  $\mu$ M for two hours), ERK phosphorylation was assessed after four minutes of incubation with the drugs using the in-cell western assay. THC stimulated ERK phosphorylation in a dose-dependent manner (1  $\mu$ M, 140  $\pm$  8% over basal). Coincubation with SR141716 inhibited this stimulation (110  $\pm$  1.8%). Similarly, THCA-A induced a dose-dependent ERK phosphorylation (1  $\mu$ M, 134  $\pm$  9% over basal) that was inhibited in the presence of 1  $\mu$ M SR141716A (121  $\pm$  7% over basal). In conclusion, in our hands, both THC and THCA-A could stimulate CB1-dependent signaling in the N18TG2 neuroblastoma cell line. Future studies will explore other signaling pathways and binding targets (e.g., PPARs, GPR-55) that may be involved in the analgesic effects of this agent.

This research was funded by NIH grants R01-DA042157

# Optimization of a Novel D2 Dopamine Receptor-Selective Antagonist into Lead Candidates for the Treatment of Neuropsychiatric Disorders

Ashley Nilson,<sup>1</sup> John Hanson,<sup>2</sup> Andres E. Dulcey,<sup>3</sup> Xin Wen,<sup>3</sup> R. Benjamin Free,<sup>4</sup> Raul R. Calvo,<sup>3</sup> Juan J. Marugan,<sup>3</sup> and David R. Sibley<sup>5</sup>

<sup>1</sup>NINDS; <sup>2</sup>National Institute of Neurological Disorders and Stroke; <sup>3</sup>National Center for Advancing Translational Sciences; <sup>4</sup>NINDS/NIH; and <sup>5</sup>National Institutes of Health

Abstract ID 19484

Poster Board 566

Schizophrenia is a devastating neuropsychiatric illness impacting approximately 1% of the global population and is the 15<sup>th</sup> leading cause of disability worldwide. Schizophrenia is characterized by positive (hallucinations, delusions, paranoia), negative (flat affect, decreased motivation) and cognitive symptoms. Current therapies treat mostly the positive symptoms and are associated with a plethora of off-target side effects such as sedation, weight gain, and diabetes, among others. All FDA-approved antipsychotic medications target the D2 dopamine receptor (D2R) but also exhibit poly-pharmacology with other receptors. Further, there are few D2R antagonists that can selectively inhibit the D2R without also antagonizing the D3 and D4 dopamine receptors (D3R, D4R, respectively). We recently identified a D2R-selective antagonist scaffold, MLS6916, from a high throughput screen of the D2R. When counter-screened against 168 GPCRs using  $\beta$ -arrestin recruitment as a functional readout, 10  $\mu$ M MLS6916 only inhibited the D2R, and to a lesser extent, the D4R. Further, using radioligand binding competition assays, MLS6916 was >200-fold D2R>D3R selective and 12-fold D2R>D4R selective. Despite its promising D2R selectivity, MLS6916 was found to exhibit poor metabolic stability when assayed using rat liver microsomes. Interestingly, we found high species variability with respect to metabolic stability using rat, mouse, and human liver microsomes. While many analogs exhibited poor metabolic stability in rat liver microsomes, we observed equal or worse stability in mouse liver microsomes, but dramatically higher stability in human liver microsomes. High metabolic stability in humans is essential for moving a compound into the clinic, but preclinical studies will require at least moderate metabolic stability in rodents to employ animal models that are predictive of antipsychotic efficacy and/or adverse side effects. Thus, to chemically optimize this scaffold and explore its structure-activity relationships, greater than 100 analogs were synthesized to identify modifications that might result in improved metabolic stability. All analogs were also evaluated for D2R, D3R, and D4R activities using radioligand binding competition and  $\beta$ -arrestin recruitment assays. Lead compounds were identified that possessed D2R  $K_i$  values of <100 nM, were highly selective versus the D3R and D4R, and exhibited improved metabolic stability in mouse and/or human liver microsomes. We further determined the pharmacokinetic profiles of the most promising compounds in mice since this species has good models for predicting antipsychotic efficacy. After injecting 30 mg/kg i.p., we found that the compounds exhibited  $t_{1/2}$  values of 5-6 hr in both plasma and brain. Importantly, the compounds exhibited 1:1 brain-plasma ratios with  $C_{max}$  values >10  $\mu$ M indicating excellent brain penetration. In summary, we have identified lead candidate compounds that have exceptional D2R-selectivity, excellent metabolic stabilities in human liver microsomes, and sufficient metabolic stability in mice to conduct behavioral studies. Future studies will investigate preclinical antipsychotic efficacy in mouse models as well as the potential for on-target side effects such as catalepsy. These advanced leads may have the potential to treat neuropsychiatric disorders with greatly reduced off-target side effects.

# N-cadherin Signaling via PI3K $\beta$ -Akt3 Stabilizes Occludin Tight Junctions in the Blood-Brain Barrier

Quinn Lee,<sup>1</sup> Kevin Kruse,<sup>2</sup> Shuangping Zhao,<sup>3</sup> Leon Tai,<sup>3</sup> and Yulia Komarova<sup>4</sup>

<sup>1</sup>Univ of Illinois Chicago; <sup>2</sup>University of Utah; <sup>3</sup>University of Illinois Chicago; and <sup>4</sup>Univ of Illinois at Chicago

**Abstract ID 19653**

**Poster Board 567**

Tight junctions (TJs) seal brain endothelial cells (BECs) to form a restrictive blood-brain barrier (BBB) to selectively control the influx of circulating substances into the central nervous system. Critical to the integrity of BBB are pericytes, cells that physically interact with BECs through Neural (N)-cadherin adhesion. Using brain samples from donors of different ages, we observed a significant loss of N-cadherin junctions in middle-aged patients. This change in N-cadherin was associated with a significant disruption of occludin TJs, suggesting a potential important crosstalk between N-cadherin and TJs. Therefore, to better understand the role of N-cadherin function in the BBB, we generated an inducible, EC-specific knockout of N-cadherin in mice. We demonstrated that mutant mice lacking N-cadherin exhibited greater BBB permeability as well as impairments in TJ ultrastructure. Analyzing different TJ proteins in the microvasculature of the brain cortex, we also found significant disruption of occludin but not claudin TJs in these mutant mice. Furthermore, analysis of occludin kinetics in BEC monolayers lacking N-cadherin adhesion revealed significantly greater internalization rates of occludin from TJs, suggesting that N-cadherin signaling stabilizes occludin TJs. We showed that N-cadherin induces the activation of phosphoinositide 3-kinase (PI3K), leading to Akt phosphorylation. Depletion of PI3K p110 $\beta$  or Akt3, but not other p110 or Akt isoforms, increased occludin internalization from TJs in BECs with intact N-cadherin adhesion. Our data indicate that N-cadherin adhesion activates PI3K p110 $\beta$ -Akt3 signaling in BECs that is essential for the stabilization of occludin TJs to strengthen the BBB.



# Cannabinoid Receptor Interacting Protein 1a (CRIP1a) Associates with $G\alpha_i$ in a $GTP\gamma S$ or Agonist Dependent Manner

Erin K. Hughes,<sup>1</sup> Audrey Chrisman,<sup>2</sup> Sandra Leone-Kabler,<sup>3</sup> Glen S. Marrs,<sup>2</sup> W. Todd Lowther,<sup>3</sup> and Allyn Howlett<sup>4</sup>

<sup>1</sup>Wake Forest Univ School of Medicine; <sup>2</sup>Wake Forest University; <sup>3</sup>Wake Forest University School of Medicine; and <sup>4</sup>Wake Forest School of Medicine

Abstract ID 24557

Poster Board 568

Cannabis usage in recent years has increased due to the legalization of both recreational and medical use, making it important to understand how psychoactive cannabinoids modulate cellular signaling in neurons. The CB1 cannabinoid receptor (CB1R) is a G-protein coupled receptor (GPCR) found in the central nervous system (CNS) and modulates neuroprogenitor development, neural commitment, and neurotransmitter release. Cannabinoid receptor interacting protein 1a (CRIP1a) is an abundant 20 kDa protein in the CNS, which we recently determined to be a beta-barrel protein similar in structure to homologous proteins that serve as intracellular carriers of lipidated proteins. In-vitro binding studies demonstrated that recombinant CRIP1a interacts directly with myristoylated  $G\alpha_i$ -derived peptides (Booth et. al. 2021). CRIP1a interacts with the CB1R to modulate its cellular signaling; however, the mechanism by which CRIP1a impacts CB1R-Gi heterotrimer interactions in neurons is unknown. We hypothesized that CRIP1a modulates CB1R signaling via an association with the  $G\alpha_i$  subunit after the  $G\alpha_i$  subunit is released from the GPCR. We tested this hypothesis by treating N18TG2 mouse neuroblastoma detergent-free cell homogenates with  $GTP\gamma S$  to dissociate  $G\alpha_i$ . After sedimentation into cytosolic versus membrane fractions, immunoprecipitated CRIP1a co-migrated on SDS-PAGE gels with  $G\alpha_i$  with a shift in mobility for these proteins. Immunoblotted CRIP1a and  $G\alpha_i$  band densities were quantitated using LI-COR Empiria software for statistical analyses. CRIP1a and  $G\alpha_i$  co-migrated as an SDS-resistant complex, consistent with the myristoylated- $G\alpha_i$  intercalating within the hydrophobic interior of the CRIP1a barrel structure. The density of the mobility-shifted complex appeared to move from the membrane to cytosolic fraction within 10 minutes of treatment of the homogenate with  $GTP\gamma S$ . The shift from membrane to cytosolic fraction is consistent with  $G\alpha_i$  disassociating from the G-protein heterotrimer after binding of the non-hydrolyzable GTP analog. The CB1R full agonist CP55940 was also used to treat N18TG2 cell homogenates within a similar time-course. We further tested the hypothesis by using a proximity ligation assay (PLA) to detect CRIP1a and  $G\alpha_i$  within 40 nm of each other, and cellular marker staining in intact N18TG2 cells. N18TG2 cell treatment with 100 nM CP55940 determined that CRIP1a and  $G\alpha_i$  co-localize near the plasma membrane (stained with Na/K-ATPase or extracellular CB1R antibodies) within 30-90 seconds of agonist treatment. Collectively, these data suggest CRIP1a is a cargo-carrying protein capable of binding the myristoylated- $G\alpha_i$  subunit near the plasma membrane in a  $GTP\gamma S$  and agonist-dependent manner.

These studies were supported by NIH grants R01-DA042157, and F31-DA056188, and the Wake Forest University Cowgill Fellowship.

# Early Life Adversity Disrupts Social Preference and Opioid Reward Mechanisms in Adolescent Mice

Malabika Maulik,<sup>1</sup> Madison Michels,<sup>2</sup> Kayla DeSchepper,<sup>3</sup> Angela Henderson-Redmond,<sup>1</sup> Daniel Morgan,<sup>1</sup> and Swarup Mitra<sup>3</sup>

<sup>1</sup>Marshall Univ; <sup>2</sup>Davis and Elkins College; and <sup>3</sup>Marshall University

**Abstract ID 22240**

**Poster Board 1**

Early life adversity in form of poor postnatal care is a major developmental stressor impacting behavior later in life. Previous studies have shown the impact of early life stress on behavioral and neural abnormalities. Specifically, research have demonstrated how early life stress in form of reduced bedding and nesting materials can result in sex-specific behavioral deficits and aberrations in the cerebellar regions of adult rodents. Little is known about how such alterations in cerebellar regions due to early developmental stress impact drug-seeking and reward mechanisms. To address this question, we assessed behavioral outcomes in adolescent C57/BL6 mice who were exposed to limited bedding and nesting materials at postnatal days 2–9. The animals were tested for a battery of behaviors including open field, novel object recognition, social preference, elevated plus maze, and morphine-induced conditioned place preference. There was a significant reduction in social preference in animals that underwent early-life stress compared to normally reared animals (t-test,  $p < 0.05$ ). Our results also indicated that animals undergoing post-partum adversity had increased preference towards the morphine-paired chamber in the morphine-induced conditioned place preference test (t-test,  $p < 0.05$ ). No differences were observed between the groups in novel object recognition or elevated plus maze. To identify cerebellar epigenetic markers that might underlie these behavioral deficits, we performed mRNA analysis of deep cerebellar nuclei and identified putative factors that might have a role in these behaviors. The current study aims to further understand how stress-induced neurodevelopmental changes can influence neuronal remodeling and affect addiction vulnerability in adolescents.

This project was funded by grants R01DA044999 and P20GM103434 from the National Institutes of Health.

# Nicotinamide Adenine Dinucleotide (NAD) Attenuates the Rate-Decreasing Effects of Oxycodone Withdrawal in Rats with No Apparent Abuse Liability

Sarah Melton,<sup>1</sup> Tamara Morris,<sup>1</sup> Ashley Henderson,<sup>1</sup> Aslan Abdurrahman,<sup>2</sup> Will Smith,<sup>3</sup> Ashton Friend,<sup>3</sup> Richard Mestayer,<sup>4</sup> and Peter J. Winsauer<sup>5</sup>

<sup>1</sup>Louisiana State Univ Hlth Sci Ctr; <sup>2</sup>James J. Peter's VA Medical Center; <sup>3</sup>Louisiana State University Health Science Center; <sup>4</sup>Springfield Wellness Center; and <sup>5</sup>Louisiana State Univ Health Science Ctr

Abstract ID 56040

Poster Board 2

**Background:** Two current treatments for opioid use disorder (OUD) are the chronic administration of buprenorphine (partial opioid receptor agonist) or methadone (full opioid receptor agonist), as both of these agonists can alleviate withdrawal symptoms. However, neither of these drugs transition individuals with OUD to abstinence, and they both have an abuse liability. We examined whether the intravenous administration of the small molecule NAD<sup>+</sup> could effectively attenuate withdrawal and transition individuals to abstinence (Experiment 1) while also having no abuse liability (Experiment 2).

**Methods:** In Experiment 1, prior to establishing oxycodone dependence, seven Long-Evans rats (4 male and 3 female) were trained to lever press under a fixed-ratio 30 schedule for food reinforcers. When responding stabilized, subjects were administered an increasing chronic regimen of oxycodone (i.e., 3.2 mg/kg of oxycodone once daily, 3.2 mg/kg twice daily, and 10-18 mg/kg twice daily) until both spontaneous and precipitated withdrawal were reflected by disruptions in overall response rate (responses/second) and pre-ratio pausing (seconds). Precipitated withdrawal was demonstrated by administering increasing cumulative doses of naltrexone i.p. (0.32-3.2 mg/kg). After disruption of behavioral responding (withdrawal) was demonstrated consistently, indicating dependence, surgery was performed to implant a catheter and port. Twenty-four hours following catheterization, the chronic oxycodone regimen was restarted for the recovery period from surgery and for reestablishing responding under the operant schedule. When responding stabilized, the chronic regimen of oxycodone was permanently discontinued, and subjects were infused i.v. with either saline or 180 mg/kg of NAD<sup>+</sup> each night for 10 hours per day for 10 consecutive days. Subjects responded under the operant task every afternoon during the 10 days to assess the disruptions in behavior. In Experiment 2, four male Sprague-Dawley rats were trained to respond under a fixed-ratio 10 schedule of oxycodone reinforcement after catheterization. During these sessions, overall response rate and pre-ratio pausing (PRP) were recorded. After self administration was established for an oxycodone training dose of 0.032 mg/kg/infusion, saline or NAD<sup>+</sup> (1.57 or 3.2 mg/kg/infusion) was substituted for oxycodone until one of three criteria were met.

**Results:** In Experiment 1, precipitated and spontaneous withdrawal from oxycodone decreased response rate and increased PRP. When oxycodone was permanently discontinued, subjects given 10 days of i.v. NAD<sup>+</sup> recovered their pre-chronic baseline of responding after 2 days of oxycodone cessation, while the saline group recovered their pre-chronic baseline after 4 days. PRP was also restored more quickly in the NAD<sup>+</sup> group than the saline group. In Experiment 2, the mean number of oxycodone infusions was  $23.6 \pm 7.6$ , whereas the number of infusions was markedly reduced when saline (6.7) or NAD<sup>+</sup> ( $6.2 \pm 3.7$  and  $1.6 \pm 0.89$ ) was substituted for oxycodone.

**Conclusion:** In our rodent model of opioid-dependence, i.v. NAD<sup>+</sup> infusions reduced the duration and magnitude of the rate-decreasing effects of oxycodone, which were a direct reflection of withdrawal. Of the NAD<sup>+</sup> infusion doses tested, neither dose substituted for oxycodone and produced levels of responding closer to those for saline. These results reveal that NAD<sup>+</sup> may have promising potential as a treatment for dependence.

# R-(-)-2,5-dimethoxy-4-iodoamphetamine [(-)-DOI] decreases cocaine demand in a 5-HT<sub>2A</sub>R-mediated manner

Leah Salinsky,<sup>1</sup> Christina R. Merritt,<sup>1</sup> Noelle C. Anastasio,<sup>1</sup> and Kathryn A. Cunningham<sup>1</sup>

<sup>1</sup>Univ of Texas Medical Branch

Abstract ID 27882

Poster Board 3

**Aims:** Drug overdose deaths within the U.S. reached an unprecedented high, surpassing 100,000 in 2021. Cocaine overdoses account for ~15,000 deaths each year and cocaine use disorder (CUD) remains a challenge to treat, with the current standard of care reliant primarily on psychosocial interventions, such as cognitive behavioral therapy. Efficacious pharmacotherapeutic support for CUD is an important goal in our field. In the last decade, there has been a resurgence of interest in serotonergic psychedelics as potential therapeutics for substance use and mental disorders, including CUD. Agonist actions at the serotonin (5-HT) 5-HT<sub>2A</sub> receptor (5-HT<sub>2A</sub>R) contribute importantly to psychedelic mechanisms of action, and the efficacy of these compounds in limiting cocaine intake is unknown. In the present studies, we tested the hypothesis that the psychedelic 5-HT<sub>2A</sub>R agonist R-(-)-2,5-dimethoxy-4-iodoamphetamine (DOI) will decrease cocaine demand in a rodent behavioral economics model.

**Methods:** Male, Sprague-Dawley rats (n = 28) were trained to self-administer cocaine (0.75 mg/kg) for daily 180-min sessions until stability on an FR3 schedule of reinforcement. Upon stability, daily sessions on the threshold procedure were initiated. During each 110-min session, progressively smaller doses of cocaine were available. The duration of infusion decreased by 0.25 log per block across 11 blocks lasting 10-min each, decreasing the dose of drug earned per infusion from 0.75 mg/kg/inf to 0.003 mg/kg/inf. Pharmacological testing with DOI treatment (0.03, 0.1, 0.3 mg/kg; s.c., 20 min prior to session) began upon establishment of stable demand elasticity ( $\alpha$ ) and demand intensity ( $Q_0$ ). Treatment with the selective 5-HT<sub>2A</sub>R antagonist M100907 (0.01 mg/kg; i.p., 30 min prior) was employed to assesses the role of the 5-HT<sub>2A</sub>R in the behavioral effects of DOI. Demand curves for each subject were plotted with number of reinforcers earned[KC1] (consumption, mg) as a function of FR requirement (price) and the data were fitted using an exponential model. The effect of DOI on measurements of cocaine demand was analyzed with an experiment-wise error rate of  $\alpha=0.05$ .

**Results:** Analysis indicated that DOI treatment dose-dependently decreased cocaine demand elasticity, price point at maximum expenditure, maximum expenditure, essential value, breakpoint, and the area under the demand curve ( $p < 0.05$ ) without altering measurements of task disruption. DOI did not significantly alter cocaine demand intensity. The selective 5-HT<sub>2A</sub>R antagonist M100907 prevented DOI-induced suppression of most measures in the cocaine demand paradigm ( $p < 0.05$ [KC2]).

**Conclusions:** The current studies reveal that the psychedelic DOI decreases the motivational effects of cocaine, which were reversed by the 5-HT<sub>2A</sub>R antagonist M100907. These data suggest that while cocaine may still be reinforcing[ANC3] at minimal prices, the rats are less willing to work for cocaine after DOI pretreatment, and provide support for expanded interrogation of the efficacy of 5-HT<sub>2A</sub>R agonist psychedelics in counteracting the behavioral effects of cocaine.

This work was supported by Center for Addiction Research at the University of Texas Medical Branch.

# Opioid-related discriminative stimulus, antinociceptive and respiratory depressant effects of substituted 3-hydroxy-N-phenethyl-5-phenylmorphans

Carol Paronis,<sup>1</sup> Tyler J. Lee,<sup>1</sup> Mauricio Ruiz Soler,<sup>1</sup> Dana R. Chambers,<sup>2</sup> Joshua Lutz,<sup>2</sup> Dan Luo,<sup>3</sup> Thomas Prisinzano,<sup>4</sup> Agnieszka Sulima,<sup>2</sup> Arthur Jacobson,<sup>2</sup> Kenner Rice,<sup>2</sup> and Jack Bergman<sup>1</sup>

<sup>1</sup>McLean Hospital/Harvard Medical School; <sup>2</sup>NIDA and NIAAA; <sup>3</sup>University of Kentucky; and <sup>4</sup>Univ of Kentucky

Abstract ID 18116

Poster Board 4

**Aim:** Delta opioid receptor (DOR) signaling mechanisms have been proposed to decrease the side effect liability associated with morphine-like prescription opioids. We evaluated this proposition by determining the acute effects of six novel opioid agonists in assays of morphine discrimination in rats, and antinociception, operant performance and respiratory function in nonhuman primates.

**Methods:** 6 novel 3-hydroxy-N-phenethyl-5-phenylmorphans (C9-alkyl substituted compounds with varying stereochemistry) were synthesized at the NIDA and NIAAA IRP. In vitro assays using commercially available kits (e.g. HitHunter for cAMP accumulation) indicated the compounds have no efficacy at kappa opioid receptors (KOR), no to low efficacy at DOR, and some inhibitory effects at DOR or KOR. The compounds had efficacy ranging from low (105) to moderate (76a, 111, 90b) to high (76b, 142) at mu opioid receptors (MOR). In behavioral studies, full dose-effect functions for all six compounds were first determined in rats (n=7-9) trained to discriminate 3 mg/kg morphine from saline. Next, effects in squirrel monkeys (n=3-5/group) were determined using cumulative dosing procedures in two assays. In one set of studies, tail-withdrawal latency from 52°C water (antinociception) and effects on food-maintained operant responding (behavioral disruption) were concurrently evaluated. In other studies, whole body plethysmography in the presence of normal air and air mixed with 5% CO<sub>2</sub> was used to obtain respiratory parameters (breathing frequency, tidal volume, minute volume).

**Results:** Four compounds (76b, 105, 142, and 111) fully substituted for morphine in discrimination studies; one compound (76a) partially substituted (>70% drug-lever responding), and one compound (90b) did not generalize from the morphine stimulus (~25% drug-lever responding). All morphine-like discriminative stimulus effects were attenuated by pretreatment with 0.1 mg/kg naltrexone. In squirrel monkeys, compounds 76b and 142 had antinociceptive effects, behaviorally disruptive, and ventilatory effects similar to those of morphine. The remaining compounds had similarly disruptive effects on food-maintained operant responding but produced only limited effects on ventilation. Only three of the four (111, 90b, and 76a) had moderate to full antinociceptive effects.

**Conclusion:** These data demonstrate that the presence of agonist or antagonist activity at DOR may have greater influence on the effects of partial MOR agonists (76a, 111, and 90b) than on either full agonists (76b, 142) or very low efficacy agonists (105).

Supported by NIH Grant DA047574

# Behavioral and Neurochemical Effects of Extended Access to Stimulant Self-Administration in Rats

Robert Seaman,<sup>1</sup> Kariann Lamon,<sup>2</sup> Nicholas Whitton,<sup>2</sup> Agnieszka Sulima,<sup>3</sup> Kenner Rice,<sup>3</sup> Kevin Murnane,<sup>2</sup> and Gregory T. Collins<sup>1</sup>

<sup>1</sup>Univ of Texas Health Science Center at San Antonio; South Texas Veterans Health Care System; <sup>2</sup>Louisiana State Univ Health Sciences Center - Shreveport; and <sup>3</sup>Molecular Targets and Medications Discovery Branch, Drug Design and Synthesis Section

Abstract ID 15027

Poster Board 5

Approximately 20 million people in the United States are classified as having a substance use disorder. Given the chronicity of this disorder, it is crucial to gain a better understanding of the toxicity associated with prolonged drug use. Regarding stimulants, monoamine releasers (e.g., methamphetamine) rather than monoamine reuptake inhibitors (e.g., cocaine) are typically associated with neuroinflammatory and neurodegenerative effects that are thought to underlie cognitive dysfunction. Interestingly, recent data suggest that MDPV (a synthetic cathinone that functions as a monoamine reuptake inhibitor), has neurotoxic effects; however, the cognitive and neurochemical consequences of MDPV self-administration remain largely unexplored. Furthermore, despite the fact that drug preparations that contain MDPV often also contain caffeine, little is known regarding the toxic effects produced by co-use of these two stimulants. The current study aims to investigate the degree to which self-administered MDPV and a mixture of MDPV+caffeine can produce deficits in recognition memory relative to methamphetamine and cocaine. Male Sprague-Dawley rats (n=8/group) were allowed 90-min or 12-h access to grain pellets on one lever and infusions of either MDPV (0.032 mg/kg/inf), MDPV+caffeine (0.032 mg/kg/inf + 0.11mg/kg/inf, respectively), methamphetamine (0.1 mg/kg/inf), cocaine (0.32 mg/kg/inf), or saline on the other lever for 5 days per week, for 6 weeks. Novel object recognition was evaluated prior to any drug self-administration history, 3 and 6 weeks after rats had begun self-administering, and once more following a 3-week drug-free period. Rats that had 12-h access to MDPV, MDPV+caffeine, or methamphetamine exhibited time-dependent deficits in the novel object recognition assay relative to rats given access to saline. No deficits were observed in rats that self-administered cocaine in 12-h sessions. Rats provided 90-min access to a mixture of MDPV+caffeine also exhibited deficits in recognition memory, whereas 90-min access to other reinforcers did not result in recognition memory deficits. Degrees of monoamine depletion largely coincided with recognition memory deficits. These data suggest that unlike cocaine, the prototypical monoamine reuptake inhibitor, MDPV is capable of producing memory deficits often associated with neuroinflammation and/or neurodegeneration. These data also demonstrate that mixtures of MDPV+caffeine produce deficits in recognition memory following both 90-min and 12-h access, suggesting that caffeine might be enhancing toxicity produced by MDPV. Future studies will evaluate markers of neuroinflammation in these rats and explore pharmacological avenues to mitigate stimulant-induced cognitive deficits.

Supported by NIH/NIDA [(R01DA039146; GTC), (P20GM121307, R01NS120676; KSM)], and the IRPs of NIDA and NIAAA (KCR).

# Eating a High Fat/High Carbohydrate or Ketogenic Diet Does Not Impact Sensitivity to Morphine-induced Antinociception in Rats with Hindpaw Inflammation

Katherine M. Serafine,<sup>1</sup> Madeline K. Elsey,<sup>2</sup> Nina M. Beltran,<sup>1</sup> and Vanessa Minervini<sup>3</sup>

<sup>1</sup>Univ of Texas at El Paso; <sup>2</sup>Univ of Texas, El Paso; and <sup>3</sup>Creighton University

Abstract ID 56470

Poster Board 6

The obesity epidemic continues to be a pervasive, global concern, and individuals diagnosed with obesity have a higher prevalence of chronic pain. While obesity is thought to be caused by a multitude of factors, one contributing factor that has received attention in recent years is the overconsumption of high fat/high carbohydrate foods. Previous literature has demonstrated that eating high fat/high carbohydrate diets can increase sensitivity of rats to stimulant drugs, such as cocaine, but it is not known if eating a high fat/high carbohydrate diet might impact sensitivity to other drugs, such as opioids (e.g., morphine) in the context of inflammatory pain-relief. Further, not all high fat diets are associated with increased weight gain or obesity. For example, the ketogenic diet (which is high in fat and very low in carbohydrates) has been associated with weight loss. To explore whether these dietary manipulations impact sensitivity of rats to morphine-induced antinociception in a model of inflammatory pain, in the present study 24 female Sprague Dawley rats ( $n=8$ /group) ate a standard laboratory chow (17% kcal from fat), a traditional high fat/high carbohydrate chow (60% kcal from fat), or a ketogenic (high fat/low carbohydrate) chow (90.5% kcal from fat). It was hypothesized that rats eating high fat chow would be more sensitive to the effects of morphine than rats eating other diets. Rats ate their assigned diets for 5 weeks before the experimental testing began. Approximately 24-hours before the first test, unilateral hindpaw inflammation was induced by injecting 0.1mL of complete Freund's adjuvant (CFA) or saline into the footpad. A saline injection, followed by 4 cumulative injections of morphine (1.0-17.8 mg/kg IP) were administered every 15 minutes, and 13 minutes after each injection, the force that resulted in paw withdrawal was recorded. Morphine tests were repeated once per week, for 4 consecutive weeks. Morphine dose-dependently increased paw withdrawal force across all groups for both the CFA- and saline-injected paws; however, there were no group differences between rats eating different diets during any of the 4 weeks of morphine testing. These results suggest that while dietary factors can impact neurochemistry and sensitivity to other types of drugs, the antinociceptive effects of morphine appear to be comparable regardless of the type of food an individual might consume. Future studies will explore potential sex-differences and assess the impact of dietary manipulation on other opioid-induced effects, including their rewarding and reinforcing effects.

M.E. was supported by NIGMS linked awards RL5GM118969, TL4GM118971, and UL1GM118970 and by an ASPET SURF award.

K.M.S., was supported NIDA award R25DA033613, and this project was also sponsored by a NIDA RCMI supplement under award 3U54MD007592-29S4.

# GPR183 Activation in the Peripheral Nervous System Induces Behavioral Hypersensitivities in Rats

Kyle Oberkrom,<sup>1</sup> Kathryn Braden,<sup>2</sup> Zhoumou Chen,<sup>1</sup> Luigi A. Giancotti,<sup>1</sup> Christopher K. Arnatt,<sup>3</sup> and Daniela Salvemini<sup>4</sup>

<sup>1</sup>Saint Louis University; <sup>2</sup>Washington University in Saint Louis; <sup>3</sup>Saint Louis Univ; and <sup>4</sup>Saint Louis Univ Sch of Medicine

**Abstract ID 25203**

**Poster Board 7**

Neuropathic pain is a global health concern. Neuropathic pain is poorly managed; current pharmacological therapies have limited efficacy and multiple side effects. Novel therapeutic approaches are needed. Our group has identified the G-protein coupled receptor (GPCR), GPR183, as a non-opioid based target for therapeutic intervention with selective GPR183 antagonists. GPR183 is expressed in a number of immune cells known to be involved in neuropathic pain states such as T cells, as well as in glia and neurons. Interestingly, this expression in the nervous system correlates with key areas of the pain neuroaxis including in human spinal cord and dorsal root ganglia. We have recently reported that GPR183 plays a role in central sensitization. However, the role of GPR183 in peripheral sensitization is not known and was the subject of our investigation. In rats, intraplantar injection of  $7\alpha,25$ -dihydroxycholesterol ( $7\alpha,25$ -OHC), the most potent ligand for GPR183, induced behavioral hypersensitivities associated with neuropathic pain states (i.e. thermal hyperalgesia and mechano-allodynia). These effects were blocked by an inhibitor of GPR183, SAE14. At the molecular level, we found that GPR183 induced hypersensitivities were driven by the mitogen activated protein kinase, ERK. Indeed, U0126, a well characterized MEK/ERK inhibitor blocked  $7\alpha,25$ -OHC-induced behavioral hypersensitivities. Our results provide the first evidence implicating GPR183 signaling in the development of peripheral sensitization and first mechanistic insight on molecular pathways engaged downstream, of this GPCR opening the doors for future investigations into this novel pathway.

Supported by start-up funds of Dr. Salvemini and Dr. Arnatt, the National Institutes of Health (NIH) Grant R01NS128004, and the NIH Training Grant T32 GM141602-01 A1 (KDO)



# KATP channel prodrugs reduce hypersensitivity in neuropathic and inflammatory pain models, morphine-induced hypersensitivity, and reduce withdrawal behaviors in mice

Amanda Klein,<sup>1</sup> Alexis Doucette,<sup>1</sup> Kayla Johnson,<sup>1</sup> Shelby Hulke,<sup>1</sup> Sunna Mujteba,<sup>1</sup> Elena Miller,<sup>1</sup> and Peter I. Dosa<sup>1</sup>

<sup>1</sup>University of Minnesota

Abstract ID 16640

Poster Board 8

Pharmaceutical strategies to utilize KATP channels for therapeutics have been hindered due to low solubility and/or ability to be delivered systemically. Recently developed novel prodrugs with high aqueous solubility, called cromakalim prodrugs (CKLP), are based on the structure of the KATP channel opener cromakalim. Cromakalim, and other KATP channel openers, has been shown to reduce hyperalgesia in various chronic pain models in rodents. KATP channels are also downstream of mu-opioid receptor signaling, and opioid antinociception can be attenuated after blocking or downregulating KATP channel function. The objective of this study is to test novel KATP channel-targeting prodrugs in rodent models of neuropathic and inflammatory pain in addition to opioid tolerance after chronic morphine administration. Male and female mice were subjected to spinal nerve ligation (SNL) or intraplantar injection of Complete Freund's Adjuvant (CFA) to induce a model of neuropathic and inflammatory pain, respectively. Intrathecal administration of either of the KATP channel prodrugs, CKLP1, CF3-CKLP1, or CKLP2 (0-60ug) attenuated mechanical hypersensitivity after SNL or CFA compared to vehicle (saline). Mechanical hypersensitivity was improved in mice during chronic morphine treatment (15mg/kg, twice daily, 5 days) with administration of either CKLP1, CF3-CKLP1, or CKLP2. Naloxone precipitated withdrawal behaviors, were improved after CKLP2 administration, including jumping and rearing measured one day after the completion of morphine tolerance. These results are consistent with our previous data indicating non-water soluble KATP channel agonists produce analgesia and attenuate morphine tolerance in mice. Newly developed, cromakalim prodrug 1 (CKLP1), CF3-CKLP1, and CKLP2 are water-soluble KATP channel openers that could be useful to reduce chronic pain, opioid tolerance, and withdrawal.

This research was funded by National Institutes of Health (K01DA042902, R01DA051876 to Klein) and the University of Minnesota Pain Consortium. This work was also partially funded by the Summer Undergraduate Research Program from the UMD Chemistry and Biochemistry Department and the Undergraduate Research Opportunity Program from the University of Minnesota.

# Differential effects of kappa opioid receptor activation and blockade on the development of methamphetamine-induced sensitization in adult male and female rats

Manoranjan D'Souza,<sup>1</sup> Madison Snyder,<sup>2</sup> and Sarah Seeley<sup>2</sup>

<sup>1</sup>Ohio Northern Univ; and <sup>2</sup>Ohio Northern University

Abstract ID 16371

Poster Board 9

Over the last decade the illicit use and abuse of methamphetamine has increased in the United States. Repeated and intermittent use of methamphetamine can lead to sensitization of brain circuits, which can promote continued abuse of methamphetamine. However, neural substrates underlying methamphetamine-induced sensitization are not fully understood. In this proposal, we specifically evaluated the role of kappa opioid receptors (KORs) in the development of methamphetamine-induced sensitization in adult male and female rats. In animals, methamphetamine-induced sensitization manifests as enhanced behavioral response to a dose of methamphetamine after a period of repeated intermittent methamphetamine treatment compared to response to the same dose of methamphetamine prior to exposure to repeated methamphetamine treatment. The experiment was conducted over 28 days and locomotor activity (primary dependent measure) was measured on Days 1, 2, and 28. All animals received saline on Day 1. Animals then received methamphetamine (0.5 mg/kg; i.p.) on Day 2 and Day 28. Animals were treated daily with a single injection of methamphetamine (1 mg/kg; i.p.) for 6 days (Days 3-8; period of repeated intermittent exposure). Animals received no methamphetamine treatment between Days 9-27 (drug-free period). This drug-free period allows for methamphetamine-induced neurobiological changes to take place, which are hypothesized to play a role in the sensitized response to methamphetamine. To assess the role of KOR receptors, animals received a single injection of either the KOR agonist (U50488; 1.5 mg/kg; s.c.) or saline (1 ml/kg; s.c.; control) daily for 6 days (Days 3-8), 30 minutes prior to receiving methamphetamine (1 mg/kg; i.p.). Other groups of animals received either the KOR antagonist (norBNI; 15 mg/kg; s.c.) or saline (1 ml/kg; s.c.; control) on Day 2 after measurement of methamphetamine-induced locomotor activity. Animals received only one injection of the KOR antagonist (norBNI) because of its long duration of action (~28 days). Data obtained from the study suggests that activation of the KORs using the KOR agonist (U50488; 1.5 mg/kg; i.p.) significantly decreased methamphetamine-induced sensitization in adult female, but not male rats, compared to respective controls. In contrast, blockade of the KORs using the KOR antagonist (norBNI, 15 mg/kg; s.c.) significantly increased methamphetamine-induced sensitization in adult male, but not female rats, compared to respective controls. Based on the data we can suggest an inhibitory role of KORs in the development of methamphetamine-induced sensitization in adult male rats, which was unmasked by blocking KORs prior to methamphetamine exposure. Together, the data suggest a sex-dependent differential role for KORs in the development of methamphetamine-induced sensitization in adult male and female rats.

Dr. D'Souza was supported by an endowed fellowship (Pharmacy Centennial Alumni Chair) and a Bower, Bennett and Bennett summer grant awarded by the Raabe College of Pharmacy, Ohio Northern University (ONU), Ada, Ohio.

# Inhibition of ACAT as a Therapeutic Target for Alzheimer's Disease is Independent of ApoE4-lipidation

Ana Valencia,<sup>1</sup> Deebika Balu,<sup>2</sup> Naomi Faulk,<sup>1</sup> Jason York,<sup>1</sup> and Mary Jo LaDu<sup>3</sup>

<sup>1</sup>University of Illinois at Chicago; <sup>2</sup>Univ of Illinois at Chicago; and <sup>3</sup>Univ of Illinois-Chicago

Abstract ID 24886

Poster Board 10

**Background:** While the mechanism(s) underlying *APOE4*-induced AD risk remains unclear, apoE4 levels in the brains of humans and transgenic mice (Tg) expressing human *APOE4* are lower than those expressing *APOE3*, and apoE4-lipoproteins are poorly lipidated compared to apoE3-lipoproteins. Increasing the lipidation of apoE4 can stabilize apoE4-lipoproteins, thus making this process an attractive therapeutic target. Several enzymes affect CNS cholesterol levels including ACAT (acyl-CoA:cholesterol-acyltransferase), which catalyzes the formation of intracellular cholesteryl-ester droplets, reducing the intracellular free cholesterol (FC) pool. Inhibition of ACAT increases the FC pool, making the lipids available for secretion to extracellular apoE-containing lipoproteins. Previous studies using commercially available ACAT inhibitors, including Avasimibe (AVAS), as well as ACAT-knock out (KO) mice, demonstrate reduced plaque burden, gliosis, amyloid-beta peptide (A $\beta$ ), and altered amyloid precursor protein (APP) processing in familial AD (FAD)-Tg mouse models. However, the effects of AVAS in the presence of human apoE4 remain unknown. Our hypothesis is that AVAS, via inhibition of ACAT, will increase the FC pool, promoting ABCA1-mediated efflux of cholesterol to nascent apoE4-lipoproteins. This correction of apoE4 structure via lipidation will restore its function in the CNS, including clearance of oA $\beta$  and reducing neuroinflammation.

**Methods:** Male E4FAD-Tg mice (5xFAD<sup>+/-</sup>/*APOE4*<sup>+/+</sup>) were treated by oral gavage with AVAS from 6-8 months. Synaptic proteins were measured by Western blot and learning and memory by Morris Water Maze (MWM). Lipid droplets/cell were analyzed by staining with LipidSpot. Ab pathology was evaluated by measuring Ab solubility (3-step sequential extraction followed by ELISA) and Ab/amyloid deposition (immunostaining). Neuroinflammation (astrogliosis and microgliosis) were evaluated by immunohistochemistry. ApoE levels and lipidation were analyzed by apoE-ELISA and native gels.

**Results:** AVAS treatment significantly reduced intracellular lipid droplets, demonstrating indirect target engagement, increased MWM measures of memory and postsynaptic protein levels, indicating surrogate efficacy, and reduced pathological changes in A $\beta$  solubility/deposition, and neuroinflammation, all critical components of *APOE4*-modulated AD pathology. However, there was no increase in apoE4 levels or lipidation, while amyloidogenic processing of APP was significantly reduced.

**Conclusion:** This study suggests that the AVAS-induced reduction in A $\beta$  via reduced APP processing was sufficient to reduce AD pathology, while apoE4-lipoproteins remained poorly lipidated.

This study was partially sponsored by AbbVie, Inc. AbbVie contributed to the study design, research, and interpretation of data, reviewing, and approving the manuscript.

# Characterizing a Mesolimbic Circuit for Opioid Reward

Ruben A. Garcia-Reyes,<sup>1</sup> and Daniel Castro<sup>2</sup>

<sup>1</sup>*Biophotonics Research Center, Mallinckrodt Institute of Radiology Washington University School of Medicine in St. Louis; and*

<sup>2</sup>*Washington University School of Medicine in St. Louis*

**Abstract ID 17668**

**Poster Board 11**

A circuit mechanism was recently identified by our lab in which mu opioid peptide receptors (MOPRs) act to control reward consumption. We found that MOPRs are expressed on the lateral dorsal raphe nucleus (LDRN) terminals that project to the nucleus accumbens medial shell (mNAcSh) and are activated by retrogradely released enkephalin from mNAcSh itself (LDRN→mNAcSh). While MOPRs in mNAcSh are important for reward consumption, MOPRs necessarily act in concert with other neurochemical actuators. Recent data demonstrated that stimulation of non-specific LDRN→mNAcSh terminals could evoke either inhibitory or excitatory postsynaptic potentials in mNAcSh neurons, indicating that both GABAergic (vGAT) and glutamatergic (vGlut2) subpopulations are included in the LDRN→mNAcSh circuit. Whether vGAT or vGlut2 subcircuits have distinct roles in reward consumption is unknown. To isolate the potential subpopulation driving the expression of reward consumption behaviors, we simultaneously recorded vGlut2 and vGAT terminal activity using two calcium biosensors via dual-color fiber photometry in a sucrose consumption task. In this task, mice were allowed to consume sucrose pellets that were non-contingently delivered throughout the test session. Mice were tested ad libitum or after 24 hours of acute food deprivation. Additionally, mice were tested after systemic administration of the opioid antagonist naloxone to test if terminal activity depended on endogenous opioid receptors. We hypothesized that vGlut2, but not vGAT, terminal activity would decrease at the onset of sucrose consumption, and this decrease would be opioid dependent. Our rationale was informed by extensive literature indicating that consummatory behavior in mNAcSh is primarily mediated by decreased neural activity. Preliminary data suggests that vGlut2 terminal activity was reduced during reward consumption. Oppositely, vGAT terminal activity appears to slightly increase activity during the same behavioral epoch. While these results were represented across all conditions, the decrease in vGlut2 terminal activity was more robust during the food deprivation state. These findings provide initial, but greater understanding of the complex transient interactions glutamate could be playing in our LDRN→mNAcSh circuit. In the future, we will target each neural subpopulation via optogenetic stimulation to modulate reward consumption.

# Characterizing How Lesioning of Cocaine Activated Ensembles in the Nucleus Accumbens Affects Cocaine Related Behaviors

Rishik Bethi,<sup>1</sup> Kim Thibeault,<sup>2</sup> and Erin Calipari<sup>2</sup>

<sup>1</sup>Vanderbilt Univ; and <sup>2</sup>Vanderbilt University

Abstract ID 15709

Poster Board 13

As a brief background, substance use disorder (SUD) is fundamentally a learning disorder that affects millions across the nation. Within the mesocorticolimbic system, the nucleus accumbens (NAc) is ideally situated to process reward information which makes it a key region involved in SUD. Moreover, recent studies have shown that neuronal ensembles, coordinated populations of neurons, within the NAc can be activated to specific stimuli, including drugs of abuse. This developing ensemble theory has made these neuronal ensembles potential therapeutic targets for treating maladaptive drug seeking. Our project aims to characterize these neuronal ensembles activated by cocaine to assess their role in cocaine use disorder. Specifically, we plan to characterize how lesioning of these cocaine activated ensembles in the NAc affects cocaine related behaviors. New technological advances have led to the development of genetic mouse lines that allow for activity-dependent expression of viruses, which we use to modulate ensemble activity. Using an Arc-CreER<sup>T2</sup> mouse line, a Cre-dependent diphtheria toxin was injected into the NAc to lesion neuronal ensembles specifically activated to chronic cocaine and withdrawal. Using these two groups and a control, we sought to characterize the role of this ensemble in reinforcement learning and other cocaine-related behaviors. We had mice perform a positive reinforcement task for sucrose and determined the active pokes after acquisition and the total average sucrose infusions. Interestingly, we found that lesioning either the ensemble recruited by chronic cocaine or withdrawal does not attenuate reinforcement learning or motivated behavior, as there was no significant difference in the days to acquire the task or the average infusions. Next, we also had mice perform a negative reinforcement task for shock avoidance and determined the percent correct trials, the days to >75% correct trails, total shocks, and escapes. Here, we also found that lesioning either ensemble does not attenuate reinforcement learning or motivated behavior, with no significant difference among the 3 groups. Lastly, in animal models, cocaine use is also associated with locomotor disturbances, where mice move significantly more after repeated exposure to cocaine. Therefore, we also investigated whether there were any effects of lesioning the cocaine ensembles on cocaine locomotor sensitization. Here we found that both the control group and the group lesioned to withdrawal were sensitized to a challenge injection of cocaine. However, lesioning the chronic cocaine ensembles resulted in the group not being sensitized, as they did not have a significant difference in locomotion from the initial cocaine injection to a final injection on the sensitization day. Together, these results suggest that the ensembles recruited after a history of cocaine are not necessary for reinforcement learning and motivated behavior. However, the chronic cocaine ensemble may be critically in the pathways that underlie locomotor behaviors associated with repeated cocaine use. Characterizing the role of these ensembles in the brain sheds light on how reinforcement learning processes are dysregulated and will provide crucial insight in finding effective treatment strategies.

# Social Isolation Stress Leads to Synaptic Changes in Locus Coeruleus Noradrenergic Neurons

Jenny Kim<sup>1</sup>

<sup>1</sup>Washington University in St. Louis

**Abstract ID 54009**

**Poster Board 14**

Stress critically affects nociceptive processing. Although studies have shown that noradrenergic neurons in the locus coeruleus (LC-NE) are key to both the stress and pain response, the role of the LC-NE system in stress-induced changes to pain processing is yet unclear. Here, we aimed to investigate the effects of chronic social isolation stress on nociception, and whether isolation stress leads to changes in LC-NE activity. Synaptic transmission is vital in maintaining baseline LC activity, and synaptic plasticity can alter LC dynamics in response to external stimuli. Thus, by isolating and measuring miniature excitatory postsynaptic currents (mEPSCs) to determine changes in excitatory synaptic input to these cells, we can provide insight into the effects of social isolation on the LC-NE system. After 10-12 days of social isolation, we conducted Von Frey and hot plate experiments to test mechanical and thermal sensitivity, respectively. Socially isolated adult mice displayed both mechanical and thermal antinociception compared to group-housed controls. To determine whether synaptic changes to LC-NE neurons may have contributed to this stress-induced antinociception, we conducted whole-cell voltage clamp recordings of LC neurons in acute brain slices. mEPSCs were pharmacologically isolated by blocking voltage-gated sodium channels (TTX; 1  $\mu$ M), blocking GABA<sub>A</sub> receptors (picrotoxin, 100  $\mu$ M), and glycine (1  $\mu$ M strychnine) receptors. We found that social isolation causes greater probability of higher amplitude mEPSCs and decreased event frequency. Our results suggest that heightened excitatory input to the locus coeruleus neurons may contribute to the antinociception caused by social isolation. These findings provide key insight into how LC-NE neurons may modulate an integrated stress-pain response.

This project was funded by NIH/NINDS: R01NS117899.

# Genetic Brain Serotonin Deficiency Significantly Impacts a Subset of Behavioral and Molecular Responses to Psychostimulants in Mice

Benjamin Sachs,<sup>1</sup> Madeline Wujek,<sup>2</sup> Michelle M. Karth,<sup>2</sup> Melinda D. Karth,<sup>2</sup> Gianna M. Perez,<sup>2</sup> and Davis J. Van Dyk<sup>2</sup>

<sup>1</sup>Villanova Univ; and <sup>2</sup>Villanova University

Abstract ID 18359

Poster Board 15

Chronic use of psychostimulants, such as cocaine and amphetamine, has been linked to numerous adverse health consequences, including cardiovascular complications. An improved understanding of the causes of excessive psychostimulant intake has the potential to facilitate efforts to reduce the consumption of these drugs and improve human health. Both genetic and environmental factors are thought to influence responses to psychostimulants, but the precise genetic alterations that make individuals differentially sensitive to the effects of these drugs have not been completely defined. Psychostimulants are known to increase the extracellular levels of several neurotransmitters, including dopamine and serotonin (5-HT), and thus genetic alterations in either of these neurotransmitter systems could be predicted to lead to aberrant responses to these drugs. Based on the results of published pharmacological studies, we hypothesized that genetic brain 5-HT deficiency would reduce locomotor sensitization to cocaine and amphetamine. To model brain 5-HT deficiency, we used the tryptophan hydroxylase 2 (R439H) knock-in (KI) mouse line, which harbors a partial loss of function mutation in the brain 5-HT synthesis enzyme, tryptophan hydroxylase 2 (Tph2). Homozygous Tph2KI mutant animals (KI mice) have been shown to exhibit 60-80% reductions in the levels of brain 5-HT compared to their wild-type littermates. Our data reveal that brain 5-HT deficiency does not appear to influence locomotor responses to acute or repeated administration of cocaine or amphetamine. However, our preliminary data suggest that low brain 5-HT reduces sensitivity to amphetamine-induced conditioned place preference. Real-time PCR reveals that several psychostimulant-induced changes in gene expression were unaffected by brain 5-HT deficiency, but a significant genotype by drug interaction was observed for one of the candidate genes tested in the nucleus accumbens. This gene, anaplastic lymphoma kinase (Alk), has been previously implicated in cocaine sensitization and was upregulated in wild-type mice, but not KI animals. Overall, these data provide new insight into the importance of brain 5-HT levels in determining some of the behavioral and molecular responses to psychostimulants.

This study was supported by a Small Research Grant from the Villanova Institute for Research and Scholarship to BDS.

# Mitochondria as key mediators of behavioral and metabolic effects of stress

Erin Gorman-Sandler,<sup>1</sup> Breanna Robertson,<sup>2</sup> Jesseca Crawford,<sup>2</sup> Gabrielle Wood,<sup>2</sup> Noelle Frambes,<sup>3</sup> Marnie McLean,<sup>4</sup> Jewel Scott,<sup>5</sup> Michael J. Ryan,<sup>3</sup> Susan Wood,<sup>2</sup> Abbi Lane,<sup>4</sup> and Fiona Hollis<sup>2</sup>

<sup>1</sup>University of South Carolina; <sup>2</sup>University Of South Carolina School Of Medicine; <sup>3</sup>Columbia VA Healthcare System; <sup>4</sup>University of South Carolina Arnold School of Public Health; and <sup>5</sup>University of South Carolina College of Nursing

**Abstract ID 21427**

**Poster Board 16**

Postpartum depression (PPD) affects up to 20% of mothers yet remains understudied. Mitochondria are dynamic organelles that are crucial for cell homeostasis and share a link with many of the proposed mechanisms underlying PPD pathology. The brain relies on mitochondrial energy production to function, and stress, a major risk factor for PPD, amplifies brain energy demands. In turn, brain mitochondrial function is also affected by stress and linked to anxiety-like and social behaviors. We recently found that gestational stress in rats decreased mitochondrial complex I respiration in the prefrontal cortex (PFC) in association with depressive-like behaviors. We hypothesized that enhancing complex I respiration during stress exposure would prevent these stress-induced PPD-relevant behaviors. Nulliparous and time-mated adult female Wistar rats received nicotinamide (NAM, a NAD<sup>+</sup> precursor that stimulates complex I respiration, 3mM) or vehicle (VEH) in the drinking water from gestational day 8-21. On gestational day 10, females were exposed to 10 consecutive days of chronic mild unpredictable stress or handling (CON). Sucrose preference, maternal care, anxiety-like and passive coping behaviors were assessed from postpartum day 2 (PD2) – PD10. Rats were euthanized on PD11, and the PFC was extracted and assessed for mitochondrial respiration. Gestational stress significantly decreased postpartum sucrose preference and maternal care, which was prevented by NAM. Notably, these data suggest that targeting complex I respiration may be a viable approach to prevent behavioral features of PPD in the face of stress. Because stress increases the risk of PPD in women, which is associated with cardiovascular risk, we also explored the effects of stressors on cardiometabolic measures during an in-person lab visit in a preliminary study of postpartum women. Perinatal stress load was calculated from demographic, risk factors, and pregnancy experience to serve as a PPD risk score. Women with higher stress loads had lower resistance vessel endothelial function and higher BMI. Taken together, our preclinical data point to an active role for PFC mitochondrial function in gestational stress-induced PPD-relevant behaviors. Further, these animal and human studies highlight stress as a key mediator of postpartum health, and animal studies suggest mitochondria as a potential protective therapeutic target.

This work was supported by NIH grants P20GM109091 (F.H.), and R01 MH129798 (SKW); VA grants: VISN7 RDA (F.H.), Merit awards: BX002604 (M.J.R.), and the American Heart Association 18CDA34110038 (A.L.). The funders had no role in study design, data collection and analysis, decision to publish, or preparation of the abstract.



# Methamphetamine Route of Administration has a Disproportionate Impact on Females than Males

M. Frances Vest,<sup>1</sup> Alexandru M. Dumitrescu,<sup>1</sup> Christina Ledbetter,<sup>1</sup> Vinita Batra,<sup>1</sup> Elliott Thompson,<sup>1</sup> Nicholas Goeders,<sup>1</sup> James C. Patterson,<sup>1</sup> and Kevin Murnane<sup>1</sup>

<sup>1</sup>Louisiana State University Health Science Center Shreveport

**Abstract ID 56700**

**Poster Board 17**

Methamphetamine is a highly addictive psychostimulant that upon chronic use can be associated with maladaptive behavior and cognitive impairment. Methamphetamine is almost equally used by both sexes; however, little has been done thus far to investigate the influence of sex on behavioral outcomes associated with chronic methamphetamine use. Likewise, methamphetamine can be administered through various routes, with the most popular being inhalation, but another common route being intravenous injections. We aimed to investigate how route of administration and sex influence behavioral outcomes, subjects (N = 49) were recruited from local in-patient addiction treatment facilities, and once consented, screened, and determined eligible for participation, subjects completed questionnaires about their drug use history as well as a cognitive battery including tasks of various executive functions such as cognitive flexibility and response inhibition. At the group level, there was no difference in task performance between males and females. Interestingly, when route of administration was considered, only females were affected, such that females who administer methamphetamine intravenously performed worse on cognitive tasks than females who inhale methamphetamine. Male methamphetamine users, however, did not exhibit this same pattern. Route of methamphetamine administration did not affect task performance in males. These results suggest that males and females are differentially affected by drug use patterns, and therefore should be managed differently in treatment. Further research should be to characterize this phenomenon of sex differences revealed by route of administration's impact on executive function tasks. Including neuroimaging in future studies will be important in fully characterizing this sex difference found with route of methamphetamine administration.

This work was supported by the Louisiana Addiction Research Center, the LSU Health Shreveport Office of Research, the Department of Pharmacology, Toxicology & Neuroscience, and the Center of Biomedical Research Excellence in Redox Biology and Cardiovascular Disease (P20GM121307).

# Reversal of a Scopolamine-Induced Cognitive Deficit in Group-Housed Monkeys Who Drink Ethanol

Lindsey Galbo-Thomma,<sup>1</sup> Phillip Epperly,<sup>2</sup> and Paul Czoty<sup>3</sup>

<sup>1</sup>Wake Forest Univ Graduate School of Arts & Sciences; <sup>2</sup>Wake Forest University School of Medicine; and <sup>3</sup>Wake Forest School of Medicine

**Abstract ID 17554**

**Poster Board 18**

Individuals who experience chronic social stress are vulnerable to developing problematic drinking behaviors that can impair important executive function behaviors, ultimately contributing to the development of alcohol use disorder (AUD). Interestingly, the basal forebrain cholinergic pathway to the prefrontal cortex (PFC), the brain region mediating cognitive flexibility, is sensitive to both stress and alcohol. The purpose of the present study was to examine the efficacy of M1/4 muscarinic and  $\alpha$ 4B2 nicotinic cholinergic receptor [partial] agonists in reversing a scopolamine-induced deficit of a PFC-mediated task in group-housed monkeys with ethanol self-administration histories. Twelve male cynomolgus macaques formed three established social groups and became dominant, experiencing chronic social enrichment, or subordinate, experiencing chronic social stress. Monkeys self-administered ethanol for one year and were trained to perform a serial stimulus discrimination reversal learning task. Subsequently, sensitivity to scopolamine's cognitive impairing effects was determined followed by the pro-cognitive and scopolamine-reversal potential of xanomeline and varenicline alone and when co-administered with scopolamine. We hypothesized that subordinate monkeys, whom had greater mean daily ethanol intakes across one year of ethanol self-administration, would be more sensitive to the cognitive impairing effects of scopolamine and require greater doses of xanomeline and varenicline to reverse a scopolamine-induced cognitive deficit. Across one year of ethanol self-administration, subordinate monkeys had greater mean daily ethanol intakes than dominant monkeys in 2 of 3 groups. Scopolamine dose-response curves indicate that heavy drinkers, but not subordinate monkeys, were more sensitive to scopolamine's cognitive impairing effects ( $p < 0.005$ ). Xanomeline and varenicline dose-response curves when administered alone or with scopolamine are presently being collected. These findings will characterize the role of cholinergic receptor subtypes involved in mediating reversal learning, ultimately contributing to identification of putative pharmacotherapeutic targets for remediating AUD-induced cognitive deficits.

This research was supported by grants from the National Institute on Alcohol Abuse and Alcoholism (R01 AA027556, P50 AA026117, F31 AA029588, T32 AA07565).

# Microglia-Oligo Cross-Talk: PLX5622 Rescues Susceptibility to Stress, Decreases Inflammatory Markers, and Reduces Numbers of ImOL Present in mPFC

Miguel Madeira,<sup>1</sup> Zachary Hage,<sup>2</sup> Styliani-Anna (Stella) E. Tsirka,<sup>1</sup> and Alexandros Kokkosis<sup>1</sup>

<sup>1</sup>Stony Brook Univ; and <sup>2</sup>Stony Brook University

Abstract ID 19298

Poster Board 63

**Background:** Major Depressive Disorder (MDD) is a complex and heterogenous psychiatric disorder affecting more than 350 million people worldwide. Though the mechanisms underlying MDD are not fully understood, a subset of depressive patients can manifest chronic neuroinflammatory responses. In addition, brain-imaging studies in MDD patients have provided evidence of white matter reductions and such changes are hypothesized to lead to disruption of Oligodendroglial (OLN) homeostatic mechanisms, resulting in destabilization of emotional/cognitive circuitry. Recent work shows that a subset of OLN may adopt immune phenotypes (ImOL). The present goal of the study is to investigate whether these histopathological alterations are linked with chronic inflammation through a culture systems and a mouse model of depression.

**Methods *In vivo*:** The Repeated Social Defeat Stress (RSDS) paradigm (10 days) was used to induce depressive-like behavior in 8–12-week-old male *CX3CR1*-GFP<sup>+</sup> and *CSPG4*-EGFP<sup>+</sup> mice. Behavioral tasks (BH) were performed to stratify the defeated mice to susceptible (S; depressive-like) and resilient (R; non-depressive) to stress groups. The study focuses on the stress-affected prefrontal cortex (mPFC) area. PLX5622 treatment was conducted for 7 days post RSDS. ***In vitro*:** Primary OPCs were isolated from neonatal (P1-P3) mouse pups. OPCs were treated with 100 U/mL IFN $\gamma$  for 48 hours before being fixed or lysed.

**Results *In vivo*:** Our results show that microglia become activated, expressing higher levels of pro-inflammatory markers like iNOS and CD86 in S as compared to R and Control (C) mice. We have also demonstrated that in S mice, compared to C and R, hypomyelination occurs and O4+ OLN express MHCII, P2RY12, and C3, markers typically expressed by innate immune cells. Interestingly, when treated with PLX5622, all S mice become R. In line with this, inflammatory cytokines are decreased, numbers of ImOL are rescued to control levels and hypomyelination is rescued. ***In vitro*:** OPC culture work shows that IFN $\gamma$  treatment is enough to cause expression of MHCII in NG2+ OPCs.

**Conclusions** Together, our computational data in MDD patients and depression mouse model, show that OLN can adopt an immune-like phenotype which is rescued when 90-95% of microglia are ablated. Additionally, our culture work confirms that the ImOL phenotype does occur in response to inflammatory cytokines.

This work was supported by:

- R01MH123093-01S1

- T32GM007518

# Modifying the Conditioned Reinforcing Properties of Cocaine in the New Response Acquisition Procedure

Lauren Rysztak,<sup>1</sup> and Emily M. M Jutkiewicz<sup>2</sup>

<sup>1</sup>Univ of Michigan; and <sup>2</sup>Univ of Michigan Medical School

**Abstract ID 26223**

**Poster Board 64**

One contributor to relapse is the ability of environmental cues that have been associated with drug-taking behavior to evoke drug-craving and -seeking behaviors. Often, the conditioned reinforcing properties of drug-paired cues are evaluated following contingent drug-self administration in reinstatement procedures. Various drugs of abuse, such as cocaine, increase responding for drug-paired cues, both within and across drug classes, under these conditions. We sought to evaluate whether compounds that induce reinstatement or drug-seeking behavior also increase responding for cocaine-paired cues in a stringent test of cocaine conditioned reinforcement (New Response Acquisition). We hypothesized that indirect dopamine agonists and other drugs that induce cocaine-seeking behavior would increase responding for cocaine-paired cues in the New Response Acquisition procedure. This procedure begins with Pavlovian Conditioning in which subjects receive five infusions of cocaine (320 ug/kg/inf) and either simultaneous (Paired) or separate (Unpaired) presentations of a light+tone stimulus per day for 10 days. Then, novel operant manipulanda are introduced into the chamber, and responses produce presentations of cues formerly associated with cocaine (Acquisition). On the fourth day of Acquisition, a drug pre-treatment was administered acutely before the start of the session and responding was evaluated. Consistent with previous findings, subjects in the Paired group make more active responses than inactive responses for cue presentations than Unpaired subjects. Interestingly, cocaine (10 and 18 mg/kg), amphetamine (1 mg/kg), or nicotine (0.3 mg/kg) either did not alter or decreased responding for cocaine-paired cues in Paired and Unpaired groups. However, the delta opioid receptor agonist SNC80 (3.2 mg/kg) and the muscarinic receptor antagonist scopolamine (0.32 mg/kg) produced robust increases in responding for the cocaine-paired cues in the Paired group but not in the Unpaired group. These data suggest the two behavioral assays to measure the conditioned reinforcing properties of drug-paired cues may evaluate different aspects of conditioned reinforcement with potentially different underlying mechanisms. This work may provide insight into the underlying neurobiology mediating the conditioned reinforcing effects of drug-paired cues and identify novel ways to evaluate treatment for relapse to substance use disorders.

Funding for this work was provided by: R01DA042092, F31DA053697-01, and T32DA007281-23.

# Aged mice exhibit more rapid acquisition of remifentanil self-administration and an up-shifted dose-response curve

Darius Donohue,<sup>1</sup> Kelsey Carter,<sup>1</sup> Patricia Vangeneugden,<sup>1</sup> Kylie Handa,<sup>1</sup> Sofia Weaver,<sup>1</sup> Amanda L. Sharpe,<sup>1,2</sup> and Michael J. Beckstead<sup>1,3</sup>

<sup>1</sup>Department of Aging & Metabolism, Oklahoma Medical Research Foundation; <sup>2</sup>Department of Pharmaceutical Sciences, Oklahoma University Health Sciences Center; and <sup>3</sup>Oklahoma City VA Medical Center

Abstract ID 21544

Poster Board 65

Opioid use disorder is a chronic, relapsing condition characterized by cycles of voluntary abstinence, the appearance of withdrawal symptoms, and subsequent reinstatement of intake. Current medical approaches are not sufficient to help abstinent addicts that wish to prevent entering their next cycle of use. Although opioid use disorder is more common in the young, aged individuals are more likely to experience chronic pain, predisposing them to increased risk of becoming addicted to prescription or illicit painkillers. However, drug self-administration studies in rodents have historically only used young animals, and to our knowledge no study has explored intravenous opioid self-administration in an aged rodent model. Here we trained young (3-4 month) and old (20-24 month) C57Bl/6N mice to operantly respond for intravenous infusions of the fast-acting opioid remifentanil (3 or 10  $\mu\text{g}/\text{kg}/\text{infusion}$  during training). Nearly all mice acquired self-administration at both doses, however acquisition was significantly more rapid in old mice at the 3  $\mu\text{g}/\text{kg}/\text{infusions}$  dose ( $P = 0.015$ ). We then put mice through a multi-day dose-response curve in 3-hr FR3 sessions (1-100  $\mu\text{g}/\text{kg}/\text{infusion}$ , 2-3 days per dose). Old mice exhibited significantly up-shifted responding and intake compared to young mice ( $P = 0.0008$ ). Finally, mice were given a single 3-hr session where correct responses elicited light and sound cues previously associated with remifentanil after either 1 or 30 days of forced abstinence, but no drug infusion occurred. Both young and old mice showed significantly more responding for cues at 30 days versus 1 day of abstinence ( $P = 0.018$ ) with no main effect of age. No sex differences were apparent in any measure. This is the first demonstration of incubation of remifentanil craving in any rodent model of self-administration and indicates increased drug seeking following forced abstinence. The up-shifted dose-response relationship is consistent with differences in hedonic setpoint and could indicate a general phenotype of drug abuse vulnerability in the aged population. Further work will be needed to test the applicability to other opioids and other classes of abused drug.

Funded by NIH R21 AG072811 and VA Merit Review Award I01 BX005396.

# GPR55 Antagonist KLS-13019 Reverses Chemotherapy-Induced Peripheral Neuropathy (CIPN) in Rats

Michael Ippolito<sup>1</sup>

<sup>1</sup>Temple University

**Abstract ID 24830**

**Poster Board 66**

Michael Ippolito, Hajra Sohail, Ian Barckhausen, Eleanor Labriola, Sara Jane Ward

Neuropathic pain is a form of chronic pain that develops as a consequence of damage to the nervous system. Treatment of neuropathic pain is often incompletely effective, and most of the available therapeutics have only moderate efficacy and present side effects that limit their use. Opioids are commonly prescribed for the management of neuropathic pain despite equivocal results in clinical studies and significant potential for addiction and abuse. Thus, neuropathic pain represents an area of critical unmet medical need to be addressed by the global medical and pharmaceutical communities. Novel classes of therapeutics with improved efficacy and safety profiles are urgently needed for the treatment of neuropathic pain. Novel antagonist of GPR55, KLS-13019, was screened in rat models of neuropathic pain and morphine discrimination. Peripheral neuropathy was induced in 16 rats with once daily 1mg/kg paclitaxel injections for 4 days. Rats were then administered 0, 3, 10, or 30 mg/kg KLS-13019 on days 7 and 14 and allodynia was assessed by a Von Frey test. Allodynia was reversed in a dose dependent manner in the rats treated with KLS-13019, with the highest dose reverting the response to pre-paclitaxel injection baseline levels. Additionally, in an effort to characterize the *in vivo* pharmacology of KLS-13019 compared to opioid-class drugs, a cohort of rats was trained to discriminate between morphine and saline via alternative and mutually exclusive lever presses as the “correct response” to treatment. After training, rats dosed with KLS-13019 did not respond as though they had received morphine. Together, these data suggest that KLS-13019 represents a new class of drug that would be potentially useful for the treatment of neuropathic pain, and these animal models in combination with molecular techniques will describe the role of GPR55 in neuropathic pain to provide the proof-of-concept for a novel therapeutic strategy for this affliction.

# Effects of a highly G Protein-Biased Mu Opioid Receptor Agonist, SR-17018, in Non-human Primates

Mei Chuan Ko,<sup>1</sup> Huiping Ding,<sup>1</sup> Norikazu Kiguchi,<sup>2</sup> Dehui Zhang,<sup>3</sup> and Yanan Zhang<sup>3</sup>

<sup>1</sup>Wake Forest University School of Medicine; <sup>2</sup>Wakayama Medical University; and <sup>3</sup>Research Triangle Institute

**Abstract ID 20391**

**Poster Board 67**

SR-17018 was identified as a G protein-biased mu opioid peptide (MOP) receptor agonist with the highest bias factor and lacked MOP agonist-associated adverse effects in mice. The aim of this study was to determine the functional profile of spinal and systemic delivery of SR-17018 in non-human primates. Effects of SR-17018 were compared with those of MOP agonists in different intrinsic efficacies, DAMGO, morphine, heroin, and buprenorphine, in a series of behavioral assays established in rhesus monkeys (*Macaca mutatta*). Following intrathecal administration, SR-17018 (30-300 ug), buprenorphine (3-10 ug), morphine (10-30 ug), and DAMGO (1-3 ug), dose-dependently attenuated capsaicin-induced thermal allodynia. However, unlike DAMGO and morphine eliciting robust itch-scratching activities, intrathecal SR-17018 and buprenorphine only elicited mild scratching activities, indicating that SR-17018 has low efficacy for activating MOP receptors. In the intravenous drug self-administration assay, heroin (0.3-10 ug/kg/infusion) produced a higher reinforcing strength as compared to lower reinforcing strengths by SR-17018 (3-30 ug/kg/infusion) and buprenorphine (1-10 ug/kg/infusion) in primates under the progressive-ratio schedule of reinforcement. The intrathecal opioid-induced itch scratching and intravenous drug self-administration are well known to distinguish MOP agonists with different intrinsic efficacies in primates. Our findings reveal that *in vivo* apparent low efficacy of SR-17018 is similar to that of a MOP *partial* agonist buprenorphine measured by the primate assays with translation relevance. Such a low intrinsic efficacy contributes to its improved side-effect profile of a highly G protein-biased MOP agonist, SR-17018, in primates.

Support/Funding Information: The US-PHS grants DA049580, DA053343, and DA044775.

# Ventilatory Effects of *Mu* Opioid Receptor Agonist Mixtures

Shawn Flynn,<sup>1</sup> and Charles P. France<sup>1</sup>

<sup>1</sup>Univ of Texas Health San Antonio

Abstract ID 14245

Poster Board 68

The opioid epidemic remains a major public health challenge, with over 80,000 opioid overdose deaths reported in 2021. Over 70,000 of these deaths involved synthetic opioids, primarily fentanyl and fentanyl analogs such as carfentanil, which is reportedly 100-fold more potent than fentanyl. Highly potent synthetic opioids such as fentanyl and carfentanil are primarily encountered as adulterants of other drugs, most commonly other opioids such as heroin. Some clinical reports suggest that larger doses of naloxone are necessary to reverse overdoses involving carfentanil. As opioid overdose causes death primarily through suppression of ventilation, this study used whole-body plethysmography in rats to determine possible interactions between opioid agonists that might contribute to their apparent increased lethality, in humans. The primary outcome of this study was minute volume (the volume of air ventilated per minute, product of tidal volume and respiratory rate). First, dose-effect curves for the ventilatory depressant effects of fentanyl (0.0056-0.178 mg/kg; i.v.), carfentanil (0.00056-0.0056 mg/kg; i.v.), and heroin (0.178-1.78 mg/kg; i.v.) were determined in male and female Sprague-Dawley rats. Then, dose-effect curves were determined for binary mixtures of *mu* opioid receptor agonists at three fixed-dose ratios (3:1, 1:1, 1:3) relative to the potency of each drug alone to suppress ventilation to 75% of baseline. Experimentally determined dose-effect curves for opioid agonist mixtures were then compared to the predicted dose-effect curves based on the effects of each drug alone using dose-addition analysis. All opioid agonists dose-dependently reduced minute volume in male and female rats. Fentanyl was significantly more potent at reducing minute volume in females than males, though there was no difference in the potency of carfentanil or heroin across sexes. Fentanyl was 10-fold more potent than heroin in male rats, but 50-fold more potent than heroin in female rats. Carfentanil was approximately 300-fold more potent than heroin in both males and females. Analysis of the effects of agonist mixtures suggests that interactions between the effects of *mu* opioid receptor agonists on ventilation are simply additive in nature. This study determined the relative potencies of fentanyl, carfentanil, and heroin to suppress ventilation in male and female rats. Observed sex differences in the potency of fentanyl to suppress ventilation warrants further study.

Support/Funding Information: Welch Foundation AQ-0039



# Behavioral effects of fentanyl in presence or absence of chronic neuropathic pain in male and female rats

Gwendolyn Burgess,<sup>1</sup> Hailey Y. Rizk,<sup>2</sup> Shane M. Sanghvi,<sup>2</sup> Melanie R. Vocelle,<sup>2</sup> and Emily M. M Jutkiewicz<sup>3</sup>

<sup>1</sup>Univ of Michigan; <sup>2</sup>University of Michigan; and <sup>3</sup>Univ of Michigan Medical School

Abstract ID 23939

Poster Board 201

Mu opioid receptor (MOR) agonists are used clinically at times to treat chronic pain, yet there is debate about whether or not chronic pain alters the effects of opioid analgesics and their abuse liability. This project examined the extent to which chronic neuropathic pain altered the reinforcing, interoceptive, antihyperalgesic, and rate decreasing effects of fentanyl in male and female Sprague Dawley rats. It has been proposed that chronic pain causes opioid peptide release and tolerance due to continuous MOR activation; therefore, we hypothesized that chronic neuropathic pain would decrease the potency of fentanyl over the duration of chronic pain in all these behavioral measures and that the shift in the fentanyl dose effect curve would be greater in female than male rats. We surgically induced a spared nerve injury (SNI) that produces a persistent hyperalgesic state for at least 18 mo. Fentanyl dose response curves (and other drugs) in each behavioral assay were evaluated before surgery and after surgery for 2-6 months. We measured (a) fentanyl self-administration behavior by evaluating within session fentanyl dose effect curves on a fixed ratio 5 (FR5) schedule of reinforcement, (b) the discriminative stimulus effects of fentanyl in rats trained to discriminate 0.032 mg/kg fentanyl from saline, (c) the antihyperalgesic and antinociceptive effects of fentanyl as withdrawal latencies from a mechanical stimulus (Randall Selitto), and (d) the fentanyl-induced decreases in rates of responding under a FR5 schedule of reinforcement for sucrose-maintained responding. Fentanyl maintained self-administration behavior in all rats prior to sham ( $ED_{50}=1.04 \pm 0.04$  mcg/kg) or SNI surgery ( $ED_{50}=1.30 \pm 0.10$  mcg/kg); data are presented as intake (mcg earned/dose). While there was an initial decrease in responding post-surgery, fentanyl-maintained responding increased over 3-4 d to reach the pre-surgical average. These  $ED_{50}$  values did not significantly change over 8 wks of chronic pain. Fentanyl produced dose-dependent increases in % fentanyl responding prior to sham ( $ED_{50}=0.01 \pm 0.001$  mg/kg) and SNI surgery ( $ED_{50}=0.013 \pm 0.001$  mg/kg). We observed no significant changes in these  $ED_{50}$  values over 6 mo of chronic pain. Fentanyl produced dose-dependent increases in withdrawal pressure prior to sham surgery ( $ED_{50}=0.019 \pm 0.002$  mg/kg) and SNI surgery ( $ED_{50}=0.023 \pm 0.002$  mg/kg) prior to SNI. The antihyperalgesic effects of fentanyl were not altered up to 6 months after either surgery. Fentanyl dose-dependently decreased rates of responding prior to sham surgery ( $IC_{50}=0.022 \pm 0.001$  mg/kg) and SNI surgery ( $IC_{50}=0.019 \pm 0.001$  mg/kg). The rate decreasing effects of fentanyl were not altered up to 6 mo. after either surgery. In conclusion, SNI-induced chronic pain did not alter the antihyperalgesic effects, rate decreasing effects, interoceptive effects, or reinforcing effects of fentanyl. In addition, there were no significant differences in the potency of fentanyl between males and females in any of the behavior measures. These results suggest that chronic pain alone likely does not alter the behavioral effects or the abuse potential of fentanyl. Ongoing and future experiments are evaluating the effects of partial MOR agonists and will evaluate motivation for fentanyl in the presence or absence of chronic pain.

# Genetic deletion of atypical VGLUT3 rescues Huntington's disease phenotype and neurodegeneration in zQ175 mice

Karim Ibrahim,<sup>1</sup> Khaled Abd-Elrahman,<sup>2</sup> and Stephen S. Ferguson<sup>1</sup>

<sup>1</sup>Univ of Ottawa; and <sup>2</sup>University of British Columbia

Abstract ID 18502

Poster Board 202

Huntington's disease (HD) is an incurable, fatal neurodegenerative disease caused by an abnormal expansion in the huntingtin protein (mHTT) leading to progressive motor and cognitive impairments in patients. HD pathophysiology involves evident dysfunctions in glutamatergic neurotransmission leading to severe striatal neurodegeneration. In this context, vesicular glutamate transporter subtype-3 (VGLUT3) represents a promising therapeutic target, being a modulator of glutamate release from selected glutamatergic and non-glutamatergic neurons that are affected by HD. Nevertheless, current evidence on the role of VGLUT3 in HD pathophysiology remains largely unknown. Here, we employed two genetically modified mice in which the *Slc17a8* gene is deleted in both male and female wild-type (VGLUT3<sup>-/-</sup>) and zQ175 knock-in mouse model of HD (zQ175:VGLUT3<sup>-/-</sup>). Longitudinal assessment of motor and cognitive function reveals that VGLUT3 deletion rescues the deficits in motor coordination and working memory in both male and female zQ175 mice throughout 15 months of age. Furthermore, VGLUT3 deletion rescues the neuronal loss and promotes the activation of Akt and ERK1/2 cellular pro-survival signaling in the striatum of zQ175 mice of both sexes. Interestingly, the rescue in zQ175:VGLUT3<sup>-/-</sup> mice is accompanied by a reduction in nuclear accumulation of mHTT aggregates with no change in the total aggregate burden in striatal neurons. Collectively, these findings provide novel evidence that VGLUT3 neurotransmission, despite its limited expression, can be a vital contributor to HD progression in a sex-independent fashion and a viable target for HD therapeutics.

This study was supported by CIHR grants (PJT-148656, PJT-165967, and PJT-178060) and Funding from Krembil Foundation to Dr. Stephen Ferguson.

# The serotonergic psychedelic *N,N*-Dipropyltryptamine prevents seizures in a mouse model of fragile X syndrome via an apparent non-serotonergic mechanism

Richa Tyagi,<sup>1</sup> Tanishka S. Saraf,<sup>2</sup> and Clinton E. Canal<sup>2</sup>

<sup>1</sup>*Mercer Univ Atlanta; and* <sup>2</sup>*Mercer Univ*

Abstract ID 14531

Poster Board 203

Serotonergic psychedelics (SPs) are well-known as serotonin 2 receptor (5-HT<sub>2</sub>R) agonists. Tryptamine-based SPs, e.g., psilocin, also possess agonist activity at 5-HT<sub>1</sub>-type receptors and bind tightly to other 5-HTRs. Recent studies report that psilocybin, a prodrug for psilocin, has efficacy in treating various neuropsychiatric disorders. We and others have shown that 5-HT<sub>1</sub>R agonists prevent audiogenic seizures (AGS) in an *Fmr1* knockout (KO) mouse model of fragile X syndrome, a monogenic disorder typified by cognitive rigidity, anxiety, intellectual disability, and often seizures. Here we report that the SP, *N,N*-Dipropyltryptamine (DPT), is an anticonvulsant in *Fmr1* KO mice, and we report our efforts to dissect the pharmacology underlying this effect. From radioligand competition binding assays in vitro, we determined the affinity of DPT at [<sup>3</sup>H]Lysergic acid diethylamide-labeled human 5-HT<sub>2A</sub>R and its affinities at [<sup>3</sup>H]5-Carboxamidotryptamine-labeled 5-HT<sub>1A</sub> and 5-HT<sub>1B</sub>R. The rank order of binding potencies of DPT was 5-HT<sub>2A</sub>>5-HT<sub>1A</sub>>5-HT<sub>1B</sub>R; K<sub>i</sub> values were 152 nM (pK<sub>i</sub>=6.82 ± 0.116), 1640 nM (pK<sub>i</sub>=5.78 ± 0.05) and 8081 nM (pK<sub>i</sub>=5.09 ± 0.03). The affinities of 5-HT—used as a positive control—at 5-HT<sub>2A</sub>, 5-HT<sub>1A</sub>, and 5-HT<sub>1B</sub>R were 41 nM (pK<sub>i</sub>=7.38 ± 0.002), 26 nM (pK<sub>i</sub>=7.59 ± 0.07) and 18 nM (pK<sub>i</sub>=7.75 ± 0.13), respectively. We next determined the in vitro functional activities of DPT at 5-HT<sub>2A</sub>, 5-HT<sub>1A</sub>, and 5-HT<sub>1B</sub>R using TRUPATH G-protein biosensor technology. The rank order of functional potencies of DPT was 5-HT<sub>2A</sub>>5-HT<sub>1B</sub>>5-HT<sub>1A</sub>R; EC<sub>50</sub> values were 445 (pEC<sub>50</sub>=6.35 ± 0.12), 1710 (pEC<sub>50</sub>=5.77 ± 0.13), and 2400 nM (pEC<sub>50</sub>=5.61 ± 0.06). 5-HT's potencies at 5-HT<sub>2A</sub>, 5-HT<sub>1B</sub> and 5-HT<sub>1A</sub>R were 12 (pEC<sub>50</sub>=7.92 ± 0.05), 1.4 (pEC<sub>50</sub>=8.88 ± 0.1) and 73 nM (pEC<sub>50</sub>=7.14 ± 0.05), respectively. DPT displayed full agonist activity at 5-HT<sub>2A</sub>R and partial agonist activity at 5-HT<sub>1A</sub>R (52%) and 5-HT<sub>1B</sub>R (85%). To estimate the dose of DPT that effectively engages 5-HT<sub>2A</sub>R in vivo, we assessed DPT's activity (3, 5.6, 10, 15, and 20 mg/kg, i.p., N=5/group) in juvenile and adult wild-type (WT) mice in the 5-HT<sub>2A</sub>R-dependent head-twitch response (HTR) assay. We also estimated the dose of DPT that effectively engages 5-HT<sub>1A</sub>R in vivo by assessing its activity to elicit 5-HT<sub>1A</sub>R-dependent behaviors, including hind limb abduction and flat body posture. DPT elicited the HTR with peak effects at 10 mg/kg, suggesting 5-HT<sub>2A</sub>R engagement at this dose, and we observed behaviors indicative of 5-HT<sub>1A</sub>R activation at 20 mg/kg only. We next investigated the anticonvulsant activity of DPT (3, 5.6, and 10 mg/kg, i.p., N=8-12/group) in juvenile *Fmr1* KO mice by AGS testing. DPT at 3 and 5.6 mg/kg was ineffective at blocking AGS; however, at 10 mg/kg, DPT completely prevented AGS in *Fmr1* KO mice (0% vs. 72%, vehicle-treated; P<0.0001). Aligning these results with our in vivo receptor engagement tests, they suggested that DPT's anticonvulsant effects could be mediated by 5-HT<sub>2A</sub>, but likely not 5-HT<sub>1A</sub>R. To further evaluate DPT's anticonvulsant mechanisms, we pretreated mice with pimavanserin (3 and 10 mg/kg), WAY100635 (0.1 mg/kg), and SB224289 (5 mg/kg), selective 5-HT<sub>2A/2C</sub>, 5-HT<sub>1A</sub>, and 5-HT<sub>1B</sub>R antagonists, respectively, and methiothepin (4 mg/kg), a pan-5-HTR antagonist (N=4-8/group). None of the 5-HTR antagonists blocked the anticonvulsant effects of DPT. Our results suggest that DPT prevents seizures in *Fmr1* KO mice via a non-serotonergic mechanism, which we are currently investigating.

Support: R15NS118352, FRAXA

# Mitochondrial SIRT3 and morphine induced hyperalgesia and tolerance: the effect of polyphenol fraction of bergamot

Sara S. Ilari,<sup>1</sup> Filomena A. Lauro,<sup>2</sup> Luigino Giancotti,<sup>2</sup> Concetta Dagostino,<sup>1</sup> Valentina Malafoglia,<sup>3</sup> Lucia C. Passacatini,<sup>1</sup> Cinzia Garofalo,<sup>4</sup> Marco Tafani,<sup>5</sup> Ernesto Palma,<sup>1</sup> Carlo Tomino,<sup>6</sup> Daniela Salvemini,<sup>2</sup> Vincenzo Mollace,<sup>1</sup> and Carolina Muscoli<sup>1</sup>

<sup>1</sup>Department of Health Science, Institute of Research for Food Safety & Health (IRC-FSH), University; <sup>2</sup>Department of Pharmacology and Physiology, Saint Louis University School of Medicine, 1402 S. Grand; <sup>3</sup>Institute for Research on Pain, ISAL Foundation, Torre Pedrera, 47922 Rimini, Italy; <sup>4</sup>Department of Health Science, Institute of Research for Food Safety & Health (IRC-FSH), University; <sup>5</sup>Department of Experimental Medicine, University of Rome "Sapienza", Italy; and <sup>6</sup>Scientific Direction, IRCCS San Raffaele Roma, 00166 Rome, Italy

**Abstract ID 55336**

**Poster Board 204**

Chronic pain and oxidative stress are two pathophysiological conditions that can induce each other, causing alteration of normal cellular physiology and both contribute to the development and progression of chronic degenerative diseases.

Morphine is the leading pain management drug in conditions ranging from acute to chronic pain and its prolonged use leads to antinociceptive tolerance and development of oxidative stress. It is well known that excessive ROS generation, during morphine tolerance, can damage proteins, nucleic acids, and further alter mitochondrial homeostasis, particularly affecting the oxidation of specific proteins.

Lipid peroxidation is the primary consequence of cellular oxidative stress. Furthermore, it generates reactive species (e.g., 4-hydroxynonenal (4-HNE) and malonaldehyde (MDA)) that may contribute to toxicity and cellular signaling and have been linked to neurodegeneration.

The increase in lipid peroxidation products is also closely linked to the formation of hyperacetylated proteins at the mitochondrial level. In particular, protein acetylation plays a crucial role in cells by modifying some enzymes and substrates' activity and/or specificity, thus regulating glucose metabolism, lipids, and amino acids.

SIRT3 is the principal regulator of mitochondrial function and can deacetylate several proteins involved in the maintenance of the mitochondrial function in the antioxidant pathway, energy metabolism, ATP production, and mitochondrial dynamics.

Our recent studies showed the critical role of SIRT3 during inflammatory and neuropathic pain, highlighting the beneficial role of natural antioxidants in restoring cellular homeostasis.

Here, we observed that repeated doses of morphine for 4 days in mice developed antinociceptive tolerance, associated with superoxide production. Co-administration of morphine with BPF (25mg/Kg) or MnTBAP (10mg/Kg) is able to inhibit these effects.

Furthermore, we observed that superoxide production is associated with the nitration and inactivation of glutamine synthetase (GS), GLT1, mitochondrial SIRT3 and MnSOD, leading also to a condition of nitration and acetylation of the overall mitochondrial proteins. Co-administration of morphine and BPF (25mg/Kg) or MnTBAP (10mg/Kg) prevented the nitration of SIRT3, MnSOD, GS and GLT-1 by inhibiting the development of hyperalgesia during opioid tolerance. Results of our study support the hypothesis according that post-translational modifications of sirtuins is an important pathway used by superoxide/peroxynitrite to mediate the development and maintenance of opioid induced hyperalgesia. Prevention of post-translational modifications, such as nitration, and hyperalgesic response by antioxidants indicate the importance of the development of new therapeutic approach that can modulate the glutamate transmission without directly blocking glutamate actions.

Furthermore, our data showed that co-administration of morphine and BPF can be a good therapeutic approach for rehabilitation and treatment of chronic pain thanks to its ability to inhibit the development of tolerance preserving analgesic-morphine property.

These findings demonstrate that activation of SIRT3 by antioxidants is beneficial during oxidative stress during opioid tolerance.

Support/Funding Information: PON03PE\_00078\_1, PON03PE\_00078\_2, GR-2021-12375174 and SG-2021-1237555.

# Effects of Cannabinoids on Fentanyl Antinociception

Dalal Alkhelb,<sup>1</sup> Christos Iliopoulos-Tsoutsouva,<sup>1</sup> Spyridon P. Nikas,<sup>1</sup> Michael S. Malamas,<sup>1</sup>  
Alexandros Makriyannis,<sup>2</sup> and Rajeev I. I. Desai<sup>1</sup>

<sup>1</sup>Center for Drug Discovery, Northeastern University; and <sup>2</sup>Center for Drug Discovery, Northeastern Univ

**Abstract ID 26414**

**Poster Board 205**

Extensive evidence suggests the existence of a functional interaction between endogenous cannabinoids and opioid systems. Thus, targeting cannabinoid CB1 receptors (e.g., opioid-sparing) may be a promising approach to overcome the current opioid public health crisis. The present studies were undertaken to evaluate the effects of CB1 ligands alone and in combination with the highly potent  $\mu$ -opioid receptor agonist fentanyl in male mice. The warm water tail-withdrawal procedure ( $52\pm 0.5^\circ\text{C}$ ) and the chemically induced pain assay (2.5% formalin) were utilized to compare the antinociceptive effects of the principal psychoactive component of cannabis ( $\Delta 9$ -THC) as well as a full (AM8936) and partial (AM11101) synthetic CB1 agonists alone, and in combination with fentanyl. Results show that the  $\mu$ -opioid receptor agonist fentanyl as well as the CB1 ligands  $\Delta 9$ -THC, AM8936, and AM11101 produced a dose-dependent increase in antinociceptive effects in both assays. Pretreatment with subthreshold or lower doses of the CB1 ligands ( $\Delta 9$ -THC, AM8936, or AM11101) shifted the fentanyl dose-response curve to the left in a dose-dependent manner, demonstrating that CB1 ligands enhance the antinociceptive effects of opioids in thermal and chemical pain assays. Isobolographic analysis showed a better synergistic profile for the interaction between the synthetic partial CB1 agonist AM11101 in combination with fentanyl compared to  $\Delta 9$ -THC and AM8936. These data suggest that using partial CB1 agonists might be a better approach to augment fentanyl's antinociceptive effects. Future work will further evaluate the interaction between cannabinoids and opioids using behavioral (e.g., conditioned place preference), physiological (e.g., fentanyl-induced respiratory depression), and neurochemical studies (e.g., fentanyl-induced DA changes in the brain).

# Clozapine, but Not Ziprasidone, Decreases the Discriminative Stimulus Effects of 22 Hours Deprivation in Sprague-Dawley Rats

Simon Tangen,<sup>1</sup> Sydney K. Wenzel,<sup>1</sup> Erika K. Cedarbloom,<sup>1</sup> Giulia Lelli,<sup>1</sup> and David Jewett<sup>2</sup>

<sup>1</sup>University of Wisconsin - Eau Claire; and <sup>2</sup>Univ of Wisconsin-Eau Claire

Abstract ID 23235

Poster Board 206

We sought to determine if medications used as atypical antipsychotics in humans affect food-related discriminative stimuli in adult and aged animals. We examined the ability of the atypical antipsychotics clozapine and ziprasidone to alter discriminative stimuli associated with 22 hr food deprivation.

Rats were trained to discriminate between 22 and 2 hours food deprivation in an operant choice procedure. Under 22 hr deprivation conditions, left lever presses were reinforced with the delivery of a 45 mg food pellet under a Fixed Ratio 15 reinforcement schedule (FR 15). Incorrect lever presses induced 8 seconds of darkness under the FR 15. Experimental contingencies were reversed under 2 hr deprivation conditions. Training continued until rats emitted 80% or greater condition-appropriate responses both before the first consequence and for the entire training session (10 reinforcers earned of 15 minutes elapsed) for 8 out of 10 consecutive sessions.

After acquisition of the discrimination, tests sessions began. During test sessions, responses to both levers were reinforced under FR 15s and 5 reinforcers could be earned in a 5 minute trial. Test trials were conducted every 15 minutes for 2 hours. Test sessions were preceded by subcutaneous injection of vehicle, clozapine (1.0-5.6 mg/kg), or ziprasidone (0.1 to 1.0 mg/kg).

Under 2 hr deprivation condition, atypical antipsychotic pretreatment did not induce 22-hr deprivation-like responding (e.g., the drug did not induce stimuli associated with "hunger"). Under 22 hr deprivation conditions, clozapine reduced the discriminative stimulus effects of food deprivation (1.0 – 5.6 mg/kg) and reduced rates of lever pressing (5.6 mg/kg). Under both 2 and 22 hr food deprivation conditions, clozapine reduced food intake (3.2 -5.6 mg/kg). The effects of clozapine were assessed again six months later. Clozapine (1.0 mg/kg) produced rate decreasing effects and eliminated responding in several subjects. At time points where rates were not suppressed, the discriminative stimulus effects of 22 hr deprivation were not altered. Later, the effects of ziprasidone were assessed. Ziprasidone did not alter discriminative stimuli associated with 22 hr food deprivation or reduce 22 hr deprivation-induced food intake. Ziprasidone (1.0 mg/kg) significantly reduced rates of lever pressing.

We noticed differences in the stability of the discriminative stimulus effects of 22 hr deprivation during the test sessions. With younger subjects (age ~ 12 months) and under conditions with the vehicle for clozapine (30% DMSO), the discriminative stimulus effects of 22 hr food deprivation were stable for the entire 2 hr session (on average, performance was not different than criterion levels). In older subjects (~24 months) administered with the vehicle for ziprasidone, test performance was less stable, especially during the second hour of assessment. Initial assessments of accuracy during training sessions have not revealed differences in performance between ~12 month old subjects and ~24 month old subjects.

Medications used as atypical antipsychotics can have different effects in rodent models of eating. Clozapine, but not ziprasidone, reduced both 22 hr deprivation-induced discriminative stimuli and 22 hr deprivation-induced food intake. Clozapine's rate decreasing effects were more pronounced in older rats. The deprivation discrimination can be used to assess food-related phenomenon throughout the life span of rodents.

# Fentanyl-Targeting Monoclonal Antibodies Block Fentanyl-Induced Respiratory Depression in Non-Human Primates

Emily Burke,<sup>1</sup> Paul T. Bremer,<sup>2</sup> and Rajeev Desai<sup>3</sup>

<sup>1</sup>McLean Hosp; <sup>2</sup>Cessation Therapeutics; and <sup>3</sup>McLean Hospital/Harvard Medical School

Abstract ID 16680

Poster Board 207

Fentanyl is a synthetic opioid that is routinely abused for its pleasurable psychoactive effects, which can lead to substance use disorder (SUD) and subsequent overdose. Although treatments for fentanyl overdose exist, like  $\mu$ -opioid receptor antagonists naloxone and naltrexone, they can be ineffective and are short acting. Thus, antibody-based therapeutics have emerged as a new approach to prevent fentanyl overdose due to their specificity, low toxicity, and immediate effects post-infusion. The present experiments were conducted to examine the ability of a novel fentanyl-targeting monoclonal antibody, CSX-1004, to block fentanyl's respiratory depressant effects. Eight squirrel monkeys were treated with either 10 or 40 mg/kg CSX-1004 via IV infusion and were cumulatively given fentanyl on days 0, 2, 7, 14, 21, and 28 post-infusion. The eight subjects also received a second infusion of either 10 or 40 mg/kg CSX-1004 after a 2-month washout period to determine the magnitude of fentanyl antagonism. Respiratory depression was examined using a ventilation chamber in which subjects were exposed to air and a mixture of air with 5% CO<sub>2</sub> in 10-minute alternating increments. The volume of breaths per minute was measured and used to generate dose-response functions. Results show that CSX-1004 successfully blocked fentanyl's respiratory depressant effects in both a dose- and time-dependent manner. Fentanyl challenge on Day 0 post-CSX-1004 infusion resulted in no fentanyl-associated reductions in minute volume, and these effects continued through Day 28, although efficacy gradually diminished starting at Day 14. Subjects that received the 10 mg/kg dose returned to baseline levels faster than those that received the 40 mg/kg dose, with efficacy beginning to diminish at day 7. The 40 mg/kg CSX-1004 dose also produced a substantial ~14-fold rightward shift in the dose-response function of fentanyl but did not block the effects of other  $\mu$ -opioid agonists. The 10 mg/kg CSX-1004 dose also produced a rightward shift in the dose-response function of fentanyl, but this was only about a ~5-fold rightward shift. These studies provide strong evidence that monoclonal antibodies could be a promising treatment in preventing fentanyl overdose while not disrupting the efficacy of other opioids that are often prescribed for pain management.

Supported by NIDA Grant 1U01DA051071-01A1

# Dramatic increase in lever pressing activity in rats following cocaine self-administration on high fixed ratio schedules

Jhanvi N. Desai,<sup>1</sup> Abigail Muccilli,<sup>2</sup> Luis Tron Esqueda,<sup>1</sup> Andrew Norman,<sup>1</sup> and Jeffrey A. Welge<sup>1</sup>

<sup>1</sup>University of Cincinnati College of Medicine; and <sup>2</sup>Rowan University

Abstract ID 14745

Poster Board 208

Cocaine self-administration in rats is a model of cocaine use disorder. The rate of acquisition is highest under fixed ratio (FR) 1 schedule, where every lever press results in a cocaine injection. While FR1 is good for training, it is not considered good for measuring the positive reinforcing effects of cocaine. Progressive ratio (PR) schedules, where the number of lever presses required to get the next cocaine dose gradually increases, are considered a better method for measuring cocaine's reinforcing efficacy. PR schedules are known to increase the rate of lever pressing activity compared with FR1. Both FR1 and PR schedules of cocaine self-administration follow the compulsion zone theory which states that cocaine induces lever pressing behavior only when cocaine levels are below the satiety threshold and above the priming/remission threshold. We now explore whether cocaine self-administration on FR magnitudes greater than 1 also increases lever pressing activity compared with FR1. Male Sprague Dawley rats (n=8) were trained to self-administer cocaine (i.v.) on an FR1 schedule at different doses. Next, they self-administered cocaine on FR 5, 10, 20 and 50 at a unit dose of 3  $\mu$ mol/kg until they acquired maintained self-administration at FR50. Standard FR1 sessions were performed before and during FR50 training. Number of lever presses during unloading was lognormally distributed and the geometric mean was calculated. The number of unloading lever presses increased approximately sevenfold from pre-FR50 FR1 sessions (23) to during-FR50 FR1 sessions (158) and increased about elevenfold from pre-FR50 FR1 sessions to FR50 sessions (245). The number of unloading lever presses in FR50 sessions were approximately 1.5-fold higher than during-FR50 FR1 sessions. After completion of FR50 sessions, the standard FR1 sessions were performed on 5 rats twice a week for 4-7 weeks. The number of lever presses significantly decreased from FR50 sessions and reduced by 75% in post-FR50 FR1 sessions (59). However, number of lever presses remained 2.5 times higher in post-FR50 FR1 sessions compared to pre-FR50 FR1 sessions and lever pressing activity did not return to baseline. Despite the differences in number of lever presses, there was no significant difference in the duration of unloading lever pressing activity between all sessions. Inter-press intervals (IPI) were lognormally distributed, and shifted from bimodal to unimodal after exposure to FR50. The number of long IPIs decreased and the number of short IPIs substantially increased resulting in the dramatic increase in lever presses. The increase in rate of unloading lever pressing activity following high FR training may account for reports that cocaine is a positive reinforcer. However, the satiety and remission thresholds, the calculated cocaine level at the first and last unloading lever press, respectively, were similar in all sessions. This confirms that the compulsion zone is not altered after exposure to high FR magnitude and the dramatic increase in the frequency of lever presses improves the resolution of these calculated threshold values.

Supported by NIDA grant U01DA050330 (to ABN)



# Role of Opioid Analgesic Efficacy in the Treatment of Pain-Related Disruption of Behavior in Male and Female Mice

Laurence Miller,<sup>1</sup> Jamani Garner,<sup>2</sup> Kelly Roen,<sup>3</sup> and Gabrielle Pollard<sup>3</sup>

<sup>1</sup>Augusta Univ; <sup>2</sup>Georgia State University; and <sup>3</sup>Augusta University

Abstract ID 23576

Poster Board 209

A key goal in preclinical pain research is improvement of the translational value of findings by modeling pain states elicited in humans. Examining the expression and treatment of pain-related disruption of behavior represents one approach to improving the alignment between preclinical pain research and clinical settings. Past studies support the ability of the opioid, analgesic morphine to restore pain-related depression of behavior in mice and rats. The goal of the present study was to examine the role of mu opioid receptor agonist efficacy in the treatment of pain-related depression of behavior. The partial mu opioid receptor agonist buprenorphine, and the full mu opioid receptor agonist methadone were examined for their ability to block lactic-acid induced depression of Nestlet shredding in male and female ICR mice. At the start of test sessions, a 5 × 5 cm Nestlet was weighed and suspended from the wire lid of the home cage. Under control conditions, mice removed pieces of the suspended Nestlet to build nests. Intraperitoneal injection of 0.18% lactic acid disrupted Nestlet shredding. Unlike morphine, buprenorphine failed to restore acid-induced depression of shredding. In contrast, methadone significantly blocked acid-induced depression of shredding. In the absence of acid, both buprenorphine and methadone significantly depressed shredding. These findings suggest that opioid effects on nestlet shredding in the presence and absence of pain stimuli require different levels of MOR efficacy. Disruption of shredding in the absence of a pain stimulus has lower efficacy requirements than treatment of pain-related depression of behavior.

Support/Funding Information: NIA Grant R15AG055041

# Positive Allosteric Modulation of the Mu Opioid Receptor Does Not Potentiate Opioid-Mediated Side Effects

Kelsey Kochan,<sup>1</sup> Thomas Prince,<sup>1</sup> and John Traynor<sup>1</sup>

<sup>1</sup>University of Michigan

Abstract ID 18014

Poster Board 210

Opioid therapeutics, such as morphine, that act at the mu-opioid receptor (MOR) are the clinical standard for managing pain. Although opioids are effective, their use leads to severe adverse effects, such as constipation, addiction, and respiratory depression. Thus, there is a clear need for safer alternatives to manage pain. One promising approach is to enhance the effects of the endogenous opioid system by the use of positive allosteric modulators (PAMs) of MOR. A known PAM, BMS-986122, enhances MOR agonist potency in cellular models. In mouse models, BMS-986122 promotes the antinociceptive activity of endogenous opioid peptides and exogenous opioid drugs in various pain assays. Moreover, at an effective antinociceptive dose in mice, BMS-986122 produces less severe adverse effects than morphine, as determined by measures of constipation, respiratory depression, and conditioned place preference. However, we do not yet know if the side effects of traditional exogenous opioids are increased by PAM modulation. Here we compare the ability of BMS-986122 to enhance the action of three structurally diverse opioid therapeutics, morphine, methadone, and fentanyl. We find that BMS-986122 increases the antinociceptive effects of the drugs in the warm water tail withdrawal and hot plate assays without promoting constipation, respiratory depression, or reward in CD1 male and female mice. Future work will assess the effects of BMS-986122 in chronic pain models. If BMS-986122 enhances MOR-mediated antinociception but not MOR-mediated adverse effects, the development of PAMs as standalone pain medications and opioid-sparing drugs will be a valuable approach to effective pain management.

This work was funded by R37 DA039997. KEK was also supported by T32 GM007767 and a Rackham Predoctoral Fellowship.

# Allosteric Dopamine transporter modulator inhibits cocaine-induced behaviors

Yibin Xu, Stacia Lewandowski,<sup>1</sup> Christina Besada,<sup>2</sup> and Ole Mortensen<sup>3</sup>

<sup>1</sup>Drexel University; <sup>2</sup>Drexel College of Medicine; and <sup>3</sup>Drexel Univ College of Medicine

**Abstract ID 52443**

**Poster Board 211**

The neurotransmitter dopamine (DA) is involved in motivation, reward mechanisms, and many central nervous system diseases. DA is transported into the presynaptic neurons by a protein called dopamine transporter (DAT). The psychostimulant cocaine is an inhibitor of DAT. When DAT is inhibited by cocaine, the DA in the synaptic cleft increases and this leads to amplified downstream dopaminergic signaling primarily in the mesolimbic pathway. This increase in cocaine-induced DA signaling is responsible for the addictive properties of cocaine. Because DAT is the primary target of cocaine, compounds acting on the DAT in novel ways could potentially treat cocaine use disorders. We previously found a novel compound—KM822 and characterized it as an allosteric modulator of DAT function. KM822 significantly decreases cocaine-induced locomotive response in planarians. To test if KM822 has similar effects in mammals, we administered KM822 and cocaine intracranially into nucleus accumbens (NAc) area in Long Evans rats and measured the locomotion changes. We targeted the NAc as it is a part of the brain that plays a crucial role in the mesolimbic dopaminergic pathway and has been recognized by its high density of DAT. Our results showed that KM822 significantly decreased hyper-locomotion induced by cocaine and notably did not cause any locomotion changes by itself. We also examined KM822's ability to interfere with cocaine's rewarding effect using the conditioned place preference (CPP) assay. In this assay, animals are tested for their preference for a cocaine-associated environment as a model of cocaine seeking. Unlike the locomotion assay, this assay is more relevant to behaviors associated with cocaine addiction and therefore has higher translational value. CPP is also utilized to determine the addictive liability of KM822. c-Fos expression is frequently utilized as a functional marker to investigate neuronal processes in response to a stimuli. To determine how KM822 affects neuronal activity in the NAc, c-Fos staining was conducted, and the expression of c-Fos was compared between animals pre-treated with KM822 and those pre-treated with vehicle before cocaine infusion. In the future, we plan to further assess the impact of KM822 in extinction and relapse utilizing CPP. Overall, these studies demonstrate the ability of KM822 to block DAT inhibitor-induced behaviors in rats and provide strong evidence that the novel allosteric DAT modulator KM822 has significant potential for treating cocaine addiction.

Support/Funding Information: NIH R01- MH121453

# Commonalities of Ginseng Extract (*P. quinquefolius*) and Exercise Mimetic $\beta$ -GPA for Reducing Age-related Cognitive Deficits and Modulating the Autophagy-Lysosomal Pathway

Ben Bahr,<sup>1</sup> Michael Almeida,<sup>2</sup> and Stephen Kinsey<sup>3</sup>

<sup>1</sup>Univ of North Carolina - Pembroke; <sup>2</sup>Univ of North Carolina at Pembroke; and <sup>3</sup>University of North Carolina – Wilmington

Abstract ID 23079

Poster Board 212

Neuronal disturbances signify brain vulnerability that fosters cognitive impairment, whether facilitated by excitatory over-activation, toxin exposures, metabolic distress, trauma-inducing events, or aging. Across such dementia risk factors, negative effects on proteostasis and synaptic integrity gradually increase the risk for mild cognitive impairment (MCI) and the continuum to dementia. Removal of old and damaged proteins by the autophagy-lysosomal pathway clearly becomes compromised with aging, and the altered proteostasis has been linked to the gradual deterioration of synaptic connections important for cognition. Poor nutrition is known to impact cognition and many studies suggest natural products promote cognitive health. Here, a dozen natural products were tested for their ability to amplify cathepsin B (CatB), a lysosomal enzyme that has been found to degrade pathogenic proteins and to be synaptoprotective in models of aging-related neurodegenerative disorders. After three daily infusions into hippocampal explants, extracts of bacopa (*Bacopa monnieri*) and the specific ginseng *Panax quinquefolius* enhanced the 30-kDa active form of the CatB protease (CatB-30) by over 3-fold, whereas only small increases were produced by another ginseng extract (*Panax ginseng*) and wild blueberry extract (*Vaccinium corymbosum*). Only *P. quinquefolius* treatment produced a correlation between enhanced CatB-30 levels and levels of the synaptic proteins GluA1 and synaptophysin. This ginseng extract was also the most effective natural product tested for increasing the autophagy marker LC3-II. To further address the hypothesis that dietary agents activate the CatB autophagy-lysosomal component and enhance synaptic resilience, we tested plant extracts and the exercise mimetic  $\beta$ -GPA in long-term hippocampal slice cultures subjected to a week of proteostatic stress induced by the lysosomotropic compound chloroquine. Note that, similar to the benefits of a healthy diet, exercise is well-known for reducing dementia risk, and the exercise mimetic  $\beta$ -GPA was previously shown in our lab to positively modulate the CatB protease. In the chloroquine-insulted tissue, both *P. quinquefolius* and  $\beta$ -GPA treatments resulted in significant protection of hippocampal synapses, and *V. corymbosum* extract protected marginally. These results indicate synaptic resilience as being a key factor for brain health through diet and exercise. In recent *in vivo* studies, our translational research identified selective cognitive defects in middle-aged rodents as compared to respective young groups, and the aging-induced cognitive decline was offset by two tested treatments. The same ginseng extract found to be an effective CatB positive modulator improved behavioral performance in middle-aged Fisher rats (12 months) when supplemented into supplied food pellets for 6 weeks. In a separate study,  $\beta$ -GPA was found to enhance memory in 10-month-old mice when supplemented into a 6-week feeding schedule. Interestingly, the commonality the two agents have for reducing the aging-related cognitive deficits is similar to the common modulation the agents elicit towards key elements of the autophagy-lysosomal system.

# Evaluating Serotonin 2C and Dopamine D3 Receptor Ligands, Alone and in Mixtures, as Candidate Medications for Substance Use Disorders

Briana Mason,<sup>1</sup> Anona Thomas,<sup>2</sup> Yonggong Shi,<sup>2</sup> Christina George,<sup>2</sup> Jianjing Cao,<sup>3</sup> Amy Newman,<sup>3</sup> and Gregory T. Collins<sup>1</sup>

<sup>1</sup>Univ of Texas Health Science Center at San Antonio; <sup>2</sup>University of Texas Health Science Center at San Antonio; and  
<sup>3</sup>NIDA-IRP

Abstract ID 22400

Poster Board 213

Substance use disorders (SUDs) remain debilitating public health crises that have only escalated in economic severity and lethality over the last decade. Serotonin 2C (5-HT<sub>2C</sub>) and dopamine D3 (DAD3) receptor ligands have shown promise as candidate SUD medications, as they can attenuate drug-taking in preclinical SUD models. However, their potential for adverse side effects and ineffectiveness in clinical trials represent translational hurdles. Two potential approaches to circumvent these issues are to enhance the selectivity of the ligands and/or develop polypharmacy approaches targeting multiple receptors. Therefore, the first goal of this study was to characterize the potential of a selective 5-HT<sub>2C</sub> receptor agonist (CP-809,101; 0.32-10 mg/kg, IP) and a selective DAD3 receptor partial agonist (VK4-40, 1-32 mg/kg, IP) and a DAD3 receptor antagonist (VK4-116, 1-32 mg/kg, IP) to reduce responding for cocaine (0.32 mg/kg/inf), methamphetamine (0.056 mg/kg/inf), fentanyl (0.0032 mg/kg/inf), and sucrose (1 sucrose pellet) in male (n=6-8 per group) and female (n=6-8 per group) Sprague Dawley rats. Rats were trained to receive a delivery of each reinforcer under a progressive ratio schedule of reinforcement. Once responding stabilized ( $\leq 2$  reinforcers earned over two consecutive sessions), rats were pretreated with each compound 15 min prior to test sessions to generate inhibition functions. CP-809,101 reduced responding across drug conditions, was more potent than either of the DAD3 receptor ligands, and had a lesser effect on rats responding for sucrose reinforcers. VK4-40 was more effective at reducing responses for fentanyl than VK4-116, but VK4-116 was more effective than VK4-40 in rats that self-administered cocaine. These data informed our approach to evaluating mixtures. Next, we sought to evaluate the effectiveness of 5-HT<sub>2C</sub> and DAD3 receptor ligand mixtures to reduce drug taking, with the hypothesis that such a polypharmacy approach would be more potent and/or effective at reducing drug taking than would be expected based on the effects of the ligands alone. When the compounds were evaluated as mixtures, combinations of CP-809,101 and VK4-40 as well as CP-809,101 and VK4-116 effectively produced reductions in drug taking at doses indicating additive or synergistic interactions. Mixtures of 5-HT<sub>2C</sub> and DAD3 ligands were more potent in the reduction of responding for intravenous drugs as compared to responding for sucrose reinforcers. These studies show that selective 5-HT<sub>2C</sub> and DAD3 receptor ligands can be useful for the reduction of drug-taking in rats, and suggest that a polypharmacy approach targeting these two receptors may provide a novel, and broad-spectrum strategy to treat SUDs.

This research is supported by the U.S. Department of Veterans Affairs (I01BX004550; BM, GTC).

# Novel Sigma Receptor Dual Modulator Enhances Memory Behavior in the Senescence-Accelerated Prone Mouse (SAMP8) Model of Age-Related Cognitive Decline

Ariel Magee,<sup>1</sup> Susan A. Farr,<sup>2</sup> Mike Niehoff,<sup>2</sup> Ivonne Larrea,<sup>2</sup> Yoan Ganey,<sup>2</sup> Ken Witt,<sup>3</sup> and Justin Samanta<sup>4</sup>

<sup>1</sup>Southern Illinois Univ; <sup>2</sup>Saint Louis University School of Medicine; <sup>3</sup>Southern Illinois Univ School of Pharmacy; and <sup>4</sup>Saint Louis University College of Arts and Sciences

Abstract ID 52588

Poster Board 214

Alzheimer's disease (AD) is the leading cause of dementia, affecting nearly 50 million people worldwide. Despite an increased understanding of AD pathogenesis, the search for viable disease-modifying therapeutics continues. Sigma-1 and sigma-2 receptors, which are found in regions of the brain highly affected by AD, present novel targets with disease-modifying potential. While little is known about the mechanism of action of the sigma receptors, they are proposed to be involved with the regulation of many AD hallmarks. Investigations of sigma-1 receptor and sigma-2 receptor modulators have independently shown to improve learning and memory behaviors, as well as reduce neuroinflammation and amyloid-beta brain levels in AD mouse models (Antonini et al., *Journal of Alzheimer's Disease*, 24(3), 569–586, 2011; Izzo et al., *PLoS ONE*, 9(11), 2014). Herein, we investigated a novel molecule (BBZI) with high receptor affinity for both sigma-1 (Ki = 0.8nM) and sigma-2 (Ki=2.5nM) receptors as to learning and memory behavioral responses with chronic dosing in the senescence-accelerated prone mouse (SAMP8) model of age-related cognitive decline and AD.

Twelve-month old SAMP8 were treated with BBZI over 28-days, i.p. daily dosing (0.001, 0.01, 0.1, 1.0, and 10 mg/kg) and vehicle controls. Testing battery included investigation of locomotion and anxiety through the open field activity test (day 15) and the elevated plus test (days 16-17), Y-maze for short term spatial memory (day 22), novel object recognition to test recognition memory (days 23-24), and the T-maze foot-shock avoidance test for long term spatial memory (days 20 & 27). The results indicated there is no difference in distance traveled or level of anxiety like behavior across the dosing groups as indicated by the open field activity test and the elevated plus test, respectively. There was also no significant improvement in Y-maze tested spatial memory or recognition memory as indicated novel object recognition test results. However, the T-maze foot-shock avoidance test results indicated BBZI treatment of 1.0 mg/kg with i.p. injection displayed significant positive results with acquisition learning testing (9.25 +/- 0.91 trials to first avoidance,  $p < 0.05$ ) and retention memory testing (6.42 +/- 0.84 trials to criterion,  $p < 0.001$ ). Additionally, BBZI treatment of 0.1 mg/kg with i.p. injection yielded positive results with retention memory testing (8.46 +/- 0.86 trials to criterion,  $p < 0.05$ ).

Our study revealed that at the doses specified, BBZI promotes enhanced long term memory effectiveness with the T Maze foot-shock avoidance test in a mouse model of AD, while having no impact on general activity or anxiety. This corroborates the hypothesis of sigma receptors' involvement in learning and memory behaviors and further supports the potential of Sigma receptor target therapeutics for AD treatment.

# Effects of a two-hit model of early life adversity on oral ethanol self-administration and adrenergic receptor expression in adolescent rats

Brian Parks,<sup>1</sup> Paloma Salazar,<sup>1</sup> Madison McGraw,<sup>1</sup> Lindsey Morrison,<sup>2</sup> Julia Tobacyk,<sup>1</sup> Lisa Brents,<sup>1</sup> and Michael Berquist<sup>1</sup>

<sup>1</sup>Univ of Arkansas for Medical Sciences; and <sup>2</sup>University of Arkansas for Medical Sciences

Abstract ID 24021

Poster Board 215

Alcohol (EtOH) use significantly contributes to the three leading causes of death among adolescents: unintentional injuries, suicide, and homicide. Adolescents consume more EtOH per drinking occurrence than adults. Early life adversities (ELA), including prenatal opioid exposure (POE) and postnatal adverse experiences, increase the risk of problematic EtOH use among adolescents. POE is any exposure to opioids during gestation and postnatal adverse experiences include abuse, neglect, or household dysfunction, such as parental substance use disorder. Because they often co-occur and are risk factors for early EtOH use, we investigated the relationship between POE, postnatal adversity, and adolescent EtOH. We also aimed to determine how  $\alpha$ -adrenoceptor activity is affected by these ELAs to in turn affect adolescent EtOH intake. To model POE, pregnant rats received 15 mg/kg/day morphine or vehicle via subcutaneous minipumps from gestational day 9 to birth. To model postnatal adversity, we used limited bedding and nesting (LBN) procedures in which dams and litters were restricted to 20% of normal bedding and nesting materials from postnatal day (PD) 3 to 11. LBN increases maternal stress and decreases maternal care quality. Starting on PD 31 or 33, rats were given access to bottles containing either a 20% EtOH (v/v) solution or water under an intermittent-access, two-bottle choice procedures for 24-hour sessions, three days per week for four weeks (12 sessions). Rats received either yohimbine (1 mg/kg; ip) or vehicle 30-min prior to each EtOH access session to determine if pharmacologically-induced sympathomimetic activity enhances the acquisition of EtOH in adolescent rats and to assess for altered  $\alpha_2$ -adrenoceptor activity in rats that experienced POE and/or LBN. Cortices and brainstems from littermates without EtOH exposure were harvested on either PD 30 or PD 70 and used in radioligand receptor binding assays to quantify  $\alpha_1$ - and  $\alpha_2$ -adrenoceptor density. We hypothesized that adolescents with a history of combined POE and LBN ("two-hit" group) will consume more EtOH, have higher brain densities of  $\alpha_1$ -adrenoceptor, and have lower brain densities of  $\alpha_2$ -adrenoceptor than adolescents with either condition alone. In general, female rats drank more EtOH than male rats, and EtOH consumption was more affected by treatment condition in females than males. For example, female rats, more so than male rats, in the two-hit treatment group drank more EtOH after administration of yohimbine. Also, in the two-hit group, there was a decrease in EtOH consumption compared to the LBN and control groups within each sex. In our adrenoceptor density study, there was no difference in  $\alpha_1$ -adrenoceptor expression between males and females and across treatment groups. However, in the female cortex, there was high variability and a main effect of sex in  $\alpha_2$ -adrenoceptor expression with male expression being greater. Together, these results indicate a complex interaction between ELA, sex, and  $\alpha$ -adrenoceptor activity that may support a stress inoculation hypothesis.

Support/Funding Information: NIDA 5T32DA022981 ABI/ACRI Grant Award

# Pentobarbital More Potently Disrupts Learning in Females Than Males Compared to Other Allosteric Modulators of the GABA<sub>A</sub> Receptor Complex

Ashley Henderson,<sup>1</sup> Tamara Morris,<sup>2</sup> Sarah Melton,<sup>2</sup> and Peter J. Winsauer<sup>2</sup>

<sup>1</sup>Louisiana State Univ Hlth Sci Ctr; and <sup>2</sup>LSUHSC Department of Pharmacology

Abstract ID 25346

Poster Board 216

**Background:** Understanding sex differences in drug effects leads to improved clinical outcomes and a better understanding of drug mechanisms. For this reason, several positive allosteric modulators and a negative allosteric modulator of the GABA<sub>A</sub> receptor complex were administered to male and female Long-Evans rats responding in a learning task. The positive allosteric modulators were ethanol, pentobarbital, and alprazolam, whereas the negative allosteric modulator was FG-7142.

**Methods:** Learning was assessed using a repeated-acquisition procedure in which subjects responded on three response keys to acquire a different four-response sequence each session for food reinforcement. More specifically, sequence completions were reinforced under a second-order variable ratio 2 (VR-2) schedule, and incorrect responses resulted in a 5-sec timeout. Data were analyzed in terms of the overall response rate (responses/min, not including timeouts) and the percentage of errors ((incorrect responses/total responses) x 100). After responding under the repeated acquisition baseline stabilized, dose-effect curves were obtained for each of the drugs. ED50 values were calculated for each subject and the group by linear regression using two or more data points in the descending (response rate) and ascending (percent errors) portion of the dose-effect curves.

**Results:** With a few exceptions, all of the drugs were equally potent in both males and females compared to their respective controls, and dose-dependently decreased the overall response rate and increased the percentage of errors as the dosage increased. Overall response rate and percent errors were both significantly affected at the same dose for FG-7142 (1.0-10 mg/kg) and ethanol (0.32-1.33 mg/kg). Alprazolam (1.0-18 mg/kg) more potently decreased response rate than it increased percent errors. In contrast, pentobarbital (1.0-18 mg/kg) was unlike the other drugs in that it more potently decreased response rate and increased errors in female rats compared to males by a quarter-log unit. This difference was also reflected in the ED50s calculated from individual animal data and ED50s from grouped data. Pentobarbital also significantly increased percent errors at a lower dose than the dose affecting response rate in males, while response rate and percent errors were significantly disrupted at the same dose in females.

**Conclusions:** Whereas ethanol, pentobarbital, alprazolam, and FG-7142 all allosterically modulate the GABA<sub>A</sub> receptor complex, they can produce very distinctive disruptions of rate and accuracy of responding under a repeated-acquisition procedure. Furthermore, these drugs can produce distinctive disruptions of these measures in males versus females. In this study pentobarbital decreased accuracy at doses lower than those that decreased response rate in males, whereas it decreased both measures at the same dose in females. These data, therefore, expand our understanding of allosteric GABA<sub>A</sub> modulators and reveal sex differences in pentobarbital's potency for disrupting learning.



# The ascending limb of the dose-response curve for cocaine self-administration is an experimental artifact

Luis Tron Esqueda,<sup>1</sup> Jhanvi N. Desai,<sup>1</sup> and Andrew Norman<sup>1</sup>

<sup>1</sup>University of Cincinnati College of Medicine

Abstract ID 24934

Poster Board 217

Cocaine self-administration is a model of cocaine use disorder and is considered an example of positive reinforcement. Agonist dose-response curves are fundamental to understanding the mechanisms underlying agonist induced responses. According to operant behavior theory, a greater positive reinforcement (higher cocaine unit dose) produced by a stimulus (cocaine injection) would increase the probability of performing the operant behavior (lever press) and result in a higher frequency of lever pressing. Conversely, it is observed that as the cocaine unit dose increases, the rate of cocaine self-administration decreases, particularly at a fixed ratio (FR) 1 schedule, thus creating a paradox. However, at smaller unit doses the rate of cocaine self-administration is reported to increase as the unit dose increases up to a maximum. This ascending limb of the cocaine dose-response curve is considered to represent the positive reinforcing effects of cocaine. FR1 schedule of cocaine self-administration follows the compulsion zone theory which states that cocaine induces lever pressing behavior only when cocaine level is below the satiety threshold and above the remission threshold. This theory explains FR1 and progressive ratio schedules over a range of cocaine unit doses but has not been applied to high FR schedules. We examined the cocaine dose-response relationship through cocaine self-administration on FR1 and FR50 at different unit doses (0.1, 0.3, 0.5, 0.75, 1.5 and 3  $\mu\text{mol/kg}$ ). Rats ( $n=5$  completed all phases of the study) were trained to self-administer cocaine on FR1 at different unit doses, and on FR50 at 3  $\mu\text{mol/kg}$  unit dose. Next, they self-administered cocaine in sessions that started with FR1, then proceeded to FR50 across the range of unit doses. Only one dose was used in a session, and three sessions were performed for each dose. Rats completed all injections on FR1 but could not complete all injections on FR50 at doses lower than 1.5  $\mu\text{mol/kg}$ . The ratio of the number of injections completed on FR50 relative to FR1 was 0.03, 0.43, 0.62, 0.72, 1 and 1 at 0.1, 0.3, 0.5, 0.75, 1.5 and 3  $\mu\text{mol/kg}$  cocaine doses respectively. Rats were able to maintain cocaine level at or above the satiety threshold for all unit doses on FR1 as an injection follows one lever press. However, on FR50, they could maintain cocaine level above the satiety threshold only at 1.5 and 3  $\mu\text{mol/kg}$  doses. During cocaine self-administration on FR50 at 0.1, 0.3, 0.5 and 0.75  $\mu\text{mol/kg}$  doses, cocaine levels gradually declined through the compulsion zone while rats completed the 50 required presses. The injection of a small unit dose was not enough to maintain cocaine level within the compulsion zone. This ascending limb of the dose-response curve appears due to rats being unable to complete all injections in the compulsion zone on FR50 before cocaine level falls below the remission threshold. In cocaine self-administration sessions where session time is kept constant, the duration of responding increases with increasing unit doses until responding persists for the entire session. This results in an artifactual increase in the rate of responding as a function of a narrow range of lower unit doses and is exacerbated at FR50. There is no part of the dose-response function that is consistent with the positive reinforcing effects of cocaine.

Supported by NIDA grant U01DA050330 (to ABN)

# Organic Cation Transporter 3 is a Crucial Modulator of Serotonin Clearance in Basolateral Amygdala and Sex-Dependently Modulates Fear Behaviors

Nikki Clauss,<sup>1</sup> Lauren Honan,<sup>2</sup> William A. Owens,<sup>3</sup> Rebecca Horton,<sup>2</sup> Glenn Toney,<sup>4</sup> and Lynette C. Daws<sup>5</sup>

<sup>1</sup>Univ of Texas Health Science Center At San Antonio; <sup>2</sup>University of Texas Health Science Center At San Antonio; <sup>3</sup>UT Health Science Ctr-San Antonio; <sup>4</sup>Univ of Texas Health San Antonio; and <sup>5</sup>Univ of Texas Health Science Ctr

Abstract ID 29086

Poster Board 265

Dysregulation of serotonergic neurotransmission has long been implicated in neuropsychiatric illness, including stress related disorders, therefore understanding the role serotonin (5-HT) plays in circuitry relevant to emotion could open new avenues for improving treatment of stress-related disorders. Considerable research has investigated the role of the high-affinity, low-capacity 'uptake-1' 5-HT transporter (SERT) in modulation of emotion-regulating circuitry. To date, pharmacological targeting of SERT has shown variable clinical efficacy, suggesting a role for other mechanisms in manifestation of disorders associated with serotonergic dysregulation. Evidence from our laboratory and others suggests that the corticosterone-sensitive, organic cation transporter 3 (OCT3), a low-affinity, high-capacity 'uptake-2' transporter of 5-HT, has a significant impact on serotonergic homeostasis and may play a major role in stress-related disorders. Here we used genetic and viral approaches to test the hypothesis that OCT3 is an important mechanism for 5-HT clearance in basolateral amygdala (BLA, a brain region essential to processing and consolidation of fear memory), and strongly modulates fear related behaviors in adult male and female mice. Oct3 floxed mice were crossed with either ePet-cre mice to knockout (KO) OCT3 from 5-HT neurons during development, or with Nestin-cre/ERT2 mice, to allow tamoxifen induced global depletion of OCT3 from neurons and glia. To assess involvement of OCT3 primarily on post-synaptic neurons in BLA, we bilaterally injected AAV5-EF1a-mCherry-IRES-WGA-Cre, or control virus, into BLA of OCT3 floxed mice. We characterized 5-HT clearance in BLA using *in vivo* high-speed chronoamperometry. Consistent with OCT3 being an important regulator of 5-HT homeostasis, we found 5-HT clearance in BLA to be impaired in mice of both sexes regardless of constitutive KO (OCT3 floxed x ePet1-cre) or conditional (tamoxifen-inducible) depletion. Preliminary data from mice injected with virus are showing similar trends. Mice constitutively lacking OCT3 on 5-HT neurons of either sex showed no differences in fear acquisition or memory. Mice with conditional OCT3 global depletion or virally induced OCT3 depletion in BLA, likewise showed no difference in fear acquisition compared to relevant control mice. However, these mice showed dramatic sex-dependent differences in fear memory. Tamoxifen-inducible OCT3 depletion resulted in poorer contextual fear memory in males, but increased contextual fear memory in females, such that freezing behavior remained at almost 100% across the test period. Preliminary data from mice with viral depletion of OCT3 in BLA reveal no consequence for fear acquisition and memory in males, whereas females show both increased contextual and cued fear memory. The lack of behavioral consequence for fear acquisition and memory in mice with constitutive loss of OCT3 from 5-HT neurons suggests compensation may be involved. Alternatively, OCT3 located on other neuronal types and/or glia may be more important for these behavioral effects. Together, these data support the hypothesis that OCT3 is an important mechanism for 5-HT clearance in BLA, and plays a critical, sex-dependent role in fear memory, though the underlying mechanism(s) remain to be elucidated.

Supported by R01 MH093320 to LCD and GMT, NJC is supported by T32 DA031115.

# Ethanol Vapor Self-administration Reveals that Female Wistar Rats are More Likely to Become High Intensity Binge Users than Male Rats

Alicia Avelar,<sup>1</sup> Kareena Narula,<sup>2</sup> Kalie A. Quon-adams,<sup>2</sup> Stephanie Krause,<sup>3</sup> Amanda Roberts,<sup>3</sup> Giordano de Guglielmo,<sup>2</sup> and Olivier George<sup>2</sup>

<sup>1</sup>Univ of California San Diego; <sup>2</sup>University of California San Diego; and <sup>3</sup>The Scripps Research Institute

Abstract ID 18546

Poster Board 266

Alcohol misuse has long been a serious health and social concern. Alcohol binge use can increase escalation of alcohol use in humans, and National Institute on Alcohol Abuse and Alcoholism (NIAAA) has described High Intensity (HI) binge drinking which is consuming twice the alcohol as a binge user in a 2-hour period. Binge and HI binge drinking increase negative health and social outcomes for humans, however there are few animal models exhibiting voluntary self-administration of similar amounts of alcohol. Previous work shows that male rats escalate self-administration of ethanol vapor to the point of becoming dependent and that ~25% of male Wistar rats binge ethanol vapor to reach blood alcohol levels (BALs) in the 300-450 mg% range (de Guglielmo et al., 2017, George lab unpublished data). However, this study was performed only in male rats and it is unclear if the same phenomenon occurs in females. To address this gap, we evaluated sex differences in ethanol vapor self-administration (EVSA) in Wistar rats. **Our hypothesis was that some rats that self-administer ethanol vapor will be High Intensity binge users.** Rats were tested under a fixed ratio 1 schedule of reinforcement for 8 hr sessions every other day and the duration of alcohol vapor puff increased every 8 sessions from 2, to 5, to 10 minutes. Rats received 1 puff of ethanol vapor with a 20 s time out period for each nosepoke into the drug associated nosepoke port. Tail blood was collected throughout the experiment and blood alcohol levels (BALs) were measured by gas chromatography. Female rats learned to discriminate between active and inactive nosepokes earlier and more accurately than males. Female rats self-administered more ethanol vapor than males. BALs increased throughout the ethanol vapor sessions, with female levels being higher than males. Our criteria for High Intensity binge use of ethanol vapor is that rats have BALs over 160 mg/dL, which is twice the BAL for meeting binge use criteria (80 mg/dL), after their final 8 hr session of self-administering 10 minute long ethanol vapor puffs. Overall, the present results show that female rats discriminate better between active and inactive nosepokes, have faster acquisition of ethanol vapor self-administration, and binge more than males. These results demonstrate the relevance of the ethanol vapor self-administration model to study binge ethanol use and demonstrate that females are particularly vulnerable to High Intensity binge use of alcohol.

Support/Funding Information: 5T32AA007456-39, Dr. Marisa Roberto, The Scripps Research Institute, Neuropsychopharmacology:Multidisciplinary Training 5R01AA022977-08, Dr. Olivier George, University of California San Diego, Alcohol Vapor Self-Administration in Rats, P60AA006420 Scripps Research Alcohol Research Center's Animal Models Core

# Effects of Cannabinoids and a Cannabinoid Extract on Thermal Nociception and Conditioned Behavior

Tamara Morris,<sup>1</sup> Peter J. Winsauer,<sup>2</sup> Scott Edwards,<sup>3</sup> and Jessica Cucinello-Ragland<sup>3</sup>

<sup>1</sup>Louisiana State Univ Hlth Sci Ctr; <sup>2</sup>Louisiana State Univ Health Science Ctr; and <sup>3</sup>LSU Health Sciences Center

Abstract ID 25413

Poster Board 267

**Introduction:** Cannabinoids, both alone and in combination with opioids, have been tested as potential therapeutics for the mitigation of pain. Therefore, our research examined the antinociceptive, behavioral, and antihyperalgesic effects of  $\Delta^9$ -tetrahydrocannabinol (THC), CP 55,940 (CP), cannabidiol (CBD), and a cannabis-derived mixture (NEPE14). Both THC and CP were also administered in combination with the cannabinoid type-1 receptor (CB1R) antagonist, AM251, to determine the role of CB1Rs in their antinociceptive, behavioral, and antihyperalgesic effects.

**Methods:** Nine male Sprague Dawley (SD) rats were trained to respond under a fixed-ratio 30 (FR-30) schedule for food reinforcers. During these sessions, overall response rate, running rate, and pre-ratio pauses (PRP) were recorded. Nociception was assessed after the session with warm-water tail-withdrawal latency (in seconds) from 40 or 50 °C water. Subjects received the cannabinoids or NEPE14 30 minutes prior to the behavior sessions once or twice per week until complete dose-effect curves were established. When administered, AM251 (3.2 mg/kg) preceded cannabinoid administration by 10 minutes (i.e., 40 minutes pre-session). In two separate groups of male and female Wistar rats, complete Freund's adjuvant (CFA; n= 6-8) or saline (n= 4-7) was administered into the hind paw to induce inflammation. After CFA or saline injection, probing of the hind paw with von frey filaments was used to assess mechanical hypersensitivity and a Thermal Probe Test was used to assess thermal hyperalgesia. The cannabinoids (i.p.) or NEPE14 (i.p. or via the oral mucosa) were administered 30 minutes prior to testing.

**Results:** Acute THC (1-5.6 mg/kg) and CP (0.032-0.18 mg/kg) significantly and dose-dependently decreased overall response rate and running rate, but not PRP. Both drugs also increased tail-withdrawal latency compared to vehicle. While AM251 produced a small, but significant, rate-decreasing effect alone, it also significantly antagonized the rate-decreasing effects of both THC and CP, and the antinociceptive effects of CP. In contrast, CBD (10-100 mg/kg) or NEPE14 (3.7-20.7 ml/kg i.p., or 0.1-1 ml o.m.) did not significantly decrease response rates or increase tail-withdrawal latency. In rats administered CFA, mechanical and thermal paw-withdrawal thresholds were significantly decreased compared to control rats (main effect), and NEPE14 (6.6 and 20.7 ml/kg) significantly reduced the mechanical and thermal hypersensitivity by returning those thresholds to control levels (main effect). Similarly, NEPE14 (o.m.) significantly reduced mechanical and thermal hypersensitivity in both male and female rats injected with CFA, as indicated by either main effects or an interaction.

**Conclusion:** Of the cannabinoids tested, only THC and CP significantly reduced thermal nociception. However, the antinociceptive doses of each drug in SD rats were less potent (THC), or more potent (CP), than the doses that disrupted conditioned behavior. The antagonism of the antinociceptive and behavioral effects of THC and CP by AM251 indicated that these effects were predominately mediated by CB1Rs. Finally, NEPE14 did not significantly affect thermal nociception or conditioned behavioral responding, but it significantly reduced CFA-induced mechanical and thermal hyperalgesia. These data suggest that NEPE14 may have effects that are distinct from those of many individual cannabinoids.

# Hypothalamic nociceptin neurons modulate stress-induced binge eating behaviors

Kyle Parker,<sup>1</sup> Vincent Duong,<sup>1</sup> Wenxi Yang,<sup>1</sup> and Lamley Lawson<sup>1</sup>

<sup>1</sup>Washington Univ Sch of Med

**Abstract ID 26311**

**Poster Board 268**

Homeostatic regulation of food consumption and stress is critical to survival, yet certain environmental conditions facilitate aberrant feeding behaviors. Nociceptin and its receptor, nociceptin opioid peptide (NOP) receptor have a vast neuromodulatory network spanning multiple stress and reward-related brain nuclei and have been demonstrated to modulate feeding and stress regulation. Previous data has shown that stimulation of nociceptin-expressing neurons in the arcuate nucleus of the hypothalamus (ARC) increases food consumption. Similarly, stimulation of these neurons afferent projections within the bed nucleus of the stria terminalis (BNST) also increases food consumption. Here, we examined how this nociceptinergic neurocircuitry controls palatable food consumption in a model of stress-induced binge eating behavior where animals are given intermittent food restriction and palatable food access similar to "yo-yo" dieting. We used inhibitory opsin, parainopsin (PPO) in *Prnc-Cre* mice to inhibit nociceptin-expressing ARC projections in the BNST during food stress and palatable food access. We found that BNST-afferent  $ARC^{Pnoc}$  neuron inhibition reduces stress-induced food consumption in animals previously exposed to cycles of food restriction and ad libitum palatable food access.

Supported by NIH grant P30 DK056341 (Nutrition Obesity Research Center)

# Role of Neuromedin S-expressing Ventral Tegmental Area Neurons in Morphine Behavior

Cristina Rivera Quiles,<sup>1</sup> Milagros Alday,<sup>2</sup> Olivia Dodson,<sup>2</sup> and Michelle Mazei-Robison<sup>1</sup>

<sup>1</sup>Michigan State Univ; and <sup>2</sup>Michigan State University

Abstract ID 13625

Poster Board 269

**Objective:** Opioid dependence and addiction constitute a major health and economic burden, but our limited understanding of the underlying neurobiology limits better interventions. Alteration in the activity and output of dopamine (DA) neurons in the ventral tegmental area (VTA) is known to contribute to drug effects, but the mechanisms underlying these changes remain relatively unexplored. We used TRAP to identify gene expression changes in VTA DA neurons following chronic morphine and found that Neuromedin S (NMS) is enriched in VTA DA neurons, and its expression is robustly increased by morphine. However, whether all VTA DA neurons express NMS, and their potential functional impact has yet to be determined. We hypothesize that NMS neurons represent a novel subset of VTA neurons that contribute to morphine-elicited behavior. Specifically in these studies, we hypothesize that activating and inhibiting VTA-NMS neurons will promote and inhibit morphine behaviors, respectively.

**Methods:** To test this, adult male and female NMS-Cre mice and wild-type littermates were used. Cre-dependent viral vectors were stereotaxically injected into the VTA to allow for DREADD-mediated activation (Gq) or inhibition (Gi) of VTA-NMS neurons. Behavioral analyses were completed two weeks after surgery. Locomotor activity was assessed following saline (d1), saline + Clozapine-N-oxide (CNO, 0.3mg/kg, ip, d2-d3), and morphine (15mg/kg) + CNO (d4-d8). A morphine + CNO challenge was done 1 week following d8. Conditioned place preference (CPP) was also performed. Mice underwent a 20 min. pre-test, followed by conditioning sessions where they received vehicle + saline in the morning and CNO + morphine (0.3mg/kg and 15mg/kg, respectively) in the afternoon for 4 days. Morphine preference was assessed during a 20 min. post-test. Significant differences ( $p < 0.05$ ) were determined using a repeated-measures two-way ANOVA for locomotor behavior and paired t-tests for CPP (pre-test vs. post-test).

**Results:** We find that both male and female NMS-Gq mice exhibit increased morphine-induced locomotor activity compared to controls. Additionally, locomotor response to a challenge morphine + CNO injection was significantly increased in NMS-Gq mice compared to controls. NMS-Gi mice show a trend for the opposite effect, with a decreased locomotor response to a challenge morphine + CNO injection. In CPP assays, NMS-Gq mice displayed a similar morphine-CNO CPP to controls. However, NMS-Gi mice exhibited decreased morphine-CNO CPP compared to controls.

**Conclusions:** Thus, manipulation of VTA-NMS neuronal activity alters morphine-elicited behaviors including locomotion, sensitization, and CPP. Future studies will determine whether VTA-NMS neuronal activity modulates other morphine behaviors. Our current data suggest that VTA-NMS neurons represent a subset of neurons that may be functionally relevant for morphine responses.

Financial support provided by NIDA (R01 DA039895, MMR), the McManus Foundation, NSF (DGE-1848739, CMRQ) and the Howard Hughes Medical Institute.

# Self-administration of G-protein biased mu opioid agonists in nonhuman primates

Carol Paronis,<sup>1</sup> Kristen E. George,<sup>1</sup> Eric W. Bow,<sup>2</sup> Eugene S. Gutman,<sup>2</sup> Agnieszka Sulima,<sup>2</sup> Kenner Rice,<sup>2</sup> Arthur Jacobson,<sup>2</sup> and Jack Bergman<sup>1</sup>

<sup>1</sup>McLean Hospital/Harvard Medical School; and <sup>2</sup>NIDA and NIAAA

Abstract ID 21458

Poster Board 270

**Aim:** Biased signaling by *mu*-opioid agonists has been proposed to result in fewer opioid side effects and, consequently, an improved safety profile compared to conventional prescription opioids. We evaluated the acute effects of novel G-protein preferring opioid agonists in an assay of self-administration in nonhuman primates to determine whether G-protein preferring opioid agonists have reduced abuse liability.

**Methods:** Squirrel monkeys (*Saimiri sciureus*, n=3) surgically implanted with IV catheters were trained to respond on one lever for a food reinforcer (20% sweetened condensed milk) and on another lever for an IV injection of 0.01 mg/kg heroin under concurrent fixed ratio schedules. Once trained, heroin dose-effect functions were established in each subject by varying the unit dose of heroin available for injection, from 0.001 to 0.032 mg/kg/inj, under a modified double alternation schedule. Next, under similar conditions, the reinforcing effects of the novel *mu*-opioid agonists EWB-3-1, EWB-2-189 and EG-1-203 were evaluated, as were the effects of the rapid acting opioid agonist, remifentanyl. The reinforcing effects of heroin were periodically redetermined to ensure stability of performance.

**Results:** Under the concurrent schedules of reinforcement, responding was primarily distributed to the food-associated lever when saline was available and was increasingly allocated to the injection-associated lever with increasing doses of heroin. Heroin maintained self-administration over the dose range of 0.0032 to 0.032 mg/kg/inj, with peak number of injections, 26±13, obtained at 0.0032 mg/kg/inj heroin. Higher doses maintained fewer injections, resulting in an inverted-U shaped dose response function. Remifentanyl had qualitatively and quantitatively similar effects to heroin, although it was more potent with peak effects occurring at the unit dose of 0.00032 mg/kg/inj. The three novel opioids also maintained self-administration behavior: responding on the injection-associated lever increased with the unit dose of each novel compound, the peak number of injections was similar across drugs, ranging from 22±4 (EWB-1-203) to 29±3 (EWB-2-189), and inverted U-shaped functions were obtained with EWB-3-1 and EG-2-189. Solubility limits precluded testing doses of EWB-1-203 on the descending portion of the dose-effect curve.

**Conclusion:** EWB-3-1, EG-1-203, and EWB-2-189 all had reinforcing effects in a self-administration procedure, indicative of potential abuse liability. These data demonstrate that the absence of  $\beta$ -arrestin recruitment by *mu*-opioid agonists does not necessarily predict lower abuse liability of opioid agonists.

Funded by NIH/NIDA DA047574

# Targeting A3 Adenosine Receptor (A3AR) Attenuates Paclitaxel-induced Cognitive Impairment

Silvia Squillace,<sup>1</sup> Timothy Doyle,<sup>1</sup> Michael Niehoff,<sup>2</sup> Kenneth Jacobson,<sup>3</sup> Susan A. Farr,<sup>4</sup> and Daniela Salvemini<sup>1</sup>

<sup>1</sup>Department of Pharmacology and Physiology and Institute for Translational Neuroscience (ITN), Saint Louis University School of Medicine; <sup>2</sup>Department of Internal Medicine-Geriatrics, Saint Louis School of Medicine; <sup>3</sup>NIDDK/NIH; and <sup>4</sup>Department of Internal Medicine-Geriatrics and Institute for Translational Neuroscience (ITN), Saint Louis School of Medicine

Abstract ID 20618

Poster Board 400

Paclitaxel, standard-of-care first-line chemotherapy for epithelial ovarian cancer and triple negative breast cancer, was shown to impair learning and memory functions in >50% of cancer survivors. Underpinning mechanisms of this major neurotoxicity are still mostly unknown, and there are no FDA-approved interventions. We developed a mouse model of paclitaxel-induced cognitive impairment whose cumulative dose is comparable to the total dose per cycle used in breast cancer patients. Paclitaxel-treated mice showed significant cognitive impairment in different hippocampal tests (T-maze, Novel Object Place Recognition test, NOPRT). Learning and memory functions were improved by co-administration of the selective A3 adenosine receptor (A3AR) agonist, MRS5980, without adversely affecting anxiety-like behavior and locomotor activity. Noteworthy, A3AR agonists possess anticancer activity and enhance the antitumor effects of paclitaxel. Moreover, we previously shown that targeting A3AR successfully improved neurocognitive functions after cisplatin, another widely used chemotherapeutic. Our previous studies in chemotherapy-induced peripheral neuropathy showed that Paclitaxel treatment caused a strong neuroinflammation in the central nervous system through the dysregulation of adenosine signaling. Adenosine kinase (ADK) is a key regulator of the adenosine signaling at its receptors. Here we demonstrated that the ADK inhibitor, ABT-702, attenuated paclitaxel-induced cognitive dysfunctions in mice. Mechanistically, these data suggest that paclitaxel-induced ADK dysregulation leads to a reduction of adenosine signaling at the A3AR and it is functionally linked to the development of cognitive dysfunctions. Collectively, the A3AR is emerging as an exciting novel approach in the treatment of a major chemotherapy-induced neurotoxicity.

**Keywords:** Chemotherapy-induced cognitive impairment; A3 Adenosine receptor (A3AR); hippocampus; Paclitaxel; MRS5980.

**Fundings:** This study was funded by the National Institutes of Health Grant RO1CA230512 (NIH) to Daniela Salvemini. Daniela Salvemini is a co-founder of Biolntervene Inc. All other authors claim no conflicts of interest.



# Dynorphin release in the dorsal nucleus accumbens drives decreased feeding and consummatory reward behavior in mice

Nathanyal Ross,<sup>1</sup> Sineadh Conway,<sup>1</sup> and Ream Al-Hasani<sup>2</sup>

<sup>1</sup>Washington Univ; and <sup>2</sup>Washington Univ in St Louis

Abstract ID 54636

Poster Board 401

The nucleus accumbens (NAc) has been shown to be involved in reward-seeking behavior and feeding, and endogenous opioids, including kappa opioid receptors (KOR) and its endogenous ligand dynorphin (dyn), play a vital role in regulating reward and affective behavior within the NAc (Gendelis et al., 2021).

However, little is known about the role of the endogenous KOR/dyn system in feeding behaviors, specifically in the NAc. We hypothesized that dynorphin would dysregulate feeding in mice. To test this hypothesis, we optogenetically stimulated dynorphin neurons in the dorsal (dNAcSh) and ventral nucleus accumbens shell (vNAcSh). We found that photostimulation of dynorphin in the dNAcSh decreased chow consumption in a free-feeding paradigm. To determine whether dynorphin might also decrease operant responding and consumption of a palatable reward, mice were allowed to nosepoke for sucrose pellets in an operant task. We observed a decrease in the number of nose pokes and sucrose pellets consumed during dNAcSh dynorphin neuron photostimulation. Based on this data we wanted to determine whether dynorphin neuron activation drives a decrease in consumption regardless of motivated hunger state. To do this, we food-restricted and food-deprived the mice prior to the operant sucrose task and showed that dynorphin neuron activation decreased feeding post-food restriction and deprivation, as compared to controls, suggesting that dynorphin in the dNAcSh decreases feeding behavior regardless of motivated hunger state. Stimulation of vNAcSh dynorphin neurons showed no effect on feeding behavior, suggesting that there is a regionally distinct effect of dynorphin neuron activation within the NAc. To determine whether this decrease in feeding is dependent on the caloric value of the reward, we used a two-bottle choice task where mice have the option between water or saccharin, which has no caloric value but is still rewarding. We found that chemogenetic activation of dNAcSh dynorphin neurons through the use of excitatory Gq designer receptors exclusively activated by designer drugs (DREADDs) decreased saccharin preference, suggesting that dynorphin decreases palatable liquid consumption regardless of caloric value.

Together these findings illustrate a newfound role of dNAcSh dynorphin neurons in modulation of feeding and consummatory reward behavior.

Support/Funding Information: NIH/NIDA K99/R00 DA038725 (to R.A.), NIH/NIDA R21 DA048650 (to R.A.), NARSAD Young Investigator Grant from the Brain and Behavior Research Foundation, grant no. 28243 (to R.A.)

# A Role of NOD2 in CARTp-mediated Behavioral Hypersensitivities

Rachel Schafer,<sup>1</sup> Luigi A. Giancotti,<sup>1</sup> Zhoumou Chen,<sup>1</sup> Timothy Doyle,<sup>1</sup> Jinsong Zhang,<sup>2</sup> and Daniela Salvemini<sup>1</sup>

<sup>1</sup>Department of Pharmacology and Physiology, and Institute for Translational Neuroscience, Saint Louis University School of Medicine, St. Louis, MO; and <sup>2</sup>Department of Pharmacology and Physiology, Saint Louis University School of Medicine, St. Louis, MO

Abstract ID 24468

Poster Board 402

Neuropathic pain is a debilitating chronic condition that is severe and remains difficult to treat. While opioids are widely used to treat chronic pain, long-term use can cause severe side-effects and the risk of overdose. Therefore, there is a high priority to identify novel non-opioid-based therapeutic targets. Our lab discovered G-protein coupled receptor 160 (GPR160) as a potential novel therapeutic target for neuropathic pain and orphanized it as a receptor for cocaine- and amphetamine-regulated transcript peptide (CARTp). The molecular and biochemical mechanisms underpinning CARTp-induced behavioral hypersensitivities remain poorly understood. Intrathecal (i.th.) injections of CARTp in mice lead to GPR160-dependent and dose- and time-dependent behavioral hypersensitivities similar to those seen in neuropathic pain states (i.e. mechano- and cold allodynia). Unbiased RNA transcriptomics analysis of dorsal horn spinal cord (DH-SC) tissues harvested at time of peak hypersensitivities identified nucleotide-binding oligomerization domain-containing protein 2 (*Nod2*) as a gene that was significantly upregulated in response to CARTp. This led to our hypothesis that CARTp causes behavioral hypersensitivities through NOD2. NOD2 is a cytosolic pattern recognition receptor that is involved in activating the immune system in response to bacterial pathogens by directly binding to a bacterial peptidoglycan component, muramyl dipeptide (MDP). Once NOD2 is bound to MDP, RIPK2, a kinase shown to be critical for MDP-induced NOD2 signaling, binds to NOD2, activating multiple proinflammatory pathways. When compared to wild type mice (WT, C57BL/6), the development of mechano- and cold-allodynia following i.th. injections of CARTp was significantly attenuated in *NOD2*<sup>-/-</sup> mice, implicating NOD2 in the pharmacological actions of CARTp. To further validate our findings, we used a genetic approach to inhibit NOD2 in the DH-SC of mice. Knocking down *Nod2* using targeted-specific siRNA delayed CARTp-induced behavioral hypersensitivities, further confirming our knockout results. To explore further the CARTp/NOD2 signaling pathway, we tested whether knocking down RIPK2 attenuates the CARTp behavioral phenotype. Unexpectedly, genetic (i.e. *Ripk2*-targeted siRNA) or pharmacological (i.e. using a selective RIPK2 antagonist, WEHI-345) failed to block CARTp-induced behavioral hypersensitivities suggesting that RIPK2 is not required in CARTp/NOD2 signaling. In contrast and as expected, blocking RIPK2 blocked MDP-induced NOD2 signaling. These results indicate that CARTp causes sensitization through NOD2 but independent of RIPK2. Our results identify a novel pathway by which CARTp causes behavioral hypersensitivities and a novel mechanism by which NOD2 is activated in non-pathogenic settings.

Support/Funding Information: T32 GM 8306-29 and NIH/NINDS grant R01NS1132257 (DS).

# Effect of Methylphenidate on Motor Skill Learning and Consolidation

Cecilia Lee, Kaitlin R. Van Alstyne,<sup>1</sup> and Stephan G. Anagnostaras<sup>1</sup>

<sup>1</sup>University of California, San Diego

Abstract ID 53887

Poster Board 403

**Problem:** Methylphenidate (MPH) is one of the most commonly prescribed drugs to treat attention-deficit and hyperactivity disorder (ADHD), but the effect of methylphenidate, especially at low, cognitive-enhancing doses, on motor learning has not been explored in depth. Existing literature shows numerous experiments using high doses of methylphenidate that greatly exceed human therapeutic doses. This study addresses a gap in existing literature surrounding methylphenidate's effect on motor learning and memory; if methylphenidate enhances motor skill acquisition it could be useful in therapeutic settings where motor skills are being trained or rehabilitated. This experiment seeks to explore whether methylphenidate enhances motor learning as measured by Rotarod acquisition and retention.

**Methodology:** C57BL/6J x 129S1/SvImJ (129B6) hybrid mice were randomly assigned to drug (n=10) and control (n=9) groups. Both sexes were represented in both groups. Mice were given 1 mg/kg methylphenidate HCl, i.p., or an equivalent injection of saline vehicle (10 ml/kg). This dose was chosen from our lab's previous work finding this dose enhanced fear conditioning and water maze retention (Carmack et al., 2014, a, b). 15 min later, mice were placed on a 5-slot accelerating Rotarod (3 to 30 rpm across 5 min). Three training trials were completed within 90 min of injection, and the subjects' Rotarod positions were counterbalanced to control for any unknown differences in slot environment. One week later, two retention tests, one with drug and one without, were held on separate days to examine any differences in motor learning and retention of mice trained with and without methylphenidate.

**Major Findings:** Mice given methylphenidate during training showed improved motor memory at 7 days retention compared to the saline control mice. Although only minor improvements were exhibited during training, when tested one week later mice given methylphenidate during training showed substantial enhanced retention regardless of whether they were tested on or off drug. This suggests that methylphenidate given during motor skill acquisition may enhance consolidation of motor memory.

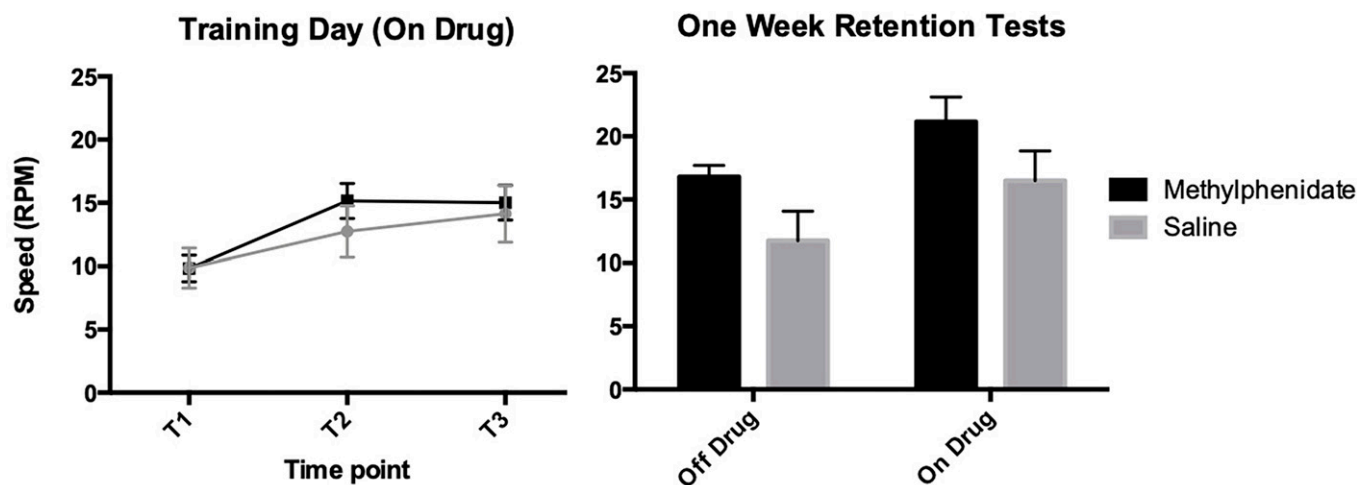


**Figure 1:** Average speed is shown for each of 3 training trials (on drug) and 2 one week retention tests. Mice given 1 mg/kg methylphenidate showed improved motor skill retention one week after training, regardless of whether or not they were tested on or off drug.

# Nicotine Withdrawal During Contextual Fear Extinction Causes Sex Specific Impacts in the Murine Dorsal and Ventral Hippocampus

Jack Keady,<sup>1</sup> and Jill Turner<sup>1</sup>

<sup>1</sup>Univ of Kentucky

Abstract ID 15496

Poster Board 404

Over 30 million Americans are smokers and more than 16 million have been diagnosed with a disease caused by smoking. The negative health risks of smoking are well known, and 70% of smokers express a desire to quit. However, the two current FDA approved medications for smoking cessation, Varenicline and Bupropion, have a maximal 25% quit success rate in a 1 year follow up. The lack of long-term efficacy of these drugs is often attributed to their ineffectiveness on non-craving related withdrawal symptoms such as cognitive deficits and affective dysfunction, both of which are predictors of smoking relapse. The hippocampus has well-defined roles in both contextual memory and affective responding, the dorsal hippocampus (DHIPP) and ventral hippocampus (VHIPP) respectively, suggesting these subregions are potential targets for mechanistic evaluation of two major predictive factors of smoking relapse. Previous data from our lab demonstrates that both male and female mice experience anxiety-like phenotypes following spontaneous nicotine withdrawal, which can be attenuated by knocking down the transcription factor CREB in the VHIPP, but not the DHIPP. However, we have yet to evaluate the mechanism that underlies the cognitive impairments associated with nicotine withdrawal. In order to study the impacts of chronic nicotine exposure and withdrawal on contextual memory, we chronically treated male and female 7 to 12-week-old mice with either saline or intermittent nicotine (18 mg/kg/day) via osmotic minipumps (Alzet 1002 model). On the twelfth day of treatment, the subjects were trained in a fear conditioning paradigm with two CS-US pairings (CS 89 dB tone and US 0.5 mA shock). The next morning the mice underwent the baseline assessment for contextual fear extinction, then in the afternoon had spontaneous withdrawal from nicotine via minipump removal or sham control surgery. The mice then underwent 5 days of contextual fear extinction. Following the 5<sup>th</sup> extinction session, the DHIPP and VHIPP were collected and assessed for transcriptomic and proteomic changes. Female mice undergoing nicotine withdrawal had modest deficits in contextual fear extinction, but there were no impacts of drug treatment observed in males. Preliminary transcriptomic results suggest males have higher baseline expression of Immediate Early Genes and Neuregulin Signaling Pathway genes in the DHIPP than females, which is attenuated by withdrawal from nicotine. Further examination of treatment by sex effects in the VHIPP are ongoing to determine if changes so far observed are subregion specific within the hippocampus.

Support/Funding Information: NIH/NIDA grant DA044311

# Widening the Opioid Analgesia Therapeutic Window with a Dual Pharmacology Strategy

Indu Mithra Madhuranthakam,<sup>1</sup> Sarah Uribe,<sup>1</sup> Danya Aldaghma,<sup>1</sup> Drew Kwitchoff,<sup>1</sup> Jonathan Philip,<sup>1</sup> Aela A. Williams,<sup>1</sup> Rohit A. Nambiar,<sup>1</sup> Dishary Sharmin,<sup>2</sup> James Cook,<sup>2</sup> Bradford Fischer,<sup>3</sup> and Thomas Keck<sup>1</sup>

<sup>1</sup>Rowan University; <sup>2</sup>University of Wisconsin Milwaukee; and <sup>3</sup>Cooper Medical School of Rowan University

**Abstract ID 26924**

**Poster Board 405**

Opioids are effective in managing acute and chronic pain but have serious side effects like constipation, tolerance, abuse liability, and respiratory depression. To provide safer analgesic options to patients, it is critical to identify new pharmacotherapeutic strategies to treat pain. In addition to central and peripheral nociceptive pathways, antinociception can also be achieved by selective enhancement of GABAergic signaling at ionotropic GABA<sub>A</sub> receptors. These receptors can be selectively targeted by MP-III-024, a novel  $\alpha 2/\alpha 3$  subunit-selective positive allosteric modulator (PAMs). We previously demonstrated that morphine/MP-III-024 co-administration produced synergistic antinociceptive and antihyperalgesic effects. In this follow-up study, we investigated whether co-administration of MP-III-024 with morphine generates synergistic effects in behavioral tests susceptible to morphine side effects. Herein, we report that co-administration of MP-III-024 with morphine at a 0.94:1 ratio (synergistic in antinociception models) induced only additive or sub-additive effects on morphine-induced hyperlocomotion, behavioral disruption measures in food-maintained operant responding, and conditioned place preference. Co-administration of MP-III-024 also does not affect the development of analgesic tolerance caused by chronic morphine. Studies evaluating the effects on respiratory depression are ongoing. These findings suggest that a dual medication strategy may widen the therapeutic window for opioid analgesia and lower the risk of negative effects, including opioid dependence.

# Blockade of selective $G\beta\gamma$ signaling pathway by gallein decreases development of opioid tolerance

Alan V. Smrcka,<sup>1</sup> Gissell Sanchez,<sup>2</sup> and Emily M. M Jutkiewicz<sup>3</sup>

<sup>1</sup>Univ of Michigan Med Sch; <sup>2</sup>Univ of Michigan; and <sup>3</sup>Univ of Michigan Medical School

Abstract ID 18253

Poster Board 406

The  $\mu$ -opioid receptor (MOR) is a  $G_i$ -protein-coupled receptor (GPCR) responsible for opioid-induced analgesia and undesired effects such as constipation, respiratory depression, and addiction. Upon binding of an agonist to MOR, intracellular  $G\alpha$  and the  $G\beta\gamma$  subunits dissociate to signal, and the signaling cascade that follows  $G\beta\gamma$  activation by MOR is necessary for opioid-mediated antinociception. However, phospholipase- $C\beta 3$  (PLC $\beta 3$ )—one effector of  $G\beta\gamma$  and  $G\alpha_q$ —has been shown to limit the antinociceptive effects of morphine since genetic deletion of PLC $\beta 3$  potentiates the antinociceptive effects of morphine in mice. Gallein is a small-molecule that binds to  $G\beta\gamma$ , and it prevents protein-protein interactions between  $G\beta\gamma$  and select effectors such as PLC $\beta$  and GRK2. We hypothesize that preventing  $G\beta\gamma$ -PLC interactions potentiates antinociceptive effects of opioids and decreases the development of morphine tolerance. The warm water tail withdrawal (WWTW) assay is used to measure antinociceptive response in mice by timing the latency of tail withdrawal from 55°C water. In these studies, we used a paradigm of repeated administration of morphine or saline (3 times daily) for 6 days to induce morphine tolerance. After repeated morphine administration, the development of opioid tolerance is determined by a rightward shift in the morphine dose-response on day 6 compared to day 1. Repeated administration of 10 mg/kg morphine produced a 5x-fold rightward shift in ED<sub>50</sub> values comparing day 1 and day 6. Gallein (50mg/kg) treatment on day 1 and day 3 of repeated morphine administration prevented the rightward shift in the morphine dose-response curve on day 6. We also tested gallein's ability to potentiate morphine antinociception in a physiological state of tolerance. Gallein (100mg/kg) administered 15hrs prior to day 6 assay shifted the morphine dose-response curve to the left, increasing the potency and efficacy of morphine. These data suggest that gallein treatment prevents the development of opioid tolerance, and that after development of tolerance, gallein can enhance opioid-mediated antinociception. Overall, these studies show that inhibition of  $G\beta\gamma$ -PLC pathway may have therapeutic potential to decrease the development of opioid tolerance and/or provide opioid-sparing effects.

Support/Funding Information: DA 0418625

# M1 Positive Allosteric Modulators Enhance Domains of Cognitive Function by Activation of ssT-expressing Interneurons in the Prefrontal Cortex

Jerri Rook,<sup>1</sup> Zixiu Xiang,<sup>2</sup> Jonathan Dickerson,<sup>1</sup> Shalini Dogra,<sup>1</sup> Kendall Jensen,<sup>3</sup> Insung Kim,<sup>3</sup> Megan Ohler,<sup>3</sup> Kelly Weiss,<sup>3</sup> and P. Jeffrey Conn<sup>1</sup>

<sup>1</sup>Vanderbilt Univ; <sup>2</sup>Vanderbilt University Medical Center, Dept of Pharmacology; and <sup>3</sup>Vanderbilt University

Abstract ID 25301

Poster Board 407

Recent studies suggest that highly selective positive allosteric modulators (PAMs) for muscarinic acetylcholine receptor subtype 1 (M1) have exciting potential as novel treatments for the negative symptoms and cognitive impairments in patients suffering from schizophrenia. However, the precise mechanisms by which M1 regulates brain circuits that are relevant for the major symptom clusters associated with schizophrenia are unknown. Early stages of schizophrenia are associated with hyperactivity of the prefrontal cortex (PFC) and this is important for some of the cognitive and negative symptoms associated with the disease. Previously, we demonstrated that M1 PAMs can ameliorate the behaviors relevant for negative symptoms and cognitive disruptions in preclinical models. Additionally, we found that M1 PAMs enhance M1-mediated long-term depression (LTD) and postulated that this may be involved in M1-mediated effects of prefrontal cortex (PFC)-dependent cognitive function. However, this hypothesis has not been directly tested. Here we utilize genetic knockout animals to selectively delete M<sub>1</sub> from specific neuronal populations to test the hypothesis that M<sub>1</sub>-LTD requires activation of M<sub>1</sub> in PFC pyramidal cells and does not require activation of M<sub>1</sub> in inhibitory interneurons. M1 activation can increase activity of both somatostatin (ssT)-expressing inhibitory interneurons (ssT-INs) and parvalbumin (PV)-expressing interneurons (PV-INs) in the PFC, and we have performed exciting studies suggesting that activation of M1 can induce an especially robust and long-lasting increase in excitability of ssT-INs in this region. Additionally, utilizing transgenic mice along with optogenetic approaches we demonstrate that neither somatostatin (ssT) or parvalbumin (PV) interneurons (IN) had significant effects on mLTD. Interestingly, our data suggests that activation of ssT-INs is independent of M1-LTD and M1-LTD requires activation of M1 in pyramidal cells but not ssT-INs. Based on this, we performed studies to determine whether M1 in ssT-INs are required for effects of M1 PAMs on cognitive function. Our results point to a critical role for M1 in ssT-INs rather than M1-LTD in enhancing cognitive function.

Support/Funding Information: NIMH MH073676 (JMR)

# Behavioral Performance Characterization of the Putative Neuroinflammation Inhibitor 1-Methyl-Tryptophan Following Acute Traumatic Stress in Rats

Rachel M. Taylor,<sup>1</sup> Fred L. Johnson,<sup>1</sup> Emily M. Scott,<sup>1</sup> Aurian Naderi,<sup>1</sup> Kacie M. McKinney,<sup>1</sup> Kilana D. Coachman,<sup>1</sup> Laurence P. Simmons,<sup>1</sup> James C. DeMar,<sup>1</sup> Peethambaran Arun,<sup>1</sup> Joseph B. Long,<sup>1</sup> Liana M. Matson,<sup>1</sup> and Emily G. Lowery-Gionta<sup>1</sup>

<sup>1</sup>Walter Reed Army Institute of Research

Abstract ID 52631

Poster Board 408

Of US Soldiers exposed to psychological trauma during deployment in current conflicts, 12-25% develop Post-Traumatic Stress Disorder, with greater numbers estimated for developing Acute Stress Reactions (ASR) or Acute Stress Disorder (ASD). At present there are no FDA-approved pharmacotherapies for the treatment of ASR or ASD, thus novel therapeutics are needed. One target of interest is a component of the kynurenine pathway of tryptophan metabolism, as increased expression of the pathway protein indoleamine-2,3-dioxygenase-1 (IDO-1) is found in the acute aftermath of traumatic stress exposure. The overall outcome of increased expression of IDO-1 and kynurenine metabolites is increased neuroinflammation, which also plays a role in stress-related disorders. 1-methyl-tryptophan (1MT) is a reported inhibitor of IDO-1 as well as a putative anti-inflammatory drug candidate. We sought to evaluate the efficacy of 1MT to prevent behavioral performance decrements using a rodent model of military-relevant complex traumatic stress (MRCTS). This preclinical model incorporates combat-relevant facets of traumatic stress events. Briefly, adult male and female Sprague-Dawley rats were exposed to MRCTS procedures (e.g., predator exposure, inescapable foot shock, & underwater immersion) or left undisturbed in their home-cage. Rats were then administered 1MT (10 or 30 mg/kg, i.p.) or vehicle. At 24-h post-stress exposure, all rats were evaluated in a behavioral battery: elevated plus maze (EPM), open field (OF), and acoustic startle response (SR) tests. Data were analyzed in separate 2-way ANOVAs, based on *a priori* hypotheses. On the EPM, female rats traveled greater overall distance and distance on the open arms than males and stress exposure negatively impacted performance for both sexes ( $p < 0.05$ ). Significant ( $p < 0.05$ ) main effects of various factors were observed for different EPM outcome measures and post-hoc analyses revealed a significant dose-dependent decrease in open arm distance in stress-exposed groups. Similarly, on the OF, females traveled significantly greater overall distance ( $p < 0.001$ ) and distance in the center area ( $p < 0.01$ ) than males. However, there was a lack of significant main effects of stress and 1MT treatment in most analyses. For SR, males significantly startled to a greater degree than females under both control ( $p < 0.001$ ) and stressed ( $p < 0.0001$ ) conditions; however, there was a lack of a significant effect of 1MT treatment in both conditions. Together, the present results demonstrate limited efficacy of 1MT for the prevention of stress-related decrements in behavioral performance in rats. Importantly, the present data demonstrate that sex differences are present under basal & stressed conditions. Trends in low dose-treated groups also highlight that MRCTS exposure influences the kynurenine pathway to some degree.

Material has been reviewed by the Walter Reed Army Institute of Research. There is no objection to its presentation and/or publication. The opinions or assertions contained herein are the private views of the author, and are not to be construed as official, or as reflecting true views of the Department of the Army or the Department of Defense. Research was conducted under an IACUC-approved animal use protocol in an AAALAC International-accredited facility with a Public Health Services Animal Welfare Assurance and in compliance with the Animal Welfare Act and other federal statutes and regulations relating to laboratory animals.



# Investigation of the Contribution of Glucose Transport to Detection of Glucose Taste by Human Subjects in a Rapid Throughput Taste Discrimination Assay

R. Kyle Palmer,<sup>1</sup> and Anna K. Nechiporenko<sup>2</sup>

<sup>1</sup>Opertech Bio, Inc., Philadelphia, Pennsylvania, USA; and <sup>2</sup>Opertech Bio, Inc.

Abstract ID 21690

Poster Board 409

The GPCR heterodimer TAS1R2/TAS1R3 expressed in specialized cells in the taste bud is known to be the principle mediator of sweet taste signaling to agonists such as glucose. Recent evidence has suggested an additional taste signaling pathway specific to glucose and potentially other metabolizable saccharides through a sodium-dependent glucose transporter protein (SGLT) also in taste cells. We previously used a rapid throughput taste discrimination assay for human subjects to characterize concentration-dependence of the taste of agonists of TAS1R2/TAS1R3 (Palmer et al, 2021, JPET, 377:133-145). In this assay, subjects self-administer 200  $\mu$ l of tastant solution drawn by an electronic pipette from randomly presented wells of a 96-well plate. Responses to taste stimuli are registered by touching pre-designated targets on a touch-sensitive laptop display, and are reinforced by the immediate appearance of a virtual poker chip that carries actual monetary value. We now are using this approach to pharmacologically investigate the contribution of the proposed SGLT taste signaling pathway by testing the effects of sodium (co-transported with glucose) and the non-selective SGLT inhibitor phlorizin on glucose taste discrimination. Two male and 2 female adults served as subjects in a rapid throughput discrimination between glucose and water taste stimuli presented randomly across 96 trials per test. The test followed a forced choice method of constant stimuli (MCS) design to determine the discriminability of 5 different randomly presented concentrations of glucose (20, 40, 60, 80 and 100 mM; 12 trials each per test) from water (36 trials per test). Touch responses on a “sweet”-designated target during trials of any glucose concentration were reinforced with a 20-cent poker chip, as were responses on a “water”-designated target on trials of water. Errors (i.e., touching the “sweet” target on water trials, or “water” target on glucose trials) were penalized by a 10-cent subtraction from the subject’s cumulative score. Each subject was tested 6 times on this design. Signal detection analysis of the resulting dataset averaged across all subjects and all tests yielded a  $d'$  value for discriminability 0.55 for 20 mM glucose, indicating that this concentration was near an empirical threshold for detection. The test was repeated with 20 mM NaCl replacing water as a stimulus and as the solvent for all glucose concentrations. Discriminability of glucose was increased when dissolved in 20 mM NaCl; the  $d'$  value for 20 mM glucose under these conditions increased to 1.01, indicating that the presence of sodium enhanced detection of glucose. However, and in contrast to a recent publication (Breslin et al, 2021, PLoS One, 16(10):e0256989), addition of 200  $\mu$ M phlorizin had no impact on discriminability of any concentration of glucose dissolved in water. Thus, the enhancing effect of sodium on discriminability of low glucose concentrations does not appear to involve an SGLT.

## Discriminative Stimulus Properties of Lorcaserin in C57BL/6 mice

Fan Zhang,<sup>1</sup> Katherine Nicholson,<sup>1</sup> Keith L. Shelton,<sup>1</sup> Todd M. Hillhouse,<sup>2</sup> Herbert Y. Meltzer,<sup>3</sup> and Joseph Porter<sup>1</sup>

<sup>1</sup>Virginia Commonwealth Univ; <sup>2</sup>Univ of Wisconsin Green Bay; and <sup>3</sup>Northeastern Univ FSM

Abstract ID 21838

Poster Board 410

The serotonin 2C receptor (5HT<sub>2C</sub>) has been investigated as a potential therapeutic target for a variety of psychiatric disorders as well as treatment of obesity. A stumbling block in the development of these medications is identifying agonists with selectivity for 5HT<sub>2C</sub> over 5HT<sub>2A</sub> and 5HT<sub>2B</sub>. Lorcaserin (Belviq<sup>®</sup>) is a serotonin agonist that was previously marketed as a weight-loss medication. While *in vitro* binding suggests that its pharmacological actions are due to a high binding affinity at 5-HT<sub>2C</sub> receptors, a drug discrimination study in rats suggested that its discriminative stimulus properties also included activity at 5-HT<sub>2A</sub> and 5-HT<sub>1A</sub> receptors (Serafine et al. 2016). The present study used adult male C57BL/6 mice to further examine the discriminative stimulus properties of lorcaserin in a two-lever drug discrimination assay. The mice were trained to discriminate 2.0 mg/kg lorcaserin (s.c., 30 min prior to session onset) from saline under a fixed ratio (FR)12 schedule reinforced with 0.02 ml sweetened milk deliveries. A generalization curve with lorcaserin (0.125 – 4.0 mg/kg) yielded an ED<sub>50</sub> = 0.78 mg/kg (95% C.I. = 0.59 - 1.04 mg/kg) for substitution for the training dose. The 5-HT<sub>2C</sub> agonist mCPP (s.c., 15 min) fully substituted for lorcaserin with an ED<sub>50</sub> = 0.49 mg/kg (95% C.I. = 0.28 - 0.86 mg/kg). Conversely, the 5-HT<sub>1A</sub> agonist 8-OH-DPAT (s.c., 15 min pre-session) did not substitute for lorcaserin producing a maximum of 24.50% drug-lever responding (DLR) at 0.5 mg/kg with a reduction in response rate. Administration of the 5-HT<sub>2C</sub> antagonist SB 242084 (0.5 mg/kg) prior to 2 mg/kg lorcaserin significantly reduced lorcaserin-lever selection to 24.54% DLR but did not change response rates. In agreement with previous drug discrimination results in rats (Serafine et al. 2016), the importance of 5-HT<sub>2C</sub> agonism for lorcaserin's discriminative stimulus properties was shown by mCPP (5-HT<sub>2C</sub> agonist) substituting for lorcaserin and the attenuation by SB 242084 (5-HT<sub>2C</sub> antagonist) of drug-appropriate responding following administration of the lorcaserin training dose. In contrast, the 5-HT<sub>1A</sub> agonist 8-OH-DPAT did not share any discriminative stimulus properties with lorcaserin in mice, which may reflect increased specificity of the cue associated with a higher lorcaserin training dose and/or species related differences. Additional studies need to be conducted to determine the role of 5-HT<sub>2A</sub> receptor activity in mice with lorcaserin drug discrimination. These preliminary results suggest that lorcaserin drug discrimination in C57BL/6 mice is a useful *in vivo* assay for future development of psychotherapeutic drugs with selective 5-HT<sub>2C</sub> agonist activity.

# Antinociceptive Effects of Fentanyl and Non-opioid Drugs in Methocinnamox-treated Rats

Saba Ghodrati,<sup>1</sup> Lawrence Carey,<sup>2</sup> and Charles P. France<sup>3</sup>

<sup>1</sup>Univ of Texas Health Science Center at San Antonio at; <sup>2</sup>Univ of Texas Health Science Center, San Antonio; and <sup>3</sup>Univ of Texas Hlth Sci Ctr

Abstract ID 17113

Poster Board 411

Methocinnamox (MCAM) is a long acting  $\mu$ -opioid receptor antagonist and potential novel treatment for opioid use disorder. MCAM antagonizes the antinociceptive effects of  $\mu$ -opioid receptor agonists for 2 weeks or longer. However, this long duration of action could make the clinical use of MCAM challenging as  $\mu$ -opioid receptor agonists are frequently used for pain management. Therefore, alternative drugs to provide pain relief would need to be identified. In this experiment, 24 male Sprague Dawley rats were used to study the antinociceptive effects of fentanyl and non-opioid drugs, in the presence and absence of MCAM, using the complete Freund's adjuvant (CFA) model of inflammatory pain. For these studies, 12 rats received MCAM and 12 rats received 10%  $\beta$ -cyclodextrin vehicle. Half of the animals from each of these treatment groups were treated with CFA i.pl. (n=6/group), or saline i.pl. (n=6/group). Hypersensitivity to mechanical stimulation was measured using a von Frey anesthesiometer. The antinociceptive effects of fentanyl (0.01-0.1 mg/kg, i.p.), ketamine (17.8-56 mg/kg, i.p.), gabapentin (32-100 mg/kg, i.p.), meloxicam (3.2-10 mg/kg, i.p.), and  $\Delta^9$ -tetrahydrocannabinol (THC, 1-10 mg/kg, i.p.) were tested in all animals in a pseudorandom order every 3 days following a single s.c. administration of MCAM (10 mg/kg) or vehicle. Following completion of antinociception studies, the same doses of each drug were studied for effects on motor performance using a rotarod apparatus. Intraplantar administration of CFA induced hypersensitivity to mechanical stimulation. Fentanyl dose-dependently alleviated CFA-evoked mechanical hypersensitivity (i.e., antinociception) in vehicle-treated rats (up to 105% reversal), but not in MCAM-treated rats. Fentanyl did not impair motor performance in either group. THC (up to 82% reversal), ketamine (up to 66% reversal), and gabapentin (up to 46% reversal) dose-dependently alleviated CFA-evoked mechanical hypersensitivity in both the MCAM- (n=6), and vehicle-treated groups (n=6). Meloxicam failed to alter CFA-evoked mechanical hypersensitivity in either group. THC, gabapentin, and meloxicam did not affect motor performance in either group. Ketamine dose-dependently impaired motor performance in both the MCAM- and vehicle-treated groups (up to 71% reduction in latency to fall). These data suggest that ketamine, gabapentin and THC could be effective treatments for inflammatory pain under conditions of long term  $\mu$ -opioid receptor antagonism.

This work was supported by grant AQ-0039 from the Welch Foundation, and NIDA grant T32DA031115 (CPF).

# Microglia in the Locus Coeruleus Mediate the Behavioral and Neuronal Consequences of Social Stress in Females

Cora Smiley,<sup>1</sup> Samantha Bouknight,<sup>2</sup> Brittany Pate,<sup>3</sup> Alexandria Nowicki,<sup>4</sup> Evelyn Harrington,<sup>3</sup> and Susan Wood<sup>4</sup>

<sup>1</sup>Univ of South Carolina Sch of Med; <sup>2</sup>Univ of South Carolina; <sup>3</sup>University of South Carolina School of Medicine; and <sup>4</sup>Univ of South Carolina School of Medicine

Abstract ID 28676

Poster Board 412

Neuropsychiatric disorders that result from stress, especially post-traumatic stress disorder, are highly detrimental to both the patient and society and disproportionately affect females. One hallmark symptom of this disorder, that is also more often observed in females, is hypervigilance in response to reminders of the initial stressful/traumatic event. Recent evidence points towards heightened neuroimmune signaling in response to stress as a mechanistic factor underlying this behavioral dysfunction. Previous experiments in our lab have determined that social stress, specifically vicarious witness stress (WS), leads to increases in neuroimmune signaling within the locus coeruleus (LC) of females, as indicated by increased microglial activation and IL-1b proinflammatory cytokine release. Further, neuroimmune factors are known to activate LC neurons while hyperactivity of LC neurons has been identified as a maladaptive factor in clinical and preclinical studies of anxiety. Taken together, increased proinflammatory signaling may be a key factor in the increased susceptibility to developing neuropsychiatric disorders following stress exposure that is observed in females. Therefore, the goal of this project was to determine the functional and behavioral impact of blocking microglial activity within the LC during WS exposure on subsequent hypervigilance-related outcomes. These experiments utilized chemogenetic DREADDs techniques with a virus engineered to specifically target microglia (AAV-CD68-Gi). The first experiment was designed to determine the impact of intra-LC microglial inactivation on anxiety-like behavior during stress exposure. Female rats were injected with this inhibitory virus and, following 3-4 weeks to allow for viral expression, rats were injected with either CNO to activate the DREADDs virus or vehicle one hour prior to exposure to a single session of WS. Brain tissue was collected two hours following stress exposure and behavior during the session along with the activation state of the microglia was analyzed. A second study treated female rats with AAV-CD68-Gi within the LC prior to five daily WS exposures with CNO/vehicle injections before each session. Subsequently, rats underwent testing in marble burying and the stress context to determine the impact of microglial blockade on subsequent hypervigilant responses to stress-related stimuli. Finally, a separate subset of surgically naïve rats were solely treated with CNO or vehicle to ensure that CNO alone had no effect on behaviors during stress. Importantly, these studies quantified microglial morphology using Iba1 and confirmed that DREADD activation with CNO prevented microglial activation and further verified that CNO did not affect behaviors during stress. Additionally, these experiments concluded that DREADD-mediated microglial inhibition prevents the emergence of the hypervigilant burying behaviors we have previously observed both during stress and in response to the stress context. Finally, cfos immunohistochemistry is currently being completed to determine if DREADD-mediated microglial inhibition inhibits LC activity, as anticipated, and the related behavioral output. Taken together, these experiments have identified neuroimmune activity within the LC as a key factor involved in mediating hypervigilant burying behavior in females and may provide a novel treatment target for the prevention of stress-related pathologies following trauma exposure.

This work was supported by R01 grant MH113892 and VA Merit BX005661 (SKW).

# Role of ventral tegmental area SGK1 phosphorylation and activity in drug-associated behaviors

Samantha Caico<sup>1</sup>

<sup>1</sup>Michigan State Univ

Abstract ID 13647

Poster Board 413

The mesolimbic dopamine system, which plays an important role in motivated promotes[MRM1] rewarding[MRM2] behavior, is modulated by drugs of abuse. Drugs can alter cellular activity and gene expression within the ventral tegmental area (VTA), promoting behaviors associated with addiction. Previous work in our lab found that chronic cocaine and morphine administration increased both the activity and phosphorylation (at Ser78) of serum- and glucocorticoid-inducible kinase 1 (SGK1) in the VTA.[MRM3] Using a viral vector strategy to overexpress a catalytically inactive SGK1 mutant (K127Q), we have found that decreasing SGK1 activity in VTA dopamine neurons is sufficient to reduce cocaine conditioned place preference (CPP), supporting that our biochemical changes are functionally relevant. However, it is unclear whether SGK1 phosphorylation also alters drug-elicited behavior. Here, we present data that decreasing VTA SGK1 phosphorylation is also sufficient to reduce drug responses. We utilized viral vectors to overexpress SGK1 mutants that either prevent (S78A) or mimic (S78D) SGK1 Ser78 phosphorylation in the VTA. We found that preventing SGK1 phosphorylation (via S78A) decreased cocaine CPP and morphine preference in a two-bottle choice assay, while mimicking S78 phosphorylation (via S78D) did not alter either behavior ( $n = 14-21$  mice/group for CPP with  $p < 0.001$ ,  $n = 16-18$  mice/group for morphine preference with  $p < 0.05$ ). Together, these data support that decreasing either VTA SGK1 catalytic activity or phosphorylation is sufficient to reduce drug-elicited behavior. Thus, we hypothesized that SGK1 pharmacological inhibition may be a translational approach to decrease drug behavior. Using Neuro2A cells, we validated that the SGK1 inhibitor GSK650349 dose-dependently decreased phosphorylation of the exclusive SGK1 substrate, NDRG. Interestingly, we also observed that GSK650349 decreased SGK1 S78 phosphorylation, suggesting pharmacological inhibition may decrease both SGK1 catalytic activity and phosphorylation. To assess whether GSK650349 could prevent drug-induced changes in VTA SGK1 activity and phosphorylation, we pretreated mice for 7 days with GSK650349 (5mg/kg, i.p.) or vehicle, then administered GSK650349 for 7 days with morphine (20mg/kg) or saline. Via western blot, we found that morphine treatment significantly increased VTA SGK1 catalytic activity and S78 phosphorylation in vehicle-treated mice as expected, while morphine mice treated with GSK650349 did not differ from saline controls ( $n = 11-15$  mice/group). These data support that systemic GSK650349 administration is sufficient to alter SGK1 activity within the brain. We are now determining whether systemic GSK650349 can reduce drug-elicited behavior. I will investigate the effects of GSK650349 administration on cocaine locomotor sensitization, cocaine CPP, and morphine preference using a two-bottle choice test. Our preliminary data suggest that GSK650349 (5mg/kg) is sufficient to blunt cocaine-induced locomotor activity, but not cocaine CPP. Together, our data support a role for SGK1 activity and phosphorylation in drug responses and suggest that SGK1 inhibition could provide a novel avenue for therapeutic intervention.

# Veterinary anesthetic xylazine produces synergistic antinociceptive effects with the opioid fentanyl in mice

Ellen Walker,<sup>1</sup> Jumar Etkins,<sup>2</sup> Karen Gonzalez,<sup>2</sup> and Gabriel Vivas<sup>2</sup>

<sup>1</sup>Temple Univ School of Pharmacy; and <sup>2</sup>Temple University School of Pharmacy

**Abstract ID 55131**

**Poster Board 414**

A recent twist to the ongoing tragedy of the opioid epidemic is the combination of fentanyl with the veterinary tranquilizer xylazine known on the street as “tranq dope.” Xylazine is an  $\alpha_2$  adrenoreceptor agonist used for sedation in large animals. In Philadelphia and other major cities, illicit bags of fentanyl are increasingly adulterated with xylazine significantly adding further insult to current toxicity of the opioid crisis. One key pharmacological feature of xylazine may be the potential to increase the duration of action, or high, of fentanyl which has a notoriously shorter half-life than other abused opioids. In addition, we hypothesize that xylazine potentiates the pharmacological effects of fentanyl through opioid and norepinephrine synergistic mechanisms. To examine this hypothesis, Swiss-Webster mice were tested for their baseline sensitivity to a 52.5°C hot-plate as measured by a hind-paw lick or jump with a 60 sec cut-off period. After baseline measures, mice were injected (IP) with either fentanyl alone, xylazine alone, or combinations of fentanyl and xylazine in ratios of 1:1, 1:3 and 3:1 fentanyl to xylazine. After a 10 min pretreatment, mice were tested again on the hot plate. Both fentanyl and xylazine produced full, dose-dependent increases in antinociception although fentanyl was 10-fold more potent than xylazine at doses without motoric effects. When combined, simple additivity was observed with the 3:1 ratio of fentanyl to xylazine. However, synergistic effects were observed for the ratios of 1:1 and 1:3 fentanyl to xylazine. In conclusion, when combining fentanyl and xylazine in a 1:1 and 1:3 ratios, xylazine augments the pharmacological effects of fentanyl if the xylazine administered is equal to or greater than the relative potency of fentanyl. This augmentation may help to explain the recent trend to combine these two agents for illicit sale despite the increasing toxicity. The underlying mechanisms of this synergism will be investigated further through opioid and norepinephrine competitive antagonism and time-course studies.

Supported by Pilot Project Core from NIH 5P30DA013429 to EAW

# Sprague Dawley Rats from Different Vendors Vary in the Modulation of Prepulse Inhibition of Startle (PPI) by Dopamine, Acetylcholine, and Glutamate Drugs

S. Barak Caine,<sup>1</sup> and Morgane Thomsen<sup>2</sup>

<sup>1</sup>McLean Hospital; and <sup>2</sup>Mental Health Services, Capital Region of Denmark

Abstract ID 53081

Poster Board 415

**Rationale:** Rodent vendors are often utilized interchangeably assuming that the phenotype of a given strain remains standardized between colonies. Several studies, however, have found significant behavioral and physiological differences between Sprague Dawley (SD) rats from separate vendors. Prepulse inhibition of startle (PPI), a form of sensorimotor gating in which a low-intensity leading stimulus reduces the startle response to a subsequent stimulus, may also vary by vendor. Differences in PPI *between* rat strains are well known, but divergence between colonies *within* the SD strain lacks thorough examination.

**Objectives:** We explored intrastrain variation in PPI by testing SD rats from two vendors: Envigo and Charles River.

**Methods:** We selected drugs acting on four major neurotransmitter systems that have been repeatedly shown to modulate PPI: dopamine (apomorphine; 0.5, 1.5, 3.0 mg/kg), acetylcholine (scopolamine; 0.1, 0.5, 1.0 mg/kg), glutamate (dizocilpine; 0.5, 1.5, 2.5 mg/kg), and serotonin (2,5-Dimethoxy-4-iodoamphetamine, DOI; 0.25, 0.5, 1.0 mg/kg). We determined PPI and startle amplitude for each drug in male and female Envigo and Charles River SD rats.

**Results:** SD rats from Envigo showed dose-dependent decreases in PPI after apomorphine, scopolamine, or dizocilpine administration, without significant effects on startle amplitude. SD rats from CR were less sensitive to modulation of PPI and/or more sensitive to modulation of startle amplitude, across the three drugs.

**Conclusions:** SD rats showed vendor differences in sensitivity to pharmacological modulation of PPI and startle. We encourage researchers to sample rats from separate vendors before experimentation to identify the most suited source of subjects for their specific endpoints.

McLean Hospital funding to SB Caine; NIH grant R01AA025071 to M Thomsen

# Discriminative Stimulus Effects of 30.0 and 300.0 mg/kg Gabapentin in Rats: Substitution Testing with Morphine and Fentanyl

Alexia G. Dalton,<sup>1</sup> Madeline T. Van Fossen,<sup>1</sup> Alexandria Iannucci,<sup>1</sup> Joshua Prete,<sup>1</sup> Taylor Galaszewski,<sup>1</sup> Dillon S. Shekoski,<sup>1</sup> Bethany E. Beavers,<sup>1</sup> and Adam J. Prus<sup>1</sup>

<sup>1</sup>Northern Michigan University

Abstract ID 56087

Poster Board 416

Gabapentin is a blocker for Ca<sup>2+</sup> channels that contain an  $\alpha 2\Delta$ -1 or  $\alpha 2\Delta$ -2 subunit and is prescribed for neuropathic pain, anxiety, fibromyalgia, and epilepsy. There are increasing reports of abuse with gabapentin, particularly when also used with opioids. These observations suggest that gabapentin may produce positive subjective effects and that these effects may be similar, to some extent, with opioids. In order to examine the subjective effects of gabapentin, the present study utilized a drug discrimination procedure in 22 male adult Sprague Dawley rats trained to discriminate either a 30.0 (30GPN) or 300.0 mg/kg dose (300GPN) of gabapentin versus saline in a two choice operant task for food reinforcement. All rats met the training criteria, consisting of 5 out of 6 consecutive sessions of at least 80% condition-appropriate responding. Gabapentin produced full-substitution (>80% drug-lever responding) for 30GPN beginning at a 15.0 mg/kg dose and for 300GPN beginning at a 100.0 mg/kg dose. Morphine produced partial substitution (>20% drug-lever responding) for both training doses, with a 5.0 mg/kg dose of morphine producing partial substitution for both 30GPN (40.9% drug-lever responding) and 300GPN (31.7%). A 10.0 mg/kg dose of morphine also partially substituted for the lowest training dose, 30GPN (64.8%), which significantly reduced response rates (0.5 responses per second [RPS]), but this dose was highly rate suppressant for the 300GPN group (0.02 RPS), which precluded determination of percent drug responding for this dose. A 0.08 mg/kg dose of fentanyl partially substituted for 30GPN (45.6%) and for 300GPN (33.2%). Pretreatment with a 3.0 mg/kg dose of the opioid receptor antagonist naltrexone partially blocked the discriminative stimulus effects of 30GPN (69.5%) and 300GPN (69.8%). The present findings indicate that gabapentin can be readily established as a discriminative cue and that the properties of this cue may be partially mediated by opioid receptors.



# The Effects of Eating a Traditional High Fat or a Ketogenic Diet on Sensitivity of Female Rats to Morphine-Induced Antinociception, Tolerance and Withdrawal

Nina M. Beltran,<sup>1</sup> Alyssa N. Parra,<sup>1</sup> Isabella M. Castro,<sup>1</sup> Madeline K. Elsey,<sup>1</sup> Ana Paulina Serrano,<sup>1</sup> Jazmin R. Castillo,<sup>1</sup> Vanessa Minervini,<sup>2</sup> and Katherine M. Serafine<sup>1</sup>

<sup>1</sup>The University of Texas at El Paso; and <sup>2</sup>Creighton University

Abstract ID 27565

Poster Board 417

Opioid drugs like morphine are used for pain relief but also have high abuse potential. Further, individuals diagnosed with obesity are at a greater risk for opioid overdose. While overconsumption of a high fat diet can lead to obesity, it is not known if diet impacts sensitivity of individuals to morphine. To explore this possibility, the effects of morphine under acute and chronic conditions, as well as non-precipitated withdrawal were assessed in 24 female Sprague Dawley rats ( $n=8$ /group) eating a standard laboratory chow (17% kcal from fat), a traditional high fat/high carbohydrate chow (60% kcal from fat), or a ketogenic (high fat/low carbohydrate) chow (90.5% kcal from fat). Morphine-induced antinociception was measured using the warm water tail withdrawal procedure. To explore the adverse effects of morphine, body weight, food consumption, fecal output, respiration, and body temperature were recorded periodically throughout the study. To study the effects of chronic morphine exposure, morphine was administered intraperitoneally (IP) twice daily for 19 days (3.2-56 mg/kg) increasing in  $1/4$  log doses every 3 days. Finally, after chronic morphine administration, observational signs of non-precipitated withdrawal and changes in body weight were measured following morphine discontinuation. It was hypothesized that rats eating high fat chow would be more sensitive to the acute effects of morphine (0.32-17.8 mg/kg IP) than rats eating other diets. It was further hypothesized that rats eating high fat chow would also be more sensitive to the development of tolerance to the antinociceptive effects (3.2-56 mg/kg IP) and withdrawal symptoms following chronic morphine administration, as compared to rats eating a ketogenic or standard chow. Morphine-induced antinociception was comparable among rats eating different diets when tested under acute conditions, and there were also no group differences in morphine-induced changes to respiration or body temperature. Fecal output was consistently greater for rats eating standard chow as compared to rats eating high fat or ketogenic chow following saline injections, as well as following acute or chronic morphine administration. After chronic morphine administration, all rats developed tolerance to morphine-induced antinociception. Specifically, the antinociception dose-response curves shifted rightward 8.2-fold for rats eating standard and high fat chow, and 4.4-fold for rats eating ketogenic chow. That is, tolerance was reduced (or less developed) for rats eating ketogenic chow as compared to other groups. Finally, morphine discontinuation resulted in observable withdrawal signs among all rats; however, there were no group differences except regarding withdrawal-related weight loss. Specifically, rats eating ketogenic chow experienced less withdrawal-related weight loss as compared to the other groups. These results suggest that tolerance to the pain relieving effects of opioid medications, as well as withdrawal symptoms, might be blunted by consuming a ketogenic diet. Future studies will examine the effects of dietary manipulation on drug sensitivity in the context of inflammatory pain.

M.K.E. was supported by the NIGMS of the NIH under linked award numbers RL5GM118969, TL4GM118971, and UL1GM118970 and by an ASPET SURF award. K.M.S., A.N.P., A.P.S., and J.R.C., were supported by the NIDA of the NIH under award R25DA033613. K.M.S was supported by a NIDA RCMI supplement under award number 3U54MD007592-29S4.

# The compulsion zone theory of cocaine self-administration behavior in rats explains the effects of fixed ratio magnitude on inter-injection intervals

Abigail Muccilli,<sup>1</sup> Jhanvi Desai,<sup>2</sup> and Andrew Norman<sup>3</sup>

<sup>1</sup>Rowan Univ; <sup>2</sup>Univ of Cincinnati; and <sup>3</sup>Univ of Cincinnati College of Medicine

Abstract ID 17002

Poster Board 464

Cocaine self-administration paradigm in rats is an established animal model of cocaine use disorder and is integral to medication development. Since the inception of the field, self-administration schedules have been used as a measure of “reinforcing efficacy” under the belief that altering schedules modifies the reinforcement magnitude of cocaine. This approach has failed to predict the clinical effectiveness of any medications. Cocaine is a drug and would be expected to elicit its effects according to the principles of pharmacology. It activates dopaminergic mechanisms underlying stereotypy. The compulsion zone theory of acquired cocaine self-administration behavior states that cocaine induces stereotypic lever-pressing behavior only when cocaine levels are below the satiety threshold and above the priming/remission threshold. This theory explains both Progressive Ratio and Fixed Ratio (FR) 1 schedules of cocaine delivery and was applied to different magnitude FR schedules. Eight Male Sprague-Dawley rats were trained to acquire cocaine self-administration behavior on an FR1 schedule at different unit doses (i.v). Next, they were trained to self-administer cocaine on other FR schedules. Daily sessions began with 4 contingent cocaine priming injections of 1.5  $\mu\text{mol/kg}$  followed by 15 injections on FR1 and then switched to 15 injections of FR5, 10, 20 or 50 schedules at a unit dose of 3  $\mu\text{mol/kg}$ , ending with unloading where lever presses had no consequences. The inter-injection intervals were regular at all FR values, but the mean values were significantly longer at FR50 (7.7 min) compared to FR1 (5.7 min). The 34% increase in inter-injection intervals could be accounted for by the additional time that it took to complete the 50 presses (approximately 2.3 min). The mean calculated cocaine level at the time of injection was 31% lower at FR50 relative to FR1, again because it took longer to complete the 50 presses. However, the concentration of cocaine at the time of the first lever press in the sequence of 50 was similar to the concentration at the time of injection at FR1 suggesting that satiety threshold is not altered by increased FR value. Once rats perform the first lever press at the satiety threshold on FR50, the 50 lever presses occur at a high rate (20.8 presses/min) within the compulsion zone until the last press results in an injection. All lever pressing behavior, regardless of FR value, occurred at or below the satiety threshold in accordance with the compulsion zone theory. There is no reason to assume that the FR value alters the reinforcing efficacy of cocaine. Increased rate of lever pressing at FR50 occurs only because rats are compelled to press the lever when cocaine levels are below the satiety threshold, and lever pressing behavior does not stop until it results in an injection that raises cocaine levels above the satiety threshold. A higher FR value does not affect how cocaine induces lever pressing behavior and does not convey any different information than FR1. It simply acts as a time-out period and adds noise to maintained cocaine-self administration. Thus, the compulsion zone theory appears to provide a unified theory of schedules of cocaine delivery and provide a rational basis for advancing medications development.

Supported by NIDA grant U01DA50330 (to ABN).

# A Behavioral Economic Analysis of Polysubstance Use: Studies with Cocaine, Fentanyl, and Cocaine–Fentanyl Mixtures in Sprague–Dawley Rats

Harmony Risca,<sup>1</sup> and Gregory T. Collins<sup>2</sup>

<sup>1</sup>Univ of Texas Health Science Center; and <sup>2</sup>Univ of Texas Health Science Center at San Antonio

Abstract ID 24299

Poster Board 465

The co-use of stimulants and opioids has become increasingly evident in recent years, yet few studies have systematically investigated the reinforcing effects of cocaine-fentanyl mixtures. Behavioral economic demand analyses provide a translational approach to quantify the relative value of drug reinforcers across different classes (stimulant vs opioid), making it a viable method to help ascertain factors which promote polysubstance use in humans. The current study used a multiple component schedule of drug self-administration to assess economic demand for cocaine (0.032, 0.1, 0.32, 1.0 mg/kg/inf), fentanyl (0.00032, 0.001, 0.0032, 0.01 mg/kg/inf), and mixtures of cocaine:fentanyl (in 10:1, 3:1, 1:1, 1:3, 1:10, relative to the dose ranges above) in male and female rats. Available unit-doses of drug increased across 4, 20-min drug components, with increases in the response requirement (fixed ratio) occurring across sessions. Demand curves for cocaine, fentanyl, and their respective mixtures were generated by normalizing consumption (number of infusions earned) to  $Q_0$  (estimate of unconstrained demand) and plotted as a function of standardized price ( $FR \times Q_0$ ). Elasticity coefficients ( $\alpha$ ) generated from demand curve analyses were used to assess the relative value of each drug and mixture preparation. The elasticity coefficient of fentanyl was greater than that of cocaine (i.e., cocaine had a greater “essential value”). Similarly, demand for the 10:1 mixture of cocaine + fentanyl was found to be greater than demand for fentanyl alone but comparable to cocaine. Mixtures of 1:3 and 1:10 cocaine + fentanyl produced alpha values that were greater than that of cocaine but not that of fentanyl, further suggesting that interactions may be strictly additive in respect to their reinforcing effects. Results from the current study compliment reports from nonmedical opioid users who combine opioids with stimulants to “enhance the high”. Taken together, the co-use of cocaine and fentanyl may increase the risk for developing a substance use disorder. Additionally, treatment targeting opioid use may be less effective in individuals who co-use stimulants such as cocaine with opioids. Future studies are warranted to assess how opioid dependence and withdrawal may impact the reinforcing effectiveness of cocaine-fentanyl mixtures compared to either drug alone.

This research was funded by the National Institutes of Health (R01 DA039146) and NIH/NIDA T32 (DA031115) postdoctoral research fellowship.

## A Reinforcer Worth its Salt?

Lee Gilman,<sup>1</sup> Marissa M. Nicodemus,<sup>2</sup> Allianna K. Hite,<sup>2</sup> Cameron N. Russell,<sup>2</sup> Lauren R. Scrimshaw,<sup>2</sup> Jasmin N. Beaver,<sup>2</sup> and Brady L. Weber<sup>2</sup>

<sup>1</sup>Kent State Univ; and <sup>2</sup>Kent State University

Abstract ID 56509

Poster Board 466

Excess salt (NaCl) intake is an established risk factor for cardiovascular diseases. But excess salt intake persists despite these known adverse outcomes. Why do we keep eating those chips, pretzels, cheese, etc., even when we're not hungry nor deficient in salt? Surprisingly, studies have not systematically evaluated how much 'work' salt- and food satiated mammals will exert for sweet reinforcers (31% sucrose) with increasing amounts of salt (1, 2, or 4% NaCl) upon initial or repeated exposure. Using adult C57BL/6J mice of both sexes, we have commenced evaluating this question using operant conditioning. Mice were trained with increasing fixed ratios (1, 3, 5) then transitioned to a progressive ratio to identify stable breakpoints. This allowed us to use a within-subjects design to 'ask' mice how much 'work' reinforcers are worth depending upon their salt content. When stable breakpoints were reached for the sweet reinforcers (0% NaCl), mice were sequentially transitioned to sweet reinforcers containing 1, 2, or 4% NaCl. A return to 0% NaCl sweet reinforcers preceded each increase in salt content. This process was repeated once more to determine how repeated exposure to higher salt levels impacts effort to obtain reinforcers with lower salt levels. All mice were salt-replete and were not food restricted. Though experiments are ongoing, early evidence in males indicates initial exposure to sweet reinforcers containing salt devalues subsequent sweet reinforcers (0% NaCl). Given known sex differences in operant conditioning acquisition, outcomes in females are currently too preliminary to make confident conclusions. These longitudinal investigations will set a baseline for subsequent study of voluntary excess salt consumption when mammals are in a salt-replete and food satiated state. By assessing how reinforcer salt content affects willingness to work, we can begin to identify neural circuitry that drives persistent salt consumption in the absence of need for either salt or food. Similarly, establishment of this paradigm will facilitate determination of cellular and/or molecular targets for therapeutics to attenuate excess salt intake.

This work was supported by Kent State University, and by NIMH R15MH118705 to TLG.

# Opposing Roles of Enkephalin and Dynorphin in the Amygdala on Resilience to Social Stress in Females

Alexandria Nowicki,<sup>1</sup> Cora Smiley,<sup>2</sup> Brittany Pate,<sup>3</sup> Samantha Bouknight,<sup>4</sup> and Susan Wood<sup>1</sup>

<sup>1</sup>Univ of South Carolina School of Medicine; <sup>2</sup>Univ of South Carolina Sch of Med; <sup>3</sup>University of South Carolina School of Medicine; and <sup>4</sup>Univ of South Carolina

Abstract ID 25994

Poster Board 467

With over 50 million people affected in the US alone, mental health disorders take a high toll on our country. Further, women have a predisposition to developing stress-related disorders and demonstrate more anxiety-like behaviors following stress cues compared with men. Anxiety and fear responses are heavily regulated by the amygdala, a brain region that plays a crucial role in mood behaviors and emotional memory processes. Mu (MOR), kappa (KOR), and delta (DOR) opioid receptors are present in high concentrations in such stress-related areas of the brain and mediate communication with specific neurotransmitters involved in emotional processing and stress responses. Enkephalin (ENK), an agonist at both MOR and DOR, promotes a basal hedonic state and is known to attenuate stress-induced anxiety-like behavior. In contrast, the endogenous KOR agonist dynorphin (DYN) promotes an “anti-reward” response, through inhibition of dopamine release and initiation of a dysphoric cycle that leads to irritability, anxiety, anhedonia, and loss of reward motivation. Accordingly, KOR neurotransmission mediates the effects of stress and leads to heightened drug reinstatement in rodent models. This study utilized a highly validated, ethologically relevant model, witness stress (WS), whereby females observed social defeat between two males from a confined region of an aggressive resident's cage. Previous data from our lab suggests that WS increases anxiety-like responding in females as determined by increases in hypervigilant burying responses during stress exposure as well as during re-exposure to the stress context. Further, we determined that these behavioral responses were paralleled by increases in KOR expression within the amygdala, supporting the involvement of the opioid receptor systems in the stress susceptibility of females. We next aimed to determine if exposure to witness stress (WS)-related cues alters ENK and DYN consistent with maintenance of anxiety-like behaviors in two regions of the amygdala, the basolateral amygdala (BLA) and the central amygdala (CeA), in females with a history of WS. This is an especially important consideration considering research regarding females within this topic has not yet been explored. To test this hypothesis, we first exposed female rats to a single WS exposure and brain tissue was collected two hours later. In the second experiment, rats experienced five days of WS and were subsequently exposed to WS-related cues prior to tissue collection. Immunofluorescence was used to detect levels of ENK and DYN in the CeA and BLA in response to both acute stress and to the WS context. In alignment with previous literature and current rationale, we expect that ENK expression will be lower in the BLA of stressed females while, in turn, DYN expression should be increased in the CeA of these same rats to create a dysphoric effect following stress-cue exposure. In correspondence with these results, future studies will employ behavioral pharmacology to determine if injecting the MOR agonist DAMGO and/or the KOR agonist norBNI into the amygdala will increase resilience to witness stress in females. In summary, our data indicates that the opioid receptor system is associated with the hypervigilant burying responses observed in females during both stress and stress cue exposure, elucidating a promising target for the treatment of stress susceptibility in females.

Funding Info:

R01MH113892 & VA Merit BX005661 - SKW

Magellan Scholar & Honors College SURF - AVN

# The Synthetic Psychedelic 2,5-methoxy-4-iodoamphetamine (DOI) Attenuates the Positive Appetitive and Reinforcing Effects of Methamphetamine

Bo J. Wood,<sup>1</sup> and Kevin Murnane<sup>1</sup>

<sup>1</sup>Louisiana State Univ Health Sciences Center - Shreveport

Abstract ID 56697

Poster Board 468

**INTRO:** Methamphetamine is a highly addictive psychomotor stimulant, which despite posing a growing public health threat, has no Food and Drug Administration approved pharmacotherapies. Psychedelics, whose early studies have had success in addiction and other psychiatric conditions, offer a new approach to treating methamphetamine addiction. Despite the growing examination of these psychedelics in clinical research, these compounds have not been evaluated in the context of attenuating the positive appetitive and reinforcing effects of methamphetamine.

**METHODS:** To investigate this, the synthetic phenethylamine R(-) 2,5-methoxy-4-iodoamphetamine (DOI) was used in two well validated behavioral models, conditioned place preference (CPP) and operant self-administration, to evaluate its capacity to attenuate the positive appetitive and reinforcing effects of methamphetamine, respectively. For the positive appetitive effects of methamphetamine, CPP was utilized, where animals were administered DOI intraperitoneally directly following each methamphetamine conditioning session. For the reinforcing effects of methamphetamine, operant self-administration was used where animals were trained to respond at a fixed ratio 5 schedule of reinforcement. Once stably responding, animals received a pre-treatment of DOI 15 minutes prior to the start of the operant session. To ensure any potential decrease in drug-associated responding, a food-maintained control was used.

**RESULTS:** At the peak dose in CPP of methamphetamine (0.56mg/kg), DOI blocked the development of a methamphetamine place preference. DOI (3.2 mg/kg) significantly reduced the percent change of time spent in the methamphetamine-paired side compared to animals who received saline as a post-treatment. Additionally, DOI (0.32 mg/kg) produced a robust decrease in operant responding for methamphetamine. When evaluating food-maintained behavior, we found that DOI more potently suppresses methamphetamine self-administration compared to the food-maintained control.

**DISCUSSION:** Although psychedelics such as psilocybin have shown promise in both preclinical and clinical settings for addiction and various psychiatric disorders, there is a large gap of this research in the context of methamphetamine addiction. Consistent with previous findings from our lab showing that DOI suppresses alcohol CPP and decreases voluntary drinking, DOI suppressed methamphetamine CPP and voluntary methamphetamine self-administration. Together the data presented here demonstrate that DOI attenuates the positive appetitive and reinforcing effects of methamphetamine. These results indicate the potential that psychedelics have in the treatment of methamphetamine addiction.

This work was supported by the Louisiana Addiction Research Center, the Department of Pharmacology, Toxicology & Neuroscience, and the Center of Biomedical Research Excellence in Redox Biology and Cardiovascular Disease (P20GM121307).

# Corticotropin-releasing factor pathways facilitate hypervigilant behavioral and physiological responses to social stress in female rats

Brittany Pope,<sup>1</sup> Sarah Mott,<sup>2</sup> Evelyn Harrington,<sup>3</sup> Cora Smiley,<sup>4</sup> Jim Fadel,<sup>3</sup> and Susan Wood<sup>5</sup>

<sup>1</sup>Univ of South Carolina; <sup>2</sup>Univ of North Carolina at Chapel Hill; <sup>3</sup>University of South Carolina School of Medicine; <sup>4</sup>Univ of South Carolina Sch of Med; and <sup>5</sup>Univ of South Carolina School of Medicine

Abstract ID 28262

Poster Board 469

Psychosocial stress is a common risk factor for comorbid anxiety and cardiovascular disease with women exhibiting increased susceptibility compared to men. Interestingly, this increased risk among women is confined between the onset of puberty and menopause, suggesting a role for cycling ovarian hormones. However, the underlying mechanism linking stress and ovarian hormones to the disproportionate risk of stress-related disorders among women remains unclear, making it difficult to develop targeted and effective pharmacotherapies. Using witness stress (WS), a social stress model in which a female rat observes an aggressive social defeat encounter between two male rats, we previously found that intact females are highly susceptible to this form of stress as evidenced by persistent hypervigilant behavioral and autonomic responses. Interestingly, ovariectomized (OVX) rats are resistant to WS-evoked behavioral and autonomic shifts, while 17- $\beta$  estradiol (17- $\beta$ E) replacement reinstates this hypervigilant phenotype. Therefore, interrogating systems regulated by stress and 17- $\beta$ E may reveal novel pharmacological targets to treat stress-related hypervigilant disorders. The corticotropin-releasing factor (CRF)-rich central amygdala (CeA) is one stress- and estrogen-sensitive brain region that can regulate these responses. Specifically, the prominent CRF projections to the locus coeruleus (LC) facilitate burying behavior and increased sympathetic drive and vagal withdrawal, autonomic features of hypervigilance. Therefore, this study aimed to examine whether 17- $\beta$ E regulates CRF expression in the CeA paired with the functional implications indicated by LC neuronal activity, hypervigilant behavior, and peripheral epinephrine (EPI) responses in the presence and absence of WS. Female rats, implanted with a catheter in the right jugular vein, were either left intact (sham) or OVX. One hour after injection (vehicle or 17- $\beta$ E (10  $\mu$ g/rat, s.c.)), rats underwent WS or control handling (CON). Behavior was recorded during WS/CON (15 min) and blood was collected via i.v. catheter immediately following. Brains were collected 2 hours later, and immunohistochemistry was used to quantify CRF expression in the CeA and *cfos* expression in both the CeA and LC. WS-evoked burying behavior was blunted in OVX rats and reinstated by 17- $\beta$ E, but 17- $\beta$ E had no effect on rearing and freezing behavior. Accordingly, plasma EPI levels were also regulated by 17- $\beta$ E as OVX blocked WS-evoked increases in EPI, and this response was reinstated by 17- $\beta$ E replacement. In the brain, 17- $\beta$ E selectively enhanced activation of CeA CRF+ neurons among WS rats. Further, OVX attenuated WS-evoked increases in LC *cfos*, but 17- $\beta$ E reinstated this WS-evoked increase in LC activity. Taken together with evidence from clinical trials implicating the role of LC hyperactivity in stress-related disorders, these findings demonstrate that CRF and LC signaling in the brain may represent a novel therapeutic target for promoting stress resilience among women.

This work was supported by RO1 grant MH113892 and VA Merit BX005661 (SKW) and American Heart Association Predoctoral Fellowship #915364 (BSP).

# Bidirectional ERK1/2 Modulation in Dopaminergic Neurons Regulates DAT Expression and Function

Christina Besada,<sup>1</sup> Stacia I. Lewandowski,<sup>2</sup> and Ole Mortensen<sup>3</sup>

<sup>1</sup>Drexel College of Medicine; <sup>2</sup>Drexel University College of Medicine; and <sup>3</sup>Drexel Univ College of Medicine

Abstract ID 16668

Poster Board 69

Dopamine (DA) is a neurotransmitter that plays a critical role in motivation, reward, and learning. The dopamine transporter (DAT) is responsible for the reuptake of released DA, making it a central regulator of DA neurotransmission. DAT is a target for psychostimulants such as cocaine, giving DAT a key role in psychostimulant-use disorders. Two signaling pathways that contribute to DAT regulation and trafficking to and from the plasma membrane involve the protein kinase C (PKC) and the mitogen activated protein kinase (MAPK) ERK1/2. ERK1/2 is inactivated by the MAPK phosphatase MKP3, which specifically dephosphorylates ERK1/2. Prior *in vitro* data demonstrated that activation of PKC by phorbol 12-myristate 13-acetate (PMA) results in decreased DAT surface-expression; MKP3 overexpression attenuates this effect. Furthermore, related studies have shown that ERK1/2 activation may lead to phosphorylation of DAT on threonine 53 (Thr53), however, the significance of this phosphorylation is not completely understood, but it is thought to play a significant role in DAT function and trafficking. *In vivo* data from our lab shows exogenous overexpression of MKP3 and resulting ERK1/2 inactivation increases DAT surface-expression, but interestingly reduces DAT transcript levels. This suggests that post-transcriptional regulation of DAT, such as proteasomal degradation, may be affected by ERK1/2. Additionally, MKP3 overexpression reduced Thr53 phosphorylation levels despite the overall increase of DAT surface-expression. To further characterize the contributions of ERK1/2 to DAT regulation and trafficking *in vivo*, we will use two viral constructs: AAV9-FLEX-MKP3-R (MKP3) and AAV9-FLEX-OptoSOS-R (OptoSOS). OptoSOS is an optogenetic tool that enables blue-light activation of ERK1/2. Both constructs enable cre recombinase-dependent expression in DA neurons of the VTA, allowing for spatiotemporal inactivation or activation of ERK1/2. We have confirmed that ERK1/2 is activated by blue-light in a cre-dependent manner, and similar to our results with MKP3 overexpression, ERK1/2 activation results in changes in DAT surface-expression and phosphorylation. Additionally, ERK1/2 activation results in increased phosphorylation of tyrosine hydroxylase – the rate limiting enzyme in DA synthesis. We will utilize these constructs to better understand the role of ERK1/2 signaling in regulation of DAT phosphorylation and membrane trafficking, and DA neurotransmission. Taken together, our results indicate that ERK1/2 serves a critical physiological role in DAT regulation, and these studies will provide important information regarding the mechanistic relationship between DAT trafficking, phosphorylation, and activity. These tools could help to reveal novel therapeutic strategies for psychostimulant-use disorders.



# Pharmacology of Memory Dysfunction in Alzheimer's Disease (AD)

Marcia Ratner,<sup>1</sup> and David H. Farb<sup>1</sup>

<sup>1</sup>*Boston Univ School of Medicine*

**Abstract ID 28694**

**Poster Board 70**

The biological basis for memory continues to be actively investigated yet, as contrasted with cardiovascular pharmacology, an overarching pharmacological theory for the modulation of memory in healthy and diseased states remains largely unknown. To address this need for developing a platform for the interrogation of memory by probe drugs, we have focused on developing a paradigm for within subject interrogation of memory circuitry *in vivo* in awake ambulating animals as a basis for future discovery in a precision medicine approach to neurotherapeutics.

The hippocampal trisynaptic circuit (HTC) is formed by synapses between neurons in the entorhinal cortex (EC) synapsing on dentate granule cells (DC) that synapse upon pyramidal cells in the CA3 pyramidal neurons (Ca3 Pyr), which then synapse upon CA1 pyramidal neurons (CA1 Pyr): EC > DC > CA3 Pyr > CA1 Pyr which is recognized as a core module in mammalian memory systems function. Disorders of aging such as mild cognitive impairment and AD are associated with HTC hyperactivity (Wilson et al., 2006; Yassa et al., 2010; Baker et al., 2015; Robitsek et al., 2015; Sosulina et al., 2021). We demonstrated that acute systemic administration of low dose levetiracetam + valproic acid reduced HTC hyperactivity and increased the spatial information content encoded by HTC place cells (Robitsek et al., 2015). We have also shown that the dose-dependent ripple band response to administration of an orally bioavailable negative allosteric modulator of alpha5-type GABA-A receptors (alpha 5IA) is attenuated or eliminated in awake immobile TgF344-AD rats with elevated plasma AB42 and AB40 (Ratner et al., 2021).

Here, we ask whether Abeta42 that is produced in a transgenic rat model of AD (TgF344-AD) disrupts synchronous firing of subsets of CA1 Pyr that comprise sharp wave ripples (SPW-Rs) at 140 - 200 Hz. SPW-Rs are likely a functional elementary process in memory consolidation (Buzsaki 2015). Epsilon band (90 to 130 Hz) oscillations are smaller in amplitude than SPW-Rs and both emanate from CA3 Pyr oscillations. The boundary between these two frequency bands is defined by a characteristic dip between 130 and 150 Hz in power spectral density plots, surrounded by distinct peaks at 170-180 and 110 Hz. We have shown that this type of synchronous high frequency circuitry activity is disrupted in awake immobile TgF344-AD rats (Ratner et al., 2021).

We now show that administration of alpha5IA differentially modulates these two high frequency bands. In WT F344 CA1, alpha5IA dramatically potentiates SPW-Rs but has little effect on epsilon. Moreover, in TgF344-AD rats, where alpha5IA now fails to enhance the SPW-Rs, epsilon is largely unaffected by the overexpression of Abeta 42 and 40 and its sensitivity to alpha 5IA is not measurable in this respect like the ripple band. These observations suggest alpha-5 subunit-containing GABA<sub>A</sub> receptors, which are highly expressed in CA1 Pyr neurons play a role SPW-R modulation but not high frequency oscillations in the adjacent epsilon band. The results demonstrate that alpha5IA modulation can be used to differentiate between high frequency oscillations in the ripple band from those in the epsilon band. Further research will explore the relevance of this preferential modulatory effect in terms of the behaviorally demonstrated nootropic effects of alpha 5IA.

David H Farb was supported by National Institute on Aging

(R21AG056947, P01AG9973).

Marcia H. Ratner was supported by National Institute on Aging

(T32AG00115).

# Unconventional Mechanisms of Novel Positive Allosteric Modulators of NMDA Receptors

Elijah Ullman,<sup>1</sup> Riley Perszyk,<sup>1</sup> Jing Zhang,<sup>2</sup> Nick Akins,<sup>2</sup> Russell Fritzscheier,<sup>2</sup> Srinu Paladugu,<sup>2</sup> Dennis Liotta,<sup>2</sup> and Stephen Traynelis<sup>1</sup>

<sup>1</sup>Emory Univ; and <sup>2</sup>Emory University

**Abstract ID 53705**

**Poster Board 71**

The N-methyl-D-aspartate receptor (NMDAR) is a ligand gated ion channel that is permeable to Na<sup>+</sup> and Ca<sup>2+</sup> and mediates a slow component of excitatory neurotransmission. NMDARs are implicated in synaptic plasticity and disease states such as in Parkinson's, Alzheimer's, Schizophrenia, and stroke. Here we have evaluated the characteristics at the single channel level of three series of allosteric modulators with structural determinants of bindings in regions that participate in NMDAR channel gating. We have generated two series of positive allosteric modulators (PAMs), EU1622 and EU1794 that generate two and three subconductance states respectively, and reduce the Ca<sup>2+</sup>:Na<sup>+</sup> permeability ratio (Perszyk et al., 2018, 2020) – a first in class features of NMDAR modulators. We are exploring the mechanisms underlying these two classes of unique conductance-modifying allosteric modulators. Specifically, we are measuring effects on open probability, conductance, mean open time, deactivation time course, and agonist potency for conductance modifying modulators for comparison to modulators (EU1180 series) that do not alter conductance. In addition, the reduction of calcium permeability holds interesting therapeutic potential due to reduced neurotoxic risk of NMDA receptor potentiation compared to non-conductance modifying modulators. Ongoing efforts by our group are working to identify the mechanisms by which these modulators mediate changes in calcium permeability, which may be related to changes in calcium binding affinity to residues within or near the pore, or changes in pore diameter.

S.F.T. is a PI on a research grants from Janssen to Emory, is a member of the SAB for Sage Therapeutics, Eumentis Therapeutics, and CombinedBrain, a senior advisor for GRIN Therapeutics, is on the Medical Advisory Board for the CureGRIN Foundation and the GRIN2B Foundation, is co-founder of NeurOp Inc and Agrithera, is on the Board of Directors for NeurOp Inc. S.F.T and D.C.L are co-inventors on Emory-owned Intellectual property that includes the allosteric modulators discussed in this work. D.C.L is a member of the Board of Directors for NeurOp Inc

# Agmatine inhibits NMDA Receptor-mediated Calcium Transients in Spinal Cord Dorsal Horn

Tongzhen Xie,<sup>1</sup> Rachel E. Schorn,<sup>1</sup> Cristina D. Peterson,<sup>2</sup> Lucy Vulchanova,<sup>1</sup> George L. Wilcox,<sup>3</sup> and Carolyn A. Fairbanks<sup>2</sup>

<sup>1</sup>University of Minnesota; <sup>2</sup>Univ of Minnesota; and <sup>3</sup>Univ of Minneapolis Medical School

Abstract ID 17771

Poster Board 72

**Aims, and Hypothesis:** The activation of N-methyl-D-aspartate receptors (NMDARs) in the spinal cord dorsal horn, and the subsequent  $\text{Ca}^{2+}$  permeation into neurons, are established contributions to chronic pain. Specifically, antagonism of the GluN2B subunit-containing NMDARs (GluN2B-NMDARs) is involved in the development of chronic pain. Our previous studies have shown that the intrathecal administration of Agmatine, an endogenous decarboxylated form of L-arginine that selectively antagonizes GluN2B-NMDARs, inhibits and reverses the pain behaviors in animal models of chronic pain. However, the mechanism of Agmatine's inhibition on  $\text{Ca}^{2+}$  transients in the spinal cord dorsal horn is still unknown.

**This study aims** to define the modulatory effect of agmatine on NMDARs-mediated  $\text{Ca}^{2+}$  transients in ex vivo mouse spinal cord slices. **The hypothesis** is that 1) agmatine can concentration-dependently inhibits NMDARs-mediated  $\text{Ca}^{2+}$  transients, similar to other NMDAR antagonists. 2) agmatine's inhibitory effect can be reversed by GluN2B knock-down.

**Methods:** Female and male ICR mice (4-6 weeks) were perfused before spinal cord extraction, and ex vivo spinal slices were incubated with the calcium indicator dye Fluo-4. For GluN2B knock-down mice (GluN2B-KD), intraspinal injections of Cre-containing AAV9-hSyn-GCaMP6s-cre and control AAV9-hSyn-GCaMP6s-Δcre viruses were performed on C57 GluN2Bfl/fl mice. Both viruses encoded a  $\text{Ca}^{2+}$  indicator, GCaMP6s, to visualize  $\text{Ca}^{2+}$  transients. 4 weeks after injection, laminectomy was conducted and spinal neurons expressing Cre recombinase were distinguished by GCaMP6s expression. Intracellular  $\text{Ca}^{2+}$  was visualized by single-plane two-photon microscopy. Time-lapse of images were acquired and the peak amplitude of fluorescence intensity was analyzed by Student's t-test.

**Results:** 2 minutes incubation of APV (2, 10, 50  $\mu\text{M}$ ), ifenprodil (30, 100, 300  $\mu\text{M}$ ), and Agmatine (1, 3.3, 10 mM) concentration-dependently attenuated the NMDARs-mediated  $\text{Ca}^{2+}$  transients. For ifenprodil, we also found that longer incubation (15 min) resulted in significantly higher inhibition of NMDAR-mediated  $\text{Ca}^{2+}$  transients ( $n=3$ ,  $P < 0.01$ ). In the GluN2B-KD study, NMDA (30, 100, 300  $\mu\text{M}$ ) application without antagonist showed no significant difference in  $\text{Ca}^{2+}$  response between GluN2B-KD and control ( $n=6$ ). The GluN2B-KD significantly reversed the inhibition of amplitude of NMDAR-mediated  $\text{Ca}^{2+}$  response by 15 minutes incubation of 100  $\mu\text{M}$  ifenprodil ( $n=4$ ,  $P < 0.01$ ) but not in 15 minutes incubation of 3.3mM Agmatine.

**Conclusions:** APV and ifenprodil significantly attenuated the intracellular NMDARs-mediated  $\text{Ca}^{2+}$  signals, indicating that the NMDARs-mediated  $\text{Ca}^{2+}$  transients' assay is specific to NMDARs. Agmatine's concentration-dependent inhibition of NMDARs-stimulated  $\text{Ca}^{2+}$  transients suggests that Agmatine is an effective antagonist of NMDARs in the spinal cord dorsal horn, which is consistent with our electrophysiological and neuropharmacological research showing that Agmatine is an effective inhibitor of NMDARs in the spinal cord dorsal horn. GluN2B-KD and controls had similar NMDAR-mediated  $\text{Ca}^{2+}$  transients, and GluN2B-KD reversed the attenuation of NMDARs-mediated  $\text{Ca}^{2+}$  transients by ifenprodil but did not with Agmatine. These results further defined the Agmatine's effect on NMDAR-mediated  $\text{Ca}^{2+}$  transients, which will help the development of agmatine-based chronic pain therapeutics.

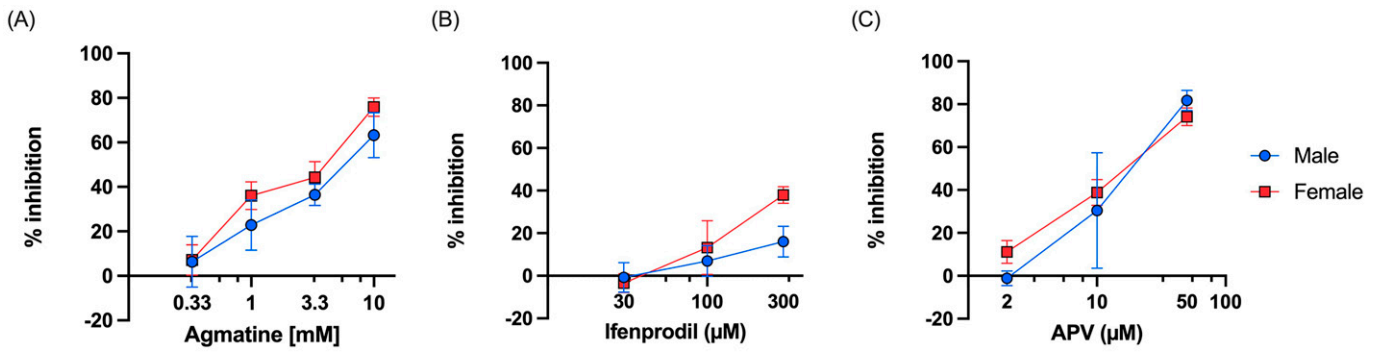


Figure 1. Agmatine (A), ifenprodil (B), and APV (C) concentration-dependently inhibit NMDAR-mediated  $Ca^{2+}$  transients.

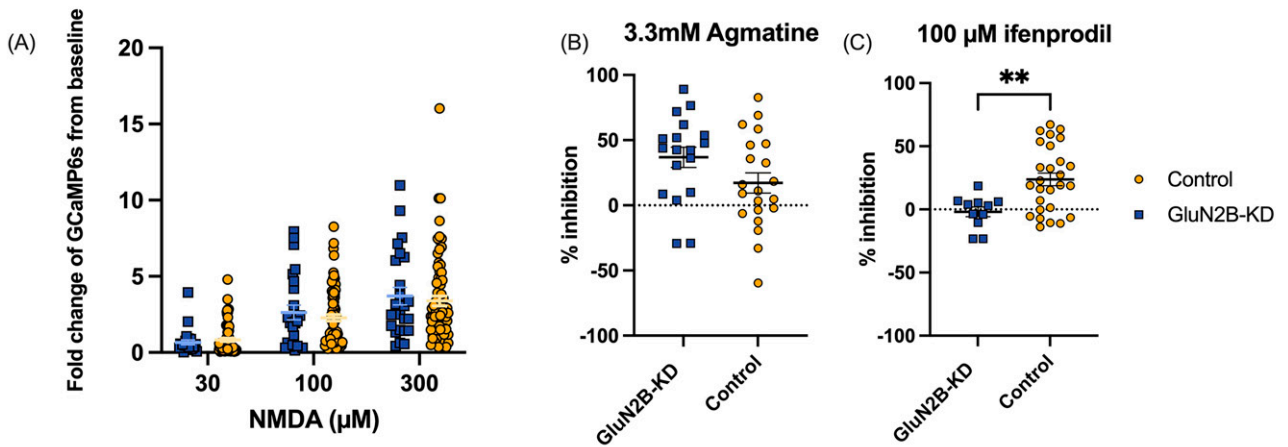


Figure 2. (A) GluN2B-containing NMDARs knock down (GluN2B-KD) animals show similar amplitude of NMDARs-mediated  $Ca^{2+}$  transients compared to control, and (B) GluN2B-KD reversed the NMDAR-mediated  $Ca^{2+}$  transients' attenuation by ifenprodil ( $n=4$ ,  $P<0.01$ ), (C) but not with Agmatine.

# Real-time pharmacokinetic measurements of vancomycin in the brain of mice via electrochemical aptamer-based sensors

Karen KS. Scida,<sup>1</sup> Miguel A. Pellitero,<sup>2</sup> Netzahualcoyotl Arroyo-Curras,<sup>3</sup> and Gregory Carr<sup>1</sup>

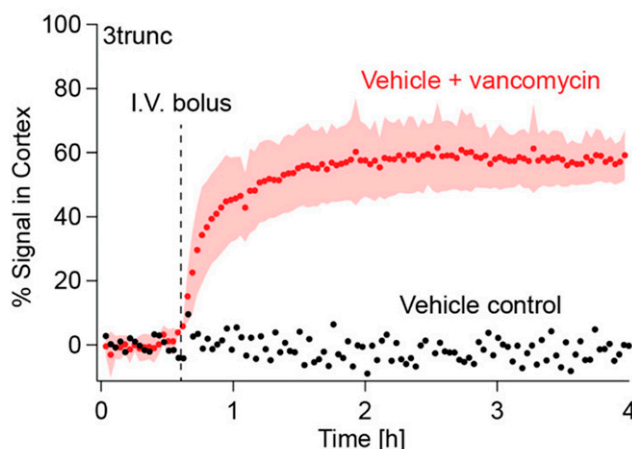
<sup>1</sup>Lieber Institute for Brain Development; <sup>2</sup>Universidad de Oviedo; and <sup>3</sup>Johns Hopkins School of Medicine

Abstract ID 17697

Poster Board 73

Disease treatment and prevention are currently based on population-averaged pharmacological data obtained from a limited number of patients. Additionally, clinical dose estimations are based on physical parameters like body mass, age, and pharmacogenetic markers that do not consider idiosyncratic or state-dependent variables (e.g., exercise, hydration, eating habits, etc.). As can be expected, these pharmacokinetic approximations can lead to large variability in efficacy for individual patients. Moreover, current methods for measuring drug plasma exposures require offline measurement of analytes and the actual site of action (e.g., the brain) is often completely inaccessible for measurements from awake behaving animals. Therefore, pharmacokinetic-pharmacodynamic correlations are often based on low-accuracy data. The latter is a common scenario in brain-related disease and injury treatment as there is limited information about drugs that permeate the blood-brain barrier (BBB) and even less regarding drug distribution across different brain regions. For example, the aminoglycoside vancomycin is a common antibiotic used in perioperative neurosurgery and the management of penetrating brain injury, and the standard of care requires its delivery via intravenous (I.V.) injection. Vancomycin has poor permeability across the BBB (CSF-to-plasma ratios of 0.07-0.30); therefore, high vancomycin intravenous dosing is required to achieve brain concentrations above minimum inhibitory concentrations. To our knowledge, however, there are no published reports showing measurable concentrations of vancomycin in the brain after intravenous administration. Consequently, prophylaxis dosing regimens remain highly speculative.

Electrochemical aptamer-based (E-AB) sensors, an emerging technology in the field of pharmacology, have shown great success at measuring full pharmacokinetic profiles of small molecule drugs in-situ in the vein of rodents with unprecedented accuracy, precision and temporal resolution. The E-AB sensor platform is reagentless and has recently enabled the real-time tracking of vancomycin concentrations in the blood of rats. In this work, we expand the use of E-AB sensors to the measurement of vancomycin in the brain of mice. We demonstrate that following an I.V. injection of 75 mg/kg (tail vein bolus), the concentration of vancomycin reaches a  $C_{max}$  of 8  $\mu$ M in the cortex in 1.5 h, plateauing at that level for the remaining of the experiment ( $\sim$ 2 h). To our knowledge this the first real-time in vivo measurement of vancomycin in the brain. Future experiments in this project will measure vancomycin concentrations in different brain regions following multiple I.V. doses and validate the concentration measurements using gold-standard mass spectrometry methods.



Vancomycin pharmacokinetics in mice brain cortex following an intravenous tail injection of 75 mg/kg bolus measured via electrochemical aptamer-based sensors

# Role of Glucagon-like peptide-1 Expressing Ventral Tegmental Area Neurons in Morphine Behavior

Olivia Dodson,<sup>1</sup> Cristina Rivera Quiles,<sup>1</sup> and Michelle Mazei-Robison<sup>1</sup>

<sup>1</sup>Michigan State Univ

Abstract ID 17034

Poster Board 74

Although opioid dependence and addiction continue to constitute a major health and economic burden, our limited understanding of the underlying neurobiology limits better diagnostics and interventions. Dysregulation of the mesocorticolimbic reward circuit is acknowledged to contribute to various aspects of drug addiction, with alteration in the activity and output of dopamine (DA) neurons in the ventral tegmental area (VTA) known to contribute to the rewarding aspects of drug use. However, the molecular mechanisms underlying these changes in VTA DA function remain relatively unexplored. Thus, we used translating ribosome affinity purification (TRAP) to identify gene expression changes in mice that specifically occur in VTA DA neurons following chronic morphine exposure. We found that expression of several neuropeptides not traditionally described in the VTA are robustly induced by morphine exposure. Glucagon-like peptide-1 (GCG) was of particular interest as it was enriched in VTA DA neurons and its expression was robustly increased following chronic morphine exposure. These data support increased GCG expression in the VTA following multiple types of opioid exposure and form a strong premise for studying GCG function. Thus, we hypothesize that activity of VTA GCG neurons contributes to morphine-elicited behaviors. To test this, we have begun to characterize the expression and functional impact of VTA DA neurons that co-express GCG using GCG-Cre mice and Cre-dependent viral vectors. Specifically, we are using DREADDs, designer receptors exclusively activated by designer drugs, to selectively activate or inhibit VTA-GCG neurons. We stereotaxically injected the excitatory DREADD hM3Dq (AAV-DIO-hM3Dq-mCherry) into the VTA of male and female wild-type and GCG-Cre mice and found that acute activation of VTA-GCG neurons via i.p. injection of clozapine-N-oxide (CNO, 0.3 mg/kg) does not affect general locomotor activity or elicit conditioned place preference or aversion (n = 5,9). We are now assessing whether activation of VTA-GCG neurons alters morphine-elicited behaviors (conditioned place preference, locomotor sensitization). Our preliminary data suggest there's a decrease in morphine-induced locomotion and morphine CPP in animals whose VTA-GCG neurons were activated. Studies are currently underway to assess these behaviors in a second cohort of mice. Together, these studies are expected to set the stage for future work investigating the role of specific VTA-DAGCG circuits, their activity during behavior, and their potential as targets for therapeutic intervention.

# Regulated Trafficking of GABA Transporters, GAT1 and GAT3, in Response to Methamphetamine

Hannah R. Grote,<sup>1</sup> Susan G. Amara,<sup>1</sup> and Suzanne M. Underhill<sup>1</sup>

<sup>1</sup>National Institute of Mental Health

Abstract ID 55152

Poster Board 75

As the main inhibitory neurotransmitter in the CNS, GABA is vital for neuronal signaling. Dysregulation of GABA has been implicated in a variety of conditions, from epilepsy to schizophrenia. The main GABA transporters in the CNS, GAT1 and GAT3, are responsible for the maintenance of inhibition within these systems via reuptake of GABA released during neurotransmission. GAT1 is robustly expressed by neurons but is also expressed on astrocytes while GAT3 is largely localized to peri-synaptic astroglia. GABA signaling is also dependent on glutamate uptake since glutamate is required for GABA synthesis. The neuronal excitatory amino acid transporter EAAT3 is responsible for glutamate transport into GABAergic neurons. Previous work from this laboratory has demonstrated that psychostimulants such as methamphetamine induce the internalization of the catecholamine transporters DAT and NET as well as EAAT3. This process involves methamphetamine stimulation of the G-protein coupled receptor TAAR1 and activation of the small GTPase RhoA that facilitates internalization of the transporters.

To examine whether GABA transporters are also internalized through a TAAR1-dependent mechanism, we measured the uptake of radiolabeled GABA into mixed cultures of primary striatal neurons and glia. In these cultures, which express both GAT1 and GAT3, neither amphetamine nor methamphetamine co-application had any measurable effect on GABA uptake, consistent with their reported low affinity for GABA transporters. However, pre-treatment with methamphetamine led to a significant decrease in GABA uptake. Inhibitors of RhoA, RhoA kinase (ROCK), and G-13-mediated GPCR signaling all prevented the methamphetamine-induced loss of GABA uptake. Together, these data suggest that GAT internalization is dependent on TAAR1 mediated signaling, as with other neurotransmitter transporters. Further studies using selective GAT inhibitors are underway to resolve the relative contributions of different GAT subtypes to the observed effects. In addition, GAT1 and GAT3 constructs containing GFP at the amino terminus have been generated and are being used to assess the trafficking of the two GAT subtypes directly.

Our findings show that methamphetamine can regulate GAT activity through TAAR1-mediated activation of RhoA signaling. Thus, TAAR1 and its downstream signaling cascades are important therapeutic targets for a wide variety of conditions and neurodegenerative diseases. GAT inhibitors are currently used as anticonvulsants and off-label anxiolytic treatments, despite the subsequent learning and long-term memory deficits. These findings suggest alternative methods for modulating GABA transport via TAAR1 which could prove to be vital for reevaluating current treatments.

This work was supported by Intramural Research at the NIH, NIMH.

# Characterizing Glutamate Stimulated Noradrenaline Release in Rat Cerebral Cortex Brain Slices: Release Mediating Receptors and their Subunits Composition

Yousef ALJOHANI,<sup>1</sup> Ghazaul Dezfuli,<sup>1</sup> and Kenneth J. Kellar<sup>1</sup>

<sup>1</sup>Georgetown University School of Medicine

Abstract ID 22062

Poster Board 76

Aging affects virtually all organs of the body. However, perhaps most profound are its deteriorating effects on the brain, where it often affects a wide array of crucial functions, such as attention, focus, mood, neuroendocrine regulation, sleep cycles, and autonomic movements (including those affected in Parkinson's disease). All these functions and fundamental cognitive processes, such as memory/recall and processing speed, rely on neuronal circuits governed by neurotransmitters signaling between neurons. Glutamate (Glu) is the main excitatory neurotransmitter in the central nervous system. It is involved in most neuronal functions that stimulate other neurons to release their neurotransmitters, such as norepinephrine (NE), dopamine, acetylcholine, and many others. Previous studies from our lab have confirmed that Glu-stimulated NE releases in the cerebral cortex and hippocampus tissue slices from aged Fischer 344 rats (20 - 24 months old) is significantly decreased (by approximately 30%) compared to release from young control rats (3 - 4 months-old). Importantly, the age-associated decrease in NE release can be fully rescued by amphetamine or methylphenidate *in Vitro*. We also showed that tonically active inhibitory alpha-2 receptors modulate the Glu-stimulated NE release, suggesting a promising target for restoring age-related decrease in NE release. Herein, we are further investigating the glutamate receptors subtypes that mediate NE release and their subunits composition. We found that most Glu-stimulated NE release is mediated by NMDA receptors (approximately 85-90%), whereas a small fraction of Glu-stimulated NE release is mediated by non-NMDA Glu receptors subtypes (i.e., AMPA and/or Kainate receptors subtypes). We also found that adding exogenous glycine or D-Serine, obligatory co-agonists required for NMDA receptor activation did not potentiate NE release. However, the highly competitive NMDA receptor antagonist at the glycine binding site, 7-Chlorokynurenic acid, significantly inhibits the Glu-stimulated NE release, whereas glycine or D-Serine outcompeted that inhibition in a dose-dependent manner. Moreover, PEAQX, a drug that inhibits NR2A subunit-containing NMDA receptors at nanomolar concentrations and inhibits NR2B subunit-containing NMDA receptors only at higher concentrations, exhibits an inhibitory profile best described by two distinct NMDA neuronal populations. The population of NMDA receptors with high affinity for PEAQX mediates ~ 15% of the release, and the population with low affinity mediates ~85% of the release. Consistent with this assignment of the NMDA receptors with high and low affinity for PEAQX, the drug Ifenprodil, which is highly selective for NMDA receptors containing NR2B subunits, inhibits ~ 85% of Glu-stimulated NE release, confirming that most of Glu-stimulated NE release is mediated by NR2B subunit-containing NMDA receptor.



# Redox-dependent Activation of Protein Kinase C and Neurotransmitter Transporter Trafficking

Saranya Radhakrishnan,<sup>1</sup> and Susan G. Amara<sup>1</sup>

<sup>1</sup>National Institute of Mental Health

Abstract ID 55201

Poster Board 133

Plasma membrane neurotransmitter transporters clear neurotransmitters from the extracellular space and play a key role in regulating neuronal signaling. The neuronal excitatory amino acid transporter 3, EAAT3, is essential for glutamate clearance and modulation of glutamatergic tone. However, EAAT3 also transports cysteine into the cell where it serves as a rate-limiting substrate for the synthesis of glutathione, a key neuronal antioxidant. EAAT3 mutations are associated with several neuropsychiatric disorders such as schizophrenia and obsessive-compulsive disorders that may be due to its role in glutamate or cysteine transport.

The activity of plasma membrane transporters can be altered by changes in transport kinetics, expression levels and trafficking to and from the plasma membrane. Using surface biotinylation assays in Neuro2A cells and mouse primary cortical neurons we confirmed that activation of protein kinase C (PKC) can increase cell surface localization of EAAT3, as previously reported in other cell lines. Redox-triggered mechanisms can influence signaling through PKC by altering the catalytic properties or the subcellular compartmentalization of various PKC isoforms. This suggests a mechanism whereby EAAT3 trafficking could be modulated by cellular redox stress and PKC activation to increase cysteine import and stimulate glutathione biosynthesis.

To study this, we examined whether oxidizing agents such as hydrogen peroxide can enhance PKC activation and increase EAAT3 plasma membrane localization. Using a genetically encoded PKC activity sensor, CKAR, we found that application of oxidizing agent, hydrogen peroxide increased PKC activation and enhanced surface expression of EAAT3 in both EAAT3-transfected Neuro2A cells and in primary cultures of mouse cortical neurons that express EAAT3 endogenously. To further understand the specific subcellular localization of this PKC activation, we generated sensors that were targeted to lipid raft and non-lipid raft using a Lyn Kinase and KRAS targeting motif. The activation of PKC with hydrogen peroxide caused an increase in PKC activation at the non-lipid raft but did not cause a significant increase near the lipid raft. From previous research, we also know that EAAT3 associates with non-lipid raft suggesting that this targeted PKC activation could be relevant to understanding the redox mediated increase of EAAT3 at the membrane. Taken together our observations suggest specific subcellular localization for the redox mediated activation of EAAT3 trafficking to the membrane.

# Intrinsic Alterations of Dopaminergic Neurons in the 3xTg-Alzheimer's Disease Mouse

Harris E. Blankenship,<sup>1</sup> Kylie Handa,<sup>1</sup> Willard M. Freeman,<sup>1</sup> and Michael J. Beckstead<sup>1</sup>

<sup>1</sup>Oklahoma Medical Research Foundation

**Abstract ID 55249**

**Poster Board 134**

Amyloid- $\beta$  and tau accumulation accompanied by cortico-hippocampal degeneration comprise the pathological hallmarks of late-stage Alzheimer's disease (AD) but do not readily explain all behavioral phenotypes present in Alzheimer's patients. Decades of anecdotal and recent experimental evidence implicate dopamine dysfunction in prodromal stages of AD, suggesting dopaminergic circuits could be potential therapeutic targets. Insight into alterations in structure, function, and molecular phenotype of single living dopamine neurons of the ventral midbrain is vital to understanding the prodromal pathophysiology of AD. Here, we used acute slice patch-clamp electrophysiology, single cell RNA-sequencing, pharmacology, and morphological reconstruction to assess single dopaminergic neuron structure and function in triple transgenic 3xTg-AD mice, a model that expresses both amyloid- $\beta$  and tau in a characterized spatiotemporal manner. Electrophysiological recordings from 3xTg-AD dopaminergic neurons of the ventral tegmental area displayed hypersensitivity, measured both by gain and number of action potentials generated, to direct-current injections as early as three months of age. Tonic firing rhythmicity of dopamine neurons in transgenic mice significantly deviated from controls by six months of age. Voltage clamp experiments indicated a decreased small conductance calcium activated potassium channel (SK) current may underly both the irregularity in pacemaking and the hypersensitivity of phasic action potential generation. Interestingly, irregularity was recapitulated by a partial block of SK, though not completely recovered by positive allosteric modulation of the same channel. Additionally, we observed diminished neurite complexity in single dopamine neurons from 3xTg-AD mice, when measured using Sholl analysis. Tandem patch-clamp single-cell RNA-sequencing (Patch-seq) data suggests dopamine neurons with impaired physiology deviate drastically from the molecular profile of their healthy wildtype controls. These results suggest functional and structural degeneration in subpopulations of single dopaminergic neurons across the lifespan of 3xTg-AD mice.

Support/Funding Information: R01AG052606 and R21AG072811 to MJB and F31AG079620 to HEB

# Alternatively Spliced Variants of the Mu Opioid Receptor Gene, *Oprm1*, Differentially Mediate Opioid-Induced Respiratory Depression in Rats

Ayma F. Malik<sup>1</sup>

<sup>1</sup>Rutgers, The State Univ of New Jersey

Abstract ID 53836

Poster Board 135

Opioid overdose deaths have skyrocketed by 3.5x in the last decade, mainly due to “opioid-induced respiratory depression (OIRD).” Understanding the mechanisms underpinning this is essential towards prevention and the development of new effective interventions. Mu opioid actions, including analgesia, tolerance, addiction and OIRD, are primarily mediated through mu opioid receptors (MOR). The single-copy MOR gene, *Oprm1*, undergoes extensive alternative splicing to generate two classes of MOR splice variants: Exon 1- (E1) and Exon 11- (E11) associated variants. The functional relevance of these splice variants has been demonstrated in mediating the actions of various mu opioids, including analgesia, tolerance, physical dependence, and reward. However, it remains unknown how the two sets of *Oprm1* splice variants influence OIRD. To address this question, we used two *Oprm1* gene targeted rat models, in which E1- or E11-associated variants are floxed with loxPs and can be conditionally disrupted by Cre-loxP recombination. We measured OIRD induced by morphine and fentanyl in these rat models under awake and unrestricted conditions using Whole-Body Plethysmography (WBP) technology that can define specific changes in respiration from opioids. The results demonstrated that E1- and E11- associated variants differentially influence OIRD, with varied responses from morphine and fentanyl administrations, as well as between male and female rats. Additionally, OIRD responses in rats differed from those in mice, suggesting species differences in OIRD. Together, this study not only provides a deeper understanding of the unique role of E1- and E11-associated variants on OIRD, but also enables the development of potential therapeutic strategies to reduce unnecessary opioid-related deaths.

Supported in part by grants from NIH (DA042888 and DA007242).

# Dopamine Dysregulation and Beyond: Exploring Methamphetamine-Induced Neuropathology

Nicole Hall,<sup>1</sup> Kariann Lamon,<sup>2</sup> Nicholas Whitton,<sup>2</sup> and Kevin Murnane<sup>1</sup>

<sup>1</sup>Louisiana State Univ Health Sciences Center - Shreveport; and <sup>2</sup>Louisiana State University Health Sciences Center - Shreveport

Abstract ID 23437

Poster Board 136

Methamphetamine misuse is a growing health crisis devastating the lives of millions throughout the world. Decades of research has focused on modulating the mesolimbic dopamine pathway as a target for methamphetamine medications development due to the known rewarding and reinforcing effects, yet no treatment is presently available. Recent evidence, however, indicates that methamphetamine induces widespread neuroinflammation which has been linked to both neurovascular damage and dopamine dysregulation. The aim of this research is to investigate a broadened neuropathology in an established model of methamphetamine binge dosing known to produce substantial and sustained dopamine dysregulation. For this study, we administered four intraperitoneal injections spaced two hours apart. Neurocognitive effects on learning and memory were assessed by passive avoidance assay and cerebral perfusion was evaluated using laser speckle contrast analysis (LASCA). Five days after the dosing regimen, we collected brain tissue for postmortem analysis which included high performance liquid chromatography (HPLC), quantitative polymerase chain reaction, and western blot analysis. HPLC analysis revealed that the dosing regimen induced a more than two-fold decrease in striatal dopamine levels when compared to saline controls. Methamphetamine exposed animals showed an absolute change in latency from training to testing in the passive avoidance assay that was fifty percent lower than that of control animals. Significant upregulation of gene expression of the cytokine interleukin 1 beta and the chemokine monocyte chemoattractant protein 1 was observed in striatal tissues obtained from mice administered methamphetamine. LASCA revealed a slight decrease in cerebral perfusion acutely following a bolus injection of MA; however, an increase in perfusion was detected one hour following the dosing regimen. Although much is known about the effects of dopamine and its dysregulation in the context of methamphetamine addiction, the role of extended neuropathology is understudied. Together the data presented here demonstrate that the binge dose regimen produces significant decreases in striatal dopamine and related cognitive deficits consistent with well-known effects of MA, and furthermore elucidates neurovascular damage and associated neuroinflammation not as frequently explored.

These studies were supported by the Louisiana Addiction Research Center, the Center of Biomedical Research Excellence in Redox Biology and Cardiovascular Disease (P20GM121307), and an RO1 (R01NS120676) to KSM and a Multidisciplinary Training in Cardiovascular Pathophysiology fellowship through the Center for Cardiovascular Diseases and Sciences (T32HL155022) to NMH.

# Novel Somatostatin Receptor Subtype-4 Agonist Enhances Memory and Neprilysin Enzyme Activity in Senescence Accelerated Mouse-Prone 8 Model of Cognitive Decline

Kuber Bajgain,<sup>1</sup> Karin Sandoval,<sup>1</sup> Ariel Magee,<sup>2</sup> Susan A. Farr,<sup>3</sup> Michael Niehoff,<sup>4</sup> and Ken Witt<sup>5</sup>

<sup>1</sup>Southern Illinois Univ Edwardsville; <sup>2</sup>Southern Illinois Univ; <sup>3</sup>Saint Louis University School of Medicine; <sup>4</sup>Saint Louis University; and <sup>5</sup>Southern Illinois Univ School of Pharmacy

Abstract ID 53923

Poster Board 137

Alzheimer's disease (AD) is a progressive neurodegenerative disorder characterized by cognitive impairments and brain amyloid-beta ( $A\beta$ ) aggregation. Neprilysin (NEP) is a primary  $A\beta$ -degrading enzyme, activated by the neuropeptide somatostatin (ssT) through a receptor mediated action (Saito et al., 2005, Nat Med 11(4):434-439). Of the five ssT receptors, the subtype-4 (ssTR4) shows the greatest promise for AD treatment targeting. ssTR4 has optimal brain localization, being highly expressed in neurons of the neocortex, and hippocampus (Viollet et al., 2008, Mol Cell Endocrinol 286(1-2):75-87). We previously showed ssTR4 agonist actions increase spatial and recognition memory in Senescence Accelerated Mouse-Prone 8 (SAMP8) and APP<sup>swe</sup> mouse models of AD, with capacity to reduce  $A\beta$ -oligomer protein expression (Sandoval et al., 2012 Eur J Pharmacol 683(1-3):116-124; Sandoval et al., 2013, Brain Res 1520:145-56).

Herein, we evaluated the novel ssTR4 agonist SM-I-26 on memory behavior and NEP activity in SAMP8 mice. SM-I-26 has high ssTR4 affinity ( $K_i=12$  nM), selectivity (>400-fold selective over other ssTR subtypes), and activity ( $EC_{50}=17$  nM). Male 12-month-old SAMP8 mice were administered 0.01, 0.1, or 1.0  $\mu$ g (i.c.v.) of SM-I-26 or vehicle for memory retention testing using the T-maze foot-shock avoidance test (memory retention 1-week post-injection,  $n = 7-8$ /group). NEP activity was tested at 1.0  $\mu$ g (i.c.v.) against vehicle control in cortical and hippocampal tissue 24-h post injection ( $n = 7$ /group).

SM-I-26 improved behavioral retention of the T-maze shock avoidance task in a dose-responsive manner ( $P<0.0001$ , one-way ANOVA), with 0.1 and 1.0  $\mu$ g SM-I-26 significantly reducing the mean trials to criterion when compared to vehicle ( $P<0.0001$ , Dunnett's T3). Within cortical tissue, SM-I-26 increased NEP activity ( $P < 0.05$ , independent t-test) compared to vehicle controls. A similar but non-significant trend between SM-I-26 and NEP activity was observed in hippocampal tissue.

Data shows i.c.v. administration of the ssTR4 agonist SM-I-26 improves memory behavior in SAMP8 mice and increases NEP activity in primary tissues associated with AD impairments. The potential of a ssTR4 agonist therapeutic for AD treatment is supported by this work.

This work has been supported by the National Institutes of Health, National Institute on Aging, R01AG047858.

# $\beta$ -Arrestins Mediate Rapid 5-HT<sub>2A</sub> Receptor Endocytosis to Control the Efficacy and Kinetics of Serotonin and Psychedelic Hallucinogen Signaling

Hudson Smith,<sup>1</sup> Daniel E. Felsing,<sup>2</sup> Ashley Nilson,<sup>2</sup> and John A. Allen<sup>2</sup>

<sup>1</sup>The University of Texas Medical Branch at Galveston; and <sup>2</sup>The University of Texas Medical Branch

138

Abstract ID 56096

Poster Board 138

Serotonin 5-HT<sub>2A</sub> receptors (5-HT<sub>2A</sub>Rs) regulate mood and perception in the central nervous system, and are a molecular target for psychedelic hallucinogens, atypical antipsychotics, antidepressants, and anxiolytics. The 5-HT<sub>2A</sub>R is a seven transmembrane, G protein-coupled receptor (GPCR) that primarily signals via the G<sub>αq</sub> family of heterotrimeric G proteins. Activation of the 5-HT<sub>2A</sub>R ultimately results in the intracellular release of Ca<sup>2+</sup> following G<sub>αq</sub>-mediated activation of phospholipase C (PLC) and the formation of inositol phosphates. In addition to G-protein dependent signaling, many GPCRs are now known to signal through G protein independent pathways.  $\beta$ -Arrestins are intracellular effector proteins that may mediate G protein independent signaling and are known to regulate G protein dependent signaling via receptor endocytosis and recycling at the plasma membrane. However, when compared to other GPCRs, the importance of  $\beta$ -arrestins for controlling the efficacy and duration of 5-HT<sub>2A</sub>R signaling is less defined. Live cell confocal imaging utilizing a FLAG-5-HT<sub>2A</sub>R and  $\beta$ -arrestin2-GFP was utilized to determine if agonist activation of 5-HT<sub>2A</sub>R receptors resulted in the recruitment of  $\beta$ -arrestin to the plasma membrane. Treating cells with either 5-HT (10mM) or the selective 5-HT<sub>2R</sub> agonist and hallucinogen DOI (10mM) induced a robust and rapid (within 30 secs) translocation of  $\beta$ -arrestin2-GFP from the cytoplasm to the plasma membrane, where it colocalized with FLAG-5-HT<sub>2A</sub>R. To determine the contributions of  $\beta$ -arrestin isoforms in 5-HT<sub>2A</sub>R signaling and trafficking, we utilized CRISPR/Cas9 genome editing to stably knockout (KO)  $\beta$ -arrestins 1 and 2. Western blots confirmed a complete loss of the  $\beta$ -arrestin 1 and 2 proteins in KO cells versus parent cells (WT). Using a receptor cell surface ELISA assay, we confirmed a DOI treatment (5 min) resulted in a rapid loss (~35%) of receptors from the plasma membrane in WT cells. By comparison, 5-HT<sub>2A</sub>R endocytosis (3 min to 45 min) was significantly reduced in  $\beta$ -arrestin 1/2 KO cells. Kinetic live-cell Ca<sup>2+</sup> release by the 5-HT<sub>2A</sub>R agonists (5-HT and DOI) was measured using a FLIPR assay.  $\beta$ -arrestin 1/2 KO cells exhibited a prolonged duration of Ca<sup>2+</sup> signaling when compared to WT cells. Additionally, the maximal effect (E<sub>max</sub>) of 5-HT and DOI was significantly increased (45% and 46%, respectively) in KO cells, although agonist potency was unchanged. Re-expression of  $\beta$ -arrestin 1 and 2 in KO cells reduced elevated agonist-mediated Ca<sup>2+</sup> responses to that of WT cells. In addition, knockout of  $\beta$ -arrestin1/2 increased and prolonged the duration of 5-HT<sub>2A</sub>R agonist-mediated ERK phosphorylation. Taken together, these data indicate rapid 5-HT<sub>2A</sub>R endocytosis following activation a serotonin or hallucinogen agonist is dependent on  $\beta$ -arrestins, and that  $\beta$ -arrestins rapidly interact with 5-HT<sub>2A</sub>R receptors to limit both the intensity and duration of G<sub>αq</sub>-mediated signal transduction. Taken together, these studies suggest an essential role of  $\beta$ -arrestins in regulating 5-HT<sub>2A</sub>R pharmacodynamics and the signaling responses to both serotonin and a psychedelic hallucinogen.

# Gain Modulation by Mouse Prefrontal Cortex Diminishes Fentanyl-Induced Respiratory Depression

Daniel P. Woods,<sup>1</sup> Ryan S. Herzog,<sup>2</sup> Qiwei W. Sun,<sup>3</sup> Zachary T. Glovak,<sup>4</sup> Helen A. Baghdoyan,<sup>2</sup> and Ralph Lydic<sup>5</sup>

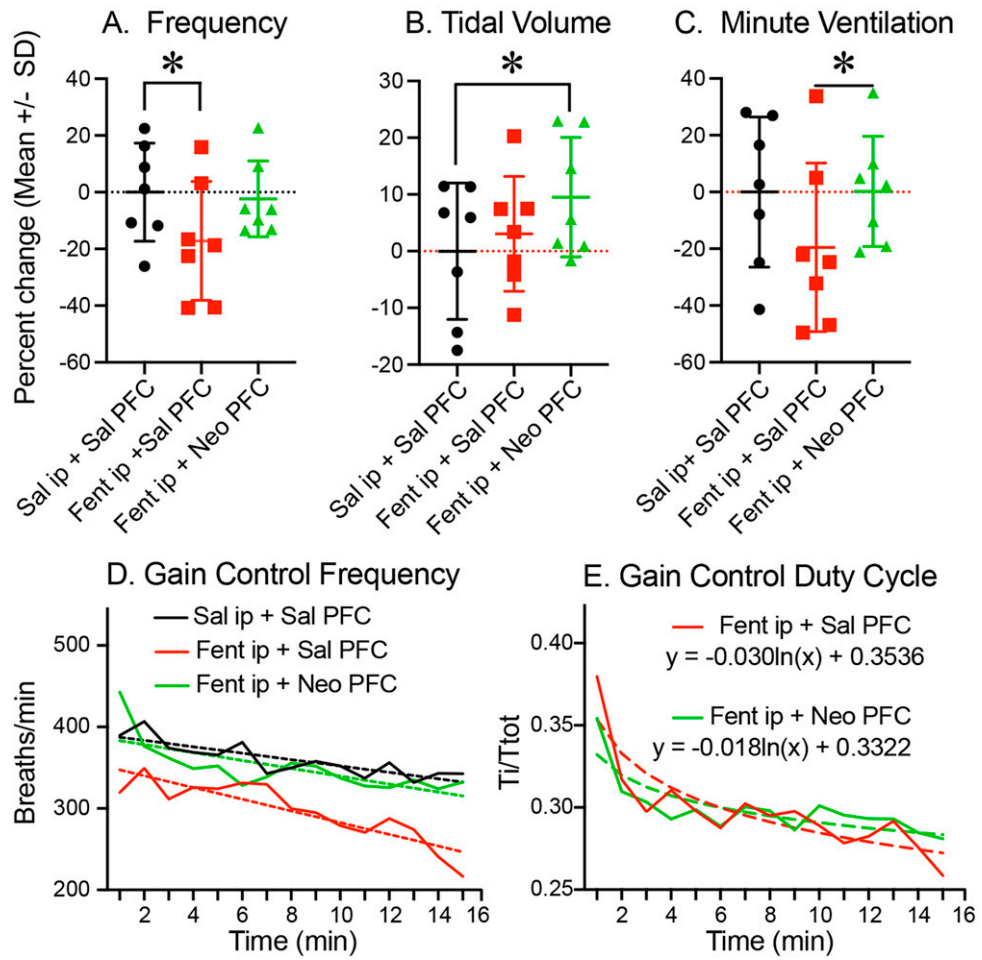
<sup>1</sup>University of Tennessee Knoxville; <sup>2</sup>Univ of Tennessee; <sup>3</sup>Yale Medical School; <sup>4</sup>Seattle Children's Hospital; and <sup>5</sup>University of Tennessee

Abstract ID 53000

Poster Board 139

Breathing is generated by pontomedullary brain stem nuclei and modulated by limbic and cortical nuclei. Recent data show that neostigmine delivered into the prefrontal cortex (PFC) significantly modulates breathing of intact, behaving C57BL/6J (B6) mice (10.1016/j.resp.2022.103924). Although the PFC contains no respiratory neurons, it projects to brain stem neurons that regulate arousal and breathing. This study is evaluating the hypothesis that PFC neostigmine enhances gain modulation of breathing. Gain modulation is the process by which the responsiveness of a neural circuit or neuron is altered by activity of other neurons. These studies were approved by University of Tennessee IACUC and adhered to the ARRIVE guidelines. Mice ( $n = 7$ ) were implanted with a 26-gauge guide cannula aimed at the medial PFC (histology pending). A week after surgical recovery, whole body plethysmography was used to measure breathing during wakefulness after three treatment conditions: 1) Intraperitoneal (ip) administration of saline (control) plus PFC microinjection of saline (black), 2) ip fentanyl (0.1 mg/kg) plus PFC saline (red), and 3) ip fentanyl (0.1 mg/kg) plus PFC neostigmine (0.016 nmol/50 nL) (green). As anticipated, fentanyl decreased respiratory frequency (Fig. 1A). PFC neostigmine caused an increase in tidal volume (Fig. 1B). PFC neostigmine also significantly ( $*P < 0.05$ ) diminished the depression in minute ventilation caused by fentanyl (Fig. 1C). These results were then quantified using a previous pharmacological model of gain modulation (10.1016/s1569-9048(02)00042-3). Gain was expressed as  $F_o = (1 + F_{tonic}k)F_i$ . In this equation,  $F_i$  indicates pre- and  $F_o$  post-neostigmine measures of breathing,  $F_{tonic}$  represents baseline respiratory frequency, and ( $k$ ) is a unitless multiplicative modulation coefficient. Fig. 1D shows time-dependent differences in respiratory frequency among three injection conditions via linear regression analysis. Minute 1 indicates recording onset after PFC injection. Trendline slopes (dashed lines) for frequency were used to determine treatment condition-dependent  $k$  values for condition 1 (-3.9), condition 2 (-7.2), and condition 3 (-4.8). Fig. 1E shows similar analyses applied to measures of respiratory duty cycle (inspiratory duration divided by duration of inspiration + expiration) considered to reflect respiratory effort. Fig. 1E shows that duty cycle was modulated logarithmically with multiplicative coefficient  $k = -0.030$  when the PFC was injected with saline and  $k = -0.018$  when the PFC was injected with neostigmine. This inverse exponential slope change reveals a 60% relative scalar increase in duty cycle due to PFC neostigmine administration.  $R^2$  values show a high percent of variance in duty cycle modulation accounted for by treatment conditions 2 (77%) and 3 (68%). These results support the interpretation that PFC neostigmine administration influences breathing, in part, by enhancing the gain of PFC input to brain stem nuclei that regulate breathing (10.1152/jn.00017.2021).

Support: The University of Tennessee





# Ethanol Effects on Synaptic Transmission: Implications for Motor Learning and Memory

Grace Nelson,<sup>1</sup> Armando Salinas,<sup>2</sup> Charles Levy,<sup>2</sup> and Logan Slade<sup>2</sup>

<sup>1</sup>Kansas State Univ; and <sup>2</sup>LSU Health Shreveport

**Abstract ID 18444**

**Poster Board 140**

Alcohol is one of the most widely used and abused drugs in the United States, with the National Survey on Drug Use and Health reporting that alcohol misuse costs the country 249 billion dollars a year. The majority of these costs are attributed to binge drinking, which 25.8% of surveyed adult participants had recently participated in. Given its widespread abuse, discerning the specific consequences of alcohol ingestion helps to better quantify its effects on society. One of alcohol's well-known effects is its inhibition of coordination and motor learning during intoxication. The exact mechanism of how alcohol affects motor learning is unknown but is likely linked to the inhibition of excitatory signaling, particularly in the striatum, a brain region essential for coordinated movement. To further investigate this effect, excitatory field potentials were taken from the striatum of acutely prepared brain slices. We first determined that the field potentials were AMPA mediated via the application of DNQX, an AMPA receptor antagonist. Upon application of DNQX, field potentials were extinguished. Other slices were treated with ethanol to examine its effects on synaptic transmission. Differing concentrations of ethanol were used for comparison. Ethanol-treated slices demonstrated dose-dependent inhibition of transmission. Ongoing efforts will determine how ethanol-mediated inhibition of synaptic transmission affects synaptic plasticity, the molecular substrate of motor learning and memory.

# Metabotropic glutamate receptor 3 activation modulates thalamic inputs to the nucleus accumbens and rescues schizophrenia-like physiological and behavioral deficits

Shalini Dogra,<sup>1</sup> and P. Jeffrey Conn<sup>1</sup>

<sup>1</sup>Vanderbilt Univ

Abstract ID 19574

Poster Board 141

Accumulating evidence suggests that some symptoms of schizophrenia are associated with dysregulated excitatory neurotransmission in the central nervous system (CNS), and recent clinical trials have revealed beneficial effects of nucleus accumbens (NAc) deep brain stimulation in schizophrenia patients. One exciting target that regulates the excitatory transmission in the CNS is metabotropic glutamate receptor 3 (mGlu<sub>3</sub>) and polymorphisms in *GRM3* (the gene encoding the mGlu<sub>3</sub> receptor) are associated with an increased likelihood of schizophrenia diagnosis. But the mechanisms by which *GRM3* modulates brain circuits involved in schizophrenia are not clear. Interestingly, using newly developed highly selective negative allosteric modulators of mGlu<sub>3</sub> receptor, we provide an evidence that mGlu<sub>3</sub> receptor activation induces robust depression of excitatory neurotransmission in the NAc. Therefore, we propose a hypothesis that mGlu<sub>3</sub> receptor activation can ameliorate schizophrenia-like glutamatergic abnormalities and behavioral deficits, in part, through actions on specific glutamatergic inputs within the NAc. To test this hypothesis, we performed a series of electrophysiological and behavioral studies using a combination of genetically modified mice, optogenetic approaches, and novel pharmacological tools in male and female c57BL6j mice treated with saline or phencyclidine (PCP, 10 mg/kg; s.c., 7 day treatment followed by 7-day washout). Using *ex vivo* whole-cell patch-clamp electrophysiology, we showed that treatment with PCP enhanced the frequency of excitatory postsynaptic currents onto D1 medium spiny neurons (MSNs), but not onto D2 MSNs in the NAc shell indicating increased glutamatergic signaling in the PCP-treated mice. Interestingly, these effects of PCP were normalized by bath application of mGlu<sub>2/3</sub> receptor agonist, LY379268 (100 nM). To evaluate the specific glutamatergic projections affected by PCP, we injected adeno-associated virus expressing Channelrhodopsin (ChR2) into medial thalamus (mThal), or basolateral amygdala, or ventral hippocampus. Our slice optogenetics experiments revealed that PCP treatment specifically enhanced transmission from thalamic inputs to the D1 MSNs of the NAc (Thal-D1 NAc shell). Excitingly, treatment with LY379268 blocked the PCP-induced changes in excitatory transmission at Thal-D1 NAc shell synapse and the effects of LY379268 were blocked by mGlu<sub>3</sub> receptor specific negative allosteric modulator (VU650786; 30 mg/kg; *i.p.*). These studies suggest that activation of mGlu<sub>3</sub> receptors can rescue PCP-induced abnormalities in the glutamatergic signaling the NAc of mice modeling schizophrenia-like pathophysiology. We also found that activation of mGlu<sub>3</sub> receptors or chemogenetic silencing of Thal-NAc projections rescued the sociability deficits (a behavior relevant for negative symptoms of schizophrenia) in PCP-treated mice. Collectively, these data provide a novel insight into potential mechanisms by which activation of mGlu<sub>3</sub> receptors can rescue schizophrenia-like pathophysiology and suggest that targeting these receptors could provide a viable approach for developing new therapeutics for treating schizophrenia.

# Characterization of Novel Tryptamines' Anxiolytic and Anti-Inflammatory Effects in Relation to their Psychoactive Effects

Catharine Carfagno,<sup>1</sup> M. F. Vest,<sup>2</sup> Kevin Murnane,<sup>3</sup> Kariann Lamon,<sup>2</sup> and Bo J. Wood<sup>2</sup>

<sup>1</sup>Louisiana State Univ-Shreveport; <sup>2</sup>Louisiana state university shreveport; and <sup>3</sup>Louisiana State Univ Health Sciences Center - Shreveport

Abstract ID 19236

Poster Board 142

Psychedelics are a class of drugs characterized by their psychoactive properties through primary action of the serotonin system, specifically the serotonin 2A receptor (5-HT<sub>2A</sub>R). Recent clinical research has shown efficacy for treatment-resistant depression, end-of-life anxiety, and substance use disorders. There are two main classes of psychedelics, phenethylamines and tryptamines, that have slightly different affinities for the various 5-HT receptors, and therefore display slightly different effects. The purpose of the current research is to distinguish the anti-inflammatory, anxiolytic, and psychoactive effects of an established phenethylamine, DOI, and three novel tryptamines, compound 1, 2, and 3, that are structural analogs of psilocybin. To evaluate the anti-inflammatory effects of these compounds, RAW macrophages were exposed to lipopolysaccharide (LPS) and treated with a range of concentrations of each psychedelic. After 24 hours the supernatant was evaluated for NO<sub>x</sub> levels (Griess assay) and TNF- $\alpha$  (Elisa). To investigate the potential role of the 5-HT<sub>2A</sub>R in the anti-inflammatory response, the same assays were run using the 5-HT<sub>2A</sub>R antagonist, M100907. Differences in psychoactive effects were established by the Head Twitch Response (HTR). Differences in anxiolytic properties were established using the elevated zero maze (EZM) with acute and chronic administration of psychedelics, evaluating the role of downregulation of the 5-HT<sub>2A</sub>R on anxiety. The results suggest that DOI produces the most robust anti-inflammatory response in both NO<sub>x</sub> and TNF- $\alpha$  assays of all four compounds, while compound 2 showed the most robust anti-inflammatory response out of the three novel tryptamines. In vivo DOI displayed the most robust HTR while also demonstrating robust anxiolytic effects. Of the three tryptamines, compound 1 & 3 had the most robust HTR and anxiolytic response while compound 2 had the inverse. These results suggest that the magnitude of the anxiolytic response relies on the magnitude of the psychoactive effects, but further studies are needed to determine this.

# Role and Regulation of BNST GluN2D-containing NMDARs in a Continuous Access Ethanol Task

Marie A. Doyle,<sup>1</sup> Megan E. Altemus,<sup>1</sup> Gregory J. Salimando,<sup>1</sup> Justin K. Badt,<sup>1</sup> Michelle N. Bedenbaugh,<sup>1</sup> Anika S. Park,<sup>1</sup> Danielle N. Adank,<sup>1</sup> Richard B. Simerly,<sup>1</sup> and Danny G. Winder<sup>1</sup>

<sup>1</sup>Vanderbilt University

Abstract ID 16515

Poster Board 143

Alcohol use disorder (AUD) is a chronic, relapsing disease, highly comorbid with anxiety and depression. These states of negative affect experienced during withdrawal are hypothesized to drive alcohol seeking and relapse behavior. The bed nucleus of the stria terminalis (BNST) is a brain region responsible for the integration of negative affect and alcohol-related behaviors. Within this region, NMDARs are a major target of ethanol, capable of modulating ethanol-induced synaptic plasticity and transmission. Specifically, GluN2D subunit-containing NMDARs have recently emerged as a target of interest. Using a continuous access two-bottle choice mouse model of chronic ethanol intake followed by forced abstinence (CDFA), we demonstrated that dorsolateral BNST (dlBNST) GluN2D mRNA (*grin2d*) expression is decreased during periods of forced abstinence in female mice. However, the role of dlBNST GluN2D expression in the context of negative affect- and ethanol-related behaviors remains unknown. To answer this question, open field, elevated zero maze, and forced swim tasks were used to measure anxiety- and depressive-like behaviors in FlxGluN2D mice with bilateral intra-dlBNST injections of Cre recombinase- or GFP-expressing virus, and we found that conditional knockdown of dlBNST GluN2D in female mice does not affect these assays of negative affect. However, in a continuous access ethanol two-bottle choice task, preliminary data suggest that female mice lacking dlBNST GluN2D display decreased ethanol intake and preference across the six-week paradigm as well as during an assessment of aversion-resistant ethanol intake, using increasing concentrations of quinine in the ethanol. These data propose a role for dlBNST GluN2D expression in mediating ethanol-related behaviors. However, as the BNST is a highly heterogeneous region, it remains unknown if neuronal subpopulations drive changes in expression. Notably, BNST neurons expressing corticotropin-releasing factor (BNST<sup>CRF</sup>) have been implicated in both negative affect and stress-induced alcohol-seeking behaviors and exhibit a significant level of *grin2d* labeling. Current studies investigate counts of *grin2d* puncta in BNST<sup>CRF</sup> cells following protracted withdrawal in the CDFa paradigm. In addition to regulation of subunit expression by forced abstinence, parallel studies investigate the role of GluN2D-containing NMDARs in modifying ethanol sensitivity of BNST<sup>CRF</sup> neurons. Together, given the restricted CNS expression of this subunit, exploration of GluN2D control of ethanol circuit actions may lead to a novel therapeutic target to consider in AUD treatment.

MAD was supported by T32s (T32 NS007491 and T32 MH065215) and an F32 from NIAAA (MAD, AA029592). The research was supported by an R37 from NIAAA (DGW, AA019455).

# Uncovering the release dynamics of enkephalins following acute stress and opioid exposure

Marwa Mikati,<sup>1</sup> Petra Erdmann-Gilmore,<sup>2</sup> Rose Connors,<sup>2</sup> Sineadh Conway,<sup>2</sup> Justin Woods,<sup>2</sup> Robert Sprung,<sup>2</sup> Reid Townsend,<sup>2</sup> and Ream Al-Hasani<sup>3</sup>

<sup>1</sup>Washington Univ in St. Louis School of Medicine; <sup>2</sup>Washington University in St. Louis; and <sup>3</sup>Washington Univ in St Louis

**Abstract ID 28409**

**Poster Board 144**

Opioid peptides are key modulators of natural reward and threat processing. It has been shown in the rodent models that enkephalinergic neurons in the nucleus accumbens (NAc) shell may play a modulatory role in stressful situations specifically as anti-stress agents, for example after exposure to predator odor and in the vulnerability to social defeat stress. However, it has been challenging to identify the specific roles of Met- and Leu-enkephalins due to the difficulty in their detection. Here, we show that enkephalinergic neurons in the ventral NAc shell are activated following exposure to predator odor and experimenter handling using fiber photometry. To get a deeper insight into enkephalin release dynamics we couple microdialysis and nano-liquid chromatography/mass spectrometry (nLC-MS) to allow the detection of endogenous Leu- and Met-enkephalin *in vivo*. With this approach, we can detect and distinguish between Met- and Leu- Enkephalin release in awake behaving mice. We show that enkephalins are released following exposure to predator or handling stress. We also demonstrate the dynamics of Met- and Leu-Enkephalin release as well as how they correlate to one another in the ventral NAc shell. Due to the success of this method in measuring peptide dynamics following stress, we wanted to expand our investigation into how exogenous opioids alter the release of enkephalins. Since enkephalins activate the mu and delta opioid receptors, we chose to focus on fentanyl, a mu-opioid receptor agonist that has high abuse liability. Using fiber photometry, we show that fentanyl silences enkephalinergic neurons. We also show that fentanyl attenuates the release of enkephalins using nLC-MS, and that this effect is reversible by artificially evoking neuronal activity in the ventral NAc shell, thereby driving peptide release. Our findings suggest that exogenous opioids alter endogenous opioid peptide release dynamics which may alter reward circuitry. Overall, we show distinct roles for Met- and Leu-enkephalins following acute stressors and exogenous opioid administration, allowing us for the first time to correlate real-time behavioral manipulations with opioid peptide release.

Support/Funding Information: •Cognitive, Computational, and Systems Neuroscience Fellowship (WUSTL Med) •Al-Hasani R21DA048650 •Al-Hasani R00DA038725

# TRPA1 Receptor Expressed by the Edinger-Westphal Nucleus (EWcp) is Involved in Stress Adaptation

Dr. Erika Pinter, Viktória Kormos,<sup>1</sup> Dóra Zelena,<sup>1</sup> János Konkoly,<sup>1</sup> Balázs Gaszner,<sup>1</sup> and Miklós Kecskés<sup>1</sup>

<sup>1</sup>University of Pecs

Abstract ID 16795

Poster Board 145

The Transient Receptor Potential Ankyrin 1 (TRPA1) non-selective cation channel expressed by the primary sensory neurons mediates pain sensation and neurogenic inflammation. It is also expressed in the brain, but little is known about its specific physiological and pathological roles. Our earlier studies using TRPA1 knockout mice revealed that the genetic lack of the receptor inhibits the neurodegeneration in murine models of multiple sclerosis, Alzheimer disease and aging. TRPA1 mRNA expression was previously shown in mouse and human EWcp urocortin1 (UCN1) positive neurons and reacted to chronic variable stress. In the present study we hypothesized that TRPA1 receptor mediated events may participate in posttraumatic stress disorder (PTSD).

A selective, covalent TRPA1 agonist, JT010 was used on acute EWcp slices of C57BL/6J male mice for electrophysiological measurements. Male *Trpa1* WT and KO mice were used in a PTSD model, single prolonged stress (SPS). Two weeks later the behavioral tests, forced swim test (FST) and restraint were performed. The *Trpa1* and *Ucn1* mRNA expression and the UCN1 peptide content were visualized by RNAscope in situ hybridization combined with immunohistochemistry in EWcp.

JT010 activated TRPA1 channels of urocortinergic cells in acute slices proving its functionality. *Trpa1* KO animals showed significantly reduced immobility after SPS compared to WT mice, both in the FST and restraint stress. Expression of *Trpa1* mRNA was significantly decreased in EWcp of WT animals in response to SPS. Higher basal *Ucn1* mRNA expression was observed in the EWcp of KO animals, that was not affected by SPS exposure. Urocortinergic cells of WT animals responded to SPS with strong increase of UCN1 peptide content compared to the controls, however, this was not noticeable in the KO animals. We proved the presence of functional TRPA1 receptors on EWcp/UCN1 neurons.

Since the decreased *Trpa1* mRNA expression in the SPS model of PTSD associated with increased neuronal UCN1 peptide content we presume that TRPA1 participates in the regulation of stress adaptation and plays role in the development of PTSD.

TKP2021-EGA-16 support provided from the National Research, Development and Innovation Fund of Hungary, financed under the EGA 16 funding scheme. RRF-2.3.1-21-2022-00015 support provided by the European Union. Hungarian Brain Research Program 3.0 (NAP 3.0) 2022-2025.

# Diurnal Variation in Acetylcholine Modulation of Dopamine Dynamics Following Chronic Cocaine Intake

Melody Iacino,<sup>1</sup> and Mark Ferris<sup>2</sup>

<sup>1</sup>Wake Forest Univ; and <sup>2</sup>Wake Forest Sch of Med

Abstract ID 14368

Poster Board 146

In 2020, approximately 5.2 million Americans reported using cocaine with 1.3 million of those individuals meeting the criteria for Cocaine Use Disorder (CUD). Despite the increasing need, there are no FDA-approved treatments for CUD. One variable that is often overlooked in CUD research is cocaine-induced disruption of circadian (24-hour) and diurnal (night/day) rhythms, which may reinforce the cycle of continued drug use. The mesolimbic dopamine (DA) system is an important mediator of motivated and reward-associated behaviors that are maladapted in CUD. Striatal cholinergic interneurons (CINs) modulate mesolimbic DA release via nicotinic acetylcholine receptors (nAChRs) on DA terminals, thus providing a critical mechanistic target for diurnal disruptions of DA release. Though the effect of cocaine on DA signaling has been extensively studied at single time points, cocaine-induced disruptions of DA release across time-of-day as well as their mechanisms have not been investigated. Here, we utilized fast scan cyclic voltammetry in a rat model of cocaine self-administration following various access schedules [(short continuous access (ShA), long continuous access (LgA), or intermittent access (IntA)] to examine diurnal variations in DA release based on local modulators and cocaine history. We hypothesize that the pattern of cocaine intake will differentially affect diurnal rhythms of DA release and elucidate a potential mechanism for CIN modulation of diurnal rhythms in nucleus accumbens core (NAc) DA signaling. We found that IntA increased DA release midway through the dark cycle compared to ShA or LgA at the same time point. Additionally, antagonizing  $\beta_2$  nAChRs revealed greater ACh contribution in IntA and LgA conditions. Further investigation into the role of diurnal rhythms underlying DA release and CIN modulation in CUD will highlight novel neurochemical targets and outline *when* during the day that individuals might be more susceptible to cocaine relapse.

Support/Funding Information: R01 DA052460; K99/R00 DA311791; P50 DA006634; P50 AA026117; Peter F. McManus Charitable Trust

# Concomitant Mild Traumatic Brain and Burn Injury Elicits a Unique Gene Expression Profile within the Brain

Christopher O'Connell,<sup>1</sup> Evan Reeder,<sup>1</sup> Ryan Brown,<sup>1</sup> Matthew Robson,<sup>1</sup> and Jason Gardner<sup>2</sup>

<sup>1</sup>University of Cincinnati James L Winkle College of Pharmacy; and <sup>2</sup>University of Cincinnati College of Medicine

Abstract ID 20802

Poster Board 165

Mild Traumatic Brain Injuries (mTBI) and Burn Injuries (BI) present monumental public health burdens that have been independently linked to long term nervous system-related morbidity and negative patient outcomes. Military service members in active combat theaters are among the most at risk for sustaining concomitant mTBI and BI, in most cases due to detonation of improvised explosive devices. Previous studies have provided evidence that mTBI and BI independently induce inflammation, through the induction of innate inflammatory cascades, however the concomitant effects of simultaneous mTBI and BI on early post-injury molecular processes, gene expression alterations, neuronal signaling within the brain and ultimately outcomes are currently unknown. This lack of data, coupled with an overt lack of studies conducted in human subjects, has left large gaps in the knowledge required and the available capability to successfully treat complicated polytrauma cases involving mTBI and BI. We hypothesize that concomitant mTBI and BI act in exaggerating early neuroinflammatory responses within the CNS, an effect that leads to worse long-term health and behavioral outcomes, when compared to mTBI or BI alone. To test this hypothesis, adult, wild type C57Bl/6J mice were subjected to a single, blast induced mTBI and full thickness BI (mTBI/BI), a single, blast induced mTBI alone, a full thickness BI alone, or sham treatment followed by RNA-sequencing of ipsilateral brain parenchyma conducted at six hours post-injury (hpi). Bioinformatic analysis of the RNA-sequencing results and subsequent pathway, overrepresentation, and protein-protein interaction analyses identified a large array of unique gene expression profiles specific to the combined mTBI/BI condition and identified gene-sets relevant to neuroinflammation, extracellular matrix organization and vascular integrity that are highly enriched within the data. Notably, significant, exclusive, upregulation of genes canonically expressed during mesenchymal-epithelial transition occurred within the brains of mTBI/BI subjects. Cumulatively, these data suggest that concomitant mTBI/BI results in a profound, combinatorial exacerbation of modality-specific disruptions in the blood-brain-barrier and neuro-vascular stability and may provide viable mechanism derived targets for pharmacotherapeutic development. Studies contained herein provide the first characterization of a synergistic effect of concomitant mTBI and BI on early transcription and inflammation within the CNS and afford insight into the specific molecular events involved in observed synergism. Further, our studies are anticipated to identify potential targets for the development of pharmacotherapeutics to improve neurologic outcomes in those subjected to polytrauma.

Support/Funding Information: Department of Defense CDMRP Award #W81XWH2210849.



# Delta Opioid Receptor Activation Blocks Allodynia in a Model of PACAP-induced Headache

Elizaveta Mangutov,<sup>1</sup> Isaac Dripps,<sup>2</sup> Kendra Siegersma,<sup>2</sup> Rebecca Bocian,<sup>2</sup> Sarah Asif,<sup>2</sup> Wiktor Witkowski,<sup>2</sup> and Amynah Pradhan<sup>1</sup>

<sup>1</sup>Washington University in St. Louis; and <sup>2</sup>University of Illinois at Chicago

Abstract ID 16687

Poster Board 166

**Background and purpose:** Pituitary adenylate cyclase activating polypeptide (PACAP) is a known human migraine trigger and antibodies against the peptide and its receptor (PAC1) are being tested for the treatment of migraine. We have previously identified the delta opioid receptor (DOR) as a novel therapeutic target for headache disorders. However, it is still unclear how DORs regulate migraine-associated symptoms. One of the aims of this study was to develop a mouse model of PACAP-induced headache, and to determine the effect of DOR agonist in this model. A further goal was to investigate co-expression of DOR with PACAP and PAC1 receptor.

**Experimental approach:** To develop the PACAP model in mice, the effect of increasing doses of acute and chronic PACAP was assessed on mechanical responses measured by manual von Frey hair stimulation of the periorbital region. We also tested established headache therapies in this model, including the acute treatment sumatriptan, and a calcitonin gene related peptide (CGRP) antagonist, as well as the DOR agonist, SNC80. Expression of DOR and the PACAPergic system was determined using in situ hybridization to identify co-expression of PACAP, its receptor PAC1, and DOR mRNA. The somatosensory cortex, hippocampus, trigeminal nucleus caudalis, and trigeminal ganglia was analyzed.

**Key results:** PACAP caused acute and chronic dose-dependent cephalic allodynia. Our maximum dose of PACAP was blocked by sumatriptan and DOR agonist SNC80, but not olcegepant. Correspondingly, in a model of chronic CGRP-induced allodynia, the PAC1 antagonist M65 was ineffective. Chronic administration of SNC80 blocked the development of chronic PACAP-induced allodynia, suggesting its promise as a preventive treatment. There was some coexpression of PACAP and DOR in all brain regions but it was relatively low. In contrast, there was very high coexpression (>75%) of PAC1 and DOR in the somatosensory cortex, hippocampus, and trigeminal nucleus caudalis.

**Conclusion and implications:** We have developed a novel model of PACAP-induced allodynia in mice, which is blocked by known migraine therapeutics. Its mechanism of action is separate to CGRP-related responses. DOR agonists were effective in this model and DOR was highly co-expressed with the PACAPergic system. Future studies will determine the functional relationship between DOR and PACAP-PAC1.

Support/Funding Information:

NIH-NIDA R01DA040688

T32 training grant T32AA026577 from NIH-NIAAA.

# Antisense oligonucleotides targeting microRNA binding sites in the GRN mRNA increase progranulin translation: potential therapeutic strategy for frontotemporal dementia

Spencer Jones, Geetika Aggarwal,<sup>1</sup> Yousri Benchaar,<sup>2</sup> Jasmine Bélanger,<sup>2</sup> Myriam Sévigny,<sup>2</sup> Denise Smith,<sup>1</sup> Michael Niehoff,<sup>1</sup> Ian Mitchell de Vera,<sup>1</sup> Terri Petkau,<sup>3</sup> Blair Leavitt,<sup>3</sup> Karen Ling,<sup>4</sup> Paymaan Jafar-Nejad,<sup>4</sup> Frank Rigo,<sup>4</sup> John Morley,<sup>1</sup> and Andrew Nguyen<sup>1</sup>

<sup>1</sup>Saint Louis University; <sup>2</sup>Laval University; <sup>3</sup>University of British Columbia; and <sup>4</sup>Ionis Pharmaceuticals

Abstract ID 24673

Poster Board 167

Heterozygous GRN mutations cause frontotemporal dementia (FTD) due to haploinsufficiency of progranulin. The microRNA, miR-29b, negatively regulates progranulin protein levels. Antisense oligonucleotides (ASOs) are emerging as a promising therapeutic modality for neurological diseases, but strategies for increasing target protein levels are limited. Here, we tested if ASOs can increase progranulin levels by sterically blocking the miR-29b binding site in the 3' UTR of the human GRN mRNA. We found 16 ASOs that increase progranulin protein levels in a dose-dependent manner in neuroglioma cells. A subset of these ASOs also increased progranulin levels in iPSC-derived neurons and in a humanized GRN mouse model. While the ASOs did not increase GRN mRNA levels, polysome profiling experiments revealed that the ASOs increase progranulin translation. Consistent with this, ASO treatment increased levels of newly synthesized progranulin protein. In FRET-based assays, the ASOs effectively competed miR-29b from binding to the GRN 3' UTR RNA. Together, these studies establish the mechanism of action is that these ASOs displace miR-29b from its binding site and thereby de-repress translation, resulting in increased synthesis of progranulin protein. Our results demonstrate that ASOs can be used to effectively increase target protein levels by partially blocking miR binding sites; this ASO strategy may be therapeutically feasible for progranulin-deficient FTD as well as other conditions of haploinsufficiency.

# A Novel Clinical-stage Small Molecule Targeting the ‘Dark Side’ of Opioid Addiction

Rhianne Scicluna,<sup>1</sup> Tylah Ms. Doolan,<sup>2</sup> Erin Lynch,<sup>2</sup> Nicholas Everett,<sup>2</sup> and Michael Bowen<sup>3</sup>

<sup>1</sup>The Univ of Sydney; <sup>2</sup>The University of Sydney; and <sup>3</sup>The Univeristy of Sydney

**Abstract ID 26262**

**Poster Board 168**

The ‘dark side’ of addiction refers to the temporary relief drug-taking provides from the persistent negative emotional state that emerges as a person develops a substance use disorder. In the context of opioid use disorder, negative affect and craving during acute and protracted withdrawal present major barriers to recovery. There is only one non-opioid treatment for acute opioid withdrawal, associated with limited efficacy and serious side effects, and no treatment for protracted withdrawal. KNX100 is a novel, clinical stage small molecule being developed for the treatment of opioid use disorder. KNX100 has an undisclosed pharmacological mechanism of action but has been shown to act in the nucleus accumbens shell to reduce neuronal hyperexcitability and signalling in the pDYN/DYN/KOR receptor pathway during opioid withdrawal in mice, demonstrating highly disease-relevant neural and molecular actions. Moreover, KNX100 reduced the negative affective symptoms of acute naloxone-precipitated oxycodone withdrawal and inhibited the acquisition of withdrawal-induced conditioned-place aversion in mice. Here, the effects of KNX100 on irritability during spontaneous oxycodone withdrawal and cue-induced reinstatement of oxycodone-seeking during abstinence were examined in rats. Prior to oxycodone self-administration, rats were tested for their baseline irritability (aggressive and defensive behaviours on the bottle brush test) and were assessed for baseline somatic symptoms (wet dog shakes). Rats were then trained to self-administer oxycodone for 15h/day for 44-48 days through a surgically implanted intravenous catheter. Each infusion was accompanied by a light+tone. To elicit spontaneous withdrawal, rats underwent 24-hour without a self-administration session. Spontaneous withdrawal symptoms (irritability and somatic symptoms) were assessed during two counterbalanced withdrawal sessions, once treated with vehicle and once with KNX100. For assessment of cue-induced reinstatement, rats underwent a 15-day protracted abstinence period and were tested for reinstatement on day 2 and 15, with rats receiving KNX100 or vehicle prior to reinstatement testing on day 15. KNX100 treatment significantly reduced withdrawal-induced irritability-like behaviour, but not wet dog shakes, in male and female rats. KNX100 markedly inhibited cue-induced reinstatement of drug seeking 15 days into abstinence. These data further indicate KNX100 may alleviate the negative psychological state that emerges during withdrawal and persists into abstinence that contributes to drug craving and relapse and suggest KNX100 may be a viable therapeutic for alleviating the negative affective aspects of acute withdrawal and promoting abstinence.

This work was funded by Kinosis Therapeutics Pty Ltd under a Master Research Services Agreement with the University of Sydney.

# Multiplexed pharmacological calcium imaging reveals distinct GPCR-mediated response profiles of locus coeruleus neurons

Chao-Cheng Kuo,<sup>1</sup> and Jordan McCall<sup>1</sup>

<sup>1</sup>Washington University in St. Louis

Abstract ID 23754

Poster Board 169

The noradrenergic neurons in locus coeruleus (LC) are the main source of norepinephrine (NE) for the central nervous system. Potential modular organization of the LC could provide functional differentiation during distinct behaviors. This organization would suggest that different LC modules should act differentially according to the behavioral state. The LC is enriched in many G-protein coupled receptors (GPCRs) that are likely endogenously activated during behavior to regulate activity among LC modules, but the detailed mechanisms remain unclear. Here we perform GCaMP8f calcium imaging of LC-NE neurons in acute brain slices in concert with a large-scale pharmacological scan of multiple GPCR agonists. We use modified image processing algorithms, CNMF-E and CASCADE, for automatic region of interest (ROI) extraction and machine learning-based spike deconvolution, respectively. Approximately five hours of simultaneous cell-attached electrophysiological recordings and calcium imaging are used to train the spike prediction model. This model can deconvolute individual LC-NE action potentials with firing rates below 4 Hz with almost 100% accuracy. Deconvolution accuracy stays about 85% while cells are firing at 5 Hz. In addition, the significantly lower rate (<2%) of prediction errors further improves the practicality of our model. To determine the pharmacological profile among different population of LC-NE neurons, we inject cholera toxin subunit b conjugated to CF dye-594 (CTB-594), a widely used retrograde neuronal tracer, into either medial prefrontal cortex (mPFC), basolateral amygdala (BLA), or spinal cord. This enables reconstruction of tissue morphology and fine alignment between GCaMP8f and CTB-594 signals by post-hoc immunohistochemistry to register extracted ROIs into either CTB-594-positive or CTB-594-negative classifications. Our results show pharmacological profiles among populations of LC-NE neurons which send their axons to either mPFC, BLA or spinal cord. Interestingly, the activation of some GPCRs brings a differential effect among distinct cell populations. For example, the application of adenosine, a natural ligand of adenosine receptors, causes a stronger excitation in non-mPFC projecting population compared to those mPFC projecting cells. In this study, we introduce a novel, highly efficient method of slice calcium imaging to investigate pharmacological profile in acute brain slices. This approach could be adopted in other cell types to define responses to activation of any receptor capable of altering downstream intracellular calcium fluctuations. Here our findings imply that the release of endogenous GPCR ligands could enable modularity in LC-NE system to drive functional differentiation during distinct behaviors. Moreover, the pharmacological profiles we revealed could also bring a possibility of subpopulation-selective pharmacological modulation by cocktails containing multiple compounds.

# Fatty Acid Binding Protein 5 Modulates Brain Endocannabinoid Tone and Retrograde Signaling in the Striatum and Hippocampus

Mohammad Fauzan,<sup>1</sup> Saida Oubraim,<sup>2</sup> Mei Yu,<sup>3</sup> Sherrye T. Glaser,<sup>4</sup> Martin Kaczocha,<sup>3</sup> and Samir Haj-Dahmane<sup>5</sup>

<sup>1</sup>Stony Brook Univ; <sup>2</sup>University at Buffalo; <sup>3</sup>Stony Brook University; <sup>4</sup>Kingsborough Community College; and <sup>5</sup>Univ at Buffalo

Abstract ID 25321

Poster Board 170

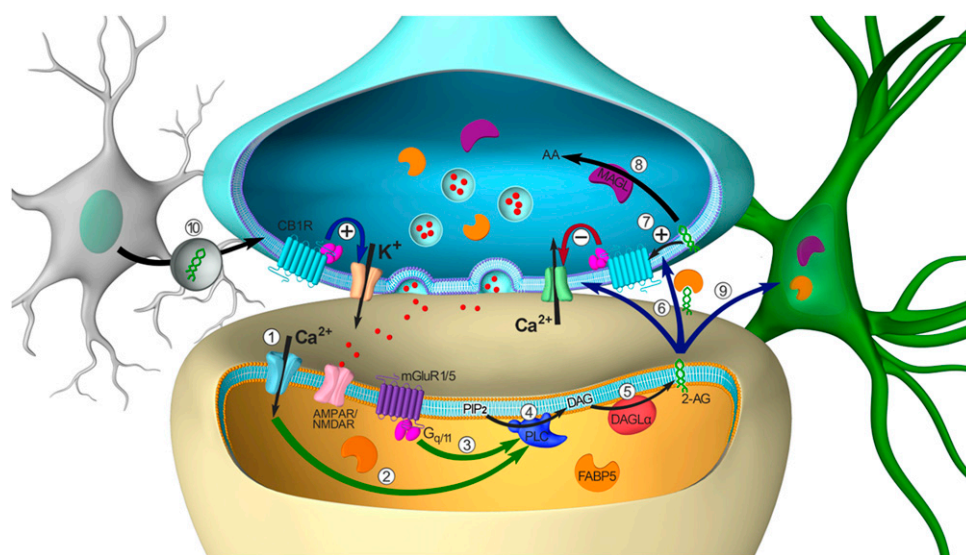
**Background:** The endocannabinoids (eCB) anandamide (AEA) and 2-arachidonoylglycerol (2-AG) are lipid neurotransmitters that regulate an array of physiological functions including pain, stress homeostasis, and reward. Fatty acid binding protein 5 (FABP5) is a key modulator of intracellular eCB transport and inactivation. Recent evidence suggests that FABP5 controls synaptic 2-AG signaling at excitatory synapses in the dorsal raphe nucleus. However, it is currently not known whether this function extends to other brain areas, has a cell specific role, or aids in synaptic transport.

**Methods:** Striatal and hippocampal FABP5 in the mouse brain were visualized using immunohistochemistry with antibody specific labeling for neurons, astrocytes, and FABP5 from microtome brain sections. hSynapsin and GFAP driven AAVs were injected into the hippocampus in FABP5 KO mice, via stereotaxic surgery. Brain regions were micro dissected from wild-type and FABP5 KO mice for qPCR and mass spectrophotometry analysis of various proteins and lipids in the eCB pathway. Lastly, electrophysiology was performed to examine the effects of FABP5 inhibition and re-expression upon eCB signaling.

**Results:** FABP5 deletion elevates AEA levels in the striatum, PFC, midbrain, & thalamus, as well as midbrain 2-AG levels. The expression of eCB biosynthetic and catabolic enzymes was largely unaltered in these regions, although minor sex and region-specific changes in the expression of 2-AG catabolic enzymes were observed in female FABP5 KO mice. Robust FABP5 expression was observed in the striatum. Re-expression of FABP5 in astrocytes rescues eCB signaling better in FABP5 KO mice, as compared to re-expression in neurons. Deletion of FABP5 impaired tonic 2-AG and AEA signaling at striatal GABA synapses of MSNs and blunted phasic 2-AG mediated short-term synaptic plasticity without altering CB1R expression or function

**Conclusion:** Collectively, these results support the role of FABP5 as a key regulator of eCB signaling at excitatory and inhibitory synapses in the brain.

Funded by NIH (Grant. no. MH122461 & DA035949)



Model of synaptic eCB transport by FABP5 with role specificity to brain regions and cell types. FABP5 is secreted into synapses by glial cells. Activation of postsynaptic neurons leads to the biosynthesis of the eCB 2-AG, which is transported across the synapse by FABP5 and subsequently activates presynaptic CB1 receptors. This attenuates release of neurotransmitters. Alternatively, 2-AG gets catabolized by MAGL in the pre-synaptic neuron (Kaczocha and Haj-Dahmane, 2021).

# Antidepressants and Dopamine Levels Induced by Substance Misuse Regulate Inflammation and HIV in Myeloid Cells

Stephanie Matt,<sup>1</sup> Rachel Nolan,<sup>1</sup> Breana Channer,<sup>2</sup> Joanna Canagarajah,<sup>2</sup> Samyuktha Manikandan,<sup>1</sup> Yash Agarwal,<sup>1</sup> Krisna Mompho,<sup>1</sup> Oluwatofunmi Oteju,<sup>1</sup> Kaitlyn Runner,<sup>1</sup> Alexis Brantly,<sup>1</sup> Emily Nickoloff-Bybel,<sup>1</sup> and Peter Gaskill<sup>1</sup>

<sup>1</sup>Drexel Univ College of Medicine; and <sup>2</sup>Drexel Univ

Abstract ID 17802

Poster Board 271

Neurological complications of HIV infection (neuroHIV) remain prevalent even in individuals on antiretroviral therapy (ART). Inflammation is central to the development of HIV neuropathogenesis and myeloid cell populations such as microglia and macrophages are the primary targets for HIV in the central nervous system (CNS) that also drive this inflammation. In addition, inflammation can be exacerbated by substance use disorders (SUDs), which are highly comorbid with HIV infection and worsen clinical outcomes. Despite distinct mechanisms of action, all substances of misuse increase CNS dopamine, suggesting that dopamine is a common mechanism by which addictive drugs potentiate neuroHIV. Our data show that dopamine increases IL-1 $\beta$  production in microglia and macrophages, and that the levels of different myeloid dopamine receptors drive changes in IL-1 $\beta$ . We also provide evidence that dopamine can synergistically increase IL-1 $\beta$  and alter inflammasome components in the presence of HIV infection.

In addition to SUDs, depression is another increasingly common complication that can substantively affect HIV disease progression. Although myeloid cells are primary HIV targets and their activation has been shown to mediate depression-associated inflammation, myeloid inflammatory links between neuroHIV, depression, and the drugs used to treat them are not well understood. Many antidepressants such as bupropion (Wellbutrin) and sertraline (Zoloft) act on receptors and associated proteins that alter monoaminergic neurotransmission, and monoamine receptor activity on immune cells can influence inflammatory signaling. Therefore, we hypothesize that antidepressants could promote myeloid activation, influencing the progression of HIV infection. Using high-throughput, high-content cellular analysis, our studies indicate that physiologically relevant concentrations of antidepressants with distinct mechanisms of action including bupropion, sertraline, venlafaxine, trazodone, and mirtazapine differentially modulate NF- $\kappa$ B nuclear translocation in primary human macrophages. NF- $\kappa$ B activation is associated with increased HIV transcription, potentially providing a favorable environment for HIV replication, and we also show that some antidepressants can increase HIV replication and may weaken ART efficacy. Ongoing studies are examining the impact of antidepressants in the presence of HIV/ART and combination antidepressant treatment on modulating monoamine and inflammatory signaling. Due to the high prevalence of both SUDs and the increasing use of other monoamine-modulating therapeutics like those used for depression, a detailed understanding of dopamine and antidepressant-mediated changes in inflammation and viral dynamics will be critical for identifying efficacious therapies to mitigate treatment-resistant depression, suboptimal ART efficacy, and persistent cognitive symptoms in people living with HIV.

We would like to thank everyone in the Gaskill Lab for their support with this work. This project was supported by grants from the National Institutes of Drug Abuse, R01DA052859, R01DA057337, R01DA039005, and R21DA049227 (PJG), the W.W. Smith Charitable Trust Foundation Grant A2003 (PJG), the Brody Family Medical Trust Fund (SMM), the Cotswold Foundation Fellowship (SMM), and the Department of Pharmacology and Physiology at Drexel University College of Medicine.

# Is Ketamine a rapid acting antidepressant in juvenile rats?

David Middlemas,<sup>1</sup> Brianna Stanley,<sup>1</sup> and Alexis Klinner<sup>1</sup>

<sup>1</sup>AT Still University

**Abstract ID 26856**

**Poster Board 272**

Ketamine and Esketamine are rapid-acting antidepressants. Esketamine is approved for the treatment of treatment resistant depression in adults, but not for the treatment of adolescent depression. Further investigation of Ketamine's rapid acting antidepressant effect in juvenile rodent models are warranted. This study tests whether Ketamine is a rapid acting antidepressant in juvenile rats. The dose-response and time course of ketamine's antidepressant-like effects in juvenile rats was assessed using the Tail Suspension Test and the Forced Swim Test. Juvenile rats were injected once with varying doses of Ketamine and tested at 2, 24, and 72 hours. Our findings indicate that ketamine has antidepressant-like action at the 2 hours and 24 hours at doses from 40 to 60 mg/ml. No significant change in antidepressant-like activity was observed at 72 hours for any dose. In future studies, we will delineate whether there are pharmacokinetic differences in rapid antidepressant and dissociative effects of ketamine in juvenile rats.

This work was funded by a Warner Fermaturo grant #501-501 and 560-760 awarded by AT Still University, Kirksville, MO, USA and a Biomedical Sciences Graduate Program Award #851-059 awarded by Kirksville College of Osteopathic Medicine, AT Still University, Kirksville, MO, USA.

# Impact of Maternal Overnutrition in Central Nervous System Circuits that Regulate Feeding

Sai Shilpa Kommaraju,<sup>1</sup> Ming Gao,<sup>1</sup> Elaine Cabrales,<sup>1</sup> Chelsea Faber,<sup>1</sup> and Zaman Mirzadeh<sup>1</sup>

<sup>1</sup>Barrow Neurological Institute

Abstract ID 26676

Poster Board 273

Maternal obesity influences susceptibility of offspring to Obesity and Type-II diabetes (T2D). Animal studies of maternal overnutrition have demonstrated alterations in the circuits driving metabolic homeostasis. More specifically, hypothalamic circuits that regulate energy expenditure and food intake. Previously, we reported on a subset of neurons (Agouti-related Peptide-AgRP/Neuropeptide Y – NPY), that are essential to metabolic homeostasis in the mediobasal hypothalamic arcuate nucleus (ARC). These neurons are uniquely enmeshed by perineuronal net (PNN)- like structures, which coincides with the critical-period (before postnatal day 28 or P28) closure in this area. To study the consequence and impact of maternal overnutrition on AgRP neurons, we subjected nursing dams to either high fat diet (maternal High Fat diet- mHFD) or normal chow diet (maternal Normal Chow diet- mNCD) during their lactation period. We found ARC PNNs formed earlier (premature) and a leptin surge observed sooner and at higher levels in pups subjected to mHFD compared to mNCD. Through indirect calorimetry studies we showed that mHFD exposed mice reduced their food intake but no change in their energy expenditure was observed. These results suggest that mHFD may influence the inhibitory synaptic transmission of AgRP/NPY neurons. In slice electrophysiology studies probing the synaptic transmission and neuronal excitability of AgRP/NPY neurons, we found that AgRP/NPY neurons in mHFD mice at P21 displayed a lower firing rate, and higher amplitude of spontaneous and miniature inhibitory postsynaptic currents (sIPSC and mIPSC), but no effect on spontaneous and miniature excitatory postsynaptic currents (sEPSC and mEPSC). Overall, we infer that maternal overnutrition altered the activity of AgRP neurons, thereby modifying hypothalamic arcuate circuits, leading to metabolic dysfunction. Future work regarding the impact of early maturation of PNNs as a result of maternal overnutrition during postnatal development are being explored.

This project is funded by DOD grant.



# Effects of Cannabinoid CB<sub>1</sub> agonists on extracellular levels of dopamine in the nucleus accumbens shell of male mice

Evan Smith,<sup>1</sup> Dalal Alkhelb,<sup>1</sup> Christos Iliopoulos-Tsoutsouvas,<sup>1</sup> Spyros Nikas,<sup>1</sup> Rajeev Desai,<sup>2</sup> and Alexandros Makriyannis<sup>1</sup>

<sup>1</sup>Center for Drug Discovery, Northeastern Univ; and <sup>2</sup>McLean Hospital/Harvard Medical School

**Abstract ID 25747**

**Poster Board 274**

The use of cannabis has led to a dramatic increase in cannabinoid (CB) abuse during the past decade, presenting a major public health challenge. Despite significant research there is a lack of full understanding on how cannabinoids that vary in efficacy and affinity at CB<sub>1</sub> receptors alter key neurotransmitters like dopamine (DA) in reward-related brain regions to impact behavior. Mounting evidence suggests that actions at CB<sub>1</sub> receptors modulate DA within the nucleus accumbens shell—a key brain region involved in the abuse-related neurobiological actions of most drugs of abuse. Here, we utilized *in vivo* microdialysis and liquid chromatography-mass spectrometry (LC-MS/MS) to quantify changes in DA within the nucleus accumbens shell of mice administered (*i.p.*) the synthetic full CB<sub>1</sub> agonist AM8936 (0.01-1.0 mg/kg), the synthetic partial CB<sub>1</sub> agonist AM11101 (0.1-3.2 mg/kg), or the phytocannabinoid partial CB<sub>1</sub> agonist  $\Delta^9$ -THC (0.1-3.2 mg/kg). At lower doses, AM8936, AM11101, and  $\Delta^9$ -THC administration increased extracellular levels of DA within the nucleus accumbens shell reaching a maximum of 134%, 140%, and 161% of baseline levels after 0.032, 0.32, and 0.32 mg/kg, respectively. AM11101 and  $\Delta^9$ -THC produced peak increases in DA at 20 minutes post-injection, which remained elevated for approximately 2 hours and then returned toward baseline levels. Conversely, the peak increases in DA after administration of 0.032 mg/kg AM8936 was observed at about 140 minutes post-injection, and DA remained elevated until the end of the experiment (5 hours post injection). At 10-fold higher doses, AM8936, AM11101, and  $\Delta^9$ -THC decreased DA to 62%, 72%, and 62% of baseline levels after 0.32, 3.2, and 3.2 mg/kg, respectively; for all drugs these decreases persisted until the end of the experiment. The calculated area under the curve for a 100-minute window centered around the peak DA increase for each agonist showed that low doses of AM8936 (0.01-0.032 mg/kg) AM11101 (0.1-0.32 mg/kg) and  $\Delta^9$ -THC (0.1-0.32 mg/kg) increased DA levels, whereas higher doses of AM8936 (0.1-1.0 mg/kg) AM11101 (1.0-3.2 mg/kg) and  $\Delta^9$ -THC (1.0-3.2 mg/kg) decreased extracellular levels of DA. Together, these results demonstrate that while AM11101 and  $\Delta^9$ -THC DA effects have quicker onset and shorter duration compared to AM8936, CB<sub>1</sub> partial and full agonists have similar, biphasic effects on DA within the nucleus accumbens shell.

# Dopaminergic Immunomodulation May Amplify Macrophage Inflammation in the Context of HIV Infection

Breana Channer,<sup>1</sup> Dayna Robinson,<sup>1</sup> Oluwatofunmi Oteju,<sup>1</sup> Stephanie Matt,<sup>1</sup> and Peter Gaskill<sup>1</sup>

<sup>1</sup>*Drexel University College of Medicine*

**Abstract ID 20808**

**Poster Board 275**

Human immunodeficiency virus (HIV) is a global pandemic that results in dysregulated immune function in both the periphery and central nervous system (CNS). In the CNS, this immune dysregulation can lead to chronic neuroinflammation and increase the susceptibility of individuals to comorbid inflammatory diseases. Although antiretroviral therapy (ART) can stop HIV replication, it does not fully suppress HIV-associated neuroinflammation, which is largely sustained by myeloid cells such as macrophages and microglia. The prevalence of comorbid disease is increased in individuals with substance use disorders (SUD), which are disproportionately greater in people living with HIV (PLWH) and are a major risk factor for neurological disease. This suggests SUD could exacerbate myeloid associated neuroinflammation, although the mechanisms by which this occurs are not clear. However, all addictive substances increase extracellular dopamine, and we have shown that dopamine dysregulates immune activity and promotes inflammation in human macrophages.

Therefore, we hypothesize that stimulant induced dopamine concentrations will have more robust inflammatory effects in HIV-infected human macrophages than uninfected cells. To test this, primary human macrophages, and human, induced pluripotent stem cell derived macrophages were infected or mock-infected with HIV and treated with dopamine. Changes in inflammatory profiles were assessed by measuring NF- $\kappa$ B nuclear translocation, Nod-like receptor (NLR) inflammasome activity and cytokine production using high content imaging, Western blotting and AlphaLISA analysis. Dopamine significantly increased the production of IL-6 and IL-1 $\beta$ , and these effects were exacerbated in HIV infected cells. Our data suggest that dopamine may be acting through dopaminergic and adrenergic receptors, and receptor activation drives NF- $\kappa$ B activity, alterations in inflammasome transcripts and Akt phosphorylation, suggesting multiple pathways by which dopamine could influence macrophage function. Understanding the immunological effects of dopamine could usher initiatives to develop or repurpose dopaminergic therapeutics as adjuvant ART therapy as well as treatment for other neuroinflammatory diseases.

We would like to thank everyone in the Gaskill lab for their support with this work. This project was funded by the National Institutes of Drug Abuse (R01DA052859, R01DA057337, R21DA049227 to PJG), Cotswald Foundation Fellowship (SMM) and T32 (MH079785 to BC).

# Prenatal Stress Alters Transcription of NMDA Receptors in the Frontal Cortex and Hippocampus

Tristram Buck,<sup>1</sup> and Monsheel Sodhi<sup>1</sup>

<sup>1</sup>Loyola University Chicago

Abstract ID 25885

Poster Board 276

Prenatal stress results in abnormal neurodevelopment, including deficits in social behavior. Social behavioral deficits are also symptoms of several psychiatric disorders. Previous studies have shown that the N-methyl-D-aspartate (NMDA)-type glutamate receptor is abnormally regulated after prenatal stress, which could be functionally significant because glutamate neurons transmit the majority of excitatory signals within the corticolimbic system, and are required for cognitive behaviors including social interaction. We have tested the hypothesis that prenatal stress modifies the expression of the NMDA-type glutamate receptor (NMDAR) subunits and that this modification triggers deficits in social behavior. We performed the prenatal stress exposure by restraining pregnant mice for 45 minutes three times daily during the 2<sup>nd</sup> and 3<sup>rd</sup> weeks of gestation. When male offspring reached adulthood (P70), we administered i.p. injections of haloperidol (1 mg/kg), clozapine (5 mg/kg), or saline twice daily for 5 days. Subsequently, we measured the social behavior (SI) of each mouse using the three-chamber social interaction test and we measured locomotor activity in an open field. After testing, mice were euthanized and their brains were dissected and stored at -80 °C. We extracted RNA from the hippocampus and frontal cortex of each mouse and used qPCR to measure the transcription of the NMDAR subunits, GluN1, GluN2A, GluN2B, and GluN3A in each region. Vehicle-treated prenatally stressed (PRS-Veh) mice exhibited a reduction in SI compared to vehicle-treated non-stressed controls (NS-Veh) ( $p < 0.01$ ). PRS mice treated with clozapine (PRS-Clz) did not display SI deficits relative to NS-Veh mice. PRS mice treated with haloperidol (PRS-Hal) showed similar social behavior to PRS-Veh mice. Neither PRS nor medication reduced locomotor activity. Our results showed that PRS and antipsychotic treatment were associated with altered transcription of NMDAR subunits in both the hippocampus and frontal cortex. In the frontal cortex, transcription of NMDAR subunits was positively correlated with social interaction (GRIN1, GRIN2A, GRIN2B,  $R = 0.42-0.45$ ,  $p < 0.01$ ) and negatively correlated with locomotor activity (GRIN1, GRIN2A, GRIN2B, GRIN3A,  $R = -0.35 - -0.46$   $p < 0.05$ ). In the hippocampus, transcription of NMDAR subunits was negatively correlated with social interaction (GRIN2A,  $R = -0.33$  and  $p < 0.05$ , GRIN2B,  $R = -0.47$  and  $p < 0.01$ ). These data indicate abnormal transcription of NMDAR subunits in the hippocampus and frontal cortex occurs after exposure to PRS in mice, and that this dysregulation correlates with deficits in social interaction behavior. The subunit composition of the NMDAR affects the receptor's affinity for glutamate, kinetics, single-channel conductance, its sensitivity to magnesium blockade, calcium permeability, pH sensitivity, and drug sensitivity. Clearly altering the transcription levels of different NMDAR subunits would have a significant impact on the excitatory transmission in the corticolimbic circuit. In conclusion, these results suggest that altered transcription of NMDAR subunits may be a novel molecular pathway by which prenatal stress leads to life-long deficits in social behavior, which are a feature of several psychiatric disorders including autism, schizophrenia, and social anxiety disorder.

# Spinal Aha1 inhibition improves morphine therapy for pain management

Wei Lei,<sup>1</sup> Valentin M. Kliebe,<sup>2</sup> Katherin Gabriel,<sup>3</sup> Christopher S. Campbell,<sup>3</sup> John M. Streicher,<sup>3</sup> Brian S.J. Blagg,<sup>4</sup> and Lauren Ball<sup>5</sup>

<sup>1</sup>Manchester University College of Pharmacy, Natural and Health Sciences; <sup>2</sup>Med Univ of South Carolina; <sup>3</sup>Univ of Arizona;

<sup>4</sup>University of Notre Dame; and <sup>5</sup>Medical Univ of South Carolina

**Abstract ID 27432**

**Poster Board 277**

Opioids, such as morphine, are effective at treating moderate or severe pain. However, the side effects, such as the risk of addiction, respiratory depression, and tolerance, limit the use of opioids for pain relief. Therefore, developing an approach to improve opioid analgesia is highly demanded. Our previous studies have shown that heat shock protein 90 (Hsp90) inhibition can enhance morphine antinociception and reduce tolerance. However, universal Hsp90 inhibition causes severe side events, such as liver toxicity. Therefore, a more selective approach that targets the Hsp90 mechanism is desired for improving opioid therapy. Most recently, we found that inhibiting the activator of Hsp90 ATPase homolog 1 (Aha1), a co-chaperone of Hsp90, showed a similar beneficial effect as that from Hsp90 universal inhibitor, however, the mechanism is unknown. In this study, we sought to explore the effect of the Aha1 inhibitor, KU-177, on morphine analgesia and side effects in the tail-flick pain model. Male and female CD-1 mice were treated with 0.1 nmol KU-177 intrathecally. After recovering for 24 hours, mice were treated with morphine subcutaneously, and the tail-flick was performed to determine the thermal threshold. We also tested the impact of KU-177 on morphine tolerance. In addition, proteomics and phosphoproteomics were performed to determine the potential mechanisms by which Aha1 inhibition regulates opioid signaling in the spinal cord. We found that treatment of KU-177 enhanced the morphine analgesia but reduced the morphine tolerance. Our quantitative proteomics studies demonstrate that inhibiting Aha1 by KU-177 upregulates or downregulates 114 proteins in the spinal cord. Several proteins altered by the treatment of KU-177, such as Gpr37 and Rab5c, are associated with the function of G-protein coupled receptors (i.e., opioid receptors). These findings provide evidence that developing Aha1 inhibitors as adjunct pain medications may improve the efficacy and safety of opioid pain management.

This study was funded by South Carolina IDeA Networks of Biomedical Research Excellence Developmental Research Project Program (NIGMS 2P20GM103499).

# Nucleus Accumbens Single Nucleus RNA Sequencing Identifies Cell Subtype-Specific Maladaptations after Prolonged Spared Nerve Injury

Randal Serafini,<sup>1</sup> Aarthi Ramakrishnan,<sup>2</sup> Molly Estill,<sup>2</sup> Vishwendra Patel,<sup>2</sup> John Fullard,<sup>2</sup> Robert Blitzer,<sup>2</sup> Schahram Akbarian,<sup>2</sup> Panos Roussos,<sup>2</sup> Venetia Zachariou,<sup>2</sup> and Li Shen<sup>2</sup>

<sup>1</sup>*Icahn School of Medicine at Mt Sinai*; and <sup>2</sup>*Icahn School of Medicine at Mount Sinai*

Abstract ID 14714

Poster Board 278

Chronic pain is a highly prevalent condition that is difficult to treat because of molecular maladaptations that occur at several levels of the nociceptive circuitry. Currently prescribed therapeutics show limited efficacy and cause substantial side effects after prolonged use. Several regions of the mesocorticolimbic circuit, such as the medial prefrontal cortex, nucleus accumbens (NAc), and ventral tegmental area play a key role in the maintenance of sensory hypersensitivity, pain perception, and chronic pain-associated affective comorbidities, such as depression and addiction vulnerability. Here, we performed single nucleus RNA sequencing (snRNA-seq) on NAc tissue from adult male DBA/2J mice three months after spared nerve injury (SNI). Cell clusters were annotated against a publicly-available single cell RNA-seq NAc dataset by Avey et al. ("Single-Cell RNA-Seq Uncovers a Robust Transcriptional Response to Morphine by Glia"). Bioinformatic analysis identified the following cell clusters with >100 differentially-expressed genes (DEGs; p-nominal < 0.05): Astrocyte\_1, Astrocyte\_2, Endothelial, Microglia, Neuron\_1, Neuron\_2, Neuron\_3, NSC\_1, OL\_2, OL\_3, OL\_4, OPC, VLMC. When considering neuronal clusters, we identified Ingenuity Pathway Analysis (IPA)-generated Top 15 Canonical Pathways that were directionally conserved across at least two of the three clusters, including impaired "Synaptogenesis Signaling" and "Synaptic Long-term Potentiation". Unpublished work from our group also suggests that NAc medium spiny neurons become hyperexcitable at 1.5-2 months post-SNI. A key transcription factor that negatively regulates excitatory synaptic plasticity in adult neurons is MEF2C. At three months post-SNI we observed a decrease in *Drd1+/-Drd2+/-Mef2c+* co-expressing neurons. Taken together, we hypothesized that overexpression of *Mef2c* in NAc neurons with an AAV8-hSyn-*Mef2c-Gfp* viral vector would modulate these maladaptations. Indeed, virus-mediated overexpression of *Mef2c* in NAc MSNs reversed SNI-induced hyperexcitability and reduced miniature excitatory post-synaptic current amplitudes relative to SNI-*Gfp* animals. IPA analysis of NAc bulk RNA-seq comparing SNI-*Mef2c* and SNI-*Gfp* conditions (2 months post-SNI) predicted an upregulation of the "Synaptic Long-term Potentiation" pathway. These *Mef2c* overexpression-induced counteractions of SNI maladaptations were associated with a reversal of SNI-induced punctate mechanical hypersensitivity and anxiety-like behavior in the marble burying assay. Future directions include assessing circuit-level effects on neurotransmitter levels upon *Mef2c* overexpression in the NAc by use of voltammetry. Overall, this work emphasizes that prolonged peripheral nerve injury induces transcriptional changes in a majority of cell subtypes in the NAc, and cell subtype-specific therapeutic strategies can alleviate behavioral manifestations of SNI.

**Support/Funding Information:** R01 NS086444 (VZ), R01 NS086444-07S1 (VZ & RAS), ASRA Graduate Student Award (RAS)

# The Ventral Tegmental Area and Medial Habenula Differentially Control Reward, Reinforcement, and Intake of Nicotine

Brandon Henderson,<sup>1</sup> Nathan A. Olszewski,<sup>2</sup> and Samuel J. Tetteh-Quarshie<sup>2</sup>

<sup>1</sup>Marshall Univ Joan C. Edwards School of Medicine; and <sup>2</sup>Joan C Edwards School of Medicine at Marshall University

**Abstract ID 20494**

**Poster Board 335**

For years, prior research has established the scientific premise that the ventral tegmental area (VTA) and the medial habenula (MHb) mediate aspects of nicotine reward, reinforcement, aversion, and intake. To examine how both the VTA and MHb are involved in nicotine reinforcement-related behavior, we used genetically modified mice (males and females) that express fluorescent nAChRs in a mouse model of vapor self-administration. Mice were trained to acquire self-administration on a FR1 and FR3 schedule using nicotine with or without flavors (menthol or green apple). Green apple and menthol enhanced nicotine vapor self-administration in both male and female mice but in a sex-dependent manner (males at 6 mg/mL nicotine and females at 60 mg/mL nicotine). Following vapor self-administration, brain slices containing the VTA and MHb were prepared to examine self-administration-induced changes in baseline firing and intrinsic excitability. To examine intrinsic excitability, we used a current-step protocol to determine rheobase (current necessary to elicit an action potential) and maximum spikes during current steps. We correlated FR3 active nose pokes (mean of 5 FR3 sessions) to electrophysiological measures to examine how neuronal excitability in the VTA and MHb was linked to reinforcement-related behaviors. We observed that intrinsic excitability of VTA dopamine neurons did not correlate to FR3 active nose pokes; but it did correlate to active and inactive nose poke distinction. We observed that the intrinsic excitability of medial MHb neurons correlated inversely to FR3 active nose pokes (high FR3 nose pokes, lower intrinsic excitability). Correlations were consistent between unflavored or flavored nicotine assignments; but menthol and green apple exhibited greater changes in intrinsic excitability of neurons. These data suggest that the MHb may be critical for the magnitude of nicotine intake while VTA dopamine neurons may regulate the learning-related behavior associated with nicotine intake.

This work was supported by funding from the National Institutes of Health (DA050717 and DA046335 to BJH).

# Alkoxy Chain Length Governs the *In Vitro* and *In Vivo* Potency of 2-Benzylbenzimidazole Opioids Implicated in Human Overdose Deaths

Michael Baumann,<sup>1</sup> Donna Walther,<sup>1</sup> Marthe M. Vandeputte,<sup>2</sup> Meng-Hua M. Tsai,<sup>1</sup> Li Chen,<sup>1</sup> Christophe P. Stove,<sup>2</sup> and Grant Glatfelter<sup>1</sup>

<sup>1</sup>NIDA Intramural Research Program; and <sup>2</sup>University of Ghent

Abstract ID 17915

Poster Board 336

Illicitly manufactured fentanyl plays a major role in the current opioid crisis, but non-fentanyl mu-opioid receptor (MOR) agonists are emerging in drug markets worldwide. Synthetic 2-benzylbenzimidazole opioids, also known as “nitazenes”, are examples of non-fentanyl MOR agonists linked to human fatalities. Here, we characterized the pharmacological effects of nitazene analogs that differ in their alkoxy chain length, including metonitazene (O-methyl), etonitazene (O-ethyl), protonitazene (O-propyl), isotonitazene (O-isopropyl), and butonitazene (O-butyl). We first examined the effects of the analogs in assays measuring MOR binding in rat brain membranes and forskolin-stimulated cAMP accumulation in MOR-transfected human embryonic kidney cells. Next, we examined the antinociceptive, locomotor, and body temperature effects of subcutaneously (s.c.) administered drugs in male C57Bl/6J mice fitted with surgically-implanted temperature transponders. Radioligand binding data demonstrated that all nitazenes display selective affinity for MOR ( $K_i$  range=3.6-53.1 nM) versus delta- and kappa-opioid sites. Increasing alkoxy chain length from methyl to ethyl, propyl, and butyl led to a stepwise decrease in MOR affinity. All of the nitazenes were agonists for MOR-mediated inhibition of cAMP accumulation ( $EC_{50}$  range=0.03-0.50 nM), with the O-ethyl compound being the most potent. In the cAMP assay, the O-ethyl, O-isopropyl, and O-propyl analogs were more potent than fentanyl ( $EC_{50}$ =0.10 nM) and much more potent than morphine ( $EC_{50}$ =1.22 nM). The mouse experiments revealed that nitazenes induce dose-dependent antinociception ( $ED_{50}$  range=0.01-1.4 mg/kg), locomotor stimulation, and hypothermia, with etonitazene having the highest potency. In the hot plate assay, the O-ethyl, O-isopropyl, and O-propyl analogs were more potent than fentanyl ( $ED_{50}$ =0.15 mg/kg), and much more potent than morphine ( $ED_{50}$ =10.19 mg/kg). Correlation analysis showed that *in vivo*  $ED_{50}$  potencies were positively correlated with the *in vitro*  $EC_{50}$  potencies for inhibition of cAMP but not  $K_i$  affinities at MOR. Overall, our findings reveal that alkoxy chain length governs potency of nitazenes *in vitro* and *in vivo*, whereby the ethyl and isopropyl chain lengths provide optimal pharmacological activity at MOR. Three of the tested nitazenes are more potent than fentanyl, and all are much more potent than morphine. Thus, nitazenes may pose serious risks to human users who are unknowingly exposed to the compounds.

Funded by the Intramural Research Program of NIDA, NIH

# Coronaridine Congeners Attenuate Fentanyl Seeking During Prolonged Abstinence, Possibly Through Inhibiting Dopamine Release in the Nucleus Accumbens

Jacob D. Layne,<sup>1</sup> Mason J. Hochstetler,<sup>1</sup> Brandon M. Curry,<sup>1</sup> Benjamin M. Williams,<sup>2</sup> Christina A. Small,<sup>2</sup> Scott C. Steffensen,<sup>2</sup> Hugo R. Arias,<sup>1</sup> and Craig T. Werner<sup>1</sup>

<sup>1</sup>Oklahoma State University Center for Health Sciences; and <sup>2</sup>Brigham Young University

Abstract ID 54260

Poster Board 337

**Background:** The prevalence of opioid use disorder (OUD) has reached epidemic proportions with a record-breaking number of overdose deaths. Over 70% of the record-breaking number of overdose deaths are caused by synthetic opioids, including fentanyl. Fentanyl is commonly administered intravenously or by inhalation (smoking/vaping), which results in rapid drug bioavailability in the brain. There is a current need to identify a novel pharmacologic therapy to treat OUD, and there is increasing evidence to support the use of novel compounds referred to as coronaridine congeners to treat OUD and other psychiatric illnesses. In preclinical models, coronaridine congeners have been shown to decrease self-administration of drugs of abuse and induce antidepressant and anxiolytic effects. Here we used a preclinical fentanyl vapor self-administration model and fast-scan cyclic voltammetry (FSCV) to study the anti-addictive effects of two coronaridine congeners, 18-methoxycoronaridine (18-MC) and catharanthine (Cath).

**Methods:** C57BL/6J mice were trained to self-administer vaporized fentanyl (5 mg/mL) or vehicle in air-tight operant chambers. Mice self-administered vapor for 1 hour per day for 10 days (sessions were conducted for 5 consecutive days, followed by 2 days off). Chambers were equipped with two nosepeaks, one active and one inactive. A successful response in the active nosepoke resulted in a vapor delivery that coincided with the presentation of a cue light, followed by a 1-minute timeout period. Mice learned to self-administer vapor with 3-second vapor deliveries for the first 3 days of training, which was then reduced to 1.5-second vapor deliveries the remaining 7 days. After training, mice were returned to their home cages for a forced abstinence period. Cue-induced drug seeking tests were conducted on abstinence days (AD) 20 and 25. During cue-induced seeking tests, successful responses in the active nosepoke resulted in presentation of the drug-associated cue, but no vapor was delivered (i.e. extinction conditions). Cue-induced drug seeking tests were conducted using a crossover design where half of subjects received coronaridine treatment (18-MC or Cath), while the other half received vehicle (ddH<sub>2</sub>O), on AD20. On AD25, subjects received the opposite treatment compared to AD20. Mice were injected (i.p.) with either vehicle or coronaridine treatment 1 hour before seeking tests. To examine the molecular mechanism of coronaridine congeners, FSCV was conducted on dopaminergic pre-synaptic terminals in the nucleus accumbens (NAc) neurons to measure dopamine (DA) release in the presence of 18-MC and Cath with or without nicotinic acetylcholine receptor antagonists.

**Results:** We found that both 18-MC and Cath significantly reduced fentanyl seeking during prolonged abstinence with no effect on mice that had previously self-administered vehicle. Furthermore, FSCV revealed that 18-MC and Cath significantly reduced DA release onto NAc neurons.

**Conclusion:** In this study, we report that both 18-MC and Cath decrease fentanyl seeking during prolonged abstinence. DA release is important for opioid-related behaviors, and we found that 18-MC and Cath reduce DA release in the NAc, a mechanism that may underlie the effect of coronaridine congeners on fentanyl seeking. Together, these results provide evidence that coronaridine congeners may be promising novel compounds for the pharmacotherapeutic treatment of OUD.



# Effects of Aripiprazole on Nicotine Withdrawal-Like Behaviors and Murine Neuregulin 3-ErbB4 Signaling

Emily Prantzas,<sup>1</sup> and Jill Turner<sup>1</sup>

<sup>1</sup>Univ of Kentucky

Abstract ID 29150

Poster Board 338

The World Health Organization estimates that 1.3 billion people worldwide are tobacco users and, without cessation support, only 4% of attempts to quit tobacco will succeed. Additionally, the NIH reports a 7.5-fold increase in rates of nicotine dependence among patients with schizophrenia compared to the general population. Both nicotine dependence and schizophrenia have been shown to have strong genetic influences, with similar variations in the gene for Neuregulin 3 (NRG3), a member of the EGF superfamily and the cognate ligand for ErbB4 receptors. Moreover, NRG3 protein and mRNA have been found to be highly enriched following chronic nicotine exposure and withdrawal. However, specific mechanisms underpinning NRG3's association with both increased schizophrenia risk and increased nicotine withdrawal symptomology are unknown.

Studies show conflicting evidence that 2<sup>nd</sup> and 3<sup>rd</sup> generation antipsychotic use may improve outcomes of substance use disorder. Aripiprazole is a common 3<sup>rd</sup> generation antipsychotic used to treat schizophrenia with multiple other indications. There is anecdotal evidence suggesting that aripiprazole may improve smoking cessation rates, though no studies have conclusively identified this drug as a smoking cessation therapy. The effect of aripiprazole on the neuregulin signaling pathway and related processes is also unknown.

The purpose of this experiment is to determine the efficacy of aripiprazole in ameliorating nicotine withdrawal behavioral phenotypes, with an overarching goal to characterize the expression patterns of NRG3-ErbB4 signaling within the PFC and identify the molecular alterations induced during chronic nicotine and withdrawal that may be used as novel drug targets for smoking cessation therapies. Animals treated chronically with nicotine and aripiprazole followed by spontaneous nicotine withdrawal were examined in the alternating Y-maze, social interaction test, and open field test for efficacy in reducing behavioral endophenotypes common to both nicotine withdrawal and schizophrenia in our model. Following behavioral testing, PFC tissues were analyzed to determine mRNA and protein expression of factors in the NRG3 signaling pathway. Our data suggest that chronic nicotine, 24h nicotine withdrawal, and aripiprazole treatment result in differential changes in mRNA expression associated with Neuregulin 3 and glutamatergic signaling in the mPFC, OFC, and hippocampus. These findings will provide insight into the underlying mechanisms linking the NRG3 signaling pathway and nicotine dependence and may provide a novel link between nicotine use and its highly co-morbid psychiatric disorder, schizophrenia. Findings from these highly translational studies may lead to novel therapeutic development for both nicotine dependence and schizophrenia.

This study was supported by NIH/NIDA grant DA044311 (JRT).

# Effect of Inhibition of Xenobiotic Transporter MRP5/ABCC5 on Neurite Elongation: Screening for MRP5 Inhibitors among Clinically Used Drugs

Takahiro Ishimoto,<sup>1</sup> Hirofumi Yagi,<sup>1</sup> Yusuke Masuo,<sup>1</sup> and Yukio Kato<sup>1</sup>

<sup>1</sup>Kanazawa University, Faculty of Pharmacy

Abstract ID 17323

Poster Board 339

**Aim:** We have previously reported that expression of multidrug resistance associated protein 5 (MRP5/ABCC5) in murine primary cortical neurons (PCNs) is much higher than other ABCC family transporters. However, its physiological function remains uncertain. We hypothesized that inhibition of MRP5 would promote neurite elongation because MRP5 efflux the second messengers such as cGMP and cAMP, which are important modulators of neurite elongation. The present study aimed to evaluate the effect of the knockdown of MRP5 on neurite outgrowth and to screen for MRP5 inhibitors among clinically used drugs acting in the central nervous system.

**Methods:** Protein expression of MRP5 in PCNs was examined by immunocytochemical analysis. To evaluate the effect of MRP5 knockdown on neurite elongation, a neuronal cell line Neuro2A was transfected with siRNA for *Mrp5* (siMrp5), followed by counting cells with neurites longer than the cell diameter. To check the efflux activity of MRP5 in Neuro2A, we used CMFDA, which is metabolized inside the cells to become a fluorescent substrate of MRP5; Neuro2A was incubated with CMFDA, and intracellular fluorescence intensity was measured.

**Results and Discussion:** Immunocytochemical analysis showed that MRP5 was expressed in the PCNs and Neuro2A, which are positive for the neuronal marker  $\beta$ III-tubulin. Transfection with siMrp5 in Neuro2A showed significantly lower mRNA expression of *Mrp5* compared to negative siRNA-treated cells. The siMrp5 transfection significantly increased the number of cells with longer neurites and mRNA expression of neurite marker *gap43* compared to negative siRNA transfection. The *Mrp5* knockdown increased the expression of cGMP-dependent protein kinase (PKG), whereas a PKG inhibitor KT5823 significantly suppressed the neurite elongation induced by the knockdown with a concomitant decrease in the expression of PKG. These results suggest that inhibition of MRP5 promotes neurite elongation by activating PKG. Furthermore, we performed the screening for MRP5 inhibitors among clinical drugs. Neuro2A transfected with siMrp5 showed a higher intensity of intracellular fluorescence of CMFDA metabolite during incubation with CMFDA compared to negative siRNA. In addition, a typical inhibitor for MRP5 zaprinast also increased the fluorescent intensity, confirming that the assay is useful to assess the efflux activity of MRP5. Midazolam, perampanel, and nizatrazepam remarkably increased the intracellular fluorescent intensity of the CMFDA metabolite. Exposure to midazolam or perampanel significantly promoted neurite elongation in PCNs. These drugs may thus potentially affect the neurite elongation by MRP5 inhibition and would be useful for the regulation of neurite outgrowth. Further studies are needed to elucidate the detailed mechanisms and to evaluate the possible involvement of clinically used MRP5 inhibitors in neurite elongation.

**Conclusion:** Inhibition of MRP5 promotes neurite elongation by activating PKG. Midazolam and perampanel have been found to be novel MRP5 inhibitors, which promote neurite elongation in PCNs.

# Deferiprone Decreases Labile Iron in Brain and Ameliorates Abnormal Emotional Behavior in Mice with Brain Iron Accumulation

Ruiying Cheng,<sup>1</sup> Yingfang Fan,<sup>2</sup> Rajitha Gadde,<sup>3</sup> Swati Betharia,<sup>3</sup> and Jonghan Kim<sup>1</sup>

<sup>1</sup>Univ of Massachusetts Lowell; <sup>2</sup>Massachusetts General Hospital; and <sup>3</sup>Massachusetts College of Pharmacy and Health Sciences

Abstract ID 22389

Poster Board 340

Iron is an essential nutrient for multiple biological functions, including oxygen transport, redox action, and DNA synthesis. However, excess iron in the brain is neurotoxic due to its ability to produce reactive oxygen species (ROS) and resultant oxidative stress, which can further increase the risk of neurodegeneration diseases such as Parkinson's Disease and Alzheimer's Disease. We have previously demonstrated that impulsivity and hyperactivity behavior of mice with brain iron accumulation were associated with increased labile iron, and not with total iron, in the brain, suggesting a causative relationship between labile iron-induced oxidative stress and abnormal emotional behavior. Deferiprone (DFP) is a commonly used oral iron chelator to remove excess iron from the body in patients with secondary iron overload, such as thalassemia and sickle cell disease. DFP is capable of transporting iron across cell membranes and across the blood-brain barrier, making it a potential clinical treatment for patients with neurodegeneration associated with brain iron accumulation. In particular, DFP has demonstrated the ability *ex vivo* to oxidize iron from its ferrous (toxic, labile) form to ferric (physiologic) form, thus removing toxic iron and preventing oxidative stress. However, the efficacy of DFP on *in vivo* labile iron chelation and affective disorder has not been tested. To examine the labile iron chelation potential of DFP, we first treated iron overloaded SH-SY5Y neuroblastoma cells with DFP and found that DFP decreased intracellular labile iron levels, as determined by Calcein-AM assay, as well as ROS production, as determined by DCF-DA fluorescence assay. We then evaluated if DFP reverses excess labile iron from the iron-loaded brain and ameliorates iron-induced oxidative stress using Hfe H67D mutant mice, a mouse model of brain iron accumulation. While oral gavage of DFP to H67D mice for 6 weeks showed significant decrease in systemic iron overload, as determined by liver non-heme iron, non-heme iron levels in the brain did not decrease. Notably, DFP treatment decreased labile iron in the cortex along with decreased oxidative stress, as determined by isoprostane levels. In addition, H67D mice showed increased impulsivity and hyperactivity and decreased anxiety-like behavior, as assessed by Elevated Plus Maze (EPM) task, which was corrected by DFP treatment. Taken together, our results provide a potential therapeutic option for psychiatric disorders that are associated with increased labile iron and oxidative stress.

# High-throughput, microplate reader detection of the ASP<sup>+</sup> fluorescent substrate to identify novel inhibitors of organic cation transporter-3

Rheaclare Fraser-Spears,<sup>1</sup> Ann Decker,<sup>2</sup> Bruce Blough,<sup>2</sup> and Lynette C. Daws<sup>3</sup>

<sup>1</sup>Univ of the Incarnate Word Feik School of Pharmacy; <sup>2</sup>RTI International; and <sup>3</sup>Univ of Texas Health Science Ctr

Abstract ID 54516

Poster Board 341

We optimized a high-throughput fluorescent-based assay to assess transporter activity by measuring uptake of the substrate, ASP<sup>+</sup> - 4-(4-(dimethylamino)styryl)-N-methylpyridinium. ASP<sup>+</sup> is the fluorescent derivative of the neurotoxin 1-methyl-4-phenylpyridinium MPP<sup>+</sup>, both of which have been used to study various transporter properties. The ASP<sup>+</sup> microplate method offers an easily teachable platform for microscale adaption to conduct high-throughput screens in 96-well plates. Our current work focuses on organic cation transporters (OCTs), proteins expressed in the brain and throughout the body with vital roles in normal physiology and drug responses. OCTs have a low-affinity and high-capacity to transport substrates across the cell membrane, and can quickly take up a broad range of compounds that include pharmacological drugs, endogenous neurotransmitters like dopamine, norepinephrine, and serotonin, and experimental substrates like ASP<sup>+</sup>. OCT research is limited by the lack of selective ligands for each of the three OCT subtypes (OCT1, 2, and 3). Saturation binding of ASP<sup>+</sup> was measured in human embryonic kidney (HEK) cells that overexpress human OCT3 to determine the K<sub>D</sub> for ASP<sup>+</sup> in this model. Validation competition analysis was conducted to measure the displacement of ASP<sup>+</sup> uptake and reduced fluorescence by known OCT3 inhibitors, corticosterone and normetanephrine. A primary screen testing nearly 1500 compounds (at 10 μM) and a subsequent confirmatory screen testing 100 compounds (at 10 μM and 1 μM) were conducted to identify hit compounds that were selected based on their ability to inhibit maximum binding of ASP<sup>+</sup> at < 75%, similarly to blockade measured by normetanephrine. Screening parameters such as z-factor, % coefficient of variation, and the signal-to-background ratio were within acceptable ranges for this fluorescent ASP<sup>+</sup> uptake microplate method, confirming its utility for high throughput screens. Twenty-seven compounds had confirmed activity at human OCT3 and were used in further competition analysis studies to determine their IC<sub>50</sub> values and identify trends in structure-activity-relationships. Experiments are ongoing to also evaluate the selectivity of lead compounds by testing their inhibition of fluorescent ASP<sup>+</sup> uptake in cell lines that express human OCT1 or OCT2 for comparison to data obtained in the human OCT3 cell line. Identifying novel experimental selective inhibitors will propel the study of broadly expressed OCTs and expand the utility of the ASP<sup>+</sup> microplate assay as a rapid and versatile approach to studying ligand interactions and the transport function of OCTs.

This work was supported by a pilot, NIDA-funded grant (U18DA052527-01 awarded to LD and BB) and an FSOP internal research award (RFS).

# Therapeutic Efficacy of Macamides on Fragile X Tremor/Ataxia Syndrome (FXT/AS)

Collis Brown,<sup>1</sup> Sonya Sobrian,<sup>1</sup> and Tamaro Hudson<sup>1</sup>

<sup>1</sup>Howard University

Abstract ID 20175

Poster Board 342

Fragile X-associated tremor/ataxia syndrome (FXT/AS) is a late-onset neurodegenerative disease associated with movement and memory problems, affecting 1 in 3000 males over 50 years of age. This syndrome is characterized by excess CGG (55-200) repeats of a trinucleotide sequence in the DNA for the Fragile X Messenger Ribonucleoprotein 1 (*FMR1*). It is suspected to induce mitochondrial dysfunction in the CNS. Currently, no effective pharmacological treatments exist for FXTAS. The goal of this research was to test the ability of synthetic macamides, which are endocannabinoid like-compound, to restore mitochondrial viability. Macamides were chosen as they have been shown to prevent mitochondrial membrane toxicity in Parkinson's disease. To establish a rapid screening cell model to study the pharmacological efficacy of macamides, fibroblast baby hamster kidney (BHK-21) cell lines were treated with glucose oxidase (GluOx) at varying concentrations and times. Mitochondrial viability was assessed by the colorimetric Janus B Green Assay, which stains the mitochondria and enables assessment of cell numbers and the presence of oxygen in anchorage-dependent cell culture. GluOx treatment of BHK-21 cells caused a dose- and time-dependent increase in oxidative stress. There was a significant disruption in the morphology of BHK-21 cells at a high glucose concentration, i.e., 40 nM, between 2 and 24 hours post-exposure. The Janus B Green colorimetric assay confirmed the morphology data. In examining the effects of glucose on mitochondrial viability, we demonstrated that at 15, 30, 35, and 40 nM, glucose significantly decreased mitochondria viability compared to the untreated, with 40 nM having the most significant effect. Upon establishing this model of mitochondrial dysfunction, we next investigated the ability of three novel mitochondrial antioxidants (e.g., macamides) to protect mitochondrial viability. Macamides preserved the morphology of the BHK-21 cells at concentrations of 0.5uM, 1uM, and 5uM. Furthermore, in the presence of glucose, macamides at a low concentration of 0.5uM prevented the reduction of mitochondria viability. This study provides evidence of the efficacy of macamides as novel therapeutic candidates in the treatment of mitochondrial dysfunction associated with FXTAS.

**Support/Funding Information:** Award Number TL1TR001431

# Ethanol-induced suppression of GIRK-dependent signaling in the basal amygdala

Ezequiel Marron,<sup>1</sup> Megan E. Tipps,<sup>1</sup> Bushra Haider,<sup>1</sup> Tim R. Rose,<sup>1</sup> Baovi N. Vo,<sup>1</sup> Margot C. DeBaker,<sup>1</sup> and Kevin Wickman<sup>1</sup>

<sup>1</sup>University of Minnesota

Abstract ID 25419

Poster Board 343

Ethanol exposure fosters neuroadaptations that regulate mood, learning, and goal-directed behavior. The basolateral amygdala (BLA) regulates mood and associative learning and has been linked to the development and persistence of alcohol use disorder (AUD). The GABAB receptor (GABABR) is a promising therapeutic target for AUD, and previous work suggests that exposure to ethanol and other drugs can alter neuronal GABABR-dependent signaling. The impact of ethanol on GABABR-dependent signaling in the BLA was examined using slice electrophysiology following repeated ethanol injection and/or chronic intermittent exposure to ethanol vapor in mice. The relevance of ethanol-induced plasticity in the BLA was explored using tests of mood-related behavior and associative learning, combined with neuron-specific, viral genetic manipulations. The inhibitory effect of GABABR activation on principal neurons in the basal (BA) but not lateral (LA) sub-region of the mouse BLA was diminished following repeated ethanol exposure ( $t_{58}=5.072$ , \*\*\*\* $P<0.001$ ;  $N=30$ /group; unpaired Student's t-test). This adaptation was attributable to the suppression of the G protein-gated inwardly rectifying K<sup>+</sup> (GIRK) channel activity. While GIRK1 and GIRK2 subunits are critical for GIRK channel formation in BA principal neurons, GIRK3 was necessary for the ethanol-induced plasticity as the adaptation was not present in GIRK3KO mice exposed to ethanol ( $t_{42}=0.3170$ ,  $P=0.7528$ ,  $N=22$ /group; unpaired Student's t test). In wild type mice, exposure to ethanol altered several mood-related behaviors. In the light-dark box test ethanol-exposed animals spent less time on the light side ( $t_{22}=3.208$ , \*\* $P=0.0041$ ,  $N=12$ /group; unpaired Student's t-test). In the marble burying test ethanol-exposed animals buried more marbles ( $t_{22}=3.174$ , \*\* $P=0.0044$ ,  $N=12$ /group; unpaired Student's t-test). In the bottle-brush test ethanol-exposed animals had an increased irritability ( $t_{22}=12.19$ , \*\*\*\* $P<0.0001$ ,  $N=12$ /group; unpaired Student's t test). Importantly, all these behavioral effects were absent in ethanol exposed GIRK3KO mice: light-dark box ( $t_{16}=1.719$ ,  $P=0.1048$ ,  $N=8-10$ /group; unpaired Student's t test); marble burying ( $t_{16}=0.2327$ ,  $P=0.8189$ ,  $N=8-10$ /group; unpaired Student's t test); bottle-brush ( $t_{16}=0.8220$ ,  $P=0.4232$ ,  $N=8-10$ /group; unpaired Student's t test). Finally, some, but not all, of these ethanol exposure-dependent behavioral effects could be mimicked in ethanol naive mice by the selective suppression of GIRK channels in BA principal neurons. Therapeutic approaches designed to prevent this plasticity and/or enhance GIRK channel activity may prove useful for treatment of AUD.

## Grant Support

KW: NIDA-DA034696, NIAA-AA027544; MET: NIAAA-AA025978; TRR: NIDA-DA007234; TRR & BNV: UMN Doctoral Dissertation Fellowships; Viral Vector and Cloning Core/Viral Innovation Core: NIDA-DA048742-01A1; KW: Wallin Neuroscience Discovery Fund award.

# Identification of Small Molecule Therapeutics and Neuroprotective Gene Targets via High Throughput Screening and RNA Interference in *C. elegans* Parkinson's Disease Models

Carl T. Ash,<sup>1</sup> Emily E. Anderson,<sup>1</sup> Amy E. Moritz,<sup>1</sup> Patricia K. Dranchak,<sup>2</sup> R. Benjamin Free,<sup>1</sup> James Inglese,<sup>2</sup> Joseph P. Steiner,<sup>1</sup> David R. Sibley,<sup>1</sup> and Emmanuel O. Akano<sup>1</sup>

<sup>1</sup>NIH/NINDS; and <sup>2</sup>NIH/NCATS

Abstract ID 17834

Poster Board 344

Parkinson's disease (PD) is a neurodegenerative disorder characterized by the necrosis of midbrain dopaminergic neurons and subsequent deficiencies of dopamine (DA) signaling, resulting in tremors, rigidity, and bradykinesia among a range of other motor and non-motor complications. Despite its high prevalence and considerable economic burden, driven by a rapidly growing aging population, the underlying molecular mechanisms of PD remain poorly understood, and robust, translational models of the disease have yet to be fully established. These limitations in our collective understanding of PD warrant an urgent need for discovering and interrogating PD-associated druggable targets to address the lack of effective, neuroprotective therapeutics with minimal side effect profiles. Here, we report the development of two high throughput *in vivo* assays for the discovery of small molecule compounds with therapeutic potential and for probing genes potentially involved in dopaminergic neuroprotection. Transgenic mutant *Caenorhabditis elegans* (*C. elegans*) carrying human PD-linked genes were used, one expressing mutant (G2019S) leucine-rich repeat kinase 2 (LRRK2), and the other expressing mutant (A53T)  $\alpha$ -synuclein (SNCA). Both strains express GFP exclusively within their dopaminergic neurons allowing for fluorescent signal intensity to serve as a proxy for monitoring dopaminergic neurodegeneration. A control strain (BY250) was used that expressed only dopaminergic neuronal GFP in the absence of PD-linked transgenes. Daily laser cytometry and high-content imaging readings of GFP intensity revealed a robust temporal dopaminergic neurodegeneration in both PD strains, mirroring that which is seen in human PD, within the first seven days of adulthood. By day seven, GFP fluorescent intensity had decreased by 30-50% and 75-85% in the SNCA and LRRK2 worms, respectively; such an effect was not observed in the wild-type control worms. In the LRRK2 mutant worms, we have identified a set of selective LRRK2 kinase inhibitors that may serve as positive controls for neuroprotection. Assay validation and optimization studies are ongoing with the goal of conducting a high throughput screen of small molecules that may confer neuroprotection in our LRRK2 model and serve as scaffolds for the development of drug leads. We have also established effective knockdown of GFP fluorescent signal intensity by the administration of RNA interference (RNAi) via engineered vector bacterial feeding. Due to the low penetrance of RNAi in neurons, we crossed our control and mutant worms into three RNAi hypersensitive backgrounds carrying *eri-1*, *eri-1*; *lin-15B*, and *rif-3* mutations. In a preliminary screen of RNAi vectors, three (*ceh-43*, *unc-62*, and *ama-1*) conferred robust knockdown of GFP signal in both the control and mutant  $\alpha$ -synuclein-expressing strains, averaging  $\geq 75\%$  knockdown by day seven of treatment when compared to an empty vector control RNAi. In the future, we hope to use this assay to screen *C. elegans* RNAi libraries to elucidate genes that may be neuroprotective in worms expressing the PD transgenes and may serve as potential drug targets for PD therapeutics. A synergistic application of these two approaches may also prove fruitful in that we may deploy RNAi to interrogate potential targets of drugs identified in our high throughput screen or, conversely, use our neuroprotective controls to assess the efficacy of druggable targets related to genes identified by RNAi screening.

# The Cannabinoid 1 Receptor Allosteric Modulator GAT211 Impacts Behavior in a Sex-Dependent Manner

Alyssa Lauer,<sup>1</sup> and Erin Bobeck<sup>1</sup>

<sup>1</sup>Utah State Univ

Abstract ID 16759

Poster Board 345

**Background:** Drugs that target the endocannabinoid system are gaining significant attention in the field of neuropharmacology. Cannabinoid 1 Receptors (CB1Rs) are of special interest due to their implication in a wide array of neuropsychiatric disorders.

Allosteric modulators (AMs) of the Cannabinoid 1 Receptor (CB1R) alter endocannabinoid binding at the orthosteric binding site. CB1R AMs present a promising new avenue for the development of therapeutics. However, sex differences in the endocannabinoid system have been detailed in a growing body of literature. Despite this, few research studies have examined whether sex impacts the efficacy of CB1R AMs.

**Methods:** GAT211 is an allosteric agonist and positive AM of CB1Rs. This compound increases the binding of endocannabinoids to CB1Rs. In the present study, male and female mice were given I.P. injections of either GAT211 or vehicle and tested on the elevated plus maze (EPM) and open field test (OFT).

The EPM is a behavioral test that is used to test anxiety behaviors. The OFT is used to assess locomotion and exploratory behavior.

**Results:** Male mice exposed to GAT211 spent significantly more time in the open arms of the elevated plus maze when compared to mice within the control group. Female mice exposed to GAT211 performed similarly to both male and female control animals. There was no significant difference on the open field test, which suggests that GAT211's effect on males is not simply the result of increased locomotion.

**Conclusion:** These findings suggest that the effects of CB1R AMs may be sex-dependent. This presents an important consideration for evaluating the translational potential of these molecules. Furthermore, the results presented here highlight the importance of research examining sex as a biological variable.



# Dynamic Role of Intra-Locus Coeruleus Mu Opioid Receptors in Nociception

Makenzie Norris,<sup>1</sup> Chao-Cheng Kuo,<sup>1</sup> Jenny Kim,<sup>1</sup> Samantha Dunn,<sup>1</sup> Gustavo Borges,<sup>1</sup> and Jordan McCall<sup>1</sup>

<sup>1</sup>Washington University in St. Louis

**Abstract ID 24694**

**Poster Board 346**

The locus coeruleus (LC) provides the largest noradrenergic innervation to the central nervous system and is a major node in pain neural circuitry. LC noradrenergic neurons directly project to the dorsal horn of the spinal cord. It is through these direct spinal projections LC neurons leverage their antinociceptive influence locally via alpha-2 adrenoreceptor activation to inhibit nociceptive afferents. The LC responds to noxious stimuli with a shift from low tonic to phasic activation and stimulation of the LC has been shown to be antinociceptive. Paradoxically, however, here we show that optogenetic inhibition of LC activity is also acutely antinociceptive - a finding opposite of the canonical role of LC neurons in nociceptive processing. To determine the mechanistic underpinnings of this novel phenomenon, we focused on the dense concentration of mu opioid receptors (MORs) in the LC. Intra-LC MORs have been implicated in several biological processes including, neuropathic pain and stress. Literature suggests intra-LC MORs may be particularly critical for LC-mediated changes in nociception. Pharmacological activation of these MORs has been shown to dose-dependently inhibit LC neuronal activity and promote antinociception. To determine the role of intra-LC MORs in nociceptive processing we developed a MOR conditional knockout (cKO) mouse line. In these mice, MORs are conditionally deleted in cells where MORs are coexpressed with the critical enzyme required to produce norepinephrine (dopamine beta hydroxylase). Furthermore, conditional deletion of MORs in dopamine beta hydroxylase cells, decreased nociceptive thresholds at baseline. To determine whether intra-LC MORs are sufficient to return lower withdrawal thresholds in MOR cKO mice back to baseline, we cell-type selectively rescued MOR function in these mice using a light sensitive MOR, opto-MOR. Finally, to determine whether the LC's pronociceptive function is conserved in neuropathic pain states, we found optogenetic inhibition of the LC 1-week post spared nerve injury resulted in contralateral allodynia. Interestingly, however, inhibition 4 weeks after injury became ipsilaterally antinociceptive suggesting LC activity shifted from pronociceptive to analgesic when neuropathic injury became more chronic. Together, our results suggest the LC controls basal nociception in a MOR-dependent manner that becomes highly dynamic in neuropathic pain states.

# Effectiveness of GPR171 Agonist with Morphine and Identification of GPR171 Signaling Profile

Callie Porter,<sup>1</sup> and Erin Bobeck<sup>2</sup>

<sup>1</sup>Utah State University; and <sup>2</sup>Utah State Univ

**Abstract ID 21730**

**Poster Board 347**

Pain is one of the most common motives for seeking medical attention. Opioid pharmaceuticals are among the most effective for treating pain, yet are limited due to adverse side effects, addiction, dependence, and tolerance. Recently, a novel G protein-coupled receptor, GPR171, and a GPR171 agonist, MS15203, have been identified. Activation of GPR171 via MS15203 in combination with morphine has been shown to enhance morphine antinociception in acute pain. This finding suggests GPR171 is a potential candidate for pain therapeutics, however, additional research on GPR171 is needed. Two ongoing studies intend to further understand GPR171's role in nociception. The first study aims to further assess GPR171's role in antinociception with the use of differing MS15203 and morphine combinations. The increase in antinociception by MS15203-induced GPR171 activation shows the potential to decrease morphine dosages while achieving the same analgesic effect as a higher dosage of morphine. With the addition of MS15203 and reduction in morphine amounts, this would provide the same pain relief for an individual and substantially decrease opioid adverse side effects. In this study, two combinations of morphine and MS15203 were used. The first consisting of 0.10mg/kg morphine plus 50mg/kg MS15203 and the second being 1.0 mg/kg morphine with 25 mg/kg MS15203. Each dose of morphine and MS15203 were also tested independently. Mice were injected once with a randomly assigned treatment and tested using the hot plate and tail flick methods at five time intervals (0, 15, 30, 60, 90, and 120 minutes). Data indicates treatment of MS15203 does not enhance antinociception with lower morphine dosages. However, minimal antinociception following injection was achieved in subjects treated with the combination and MS15203 alone. Yet, the mechanisms used to achieve and enhance antinociception by GPR171 remain unknown. Thus, the second study seeks to elucidate the de-orphaned receptor's signaling mechanisms during chronic agonism. Within this study, mice received repeated twice-daily injections of either 10 mg/kg of MS15203 or 0.9% saline for five continuous days. Subjects were euthanized and brain removal and collection quickly followed. Immunohistochemistry and co-immunoprecipitation will be utilized to determine whether GPR171 under chronic agonism signals via the G-protein or  $\beta$ -arrestin pathway. Determining GPR171's signaling mechanism is essential for drug development. This de-orphaned receptor is a promising target for pain therapeutics and will serve as a better alternative to traditional pain management drugs.

# Presynaptic Regulation of Monoamine Release in the Dorsal Raphe Nucleus by Alpha2-adrenergic Receptors

Aleigha Gugel,<sup>1</sup> and Stephanie C. Gantz<sup>1</sup>

<sup>1</sup>University of Iowa

Abstract ID 23263

Poster Board 348

The dorsal raphe nucleus is the largest serotonergic nucleus in the brain and the predominant source of central serotonin (5-HT). Here, synaptic activation of G<sub>q</sub> protein-coupled alpha1-adrenergic receptors (alpha1-A<sub>R</sub>s) produces a long-lasting excitatory postsynaptic current (alpha1-A<sub>R</sub>-EPSC) that drives action potential firing. Alpha2-adrenergic receptors (alpha2-A<sub>R</sub>s) are presynaptic autoreceptors that when activated limit further noradrenaline release. How activation of alpha2-A<sub>R</sub>s affects the alpha1-A<sub>R</sub>-EPSC and ultimately serotonin neuron excitability is unknown. In the present study, whole-cell patch-clamp recordings were made from serotonin neurons in the dorsal raphe nucleus in acute mouse brain slice to determine the effects of alpha2-A<sub>R</sub> activation on the alpha1-A<sub>R</sub>-EPSC. Application of the alpha2-A<sub>R</sub> agonists, UK-14,304 and clonidine, abolished the alpha1-A<sub>R</sub>-EPSC. Exogenous application of noradrenaline produced an inward current in serotonin neurons, that was unaffected by UK-14,304, demonstrating that activation of alpha2-A<sub>R</sub>s eliminates the alpha1-A<sub>R</sub>-EPSC via a presynaptic mechanism. In addition, UK-14,304 and clonidine also produced a significant reduction in the 5-HT1A receptor-mediated inhibitory postsynaptic current (5-HT1A<sub>R</sub>-IPSC). Application of UK-14,304 also produced an outward current and a decrease in membrane resistance in some serotonin neurons due to activation of postsynaptic alpha2-A<sub>R</sub>s activating G protein-coupled inwardly rectifying potassium (GIRK) channels. In conclusion, activation of alpha2-A<sub>R</sub>s reduces both excitatory and inhibitory synaptic transmission in dorsal raphe serotonin neurons. The net effect on serotonin neuron excitability *in vitro* and *in vivo* will be discussed.

# Chronic Morphine and Fentanyl Induce Intestinal Dysbiosis by Decreasing the Antimicrobial Activity of the Ileum

Karan Hitesh Muchhala,<sup>1</sup> Grace K. Mahon,<sup>1</sup> Eda Koseli,<sup>2</sup> Jaelen Bethea,<sup>2</sup> Minhoo Kang,<sup>2</sup> and Hamid I. Akbarali<sup>3</sup>

<sup>1</sup>Virginia Commonwealth Univ; <sup>2</sup>Virginia Commonwealth University; and <sup>3</sup>Virginia Commonwealth Univ, Med College of Virginia

Abstract ID 19075

Poster Board 368

**Introduction:** Recently, evidence from both preclinical<sup>1</sup> and clinical<sup>2</sup> studies indicates that chronic opioid use results in intestinal dysbiosis; eliminating the dysbiotic bacteria with antibiotics prevents the onset of tolerance to the antinociceptive effects<sup>1</sup>. However, the mechanism underlying opioid-induced dysbiosis (OID) is unclear. One mechanism by which the intestinal epithelium maintains the microbiota is through the release of antimicrobial peptides (AMPs). In the present study we tested if chronic morphine or fentanyl altered the antimicrobial activity of the intestinal epithelium. We also tested if the short-chain fatty acid, butyrate, a bacterial fermentation product known for its protective effects on the intestinal epithelium<sup>3</sup>, can prevent OID and tolerance.

**Methods:** Male Swiss Webster mice (6-8 weeks) were implanted for 7-days with a morphine (75-mg) or placebo pellet and orally administered sodium butyrate (275 mg/kg) b.i.d. Tolerance to antinociception was tested on day-7 using the warm-water tail-withdrawal assay. Resected ileum tissue was incubated in DMEM/F12 for 15-18-hours to allow for the dissolution of AMPs into the media. %Antibacterial activity of the conditioned media was determined by counting the colonies of *E.coli* (Gram-negative) or *L.reuteri* (Gram-positive) on agar plates. AMPs, Regenerating islet-derived protein 3-gamma (Reg3g), active against Gram-positive bacteria, and alpha-defensin-5 (Defa5), active against Gram-positive and Gram-negative bacteria, were measured in the ileum using qRT-PCR. Experiments were also conducted in mice treated for 6 days with 0.3 mg/kg fentanyl ± butyrate (275 mg/kg) i.p. b.i.d.

**Results:** %Antibacterial activity against *E.coli* or *L.reuteri* of ileum tissue supernatants from chronic morphine-treated mice was significantly reduced compared to that from placebo controls. Chronic morphine or fentanyl administration also significantly down-regulated Reg3g and Defa5 in the ileum. Butyrate prevented opioid-induced decrease in %antibacterial activity and down-regulation of AMPs in the ileum. Butyrate-treated mice also did not exhibit tolerance in the warm-water tail-withdrawal assay.

**Conclusion:** Chronic opioid treatment reduced AMPs in the ileum, implicating a potential mechanism underlying OID. Preventing the opioid-induced decrease in antibacterial activity with sodium butyrate precluded the development of tolerance to antinociception, thus implicating sodium butyrate as a prophylactic treatment for OID.

## References

1. Kang M, Mischel RA, Bhawe S, et al. The effect of gut microbiome on tolerance to morphine mediated antinociception in mice. *Sci Rep*. 2017;7(1):42658. doi:10.1038/srep42658
2. Cruz-Lebrón A, Johnson R, Mazahery C, et al. Chronic opioid use modulates human enteric microbiota and intestinal barrier integrity. *Gut Microbes*. 2021;13(1). doi:10.1080/19490976.2021.1946368
3. Tan J, McKenzie C, Potamitis M, Thorburn AN, Mackay CR, Macia L. The role of short-chain fatty acids in health and disease. *Adv Immunol*. 2014;121:91-119. doi:10.1016/B978-0-12-800100-4.00003-9

This work was supported by the National Institute of Health grant: P30 DA033934

# Cellular Mechanisms of Amyloid $\beta$ Oligomers Suppressing GABAB-GIRK Signaling

Haichang Luo,<sup>1</sup> Kevin Wickman,<sup>1</sup> and Ezequiel Marron Fernandez de Velasco<sup>2</sup>

<sup>1</sup>Univ of Minnesota; and <sup>2</sup>University of Minnesota

Abstract ID 21794

Poster Board 369

Amyloid  $\beta$  oligomers (A $\beta$ Os) are one of the primary pathogenic factors in Alzheimer's Disease and have been shown to induce excitotoxicity in the hippocampus in both acute and chronic models. While many studies have elucidated A $\beta$ Os' pathological effects on glutamatergic signaling, limited studies focus on the impacts of A $\beta$ Os on GABAergic inhibitory signaling and its possible role in pathogenesis. Our group and others have established G protein-coupled inwardly-rectifying K<sup>+</sup> (GIRK) channels as critical mediators of GABAB receptor-dependent signaling, impacting neuronal excitability, synaptic plasticity, and cognitive function. A $\beta$ Os are shown to downregulate GIRK channel mRNA and protein expression in the rodent hippocampus, but no mechanistic studies have been done to verify the link between GIRK channel downregulation and A $\beta$ O-induced synaptic and cognitive deficits. To study whether GIRK channels are one of A $\beta$ Os' early targets whose changes contribute to the downstream pathology, we investigate the effects of synthetic A $\beta$ Os on cultured mouse hippocampal neurons. Data were analyzed using Welch's t-test or one-way ANOVA with Tukey's multiple comparisons test (n = 16-18), as appropriate. We found that both GABAB-evoked somatodendritic whole-cell currents (100  $\mu$ M baclofen) and directly-activated GIRK channel-mediated currents (10  $\mu$ M ML297) were significantly suppressed following A $\beta$ O incubation (0.5  $\mu$ M) in neurons (baclofen: p = 0.0391, ML297: p = 0.0412). The effect was seen after only 3 hours of incubation. The suppression observed was successfully blocked by co-incubating with a metabotropic glutamate receptor 5 (mGlu5R) antagonist (10  $\mu$ M MTEP, baclofen: p > 0.9999), suggesting that the suppression of GABABR-GIRK currents is likely through A $\beta$ O-induced mGlu5R activation. In addition, incorporating phosphatidylinositol 4,5-bisphosphate (PIP2) in the pipette solution rescued the current suppression evoked by A $\beta$ Os (30  $\mu$ M diC8PIP2, baclofen: p > 0.9999), indicating that a possible reduction in PIP2 (essential for GIRK activation) in the plasma membrane is involved in the early effects of A $\beta$ Os on GIRK-dependent signaling and is likely the consequence of mGlu5R activation. It is the first time that a possible mechanism for the action of A $\beta$ Os on GIRK-dependent signaling is investigated, and the behavioral consequences of the GIRK adaptation are also being tested at the moment.

# Dopamine transporter activity regulates neuroimmune communication

Adithya Gopinath,<sup>1</sup> Phillip M. Mackie,<sup>1</sup> Emily Miller,<sup>2</sup> Leah T. Phan,<sup>2</sup> Stephen Franks,<sup>2</sup> Tabish Riaz,<sup>2</sup> Aidan R. Smith,<sup>2</sup> Michael Okun,<sup>2</sup> and Habibeh Khoshbouei<sup>3</sup>

<sup>1</sup>Univ of Florida; <sup>2</sup>University of Florida; and <sup>3</sup>McKnight Brain Inst of the Univ of Florida

**Abstract ID 52323**

**Poster Board 370**

Dopamine transporter (DAT) is a master regulator of dopamine transmission in the brain. Mutation in DAT structure is implicated in familial Parkinson's disease. In addition, DAT is one of the main targets of psychostimulants, therefore, DAT is conventionally studied in central nervous system (CNS) and in the context of neurological and neuropsychiatric diseases. But, in addition to the brain, DAT is also expressed at the plasma membrane of myeloid and lymphoid cells in the periphery. We found DAT activity reduces macrophage responses to immune stimulation through autocrine/paracrine signaling. In human monocyte-derived macrophages, we identified an immunosuppressive role for DAT, where inhibition of DAT activity exaggerated macrophages' phagocytic response and enhanced production of inflammatory mediators such as IL-6, CCL2, and TNF $\alpha$ . Consistent with our ex-vivo studies, our in vivo data in a mouse model with genetic deletion of DAT (DAT KO) also showed an immunosuppressive role for DAT. Unlike WT littermates, LPS-induced immune stimulation in DAT KO mice resulted in elevated baseline inflammation, exaggerated phagocytosis, increased B-cell and T-cell responses. In addition, our studies in 96 PD patients and mouse models of PD revealed the disease relevance of increased DAT activity as measured by increased number of DAT expressing monocytic suppressor cells. These data collectively point to the importance of DAT activity in peripheral immune responses. Our current and ongoing studies seek to determine the impact of DAT deletion and its restoration on the CNS immune landscape and the ensuing changes in peripheral immunity. We will first determine whether DAT deletion and/or LPS-mediated immune stimulation alters microglial number, morphology, and their contact with dopaminergic nuclei in DAT-expressing brain regions such as midbrain, striatum, median forebrain bundle and hypothalamus. To determine which dopaminergic nuclei is critical for top-down (CNS  $\square$  periphery) regulation of peripheral immunity, we will virally restore DAT in each brain region and monitor peripheral immunity, as described above. The completion of this study will reveal the contribution of DAT activity in the regulation of CNS-to-periphery neuroimmune interactions, providing a key opening into a new field for dopamine transporter biology.

# Chronic intermittent ethanol exposure induces spatial changes in lipid raft localization of G-proteins and their interacting proteins in rat prefrontal cortex

Anna Neel,<sup>1</sup> James D. Miller,<sup>1</sup> Shiyu Wang,<sup>1</sup> Minghao Li,<sup>1</sup> Jonathan C. Mayer,<sup>1</sup> Haiguo Sun,<sup>1</sup> Brian McCool,<sup>1</sup> and Rong Chen<sup>1</sup>

<sup>1</sup>Wake Forest Univ Hlth Sciences

Abstract ID 25402

Poster Board 371

**Background:** The trimeric G-proteins, composed of a G $\alpha$  and a dimeric G $\beta\gamma$  subunit, function to relay extracellular stimuli from G-protein-coupled-receptors (GPCRs) and transduce intracellular signaling cascades by directly interacting with their cognate coupling partners in confined membrane microdomains. Chronic intermittent ethanol (CIE) exposure alters the function of many GPCRs, although the molecular mechanism is largely unknown. Our preliminary data indicate that CIE exposure increases membrane cholesterol content in the brain. Membrane cholesterol critically regulates the compartmentalization of membrane proteins and the assembly of signaling complexes. Thus, this project aimed to test the hypothesis that CIE exposure may result in spatial alterations of membrane localization of G-proteins and their coupling partners within lipid raft and non-raft microdomains, disrupting GPCR-stimulated G-protein and downstream signaling.

**Method: Ethanol Vapor Exposure:** Male Sprague Dawley rats were exposed to either ethanol vapor (CIE) or room air (AIR) during the light cycle (12 hr/day) for seven consecutive days. Following 24 hr withdrawal from the last ethanol exposure, all animals were euthanized, and prefrontal cortex (PFC) tissue was dissected.

**Sucrose Density Gradient Ultracentrifugation:** PFC tissue was homogenized and then fractionated by discontinuous sucrose density (5%/30%/40%) ultracentrifugation. Fifteen fractions were collected along the sucrose density gradient for each sample. Western blotting was performed to determine the localization of G-protein subunits and their interacting proteins within lipid raft and non-lipid raft microdomains.

**Results:** We found that CIE induced differential changes in the localization of G-protein subunits within lipid rafts and non-raft regions. In CIE-exposed animals, G $\alpha_i$  and G $\alpha_o$  subunits, but not G $\alpha_s$  and G $\alpha_q$  subunits, translocated from lipid rafts toward non-rafts, while G $\beta\gamma$  subunits translocated from non-rafts toward lipid rafts when compared to AIR-exposed control animals. Interestingly, CIE exposure did not alter the compartmentalization of the protein kinases adenylyl cyclase type 1 and phospholipase C $\beta$ 1, which are direct G-protein interacting proteins. Further, CIE exposure induced an increase in lipid raft localization of mGluR2, a G $\alpha_i/o$ -interacting protein, and Kv1.2, a G $\beta\gamma$ -interacting protein, but had no effect on G $\alpha_q$ -coupled mGluR1 localization. Finally, CIE exposure significantly increased rat PFC membrane cholesterol content.

**Conclusions:** Our data suggest that spatial localization of G-proteins and their interacting proteins is susceptible to regulation by CIE. Importantly, the present study highlights a potential role of lipid metabolism in GPCR dysregulation and may open a new avenue for targeting cholesterol metabolism as a treatment for alcohol use disorder.

Support/Funding Information:

T32-AA007565

R21DA056857

R01DA042862

# Cyclodextrins decrease TRPV1 and TRPA1 ion channel activation via lipid raft disruption

Éva Szőke,<sup>1</sup> Andrea Nehr-Majoros,<sup>1</sup> Ádám Horváth,<sup>1</sup> Anita Steib,<sup>1</sup> Levente Szócs,<sup>2</sup>  
Éva Fenyvesi,<sup>2</sup> and Zsuzsanna Helyes<sup>1</sup>

<sup>1</sup>University of Pécs; and <sup>2</sup>Cyclolab R&D Ltd

Abstract ID 16855

Poster Board 372

Transient Receptor Potential Ankyrin 1 (TRPA1) and Vanilloid 1 (TRPV1) are nociceptive ion channels involving in pain sensation and development of neurogenic inflammation. These non-selective channels are located in the lipid rafts, the cholesterol-rich membrane domains of the plasma membrane of primary sensory neurons and peripheral nerve terminals. Cyclodextrins (CDs) are able to form inclusion complexes with cholesterol and deplete it from lipid rafts. We have already described that lipid raft disruption by Methyl- $\beta$ -cyclodextrin (MCD) inhibited TRP ion channel function and has analgesic effect in animal models.

We tested five different CD derivatives (Randomly methylated  $\beta$ -cyclodextrin: RAMEB, (2-Hydroxypropyl)- $\gamma$ -cyclodextrin: HPGCD, (2-Hydroxypropyl)- $\beta$ -cyclodextrin: HPBCD, Sulfobutylated  $\beta$ -cyclodextrin sodium salt: SBECD and (2-Hydroxy-3-N,N,N-trimethylamino) propyl- $\beta$  cyclodextrin: QABCD; CycloLab Ltd.) in respect of their cytotoxicity (1, 3, 10, 50, 100 mM; 24 h) on chinese hamster ovary (CHO) cells with CellTiter-Glo® Luminescent Cell Viability Assay. MitoTracker™ Red CMXRos fluorescent dye was used to reveal the effect of 24-hour CD treatment on mitochondrial functioning of CHO cells. We performed radioactive  $^{45}\text{Ca}^{2+}$ -uptake measurements on TRPA1 and TRPV1 receptor-expressing CHO cells to detect alterations in receptor activation after CD treatment.

In CellTiter-Glo® Luminescent Cell Viability Assay the methylated derivative RAMEB showed significant cytotoxic effect in 3.5 mM concentration, but none of the non-methylated derivatives decreased cell viability in 10 mM concentration.

HPBCD treatment (1 mM and 10 mM) and QABCD treatment (10 mM) resulted in significantly increased fluorescence intensities of CHO cells' mitochondria labeled with MitoTracker™ Red CMXRos. All of the investigated CDs were able to inhibit the  $^{45}\text{Ca}^{2+}$ -uptake in TRPA1 and TRPV1 receptor-expressing CHO cells in a concentration dependent manner.

In conclusion, non-methylated derivatives have much lower cytotoxicity compared to RAMEB. HPBCD and QABCD affected significantly the mitochondrial function and all investigated CD derivatives were able to inhibit TRPA1 and TRPV1 channel activation, presumably via the disruption of lipid rafts. Targeting hydrophobic interactions of the protein-lipid interface might be promising as a novel mechanism of action in analgesia.

**Support/Funding Information:** TKP2021-EGA-16, TKP2021-EGA-13, NKFIH-138936, RRF-2.3.1-21-2022-00015, KTIA\_NAP\_20017-1.2.1-NKP-2017-00002, ÚNKP-21-3-II New National Excellence Program of the Ministry for Innovation and Technology, Gedeon Richter Talentum Foundation



# Estrogen Depletion Alters Cortical NMDAR Function in Ovariectomized Rats

Kimberly Holter,<sup>1</sup> McKenna G. Klausner,<sup>2</sup> Bethany Pierce,<sup>1</sup> Owen Ghaphery,<sup>2</sup> Ashlyn Stone,<sup>1</sup> and Robert W. Gould<sup>1</sup>

<sup>1</sup>Wake Forest University School of Medicine; and <sup>2</sup>Wake Forest University

Abstract ID 20567

Poster Board 373

Despite similar overall prevalence of schizophrenia diagnoses in males and females, >75% of patients diagnosed between 45-50 years of age are female, an age range that corresponds with the menopause transition. Evidence suggests that decreased circulating estrogen associated with menopause may contribute to this late stage onset in females. For example, perimenopausal and postmenopausal women exhibit heightened symptom severity, risk of relapse, and poorer treatment response to some antipsychotic medications compared to premenopausal women. However, mechanisms contributing to these alterations are not well understood. Administration of *N*-methyl-D-aspartate receptor (NMDAR) antagonists, including MK-801, is frequently used to disrupt cognition and induce hyperlocomotion, modelling the cognitive and positive symptoms of schizophrenia, respectively, in animals. MK-801 also induces excessive increases in high frequency gamma power recorded via electroencephalography (EEG) which corresponds with cognitive disruptions and positive symptoms. Gamma power reflects a balance of cortical GABA and glutamate signaling and, thus, these increases are hypothesized to be driven by inhibition of NMDARs on cortical PV-containing interneurons. This ultimately causes disinhibition of glutamatergic pyramidal neurons and increased excitability. Oscillations within the beta frequency range are also altered in schizophrenia and are sensitive to inhibition of NMDARs on PV-containing interneurons. Beta power is commonly reduced following NMDAR antagonist administration in rodents and humans and corresponds with cognitive impairment. However, few preclinical studies have examined the influence of hormones including 17 $\beta$ -estradiol (E2), the most potent form of circulating estrogen, in conjunction with the NMDAR antagonist model. Using surface electrodes and wireless EEG detection, we directly tested the hypothesis that E2 depletion reduces NMDAR function and increases associated cognitive impairments. MK-801 (0.03-0.18 mg/kg, sc) was administered to 3-month-old female rats who were ovariectomized (Ovx; a rodent model of surgical menopause) and implanted with an empty silastic capsule (Ovx rats) or a capsule containing E2, a well-established method of chronic E2 delivery (Ovx+E rats). Data suggests, while there are no significant baseline differences, Ovx rats are more sensitive to MK-801-induced changes in gamma and beta power compared to Ovx+E rats. Ongoing studies are examining the ability of olanzapine (0.3-1.8 mg/kg, IP), an atypical antipsychotic, to attenuate MK-801-induced functional EEG changes. We also investigated cognitive performance of Ovx and Ovx+E rats on a touchscreen paired-associates learning (PAL) task to evaluate visual learning and working memory. While MK-801 dose-dependently decreased accuracy, no significant differences were noted between Ovx and Ovx+E groups. Ongoing studies are assessing other cognitive domains (attention and vigilance) using the touchscreen 5-choice serial reaction time task. Ultimately, these studies aim to establish a relationship between estradiol, NMDAR function, and antipsychotic-like activity using a translational biomarker of brain function to inform menopause-related differences in patients with schizophrenia to pursue development of novel antipsychotic medications.

**Support/Funding Information:** AG077271 (R21)

# TrkB-containing Serum Extracellular Vesicles as a Potential Biomarker for Cognitive Improvement

Reiya Yamashita,<sup>1</sup> Takahiro Ishimoto,<sup>1</sup> Satoshi Matsumoto,<sup>2</sup> Yusuke Masuo,<sup>1</sup> Makoto Suzuki,<sup>2</sup> and Yukio Kato<sup>1</sup>

<sup>1</sup>Kanazawa University, Faculty of Pharmacy; and <sup>2</sup>L•S Corporation Co. Ltd.

Abstract ID 21807

Poster Board 470

**Aim:** One of the essential factors for memory formation through neuroplasticity is brain-derived neurotrophic factor (BDNF)/TrkB signaling. Therefore, the evaluation of TrkB activity could be a biomarker of cognitive improvement by drugs, but a non-invasive method to evaluate TrkB activity has not yet been established in humans. We focused on extracellular vesicles (EVs), which are released from various tissues and reflect the contents of the derived cells. The present study aimed to evaluate the release of TrkB-containing EVs from the brain into the circulating blood and its potential as a biomarker for cognitive improvement using food-derived amino acid ergothioneine (ERGO), which activates TrkB and improves cognitive function.

**Methods:** EVs were isolated by ultracentrifugation from culture medium and serum. In the clinical study, healthy volunteers and subjects with mild cognitive impairment were divided into two groups: ERGO (5 mg/day)-containing food extract tablets treated group (ERGO group) and the placebo group. Serum collection and cognitive function test (Cognitrix) were performed at weeks 0, 4, 8, and 12. Expression of phosphorylated TrkB, an active form of TrkB, in serum EVs was quantified by Western blotting, and the correlation between the expression and each cognitive domain score of Cognitrix was analyzed. To confirm the involvement of TrkB phosphorylation and ERGO-induced cognitive improvement, mice were treated with ERGO with/without a TrkB inhibitor ANA-12, three times a week.

**Results and Discussion:** First, we checked the expression of TrkB in EVs derived from the neuronal cells Neuro2A transfected with a plasmid encoding a FLAG-tagged mouse TrkB (TrkB-FLAG). Expression of TrkB-FLAG and EVs markers CD63 was confirmed in EVs isolated from the cultured medium. Interestingly, TrkB-FLAG was detected in serum EVs after intrahippocampal injection of adeno-associated virus serotype PHP.eB vector encoding the TrkB-FLAG gene in mice. This result suggests that TrkB-expressing EVs are secreted from the brain into the bloodstream. In the clinical study, the expression ratio of p-TrkB to TrkB (p-TrkB/TrkB) in serum EVs in the ERGO group was significantly higher than that in the placebo group at week 12. Analysis of the correlation between p-TrkB/TrkB and cognitive improvement in serum EVs showed that p-TrkB/TrkB positively correlated with blood ERGO concentration and some cognitive domains such as composite memory and verbal memory. In mice, the oral ERGO administration increased cognitive function assessed by a novel object recognition test, while simultaneous administration of a TrkB inhibitor significantly suppressed such increase. These results suggest that TrkB phosphorylation may be involved in ERGO-induced cognitive improvement, and p-TrkB/TrkB would be a biomarker for cognitive improvement.

**Conclusion:** TrkB-containing EVs are secreted from the brain into the circulating blood, and TrkB phosphorylation would be a potential biomarker for ERGO-induced cognitive improvement.

# IRX4204 enhances gait recovery in mice subjected to experimental autoimmune encephalomyelitis

Gracious Kasheke,<sup>1</sup> Scott P. Holman,<sup>1</sup> Kaitlyn Fraser,<sup>1</sup> Arul Asainayagam,<sup>1</sup> Sagar Vuligonda,<sup>2</sup> Martin Sanders,<sup>2</sup> and George Robertson<sup>3</sup>

<sup>1</sup>Dalhousie University; <sup>2</sup>Io Therapeutics Inc; and <sup>3</sup>Dalhousie Univ

Abstract ID 14678

Poster Board 471

**Introduction:** Current immune-based therapies for multiple sclerosis (MS) reduce relapses but have limited value in slowing disease progression. Remyelination is considered essential for functional recovery in MS. Activation of the retinoid X receptor (RXR) enhances remyelination by increasing the production of myelin-producing oligodendrocytes. 3-Methyl-5-[(1S,2S)-2-methyl-2-(5,5,8,8-tetramethyl-5,6,7,8-tetrahydronaphthalen-2-yl)cyclopropyl]-2(E),4(E)-pentadienoic acid (IRX4204) is an investigational drug that preferentially activates the RXR.

**Objective:** The purpose of this study was to determine if IRX4204 administration improves motor recovery and remyelination in a mouse model of MS termed experimental autoimmune encephalomyelitis (EAE).

**Methods:** Female C57Bl/6 mice (20-25 g) were subjected to EAE by immunization with a peptide corresponding to amino acids 35-55 of myelin oligodendrocyte glycoprotein. A solution containing 3 mg/mL of this peptide in phosphate buffered saline (PBS; pH 7.4) was emulsified (1:1 ratio) in Complete Freund's Adjuvant (CFA). Each mouse received two 100 µL injections of the emulsified mixture subcutaneously. Additionally, each mouse received a 200 µL injection of pertussis toxin dissolved in PBS (1.5 ng/µL) on the day of immunization and again on day post-immunization 2. Mice were then treated orally with either vehicle (NEOBEE; 8 ml/kg/day; n = 10) or IRX4204 (12 mg/kg/day; n = 10) beginning at peak disease (day post-immunization 16). Disease severity was assessed using a clinical scoring scale and white matter loss was assessed following the staining of spinal cord sections with eriochrome cyanine and neutral red. Motor function was assessed weekly using kinematic gait analysis to measure hindleg movements in the sagittal plane while mice walked on a treadmill. Spinal cord concentrations of IRX4204 following daily doses were measured using liquid chromatography in tandem with mass spectrometry.

**Results:** Relative to vehicle, IRX4204 reduced clinical scores and reversed gait deficits in EAE mice. Gait improvements in IRX4204-treated EAE mice were characterized by increased toe heights and the recovery of knee joint movements. These gait improvements were associated with reduced white matter loss in the spinal cord suggestive of enhanced remyelination. Furthermore, spinal cord concentrations of IRX4204 reached levels known to stimulate the differentiation of oligodendrocyte progenitor cells into myelin-making oligodendrocytes.

**Conclusion:** These results support and extend findings from other laboratories which have reported that RXR activation enhances remyelination and reduces motor deficits in mice subjected to EAE. Our findings suggest that IRX4204 may reverse motor deficits in MS by stimulating remyelination.

# The synaptic protein phosphatase 1 targeting protein, spinophilin, mediates striatal neuroadaptations underlying motor function

Anthony J. Baucum,<sup>1</sup> Darryl S. Watkins,<sup>1</sup> Basant Hens,<sup>1</sup> Nikhil R. Shah,<sup>1</sup> and Cameron W. Morris<sup>1</sup>

<sup>1</sup>Indiana University School of Medicine

Abstract ID 17909

Poster Board 472

The striatum is part of the striatal-thalamic-cortical-striatal loop and is one brain region that integrates signals to regulate myriad behaviors, including motor learning, locomotor sensitization to drugs of abuse, and repetitive motor outputs observed in obsessive-compulsive spectrum disorders. We have found that global loss of the post synaptic density-enriched protein phosphatase 1 (PP1) targeting protein, spinophilin, mediates multiple striatal-associated behaviors, including rotarod motor learning and psychostimulant-induced locomotor sensitization. Moreover, using recently characterized cell type-specific spinophilin knockout mice, we have observed that loss of spinophilin in specific striatal neurons, direct or indirect pathway medium spiny neurons, attenuates pathological grooming associated with excessive metabotropic glutamate receptor 5 (mGluR5) function. Interestingly, it has previously been suggested that spinophilin is highly locally translated; however, our preliminary data suggest that this local translation may be different in different brain regions. Therefore, these data position spinophilin specifically in the striatum, as a critical regulator of striatal neuroadaptations; however, how spinophilin mediates striatal neuroadaptations is unclear. Herein, we discuss mechanisms by which spinophilin regulates striatal neuroadaptations underlying motor output changes associated with striatal pathophysiology, including locomotor responses to psychostimulant drugs of abuse and dopamine receptor agonism.

**Support/Funding Information:** R21/R33DA041876; Department of Pharmacology and Toxicology, Stark Neurosciences Research Institute, and Strategic Research Initiative Indiana University School of Medicine; Department of Biology

# Calmodulin Dependent Protein Kinase II: An Effector in the Signaling Pathway of Antidepressant-like Behavior Elicited by Ketamine in Combination with Melatonin

Gloria Benítez-King,<sup>1</sup> Armida Miranda-Riestra,<sup>1</sup> Rosa Estrada-Reyes,<sup>1</sup> Citlali Trueta,<sup>2</sup> Jesús Argueta,<sup>3</sup> Julián Oikawa-Sala,<sup>3</sup> Luis Alejandro Constantino-Jonapa,<sup>3</sup> and Montserrat G. Cercós<sup>1</sup>

<sup>1</sup>Instituto Nacional de Psiquiatría Ramón de la Fuente Muñiz; <sup>2</sup>Instituto Nacional de Psiquiatría Ramón de la Fuente Muñiz; and <sup>3</sup>Instituto Nacional de Psiquiatría Ramón de la Fuente Muñiz

Abstract ID 21584

Poster Board 473

Melatonin (MEL; *N*-acetyl-5-hydroxytryptamine) and ketamine (KET; 2-(2-chlorophenyl)-2-(methylamino) cyclohexan-1-one) elicit antidepressant-like effects in mice and increases neurogenesis in the hippocampus (HP) through stimulation of MEL receptors or by blocking the NMDA receptors, respectively. Non-effective doses KET administered with non-effective MEL doses, increases both processes.

The alpha isoform of Calmodulin-dependent kinase II (CaMKII) is a downstream effector in both KET and MEL signaling pathways. MEL activates CaMKII and stimulates dendrite formation and complexity, as well as neurogenesis in the hippocampus (HP). On the other hand, KET through NMDA receptor antagonism increases phospho-CaMKII (p-CaMKII) levels, and glutamate receptor (GluR1) expression and phosphorylation in the prefrontal cortex (PC). The goal of this study was to determine whether MEL in combination with KET at doses that elicit the anti-depressant-like behavior in mice activates CaMKII and GLUR1 signaling pathways in the HP and PC.

Male Swiss Webster mice (25–35 g) were managed under the laboratory animal care rules (NIH-85-23, 1985). Vehicle (VEH), or either MEL (16 mg/kg), or KET (1.5 mg/kg) alone or KET in combination with MEL (1.5/16 mg/kg; KET/MEL) were intraperitoneally administered in 10.0 mL/kg body weight, and 30 min later were submitted to the forced swimming test (FST). Mice were decapitated, and the HP and the PC dissected, homogenized, separated by two- or one-dimensional electrophoresis, and assayed by Western blot. We detected  $\alpha$ CaMKII, anti-pCaMKII, GluR1 with specific primary and secondary antibodies coupled to either FITC or RITC. Another group of mice, treated as described above were intracardially perfused with 4% paraformaldehyde after the FST. We sectioned brains with a cryostat at -20°C in slices of 30–35  $\mu$ m. Slices were stained with the antibodies mentioned above and nuclei with DAPI. Data were analyzed with a Student's t-test or a one-way analysis of variance (ANOVA). p-values  $\leq$  0.05 was considered as significant.

We separated and identified CaMKII and GluR1 by molecular weights and isoelectric point by two-dimensional electrophoresis. The relative amount of CaMKII were increased in mice treated with MEL or KET/MEL in the HP. In the PF, the relative amount of this protein was solely increased in mice treated with KET/MEL. Also, the acidic isoforms of GluR1 were significantly increased in the HP of mice treated with MEL or KET/MEL and in the PC of mice treated with KET or KET/MEL.

We showed by Western blot that the relative amount of  $\alpha$ CaMKII and pCaMKII were increased in HP of mice administered with KET or the combination of KET/MEL. This result was confirmed by immunostaining of pCaMKII in HP. No differences were observed in the PC. These results indicate that CaMKII expression and activation is selectively caused in the HP by MEL, KET and KET/MEL after an acute administration. Also, we showed that in PF, the amount of the acidic isoforms of GluR1 were increased by KET/MEL. Importantly, KET at the dosage tested *per se* does not produce the antidepressant-like behavior in mice. Data suggest that the antidepressant-like behavior observed after an acute administration of KET/MEL could be mediated by increasing phosphorylation of both CaMKII and the glutamate receptor GluR1. More experiments are necessary to go deeper into the mechanism of KET/MEL combination.

Supported by CONACyT Grant 290526 (GBK) and Grant 252935 (CT).

# Sex-differences in acute $\Delta^9$ -THC-induced antinociception are strain-specific

Courtney Lulek,<sup>1</sup> Malabika Maulik,<sup>2</sup> Swarup Mitra,<sup>1</sup> Daniel Morgan,<sup>2</sup> and Angela N. Henderson-Redmond<sup>1</sup>

<sup>1</sup>Marshall University; and <sup>2</sup>Marshall Univ

Abstract ID 55573

Poster Board 474

Though cannabinoids are being increasingly used for their pain-relieving effects, tolerance to these effects, including those of delta-9-tetrahydrocannabinol ( $\Delta^9$ -THC), may limit their clinical efficacy. With more women than men now using medical cannabis for pain relief, it is crucial we understand how biological sex may influence cannabinoid-mediated antinociception and subsequent tolerance. Likewise, few studies have considered whether the efficacy of cannabinoids may vary as a function of genetics. Though studies in rats consistently find female rats to be more sensitive to the acute antinociceptive effects of cannabinoids than males, work in our lab consistently finds the converse. Studies in our lab primarily utilize mice on a C57BL6/J (B6) background. Consequently, not only is there is little genetic variation among our B6 mice, but it remains unknown whether the sex-specific effects we observe in B6 mice extend to other mouse strains. Therefore, the purpose of the present study is to examine whether our observed sex differences in  $\Delta^9$ -THC-induced antinociception and tolerance are strain-dependent. Male and female B6, DBA, AKR, and CBA mice were assessed for differences in acute  $\Delta^9$ -THC-induced antinociception and hypothermia prior to and following seven days of once-daily  $\Delta^9$ -THC administration. Consistent with our previous studies, male B6 mice were more sensitive to the acute antinociceptive effects of  $\Delta^9$ -THC than female B6 mice, an effect which correlated with differences in B6 CB<sub>1</sub> mRNA expression in the PAG and dissipated with age. While DBA and CBA female mice showed increased  $\Delta^9$ -THC-antinociception compared to male littermates at 30 and 10 mg/kg  $\Delta^9$ -THC, respectively, these effects dissipated at higher doses, revealing that dose of  $\Delta^9$ -THC may also be important. Overall, CBA mice were much more sensitive to  $\Delta^9$ -THC-induced antinociception while AKR mice were much less responsive. Despite the heterogeneity in  $\Delta^9$ -THC-induced antinociception, there was little variability in  $\Delta^9$ -THC-induced hypothermia as a function of either sex or mouse strain. Likewise, across all strains, female mice were faster to develop tolerance or developed tolerance at the same rate as male littermates. Taken together, these studies highlight the therapeutic potential of  $\Delta^9$ -THC in pain management and underscore the importance of considering not only  $\Delta^9$ -THC dose as a function of sex, but potentially genetic differences among various populations when evaluating their clinical utility.

Support/Funding Information: DA044999

# Regulation of cAMP Signaling by Endothelin-A Receptor Antagonist, BQ123 in Morphine Tolerance in SH-SY5Y Human Neuroblastoma Cells

Shaifali Bhalla,<sup>1</sup> Margi Sheth,<sup>2</sup> and Zhong Zhang<sup>2</sup>

<sup>1</sup>Midwestern Univ College of Pharmacy–Downers Grove Campus; and <sup>2</sup>Midwestern University College of Pharmacy–Downers Grove Campus

Abstract ID 15499

Poster Board 475

**Purpose:** Endothelin-A receptor (ETAR) antagonist, BQ123 augments opioid analgesia, mitigates tolerance, and reduces withdrawal symptoms. Opioid-induced activation of GPCRs inhibits adenylyl cyclase and decreases 3',5'-cyclic adenosine monophosphate (cAMP). On the other hand, cAMP upregulation is observed in opioid tolerance and withdrawal. However, the signaling mechanisms involved in the effects of BQ123 on opioids are unknown. The objective of this study was to determine the effect of BQ123 on morphine-induced changes in cAMP signaling in SH-SY5Y neuroblastoma cells.

**Methods:** A stably transfected SH-SY5Y cell line (ATCC®) was established with GloSensor™ -23F cAMP plasmid (Promega™) containing the hygromycin-resistance gene, using ViaFect™ (Promega™) as transfection reagent. Cells were maintained and seeded in 96-well white, opaque-bottom plates ( $5 \times 10^4$  cells/well) in DMEM/10% FBS at 37°C/5% CO<sub>2</sub>. Promega's real-time cAMP-GloSensor™ assay was optimized and used to measure cAMP response in live cells. Transfected cells were incubated with equilibrium buffer [cAMP GloSensor™ reagent (2% (v/v)), 88% CO<sub>2</sub> independent medium, 10% FBS]. cAMP levels were determined by changes in luminescence using EnSpire™ multimode microplate reader (PerkinElmer). Cells were treated with morphine ( $10^{-5}$  – 10 μM) and BQ123 (1 μM) for 2 h in acute experiments, and with morphine (1 μM) in presence and absence of BQ123 (1 μM) for 24 h in chronic studies. Two challenge doses of morphine (10 μM and 20 μM) were tested in cells treated chronically with morphine. cAMP signaling was stimulated with isoproterenol ( $10^{-8}$  – 1 μM) as positive control. Experiments were repeated in triplicate and data was analyzed in GraphPad Prism version 9.00 (GraphPad Software, San Diego, CA).

**Results:** The positive control, isoproterenol, produced a concentration-dependent increase in cAMP in -23F cAMP plasmid transfected SH-SY5Y cells. Acute morphine treatment ( $10^{-5}$  – 10 μM for 2 h) decreased cAMP, while acute treatment with BQ123 (1 μM) further decreased cAMP response. It was intriguing to note that BQ123 (1 μM) enhanced morphine-induced reduction of cAMP responses. Chronic morphine (1 μM for 24 h) increased cAMP response by 53% ( $p < 0.05$ ) compared to acute treatment, confirming the development of tolerance. Chronic treatment with combination of morphine (1 μM) and BQ123 (1 μM) resulted in dose-dependent inhibition of cAMP levels in response to challenge doses of morphine.

**Conclusion:** The present study provided insight into the mechanism by which ETAR antagonists decrease morphine tolerance in SH-SY5Y cells. BQ123 enhanced morphine-induced cAMP signaling through G<sub>i</sub>-coupled mu opioid receptors (MORs) in both acute and chronic studies in SH-SY5Y cells, which support our previous work. These findings suggest that cAMP is involved in the effect of BQ123 on morphine tolerance. Detection of the MOR is essential to ensure that cAMP signaling is regulated by MOR agonists. We are presently confirming these effects by detection of MORs in SH-SY5Y cells using flow cytometry. *In vitro* experiments are ongoing to determine effects of BQ123 on intracellular calcium response to morphine treatment using fluorescent imaging. In future studies, we plan to investigate ETAR expression and explore potential interactions between MORs and ETARs in SH-SY5Y cells.

**Funding Info:** Faculty Research Grant, Midwestern University College of Pharmacy; Biomedical Sciences Program, College of Graduate Studies, Downers Grove, IL.

# Calcium Imaging Alongside Deep Behavior Learning in Fentanyl Vapor Self-Administration

Mason J. Hochstetler,<sup>1</sup> Jacob D. Layne,<sup>1</sup> Brandon M. Curry,<sup>1</sup> and Craig T. Werner<sup>1</sup>

<sup>1</sup>Oklahoma State University - Center for Health Sciences

Abstract ID 54277

Poster Board 476

The prevalence of opioid use disorder (OUD) and overdose deaths have reached epidemic proportions and constitute a global crisis. In 2019 synthetic opioids, including fentanyl, were being used by 1.2% of the worldwide population and contributed to more than 70% of the record-breaking number of overdose deaths. Fentanyl, which is often used clinically for anesthesia and analgesia, is commonly administered intravenously or by inhalation (smoking/vaping), which results in rapid drug bioavailability in the brain. Technical challenges have contributed greatly to our lack of understanding of the neurobiology of OUD, including limitations of behavioral models, difficulty tracking individual neurons longitudinally in freely behaving animals, and inadequate behavioral analysis tools. Intravenous drug self-administration is considered the “gold standard” model to investigate the neurobiology of OUD preclinically, but it remains difficult to perform *in vivo* electrophysiology or calcium imaging during drug self-administration due to the tangling of drug catheter and recording cable. This technical challenge was overcome with the development of a noninvasive mouse model of opioid self-administration using vaporized fentanyl that recapitulates key features of OUD. Imaging freely behaving animals is difficult, and conventional single-unit recordings can neither distinguish neuron subtypes nor track individual neurons longitudinally. In contrast, *in vivo* imaging using miniaturized fluorescence microscope (miniscope) systems allows for examining spatially and temporally coordinated activity in hundreds of individual neurons longitudinally in freely behaving animals. Complex behavioral analysis is infrequently incorporated in preclinical models, which likely contributes to limited translational impact. Recent computational advances in convolutional neural networks, pose estimation, and machine learning analysis has overcome these challenges to provide tools for computational neuroethology. We are leveraging these cutting-edge imaging technologies and behavioral analysis tools to gain a deeper insight into the neuronal ensembles that encode opioid-related behaviors during fentanyl self-administration and relapse.

**Keywords:** Opioid use disorder, self-administration, relapse, fentanyl, imaging



# Engagement of Beta-Arrestin 2 at the $\mu$ -opioid receptor reduces the abuse liability of opioids in mice during operant self-administration

Lindsey Felth,<sup>1</sup> Sarah W. Gooding,<sup>2</sup> Randi Foxall,<sup>3</sup> Zachary Rosa,<sup>2</sup> Izabella Sall,<sup>3</sup> Joshua Gipoor,<sup>2</sup> Anirudh Gaur,<sup>2</sup> Cheryl Whistler,<sup>3</sup> and Jennifer Whistler<sup>2</sup>

<sup>1</sup>Univ of California-Davis; <sup>2</sup>University of California-Davis; and <sup>3</sup>University of New Hampshire

Abstract ID 27678

Poster Board 477

In the United States, opioid overdoses claim the lives of 254 people daily. Despite their significant risks, opioid analgesics, including morphine, codeine, Vicodin and Oxycontin, are still regarded as the gold standard for alleviating pain clinically. There is still much unknown about what cellular mechanisms could improve the safety margin of these drugs, including reducing abuse liability. All of these drugs exert their analgesic effects through activation of the G<sub>i</sub> coupled  $\mu$ -Opioid receptor (MOR). When MOR is activated by its endogenous ligand, a regulatory molecule called  $\beta$ Arrestin-2 ( $\beta$ AR2) is recruited to the receptor, causing titration of signal transduction and subsequent internalization and recycling of the receptor. Conversely, when MOR is activated by many clinically relevant opioid drugs, such as morphine, it does not effectively recruit  $\beta$ AR2. The lack of  $\beta$ AR2 recruitment results in receptors remaining present on the membrane without being internalized and recycled back to the membrane. Continuous signaling from the membrane results in cAMP superactivation, a homeostatic adaptation meant to dampen the signaling. This cAMP superactivation has been implicated in neuronal and behavioral plasticity associated with compulsive drug seeking, the correlate of Opioid Use Disorders (OUDs) in mice. We hypothesize that effective recruitment of  $\beta$ AR2 to activated MORs will prevent cAMP superactivation, therefore preventing the neuronal and behavioral plasticity that result in compulsive drug seeking behavior. To investigate this hypothesis, this study utilizes four different genotypes of mice, with varying  $\beta$ AR2 recruitment profiles in response to morphine: WT (poorly recruits  $\beta$ AR2), RMOR (strongly recruits  $\beta$ AR2),  $\beta$ AR2-KO (does not recruit  $\beta$ AR2),  $\beta$ AR2-KO/RMOR (does not recruit  $\beta$ AR2). We utilized a novel oral operant self-administration paradigm for 17 weeks to model the transition from impulsive to compulsive drug use. At the end of 17 weeks, operant self-administration was extinguished and reinstatement was assessed to model OUDs. We calculated a composite compulsivity score to encapsulate behavior throughout the paradigm and classify each subject as compulsive or non-compulsive. Our results show that genotypes that effectively recruit  $\beta$ AR2 engaged in compulsive drug seeking less. We also show that compulsive drug seeking is not dependent on the amount of opioid consumed, nor the preference for opioid over other rewards. These results imply that drugs which effectively recruit  $\beta$ AR2 in response to activation at MOR have therapeutic utility as analgesics with reduced abuse liability.

**Support/Funding Information:** R21 DA 049565

# Retrospective Analyses of Dementia Outcomes in Patients Prescribed Immunosuppressants

Jacqueline Silva,<sup>1</sup> Daniel Jupiter,<sup>2</sup> and Giulio Taglialatela<sup>2</sup>

<sup>1</sup>Univ of Texas Medical Branch at Galveston; and <sup>2</sup>University of Texas Medical Branch

Abstract ID 28934

Poster Board 534

**Background:** The prevalence of dementia is approximately 11% in patients aged 65 and over in the US. Evidence suggests that patients treated with immunosuppressive calcineurin inhibitors (**CNI**) have a lower prevalence of dementia compared to the general population. Whether the observed effects are due to general immunosuppression or specifically to calcineurin inhibition remains unresolved. In this project we use electronic medical records (**EMR**) obtained from the TriNetX database to test the hypothesis that patients prescribed the CNI immunosuppressant tacrolimus have a lower prevalence of dementia relative to patients prescribed the non-CNI immunosuppressant sirolimus.

**Methods:** EMRs of patients prescribed tacrolimus or sirolimus were downloaded from the TriNetX Diamond Network, a longitudinal dataset of linked primary care, medical, and pharmacy claims data for over 200 million patients. Patients aged 65 and over who were prescribed the drug of interest for at least one year were analyzed. Patients prescribed both drugs or who were diagnosed with dementia before first recorded drug prescription were excluded from analysis. Patients prescribed tacrolimus were propensity-score matched, by demographics and several dementia risk factors, to those prescribed sirolimus, in a one-to-one ratio. We then retrospectively examined dementia outcomes using bivariate, survival, and competing risk analyses. All analyses were conducted using R version 4.2.0.

**Results:** Of the 2950 patients in each cohort, 190 (6.4%) prescribed tacrolimus and 202 (6.9%) prescribed sirolimus later developed dementia. Survival and competing risk analyses revealed no significant difference in dementia prevalence between cohorts. However, patients prescribed sirolimus were more likely to experience death relative to patients prescribed tacrolimus (HR = 1.37,  $p < 0.001$ ).

**Conclusion:** Our results do not support the hypothesis that patients prescribed tacrolimus have a lower prevalence of dementia relative to patients prescribed sirolimus. Nevertheless, both cohorts have a reduced prevalence of dementia compared to all patients aged 65 and over in the US. We suspect that the decreased prevalence of dementia can be attributed to an alternative converging impact of the diverse mechanisms of action of the two drugs rather than to general immunosuppression. However, the increased risk of death in patients prescribed sirolimus relative to tacrolimus may obscure result interpretation since dead patients are unable to develop dementia. While not significant, these results showcase the importance of presenting the null hypothesis to inform future studies and give mechanistic insight into potential treatments for dementia.

**Support/Funding Information:** NIH/NIA grant R01AG060718 to GT

# Who Knew? Dopamine Transporter Activity Is Critical in Innate and Adaptive Immune Responses

Emily Miller,<sup>1</sup> Adithya Gopinath,<sup>2</sup> Phillip M. Mackie,<sup>2</sup> Leah T. Phan,<sup>2</sup> Rosa Mirabel,<sup>2</sup> Aidan R. Smith,<sup>2</sup> Stephen Franks,<sup>2</sup> Ohee Syed,<sup>2</sup> Tabish Riaz,<sup>2</sup> Brian K. Law,<sup>2</sup> Nikhil Urs,<sup>2</sup> and Habibeh Khoshbouei<sup>3</sup>

<sup>1</sup>Univ of Florida; <sup>2</sup>University of Florida; and <sup>3</sup>McKnight Brain Inst of the Univ of Florida

**Abstract ID 54347**

**Poster Board 536**

The dopamine transporter (DAT) regulates the dimension and duration of dopamine transmission. DAT expression, its trafficking, protein-protein interactions, and its activity are conventionally studied in the CNS and within the context of neurological diseases such as Parkinson's Diseases and neuropsychiatric diseases such as drug addiction, attention deficit hyperactivity and autism. However, DAT is also expressed at the plasma membrane of peripheral immune cells such as monocytes, macrophages, T-cells, and B-cells. DAT activity via an autocrine/paracrine signaling loop regulates macrophage responses to immune stimulation. In a recent study, we identified an immunosuppressive function for DAT, where blockade of DAT activity enhanced LPS-mediated production of IL-6, TNF- $\alpha$ , and mitochondrial superoxide levels, demonstrating that DAT activity regulates macrophage immune responses. In the current study, we tested the hypothesis that in the DAT knockout mice, innate and adaptive immunity are perturbed. We found that genetic deletion of DAT (DAT<sup>-/-</sup>) results in an exaggerated baseline inflammatory phenotype in peripheral circulating myeloid cells. In peritoneal macrophages obtained from DAT<sup>-/-</sup> mice, we identified increased MHCII expression and exaggerated phagocytic response to LPS-induced immune stimulation, suppressed T-cell populations at baseline and following systemic endotoxemia and exaggerated memory B cell expansion. In DAT<sup>-/-</sup> mice, norepinephrine and dopamine levels are increased in spleen and thymus, but not in circulating serum. These findings in conjunction with spleen hypoplasia, increased splenic myeloid cells, and elevated MHC-II expression, in DAT<sup>-/-</sup> mice further support a critical role for DAT activity in peripheral immunity. While the current study is only focused on identifying the role of DAT in peripheral immunity, our data point to a much broader implication of DAT activity than previously thought. This study is dedicated to the memory of Dr. Marc Caron who has left an indelible mark in the dopamine transporter field.

# Discovery of an Allosteric Agonist for Schizophrenia Risk Gene GPR52 with Antipsychotic Activity

Ryan E. Murphy,<sup>1</sup> Daniel E. Felsing,<sup>1</sup> Nolan M. Dvorak,<sup>1</sup> Fernanda Laezza,<sup>1</sup> Kathryn A. Cunningham,<sup>1</sup> and John A. Allen<sup>1</sup>

<sup>1</sup>University of Texas Medical Branch

Abstract ID 27887

Poster Board 537

GPR52, recently identified by GWAS as a schizophrenia risk gene, is a brain orphan G protein-coupled receptor. GPR52 is primarily expressed in D2 medium spiny neurons in the human striatum, particularly the nucleus accumbens. This unique expression profile of GPR52 suggests that the receptor may functionally regulate cAMP signaling to oppose the activity of dopamine D2 receptors. This distinguishes GPR52 as an attractive target for numerous psychiatric disorders, including schizophrenia and substance use disorders. Here we report our efforts to elucidate GPR52 neuronal signaling and to discover selective agonists for this receptor. In molecular signaling studies, expression of low levels of human GPR52 in wildtype HEK293 cells elevated basal cAMP levels over 100-fold, with further elevation of cAMP in response to the agonist FTBMT. This cAMP response was eliminated by stable knockout of  $G_{s/olf}$  proteins using CRISPR/Cas9 genome editing. Iterative medicinal chemistry design and pharmacological evaluation of novel small molecules led to the optimized GPR52 agonist PW0787. PW0787 increased GPR52 cAMP signaling with good potency (EC<sub>50</sub>: 135nM) and efficacy (300% over basal), while exhibiting excellent target selectivity, brain penetrance, and serum concentration. Molecular docking of PW0787 into the GPR52 crystal structure suggested compound binding with extracellular loop 2 (ECL2) and an allosteric mode of action. In a whole cell patch clamp study using mouse brain slices, PW0787 increased the frequency and number of evoked action potentials in D2, but not D1, medium spiny neurons of the nucleus accumbens. In this study, PW0787 also rescued neuronal excitability to basal levels after treatment with the dopamine D2 receptor agonist quinpirole. Dose-dependent testing of PW0787 revealed 3 and 10 mg/kg treatments in mice significantly reduced amphetamine-induced hyperlocomotion, indicating antipsychotic-like activity. Together, these findings indicate that GPR52, via  $G_{s/olf}$  cAMP signaling, is a highly constitutively active, excitatory receptor selectively expressed in D2 medium spiny neurons. Our drug discovery effort has resulted in novel GPR52 activators with PW0787 being a potent, selective, orally bioavailable, brain-penetrant agonist that excites D2 medium spiny neurons and shows antipsychotic-like activity. Functional alterations of striatal cAMP signaling by GPR52 may help explain why the receptor is a schizophrenia risk gene. These findings further support that GPR52 is a druggable target with therapeutic potential for treating psychiatric disorders.

**Acknowledgements:** The UTMB Center for Addiction Research, NIDA 1U18DA052543-01 (JAA), and 2022 PhRMA Foundation Pre-Doctoral Fellowship in Drug Discovery (REM).

# Structure based approaches on fentanyl template to design novel mu opioid modulators

Rohini Ople,<sup>1</sup> Haoqing Wang,<sup>2</sup> Qiongyu Li,<sup>3</sup> Ben Polacco,<sup>3</sup> Sarah Bernhard,<sup>4</sup> Kevin Appourchaux,<sup>5</sup> Sashrik Sribhashyam,<sup>4</sup> Shainnel Eans,<sup>6</sup> Ruth Huttenhain,<sup>3</sup> Jay McLaughlin,<sup>6</sup> Brian Kobilka,<sup>7</sup> and Susruta Majumdar<sup>4</sup>

<sup>1</sup>Univ of Health Science and Pharmacy; <sup>2</sup>Stanford University School of Medicine, Stanford, CA, USA; <sup>3</sup>University of California; <sup>4</sup>University of Health Sciences & Pharmacy & Washington University School of Medicine; <sup>5</sup>University of Health Sciences & Pharmacy; <sup>6</sup>University of Florida; and <sup>7</sup>Stanford Univ Medical Ctr

Abstract ID 52769

Poster Board 538

Opioids are used for the treatment of acute to severe pain. Usage of opioids also produces liabilities like respiratory depression and addiction, which in combination with illicit use of fentanyl and designer analogs has contributed to the opioid epidemic. Most approaches to design safer opioids have been restricted to targeting the orthosteric binding sites. We have recently reported a novel strategy to design functionally selective opioids by targeting the sodium binding allosteric site in the mu opioid receptor (MOR). The lead ligand C6 guano engages a key residue Asp<sup>250</sup> in the sodium site through a salt bridge with a guanidine group in the ligand. C6 guano shows MOR dependent antinociception with reduced adverse effects seen with clinically used opioids (Faouzi et al., *Nature* 2023, **613**, 767–774). While representing a significant advance in the design of opioids, C6 guano is supra-spinally active because of the polar and charged guanidine group. Using the cryo-EM structure of C6 guano bound to MOR, we designed second generation analogs to optimize the systemic activity of C6 guano. Characterization of analogs led to the identification of a fentanyl-derived compound named RO-76 which in TRUPATH assays showed reduced efficacy at all Gi/o/z subtypes and no measurable efficacy at  $\beta$ -arrestin-1/2 and labelled unique transducers in APEX2 proximity labeling assays. Unlike C6 guano which showed direct engagement of the sodium site, RO-76 interacted with the sodium site residues through a water in cryo-EM of RO-76 bound to MOR-Gi complex. Previous high-resolution structures of MOR have predicted the presence of a polar cavity in the sodium binding pocket, but these waters have not been rationally targeted before at MOR or other GPCRs to the best of our knowledge. In mice, the drug was systemically active in tail withdrawal assays, and showed reduced respiratory depression and conditioned place preference compared to morphine.

In summary, we envision that targeting the sodium binding site may be a potential avenue to both probe the role of the sodium site in MOR function as well as development of a new class of analgesics in the near future.

## **Support and sponsors:**

Center for Clinical Pharmacology

University of Health Sciences and Pharmacy at St. Louis

National Institute of Drug Abuse

# Comparative Analysis of Neuro-markers in Angiotensin II High Salt Diet Hypertensive Rats

Helmut Gottlieb,<sup>1</sup> Cynthia Franklin,<sup>2</sup> Jeffrey Angell,<sup>2</sup> Nikhil Joseph,<sup>2</sup> Clayton Townsend,<sup>2</sup> Anita Nancherla,<sup>2</sup> David Yzquierdo,<sup>2</sup> and Jessica Bradley<sup>3</sup>

<sup>1</sup>Univ of Incarnate Word Feik School of Pharmacy; <sup>2</sup>UIW Feik School of Pharmacy; and <sup>3</sup>UIW School of Osteopathic Medicine

**Abstract ID 21860**

**Poster Board 539**

Chronic heart failure produces a marked increase in renin-angiotensin-aldosterone system (RAAS) which contributes to changes in cardiovascular and renal system. This study examines the changes in cFOS, FosB, and inducible cAMP element repressor (ICER) immunostaining expression in supraoptic nucleus (SON) and hypothalamic paraventricular nucleus (PVN) of Ang II infused rats on a high salt diet (AngII/NaCl) as compared to normal rats. FosB and cFos have been well established as neuronal markers for excitation, chronically and acutely respectively. ICER has shown to inhibit cAMP in neuroendocrine cells, thus serving as a potential marker for neuro-inhibition. Alternate sets of forebrain sections were processed using a commercially available antibody. Sections were also double labeled with vasopressin to anatomically define specific brain regions. FosB and cFos expression was significantly increased in both PVN and SON as compared to control animals. ICER expression decreased in Ang II/NaCl compared to control animals. There was no significant change in urine and sodium excretion between AngII/NaCl and control animals. Altogether, this data provides new information concerning the use of neuronal markers used to identify CNS changes in normal vs pathophysiological conditions.

*Supported by NIH R16GM145433*

# Protein kinase D2 confers neuroprotection by promoting AKT and CREB activation in ischemic stroke

Jaclyn Connelly,<sup>1</sup> Xuejing Zhang,<sup>1</sup> Yapeng Chao,<sup>1</sup> Yejie Shi,<sup>1</sup> Tija Jacob,<sup>1</sup> and Qiming Wang<sup>1</sup>

<sup>1</sup>Univ of Pittsburgh School of Medicine

**Abstract ID 54838**

**Poster Board 540**

Ischemic stroke, constituting 80-90% of all strokes, is a leading cause of death and long-term disability in adults. There is an urgent need to discover new targets and therapies for this devastating condition. Protein kinase D (PKD), as a key target of diacylglycerol long-known for its involvement in ischemic responses, has not been well studied in ischemic stroke, particularly PKD2. In this study, we found that PKD2 expression and activity were significantly upregulated in the ipsilateral side of the brain after transient focal cerebral ischemia, which coincides with the upregulation of PKD2 in primary neurons in response to in vitro ischemia, implying a potential role of PKD2 in neuronal survival in ischemic stroke. Using kinase-dead PKD2 knock-in (PKD2-KI) mice, we examined whether loss of PKD2 activity affected stroke outcomes in mice subjected to 1 h of transient middle cerebral artery occlusion (tMCAO) and 24 h of reperfusion. Our data demonstrated that PKD2-KI mice exhibited larger infarction volumes and worsened neurological scores, indicative of increased brain injury, as compared to the wild-type (WT) mice, further confirming a neuroprotective role of PKD2 in ischemia/reperfusion (I/R) injury. Mouse primary neurons obtained from PKD2-KI mice also exhibited increased cell death as compared to the WT neurons when subjected to in vitro ischemia. We have further identified AKT and CREB as two main signaling nodes through which PKD2 regulates neuronal survival during I/R injury. In summary, PKD2 confers neuroprotection in ischemic stroke by promoting AKT and CREB activation and targeted activation of PKD2 may benefit neuronal survival in ischemic stroke.

**Support/Funding Information:** American Heart Association award 19TPA34850096

# Sex Differences in Stimulant Action at the Dopamine Transporter

Jennifer Tat,<sup>1</sup> Lillian Brady,<sup>2</sup> and Erin Calipari<sup>1</sup>

<sup>1</sup>Vanderbilt Univ; and <sup>2</sup>Vanderbilt University

**Abstract ID 15167**

**Poster Board 541**

Substance use disorder (SUD) is a chronic, relapsing brain disease characterized by irregularities in motivation and reward processing. In humans, women transition from recreational to chronic substance abuse more rapidly than men and are more likely to relapse following abstinence. Thus, understanding the biological basis of these differences is critical for improved SUD treatment in women. The reinforcing properties of nearly all drugs of abuse are dependent on their ability to increase dopamine levels in the nucleus accumbens (NAc) – a brain region involved in reward processing and motivation. For stimulant drugs of abuse, this occurs via their ability to alter the function of the dopamine transporter (DAT). Three notable stimulants - cocaine, amphetamine, and methylphenidate - all can bind to the DAT and thus decrease dopamine clearance and increase the magnitude and time course of synaptic dopamine levels. However, unlike cocaine and methylphenidate, amphetamine can also drive active dopamine release through reversal of the DAT. The goal of this study was to understand exactly how biological sex alters the ability of these drugs to alter dopamine dynamics in the NAc depending on their mechanism of action. There are a variety of factors that could contribute to sex differences in stimulant effects on reward circuitry, one being estrous cycle-dependent ovarian hormone fluctuations. Previous studies have demonstrated that cocaine has an enhanced ability to inhibit the DAT in females during estrus (high circulating hormones) as compared to females in diestrus (low circulating hormones) and males, but it is unclear as to whether this effect is unique to cocaine or generalizes across all stimulant drugs. To this end, *ex vivo* fast-scan cyclic voltammetry (FSCV) combined with site-specific pharmacology was utilized to measure the effect of cocaine, amphetamine, and methylphenidate on sub-second dopamine release in males and freely-cycling females. We found that amphetamine's ability to inhibit dopamine uptake was higher in estrus females than diestrus females and males, suggesting that the effects are hormone-mediated. However, methylphenidate's ability to inhibit dopamine uptake was higher in females than males, regardless of cycle stage. Together, these data suggest that sex differences in the primary mechanism of action of stimulant drugs exist and may play a key role in SUD development in males and females.

Funding was provided by startup funds from V.U. School of Medicine, Department of Pharmacology and the National Institutes of Health (NIH) (to E.S.C.). Funds from the National Institute of Drug Abuse (NIDA) DA042111 and DA048931, the Brain and Behavior Research Foundation, Whitehall Foundation, and the Edward J Mallinckrodt Jr. Foundation (E.S.C) also supported this work.



# Mediation Analysis Reveals that Opioid-Induced Sleep Disruption is Partially Mediated by Increased Motor Activity in C57BL/6J (B6) Mice

Diana Zebadúa Unzaga,<sup>1</sup> Xiaojuan Zhu,<sup>2</sup> Joshua M. Price,<sup>2</sup> Michael A. Oneil,<sup>2</sup> Ralph Lydic,<sup>2</sup> and Helen A. Baghdoyan<sup>2</sup>

<sup>1</sup>Univ of Tennessee; and <sup>2</sup>University of Tennessee

Abstract ID 19255

Poster Board 542

Opioids are essential for pain management yet cause unwanted side effects in humans and mice, such as sleep disruption (O'Brien et al., 2021; doi:10.1152/jn.00266.2021) and hypothermia (Baker & Meert, 2002; doi:10.1124/jpet.102.037655). Some opioid effects in B6 mice differ from effects in humans. For example, opioids cause a dose-dependent increase in motor activity in mice (Haouzi et al., 2021; doi:10.1152/jn.00711.2020) but not in humans. Preliminary data previously showed that in B6 mice fentanyl significantly and dose-dependently increased wakefulness, disrupted sleep, increased motor activity, and decreased body temperature (Zebadúa Unzaga et al., 2022; <https://doi.org/10.1096/fasebj.2022.36.S1.R2168>). The present IACUC-approved study increased the sample size, included morphine, and applied mediation analyses (Vuurde & Bolger, 2018; <https://doi.org/10.3758/s13428-017-0980-9>) to determine whether opioid-induced changes in motor activity or body temperature mediated the increase in wakefulness.

Adult B6 males (n=12) were housed in a 12:12h light:dark cycle. Mice were implanted with subcutaneous telemeters (DSI HD-X02) to simultaneously record electroencephalogram (EEG), electromyogram (EMG), motor activity, and body temperature. Using a crossover design all mice received subcutaneous injections (0.3 mL) of saline (control) and increasing half-log doses of fentanyl (0.001 to 3 mg/kg) and morphine (0.01 to 30 mg/kg) within 90 min after lights on. EEG and EMG signals were recorded for 4 h post injection to quantify percent of recording time spent in wakefulness (Wake), rapid eye movement (REM) sleep, and non-REM sleep. Within-subject multi-level mediation regression analyses assessed whether motor activity and/or body temperature affected the relationship between opioid dose and percent of time spent awake (%Wake). The mediation model (Fig. 1, modified from Vuurde & Bolger, 2018) illustrates that opioid dose is the hypothesized causal independent variable, %Wake is the measured outcome, and motor activity (Motor) or body temperature (Temp) are measured variables that may mediate the effect of opioid dose on %Wake. Mediation analyses were performed using Stata 17 (StataCorp, 2021). A log transformation of motor activity was performed to meet the assumptions of normality of the model residuals.

The results revealed that doses of fentanyl  $\geq 0.1$  mg/kg and doses of morphine  $\geq 1$  mg/kg were significant predictors of increased %Wake ( $p < 0.001$ ). Doses of fentanyl  $\geq 0.1$  mg/kg and morphine  $\geq 3$  mg/kg also were significant predictors of increased motor activity ( $p < 0.001$ ). Motor activity significantly mediated the effect of fentanyl dose ( $p < 0.001$ ) and morphine dose ( $p < 0.001$ ) on %Wake. Body temperature did not significantly mediate the effect of opioid dose on %Wake.

Thus, mediation analyses showed that the fentanyl- and morphine-induced increases in wakefulness were partially mediated (15.9% and 21.7%, respectively) by motor activity. Whether opioids act directly to enhance wake-promoting mechanisms and/or inhibit sleep-generating neuronal circuits remains to be determined. The present findings encourage quantifying the effects of systemically administered opioids on wake- and sleep-promoting neurotransmitters.

**Support/Funding Information:** University of Tennessee

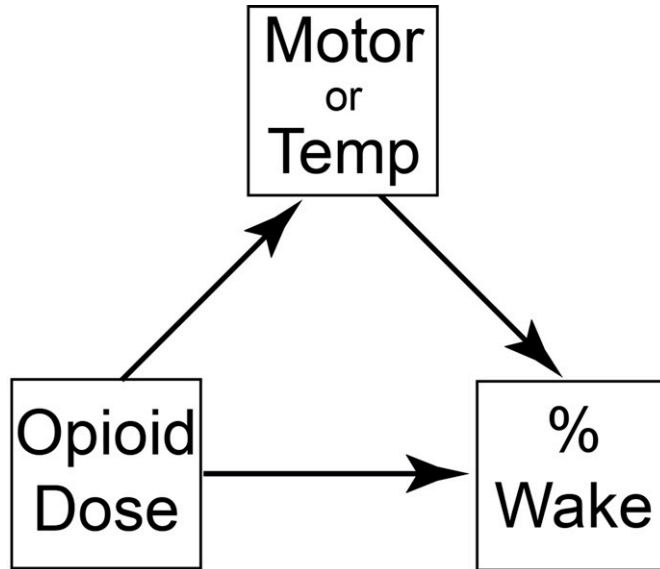


Figure 1. Mediation model

# Sex Differences in GABA Regulation of Dopamine Release in the Nucleus Accumbens and its Role in Cocaine Use Disorder

Brooke Christensen,<sup>1</sup> Addison R. Van Namen,<sup>2</sup> and Erin Calipari<sup>1</sup>

<sup>1</sup>Vanderbilt Univ; and <sup>2</sup>Vanderbilt University

Abstract ID 20953

Poster Board 543

**Background:** While sex differences in the pervasiveness and prognosis of neuropsychiatric disorders have long been known to exist, there are few instances where approaches to pharmacological treatment of these disorders differ between the sexes, which likely contributes to ineffective treatments in women. In substance use disorder (SUD), women exhibit increased propensity to use drugs, a faster transition to addiction from first use, greater problems maintaining abstinence, and relapse at a higher rate than men. At the center of sex-differences in addiction vulnerability is the mesolimbic dopamine system. While work has focused on sex differences in the anatomy of dopamine neurons and relative dopamine levels, an important characteristic of dopamine release from axon terminals in the nucleus accumbens (NAc) is that it is rapidly modulated by local regulatory mechanisms independent of somatic activity. GABA released from local microcircuitry in the NAc has been shown to play a critical role in regulating dopamine release at the terminals through ionotropic GABA-A and G<sub>i</sub>-coupled GABA-B receptors and has also been implicated in cocaine-induced processes. Here we define basal sex differences in dopamine release regulation via GABA in the NAc and show how this is dysregulated by chronic cocaine exposure.

**Methods:** To dissociate dopamine terminal regulation from somatic regulation, we utilize *ex vivo* fast scan cyclic voltammetry and optogenetics in striatal brain slices. Dopamine release was evoked from terminals, and GABA receptor modulation of this signal was determined via bath application of picrotoxin (GABA-A antagonist), muscimol (GABA-A agonist), saclofen (GABA-B antagonist), and baclofen (GABA-B agonist) to slices. This was done at baseline in both males and females as well as after chronic cocaine exposure.

**Results:** First, we found that both GABA-A and GABA-B receptors modulate dopamine release on a rapid time scale directly at the terminals in the NAc. There were sex differences in this regulation, with enhanced GABA-A-mediated inhibition observed in females and greater GABA-B-mediated inhibition observed in males. Additionally, GABAergic modulation of dopamine release was blunted in males following chronic cocaine exposure.

**Conclusion:** The results of these studies will contribute to the understanding of how sex fits into the comprehensive framework for dopamine release regulation and how dysregulation of these processes influences the trajectory of CUD in both males and females.

Funding was provided by startup funds from V.U. School of Medicine, Department of Pharmacology and the National Institutes of Health (NIH) (to E.S.C.). Funds from the National Institute of Drug Abuse (NIDA) DA042111, DA048931, DA056221, the Brain and Behavior Research Foundation, Whitehall Foundation, and the Edward J Mallinckrodt Jr. Foundation (E.S.C) also supported this work.

# Comparison of the mu-opioid receptor antagonists methocinnamox (MCAM) and naloxone to reverse the ventilatory-depressant effects of fentanyl and heroin in male rats

Takato Hiranita,<sup>1</sup> Nicholas P. Ho,<sup>2</sup> and Charles P. France<sup>3</sup>

<sup>1</sup>Univ of Texas Hlth San Antonio; <sup>2</sup>UT Health San Antonio; and <sup>3</sup>Univ of Texas Hlth Sci Ctr

Abstract ID 15541

Poster Board 544

The number of opioid overdose deaths has increased significantly over the past decade. The life-threatening effect of opioids is ventilatory depression and the  $\mu$ -opioid receptor (MOR) antagonist naloxone is the only medication approved by the United States Food and Drug Administration for treating opioid overdose. However, the short duration of action of naloxone limits its effectiveness to reverse and protect against opioid overdose. A longer-acting MOR antagonist could improve treatment of opioid overdose. The MOR antagonist methocinnamox (MCAM) antagonizes the ventilatory-depressant effects of the non-morphinan MOR agonist fentanyl in rats with an unusually long duration of action. The present study extended previous studies and compared the potency and effectiveness of MCAM to naloxone for reversing the ventilatory-depressant effects of fentanyl and the morphinan heroin in eight male Sprague-Dawley rats in a within-subjects design. Whole-body plethysmography was employed (normal air) to assess ventilatory parameters every minute continuously throughout sessions [ventilatory frequency ( $f$ , breaths/minute); tidal volume ( $V_T$ , mL/breath/kg); and minute volume ( $V_E$ , mL/minute/kg), the product of  $f$  and  $V_T$ ]. Chambers were equipped with towers and swivels that allowed automated i.v. infusions through a chronic indwelling catheter without breaking the seal of the chamber. Immediately after a 45-minute habituation period, saline or an acute dose of heroin or fentanyl was administered i.v. Five minutes later rats received a second infusion of MCAM, naloxone, or vehicle (10%  $\beta$ -cyclodextrin in water). Heroin (0.32-3.2 mg/kg) and fentanyl (0.0032-0.1 mg/kg) dose-dependently and significantly decreased ventilation (e.g., area under the curve, 1-10 minutes) of  $V_E$  up to 27.0% (One Way Repeated Measures Analysis of Variance followed by Bonferroni  $t$ -test,  $t=16.5$ ,  $P<0.001$ ) and 29.4% ( $t=24.6$ ,  $P<0.001$ ) of saline control, respectively. Heroin ( $ED_{50}$  values: 4.81 micromol/kg, i.v.) was 36.2-fold less potent than fentanyl in decreasing  $V_E$ . Both MCAM and naloxone (0.0001-0.01 mg/kg) dose-dependently and significantly reversed ventilatory depression ( $V_E$ ) by heroin (3.2 mg/kg) or fentanyl (0.1 mg/kg) compared with vehicle control ( $t$  values  $\geq 15.1$ ,  $P$  values  $< 0.001$ ). MCAM and naloxone reversed the ventilatory-depressant effects of heroin (3.2 mg/kg, i.v.) up to 67.7% and 94.0% of vehicle control (i.e. saline followed by vehicle), respectively. MCAM and naloxone reversed the ventilatory-depressant effects of fentanyl (0.1 mg/kg, i.v.) up to 58.9% and 129.2% of vehicle control, respectively. The potency of MCAM [ $ED_{50}$  values: 0.0141 (95% confidence interval: 0.0121, 0.0166) and 0.0158 (0.0139, 0.0184) micromol/kg, i.v.] did not significantly differ from that of naloxone to reverse the ventilatory-depressant effects of heroin and fentanyl (potency ratios: 1.25 and 1.96), respectively. The present study demonstrates that MCAM is as potent and effective as naloxone to reverse the ventilatory-depressant effects of morphinan and non-morphinan MOR agonists. Supported by USPHS grant UG3DA048387-S1 and the Welch Foundation (Grant AQ-0039).

# Regulation of Neuronal Activity by GluD1 Current in Brain Slices

Stephanie Gantz,<sup>1</sup> Daniel Copeland,<sup>1</sup> and Aleigha Gugel<sup>1</sup>

<sup>1</sup>University of Iowa

**Abstract ID 28219**

**Poster Board 545**

Ion channel function of native delta glutamate receptors (GluD<sub>R</sub>s) is incompletely understood. Previously, we and others have shown that activation of G<sub>q</sub> protein-coupled receptors (GPCR) produces a slow inward current carried by GluD<sub>1R</sub>. GluD<sub>1R</sub> also carry a tonic cation current of unknown origin. Here, using voltage-clamp electrophysiological recordings from adult male and female mouse brain slices containing the dorsal raphe nucleus, we find no role of on-going G protein-coupled receptor activity in generating or sustaining tonic GluD<sub>1R</sub> current. Neither augmentation nor disruption of G protein activity affected tonic GluD<sub>1R</sub> current, suggesting that on-going G protein-coupled receptor activity does not give rise to tonic GluD<sub>1R</sub> current. Further, tonic GluD<sub>1R</sub> current was unaffected by the addition of external glycine or D-serine, which influence GluD<sub>2R</sub> current at millimolar concentrations. Instead, GPCR-stimulated and tonic GluD<sub>1R</sub> current is regulated by external calcium. In current-clamp recording, block of GluD<sub>1R</sub> channels hyperpolarized the membrane by ~10 mV at subthreshold potentials, reducing excitability. Thus, GluD<sub>1R</sub> carry a G protein-independent tonic current that contributes to subthreshold neuronal excitation in the dorsal raphe nucleus.

# Acute and Subchronic GPR171 Agonism Affects Anxiety and Depression in Female Mice

Megan Raddatz,<sup>1</sup> and Erin Bobeck<sup>1</sup>

<sup>1</sup>Utah State Univ

Abstract ID 26904

Poster Board 546

G-protein coupled receptors (GPCRs) are one of the most promising targets for pharmaceutical intervention in psychiatric disorders. GPR171, a newly orphanized GPCR, is of particular interest as a novel therapeutic as it is highly expressed in areas directly involved in anxiety and depression. In males, acute treatment with a GPR171 antagonist decreased anxiety-like behavior compared to vehicle-treated mice but did not affect depressive or fear behaviors. This research has not been extended to females despite females representing approximately two-thirds of those afflicted with anxiety and/or depression. To address the need to develop and test treatments in the larger clinical population, the aim of our research was to determine the role of GPR171 in depression and anxiety in females. We also sought to determine whether the effects of GPR171 were dependent on treatment length, as the long-term effects of treatments are generally neglected in studies exploring depression and anxiety in mice. To explore acute treatment effects, female mice were subjected to a single injection of a GPR171 agonist, antagonist, or vehicle and immediately tested for depressive symptoms in the forced swim test (FST). A separate cohort of females were injected with either a GPR171 agonist, antagonist, or vehicle for 6 days, followed by testing in the elevated plus maze (EPM), and FST to assess anxiety and depression. Time spent in the closed arms vs. open arms in the EPM was automatically recorded using ANYmaze software and immobility time in the FST was manually recorded by a blind reviewer. Results indicate that acute agonist treatment reduced immobility time in the FST in females, while the antagonist did not have any measurable effect compared to the vehicle. Subchronic treatment with the agonist also reduced immobility time in the FST as compared to the vehicle treated mice, indicating that the agonist had an antidepressant effect that was consistent regardless of treatment length. Interestingly, results indicate that subchronic agonist-treated mice had a higher ratio of time spent in the closed vs. open arms in the EPM when compared to vehicle treated mice, suggesting that subchronic treatment of the agonist increased anxiety compared to the vehicle treated mice while the antagonist had no effect. These effects are unlikely to be attributed to any differences in movement seeing as mice did not differ significantly in total distance traveled in the open field test, regardless of treatment group. Together, these findings identify a GPR171 agonist as a potential antidepressant target in females, but future studies are needed to elucidate on the mechanisms underlying the increase of anxiety behaviors under subchronic agonist treatment.

# Involvement of the Rat Medial Prefrontal Cortex 5-HT<sub>2A</sub> Receptor in Impulsive Action

Juliana L. Giacomini,<sup>1</sup> Christina R. Merritt,<sup>1</sup> Kathryn A. Cunningham,<sup>1</sup> and Noelle C. Anastasio<sup>1</sup>

<sup>1</sup>Univ of Texas Medical Branch

Abstract ID 24537

Poster Board 547

Transmission via 5-HT<sub>2A</sub> receptors (**5-HT<sub>2A</sub>R**) in medial prefrontal cortex (**mPFC**) is implicated in the regulation of impulsive action which can be assessed in models which evaluate inhibitory control over prepotent motor responses. Systemic administration of a selective 5-HT<sub>2A</sub>R antagonist consistently attenuates impulsive action in choice serial reaction time (**CSRT**) tasks of motor impulsivity. Intra-mPFC 5-HT<sub>2A</sub>R blockade induces subtle enhancements in inhibitory control. Intriguingly, high-impulsive rats exhibit higher levels of 5-HT<sub>2A</sub>R expression and function. Here, we tested the hypothesis that stable knockdown of the 5-HT<sub>2A</sub>R locally in the mPFC regulates inhibitory control involving cues in the sucrose-reinforced 1-choice CSRT task.

**Methods:** A short hairpin RNA (**5-HT<sub>2A</sub>R-shRNA**) that efficiently knocks down over 90% of 5-HT<sub>2A</sub>R mRNA *in vitro* was designed, validated, and packaged into an adeno-associated viral (**AAV**) vector; a non-silencing control (**NSC**) hairpin was designed and assessed to have no effect on 5-HT<sub>2A</sub>R mRNA expression. Male Sprague-Dawley rats were trained to stability in a sucrose-reinforced 1-CSRT task with a cued inter-trial interval (**ITI**) of 5-sec (**ITI-5s**) and challenged in sessions with ITI 8-sec (**ITI-8s**) prior to surgical delivery of viral vectors. Rats received bilateral stereotaxic infusions of 5-HT<sub>2A</sub>R-shRNA-eGFP AAV (n=8) or NSC-eGFP-AAV (n=8) into the mPFC (AP: +3.0 mm; ML: +1.4 mm; DV: -5.1, -4.1, -3.1 mm; relative to Bregma). After recovery, rats were restabilized in the 1-CSRT task with ITI-5s with two post-surgery probes in ITI-8s.

**Results:** Statistical analysis of performance on the ITI-5s and ITI-8s parameters did not yield significant effects of the knockdown of 5-HT<sub>2A</sub>R in mPFC. Further analysis centered on the effects of increased ITI challenges revealed that, normalized to the ITI-5s baseline, intra-mPFC 5-HT<sub>2A</sub>R knockdown significantly increased ITI-8s premature responding as compared to pre-surgery baselines. Thus, intra-mPFC 5-HT<sub>2A</sub>R knockdown revealed an increased impact of longer cued ITIs (ITI-8s) relative to baseline (ITI-5s) on premature responding for sucrose in 1CSRT task.

**Conclusions:** These results suggest that 5-HT<sub>2A</sub>R transmission in the mPFC modulates impulsive action related to cues associated with a task and/or reward. Therefore, identification of 5-HT<sub>2A</sub>R distribution along neural circuits governing inhibitory control of motivated behavior could lead to a new mechanistic understanding of behavioral impulsivity. We are currently conducting tract-tracing studies to determine the anatomical distribution of 5-HT<sub>2A</sub>R-containing mPFC afferents to uncover the involvement of downstream connectivity that regulates impulsive behavior.

**Financial Support:** T32DA07287, P50DA033935

# Butyrate Prevents Opioid Induced Peripheral Hypersensitivity via a Gut Dependent Mechanism

Donald Jessup,<sup>1</sup> and Hamid I. Akbarali<sup>2</sup>

<sup>1</sup>Virginia Commonwealth Univ; and <sup>2</sup>Virginia Commonwealth Univ, Med College of Virginia

Abstract ID 16983

Poster Board 569

**Background:** Recent evidence has shown that changes in the gut microbiome occur with chronic opioid use in both rodent and human models (1-2). Opioid induced dysbiosis has been implicated in some of the pharmacological effects of opioids. However, it is unclear how chronic opioid use alters the gut microbiome. Interestingly, studies have also shown that the gut epithelial barrier is disrupted by chronic morphine (2). An important constituent of the commensal microbiome are bacterial species that ferment fibers into short chain fatty acids (SCFA). The SCFA butyrate is known to improve the integrity of the epithelium and enhance antimicrobial peptide release. Based on this, we hypothesized that sodium butyrate can relieve peripheral hypersensitivity as well as reduce primary nociceptor hyperexcitability in experimental models of opioid induced peripheral hypersensitivity.

**Methods:** Animals were administered a ramping dose of morphine (Mor), and organized into the following treatment groups: Mor (20mg/kg i.p b.i.d on day 1 to 80mg/kg i.p b.i.d on day 4) ± sodium butyrate (NaBut) (250mM p.o b.i.d), and Saline ± NaBut (250mM p.o b.i.d). Animals were assayed using a 50°C hot-plate for opioid-induced hyperalgesia, and primary nociceptors from L4-S1 dorsal root ganglia were collected for whole-cell patch clamp electrophysiological recordings.

**Results:** Chronic opioid exposure induced thermal hypersensitivity (14.8s ± 0.568 Mor vs 28.16s ± 0.848 saline), which was reversed by NaBut (250mM p.o b.i.d) (24.84s ± 0.675) (N=14 per treatment group). Electrophysiological recordings demonstrated Mor treated animals elicited a greater number of action potentials (APs) compared to controls (Mor: 4.44 ± 0.532 vs 2.1 ± 0.182 APs Saline), indicating enhanced excitability. NaBut treatment attenuated this enhanced excitability (Mor + NaBut 2.29 ± 0.354 APs) (N=6 n=17 per treatment). Phase plane analysis of hyperexcitable cells indicated significant changes in sodium channel kinetics which was prevented by in-vivo butyrate administration but not by direct application of butyrate to DRG neurons. In order to investigate the specific contribution of the gastrointestinal tract on Mor-induced neuronal hyperexcitability, conditioned media was collected from colonic tissues (colonic conditioned media (CCM)) and applied to naïve DRG neurons. CCM from Mor-treated colons enhanced excitability (Mor 5.6 vs Saline 2.47 APs) that was absent in CCM from the Na-butyrate treatment group (3.15 APs).

**Discussion/Conclusion:** In both the in-vivo behavioral assays of peripheral hypersensitivity and in ex-vivo electrophysiological experiments, butyrate reversed the enhanced excitability and hypersensitivity of Mor-treated animals. These findings demonstrate that the SCFA butyrate, a major metabolite of the gut microbiome plays an important role in preventing the development of opioid-induced peripheral hypersensitivity.

## References

- 1.) Kang M, Mischel RA, Bhawe S, Komla E, Cho A, Huang C, Dewey WL, Akbarali HI. The effect of gut microbiome on tolerance to morphine mediated antinociception in mice. *Sci Rep.* 2017 Feb 17;7:42658.
- 2.) Cruz-Lebrón A, Johnson R, Mazahery C, Troyer Z, Joussef-Piña S, Quiñones-Mateu ME, Strauch CM, Hazen SL, Levine AD. Chronic opioid use modulates human enteric microbiota and intestinal barrier integrity. *Gut Microbes.* 2021 Jan-Dec;13(1):1946368.

Funding for this research generously provided by the following NIH grants:

P30DA033934, T32DA007027



# Metabotropic mGlu<sub>1</sub> Receptor Regulation of Cortical Inhibition and Cognitive Function: Implications in Adolescent Cocaine Exposure

Deborah Luessen,<sup>1</sup> Isabel Gallinger,<sup>1</sup> Brenna Wolfe,<sup>1</sup> and P. Jeffrey Conn<sup>1</sup>

<sup>1</sup>*Vanderbilt Univ*

Abstract ID 13858

Poster Board 570

**Aim:** Exposure to psychostimulants, such as cocaine, during adolescence produces persistent changes in the prefrontal cortex (PFC) which parallel cognitive deficits seen in adulthood. Further, adolescent exposure to psychostimulants impairs inhibitory transmission in the PFC in adulthood, suggesting that enhancing PFC inhibitory transmission may be a promising strategy to reverse drug-induced cognitive deficits. Activation of the mGlu<sub>1</sub> subtype of metabotropic glutamate receptor increases inhibitory transmission in the PFC and working memory by selective excitation of somatostatin-expressing GABA interneurons (sst-INs). Therefore, we hypothesize that repeated exposure to cocaine during a critical developmental period in adolescence disrupts PFC inhibition via sst-INs and drives working memory impairments in adulthood which can be mitigated by activation of mGlu<sub>1</sub>.

**Methods:** Male and female mice were injected once daily with cocaine (20 mg/kg, i.p.) for 7 days (PND 35-42). Behavioral and electrophysiological testing was conducted between 10-12 weeks of age. mGlu<sub>1</sub> positive allosteric modulators (PAMs), sst- and PV-Ai9 tdTomato mice, whole-cell patch-clamp electrophysiology, maze- and touchscreen-based automated cognition testing.

**Results:** We found that repeated administration of cocaine during a critical adolescent period impaired PFC sst-IN, but not parvalbumin-expressing interneuron (PV-IN), firing compared to saline-treated mice. Adolescent cocaine exposure significantly decreased the frequency of spontaneous excitatory postsynaptic currents onto sst-INs but not PV-INs. These findings were paralleled by adolescent cocaine-induced impairments in spatial working memory in adulthood. Importantly, these physiological and behavioral effects of adolescent cocaine exposure were reversed by selective mGlu<sub>1</sub> activation. Lastly, repeated amphetamine administration during the same adolescent critical period did not result in impaired sst-IN function or spatial working memory in adulthood.

**Conclusions:** These studies show that: 1) cocaine, but not amphetamine, exposure during an adolescent critical period induces persistent and selective deficits in PFC sst-IN function and cognition in adulthood and 2) selective activation of mGlu<sub>1</sub> with PAMs represents a novel strategy for reversing cocaine-induced cognitive impairments.

This work is supported by MH119673, NS031373, MH062646, MH073676, MH065215

# Development of a Mouse Model to Study Alcohol Withdrawal-Induced Allodynia

Jhoan S. Aguilar,<sup>1</sup> Amy Lasek,<sup>2</sup> Luana Martins de Carvalho,<sup>2</sup> and Arynah Pradhan<sup>1</sup>

<sup>1</sup>Washington University in St. Louis; and <sup>2</sup>Virginia Commonwealth University

**Abstract ID 16458**

**Poster Board 571**

Alcohol use disorder is a prevalent psychiatric disorder affecting nearly 15 million people in the United States. Individuals who wish to cease to consume alcohol are often met with the effects of the dark side of addiction after alcohol withdrawal. One detrimental withdrawal symptom is increased pain sensitivity, which may contribute to relapse to attain the analgesic effect of alcohol. The present study investigated alcohol withdrawal-induced allodynia in a mouse model of chronic ethanol administration and assessed the effectiveness of a histone deacetylase inhibitor in preventing the development of allodynia. Male and female C57BL/6J mice were first given Lieber-DeCarli control liquid diet for 5 days. The mice were then separated into control and ethanol (5% vol/vol) diet groups and fed their respective diets for 10 days. On day 11, the ethanol and control diet-fed mice were given an oral gavage of either ethanol (5 g kg<sup>-1</sup> body weight) or an isocaloric maltose/dextran solution, respectively. Ethanol diet-fed mice then underwent ethanol withdrawal for 24 hours. We found that mice given ethanol diet plus withdrawal exhibited allodynia compared to control mice. The allodynic response persisted for at least 48 hours and then slowly returned to baseline levels. Finally, we performed an experiment in which we treated mice during ethanol withdrawal with suberoyl anilide hydroxamic acid (SAHA), a pan-histone deacetylase (HDAC) inhibitor and found that SAHA attenuated the allodynic response in ethanol diet-fed plus withdrawal mice. These results demonstrate that chronic ethanol diet plus withdrawal induces allodynia, and SAHA prevents the development of this pain. This model can be used to further understand the molecular mechanisms and the effectiveness of pharmacological interventions in ethanol withdrawal-induced pain sensitivity.

Supported by NIAAA U01 AA020912 and P50 AA022538 (AWL).

# Interactions between Biological Sex and Hormonal Cycles in Stimulant Effects on Motor Behavior

Abigail Carr,<sup>1</sup> Jennifer Tat,<sup>2</sup> Erin Calipari,<sup>2</sup> and Kristy R. Erickson<sup>1</sup>

<sup>1</sup>Vanderbilt University; and <sup>2</sup>Vanderbilt Univ

Abstract ID 18982

Poster Board 572

Substance use disorder (SUD) is a chronic neuropsychiatric disease characterized by long-lasting changes in behavior in response to drugs of abuse. These behavioral changes have previously been linked to drug-induced alternations in dopamine signaling. Although women are more susceptible to developing SUD and are more likely to relapse following periods of abstinence, a majority of work on the behavior basis of SUD has focused on male subjects. Emerging data has identified that estrous cycle-dependent hormone fluctuations play a key role in dopamine release regulation and may also play a role in sex differences in motor behavior in response to stimulant administration. Previous studies have shown that females display enhanced locomotor activity after cocaine exposure, but it is unclear if this increase is cycle-stage dependent and if this effect is similar across structurally dissimilar psychostimulants. Here we investigated a range of doses of each stimulant – cocaine (3, 10, or 30 mg/kg), amphetamine (1, 3, or 10 mg/kg), and methylphenidate (3, 10, or 30 mg/kg) – in males and freely cycling females to analyze the psychostimulant's effect on locomotor activity. For cocaine, we observed a dose-dependent effect of cycle stage, where females in estrus (high circulating hormones) showed elevated motor responses as compared to females in diestrus (low circulating hormones) and males at the high doses. In contrast, for amphetamine, females were more responsive than males at the lower doses, but these effects were less sensitive to changes in estrous cycle. Finally, for methylphenidate, there was an upward shift in the dose-response curve in males but not females. Interestingly, there was also an estrous-cycle effect in females with diestrus females showing more motor activity than males. Together, these data suggest each psychostimulant displays unique sex- and cycle stage-dependent differences depending on its dose. In the future, it will be critical to directly link these differences to reward processing for the development of sex-specific pharmacotherapies for SUD.

**Acknowledgements:** Funding was provided by startup funds from V.U. School of Medicine, Department of Pharmacology and the National Institutes of Health (NIH) (to E.S.C.). Funds from the National Institute of Drug Abuse (NIDA) DA042111 and DA048931, the Brain and Behavior Research Foundation, Whitehall Foundation, and the Edward J Mallinckrodt Jr. Foundation (E.S.C) also supported this work. Personal funding was provided by NIH's MARC START program.

# Ligand and G Protein Selectivity in Kappa Opioid Receptor Revealed by Structural Pharmacology

Jianming Han,<sup>1</sup> Jingying Zhang,<sup>2</sup> Sarah Bernhard,<sup>2</sup> Lei Zhao,<sup>3</sup> Peng Yuan,<sup>2</sup> Jonathan F Fay,<sup>4</sup> and Tao Che<sup>2</sup>

<sup>1</sup>Washington University School of Medicine in St.Louis; <sup>2</sup>Washington University School of Medicine; <sup>3</sup>Washington Universtiy in St.Louis; and <sup>4</sup>University of Maryland Baltimore

**Abstract ID 18996**

**Poster Board 573**

The kappa opioid receptor (KOR) represents a highly desirable therapeutic target for treating not only pain but also addiction and affective disorders. The development of KOR analgesics, however, has been hindered by the hallucinogenic side effects mediated by KOR signaling. The initiation of KOR signaling requires the Gi/o family proteins. However, how hallucinogens exert their actions via KOR and how KOR determines the G protein subtype selectivity are not well understood. Here we determined the active-state structures of KOR in complex with G protein heterotrimers by cryo-electron microscopy (Cryo-EM). Comparisons of these structures reveal molecular determinants critical for KOR-G protein interactions as well as key elements governing Gi/o family subtype selectivity and KOR ligand selectivity. These results provide novel insights into the actions of opioids and G protein-coupling specificity at KOR and establish a foundation to explore the therapeutic potential of pathway-selective agonists of KOR.

# Characterizing the Role of Nicotine on Sex-Specific Neural Circuit Mechanisms Underlying Sensory Reinforcement

Grace Bailey,<sup>1</sup> Jennifer Tat,<sup>1</sup> Janet Mariadoss,<sup>1</sup> Lillian Brady,<sup>1</sup> and Erin Calipari<sup>1</sup>

<sup>1</sup>Vanderbilt Univ

Abstract ID 23911

Poster Board 574

Substance use disorder is characterized by motivational circuit dysfunction that leads to maladaptive behaviors associated with reward processing and drug consumption. Men and women are differentially vulnerable to the harmful effects of substances of abuse, and women are most at risk. The goal of this study was to understand how sex contributed to the behavioral effects of nicotine in mice. In both animals and humans, nicotine is shown to be a weak primary reinforcer in the absence of cues, but in the presence of cues produces high rates of responding in reinforcement tasks. Thus, defining the mechanism underlying the interaction between sensory stimuli in the environment and nicotine's pharmacological effects are important for understanding nicotine addiction. We took a multifaceted approach to determine sex-dependent neurochemical mechanisms that underlie the role of repeated nicotine exposure on sensory reinforcement in male and female mice. First mice were trained for sensory reinforcement, where they emitted a nose poke for the presentation of visual and auditory stimuli. Mice showed rates of responding that were significantly higher than the unreinforced condition. Interestingly, sensory stimuli were more reinforcing in females compared to males. Next, mice were treated with saline or nicotine via subcutaneous injection for five days. We found a significant increase in sensory reinforcement in response to nicotine in males, but not females. Sensory reinforcement is dependent on dopamine release in reward-related brain regions such as the nucleus accumbens, thus, to understand potential mechanisms by which this occurred we assessed dopamine release dynamics and the effects of nicotine on these dynamics using fast scan cyclic voltammetry. We then correlated the effects of nicotine on dopamine release with behavior in the same animals during sensory reinforcement. There was a significant positive correlation between the rate of responding in the sensory reinforcement task and the effects of low dose nicotine on dopamine release in females, but not males. Further, we found that reinforced responses to sensory cues after repeated nicotine injections positively predicted dopamine release in response to tonic and phasic stimulation parameters following bath application of a higher desensitizing nicotine dose. Interestingly, this effect was not sex-specific, suggesting that nicotine's ability to activate vs desensitize receptors may play differential roles in sex-specific behavioral effects. Overall, these data suggest that sex differences in nicotine regulation of dopamine neurotransmission underlies sex-specific behavior in sensory reinforcement. Determining the effect of nicotine on sex differences in the interaction between cues and nicotine effects on behavior, as well as understanding the neural circuitry controlling the differences in reward processing and behavior between males and females will aid in the development of sex-specific treatment interventions for nicotine dependence and broad substance use disorders.

Funding for this project was provided by funds from Vanderbilt University School of Medicine (E.S.C.), and funding from the National Institute of Health (NIH). Funds from the National Institute on Drug Abuse (NIDA) DA042111 (E.S.C.), the Brain & Behavior Research Foundation (E.S.C.), the Vanderbilt University Academic Pathways Postdoctoral Research Fellowship (L.J.B.) and the NIH / NIDA (1K99DA052641) MOSAIC K99/R00 (L.J.B.) also supported this work.

# Structure, Function, and Pharmacology of Delta Opioid Receptor Bitopics

Sarah Bernhard,<sup>1</sup> Balazs R. Varga,<sup>1</sup> Amal El Daibani,<sup>1</sup> Jordy H. Lam,<sup>2</sup> Saheem Zaidi,<sup>2</sup> Kevin Appourchaux,<sup>1</sup> Shainnel Eans,<sup>3</sup> Vsevolod Katritch,<sup>2</sup> Jay McLaughlin,<sup>3</sup> Susruta Majumdar,<sup>1</sup> and Tao Che<sup>1</sup>

<sup>1</sup>Washington University School of Medicine; <sup>2</sup>University of Southern California; and <sup>3</sup>University of Florida

**Abstract ID 17740**

**Poster Board 89**

Opioid receptor ligands like morphine are effective targets for pain relief. However, these pain relievers can cause severe negative side effects via downstream signaling pathways. The sodium ( $\text{Na}^+$ ) binding site has been found to be conserved among many G protein-coupled receptors (GPCRs) including opioid receptors where  $\text{Na}^+$  acts as a negative allosteric modulator of GPCR activation and signaling. Targeting the  $\text{Na}^+$  binding site could alter downstream signaling pathways and reduce common side effects. We explored the functional effect of engaging both the delta opioid receptor (DOR) allosteric  $\text{Na}^+$  site and orthosteric site using structure-based design of bitopic ligands. To validate our design strategy of targeting the  $\text{Na}^+$  site, we solved cryoEM structures of two lead compounds, C5 and C6, bound to DOR. The structures highlight key gatekeeper and ligand- $\text{Na}^+$  site interactions which control efficacy and potency at two key GPCR signaling pathways, G-protein and beta-arrestin. While C5 is a full agonist that activates both pathways at DOR, C6 behaves as a partial agonist with less liability to promote potent side-effects. In mice, C6 showed analgesic actions in a neuropathic pain assay without convulsions. Convulsions have prevented the clinical usage of first-generation classical DOR agonists, supporting the idea that targeting the sodium site may be an avenue toward developing safer analgesics.

# Dual sEH/FAAH Inhibitors as a Promising Therapeutic Strategy for the Treatment of Chronic Pain

Jeannes Angelia,<sup>1</sup> Ram Kandasamy,<sup>2</sup> Xiaohui Weng,<sup>1</sup> and Stevan Pecic<sup>3</sup>

<sup>1</sup>California State University Fullerton; <sup>2</sup>California State University, East Bay; and <sup>3</sup>California State Univ Fullerton

**Abstract ID 21553**

**Poster Board 90**

Chronic pain is the primary cause of disability worldwide. According to the National Institutes of Health, nearly 25.3 million Americans suffer from daily pain, and another 23.4 million Americans report significant pain. In this project we developed dual inhibitors, single small molecules that simultaneously inhibit two enzymes: soluble epoxide hydrolase (sEH) and fatty acid amide hydrolase (FAAH), both playing significant roles in pain and inflammation. Using an environmentally friendly four steps synthetic route, we were able to identify several very potent dual inhibitors, and one was tested in a rat model of acute inflammatory pain. We established a structure-activity relationship and discovered that fluoro- and chloro- groups in the ortho position are important for potent inhibition and are well-tolerated in the binding site of both enzymes. All dual inhibitors were significantly less potent on the mouse sEH enzyme than on human and rat enzymes. The sequence alignment of human, mouse, and rat enzymes shows high sequence similarity and contains many conserved amino acid residues located in the catalytic site of sEH; thus, we believe the species selectivity might be due to the different shapes of active sites and binding modes of analogs. Nonetheless, our findings indicate that modeling pain and other behaviors in rats are the best models to evaluate these dual inhibitors given the similar potencies at inhibiting both rat and human sEH enzymes. Finally, we evaluated the most potent compounds in human, mouse, and rat microsomal liver assays (MLA), which is a good predictor of in vivo metabolism and is an important tool in drug development. All tested compounds showed poor metabolic profiles in human, mouse, and rat MLA. In future work, we will try to use various medicinal chemistry approaches, such as the inclusion of deuterium atom, modifying labile functional groups, and deactivating aromatic rings in order to improve the microsomal stability. Dual sEH/FAAH inhibitors described here have the potential to be used as a promising novel non-opioid therapeutic strategy in pain management and our studies may provide a foundation for the future investigation of the benefits of using the dual ligand strategy in analgesia.

Research reported in this publication was supported by the National Institute of General Medical Sciences of the National Institutes of Health under Award Number SC2GM135020

# Preclinical Assessment of CSX-1004: A High Affinity, Humanized Monoclonal Antibody for Mitigating the Effects of Fentanyl

Paul T. Bremer,<sup>1</sup> Nicholas T. Jacob,<sup>1</sup> Bin Zhou,<sup>2</sup> Lisa M. Eubanks,<sup>2</sup> and Kim D. Janda<sup>2</sup>

<sup>1</sup>Cessation Therapeutics; and <sup>2</sup>Scripps Research Institute

Abstract ID 24310

Poster Board 91

**Objective:** Fentanyl abuse is a major public health issue in the United States, with fentanyl and fentanyl analogs being responsible for the majority of the drug overdose deaths that now exceed 100,000 per year. While naloxone is an effective opioid overdose reversal medication via antagonism of the respiratory depressant action of fentanyl at brain stem mu-opioid receptors, many fentanyl-related deaths occur within minutes before life-saving medication can be administered, and some toxic fentanyl-mediated effects (e.g., laryngospasm) are insensitive to naloxone. Thus, an unmet medical need exists for a long-acting drug that can prevent recurrent fentanyl overdose events in at-risk patients. Herein, we present in vitro and in vivo data for an IgG1 monoclonal antibody (mAb), known as CSX-1004, that can antagonize the effects of fentanyl by sequestering fentanyl in peripheral circulation.

**Methods:** Affinity of CSX-1004 for fentanyl and fentanyl analogs was evaluated in a surface plasmon resonance (SPR) assay. The ability of CSX-1004 to attenuate the antinociceptive and respiratory effects of fentanyl was evaluated in mouse hot-plate/tail-flick and plethysmography assays, respectively. To establish IND-readiness, a manufacturing process was developed for CSX-1004, which included analytical testing of the resulting GMP-grade drug product. Moreover, a repeat-dose, GLP-compliant study in rats was also conducted to assess the pharmacokinetics and potential toxicological effects of CSX-1004.

**Results:** The SPR assay revealed picomolar affinity of CSX-1004 for fentanyl and related analogs without cross-reactivity to other opioids. In mice, CSX-1004 (30 mg/kg, IV) produced a rapid and robust reversal of a dose of fentanyl (0.2 mg/kg, IP) that produced maximal or near maximal antinociceptive effects in the hotplate and tail flick assays. Similarly, in the plethysmography assay, CSX-1004 (60 mg/kg, IV) rapidly and robustly reversed the effects of a dose of fentanyl (0.135 mg/kg, IV) and carfentanil (0.01 mg/kg, IV) that reduced minute volume to <25% of baseline. In mice pretreated with either saline or CSX-1004, high doses of fentanyl (15 mg/kg, IV) produced lethality in 80% of saline-treated mice vs. 50% of CSX-1004-treated mice. For purposes of IND filing and establishing clinical trial material, testing of vial drug product demonstrated adequate quality, purity, potency and safety that was maintained for over 6 months at refrigerated and frozen storage conditions. Lastly, a toxicology/pharmacokinetic study in rats revealed a long terminal half-life (~8 days) of CSX-1004 without any adverse mAb-related effects even when administered repeatedly (once every 3 weeks for 12 weeks) at high doses (up to 400 mg/kg).

**Conclusion:** Taken together, these findings support the preclinical safety and efficacy of CSX-1004 for fentanyl overdose prevention and reversal and suggest that CSX-1004 has the potential to be clinically useful in mitigating the death toll caused by fentanyl.

Supported by NIDA Grant 1U01DA051071-01A1



# HBW-008-A, a Novel, Potent, Selective, Safe and Bioavailable p21-Activated Kinase 4 (PAK4) Inhibitor, is an Efficacious Adjuvant Agent for PD-1 Therapy in Mice

Ning Lee,<sup>1</sup> Yingfu Li,<sup>1</sup> Guanfeng Liu,<sup>1</sup> and Mao Yang<sup>1</sup>

<sup>1</sup>Chengdu Hyperway Pharmaceuticals

Abstract ID 18690

Poster Board 92

PAK4, a member of the serine-threonine PAK kinase family involved in a wide range of cellular functions, is often dysregulated across diverse cancer types. PAK4 may promote cancer progression, through altering biological capabilities such as proliferation, epithelial-mesenchymal transition (EMT), invasion, metastasis and tumor microenvironment conditioning. Lately, it has been shown that a PAK4 inhibitor (PAK4i) may enhance the efficacy of PD-1 blockade and CAR-T cells, and provide a novel adjuvant agent for the current immunotherapy, a prime-time cancer treatment yet struggled with low response rate. Furthermore, a PAK4i may sensitize cancer cells to chemotherapy and radiotherapy. With over 20 years in development, many PAK4is have been published but only few entered clinical, and none is approved by far. Issues of existing compounds include unfavorable pharmacokinetic (PK) profiles and the lack of selectivity due to high homology among PAK family members. Through our medicinal chemistry efforts, we have discovered a novel orally bioavailable small-molecule PAK4i, HBW-008-A, that has a superior PAK4 inhibition and selectivity against PAK2 (cardiovascular liability) as compared with other known PAK4is. In a mouse MC38 colon cancer model, as combined with mPD-1, HBW-008-A demonstrated an enhanced anti-tumor efficacy than mPD-1 mono therapy, without any toxicity issue. HBW-008-A exhibited a good hepatic microsomal stability, as well as plasma stability in several animal species including human. In a head-to-head rat PK study, HBW-008-A displayed comparable exposures to the pan-PAK inhibitor PF-3758309. In addition, HBW-008-A had higher exposures in liver, lung, kidney, intestine, stomach, and pancreas than those in blood. In a 14-day toxicity study in rats using doses up to 300 mg/kg, HBW-008-A showed no sign of safety concern. Taken together, we have demonstrated that HBW-008-A is a validated candidate for future clinical studies in cancer patients.

**SIGNIFICANCE STATEMENT** The novel orally bioavailable small-molecule PAK4i, HBW-008-A, produced an enhanced anti-tumor efficacy as combined with mPD-1 in a mouse MC38 colon cancer model. HBW-008-A also presented a better safety and PK profile than other known PAK4is. These preclinical studies have established HBW-008-A a more advantageous PAK4i to be tested clinically as a potential adjuvant agent for immunotherapy in treating cancers.

All authors are employees of Chengdu Hyperway Pharmaceuticals.

# Identification of Inhibitors of the TMPRSS2 and SPIKE Interaction Through Novel uHTS Assays and Molecular Docking

Danielle Cicka,<sup>1</sup> Andrey A. Ivanov,<sup>2</sup> Sophie West,<sup>2</sup> Dacheng Fan,<sup>2</sup> Qiankun Niu,<sup>2</sup> Yuhong Du,<sup>2</sup> and Haiyan Fu<sup>2</sup>

<sup>1</sup>Emory University; and <sup>2</sup>Emory University

**Abstract ID 53428**

**Poster Board 93**

The few therapies available for SARS-CoV-2 have limited areas of effectiveness and resistance is inevitable. Identification of inhibitors of viral entry has been challenging and have focused on the strong interaction between ACE2 and SPIKE. However, the interaction between TMPRSS2 and SPIKE is also critical for viral entry and identification of inhibitors of this interaction could be therapeutic starting points. Therefore, we seek to develop ultra high-throughput assays for identification of inhibitors of the TMPRSS2 and SPIKE interaction and prioritize top-hit compounds based on biophysical and molecular docking.

We first created a Time Resolved-Förster/Fluorescence Energy Transfer (TR-FRET) assay utilizing fluorescently labeled antibodies to detect interactions between overexpressed SPIKE and TMPRSS2 proteins in cell lysates. To further narrow the hits from this TR-FRET screen, we developed an orthogonal uHTS Nanoluciferase Binary Technology (NanoBIT) assay to detect the interaction between tagged SPIKE and TMPRSS2 in live cells. With these orthogonal assays, we expanded our TR-FRET screen to over 100,000 compounds. Several compounds were found to show activity in both the TR-FRET and the NanoBIT assay. Thermal shift assays further narrowed down compounds by identifying compounds that bound to either SPIKE or TMPRSS2 purified recombinant proteins, prioritizing potential compounds of interest.

Next, molecular docking was done to identify which of the top compounds may directly disrupt the SPIKE/TMPRSS2 interaction. MM-GBSA binding energies were calculated to determine potential ligand binding sites for each compound on the interface of TMPRSS2 and SPIKE. Binding energies were also calculated for compound binding to allosteric sites on SPIKE or TMPRSS2, based on which protein they interacted with in thermal shift data. SiteScores were also calculated for each binding site of the compounds to identify at which binding site they were most likely to interact with the protein of interest. A detailed evaluation of the binding energies at each site revealed the contributions of various types of bonds contributing to the binding energy of the compounds at each binding site and the residues important for the ligand and protein interaction. This revealed a potential mechanism of action for these candidate TMPRSS2/SPIKE interaction disruptors. For example, eltrombopag was found to have favorable energy for being an allosteric modulator of the interaction, but also may act as direct disruptor of the interaction.

Thus, we have identified several potential inhibitors of the SPIKE/TMPRSS2 interaction through the use of our newly developed orthogonal TR-FRET and NanoBIT uHTS assays and characterized the binding sites via molecular docking. These uHTS assays may be a tool for future TMPRSS2/SPIKE disruptor discovery and the identified candidate compounds could provide promising groundwork for further development of inhibitors of SARS-CoV-2.

This research was supported in part by The Emory School of Medicine COVID Catalyst-13 award, the NCI Emory Lung Cancer SPORE (HF, P50CA217691) Career Enhancement Program (AAI, P50CA217691), Emory initiative on Biological Discovery through Chemical Innovation (AAI).

# Characterization of OJT008 As a Novel Inhibitor of *Mycobacterium tuberculosis*

Kehinde Idowu, Collins Onyenaka,<sup>1</sup> Ngan Ha,<sup>2</sup> Edward A. Graviss,<sup>2</sup> and Omonike Olaleye<sup>1</sup>

<sup>1</sup>Texas Southern Univ; and <sup>2</sup>Houston Methodist Research Institute

Abstract ID 26564

Poster Board 94

Despite recent progress in the diagnosis of Tuberculosis (TB), the chemotherapeutic management of TB is still challenging. *Mycobacterium tuberculosis* (*Mtb*) is the etiological agent of TB, and TB is classified as the 13th leading cause of death globally. It is estimated that 558,000 people were reported to develop multi-drug resistant TB globally. Our research focuses on targeting Methionine Aminopeptidase (MetAP), an essential protein for the viability of *Mtb*. MetAP is a metalloprotease that catalyzes the N-terminal methionine excision (NME) during protein synthesis. This essential role of MetAPs allows this enzyme an auspicious target for the development of novel therapeutic agents for the treatment of TB. *Mtb* possesses 2 MetAP1 isoforms: MtMetAP1a and MtMetAP1c. In our study, we cloned, overexpressed recombinant MtMetAP1c, and investigated the *in vitro* inhibitory effect of OJT008 on cobalt and nickel ion activated MtMetAP1c and the mechanism of action was elucidated through an *in-silico* approach. The compound's potency against replicating and multidrug-resistant (MDR) *Mtb* strains was also investigated. The induction of the overexpressed recombinant MtMetAP1c was optimized at 8 hours with a final concentration of 1mM Isopropyl  $\beta$ -D-1-thiogalactopyranoside. The average yield for MtMetAP1c was 4.65mg mg/L of *Escherichia coli* culture. A preliminary MtMetAP1c metal dependency screen Provided optimum activation with nickel and cobalt ions at 100 $\mu$ M. The half maximal inhibitory concentration (IC<sub>50</sub>) values of OJT008 against MtMetAP1c activated with CoCl<sub>2</sub> and NiCl<sub>2</sub> were 11 $\mu$ M and 40  $\mu$ M respectively. The *in-silico* study showed OJT008 strongly binds to both metals activated MtMetAP1c, as evidenced by strong molecular interactions and higher binding score thereby corroborating our result. This *in-silico* study validated the pharmacophore's metal specificity. The potency of OJT008 against drug sensitive and MDR *Mtb* was < 0.063  $\mu$ g/mL. Our study reports OJT008 as an inhibitor of MtMetAP1c which is potent at low micromolar concentrations against both drug-sensitive and MDR-*Mtb*. These results suggest OJT008 is a potential lead compound for the development of novel small molecules for the therapeutic management of TB.

This project is sponsored by NIH-RCMI (U54MD007605) Grants.

# Antioxidant Effects of Cardamonin in BV-2 Microglial Cells Through the Modulation of Keap1/Nrf2 Signaling Pathway

Kimberly Barber,<sup>1</sup> Patricia Mendonca,<sup>2</sup> and Karam F. Soliman<sup>3</sup>

<sup>1</sup>Florida A&M University; <sup>2</sup>Florida A&M Univ; and <sup>3</sup>Florida A&M Univ College of Pharmacy

Abstract ID 21727

Poster Board 95

The transcription factor Nrf2 and its endogenous inhibitor Keap1 are crucial in maintaining cellular redox homeostasis by regulating over 200 gene expressions of networks of antioxidant, anti-inflammatory, and detoxification enzymes. Therefore, activation of Nrf2 provides cytoprotection against numerous pathologies, including age-related diseases. Much evidence shows that oxidative stress (OS) and inflammation are critical factors in the pathogenesis of neurodegenerative diseases. Clinical and preclinical studies indicate that neurodegenerative disorders, such as Alzheimer's disease, are characterized by higher levels of OS and lower levels of antioxidant defense in the brain. Neuroinflammation with increased production of nitric oxide (NO) and reactive oxygen species is among the many factors associated with microglial cell activation. The current study investigated the effect of the flavonoid cardamonin, a natural compound, on LPS-activated BV-2 microglial cells. Results show that cardamonin induced a dose-response cytotoxic effect in concentrations ranging from 0.78 to 200  $\mu$ M. Cardamonin concentrations of 6.25 to 50  $\mu$ M reduced over 95% the release of NO, compared to the cells treated with LPS only. There was a significant decrease in the cellular production of SOD and increased levels of expression of CAT and glutathione. In RT-PCR arrays, cardamonin decreased the mRNA expression of *NOS2*, *CCL5/RANTES*, *SLC38A1*, and *TXNIP*. RT-PCR with individual primers showed that cardamonin decreased the levels of *Keap1* and increased the expression of *Nrf2*, which was confirmed utilizing the protein levels assayed with WES analysis. The data show cardamonin efficacy in modulating proteins and genes involved in inflammation and controlling elevated intracellular levels of ROS, suggesting that Keap1/Nrf2 signaling may be responsible for the upregulation of antioxidant factors observed in this study. In conclusion, these findings indicate that cardamonin may have a potential in the therapy of microglia-derived neurodegeneration, helping to prevent or slow the progression of the disease in the CNS.

Support/Funding Information: National Institute of Minority Health and Health Disparities of the NIH U54 MD007582.

# Identification of Transfer RNA Modification Enzymes That Regulate a Bacterial RNA Chaperone Known as Hfq

Jalisa Nurse,<sup>1</sup> Karl Thompson,<sup>1</sup> Joseph Aubee,<sup>2</sup> and Valerie de Crecy-Legard<sup>3</sup>

<sup>1</sup>Howard University; <sup>2</sup>Memorial Sloan Kettering Cancer Institute; and <sup>3</sup>Gainesville, University of Florida

Abstract ID 52257

Poster Board 96

Hfq is an RNA chaperone found in many bacteria that plays an important role in regulating gene expression. Hfq associates with small RNA molecules to form ribonucleoprotein (RNP) complexes, which can target and silence specific mRNAs by altering their stability or translation. Due to its important role in the cell, it is important that we understand the regulation of *hfq* expression at multiple levels. In this work, we are investigating the regulation of *hfq* expression by RNA modifications.

RNA modifications are chemical changes to RNA molecules that ensure accuracy of the translation of the genetic code. These chemical modifications promote tight codon-anticodon interactions and stabilize the tRNA molecule, decreasing the probability of so that it is translation errors. We constructed an *hfq-lacZ* translation fusion in *Escherichia coli* K12 MG1655 and executed a targeted genetic screen for RNA modification mutants that may affect *hfq* expression.

We compared the activity of wild type and mutant (in RNA modification genes) *hfq-lacZ* translational fusion in the absence of these RNA modification mutants. We measured *hfq-lacZ* activity in RNA modification mutants using high-throughput kinetic  $\beta$ -galactosidase assays. Finally, we measured Hfq protein levels in wild type and RNA modification mutant backgrounds using Western blot analysis. Our study shows the tRNA uridine 5-carboxymethylaminomethyl synthase, encoded by the *mnmG* gene, is necessary for full expression of *hfq* in *E. coli*. These RNA modification enzymes are highly conserved in bacterial and humans. Further, the lack of many RNA modifications have been associated with neurological diseases, cancer, and antibiotic resistance possibly due to defective gene expression.

# Comparative LC/MS Analysis of the Extraction of Cocaine and its Metabolites Using QuEChERS and Column Extraction Methods

Zhen-Hin E. Chan,<sup>1</sup> and Rose Webster<sup>2</sup>

<sup>1</sup>Northern Kentucky University; and <sup>2</sup>University of Cincinnati

Abstract ID 56031

Poster Board 97

Cocaine abuse is a major public health problem worldwide and monoclonal antibodies are at the forefront as a possible treatment for its abuse. Our laboratory has developed a recombinant humanized anti-cocaine monoclonal antibody, known as h2E2, and a Fab fragment that has shown promising results in animal studies. In order to study the efficacy of this antibody against cocaine, we have also developed methods to measure cocaine and its metabolites in rodent tissue and fluids such as brain, blood, or urine. We compared two cocaine extraction methods, the Quick Easy Cheap Effective Rugged Safe (QuEChERS) salt mix of NaCl, MgSO<sub>4</sub>, sodium citrate (dihydrate + sesquihydrate); and United Chemical Technologies (UCT) Clean Screen DAU columns. Cocaine extracted from urine by both methods was quantified via a Shimadzu LCMS 8060. Our objective was to find a quick and reproducible extraction method. We used 3D printing to develop custom holding stands for the columns. QuEChERS is a dispersive solid-phase extraction method for sample preparation. For this comparison, we used urine from a study examining the effect of the Fab fragment of h2E2 on the distribution of cocaine and its metabolites in Sprague-Dawley rats per IUACUC regulations. We selected a subset of urine samples (n=9) that would have high (>1000ng/mL), mid (≤100ng/mL), and low (≤10ng/mL) levels of cocaine.

We compared a 10-fold dilution of the extracts obtained by the two methods. The urine samples were extracted with 50mg of pre-weighed QuEChERS and 200 uL acetonitrile. The organic supernatant (150uL) of cocaine and its metabolites was used for the analysis. For the initial estimates, the standards used ranged from 3.2-7000ng/mL. Six months later, a 10-fold dilution of the samples, with a similarly diluted standard set, was analyzed (0.3-700ng/mL). The columns utilize both a reverse (C8) phase and an ion exchange (benzenesulfonic acid) phase bonded to silica gel. The extraction of cocaine and its metabolites was carried out as recommended by the manufacturer's instructions. Fused deposition modeling (FDM), commonly known as 3D printing, was used to make custom holders for the extraction columns through design iteration. The final eluate was collected with the 3D printed stands and then evaporated with a Reacti-Therm III Heating Module(using air). This was reconstituted in 150uL of acetonitrile and stored in vials for analysis. For both extraction methods, 0.5uL of each sample was injected into the instrument. Samples (n=48) in duplicate were analyzed twice over 41 days between experiments using the QuEChERS method. Each sample concentration was within 25% over the two days. The three sample levels were reanalyzed at a 10x dilution using the two methods. All but one (20.7%) of the high samples were within 20% of the first run for both methods. For the mid to low concentrations, none of the values fell within 25% of the earliest run for either method which needs further investigation. This will be done with naive urine spiked with similar concentrations of cocaine and its metabolites. For the QuEChERS method, the most tedious step was weighing the salts. Comparatively, the other process needed conditioning, application, washing, and elution of the column before drying and reconstituting the sample. Overall, we found the QuEChERS method of extracting cocaine and its metabolites to be easier to implement with fewer required steps.

Thanks to United Chemical Technologies for providing the columns used

Supported by NIDA grant U01DA050330

# Identifying the Anticancer Properties and Mechanisms of Action of Anthocyanin-rich Extracts from the *Aponogeton madagascariensis* on Triple Negative Breast Cancer Cells

Shanukie Embuldeniya,<sup>1</sup> Kerry Goralski,<sup>2</sup> and Arunika Gunawardena<sup>2</sup>

<sup>1</sup>Dalhousie Univ; and <sup>2</sup>Dalhousie University

Abstract ID 16711

Poster Board 98

**Introduction:** Breast Cancer is one of the leading causes of death from cancer among women, with Triple Negative Breast Cancer (TNBC) accounting for 10 – 20% of all breast cancers. Due to the aggressiveness and multi-drug resistant nature of TNBC cells, more effective and targeted treatments are needed. Studies show that bioactive flavonoids from plant extracts can reduce cancer cell viability, proliferation, and metastasis. However, the exact pharmacological mechanisms responsible for these anticancer properties remain unclear. The present work aims to identify the anticancer properties and the pharmacological mechanisms of action of anthocyanin-rich extracts from young and mature leaves of the aquatic plant *Aponogeton madagascariensis* (Lace Plant) on MDA-MB-231 triple negative, human breast cancer cells.

**Methods:** Anthocyanin-rich crude extracts were prepared from young and mature leaves of lace plants grown in axenic cultures. Cell viability of MDA-MB-231 cells and control breast epithelial MCF-10A cells were measured using MTT cell viability assays ((3-(4,5-dimethylthiazol-2-yl)-2,5-diphenyltetrazolium bromide). Cell proliferation was measured using a fluorescent based CyQuant® proliferation assay. A CM-H<sub>2</sub>DCF-DA fluorescent assay was used to test for intracellular Reactive Oxygen Species (ROS) levels. Quadruplicates of each experimental condition was measured with a minimum of three separate assays performed for each test. A two-way ANOVA was performed followed by a Tukey's multiple comparison test to determine significant pairwise comparisons.

**Results:** Treatments with anthocyanin-rich extracts from young and mature lace plant leaves (25 – 250 µg/mL) for 48 hrs reduced MDA-MB-231 cell viability by 20 – 30 percent, in a dose-dependent manner, while having no significant cytotoxic effect on control breast epithelial, MCF-10A cells. Treatments with anthocyanin-rich extracts from young and mature lace plant leaves (12 – 250 µg/mL for 24 and 48 hrs) reduced cell proliferation of MDA-MB-231 by 20 – 40 percent compared to vehicle treated cells. Preliminary data showed that extracts (50 – 250 µg/mL treated for 24 hrs) from mature lace plant leaves increased ROS activity by 1.5 – 2-fold compared to their vehicle controls.

**Conclusion:** Our work to date shows that anthocyanin-rich crude extracts from young and mature leaves of the lace plant displays cytotoxic and anti-proliferative effects in MDA-MB-231 triple negative cells which could be due to elevated intracellular ROS.

# Patient iPSC-based high throughput drug screening identifies drug candidates involved in reduced tauopathy associated with Alzheimer's disease

Dhruv Gohel,<sup>1</sup> Yichen Li,<sup>1</sup> and Feixiong Cheng<sup>1</sup>

<sup>1</sup>Cleveland Clinic Lerner Research Institute

Abstract ID 53201

Poster Board 111

## Abstract

**i. Background:** Alzheimer's disease (AD) is a commonest neurodegenerative and dementing disease caused by accumulation of phosphorylated Tau (pTau) and amyloid-beta (A $\beta$ ) in brain. Effective strategies to remove A $\beta$  in AD-patient brains have been developed but have limited effects to effectively improve cognitive functions in clinical trials. Differentiated neurons from patient-induced pluripotent stem cells (iPSCs) provide an effective drug discovery model compared to traditional AD models. We therefore used drug repurposing approach and performed high throughput screening with Food and Drug Administration (FDA)-approved drugs to identify novel drugs showing reduced pTau levels in iPSC derived neurons from AD patients.

**i. Method:** We selected two AD patient derived iPSC cell lines having mutated APP and differentiated them to neurons using well-established protocols. We used pTau231/total Tau ratio as readout as pTau231 is an early marker of AD pathology and also related with cognitive decline. To identify compounds that reduce pTau231 accumulation in these Familial AD (FAD) neurons, we screened a collection of 960 FDA approved drugs for their efficacy to lower neuronal pTau231 levels by performing multiplex-ELISA.

**i. Results:** We successfully differentiated patients' iPSC to neuronal progenitor cells (NPC) followed by mature neurons as evident by western blotting and microscopy results using neuron specific markers. Apparently, in our primary screening 59/960 (6.1%) and 69/960 (7.2%) compounds showed significantly reduced pTau231/total Tau by a Z score <-5 in both the patient-derived iPSC lines respectively. From both of the primary screening, we identified 41 common hits and classified them in to various drug groups. As expected, our classification showed most of the drugs were antimicrobial and anti-cancer drugs. Interestingly, we did identify several drugs for cardiovascular diseases (i.e., gemfibrozil), immune modulators and various other pathologies reducing pTau231/total Tau. In addition, we identified potential mechanism-of-action of hit drugs in AD after RNA-sequencing analysis of drug-treated iPSC-derived neurons.

**i. Conclusion / future perspectives:** Here, we successfully utilized AD-patient iPSC-derived neurons for phenotypic drug screen to identify FDA approved drugs that reduce pathological pTau accumulation in FAD neurons, offering potential treatment for AD.



# Assessment of Dextromethorphan on Compulsive Behavior Using the Schedule-Induced Polydipsia Paradigm in Rats

Madeline T. Van Fossen,<sup>1</sup> Alexia G. Dalton,<sup>2</sup> Bethany E. Beavers,<sup>2</sup> Dillon S. Shekoski,<sup>2</sup> Taylor Galaszewski,<sup>2</sup> and Adam J. Prus<sup>2</sup>

<sup>1</sup>Northern Michigan Univ; and <sup>2</sup>Northern Michigan University

Abstract ID 27875

Poster Board 112

Dextromethorphan (DM) is a sigma1 receptor agonist, 5-HT2A receptor agonist, and NMDA receptor antagonist FDA-approved for pseudobulbar affect and, in combination with the dopamine reuptake inhibitor bupropion, for the treatment of major depressive disorder. Antidepressant drugs that exhibit pharmacological actions similar to DM can attenuate symptoms of obsessive-compulsive disorder. The present study aimed to evaluate the effects of DM in rats using the schedule-induced polydipsia procedure, a model of compulsive behavior. In this paradigm, food-, but not water-, restricted animals drink excessive amounts of water when food is delivered on a fixed schedule. This study examined male Wistar rats (food restricted to 85% of free-feed weights) during 60 min sessions with fixed-time 60 second schedules and free access water. Following 20 consecutive daily training sessions, rats were divided into high or low drinker groups. DM (15.0 - 60.0 mg/kg) dose-dependently reduced water consumption and frequency of licks in both the low and high drinker groups. DM reduced food-receptacle head entries in only the low drinker group. Further, the 5-HT2A/2C agonist DOI (0.5 - 2.0 mg/kg) also inhibited water consumption in both low and high drinkers and reduced frequency of head entries in only the low drinker group. Based on these findings, DM may be effective for treating compulsive behavioral disorders and these effects may be facilitated by activation of 5-HT2A receptors.

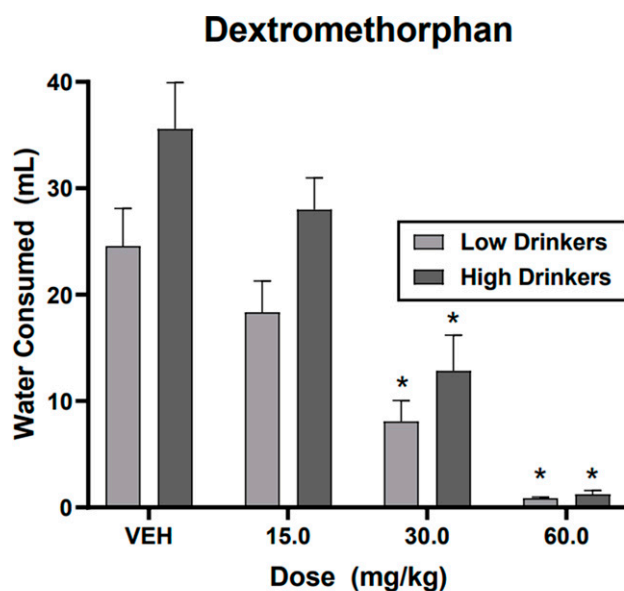


**Figure:** Dextromethorphan significantly reduced water consumption within the low drinker (light bars) and high drinker (dark) groups. \*p<0.05 versus VEH control.

# Bioisosteric Replacement of Amides Linkers with 1, 2, 3-Triazoles for Improved Pharmacokinetics Without Losing Dopamine D<sub>4</sub> Receptor Potency or Selectivity

Diandra Panasis,<sup>1</sup> Mohammad Alkhatib,<sup>1</sup> Julianna Saez,<sup>1</sup> John Hanson,<sup>2</sup>  
Ashley N. Nilson,<sup>2</sup> Franziska M. Jacobs,<sup>3</sup> Nitish Kasarla,<sup>1</sup> Bryant Wang,<sup>1</sup> Maria Ladik,<sup>1</sup>  
Abigail Muccilli,<sup>1</sup> Kaylen Hong,<sup>1</sup> R. Benjamin Free,<sup>2</sup> David R. Sibley,<sup>2</sup> Comfort A. Boateng,<sup>3</sup> and  
Thomas Keck<sup>1</sup>

<sup>1</sup>Rowan University; <sup>2</sup>National Institute of Neurological Disorders & Stroke, NIH; and <sup>3</sup>Fred Wilson School of Pharmacy, High Point University

Abstract ID 26198

Poster Board 113

The neurotransmitter dopamine signals through G protein-coupled receptors that regulate a variety of neurophysiological functions, including movement, emotional regulation, motivation, and cognition. There are five unique receptors for dopamine that can be classified into two subfamilies based on their structure, pharmacology and signaling properties: D<sub>1</sub>-like, consisting of the D<sub>1</sub> and D<sub>5</sub> receptors (D<sub>1</sub>R and D<sub>5</sub>R), and D<sub>2</sub>-like, consisting of the D<sub>2</sub>, D<sub>3</sub> and D<sub>4</sub> receptors (D<sub>2</sub>R, D<sub>3</sub>R, and D<sub>4</sub>R). D<sub>4</sub>Rs are enriched in the hippocampal and prefrontal cortical regions of the brain that are critical to attention, cognition, memory formation, and decision-making. While the physiological relevance of D<sub>4</sub>R signaling in the brain is not fully understood, preclinical studies indicate that D<sub>4</sub>R-selective ligands can improve outcomes in animal models of neuropsychiatric disorders with deficits in cognition and behavioral control, including Alzheimer's disease, ADHD, and substance use disorders. We have recently reported a library of novel D<sub>4</sub>R-selective ligands of varying efficacies, based on a phenylpiperazine scaffold, to investigate D<sub>4</sub>R function in preclinical models. However, the *in vivo* utility of some ligands was limited by rapid phase I metabolism, which cleaved an amide bond in the molecular template. Herein we report the development and structure-activity relationship of novel ligands featuring a bioisosteric replacement of the amide linker with a 1,2,3-triazole moiety using click chemistry methods. Comprehensive *in vitro* analyses indicate that this substitution is well tolerated and 1,2,3-triazole compounds maintain binding and functional profiles similar to their matching amide analogs. The 1,2,3-triazole moiety should be more resistant to drug metabolism. Studies evaluating analog stability in rat and human liver microsomes are presently underway.

Support/Funding Information: NIH (DA050896, GM136492), AACP, the National Institute of Neurological Disorders and Stroke-Intramural Research Program, internal funds from Rowan University and High Point University, Fred Wilson School of Pharmacy.

# Development of GPR183 antagonists for the treatment of neuropathic pain

Vanja Kalajdzic,<sup>1</sup> Israel Olayide,<sup>2</sup> Kathryn Braden,<sup>3</sup> Daniela Salvemini,<sup>4</sup> and Christopher K. Arnatt<sup>2</sup>

<sup>1</sup>Saint Louis University; <sup>2</sup>Saint Louis Univ; <sup>3</sup>Washington University in Saint Louis; and <sup>4</sup>Saint Louis Univ Sch of Medicine

**Abstract ID 54213**

**Poster Board 114**

Neuropathic pain is a difficult condition affecting millions of people in the United States and occurs as a result of neurological conditions (i.e. multiple sclerosis), metabolic conditions (i.e. diabetes), and trauma, among others. Current treatment of neuropathic pain involves the usage of opioids, which may cause serious side effects, such as addiction and death. The need for a safer and more efficient non-opioid treatment is increasing daily and is becoming more urgent. The G-protein coupled receptor (GPCR), GPR183, also known as Epstein-Barr virus (EBV) induced gene 2 (EBI2), is a therapeutic target for neuroinflammatory and metabolic diseases. The endogenous ligand for GPR183 is  $7\alpha,25$ -dihydroxycholesterol ( $7\alpha,25$ -OHC), a metabolite of cholesterol, that induces behavioral hypersensitivity in rodents. Using in silico method, over 5 million compounds were screened, and several compounds showed strong inhibition of  $7\alpha,25$ -OHC, including SAE-1. Our study focuses on the synthesis and biological evaluation of SAE-1 derivatives as GPR183 antagonists. Using 12 different acids and 8 different amine precursors, a total of 96 compounds are being synthesized via amide coupling reactions. The optimal synthesis conditions were explored to obtain the best reaction yield and purity of the compounds. The development of these compounds will allow us to test multiple functional groups' subsequent effects on their agonism/antagonism of GPR183.

# Novel Axin Stabilizer YA6060 is a Promising Therapy for Liver Fibrosis

Yan Shu,<sup>1</sup> Shiwei Zhou,<sup>2</sup> Yong Ai,<sup>2</sup> Shaoteng Wang,<sup>2</sup> Amanda Xu,<sup>2</sup> and Fengtian Xue<sup>2</sup>

<sup>1</sup>Univ of Maryland School of Pharmacy; and <sup>2</sup>University of Maryland School of Pharmacy

Abstract ID 17628

Poster Board 115

Both Wnt/ $\beta$ -catenin and AMPK signaling pathways play an important role in liver fibrosis. We have previously synthesized a class of novel compounds that show dual activities of Wnt/ $\beta$ -catenin inhibition and AMPK activation *via* the mechanism of Axin stabilization. With our most recent lead compound YA6060, the aim of this study was to test the hypothesis that simultaneous Wnt/ $\beta$ -catenin inhibition and AMPK activation by a small molecule was a promising therapeutic strategy to treat liver fibrosis. The hepatic stellate cell line LX-2 was used to test the anti-fibrotic effects of YA6060 *in vitro*. The proliferation of LX-2 cells was determined by cell viability assay and wound healing assay. A mouse liver fibrosis model, established by intraperitoneal injection of dimethylnitrosamine (DMNA), was employed to validate the pharmacological effects of YA6060 *in vivo*. The expression of key proteins and genes were detected by Western blot and RT-PCR. Liver fibrosis was examined by Sirius Red staining. YA6060 treatment was found to suppress the proliferation of LX-2 cells and reduce the fibrotic and inflammatory gene expression. YA6060 treatment could also down-regulate the expression of  $\beta$ -catenin by stabilizing AXIN, leading to Wnt signaling inhibition, and simultaneously activate the AMPK pathway in LX-2 cells. Furthermore, YA6060 administration could significantly reduce the degree of liver fibrosis in mice, with the alteration in gene and protein expression that was consistent with the mechanism of Wnt inhibition and AMPK activation. In conclusion, our studies have showed that YA6060 can inhibit liver fibrosis by simultaneously inhibiting the Wnt/ $\beta$ -catenin signaling pathway and activating APMK signaling pathway. The findings have established that small molecule with dual activities of Wnt inhibition and AMPK activation *via* Axin stabilization is a valid strategy to the development of anti-fibrosis agents.

# Efficacy of HS-10382 (TERN-701) in tumor xenograft models, a new investigational allosteric ABL1 kinase inhibitor as a potential treatment for CML

Yuanfeng Zhou,<sup>1</sup> Benjamin Parsons,<sup>2</sup> Danni Sun,<sup>3</sup> Yunfan Li,<sup>3</sup> Guoliang Chen,<sup>3</sup> Mingjie Luo,<sup>3</sup> Christopher Jones,<sup>2</sup> Xiaogang Lian,<sup>4</sup> Xiaolei Wang,<sup>4</sup> Yundong Sun,<sup>4</sup> Jeffrey Jasper,<sup>2</sup> and Huifeng Niu<sup>5</sup>

<sup>1</sup>Shanghai Hansoh Biomedical Company Ltd; <sup>2</sup>Terns Pharmaceuticals; <sup>3</sup>Shanghai Hansoh Biomedical Co Ltd; <sup>4</sup>Jiangsu Hansoh Pharmaceutical Group Co, Ltd; and <sup>5</sup>Shanghai Hansoh Biomedical Co. Ltd.

Abstract ID 53328

Poster Board 116

The chromosomal translocation resulting in the generation & expression of the BCR-ABL1 oncogene is a hallmark of chronic myeloid leukemia (CML). HS-10382 (TERN-701) is a potent, selective, and orally bioavailable BCR-ABL1 kinase inhibitor with  $IC_{50}=0.4$  nM at the non-autoinhibited N-terminally truncated wild-type (WT) ABL1 protein (64-515 aa), with no significant inhibition at 375 protein kinases tested (including full-length WT ABL1). Additionally, TERN-701 is active against several BCR-ABL mutations in cells that are resistant to active site tyrosine kinase inhibitors (TKIs). In contrast to competitive type I TKIs that inhibit the transphosphorylation activity of the BCR-ABL1 oncoprotein by binding the ATP-binding site of the catalytic domain of the kinase, HS-10382 (TERN-701) targets the C-terminal myristoyl allosteric site of BCR-ABL1 to inhibit enzymatic activity, similar to asciminib.

In the KCL22-s mouse subcutaneous xenograft tumor efficacy model of CML, imatinib mesylate at 75 mg/kg, flumatinib mesylate at 75 mg/kg and HS-10382 (TERN-701) at 3 mg/kg were given respectively, QD, for 15 days; positive control asciminib at 3 mg/kg and HS-10382 (TERN-701) at 1.5, 3 and 7.5 mg/kg were given, BID, for 15 days (all oral (PO) administration). The obtained tumor growth inhibition values (TGI%) were 56.03%, 193.24%, 127.26%, 87.29%, 98.20%, 187.08%, and 190.62%, respectively. The anti-tumor effect of HS-10382 (TERN-701) was higher than that of asciminib at equivalent dosing frequency and dosage (TGI% = 187.08% vs. 87.29%,  $p = 0.02$ ). Once daily dosing at 3 mg/kg HS-10382 (TERN-701) also produced a significant anti-tumor effect compared to the twice-daily equivalent dose of asciminib. The minimum effective dose of HS-10382 (TERN-701) on the KCL22-s tumor model was 1.5 mg/kg (BID), which produced a comparable response to the positive control asciminib.

Further xenograft studies using the K562 CML cell line confirmed the potency of HS-10382 (TERN-701) at the WT BCR-ABL1 kinase. Treatment with asciminib at 3 mg/kg QD or HS-10382 (TERN-701) at 1 mg/kg (QD), 3 mg/kg (QD or BID), and 10 mg/kg (QD) led to TGI values of 34.01%, 40.64%, 50.59%, 87.39%, and 120.84%, respectively. As in the KCL22-s model, treatment with HS-10382 (TERN-701) demonstrated an effective dose-response relationship with regards to tumor growth inhibition. QD treatment with 3 mg/kg HS-10382 (TERN-701) exhibited a superior anti-tumor effect ( $p = 0.04$ ) over QD treatment with 3 mg/kg asciminib ( $p = 0.17$ ) relative to the vehicle control.

The BCR-ABL1 T315I mutant is resistant to several approved competitive TKIs in the clinic. In the Ba/F3 BCR-ABL1-T315I model, flumatinib mesylate at 75 mg/kg, asciminib at 50 mg/kg, and HS-10382 (TERN-701) at 25, 50, and 75 mg/kg were dosed BID for 14 days (all PO administration); the corresponding tumor growth inhibition values (TGI%) were 20.25%, 9.33%, 23.28%, 51.80%, and 48.69%, respectively. The anti-tumor effect of HS-10382 (TERN-701) was greater than that of asciminib (TGI%=51.80% vs. 9.33%,  $p = 0.0004$ ) at the equivalent dose and dosing frequency. The minimum effective dose of HS-10382 (TERN-701) in the Ba/F3 BCR-ABL1-T315I model was 50 mg/kg (BID).

The anti-tumor effects of HS-10382 (TERN-701) in mouse xenograft models of human CML indicate that the molecule is a potent inhibitor of tumor growth with potential for efficacious once-daily dosing. HS-10382 (TERN-701) holds promise of translation to treatment of human CML.

# Enhancement of Muscarinic Receptor-Induced Contractions by Hydrogen Sulfide-Releasing Compounds in Bovine Isolated Irides

Fatima Muili,<sup>1</sup> Anthonia Okolie,<sup>2</sup> Shervin Aghaabbasi,<sup>2</sup> JD Fontenot,<sup>2</sup> Reem Matti,<sup>2</sup> Kalu Ngele,<sup>2</sup> Catherine Opere,<sup>3</sup> Sunny Ohia,<sup>2</sup> and YA FATOU NJIE MBYE<sup>2</sup>

<sup>1</sup>Texas Southern Univ; <sup>2</sup>Texas Southern University; and <sup>3</sup>Creighton University

Abstract ID 53481

Poster Board 117

In the eye, hydrogen sulfide (H<sub>2</sub>S)-releasing compounds have been reported to lower intraocular pressure and relax precontracted porcine irises, *in vitro* [Ohia et al. 2018. J. Ocul Pharmacol. Ther. 34:61-69]. The aim of the present study was to investigate the pharmacological actions of H<sub>2</sub>S-releasing compounds on muscarinic receptor-mediated contractions in bovine isolated irises. Isolated bovine iris muscle strips were set up in organ baths and prepared for measurement of isometric contractile tension using a Grass FT03 force-displacement transducer coupled to the PolyView Computer Software. Contractile tone was induced in muscle strips using concentrations of carbachol (300 nM – 1000 nM) in the absence and presence of H<sub>2</sub>S-releasing compounds, GYY 4137 [morpholin-4-ium-4-methoxyphenyl (morpholino) phosphinodithioate], S-allyl-cysteine and the substrate for H<sub>2</sub>S biosynthesis, L-cysteine. When used, an inhibitor of H<sub>2</sub>S biosynthesis, amino-oxyacetic acid, AOAA (10 μM) was present in the buffer solution before and after treatment of tissues with the H<sub>2</sub>S-releasing compounds. All three H<sub>2</sub>S-releasing compounds examined had no contractile effects on basal tone in the bovine isolated irides. However, when present in the buffer solution, GYY 4137 (10 nM – 300 nM), S allyl-cysteine (10 nM – 300 nM) and L-cysteine (300 nM – 30 μM) produced leftward shifts of concentration-response curves to carbachol. For instance, GYY 4137 (10 nM) decreased the EC<sub>50</sub> value for carbachol from 224.3 ± 25.2 nM to 47.1 ± 8.1 nM (n = 14) (p<0.001). Furthermore, L-cysteine (300 nM) also reduced EC<sub>50</sub> value of carbachol from 224.3± 25.2 nM to 44.7 ± 3.5 nM (n = 7) (p<0.001). The leftward shifts of carbachol concentration-response curves produced by L-cysteine (300 nM) was blocked by AOAA (10 μM). We conclude that H<sub>2</sub>S-releasing compounds can enhance muscarinic receptor-induced contractions of bovine isolated irises, an effect that is dependent upon the endogenous production of H<sub>2</sub>S in this muscle.

Support/Funding Information: NATIONAL INSTITUTES OF HEALTH/ NATIONAL EYE INSTITUTE R15EY032274

# High brain-blood barrier permeability highlights a new class of neurolysin activators as promising candidates for stroke treatment: a pilot pharmacokinetic study in mice

Yong Zhang,<sup>1</sup> Sejal Sharma,<sup>2</sup> Shiva H. Esfahani,<sup>3</sup> Shirisha Jonnalagadda,<sup>4</sup> Aarfa Queen,<sup>4</sup> Saeideh Nozohouri,<sup>2</sup> Dhavalkumar Patel,<sup>2</sup> Paul C. Trippier,<sup>4</sup> Vardan T. Karamyan,<sup>3</sup> and Thomas J. Abbruscato<sup>2</sup>

<sup>1</sup>Texas Tech Univ Health Sciences Center; <sup>2</sup>Texas Tech University Health Sciences Center; <sup>3</sup>Texas Tech University Health Sciences Center, Oakland University William Beaumont School of Medicine; and <sup>4</sup>University of Nebraska Medical Center

Abstract ID 53312

Poster Board 118

Neurolysin (Nln) is a peptidase that broadly distributes in the brain and functions to cleave various neuropeptides. Activation of Nln after ischemic stroke has been documented as a critical cerebroprotective mechanism and a promising pharmaceutical target for post-stroke treatment. Yet, drug development for stroke treatment remains challenging due to the additional protection afforded to the brain by the blood-brain barrier (BBB). Evaluation of BBB permeability and brain availability is an indispensable step for discovering new candidates for stroke treatment. Herein, we report a new class of Nln activators that show intriguing brain-drug-like properties. *In vitro* permeability assays suggest KS52 and KS73 out of this class compounds have significantly high BBB permeability (49.2-fold and 84.8-fold,  $p < 0.05$  and  $p < 0.01$ , respectively) compared to the endogenous Nln activator histidine-tyrosine dipeptide (His-Tyr). Consistently, after a single dose of intravenous (*i.v.*) administration at 4 mg/kg, KS52 and KS73 rapidly enter healthy brains of mice, reach cerebral concentrations at 17.8 and 10.5 %injection dose/ml (%ID/ml) at 5 minutes, and maintain similar levels till 30 minutes. After 1 hour of post-administration, brain concentrations for the two compounds went down to 11.9 and 6.7 %ID/ml, respectively. It is worthy of note that, even at 4 hours the longest time point in this study, brain concentrations for KS52 and KS73 remain 7.9-fold and 13.0-fold higher than the  $A_{50}$  (minimal concentration required for increasing 50% peptidase activity of Nln). Compared to KS73, KS52 show a comparable half-life (~100 vs. ~110 minutes) but a relatively higher uptake rate (~50% more) in brains, which might be due to the slight difference between their chemical structures. Furthermore, brain availability of these compounds will also be tested in the ischemic brains of mice. Overall, the present study reports a new class of Nln activators with high BBB permeability, rapid brain uptake and optimal brain retention time, providing valuable pharmacokinetic evidence supporting the future development of these agents as promising candidates for post-stroke treatment.

*This project was supported by NIH grant R01NS106879 to P.C.T., V.T.K. and T.J.A.*

# TLR Agonist INI-4001 Improves Efficacy of Heroin Vaccine Intended for Clinical Treatment of Opioid Use Disorder

Michael Raleigh,<sup>1</sup> Karthik Siram,<sup>2</sup> David Burkhart,<sup>2</sup> Jennifer Vigliaturo,<sup>1</sup> Carly Baehr,<sup>1</sup> Ann Gebo,<sup>1</sup> Scott Winston,<sup>3</sup> and Marco Pravetoni<sup>4</sup>

<sup>1</sup>University of Minnesota; <sup>2</sup>University of Montana; <sup>3</sup>Winston Biopharmaceutical Consulting; and <sup>4</sup>University of Washington School of Medicine

**Abstract ID 53470**

**Poster Board 119**

A heroin vaccine (M-sKLH) to treat opioid use disorder (OUD) is being prepared for clinical testing. Currently, a TLR7/8 agonist, INI-4001, is being studied for its ability to increase vaccine efficacy in opioid use disorder vaccines. To study its effects on increasing vaccine efficacy, INI-4001 was added to M-sKLH adsorbed to aluminum and tested in rats. Male Sprague Dawley rats were vaccinated with M-sKLH adsorbed to aluminum adjuvant with either buffer or INI-4001 and compared against controls consisting of aluminum alone. Cumulative doses of heroin (from 0.5 up to 4 mg/kg, s.c.) were given every 15 minutes and then rats were tested for antinociception via hotplate and respiratory depression via oximetry. Following the final dosing, rats receive a dose of naloxone. Morphine-specific antibody titers were doubled in the group containing INI-4001. Both M-sKLH with aluminum and M-sKLH with aluminum and INI-4001 showed protection against heroin-induced antinociception. However, only M-sKLH with aluminum and INI-4001 was protective against heroin-induced respiratory depression (as measured by % reduction of oxygen saturation). Naloxone reversed heroin-induced effects in all groups, demonstrating that antagonist activity is preserved in M-sKLH vaccinated animals. These data demonstrate that addition of INI-4001 improves the efficacy of M-sKLH adsorbed to aluminum and support the use of M-sKLH adsorbed to aluminum and mixed with INI-4001 for treatment of opioid use disorder in humans.

This work was supported by National Institutes of Health National Institute on Drug Abuse grants UG3DA047711 and BAA-DAIT-75N93019R00009.



# Efficacy of LSD1 Directed Agents is Enhanced with Kinase Signaling Inhibition in Glioblastoma Stem Cells

Lea Stitzlein,<sup>1</sup> Jack Adams,<sup>2</sup> Matthew Luetzen,<sup>2</sup> Melissa Singh,<sup>2</sup> Xiaoping Su,<sup>2</sup> Yue Lu,<sup>2</sup> Ravesanker Ezhilarasan,<sup>3</sup> Joy Gumin,<sup>2</sup> Frederick F. Lang,<sup>2</sup> Erik Sulman,<sup>3</sup> Joya Chandra,<sup>2</sup> and Michelle Monje-Deisseroth<sup>4</sup>

<sup>1</sup>Univ of Texas MD Anderson Cancer Center UT Health GSBS; <sup>2</sup>MD Anderson Cancer Center; <sup>3</sup>NYU Langone Medical Center; and <sup>4</sup>Stanford University

Abstract ID 17899

Poster Board 120

Lysine-specific demethylase 1 (LSD1) is an epigenetic eraser that removes methyl marks from lysine residues on histones (H3K4 and H3K9) and is implicated in the regulation of tumor initiating cells. In glioblastoma (GBM), LSD1 is overexpressed in the tumor initiating cells, glioblastoma stem cells (GSCs), and LSD1 directed therapy via small molecule inhibition can affect tumorigenicity. However, there is no clinically viable strategy to treat GBM with LSD1 inhibition yet. To design an effective LSD1 treatment approach for clinical use, treatment strategies should proactively evade resistance and prevent tumor regrowth, such as the concurrent inhibition of LSD1 with inhibition of compensatory effects. In liquid cancer models, mitogen-activated protein kinase (MAPK) signaling activation functions as a resistance mechanism to LSD1 inhibition. We find this pathway relevant in GBM as it is frequently hyperactivated, in part via mutations and/or amplification of receptor tyrosine kinases (RTKs). Therefore, the present study sought to understand the relationship between LSD1 and RTK/MAPK signaling and to evaluate the combination efficacy of LSD1 inhibition and kinase signaling inhibition in GBM.

Upon LSD1 knockdown in human GBM cells, transcriptional changes were examined using RNA-seq and GSEA. The GSEA identified several kinase signaling processes that were enriched for LSD1 expression, including those related to transmembrane RTK activity and RTK binding. Western blot analysis was used to determine effect of LSD1 inhibition on components of the MAPK signaling pathway in GSCs and a pediatric high-grade glioma cell model. Pharmacological inhibition of LSD1 was assessed as a single agent with five candidates, including GSK-LSD1, ORY-1001, ORY-2001, IMG-7289 and tranlycypromine. Next, we evaluated the effect of LSD1 inhibition combined with osimertinib, a kinase inhibitor directed against the epidermal growth factor receptor (EGFR).

Our results demonstrate that MAPK activity can be modulated via inhibition of LSD1, and perhaps support the emergence of a resistant subpopulation. We observed an increase in phosphorylated ERK1/2 (pERK) following pharmacological LSD1 inhibition in GSC17 and SU-DIPG-XIII cells. The LSD1 inhibitor, ORY-2001, caused increased pERK relative to an untreated control in both the GSC17 and SU-DIPG-XIII cells (mean = 11.9 and 2.17, respectively). To further understand the relationship between LSD1 and kinase signaling, we found several protein tyrosine phosphatases non-receptors (PTPNs) downregulated upon LSD1 knockdown, including PTPN16/7 (fold change = -0.39, -0.89, and -1.64, respectively). PTPNs act as negative regulators of kinase signaling cascades and can regulate the activity of RTKs and their downstream signaling components. Lastly, the concurrent inhibition of LSD1 and EGFR showed synergy *in vitro* compared to single agent inhibition. The combination of ORY-1001 and osimertinib had the highest synergy score of 38.7 in the GSC17s.

In summary, the results from this study emphasize the importance of preemptive therapeutic strategies to improve efficacy and avoid therapeutic resistance that is common in GBM. Future studies are aimed at defining the mechanism by which LSD1 regulates kinase signaling at the EGFR and to evaluate the combination treatment *in vivo* using orthotopic xenograft models of the GSCs.

This work was supported by NIH awards R21 NS093387, P50 CA127001, R21 NS111058, and R33 NS111058 and by CPRIT award DP160014.

# Optimizing Tuberculosis Treatment Efficacy: comparing the Standard Regimen with Moxifloxacin-containing Regimens

Maral Budak,<sup>1</sup> Jennifer Linderman,<sup>1</sup> JoAnne Flynn,<sup>2</sup> and Denise Kirschner<sup>3</sup>

<sup>1</sup>University of Michigan; <sup>2</sup>University of Pittsburgh; and <sup>3</sup>University of Michigan Medical School

Abstract ID 19313

Poster Board 151

Tuberculosis (TB) continues to be one of the deadliest infectious diseases in the world, causing ~1.5 million deaths every year. The World Health Organization initiated an *End TB Strategy* that aims to reduce TB-related deaths in 2030 by 90%. Recent research goals have focused on discovering more effective and more patient-friendly antibiotic drug regimens to increase patient compliance and decrease the emergence of resistant TB. Moxifloxacin is one promising antibiotic that may improve the current standard regimen by shortening treatment time. Clinical trials and *in vivo* mouse studies suggest that regimens containing moxifloxacin have better bactericidal activity. However, testing every possible combination regimen with moxifloxacin either *in vivo* or clinically is not feasible due to experimental and clinical limitations. To identify better regimens more systematically, we simulated pharmacokinetics/pharmacodynamics of various regimens (with and without moxifloxacin) to evaluate efficacies, and then compared our predictions to both clinical trials and nonhuman primate studies performed herein. We used *GranSim*, our well-established hybrid agent-based model that simulates granuloma formation and antibiotic treatment, for this task. In addition, we established a multiple-objective optimization pipeline using *GranSim* to discover optimized regimens based on treatment objectives of interest, i.e., minimizing the total drug dose and lowering the time needed to sterilize granulomas. Our approach can efficiently test many regimens and successfully identify optimal regimens to inform pre-clinical studies or clinical trials and ultimately accelerate the TB regimen discovery process.

# Pharmacological evaluation of *N*-hydroxypyridinediones to support optimization as HBV ribonuclease H inhibitors

Molly Woodson,<sup>1</sup> M. Abdul Mottaleb,<sup>2</sup> Grigoris Zoidis,<sup>3</sup> and John Tavis<sup>4</sup>

<sup>1</sup>*Saint Louis Univ;* <sup>2</sup>*St Louis University;* <sup>3</sup>*University of Athens;* and <sup>4</sup>*Saint Louis University*

Abstract ID 19353

Poster Board 152

Hepatitis B Virus (HBV) chronically infects ~300 million people worldwide, resulting in > 880,000 deaths annually. Current treatment employs a combination of nucleos(t)ide analogs and interferon- $\alpha$ . While these drugs suppress viremia up to 5-6 log<sub>10</sub> in most patients, they are not curative and treatment is lifelong. HBV replicates by reverse transcription, which is catalyzed by the reverse transcriptase (RT) and ribonuclease H (RH) domains of the polymerase (P) protein. We have identified the HBV RH as a promising drug target and have ~300 RH inhibitors within a growing library of >2500 experimental compounds. Compounds primarily belong to 3 chemotypes: The  $\alpha$ -Hydroxytropolones ( $\alpha$ -HT), the *N*-hydroxypyridinediones (HPD), and the *N*-hydroxynaphthyridinones (HNO). The most potent HBV RH inhibitors are HPDs with low cytotoxicity (EC<sub>50</sub> <100 nM, selectivity indexes >1100). However, we lack critical knowledge that is essential for preclinical to clinical studies. Therefore, our goal was to understand factors that modulate HPD potency and to assess their potential to cause drug-drug interactions. The 16 compounds tested to date were highly soluble (> 200  $\mu$ M) with high P<sub>appS</sub> (> 1\*10<sup>-6</sup> cm/sec) in PAMPA at pHs 5 and 6.5, but not at pH 7.4. The two most potent compounds were tested in MDCK-MDR1 permeability assays. They had low P<sub>appS</sub> but were not actively effluxed (B-A/A-B < 2). Five HPDs were tested in microsome and hepatocyte assays, and all had t<sub>1/2</sub> > 30 min and > 2 hr, respectively. Plasma protein binding studies are ongoing, which employs an innovative EC<sub>50</sub> shift assay. To assess drug-drug interaction potential, 10 structurally diverse compounds were screened at 10  $\mu$ M against CYP3A4, CYP2C19, CYP1A2 and CYP2C9 in competitive inhibition assays. No compounds significantly inhibited CYP3A4 activity (< 25%), 3 of 10 significantly inhibited CYP1A2, and all 10 significantly inhibited CYP2C19 and CYP2C9. CYP3A4 and CYP2C19 induction was assessed for 4 HPDs so far by quantifying changes in mRNA expression, and none significantly increased CYP3A4 or CYP2C19 expression (fold change <2). CYP2C9 induction studies are ongoing. These results indicate the HPDs have desirable ADME parameters for preclinical to clinical testing, and they help inform structure-activity relationship studies as the HPDs are optimized to become clinical candidates for anti-HBV therapy.

# Development of highly potent and selective inhibitors for GRK5

Yueyi Chen<sup>1</sup>

<sup>1</sup>Purdue University

Abstract ID 14062

Poster Board 153

G protein-coupled receptor kinases (GRKs) regulate cell signaling by triggering receptor desensitization via phosphorylation on G protein-coupled receptors (GPCRs). The seven human GRKs (GRK1–GRK7) are classified into three subfamilies: GRK1 (GRK1 and GRK7), GRK2 (GRK2 and GRK3), and GRK4 (GRK4, GRK5, and GRK6). GRK2 and GRK5 are the most abundant in cardiovascular tissue, where they are potential targets for treatment of cardiovascular disease. GRK5 also undergoes Ca<sup>2+</sup>/calmodulin-dependent nuclear localization, where it phosphorylates histone deacetylase 5 (HDAC5), inducing an increase in transcription of cardiac hypertrophy-related genes. In GRK5-knockdown mice, cardiomyocytes are protected from hypertrophy; however, the specific roles of GRK5 in heart failure and hypertrophic cardiomyopathy are still unclear. Furthermore, GRK5 is required for cancer progression in various cancer types. Depletion of GRK5 has been shown to suppress prostate cancer, breast cancer, and non-small-cell lung cancer. Therefore, targeting GRK5 can also be a chemotherapeutic strategy. Here we are testing a series of inhibitors for GRK5/6 derived from the indolinone scaffold, utilizing Cys474 residue unique in GRK5/6 to enhance selectivity by covalent capture. We have been exploring different inhibitor warheads for improving potency and selectivity without potentially toxic functional groups. So far, we have identified several highly potent and selective GRK5 inhibitors. We are also in the progress of solving the co-crystal structure of GRK5 with the inhibitors for a better understanding of the inhibition mechanisms and facilitating improvement of inhibitors. Recently, we have also resolved the structure of an apo-GRK5, which will greatly enhance our understanding of the enzymatic mechanisms of GRK5 and improve the chance for ligand soaking. Overall, discovery of the inhibitors can significantly facilitate understanding and treatment of cardiovascular diseases and cancers.

Compound	GRK5 (μM)	GRK2 (μM)	GRK2/GRK5*
Sunitinib	0.83±0.07	130±200	157
018-21	0.010±0.008 (4)	>1000(3)	>100,000
021-21	0.06±0.04 (3)	90±20 (3)	1500
041-21	0.11±0.07 (3)	>1000(3)	>9090
045-21	0.8±0.5 (3)	>1000(3)	>1250
001-22	0.013±0.004 (3)	50±30 (3)	>3846
004-22	0.035±0.008 (3)	90±20 (3)	2571
010-22	0.010±0.0002 (3)	18±4 (3)	1800
030-22	0.06±0.01 (3)	>1000 (3)	>16,667

**Table 1.** IC<sub>50</sub> values (μM ± SD) of sunitinib and the most potent and selective chemical probes. Number of replicates shown in parentheses. \*Selectivity for GRK5 over GRK2 using the ratio of corresponding IC<sub>50</sub> values. Results are obtained using the single-endpoint radiometric kinase.

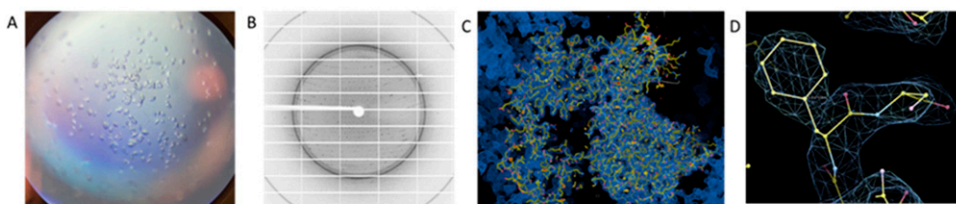


**Figure 2.** A) Crystallization of hGRK5-D311N mutant with Sgv. B) 2D diffraction map obtained using X-ray at Argonne National Lab synchrotron. C) Molecular replacement of GRK5 into the ligand-free density map. D) A single residue in the 3D structure solved with molecular replacement indicating

# Natural Products as a Source of Chemical Diversity in cyclic-AMP dependent Protein Kinase A (PKA) Inhibitor Discovery

Brice Wilson,<sup>1</sup> Ning Li,<sup>1</sup> Juliana Martinez Fiesco,<sup>1</sup> Masoumeh Dalilian,<sup>1</sup> Dongdong Wang,<sup>1</sup> Sarath Senadeera,<sup>1</sup> Lin Du,<sup>1</sup> Richard W. Fuller,<sup>1</sup> Rohan Shah,<sup>1</sup> Emily A. Smith,<sup>1</sup> Ekaterina I. Goncharova,<sup>1</sup> John A. Beutler,<sup>1</sup> Tanja Grkovic,<sup>1</sup> Ping Zhang,<sup>1</sup> and Barry R. O'Keefe<sup>1</sup>

<sup>1</sup>National Cancer Institute

**Abstract ID 52134**

**Poster Board 154**

3',5'-cyclic monophosphate (cAMP)-dependent protein kinase A (PKA) dysfunction underlies a number of human diseases, including a recently identified rare gene fusion which acts as an oncogene for fibrolamellar hepatocellular carcinoma (FLHCC). These important disease associations have led to a renaissance in drug development interest targeting this kinase. We therefore have established a suite of biochemical, cell-based, and structural biology assays for identifying and evaluating new pharmacophores for PKA inhibition. This discovery process entails a 384-well high throughput screen of more than 300,000 substances, focusing on fractionated natural product extracts. Validated active compounds were subsequently characterized using biochemical, biophysical, and cell-based assays. This detailed assessment identified several previously unrecognized PKA pharmacophores and led to the generation of new x-ray crystallography structures demonstrating unique interactions between PKA and bound inhibitor molecules.

This research was supported in whole or in part with Federal Funds from National Cancer Institute, Center for Cancer Research, National Institutes of Health, Department of Health and Human Services, Intramural Program, under project number ZIA BC 011744 (P.Z.), contract number 75N91019D00024 (M.D., E.A.S., and A.W.), the Cancer Moonshot Program- NCI Program for Natural Product Discovery (ZIA BC 011854 (B.R.O.)), Cell-free assay technologies for the identification of active compounds (ZIA BC 011471, (B.R.O.)), and Assay development and screening for molecular targets and discovery (ZIA BC 011904 (B.R.O.)).

# Pharmacological and Genetic Preclinical Models of Ghrelin Receptor Functional Selectivity to Investigate Metabolic Disease Pathophysiology

Joshua Gross,<sup>1</sup> Lara Kohlenbach,<sup>2</sup> Yang Zhou,<sup>1</sup> Juan J. Marugan,<sup>3</sup> and Lawrence S. Barak<sup>1</sup>

<sup>1</sup>Duke University School of Medicine; <sup>2</sup>Duke University; and <sup>3</sup>National Center for Advancing Translational Sciences (NCATS), National Institutes of Health (NIH)

Abstract ID 17517

Poster Board 161

The growth hormone secretagogue receptor-1a (GHSR<sub>1a</sub>) is an attractive pharmacological target for several prevalent metabolic diseases, including obesity, diabetes, and neurodegeneration. The GHSR<sub>1a</sub> acts pleiotropically during caloric restriction and/or environmental stress to restore physiological homeostasis through both central and peripheral metabolic processes, such as those mediating food-seeking behavior, glucose homeostasis, and energy expenditure. GHSR<sub>1a</sub> signaling is primarily regulated by the orexigenic hormone ghrelin, the anorexigenic antagonist liver-derived anti-microbial protein-2 (LEAP2), and allosteric interactions with intracellular G proteins or  $\beta$ -arrestins ( $\beta$ arr). G protein- and  $\beta$ arr-dependent signaling pathways downstream of the GHSR<sub>1a</sub> produce dissociable physiological effects that can be evaluated according to their similarity and strength, *i.e.*, 'signaling bias' or 'functional selectivity'. To discover biased GHSR<sub>1a</sub> drug candidates, we screened a 50,000 compound library and identified a novel chemotype of small molecule GHSR<sub>1a</sub> agonists. Further investigation and optimization led to the discovery of a GHSR<sub>1a</sub>-selective, brain penetrant, G protein-biased agonist, N8279 (NCATS-SM8864; Gross et al. 2022, PNAS). In a parallel genetic-based effort, we engineered transgenic mice expressing contiguous GHSR<sub>1a</sub> point mutations that elicit either complete G protein or  $\beta$ arr-dependent signaling bias. Thus, these two strategies together enable an orthogonal, pharmacological-genetic evaluation of GHSR<sub>1a</sub> signaling bias *in vivo*. Our metabolic and physiological studies with GHSR<sub>1a</sub><sup>Gprotein</sup> and GHSR<sub>1a</sub> <sup>$\beta$ arr</sup> mice demonstrate distinct differences in homeostatic and hedonic food intake, glucose/insulin homeostasis, and body weight in an energy state-dependent manner (e.g., fasted, fed, obesogenic diet). Therefore, these results provide proof-of-concept that leveraging GHSR<sub>1a</sub> functional selectivity pharmacologically may be a viable strategy for generating targeted, GHSR<sub>1a</sub>-directed therapies that are superior to unbiased drugs. Lastly, we have also engineered a humanized GHSR<sub>1a</sub> mouse that will enable efficacy testing of N8279 and its analogues in a more clinically-relevant animal model. Collectively, our approach employing complementary pharmacologic and genetic tools can provide important insights into basic mechanisms of GPCR signaling; and moreover, illustrate the potential of biased GHSR<sub>1a</sub> pharmacotherapy to ameliorate pathological disruptions in metabolic homeostasis.

Support/Funding Information: F32DA051139 (JDG), U18DA052417 (LSB), ZIATR000083 (JJM)

# Design, Synthesis and Biological Evaluation of Benzothiazole-Phenyl Analogs as Multi-Target Directed Ligands for Treating Pain

Stevan Pecic,<sup>1</sup> Jeannes Angelia,<sup>1</sup> and Xiaohui Weng<sup>1</sup>

<sup>1</sup>California State University Fullerton

Abstract ID 14305

Poster Board 162

Soluble epoxide hydrolase (sEH) and fatty acid amide hydrolase (FAAH) are potential targets for several diseases. Previous studies have reported that concomitant selective inhibition of sEH and FAAH produced antinociception effects in an animal model of pain. However, the co-administration of a selective sEH inhibitor and a selective FAAH inhibitor might produce serious side effects due to drug-drug interactions that could complicate drug development in the long term. Thus, discovering dual sEH/FAAH inhibitors, single small molecules that can simultaneously inhibit both sEH and FAAH, would be a significant accomplishment in the medicinal chemistry field. Herein, we report the synthesis and biological evaluation of benzothiazole-phenyl-based analogs as potential dual sEH/FAAH inhibitors. This work represents a follow-up structure activity relationship (SAR) and metabolic-stability studies of our best dual sEH/FAAH inhibitor identified previously. Our SAR study indicates that trifluoromethyl groups on the aromatic rings are well tolerated by the targeted enzymes when placed at the ortho and para positions; however, they, surprisingly, did not improve metabolic stability in liver microsomes.

Support/Funding Information: National Institute of General Medical Sciences of the National Institutes of Health under Award Number SC2GM135020

# Pulmonary delivery of nanochelators decreases lung iron accumulation and alleviates bleomycin-induced lung fibrosis in rats

Mayuri Patwardhan,<sup>1</sup> Wesley Stiles,<sup>2</sup> Homan Kang,<sup>3</sup> Hak Soo Choi,<sup>3</sup> and Jonghan Kim<sup>1</sup>

<sup>1</sup>Univ of Massachusetts Lowell; <sup>2</sup>Gordon Center for Medical Imaging, Massachusetts General Hospital (MGH); and <sup>3</sup>Gordon Center for Medical Imaging, Massachusetts General Hospital

Abstract ID 17759

Poster Board 291

Idiopathic pulmonary fibrosis (IPF) is a fatal condition with no known cure. Patients with IPF have a poor prognosis; the estimated mean survival time is 2-5 years after diagnosis. The disease is characterized by progressive collagen accumulation in the lungs, which causes alveolar damage and scarring, though the exact molecular mechanism is unknown. Dysregulated iron homeostasis is considered to be a key mediator in the pathogenesis of the disease. Furthermore, pulmonary iron accumulation is linked to fibrosis and lung function decline in bleomycin-induced rodent models of IPF. Molecular studies have shown that excess iron induces oxidative stress in the lung, which causes structural destruction, epithelial-mesenchymal transition, and collagen accumulation. While deferoxamine conjugated nanoparticles (DFO-NPs; nanochelators) have shown superior efficacy and safety in various systemic iron overload models, we examined in the present study if DFO-NPs decrease lung iron overload associated with IPF using bleomycin-exposed rats, a well-established rodent model of IPF. Intratracheal (IT) instillation of bleomycin (2.5 mg/kg) causes lung fibrosis in rats, as evidenced by an increase in collagen content, alveolar structure damage, and iron accumulation. IT administration of DFO-NP (2  $\mu$ mole/kg) improved body weight loss caused by bleomycin treatment and restored lung iron accumulation ( $p < 0.05$ ) in bleomycin-challenged rats. Moreover, DFO-NPs treatment reversed fibrosis and oxidative stress associated with bleomycin. An equimolar dose of native deferoxamine also reduced lung injury markers, but the effects were not statistically significant ( $p = 0.88$ ), while empty NPs (with no DFO) did not show anti-fibrotic effects, verifying that therapeutic benefits of DFO-NPs are associated with iron chelation. Although IT administration of nintedanib, the current treatment for IPF, showed anti-fibrotic activity, it demonstrated several side effects such as liver injury, whereas DFO-NPs did not exhibit any toxicity. These data suggest that the pathogenesis of pulmonary fibrosis and the decline in lung function are influenced by increased pulmonary iron accumulation. Furthermore, these findings emphasize the potential therapeutic benefit of pulmonary iron chelation for IPF via nanomedicine delivery.



# Virtual Screening for Potential Hepatitis B Virus Non-Nucleoside Reverse Transcriptase Inhibitors

Emma Inmon,<sup>1</sup> Razia Tajwar,<sup>1</sup> Qilan Li,<sup>1</sup> Marvin J. Meyers,<sup>1</sup> and John Tavis<sup>1</sup>

<sup>1</sup>*Saint Louis University*

**Abstract ID 23309**

**Poster Board 292**

Hepatitis B virus (HBV) is a major global health problem. Current HBV therapies are not curative, so improved therapeutics are urgently needed to develop combinations of novel drugs to achieve a cure. HBV replication is catalyzed by the viral polymerase (P) protein with reverse transcriptase and ribonuclease H activities. The P protein is vital for HBV replication and provides a great target for new therapies against HBV. We recently predicted and validated the structure of P for the first time (Tajwar et al., *Protein Science* 31:e4421). Using SiteMap from the Schrödinger Suite software, we found three potential non-active site targets on the HBV P protein analogous to the targets for HIV non-nucleoside reverse transcriptase (NNRTI) drugs. We conducted a three-tier high throughput virtual screen using the Chembridge CORE library of 830,000+ compounds against the three target sites. The top scoring 300 compounds per site were re-scored using induced-fit docking. Docking scores were as low as -12.6 kCal/mol. We then examined the top hits for ligand uniqueness, binding poses, compound conformational stability and rigidity, cLogP values, and chemotype clustering, followed by manual selection of ~50 compounds per target site for wet-bench testing. The chosen compounds are being assayed for toxicity and ability to inhibit HBV replication in cells. The long-term goals are to launch medicinal chemistry optimization campaigns to generate novel HBV NNRTI drugs and to develop tool compounds for mechanistic analysis of HBV reverse transcription.

Support/Funding Information: Seed grant from the Saint Louis University Liver Center

# Preclinical and Phase I Clinical Development of a Novel Multi-target Drug Candidate for Neuropathic Pain

Zsuzsanna Helyes,<sup>1</sup> Adam Horvath Horvath,<sup>2</sup> Nikolett Szentes,<sup>2</sup> Valeria Tekus,<sup>2</sup> Szilard Pal,<sup>3</sup> Tamás Kálai,<sup>2</sup> and Péter Mátyus<sup>4</sup>

<sup>1</sup>University of Pécs, Medical School; <sup>2</sup>University of Pécs, Medical School; <sup>3</sup>University of Pécs, Faculty of Pharmacy; and

<sup>4</sup>University of Pécs, Medical School & E-Group

**Abstract ID 16166**

**Poster Board 293**

SZV-1287 (3-(4,5-diphenyl-1,3-oxazol-2-yl)propanal oxime) is a unique, novel multi-target drug, which irreversibly inhibits the semicarbazide-sensitive amine oxidase (ssAO) enzyme. ssAO metabolizes primary amines to irritants like methylglyoxal and formaldehyde activating the transient receptor potential ankyrin 1 (TRPA1) and vanilloid 1 (TRPV1) non-selective cation channels. SZV-1287 also directly antagonizes TRPA1 and TRPV1 receptors located predominantly on nociceptive primary sensory neurons, immune cells and several central nervous system regions. Furthermore, its main metabolite, oxaprozin, is a clinically used cyclooxygenase inhibitor, which might have synergistic effect with the mother compound in several pain conditions.

We provided proof-of-concept for the ability of single SZV-1287 administration (10-50 mg/kg i.p.) to significantly reduce acute and chronic pain behaviors including the sciatic nerve injury-induced neuropathic hyperalgesia in mice via inhibiting TRPA1 and TRPV1 activation. Repeated 20 mg/kg SZV-1287 injections attenuated chronic arthritis (edema, myeloperoxidase activity, histopathological changes) and related hyperalgesia, L4-L6 spinal dorsal horn neuroinflammation (microgliosis) even in the late phase of the model when neuropathic mechanisms are important. Since under the acidic conditions of the stomach, SZV-1287 is transformed to oxaprozin, which is ineffective for neuropathic pain, enterosolvent capsule was formulated and tested during the preclinical development. SZV-1287 was quickly absorbed, its plasma concentration was stable for 2 h, and entered the brain. Although SZV-1287 significantly decreased proton-induced TRPV1-mediated calcium-influx potentially leading to hyperthermia, it did not alter the deep body temperature. It did not induce any considerable toxicity either in rodents or in dogs.

After the approval of the preclinical dossier by the Hungarian authority, the phase IA trial (single ascending dosing: 75, 150, 300, 450 mg) has successfully been completed without any considerable side effects. SZV-1287 plasma concentration was stable for 4 h and oxaprozin concentration continuously increased during 24 h. If the candidate proves to be safe in humans after repeated dosing for 7 days with favorable kinetic profile, the compound can progress to the phase II. studies in neuropathic pain patients. This project is a good example for successful early development of a novel compound originating from the academia together with industrial partners.

Support/Funding Information: GINOP-2.2.1-15-2016-00020, Eotvos Lorand Research Network, OTKA-K138046, National Laboratory for Drug Research and Development, TKP2021-EGA-16, National Brain Research Program-3

# The Modulatory Effects of Citrus Flavonoid Hesperetin on Nrf2 Expression and NF- $\kappa$ B Signaling Pathway in LPS-Activated BV-2 Microglial Cells

Karam F. Soliman,<sup>1</sup> Jasmine A. Evans,<sup>2</sup> and Patricia Mendonca<sup>2</sup>

<sup>1</sup>Florida A & M Univ College of Pharmacy; and <sup>2</sup>Florida A&M University

Abstract ID 16737

Poster Board 294

Neurodegenerative diseases have become more prevalent as the population ages. Oxidative stress and neuroinflammation have been suggested as critical factors in the progression of these diseases. Chronic neuroinflammation is a crucial part of the immune response against various pathogens in the central nervous system. The chronic production of proinflammatory mediators and activation of microglial cells may lead to the onset of neurodegenerative diseases, such as Alzheimer's. Studies have shown that flavonoids can reduce neuroinflammation by modulating specific genes of the NF- $\kappa$ B signaling pathway, which is associated with inflammation in the brain. These natural compounds also upregulate Nrf2, which is a critical transcription factor that combats oxidative stress by inducing the transcription of multiple antioxidant genes. The present study evaluated the effect of hesperetin, a flavonoid, on LPS-activated BV-2 microglial cells. The objective was to investigate the hesperetin modulatory effect on inflammation and oxidative stress. The results show the expression of hesperetin-induced catalase (CAT) and superoxide dismutase (SOD) after 48-h treatment, even after the cells were stimulated with LPS. The same effect was obtained in glutathione (GSH), showing that hesperetin induced the expression of glutathione on LPS-activated BV-2 cells. Data from PCR arrays showed that 100  $\mu$ M of hesperetin modulated numerous genes that regulate oxidative stress and inflammatory processes. Hesperetin down-regulated mRNA expression of proinflammatory genes *ERCC6*, *NOS2*, and *NCF1* and upregulated the expression of *HMOX1*, a critical antioxidant gene that aids in reducing excessive oxidative stress. RT-PCR also showed that hesperetin upregulated Nrf2 mRNA expression, which is involved in the transcription of several antioxidant genes. In addition, hesperetin modulated the expression of genes associated with NF- $\kappa$ B signaling, including *RELA*, *NF- $\kappa$ B1*, *NF- $\kappa$ B2*, and *NF- $\kappa$ BIA*. The lack of expression of these genes has been associated with increased neuroinflammation observed in Alzheimer's disease. The findings obtained in this study indicate that hesperetin may be a potential candidate for neurodegenerative diseases therapy by upregulating Nrf2 expression and subsequent transcription of antioxidant genes and also by reducing neuroinflammation through the modulation of the NF- $\kappa$ B signaling, which could slow the onset and progression of AD.

Support/Funding Information: National Institute of Minority Health and Health Disparities of the NIH U54 MD007582

# Effect of Topical Application of cannabis fixed Oil on Imiquimod-Induced Psoriasis-like Lesions in the Thin Skin of Adult Male Albino rabbits

Youness Kadil,<sup>1</sup> Hasnaa Bazhar,<sup>2</sup> Ibtihal Segmani,<sup>2</sup> afaf Banid,<sup>2</sup> Fatimaezzahra kabbali,<sup>2</sup> and Houda FILALI<sup>2</sup>

<sup>1</sup>Faculty of Medecine and Pharmacy of Casablanca; and <sup>2</sup>Faculty of Medicine and Pharmacy, University of Hassan II Casablanca

**Abstract ID 23613**

**Poster Board 295**

Psoriasis is a chronic autoimmune inflammatory skin disease with no clear cause. Cannabis sativa is a medicinal plant with significant pharmacological properties based on the existence of pharmacologically relevant chemicals. The aim of this investigation was to explore the effect of fixed cannabis oil on psoriasis-like skin lesions induced by Imiquimod. To this end, 16 male Albino rabbits were divided into 4 groups. The 3 psoriasis-inducing groups received twice-daily topical applications of Imiquimod cream (5%) to the skin of the shaved back for 10 consecutive days.

Following treatment, samples obtained from the mid-back skin were collected, and processed for immunohistochemical and histological investigation.

Application of imiquimod resulted in epidermal inflammation, hyperplasia, and changes in the usual appearance of keratinocytes with degenerative changes observed at the light microscopic level.

Nonetheless, the topical application of fixed cannabis oil significantly attenuated the Imiquimod-induced psoriasis-like inflammation and all epidermal and other dermal alterations, which leads us to conclude that fixed cannabis oil can be used as an adjuvant topical therapy to treat psoriasis.

# Herbal microbiomes are plant-specific and rich in immune-stimulating pathogen-associated molecular pattern molecules

Elizabeth Mazzio,<sup>1</sup> Andrew BArnes,<sup>1</sup> Ramesh Badisa,<sup>1</sup> Henry Williams,<sup>1</sup> and Karam F. Soliman<sup>2</sup>

<sup>1</sup>FLORIDA A&M UNIVERSITY; and <sup>2</sup>Florida A & M Univ College of Pharmacy

Abstract ID 14491

Poster Board 296

For thousands of years, humans have been orally consuming herbal botanical medicines, ascribing the beneficial effects to the plant itself. Oddly, we have not yet realized the impact of ingesting dead/live microorganisms in these plants. The residual dead remains of the herbal microbiome can and do leave a trail of thermal and pH-stable immune-stimulating antigenic epitopes with the capacity to act in the human gut. The current study employs a high throughput screening to elucidate the immune-stimulating properties of over-the-counter (OTC) / point-of-sale (POS) herbs. The findings illustrate the existence of an immune active herbal bioactive microbiome, which is plant specific but independent of the plant itself. In this study, an initial high throughput screening of 2535 phytochemicals and OTC/POS'S botanicals was carried out to elucidate pro-inflammatory effects in RAW 264.7 macrophages, with many as potent as positive controls: lipopolysaccharide (LPS) (E.coli 0111:B4). Microbial pathogen-associated molecular pattern molecules (PAMPS) in bio-active herbs were removed from the plants by spin column application, extracts were retested for a bioactive response, and the pH stability of LPS analyzed using a stomach simulation model. Lastly, we reverse cultured the "residual remains" in 7 OTC/POS herbs which were isolated, colonized, and sequenced using Illumina targeting the V4 region of the 16S rRNA gene and the V1-V3 region of the 18S rRNA gene. The obtained results show that Out of 2535 compounds screened, not a single phytochemical or drug (>500 tested) could mimic LPS, which was only observed for 65 "specific" herbal medicine plants, having high concentrations of PAMPS, dominating in roots and oceanic marine sea kelps /algae's [e.g., Roots of Burdock, Hydrangea, Poke, Madder, Sarsaparilla, Calamus, Rhaponticum, Pleurisy, Aconite], [e.g., Marine products: Bladderwrack, Chlorella, Spirulina, Kelp, and product combinations sold as Sea moss (Irish Moss, Bladderwrack, Burdock Root)] and Misc. (Cleavers, Watercress, Cardamom seed, Tribulus Fruit, Duckweed, Puffball, Hordeum, Pu Huang /Pollen). Microbial PAMPS in bioactive herbs, removed by spin column application, established herbs as biologically inert, with sea alginates having a greater affinity for PAMPS than the removal column. These findings suggest sea alginates as a natural reservoir of microbes. A stomach simulation model showed LPS maintained full activity after a 4-hour retention time in up to 2 N HCL. Reverse culture studies provided evidence for diverse gram-negative presence, not from the E. Coli strain. Conclusions: The findings from this work suggest dead active microorganism communities are abundant in specific medicinal OTC/ POS botanical supplements and responsible for immune stimulation. Given pH stability, these could pass through the stomach and work to signal the upper GI-immune axis. It is well known that herbal microbial debris is not removed or assessed for by scientific protocols in standard laboratories, which could lead to false positives attributed to the herbs. Research into the bioactive microbial debris in herbal medicine is needed, as would its relevance to cancer and auto-immune diseases.

This work was supported by NIMHD grant U54 MD 007582

# Targeting the TAK1/TNF signaling pathway with novel pharmacological inhibitors

Scott Scarneo,<sup>1</sup> Timothy Haystead,<sup>2</sup> Philip Hughes,<sup>3</sup> and Robert Freeze<sup>3</sup>

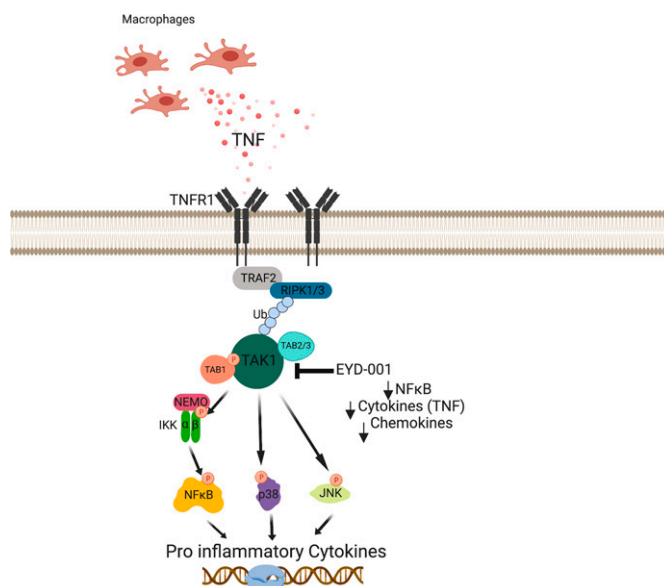
<sup>1</sup>EydisBio Inc; <sup>2</sup>Duke Univ; and <sup>3</sup>EydisBio Inc.

Abstract ID 13594

Poster Board 297

The serine/threonine protein kinase transforming growth factor- $\beta$ -activated kinase 1 (TAK1) is a key regulatory signaling node in the tumor necrosis factor (TNF) pathway, mediating proinflammatory cytokine responses in immune cells. To date very few selective TAK1 inhibitors have been developed and none have advanced into the clinic for the treatment of autoimmune diseases. Our group is the first to develop a selective orally bioavailable TAK1 inhibitor for the treatment of autoimmune diseases such as rheumatoid arthritis (RA). Our work has identified a low nM (IC<sub>50</sub>=2.5nM) inhibitor of TAK1 with 98% oral bioavailability. Furthermore, EYD-001 is selective within the human kinome. To test the effects if TAK1 inhibition in disease relevant animal models, we next sought to test the drug efficacy of EYD-001 in the collagen induced arthritis (CIA) pre-clinical mouse model of RA. In the CIA model, TAK1 inhibition led to a significant reduction in disease score, evidenced by histological reductions in edema and inflammation in the knee as well as significant reduction of TNF expression in the serum, paw and knee synovial fluid. Compared to Enbrel (anti-TNF monoclonal antibody) treated animals, TAK1 inhibition with EYD-001 performed equally or better. Based on our findings we posit that the development of novel TAK1 inhibitors will expand the therapeutic options available to patient suffering from auto immune diseases such as RA.

This work is supported by NIH grant R44AR076772 to Scott Scarneo and Timothy Haystead.



The TNF/TAK1 signaling pathway. Inhibition of TAK1 with EYD-001 represents a novel drug target for the treatment of TNF mediated autoimmune diseases.

# Development and Validation of a Simple and Selective HPLC-MS/MS Method for Simultaneous Quantification of GS-441524 and its Prodrug Remdesivir

Su Guan,<sup>1</sup> Meijuan Tu,<sup>2</sup> Samantha Evans,<sup>3</sup> and Aiming Yu<sup>4</sup>

<sup>1</sup>Univ of California Davis Health; <sup>2</sup>Univ of California, Davis; <sup>3</sup>The Ohio State University; and <sup>4</sup>UC Davis School of Medicine

Abstract ID 52032

Poster Board 298

Remdesivir is the first antiviral drug approved by the U.S. Food and Drug Administration to treat COVID-19. GS-441524 is the active metabolite of remdesivir, and its antiviral activity against COVID-19 has been confirmed. The aims of this study were to develop and validate an HPLC-MS/MS method for the quantification of GS-441524 in commercial injectable products and to determine the level of its prodrug remdesivir, if any. A rapid, sensitive, and reliable method was thus developed for simultaneous determination of GS-441524 and remdesivir. An isotope labeled analog, remdesivir-D5, was used as the internal standard. Chromatographic separation was performed on a Thermo® AQUASIL C18 (50 × 4.6 mm, 3 μm) column by gradient elution. Multiple reaction monitoring transitions in electrospray positive ion mode were m/z 292.3@202.1 for GS-441524, 603.4@402.3 for remdesivir, and 608.6@407.2 for the internal standard. The total running time was within 5 min, with baseline separation of the prodrug and active metabolite. The calibration curves were linear over the range of 100-4000 ng/mL for GS-441524 and 10-400 ng/mL for remdesivir, with the mean correlation coefficients greater than 0.99. Acceptable precision and accuracy were achieved by using this method. Precisions evaluated at 150, 500, and 3000 ng/mL for GS-441524 and 15, 50, 300 ng/mL for remdesivir, respectively, were lower than 2.7%, and accuracy was in the 90.0-106.7% range. The validated HPLC-MS/MS method was successfully applied to examine the contents of GS-441524 and remdesivir among some commercially available products.

# Marine-Derived Pharmaceuticals in Clinical Trials in 2022

Alejandro MS. Mayer,<sup>1</sup> Marsha Pierce,<sup>2</sup> Maria Reji,<sup>3</sup> Alex C. Wu,<sup>3</sup> Karolina K. Jekielek,<sup>3</sup> Henry Q. Le,<sup>3</sup> Katelyn Howe,<sup>3</sup> Maryam Butt,<sup>2</sup> Sujin Seo,<sup>3</sup> David J. Newman,<sup>4</sup> and Keith B. Glaser<sup>5</sup>

<sup>1</sup>Midwestern Univ, College of Graduate Studies; <sup>2</sup>Midwestern Univ; <sup>3</sup>Midwestern University; <sup>4</sup>NIH Special Volunteer, Natural Products Branch; and <sup>5</sup>AbbVie, Inc

Abstract ID 52701

Poster Board 299

**Objective:** Natural products contribute substantially to clinical pharmaceuticals, with an estimated 60-70% of active compounds derived from or inspired by natural products. Due to adaptation to their unique habitat, the marine environment is a rich source of biologically active primary and secondary metabolites not represented in synthetic compound libraries. To track progress of the clinical development of marine pharmaceuticals, we maintain the website [www.marinepharmacology.org](http://www.marinepharmacology.org) as a reference for those with an interest in the preclinical and clinical development of marine compounds, which has nearly 10,000 views since its redesign in 2021. In 2022, there were 15 marine-derived drugs approved by the FDA, two approved in Australia, and one approved in China.

**Hypothesis:** There has been progress in the clinical development of marine-derived pharmaceuticals in 2022.

**Methodology:** To identify new marine-derived compounds and track their advancements, the following websites were researched: (a) USA: <https://www.accessdata.fda.gov/scripts/cder/daf/> United States Food and Drug Administration (FDA); (b) Europe: <https://www.clinicaltrialsregister.eu/ctr-search/> search European Clinical Trials register; (c) China: <https://www.chictr.org.cn/enindex.aspx> Chinese Clinical Trials register; and (d) [www.clinicaltrials.gov](http://www.clinicaltrials.gov) to determine the current status of marine-derived compounds in clinical trials.

**Results:** Several marine-derived compounds targeting the receptors and proteins (shown in brackets), have been added to the marine-derived pharmaceutical pipeline or progressed in their development in 2022: E7130 (microtubules), and antibody-drug conjugates (ADCs) BT5528 (EPhA2 with Monomethyl Auristatin E, MMAE, which blocks tubulin polymerization) and BT8009 (Nectin-4 with MMAE) all for cancer therapy have initiated Phase I clinical trials. The ADCs MORAb-202 (FRalpha with Eribulin), MRG003 (EGFR with MMAE), A-166 (HER-2 with Duostatin 5), RC-88 (mesothelin with MMAE) for cancer therapy and STI-6129 (CD38 with Duostatin 5.2) for refractory amyloidosis therapy have ongoing Phase I and Phase II clinical trials. The ADCs ARX-788 (HER-2 with Amberstatin269) and Upifitamab rilsodotin (NaPi2b with Auristatin F- hydroxypropylamide) for cancer therapy moved from Phase I into Phase II and III clinical trials. At the end of 2022, there were 34 marine-derived compounds in active clinical trials: 6 marine-derived compounds were in Phase III, 15 compounds in Phase II, and at least 19 compounds in Phase I.

**Conclusions:** In 2022, the clinical development of marine-derived drugs remained very active with several compounds entering Phase I, and others advancing to Phase II and Phase III.

This work was supported by Midwestern University Intramural Funds.



# An Elastin-like Polypeptide-fused Peptide Inhibits MMP-2 Activity at nM Concentrations with High Specificity

Adesanya A. Akinleye,<sup>1</sup> Richard J. Roman,<sup>1</sup> and Gene L. Bidwell<sup>1</sup>

<sup>1</sup>University of Mississippi Medical Center

Abstract ID 20222

Poster Board 300

Chronic kidney disease (CKD) is a growing health concern. Renal fibrosis results from buildup of extracellular matrix (ECM) proteins replacing functional tissue. Matrix metalloproteinases (MMP) are endopeptidases that maintain ECM homeostasis. Studies suggest that in early stages of CKD, increases in MMP-2 activity can promote activation of inflammatory and pro-fibrotic cytokines, driving renal fibrosis. Our lab has recently created a chimeric fusion protein between an MMP-2 inhibitory peptide (MMP-2i) and the Elastin like polypeptide (ELP) drug carrier. ELP is a biopolymer created using a repetitive pentapeptide motif (VPGXG) that we've shown to stabilize peptide cargo in circulation and mediate delivery to the kidneys. We hypothesized the MMP-2i peptide would maintain potent and specific MMP-2 inhibition, when fused to the ELP carrier. We utilized variously sized ELP carriers, created using 63, 127, or 255 pentapeptide repeats, resulting in carrier molecular weights of 26, 50, and 99 kDa, respectively. The aims of the current study are: 1) to determine if changes in the ELP carrier size affect the inhibitory activity of MMP-2, 2) to validate that ELP-MMP2i specifically inhibited MMP-2 compared to other renally expressed MMPs, and 3) to optimize the renal delivery of ELP-MMP2i by testing various sizes of the ELP carrier. Using a fluorescent resonance energy transfer assay, the activity of MMP2 (20 ng/mL) was determined in the presence of ELP-MMP-2i or ELP control of each molecular weight. All ELP-MMP2i constructs were potent inhibitors of MMP-2 activity, and the potency of inhibition increased as the size of the ELP carrier decreased ( $IC_{50}$  = 10.5, 96.8, and 361.7 nM for the 26, 50, and 99 kDa proteins, respectively). The most potent inhibitor of MMP2, ELP<sub>63</sub>-MMP2i, was also tested for inhibition of five additional renally-expressed MMPs (20 ng/mL). ELP-MMP2i had no detectable inhibition of MMP-9, and the  $IC_{50}$  for inhibition of MMP-3, MMP-7, and MMP-10 was 85.1, 165.9, and 84.1 nM, respectively. ELP-MMP2i did not inhibit MMP14 at low micromolar concentration, though an  $IC_{50}$  could not be accurately determined. These data demonstrate that ELP-MMP2i is over 8,000x more potent for inhibition of MMP2 than most other renally-expressed MMPs. To assess plasma pharmacokinetics and biodistribution, Sprague Dawley rats (n=4/group) were dosed (600nmol/kg) either intravenously (IV) or subcutaneously (SC) with each of the ELP-MMP-2i proteins labelled with a fluorescent marker. Plasma clearance among the three proteins was size dependent in both routes of administration. Peak plasma levels were greatest with the 26 kDa protein. Bioavailability after SC administration was also greatest for the 26 kDa protein (55.3, 25.1, and 16.7% for 26, 50, and 99 kDa proteins). All proteins localized exclusively in the kidney after both IV and SC injection, and renal levels negatively correlated with the size of the ELP carrier (renal tissue concentrations of  $6.2 \pm 1.9$ ,  $3.6 \pm 0.2$ , and  $2.5 \pm 0.4$  mM for the 26, 50, and 99 kDa proteins, respectively, following IV administration (two-way ANOVA  $p < 0.0001$ ), and  $2.0 \pm 0.7$ ,  $0.6 \pm 0.1$ , and  $0.5 \pm 0.1$  mM following SC administration (two-way ANOVA  $p < 0.0001$ ). This study demonstrates that the ELP-fused MMP-2 inhibitory peptide maintains potent and specific MMP-2 inhibition, and the therapeutics localize to the kidney with high specificity after systemic administration.

This work was supported by NIH grants R01HL095638 to GLB, R01HL138685 to RJR and F31DK130598 to AAA.

# ***In vitro* antiglycation and protein cross-link breakage effects of *Murraya koenigii* leaf extracts and their phytochemical composition**

Oluwaseyefunmi Adeniran,<sup>1</sup> and Sechene S. Gololo<sup>2</sup>

<sup>1</sup>Sefako Makgatho Hlth Sci Univ; and <sup>2</sup>Sefako Makgatho Health Sciences U

Abstract ID 28622

Poster Board 313

*Murraya koenigii* (curry leaf) is a well-known spice and herb with several pharmacological benefits. Information regarding its ability to break cross-links formed between advanced glycation end products (AGEs) or prevent formation of advanced glycation end-products are limited. These AGEs are linked to vascular complications of diabetes and other age-related diseases.

Mixture of glucose and bovine serum albumin (BSA) were incubated with and without plant extracts (*Murraya koenigii* leaf *n*-hexane, ethyl acetate, methanol and water) or control (aminoguanidine) at 37°C for 40 days. AGEs inhibition and protein cross-link breakage effects of *Murraya koenigii* (*M. koenigii*) were assessed using enzyme-linked immunosorbent assay (ELISA) and spectrofluorometry. Their phytochemical compositions were determined using gas chromatography mass spectrometry (GC-MS) and standard chemical tests. Cell viability test of the leaf extracts were investigated using H-4-II-E liver cells.

All *M. koenigii* leaf extracts significantly inhibited the formation of BSA-glucose derived total immunogenic AGEs (TIAGEs) than aminoguanidine used as positive control ( $p < 0.0001$ ). Methanol and water extracts of the plant showed significantly higher anti-glycation effect ( $p < 0.001$ ) against carboxymethyl lysine formation than the control, aminoguanidine. Of the extracts, the highest anti-glycation effect against fluorescent AGEs was demonstrated by the methanol extract. Only the *n*-hexane, ethyl acetate and water extracts showed cross-link breakage ability. Methanol leaf extract of *M. koenigii* displayed 100% cell viability for concentrations ranging from 7.8 – 1000  $\mu\text{g/mL}$ .

The results of the study suggest that *Murraya koenigii* leaf extracts have both antiglycative and protein cross-link breakage effects. Phytochemical screening of the extracts gave an indication of secondary metabolites and compounds which may be responsible for the observed effects. Demonstration of the anti-glycation and AGEs-protein cross-link breaking effects of these extracts may lead to the identification and isolation of novel antiglycation phytochemicals and eventual new drug discovery and synthesis.

Support/Funding Information:

National Research Foundation (NRF), South Africa

Health and Welfare Sector Education and Training Authority (HWSETA), South Africa

Sefako Makgatho Health Sciences University (SMU), South Africa

# A Selective TRPC3 Antagonist Rescues Neuronal Loss and Facilitates Spatial Learning and Memory in Alzheimer's Model

Jiaxing Wang,<sup>1</sup> Sicheng Zhang,<sup>1</sup> Vijay K. Boda,<sup>1</sup> Zhongzhi Wu,<sup>1</sup> and Wei Li<sup>1</sup>

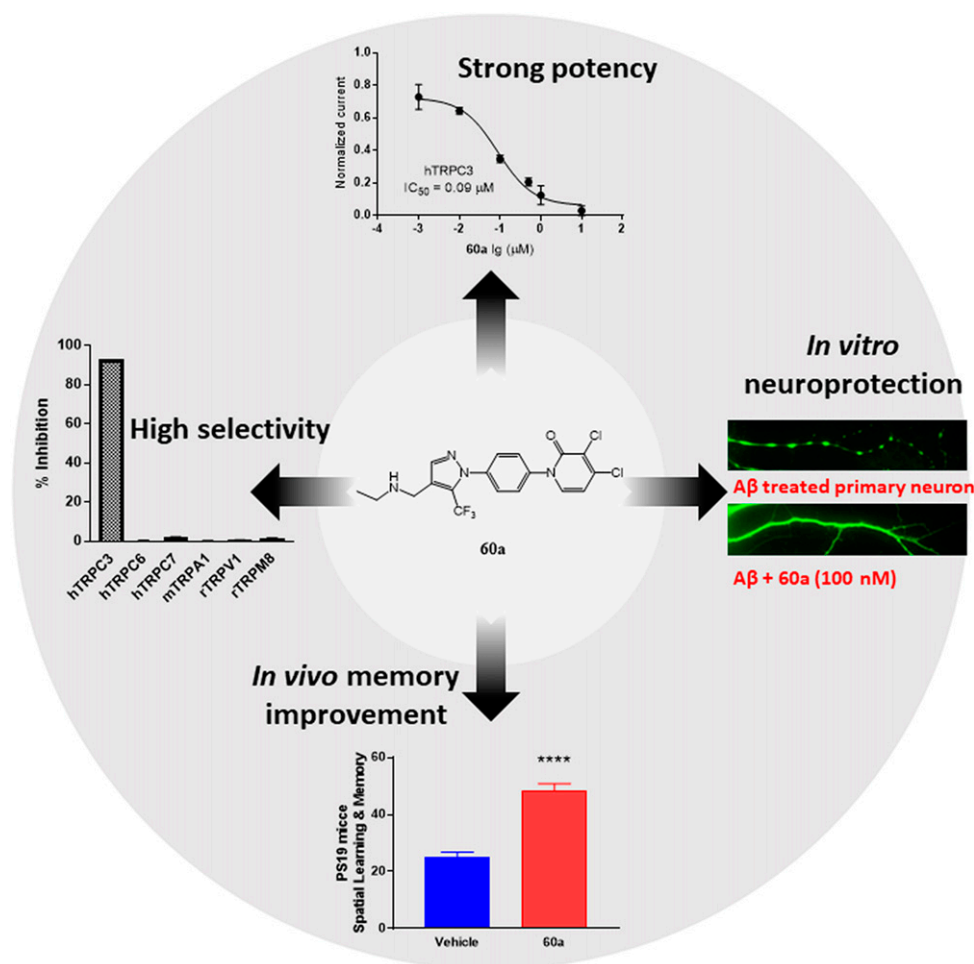
<sup>1</sup>University of Tennessee Health Science Center

Abstract ID 14268

Poster Board 314

Aberrant calcium signaling has intimate associations with multiple diseases. Upregulation of transient receptor potential canonical 3 (TRPC3), which is an ion channel that essentially mediates calcium influx, drives the progression of neurodegenerative diseases. We previously designed **JW-65**, a selective TRPC3 inhibitor with a favorable safety profile and good metabolic stability. However, **JW-65** has moderate potency ( $IC_{50} = 330$  nM) and selectivity for TRPC3 inhibition. Here we report a synthetic **JW-65** analog, **60a**, with significantly improved potency and selectivity. **60a** is a potent TRPC3 inhibitor ( $IC_{50} = 90$  nM) with no detectable inhibitory effect on the close homologs TRPC6/7, highlighting **60a** as the first truly selective TRPC3 inhibitor. *In vitro* evaluations of **60a** reveal its rescuing abilities on neuronal damage. *In vivo* studies indicate **60a** is a promising candidate for further development as a potential AD therapy with a novel mechanism of action.

This work was supported by the University of Tennessee College of Pharmacy Drug Discovery Center and NIH grant R61NS124923 to WL.



## Determination of Strychnine Levels in Serum and Brain via LC-MS/MS in Mice Vaccinated Against Strychnine

Jennifer Vigliaturo,<sup>1</sup> Carly Baehr,<sup>2</sup> Andrew Kassick,<sup>3</sup> Diego Luengas,<sup>1</sup> Aaron khaimraj,<sup>1</sup> Marco Pravetoni,<sup>4</sup> Saadyah Averick,<sup>5</sup> and Michael Raleigh<sup>1</sup>

<sup>1</sup>University of Minnesota; <sup>2</sup>Univ of Minnesota; <sup>3</sup>Allegheny Health Network Research Institute; <sup>4</sup>University of Washington School of Medicine; and <sup>5</sup>Allegheny Health Network Research Institute

**Abstract ID 53762**

**Poster Board 315**

Strychnine is an extremely toxic compound that can cause seizures, respiratory failure, and death with no available treatment. To determine if strychnine-specific antibodies could protect against strychnine-related effects and alter strychnine distribution in serum and brain, mice were vaccinated once every two weeks with a strychnine conjugate vaccine (Strychnine-sKLH adsorbed to aluminum) or aluminum alone. One week later, mice received a 0.9 mg/kg IP strychnine dose and blood and brain were collected 30 minutes. To quantitatively determine the strychnine in mouse serum and brain, a sensitive method has been developed and validated on liquid chromatography-tandem mass spectrometry (LC-MS/MS) in Electrospray ionization (ESI) inlet with dynamic multiple reaction monitoring (DMRM) mode. The method consists of a protein precipitation spiked with internal standard followed by solid phase extraction (SPE) using a Bond Elut PCX 96 well plate. Serum and brain supernatant samples of 200  $\mu$ L were pretreated via protein precipitation and internal standard. Chromatographic separation was carried out on a Poroshell EC C18 2.1 x 50mm 2.7u column. The method is linear in the range of 2.5-500 ng/mL and a relative standard error of 4.8%. Maximum detected strychnine in vaccinated mouse serum ranged from 79 to 471 ng/mL, 19 to 124 ng/mL in unvaccinated mice. Strychnine concentrations in vaccinated mouse brains ranged from 10 to 34 ng/gm, 46 to 97 ng/gm in unvaccinated mice. The results of this study showed that strychnine-sKLH reduced brain strychnine concentrations and demonstrate that a strychnine-immunotherapy could be developed to protect against strychnine-related effects.

# Analgesic and Side Effect Profiles of Novel Alpha-2 Adrenergic Receptor Agonists

Cristina D. Peterson,<sup>1</sup> Lukas Caye,<sup>1</sup> Kelley Kitto,<sup>2</sup> George L. Wilcox,<sup>3</sup> Laura Stone,<sup>2</sup> Swati More,<sup>2</sup> and Carolyn A. Fairbanks<sup>1</sup>

<sup>1</sup>Univ of Minnesota; <sup>2</sup>University of Minnesota; and <sup>3</sup>Univ of Minneapolis Medical School

Abstract ID 24150

Poster Board 316

Alpha 2 adrenergic receptor ( $\alpha_2$ -AR) agonists are effective analgesics while avoiding concerns surrounding opioid analgesia including misuse, diversion, and overdose. Clonidine, the best characterized  $\alpha_2$ -AR agonist, is limited in widespread use for analgesia by side effects including hypotension and sedation. We therefore developed a series of novel, non-opioid  $\alpha_2$ -AR agonists and assessed their kinetics, analgesic efficacy,  $\alpha_2$ -AR subtype affinity, and side effects.

**Methods:** We designed and synthesized novel  $\alpha_2$ -AR agonists, then determined dose ranges in female and male ICR mice (21-30 g) by intrathecal injection of the agonists with substance P to induce quantifiable transient nociceptive behaviors. Mice were pretreated with either an in-class control or the newly developed  $\alpha_2$ -AR agonists as single agents or in combinations and the maximum percent effect (%MPE) in reduction of the Substance P (SP)-induced nociception was calculated as compared to saline control. Following MPE calculation, motor impairment was assessed by administration of high effective doses in the open field and rotarod assays. In parallel, the novel agonists were administered in spared nerve injury (model of neuropathic pain), and in SPARC-null transgenic mice (model of low back pain).

**Results:** The novel  $\alpha_2$ -AR agonists, delivered either singly or in combination, were effective in reducing nociceptive behaviors in the SP assay. The efficacy of the novel compounds was inhibited by idazoxan or efaroxan, but not naloxone, supporting action at  $\alpha_2$ -AR and not opioid receptors. Additionally, the novel  $\alpha_2$ -AR agonists were also effective at reducing expression of pain behavior in chronic rodent models of neuropathic and low back pain. Additionally, the compounds showed attenuated sedation as compared to in-class controls. The pursuit of  $\alpha_2$ -AR agonists may represent an improved non-opioid analgesic strategy.

**Acknowledgments:** These studies were conducted with support from the College of Pharmacy, Winston and Maxine Wallin Neuroscience Discovery Fund, Center for Drug Design and the Dept of Anesthesiology.

# How ligands achieve biased signaling at opioid receptors

Joseph M. Paggi,<sup>1</sup> Deniz Aydin,<sup>1</sup> Yianni D. Laloudakis,<sup>1</sup> Carl-Mikael Suomivuori,<sup>1</sup> Tao Che,<sup>2</sup> and Ron O. Dror<sup>1</sup>

<sup>1</sup>Stanford University; and <sup>2</sup>Washington University in Saint Louis

**Abstract ID 27497**

**Poster Board 317**

Some drugs targeting the  $\kappa$ -opioid or  $\mu$ -opioid receptors induce fewer hazardous side effects than others. This is likely because these drugs preferentially stimulate G protein signaling over arrestin signaling, a phenomenon known as biased signaling. Ligands with more finely tuned biased signaling profiles are highly sought after in order to further decrease side effects while increasing efficacy, but the design of such ligands has proven challenging because the molecular mechanism of biased signaling has remained unclear. To determine this mechanism, we used molecular dynamics simulations to identify differences between receptor conformations favored by ligands with distinct signaling profiles, and then validated the results experimentally. In two parallel studies, we compared the relatively safe opioids nalfurafine, targeting the  $\kappa$ -opioid receptor, and mitragynine pseudoinoxyl, targeting the  $\mu$ -opioid receptor, to ligands known to induce severe side effects at each respective receptor. We found that, in both receptors, ligands achieve biased signaling by selecting among distinct receptor conformations. In particular, differently biased agonists differentially favor three active receptor conformations: a conformation that couples effectively to both G proteins and arrestins, a conformation that couples preferentially to G proteins, and a conformation that couples preferentially to arrestins. These conformations differ most notably in the orientation of the intracellular part of transmembrane helix 7, far from the ligand binding pocket but close to the binding surfaces of G proteins and arrestins. We identified several protein–ligand interactions that act together to determine the observed conformational ensemble. We validated our computationally derived mechanism using mutagenesis experiments and functional assays. Our work not only illuminates the structural basis for biased signaling at opioid receptors and related GPCRs, but also promises to guide the design of ligands with desired signaling profiles.

An award of computer time was provided by the INCITE program. This research used resources of the Oak Ridge Leadership Computing Facility, which is a U.S. Department of Energy Office of Science User Facility supported under contract DE-AC05-00OR22725.

# Development and Validation of a High-Throughput Cell-Based AlphaLISA Assay to Identify Small Molecule 20S Proteasome Modulators

Erika Lisabeth,<sup>1</sup> Sophia Staerz,<sup>2</sup> Evert Njomen,<sup>2</sup> Thomas Dexheimer,<sup>2</sup> Richard Neubig,<sup>1</sup> and Jetze Tepe<sup>1</sup>

<sup>1</sup>Michigan State Univ; and <sup>2</sup>Michigan State University

**Abstract ID 54242**

**Poster Board 318**

Intrinsically Disordered Proteins (IDPs) comprise a large fraction of the human proteome, and the regulation of IDPs is exquisitely modulated through protein synthesis and degradation mechanisms. Alterations in IDP homeostasis have been implicated in many diseases, including cancer, neurodegenerative diseases and diabetes. IDPs inherently lack a folded domain and can be degraded by the 20S proteasome core without previous ubiquitination. However, aggregation of IDPs due to oligomerization is a major contributor to neurodegenerative diseases, in part due to a decline of 20S proteasome activity as age increases. Therefore, enhancing 20S proteasome activity by small molecules is an attractive therapeutic target. Although several *in vitro* screens have been performed for 20S proteasome activators, no high-throughput cell-based assay was available to screen for 20S proteasome activators using an IDP as a target protein. In collaboration with the Assay Development and Drug Repurposing Core (ADDRC) at Michigan State University, we took advantage of the AlphaLISA bead technology to determine the protein levels of a GFP:ODC fusion protein in stably transfected HEK293T cells as a readout for 20S proteasome activity. We optimized this assay to a 384 well format and a  $Z' > 0.6$  and then validated this assay with our current 20S proteasome activator, TCH-165. This assay was used to screen the FDA Prestwick Library and NIH Clinical Library to identify compounds that could increase 20S proteasome activity in cells. After cell-based validation, these compounds were also tested *in vitro* against both the 20S and 26S proteasomes using standard fluorogenic small peptide assays to select for 20S proteasome specific small molecules. Finally, we validated these compounds in western blots against another IDP,  $\alpha$ -synuclein. Overall, our results show that this assay is robust, high-throughput and useful for identifying proteasome modulators in a cellular environment.

This work was supported by the National Institutes of Aging, NS111347

# A Computational Approach to Identify Small Molecules Interact with Crystal Structure of Programmed Cell Death Protein 1 as Potential Therapeutics for Cancer Immunotherapy

Hubert Chen,<sup>1</sup> and Mustafa Gabr<sup>2</sup>

<sup>1</sup>Vanderbilt University; and <sup>2</sup>Weill Cornell Medicine

Abstract ID 54817

Poster Board 319

**Objective:** Globally, cancer is a major burden of disease threatening human health. To date, immune checkpoint inhibitors are monoclonal antibodies that cover various cancer indications as monotherapy or in combination, have revealed remarkable clinical success in a wide range of solid tumors and hematologic malignancies. Due to the inherent limitations of antibodies, it is reasonable to consider discovering orally bioavailable small molecule inhibitors that target programmed cell death protein 1/programmed death-ligand 1 (PD-1/PD-L1) signaling pathway as alternative. The aim of this study is to mainly focus on computer aided drug design (CADD) process to predict the possible small molecules that can interact with PD-1, and further serve as starting points to design potential safe and efficacious compounds in cancer treatment.

**Methods:** Possible ligand binding sites on the PD-1 protein were initially predicted by DoGSiteScorer, FTsite and PrankWeb servers. The 6 highest-ranked clusters based on the “druggability” score from PocketQuery were selected as queries for pharmacophore-based virtual screening using ZincPharmer. Drug likeness property assessment and ADME-tox prediction have been performed by using SwissADME and ADMETlab.

**Results:** 30 hit compounds were initially retrieved by pharmacophore-based virtual screening. Thereafter, 5 compounds with lowest Gibb's free energy ( $\Delta G$ ) values, namely ZINC85867378, ZINC16267039, ZINC64219346, ZINC68604154 and ZINC20576138, have been chosen for further evaluation. ZINC68604154 showed  $\Delta G$  of -9.07 kcal/mol and appeared to have reasonable oral bioavailability, low drug-drug interaction potential, and low toxicity risk.

**Conclusion:** This study establishes the workflow combining pharmacophore virtual screening, molecular docking, and absorption, distribution, metabolism, excretion - toxicity (ADMET) prediction to identify possible small molecules that can interact with PD-1. The identified compounds might serve as starting points to design potential safe and efficacious molecules in cancer immunotherapy. Further evaluation through in vitro and in vivo is necessary to optimize drug properties.



# Venglustat Analogues with Enhanced Inhibition for Protein N-Terminal Methyltransferases 1/2

Rong Huang,<sup>1</sup> Youchao Deng,<sup>1</sup> and Ying Meng<sup>1</sup>

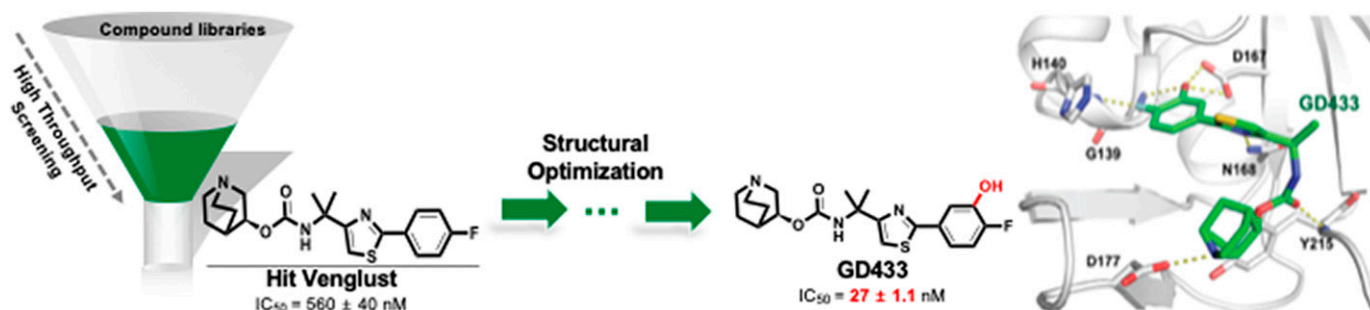
<sup>1</sup>Purdue University

Abstract ID 23315

Poster Board 320

Venglustat is a known allosteric inhibitor for ceramide glycosyltransferase, investigated in diseases caused by lysosomal dysfunction. We identified venglustat as a potent inhibitor ( $IC_{50} = 0.42 \mu\text{M}$ ) of protein N-terminal methyltransferase 1 (NTMT1) by high throughput screening. Furthermore, venglustat exhibited selectivity for NTMT1 over 36 other methyltransferases. The crystal structure of NTMT1-venglustat and inhibition mechanism revealed that venglustat competitively binds at the peptide substrate site. Meanwhile, venglustat potently inhibited protein N-terminal methylation levels in cells ( $IC_{50} = 0.5 \mu\text{M}$ ). Further structure-guided optimization of venglustat produced **GD433** ( $IC_{50} = 27 \pm 1.1 \text{ nM}$ ), displaying improved potency and selectivity than venglustat across biochemical, biophysical, and cellular assays. **GD433** also shows good oral bioavailability and can serve as an *in vivo* chemical probe to dissect the pharmacological roles of Na methylation. In addition, we also identified a close analogue that is inactive against NTMT1. The active inhibitor and negative control will serve as valuable tools to examine the physiological and pharmacological functions of NTMT1 catalytic activity. Additionally, this is the first disclosure of NTMT1 as a new molecular target of venglustat, which would cast light on its mechanism of action to guide clinical investigations and enhance its selectivity to ceramide glycosyltransferase.

Support/Funding Information: NIH grant U01CA214649 (RH), R01GM117275 (RH)



# Targeting human melanocortin type 2 receptor (MC2R) with small molecules and designed peptides for the treatment of congenital adrenal hyperplasia

Amit Pandey,<sup>1</sup> Shaheena Parween,<sup>2</sup> and Shripriya Singh<sup>2</sup>

<sup>1</sup>Univ of Bern; and <sup>2</sup>University of Bern

Abstract ID 24264

Poster Board 321

**Background:** The adrenocorticotrophic hormone (ACTH) is a 39 amino acid polypeptide secreted by the anterior pituitary and regulates cortisol secretion from the adrenal cortex. Cortisol has negative feedback and regulates the synthesis and secretion of ACTH. Excess ACTH is associated with a wide range of diseases including congenital adrenal hyperplasia (CAH). Classic CAH due to the 21-hydroxylase (CYP21A2) deficiency causes a reduction or loss of cortisol synthesis. Here the negative feedback is removed, causing an excess of ACTH which then leads to an increase in the production of adrenal androgens. This high level of androgens compromises both the growth and the fertility in CAH patients and remains a challenging side effect even under steroid treatment. Blocking the ACTH action by targeting MC2R may be a potential treatment option in patients with CAH.

**Methods:** We modeled the interaction of ACTH with MC2R and designed peptides to understand ACTH binding and activation of MC2R. A model of MC2R was made using the recently described structure of the MC4R protein. We docked the ACTH into the MC2R structure using AUTODOCK-VINA and performed Molecular dynamics simulations of ACTH binding to MC2R that provided hints for the design of peptides to block ACTH-MC2R interaction. *In-vitro* assays were performed to test the potency of designed peptides which were then optimized further to produce a second batch of antagonists. For assays, the OS3 cells transfected with MC receptor constructs were used and cyclic AMP (cAMP) was measured by luciferase assay. The potential to shift the ACTH concentration-response curve (CRC) was evaluated to characterize the antagonist activity of the designed peptides. Several natural compounds were also screened by computational docking and activity assays to screen for potential ACTH antagonism.

**Results:** We have analyzed the MC receptors and aligned the sequences of MC1R, MC2R, MC3R, MC4R, and MC5R to study the similarities and differences between these receptors. Sequence analysis identified two specific regions that are distinct for MC2R compared to other MC receptors and are also critical for the binding of ACTH to MC2R. After three rounds of peptide design, we made 4, 6, and 8 residue linear as well as circular peptides for targeting MC2R. A sequence optimization of peptides and ACTH residues was performed to improve the peptide binding to MC2R and to improve peptide stability. Mutation in the core sequence (M4, R8) of ACTH abolished MC2R activation as predicted. One lead peptide inhibitor was identified which shifted the ACTH CRC towards the right by half log, indicating antagonism. We identified several chemical leads for the further development of ACTH antagonists.

**Conclusion:** We have modeled the binding of ACTH to MC2R and designed peptides that could target the ACTH-MC2R interaction and signaling. Three rounds of peptide designs were made which provided information about key residues involved in ACTH-MC2R interaction and created more specific and tighter binding peptides to MC2R that can be used to block ACTH-MC2R interaction. Further optimization of our designed peptides as well as modification of small molecules identified in our screening could be used for developing specific inhibitors of ACTH-MC2R interaction to suppress the action of ACTH and elevated androgen production in CAH and other disorders of steroid biosynthesis.

This study was funded in part by a Swiss Government Excellence Scholarship and from a grant by IFCAH Foundation, France.

# Marine Carotenoid Fucoxanthin as a Promising Anticancer Therapeutic Against Triple-Negative Breast Cancer (TNBC)

Shade Ahmed,<sup>1</sup> Patricia Mendonca,<sup>2</sup> Samia S. Messeha,<sup>2</sup> and Karam F. Soliman<sup>3</sup>

<sup>1</sup>Florida A&M University; <sup>2</sup>Florida A&M Univ; and <sup>3</sup>Florida A&M Univ College of Pharmacy

Abstract ID 17637

Poster Board 322

Breast cancer is the second most common cancer and is the leading cause of death among women in the United States. Triple-negative breast cancer (TNBC) is an aggressive subtype that accounts for about 10-15% of all breast cancers. The tumor microenvironment facilitates tumor initiation and progression, preceding invasive metastasis, increased proliferation, and angiogenesis. Therefore, the inhibition of these mechanisms may reduce cancer advancement. Various dietary natural products show the ability to fight against the aggressiveness of breast cancer progression and tumor development through the inhibition of proliferation and angiogenesis, the induction of cell cycle arrest and apoptosis, and the modulation of signaling pathway genes. In the current study, the pharmacological effects of the natural compound fucoxanthin, a xanthophyll, a subset of carotenoids in brown macroalgae, are investigated in genetically different MDA-MB-231 (Caucasian) and MDA-MB-468 (African American) TNBC cell lines. The study shows that fucoxanthin (1.56 - 300  $\mu$ M) decreased cell viability in both cell lines in a dose and time-response manner, indicating a higher potency in MDA-MB-468 cells. Fucoxanthin presented similar anti-proliferative effects in both MDA-MB-468 and MDA-MB-231 cells after 48 and 72 h. Angiogenesis studies showed that fucoxanthin (6.25  $\mu$ M) downregulates VEGF-A and VEGF-C expression in TNF- $\alpha$ -stimulated (50 ng/ml) MDA-MB-231 cells but not in MDA-MB-468 cells in the transcription and protein levels. Also, fucoxanthin induced cell cycle arrest at the G1 phase in both MDA-MB-231 and MDA-MB-468 cells, showing higher cell cycle arrest at S-phase in MDA-MB-231 cells and higher cell cycle arrest at G2-phase in MDA-MB-468 cells. Fucoxanthin induced apoptosis in MDA-MB-231 cells but had no effect in MDA-MB-468 cells. Additionally, fucoxanthin inhibited migration and invasion in both cell lines. Fucoxanthin inhibition was more effective in MDA-MB-231 cells at a shorter time. Moreover, PI3K/AKT signaling pathway RT-PCR array studies showed that in TNF- $\alpha$ -stimulated (50 ng/ml) MDA-MB-231 and MDA-MB-468 cells, fucoxanthin (6.25  $\mu$ M) modulated mRNA expression of 13 genes including *ACTB*, *FOXO1*, *RASA1*, *HRAS*, *MAPK3*, *PDK2*, *IRS1*, *EIF4EBP1*, *EIF4B*, *PTK2*, *TIRAP*, *RHOA*, and *ELK1*. The data obtained in this study indicate that fucoxanthin may be a promising candidate for breast cancer therapy by targeting VEGF-A, and VEGF-C, decreasing cell proliferation, inducing cell cycle arrest and apoptosis, inhibiting cell migration and invasion, and modulating genes of the PI3K/AKT signaling pathway.

Support/Funding Information: National Institute of Minority Health and Health Disparities of the NIH U54 MD007582.

# Multivalent Vaccination against Polydrug Use in Opioid Use Disorder

Daihyun Song,<sup>1</sup> Bethany Crouse,<sup>2</sup> Jennifer Vigliaturo,<sup>2</sup> and Marco Pravetoni<sup>3</sup>

<sup>1</sup>Univ of Minnesota; <sup>2</sup>University of Minnesota; and <sup>3</sup>University of Washington

**Abstract ID 23682**

**Poster Board 353**

More than 107,000 cases of fatal drug overdose were reported in 2021, with around 70% of cases involving opioids. Individuals with opioid use disorder often administer polydrug street mixtures that contain multiple opioids (fentanyl and oxycodone) and non-opioids (including stimulants such as methamphetamine), leading to detrimental health outcomes. Active vaccination is being pursued as a treatment against substance use disorders (including fentanyl, carfentanil, oxycodone, heroin, and methamphetamine) and has shown efficacy in preclinical models, although the efficacy against polydrug use is not well established. To develop these vaccines, conjugates consisting of haptens crosslinked to immunogenic carrier proteins induce the T-cell-dependent generation of hapten-specific antibodies. These antibodies bind to target drugs in the circulatory system and block the drugs from crossing the blood-brain barrier, attenuating drug effects in the central nervous system. Previously, four monovalent vaccines against four different opioids have been co-administered as a quadrivalent vaccine without decreasing their individual efficacy in mice. In the current study, these four monovalent vaccines were co-formulated in a single syringe and injected into Sprague Dawley rats as a new vaccination regimen. Results showed that co-formulated quadrivalent vaccination induced greater drug-specific serum IgG titers and reduced drug distribution to the brain to a greater extent than co-administering individual vaccines at different injection sites. In addition, adding a stimulant conjugate vaccine as a pentavalent formulation did not decrease the efficacy of the quadrivalent vaccine against opioids. The combined results show that different conjugate vaccines can be co-formulated as multivalent vaccines to provide protection against polydrug use by different classes of drugs and suggest a potential therapeutic to reduce overdose related to polydrug use.

This work was supported by the National Institute on Drug Abuse

Grants UG3DA048386

# Anti-allergic and anti-Inflammatory Effects of *Cornus officinalis* using Zebrafish and IgE-chip Technology

Young Sook Kim,<sup>1</sup> Yong Wan Cho,<sup>2</sup> Hye-Won Lim,<sup>2</sup> Ik Soo Lee,<sup>1</sup> and Yu-Ri Lee<sup>1</sup>

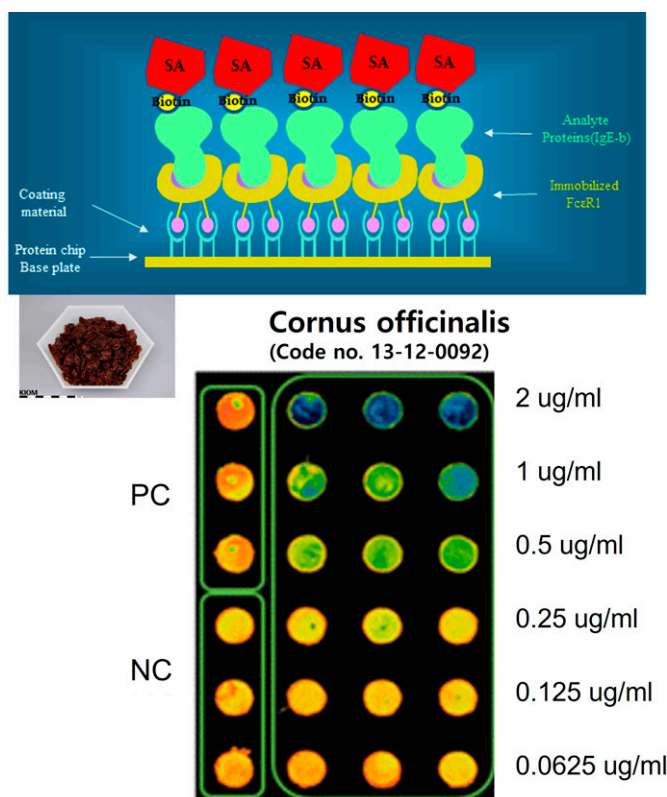
<sup>1</sup>Korea Institute of Oriental Medicine; and <sup>2</sup>Sheba Biotech Inc.

Abstract ID 53659

Poster Board 354

Atopic dermatitis (AD) is a inflammatory skin disease and itch is the most important symptom of AD. Immunoglobulin E (IgE) plays a critical role in allergic reactions. The IgE-chip technology involves the identification of allergenic proteins in natural ingredient. To find the natural products on anti-allergic effect, 229 of natural extracts were screened using IgE/FcεR1-chip assay and we selected *Cornus officinalis* extract (CO, code no. 13-12-0092). CO reduced the Compound48/80-induced histamine production in a dose dependent manner (25, 50, 100 ug/mL) and reactive oxygen species generation in MC/9 mast cells. We tested migration of neutrophils from tail fin wounds by CO in a transgenic zebrafish Tg(mpx:GFP) expressing GFP. In conclusion, the IgE/FcεR1-chip technology is a rapid method to find the effective ingredient that do not cause allergic reaction and CO is a potential anti-inflammatory mediator for treatment of allergic and inflammatory skin disease.

This article was supported by the Korea Institute of Oriental Medicine (KSN20223302) and the Technology Development Program (S3099171) funded by the Ministry of SMEs and Sartups (Mss, Korea).



Development of protein chip for IgE/FcεR1-chip reaction Schematic diagram and inhibitory effect of *Cornus officinalis* by concentration

# Investigating Birch Bark Oil Anti-Oxidative Properties in Human Keratinocytes

Esther Bonitto,<sup>1</sup> Kate-Lynn Smith,<sup>1</sup> Matthias Bierenstiel,<sup>2</sup> Rajendran Kaliaperumal,<sup>2</sup> and Kerry Goralski<sup>1</sup>

<sup>1</sup>Dalhousie University; and <sup>2</sup>Cape Breton University

Abstract ID 14365

Poster Board 355

**Background:** Inflammatory skin diseases like eczema and psoriasis are common irritating ailments for which there are few effective treatments. Anecdotal stories from the Indigenous L'nu in Cape Breton, NS, Canada suggest that their traditional birch bark oil (BBO) mixture, known as "maskwiomin," demonstrates potential therapeutic effects for the treatment of inflammatory skin diseases. We hypothesize that the mechanisms contributing to the possible beneficial effects of BBO involve anti-oxidant properties, which would ultimately reduce inflammation.

**Objective:** To determine if BBO protects human keratinocytes against oxidative stimuli.

**Methods and Results:** HaCaT human keratinocytes were treated with control cell media, 0.005% v/v BBO, or its vehicle 0.045% v/v dimethyl sulfoxide (DMSO) for 2 or 3 days, followed by 24 h treatment with the oxidative stimulus hydrogen peroxide ( $H_2O_2$ , 0-3528  $\mu$ M). MTT assays were performed to quantify subsequent percent cell viability. BBO treatment for 3 days significantly reduced  $H_2O_2$ -mediated cell death ( $IC_{50}$ ,  $3395 \pm 205.0 \mu$ M) versus DMSO ( $2729 \pm 114.8 \mu$ M) and control ( $2757 \pm 113.7 \mu$ M). Similar results were observed with BBO treatment after 2 days. Following this, media pre-treatments were repeated for 3 days, with subsequent ROS probe CM-DCFH-DA and  $H_2O_2$  (588-3528  $\mu$ M) 1 h treatment. Cytosolic ROS was quantified at  $\lambda_{ex}$  485/ $\lambda_{em}$  530 nm. Compared to control and DMSO, BBO-treated cells produced no significant change in the production of ROS. Finally, BBO was tested for the presence of endotoxins, and was found to be below 0.01 EU/mL, which is considered to be endotoxin-free.

**Conclusions:** BBO is endotoxin-free and protects human keratinocytes against the oxidative stimulus  $H_2O_2$ . However, this effect was not due to a reduction in cytosolic ROS levels. Further experiments are needed to determine the cytoprotective effects including investigation of BBO on mitochondrial ROS. Overproduction of ROS is involved in the pathogenesis of eczema and psoriasis, so it will be important to understand if BBO can mitigate these effects to potentially be used in therapeutic application.

This project is kindly supported by a Canadian Institutes of Health Research (CIHR) grant.

# Characterization of the pharmacological mechanism of OJT009 as a novel inhibitor of severe acute respiratory syndrome coronavirus 2

Tolulope Adebusuyi, Manvir Kaur,<sup>1</sup> Anuoluwapo O. Egbejimi,<sup>2</sup> Idowu Kehinde,<sup>2</sup> and Omonike A. Olaeye<sup>2</sup>

<sup>1</sup>Texas Southern Univ; and <sup>2</sup>Texas Southern University

Abstract ID 22124

Poster Board 356

The emergence of deadly SARS-CoV-2 variants with mutations on the viral genes has made it more imperative to discover therapeutics that target the host receptors for COVID-19 treatment. Our research has targeted the critical host entry receptor for SARS-CoV-2 entry into the human cells, Angiotensin-converting enzyme-2 (ACE2). Through a high-throughput screen we identified OJT009 as a novel inhibitor of SARS-CoV-2. Herein, our purpose is to identify the primary mechanism of action of OJT009 against SARS-CoV-2. The Interaction between ACE2 and the RBD region of Spike protein is the most crucial step in the viral life cycle. Therefore, the ACE2- RBD interaction has remained a key target for therapeutics in COVID19 treatment. Although ACE2 facilitates viral entry, it provides defense against acute lung injury through its physiological function of converting Ang 2 to Ang 1-7 thereby counterbalancing the effects of ACE1 in the Renin-Angiotensin pathway, The ACE2/Ang 1-7 pathway must be carefully manipulated without disrupting the balance of the renin angiotensin system. We investigated the effect of OT009 on ACE2-RBD interaction as well as its impact on the renin angiotensin pathway. To assess the impact of OJT009 on the key interaction between recombinant human ACE2 (rhACE2) and the RBD of the S protein of SARS-CoV-2, we utilized a COVID-19 Spike-ACE2 Binding Assay. To investigate the impact of OJT009 on renin angiotensin pathway we first tested the effect of OJT009 on the exopeptidase activity of ACE2 using an ACE2 activity assay. Furthermore, we tested the effect of OJT009 on ACE1 exopeptidase activity and we also examined the impact on OJT009 on expression levels of both ACE2 and ACE1.

OJT009 inhibited SARS-CoV-2 infection-induced CPE *in vitro* with a 50% Inhibitory Concentration (IC<sub>50</sub>) value at about 21.7 μm. A unique dose-response curve was observed when the effect of OJT009 on the binding affinity of rhACE2 and RBD of SARS-CoV-2 S protein was evaluated. The concentrations tested ranged from 100 nM to 100 μM. OJT009 inhibited the binding of SARS-CoV-2's S (RBD) protein to rhACE2 receptor at lower concentrations ranging from 100 nM to 10 μM; but enhanced the interaction at higher concentrations from 50 μM. Hence, the bell-shaped model generated two IC<sub>50</sub> values. OJT009 inhibited ACE 2 activity *in vitro* at very high(100 μM) concentrations but does not affect the activity at low concentrations(50 μM). The expression levels of both ACE2 and ACE1 remained unchanged after treatment with OJT009 in cell culture. Further investigations through additional computational modelling studies validated our *in vitro* findings that OJT009 might inhibit viral attachment and entry.

The unconventional dose-response curve observed, could suggest additional binding site(s) and/or target(s), such as other sites on rhACE2 or the Spike (RBD) protein. To further understand the impact of OJT009 on the RAAS pathway we investigated its role on the exopeptidase activity and expression of both ACE1 and ACE2. At high concentrations, OJT009 inhibits the ACE2 exopeptidase activity but enhances the binding of ACE2 with RBD. While at low concentration, it does not affect ACE2 activity but disrupts the interaction of ACE2 and RBD. Although OJT009 inhibits the activity of ACE1 at concentrations above 50 μm it does not affect the expression of either ACE1 or ACE2.

Based on our findings, OJT009 represents a promising drug class that could be further evaluated as a lead series in development of COVID-19 treatment.

# Development of GPR183 antagonists to treat neuropathic pain

Elise D. Stuertz,<sup>1</sup> Israel Olayide,<sup>1</sup> Kathryn Braden,<sup>1</sup> Daniela Salvemini,<sup>2</sup> and Christopher K. Arnatt<sup>1</sup>

<sup>1</sup>*Saint Louis University; and* <sup>2</sup>*Saint Louis Univ Sch of Medicine*

**Abstract ID 54360**

**Poster Board 364**

Over thirty percent of Americans suffer from chronic pain, and in 2014 around 240 million prescriptions for opioid pain relievers were prescribed. Opioid analgesics are highly addictive, and prescriptions for these painkillers, such as oxycodone and hydrocodone, have increased dramatically. This rise in opioid prescriptions and subsequent addictions have prompted research into creating non-opioid-based analgesics to target and relieve neuropathic pain targeting GPR183. Studies have been conducted to find an antagonist that would bind to GPR183 and only cause analgesic effects without unwanted side effects. SAE-14 was identified as a promising antagonist, as it was found to reverse chronic constriction injury-induced mechano and cold allodynia in mice. To increase the efficacy of SAE-14, the morpholine ring structure of the compound was replaced with twenty different nitrogen and oxygen-containing heterocycles. This was performed using a previously developed synthetic mechanism, and the resulting compounds were tested for their antagonism against  $7\alpha,25$ -dihydroxycholesterol ( $7\alpha,25$ -OHC)-induced GPR183 signaling.



# Pharmacological Rescue of Human Disease Mutations in *KCNJ10* and *KCNJ16* by Novel Kir4.1/5.1 Potentiator, VU0493206

Samantha McClenahan,<sup>1</sup> Dongsoo Lee,<sup>2</sup> and Jerod Denton<sup>3</sup>

<sup>1</sup>Vanderbilt Univ - Med Ctr; <sup>2</sup>Berea College; Vanderbilt University; and <sup>3</sup>Vanderbilt Univ - Med Ctr

Abstract ID 29220

Poster Board 365

Heterotetrameric inward rectifier potassium (Kir) channels composed of Kir4.1 (*KCNJ10*) and Kir5.1 (*KCNJ16*) critically regulate membrane potential and ion transport in the nervous system and kidneys. Loss-of-function (LOF) mutations in *KCNJ10* lead to SeSAME/EAST syndrome, which causes epilepsy, ataxia, and renal salt wasting. LOF mutations in *KCNJ16* also cause variable renal dysfunction. To determine if some of these mutant channels might be rescuable using pharmacological approaches and generally expand the pharmacology of this channel, we carried out a high-throughput screen (HTS) of 87,475 compounds for novel activators and inhibitors of Kir4.1/5.1. Hundreds of novel activators and inhibitors were discovered, including one activator termed VU0493206 which we describe here. In whole-cell patch clamp experiments, VU0493206 exhibits a 50% effective concentration (EC<sub>50</sub>) for activating Kir4.1/5.1 of 11 μM, has a maximal activation (E<sub>max</sub>) of more than 600% at -120 mV, and is highly selective for Kir4.1/5.1 within the Kir channel family. The effects of VU0493206 on wild type Kir4.1/5.1 and disease mutant channels were evaluated in quantitative fluorescence assays. Of the nine EAST syndrome mutants evaluated, addition of 30 μM VU0493206 significantly (p<0.05) increased channel activity of six of them. Furthermore, VU0493206 significantly (p<0.05) increased the activity of Kir4.1/5.1 channels carrying the novel T64I mutation in Kir5.1. Studies using a voltage-sensitive phosphatase to deplete membrane PIP<sub>2</sub> indicate that VU0493206 does not function as a PIP<sub>2</sub> surrogate or involve modulation of channel-PIP<sub>2</sub> interactions. We anticipate that VU0493206, optimized analogs, or structurally distinct activators identified in our HTS will be useful for exploring mechanisms of Kir channel activation, in general, and the therapeutic potential for treating Kir4.1/5.1-channelopathies specifically.

Funded by NIH R01 DK120821 to J.S.D and T32NS007491 and F32DK127679 to S.J.M.

# Schizonepeta tenuifolia extract (DKB138) enhances the muscle strength in dexametasone-induced muscle atrophy mice model

Young Sook Kim,<sup>1</sup> Dong-Seon Kim,<sup>1</sup> Heung Joo Yuk,<sup>1</sup> Bongkyun Park,<sup>1</sup> Kyujyung Jo,<sup>1</sup> Yu-Hwa Park,<sup>2</sup> Do Hoo Kim,<sup>2</sup> and Seung-Hyung Kim<sup>3</sup>

<sup>1</sup>Korea Institute of Oriental Medicine; <sup>2</sup>Dongkook Pharmaceutical Co., Ltd.; and <sup>3</sup>Daejeon University

**Abstract ID 56321**

**Poster Board 490**

Sarcopenia progresses from the age of 40 and muscle mass decreases by more than 30% in the age of 70 or older. So far, there is no drug for sarcopenia, and it mainly relies on exercise and protein supplement-oriented health foods, but drugs or functional foods are needed for elderly and patients who have difficulty moving. Schizonepeta tenuifolia is a medicinal plant widely found in Korea, China, Japan and is commonly used for headaches, colds and allergies. However, preventive effect of this herb on sarcopenia have yet to be explored. Schizonepeta tenuifolia extract (DKB138) inhibited hydrogen peroxide-induced C2C12 skeletal muscle cell death. DKB138 was analyzed by UPLC-Q-ToF/MS and 9 components were identified. In the treadmill test, DKB138-treated mice group showed a significantly enhanced running time and greater running distance compared with DEX-induced mice group (control). Also DKB138 treatment led to the downregulation of inflammation-related cytokines. In conclusion, we demonstrated that DKB138 administration protected against DEX-induced muscle atrophy. DKB138 suppressed the expression of muscle degradation factors and increased muscle strength. These results highlight the potential of DKB138 as protective and therapeutic agent or functional food against muscle dysfunction and atrophy.

This research was supported by grants [KSN1823312] from Korea Institute of Oriental Medicine and by Korea Institute of Planning and Evaluation for Technology in Food, Agriculture, Forestry and Fisheries (IPET) through Technology Commercialization Support Program [Grant no. 122048-3].

# Multi-Target Directed Ligands for the Treatment of Alzheimer's Disease

Ryan West and Stevan Pecic<sup>1</sup>

<sup>1</sup>California State Univ Fullerton

Abstract ID 18315

Poster Board 491

Alzheimer's disease (AD) is the most diagnosed neurodegenerative disease, with diagnoses expected to more than double over the next 40 years. Although few treatments are available, current medications have many adverse effects and can treat only mild-to-moderate symptoms in the early stages of AD without altering its progression. The most common AD drugs are acetylcholinesterase (AChE) inhibitors, which increase the activity of acetylcholine concentrations, improving global function. Current research suggests that neuroinflammation plays a significant role in AD pathogenesis. Several recent studies have revealed that the pathophysiology of AD and neuroinflammation involves the two enzymes soluble epoxide hydrolase (sEH) and fatty acid amide hydrolase (FAAH). FAAH is responsible for breaking down anandamide which, when bound to cannabinoid receptors, produces analgesia, anti-inflammation, and neuroprotectant effects. FAAH hydrolases anandamide into arachidonic acid (ARA), an important lipid inflammatory mediator, also produced by the body during inflammation. ARA is further catalyzed to highly anti-inflammatory lipids, epoxy fatty acids (EpFA). In addition to anti-inflammatory activity, EpFAs are known to promote neurogenesis which has the potential to counteract the adverse impact of AD. However, EpFAs are broken down by sEH and produce pro-inflammatory lipids. Furthermore, sEH has been identified as being upregulated in those suffering from AD.

Therefore, inhibiting sEH and FAAH represents a novel method of targeting AD pathogenesis. We have previously discovered several potent dual sEH/FAAH inhibitors and showed anti-inflammatory effects in a rat model of acute pain. We hypothesize that simultaneously targeting FAAH, sEH, and AChE enzymes is expected to have significant anti-AD effects. This project aims to develop multi-target directed ligands (MTDLs) or a single small molecule simultaneously operating on all three of the aforementioned biological targets. We previously discovered several potent AChE, FAAH, and sEH inhibitors, with IC<sub>50</sub> values of 51 nM, 8 nM, and 10 nM, respectively. In this study, using a polypharmacological strategy, we created three libraries of analogs merging pharmacophores of the three targeted enzymes. We successfully synthesized various analogs and evaluated them in biological enzymatic assays. Surprisingly, most analogs were active in human and rat sEH but not mouse sEH. We identified several AChE/sEH/FAAH inhibitors possessing low micromolar to nanomolar range inhibitory potencies. In addition, several important ADMET predictions were performed, as well as molecular modeling studies. The most promising MTDLs will be further evaluated in an AD rat model. Our studies will provide a foundation for the future investigation of the benefits of using the MTDL strategy in the treatment of multifactorial diseases, such as cancer, pain, and other neurodegenerative diseases.

# Novel Molecules and Novel Mechanisms: Prevention of Toxic $\beta$ -Amyloid42 Oligomerization

Gary Jones,<sup>1</sup> Justin C. Leavitt,<sup>1</sup> and Mary C. Freesh<sup>1</sup>

<sup>1</sup>*Hamit-Darwin-Freesh*

Abstract ID 53227

Poster Board 492

**Background and Objectives:** Our efforts at Hamit-Darwin-Freesh, Inc are directed toward the discovery of therapeutic options that offer a credible approach to the prevention of Alzheimer's disease (AD). For more than a decade there has evolved a strong consensus that AD is the sequelae of the action of so-called "toxic **soluble**  $\beta$ -amyloid oligomers" on select neuronal populations in brain. Protofibrils (roughly equivalent to 150 monomers) are less soluble (and less toxic), and precede plaque formation. Others have shown that while  $\beta$ -amyloid42 is present in a lesser amount than  $\beta$ -amyloid40, the 42 amino acid peptide is most toxic to neurons. Also, several studies have shown that one or more forms of  $\beta$ -amyloid trigger the formation of hyperphosphorylated tau.

For these reasons, we chose to direct our efforts toward the discovery of molecules that prevent the aggregation of ss-amyloid42 monomers and oligomers. After years of exhaustive study, and drawing upon the very limited available art, our first molecule of interest (HDF2021-1) was admittedly derived largely from pharmacological intuition; and serendipity. HDF2021-1 and structural analogs in our small library are novel. That is, they do not exist in any chemical database, and there are no recorded syntheses. Here we report on HDF2021-1.

**Methods:** Initial efficacy studies were done in two distinct *E. coli* clones, each having an IPTG-inducible plasmid that expressed ss-amyloid42. Subsequent studies were done with pure synthetic ss-amyloid42, as well as a  $\beta$ -amyloid42 fluorophore. All studies utilized Western Blot, stain-free, fluorescent, and coomassie blue gel technique, as well as fluorescent spectroscopy. Methods in cell culture were also employed, utilizing the BE(2)-M17 neuron cell line. In gel methodology, individual bands and total amyloid were quantified. Cell-free studies often employed variable concentrations of protease, thermolysin and neprilysin, among others; and protease inhibitors.

**Results, Conclusion and Commentary:** Early results in transformed *E. coli* showed that HDF2021-1 decreased the concentration of  $\beta$ -amyloid42 (Western Blot), and curiously this effect was blocked by a protease inhibitor. A similar result was seen in BE(2)-M17 cell culture. Similar results were also observed in cell-free studies when thermolysin or neprilysin were added. Fluorescent spectroscopy showed amyloid self-quenching, while low concentrations of HDF2021-1 prevent this. In the absence of protease, HDF2021-1 modestly unquenches the signal. But with protease present, HDF2021-1 markedly potentiates this effect. Gel studies with protease added show that HDF2021-1 markedly reduces oligomer size. These effects show high selectivity for amyloid. We conclude that HDF2021-1 directly disaggregates  $\beta$ -amyloid42 oligomers, but more notable is its effect to increase intrinsic protease action. Presently, we do not know if the effect is mediated by a direct action on amyloid oligomers, or an effect on protease. Efforts to clarify this question are ongoing. Also, FTIR and circular dichroism studies are underway to better understand molecular mechanisms.

Other groups have studied other aggregation inhibitors, yet none have received FDA approval for AD treatment/prevention. Nonetheless, we believe that a very high therapeutic index drug having a favorable pharmacokinetic profile will emerge and be found to be very effective in the prevention of AD. Such a drug should be relatively inexpensive and widely available.

# The Dual Role of the Natural Compound Cardamonin in Triple Negative Breast Cancer

Patricia Mendonca,<sup>1</sup> and Karam F. Soliman<sup>2</sup>

<sup>1</sup>Florida A&M Univ; and <sup>2</sup>Florida A&M Univ College of Pharmacy

**Abstract ID 21802**

**Poster Board 493**

Breast cancer is the leading cause of malignancy-related death in women, with increasing prevalence worldwide. Triple-negative breast cancer (TNBC) accounts for about 10% of all breast cancers. It has an aggressive nature and is highly metastatic, and because of the lack of therapies, it continues to be a challenge. Unlike other forms of breast cancer, TNBC does not express estrogen, progesterone, or HER2 receptors. These cancer cells instead employ mechanisms to escape the immune system. One such mechanism involves the upregulation of the expression of PD-L1, a ligand encoded by the CD274 gene. Because cancer cells tend to produce higher levels of PD-L1 compared to normal cells, therapies that inhibit PD-L1 may be helpful. Evidence also shows that high levels of oxidative stress and inflammation may participate in the initiation and progression of cancer. Many dietary flavonoids found in fruits and vegetables are attracting great interest in the prevention and treatment of TNBC due to their anti-carcinogenic, anti-oxidative, and anti-inflammatory properties. Cardamonin, an aromatic enone flavonoid found in cardamom spice, has displayed an array of pharmacological activities, including modulation of different signaling molecules involved in the development and progression of cancer. Despite evidentiary support for cardamonin in tumor suppression, there is a lack of research regarding its influence on the tumor microenvironment. This work aimed to investigate the ability of cardamonin to modulate the expression of PD-L1 and Nrf2 in genetically different MDA-MB-231 (Caucasian) and MDA-MB-468 (African American) TNBC cell lines. The results show that cardamonin treatment caused a dose-dependent decrease in cell viability in both cell lines, ranging from 3.12  $\mu$ M to 200  $\mu$ M. ELISA data showed that even though MDA-MB-231 cells show a higher expression of PD-L1, cardamonin reduced protein expression in both cell lines. Furthermore, RT-PCR assays demonstrated that cardamonin downregulated PD-L1 expression in MDA-MB-231 cells in the presence or absence of IFN- $\gamma$ , showing more effectiveness after the cells were stimulated. In MDA-MB-468 cells, a cardamonin inhibitory effect was observed in the presence of IFN- $\gamma$  because of the lower levels in the non-stimulated cells. Additionally, cardamonin upregulated the expression of Nrf2 and downregulated the expression of Keap1 in both cell lines' transcription and protein levels. The results show that cardamonin may downregulate the production of PD-L1 and block the evasion of the immune system. Still, on the other hand, it may also induce the activation of Nrf2, which has a controversial role in cancer development. In conclusion, the results suggest that cardamonin may have a therapeutic potential to decrease the levels of PD-L1 in the tumor microenvironment combating the cancer cells' effectiveness in evading the immune system; however, its role in the activation of Nrf2 needs to be further investigated.

# Sustained Release of Nanochelator in Thermosensitive Hydrogel Corrects Iron Overload

Linguxe Zeng,<sup>1</sup> Seung Hun Park,<sup>2</sup> Homan Kang,<sup>2</sup> and Jonghan Kim<sup>1</sup>

<sup>1</sup>Department of Biomedical & Nutritional Sciences, Zuckerberg College of Health Sciences, University of Massachusetts Lowell, Lowell, MA, USA; and <sup>2</sup>Gordon Center for Medical Imaging, Department of Radiology, Massachusetts General Hospital, Boston, MA, USA

Abstract ID 28591

Poster Board 494

Tens of millions of individuals suffer from either primary or secondary iron overload, which are associated with iron induced diabetes, liver cirrhosis, cardiac arrhythmias, and ultimately lethal heart failure. Patients are typically treated with chelation therapy including deferoxamine (DFO), deferiprone, and deferasirox. While DFO has good therapeutic efficacy among three of them, its short half-life mandates daily infusion for 8-10 hours. This inconvenience has been overcome by oral chelators, but their use is limited by significant adverse effects including gastrointestinal tract bleeding, hepatic fibrosis, kidney failure, and neutropenia. Therefore, there is an unmet need for developing a novel chelator that has better patient compliance and reduced dose frequency with low toxicity. We previously reported that a deferoxamine-based nanochelator (DFO-NP) with selective renal excretion has shown promise in ameliorating iron overload conditions in animal models with a substantially improved safety profile and greater iron binding affinity compared to native DFO. Considering the lifelong need for iron chelation therapy, we developed an injectable thermosensitive hydrogel based on DFO-NP (DFO-NP/HG), aiming to decrease the dosing frequency of DFO for improved patients' compliance. First, we developed a second-generation DFO-NP (DFO5-NP; nanochelator) by employing efficient conjugation chemistry on the surface of  $\epsilon$ -poly-L-lysine (EPL), which resulted in increased iron binding affinity and capacity by 11.8 folds and 5 folds, respectively, compared to native DFO. We then produced DFO5-NP in hydrogel (HG) by loading DFO5-NP to hyaluronic acid (HA) and conjugating it with thermosensitive copolymer Pluronic F12. To evaluate the efficacy of nanochelator-in-hydrogel, we injected a single dose of DFO5-NP/HG subcutaneously to iron dextran-treated mice and collected tissues 2 weeks post administration to determine iron status. Iron dextran treatment increased non-heme iron content in the liver (a measure of systemic iron status) by 4.7 folds, which was corrected by DFO5-NP/HG (41% decrease in liver iron). Increased liver ferritin, a marker of tissue iron status, was also restored by DFO5-NP/HG, almost to the normal level. Iron chelation efficacy was also observed in the spleen. Since DFO5-NP exclusively excreted through urine, we further verified if decreased iron deposition in the liver and spleen by DFO5-NP was due to increased urinary excretion of iron. Notably, a single dose of DFO5-NP/HG resulted in persistent iron excretion into urine up to 7 days. These results suggest that the second-generation nanochelator with high affinity/capacity in hydrogel provides improved and prolonged therapeutic efficacy against iron overload by sustained release into the systemic circulation, followed by continuous urinary excretion. Combined, the new nanochelator-in-hydrogel has the potential to improve the compliance and adherence of patients with iron overload disease.

# Consequences of pharmacological inhibition of cathepsin C using IcatC<sub>XPZ-01</sub> on maturation of granzyme zymogens in cytotoxic lymphocytes

Roxane Domain,<sup>1</sup> and Brice Korkmaz<sup>2</sup>

<sup>1</sup>INSERM; and <sup>2</sup>Centre d'Etude des Pathologies Respiratoires, INSERM U1100

Abstract ID 16611

Poster Board 495

Granzymes are serine proteinases present in cytotoxic lymphocytes and involved in elimination of virus infected and cancerous cells. As other related immune cell serine proteinases, granzymes are matured *in vitro* by a cysteine proteinase called, cathepsin C (CatC). However, biochemical characterization of granzymes A and B in cytotoxic lymphocytes from Papillon-Lefèvre syndrome (PLS) patients with CatC deficiency allowed the highlighting of a CatC independent processing and maturing pathway. Patients with PLS retained significant granzyme activities (~50-60%) in cytotoxic lymphocytes and displayed normal cytotoxicity against cancer cells (1). These results suggested that CatC is not the unique proteinase involved in the maturation of pro-granzymes in human lymphocytes. The presence of CatC-like proteinase(s) might provide a molecular explanation for the lack of a generalized cytotoxic T-cell activity in patients with PLS. Pharmacological targeting of CatC using a nitrile cell permeable inhibitor (IcatC<sub>XPZ-01</sub>) (2) resulted in ~50% of Granzyme B inhibition in cytotoxic T-cells, showing that CatC-independent maturation was not altered.

## References:

1. Pham et al., 2004, J Immunol,173(12):7277-81. doi: 10.4049/jimmunol.173.12.7277.
2. Korkmaz et al., 2019, Biochem Pharmacol,164:349-367. doi: 10.1016/j.bcp.2019.04.006.

# Platycodon Grandifloras Reduces Weight Gain and Attenuates Hepatic Steatosis in a Diet-Induced Mouse Model of Obesity

Vitoria Mattos Pereira,<sup>1</sup> Suyasha Pradhanang,<sup>1</sup> Anne Margaret Chenchar,<sup>2</sup> Sydney Polson,<sup>2</sup> Danielle R. Bruns,<sup>2</sup> Emily E. Schmitt,<sup>2</sup> Raza Bashir,<sup>3</sup> Sidney A. Sawan,<sup>3</sup> and Sreejayan Nair<sup>1</sup>

<sup>1</sup>Univ of Wyoming; <sup>2</sup>University of Wyoming; and <sup>3</sup>Iovate Health Sciences International Inc.

Abstract ID 50581

Poster Board 496

**Background and Aim:** Obesity is growing at epidemic proportions and is an independent risk factor for diabetes and cardiovascular disease. A paucity of safe and effective anti-obesity drugs and nutraceuticals have been explored to prevent weight gain. The root of the balloon flower *Platycodon grandiflorus* (Jacquin) (PG) has been used in traditional medicine. A recent report indicates that its root extract reduces body weight and facilitates thermogenesis. The objective of this study was to evaluate the efficacy of PG in attenuating weight gain and insulin resistance in a mouse model of diet-induced obesity.

**Methods:** Five-week-old male C57BL/6J mice were randomly assigned to receive a normal diet group (ND) (10 kcal% fat), or a high-fat-diet (HFD) (60 kcal% fat), with or without 1.025 ppm PG (HFD+PG) (n=8/per group) for a period of twelve weeks. Animal weight and food intake were assessed weekly during the treatment period. In the last week of treatment, glucose tolerance was assessed by an intra-peritoneal glucose tolerance test (IPGTT), and body composition (fat mass and lean body mass) was assessed by dual x-ray absorptiometry (DEXA). Hepatic liver accumulation was assessed via H&E stain with image J analysis. Data are expressed as mean  $\pm$  S.E.M and statistically evaluated using analysis of variance followed by Tukey's multiple comparisons.

**Results:** Thirteen weeks of treatment with HFD induced weight gain ( $p < 0.0001$ ) compared to ND animals ( $47.0 \pm 1.72$  g vs.  $28.4 \pm 1.74$ g), which was attenuated by HFD + PG supplementation ( $43.0 \pm 3.8$  g;  $p < 0.0001$ ). Compared to ND animals, fat accumulation in the liver was significantly increased following HFD-feeding ( $p < 0.01$ ), which was blunted in mice that received HFD + PG by  $\sim 78.5\%$  ( $p < 0.05$ ). In contrast, PG supplementation did not alter food intake, IPGTT, or DEXA outcomes ( $p \geq 0.05$ ).

**Conclusion:** Supplementation with *P. grandifloras* attenuates weight gain and hepatic steatosis in a dietary mouse model of obesity.

**Support/Funding Information:** Iovate Health Sciences International Inc., Oakville, Canada.



# Small Molecule Anti-Inflammatory TYK2 Inhibitors Attenuate Inflammation and Clinical Symptoms in a Mouse Model of Imiquimod Induced Psoriasis

Sanchari Basu Mallik,<sup>1</sup> Amol Tandon,<sup>1</sup> Jissy Akkarapattiakal Kuriappan,<sup>1</sup>  
Jeevak Sopanrao Kapure,<sup>1</sup> Mahesh Halle,<sup>1</sup> and Abishek Iyer<sup>1</sup>

<sup>1</sup>*Alembic Pharmaceuticals Limited*

Abstract ID 54869

Poster Board 497

**Objectives:** Psoriasis is a chronic skin condition, affecting around 8 million patients in the United States of America. The role of T helper type 1 (Th1) and T helper type 17 (Th17) mediated cytokine pathways in psoriasis pathology has been validated clinically and antibodies targeting these cytokines are highly effective in moderate to severe psoriasis. However, these antibody therapeutics come with high costs and safety concerns. There is a huge unmet need for developing safe and effective non-steroidal therapies. Small molecule inhibitors of Th1/Th17 pathways with optimal drug like properties can effectively address patient needs; making TYK2 inhibitors (TYK2i) attractive candidates for treating psoriasis. However, given the high degree of structural similarity among JAK family, designing selective TYK2i have remained a challenge.

**Methods:** Using an innovative structure based approach, we designed, synthesized and characterized TYK2i optimized for ideal drug like properties and JAK family selectivity using free energy perturbation (FEP) methods and medicinal chemistry based structure-activity-relationship. Compounds identified to be potent inhibitors of TYK2 along with high selectivity for TYK2 in the human kinome, were further evaluated for bioavailability in healthy mice. Selected compounds were tested for efficacy in a mouse model of human psoriasis. Female BALB/c mice were treated with imiquimod for 5 days on depilated back skin and right ear to induce psoriasis-like pathology. Animals were treated with test and reference compounds and evaluated for effects on clinical score, skin and ear thickness and skin histology (histology scoring, epidermal thickness and pSTAT3 activation).

**Results:** Our efforts to develop selective TYK2i led to the identification of a TYK2i series with pM to low nM potencies, high selectivity for TYK2 among 468 kinases and ideal drug-like properties. These analogs dose-dependently suppressed PASI clinical scores, ear and back skin thickness and inflammation in treated mice. Additionally, back skin histology showed significant attenuation of epidermal thickening and pSTAT3 activation, comparable to known reference controls.

**Conclusion:** We have identified selective TYK2 inhibitors that attenuate inflammation and clinical symptoms in an animal model of psoriasis. This suggests that TYK2 inhibition retains anti-inflammatory activity while eliminating potential for dose-limiting side effects observed with other systemic non-selective TYK2 or other JAK inhibitors.

This research has been fully funded by Alembic Pharmaceuticals Limited.

# Assessing how Neurodegeneration and Cognitive Impairment can be Ameliorated through the Neuroprotective Effect of Thymoquinone

Chukwunonso Chukwuemeka<sup>1</sup>

<sup>1</sup>Afe Babalola Univ Ado-Ekiti

Abstract ID 14181

Poster Board 498

**Background:** Neurodegeneration is a slow but progressive loss of neuronal cells in certain brain regions and is the main pathologic feature of Alzheimer's disease and Parkinson's disease (Francis et al., 2020). Neurodegeneration can be found in the brain at various neuronal circuitry levels, from molecular to systemic. Based on the fact that there is presently no known way to reverse the progressive degeneration of neurons, these diseases are considered to be incurable. However, some research has shown that oxidative stress and inflammation contribute to neurodegeneration (Pereira et al., 2021). It is estimated that 50 million people worldwide suffer from neurodegenerative diseases at the moment and that by the year 2050, this figure will be as high as 115 million people (Rodriguez et al., 2015).

Lipopolysaccharides (LPS) which are large molecules consisting of a lipid and a polysaccharide composed of O-antigen, outer core, and inner core joined by a covalent bond, can cause an acute inflammatory response by triggering the release of a vast number of inflammatory cytokines in various cell types (Calin et al., 2017). In addition, it is widely recognized as a potent activator of monocytes and macrophages (Ngkelo et al., 2012). Bacterial LPS has sometimes been used to study inflammation because of the abundance of inflammatory effects that it generates through TLR4 signaling.

Previous studies have shown an association between neuro-inflammation and neurodegenerative diseases such as Alzheimer's disease. Therefore, the prevention of neuro-inflammation could be an alternative method or approach for the treatment of neurodegenerative diseases. Although thymoquinone has demonstrated anti-inflammatory properties in several studies. However, its neuroprotective action in LPS-induced neuro-inflammation and cognitive impairment has not been thoroughly investigated. Hence, this study investigated the neuroprotective effect of thymoquinone in LPS-induced cognitive impairment and neurodegeneration and its underlying mechanisms with lipopolysaccharide models in mice.

**Methods:** Thirty-Five mice were assigned into five groups (n=7), group 1 (Saline Group), group 2 (LPS Group), Group 3 (TQ 15mg/Kg), group 4 (TQ 30mg/Kg), Group 5 (Donepezil 5mg/Kg). Animals in different groups were administered with vehicle (Normal Saline), thymoquinone, and donepezil for fourteen days. From the 8th day, sixty minutes after administering Vehicle/thymoquinone/donepezil, animals in groups 2, 3, 4, and 5 received LPS (500µg/Kg i.p.) consecutively for seven days. The administration was completed on the 14th day. Twenty-Four hours after the final administration, behavioral tests such as; Novel Object Recognition and Y-Maze test were used to assess cognitive functions, while elevated plus maze, open field, and light and dark box tests were used to evaluate anxiety. After that, the animals were sacrificed. Tumor Necrosis Factor- $\alpha$  (TNF- $\alpha$ ) was assessed using ELISA techniques, NF-K $\beta$ , inflammasome, and amyloid beta were quantified using immunohistochemistry, while  $\beta$ -secretase was measured with qPCR. COX Golgi staining was used to evaluate hippocampal damage.

**Results:** LPS significantly impaired cognitive performance in the NORT and Y-maze while also inducing behavioral abnormalities, as opposed to the control group. The effects were all greatly improved by treatment with TQ 30mg/Kg. TQ also significantly reduced the expression of LPS-induced TNF- $\alpha$ , NF-K $\beta$ , and inflammasome in the hippocampus and prefrontal cortex. However, TQ showed no change in the levels of  $\beta$ -secretase in the hippocampus and prefrontal cortex. TQ also prevents LPS-induced degeneration of dendrites in the hippocampus and prefrontal cortex.

**Conclusion:** Result obtained suggests that TQ may possess a neuroprotective effect against LPS-induced neurodegeneration and cognitive impairment through mechanisms involving its anti-inflammatory properties.

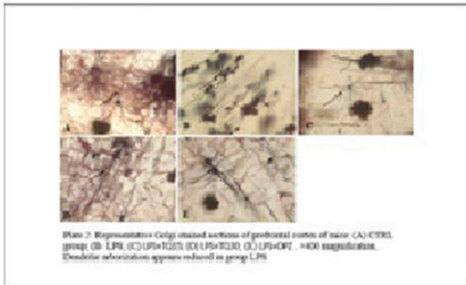


**Plate 2:** Representative Congo stained sections of prefrontal cortex of mice. CA: Control group; CTL: LPS (100µg/kg); EQ: LPS+EQ (100µg/kg); TQ: LPS+TQ (100µg/kg); EQ+DPZ: LPS+EQ+DPZ (100µg/kg); DPZ: LPS+DPZ (100µg/kg). Darker coloration appears reduced in group LPS.

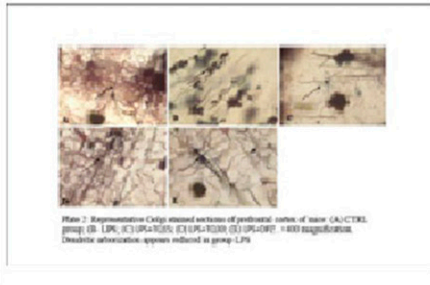


**Plate 3:** Representative Congo stained sections of prefrontal cortex of mice. CA: Control group; CTL: LPS (100µg/kg); EQ: LPS+EQ (100µg/kg); TQ: LPS+TQ (100µg/kg); EQ+DPZ: LPS+EQ+DPZ (100µg/kg); DPZ: LPS+DPZ (100µg/kg). Darker coloration appears reduced in group LPS.

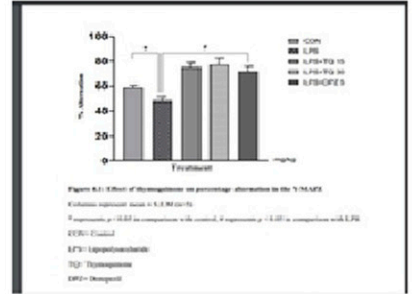


**Figure 1:** Effect of thymopentin on percentage alteration in the ThS-Aβ. Values represent mean ± SEM (n=5). \* represents  $p < 0.05$  in comparison with control, # represents  $p < 0.01$  in comparison with LPS. EQ: Equilic; LPS: Lipopolysaccharide; TQ: Thymopentin; EQ+DPZ: Desmethyl.

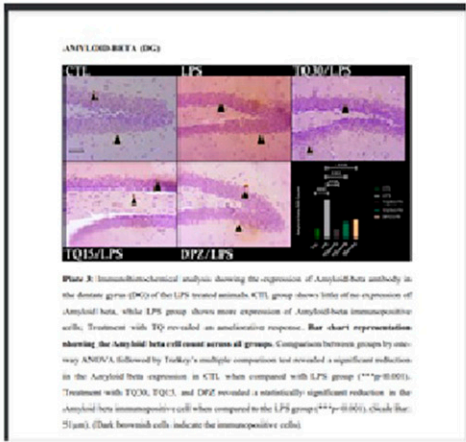


**Plate 4:** Immunohistochemical analysis showing the expression of Amyloid-beta antibody in the dentate gyrus (DG) of the LPS treated animals. CTL group shows little or no expression of Amyloid-beta, while LPS group shows more expression of Amyloid-beta immunopositive cells. Treatment with TQ revealed an ameliorative response. Bar chart representation showing the Amyloid-beta cell count across all groups. Comparison between groups by one-way ANOVA, followed by Tukey's multiple comparison test revealed a significant reduction in the Amyloid-beta expression in CTL when compared with LPS group (\*\* $p < 0.01$ ). Treatment with TQ, EQ, and DPZ revealed a statistically significant reduction in the Amyloid-beta immunopositive cell when compared to the LPS group (\*\* $p < 0.01$ , \*\*\* $p < 0.001$ ). (Scale bar: 5µm). (Dark brownish cells indicate the immunopositive cells).

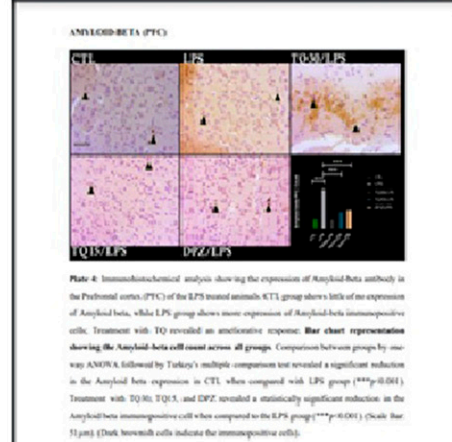


**Plate 5:** Immunohistochemical analysis showing the expression of Amyloid-beta antibody in the prefrontal cortex (PFC) of the LPS treated animals. CTL group shows little or no expression of Amyloid-beta, while LPS group shows more expression of Amyloid-beta immunopositive cells. Treatment with TQ revealed an ameliorative response. Bar chart representation showing the Amyloid-beta cell count across all groups. Comparison between groups by one-way ANOVA, followed by Tukey's multiple comparison test revealed a significant reduction in the Amyloid-beta expression in CTL when compared with LPS group (\*\* $p < 0.01$ ). Treatment with TQ, EQ, and DPZ revealed a statistically significant reduction in the Amyloid-beta immunopositive cell when compared to the LPS group (\*\* $p < 0.01$ , \*\*\* $p < 0.001$ ). (Scale bar: 5µm). (Dark brownish cells indicate the immunopositive cells).

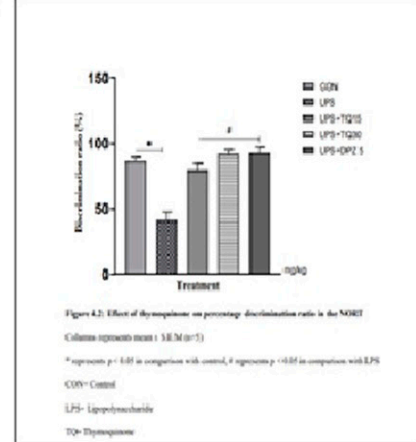


**Figure 2:** Effect of thymopentin on percentage discrimination ratio in the NOR1. Values represent mean ± SEM (n=5). \* represents  $p < 0.05$  in comparison with control, # represents  $p < 0.01$  in comparison with LPS. EQ: Equilic; LPS: Lipopolysaccharide; TQ: Thymopentin.

# Profiling Context-Dependent Activity of Allosteric Modulators at mGlu<sub>7</sub>

Xia Lei,<sup>1</sup> Alice Rodriguez,<sup>1</sup> and Colleen M. Niswender<sup>1</sup>

<sup>1</sup>*Vanderbilt University*

**Abstract ID 15381**

**Poster Board 499**

Metabotropic glutamate receptor 7 (mGlu<sub>7</sub>) is a dimeric, group III metabotropic glutamate (mGlu) receptor that acts to modulate neurotransmission across many brain structures. mGlu<sub>7</sub> is most highly expressed presynaptically in neurons and is widely distributed in the central nervous system (CNS). Mutations, deletions, or decreases in mGlu<sub>7</sub> result in symptoms and phenotypes of neurodevelopmental disorders in humans and mice, including Rett syndrome. Due to its linkage with human disorders, the receptor may be an ideal candidate for the development of therapeutics.

As mGlu<sub>7</sub> is one of the eight highly related mGlu receptors, it is difficult to develop compounds with high selectivity when targeting the orthosteric site. For this reason, our group and others are focused on developing ligands that interact with the receptor in an allosteric fashion to positive or negative modulate orthosteric agonist activity. As the activity of glutamate is very low at mGlu<sub>7</sub>, the surrogate agonist L-AP4 is often used for compound profiling. We have shown, however, that there are distinctions in the interaction of mGlu<sub>7</sub> positive allosteric modulators in the presence of glutamate versus L-AP4. Our current studies extend these findings by profiling the activity of allosteric modulators in the presence of mGlu<sub>7</sub>-interacting proteins. It is anticipated that understanding the activity of modulators in the presence of these endogenously expressed proteins will be critical to interpretation of native tissue and in vivo effects of mGlu<sub>7</sub>-targeted modulators.

Supported by NIH grant MH124671

# Effects of Simultaneous Inhibition of Fatty Acid Amide Hydrolase and Soluble Epoxide Hydrolase on Acute and Persistent Pain in Male Rats

Cassandra Yuan,<sup>1</sup> Ashley Murray,<sup>1</sup> Christopher Chin,<sup>2</sup> Alyssa Fernandez,<sup>1</sup> Stephanie Sanchez,<sup>2</sup> Stevan Pecic,<sup>3</sup> and Ram Kandasamy<sup>1</sup>

<sup>1</sup>California State University, East Bay; <sup>2</sup>California State Univ East Bay; and <sup>3</sup>California State Univ Fullerton

Abstract ID 18607

Poster Board 512

Chronic pain is the primary cause of disability worldwide. Opioids and nonsteroidal anti-inflammatory drugs (NSAIDs) are commonly used to treat persistent pain. Opioids (e.g., morphine), produce significant side effects such as addiction, constipation, and sedation. Therefore, the treatment of pain requires identifying new drugs with novel mechanisms of action to produce pain relief without these harmful side effects. Fatty acid amide hydrolase (FAAH) and soluble epoxide hydrolase (sEH) are two enzymes responsible for regulating pain and inflammation. Previous studies have demonstrated that co-administration of a FAAH inhibitor and a separate sEH inhibitor provides greater pain relief than administration of just one enzyme inhibitor alone in rodents. Thus, we synthesized a novel dual inhibitor of FAAH and sEH, SP 4-5, that inhibits both enzymes simultaneously with just one drug. This approach has several advantages including limiting the potential for drug-drug interactions. We hypothesized that simultaneous inhibition of FAAH and sEH using SP 4-5 will alleviate pain in male Sprague Dawley rats with acute and persistent inflammatory pain. We used the hot plate and tail flick tests to first assess acute pain. We administered varying doses of SP 4-5 (1 and 3 mg/kg), ketoprofen (30 mg/kg), or vehicle via intraperitoneal injection and measured the latency for the rat to respond. Administration of SP 4-5 and ketoprofen did not change the latency for the rat to flick its tail from a noxious heat source. Additionally, administration of SP 4-5 or ketoprofen did not alter the latency for a rat to respond on the hot plate test. We injected dilute formalin into the hindpaw of the rat and observed licking and guarding behavior of the injected paw in two phases of the Formalin Test. Administration of SP 4-5 and ketoprofen alleviated pain in the second, but not first, phase of the Formalin Test. To assess the efficacy of SP 4-5 in persistent inflammatory pain, rats received an intraplantar injection of 0.1 mL Complete Freund's Adjuvant (CFA) to induce hindpaw inflammation. Twenty-four hours later, the rats were administered different doses of SP 4-5 (1 and 3 mg/kg) or the nonsteroidal anti-inflammatory drug ketoprofen (30 mg/kg) and re-tested on both tests. Neither SP 4-5 nor ketoprofen alleviated pain 24 hours post-CFA. To test the effects of acute inflammatory pain, SP 4-5 and ketoprofen were injected 2.5 hours post-CFA. In this experiment, 3 mg/kg SP 4-5 and 30 mg/kg ketoprofen increased mechanical, but not thermal, withdrawal thresholds. Lastly, effective doses of SP4-5 do not depress voluntary wheel running in naive animals suggesting that the drug may not have adverse locomotor effects. Based on these data, simultaneous inhibition FAAH and sEH seems especially effective at alleviating pain against acute inflammatory pain as demonstrated using hindpaw injections of formalin and CFA. SP 4-5 is not effective against acute thermal pain, which is consistent with most NSAIDs. Further studies must establish the utility of dual FAAH/sEH inhibition on varying degrees of inflammatory pain and identify effective chemical strategies to increase the duration and magnitude of antinociception in vivo.

# Anti-Fentanyl Monoclonal Antibodies: In Vitro Characterization and In Vivo Efficacy in Reversing Apnea in Pigs

Carly Baehr,<sup>1</sup> Dustin Hicks,<sup>2</sup> Alonso Guedes,<sup>2</sup> and Marco Pravetoni<sup>3</sup>

<sup>1</sup>Univ of Minnesota; <sup>2</sup>University of Minnesota; and <sup>3</sup>University of Washington School of Medicine

**Abstract ID 54156**

**Poster Board 513**

The incidence of fatal drug overdose has increased dramatically due to the proliferation and widespread availability of fentanyl and its analogs, surpassing 100,000 in 2021 during the COVID-19 pandemic. Monoclonal antibody (mAb)-based therapeutics for opioid use disorder and overdose are in development; however, several key questions remain to be addressed relating to their safety and efficacy. Anti-fentanyl mAb have been proposed to reverse fentanyl overdose by binding fentanyl in circulation, causing fentanyl to redistribute out of brain and other organ tissue and reducing concentration of fentanyl available to activate opioid receptors. While efficacy of mAb in both prevention and reversal of fentanyl respiratory effects by mAb has been shown in rodent models, further evidence of efficacy in large animal models is required to support translation. Here, we sought to evaluate efficacy of a lead anti-fentanyl mAb in a pig model of fentanyl-induced apnea, and to assess the potential for side effects of mAb. We found that anti-fentanyl mAb did not reduce efficacy of off-target anesthetics (including propofol, droperidol and ketamine) in rats, and that mAb-bound fentanyl was unable to activate mu opioid receptors in vitro. To predict the effect of mAb on fentanyl metabolism, rat liver microsomes were incubated in vitro with fentanyl with or without an excess of mAb, and the relative rate of metabolism was determined. Finally, to evaluate efficacy of mAb in reversing fentanyl-induced apnea in pigs, Hanford miniature swine were anesthetized with isoflurane, and given an infusion of fentanyl until 2 minutes of continuous apnea occurred. Then, fentanyl infusion was discontinued, and either naloxone or the lead anti-fentanyl mAb was administered i.v. Respiratory parameters were monitored at 1-minute intervals until recovery. Whereas control subjects returned to spontaneous breathing in approximately 7-8 min, naloxone-treated subjects recovered within 1 min and mAb-treated subjects within 2 min. Concentration of fentanyl in serum was determined after apnea and during reversal, which showed that treatment with mAb increased serum fentanyl 10-20-fold within the first minute after infusion. These results support further development of anti-fentanyl mAb as a possible treatment for fentanyl overdose.

This work was supported by NIDA under CounterACT U01 DA051658 (MP) and UG3-DA057850 (MP).

# First potent macrocyclic A<sub>3</sub> adenosine receptor agonists reveal G-protein and beta-arrestin2 signaling preferences

Kenneth Jacobson,<sup>1</sup> Courtney Fisher,<sup>2</sup> Veronica Salmaso,<sup>3</sup> Tina C. Wan,<sup>2</sup> Ryan G. Campbell,<sup>4</sup> Eric Chen,<sup>3</sup> Zhan-Guo Gao,<sup>1</sup> John A. Auchampach,<sup>2</sup> and Dilip K. Tosh<sup>3</sup>

<sup>1</sup>NIDDK/NIH; <sup>2</sup>Medical College of Wisconsin; <sup>3</sup>NIDDK, NIH; and <sup>4</sup>NIH, NIDDK

Abstract ID 14834

Poster Board 514

The A<sub>3</sub> adenosine receptor (A<sub>3</sub>AR) is a therapeutic target for inflammatory diseases, ischemia, cancer, neuropathic pain, liver diseases and other chronic conditions [1]. Most reported clinical and preclinical candidate molecules acting selectively at this G-protein-coupled receptor (GPCR) are agonists of the nucleoside class. Macrocyclic derivatives of small molecules, often derived from natural products, are used increasingly in medicinal chemistry to improve absorption or to maintain conformational control to enable interaction with a target biomolecule. (N)-Methanocarba adenosine derivatives (A<sub>3</sub>AR agonists containing bicyclo[3.1.0]hexane replacing furanose) were synthesized with chains extended at N<sup>6</sup> and C2 positions with terminal alkenes for ring closure, and the compounds compared in both binding and functional assays. The resulting macrocycles of 17–20 atoms retained A<sub>3</sub> affinity in radioligand binding, indicating a spatially proximal orientation of these chains when receptor-bound, consistent with molecular modeling. C2-Arylethynyl derivative **19** was more A<sub>3</sub>AR-selective than 2-ether **12** (both 5'-methylamides, human (h) A<sub>3</sub>AR affinities (K<sub>i</sub>) 22.1 and 25.8 nM, respectively). Functional hA<sub>3</sub>AR comparison of two sets of open/closed analogues in b-arrestin2 and G<sub>i/o</sub> protein assays showed certain signaling preferences divergent from reference agonist Cl-IB-MECA. The potencies of Cl-IB-MECA at all three G<sub>α<sub>i</sub></sub> isoforms were slightly less than its hA<sub>3</sub>AR binding affinity (K<sub>i</sub> 1.4 nM), while the G<sub>α<sub>i1</sub></sub> and G<sub>α<sub>i2</sub></sub> potencies of macrocycle **12** were roughly an order of magnitude higher than its radioligand binding affinity. G<sub>α<sub>i2</sub></sub>-coupling was enhanced in macrocyclic derivative **12** (EC<sub>50</sub> 2.56 nM, ~40% greater maximal efficacy than Cl-IB-MECA). Di-O-allyl derivative **18** cyclized to form **19**, increasing the G<sub>α<sub>i1</sub></sub> potency by 7.5-fold. The macrocycles **12** and **19** and their open precursors **11** and **18** potently stimulated b-arrestin2 recruitment, with EC<sub>50</sub> values (nM) of 5.17, 4.36, 1.30 and 4.35, respectively and with nearly 50% greater efficacy compared to **1**. This example of macrocyclization altering the coupling pathways of small molecule (non-peptide) GPCR agonists is the first for potent and selective macrocyclic AR agonists. These initial macrocyclic derivatives can serve as a guide for the future design of macrocyclic AR agonists displaying unanticipated pharmacology.

1. Jacobson KA, Merighi, S, Varani, K, et al. (2018) A<sub>3</sub> adenosine receptors as modulators of inflammation: from medicinal chemistry to therapy. *Med Res Rev* 2018;38:1031-1072.

**Support/Funding Information:** NIDDK (ZIADK031117); NHLBI R01 (HL133589).

# Discovery of Potent Therapeutics for Treatment of Cryptosporidiosis

Marvin J. Meyers,<sup>1</sup> and Christopher D. Huston<sup>2</sup>

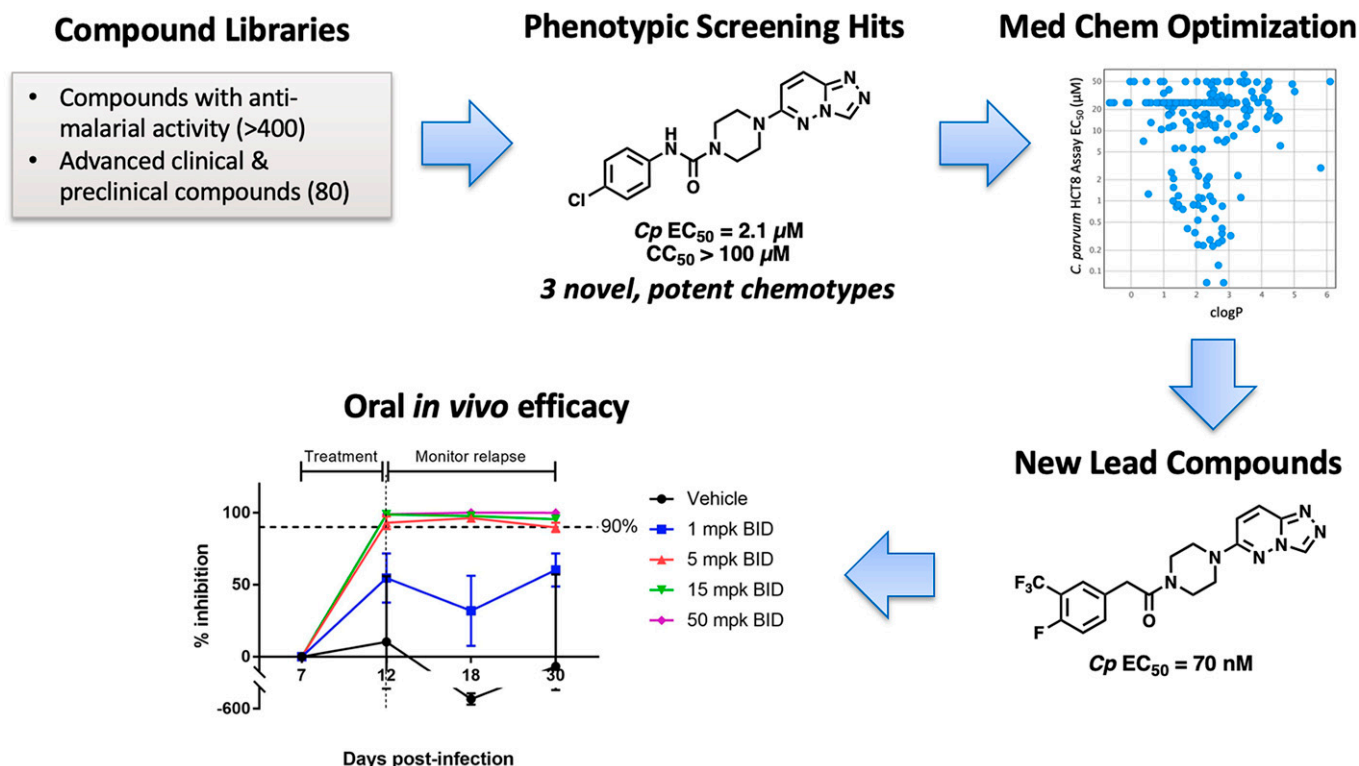
<sup>1</sup>Saint Louis University; and <sup>2</sup>University of Vermont

Abstract ID 24584

Poster Board 515

Cryptosporidiosis is a neglected diarrheal disease that is caused by infection of the intestine by the parasite *Cryptosporidium*. This disease disproportionately afflicts young and malnourished children in low-middle income countries resulting 132,000 deaths annually, greatly exceeding that of all other recognized neglected tropical diseases. The only FDA-approved therapeutic, nitazoxanide, is only marginally effective in malnourished children (34% improvement versus placebo) and is ineffective in immunocompromised adults. To address this significant unmet medical need, we have conducted screening of known anti-*Plasmodium* compounds and other advanced clinical candidates for leads for the development of novel anti-*Cryptosporidium* therapeutics. Three series of compounds, each with a unique mode of action, have been advanced to medicinal chemistry optimization. The most potent compounds identified to date have EC<sub>50</sub> values ranging from 70-200 nM in HCT-8 cells infected with *C. parvum*. Compounds from each class have oral *in vivo* efficacy in an immunocompromised mouse model of *Cryptosporidium* infection, some at doses as low as 5 mg/kg BID. Ongoing efforts to identify a safe and potent therapeutic will be discussed.

Research reported in this publication was supported by grants from the National Institute of Allergy and Infectious Diseases of the National Institutes of Health under Award Numbers R01 AI143951, R33 AI141184, and R21 AI141184.





# Sildenafil is a candidate drug for Alzheimer's disease: Real-world patient and RNA-sequencing data observations in patient-induced pluripotent stem cells-derived neurons

Yichen Li,<sup>1</sup> Dhruv Gohel,<sup>1</sup> Pengyue Zhang,<sup>2</sup> Chien-Wei Chiang,<sup>3</sup> Andrew A. Pieper,<sup>4</sup> Jeffrey Cummings,<sup>5</sup> and Feixiong Cheng<sup>1</sup>

<sup>1</sup>Lerner Research Institute, Cleveland Clinic; <sup>2</sup>School of Medicine, Indiana University; <sup>3</sup>College of Medicine, Ohio State University; <sup>4</sup>Harrington Discovery Institute, University Hospital Case Medical Center; and <sup>5</sup>School of Integrated Health Sciences, University of Nevada Las Vegas

Abstract ID 52622

Poster Board 516

**Background:** Alzheimer's disease (AD) is the main form of dementia and become one of the most expensive burdening diseases in the United States. As the traditional anti-tau or anti-amyloid selective drug discovery approaches did not benefit the AD patients, we developed an endo-phenotype disease module-based methodology for AD drug repurposing and identified sildenafil (a phosphodiesterase type 5 (PDE5) inhibitor) as a candidate drug for AD.

**Method:** We performed new patient data analyses using both the MarketScan® Medicare Supplemental database (n = 7.23 million older [ $>65$  years] subjects) and the OPTUM database (n=11.52 million older subjects). We selected a new calcium channel blocker (nifedipine) and three diuretics (bumetanide, furosemide, and spironolactone) as comparator drugs and conducted propensity score-matched observations. In total, we generated an AD patient-induced pluripotent stem cells (iPSC)-derived neuron models in this study. iPSC from six AD patients were induced to neural progenitor cells (NPCs). Neuronal precursors were generated from NPCs and matured to neurons. The AD patient-iPSC-derived neurons were treated with a concentration gradient of sildenafil and the effects were studied using ELISA, Western blotting and RNA-seq.

**Result:** We adjusted sex, age, race, and 13 comorbidities in the OPTUM analyses, as well as sex, age, geographic location, and 18 comorbidities in the MarketScan analyses. We found sildenafil usage to be associated with reduced likelihood of AD across all four drug cohorts, including bumetanide, furosemide, spironolactone, and nifedipine. Specifically, we found sildenafil vs. spironolactone was associated with a 46% reduced prevalence of AD in MarketScan (HR = 54%, 95% CI 0.32-0.66, p-value =  $3.33 \times 10^{-5}$ ) and a 30% reduced prevalence of AD in OPTUM (HR = 70%, 95% CI 0.49-1.00, p-value = 0.05). Subgroup analysis further revealed sildenafil usage in individuals with hypertension to be associated with reduced likelihood of AD across all four drug cohorts. Sildenafil treatment can reduce phosphorylated tau (pTau181 and pTau231), phosphorylated GSK-3b and CDK5 in the AD patient-iPSC-derived neuron model. mechanistically supporting its potential therapeutic effect in Alzheimer's disease. In addition, RNA-sequencing analysis of iPSC-derived neurons after sildenafil treatment revealed new mechanism-of-actions and potential biomarkers to be tested in future clinical trials.

**Conclusion:** The new patient data provide further support for reduced AD prevalence in patients exposed to sildenafil, and suggest that future experimental and clinical studies are warranted.

# Development of Mutant-Selective Allosteric EGFR Inhibitors for Drug-Resistant Lung Cancer

Tyler Beyett,<sup>1</sup> Ciric To,<sup>2</sup> David E. Heppner,<sup>3</sup> Thomas W. Gero,<sup>2</sup> Nathanael S. Gray,<sup>4</sup>  
David A. Scott,<sup>2</sup> Pasi A. Jänne,<sup>2</sup> and Michael J. Eck<sup>2</sup>

<sup>1</sup>Harvard Medical School; <sup>2</sup>Dana-Farber Cancer Institute; <sup>3</sup>University at Buffalo; and <sup>4</sup>Stanford University

**Abstract ID 16204**

**Poster Board 517**

Mutations in the epidermal growth factor receptor (EGFR) are common drivers of non-small cell lung cancer (NSCLC). Receptors harboring the most common EGFR point mutation, L858R, are effectively treated by tyrosine kinase inhibitors (TKIs), but resistance inevitably develops through additional T790M and/or C797S mutations. Acquisition of both resistance mutations renders tumors unresponsive to all clinically-approved EGFR TKIs and affects >10,000 patients per year in the US. To address this, we utilized a combination of high-throughput screening and structure-based drug design to discover and develop mutant-selective, *allosteric* EGFR inhibitors that are unaffected by common ATP-site resistance mutations.

Allosteric EGFR inhibitors work by stabilizing the inactive, “C-helix out” conformation of the kinase and are therefore antagonized by receptor dimerization, which induces the active conformation. To better understand the antagonistic effects of receptor dimerization on allosteric inhibition, we generated a constitutively dimerized pair of kinase domains suitable for biochemical assays. Using this synthetic dimer, we showed that allosteric inhibitor potency was decreased by ~500-fold upon dimerization. We also assessed the effectiveness of allosteric inhibitors against a rare kinase domain duplication (KDD) variant of EGFR associated with lung cancers. This variant was resistant to allosteric inhibition as a result of constitutive kinase domain dimerization within a single receptor. We overcame these antagonistic effects through co-administration of the dimerization-blocking antibody cetuximab or the use of a highly potent allosteric inhibitor, such as JBJ-09-063, which disrupts EGFR dimers in cells.

JBJ-09-063 displays a biochemical IC<sub>50</sub> of <100 pM and single-agent efficacy *in vivo* in a number of NSCLC models, including those harboring both the T790M and C797S resistance mutations. We have shown that JBJ-09-063 and a series of ATP-competitive TKIs can simultaneously bind EGFR kinase, resulting in inhibition synergy. Dual-targeting benefits from positive binding cooperativity between inhibitors, which partially restores binding of the frontline therapy osimertinib to the resistant C797S variant. Cooperativity is facilitated by protein conformational changes and complementary electrostatic contacts between inhibitors. Leveraging “cooperative inhibition” with other allosteric inhibitor and TKI combinations represents a novel way to target difficult to treat variants. Thus, we are utilizing structural and molecular insights of simultaneous drug binding to facilitate the identification and development of novel drug combinations.

T.S.B. is supported by a Ruth L. Kirschstein National Research Service Award (F32CA247198). This work was supported by the National Institutes of Health grant R01 CA201049 (M.J.E., N.S.G.), P01 CA154303 (M.J.E. and P.A.J.), R35 CA242461 (M.J.E.), and R35 CA220497 (P.A.J.).

# Identification of Small Molecule RGS10 Modulators in a Microglial Cell Model of Neuroinflammation

Stephanie Gonzalez,<sup>1</sup> and Benita Sjogren<sup>2</sup>

<sup>1</sup>Purdue Univ Lib Tss; and <sup>2</sup>Purdue Univ

**Abstract ID 55886**

**Poster Board 518**

Regulator of G protein signaling 10 (RGS10) has recently emerged as a prominent negative regulator of neuroinflammation in microglia, resident macrophages in the central nervous system (CNS). These are highly dynamic cells that exist in various states and elicit a protective role in the CNS. Generally, microglia exist in a “resting” state where they regulate CNS homeostasis, synaptic pruning, and neurogenesis. However, upon activation by an inflammatory stimulus, microglia will polarize to a reactive state where they are highly cytotoxic, secrete cytokines, and permeabilize the blood brain barrier. Interestingly, RGS10 is highly expressed in resting microglia and, upon microglial activation, RGS10 levels are suppressed. Furthermore, reversal of this suppression returns microglia back to a resting state and protects against dopaminergic neuronal cell death. Yet, the mechanisms of this suppression and regulation remain unknown. In addition, pharmacological tools to elucidate the role of RGS10 expression in microglia are lacking. To address this gap in knowledge, we developed a high-throughput screen to identify molecular probes that will aid in investigation of RGS10 regulation. We used BV-2 cells, a widely-used murine microglial cell line, and tagged endogenously expressed RGS10 with a split luciferase using CRISPR technology. This enabled high-throughput detection of changes in relative RGS10 protein levels. To induce the reactive state of microglia, we treated cells with an endogenous cytokine, interferon- $\gamma$  (IFN $\gamma$ ), which resulted in significant suppression of the luciferase signal. Because understanding the mechanism of RGS10 suppression is most relevant to disease pathology, we developed our high-throughput screen under conditions that identified molecular probes that reversed the IFN $\gamma$ -induced RGS10 suppression. After extensive assay optimization, we obtained a Z' of 0.51, indicating a robust screen. We screened 9,600 compounds from the ChemDiv CNS diversity library and identified 37 primary hits, that significantly reversed IFN $\gamma$ -induced suppression of RGS10 protein levels. Following initial chemical analysis and clustering, 15 of these compounds were chosen for follow-up studies. These are currently being elucidated for their potency and mechanism of action. Future studies are aimed at pursuing these hits as molecular probes to elucidate regulation of RGS10 in microglia.

# CPL-01, A Novel Extended-Release Ropivacaine, Demonstrates Consistent and Predictable Systemic Exposure Compared to Liposomal Bupivacaine in Multiple Surgical Models

Stevie Pope,<sup>1</sup> Christopher Crean,<sup>1</sup> Sarah Thrasher,<sup>1</sup> PJ Chen,<sup>2</sup> Lee Chen,<sup>2</sup> DeeDee Hu,<sup>3</sup> and Erol Onel<sup>2</sup>

<sup>1</sup>Xyzagen, Inc.; <sup>2</sup>Cali Biosciences; and <sup>3</sup>St. David's Medical Center

Abstract ID 54513

Poster Board 519

**Purpose:** Although several bupivacaine-based long-acting local anesthetics have been approved over the past decade or so, post-operative analgesia with minimal opioid use remains elusive. One reason for this may be because the pharmacokinetics (PK) from these formulations are inconsistent across multiple surgical models, leading to reluctance to use them in any surgical model where the PK curve has not already been demonstrated for fear of Local Anesthetic Systemic Toxicity (LAST) and concerns regarding inconsistent efficacy. Ropivacaine, widely considered to be safer than bupivacaine, has been developed as a novel extended-release formulation (CPL-01). As there is publicly available data demonstrating the PK of liposomal bupivacaine (LB) in several of the same surgical models as CPL-01, we compared the PK of ropivacaine from CPL-01 to that of bupivacaine from LB to better understand the consistency of their systemic exposure.

**Approach:** Data on LB's PK was used to construct a dose-normalized curve across three surgical models after a 200 mg dose. These were then graphed alongside data from CPL-01 trials in abdominoplasty, herniorrhaphy, and bunionectomy, each of which had a 200 mg dose. The curves were then compared, focusing on the consistency of the shape of the curve, the mean Cmax, and the median Tmax.

**Results:** The shape of the systemic local anesthetic curve was consistent after administration of CPL-01 across multiple surgical models but was not consistent after administration of LB (see Figure 1). The dose-normalized Cmax values were at least 4-fold lower than the accepted threshold for LAST concentration of 2,000 ng/mL (bupivacaine) or 2,200 ng/mL (ropivacaine) for all models, with little variance for either product, 268-352 ng/mL in LB and 284-455 ng/mL in CPL-01. However, when comparing median Tmax values across all three surgical models, CPL-01 showed a consistent Tmax of 8-12 h, while the Tmax for LB varied from 2-36 h.

**Conclusions:** Consistent median Tmax values across surgical models with CPL-01 indicates a more predictable release of ropivacaine over time across multiple surgical models that is not present with LB. Mean peak plasma concentration levels for both CPL-01 and LB were well below the known toxicity levels. When approved, the predictability and consistency of the PK parameters of systemic ropivacaine from CPL-01 may provide physicians with more assurance in using extended-release anesthetics, with greater confidence of more consistent efficacy and less fear of inadvertently contributing to LAST.

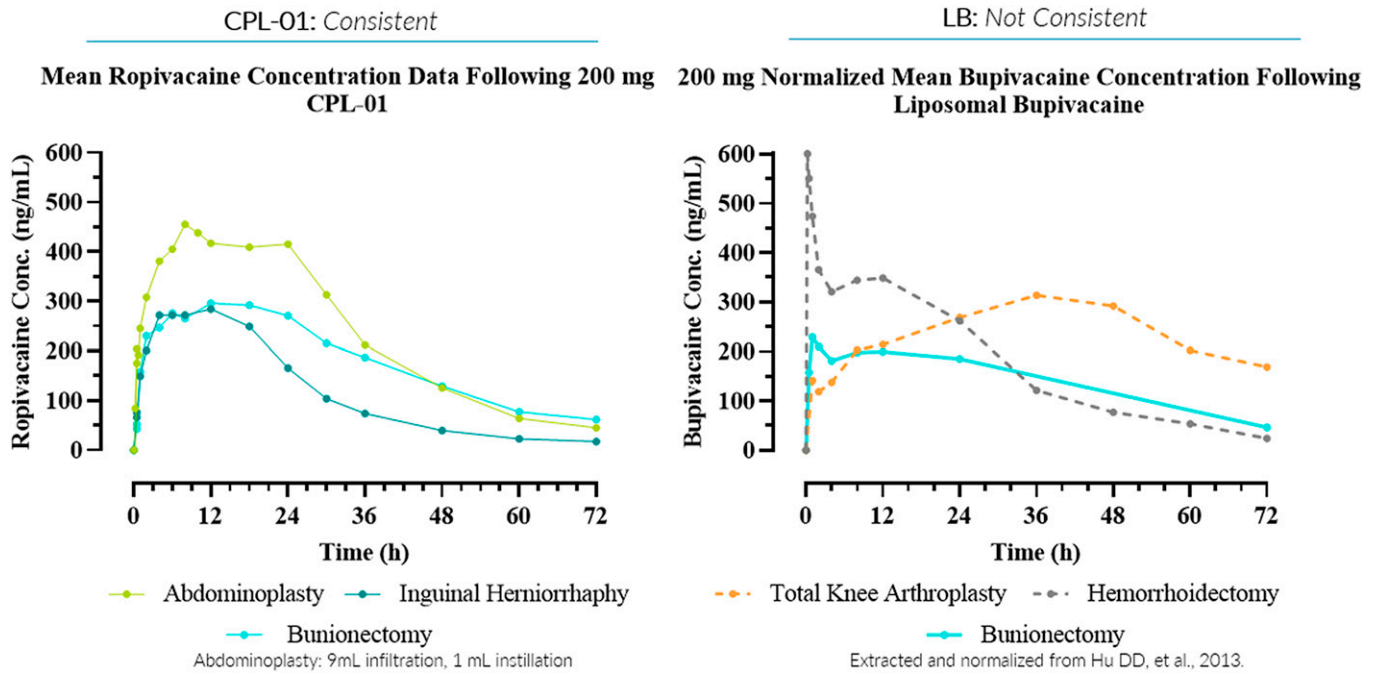


**Figure 1:** Systemic concentration of local anesthetic over time across multiple surgical models

# Development and Characterization of Third Generation MDM2 PROTACs for the Treatment of Acute Myeloid Leukemia Utilizing an Achiral Ligand for E3 Ligase Cereblon

Ira Tandon,<sup>1</sup> Qiuhua Fan,<sup>2</sup> Chunrong Li,<sup>2</sup> Nuwan Pannilawithana,<sup>2</sup> Haibo Xie,<sup>2</sup> Paulina Esguerra,<sup>2</sup> and Weiping Tang<sup>2</sup>

<sup>1</sup>Univ of Wisconsin Madison; and <sup>2</sup>University of Wisconsin Madison

Abstract ID 52646

Poster Board 520

Tumor suppressor protein p53 plays a pivotal role in the regulation of cell processes and the prevention of cancer development. The function of p53 is highly regulated by murine double minute 2 protein (MDM2); thus, the inhibition or elimination of MDM2 is a validated and robust therapeutic strategy to restore wild-type p53 function. In this work, we aim to regulate the proteostasis of MDM2 by developing PROteolysis TArgeting Chimera (PROTAC) degraders. PROTACs are heterobifunctional molecules that co-opt the ubiquitin-proteasome system to induce the degradation of target proteins. PROTACs link one ligand that recruits the protein of interest (POI) to another ligand which recruits an E3 ligase to facilitate the polyubiquitination and subsequent proteasomal degradation of the POI. Previous efforts to develop MDM2 PROTACs in our lab have yielded molecules that are capable of degrading MDM2; however, they also degrade G1 to S Phase Transition 1 (GSPT1) (degrader WB156) and/or p53 itself (degrader WB214). Due to their off-target effects, these degraders are not suitable for further therapeutic advancement. Our ongoing work focuses on the development of the third generation of MDM2 degraders featuring a novel and achiral ligand for the E3 ligase component cereblon (CRBN). The discovery of an achiral CRBN ligand from our lab provides a more stable CRBN ligand than the currently widely used molecules such as lenalidomide and has been validated for BRD4 degradation in a PROTAC setting.

A combination of NanoLuc luciferase assay and western blotting were used to screen compounds and quantify MDM2 degradation. Degradation-induced antiproliferation was quantified using Alamar Blue cell viability assay and binding affinity was measured using a fluorescence polarization assay. Preliminary results show that four compounds (QF 2-010, 2-016, 2-049, and 2-097) are capable of degrading MDM2 between 10 and 1  $\mu$ M in MOLT-4 and RS4;11 leukemia cells and have less GSPT1 degradation activity than first generation degrader WB156. Surprisingly, however, the degradation induced by third generation MDM2 PROTACs does not correspond to an upregulation in p53 levels. The PROTACs also display a limited anti-proliferation effect and low binding affinity for MDM2. Taken together, the data suggests that these degraders may work in an unexpected mechanism and will require further evaluation to understand the lack of impact on p53 protein levels. Future work will also involve the development of more achiral CRBN ligand-based MDM2 degraders in order to find a more potent PROTAC, as well as expanding our MDM2 degraders to other cancers where MDM2 is a key therapeutic target. Despite the unusual mechanism of action of the degraders, this work shows that achiral CRBN ligand-based PROTACs are capable of degrading different POIs and may be widely applicable for PROTAC development.

I.T. thanks NIH T32 GM141013 for predoctoral fellowship support. W.T. thanks the financial support from the University of Wisconsin–Madison Office of the Vice Chancellor for Research and Graduate Education with funding from the Wisconsin Alumni Research Foundation (WARF) through a UW2020 award.

# Phytochemotypic profiling and GCMS Analysis of *Viola patrinii*, a Himalayan Herb

Sajad Yousuf,<sup>1</sup> Tahira Yousuf,<sup>2</sup> Olanrewaju Morenikeji,<sup>3</sup> and Naseer A. Kutchy<sup>4</sup>

<sup>1</sup>Maharishi Univ of Information Technology; <sup>2</sup>University of Science and Technology Meghalaya; <sup>3</sup>Univ of Pittsburgh-Bradford; and <sup>4</sup>Rutgers, The State University of New Jersey

Abstract ID 24240

Poster Board 521

*Viola patrinii*, a medicinal herb belongs to the family *Violaceae*, which is a therapeutic member of traditional medicine used for the treatment of bruises, ulcers, and purification of blood. In Chinese system, it is also recommended for treating cancer and disorders related to it. Its dried flowers are used for cough, cold as well as a purgative agent. The mixture of terpenoids makes plant essential oil, obtained from aromatic and medicinal plants. These essential oils obtained from plants are also known for their therapeutic or pharmacological properties. However, the plant essential oil yielded from 200g of whole parts of *Viola patrinii* by hydrodistillation was 0.63% after the removal of moisture. Moreover, the oil yielded was having characteristic odour and yellow brownish color. Thus, GC-MS QP-2010 Ultra was used to analyze the phytochemotype in the essential oils of *Viola patrinii*. Therefore, in the current study, fifty-three compounds from *Viola patrinii* essential oil were identified, which are shown by peak areas in the chromatograph obtained during GC-MS analysis. The oil was rich in  $\alpha$ -limonene (37.12%),  $\Delta$ -carene (21.01%),  $\alpha$ -pinene (6.42%),  $\alpha$ -terpineol (5.97%), terpinolene (5.62%),  $\beta$ -terpineol (2.92%), longifolin (2.91%), camphene (2.54%), cineole (2.28%) and myrcene (1.26%). The spectra of unknown compounds in essential oils were compared with the spectra of known compounds present in the NIST and WILEY libraries. The percentage of each essential oil component was obtained by GC peaks. Thus, the structure, molecular weight, and name of the components in essential oil were described with the help of standards. Hence, the compounds like  $\alpha$ -limonene,  $\Delta$ -carene,  $\alpha$ -pinene,  $\alpha$ -terpineol, terpinolene,  $\beta$ -terpineol, longifolene, camphene, cineole acts as good antioxidants while as myrcene acts as antiviral, antibacterial and antifungal agent.

**Support/Funding Information:** Department of Biotechnology, School of Science, Maharishi University of Information Technology,

Lucknow (UP), India has supported and funded for this research work.

# Monensin and its Derivatives Exhibit Anti-Melanoma Activity *In Vitro*

Alicja Urbaniak,<sup>1</sup> Marta Jędrzejczyk,<sup>2</sup> Greta Klejborowska,<sup>2</sup> Natalia Stępczyńska,<sup>2</sup>  
Adam Huczynski,<sup>2</sup> and Alan J. Tackett<sup>3</sup>

<sup>1</sup>Univ of Arkansas for Medical Sciences; <sup>2</sup>Adam Mickiewicz University; and <sup>3</sup>University of Arkansas for Medical Sciences

**Abstract ID 15572**

**Poster Board 552**

Over the last 30 years, incidences of melanoma have increased dramatically. Although, melanoma accounts only for approximately one percent of skin cancers, it is responsible for almost eighty percent of all deaths from dermatological malignancies. Current therapeutic approaches vary depending on tumor progression and patient's health, and include tumor removal, immunotherapy, and forms of targeted therapy. Major limitations in treating melanoma are associated with adverse side effects of treatments as well as reduced drug efficiency. Therefore, new forms of therapy are needed to overcome these limitations as well as to combat the increased incidence of melanoma.

Monensin (MON) is a naturally occurring polyether ionophore which was shown to be potent and selective towards different types of cancer cells including melanoma. In order to further explore structure-activity relationship of MON and develop more potent and selective compounds based on the scaffold of MON, we synthesized an extensive library of esters and urethanes, as well as ester-carbonates, amide carbonates, tertiary amides, and esters on the C1 atom. We have identified four derivatives more potent ( $IC_{50} = 28.3 \pm 6.0 - 132.2 \pm 24.4$  nM) than parent MON ( $IC_{50} = 316.8 \pm 25.7$  nM) towards human melanoma A375 cell line, four derivatives more active ( $IC_{50} = 132.2 \pm 50.4 - 442.9 \pm 64.8$  nM) than MON ( $IC_{50} = 794.1 \pm 161.9$  nM) against human melanoma SK-MEL-5 cell line, while parent MON remained to be the most potent ( $IC_{50} = 63.2 \pm 30.9$  nM) towards mouse melanoma B16F10 cell line. Further studies revealed that these compounds significantly reduced A375 cell migration (23% vs 41% and 35% wound surface area after 53 hours control vs treatment respectively), increased Major Histocompatibility Complex-I and II presentation and Programmed Death - Ligand 1 expression in SK-MEL-5 cell line. Studies are ongoing to explore mechanism behind the activity of these promising novel drug candidates.

This work was supported by grants from the National Institutes of Health: P20GM121293 (to AJT), R24GM137786 (to AJT), and R01CA236209 (to AJT), a Barton Pilot Grant from UAMS College of Medicine (to AU), Equipment Award Program from UAMS College of Medicine (to AU).



---

# Synthesis and Structure-Activity Relationship of SAE-14 Analogs as G-Protein Coupled Receptor 183 Antagonists

Israel Olayide,<sup>1</sup> Kathryn Braden,<sup>2</sup> Daniela Salvemini,<sup>3</sup> and Christopher K. Arnatt<sup>1</sup>

<sup>1</sup>*Saint Louis Univ*; <sup>2</sup>*Washington University in Saint Louis*; and <sup>3</sup>*Saint Louis Univ Sch of Medicine*

**Abstract ID 54221**

**Poster Board 553**

The therapeutic management of neuropathic pain (NP) targets opioid receptors to modulate their signal processes. Currently, the most effective therapeutic analgesia is opioids to manage the long-term treatment of NP, and these unfortunately have associated side effects including addiction and physical dependencies. GPR183 (Epstein-Barr induced gene 2, EB12), a non-opioid G-protein coupled receptor (GPCR) revealed to be involved in the pathway of NP generation. SAE-14, a novel small molecule, is a lead compound that was shown to antagonize GPR183 and is active in vivo in a chronic constriction model of neuropathic pain. It is necessary to optimize the pharmacophores of SAE-14 to enhance its binding interactions with GPR183. Therefore, we investigated a structural activity relationship of SAE-14, to uncover improved functional groups that would augment its antagonistic activity.

# Discovery of New Agonists and Antagonists for Ectopically Expressed Olfactory Receptor OR51E1

Taylor Henry,<sup>1</sup> Qiang Wang,<sup>1</sup> Alexey Pronin,<sup>2</sup> Olena Zhuravel,<sup>3</sup> Sergey Zozulya,<sup>3</sup> and Vladlen Slepak<sup>4</sup>

<sup>1</sup>University of Miami School of Medicine; <sup>2</sup>Univ of Miami Miller School of Medicine; <sup>3</sup>Enamine, Ltd; and <sup>4</sup>University of Miami Miller School of Medicine

**Abstract ID 16032**

**Poster Board 554**

Olfactory receptors (ORs) were originally discovered in the nasal epithelium, where they mediate the sense of smell. However, members of this very large family of GPCRs (~400 genes in humans and ~1,200 in mice) were subsequently found in airways, blood vessels, gut and other tissues. These ORs are referred to as ectopically expressed ORs or "ectopic ORs". Some current evidence indicates that they are involved in sensing metabolites, cell signaling and/or other functions of ORs remain enigmatic. There are several technical obstacles that have been impeding progress in OR investigation for decades. These difficulties include the need for special chaperones necessary for OR trafficking and expression in the functional form, absence of anti-OR antibodies and lack of effective pharmacological tools. Here, we will report the results of the first high throughput screen (HTS) for molecular probes for an OR, OR51E1. We focused on this OR for several reasons, e.g., it is highly upregulated in malignant prostate cancer tumors; it was found in a subset of blood vessels and shown to be involved in regulation of blood pressure; it is one of the few ORs that was deorphanized and shown to be activated by butyrate and other short chain fatty acids. Notably, OR51E1 has an unusually high conservation (95%) between humans and other mammals, indicative of its important physiological function. Through our HTS and subsequent hit expansion, we identified ~100 novel small compound agonists which increase cAMP in a OR51E1-dependent manner, and have the EC<sub>50</sub> 10-500 times lower than butyrate. We also found several antagonists, which have a structure distinct from the two agonist chemotypes that we identified among our hits. These results demonstrate that successful discovery of drug-like compounds targeting ectopically expressed ORs is possible. Our on-going efforts are aimed at characterization of pharmacological properties of the new ligands, downstream signaling, cellular and physiological effects, and structure-function aspects of OR51E1-drug interaction. Since our expression system and hit confirmation pipeline works not only for OR51E1, but also for other ORs, our platform must be applicable for other members of this vast and untapped Class A GPCR family.

# Comparison of Mass-Action Law Dynamic Theory-based “Top-Down” Approach with Observation/Statistics-based “Bottom-Up” Approach in Biomedical R&D

Ting-chao Chou<sup>1</sup>

<sup>1</sup>PD Science LLC

Abstract ID 18532

Poster Board 555

The traditional dose-effect dynamics (DED) research and development (R&D) in biomedical sciences usually start with proposed specific aim, defined rationale and select methods/procedures. The observations and dose-effect data are then analysis using chosen method with statistical analysis for plausible conclusions. This approach is considered as the open “*bottom-up*” approach with exploratory features. However, in the absence of universal fundamental principle, this open approach frequently encounters variability and diversity issues thus require large sample size, many doses for empirical curve fittings, and may involve subjective decisions. By contrast, the general Mass-Action Law (MAL) theory-based biodynamics/pharmacodynamics/bioinformatics (BD/PD/BI) is a deterministic unified “*top-down*” approach, which is opposite to the traditional “*bottom-up*” approach, yet provides complementary alternative for ultimate goals of biomedical R&D, with excellent features of cost-effectiveness and quantitative computer simulation for digital MAL informatics. The MAL-BD/PD/BI unified theory consists of (i) Median-effect eq. (MEE), (ii) Combination Index eq. (CIE) and (iii) Dose-reduction Index eq. (DRIE), and their respective algorithms for diagnostic simulations. All *terms* of MEE, CIE and DRIE are *dimensionless relativity ratios*. Thus, the applications of MAL-unified theory is independent from: units, mechanisms, physical states; in molecular, cellular, tissue, organ, and diseases studies; and in animals, humans, clinical trials; in marine, agricultural, food and environmental sciences. Recently, the applications also extended to radiation, UV, microwave, photo- and thermo- dynamics studies. As of December 2022, the applications of MAL- BD/PD/CI/BI and its mathematical quantitative *definitions* of “PD”, synergism ( $CI < 1$ ) additive effect ( $CI = 1$ ) and antagonism ( $CI > 1$ ), and DRI have garnered over 22,000 citations in over 1,488 journals in biomedical sciences and beyond. The Michaelis-Menten, Hill, Henderson-Hasselbalch, Langmuir, and Scatchard equations are all *specific general equations*, the special cases within the domain of the MAL *unified general equation*. It worth noting here, the MAL unified theory was derived from over 300 reaction rate-equations, subjecting to the pattern analysis, combinatorial analysis, and mathematical induction and deduction, which is a completely different approach from the other five theoretical derivations as indicated above. It is noted that Top-Down and Bottom-Up approaches are opposite and complementary alternative, in *unity*, just like Yin-Yang concept in ancient philosophy, and like two sides of the same coin, or front and rear views of the same entity. Interestingly, the signals of central nerve systems are descending and the peripheral nerve systems are ascending, yet they are coordinating superbly well. It is intriguing that in the standard model of elementary particle physics, the six quarks are: top, down, bottom, up, charm and strange. This terminology of 4/6 coincidence may be by chance since it has no direct evidence yet that the mass-action law basic principle have any interplays in it. What apparent is that MAL-principle and algorithm have proven utilities in quantitative precision medicine and in digital translational medicine for biomedical R&D.

**Support/Funding Information:** NIH Grant CA18856.

# Evaluation of Influx and Efflux Transporters of Metformin in an *In Vitro* Blood-Brain Barrier Model During Normoxic and Ischemic Conditions

Sejal Sharma,<sup>1</sup> Yong Zhang,<sup>2</sup> Ali Ehsan Sifat,<sup>2</sup> Khondker Ayesha Akter,<sup>3</sup>  
Sabrina Rahman Archie,<sup>2</sup> Saeideh Nozohouri,<sup>2</sup> and Tom Abbruscato<sup>3</sup>

<sup>1</sup>Department of Pharmaceutical Sciences, School of Pharmacy, Texas Tech University Health Sciences Center; <sup>2</sup>Department of Pharmaceutical Sciences, School of Pharmacy, Texas Tech University Health Sciences Center, Amarillo, Texas; and <sup>3</sup>Texas Tech University Health Sciences Center

Abstract ID 15609

Poster Board 563

**Purpose:** Studies from our lab have shown that metformin attenuates post-ischemic brain injury through Nrf2 activation. Metformin is a small hydrophilic molecule that accumulates in the cells driven by membrane potential. Its potential interaction with transporters (uptake and efflux) is unknown. Four types of organic cationic transporters- OCT1, OCT2, OCT3, and PMAT have been identified at the luminal membrane of blood-brain barrier (BBB). MATE-1, expressed at the BBB, has also been shown to be responsible for the tubular and biliary secretion of metformin. Additionally, efflux transporters such as plasma glycoprotein (P-gp), expressed by the BBB, might influence brain access of metformin.

**Method:** A co-culture of bEnd3 cells and primary astrocytes for permeability experiments were used as an *in-vitro* BBB model. [<sup>14</sup>C] metformin treatment in presence of increasing amounts of unlabelled metformin was used to determine saturation of influx transporters. The permeability coefficient (PC) value of metformin was calculated as  $PC=(dQ/dt) * (1/(Co * A))$ . For influx transporter-specific inhibition, unlabelled metformin (10  $\mu$ M) treatment was performed in the presence of transporter-specific inhibitors. The amount of metformin in the samples was analyzed using LC-MS/MS method. For metformin's interaction with the efflux transporter, MDR1 gene-transfected P-gp overexpressing cells were used. The PC of metformin in apical-to-basolateral (A>B) and basolateral-to-apical (B>A) in the presence and absence of P-gp potent inhibitor, Cyclosporine A (CsA) was calculated. Finally, the unidirectional flux ratio (UFR) and the efflux ratio (ER) were determined.

**Result:** It was shown that with inhibitory concentrations of 10 mM and 20 mM, there was a significant decrease in [<sup>14</sup>C] metformin transport ( $p < 0.0001$ ). This suggests that influx transporters for [<sup>14</sup>C] metformin start getting saturated at an inhibitory concentration of more than 1 mM. For the transporter-specific inhibition study, with mitoxantrone, metformin showed a significant reduction in permeability ( $p < 0.005$ ). With corticosterone, there is a further reduction in permeability ( $p < 0.05$ ), which suggests that, in addition to OCT-1, OCT-2 and/or OCT-3 are involved in metformin's transport. However, there is no significant difference between corticosterone, desipramine, and MPP+, which rules out the possibility of other transporters like PMAT, SERT, or CHT involved in metformin's transport. Next, for the interaction of metformin with p-gp, the UFR, and ER was found to be 1.24 and 0.64, respectively. Studies report that compounds with UFR and ER less than 2, are poor substrates for p-gp.

**Conclusion:** Our findings suggest that metformin uses a transporter-specific mechanism for its entry across the *in vitro* BBB model. OCT-1, 2, and 3 are involved in the influx of metformin into the brain, while it does not interact with efflux transporter such as p-gp. Our ongoing and future studies are related to metformin transport using *in vitro* ischemia model of oxygen-glucose deprivation that is routinely utilized in our lab to more specifically model metformin transport into the ischemic brain.

This work was supported by NINDS R01 NS#117906

Inhibitors/Substrates	Specificity based on IC50 values for 10 $\mu$ M metformin uptake
1- methyl-4-phenylpyridinium (MPP+ )	A cationic experimental probe substrate used against the uptake of metformin in OCTs expressing cell lines and cell lines that endogenously produce OCTs. It inhibits all carrier-mediated transport at 5 mM
Desipramine	Known to inhibit OCT-1,2,3 and PMAT at 200 $\mu$ M.
Mitoxantrone	Known to inhibit OCT-1 at 25 $\mu$ M
Corticosterone	Known to inhibit OCT-1,2 and 3 at 150 $\mu$ M
Cimetidine	Known to inhibit MATE1 at 5 $\mu$ M

**Table:** Compounds and their transporter inhibition specificity.

# Directed Mutagenesis Studies Reveal Amino Acid Residues Responsible for A<sub>3</sub> Adenosine Receptor Positive Allosteric Modulator Function

Courtney Fisher,<sup>1</sup> Veronica Salmaso,<sup>2</sup> Tina C. Wan,<sup>1</sup> Balaram Pradhan,<sup>2</sup> Kenneth Jacobson,<sup>2</sup> and John A. Auchampach<sup>1</sup>

<sup>1</sup>Medical College of Wisconsin; and <sup>2</sup>NIDDK/NIH

Abstract ID 26509

Poster Board 564

The A<sub>3</sub> adenosine receptor (A<sub>3</sub>AR) is a G<sub>i</sub> protein-coupled receptor that is a therapeutic target for inflammatory diseases, ischemia, cancer, and chronic neuropathic pain. Direct agonists of the A<sub>3</sub>AR have entered late-stage clinical trials for psoriasis and inflammatory liver diseases. Unlike agonists, positive allosteric modulators (PAM) enhance A<sub>3</sub>AR signaling with spatiotemporal specificity and reduced side effect profiles. While several chemical classes have been reported to act as allosteric modulators, the lack of structural information for the A<sub>3</sub>AR has limited their development. Exploiting known species differences in A<sub>3</sub>AR PAM pharmacology, we employed a human (responding species)/mouse (non-responding species) chimeric receptor approach to localize the allosteric binding pocket for the imidazoquinolinamine derivative, LUF6000 (*N*-(3,4-dichlorophenyl)-2-cyclohexyl-1*H*-imidazo[4,5-*cj*]quinolin-4-amine), responsible for enhancement of orthosteric agonist-induced [<sup>35</sup>S]GTPγS binding and slowing of orthosteric agonist radioligand ([<sup>125</sup>I]-AB-MECA) dissociation. The regions identified from this initial screen included distal portions of transmembrane domain (TMD) 7 and Helix 8, with possible additional interactions with the distal TMD 1/intracellular loop 1 region. With this information in hand, induced fit docking was performed with LUF6000 utilizing a homology model of the A<sub>3</sub>AR constructed from the structure of an activated A<sub>1</sub>AR. LUF6000 was found to dock in several orientations, and a leading pose was selected based on consistency with structure-activity-relationship information gained from our prior work. The nearly planar imidazoquinoline ring system is predicted to lie parallel to the TMD segments, sandwiched between the “lower” (intramembrane) ends of TMDs 1 and 7. Side chains from several residues along TMD7 and Helix 8 are predicted to interact with the heterocyclic scaffold of LUF6000, the importance of which is currently being pursued. The 3,4-dichlorophenyl-4-amino group points outwards towards the lipid interface, whereas the 2-cyclohexyl group extends towards the intersection between TMD 7 and Helix 8. Notably, pi-pi stacking was predicted between a non-conserved Y284<sup>7.55</sup> (mouse = cysteine) at the tip of TMD7 and the conserved Y293<sup>8.54</sup> within Helix 8. The model also predicted hydrogen bonding between Y293<sup>8.54</sup> and the exo-cyclic nitrogen of LUF6000. Since prior SAR work showed that maximal allosteric activity of imidazoquinolinamine derivatives requires bulky hydrophobic substituents at the C-2 position, we hypothesized that this interaction might be necessary to complement a hydrophobic pocket required for LUF6000 binding. This binding mode was supported by mutagenesis experiments, wherein allosteric activity of LUF6000 was completely lost when Y284<sup>7.55</sup> was mutated to a cysteine correlating with the mouse sequence or when Y293<sup>8.54</sup> was changed to a phenylalanine. Additional mutagenesis work ruled against the importance of potential disulfide bridge formation between a non-conserved cysteine in TMD 1 (C35<sup>1.55</sup>) predicted to be in proximity to another non-conserved cysteine in Helix 8 (C300<sup>8.61</sup>). This work is the first to provide molecular information on potential binding interactions of a PAM for the A<sub>3</sub>AR, which uniquely occurs within the distal portion of TMD7 and Helix 8.

**Support/Funding Information:** NIDDK (ZIADK031117), NHLBI RO1 (HL133589), AHA (898217), NHLBI (1F31HL1600193-01A1)

# Structure-activity Exploration of Positive Allosteric Modulators of the Mu-opioid Receptor

Mengchu Li,<sup>1</sup> John Traynor,<sup>1</sup> Sherrice Zhang,<sup>2</sup> Matthew Stanczyk,<sup>1</sup> Xinmin Gan,<sup>2</sup> and Andrew White<sup>2</sup>

<sup>1</sup>Univ of Michigan; and <sup>2</sup>University of Michigan

Abstract ID 23842

Poster Board 565

Mu-opioid receptor agonists are the gold standard for pain treatment. While efficacious for moderate to severe pain, these drugs are associated with serious adverse effects including abuse liability and respiratory depression. One emerging strategy for safer pain treatments is the development of positive allosteric modulators (PAMs) of the mu-opioid receptor (mu-PAMs). Mu-PAMs can enhance analgesia by increasing the activity of endogenous neurotransmitters released during pain states. Because mu-PAMs do not activate MOR in the absence of an orthosteric agonist and the promoting effects on endogenous opioids are localized and temporal, this allosteric strategy holds the promise of analgesia with fewer side effects. Previous work has identified one molecule, BMS-986122 (Figure 1), that enhances the antinociceptive effects of endogenous opioids with a reduced ability to cause constipation, respiratory depression, and reward. However, BMS-986122 is weak with an affinity of 5mM for the mu-opioid receptor, and we do not know how the compound interacts with the receptor. Hence, the presented research aimed to explore structure-activity relationships (SAR) of the BMS986122 scaffold for the design of more potent compounds. Derivatives of BMS-986122 were synthesized and fully characterized (purity >95%). The potency and efficacy of the compounds were determined by their ability to shift the dose-response curve of the standard mu-opioid agonist DAMGO using *b*-arrestin recruitment and GTPγ<sup>35</sup>S binding assays. By altering the substitution patterns on the aromatic rings and replacing the heterocyclic core (Figure 1) we were able to identify compounds that had no effect on their own but shifted the concentration-response curve for DAMGO up to 35-fold. There was only a minor difference between individual enantiomers (\*). Our study has generated a SAR framework of BMS986122, which will facilitate the understanding of the allosteric pharmacophore and the design of better mu-PAMs.

Support/Funding Information: R37 DA039997

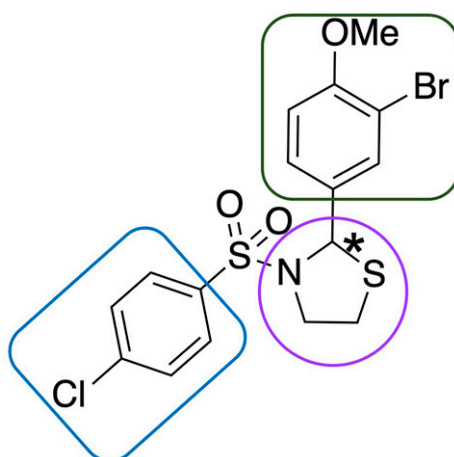


Figure 1. Structure of BMS986122.

# In Vitro Application of Hydrolase Reaction Phenotyping in Early Discovery Research

Guo Zhong,<sup>1</sup> Julie Lade,<sup>1</sup> and Armina Abbasi<sup>1</sup>

<sup>1</sup>Amgen

Abstract ID 52879

Poster Board 171

In recent years, the biotransformation profile of novel chemical entities (NCE) has evolved away from predominant cytochrome P450 (P450)-mediated metabolism and shunted toward other pathways that can contribute to small molecule drug clearance. Hydrolases are an important class of drug metabolizing enzymes, that catalyze the hydrolysis of NCE containing ester and amide functional groups. Preliminary metabolite identification in vitro (mouse, rat, dog, human hepatocytes) and in vivo (mouse, rat, dog plasma) showed that our internal NCE, denoted here as compound A1, was highly susceptible to amide hydrolysis forming the metabolite M1. To deduce the potential enzyme(s) contributing to the formation of M1, compound A1 was incubated with mouse and human plasma and whole blood, but exhibited metabolic stability suggesting the hydrolysis product was formed in tissues and not in systemic circulation. In the current study, we conducted hydrolase reaction phenotyping in tissue fractionations to investigate the relative contribution to A1 hydrolysis by carboxylesterase 1 (CES1), CES2, serine proteases, arylacetamide deacetylase (AADAC) and aldehyde oxidase (AO), all of which have been reported to catalyze amide hydrolysis in liver. Also, a workflow for hydrolase phenotyping is proposed. Our data showed that the formation of M1 was time-dependent in the incubation of 10  $\mu$ M A1 with mouse and human liver cytosol and microsomes, respectively, and the formation was significantly higher in mouse than in human liver subcellular fractions. The time-dependent formation of M1 was also observed in human intestinal S9, brain S9, and recombinant human CES1 and CES2 supersomes. Chemical inhibition studies were then performed in human liver S9 and intestinal S9 using troglitazone, a CES1 selective inhibitor, and telmisartan, a CES2 selective inhibitor, which both reduced M1 formation by >90%. In contrast to these findings, phenylmethylsulfonyl fluoride (PMSF), a reported pan inhibitor of human CES and serine proteases, did not inhibit M1 formation in either human liver S9 or intestinal S9, suggesting that some unknown hydrolase(s), the activity of which is inhibited by telmisartan and troglitazone but not by PMSF, contribute to A1 hydrolysis. Additionally, hydralazine, a selective AO inhibitor, did not cause M1 formation. Because it has been reported in literature that AADAC activity is not inhibited by telmisartan, our telmisartan inhibition data suggested that AADAC does not play a significant role in A1 hydrolysis. Taken together, serine proteases, AADAC and AO are not involved in A1 compound metabolism while CES1, CES2 and other unknown hydrolases contribute to the amide hydrolysis of A1.



# HNF4A-AS1 Alleviates Ritonavir-induced Liver Injury via HNRNPC-mediated HNF4A Degradation

Xiaofei Wang,<sup>1</sup> Jingya Wang,<sup>2</sup> Pei Wang,<sup>2</sup> Yihang Yu,<sup>2</sup> Yiting Wang,<sup>2</sup> Mengyao Yan,<sup>2</sup> Shengna Han,<sup>2</sup> and Lirong Zhang<sup>2</sup>

<sup>1</sup>Academy of Medical Sciences, Zhengzhou University; and <sup>2</sup>Department of Pharmacology, School of Basic Medical Sciences, Zhengzhou University

Abstract ID 18764

Poster Board 172

**Abstract:** A combination of ritonavir (RTV) and rifampicin (RIF) can increase the incidence of liver injury. It may ascribe to the induced expression of cytochrome P450 (CYP) 3A4. In recent years, long noncoding RNAs (lncRNAs) have been shown to be crucial for the regulation of CYPs and drug-induced liver injury. Our previous study indicated that lncRNA hepatocyte nuclear factor 4 alpha-antisense 1 (HNF4A-AS1) negatively regulates the expression of pregnane X receptor (PXR)/CYP3A4 and is involved in RTV-induced hepatotoxicity *in vitro*. However, the role of HNF4A-AS1 in RTV-induced liver injury *in vivo* and the underlying mechanism remain unraveled. In this study, Hnf4aos (a mouse lncRNA homologous to HNF4A-AS1) knockdown mice were used to confirm the crucial role of HNF4A-AS1 in RTV-induced liver injury *in vivo*. We further demonstrated that HNF4A was involved in the regulation of PXR/CYP3A4 expression mediated by HNF4A-AS1. Mechanistically, HNF4A-AS1 mediated the interaction between HNRNPC and HNF4A, whereas HNRNPC promoted HNF4A degradation through the proteasome pathway, which down-regulated the expression levels of downstream gene PXR/CYP3A4, and thus affected on RTV-induced liver injury. Overall, our findings unveil a novel mechanism by which HNF4A-AS1 regulates PXR/CYP3A4 expression through HNF4A, suggesting that HNF4A-AS1 may serve as a new indicator for the prevention and treatment of drug-induced liver injury.

**Key words:** HNF4A-AS1, hepatocyte nuclear factor 4A, pregnane X receptor, cytochrome P450 family 3 subfamily A member 4, ritonavir, liver injury

This work was supported by the National Natural Science Foundation of China [Grants 82073931 to Lirong Zhang].

# Physiologically Based Pharmacokinetic (PBPK) Modeling to Predict the Pharmacokinetics of Irbesartan in Different *CYP2C9* Genotypes

Seok-Yong Lee,<sup>1</sup> Chang-Keun Cho,<sup>1</sup> Pureum Kang,<sup>1</sup> Eunvin Ko,<sup>1</sup> and Chou Yen Mu<sup>1</sup>

<sup>1</sup>Sungkyunkwan University

Abstract ID 50858

Poster Board 173

**Introduction:** Irbesartan, a potent and selective angiotensin II type-1 receptor blocker, is mainly metabolized through oxidation and glucuronide conjugation. Its oxidation is primarily mediated by *CYP2C9*, and the genetic polymorphism of *CYP2C9* significantly affects the pharmacokinetics of irbesartan. This study aimed to establish the physiologically based pharmacokinetic (PBPK) model of irbesartan in different *CYP2C9* genotypes for individualized pharmacotherapy with irbesartan according to the genotype of *CYP2C9*.

**Methods:** The irbesartan PBPK model was established using PK-Sim<sup>®</sup> in three different *CYP2C9* genotypes (*CYP2C9*\*1/\*1, \*1/\*3, and \*1/\*13). Our pharmacogenomic data of irbesartan and a total of 15 clinical pharmacokinetic data of irbesartan with different demographic characteristics and dose regimens were leveraged to develop and validate the model. Physicochemical and ADME properties of irbesartan were obtained from previously reported data or optimized to capture the plasma concentration-time profiles in different *CYP2C9* genotypes.

**Results:** Predicted plasma concentration-time profiles were visually similar to the observed profiles in different *CYP2C9* genotypes. The ranges of fold errors for  $AUC_{inf}$  and  $C_{max}$  in development were 1.01-1.09 and 0.92-1.02 respectively, which were strictly satisfied with the evaluation criterion. The ranges of fold errors for  $AUC_{inf}$  and  $C_{max}$  in single-dose validation were 0.53-1.87 and 0.61-1.90, respectively, and in multiple-dose validation were 0.87-1.64 and 0.77-1.82, respectively, which were also within the evaluation criterion.

**Conclusion:** The PBPK model of irbesartan developed in this study can be used to predict the pharmacokinetics of irbesartan and for individualized pharmacotherapy with irbesartan in individuals of various races, ages, and *CYP2D6* genotypes.

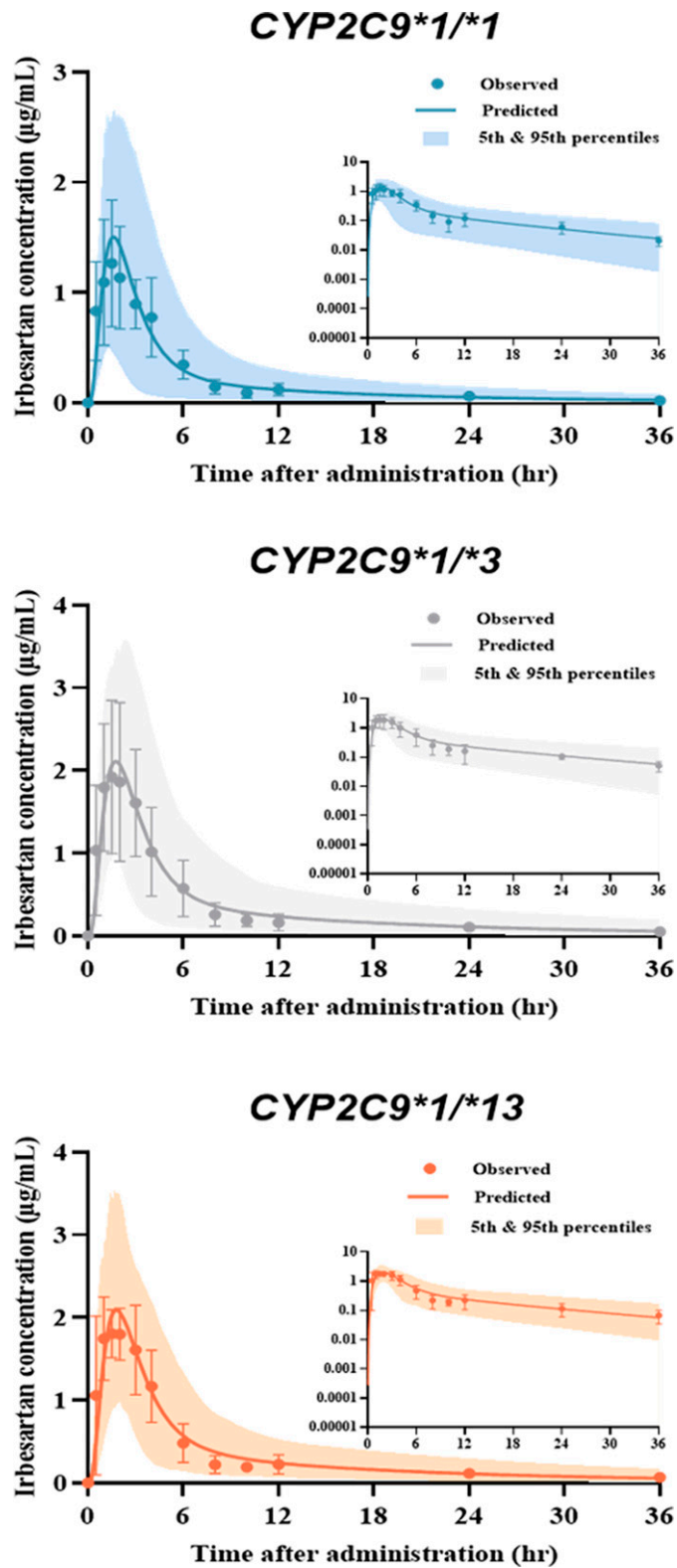


**Figure 1.** Predicted and observed plasma concentration-time profiles of irbesartan in different *CYP2C9* genotypes. Solid lines and shaded areas indicate arithmetic mean and 5<sup>th</sup>-95<sup>th</sup> percentile, respectively. Circles and error bars indicate the means and standard deviations of observed plasma concentrations, respectively. Profiles are expressed using linear and semi-logarithmic scales.

# Identification of Pazopanib as an OATP1B1 Substrate from a Competitive Counterflow Screen

Thomas Drabison,<sup>1</sup> Mike Boeckman,<sup>2</sup> Eric Eisenmann,<sup>3</sup> Sharyn D. Baker,<sup>1</sup> Shuiying Hu,<sup>4</sup> Alex Sparreboom,<sup>4</sup> and Zahra Talebi<sup>4</sup>

<sup>1</sup>The Ohio State Univ; <sup>2</sup>Ohio State University; <sup>3</sup>Ohio State Univ; and <sup>4</sup>The Ohio State University

Abstract ID 55504

Poster Board 174

**Background:** Tyrosine kinase inhibitors (TKIs) belong to a class of commonly used chemotherapeutics that impair tumor growth by interfering with the function of protein kinases and their downstream signaling cascades. Although the primary elimination pathway for most TKIs has been well established and involves hepatic CYP3A4 metabolism, the mechanism by which these agents are taken up in hepatocytes remains unclear. Experimental challenges measuring the direct uptake of TKIs contribute to this knowledge deficit, especially a relatively high level of non-specific, extracellular membrane binding of TKIs. We hypothesized that we could overcome these challenges by using a competitive counterflow (CCF) assay and this methodology would allow us to systematically re-examine TKI transport by the hepatic uptake transporter OATP1B1.

**Methods:** The CCF assay was based on the stimulated efflux of radiolabeled estradiol-17 $\beta$ -glucuronide (E $\beta$ G) in HEK293 cells engineered to overexpress OATP1B1 or a vector and was validated using E $\beta$ G as a positive control and glucose as a negative control. A total of 49 TKIs were examined for transport by OATP1B1. After identification of pazopanib as a positive hit, validation was performed by administering pazopanib to wild-type mice and mice deficient in all hepatic OATPs (OATP1A/1B-knockout mice) and measuring markers of drug-induced liver injury, including serum transaminases and histological evaluation of livers.

**Results:** Of the 49 TKIs tested, 11 compounds (22%) caused efflux of radiolabeled E $\beta$ G to a degree that was met a retrospectively determined cut off, suggesting that they are transported substrates of OATP1B1. These included the previously identified substrates axitinib and sorafenib, as well as the hepatotoxic TKI, pazopanib. Ensuing uptake studies with radiolabeled pazopanib in HEK293 cells with and without OATP1B1 overexpression confirmed that non-specific binding of TKIs compromises the use of conventional uptake assays for OATP1B1 substrate identification. In wild-type mice receiving a single oral dose of pazopanib (300 mg/kg), concentrations of the enzymes aspartate transaminase (AST) and alanine transaminase (ALT) were >200 IU/L, whereas in mice with complete deficiency of OATP1A and OATP1B isoforms, concentrations remained within the lower normal range (ALT, 25 IU/L; AST, 50 IU/L). In addition, vacuolization of hepatocytes in both the nucleus and cytoplasm in centrilobular to midzonal regions was only observed in wild-type mice, implicating OATP1B-type transport as a key mediator of pazopanib-induced liver injury.

**Conclusions:** We have successfully optimized a CCF assay for identification of OATP1B1 substrates in the class of TKIs using an overexpressed HEK293 cell-based model. Validation studies *in vivo* implicate OATP1B-type transport as a contributor to pazopanib-induced liver injury and provide a rationale for the development of intervention strategies with OATP1B1 inhibitors to prevent this debilitating side effect.

**Keywords:** OATP1B1, Pazopanib, Hepatotoxicity

# Unusual Metabolism of Benzethonium by Cytochrome P450

Ryan P. Seguin,<sup>1</sup> Libin Xu,<sup>1</sup> and Ryan Nguyen<sup>1</sup>

<sup>1</sup>Univ of Washington

Abstract ID 56418

Poster Board 175

**Introduction:** Benzethonium (BZT) is a quaternary ammonium antimicrobial used in food-processing, personal care products, antiseptics, and as a preservative in pharmaceutical formulations. BZT-containing cosmetics, creams, and ointments are commonly applied to the skin. In an ADME study conducted by the National Toxicology Program, radiolabeled BZT exhibited high dermal bioavailability (>50%) in rats, with 45% of radioactivity being recovered in feces. Furthermore, the liver contained the highest levels of radioactivity among all tissues. Radioactivity in the liver peaked at 24 hours and persisted out to 7 days after a single dermal application of [<sup>14</sup>C]-BZT. Hepatic uptake of dermally absorbed BZT followed by biliary excretion to feces can likely explain these results. Despite widespread human exposure to BZT and the above evidence for significant dermal absorption and hepatic exposure in animals, the metabolism of BZT has received no attention to date.

Our **objective** was to structurally elucidate the metabolites of BZT produced by cytochrome P450 (CYP)-mediated metabolism. Our **approach** utilized LC-MS-based investigation of the metabolite profile generated by incubating BZT in human liver microsomes (HLM) in the presence or absence of NADPH. High-resolution (time-of-flight) MS/MS fragmentation of parent BZT and the chromatographically resolved metabolites was performed.

**Results:** Incubation of BZT in HLM produced more than 10 NADPH-dependent metabolite peaks with *m/z* values corresponding to +1 or +2 oxygen atoms, both with and without loss of 2 hydrogen atoms (-2H). MS/MS fragmentation confirmed that metabolism occurs on the 2,4,4-trimethyl-pentan-2-yl (TMP) moiety of BZT. There were at least 5 chromatographically resolved hydroxy metabolites with MS/MS fragmentation supporting the addition of oxygen on the TMP moiety. However, there are only 3 unique carbon positions at which oxygen can be added to the TMP moiety. Hence, in the absence of a chiral column, it should not be possible to observe 5 unique hydroxy metabolite peaks (specifically on the TMP moiety), unless carbon-carbon (C-C) bond rearrangement occurs during the CYP-mediated metabolism of BZT. Furthermore, we observed 5 metabolite peaks corresponding to -2H metabolic modification on the TMP moiety (desaturation without addition of oxygen). However, the TMP moiety of BZT does not contain a pair of vicinal C-H bonds. This further supported a scenario where C-C bond rearrangement must have occurred within the TMP moiety of BZT prior to desaturation.

**Conclusion:** CYP-mediated metabolism of BZT appears to involve intramolecular rearrangement of C-C bonds within the TMP moiety of BZT. Our proposed mechanism begins with hydrogen atom transfer from TMP to P450 compound I (Fe<sup>IV</sup>=O) followed by intramolecular rearrangement of the carbon radical intermediate, and oxygen rebound or dehydration to form hydroxy and alkene products, respectively. This unusual metabolism led us to propose several novel metabolites of BZT.

**Significance:** This work builds upon the diverse range of CYP-catalyzed rearrangement reactions reported in the literature that serve as a cornerstone of CYP enzymology.

**Funding:** NIH NIEHS (R01ES031927, P30ES007033, and T32-ES007032)

# Metabolism of (-)- $\Delta^9$ -Tetrahydrocannabinol (THC) in Chicken and Potential Exposure of THC and Its Metabolites to Humans

Ziteng Wang,<sup>1</sup> Chock Ying Soo,<sup>2</sup> Evelyn Mei Ling Goh,<sup>2</sup> Hooi Yan Moy,<sup>2</sup> and Eric Chun Yong Chan<sup>1</sup>

<sup>1</sup>National University of Singapore; and <sup>2</sup>Health Sciences Authority

Abstract ID 15252

Poster Board 176

One recent study reported fewer cases of avian bronchitis and higher quality of meat when chicken were fed daily supplementation of cannabis.<sup>1</sup> The exposure to primary substances of cannabis, namely (-)- $\Delta^9$ -tetrahydrocannabinol (THC) and its psychoactive metabolite, 11-OH-THC, in meat and egg of these supplemented chickens rarely received attention. Notably, these substances could be consumed by humans, raising health and legal issues. To explore the potential impact, we aimed to comprehensively investigate the pharmacokinetics (PK) of THC and 11-OH-THC in chicken and humans via *in vitro* and *in silico* approaches.

*In vitro* metabolism experiments were performed to characterize metabolism of THC and 11-OH-THC using chicken liver microsomes (CLM). Kinetic parameters were calculated and compared with those derived from human liver microsomes (HLM). Thermal stabilities of THC and 11-OH-THC were further assessed by mimicking the cooking process. PK of THC and 11-OH-THC and their distribution to muscle and egg were predicted via physiologically-based pharmacokinetic (PBPK) modeling. Oral consumption of 11-OH-THC in meat or egg was simulated under fed condition to predict its exposure to humans.

The depletion of THC in CLM was slower than that in HLM (**Fig. 1A**). Intrinsic clearances ( $CL_{int}$ ) were estimated as 0.49 and 54.03 ml/min/g of chicken and human liver, respectively. Similarly, 11-OH-THC was more metabolically stable in CLM than in HLM, where UGT and P450 enzymes accounted for 67.5% and 32.5% of 11-OH-THC depletion in CLM, with  $CL_{int}$  of 0.33 and 0.16 ml/min/g liver, respectively (**Fig. 1B**). PBPK modeling predicted elimination half-lives of THC and 11-OH-THC in chicken as 79.3 and 27.2 h, respectively, demonstrating that both compounds were slowly eliminated (**Fig. 1C and D**). Their extensive distribution to chicken muscle and egg were simulated as well. However, high temperature incubation degraded most THC within 30 min, suggesting its substantial loss in a cooked chicken meal. Conversely, 11-OH-THC remained thermally stable (**Fig. 1E**). Subsequent PBPK modeling in humans simulated 1.68-fold increase in systemic exposure of 11-OH-THC in the presence of meal, suggesting food effect on systemic absorption of 11-OH-THC (**Fig. 1F**).

Our study established the PK of THC and 11-OH-THC in chicken, and revealed that 11-OH-THC may reside in chicken products even after cooking. Oral absorption of 11-OH-THC in humans could be significantly augmented by food. Considering the comparative pharmacology between 11-OH-THC and THC in men,<sup>2,3</sup> our findings hold important implications for potential human consumption of and exposure to psychoactive 11-OH-THC in the real-world. Further research is warranted to support the safe use of cannabis-supplemented chicken feeds.

## References:

1. <https://www.theguardian.com/world/2022/jun/15/cannabis-fed-chickens-may-help-cut-farmers-antibiotic-use-thai-study-shows>
2. Science 1972 177:62-4
3. J Clin Invest 1973 52:2411-7

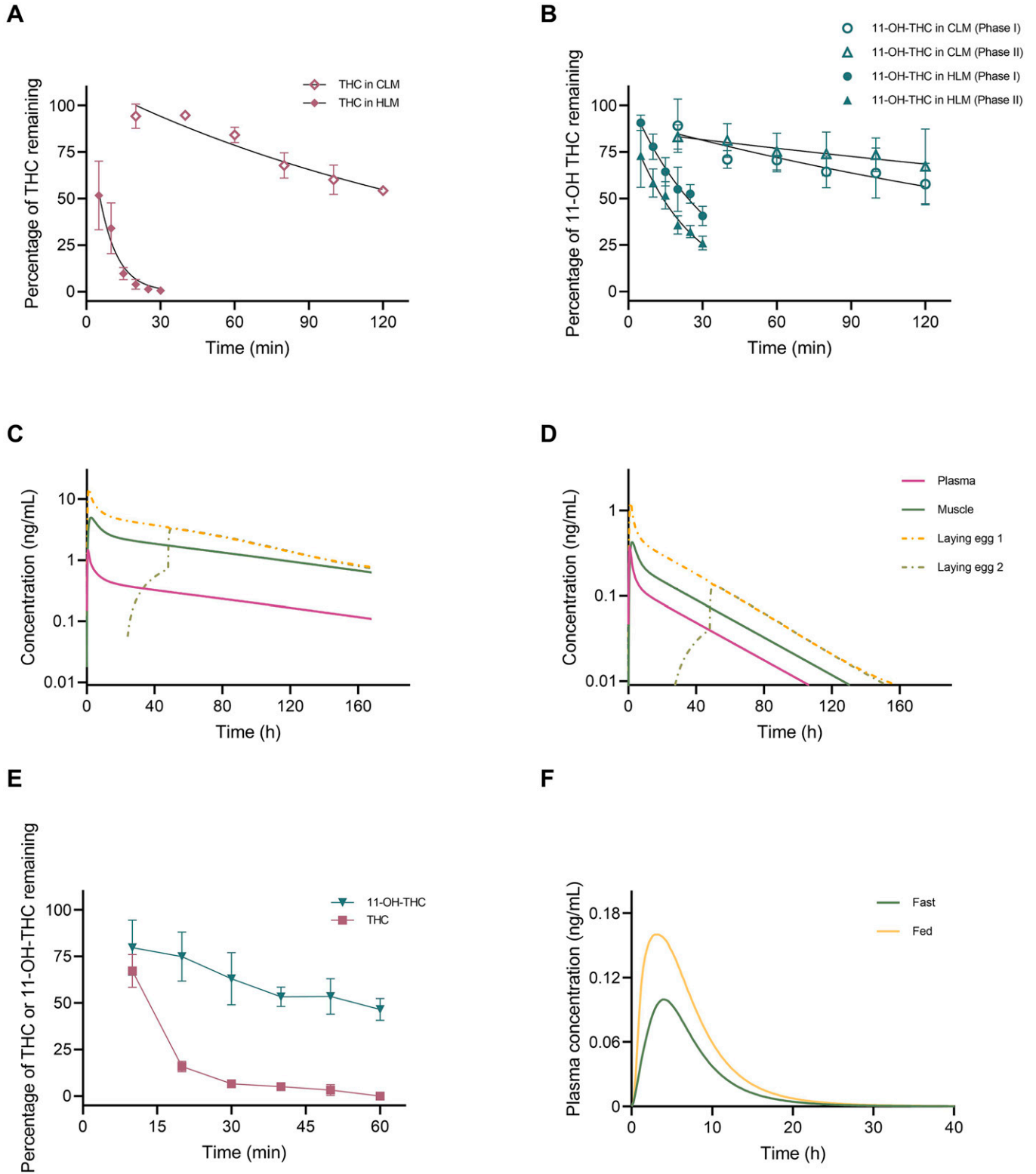


**Figure 1.** Metabolic stability of (A) THC and (B) 11-OH-THC in CLM and HLM incubation systems. Lines represent linear regression when Y-axis is natural logarithmic transformed. Simulated mean concentration-time profiles of (C) THC and (D) 11-OH-THC in plasma, muscle and eggs in chicken after oral gavage administration. (E) Stability of THC and 11-OH-THC in CLM incubation system at 90 °C. (F) Simulated mean plasma concentration-time profile of 11-OH-THC in humans after oral consumption in the presence/absence of meal.

# The CYP11A1 substrates vitamin D3 and cholesterol induce changes in protein conformation and protein-protein interactions with Adrenodoxin

Janie McGlohon,<sup>1</sup> and D. Fernando Estrada<sup>2</sup>

<sup>1</sup>University at Buffalo; and <sup>2</sup>Univ at Buffalo

Abstract ID 23103

Poster Board 177

Cytochrome P450 11A1 (CYP11A1) is a membrane associated mitochondrial enzyme that metabolizes the chemically distinct substrates cholesterol and vitamin D3, with less efficient metabolism towards the latter. CYP11A1 exerts its catalytic function by obtaining two sequential electrons from Adrenodoxin (Adx). Recent studies suggest that both substrates and Adx may play a regulatory role in CYP-mediated metabolism. This leads to my central hypothesis that the differences in the vitamin D3 chemical structure induce conformational change(s) of CYP11A1 that are relayed towards the proximal or distal regions of CYP11A1 and therefore impact Adx association to CYP11A1. Our objective is to test this hypothesis by utilizing in-solution biophysical techniques in combination with biochemical assays to assess substrate-induced conformational changes to CYP11A1 structure and determine whether vitamin D3 or cholesterol modulate CYP11A1 affinity towards Adx, thus explaining reduced efficiency towards vitamin D3. Preliminary <sup>19</sup>F-NMR spectra of CYP11A1 reveal both structural heterogeneity in CYP11A1, along with substrate-specific conformational changes. Importantly, NMR spectra reflect an interaction with vitamin D3 that otherwise is not detectible by absorbance spectroscopy. Moreover, we have combined 2D <sup>1</sup>H- and <sup>15</sup>N- Heteronuclear Single Quantum Coherence (HSQC) NMR with Biolayer interferometry (BLI) to investigate the nature of the protein-protein interaction with Adx. NMR titration of a preformed CYP11A1-Adx complex with  $\beta$ -cyclodextrin-incorporated cholesterol reveals a gradual focusing of NMR effects towards  $\alpha$  helix-3 of Adx and an overall decrease in the peak intensity remaining. The results are consistent with preliminary BLI data in which cholesterol increases the protein-protein interaction between CYP11A1 and Adx. These findings support substrate-specific induced conformational changes to CYP11A1 structure and modulation of the CYP11A-Adx complex protein-protein interaction.



# Deciphering the Zonal Distribution of Hepatic Drug Metabolizing Enzymes and Transporters in Mice by Single Cell Transcriptomics

Joe Jongpyo Lim,<sup>1</sup> Curtis Klaassen,<sup>2</sup> and Julia Yue Cui<sup>1</sup>

<sup>1</sup>Univ of Washington; and <sup>2</sup>Univ of Kansas

Abstract ID 16149

Poster Board 178

Hepatocytes are the key cell type in liver for biotransformation of drugs and other xenobiotics. The liver lobule is categorized into 3 zones: periportal (zone 1), midzonal (zone 2), and centrilobular (zone 3). There lacks a systematic characterization of the zonal distribution of drug-processing genes. Therefore, the goal of this study was to characterize the zonal distribution of drug metabolizing enzymes and transporters as well as their regulators in liver. Mouse single cell transcriptomic data (GSE192742) aligned to the mm10 reference genome were downloaded from the GEO database and subjected to zonal deconvolution. Filtering, normalization, clustering, and differential expression analyses were performed using Seurat (v4) in R (v4.1.1). Hepatocytes were identified from all the cells in the liver using known hepatocyte-specific marker genes. The hepatocytes were then assigned into one of the three zones using known zone-specific marker genes. Among the 102 mouse cytochrome P450s (Cyps), 50 were differentially enriched in the three zones. As expected, the majority of Cyps were enriched in zone 3: for example, *Cyp2e1*, which activates many hepatotoxicants was expressed 4-times higher in zone 3, and *Cyp7a1*, the rate limiting enzyme in bile acid synthesis was expressed 17-fold higher in zone 3 than zone 1. However, not all Cyps had higher expression in zone 3 than zone 1. For example, *Cyp2f2* and *Cyp2a4* were expressed 4.5- and 14-fold higher, respectively, in zone 1 than zone 3. Of the other phase-I enzymes, most aldehyde dehydrogenases were expressed more highly in zone 1 than zone 3; of the five flavin-containing monooxygenases, two were more highly expressed in the zone 2 and one in zone 1: and all six peroxidases were more highly expressed in zone 1. Phase-II conjugation enzymes such as the glucuronosyltransferases and glutathione-S transferases were more highly expressed in zone 3, whereas the sulfotransferases were enriched in zone 1. The hepatic xenobiotic uptake transporters were most highly expressed in zone 3 than zone 1: *Oatp1a1*, *1a4*, and *2b1* were 4-, 5-, and 9-fold more highly expressed in zone 3 than zone 1. The major canalicular efflux transporter *Mrp2* was 6-fold more highly expressed in zone 3 than zone 1. In contrast, the major bile acid transporters, namely, the basolateral uptake transporter *Ntcp* was evenly distributed among all three zones, whereas the canalicular efflux transporter *Bsep* was expressed higher in zones 2 and 3. The transcription factors known to regulate xenobiotic biotransformation, namely Ahr, CAR, PXR, PPAR $\alpha$ , and Nrf2 were expressed 15-, 6-, 2.5-, 4.9-fold higher in zone 3 than zone 1 hepatocytes. In conclusion, our study has unveiled unique zonal specific expression patterns of major drug-processing genes and their regulators in hepatocytes. Because many hepatotoxicants require bioactivation, our findings lay the foundation for further understanding the mechanisms of zonal specific drug-induced liver injuries.

This work was supported by the National Institutes of Health (NIH) (grants R01ES030197, and R01ES031098), the University of Washington Center for Exposures, Diseases, Genomics, and Environment (P30ES007033), Environmental Pathology/Toxicology Training Program (T32ES007032), Environmental Health and Microbiome Research Center, and the University of Washington Sheldon Murphy Endowment.

# Non-nutritive Sweeteners Acesulfame Potassium and Sucralose Competitively Inhibit P-glycoprotein

Laura Danner,<sup>1</sup> and Stephanie Olivier-Van Stichelen<sup>2</sup>

<sup>1</sup>Medical Coll of Wisconsin; and <sup>2</sup>Medical College of Wisconsin

Abstract ID 25308

Poster Board 179

Non-nutritive sweeteners (NNS) are popular sugar replacements that are used in a wide range of foods, beverages, and medications. Although NNS are recognized as safe by the Food and Drug Administration, the effects of NNS on specific patient populations and human development are not completely understood. Previously, our lab showed that mouse pups exposed to NNS during early development present compromised liver detoxification. Thus, we questioned whether NNS might disrupt detoxification in the liver, including efflux transporters such as P-glycoprotein (*ABCB1*/ PGP). **We hypothesize that two common NNS, acesulfame potassium (AceK) and sucralose (Sucr), inhibit PGP's efflux function and alter PGP expression, suggesting reduced detoxification capacity and altered distribution of certain drugs.** To investigate the effects of NNS on PGP, we first exposed the HepG2 liver carcinoma cell line to AceK and Sucr and assessed *ABCB1*/ PGP transcript and protein levels. Combined NNS treatment significantly increased *ABCB1* expression and PGP levels, an effect also commonly observed with some PGP inhibitor drugs. We, therefore, investigated NNS effects on PGP's efflux action. An *in vitro* PGP substrate retention assay performed in HepG2 and HEK293 demonstrated that combined NNS significantly increased the intracellular retention of PGP substrate Calcein-AM, confirming PGP inhibition by NNS. Individual AceK or Sucr incubation on HepG2 cells also significantly inhibited PGP efflux, validating the PGP inhibition by both compounds. In a cell-free assay measuring PGP's ATPase activity, AceK and Sucr also significantly increased PGP ATPase activity in a dose-dependent manner, revealing them as competitive inhibitors of PGP. Molecular docking experiments provided further insight into NNS interactions with PGP substrate binding pockets. Like Verapamil, Sucr was found to dock primarily in PGP's main high-affinity binding pocket. AceK shows a lower affinity for this pocket and docks mainly in two other sites within PGP's inward-facing transmembrane channel. To conclude, our results provide evidence that two common NNS, AceK and Sucr, are substrates and competitive inhibitors of PGP, impacting PGP both functionally and at the level of mRNA and protein. Most importantly, altered PGP function was observed after exposure to concentrations of NNS within expected levels from common foods and beverage consumption, suggesting risks for NNS consumers when taking medications that are PGP substrates or modulators.

# Identification and Characterization of Palmitoylation Sites in the Organic Anion Transporting Polypeptide 1B1 (OATP1B1)

Cecilia Villanueva,<sup>1</sup> Whitney Nolte,<sup>2</sup> and Bruno Hagenbuch<sup>3</sup>

<sup>1</sup>Univ of Kansas Medical Center; <sup>2</sup>Children's Mercy Hospital; and <sup>3</sup>Univ of Kansas Medical Ctr

Abstract ID 20665

Poster Board 180

**Background:** Organic Anion Transporting Polypeptide 1B1 (OATP1B1) is a hepatic transporter that mediates the uptake of numerous therapeutics like statins and antibiotics. Previous studies from our lab suggest that OATP1B1 is localized in membrane microdomains, also known as lipid rafts. Proteins in lipid rafts are frequently modified by S-acylation (also referred to as S-palmitoylation), a reversible post-translational modification that results in the addition of palmitic acid (C16:0) to cysteine residues. Using an acyl-resin-assisted capture (acyl-RAC) assay, we previously demonstrated that OATP1B1 contains S-acylated residues. We also demonstrated that 2-Bromopalmitate (2BP), a commonly used S-palmitoylation inhibitor, impacts OATP1B1 surface localization and function, suggesting that OATP1B1 is palmitoylated. Currently, nothing is known about specific palmitoylation sites in OATP1B1.

**Aim:** We hypothesize that OATP1B1 is palmitoylated at various sites and that this may impact its function and surface expression.

**Methods:** Cysteine palmitoylation was predicted using GPS-palm. Palmitoylation sites of OATP1B1 were also analyzed using mass spectrometry. Identified sites were mutated to alanine residues using site-directed mutagenesis. Transporter expression at the plasma membrane was quantified by a surface biotinylation assay. To assess the function, the uptake of the model substrate estradiol-17 $\beta$ -glucuronide was measured and then normalized for surface expression. The mutants were also analyzed using the acyl-RAC assay and western blotting.

**Results:** Positions Cys24, Cys101, and Cys691 were predicted to be palmitoylated. Palmitoylation of Cys24 was confirmed using proteomics. In addition, mass spectrometry also identified N-palmitoylation at positions Lys19 and/or Lys20. Both OATP1B1 mutants C24A and C691A have an increase in surface expression as compared to wildtype OATP1B1. Normalizing for this surface-expression increase demonstrates that their overall uptake function is decreased compared to wildtype. Mutant C101A showed no changes in both surface expression and function. Interestingly, the acyl-RAC assay demonstrated that OATP1B1 loses its S-acylated residue only when Cys24 is mutated, suggesting that Cys24 is palmitoylated in OATP1B1.

**Conclusions:** Our results show that OATP1B1 is S-palmitoylated at Cys24 and N-palmitoylated at Lys19/Lys20. Inhibition of this post-translational modification may alter the function and surface expression of this hepatic drug uptake transporter. Thus, pathological states where palmitoylation is modified could impact drug targeting and disposition.

# In vitro and In vivo Inhibition of Nicotine Metabolism by *trans*-2-Nitrocinnamaldehyde

Aiden-Hung Nguyen,<sup>1</sup> Uyen-Vy Navarro,<sup>2</sup> Ghina Moyeen,<sup>2</sup> and John Harrelson<sup>2</sup>

<sup>1</sup>Pacific Univ Sch of Pharmacy; and <sup>2</sup>Pacific Univ School of Pharmacy

Abstract ID 16923

Poster Board 181

**Background:** Pharmacogenomic studies show variation in nicotine metabolism influences smoking behaviors; slow metabolizers exhibit a decrease in smoking frequency. Thus, the design of inhibitors of nicotine metabolism is one approach for the discovery of new cessation therapies. Previous in vitro evidence demonstrate that *trans*-2-methoxycinnamaldehyde and *trans*-cinnamaldehyde are time-dependent inhibitors of human CYP2A6, the enzyme responsible for nicotine clearance. In vitro-to-in vivo extrapolation predicts a > 4-fold change in nicotine AUC (area under the curve). Here we evaluated the structural analog, *trans*-2-nitrocinnamaldehyde (NCA) in vitro, using human and mouse liver microsomes, and in vivo in C57GL/6J mice.

**Hypothesis:** The addition of the nitro group will stabilize a purported terminal formyl radical and lead to greater in vitro and in vivo inhibition potency of nicotine metabolism.

**Methods:** In vitro time-dependent inhibition studies were conducted by monitoring the remaining activity of nicotine metabolism after incubating NCA (0-120  $\mu$ M) with human (2 mg/mL) and mouse liver microsomes (2 mg/mL) for 0 to 90 minutes. An aliquot was transferred to the secondary incubation system containing NADPH (1 mM), nicotine (50  $\mu$ M), and corresponding liver cytosol (1 mg/mL) at specific time points. After incubation for 15 minutes at 37 °C, each secondary incubation was quenched with ice-cold acetonitrile and the internal standard (D<sub>3</sub>-cotinine) was added. Cotinine was quantified using a Sciex 3500 LC-MS/MS. For in vivo studies, using adult male C57BL/6J mice, two modes of administration were selected. For oral administration, NCA was dissolved in the drinking water at the concentration of 0.088 mg/mL, to which the mice had access for three days prior to intraperitoneal injection of nicotine (1 mg/kg). To compare potency with methoxsalen (a known CYP2A6 inhibitor) NCA (57.1 mg/kg) was also administered via intraperitoneal injection. Blood was collected at specific time points (5 to 120 minutes). Samples were centrifuged to isolate plasma, D<sub>3</sub>-cotinine (internal standard) and acetonitrile were added, and then centrifuged. Supernatants were analyzed on LC-MS/MS to quantify nicotine and cotinine using standard curves generated in mouse plasma. Blood concentrations from four to five mice were measured for each time point and AUC values were estimated using Phoenix WinNonlin.

**Result:** The in-vitro study using mouse liver microsomes showed that NCA time-dependently inhibited the formation of cotinine from nicotine with a  $k_{\text{inact}}$  of 0.060 min<sup>-1</sup> ( $\pm$  0.024) and a  $K_i$  of 6.0  $\mu$ M ( $\pm$  2.0). Oral administration of NCA in mice resulted in a nicotine plasma AUC of 355.9 ng\*min/mL (geometric mean; 95% CI = 151.5 – 836.6), which is estimated to be 2.5 times higher than the control nicotine plasma AUC of 143.3 ng\*min/mL (geometric mean; 95% CI: 112.2 – 183.0). Intraperitoneal injection of NCA and methoxsalen resulted in nicotine plasma AUC of 280.7 ng\*min/mL (geometric mean; 95% CI =170.7 – 474.7; AUC-fold change = 1.96) and 957.6 ng\*min/mL (geometric mean; 95% CI: 532.4 – 1665.8; AUC-fold change = 6.68), respectively.

**Conclusion:** NCA is a more potent in vitro time-dependent inhibitor of nicotine metabolism compared to *trans*-2-methoxycinnamaldehyde and *trans*-cinnamaldehyde. Greater inhibition was observed with oral administration compared to intraperitoneal injection; this is evidence that NCA is reasonably stable in water to allow for oral dosing.

# High-Resolution Mass Spectrometry Coupled with XCMS Online for High-throughput Detection and Identification of Drug Metabolites

Dilip Singh,<sup>1</sup> Vijaya S. Mettu,<sup>2</sup> Aarzo Thakur,<sup>2</sup> Anoud Ailabouni,<sup>3</sup> and Bhagwat Prasad<sup>3</sup>

<sup>1</sup>Washington State Univ Spokane; <sup>2</sup>Washington State University; and <sup>3</sup>Washington State Univ

Abstract ID 25135

Poster Board 182

Metabolite identification (MetID) studies provide critical information to elucidate the biotransformation pathways of a new chemical entity during the early stages of drug discovery and development. Liquid chromatography-high resolution mass spectrometry (LC-HRMS) is the gold-standard technique for prediction of metabolite structures, however, the current MetID studies rely on manual data processing. The goal of our study was to analyze LC-HRMS data using a high-throughput metabolomics-based MetID workflow by utilizing an in-house theoretical metabolite predictor and open-access XCMS Online ([xcmsonline.scripps.edu](http://xcmsonline.scripps.edu)). In particular, we applied this approach to detect and identify biotransformation products of cimetidine, probenecid, and imatinib in blood and urine samples collected from three rat pharmacokinetic studies. Briefly, rats ( $n = 4$  to  $8$ ) were dosed with placebo (control) or drugs [cimetidine (100 mg/kg, IP), probenecid (1000 mg/kg, IV), and imatinib (30 mg/kg, PO)], and the blood and urine samples were collected at various time points/intervals. The control and drug-treated samples were individually processed by protein precipitation followed by drying and reconstitution in LC-MS compatible solvents. The pooled blood (0.5, 1, and 2 h) and urine (0-4 h) samples of cimetidine and probenecid, and pooled blood (1, 2, and 4 h) samples of imatinib were individually analyzed using nanoLC coupled Thermo Q-Exactive HF mass spectrometer. Data-independent acquisition method was applied to allow detection of the low level metabolites. Cimetidine, probenecid, and imatinib treated samples and the corresponding controls were analyzed by XCMS Online software. Lists of all potential theoretical metabolites and their high-resolution masses were created for these three drugs using a novel in-house theoretical metabolite predictor. The output excel file was first processed to shortlist the potential metabolites using the following optimized criteria: a) metabolite elevated in the treatment group by fold difference of at least 2.5, b) accurate mass within  $\pm 5$  ppm of predicted theoretical mass, c) no detectable peak in any control samples and distinguishable peak in all treatment samples, and d) mass-defect shift and the relative retention time within a reasonable range of theoretically possible value. Then, the shortlisted data were searched against the theoretical metabolite list in a semi-automated fashion to identify drug metabolites (Figure 1). Cimetidine-treated rats showed 5 and 6 metabolite hits (3 common) in blood and urine, respectively, which included novel dihydroxyl, carboxyl, and N-acetylcysteine derivatives of cimetidine. Similarly, 6 and 14 potential metabolites (4 common) were detected in the probenecid-treated rat blood and urine, respectively. Of these, dihydroxyl, glycine and glucosylated derivatives of probenecid were detected for the first time. Five reported metabolites were detected and identified in imatinib-treated rat blood samples. Thus, a sensitive and semi-automated workflow was developed for high-throughput identification of putative biotransformation products of drugs in biological samples, which is not only applicable in drug MetID studies, but it is potentially useful in generating xenobiotic metabolite libraries to facilitate exposomics research.

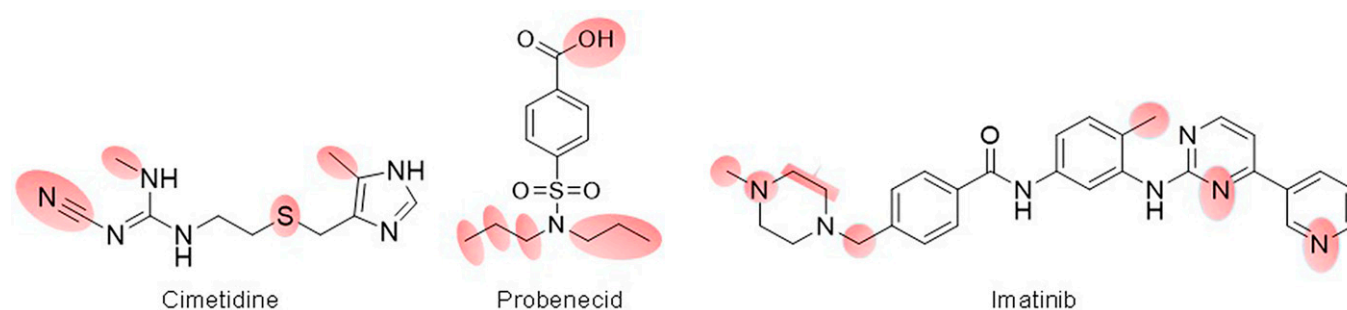


**Figure 1.** Metabolic soft spots (red highlight) in cimetidine, probenecid, and imatinib.

# The Plasma Membrane Monoamine Transporter (PMAT) is Highly Expressed in Neuroblastoma and Functions as a Mitochondrial mIBG Transporter

Leticia Vieira,<sup>1</sup> Yuchen Zhang,<sup>1</sup> Antonio J. López Quiñones,<sup>1</sup> Julie R. Park,<sup>2</sup> and Joanne Wang<sup>1</sup>

<sup>1</sup>Univ of Washington; and <sup>2</sup>Seattle Children's Hospital

Abstract ID 20301

Poster Board 183

Neuroblastoma (NB) is a pediatric cancer with low survival rates in high-risk patients. High dose <sup>131</sup>I-mIBG therapy has emerged as a promising therapy that kills tumor cells by  $\beta$  radiation. Consequently, tumor uptake and retention of <sup>131</sup>I-mIBG are a major determinant for its therapeutic efficacy. <sup>131</sup>I-mIBG enters NB cells through the norepinephrine transporter (NET) but NET expression alone cannot predict its clinical response. mIBG accumulates in mitochondria in NB cells but the underlying transport mechanism is unknown. Previously our laboratory showed that mIBG is a substrate of the polyspecific organic cation transporters (OCTs, MATEs), suggesting that transporters other than NET could play a role in tumor disposition and response to <sup>131</sup>I-mIBG. We hypothesized that besides NET, additional mIBG transporter(s) are expressed in NB cells and affect intracellular disposition and efficacy of <sup>131</sup>I-mIBG. In this study, we profiled the expression of potential mIBG transporters in NB tumor samples, explored potential association with patient overall survival (OS), and determined transporter subcellular localization and interaction with mIBG. Furthermore, using mitochondrial fraction isolated from two NB cell lines (SH-SY5Y and SK-N-BE(2)), the mechanism of mitochondrial mIBG transport was investigated. Analysis of mRNAseq data from 156 NB tissue samples from the NCI TARGET database, as well as qPCR results from NB samples from Seattle Children's Hospital consistently showed that NB tumor cells mainly expresses NET, the plasma membrane monoamine transporter (PMAT), and the vesicular membrane monoamine transporter 1/2 (VMAT1/2), with PMAT expression being the highest among all transporters analyzed. In contrast, OCTs and MATEs are minimally expressed in NB tumors. Kaplan Meier survival analysis using gene expression array data matched to clinical outcome of 243 NB patients from the TARGET database revealed that PMAT expression strongly correlates with OS of high-risk NB patients without the amplification of the MYCN oncogene. Uptake studies in PMAT-transfected HEK293 cells showed that mIBG is efficiently transported by PMAT with a  $K_m$  of  $151.7 \pm 50.7 \mu\text{M}$ . Immunostaining studies further revealed that the PMAT protein is mainly localized intracellularly in NB cells and co-localizes largely with mitochondria. Importantly, uptake studies using mitochondrial fraction isolated from cultured NB cells demonstrated that mIBG is taken up by mitochondria, and decynium-22 (a PMAT inhibitor) reduced mitochondrial mIBG uptake by 51% and 42% in SH-SY5Y and SK-N-BE(2) cells respectively. Together, our data demonstrated that PMAT is localized intracellularly in NB cells and plays a role in mitochondrial uptake of mIBG. Our results suggest that PMAT is a previously unrecognized transporter highly expressed in NB tumors and may play an important role in tumor retention, exposure, and therapeutic response to <sup>131</sup>I-mIBG.

This work is supported by NIH Grant R01GM066233

# Deciphering the role of fatty acid metabolizing CYP4F11 in lung cancer and its potential as drug target

Huiting Jia,<sup>1</sup> Sutapa Ray,<sup>2</sup> Bjoern Brixius,<sup>2</sup> and Simone Brixius-Anderko<sup>3</sup>

<sup>1</sup>Univ of Pittsburgh; <sup>2</sup>University of Pittsburgh, School of Pharmacy; and <sup>3</sup>University of Pittsburgh

Abstract ID 54081

Poster Board 184

Lung cancer is the leading cause of cancer deaths worldwide with tobacco smoke as a major driver for oncogenesis. The lipid mediator 20-hydroxyeicosatetraenoic acid (20-HETE) is known to regulate the blood pressure and promotes angiogenesis in healthy individuals. However, in cancer 20-HETE promotes cell proliferation, invasion, and migration. 20-HETE is generated by members of the cytochrome P450 family 4A/F by a selective  $\omega$ -hydroxylation of arachidonic acid. Intriguingly, the unselective inhibition of 20-HETE-producing CYP4 enzymes reduces the lung cancer tumor growth in xenograft mouse models. We conducted a bioinformatic analysis and found that the isoform CYP4F11 is the only  $\omega$ -hydroxylase which is significantly overexpressed in patients with lung squamous carcinoma. However, the exact role of CYP4F11 in lung cancer and its potential as drug target has not been established yet.

We hypothesize that CYP4F11-mediated 20-HETE production contributes to lung cancer cell proliferation and invasion. Thus, CYP4F11 could be an exciting new drug target for lung cancer therapy. To test our hypothesis, we pursue two strategies. First, we conduct cell culture studies to examine the role of CYP4F11 in lung cancer. For this, we performed a transient knockdown of CYP4F11 in lung cancer cell lines to assess the impact of CYP4F11 on cell proliferation, invasion, and migration. We found that lung cancer cell proliferation of the CYP4F11 knockdown cells was significantly decreased compared to wild type cells indicating a pivotal role of CYP4F11 in lung cancer. Excitingly, the addition of exogenous 20-HETE to the CYP4F11 knock down cells could rescue cell proliferation indicating that CYP4F11 mediated 20-HETE production impacts cancer cell proliferation. We then conducted cell migration and invasion assays and observed that a CYP4F11 knockdown attenuates the migration and invasion of lung cancer cells which emphasizes the high potential of CYP4F11 as drug target.

Second, we perform a preliminary screening for compounds inhibiting CYP4F11 which provides valuable information for lung cancer drug design. For this, we use a three-step strategy. Using recombinant human CYP4F11, we conduct spectroscopic ligand binding assays to determine compounds with a high affinity to CYP4F11. Subsequently, the half-maximal inhibitory efficiency (IC<sub>50</sub>) of compounds with a nanomolar dissociation constant (K<sub>d</sub>) will be determined. Lead compounds will then be cross evaluated in lung cancer cell lines to test their impact on cell proliferation. Using this strategy, we could successfully evaluate the CYP4A/F inhibitor HET0016 which non-selectively inhibits 20-HETE production. In spectroscopic ligand binding studies, HET0016 shows high affinity to recombinant CYP4F11. We then examined the impact of HET0016 on lung cancer cell proliferation and found that it attenuates cell proliferation in a dose dependent manner. Using this strategy, additional compounds, such as azoles and fatty acid amides, are currently evaluated

We aim to further establish the role of CYP4F11 in lung cancer and the underlying mechanism. Furthermore, we are invested to promote the exploitation of CYP4F11 as therapeutic target for a transformative lung cancer treatment option.

This research was funded by a New Investigator Award of the American Association of Colleges of Pharmacy (AACP) and start-up funds from the University of Pittsburgh School of Pharmacy.

# Understanding the cell-dependent activation of ProTides and its implications in optimizing the nucleoside antiviral prodrug design for treating pulmonary infections

Jiapeng Li,<sup>1</sup> Shuxin Sun,<sup>2</sup> Yueting Liu,<sup>2</sup> Weiwen Wang,<sup>2</sup> and Hao-Jie Zhu<sup>3</sup>

<sup>1</sup>Univ of Michigan; <sup>2</sup>University of Michigan; and <sup>3</sup>Univ of Michigan College of Pharmacy

Abstract ID 16698

Poster Board 185

Nucleoside (Nuc) analogs are an essential class of antivirals. Nuc analogs are often structurally modified into a phosphoramidate prodrug form (ProTide) to boost their intracellular activation efficiency: generating more active metabolite triphosphate Nuc (TP-Nuc). To date, three ProTides have been approved by the FDA: tenofovir alafenamide (TAF), sofosbuvir (SBV), and remdesivir (RDV). After entering cells, TAF, SBV, and RDV are hydrolyzed by the intracellular esterases carboxylesterase 1 (CES1) and cathepsin A (CatA) to release their ester moieties. The abundance of CES1 and CatA in the cells determines the amount of TP-Nuc generated. In the human lung, CatA is the major ProTide activating enzyme. We hypothesize that a higher susceptibility to CatA could improve the activation of a ProTide in the lung.

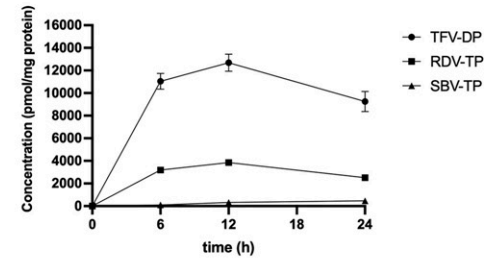
In this study, we evaluated the activation profiles of TAF, SBV, RDV in various cell lines on a molar equivalent dose basis (except for RDV in Huh-7 cells due to cytotoxicity). The cell lines tested were those commonly used in SARS-CoV-2 studies, including the human lung cell lines A549-ACE2-TMPRSS2, Calu-3, and normal bronchial epithelial cells BEAS-2B; the colon cell line Caco-2; the liver cell lines Huh-7 and HepG2; and the African green monkey kidney epithelial cells Vero E6. After 6, 12, and 24 hours of drug incubation, the intracellular concentrations of the ProTides and their active metabolites were determined by LC-MS/MS. The expression profiles of activating enzymes (e.g., CES1 and CatA) and transporters (e.g., OATP1B1 and P-gp) were retrieved from available datasets. The contribution of CatA and CES1 to the activation of TAF, SBV, and RDV in BEAS-2B cells was further evaluated using CES1 and CatA inhibitors.

The results showed that the three ProTides were activated in a cell-dependent manner. Overall, the ProTides achieved higher levels of TP-Nuc in the liver cell lines (i.e., Huh-7 and HepG2) than the other cell lines tested, which was associated with the higher expressions of OATP1B1 and CES1 in Huh-7 and HepG2 cells. In contrast, the three ProTides generated significantly less TP-Nuc in Vero E6 cells compared to the other cell lines, which was related to the abundant P-gp expression in Vero E6 cells. Among the human lung cell lines, the ProTide activation was comparable between the A549-ACE2-TMPRSS2 and BEAS-2B cells and higher than the Calu-3 cells. Similar to the type II pneumocytes, the major SARS-CoV-2 infection target, the human lung cell lines exhibit a very low abundance of CES1 but a considerable expression of CatA. Moreover, our CES1 and CatA inhibition study confirmed the predominant role of CatA in activating ProTides in BEAS-2B cells. Interestingly, in all the human lung cell lines, TAF generated 2-3- and 6-10- folds higher amounts of TP-Nuc than RDV and SBV, respectively. This observation is highly correlated with the susceptibility of the three ProTides to CatA. Moreover, the TAF prodrug had a higher accumulation in the lung cell lines than RDV and SBV, indicating that cell permeability is another important factor for intracellular prodrug activation.

In conclusion, TAF, SBV, and RDV bare considerable cell-dependent activation properties, which are associated with the expression patterns of activating enzymes and transporters across the different cell lines. Higher susceptibility to CatA and greater cell membrane permeability will enhance the activation of a ProTide in the human lung.

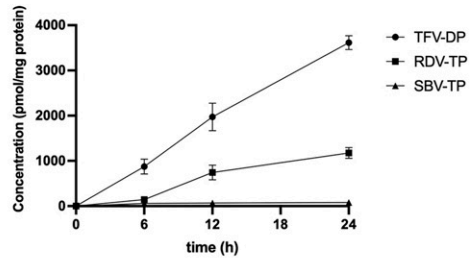


10  $\mu$ M TAF, RDV, and SBV in A549-ACE2-TMPRSS2 cells



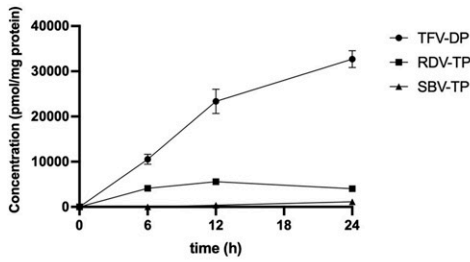
A

10  $\mu$ M TAF, RDV, and SBV in Calu-3 cells



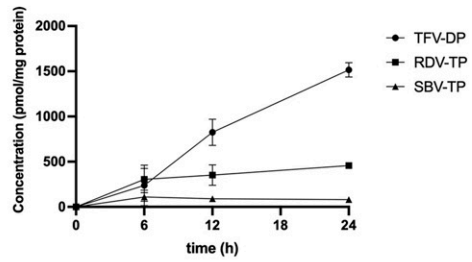
B

10  $\mu$ M TAF, RDV, and SBV in BEAS-2B cells



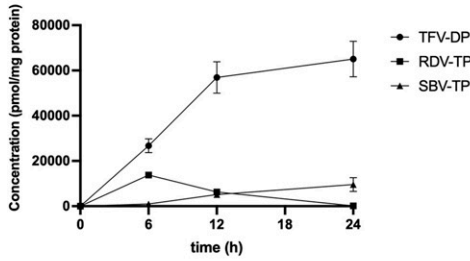
C

10  $\mu$ M TAF, RDV, and SBV in VeroE6 cells



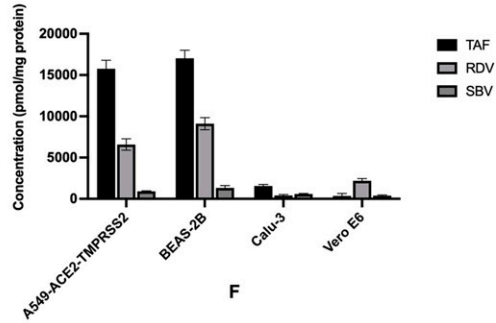
D

10  $\mu$ M TAF, SBV, and 5  $\mu$ M RDV in Huh-7 cells



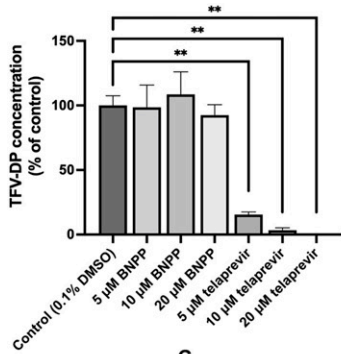
E

total drug entry of TAF, RDV, and SBV within 6 hours



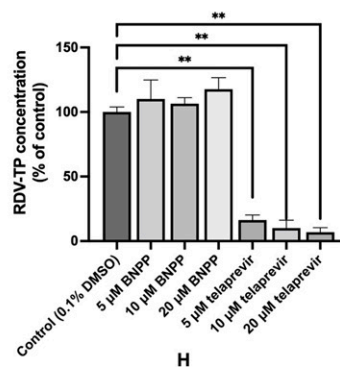
F

CES1 and CatA inhibitors for TAF in BEAS-2B cells



G

CES1 and CatA inhibitors for RDV in BEAS-2B cells



H

# PXR activation attenuates liver fibrosis by down-regulating LECT2 and disrupting $\beta$ -catenin/TCF4 interaction

Yue Gao,<sup>1</sup> Shicheng Fan,<sup>2</sup> Pengfei Zhao,<sup>1</sup> Yanying Zhou,<sup>1</sup> Huilin Li,<sup>1</sup> Xuan Li,<sup>1</sup> Chenghui Cai,<sup>1</sup> Min Huang,<sup>1</sup> and Huichang Bi<sup>1</sup>

<sup>1</sup>Sun Yat-sen University; and <sup>2</sup>Southern Medical University

Abstract ID 18908

Poster Board 186

Pregnane X receptor (PXR, NR1I2), a ligand-activated transcription factor, is relatively abundant in liver and intestine. Previous studies have demonstrated that PXR activation inhibits liver fibrosis, but the specific mechanisms still remain unclear. Leukocyte cell-derived chemotaxin 2 (LECT2), a downstream target of  $\beta$ -catenin/ T cell-specific factor 4 (TCF4) signaling, is a small-molecule protein secreted by hepatocytes. Recent study illustrated that LECT2 produced by hepatocytes participated in the progression of hepatic fibrosis by regulating angiogenesis. In the current study, we aimed to investigate whether PXR activation attenuate liver fibrosis by inhibiting LECT2 and explore its impact on  $\beta$ -catenin/TCF4 signaling. Additionally, we also aimed to unveil the critical role of  $\beta$ -catenin/TCF4-LECT2 axis in liver fibrosis and demonstrate whether PXR activation alleviates hepatic fibrosis via inhibiting  $\beta$ -catenin/TCF4-LECT2 axis.

In the current study, carbon tetrachloride (CCl<sub>4</sub>) was used to induce liver fibrosis in C57BL/6 mice. The results showed that mouse PXR agonist pregnenolone-16 $\alpha$ -carbonitrile (PCN) significantly attenuated hepatic fibrosis by suppressing the expression of  $\alpha$ -smooth muscle actin ( $\alpha$ -SMA), Collagen  $\alpha$ 1(I) and platelet endothelial cell adhesion molecule-1 (CD31). Lymphatic vessel endothelial hyaluronan receptor 1 (LYVE1) and CD31 staining indicated that PXR activation inhibited sinusoids capillarization and central angiogenesis. Besides, immunohistochemical (IHC) staining and western blot analysis indicated that LECT2 and nuclear  $\beta$ -catenin were significantly downregulated after PXR activation, while total  $\beta$ -catenin and TCF4 didn't alter significantly. Furthermore, reporter gene assay was performed and suggested that PXR activation inhibited the transcriptional activation of LECT2 by  $\beta$ -catenin/TCF4. PXR activation disrupted the interaction between  $\beta$ -catenin and TCF4. Co-Immunoprecipitation (Co-IP) assays further indicated that PXR potentially interacted with  $\beta$ -catenin and TCF4 simultaneously. Moreover, to clarify whether disrupting  $\beta$ -catenin/TCF4 interaction alleviated liver fibrosis,  $\beta$ -catenin/TCF4 inhibitor LF3 was used to evaluate its effect on liver fibrosis. The results showed the inhibition of  $\beta$ -catenin/TCF4 interaction decreased the expression level of LECT2 and alleviated liver fibrosis. In addition, AAV-*Lect2* mice was used and we found that PXR activation failed to protect liver from fibrosis in AAV-*Lect2* mice, which further confirmed that PXR attenuated hepatic fibrosis by inhibiting LECT2. Finally, we clarified that long-term treatment of PCN had no risk for carcinogenesis or promoting tumor formation induced by diethylnitrosamine (DEN), indicating the safety of long-term activation of PXR.

Taken together, this study demonstrated a new mechanism that PXR attenuated liver fibrosis by disrupting  $\beta$ -catenin/TCF4 interaction and suppressing the expression level of LECT2. The crosstalk between PXR and  $\beta$ -catenin/TCF4 signaling was also clarified. These findings provide new evidence and theoretical basis for PXR as potential drug target for liver fibrosis.

# Identification of Putative Novel Biomarkers of Organic Anion Transporter 1 and 3 for the Prediction of Transporter-Mediated Drug-Drug Interactions

Aarzo Thakur,<sup>1</sup> Dilip K. Singh,<sup>1</sup> Mary Paine,<sup>1</sup> and Bhagwat Prasad<sup>1</sup>

<sup>1</sup>Washington State University

Abstract ID 24507

Poster Board 187

Endogenous metabolites can be used as phenotypic biomarkers of solute carrier (SLC) transporters to predict transporter-mediated drug-drug interactions (DDIs). The SLC22 subfamily members organic anion transporter (OAT) 1 and 3 are expressed on the basolateral membrane of kidney proximal tubule cells. Both facilitate the uptake of several drugs and endogenous metabolites for renal secretion. Probenecid-mediated inhibition of OAT1/3 increases plasma concentrations of endogenous metabolites, including pyridoxic acid and kynurenic acid.<sup>1,2</sup> The objective of this study was to assess the effects of OAT1/3 inhibition on the metabolic profile in human plasma and urine using targeted and untargeted metabolomics approaches. Plasma and urine samples from 7 healthy adults who participated in an ongoing clinical pharmacokinetic DDI study (n=16) involving oral furosemide (OAT1/3 substrate, 5 mg) and probenecid (OAT1/3 inhibitor, 1000 mg) were selected for untargeted analysis. Plasma (pool of 1, 1.5, and 2 h collections) and urine (0-4 h) samples representing timepoints that captured maximum probenecid plasma concentrations were analyzed *via* liquid chromatography-mass spectrometry. Using XCMS Online software (xcmsonline.scripps.edu), >10,000 individual features (*m/z* values) were detected in the pooled plasma samples that were either elevated or repressed in the presence of probenecid (Fig 1). Co-administration of probenecid increased furosemide plasma concentrations by 1.5- to 3-fold ( $p < 0.05$ ), indicating a DDI. However, pyridoxic acid and kynurenic acid, known biomarkers of OATs, showed no statistically significant differences due to high interindividual variability. This variability is likely because the precursors of these biomarkers are derived from diet.<sup>1</sup> More sensitive, selective, and less variable putative OAT1/3 biomarkers were identified by shortlisting the detected features that 1) were elevated in plasma by 2- to 10-fold in presence of probenecid ( $p < 0.05$ ) and 2) showed acceptable chromatographic peak signal to noise ratios. Correlations between the fold increase in furosemide plasma concentration and fold increase in plasma concentrations of the putative hits were next evaluated. Of these hits, 16 putative biomarkers (*m/z* 100-505) that correlated with furosemide ( $r > 0.50$ ) were selected for a METLIN database search. The identified putative biomarkers were mostly anionic compounds with variable hydrophilicity (LogP: -1.0 to 6.5). Five of the putative biomarkers were carboxylic acids, two were glucuronide conjugates, three belonged to a steroidal pathway, and one each belonged to the bile acid and tryptophan metabolism pathways. A detailed pharmacokinetic analysis (0-24 h) of furosemide, pyridoxic acid, and kynurenic acid concentrations measured in plasma and urine samples from 2 participants revealed a 2.2-, 2.3-, and 1.7-fold increase in the AUC, respectively, in the presence of probenecid. Targeted metabolomics analysis of the identified metabolites in all study participants will validate their utility as biomarkers of OAT1/3 for predicting transporter-mediated DDIs.

Ref:

1. Shen *et al.*, 2019. *JPET* 368:136-45.
2. Tang *et al.*, 2021. *DMD* 49:1063-69.

This work was funded by NIH/NICHD R01HD081299.

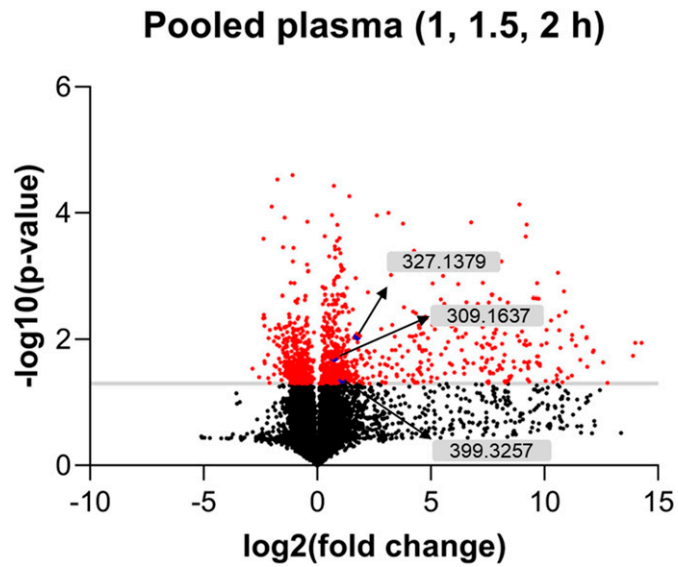


**Fig 1. Volcano plot of metabolic features detected in pooled plasma.** Red dots indicate significantly different ( $p < 0.05$ ) features (e.g.  $m/z$  values shown) in the presence of probenecid.

# Plated Hepatocyte Relay Assay for the Evaluation of the Metabolic Fates of Slowly Metabolized Compounds

Albert Li,<sup>1</sup> Binnian Wei,<sup>2</sup> and Walter Mitchell<sup>3</sup>

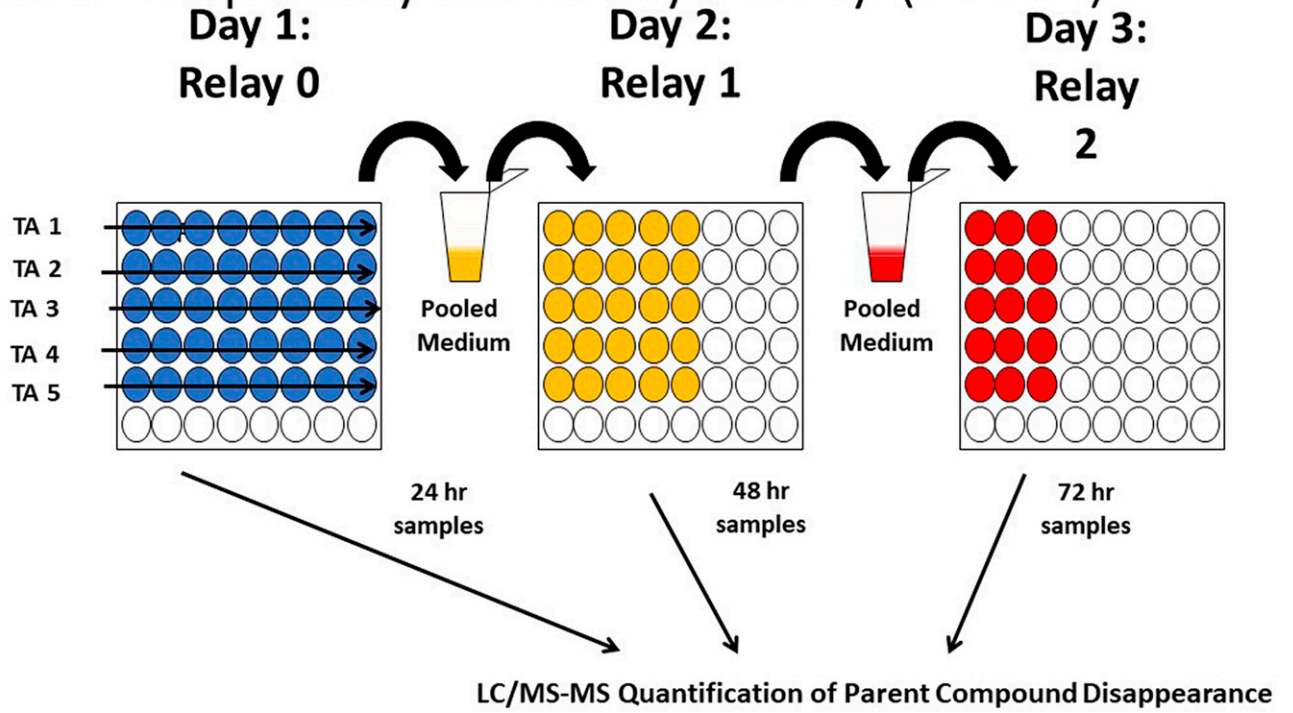
<sup>1</sup>Discovery Life Sciences In Vitro ADMET Laboratories; <sup>2</sup>Discovery Life Sciences; and <sup>3</sup>Discovery Life Sciences LLC

Abstract ID 19303

Poster Board 374

Evaluation of metabolic fates of drug candidates is a major activity in drug development, with results critical to the assessment of efficacy and safety. Due to the routine application of high throughput assays for hepatic clearance using in vitro systems such as human liver microsomes and human hepatocytes in the early phases of drug discovery and development, pharmaceutical companies have accumulated a collection of slowly metabolized compounds (SMC) as potential drug candidates. The metabolic stability of the SMC poses a challenge for further development as their metabolic fates cannot be readily defined using conventional approaches. To overcome this challenge, we have developed a plated hepatocyte relay assay (PHRA) with which SMC can be evaluated for intrinsic hepatic clearance as well as metabolite formation. PHRA is similar to the suspension hepatocyte relay assay developed by Di et al (2012) except that plated hepatocytes are employed in lieu of suspension hepatocytes, thereby extending each relay from 3 h to 24 h, and the elimination of the laborious centrifugation step required for medium transfer. The principle of the assay is to subject the SMC to metabolism by hepatocytes plated in a 96-well plate (4 hours after plating to allow cell attachment) on the day of evaluation, with medium transferred to freshly plated hepatocytes in subsequent days. Examples of the accumulative incubation durations in PHRA after each relay are as follows: 24 h (initial incubation), 48 h (1<sup>st</sup> relay), and 72 h (2<sup>nd</sup> relay), 96 h (3<sup>rd</sup> relay), and 120 h (4<sup>th</sup> relay). A validation study with 15 compounds with known human *in vivo* hepatic clearance which included the ultra low clearance compounds ( $CL_{\text{non-renal}} < 1$  mL/min/kg) meloxicam, tolbutamide, warfarin, disopyramide, and tenoxicam; and the low clearance compounds ( $CL_{\text{non-renal}} 1-5.1$  mL/min/kg) glimepiride, clozapine, riluzole, ibuprofen, prednisolone, voriconazole, quinidine, prednisone, dexamethasone and risperidone. Linear time-dependent disappearance of the parent compounds was observed for all compounds up to the longest incubation duration of 120 hrs. We further evaluated the potential applications of PHRA towards the derivation of enzyme kinetic parameters and metabolite formation of SMC using the model ultra low clearance compound, warfarin. Warfarin was evaluated at concentrations of 1, 2, 5, 10, 20 and 50  $\mu\text{M}$  for incubation durations of 24, 48 and 72 hrs in the relay assay. Linear time-dependent warfarin clearance was observed at all concentrations, with concentration-dependent metabolic clearance consistent with Michaelis-Menten enzyme kinetics, allowing the derivation of apparent  $K_m$  and  $V_{\text{max}}$  values. Furthermore, time-dependent formation of warfarin metabolites, 7-hydroxy and 7-glucuronide warfarin, were observed. Our results suggest the PHRA can be readily applied towards to evaluation of intrinsic hepatic clearance, enzyme kinetics, as well as metabolite production of SMC.

# Plated Hepatocytes Relay Assay (PHRA)



# Fluorogenic Chemical Tools to Improve Prodrug Treatment Outcomes

Michael Beck<sup>1</sup>

<sup>1</sup>*Eastern Illinois Univ*

**Abstract ID 13584**

**Poster Board 375**

Prodrugs are inactive forms of drugs that must be converted to the active drug in the body. This approach is popular as it can improve the absorption of orally administered therapeutics by increasing lipophilicity. A common approach to developing a prodrug is to mask polar hydroxyl groups with esters that can be removed once absorbed by endogenous esterases to release the active drug. Carboxylesterases (CESs) are the predominant esterases that carry out this hydrolytic activation due to their high expression in the liver and intestines. Thus, the pharmacokinetics of the active form of an ester-based prodrug greatly depends on CES activity. The activity of CESs, however, can be drastically different from person to person which has been demonstrated to influence the metabolism and, in some cases, clinical outcomes of patients treated with prodrugs that are substrates for CES1, one of the two main human CESs. The factors that contribute to this have not been fully uncovered despite the established importance of CES1 in drug metabolism. We believe that this lack of knowledge is due to the scarcity and limitations of currently available approaches to study CES1 activity in live samples. To address these challenges, we have developed new fluorogenic chemical tools that can report on CES1 activity in live cells. Subsequently, we demonstrate that these tools can identify potential CES1-mediated drug-drug interactions and can be deployed our tools in a fluorescence microscopy-based approach we created to monitor CES1 sequence-dependent activity variations in live cells. Overall, our chemical tools and approaches can help uncover factors that result in the variability of patient response to treatment with CES1-substrate drugs. We believe that the more detailed understanding of the factors that influence CES1 activity that our chemical tools can provide will lead to better patient outcomes when treated with prodrugs.

# CYP3A inhibition and induction exert limited effects on brilaroxazine pharmacokinetics

Laxminarayan Bhat,<sup>1</sup> Seema R. Bhat,<sup>2</sup> Arulprakash Ramakrishnan,<sup>2</sup> and Palaniappan Kulanthaivel<sup>2</sup>

<sup>1</sup>Reviva Pharmaceuticals, Inc.; and <sup>2</sup>Reviva Pharmaceuticals Holdings Inc.

Abstract ID 53571

Poster Board 376

**Background:** The metabolism of standard antipsychotics (e.g., aripiprazole, lurasidone, risperidone, quetiapine, cariprazine, brexpiprazole, and clozapine) involves CYP3A4. Most treatments realize significant plasma drug concentration changes when co-administered with CYP3A4 inhibitors or inducers. Such interactions are of clinical concern as schizophrenia patients take concomitant medications interacting with CYP3A4, leading to dose adjustment to ensure treatment efficacy, safety, and tolerability.

Brilaroxazine, a serotonin/dopamine modulator, is a novel compound in phase 3 development for schizophrenia. It possesses differentiated pharmacological and safety profiles over other treatments in this class. Preclinical *in vitro* work identified CYP3A as the primary enzyme involved in the metabolism of brilaroxazine. This clinical study evaluated itraconazole's (a strong CYP3A inhibitor) and phenytoin's (a strong CYP3A inducer) effects on brilaroxazine's pharmacokinetic (PK) profile.

**Methods:** This study involved a single-center, open-label, fixed-sequence, two-part, drug-drug interaction design in healthy adult male and female subjects. Part A evaluated the effects of itraconazole (200 mg QD) dosed to a steady state on the single-dose PK of brilaroxazine and metabolite RP5081 in 13 subjects. Part B assessed the effect of phenytoin (100 mg TID) dosed to a steady state on the single-dose PK of brilaroxazine and metabolite RP5081 in 16 subjects.

Determination of brilaroxazine and metabolite RP5081  $C_{max}$ ,  $AUC_{0-t}$  and  $AUC_{0-\infty}$  used noncompartmental methods and statistical inference involving log-transformation and a linear mixed-effects model with treatment as a fixed effect and subject as a random effect. The analysis involved calculating the geometric least squares mean for each treatment, the ratio of the geometric least squares means, and their 90% confidence intervals (CIs).

**Results:** Single brilaroxazine dose co-administered with itraconazole resulted in a slight increase of 8, 15 and 13% in  $C_{max}$ ,  $AUC_{0-t}$ , and  $AUC_{0-\infty}$ , respectively (90% CI within 80-125%). No difference in the brilaroxazine mean elimination half-life existed between when brilaroxazine administered alone and concomitantly with itraconazole. Alternatively, a single brilaroxazine dose with co-administered phenytoin decreased brilaroxazine  $C_{max}$ ,  $AUC_{0-t}$ , and  $AUC_{0-\infty}$  by 33, 57, and 54%, respectively.

**Conclusions:** Itraconazole (a strong CYP3A inhibitor) exerted no effect on brilaroxazine's PK. Accordingly, brilaroxazine may be co-administered with itraconazole and other strong CYP3A inhibitors. In contrast, phenytoin (a strong CYP3A inducer) decreased brilaroxazine exposure by approximately 50%. Thus, brilaroxazine dose modification may be needed when co-administering with strong CYP3A inducers. This profile presents a useful addition to the clinical management of schizophrenia to minimize the clinical risks associated with drug-drug interactions seen with other antipsychotics, particularly with CYP3A inhibitors.



# The metabolism of the 8-aminoquinolines in relation to hemolytic toxicity: exploring current understanding for future antimalarial drug discovery

Pius Fasinu<sup>1</sup>

<sup>1</sup>Univ of Alabama at Birmingham

Abstract ID 14051

Poster Board 377

First approved in 1952 for the treatment of *P. vivax* and *P. ovale* malaria, primaquine has been the only licensed 8-aminoquinoline (8AQ) until the recent approval of tafenoquine in 2018. As the only class of antimalarial drugs with activity against the dormant liver stage of the parasite, 8AQs holds the potential for global malarial eradication. However, the clinical utility of these drugs is limited due to their known hemolytic toxicity especially in individuals with genetic deficiency in the glucose-6-phosphate dehydrogenase (G6PD) enzyme. While the exact mechanism of inducing hemolysis is not clearly understood, our studies have shown that the hemolytic toxicity of 8AQs is metabolism-dependent. The involvement of CYP2D6 was confirmed by enhanced safety of primaquine in CYP2D6-knock-out mice, coadministration with CYP2D6 inhibitor and in vitro suppression of reactive oxygen species and methemoglobin generation. The metabolism of primaquine has shown enantioselectivity with the (R)-primaquine largely metabolized through the oxidation of the terminal amine on the side chain while the (S)-primaquine enantiomer is more susceptible to the CYP2D6-catalyzed ring oxidation. Our tissue distribution studies of primaquine in mice also demonstrates significant enantiomeric differences. With the in vitro generation of the reactive PQ metabolite in a non-enzymatic erythrocyte incubation, CYP2D6-mediated metabolism may only partly explain the mechanism of 8AQ-induced hemolytic toxicity. This additional pathway of generating hemolytic metabolite(s) may hamper the potential of (R)-primaquine to provide a safety advantage over the (S)-enantiomer that is more CYP2D6-dependent. Our current data showing the interplay of enzyme- and non-enzyme-dependent generation of metabolites, as well as the enantioselectivity of metabolism of drug compounds can offer insights for future antimalarial drug development.

# Production, structure, and function analyses of a recombinant miR-1291 agent

Meijuan Tu,<sup>1</sup> Zhenzhen Liu,<sup>1</sup> Tongyi Dou,<sup>2</sup> and Aiming Yu<sup>3</sup>

<sup>1</sup>Univ of California, Davis; <sup>2</sup>Biochemistry and Biophysics Center, National Heart, Lung, and Blood Institute; and <sup>3</sup>Univ of California-Davis, Sch of Med

**Abstract ID 25922**

**Poster Board 378**

MicoRNAs are a superfamily of small, regulatory noncoding RNAs that play essential roles in almost all cellular processes, including drug and nutrient transport and metabolism as well as disease progression. Previous studies have revealed that microRNA-1291-5p (miR-1291) is able to sensitize pancreatic cancer (PC) cells to chemotherapies via regulating drug efflux transporter ABCC1/MRP1 and glucose uptake transporter SLC2A1/GLUT1. Our recent studies have also shown that miR-1291 acts as a tumor suppressor, whereas it is downregulated in PC patient tissues and cell lines. In this study, we aimed to produce and characterize a recombinant miR-1291 agent to further understand miR-1291 functions and explore new therapy. Human seryl-tRNA was fused to human pre-miR-1291 to offer recombinant miR-1291 (BioRNA/miR-1291). The BioRNA/miR-1291 showed high-level expression in bacteria fermentation and was subsequently purified to high homogeneity (> 97%). While computational modeling indicated a possible rigid structure, cryogenic electron microscopy (cryo-EM) study revealed the presence of highly flexible structures for BioRNA/miRNA-1291. Further studies demonstrated that miR-1291-5p was selectively released from BioRNA/miR-1291 in PC cells to alter cell transcriptome. Moreover, PNPO, a key enzyme in vitamin B6 biosynthesis, was identified and validated as a new target for miR-1291-5p, which led to the control of VB6 homeostasis in human PC cells. In addition, the effectiveness of BioRNA/miR-1291 in improving the pharmacodynamics of another metabolic modulator 5-FU was delineated in both PC patient-derived organoid and xenograft mouse models. These results demonstrate a critical role for miR-1291 in the regulation of nutrient metabolism and provide insights into developing new therapeutic strategies.

This study was supported by the National Institute of General Medical Sciences (grant No. R35GM140835) and the National Cancer Institute (R01CA253230), National Institutes of Health.

# ***In Vitro* Characterization of CYP3A4 Inhibition and Induction of Nevirapine Analogs as Substitutes in HIV Treatment**

Emily G. Gracey,<sup>1</sup> Sylvie E. Kandel,<sup>1</sup> and Jed N. Lampe<sup>1</sup>

<sup>1</sup>University of Colorado, Skaggs School of Pharmacy

**Abstract ID 21354**

**Poster Board 379**

Nevirapine (NVP) is an HIV non-nucleoside reverse transcriptase inhibitor used both in the US and developing countries to treat and prevent HIV transmission in women and infants. NVP is generally well tolerated, but idiosyncratic drug reactions such as hepatotoxicity have been reported. NVP can cause drug-drug interactions (DDI) through both inhibition and induction of the cytochrome P450 (CYP) enzymes. NVP is metabolized by several CYPs, such as CYP3A4 and CYP2B6 and it also induces their expression. NVP is a mechanism-based inactivator (MBI) of CYP3A4, although the exact mechanism is still debated in the literature. One prominent hypothesis is that NVP forms a reactive quinone methide metabolite, through the 12-OH-NVP oxidation pathway, which can form adducts to CYP3A4.

Previous data from our lab has demonstrated several NVP analogs have similar efficacy against the target HIV-1 reverse transcriptase compared to NVP. Our hypothesis is that a structural analog of NVP with similar efficacy but reduced toxicity could be a candidate to replace NVP by decreasing the formation of the reactive quinone methide species through the 12-OH pathway, thereby reducing DDI resulting from MBI of CYP3A4.

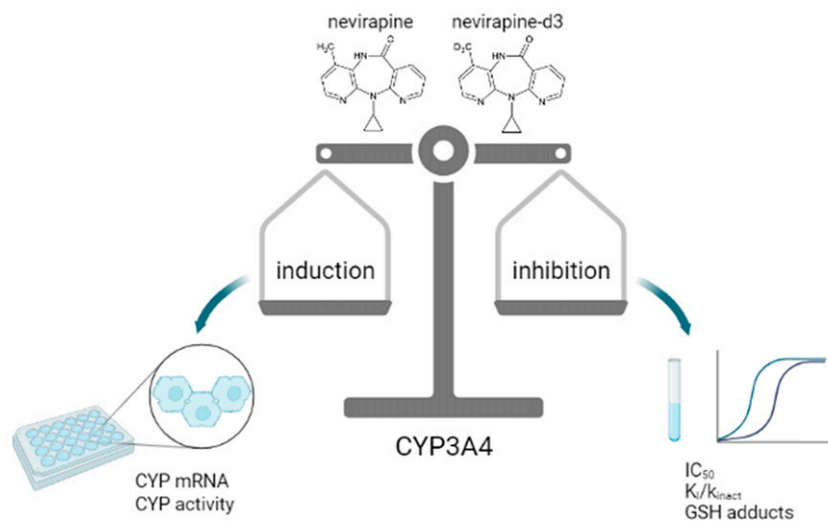
**Methods:** We analyzed three NVP analogs and NVP for their CYP induction of mRNA and activity in primary human hepatocytes. mRNA induction was analyzed via qPCR and activity was determined using probe substrate reactions and analyzed via LC-MS. We characterized the inactivation of CYP3A4 by the top candidate NVP-d3 versus NVP. IC<sub>50</sub> shift assays, K<sub>i</sub>/k<sub>inact</sub> assays, and GSH incubations were performed with recombinant CYP3A4 and analyzed via LC-MS.

**Results:** NVP and NVP-d3 demonstrated similar mRNA induction of CYP3A4 and CYP2B6. CYP3A4 activity was reduced from 25 μM to 100 μM for NVP, despite the increased mRNA levels. NVP-d3 demonstrated increased activity at 100 μM compared to 25 μM.

The CYP3A4 IC<sub>50</sub> values with a 30 minute pre-incubation were 30.0 ± 2.8 μM (- NADPH) and 5.3 ± 1.0 μM (+NAPDH) for NVP, and 9.4 ± 1.6 μM (- NADPH) and 2.9 ± 0.4 μM (+NAPDH) for NVP-d3, resulting in a shift of 5.7x for NVP and 3.2x for NVP-d3. The MBI assay resulted in a K<sub>i</sub> of 142.4 ± 10.9 μM and k<sub>inact</sub> of 0.103 ± 0.003 min<sup>-1</sup> for NVP, and a K<sub>i</sub> of 128.0 ± 18.1 μM and k<sub>inact</sub> of 0.079 ± 0.004 min<sup>-1</sup> for NVP-d3. No GSH adducts were found for NVP or NVP-d3 at the 12 position, but one likely adduct was identified at the 3 position. There was a significant difference in the metabolites produced by CYP3A4. With NVP-d3, the fold change of 12-OH metabolite formation was 0.16, while 2-OH and GSH metabolites increased by about 2 fold each.

**Discussion and Conclusions:** These results demonstrate that both NVP and NVP-d3 are MBIs of CYP3A4 with important differences in metabolite profiles. NVP-d3 demonstrated lower CYP3A4 IC<sub>50</sub> and K<sub>i</sub> values, although the difference may not be significant. Deuteration decreased the 12-OH metabolite from being formed and increased the GSH adduct formation at the 3 position, indicating reduced formation of the quinone methide reactive species at the 12 position. In rats, it was previously reported that NVP-d3 is cleared faster than NVP, indicating the induction effect may overcome inhibition, as supported by our data here. NVP-d3 may still be a candidate to replace NVP in the future, but pharmacokinetics need to be evaluated if decreasing the MBI of CYP3A4 is leading to increased clearance.

This work was supported by the NIH, NIAID Award Number R01 AI150494 (JNL).



# Development of a Cytochrome P450 CYP3A7 Quantitative Structure-Inhibitory Relationship (QSIR) Model to Assess Drug Safety in Neonates

Hannah M. Work,<sup>1</sup> Sylvie E. Kandel,<sup>1</sup> and Jed N. Lampe<sup>2</sup>

<sup>1</sup>Univ of Colorado; and <sup>2</sup>Univ of Colorado, Skaggs School of Pharmacy

Abstract ID 54628

Poster Board 380

Cytochrome P450s (CYPs) are a superfamily of human enzymes predominantly involved in the metabolism of drugs, xenobiotics, and many endogenous substrates. Assessing the inhibitory effect investigational new drugs exert on CYPs is essential because inhibition may lead to toxicity due to drug accumulation and/or adverse drug-drug interactions. Inhibition is initially predicted using adult-relevant *in silico* models (e.g., QSAR/QSIR, 3D pharmacophores, etc.). These models are based upon data obtained from previous *in vitro* high-throughput screening results. Currently, no such *in silico* model exists for CYP3A7, the predominant hepatic CYP enzyme expressed in neonates and developing infants. To help identify the risk new drugs pose to this fragile patient population prior to administration, a reliable model must be developed that can predict CYP3A7 inhibition. A subset of an FDA-approved drug library was screened *in vitro* to determine the inhibitory capacities these drugs have on CYP3A7. The activity and subsequent inhibition of CYP3A7 was monitored using a high-throughput screening assay previously developed in our lab that utilizes dibenzylfluorescein (DBF) as a probe substrate. Inhibitors identified have been further characterized by determining their half-maximal inhibitory concentration using a neonate-relevant endogenous CYP3A7 substrate probe, dehydroepiandrosterone-sulfate (DHEA-S). Here we present our findings from the high-throughput drug screen and some of the common features identified between inhibitors thus far. These findings provide insight on the promiscuity of CYP3A7 and the diversity of its inhibitors, as well as information on drug classes and structural features to avoid in neonatal drug development.

# Identification And Functional Characterization Of Alternative Transcripts Of Lncrna Hnf1a-As1 And Their Impacts On Drug Metabolism

Jing Jin,<sup>1</sup> and Xiao-bo Zhong<sup>1</sup>

<sup>1</sup>Univ of Connecticut

Abstract ID 18161

Poster Board 381

Hepatocyte nuclear factor 1 alpha antisense 1 (*HNF1A-AS1*) gene is a long non-coding RNA (lncRNA) gene physically located next to the transcription factor *HNF1A* gene in the human genome. The *HNF1A-AS1* gene encodes a lncRNA HNF1A-AS1, which has been functionally characterized as a regulatory element involved in both transcriptional and post-translational regulation of numerous critical genes involved in cancer growth, migration, and invasion. The lncRNA HNF1A-AS1 is also involved in the regulation of expression of genes encoding drug-metabolizing enzymes, including several cytochrome P450 (CYP) superfamily members (CYP1A2, 2C9, 2C19, 2E1, and 3A4) (Chen et al, 2018, PMID:29691280; Wang et al, 2019, PMID:30602592.) as well as contribution to susceptibility of drug-induced liver injury (Chen et al, 2020, PMID: 32029527; Wang et al, 2022, PMID:34949673.) through interaction with HNF1A. These conclusions are mainly made by knockdown of HNF1A-AS1 RNA with a siRNA. However, like many lncRNAs, HNF1A-AS1 has multiple annotated alternative transcripts in the human genome. Several fundamental biological questions are still not solved: (1) How many transcripts really exist? (2) Do different tissues express the same or different transcripts? (3) Do same tissues express same or different transcripts at different conditions, such as growth, development, and exposure to xenobiotics? (4) Do different transcripts have the same or different functions for gene regulation? (5) Does the siRNA used in previous studies knock down one or multiple transcripts? To address these fundamental questions, we performed polymerase chain reactions (PCR) using cDNA reversely transcribed from total RNAs isolated from HepG2 and HepaRG cells with a set of specially designed primers, which can amplify 9 annotated alternative transcripts. All amplified PCR products were purified, further sequenced, and aligned to the human genome sequence. We confirmed 3 annotated transcripts existing in both HepG2 and HepaRG cells. In addition, we identified 2 novel transcripts with additional exons, which are not annotated in the Ensembl genome database. The 5 confirmed HNF1A-AS1 transcripts have different RNA sequence information with potential to form very different RNA products. The siRNA used for knocking down experiments in previous literatures can only degrade one transcript. This result builds a foundation for us to further test the expression patterns of different transcripts in different tissues and cell lines, to further validate the dynamic expression of these 5 transcripts during liver maturation, and to further explore the mechanisms of the different transcripts in response to xenobiotic exposure. By knocking down each transcript with specially designed siRNAs, we are in the process to functionally characterize each alternative HNF1A-AS1 transcript in transcriptional and translational regulation of P450 gene expression in various conditions and their impacts on drug metabolism. The generated knowledge will help to better understand regulation of P450s-mediated drug metabolism by the alternative lncRNA transcripts and may change the current view of regulation of drug metabolism.

Support/Funding Information:NIH/NIGMS 1R35GM140862-01

# Novel Single- and Multi-Tissue Chips for Predictive Pharmacokinetic Applications

Murat Cirit,<sup>1</sup> Shiny Rajan,<sup>1</sup> Jason Sherfey,<sup>1</sup> Shivam Ohri,<sup>1</sup> Lauren Nichols,<sup>1</sup> Tyler Smith,<sup>1</sup> Paarth Parekh,<sup>1</sup> and Emily Geishecker<sup>1</sup>

<sup>1</sup>Javelin Biotech

Abstract ID 16647

Poster Board 382

Over the past decade, substantial investments of government funding and venture capital have produced novel technologies of more intact systems that represent human organ physiology. These advances include cell culture systems that go beyond single cell type monolayer cultures, such as organoids, spheroids, and co-cultures in 2D and 3D formats, and tissue chip systems that can replicate several organ systems (liver, gut, kidney).

*Human tissue chips*, aka microphysiological systems (MPS), are traditionally microfluidic devices designed to recapitulate human physiology at the tissue level and enable long-term in vitro (co-)cultures. While current microfluidic-based tissue chips are primarily used in basic research, such technologies have limited utility in pharmacokinetic applications because the flow-through fluidic design, chip material, and small media & tissue volumes do not support drug quantification.

For this unmet need, we designed single- and multi-tissue chips for pharmacokinetics applications. Javelin chips are recirculating milli-fluidic chips made of low non-specific binding thermoplastic material. Our milli-fluidic chips provide larger tissue (>200K cells) and media (>1.5ml) than microfluidic chips to enable multiple media sampling for kinetic data. The recirculatory perfusion system dramatically extends drug-tissue retention time allowing low-clearance and low-permeability drug studies.

We characterized each tissue (liver, kidney (proximal tubule) and skeletal muscle) functionality for 21+ days with single- and multi-tissue chips and demonstrated physiologically-relevant levels of enzyme and transporter activity in order to conduct pharmacokinetic studies.

A diverse set of small molecule drugs from all ECCS classes with various clearance mechanisms was evaluated on single- and multi-tissue chips. We quantified on-chip pharmacokinetic parameters, such as hepatic metabolism, uptake & disposition, tubular secretion & reabsorption, and muscle disposition. These on-chip pharmacokinetic parameters were then successfully scaled to clinical parameters for IV drugs: hepatic clearance (CL<sub>h</sub>), renal clearance (CL<sub>r</sub>) and volume of distribution (V<sub>d</sub>). The predicted PK parameters showed high correlation to clinical parameters.

This study demonstrated that this technology would offer an alternative to, and hopefully a replacement of, pharmacokinetic studies in laboratory animals for the purposes of understanding drug disposition in an intact mammal as a surrogate for human.

# Tenofovir Activation in Brain and Liver is Diminished in Creatine Kinase Brain-Type Knockout Mice

Colten D. Eberhard,<sup>1</sup> Benjamin C. Orsburn,<sup>1</sup> and Namandjé N. Bumpus<sup>1</sup>

<sup>1</sup>Johns Hopkins University

Abstract ID 16726

Poster Board 383

Tenofovir (TFV) is a nucleotide reverse transcriptase inhibitor that is administered orally as a prodrug for the treatment and prevention of HIV infection, as well as the treatment of chronic hepatitis B virus (HBV) infection. TFV must be phosphorylated intracellularly to tenofovir-monophosphate (TFV-MP) then to tenofovir-diphosphate (TFV-DP) to become pharmacologically active. The nucleotide kinases responsible for the activation of TFV remain unknown in many tissues central to viral replication and pathophysiology. In identifying TFV activating enzymes, we can interrogate whether individuals experiencing lower drug efficacy possess mutations in these enzymes. Previously, we have demonstrated that creatine kinase brain-type (CKB) is able to phosphorylate TFV-MP to TFV-DP in vitro. To determine where and to what extent CKB activates TFV in vivo, we established a *Ckb* knockout mouse model on a C57BL/6J background. Considering that the brain harbors HIV infection and our preliminary mass spectrometry-based proteomic analyses placed CKB in the top ten most abundant proteins in wild-type (WT) mouse brain, we homogenized full brains from 12-week old WT and *Ckb* knockout mice and incubated the lysates with TFV-MP and a mix of phosphodonors (ATP, phosphocreatine, and phosphoenolpyruvate). TFV metabolites were extracted and detected using ultra-high performance liquid chromatography tandem mass spectrometry (uHPLC-MS). Results showed that *Ckb* knockout male lysates formed 70.5% less TFV-DP than WT male lysates ( $n=3$  each;  $p<0.01$ ), and *Ckb* knockout female lysates formed 77.4% less TFV-DP than WT female lysates ( $n=4$  and  $3$ , respectively;  $p<0.001$ ). This indicates that CKB is the main kinase contributing to TFV-DP formation in the brain. Next, to investigate the role of CKB in the liver, 10-week old mice were dosed with a TFV prodrug (60mg/kg/day via drinking water) for 14 days. TFV metabolites were extracted from the liver and detected using uHPLC-MS. The ratio of TFV-DP to TFV was used as a metric to define TFV activation within each sample. *Ckb* knockout male mice ( $n=14$ ) had an average TFV-DP to TFV ratio 22.8% ( $p<0.05$ ) less than WT male mice ( $n=12$ ), indicating CKB contributes to TFV activation in male livers, however, to a lesser extent than in the brain. Additionally, this reveals the presence of other TFV activating kinases in the liver that have not yet been identified or characterized. Interestingly, no significant difference was observed in female livers when comparing TFV activation between genotypes. Further, in both brain and liver analyses WT female mice had significantly less TFV-DP formation than WT male mice ( $p<0.01$ ). Together, these data suggest sexual dimorphisms may exist in the TFV activation pathway in these tissues. Lastly, to examine the impact of naturally occurring mutations on CKB activity, fifteen recombinantly expressed and purified mutant CKB enzymes were incubated with TFV-MP and phosphocreatine. Eight mutations (C74S, R96P, S128R, R132H, R172P, R236Q, R292Q, and H296R) exhibited a significant reduction in the formation of TFV-DP, ranging from 69.6%-98.6% less TFV-DP formed than WT CKB ( $p<0.05$ ). In conclusion, we hypothesize that individuals possessing missense mutations that diminish TFV-DP formation may have lower levels of TFV-DP in the brain and liver, decreasing the efficacy of TFV in the treatment of HIV and HBV infections.

This work is funded by NIH R01 AG064908.



# Managing Drug Interactions Involving the Over-the-Counter Opioid Loperamide through Physiologically Based Pharmacokinetic Modeling

Zhu Zhou,<sup>1</sup> Mengyao Li,<sup>2</sup> Ping Zhao,<sup>3</sup> Jean Dinh,<sup>4</sup> and Mary Paine<sup>5</sup>

<sup>1</sup>York College, City University of New York; <sup>2</sup>Quantitative Pharmacology, Bicycle Therapeutics; <sup>3</sup>Bill & Melinda Gates Foundation; <sup>4</sup>SimCYP Ltd/Certara; and <sup>5</sup>Department of Pharmaceutical Sciences, Washington State University

Abstract ID 26621

Poster Board 384

**Background:** Loperamide is a widely used over-the-counter opioid that is indicated for the treatment of diarrhea. The recommended dose is not to exceed 16 mg/day. Loperamide is a substrate for the efflux transporter P-glycoprotein (P-gp), which prevents loperamide entry into the brain and subsequent central opioid effects. Loperamide undergoes extensive first-pass metabolism, primarily by cytochrome (CYP) 3A and CYP2C8, with minor contributions by CYP2B6 and CYP2D6. Loperamide oral bioavailability is further limited by P-gp in the intestine. Increasing case reports have described opioid and cardiac toxicities when supratherapeutic doses of loperamide are consumed alone and in combination with CYP or P-gp inhibitors. The objective of this work was to develop and verify a physiologically based pharmacokinetic (PBPK) model of loperamide that could be used to guide loperamide dosing under various drug-drug interaction (DDI) scenarios that have not been assessed clinically and thereby minimize potential toxicities.

**Methods:** A dose proportionality assessment of loperamide was first conducted at clinically relevant doses (4-16 mg loperamide•HCl). A PBPK model for loperamide in the absence and presence of select inhibitor drugs was next developed using the Simcyp™ simulator (v21). Physicochemical and pharmacokinetic properties for loperamide were collected from the literature or generated experimentally. Then the model was verified with data from published clinical DDI studies.

**Results:** Loperamide exhibited linear pharmacokinetics at clinically relevant doses. The PBPK model successfully described the pharmacokinetics of loperamide in healthy adult participants at 4, 8, and 16 mg loperamide•HCl. The predicted AUC and C<sub>max</sub> at all three doses were within 0.61- to 1.27-fold of the observed values obtained from ten clinical studies. The PBPK model independently well-captured the loperamide pharmacokinetic profile obtained from each of the eight DDI studies. The inhibitor drugs tested included quinidine (P-gp), ritonavir (CYP3A/P-gp), gemfibrozil (CYP2C8), itraconazole (CYP3A/P-gp), gemfibrozil+itraconazole, and abemaciclib (CYP1A). The predicted AUC and C<sub>max</sub> for loperamide from each DDI study were within 0.78- to 1.29-fold of observed values. The predicted AUC ratios (AUC of loperamide in the presence to absence of the inhibitor) were within 0.76- to 1.03-fold of observed ratios.

**Conclusions:** A PBPK model for loperamide was successfully developed and verified, enabling future applications. First, the model could be used to predict loperamide systemic and tissue exposure in combination with other enzyme/transporter inhibitors to assess potential safety issues at supratherapeutic exposures, including opioid and cardiac toxicities. Second, the model could be extended to assess loperamide systemic and tissue exposure in special populations, including older adults, who are particularly at risk for DDIs due to polypharmacy and co-morbidities.

This work was supported by the NIH/NIGMS (R16 GM146679), NIH/NCCIH (U54 AT008909), and PSC-CUNY Award.

# Contribution of CNT1 and CNT3 to the intestinal transport and pharmacokinetics of decitabine

Nadeen Anabtawi,<sup>1</sup> Thomas Drabison,<sup>1</sup> Mike Boeckman,<sup>1</sup> Yan Jin,<sup>1</sup> Madeline Halpin,<sup>1</sup> Alice A. Gibson,<sup>1</sup> Alex Sparreboom,<sup>1</sup> Raj Govindarajan,<sup>1</sup> and Sharyn D. Baker<sup>1</sup>

<sup>1</sup>The Ohio State University

Abstract ID 21200

Poster Board 385

**Objective:** Parenteral administration of the nucleoside analog decitabine is recognized as a valuable treatment option for various malignancies, including chronic myelomonocytic leukemia and acute myeloid leukemia. The oral bioavailability of decitabine is limited due to its degradation by cytidine deaminase (CDA) in the GI tract and liver but can be improved by concurrent administration of the CDA inhibitor, cedazuridine. Although an oral combination of decitabine and cedazuridine (ASTX727; Inqovi, Astex Pharmaceuticals) has recently been approved for the treatment of various leukemias, the mechanism by which decitabine is taken up into intestinal enterocytes after oral administration remains unknown. Here, we evaluated the hypothesis that the concentrative nucleoside transporters CNT1 (SLC28A1) and CNT3 (SLC28A3) play a role in decitabine disposition.

**Methods:** Uptake studies were performed in HEK293 cells stably transfected with CNT1, CNT3, or an empty vector using the positive control substrates uridine and gemcitabine, or varying concentrations of decitabine (0.1-10  $\mu$ M). Pharmacokinetic studies were done in C57BL/6 mice with or without a genetic deletion of CNT1 or CNT3. Decitabine (0.4 or 10 mg/kg) was administered orally or intravenously (IV) and cedazuridine (3 mg/kg) was administered by gavage immediately before decitabine. Plasma samples were taken over the course of 4 hours after dosing and analyzed by a validated method based on LC-MS/MS.

**Results:** In HEK293 cells, overexpression of CNT1 was associated with a >3-fold increase in decitabine uptake compared to vector control, while overexpression of CNT3 increased uptake by >10-fold. Decitabine uptake via CNT1 and CNT3 overexpressing cells was significantly increased up to 4 folds by co-treatment with cedazuridine. Decitabine transport by CNT1 and CNT3 was time-dependent and saturable with  $K_m$  values of  $\sim$ 1  $\mu$ M, sensitive to pH, and impaired in the absence of sodium or magnesium. Interestingly, compared to physiological temperature, CNT3 function was not impaired at 4°C. In mice, the oral bioavailability of decitabine was increased >95% by treatment with cedazuridine, compared to IV treatment without cedazuridine. In CNT1-deficient mice, the area under the curve (AUC) of decitabine was decreased compared to wild-type mice (277 $\pm$ 19 vs 344 $\pm$ 19 ng $\times$ h/mL), consistent with impaired intestinal uptake. Unexpectedly, in CNT3-deficient mice, the decitabine AUC was increased by  $\sim$ 30%, possibly due to delayed elimination as a result of defective renal tubular secretion.

**Conclusions:** In this study, we demonstrated that decitabine is a transported substrate of CNT1 and CNT3, nucleoside transporters that are expressed on intestinal enterocytes and renal tubular cells. Our preliminary pharmacokinetic studies suggest that CNT1 and CNT3 contribute jointly to the intestinal absorption of decitabine and potentially also affect its renal clearance. Currently, ongoing studies are focused on the influence of CNT3 inhibitors on the pharmacokinetics of decitabine in CNT1-deficient mice, as well as on the influence of antileukemic drugs commonly used in combination with decitabine, on its absorption and disposition properties and associated side effect profiles.

# Development of Novel DIA Based Proteomics Tools for Quantification of Drug-protein Adducts

Ellen Riddle,<sup>1</sup> Alex Zelter,<sup>2</sup> and Nina Isoherranen<sup>2</sup>

<sup>1</sup>Univ of Washington; and <sup>2</sup>University of Washington

Abstract ID 27681

Poster Board 386

Certain drugs have the potential to form reactive metabolites, which can make covalent adducts with nucleophilic amino acids in proteins. The formation of adducts has been hypothesized to cause time dependent inhibition (TDI) and toxicities that can result in drug interactions and adverse drug reactions. To date, no studies have directly quantitatively linked adduct formation to enzyme inactivation. Our hypothesis is that adduct formation on specific amino acid residues in a protein correlates directly with the inactivation of that protein. The aim of this study is to develop a method to quantify drug-protein adducts using novel DIA based proteomics tools.

To examine this hypothesis, we used raloxifene as a model drug. Raloxifene is a known TDI of CYP3A4 and CYP2C8. Previous work has shown that the reactive metabolite, a diquinone methide, covalently binds to several amino acids on CYP3A4 and CYP2C8, amongst other enzymes such as P450 reductase<sup>1,2</sup>. We used data independent acquisition (DIA) proteomics and Skyline data analysis to quantify the amount of adducts formed when human liver microsomes (HLMs) or supersomes were incubated with and without raloxifene or raloxifene-d<sub>4</sub>. Additionally, we used CYP3A4 unique “non-modifiable” peptides (peptides without cysteine, tryptophan, or tyrosine; residues that were modified by raloxifene diquinone methide in CYP3A4 purified protein<sup>2</sup>), to normalize the quantification of adducted peptides to the total amount of CYP3A4 protein present across samples within the same experiment.

Multiple peptides with raloxifene and raloxifene-d<sub>4</sub> modified cysteines were identified in HLMs, including K.GF[C]MFDME[C]HK.K, a unique CYP3A4 peptide, and R.YIDLLPTSLPHAVT[C]DIK.F, which is specific to CYP2C9. There were no observed instances where both cysteines in K.GF[C]MFDME[C]HK.K were modified by raloxifene simultaneously. For these and other adducted peptides, a clear retention time shift was observed for the adducted peptide when compared to the unadducted counterpart. The raloxifene modified and unmodified CYP3A4 peptides, K.GF[C]MFDME[C]HK.K, R.VLQNFSEFKP[C]K.E, and K.E[C]YSVFTNR.R were quantified after raloxifene and raloxifene-d<sub>4</sub> incubation in CYP3A4 supersomes and HLMs. CYP2C9 supersomes were also incubated with raloxifene and raloxifene-d<sub>4</sub> to determine if the adduct found on the CYP2C9 specific peptide was a result of the diquinone methide metabolite generated by a CYP other than CYP2C9, i.e., CYP3A4 or CYP2C8, which are both inactivated by raloxifene. Surprisingly, we found that multiple peptides were modified by raloxifene and raloxifene-d<sub>4</sub> in the CYP2C9 supersomes, even though raloxifene does not inactivate CYP2C9. In HLMs, significant interindividual variability was observed between donors in the relative quantity of adducts formed in specific peptides. Overall, this study demonstrates that DIA based proteomics tools can be used to quantify drug-protein adducts in both supersomes and in HLM, and that this method can be used to test whether the formation of adducted residues correlates quantitatively with enzyme inactivation.

## References:

1. VandenBrink, BM et al. “Cytochrome p450 architecture and cysteine nucleophile placement impact raloxifene-mediated mechanism-based inactivation.” *Mol. Pharm.* 82: (2012): 835-42.
2. Riffle, M et al. “Discovery and Visualization of Uncharacterized Drug-Protein Adducts Using Mass Spectrometry.” *Anal. Chem* 94: (2022): 3501-3509.

# The hepatocyte estrogen sulfotransferase dictates female sensitivity to T cell-mediated hepatitis independent of estrogens

Wen Xie,<sup>1</sup> and Jingyuan Wang<sup>2</sup>

<sup>1</sup>Univ of Pittsburgh School of Pharmacy; and <sup>2</sup>Univ of Pittsburgh

Abstract ID 16563

Poster Board 387

**Background & Aims:** Autoimmune hepatitis (AIH) is a typical T cell-mediated chronic liver disease with a higher incidence in females. However, the molecular mechanism for the female predisposition is poorly understood. Estrogen sulfotransferase (Est) is a conjugating enzyme best known for its function in sulfonating and deactivating estrogens. The goal of this study is to investigate whether and how Est plays a role in the female preference of AIH.

**Methods:** Mice that bear genetic or pharmacological inhibition of Est were subjected to Concanavalin A (ConA)-induced T cell-mediated hepatitis. The AIH phenotypes were characterized by the serum ALT and AST, liver histology, and the levels of cytokines and hepatic immune cells by qPCR, ELISA, and flow cytometry.

**Results:** Est was highly induced in the liver of ConA-treated mice. Systemic (EstKO) or hepatocyte-specific ablation, or pharmacological inhibition of Est protected female mice from ConA-induced hepatitis regardless of ovariectomy. In contrast, hepatocyte-specific transgenic reconstitution of Est in EstKO mice abolished the protective phenotype. ConA-treated EstKO mice exhibited a more robust inflammatory response with elevated pro-inflammatory cytokines but less toxic hepatic immune profile. Mechanistically, ablation of Est led to the hepatic induction of lipocalin 2 (Lcn2), whereas ablation of Lcn2 abolished the protective phenotype of EstKO females.

**Conclusions:** Hepatocyte Est is required for female sensitivity to ConA-induced and T-cell mediated hepatitis in an estrogen-independent manner. Est ablation may have protected female mice from ConA-induced hepatitis by upregulating Lcn2. Pharmacological inhibition of Est might be a potential strategy for the treatment of AIH.

# Regulation of Hepatic Drug Transporters by Pro-inflammatory Cytokines

Tianran Hao,<sup>1</sup> Jashvant Unadkat,<sup>1</sup> and Qingcheng Mao<sup>2</sup>

<sup>1</sup>Univ of Washington; and <sup>2</sup>Univ of Washington School of Pharmacy

Abstract ID 20942

Poster Board 388

*In vivo* studies have shown that the clearance of drugs primarily cleared by cytochrome P450 (CYP) metabolism is reduced during inflammation or infections, potentially resulting in drug toxicity. Inflammation or infectious diseases (e.g. HIV, COVID-19) are associated with increased production of pro-inflammatory cytokines which are known to down-regulate the expression or activity of CYP enzymes. However, their effect on human hepatic drug transporters has been poorly studied, primarily with individual cytokines at supraphysiological concentrations. This makes it difficult to translate these findings to *in vivo*. Therefore, the goal of this study was to systematically investigate the effect of major cytokines, individually or in combination, on the mRNA expression of hepatic drug transporters in plated primary human hepatocytes. Primary human hepatocytes (lot ZKF, YND, ADR, BioIVT) were treated with interleukin-6 (IL-6), interleukin-1 $\beta$  (IL-1 $\beta$ ), tumor necrosis factor- $\alpha$  (TNF- $\alpha$ ), and interferon- $\gamma$  (IFN- $\gamma$ ), either in combination (each at 0.1 and 1 ng/mL) or individually (0.01, 0.1, 1 and 10 ng/mL) for 72 hours with daily replenishment of media. The cytokine concentrations used encompass the *in vivo* observed plasma concentrations of cytokines in infectious diseases (e.g. HIV) and autoimmune diseases (rheumatoid arthritis). Then, the total RNA was then isolated, and the mRNA levels of 11 hepatic drug transporters were quantified by real time q-PCR, including organic anion transporting polypeptide 1B1 (OATP1B1), organic anion transporting polypeptide 1B3 (OATP1B3), organic anion transporting polypeptide 2B1 (OATP2B1), organic anion transporter (OAT2), organic cation transporter (OCT1), breast cancer resistance protein (BCRP), P-glycoprotein (P-gp), multidrug and toxin extrusion protein 1 (MATE1), multi-drug resistance protein 2,3, and 4 (MRP2/3/4). OATP1B1, OATP1B3, OAT2, P-gp, BCRP, and MATE1 mRNA expression was significantly down-regulated by the combination of cytokines in a concentration-dependent manner. OAT2 mRNA was most affected. It was down-regulated by 82% at 0.1 ng/mL and 95% at 1 ng/mL. Conversely, OCT1 mRNA expression was induced by 2-fold and 3-fold at 0.1 ng/mL and 1 ng/mL, respectively. The individual cytokines also modulated transporter mRNA expression in a concentration-dependent manner. The greatest repression (at 10 ng/ml) was of OATP1B1 by TNF- $\alpha$  (by 60%) and IFN- $\gamma$  (by 60%), OATP1B3 by IL-6 (by 75%) and IFN- $\gamma$  (by 60%), and OAT2 by TNF- $\alpha$  (by 90%) and IL-1 $\beta$  (by 90%), P-gp by IL-6 (by 50%) and TNF- $\alpha$  (by 50%). While OATP2B1 was down-regulated by IL-1 $\beta$  (by 70%) and induced by IL-6 (by 1.5-fold) at 10 g/ml, this down-regulation was abolished by the combination cytokine treatment. Our data suggested that there is an additive effect of the cytokines on the mRNA expression of most of the hepatic transporters. Similar results were obtained with plated human hepatocytes from three donors. Also, cytokines generally exhibited a greater impact on uptake transporters vs. efflux transporters. Next, we intend to determine if these observed changes in transporter mRNA expression correspond to changes in transporter activity (by transport assays) and/or abundance (by quantitative proteomics). Then, these data will be used to predict changes in transporter-mediated drug PK caused by inflammation or infectious diseases using physiologically based pharmacokinetic modeling and simulations.

This work was supported by the NIH Grant R01HD102786.

# Naturally Occurring Flavonoids Attenuate Irinotecan-Induced Intestinal Toxicity Through Anti-Inflammatory and Epithelial Barrier Activities

Imoh Etim,<sup>1</sup> Ting Du,<sup>1</sup> Abasifreke Benson,<sup>1</sup> and Song Gao<sup>1</sup>

<sup>1</sup>Texas Southern University

Abstract ID 52744

Poster Board 389

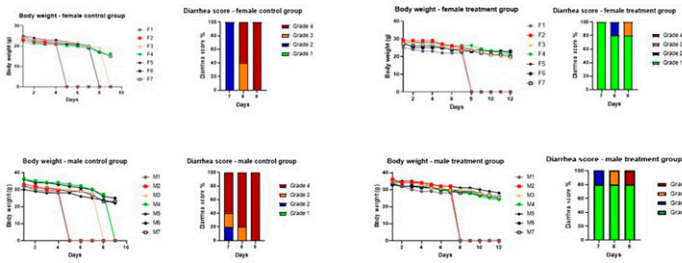
Gastrointestinal toxicity is a common dose-limiting toxicity associated with cancer chemotherapy, especially irinotecan (CPT-11) and 5-fluorouracil (5-FU). CPT-11 is a prodrug hydrolyzed to SN-38; a potent topoisomerase 1 inhibitor used in the treatment of metastatic colorectal cancer. SN-38 is further conjugated to the inactive phase II metabolite SN-38 glucuronide (SN-38G) in the presence of uridine diphosphate glucuronosyltransferases (UGT). However, SN-38G can be deconjugated back to the active drug SN-38 in the presence of intestinal  $\beta$ -glucuronidase enzyme. Naturally occurring flavonoids such as wogonin and chrysin have been reported to have several pharmacological activities, including anti-inflammatory and antioxidative properties. The purpose of this study was to investigate the attenuation of irinotecan-induced intestinal toxicity by flavonoids via the ability to modulate inflammatory cytokines and epithelial tight junction proteins in mice.

Before the dosing of CPT-11, oral gavage of wogonin/chrysin at 100 mg/kg per day was administered three days before co-administering with CPT-11. CPT-11 was administered intraperitoneally (i.p) to mice at a dose of 75 mg/kg per day for six consecutive days as a bolus injection, and then the disease activity indexes (i.e., body weight, diarrhea score, and survival analysis) were monitored. Gastrointestinal (GI) tissues were collected on day 4 (before diarrhea) and day 9 (after diarrhea) to evaluate histological changes. Also, inflammatory markers and tight junction proteins were analyzed using ELISA kit. LC-MS/MS analysis was used to quantitate the tissue drug concentrations of SN-38 and SN-38G.

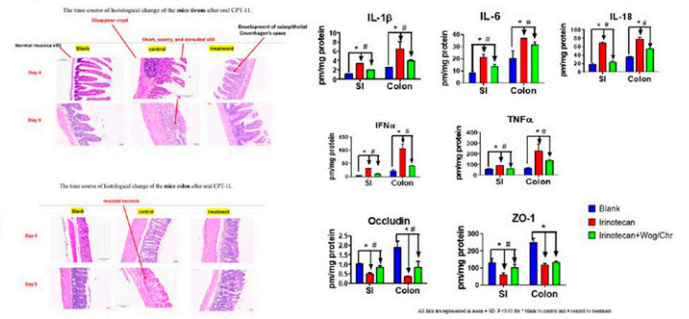
Our studies showed that the oral flavonoids (wogonin/chrysin) alleviated irinotecan-induced diarrhea damage by reducing weight loss and diarrhea score and attenuating mucositis in the small intestine and colon. Histological analysis confirmed that the oral flavonoids prevented short, scanty, and denuded villi in the ileum and colon. Compared with the control group (irinotecan only), the oral flavonoids group (irinotecan co-administered) decreased the expression of IL-1 $\beta$  by 2-folds in the small intestine and 1.5-folds in the colon. Interestingly, the expression of IL-18 was significantly downregulated in the small intestine, with almost a 4-fold decrease and a 2-fold decrease in the colon. The expressions of TNF $\alpha$  and IFN $\alpha$  were downregulated considerably, with about a 2-fold decrease in the oral flavonoids-treated group showing promising potential in reducing the expression of inflammatory cytokines in irinotecan-exposed mice. The oral flavonoids treatment also prevented disruption of the tight junction proteins, ZO-1, and occludin; we observed that the oral flavonoids upregulated ZO-1 and occludin in the small intestine by a 2-fold increase. The female treated group showed a significant difference to the control group (irinotecan only) in SN-38G tissue drug concentration in the duodenum and jejunum as the oral flavonoid-treated group showed promising potential to alleviate irinotecan-induced diarrhea pointing to gender differences between the male and female groups.

The oral flavonoids attenuated intestinal diarrhea induced by irinotecan and, therefore, could be a promising agent in the anti-tumor chemotherapy to control this GI adverse effect. Thus, increasing treatment adherence and, consequently, the chances of cancer remission.

### Body weight and diarrhea scores



### Histological evaluation, inflammatory makers and tight junction proteins



All data are represented as mean ± SD. \*P < 0.05 vs. Blank; #P < 0.05 vs. Irinotecan; ##P < 0.05 vs. Irinotecan+WogChr.

# Family 1 P450s Form Complexes that Effect Enzyme Function

J Patrick Connick,<sup>1</sup> George Cawley,<sup>1</sup> James R. Reed,<sup>1</sup> and Wayne L. Backes<sup>1</sup>

<sup>1</sup>Louisiana State University Health Sciences Center - New Orleans

**Abstract ID 25945**

**Poster Board 390**

CYP1A1, CYP1A2, and CYP1B1 share high amino acid sequence similarity, substrate selectivity, and induction characteristics. Despite this, there are significant differences in their functional characteristics. The goal of this work was to characterize the protein-protein interactions of CYP1 enzymes and to link differences in these interactions with changes in enzyme activity.

To achieve this we used bioluminescence resonance energy transfer (BRET) to study the presence and stability of CYP1 protein complexes in HEK293T cells and did kinetic analysis of CYP1 activity using recombinant protein reconstituted in liposomes with varying levels of NADPH-cytochrome P450 reductase (POR).

Using BRET, we determined that both CYP1A1 and CYP1A2 (but not CYP1B1) formed homomeric complexes. When CYP1 activity was measured while varying [POR], CYP1A1 and CYP1B1 showed a hyperbolic response while the CYP1A2 response was sigmoidal. Each family 1 P450 also appeared to form a complex with heme oxygenase-1 (HO-1), though the stability of these complexes and their effect on POR binding was unique for each P450. The presence of HO-1 generally inhibited CYP1 activity, but the kinetic data were inconsistent with simple competition for POR binding.

Differences in protein-protein interactions formed by CYP1A1, CYP1A2, and CYP1B1 appear to contribute to observed differences in enzyme function. The atypical kinetics of CYP1A2 can be explained by the presence of homomeric CYP1A2 complexes. Interestingly, homomeric CYP1A1 complexes did not appear to have a similar effect. Differences in HO-1/P450 complex formation and subsequent changes in POR binding and enzyme activity have the potential to affect the disposition of endogenous and xenobiotic compounds.

These results demonstrate that differences in quaternary structure may contribute to the unique functional characteristics of endoplasmic reticulum membrane-resident enzymes. Our understanding of P450-mediated metabolism will be incomplete if it is limited to individual P450s interacting with POR as monomers — the participation of P450 enzymes in protein complexes must also be taken into account.

Support/Funding Information:

NIGMS R01 GM123253

NIEHS P42 ES013648



---

# Development and Characterization of Chemical Tools to Study Ester Drug Metabolic Enzymes in Live Cells

Carolyn Karns,<sup>1</sup> Makenzie R. Walk,<sup>1</sup> Anchal Singh,<sup>1</sup> Mingze Gao,<sup>1</sup> Taylor P. Spidle,<sup>1</sup> and Michael Beck<sup>2</sup>

<sup>1</sup>Eastern Illinois University; and <sup>2</sup>Eastern Illinois Univ

**Abstract ID 18248**

**Poster Board 575**

Carboxylesterase-mediated metabolism of ester containing drugs can result in their activation or deactivation and enhance clearance. The two major human carboxylesterases (CEss), CES1 and CES2 play a key role in the hydrolysis of xenobiotic esters including aspirin, methylphenidate (Ritalin), oseltamivir (Tamiflu), and the illicit narcotics cocaine and heroin. Despite the established role of CEss in drug metabolism, few techniques exist to study their activity in live cells. Chemical tools have been developed to be able to expand the methods used to study CES activity, however, many existing chemical tools are not sufficiently characterized to be able to confidently study CES activity in live cells. Substrate specificity can overlap with other cellular esterases which makes it exceptionally difficult to differentiate activity between the two carboxylesterases. To address this issue, we report the development of new chemical tools to study CEss. After evaluation for suitability in live cells, we determined their ability to report on CES activity in live cells using small molecule inhibitors and shRNA. Overall, our studies will result in a library of fully characterized chemical tools for studying human carboxylesterases which can lead to improved methods for studying the role of CEss in human health and drug metabolism.

# A Novel *In Vitro* Hepatocyte Culture System (icHep) for Biliary Drug Excretion Analysis Using Permeation Assay

Yuya Nakazono,<sup>1</sup> Hiroshi Arakawa,<sup>1</sup> Natsumi Matsuoka,<sup>1</sup> Yoshiyuki Shirasaka,<sup>1</sup> and Ikumi Tamai<sup>1</sup>

<sup>1</sup>Faculty of Pharmaceutical Sciences, Institute of Medical, Pharmaceutical and Health Sciences, Kanazawa University

Abstract ID 15604

Poster Board 576

**Purpose:** Biliary excretion via drug-metabolizing enzymes and transporters is often critical as the hepatobiliary disposition is directly linked to drug efficacy and safety. Sandwich-cultured hepatocyte (SCH) is an *in vitro* model widely used to assess the biliary excretion potential of drugs. However, SCH does not allow time-dependent and quantitative evaluation because drugs accumulate in the closed bile canaliculi formed between hepatocytes and their amounts cannot be measured directly. This structural problem of SCH can be overcome by inducing a formation of an open canaliculus lumen face to a culture support. The aim of this study is to establish a novel hepatocyte culture model with open-form bile canaliculi that enables to evaluate biliary excretion of drugs by a permeation assay but not by accumulation assay.

**Methods:** Primary human hepatocytes and PXB-cells derived from liver-humanized mice were cultured on a permeable support coated with claudin, a tight junction protein. The formation of bile canaliculi was evaluated by fluorescent immunostaining of the MRP2 localized on the canalicular membrane. The permeation assay was performed using substrates for transporters (BSEP, MRP2 and P-gp) involved in biliary excretion. Human *in vivo* biliary excretion clearance of six drugs whose clearances are reported was estimated using the apparent permeability coefficient  $P_{app}$  calculated by permeation assays of each test compound.

**Results and Discussion:** When human hepatocytes were cultured on a permeable support coated with specific claudin proteins, open hemi-luminal morphology as indicated by the canalicular membrane marker MRP2 was newly formed on the surface of the permeable support. Therefore, it is considered that the surface of support coated with claudin proteins functioned as a pseudo-hepatocyte membrane for bile canaliculus formation and this culture system is termed as an induced open-form bile canaliculus hepatocyte (icHep). A continuous monolayer of hepatocytes with tight cell-to-cell contact is formed using PXB-cells. In addition, the cells maintained the functions of a wide range of liver-specific drug uptake transporters and metabolizing enzymes. Permeation assay in icHep showed unidirectional transport of taurocholate (BSEP), E<sub>2</sub>17βG (MRP2), and digoxin (P-gp) from blood to bile side. Each transport was suppressed upon treatment with the respective inhibitors. Furthermore, the estimated biliary drug excretion from the permeability obtained in icHep was well-correlated with the reported human *in vivo* values.

**Conclusions:** icHep permeation assay system established in the present study overcomes the problems of the conventional SCH method and enables easy and rapid collection of biliary excreted drugs and estimation of their biliary excretion clearance. This approach is useful to assess pharmacokinetics and drug safety during the preclinical stage of drug discovery and development.

# Identification of endogenous biomarkers of renal organic cation transporters in rats by global metabolomics analysis

Anoud Ailabouni,<sup>1</sup> Vijay Mettu,<sup>1</sup> Dilip K. Singh,<sup>2</sup> Aarzoo Thakur,<sup>2</sup> and Bhagwat Prasad<sup>1</sup>

<sup>1</sup>Washington State Univ; and <sup>2</sup>Washington State University

Abstract ID 18183

Poster Board 577

Kidney is one of the major drug-elimination organs. The total renal excretion of a compound is the net result of glomerular filtration, tubular secretion, and reabsorption. Tubular secretion is a transporter-mediated process, which is often mediated by organic cation transporters (OCT/Oct) that facilitate the active secretion of several cationic substrates including drugs such as metformin as well as endogenous cations<sup>1</sup>. Endogenous biomarkers of OCTs can help in the early assessment of drug-drug interaction without the administration of exogenous OCT probe substrates<sup>2</sup>. We hypothesize that administration of cimetidine, an OCT/Oct inhibitor, will lead to increased plasma levels and decreased renal clearance ( $CL_R$ ) of endogenous OCT/Oct substrates. Such substrates can potentially act as OCT/Oct biomarkers. We carried out a rat pharmacokinetic (PK) study where metformin (5 mg/kg, IV) was administered as an exogenous substrate of OCT (positive control) to four Sprague-Dawley rats with and without cimetidine (100mg/kg, IP) in a cross-over study design with one week washing period. Blood samples were collected from the tail vein at different time points, i.e., pre-dose, 0.17, 0.5, 1, 2, 4, 6, and 8 h, and urine samples were collected at 0-4 and 4-8 h intervals. Rat blood and urine samples were analyzed for metformin and cimetidine levels by a validated method using liquid chromatography with tandem mass spectrometry (LC-MS/MS) (Waters Xevo-TQ-XS MS; Waters, Milford, MA). Metformin area under the blood concentration-time curve ( $AUC_{(0-8h)}$ ) was significantly increased by 3.2 folds when co-administered with cimetidine (*p*-value, 0.003). Similarly, metformin  $CL_{R(0-8h)}$  was significantly decreased in cimetidine arm by 3.7 folds (*p*-value, 0.029). Further, to investigate the effect of cimetidine on endogenous metabolites, we carried out untargeted metabolomics for rat blood and urine samples using Easy Spray 1200 series nanoLC coupled Q-Exactive HF MS (Thermo Fisher Scientific, Waltham, MA). The rat blood samples were analyzed in three groups, i.e., pooled (0.5, 1, and 2h), 0.5 h, and 1 h samples, while rat urine samples were analyzed at 0-4 h interval samples. The generated data were analyzed by open-access XCMS Online software (xcmsonline.scripps.edu). Greater than 18,000 features were detected in the blood which were shortlisted using optimized selection criteria, i.e., fold differences (with versus without cimetidine) of 1.9-10 fold, *p*-value <0.05, reproducible retention time, and quality of chromatogram peak. Out of the 85 shortlisted hits, 52 were detected by METLIN software, and 30 were common in blood and urine. Among several potential compounds predicted by METLIN for each mass-to-charge ratio (*m/z*) value, only compounds containing nitrogen atoms with mass error (ppm) less than 4 were selected. Two significant hits (*m/z*, 134.06, and 233.09 corresponding to putative oxindole and robustine, respectively) were consistently found in pooled, 0.5 h, and 1h samples (Figure 1). Other putative metabolites were oxyquinoline (*m/z*, 146.09), deoxyadenosine (*m/z*, 252.11), 1-naphthylamine (*m/z*, 182.04), and 2-methylquinoline-3,4-diol (*m/z*, 176.07). A clinical study is currently being conducted to further validate these preliminary data.

This work was supported by NIH/NICHD R01HD081299

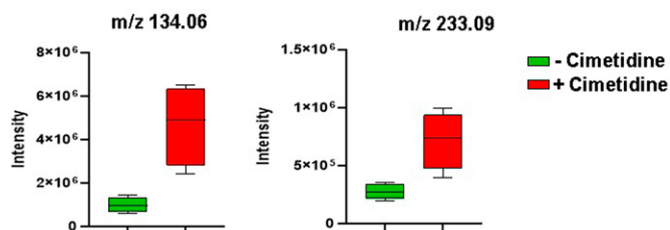


Figure 1: LCMS signal intensity with and without cimetidine of two significant hits found in the pooled, 0.5 h, and 1 h samples.

# Pharmacological Effects of Ketoconazole in the Treatment of Steroidogenesis Suppression via CYP17A1 Inhibition May Involve MicroRNA Regulation

Baitang Ning,<sup>1</sup> Dongying Li,<sup>1</sup> Bridgett Knox,<sup>1</sup> and Weida Tong<sup>1</sup>

<sup>1</sup>National Center for Toxicological Research/FDA

Abstract ID 21867

Poster Board 578

Ketoconazole, an imidazole derivative, is one of the treatment options used to treat Cushing's syndrome in adults and adolescents (>12-year-old) by suppressing steroidogenesis through its inhibition of CYP17A1 (Cyp17a1 in rodents), while Cushing's syndrome is a rare but life-threatening disease caused by cortisol hypersecretion. It is well known that microRNAs (miRNAs) influence drug metabolism by regulating the expression of CYP enzymes. Our previous liver toxicity study has shown that miRNA expressions are altered and contributed to liver toxicity by ketoconazole exposure in rats. However, it is unclear if/how miRNAs may affect Cyp17a1 levels under the treatment of ketoconazole. To that end, we used miRWalk to identify miRNA candidates that may target Cyp17a1. miRNAs with a binding probability larger than 0.95 were considered as miRNA candidates, resulting in that 135 miRNAs with a high confidence for targeting Cyp17a1 were selected. Next, we analyzed differentially expressed miRNAs (DEMs) from rats that were treated with ketoconazole for 3, 7, and 14 days, at the middle and high doses, by which we identified 11 common DEMs with log<sub>2</sub>FoldChange > 2 or < -1 across all treatment conditions. Furthermore, we overlapped the 11 common DEMs with the predicted miRNAs targeting Cyp17a1, and found that mir-22-5p, miR-671, miR-28-3p, and miR-92b-3p were significantly upregulated by ketoconazole treatment and could target Cyp17a1. Our conservation analysis based on miRNA sequences revealed that all these four miRNAs were 100% identical between rats and humans. Taken together, our work suggests that ketoconazole may upregulate mir-22-5p, miR-671, miR-28-3p, and miR-92b-3p to inhibit Cyp17A1 expression to suppress steroidogenesis in Cushing's syndrome. Wet-lab experiments that validate the molecular mechanisms are currently ongoing and will be discussed.

Support/Funding Information: FDA funded study.

# Single-dose Brilaroxazine Pharmacokinetics, Metabolism, and Excretion Profile in Animals and Humans

Laxminarayan Bhat,<sup>1</sup> Seema R. Bhat,<sup>2</sup> and Palaniappan Kulanthaivel<sup>2</sup>

<sup>1</sup>Reviva Pharmaceuticals, Inc; and <sup>2</sup>Reviva Pharmaceuticals Holdings Inc

Abstract ID 53587

Poster Board 579

**Background:** Brilaroxazine, a serotonin/dopamine modulator developed for treating schizophrenia, possesses differentiated pharmacological and safety profiles over other antipsychotic treatments. This work describes the pharmacokinetics, metabolism, and excretion (PME) of a single-dose [<sup>14</sup>C]-brilaroxazine in mouse, dog, and human studies.

**Methods:** Brilaroxazine PME profile involved three single-dose studies, two animal and one clinical. The animal studies consisted of administering a single oral dose of [<sup>14</sup>C]-brilaroxazine 10 mg/kg (400 mCi/kg) and 10 mg/kg (75 mCi/kg) to CD-1 mice and beagle dogs (both male), respectively. Each study collected serial blood and excreta samples up to 144-168 hours post-dose. The clinical study of six healthy male volunteers involved administering a single 15 mg (~163 mCi) oral dose of [<sup>14</sup>C]-brilaroxazine. This study collected serial blood and excreta samples up to 336 hours post-dose.

Radioactivity concentrations determination in blood, plasma and excreta samples utilized liquid scintillation counting (LSC) or a combination of combustion with LSC. Plasma concentrations determination of unlabeled brilaroxazine and its metabolite RP5081 used a validated LC-MS/MS method. Calculating plasma pharmacokinetic parameters of total radioactivity, brilaroxazine and metabolite RP5081 employed non-compartmental analysis (WinNonlin). Identifying brilaroxazine-related metabolite structures in biological samples involved mass spectral analysis or via direct comparison with authentic standards.

**Results:** Feces represented the predominant recovery route for administered dose for mice (77.9%), dogs (55.3%), and humans (52.3%). Urine recovery was the secondary route for mice (10.3%), dogs (15.0%), and humans (32.8%). Brilaroxazine accounted for approximately 12%, 7%, and 12% of the total circulating radioactivity, respectively, in mice, dogs and humans. A fragment of brilaroxazine, N-(2,3-chlorophenyl)-glycine (M219), was the major circulating metabolite in all species accounting for approximately 40%, 51% and 72% of the total radioactivity in mice, dogs, and humans, respectively. Human plasma showed no unique human-specific metabolite. All metabolites in human plasma were found in either mice or dogs. The major excreted metabolite identified was mono-hydroxylated brilaroxazine (M465a) in all species.

**Conclusions:** Following a single oral dose of [<sup>14</sup>C]-brilaroxazine, the administered dose was predominantly recovered in feces of all species. The major circulating metabolite was the same in all species, and there was no human-specific metabolite in plasma. Oxidation, N- or O-dealkylation with subsequent sulfation and/or conjugation with glucuronic acid were the metabolic pathways of brilaroxazine.

# Characterization of a novel bifunctional cytochrome P450 enzyme CYP107 from bacterium *Sebekia benihana*

Layne Jensen,<sup>1</sup> and D. Fernando Estrada<sup>2</sup>

<sup>1</sup>SUNY at Buffalo; and <sup>2</sup>Univ at Buffalo

Abstract ID 26055

Poster Board 580

Cytochrome P450 enzymes (CYPs) are responsible for a wide array of reactions in mammalian and bacterial cells, including hormone synthesis, steroidogenesis, and drug metabolism. In particular, we are focused on CYPs involved in vitamin D metabolism. Mammalian vitamin D-metabolizing CYPs like CYP2R1 and CYP27B1 display a narrow substrate specificity, hydroxylating vitamin D at one position. However, certain bacterial CYPs reportedly display a broader specificity and are capable of hydroxylating multiple vitamin D substrates at different positions. In particular, CYP107 from the soil organism *Sebekia benihana* has been reported to carry out hydroxylations at both the carbon-25 and the 1? positions of the hormone precursor cholecalciferol, thus combining CYP2R1 and CYP27B1 functions into a single enzyme. Our objective is to investigate structure and function in CYP107 as a way of understanding the conservation of vitamin D recognition in both bacterial and mammalian enzymes. We have successfully expressed and purified CYP107 in *E. coli* and have collected absorbance binding data with vitamin D compounds. Under low salt conditions, alfacalcidol (1 $\alpha$ -OH vitamin D) exhibits tight binding to CYP107 as a type-I ligand. Interestingly, the spin state of the heme displays salt sensitivity that is independent of ligand, with slow interconversion between high-spin (390nm) at high salt and low-spin (420 nm) at low salt. Future work will combine mutagenesis guided by mammalian substrate-CYP interactions, 1D and 2D NMR to investigate structure, and functional assays to monitor function of the protein and its mutants. This work will help elucidate the structural basis of functional conservation of CYPs across bacteria and mammals, providing insight into important active site residues and active site morphology on enzyme specificity for vitamin D.

# Identification And Functional Characterization Of Alternative Transcripts Of Lncrna Hnf4a-As1 And Their Impacts On Drug Metabolism

Le Tra Giang Nguyen,<sup>1</sup> Jing Jin,<sup>1</sup> and Xiao-bo Zhong<sup>1</sup>

<sup>1</sup>Univ of Connecticut

Abstract ID 22067

Poster Board 581

Hepatocyte nuclear factor 4 alpha antisense 1 (*HNF4A-AS1*) gene is a long non-coding RNA (lncRNA) gene physically located next to the transcription factor *HNF4A* gene in the human genome. The *HNF4A-AS1* gene encodes a lncRNA HNF4A-AS1, which has been demonstrated to be involved in negative regulation of expression of genes encoding several drug-metabolizing cytochrome P450 enzymes, including CYP1A2, 2B6, 2C9, 2C19, 2E1, and 3A4 (Chen et al, 2018, PMID:29691280; Wang et al, 2021, PMID:33674270) via interaction with HNF4A and alterations of histone modifications. By altering expression of CYPs, HNF4A-AS1 also contributes to the susceptibility of drug-induced liver injury (Chen et al, 2020, PMID: 3202952; Wang et al, 2022, PMID: 34949673). These conclusions are mainly made by knockdown of HNF4A-AS1 RNA with a siRNA. However, like many other lncRNAs, HNF4A-AS1 has 4 annotated alternative transcripts in the human genome. Several fundamental biological questions are still not solved: (1) How many transcripts do really exist? (2) Do different tissues express the same or different transcripts? (3) Do same tissues express same or different transcripts at different conditions, such as growth, development, regeneration, and exposure to xenobiotics? (4) Do different transcripts have the same or different functions for gene regulation? (5) Does the siRNA used in previous studies knock down one or multiple transcripts? To address these fundamental questions, we performed polymerase chain reactions (PCR) using cDNA reversely transcribed from total RNAs isolated from HepG2 and HepaRG cells with a set of special designed primers, which can amplify 4 annotated alternative transcripts. All amplified PCR products were purified, further sequenced, and aligned to the human genome sequence. We confirmed all 4 annotated transcripts existing in both HepG2 and HepaRG cells. In addition, we identified 2 novel transcripts, one resulted from exon skipping while another with a retained intron, which are not annotated in the Ensembl genome database. The 6 confirmed HNF4A-AS1 transcripts have different RNA sequence information with potential to form very different RNA products. The siRNA used for knocking down experiments in previous literatures can only degrade 5 out of 6 confirmed transcripts. This result builds a foundation for us to further test the expression patterns of different transcripts in different tissues and cell lines, to further validate the dynamic expression of these 6 transcripts during liver maturation, and to further explore the mechanisms of the different transcripts in response to xenobiotic exposure. By knocking down each transcript with special designed siRNAs, we are in the process to functionally characterize each alternative HNF4A-AS1 transcript in transcriptional and translational regulation of P450 gene expression in various conditions and their impacts on drug metabolism and drug-induced liver injury. The generated knowledge will help to better understand regulation of P450s-mediated drug metabolism by the alternative lncRNA transcripts and may change the current view of regulation of drug metabolism.

Support/Funding Information: NIH/NIGMS 1R35GM140862-01

# Goldenseal-mediated Inhibition of Enteric Uptake Transporters Decreases Metformin Systemic Exposure in Mice

Victoria Oyanna,<sup>1</sup> Kenisha Y. Garcia-Torres,<sup>1</sup> Baron J. Bechtold,<sup>1</sup> Katherine D. Lynch,<sup>1</sup> Ridge M. Call,<sup>1</sup> Miklos Horvath,<sup>2</sup> Preston K. Manwill,<sup>3</sup> Tyler N. Graf,<sup>3</sup> Nadja B. Cech,<sup>3</sup> Nicholas H. Oberlies,<sup>3</sup> Mary Paine,<sup>1</sup> and John D. Clarke<sup>1</sup>

<sup>1</sup>Washington State University; <sup>2</sup>SOLVO Biotechnology; and <sup>3</sup>University of North Carolina at Greensboro

Abstract ID 23219

Poster Board 582

Goldenseal (*Hydrastis canadensis* L.) is a perennial plant that is native to eastern North America. Herbal supplements made from the dried roots of the plant are commonly used to self-treat respiratory infections and digestive disorders. A recent clinical study<sup>1</sup> involving 16 healthy adult participants reported that a well-characterized goldenseal product significantly decreased metformin  $C_{max}$  (27%) and AUC (23%) but did not alter half-life or renal clearance. These pharmacokinetic data suggested goldenseal primarily altered processes involved in metformin intestinal absorption; however, the underlying mechanism(s) remain(s) unknown. Intestinal uptake of the hydrophilic metformin is dependent on several transporters, including organic cation transporter (OCT) 1, OCT3, plasma monoamine transporter (PMAT), and thiamine transporter 2 (THTR2). We hypothesized that the goldenseal-mediated decrease in metformin systemic exposure involves inhibition of one or more of these transporters. The major goldenseal alkaloids, berberine and (–)-β-hydrastine, and an extract prepared from the goldenseal product used in the clinical study (standardized to berberine) were tested as inhibitors of OCT1<sup>1</sup>, OCT3, PMAT, and THTR2 in HEK293 cells overexpressing each transporter. The goldenseal extract was the most potent against all four transporters, with an  $IC_{50}$  of 2.6, 4.9, 13.1, and 5.8 μM, respectively. A pharmacokinetic study in 8 male FVB mice compared the inhibitory effects of orally administered berberine (71 mg/kg), (–)-β-hydrastine (46 mg/kg), goldenseal extract (500 mg/kg), or imatinib (OCT inhibitor) (100 mg/kg) on orally administered metformin (10 mg/kg). Goldenseal extract and imatinib did not alter metformin half-life but significantly decreased  $C_{max}$  by 33% and 24% ( $p < 0.05$ ), respectively, consistent with the effect of goldenseal on metformin  $C_{max}$  in human participants.<sup>1</sup> Although not significant, the goldenseal extract and imatinib also decreased metformin  $AUC_{0-12h}$  (11-16%). In contrast to the goldenseal extract, berberine and (–)-β-hydrastine had no effect on metformin pharmacokinetics, indicating that neither alkaloid alone precipitated the interaction *in vivo*. The involvement of basolateral enteric/hepatic uptake transporters was next examined in 7 male FVB mice by comparing the effects of the goldenseal extract or imatinib on intravenous metformin (5 mg/kg) pharmacokinetics. Goldenseal extract and imatinib had no effect on metformin  $AUC_{0-12h}$  and half-life, suggesting lack of inhibition of basolateral enteric/hepatic uptake transporters involved in metformin disposition. Collectively, results may have implications for patients taking goldenseal with other drugs that are substrates for OCT1/3, PMAT, and THTR2, such as atenolol, verapamil, and desipramine. (Funded by the NIH/NCCIH: AT011101, AT008909)

<sup>1</sup>Nguyen *et al.* (2021) *Clin Pharmacol Ther* 109:1342-52.



# Regulation of Human Renal Drug Transporter mRNA Expression by Proinflammatory Cytokines

Yik Pui Tsang,<sup>1</sup> Jashvant Unadkat,<sup>1</sup> and Qingcheng Mao<sup>2</sup>

<sup>1</sup>Univ of Washington; and <sup>2</sup>Univ of Washington School of Pharmacy

Abstract ID 14689

Poster Board 583

Proinflammatory cytokines, which are elevated during inflammation or infections, can affect drug pharmacokinetics (PK) and pharmacodynamics in humans due to altered expression or activity of drug transporters and/or metabolizing enzymes. To date, studies have examined the effect of cytokines on the activity and/or expression of hepatic transporters and drug-metabolizing enzymes. However, many antibiotics and antivirals used to treat infections are renally cleared by transporters including the basal organic cation transporter 2 (OCT2), organic anion transporters 1 and 3 (OAT1 and 3), and the apical multidrug and toxin extrusion proteins 1 and 2-K (MATE1/2-K). Therefore, the goal of this study was to determine the effect of individual and cocktail of the major cytokines, interleukin-6 (IL-6), IL-1 $\beta$ , tumor necrosis factor (TNF)- $\alpha$ , and interferon-g (IFN-g) on the mRNA expression of human renal transporters using primary human renal proximal tubular epithelial cells (PTECs). Renal cortical tissue, excised from whole human kidneys, was subjected to enzymatic digestion, and the PTECs were isolated by density centrifugation with Percoll. Adhered PTECs on collagen-coated plates were then treated for 72 hours with the above individual or combined cytokines at concentrations of 0.1, 1, and 10 ng/mL in triplicate with daily medium change, and the experiments were conducted in PTECs isolated from 2 female, premenopausal donors. Total RNA was then isolated and subjected to qPCR analysis for multiple renal transporter genes. Exposure to the cytokine cocktail for 72 hours was found to significantly downregulate mRNA expression (in a concentration-dependent manner) of OCT2 and the organic anion transporting polypeptides 4C1 (OATP4C1), by up to 60% and 80%, respectively. An interesting trend was observed with OAT1 and 3, where their mRNA expression was first downregulated at the low cytokine concentration (0.1 ng/mL) and then increased as the cytokine concentration increased. The mRNA expression of the apical transporters, namely MATE2-K, the multidrug resistance protein 2 (MRP2), OAT4, and P-glycoprotein (P-gp), was also significantly downregulated in a concentration-dependent manner by up to 68%, 67%, 75%, and 63%, respectively. Interestingly, the mRNA expression of the novel organic cation transporter 1 (OCTN1) and MRP3 was induced in a concentration-dependent manner by up to 4- and 2.3-fold, respectively. In addition, although the effect elicited by the individual cytokines was less potent, the trend was similar as for the cytokine cocktail, except that the cytokine cocktail appeared to have a synergistic effect in regulating the transporter genes. Furthermore, the data obtained from both donors were comparable. Together, our results show that IL-6, IL-1 $\beta$ , TNF- $\alpha$ , and IFN-g likely synergistically regulate the mRNA expression of various renal uptake and efflux transporters in human PTECs. These changes could potentially translate into changes in protein abundance or activity of these transporters (our future studies), and thus alter drug PK during inflammation or infections.

This work was supported by the NIH Grant R01HD102786.

# Analysis of novel variants in the Cytochrome P450 Oxidoreductase gene found in the Genome Aggregation Database applying Bioinformatics Tools and Functional assays

Maria Natalia Rojas Velazquez,<sup>1</sup> Søren Therkelsen,<sup>2</sup> and Amit Pandey<sup>3</sup>

<sup>1</sup>Univ of Bern; <sup>2</sup>University of Copenhagen; and <sup>3</sup>Univ of Bern,

**Abstract ID 17329**

**Poster Board 584**

Cytochrome P450 oxidoreductase (POR) is the obligatory redox partner of steroid and drug-metabolizing cytochrome P450s located in the endoplasmic reticulum. Mutations in POR cause a broad range of disorders like congenital adrenal hyperplasia and alter the metabolism of clinically relevant drugs. In this study, we analyzed around 400 missense variants of the POR gene indexed in the Genome Aggregation Database (gnomAD) using eleven different *in silico* prediction tools. We identified 64 novel variants that were predicted to be disease-causing in most of the tools. We performed further population analysis of these variants and selected two of them for functional studies as proof of concept. We expressed the human POR wild type and the R268W and L577P variants in bacteria. Subsequently, we performed Kinetics assays of POR activities using model substrates. At last, POR (WT or variants) was mixed with purified cytochrome P450 proteins, and the activities of several cytochrome P450 proteins were assayed. In the kinetics studies, the rates of the reactions with the single point mutations R268W and L577P were considerably lower than the reactions with WT POR. Furthermore, we observed a decrease in the enzymatic activities of the main drug metabolizing enzymes CYP3A4, CYP3A5, CYP2C9, and CYP2C19 in a range between 35 to 85 % with variants of POR compared to WT. These results validated our method of curating a big amount of data from the wide genome projects. To be highlighted, we provided an updated and curated reference source for the diagnosis of POR deficiency. The identification and characterization of POR variants is a useful approach to studying the correlation between structural and functional changes in the POR variants and a valuable tool for clinical diagnosis and genetic counseling.

Supported by grants to Amit V Pandey from the Swiss National Science Foundation, Burgergemeinde Bern and Novartis Foundation for Medical Biological Research. Maria Natalia Rojas Velazquez is supported by a Swiss Government Excellence Scholarship (ESKAS).

# Discovery of Developmental Windows of Drug Sensitivity Using High Content Screening of Normal and Pgp-Knockout Sea Urchin Embryos

Evan Tjeerdema,<sup>1</sup> Yoon Lee,<sup>1</sup> and Amro Hamdoun<sup>1</sup>

<sup>1</sup>University of California, San Diego

Abstract ID 16745

Poster Board 585

P-glycoprotein (Pgp; MDR1; ABCB1) is central to the disposition of drugs and toxicants in adults, and is also crucial for protection of the developing embryo. Despite this fact, there are few developmental models of drug transporter biology. My research takes advantage of the sea urchin, a classical developmental model which produces millions of embryos per spawn, and which has well characterized cell lineages and regulatory networks of development. Here we recently utilized CRISPR/Cas9 mutagenesis to establish a homozygous knockout of Pgp (Pgp<sup>-/-</sup>) and leverage its unique biology to perform high-content imaging of Pgp activity during the early cleavage stages. We found that Pgp<sup>-/-</sup> embryos (n = 322) had a mean 2.67 ± 0.23-fold increase in the accumulation of 250 nM calcein-AM, a fluorescent Pgp substrate, as compared to their wildtype counterparts. In addition the Pgp<sup>-/-</sup> embryos showed increased sensitivity to the cell cycle poisons vinblastine and taxol, with respective EC<sub>50</sub> values of 3.10 μM and 7.69 μM in wildtypes (n = 55 - 787,  $\bar{x}$  = 202) compared to 2.68 μM and 5.28 μM in crispant animals (n = 355 - 806,  $\bar{x}$  = 453). This study represents the first high content pharmacological study of sea urchin embryos and sets the stage for further investigation into developmental windows of vulnerability to xenobiotics. This embryo, which has functionally differentiated cell types forming a digestive system, skeleton, immune system, and germline precursors by the first 24 hours of development, is uniquely powerful for understanding perturbations to these embryonic structures. Each embryonic cell type has a unique suite of drug transporter expression patterns, potentially resulting in differences of xenobiotic penetrance and toxicity between cell types as the embryo develops. By establishing and screening additional drug transporter knockout lines targeting the pharmacologically-relevant genes MDR3/ABCB4, MRP1/ABCC1, and BCRP/ABCG2, we aim to understand the role of these transporters in protecting specific embryonic cell types from xenobiotics during early development.

Support/Funding Information: National Institutes of Health (ES 027921) National Science Foundation (1840844)

# Human Cytochrome P450 Interactions with Redox Partner Cytochrome P450 Reductase

Sarah Burris-Hiday,<sup>1</sup> Mengqi Chai,<sup>2</sup> Michael L. Gross,<sup>2</sup> and Emily Scott<sup>1</sup>

<sup>1</sup>Univ of Michigan; and <sup>2</sup>Washington University in St. Louis

Abstract ID 26765

Poster Board 586

Cytochrome P450 enzymes are heme-containing monooxygenases metabolizing a diverse range of substrates including xenobiotics, steroids, fatty acids, eicosanoids, and vitamins. To accomplish this, 48 of the 57 human P450 enzymes require electrons delivered by the FMN-containing domain of NADPH-cytochrome P450 reductase. Naturally occurring mutations indicate different FMN domain interactions with different human P450 enzymes, but few structural details are known, likely because the complex is transient. To interrogate this interaction, the reductase FMN domain was fused to multiple P450 enzymes, both xenobiotic (CYP3A4, CYP2D6, and CYP2A6) and steroidogenic (CYP17A1 and CYP21A2). Functional studies indicate that the presence of the FMN domain indeed has a P450 isoform- and ligand-dependent effect on ligand binding. Since the FMN domain is not reduced in ligand-binding experiments, these effects are thought to be allosteric in nature. Catalytic turnover under conditions that circumvent the normal electron delivery pathway similarly indicate that FMN domain modulation is different for distinct P450 enzymes.

Mass spectrometry-based protein structural methods are employed to confirm purity and to map the P450/FMN domain interaction in these fusion proteins. Initial native MS analysis confirms the correct molecular weights for the proteins. We are using fast photochemical oxidation of proteins (FPOP) that labels residues irreversibly to footprint differentially the fusion protein, the P450 enzyme alone, and FMN domain alone. Residues protected in the fusion protein but not in the P450 or FMN domain alone should locate the specific P450/FMN domain interaction site. Current results show modest footprinting coverage with FPOP, which is being optimized to make comparisons between the fusion P450, non-fusion P450, and the non-fusion FMN domain. To complement FPOP, benzoyl fluoride (BF) footprinting of nucleophilic amino acid side chains has shown substantial coverage of lysine residues on the proximal side of the P450 where the redox partner would be expected to bind. Therefore, comparative BF footprinting of fusion and non-fusion forms should elucidate how these lysine residues are involved in the P450/FMN interaction.

The functional data demonstrate that there is intricate communication between the P450 surface where the FMN domain of reductase binds, and the buried active site where substrates and inhibitors bind. The isoform and ligand dependence suggests that the redox partner interacts with each P450 isoform in distinct ways. The allosteric effect observed here will be better understood with more structural information from the differential footprinting results. Knowledge about this protein-protein interaction could potentially be exploited to modulate the function of individual P450 isoforms selectively to improve drug metabolism and treat disease.

Funding: NIH R37 GM076343

# Predicting a Safe, Efficacious Human Dose for a Novel Anti-Cryptosporidiosis Therapeutic

Vicky Sun,<sup>1</sup> Ryan Choi,<sup>2</sup> Matthew A. Hulverson,<sup>2</sup> Wesley Van Voorhis,<sup>2</sup> and Samuel Arnold<sup>2</sup>

<sup>1</sup>Univ of Washington; and <sup>2</sup>University of Washington

Abstract ID 21181

Poster Board 587

**Introduction:** Cryptosporidiosis, the disease caused by infection with *Cryptosporidium spp.*, can lead to long-term adverse impacts and even death in malnourished children and immunocompromised patients. Specifically, in children younger than five years old, the disease has myriad detrimental effects that include persistent diarrheal episodes and impairment in cognitive development.<sup>1,2</sup> The only FDA-approved treatment, nitazoxanide, is marginally effective in the populations most impacted by the disease, and new treatment options are urgently needed.<sup>3</sup> Bumped kinase inhibitors (BKIs) represent a promising class of therapeutics that are effective against *Cryptosporidium* infection in preclinical models of disease, and BKI-1708 has emerged as a lead candidate based on its remarkable efficacy and safety profile.<sup>4</sup> Here, we use preclinical efficacy, pharmacokinetic (PK), and toxicity data to identify a safe, effective dose of BKI-1708 for the treatment of *Cryptosporidium* infection in humans.

**Methods:** To characterize the BKI-1708 exposure-response relationship for treatment of *Cryptosporidium* infection, *C. parvum*-infected IFN- $\gamma$ <sup>-/-</sup> mice were treated with a range of BKI-1708 doses. PK models were developed for BKI-1708 using data from PK studies and sparse PK data collected from efficacy studies. To estimate BKI-1708 PK parameters in humans, both allometric scaling and *in vitro* to *in vivo* extrapolation (IVIVE) were used. Allometric scaling was informed by BKI-1708 intravenous (IV) PK studies conducted in mice, rats, dogs, and non-human primates. IVIVE was supported by *in vitro* studies with hepatocytes, microsomes, and purified cytochrome P450 enzymes (CYP450s). BKI-1708 toxicity was characterized in rats and dogs after multiple-dose administration.

**Results/Conclusion:** In mice, a BKI-1708 plasma concentration of 0.12 mg/mL was associated with a 90% reduction in *Cryptosporidium* oocyst shedding in feces. Allometric scaling was used to estimate a BKI-1708 plasma clearance of 5.6 L/h, volume of distribution of 67.1 L, and half-life of 8.4 hours in humans. *In vitro* studies with hepatocytes and CYP450s suggest BKI-1708 is predominantly cleared by CYP3A4. There was a less than 3-fold difference between BKI-1708 clearance values predicted with *in vitro* data and values observed in mice, rats, dogs, and non-human primates. Toxicology studies in rats and dogs demonstrated that BKI-1708 had a safety margin greater than 22. Together, these data were used to identify a safe, efficacious dosing regimen for BKI-1708 treatment of *Cryptosporidium* infection in humans.

## References:

1. Khalil IA, et al. Morbidity, mortality, and long-term consequences associated with diarrhoea from *Cryptosporidium* infection in children younger than 5 years: a meta-analysis study. *Lancet Glob Health* **6**, e758-e68 (2018).
2. Olofin, I., et al. Associations of Suboptimal Growth with All-Cause and Cause-Specific Mortality in Children under Five Years: A Pooled Analysis of Ten Prospective Studies. *PLOS One* **8**, e64636 (2013).
3. Amadi B, et al. Effect of nitazoxanide on morbidity and mortality in Zambian children with cryptosporidiosis: a randomised controlled trial. *Lancet* **360**, 1375-1380 (2002).
4. Castellanos-Gonzalez, A., et al. A novel calcium-dependent kinase inhibitor, bumped kinase inhibitor 1517, cures *Cryptosporidiosis* in immunosuppressed mice. *J. Infect. Dis.* **214**, 1850-1855 (2016).

# Nucleotidases Exhibit Enzymatic Activities Toward the Pharmacologically Active Metabolites of Gemcitabine and Emtricitabine

Herana Seneviratne,<sup>1</sup> Nav R. Phulara,<sup>1</sup> Chiaki Ishida,<sup>2</sup> and Peter Espenshade<sup>2</sup>

<sup>1</sup>University of Maryland, Baltimore County; and <sup>2</sup>The Johns Hopkins University School of Medicine

Abstract ID 54066

Poster Board 588

Nucleoside analog drugs are used to treat HIV and a range of cancers. Emtricitabine (FTC) is a pivotal component of a widely used antiretroviral combination for HIV prevention (as pre-exposure prophylaxis) and treatment. Additionally, gemcitabine (dFdC), an important anticancer drug, is used for the treatment of a range of cancers, including pancreatic cancers. To become pharmacologically active, both FTC and dFdC must be phosphorylated into their triphosphate metabolites. Notably, interindividual variability in responses to the above drugs has been observed clinically. Unfortunately, the observed variability in treatment response can lead to poor clinical outcomes, including therapeutic failure. However, the molecular mechanisms responsible for the observed variability in the above drug responses are poorly understood. Recent studies indicate that alterations in nucleoside analog drug metabolism and disposition can contribute to the observed variabilities in drug responses. Since nucleotidases are known to contribute to nucleotide metabolism by dephosphorylating nucleoside mono, di, and triphosphates, we hypothesize that nucleotidase-mediated dephosphorylation plays a role in regulating pharmacologically active metabolites of the above drugs in tissues. To test our hypothesis, we carried out *in vitro* incubations using a range of recombinant nucleotidases, including 5'-nucleotidases (5'-NTs) and nucleoside triphosphate diphosphohydrolases (NTPDases) in the presence of the metabolites of FTC and dFdC, individually. For assays containing recombinant NTs, we used monophosphate forms of FTC and dFdC whereas triphosphate forms of the above drugs were utilized to test NTPDase activities. Following incubations, a malachite green phosphate assay was employed to determine the release of inorganic phosphate groups, a measure of dephosphorylation. From these, we observed the dephosphorylation of dFdC monophosphate in the presence of two NTs, NT5C1A and NT5C3, individually. Interestingly, only NT5C3 exhibited enzymatic activity toward FTC monophosphate. Further, NTPDase 1 showed enzymatic activity toward both dFdCTP and FTC-TP. Next, since the pancreas is a target site for dFdC treatments, we tested the presence of NT5C3, NT5C1A, and NTPDase 1 in mouse pancreatic tissue using an immunoblotting approach. The results from immunoblotting experiments revealed the presence of NT5C3 and NTPDase 1 in pancreatic tissue lysates. To determine the potential sexual dimorphisms of the expression patterns of the above proteins and to measure relative their abundance, we utilized a mass spectrometry-based proteomics strategy. From these, we detected NT5C3 and NTPDase 1 at high abundance in both male and female mouse pancreatic tissues. In summary, our data suggest that NT5C3 and NTPDase 1 may play a role in the regulation of pharmacologically active metabolites of dFdC and FTC.

# Characterization of Drug Binding to Liver Fatty Acid Binding Protein (FABP1) and Its Effect on Diclofenac Metabolism by CYP2C9

King B. Yabut,<sup>1</sup> Ben Zercher,<sup>1</sup> Matthew F. Bush,<sup>1</sup> and Nina Isoherranen<sup>1</sup>

<sup>1</sup>University of Washington

Abstract ID 27648

Poster Board 589

**Background & Objectives:** Fatty acid binding proteins (FABPs) are highly expressed intracellular proteins that solubilize and shuttle lipophilic ligands to important cellular compartments. Liver FABP(1) comprises 10% of all cytosolic protein (700  $\mu$ M) in the liver, but the role FABP1 has in drug disposition is poorly understood. Recent studies have shown that FABP1 binds the psychoactive cannabinoid THC and its metabolites. Also, FABP1-KO mice have decreased THC metabolism suggesting FABP1 may facilitate THC clearance in the liver which is primarily mediated by cytochrome P450 (CYP) 2C9. Whether human FABP1 binds different classes of drugs and how FABP1 affects drug access to metabolic enzymes like CYP2C9 is not known. We hypothesized that FABP1 binds a variety of drugs and alters their metabolism by CYPs in the liver. The aims of this study were to determine 1) the capacity of FABP1 to bind a panel of lipophilic and acidic drugs and 2) the effect of FABP1 binding on the metabolism of diclofenac, a classic substrate of CYP2C9.

**Methods:** DAUDA fluorescence displacement from FABP1 was used to determine EC<sub>50</sub> values for a panel of 12 drugs. The binding affinity ( $K_i$ ) for diclofenac with FABP1 was also measured. To test whether FABP1 could bind multiple ligands simultaneously, the stoichiometry of FABP1 and bound ligands was verified with native protein mass spectrometry (MS) which utilizes non-denaturing solution conditions to preserve non-covalent interactions. The effect of FABP1 binding on the steady-state kinetics of 4-OH-diclofenac formation was determined via incubations with CYP2C9 Supersomes. Changes in the  $k_{cat}$  and  $K_m$  for 4-OH-diclofenac formation were evaluated in the presence and absence of FABP1.

**Results:** Diclofenac, warfarin, pioglitazone, THC, 11-OH-THC and CBD bound FABP1 with micromolar EC<sub>50</sub> values in DAUDA displacement assays. The  $K_i$  determined for diclofenac binding with FABP1 was 11  $\mu$ M. Native MS studies showed FABP1 bound 2 ligands simultaneously; complexes with 2 molecules of diclofenac or DAUDA and diclofenac were observed. The apparent  $K_m$  of 4-OH-diclofenac formation by CYP2C9 increased with FABP1 ( $1.8 \pm 0.5$  to  $15.0 \pm 5.8$   $\mu$ M) suggesting FABP1 sequestered diclofenac in incubations with CYP2C9. The unbound  $K_m$ , however, was lower in the presence of FABP1 ( $0.9 \pm 0.3$  vs  $1.8 \pm 0.4$   $\mu$ M) and the  $k_{cat}$  unexpectedly decreased for CYP2C9 ( $8.5 \pm 0.7$  to  $4.6 \pm 0.4$   $\text{min}^{-1}$ ). A kinetic model incorporating FABP1 as a non-competitive inhibitor of CYP2C9 fit this data.

**Discussion:** Our studies show that FABP1 binds several lipophilic and acidic drugs with micromolar affinities and FABP1 has the capacity to bind multiple drug ligands simultaneously. Hence, based on FABP1 expression in the liver and circulating concentrations of drug ligands tested, a significant fraction of these drugs is expected to be bound to FABP1 *in vivo*. Incubations with CYP2C9 confirmed FABP1 alters diclofenac metabolism. The decrease in  $k_{cat}$  for 4-OH-diclofenac formation by CYP2C9 suggests FABP1 may directly interact with CYP2C9. These results suggest FABP1 may be a determinant of drug metabolism in the liver by having the capacity to bind multiple drug ligands and altering drug metabolism via direct protein-protein interactions with CYPs.

# Identification of 5-hydroxycotinine in the Plasma of Nicotine-treated Mice-Implications for Cotinine Metabolism and Disposition *in vivo*

Keiko Kanamori,<sup>1</sup> Syed M. Ahmad,<sup>2</sup> and Kabirullah Lutfy<sup>3</sup>

<sup>1</sup>Western Univ of Hlth Sciences; <sup>2</sup>Western Univ of Hlth Sci; and <sup>3</sup>Western Univ of Health Sciences College of Pharmacy

Abstract ID 16490

Poster Board 590

**Introduction:** Nicotine, the addictive ingredient of tobacco, is metabolized in the liver to cotinine - the stable biomarker of nicotine use. Cotinine is further oxidized to 3-hydroxycotinine (as detected in the plasma) for renal excretion. In mice, these reactions are catalyzed by the microsomal enzyme CYP2A5 which closely resembles human CYP2A6.

**Aim:** Is 3-hydroxycotinine the only major oxidation product of cotinine?

**Methods:** Mice were injected with nicotine (1 mg/kg s.c.) or exposed to e-cigarettes containing 2.4% nicotine for 4 h. Blood was collected 15 min post-injection, or 5-6 min after the end of e-cigarette exposure. Plasma nicotine metabolites were quantified by liquid-chromatography mass-spectrometry. The novel aspect of this study is that all isomers of 3-hydroxycotinine, with the same mass but different retention times, were examined.

## Results:

- 5-hydroxycotinine and cotinine N-oxide, with their peaks well resolved from that of 3-hydroxycotinine, were detected for the first time in the plasma of nicotine-treated mice (1), in addition to the previously reported 3-hydroxycotinine. 5-hydroxycotinine was as abundant as 3-hydroxycotinine in the plasma of (i) nicotine-injected mice, and (ii) in the e-cig-treated mice with plasma nicotine levels similar to those of human smokers. Plasma cotinine-N-oxide was less abundant, but readily measurable.
- The combined plasma concentration of 3-hydroxycotinine + 5-hydroxycotinine + cotinine-N-oxide was significantly higher in female than in male mice ( $n=5-6$ ), whereas for cotinine alone, the male-female difference was not significant.

## Significance:

- 5-hydroxycotinine needs to be taken into account in examining nicotine disposition *in vivo* not only in mice, but possibly also in human smokers where its presence in the urine is controversial (2). *In vitro*, 5-hydroxycotinine was detected upon incubation of human CYP2A6 with hamster liver microsomes and cotinine (3). Interestingly, the approximately equal rates of 3- and 5-cotinine hydroxylation in this *in vitro* system are in accord with our present finding that approximately equal quantities of plasma 3-hydroxycotinine and 5-hydroxycotinine are formed by mouse CYP2A5 *in vivo* upon nicotine administration. 5-hydroxycotinine may have eluded detection due to glucuronidation, and/or the lower sensitivity of the previously-used tandem mass spectrometry instead of the present direct high-resolution mass-spectrometry to monitor the parent ions.
- Because the oxidation of cotinine to 3-hydroxycotinine, 5-hydroxycotinine and cotinine N-oxide is catalyzed by a single enzyme (CYP2A5), the combined plasma concentrations of these metabolites reflect better the male/-female difference in CYP2A5 activity than the concentration of cotinine alone, which is formed from nicotine by two-step reactions. Our present results strongly suggest that 5-hydroxycotinine needs to be taken into account in future studies on sexual dimorphism of CYP2A5 activity and its regulation.

## References:

1. Kanamori K, Ahmad SM, Shin CS, Hamid A, Lutfy K. (Dec. 2022) *Drug Metab Dispos*, **50**:1454-1463.
2. Murphy SE (2021). *J Biol Chem* **296**:100722.
3. Murphy SE, Johnson LM, Pullo DA (1999) *Chem Res Toxicol* **12**:639-645.

The present studies were partly supported by the Tobacco Related Disease Research Program (TRDRP) Grant 24RT-0023 (KL) and partly by the Department of Pharmaceutical Sciences, College of Pharmacy, Western University of Health Sciences, Pomona, CA 91766



# Identifying the mechanism underlying iatrogenic intravenous paracetamol-induced hypotension

Thomas A. Jepps,<sup>1</sup> Johs Dannesboe,<sup>1</sup> Joakim Bastrup,<sup>1</sup> and Clare L. Hawkins<sup>1</sup>

<sup>1</sup>University of Copenhagen

Abstract ID 25830

Poster Board 591

**Background:** Intravenous acetaminophen (APAP; paracetamol) is used commonly in the intensive care unit or post-surgery for its analgesic effect. Intravenous administration of APAP is well documented to cause severe transient hypotension. The mechanism underlying these hemodynamic changes is still not clear, but we showed previously that the APAP metabolite N-acetyl-p-benzoquinone-imine (NAPQI) can directly and indirectly active voltage-gated Kv7 channels in vascular smooth muscle cells promoting a vasodilation.

APAP metabolism to NAPQI requires cytochrome P450 enzymes, which are also present in the vascular wall. Furthermore, another pathway of NAPQI formation is activated myeloperoxidase (MPO). MPO is a peroxidase enzyme that is primarily used by neutrophils as part of the innate immune system response and the circulating level of MPO is elevated in critically ill patients. MPO could be the missing link of why critically ill patients experience the most severe hypotension and hemodynamic instability caused by intravenous paracetamol.

**Method:** Human Coronary Artery Endothelial Cells (HCAEC) and HEK293 cells were treated with APAP (0 – 50 mM) or APAP metabolites (0 – 50  $\mu$ M) to see the effect on viability and thiol concentration levels.

The formation of APAP-adducts by cytochrome P450 and MPO was investigated by immunocytochemistry (ICC), enzyme activity assays based on thiol assays, Western Blot (WB) and Mass Spectrometry (MS).

Furthermore, individual cytochrome P450 expression and location was investigated by overexpression of CYP20A1, immunocytochemistry, Western Blot and Mass Spectrometry.

**Results:** APAP decreased viability and thiol levels in a concentration dependent manner similar to NAPQI, but not AM404 (another APAP metabolite) in HCAEC cells. The cytochrome P450 inhibitor Ketoconazole partially rescued the drop in viability and thiol levels. Using ICC, we visualized APAP-adducts, which formed when treating HCAEC cells with APAP. One of the last orphan cytochrome p450 enzymes, CYP20A1, is expressed in both HEK293 and HCAEC and are upregulated in response to treatment of APAP. By overexpressing CYP20A1 in HEK293B cells, we identify APAP as the first substrate of CYP20A1.

In addition to investigating how NAPQI is formed by CYP450 enzymes in endothelial cells, we examined the formation of NAPQI by MPO. Using thiol assays, western blot and mass spectrometry, we found that MPO can form high levels of NAPQI.

**Summary:** Our findings show that NAPQI formation from APAP can occur via two pathways: cytochrome P450 enzymes and MPO. Both of these are potential mechanisms underlying IV APAP-induced hypotension, with the MPO pathway likely driving NAPQI production in the critically ill. CYP20A1 is a potential candidate involved the metabolism of APAP in endothelial cells. By improving our understanding of the metabolism of IV APAP, we might be able to prevent the iatrogenic hypotension.

This work was support by a Department of Biomedical Sciences (University of Copenhagen) Collaboration grant.

# Redox Partner Adrenodoxin Allosterically Alters the Function of the Human Steroidogenic Cytochrome P450 11B Enzymes

Cara Loomis,<sup>1</sup> Sang-Choul Im,<sup>1</sup> Michelle Redhair,<sup>2</sup> and Emily Scott<sup>3</sup>

<sup>1</sup>University of Michigan, Division of Metabolism, Endocrinology, & Diabetes, Department of Internal Medicine, Veterans Affairs Medical Center; <sup>2</sup>University of Washington, Department of Medicinal Chemistry; and <sup>3</sup>University of Michigan, Departments of Biological Chemistry, Medicinal Chemistry, and Pharmacology

Abstract ID 28439

Poster Board 592

Cytochrome P450 (CYP) enzymes are a class of heme monooxygenases with diverse functions, including steroid hormone synthesis. The human CYP11B enzymes play key roles in steroidogenesis by producing cortisol (CYP11B1) or aldosterone (CYP11B2) and are drug targets for Cushing's disease and primary aldosteronism, respectively. Development of selective drugs for either disease state has been hindered by the 93% sequence identity between the two enzymes. Further structural and functional characterization of these enzymes is necessary to identify differences between the two enzymes that can be exploited to improve drug selectivity. Both enzymes require reduction during two transient interactions with the iron-sulfur protein adrenodoxin per catalytic cycle. Previously, equilibrium and stopped flow studies determined that adrenodoxin binding on the P450 surface allosterically modulates ligand binding in the CYP11B1 and CYP11B2 active sites  $\sim 18$  Å away (1,2). Adrenodoxin increases both substrate affinity and saturation by increasing the on rate and decreasing the off rate. Recently an orthogonal stopped-flow experiment cross-validated adrenodoxin suppression of substrate release.

The current focus is to determine the mechanism by which adrenodoxin causes these effects for both CYP11B1 where substrate binding is monophasic and CYP11B2 where substrate binding is biphasic. Thus, kinetic modeling experiments in MATLAB are being used to fit the data to specific mechanisms. These models range from adrenodoxin affecting conformational selection or induced fit, as well as more complex models considering ligand depletion, substrate reorientation, or a combination of conformational selection and induced fit. Fitting the initial data available suggests that ligand depletion is not applicable, but is insufficient to discriminate between a number of the other mechanisms. However, the data fitting process suggests optimal stopped-flow experimental conditions that can be used to distinguish between mechanisms. Thus cyclical integration of experimental and computational approaches are being used to elucidate differences in adrenodoxin effects on the substrate binding mechanism between CYP11B1 and CYP11B2. Understanding how these enzymes work and the differences between them have the potential to drive selective drug design strategies.

1. Brixius-Anderko S & Scott EE. JBC, 2021.
2. Loomis CL, Brixius-Anderko S, and Scott EE. JIB, 2022.

Support/Funding Information: NIH R01 GM135346 and F31 HD111338

# Chronic Exposure to Organophosphate Pesticides and Elevated Markers of Systemic Inflammation: Possible Neuroinflammatory and Genotoxic Effects

Dina El-Gameel,<sup>1</sup> Noha A. Hamdy,<sup>2</sup> Amira F. El-Yazbi,<sup>2</sup> Maha A. Ghanem,<sup>3</sup>  
Labiba K. El-Khordaugi,<sup>2</sup> Salwa M. Abdallah,<sup>4</sup> Yehia Mechref,<sup>5</sup> and Ahmed F. El-Yazbi<sup>6</sup>

<sup>1</sup>Alexandria University Hospitals, Alexandria, Egypt; <sup>2</sup>Faculty of Pharmacy, Alexandria University, Egypt; <sup>3</sup>Faculty of Medicine, Alexandria University, Egypt; <sup>4</sup>Central Agricultural Pesticides Lab (CAPL), Agricultural Research Center (ARC), Cairo, Egypt; <sup>5</sup>Texas Tech University, Texas, United States of America; and <sup>6</sup>Alamein International University, Alamein, Egypt

Abstract ID 19069

Poster Board 27

**Introduction:** Climate change alters not only cultivation seasons but also pest population. This led to adaptive responses in the farming industry increasing organophosphate pesticide (OP) use. This is particularly problematic in smallholder growers self-applying pesticides without the appropriate safety precautions. Several studies addressed the neurotoxic and metabolic effects of chronic exposure to OPs including delayed polyneuropathy and Gulf War Illness. Further, some studies highlighted a controversial link between chronic organophosphate exposure and the development of neurodegenerative diseases. While these neurotoxic effects were attributed to various mechanisms besides neurotoxic esterase inhibition, including inflammation, systematic examination of the inflammatory and cell damage consequences have not been forthcoming.

**Aim:** To conduct targeted, proteomic and glycomic examination of markers of inflammation, nerve damage, and metabolic dysfunction in serum samples of smallholder vegetable farmers with repeated exposure to selected OPs, as well as assessing the different potential cytotoxic effects of these OPs.

**Methodology:** Serum samples (n=31) were obtained from male farmers (18-60 years old) with chronic OP exposure, after signing an informed consent. A questionnaire was used to collect patients' demographics, years of OPs exposure, as well as their general health status, history of the types of pesticides contacted, and development of cholinergic symptoms, if any. Serum markers measured include: Interleukin 6 (IL-6) & C-Reactive protein (CRP), full lipid panel, liver enzymes (ALT & AST), and serum creatinine (sCr). These parameters were compared to values in a corresponding control group of healthy city dwellers with matched age and gender. Alongside, a fluorimetric DNA probe assay was used to determine the DNA damage kinetics induced by profenophos and chlorpyrifos, commonly used OPs. Student's *t*-test was used to compare the parameters measured. A *P*-value < 0.05 was considered significant.

**Results:** Compared to healthy controls, subjects with repeated exposure to OPs showed an elevation of liver (AST: 30.86±1.89 vs. 18.88±1.04 U/L in control) and kidney function parameters (sCr: 1.1±0.03 vs. 0.88±0.05 mg/dl in control), as well as IL-6 (5.17±0.2 vs. 3.19±0.4 pg/ml in control), indicating a subtle state of liver and renal impairment as well as chronic inflammation. No changes in serum CRP or lipids were observed. Interestingly, none of the elevated markers correlated positively with the self-reported severity of cholinergic symptoms occurring immediately after exposure, potentially precluding cholinesterase inhibition as the cause for the observed impairment. On the other hand, profenofos and chlorpyrifos were shown to induce significant DNA damage, with double strand breaks observed with concentrations as low as 200 and 400 nmol/L, respectively.

**Conclusions:** Chronic exposure to OPs appears to induce inflammation and organ impairment that are not related to cholinesterase inhibition. Potential mechanisms include possible cytotoxic effects through DNA damage. Further studies are underway to assess the apoptotic potential of OPs and to profile their proteomic and glycomic impact on subjects of chronic exposure.

# Antithrombotic Therapy Optimization in a Quaternary Care Center Anticoagulation Clinic in the Middle East

Emna Abidi,<sup>1</sup> Patricia Bon,<sup>2</sup> Ramzi Khaddage,<sup>3</sup> Antoine Cherfan,<sup>3</sup> Mohammad Kolailat,<sup>3</sup> Ziad Sadik,<sup>3</sup> and Bassam Atallah<sup>4</sup>

<sup>1</sup>Cleveland Clinic Abu Dhabi; <sup>2</sup>Cleveland Clinic Abu Dhabi, Abu Dhabi, United Arab; <sup>3</sup>Cleveland Clinic Abu Dhabi, Abu Dhabi, United Arab Emirates; and <sup>4</sup>Cleveland Clinic Abu Dhabi, Reem island, United Arab Emirates

Abstract ID 19119

Poster Board 28

**Introduction:** Antithrombotic therapy (AT) widely consists of combining anticoagulants with, one or more, antiplatelet (AP) agents. Pharmacist led anticoagulation clinics (AC) frequently focus on warfarin management. However, an overall assessment of indications and potential for combined regimens de-escalation is also needed, especially considering evidence supporting monotherapy for stable CAD in the setting of AF, to reduce bleeding risk.

**Research Hypothesis:** We hypothesize that a systematic, team-based, patient-centered, pharmacy led approach towards AT stewardship would limit the number of patients receiving potentially inappropriate combined AT and simplify regimens.

**Study Design:** This is a retrospective, observational investigation study conducted at an ambulatory AC at a quaternary care center in the Middle East.

**Methods:** A retrospective chart review was performed on all patients following in the AC between December 2020 and December 2021. We identified patients managed for warfarin monitoring, with and without concurrent AP, and assessed for appropriateness to switch to DOACs and to de-escalate combined AT. In addition to the recent trials and known indications and exclusions, relevant guidelines were utilized in the assessment including the 2022 USPSTF for primary prevention and the 2020 ACC/AHA for valvular heart disease.

**Results:** 94 patients were included, 85 (90.4%) on warfarin; 10 (11.8%) deemed candidate to switch to DOACs, 19 (22.4%) potential candidates, in need for further discussion with their treating physician, and 56 (65.9%) not candidates for switching. Moreover, 35 (37.2%) of the total patients were on combined AT; 30 (85.7%) on concurrent aspirin, 6 (17.1%) on P2Y<sub>12</sub>, and 1 (2.9%) on triple therapy. After assessing for AT de-escalation, 12 (34.3%) of the AP treated patients were deemed potential candidates after discussion with their treating physician.

**Conclusion:** This project represents a proof-of-concept to explore the utility, and later the feasibility, of a protocol based approach, switching to DOACs and de-escalating concurrent AP in a quaternary care center in the Middle East.

**Table 1 Demographics and characteristics of antiplatelets receivers vs. non-receivers in anticoagulation clinics patients**

Variables	Overall	On concurrent antiplatelet	
		No	Yes
No. (%)	94	59 (62.8)	35 (37.2)
<b>Gender, no. (%)</b>			
Male	53 (56.4)	35 (66.0)	18 (34.0)
Female	41 (43.6)	24 (58.5)	17 (41.5)
Age, mean± SD, years	53.0 ± 16.9	53.5 ± 17.6	52.1 ± 15.8
<b>Warfarin indications*, no. (%)</b>			
Atrial fibrillation	37 (39.4)	22 (59.5)	15 (40.5)
<b>Valvular disease</b>			
Bioprosthetic	13 (13.8)	4 (30.8)	9 (69.2)
Mechanical valve	31 (33)	16 (51.6)	15 (48.4)
Other valvular disease <sup>§</sup>	5 (5.3)	3 (60)	2 (40)
<b>VTE</b>			
DVT/PE	21 (22.3)	18 (85.7)	3 (14.3)
Other VTE <sup>¶</sup>	3 (3.2)	3 (100.0)	0
Cardiac thrombus	15 (16.0)	6 (40.0)	9 (60.0)
Cerebral vein thrombosis	2 (2.1)	2 (100.0)	0
Budd Chiari syndrome	1 (1.1)	1 (100.0)	0
Antiphospholipid antibody syndrome	7 (7.5)	5 (71.4)	2 (28.6)
Hypercoagulable state <sup>¶</sup>	5 (5.3)	4 (80.0)	1 (20.0)
Chronic Thromboembolic Pulmonary Hypertension	3 (3.2)	3 (100.0)	0
LVAD	1 (1.1)	0	1 (100.0)
CHA <sub>2</sub> DS <sub>2</sub> -Vasc score, mean (SD)	3.6 (1.8)	3.6 (1.8)	3.7 (1.8)
HAS-BLED score, mean (SD) <sup>§</sup>	2.1 (1.2)	2.5 (1.2)	1.6 (1.1)
<b>Potential to switch to DOAC<sup>#</sup></b>			
On Warfarin	85 (90.4)	54 (63.5)	31 (36.5)
Candidate	10 (11.8)	9 (90.0)	1 (10.0)
Potential candidate after discussion with physician	19 (22.4)	6 (31.6)	13 (68.4)
Not candidate	56 (65.9)	39 (69.6)	17 (30.4)

**Table 2: Indications and appropriateness for concurrent antiplatelet therapy**

Antiplatelets <sup>#</sup> , no. (%)	35 (37.2)
Aspirin	30 (85.7)
P2Y <sub>12</sub> , Clopidogrel	6 (17.1)
<b>Antiplatelet indications, no. (%)</b>	
Patients on antiplatelet for primary prevention and for indications other than ASCVD	7 (20.0)
Patients on antiplatelet for secondary prevention of ASCVD <sup>#</sup>	28 (80.0)
Aspirin	23 (82.1)
Clopidogrel	6 (21.4)
<b>Potential to de-escalate concurrent antiplatelets</b>	
<b>Candidate for de-escalation of antiplatelet for primary prevention</b>	
Patients on aspirin for primary prevention but not eligible as per USPSTF guidelines <sup>§</sup> , no. (%)	4 (11.4)
≥60 years old	2 (40.0)
<40 years old	2 (40.0)
<b>Candidate for de-escalation of antiplatelet for secondary prevention</b>	
Aspirin post ACS, PCI or CABG with AF > 1 year	6 (17.1)
<b>Candidate for de-escalation of antiplatelet for indication other than ASCVD</b>	
Aspirin and/or P2Y <sub>12</sub> for Mechanical valve without any other indication.	2 (5.7)

**Table 1:**

<sup>§</sup>Such as severe AR, mitral valve repair, mitral stenosis

<sup>¶</sup>Such as portal and mesenteric thrombus

<sup>¶</sup>Such as Factor V Leiden mutation, protein S deficiency, and systemic lupus erythematosus other than APLS

<sup>§</sup>Some data for HAS-BLED score calculation was missing in 16 patients.

**Percentages may not add up to 100% due to:**

\*Some patients having multiple warfarin indications.

<sup>#</sup>9 patients were already switched to DOAC.

**Table 2:**

**Numbers may not add up to 100% due to:**

<sup>#</sup> 1 patient on both clopidogrel and aspirin

<sup>§</sup> 1 patient could not be assessed for primary prevention non-eligibility due to missing data for ACC/AHA 10 years ASCVD risk calculator (cholesterol levels)

# Excessive exercise increases metabolites associated with pathophysiologic changes in ultramarathon runners

Mikolaj Marszalek,<sup>1</sup> Zofia Wicik,<sup>2</sup> Andrzej Ciechanowicz,<sup>2</sup> Disha Keswani,<sup>2</sup>  
Ceren Eyiletlen-Postula,<sup>2</sup> Szczepan Wiecha,<sup>3</sup> Lukasz Malek,<sup>4</sup> Magdalena Kucia,<sup>2</sup> and  
Marek Postula<sup>2</sup>

<sup>1</sup>Medical Univ of Warsaw; <sup>2</sup>Medical University of Warsaw; <sup>3</sup>Joseph Pilsudski University of Physical Education in Warsaw; and  
<sup>4</sup>National Institute of Cardiology

Abstract ID 19116

Poster Board 29

**Introduction:** Regular physical exercise is analogous to improved cardiovascular health and increased longevity. However, if in excess it can act as a double edged sword. Acute bouts of extreme physical activity trigger complex molecular responses reflected by changes in inflammatory markers and metabolic pathways that are believed to yield detrimental effects on the cardiovascular system (CVS)<sup>1</sup>.

**Purpose:** We aimed to assess the effects of high-intensity and long-lasting exercise prototype (100km run) on the metabolomic changes in a unique population of high-level long-term ultra-marathon runners.

**Methods:** Plasma samples were collected from ultramarathon runners (n=22) with 2-time points: before and after the run (Completion (100 km) or exhaustion (52 - 91 km, median 74 km)).

For untargeted metabolomic analysis we used ultra-high resolution Fourier-Transform Ion Cyclotron Resonance Mass Spectrometry with an electrospray ion source in direct injection. Mass spectra were analyzed by T-Rex2D algorithm in the MetaboScape5.0. Identified compounds were ontologically analyzed using MetaboAnalystR. MetscapeCytoscape plugin was used for metabolite-gene interaction analysis and gene lists were obtained from Biomart and DisGeNet.

**Results:** Mann-Whitney test (FDR<0.05) identified 1601 up and 1030 downregulated metabolites with a at least 2 fold of difference after high-intensity run. Enrichment analysis showed that the top pathways affected by analyzed metabolites were the TCA cycle (FDR=0.0442), metabolism of; Sphingolipids (p=0.00774), Glyoxylate and dicarboxylate (p=0.0249) and Butanoate (p=0.0352). Top disease phenotypes associated with differentially regulated metabolites were critical illness (major trauma, severe septic shock, or cardiogenic shock) (p=0.00154) and multiple CVS-related diseases (Fig a).

Top after the run up-regulated metabolites identified in the study included heart failure associated acetylcarnitines2 CAR(14:2) (log<sub>2</sub>FC=11.57; AUC=0.97), Dodecanoylcarnitine (2.00;0.960), 9-Decenoylcarnitine (1.78;0.95), CAR(DC8:0) (14.99;0.94), but also 2-Carboxy-5,7-dimethyl-4-octanolide (8.04;0.98), Methylmalonic acid (9.33;0.96) and cardiotoxic Cyclophosphamide (16.29;0.940)<sup>3</sup>. Top down-regulated metabolites after the run included potentially cardio-protective Gamma Glutamylglutamic acid (log<sub>2</sub>FC=-1.81; AUC=0.85), Fructose 1,6-bisphosphate (-2.42;0.88)<sup>4</sup>, Oleamide (-1.82;0.86) and gamma-Glutamylglycine (-7.98;0.85).

Interaction network analysis focused on genes associated with CVS identified atherosclerosis/ obesity-related Phospholipase A2 Group IB (PLA2G1B) as potentially the most affected gene by analyzed metabolites (Fig e).

**Conclusion:** Results show a twofold post run increase in metabolites that are both potential markers for acute exercise and that are strongly associated with CV diseases. This calls for consideration of the detrimental effects of excessive exercise and implementation of monitoring in amateur athletes.

Granted by the Medical University of Warsaw 1M9/2/M/MGED/N/22

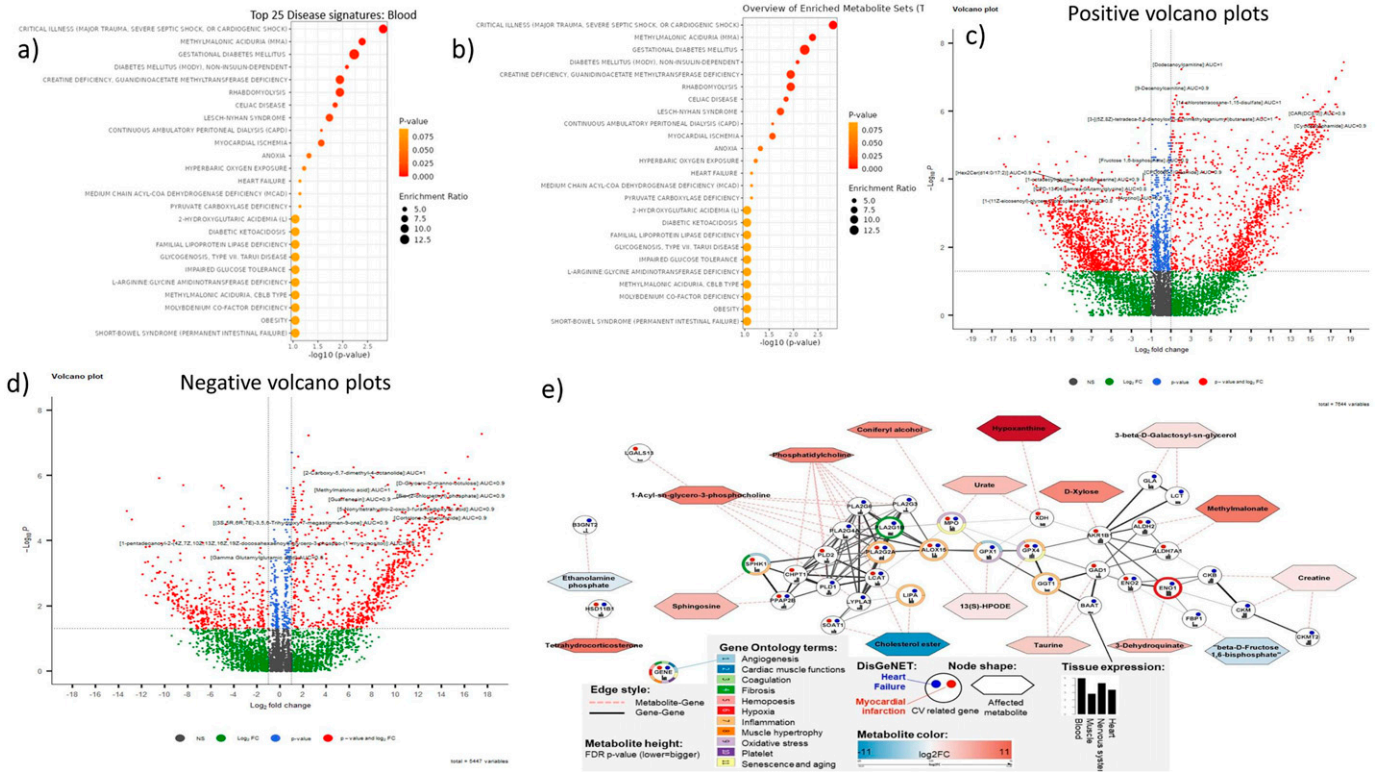


**Figure a)** Multiple CVS-related diseases signatures, **b)** overview of enriched metabolite sets with enrichment ratios, **c)** positive volcano plots, **d)** negative volcano plots, **e)** Interaction network analysis

# Social stress causes the emergence of functional Histamine H3 Receptors in urinary bladder smooth muscle

B Malique Jones,<sup>1</sup> Nathan Tykocki,<sup>1</sup> and Gerald Mingin<sup>2</sup>

<sup>1</sup>Michigan State Univ; and <sup>2</sup>University of Vermont Larner College of Medicine

Abstract ID 22897

Poster Board 30

Inflammatory hyperalgesia induced by mast cell degranulation releases histamine within the urinary bladder that disrupts the micturition reflex and alters detrusor contractility. Psychological stress also causes lower urinary tract symptoms (frequency, urgency, and hesitancy) in 4-week-old mice with a pathophysiology similar to neurogenic inflammatory hyperalgesia. Most investigations have solely focused on molecular changes to nerve sensitivity instead of direct changes to urinary bladder smooth muscle activity. Recently, our lab found that the urinary bladder smooth muscle of unstressed mice contracted and rapidly desensitized to histamine in an H1 receptor-dependent manner. We hypothesized that social stress increases histamine H1 receptor mRNA expression to prolong histamine-induced urinary bladder smooth contractions. 4-week-old C57BL/6 male (N=6) mice were randomly housed with CD1 adult male aggressor mice for 5 minutes, after which both mice were placed in barrier housing for 1 hour. Social stress was repeated with different aggressor mice for 14 days. Afterward, bladders from 6-week-old mice were dissected and cut into strips from non-stressed (N=3) and stressed (N=3) mice to measure isometric contractile force generation and changes in contractility by histamine (200  $\mu$ M). Individual bladder smooth muscle cells were also dissociated and collected for single-cell qRT-PCR. Counter to our hypothesis, histamine-induced contractions were markedly reduced in stressed as compared to non-stressed mice. Surprisingly, however, single-cell qRT-PCR performed on isolated smooth muscle cells uncovered an upregulation of histamine H3 receptor mRNA in stressed mice that was absent in non-stressed mice. H3 receptors were present and constitutively active in the tissue, as the H3 receptor antagonist ciproxifan (10  $\mu$ M) recovered the response to histamine in stressed bladders but had no effect in non-stressed bladders. In both conditions histamine-induced contractions rapidly desensitized, implying that H3 receptors do not affect this physiological mechanism. Our data aligns with previous findings that support a role for elevated histamine H3 receptor mRNA in patients with interstitial cystitis. Additionally, our data suggest that the histamine H3 receptor might have a protective role in social stress by preventing histamine-induced changes to smooth muscle contractility in stressed bladders.

This research is supported by NIH P20-DK127554 (NRT), NIH R01-DK119615 (NRT & GCM), and NIH R01 Supplement (BMJ).



# Finasteride Induces Epigenetic Alteration of TMPRSS2 Gene Expression: A Potential role in Severe Acute Respiratory Syndrome-Corona Virus-2 Inhibition

CHURCHILL IHENTUGE,<sup>1</sup> and Antonei B. Csoka<sup>2</sup>

<sup>1</sup>Texas Tech University Health Sciences Center, El Paso; and <sup>2</sup>Howard University, Washington D.C

**Abstract ID 52457**

**Poster Board 31**

SARS-COV-2 is a virus that causes the transmission of COVID-19 disease that has killed millions of people worldwide. Effort is ongoing to find a cure for this endemic disease. Recent investigations have revealed that SARS-COV-2 viral activation, penetration and multiplication in host tissue is dependent on the TMPRSS2 protein. Finasteride, a type-II 5 $\alpha$ -reductase inhibitor that decreases levels of dihydrotestosterone, is used in the treatment of benign prostatic hyperplasia. In prior work aimed at evaluating the epigenetic effects of finasteride on signaling pathways in human Leydig cells, we identified several genes in the prostatic cancer pathway that were differentially methylated. These included AR, E2F2, ERBB2, FGFR2, GSK3B, HSP90AA1, IKBKB, IL1R2, LEF1, PDGFB, PDGFC, PIK3CB, RB1 and TMPRSS2. Finasteride decreases TMPRSS gene expression through DNA methylation. We therefore suggest that finasteride could play an important role in decreasing infectivity of the SARS-COV-2 virus and inhibition of viral spike priming by inducing epigenetic changes in TMPRSS2.

# Compound 48/80 increases bladder wall mechanical compliance via activation of MMP-2

Pragya Saxena,<sup>1</sup> Sara Roccabianca,<sup>2</sup> and Nathan Tykocki<sup>1</sup>

<sup>1</sup>Michigan State Univ; and <sup>2</sup>Michigan State University

Abstract ID 26334

Poster Board 32

**Background:** Alteration in wall stiffness and bladder compliance can disrupt normal bladder function and lead to lower urinary tract symptoms (LUTS). Urinary bladder fibrosis due to inflammation is implicated in many clinical cases of LUTS. Mast cell activation represents a key target to understand the fibrotic inflammatory pathways within the bladder wall. Our lab has previously shown that mast cell activation using Compound 48/80 increases mechanical compliance and detrusor contractility, and prostaglandins and matrix metalloproteases (MMPs) released from mast cells can directly alter the mechanical properties of the bladder wall. Blocking the release of prostaglandins blocks the increase in both mechanical compliance and detrusor contractility; however, the specific MMPs responsible for driving changes in compliance are unknown. Thus, in this study we pharmacologically investigated the role of specific MMPs in driving the increase in compliance upon mast cell activation. We hypothesized that MMP-2 is present in the urinary bladder wall and is responsible for the increase in mechanical compliance caused by mast cell degranulation.

**Methods:** Whole mouse bladders from C57Bl/6 (wild-type) mice were dissected and mounted in the custom-designed pentaplanar reflected image macroscopy (PRIM) system for simultaneous measurement of transient pressure events, intravesical pressure, bladder volume, wall stress, and wall stretch during *ex vivo* bladder filling. Wall compliance was derived as a measure of the stress *versus* stretch relationship using the pressure-volume curves and associated wall geometry gathered from imaging data. Bladders were exposed to Compound 48/80 (10  $\mu$ g/ml) in the presence of vehicle, the broad-spectrum MMP inhibitor marimastat (10  $\mu$ M), or the MMP2 inhibitor ARP-100 (10 $\mu$ M) during *ex vivo* filling. MMP-2 protein expression in whole urinary bladder protein isolates was also determined using western blot analysis.

**Results:** Western blot analysis showed that MMP-2 is present in the bladder wall in both detrusor and urothelium layers. Both marimastat and ARP-100 completely abolished the increase in compliance caused by Compound 48/80. However, neither altered the increase in amplitude of transient pressure events.

**Conclusions:** These findings suggest that the effects of mast cell activation are dual in nature: mast cell activation causes a release of prostaglandins that directly alter detrusor contractility and also increase wall compliance by activating MMP-2. Increases in excitability and profound bladder wall remodeling also occur in minutes after degranulation, suggesting these mechanisms are initiated rapidly after inflammatory insult.

Support/Funding Information: R01DK119615 (NRT) and P20DK127554 (SR and NRT).

# 3D Reconstruction Reveals Changes in Mitochondrial Morphology in Mouse Skeletal Muscle Across Aging and Upon Loss of the MICOS Complex

Kit Neikirk,<sup>1</sup> Zer Vue,<sup>2</sup> Larry Vang,<sup>2</sup> Edgar Garza-Lopez,<sup>3</sup> and Antentor Hinton<sup>2</sup>

<sup>1</sup>University of Hawaii at Hilo; <sup>2</sup>Vanderbilt University; and <sup>3</sup>University of Iowa

Abstract ID 13843

Poster Board 51

Mitochondria are active organelles, undergoing harmonized cycles of fission and fusion, driven by 'mitochondrial dynamics,' to retain their morphology, distribution, and size. Mitochondrial dynamics has emerged as a critical process in maintaining cellular homeostasis. Interestingly, it has been long respected that a decrease in mitochondrial function escorts aging in specific tissues. For example, skeletal muscle gradually loses mass, strength, endurance, and oxidative capacity during aging. This decrease might, in turn, contribute to the observed age-dependent decline in organ function by mutations or alterations in mitochondrial fusion and fission proteins associated with several diseases. However, new players in regulating mitochondrial shape and cristae shape have been recently studied, such as the mitochondrial contact site and cristae organizing system (MICOS) complex. The MICOS complex is a multi-protein interaction hub that helps define cristate and mitochondria architecture. However, the MICOS complex has not been implicated in regulating organelle structure changes during aging. Thus, we hypothesized that loss of the MICOS complex during aging may increase mitochondrial fragmentation, decrease nanotunnels, and alter cristae morphology. To do this, we examined the three-dimensional morphology of mitochondria networks in young (3-month) and aged (2-year) murine gastrocnemius muscle via serial block face-scanning electron microscopy and the Amira program for segmentation, analysis, and quantification. We found differences in mitochondrial network configuration, nanotunneling, size, shape, number, contact sites, and MICOS gene expression in skeletal muscle during aging. We also found an association between OPA-1 and the MICOS complex in the gastrocnemius with mitochondrial aging. Furthermore, the loss of the MICOS complex was linked with decreased oxidative capacity and altered mitochondrial metabolism. Importantly, this highlights the importance of investigating the repair of muscle using novel mitochondrial therapies. For example, activating transcription factor-4 (ATF4) may be able to restore mitochondrial cristae integrity. Together, these results suggest a novel relationship between the MICOS complex and aging in skeletal muscle.

Support/Funding Information: The United Negro College Fund/Bristol-Myers Squibb E.E. Just Faculty Fund, BWF Career Awards at the Scientific Interface Award, BWF Ad-hoc Award, NIH Small Research Pilot Subaward to 5R25HL106365-12 from the National Institutes of Health PRIDE Program, DK020593, Vanderbilt Diabetes and Research Training Center for DRTC Alzheimer's Disease Pilot & Feasibility Program. CZI Science Diversity Leadership grant number 2022- 253529 from the Chan Zuckerberg Initiative DAF, an advised fund of Silicon Valley Community Foundation.

# Beta-hydroxyphosphocarnitine modifies the inflammation in rats with non-alcoholic steatohepatitis

Lourdes Rodriguez-Fragoso,<sup>1</sup> and Janet Sánchez-Quevedo<sup>2</sup>

<sup>1</sup>Univ Autonoma Del Estado de Morelos; and <sup>2</sup>universidad Autónoma del Estado de Morelos

Abstract ID 17031

Poster Board 52

**Objective:** To evaluate the pharmacological effect of  $\beta$ -Hydroxyphosphocarnitine ( $\beta$ -HPC) on inflammation in rats with non-alcoholic steatohepatitis.

**Introduction:** Non-alcoholic steatohepatitis (NASH) is a disease characterized by the development of steatosis and an increase in inflammatory cytokines, leading to the development of fibrosis. Currently there is no specific drug for the treatment of NASH, given its high prevalence, the development of an effective drug for the wide spectrum of alterations that characterize NASH is urgently needed.

**Method:** NASH was developed in male Wistar rats by the administration of a high fructose solution, saturated fat, and carbon tetrachloride. The rats were divided into six groups of treatment: (1) Control group, animals with no treatment; (2)  $\beta$ -HPC group (100 mg/Kg, orally for 4 weeks); (3) NASH group, animals received a fructose solution (10%, 400 kcal), a saturated fat solution (16 kcal) and carbon tetrachloride (CCl<sub>4</sub>, 30%). The animals were allowed to ingest fructose solution ad libitum in place of drinking water, from the first day until the end of the study (9 weeks); and (4) NASH +  $\beta$ -HPC group, were treated as was described above. The animals were housed in controlled ambient temperature and humidity, maintained with a standard diet and had water ad libitum. The animals were treated in accordance with the Guide for the Care and Use for Laboratory Animals. The effect of  $\beta$ -HPC on inflammation was investigated by quantifying the inflammatory cytokines (IL-1 $\beta$  and TNF- $\alpha$ ) levels by immunohistochemistry. A histopathological analysis of liver sections was also performed. The study was approved by an Institutional Review Board.

**Results:** Presence of inflammation is key in the progress of NASH. It has been reported that IL-1 $\beta$  and TNF- $\alpha$  can influence in the development of steatosis and fibrosis. Therefore, it was interesting to evaluate the effect of  $\beta$ -HPC on these cytokines. Animals with NASH showed an increase in both, IL-1 $\beta$  and TNF- $\alpha$  expression (4.2 and 4.8-fold, respectively) as compared with control group ( $p < 0.05$ ). However, in animals with NASH and treated with  $\beta$ -HPC, both IL-1 $\beta$  and TNF- $\alpha$  expression were significantly reduced (80% and 75%, respectively) as compared with NASH group ( $p < 0.05$ ). The histopathological analysis revealed presence of micro and macrovesicular steatosis in NASH group. However, animals with NASH and treated with  $\beta$ -HPC showed a significant reduction in liver steatosis and as well as an improvement in liver architecture. The decrease in steatosis could be explained by the reduction of IL-1 $\beta$  and TNF- $\alpha$  in these animals. Steatosis plays an important role for the activation of Kupffer cells and for the arriving inflammatory cells to liver. These results demonstrated the effect of  $\beta$ -HPC on inflammation in the development of NASH.

**Conclusions:** Our results showed that  $\beta$ -HPC can modify steatosis and inflammation in rats with NASH. Further studies are necessary to elucidate the mechanism of action of  $\beta$ -HPC in non-alcoholic steatohepatitis.

# Fecal microbial SN-38G metabolotypes in colorectal cancer patients are associated with irinotecan-induced delayed diarrhea

Rongrong Wu,<sup>1</sup> Junru CHEN,<sup>2</sup> Yifei JIA,<sup>2</sup> Yijia CHEN,<sup>2</sup> Yang LI,<sup>3</sup> and Ru YAN<sup>2</sup>

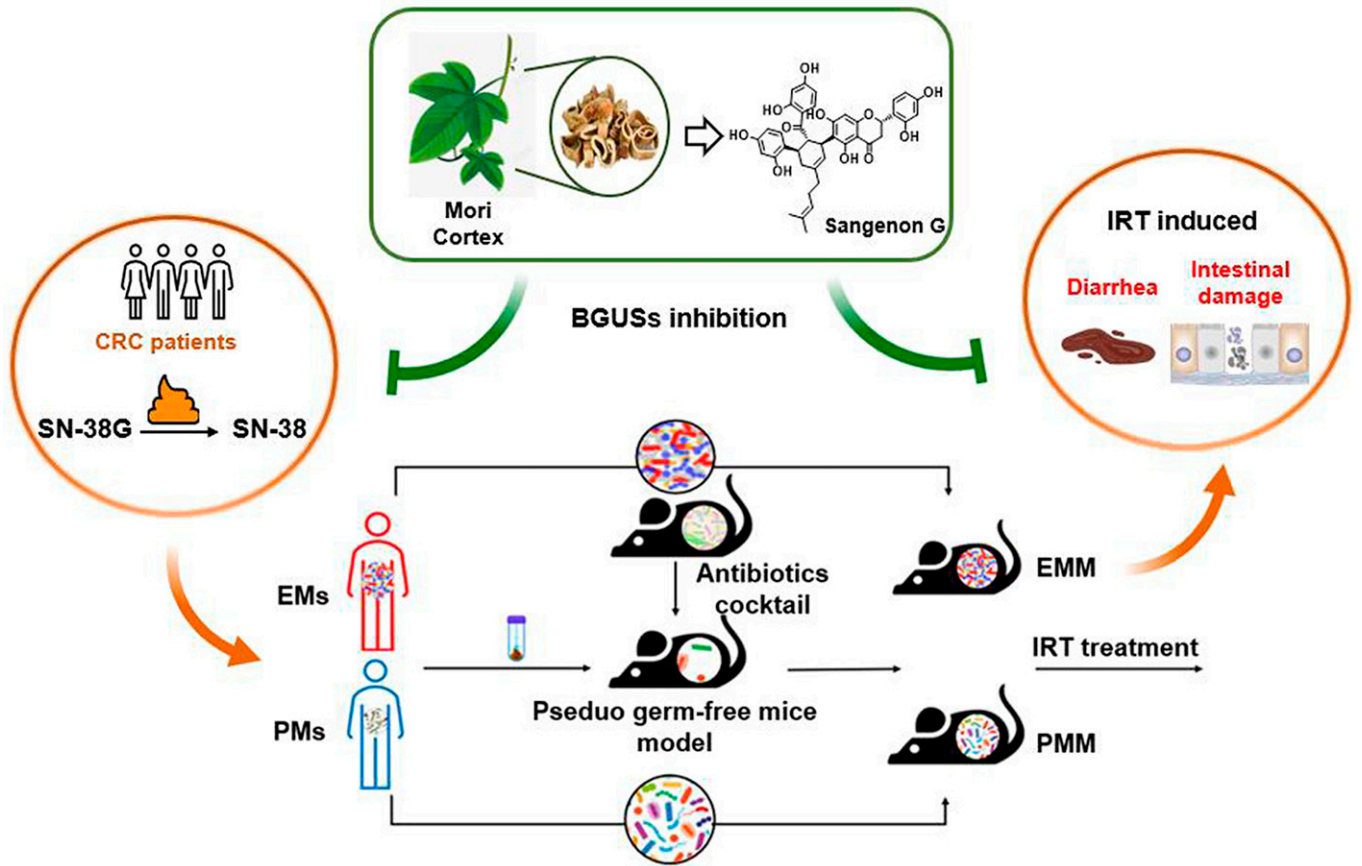
<sup>1</sup>Univ of Macau; <sup>2</sup>University of Macau; and <sup>3</sup>Shenzhen People's Hospital

Abstract ID 22189

Poster Board 53

Gut microbial  $\beta$ -glucuronidases (GUss) reactivation of the excreted, inactive metabolite SN-38G of irinotecan, a first-line chemotherapy drug in advanced colorectal cancer (CRC), caused severe late diarrhea in over 80% of CRC patients, of which 30%-40% was severe diarrhea. However, so far, the mechanistic understanding of the role of microbial GUss in differential responses of CRC patients to irinotecan is still poor. Herein, we first characterized the inter-individual variability in microbial SN-38G-hydrolyzing activity of CRC patients and assessed its impact on gastrointestinal toxicity of irinotecan using fecal microbiota transplantation. Ninety CRC patients fell into 3 distinct metabolotypes with 25 poor (PM), 38 moderate, and 27 extensive (EM) metabolizers on basis of SN-38G-hydrolyzing activity determined from *ex vivo* incubation with fecal microbiota. Notably, this metabolic activity exhibited a significant positive correlation with the TNM stages (stage IV vs I,  $p < 0.05$ ) and was higher in male patients with right-side CRC than those with left-side CRC ( $p = 0.01$ ). Shotgun metagenomic analysis of fecal microbiota revealed a clear separation of gut microbial composition between EMs and PMs. The EMs exhibited higher alpha-diversity than PMs at species level ( $p < 0.01$ ). Specifically, *Enterocloster bolteae*, and *Erysipelatoclostridium ramosum* were more abundant in PMs, while 7 species were significantly enriched in EMs, among which 4 species (*Blautia obeum*, uncultured *Blautia sp.*, uncultured *Ruminococcus sp.*, and *Lachnospiraceae bacterium*) are GUS-expressing bacteria. Pseudo-germ-free mice colonized with fecal microbiota samples from 4 representative EM patients (EMMs) displayed higher fecal SN-38G-hydrolyzing activity than those receiving fecal microbiota transplantation from 4 PMs (PMMs) ( $p < 0.05$ ). Correspondingly, animals of all EMM groups showed higher intestinal SN-38 accumulation and severer responses to irinotecan challenge (50mg/kg, i.p.) than all PMM groups, including lower survival rate, higher incidence of diarrhea and severer intestinal tissue damage. The 16s rRNA-based gene sequencing revealed no significant difference between EMM and PMM groups in alpha-diversity. Three phyla (Actinobacteriota, Proteobacteria and Verrucomicrobiota) were more abundant in PMM, while Campilobacterota showed higher relative abundance in EMM. Sangenon G, the Diel-alder adduct that isolated from Mori Cortex (*sang-bai-pi*) and strongly inhibited GUss activity in pooled human fecal microbiota, also potently suppressed SN-38G deconjugation by fecal microbiota from representative EMs (IC<sub>50</sub> 1.76-14.06  $\mu$ M) and consequently, effectively prevented irinotecan-induced adverse effects in pseudo germ-free mice receiving FMT from EMs. Taken together, these findings demonstrate the causative role of gut microbial GUss in irinotecan-induced gastrointestinal toxicity in CRC patients and highlight the potential application of SN-38G metabolotyping and GUS inhibition for targeted intervention in irinotecan therapy.

Supported by the Science and Technology Development Fund of Macao SAR (FDCT0098/2019/A2, 0091/2021/A2), Guangdong Provincial Natural Science Fund (2019A1515012195) and Shenzhen-Hong Kong-Macau Science and Technology Program Category C (SGDX20210823103805038)



Fecal microbial SN-38G metabolites in colorectal cancer patients and GUS inhibition

# Acute restoration of respiratory function in mice with botulism after treatment with aminopyridines

William T. McClintic,<sup>1</sup> Zachary D. Chandler,<sup>2</sup> Lilitha M. Karchalla,<sup>2</sup> Sean O'Brien,<sup>2</sup>  
Celinia Ondeck,<sup>2</sup> Alexis Morse,<sup>2</sup> and Patrick McNutt<sup>2</sup>

<sup>1</sup>Univ of Tennessee; and <sup>2</sup>Atrium Health Wake Forest Baptist

**Abstract ID 25349**

**Poster Board 54**

Hallmarks of botulism include toxic signs emerging 18 - 36 hours post exposure, leading to symptoms of descending flaccid paralysis resulting in paralysis of the diaphragm and asphyxiation at lethal doses. Interestingly, drugs that enhance presynaptic calcium influx, such as aminopyridines, have emerged as potential therapeutics for botulism symptoms. Indeed, we have shown the FDA-approved drugs 4-aminopyridine (fampridine) and 3,4-diaminopyridine (amifapridine) produce fast-acting symptomatic relief and prolongation of survival in animal models of lethal botulism. To quantify dose-dependent effects of aminopyridines on respiratory function, we present a plethysmography platform for characterizing respiratory function in botulism mice models treated with different aminopyridines at terminal stages of disease. Aminopyridines produce dose-dependent restoration of respiratory function that manifests between 50-100 ng/mL of 3,4-diaminopyridine and 100-200 ng/mL 4-aminopyridine. Notably, mice with severe respiratory distress show the same absolute improvement in minute volumes as mice with mild to moderate respiratory distress, indicating a biological switch for respiration governed by respiratory drive. Preliminary blood gas measurements collected 30 min after aminopyridine treatment demonstrate improved respiratory parameters are correlated with normophysiological pO<sub>2</sub> and pCO<sub>2</sub> blood levels. We will extend the platform to evaluate the potential for phrenic motor facilitation under pre-existing conditions of chronic respiratory depression as well as morphometric and biomarker assays from carotid body tissue. A platform capable of probing the mechanisms of plasticity in a model of respiratory distress has important implications for clinical and therapeutic efficacy in treating patients with neuromuscular diseases and diseases leading to loss of respiratory function.

# Non-alcoholic Fatty Liver Disease (NAFLD) causes Erythropoietin Hyporesponsiveness

Huixi Zou,<sup>1</sup> and Xiaoyu Yan<sup>1</sup>

<sup>1</sup>The Chinese Univ of Hong Kong, Sch of Pharmacy

Abstract ID 18842

Poster Board 55

Treatment with recombinant human erythropoietin (rHuEPO) may correct anemia in patients with chronic kidney disease. However, up to 10% of these patients exhibit EPO resistance or hyporesponsiveness. Non-alcoholic fatty liver disease (NAFLD) is a chronic liver disease with a high prevalence in CKD patients. NAFLD could result in TPO deficiency, iron homeostasis disorder and inflammation, which may restrict the response to EPO. Therefore, we hypothesized CKD patients with NAFLD need a higher dose of EPO to achieve the target hemoglobin levels in comparison with CKD patients without NAFLD.

To test our hypothesis, pharmacokinetic (PK) and pharmacodynamic (PD) studies of rHuEPO were performed in healthy rats and high-fat and high-calorie (HFHC) diet-induced NAFLD rats. Hematological response, endogenous hormone concentration, erythroid cells in bone marrow, inflammation biomarkers, and iron status were measured.

The results demonstrated moderate anemia and EPO hyporesponsiveness in HFHC-NAFLD rats. During the 12-week HFHC diet feeding, steady decreases in mean corpuscular hemoglobin (MCH) concentration and the mean corpuscular volume (MCV) were observed in the HFHC-NAFLD rats from week 3. At the end of the feeding, the MCH (15.5 vs 18.2 pg/cells), MCV (44.3 vs 55.2  $\mu\text{m}^3$ ), hemoglobin concentration (139.5 vs 149.3 g/L) and hematocrit levels (39.5% vs 42.7%) in HFHC-NAFLD rats were significantly lower than that in healthy rats, respectively. Then, both healthy and HFHC-NAFLD rats received rHuEPO administration (450 IU/kg, thrice weekly) for two weeks. HFHC-NAFLD rats showed significantly lower responses in hemoglobin (452.2% vs 591.8%), hematocrit (501.2% vs 651.9%), and MCV (198.7% vs 263.3%) than that in the healthy rats, respectively.

Furthermore, we investigated the underlying mechanism of EPO hyporesponsiveness in HFHC-NAFLD rats. The results showed that iron deficiency and inflammation in NAFLD caused EPO hyporesponsiveness by inhibiting erythroid progenitor cell production. Hepcidin, ferritin, and transferrin and white blood cell concentration in HFHC-NAFLD rats are 12.8, 16.4, 2.51 and 1.40-fold higher than that in healthy rats, respectively. There is no difference in the pharmacokinetics of rHuEPO, endogenous EPO and endogenous TPO concentrations between healthy and HFHC-NAFLD rats. While the number of burst-forming unit-erythroid and colony-forming unit-erythroid progenitor cells in the bone marrow of HFHC-NAFLD rats is only 74.7% and 77.7% of that in healthy rats, respectively. Also, assessed by flow cytometry, the number of erythroid precursor cells in HFHC-NAFLD rats was less than that in healthy rats.

In conclusion, our study found EPO hyporesponsiveness caused by iron deficiency and inflammation in HFHC-NAFLD rats, and it suggested NAFLD could be a covariate on EPO response in CKD patients.

This work was supported by research grants from the Hong Kong Research Grants Council, Early Career Scheme (24103120).



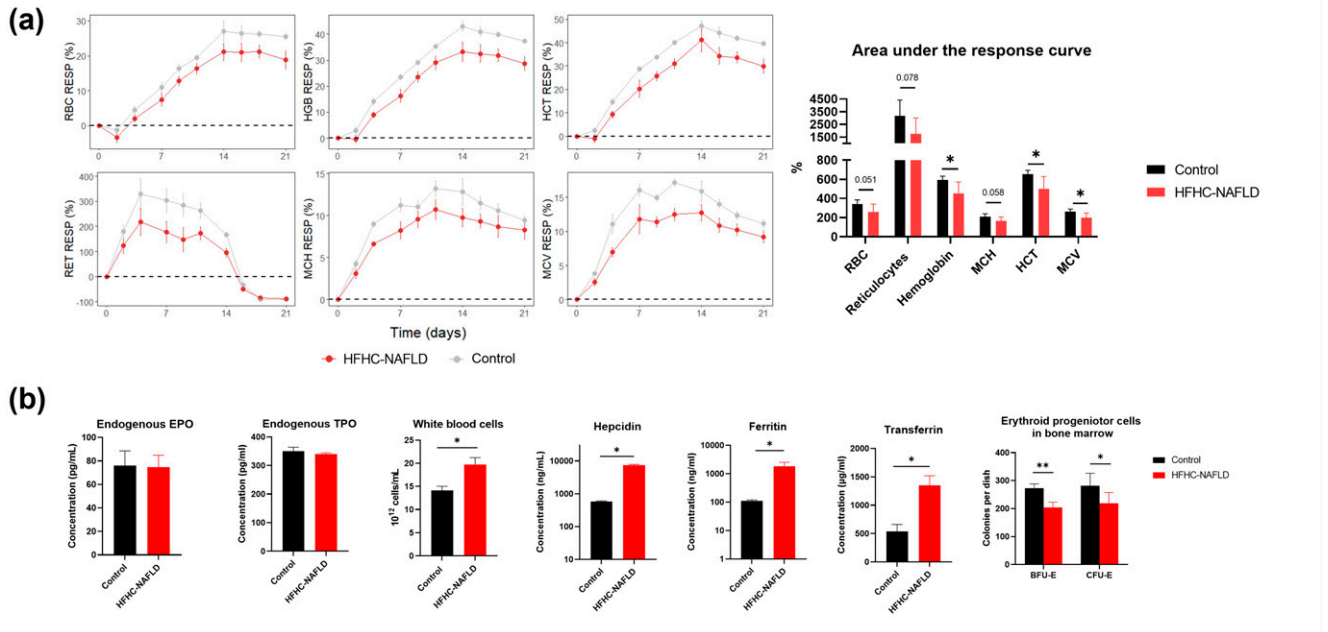


**Figure 1.** EPO hyporesponsiveness caused by iron deficiency and inflammation in HFHC-NAFLD rats. (a) the relative erythroid responses in HFHC-NAFLD rats after EPO treatment were lower than that in healthy rats, including red blood cell (RBC), hemoglobin (HGB), hematocrit (HCT), reticulocytes (RET), mean corpuscular hemoglobin (MCH) and the mean corpuscular volume (MCV). (b) Iron deficiency and inflammation in NAFLD inhibited the production of erythroid progenitor cells

# Safety Evaluation of p5RHH-p65 siRNA Nanoparticles in Mice with Colorectal Cancer Metastases

Jeremy Cho,<sup>1</sup> Luke E. Springer,<sup>1</sup> Antonina Akk,<sup>1</sup> Samuel Wickline,<sup>2</sup> Christine T. Pham,<sup>1</sup> and Hua Pan<sup>3</sup>

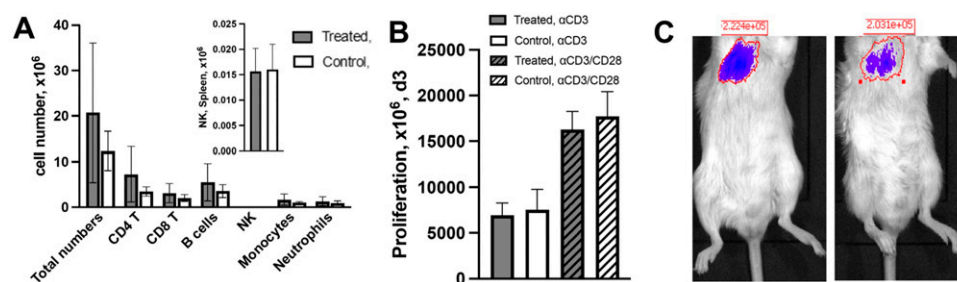
<sup>1</sup>Washington University School of Medicine; <sup>2</sup>Morsani College of Medicine; and <sup>3</sup>Washington Univ School of Medicine

Abstract ID 54814

Poster Board 227

Globally, colorectal cancer (CRC) ranks third among leading causes of cancer-related mortality, affecting more than 1.85 million people and resulting in over 850,000 deaths annually. Upon diagnosis, 20% of patients already have metastatic cancer while 25% of those initially diagnosed with localized disease will eventually develop metastases. A recent preclinical study suggested that combined anti-PD-1 and anti-PD-L1 treatment is effective in a colorectal lung metastasis mouse model but results in myocarditis, a rare but potentially life-threatening side effect that has been associated with the use of immune checkpoint inhibitors (ICIs). Studies suggest that NF- $\kappa$ B activation is involved in the development of myocarditis. Our previous studies demonstrated p5RHH-p65 siRNA nanoparticles (NPs) localize to the sites of inflammation to specifically inhibit NF- $\kappa$ B activation. Therefore, we posit that p5RHH-p65 siRNA NPs could be beneficial in mitigating ICI-induced myocarditis without affecting tumor growth. In this study, we focused on evaluating the safety of this NP in a murine colorectal lung metastasis model. Eight 4-week-old BALB/c male mice received i.v. injection of 1 million mouse colorectal (C26T-Luc) cells. Seven days after C26T-Luc cell injection, half of the mice received p5RHH-p65 siRNA NP treatment every other day for a total of three treatments. The other half of the mice served as controls. Forty-eight hours after the last treatment, mice were euthanized; blood and splenocytes were harvested for evaluation. Consistent with our previous report on normal mice, the p5RHH-p65 siRNA NP treatment (Rx) did not impair kidney function (BUN: 30.00 $\pm$ 9.00 vs 22.75 $\pm$ 3.90 mg/dL; Creatinine: 0.20 $\pm$ 0.05 vs 0.17 $\pm$ 0.01 mg/dL; Rx vs control), liver function (AST: 246.00 $\pm$ 24.00 vs 227.00 $\pm$ 48.34 U/L; ALT: 38.50 $\pm$ 0.50 vs 35.25 $\pm$ 3.77 U/L; Rx vs control), or affect blood glucose level (107.50 $\pm$ 3.50 vs 141.50 $\pm$ 18.15 mg/dL; Rx vs control). Moreover, the p5RHH-p65 NPs treatment did not alter total number of splenocytes (20.73 $\pm$ 7.67  $\times 10^6$  vs 12.35 $\pm$ 2.15  $\times 10^6$ ; Rx vs Control) or splenocyte subpopulations (B cells: 5.50 $\pm$ 2.05  $\times 10^6$  vs 3.56 $\pm$ 0.72  $\times 10^6$ ; NK cells: 0.03 $\pm$ 0.02  $\times 10^6$  vs 0.02 $\pm$ 0.002  $\times 10^6$ ; CD4+ T cells: 7.26 $\pm$ 3.04  $\times 10^6$  vs 3.48 $\pm$ 0.51  $\times 10^6$ ; CD8+ T cells: 3.09 $\pm$ 1.05  $\times 10^6$  vs 2.02 $\pm$ 0.38  $\times 10^6$ ; PMN: 1.30 $\pm$ 0.49  $\times 10^6$  vs 0.88 $\pm$ 0.24  $\times 10^6$ ; Monocytes: 1.66 $\pm$ 0.62  $\times 10^6$  vs 0.98 $\pm$ 0.14  $\times 10^6$ ; Rx vs Control) (Fig. A). Upon stimulation with aCD3/CD28 the splenocytes proliferated to the same extent (aCD3: 6927.92 $\pm$ 591.49 vs 7560.08 $\pm$ 1086.95  $\times 10^6$ ; aCD3/CD28: 16284.17 $\pm$ 988.55 vs 17725.33 $\pm$ 1236.89  $\times 10^6$ ; Rx vs Control) (Fig. B). Results represent mean $\pm$ SEM. Bioluminescence shows that lung metastases appeared relatively stable in treated mouse (Fig. C left: Day 2 and right: Day 4 after initial Rx dose). In conclusion, our results demonstrate that p5RHH-p65 siRNA NP treatment did not alter normal liver/kidney function, immune system responsiveness or promote tumor metastasis, suggesting that p5RHH-p65 siRNA NP may be further evaluated for the mitigation of ICI-induced myocarditis.

The work is supported by NIH, R21HL154009.



# Pharmacovigilance of the COVID-19 Vaccine in Ecuador During the First and Second Doses of Vaccination Campaigns

Andrea Orellana Manzano,<sup>1</sup> Fernanda B. Cordeiro,<sup>2</sup> Andrea Garcia-Angulo,<sup>1</sup>  
Diana Carvajal-Aldaz,<sup>3</sup> Elizabeth Centeno,<sup>4</sup> Maria J. Vizcaíno,<sup>3</sup> Sebastián Poveda,<sup>3</sup>  
Ricardo Murillo,<sup>3</sup> Derly Andrade-Molina,<sup>5</sup> Saurabh Mehta,<sup>4</sup> and Washinton Cardenas<sup>3</sup>

<sup>1</sup>Escuela Superior Politécnica del Litoral; <sup>2</sup>Escuela Superior Politécnica del Litoral; <sup>3</sup>Escuela Superior Politécnica del Litoral;  
<sup>4</sup>Cornell University; and <sup>5</sup>Universidad Espíritu Santo

Abstract ID 52365

Poster Board 228

**Objective:** The study aims to determine the pharmacovigilance of the Ecuadorian population during the first and second doses administered and the adverse events after 84 days of the population

**Method:** A retrospective study was conducted with 423 individuals who were administered the AstraZeneca and 66 Pfizer vaccines from April to November 2021. We compared the acute adverse reaction of the AstraZeneca and Pfizer vaccine and the long-term adverse reaction only to the AstraZeneca population, with a follow-up of 84 days—clinical and demographic data results from odds ratios and their 95% confidence interval. Survival analysis is conducted to determine the probability of surviving an adverse reaction.

**Results:** There were no differences between the sociodemographic characteristics of the population, including vaccine allergies and previous covid infection. The age and sex were significant differences, about five years (95% CI: [3, 8],  $P < 0.001$ ). The AstraZeneca sample is 38.43 (sd= 9.68), while the Pfizer sample is 33.18 (sd=10.44). The acute adverse reaction in the AstraZeneca vaccine was higher in the first dose than the second, with headache, fever, chills, muscle pain, joint pain, and generalised tiredness. Comparing AstraZeneca and Pfizer vaccine acute adverse reactions, the odds ratio for headache, muscle pain, fever, and chills are statistically higher for AstraZeneca than Pfizer in the first dose. In the second dose, only AstraZeneca presented acute adverse reactions such as local pain, general tiredness, and headache.

**Conclusions:** This is the first report about pharmacovigilance in Ecuador during the vaccination campaign with AstraZeneca and Pfizer. There was an adverse reaction mainly in the first 6 hours, but no adverse reaction in the extended period.

This study was funded by CORNELL University, ESPOL university and UEES university.

# Hepatic PKC $\beta$ promotes aging-induced obesity: potential treatment using a novel PKC $\beta$ inhibitor INST3399

Kamal D. Mehta<sup>1</sup>

<sup>1</sup>The Ohio State University Wexner Medical Center

Abstract ID 19562

Poster Board 229

Obesity and aging have both seen dramatic increases in prevalence throughout the world. In modern society, obesity is basically late-onset, and its incidence apparently increases with age, likely due to a combination of genetic and environmental factors. Available data indicates that aging is accompanied by a loss of classical brown adipocytes as well as dysfunctional liver, suggesting that loss of their functions might be connected and contribute to an obesity-prone phenotype with increased age. The underlying mechanisms are incompletely understood. Here, we demonstrate that aging induces hepatic protein kinase C $\beta$  (PKC $\beta$ ) expression under obesogenic conditions, while depletion of PKC $\beta$  specifically in hepatocytes attenuates obesity in aged mice fed high-fat diet. We show that hepatic PKC $\beta$  deficiency potentiates  $\beta$ 3-adrenergic receptor signaling to significantly enhance peripheral energy expenditure and thermogenesis, and mobilizes substrates to fuel thermogenic processes, thus favoring negative energy balance. The energy dissipation is accompanied by elevated hepatic FGF21 expression, changes in expression of hepatic metabolite/ion transporters, improved mitochondrial functions in peripheral tissues, and increases in brown adipose tissue UCP-1 and FGF21 expression, together with a shift to oxidative muscle fiber type, thereby enhancing oxidative capacity of thermogenic tissues. Taken together, loss of hepatocyte PKC $\beta$  has significant beneficial metabolic consequences by triggering liver-brain-peripheral tissue regulatory loop, linked by enhanced sympathetic  $\beta$ 3-adrenergic signaling possibly due to elevated hepatic FGF21 expression, to coordinate systemic metabolic programming. The biochemical link of hepatic PKC $\beta$  between nutrient excess and energy expenditure underscores the presence of a “thrifty system” governing metabolic cooperation among tissues promoting metabolic efficiency during lipid overload. This has potential implications for the treatment of aging-induced adiposity and related diseases. Availability of a novel PKC $\beta$  inhibitor INST3399 will allow us to examine the impact of PKC $\beta$  inhibition on aging-induced obesity and associated metabolic conditions.

Support/Funding Information: R01 HL138198

# Vitamin D3: Clueing into the crosstalk between HIF1 $\alpha$ and macrophage polarization in NASH

Basma Alaa,<sup>1</sup> Olfat Hammam,<sup>2</sup> Aiman ElKhatib,<sup>3</sup> and Yasmeen Attia<sup>1</sup>

<sup>1</sup>Department of Pharmacology, Faculty of Pharmacy, The British University in Egypt.; <sup>2</sup>Pathology department, Theodor Bilharz Research institute.; and <sup>3</sup>Department of Pharmacology and Toxicology, Faculty of Pharmacy, Cairo University.

Abstract ID 20237

Poster Board 230

**Introduction:** Hypoxia-inducible factor (HIF)-1 $\alpha$ , a crucial hypoxia sensor, presents an intriguing bridge between macrophage polarization (MP) and metabolic rewiring. The latter provides the macrophages with the plasticity to function in hostile microenvironments evolving from inflammatory settings, empowering their alternation between M1 and M2 polarization states representing the pro- and anti-inflammatory phenotypes, respectively. Accordingly, the investigation of such a link in a setting that is characterized by both metabolic dysregulation and progressive inflammation such as non-alcoholic steatohepatitis (NASH) is pre-eminent. Given its metabolic and immunomodulatory entangled roles, this study, therefore, aimed to unravel the effect of calcitriol (CAL), vitamin D3 active form, on the HIF-1 $\alpha$ /MP interplay in experimental NASH.

**Methods:** A dietary NASH model was used for the current study. Male C57BL/6 mice were allocated to the following 3 groups: (1) Normal standard chow-fed group, (2) High-fat diet (HFD)-fed group, and (3) HFD+CAL group that received CAL treatment at a dose of 5 ng/gm/day, i.p., twice weekly. Treatment started after 8 weeks of induction for a duration of 4 weeks. Livers were harvested for histopathological evaluation and subsequent assessments. Hepatic fatty acid synthase (FAS) was determined using qPCR. Immunoreactivity against toll-like receptor-4 (TLR-4) and HIF-1 $\alpha$  along with inducible nitric oxide synthase (iNOS) and Arginase-1 (Arg-1), the M1 and M2 polarization markers, respectively, were estimated using immunohistochemistry. Hepatic levels of IL-10 were measured using ELISA. All experimental procedures were approved by the Ethical Committee of the Faculty of Pharmacy, Cairo University (PT- 2734). Statistical analysis was performed using one-way ANOVA on GraphPad prism Software.

**Results:** Treatment with CAL abrogated the derangement in hepatic architecture observed in the HFD group. Additionally, hepatic FAS levels were lower in the CAL-treated group by 41.83% ( $P < 0.0001$ ), as compared to the HFD group. HIF-1 $\alpha$  immunoreactivity was curtailed by CAL reaching almost 92% ( $P < 0.0001$ ) compared to the control. The surged hepatic TLR-4 expression in the HFD group was dampened upon CAL treatment by 82% ( $P < 0.0001$ ). Regarding MP, hepatic expression of iNOS was 92% lower than its levels in the HFD group ( $P < 0.0001$ ). In contrast, hepatic Arg-1 expression was 8.15 folds higher in the HFD+CAL group compared to HFD ( $P < 0.0001$ ) suggesting the skewness of the macrophages towards the M2 phenotype. Furthermore, hepatic IL-10 levels elicited a reduction by 39.3% ( $P = 0.0225$ ) in the HFD group when compared to normal. CAL treatment, however, reversed this effect where IL-10 levels were 1.56 folds higher than its corresponding levels in the HFD group.

**Conclusion:** Overall, the present study suggests the ability of CAL to orchestrate the crosstalk between HIF-1 $\alpha$  and MP towards preventing NASH progression.

Support/Funding Info: Young investigator research grant (YIRG) from the British University in Egypt (YIRG2018-16)

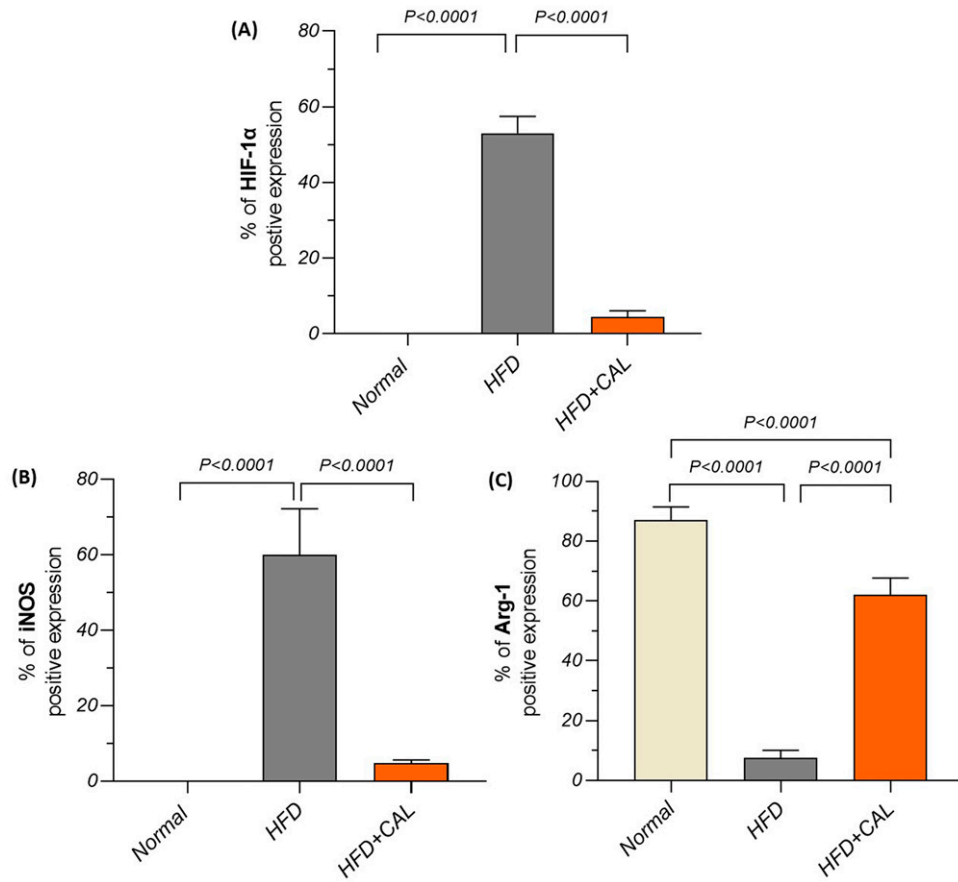


**Figure 1:** Effect of CAL on hepatic immunoreactivity against (A) HIF-1 $\alpha$ , (B) iNOS as an M1 polarization marker and (C) Arg-1 as an M2 polarization marker as estimated by immunohistochemistry. Statistical analysis was performed using GraphPad prism. Data is presented as means  $\pm$  SD. Multiple comparisons were carried out using one-way ANOVA followed by Tukey's post hoc test.

# ATI-450: A Novel MK2 Pathway Inhibitor - Preclinical & Clinical Translational Studies to Predict Human Dose

Heidi R. Hope,<sup>1</sup> Susan Hockerman,<sup>1</sup> Matt Saabye,<sup>1</sup> Loreen Stillwell,<sup>1</sup> Rakesh Basavalingappa,<sup>1</sup> Catherine Emanuel,<sup>1</sup> Steve Mnich,<sup>1</sup> Madison Bangs,<sup>1</sup> Emma Huff,<sup>1</sup> Aparna Kaul,<sup>1</sup> Anne Hildebrand,<sup>1</sup> Marco Cardillo,<sup>2</sup> Ajay Aggarwal,<sup>2</sup> and Joseph B. Monahan<sup>1</sup>

<sup>1</sup>Aclaris Therapeutics / Confluence Discovery Technologies; and <sup>2</sup>Aclaris Therapeutics

Abstract ID 54104

Poster Board 231

ATI-450 is a mechanistically novel, investigational inhibitor of the mitogen-activated protein kinase (MAPK)-activated protein kinase 2 (MK2) pathway, downstream of p38 MAPK. It selectively targets the p38MAPK/MK2 complex and locks MK2 in an inactive conformation thereby preferentially inhibiting MK2 activation relative to alternate p38 MAPK substrates. Due to p38 MAPK proinflammatory actions being largely mediated by MK2, selective blockade of this pathway bypasses p38 MAPK-regulated anti-inflammatory and negative feedback substrates. ATI-450 inhibited the p38MAPK/MK2 complex with an  $IC_{50} = 16.7 \pm 5.6nM$  while demonstrating selectivity for the p38MAPK/PRAK and p38MAPK/ATF2 complexes of  $\geq 700x$ .

ATI-450 demonstrated concentration-dependent inhibition of cytokine production and phosphorylation of the MK2 substrate HSP27 in the U937 cell line, rheumatoid arthritis synovial fibroblasts and human whole blood (HWB) following stimulation with inflammatory stimuli including LPS (TLR4), IL-1b, PolyI:C (TLR3) and R848 (TLR7/8). HWB was utilized as the most physiologically relevant cellular system to evaluate potency of ATI-450 in blocking cytokine production. ATI-450 potency for blocking TNF $\alpha$  and IL1b in HWB in response to LPS ranged in  $IC_{50}$  values from 12nM – 29nM. The biochemical efficiency for ATI-450 is high (>1) based on free-fraction corrected HWB potency relative to biochemical potency for blocking the p38MAPK/MK2 complex.

ATI-450 showed attenuation of LPS-induced cytokine production in both *in vivo* rat and mouse studies with  $EC_{80}$ 's in the 0.5-2.0 mg/kg range. In the rat streptococcal cell wall arthritis model, both edema and bone loss were reduced by ATI-450 at doses and drug levels in line with whole blood *in vitro* studies and *in vivo* acute LPS induced cytokine inhibition. An admix chow formulation of ATI-450 (1000ppm) demonstrated activity in the mouse collagen induced arthritis model with steady state drug plasma levels approximating  $IC_{80}$  concentrations in the mouse LPS study. A direct translation of ATI-450 potency from cellular HWB studies to *in vivo* rodent endotoxemia and arthritis models was observed and utilized for a human phase 1 dose projection plan.

ATI-450 was evaluated in phase 1 SAD/MAD studies at doses from 10mg to 120 mg. *Ex vivo* LPS stimulated cytokine pharmacodynamic (PD) analysis demonstrated dose- and exposure-dependency. The target PD modulation associated with phase 2 dose selection was 80+% inhibition of LPS induced TNF $\alpha$  at trough. The 50mg BID dose inhibited *ex vivo* stimulated TNF $\alpha$  production between ~85% at trough and ~93% at peak concentrations following seven days of dosing in the MAD study. The exposure/response relationship associated with the 50mg BID dose was predicted from the HWB potency of ATI-450. A 12-week rheumatoid arthritis (RA) phase 2a study was conducted using the 50mg BID dose. *Ex vivo* LPS-stimulated cytokine inhibition in blood from RA patients and volunteers dosed with ATI-450 at 50mg BID was comparable. Further, RA clinical improvement across multiple endpoints was also observed in this study. This sequence of studies demonstrates the power in utilizing translatable cellular and animal models to predict human phase 1 and 2 dosing.

# Comprehensive analysis of CYP2D6 mutations in human cancers

Kennedy Kuchinski,<sup>1</sup> Julia Driggers,<sup>2</sup> Martin Vo,<sup>3</sup> Wilber Escorcía,<sup>2</sup> and Hanna Wetzel<sup>2</sup>

<sup>1</sup>Xavier Univ; <sup>2</sup>Xavier University; and <sup>3</sup>Lake Erie College of Osteopathic Medicine

Abstract ID 24526

Poster Board 232

The cytochrome P450 (CYP) enzymes are responsible for the metabolism of many drugs. Single nucleotide polymorphisms (SNPs) have large impacts on the activity of these enzymes and result in altered metabolism for a variety of drugs. Cancer patients frequently suffer from both chronic pain and depression, leading to co-administration of selective serotonin reuptake inhibitors (ssRIs) and opioids. CYP2D6 is necessary to convert ssRIs into their inactive metabolites and to activate several prodrug opioids. Ideally, to avoid drug-drug interactions in cancer patients when prescribing ssRI-opioid combinations, careful analysis of relevant SNPs through PCR in individual patients would be employed. However, this approach remains technically and economically inaccessible to many cancer demographics and clinical settings. To address these limitations and provide genomic-based alternatives, we analyzed the frequency of CYP2D6 mutations in sequenced specimens from a varied pool of cancer patients. The primary goal of this study is to use cancer data trends linked to CYP2D6 DNA sequence disruptions to improve informed selection of ssRI-opioid treatments based on specific patient characteristics. We mined the Catalogue of Somatic Mutations in Cancer (COSMIC) from the Sanger Institute to identify CYP2D6 mutations occurring in patients with various cancers types. We also used the CHASM-3.1 and VEST-4 artificial intelligence algorithms from the Cancer-Related Analysis of Variants Toolkit (CRAVAT) to evaluate the functional significance of missense mutations. Results from CHASM reveal the probability of mutations either being drivers or passengers in cancer, while VEST indicates the likelihood of mutations being pathogenic. We found that 188 of 409 patients showed CYP2D6 mutations localized to the coding region. A majority of these (126) were missense mutations, 18 showed high pathogenicity, and no cancer drivers were identified. The three tissue types most frequently affected by CYP2D6 mutations were the large intestine (60), lung (58), and upper aerodigestive tract (49). The mean age at time of sequencing (MATS) for all tissues was 58.2 years. Three tissues showed significant age differences relative to the MATS of all tissue types: the urinary tract (mean=69.5,  $p=0.0080$ ), hematopoietic and lymphoid tissue (mean=49.1,  $p=0.0039$ ), and the stomach (mean=66.0,  $p=0.0027$ ). The primary histology associated with CYP2D6 mutations was carcinoma (327 of 409 patients). Intriguingly, cancers linked to lymphoid neoplasm histology had a significantly different MATS (mean=41.4 years,  $p=0.0002$ ) relative to all histology types (mean=58.2). The observed missense mutations in the conserved P450 domain of CYP2D6 suggest structural changes that likely affect protein function, thereby precluding effective metabolism of this enzyme's drug substrates. Therefore, these results indicate that cautious, personalized, and deliberate prescription should be used when co-administering opioids and ssRIs to patients who meet criteria associated with decreased CYP2D6 metabolism in the cancer contexts herein reported.



# Development of Humanized ACE2 Mouse and Rat Models for COVID-19 Research

Hongmei Jiang,<sup>1</sup> Emma Hyddmark,<sup>1</sup> Jianqiu Xiao,<sup>1</sup> Sara Gordon,<sup>1</sup> Angela Bartels,<sup>1</sup> Yumei Wu,<sup>1</sup> Joe Warren,<sup>1</sup> Lauren Klaskala,<sup>1</sup> Andrew Brown,<sup>1</sup> Michael Garratt,<sup>1</sup> Helmut Ehall,<sup>1</sup> and Guojun Zhao<sup>1</sup>

<sup>1</sup>Inotiv

**Abstract ID 53194**

**Poster Board 252**

Over the last 3 years, the COVID-19 pandemic has severely affected human lives and the global economy. The virus causing COVID-19 is called Severe Acute Respiratory Syndrome Coronavirus 2 (SARS-CoV-2). SARS-CoV-2 infects host cells by the binding of its spike protein to the cellular surface protein angiotensin-converting enzyme 2 (ACE2). The predicted 29 amino acid residues of ACE2 that interact with SARS-CoV-2 spike protein receptor binding domain (RBD) vary between human ACE2 and mouse or rat ACE2. Therefore, wild type mice and rats show lower SARS-CoV-2 infection rate and mild symptoms compared to what is seen in humans. Small animal models that recapitulate human COVID-19 disease are urgently needed for better understanding the transmission and therapeutic measurement. Currently, scientists use either mouse-adapted SARS-CoV-2 (SAS-CoV-2 MA) models or random transgenic mouse models that artificially express human ACE2 under the control of cytokeratin 18 promoter or a constitutive promoter. SAS-CoV-2 MA may not completely reflect all aspects of the original human-tropic SARS-CoV-2 and the current transgenic human ACE2 mouse models typically have high mortality rate caused by neuroinvasion and encephalitis due to very high human ACE2 expression. To overcome these limitations, we have developed humanized ACE2 mouse and rat models using CRISPR-Cas9. Specifically, we inserted a ~3kb human ACE2 cDNA cassette into the mouse and rat *Ace2* gene loci to ensure that human ACE2 expression is under the control of rodent *Ace2* promoter and regulatory elements, while simultaneously disabling the rodent *Ace2* gene. To accomplish this, CRISPR gRNAs targeting close to the translation initiation site of *Ace2* were screened in cultured mouse and rat cells. Then CRISPR/Cas9 complex and donor DNA were subsequently microinjected into one-cell stage embryos which were subsequently implanted into pseudo pregnant females. Resulting pups were screened for correct knockin by junction PCR and insert PCR, and the PCR products were Sanger sequenced. Targeted Locus Amplification (TLA) further confirmed the integration sites and transgene sequence. RT-qPCR and Western blot analysis data showed that, in our models, human ACE2 is expressed in tissues expressing endogenous *Ace2* (such as lung, kidney, and GI tract), while rodent endogenous *Ace2* is absent from these tissues. Further breeding data indicated that both hemizygous and homozygous humanized ACE2 animals appear to be normal and fertile. Most importantly, animals displayed symptoms after infection with SARS-CoV-2. In summary, these data suggest that our novel humanized ACE2 models can be valuable for COVID-19 research.

# Characterization of novel genetic mutations in aldehyde dehydrogenase 2 that cause alcohol flushing in humans

Freeborn Rwere,<sup>1</sup> Rafaela CR. Hell,<sup>1</sup> Xuan Yu,<sup>1</sup> and Eric R. Gross<sup>1</sup>

<sup>1</sup>Stanford University

Abstract ID 20893

Poster Board 253

Consuming alcohol can increase the risk of cancers including those of the head, neck, esophagus, bowel, breast, and liver. This cancer risk after alcohol consumption is increased several-fold for approximately 560 million East-Asian people who carry ALDH2\*2 (*rs671*, E504K) variant in aldehyde dehydrogenase 2 (ALDH2), that limits the metabolism of the alcohol break-down product acetaldehyde. This ALDH2\*2 variant is associated with the alcohol flushing syndrome and tachycardia. Whether other missense mutations in the ALDH2 gene exists that causes alcohol flushing and tachycardia remains poorly understood. Here we hypothesized other inactive ALDH2 missense mutations exists that cause acetaldehyde accumulation and alcohol flushing syndrome in humans.

After IRB approval, we used selective ion flow mass spectrometry to quantify acetaldehyde levels for wild-type ALDH2, ALDH2\*2, and other ALDH2 missense variants in humans after an alcohol challenge. In addition, we evaluated the activity of these proteins *in vitro*, and in 3T3 transiently transfected cells. Statistical analysis was performed by ANOVA and Tukey's post hoc with significance set at  $p < 0.05$ . All data are presented as mean  $\pm$  SEM.

We identified humans carrying genetic mutations in ALDH2 including *rs671* (E504K) and two novel mutations, *rs747096195* (R101G), and *rs190764869* (R114W). After subjecting volunteers to an alcohol challenge (0.25g/kg), *rs747096195* (R101G) and *rs190764869* (R114W) cause facial flushing and 2-fold higher acetaldehyde accumulation, while *rs671* causes 9-fold higher acetaldehyde accumulation relative to humans with wild type ALDH2. Further, heart rate changes after alcohol consumption correlate with inefficient acetaldehyde metabolism ( $r=0.90$ , 95% confidence 0.78-0.95,  $n=26$ ,  $p < 0.0001$ ). Characterization with ALDH2 enzyme expressed in bacterial and cultured 3T3 cells supports that *rs747096195* (R101G), *rs190764869* (R114W), and *rs671* (E504K) genetic variants in ALDH2 result in less efficient acetaldehyde metabolism relative to wild type ALDH2. Cellular reactive oxygen species (ROS) of the wild-type and mutant variants significantly increased by 2-3-fold for cells treated with ethanol compared to untreated cells.

Together, we identified genetic variants in the ALDH2 enzyme besides *rs671* that cause inefficient acetaldehyde metabolism and developed a method to non-invasively phenotype differences in acetaldehyde metabolism after an alcohol challenge in humans. This is an important step for developing precision medicine strategies to provide individualized recommendations regarding alcohol use by factoring in how genetics when coupled with phenotype may ultimately influence cancer risk from consuming alcohol.

This work was supported by GM119522 (ERG).

# Phenylacetylglutamine causes a pathologic inflammation state through the $\beta$ 2-adrenergic receptor /cAMP/PKA/NF- $\kappa$ B pathway in diabetes

Lu Huang

Abstract ID 54961

Poster Board 254

**Background:** Type 2 diabetes (T2DM) affects billions of patients and has a pathophysiologically important inflammatory component. Macrophage plasticity in diabetes is impaired, and remains in a persistent proinflammatory state; yet currently, the cause of the inflammatory state is unknown. Phenylacetylglutamine (PAGln) is an amino acid metabolism end product that rises in T2DM patients. However, the role of PAGln in the inflammatory component of T2DM remains unknown. Here, we aim to identify blood-based systemic factors for pathologic inflammation status and risk of chronic wounds as they are highly reproducible at low cost and search for effective and safe agents to attenuate diabetic inflammatory complications.

**Methods:** In vivo, phenylacetylglutamine was dissolved in normal saline and injected in mice daily (intraperitoneal, 50mg/kg). In vitro, primary mice bone marrow-derived macrophages (BMDMs) were treated with phenylacetylglutamine (100  $\mu$ M) for the indicated time. RNA-seq, Elisa, PCR, and western blot were used to characterize the impact of PAGln on BMDMs and mice wounds. Flow cytometry was taken to quantify and type immune cells in mice bone marrow, blood, spleens, and wounds. The activity of the NF- $\kappa$ B pathway was assessed by KEGG analysis, western blot, luciferase, and activity assay. Employing genetic and pharmacological tools, we detected the receptors through which PAGln mediates inflammatory events.

**Results:** Here, increased PAGln was identified in diabetes and in people suffering from chronic wounds in an independent cohort. Both conditions have been linked to a hyper-inflammatory state. In vivo, we found PAGln supplement resulted in worse wound healing and increased inflammatory gene expression in mice wounds. In vitro, PAGln leads to macrophage M1 polarization. Mechanistically, we report that in wound healing, PAGln increased in plasma upregulates cAMP levels in wound macrophages via  $\beta$ 2-adrenergic receptors and that this increase in cAMP induces NF- $\kappa$ B-mediated inflammatory gene transcription in wound macrophages via a PKA mechanism. Interestingly, we found that PAGln caused a significant increase in inflammatory macrophages in mice spleens, blood, bone marrow, as well as wounds and that this increase in inflammatory macrophages can be rescued by carvedilol ( $\beta$  blocker).

**Conclusion:** Our study unravels a novel mechanism by which PAGln disturbs the transition of macrophage phenotype from inflammatory to reparative, facilitating pathologic inflammation, and impairing wound healing by activating the  $\beta$ 2-adrenergic receptor /cAMP/PKA/NF- $\kappa$ B pathway. The negative effect of PAGln could be rescued by carvedilol ( $\beta$  blocker). Thus, our recognition of chronic inflammation in diabetes needs to be revised, and understanding these mechanisms can inform alternative treatment strategies and refine chronic wound repair therapies for diabetic patients

**Funding:** Shanghai Clinical Research Center of Plastic and Reconstructive Surgery supported by Science and Technology Commission of Shanghai Municipality (Grant No. 22MC1940300)

# Deciphering immunological mechanisms underlying the efficacy of nanoparticle-based vaccines and novel adjuvants against Opioid Use Disorder (OUD)

Fatima FH. Hamid,<sup>1</sup> Scott Schactler,<sup>2</sup> Debra Walter,<sup>3</sup> Hardik Amin,<sup>4</sup> Minh Le,<sup>4</sup> David Burkhart,<sup>4</sup> Chenming Zhang,<sup>3</sup> and Marco Pravetoni<sup>5</sup>

<sup>1</sup>University of Minnesota; <sup>2</sup>University of Washington; <sup>3</sup>Virginia Tech; <sup>4</sup>University of Montana; and <sup>5</sup>Univ of Minnesota Medical School

Abstract ID 28305

Poster Board 255

The highly complex OUD and overdose epidemic poses a public health and economic burden. In the United States, the Opioid crisis was further accelerated by COVID-19 pandemic, with more than 72,000 deaths attributed to opioid overdose in 2020, the highest number of overdose deaths ever recorded in a year. Moreover 2.7 million people were diagnosed with OUD which led to a substantial impact on the U.S economy, with the total cost of the opioid epidemic in 2020 estimated at \$1.5 trillion. There is an urgent need for safe and more effective therapeutic options to augment existing measures. Vaccines offer a highly promising strategy for OUD treatment and prevention of overdose. Vaccinating with drug-based hapten-carrier protein conjugates formulated with adjuvants, generate drug-specific polyclonal antibodies (Ab) that selectively bind targeted opioids, blocking its distribution to the brain and thus protects against opioid induced rewards, pharmacological and side effects. Preclinical testing demonstrated anti-opioid vaccines as a highly selective long-lasting treatment and prophylactic strategy for OUD and overdose in animal models. Previous clinical trials of addiction vaccines showed proof of efficacy in those subjects who achieved the highest Ab titers, highlighting the need to design more effective vaccines. Therefore, we focus on developing an improved carrier system and investigating novel adjuvants and understanding the immunological mechanisms underlying their efficacy. The generation of effective anti-drug polyclonal antibodies relies on CD4+ T cell-dependent B cell activation, highlighting the importance of dendritic cells (DC) in initiating CD4+ T cells priming and adaptive immune responses. We previously developed a lipid-poly(lactic-co-glycolic acid) (PLGA) hybrid nanoparticle (LPNP) platform that improved the efficacy of conjugate vaccines against nicotine and oxycodone. Additionally, we investigated Toll-like receptor (TLR) 7/8 agonists such as the clinically approved resiquimod (R848) and other TLR7/8 agonists, that significantly improved anti-opioid conjugate vaccine efficacy when combined with alum. Nanocarriers and TLR agonists can be exploited to potentiate antigen recognition by antigen presenting cells (APCs) and subsequently vaccination outcome. Here using an *in vitro*-flow cytometry-based activation assay, we investigated the efficacy of vaccine formulations in inducing macrophage and DCs activation, maturation and phenotypic differentiation. Using RAW264.7 and JAWS II cell line, we demonstrated that LPNP- based oxycodone vaccine is more effective in inducing macrophages activation marker (iNOS) and DCs co-stimulatory molecules and maturation markers (CD86, CD40, and MHC II) compared to conventional vaccines. Furthermore, adding TLR7/8 agonists to conjugate vaccines outperformed the alum adjuvant in inducing maturation and activation of APCs. These findings were further confirmed with RT-qPCR assays quantifying the mRNA expression of above-mentioned markers. *In vivo* flow cytometry studies are ongoing to dissect the APCs dynamics upon vaccination to identify key APCs subsets contributing to efficacy and thus a significant vaccine target.

# The Neuroprotective Effects of DPP-4 and SGLT2 Inhibitors in Type 2 Diabetes: Possible Mechanism for Halting Cognitive Deterioration

Shams T. Osman,<sup>1</sup> Noha A. Hamdy,<sup>2</sup> Amr Y. El Feky,<sup>3</sup> Labiba K. El-Khordagui,<sup>2</sup> and Ahmed F. El-Yazbi<sup>4</sup>

<sup>1</sup>Faculty of Pharmacy, Alexandria Univ; <sup>2</sup>Faculty of Pharmacy, Alexandria University; <sup>3</sup>Faculty of Medicine, Alexandria University; and <sup>4</sup>Alexandria Univ

Abstract ID 13801

Poster Board 256

Neuroinflammatory changes together with the associated alteration in cognitive dysfunction are increasingly recognized as bona fide complications of type 2 diabetes mellitus (T2DM). Moreover, research has uncovered a strong metabolic component in neurodegenerative disorders, including Alzheimer's Disease, to the extent that the former is often referred to as type 3 diabetes. Thus far, disease-modifying therapeutic interventions in cognitive disorders have not been forthcoming. However, there is mounting interest in the pleiotropic effects of novel anti-diabetic drugs, particularly their neuroprotective action. This study examines the impact of combining metformin with dipeptidyl peptidase-4 inhibitors (DPP-4i) or sodium-glucose cotransporter-2 inhibitors (SGLT2i) on cognitive decline in T2DM patients.

We designed a prospective observational cohort study, in which T2DM patients taking metformin in combination with DPP4i or SGLT2i were compared to a control group receiving metformin monotherapy. The study was conducted following approval by the Ethics Committee of the Faculty of Medicine of Alexandria University (serial number 0106970). The study was registered on ClinicalTrials.gov NCT05347459. Cognitive function was assessed using a validated Arabic version of the Montreal Cognitive Assessment (MoCA) Battery. Lab tests were conducted for glucose and inflammatory markers (CRP and IL-6) levels, as well as kidney, liver, and lipid profiles. All parameters were assessed at baseline and after six months of follow-up in the 3 treatment groups, in addition to a group of healthy non-diabetics to serve as a baseline reference. One-way ANOVA was conducted for statistical analysis using GraphPad Prism. A P-value <0.05 was considered significant.

The study began in March 2022 with a total of 89 subjects (36 males and 53 females) with a mean age of  $58.62 \pm 6.01$  years recruited after giving their written informed consent to the study. Data collected at baseline showed that patients in either combination therapy group had MoCA scores ( $19.61 \pm 1.12$  and  $19.88 \pm 1.27$  for DPP-4i and SGLT2i, respectively) that were comparable to healthy subjects ( $21.62 \pm 0.96$ ) in contrast to those on metformin monotherapy who had lower MoCA scores ( $18.64 \pm 0.63$ ). In regards to glucose levels, although HbA1c was higher in all T2DM patients, random blood glucose level was higher only in patients on metformin monotherapy and patients on metformin in combination with DPP-4i. However, neither parameter seemed to affect MoCA scores in correlation studies. Regarding the remaining laboratory tests, T2DM patients did not show abnormal liver or kidney functions nor did they show an altered lipid profile compared to healthy volunteers. Furthermore, none of these parameters appeared to be correlated with the subjects' MoCA scores. It is worth noting that similar to previous literature, neither drug class seemed to affect serum inflammatory markers (CRP & IL-6) that were associated with impaired cognition in T2DM patients.

SGLT2i and DPP-4i appear to positively impact cognitive function in T2DM patients through pathways that do not involve glycemic control, mitigation of diabetic complications, or systemic inflammation. Follow-up assessment of the patients is ongoing on the different parameters measured. An in-depth proteomic and glycomic study is underway to attempt to elucidate the potential mechanistic impact of these drug classes on neuronal function and injury parameters in diabetic patients.

# CYP4F2\*3 (V433M) Polymorphism Impacts Benzalkonium Chloride Metabolism in an Alkyl Chain Length-Dependent Manner

Linxi Zhu,<sup>1</sup> Ryan Seguin,<sup>1</sup> Nathan Alade,<sup>1</sup> Justina C. Calamia,<sup>1</sup> Kenneth Thummel,<sup>1</sup> and Libin Xu<sup>1</sup>

<sup>1</sup>University of Washington

Abstract ID 53827

Poster Board 426

Benzalkonium chlorides (BACs) are a class of quaternary ammonium compounds. They are among the most common active ingredients in disinfectants used in domestic cleaning, industrial processing, and clinical settings. BACs are primarily metabolized by cytochrome P450 (CYP) enzymes through  $\omega$ -hydroxylation by CYPs 4F2 and 4F11 and ( $\omega-1$ )-hydroxylation (or further internal oxidation) by CYPs 2D6 and 4F12. These primary metabolites are further metabolized to  $\omega$ -carboxylic acid and ( $\omega-1$ )-ketone products. We hypothesize that CYP polymorphism is a major determinant of inter-individual variability in BAC persistence in humans. CYP4F2 was previously found to be an  $\omega$ -hydroxylase of C16 BAC, but not of C12 BAC. In this work, we investigated the impact of CYP4F2 polymorphism (\*1/\*1, \*3/\*3, and \*1/\*3) on C12 and C16 BAC metabolism in 4F2-genotyped and pooled (from 10 individuals for each genotype) human liver microsomes (HLM). Wild-type (WT) (4F2\*1/\*1) HLM exhibited a 2.08-fold higher metabolic rate for C16 BAC than 4F2\*3/\*3; However, for C12 BAC, this ratio was only 1.09. The heterozygote (4F2\*1/\*3) HLM metabolic rates of both C12 and C16 BACs were close to WT, being 80% and 88% of the WT metabolic rates, respectively. The fraction metabolized (fm) of carboxylic acid for C16 BAC are 0.72 (\*1/\*1), 0.54 (\*1/\*3) and 0.22 (\*3/\*3), whereas for C12 BAC, this fm in all three variants are less than 0.05, suggesting CYP4F2 is a major contributor to the formation of  $\omega$ -carboxylic acid from C16-BAC, but not C12-BAC. The use of the specific CYP2D6 inhibitor quinidine in all three groups of 4F2-genotyped HLM confirmed the significant contribution of CYP2D6 to ( $\omega-1$ )-hydroxylation of both C16- and C12-BACs. Inhibition of CYP2D6 had a greater effect on C12 BAC metabolism than C16 BAC, reducing their ( $\omega-1$ )-hydroxy metabolites by 67% and 55%, respectively, in WT HLM. In conclusion, the impact of 4F2\*3 polymorphism on BAC metabolism in HLM was far greater for C16 BAC than for C12 BAC. Inhibition of 2D6 by quinidine was not necessary to observe this effect, indicating that the 4F2\*3 polymorphism alone can substantially reduce C16 BAC metabolism in HLM. This study suggests that individuals with the CYP4F2 poor metabolizer genotype could be more susceptible to BAC exposure.

# Impact of SULT1A1 Genetic Polymorphisms on the Sulfation of Clioquinol and Iodoquinol by Human SULT1A1 Allozymes

Mohammed Rasool,<sup>1</sup> and MING-CHEH LIU<sup>2</sup>

<sup>1</sup>University of Karbala; and <sup>2</sup>University of Toledo

Abstract ID 20293

Poster Board 427

**Background:** The phase II sulfation reaction, mediated by the cytosolic sulfotransferase (SULT) enzymes, has been proposed to be involved in the metabolism and disposal of clioquinol and iodoquinol. SULT1A1 was reported to exhibit sulfating activity with both tested compounds. The current study was intended to investigate the impact of the genetic polymorphisms of SULT1A1 on the sulfation of clioquinol and iodoquinol by SULT1A1 allozymes.

**Methods:** As a first step to clarify the effects of single nucleotide polymorphisms (SNPs) on the sulfating activity of SULT1A1, on-line SNP databases were systematically searched for SULT1A1 missense coding SNPs (cSNPs). Nine cDNAs coded by selected SULT1A1 cSNPs were generated, and the corresponding SULT1A1 allozymes were bacterially expressed and affinity-purified. The sulfating activities of the purified nine SULT1A1 allozymes toward clioquinol and iodoquinol were analyzed using an established assay procedure.

**Results:** Enzymatic assays revealed that the purified SULT1A1 allozymes exhibited differential sulfating activities toward both clioquinol and iodoquinol in comparison to the wild-type enzyme.

**Conclusion:** The obtained results may have implications in the pharmacokinetics and toxicity profiles of the tested halogenated hydroxyquinolines administered in individuals with distinct SULT1A1 genotypes. Such information may, in the future, help design individualized regimens of the investigated hydroxyquinoline drugs to improve their therapeutic efficacy and minimize their side effects.

# Amlodipine use in Mild Cognitive Impairment reduces the risk of incident dementia in National Alzheimer's Coordinating Center participants aged $\geq 55$ years from 2014-2019

Karin Sandoval

Southern Illinois Univ Edwardsville

Abstract ID 55217

Poster Board 428

There is increasing evidence that amlodipine may be useful in preventing dementia. Whether amlodipine use in mild cognitive impairment (MCI) protects against dementia remains unclear. This study evaluated the hypothesis that reported use of amlodipine in MCI would reduce the risk of incident dementia using National Alzheimer's Coordinating Center (NACC) participants aged  $\geq 55$  years from 2014-2019.

Inclusion criteria included NACC participants aged  $\geq 55$  years visiting an Alzheimer's Disease Center from 1/1/2014-12/31/2019 with a diagnosis of MCI and  $\geq 2$  visits with complete medications forms. Amlodipine use was defined as any reported use of amlodipine prior to being censored or diagnosed with dementia by a clinician. Reported medication use was based on co-participant report of participant medication use within the past 14 days. There were 3,527 participants with MCI that met inclusion criteria, with 589 (16.7 %) amlodipine users. At the initial MCI visit, significant systematic differences were found between amlodipine users and nonusers. To control for this, participants were matched at the initial MCI visit.

All amlodipine users were matched resulting in a total sample size of 1178. Following matching, amlodipine users were similar to nonusers for all variables with exception of hypercholesterolemia (amlodipine user: 463/589, 78.6%; nonuser: 430/589, 73.0%,  $p=0.0248$ , chi-square).

An extended Cox proportional hazards survival model was used to model the risk of incident dementia with amlodipine use with time following MCI diagnosis. The adjusted risk of incident dementia for amlodipine users was 32% lower (adjusted hazard ratio, HR=0.68, 95% CI: 0.53, 0.86) compared to non-users when adjusting for age category, APOE4, race, myocardial infarction, diabetes, hypercholesterolemia, type of MCI, education level and sex.

These results support the hypothesis that reported use of amlodipine in MCI reduced the risk of incident dementia.

*The NACC database is funded by NIA/NIH Grant U24 AG072122. NACC data are contributed by the NIA-funded ADRCs: P30 AG062429 (PI James Brewer, MD, PhD), P30 AG066468 (PI Oscar Lopez, MD), P30 AG062421 (PI Bradley Hyman, MD, PhD), P30 AG066509 (PI Thomas Grabowski, MD), P30 AG066514 (PI Mary Sano, PhD), P30 AG066530 (PI Helena Chui, MD), P30 AG066507 (PI Marilyn Albert, PhD), P30 AG066444 (PI John Morris, MD), P30 AG066518 (PI Jeffrey Kaye, MD), P30 AG066512 (PI Thomas Wisniewski, MD), P30 AG066462 (PI Scott Small, MD), P30 AG072979 (PI David Wolk, MD), P30 AG072972 (PI Charles DeCarli, MD), P30 AG072976 (PI Andrew Saykin, PsyD), P30 AG072975 (PI David Bennett, MD), P30 AG072978 (PI Neil Kowall, MD), P30 AG072977 (PI Robert Vassar, PhD), P30 AG066519 (PI Frank LaFerla, PhD), P30 AG062677 (PI Ronald Petersen, MD, PhD), P30 AG079280 (PI Eric Reiman, MD), P30 AG062422 (PI Gil Rabinovici, MD), P30 AG066511 (PI Allan Levey, MD, PhD), P30 AG072946 (PI Linda Van Eldik, PhD), P30 AG062715 (PI Sanjay Asthana, MD, FRCP), P30 AG072973 (PI Russell Swerdlow, MD), P30 AG066506 (PI Todd Golde, MD, PhD), P30 AG066508 (PI Stephen Strittmatter, MD, PhD), P30 AG066515 (PI Victor Henderson, MD, MS), P30 AG072947 (PI Suzanne Craft, PhD), P30 AG072931 (PI Henry Paulson, MD, PhD), P30 AG066546 (PI Sudha Seshadri, MD), P20 AG068024 (PI Erik Roberson, MD, PhD), P20 AG068053 (PI Justin Miller, PhD), P20 AG068077 (PI Gary Rosenberg, MD), P20 AG068082 (PI Angela Jefferson, PhD), P30 AG072958 (PI Heather Whitson, MD), P30 AG072959 (PI James Leverenz, MD).*



# PKM2 Deficiency in Brown Adipocytes Enhances Differentiation and the Expression of Mitochondrial Genes

Presley Dowker-Key<sup>1</sup> and Ahmed Bettaieb<sup>1</sup>

<sup>1</sup>University of Tennessee, Knoxville

Abstract ID 15100

Poster Board 429

## Abstract

The continuous rise of obesity has been associated with various comorbidities including type 2 diabetes (T2DM), cardiovascular disease (CVD), and even some types of cancer thus defining it a global health concern. Notably, brown adipose tissue (BAT) development and regulation has been more recently recognized as a potential approach to assist with patient weight loss, metabolic improvement, and obesity prevention. In previous investigations, pyruvate kinase M2 (PKM2) was identified as a novel modulator of brown adipogenesis. However, its specific molecular mechanisms and its role in brown adipogenesis remain implicit. To better understand the role of PKM2 in brown fat cell differentiation, mouse brown precursor cells were isolated and shRNA-mediated knockdown approach was employed to specifically alter PKM2 expression in brown pre-adipocytes. The effects of PKM2 deficiency on brown adipocyte differentiation and lipid accumulation were then investigated. In addition, we investigated changes in the expression of several hallmark genes of brown adipocytes. Our study demonstrates that PKM2 deficiency enhances brown fat cell differentiation and maintenance as evidenced by the markedly increased expression of differentiation and functional markers including FASN, PCB, perilipin, and UCP1. These results highlight PKM2 as a potential modulator of brown adipogenesis and suggestively, a therapeutic target for the treatment and prevention of obesity through increasing brown fat mass which may lead to enhanced energy expenditure and the subsequent prevention of excess body fat.

# Probing Adropin-Gpr19 Interactions and Signal Transduction

Robert N. Devine,<sup>1</sup> Andrew Butler,<sup>1</sup> John Chrivia,<sup>1</sup> Josef Vagner,<sup>2</sup> and Christopher K. Arnatt<sup>1</sup>

<sup>1</sup>Saint Louis University; and <sup>2</sup>University of Arizona

**Abstract ID 55063**

**Poster Board 430**

Currently, G protein-coupled receptors (GPCR) account for nearly 40% of all approved drugs. However, vital to optimal design of GPCR-targeted ligands as potential therapeutics is the understanding of the molecular basis of ligand recognition and the conformational consequences of ligand engagement that generate specific signaling responses. GPR19 is an orphan class A GPCR that has been proposed to mediate the biological actions of adropin. The propeptide (adropin) and GPR19 are highly expressed in the central nervous system relative to peripheral tissues. Adropin appears to play a role in several physiological functions that include glucose and fatty acid metabolism, brain development, and vascular function. To gain a better structural insight of the cellular signaling pathways activated by adropin, we developed a cell-based assay for assessing signal transduction and SAR (structure-activity relationship) studies. We used nanoluciferase complementation to identify cell-surface GPR19 expression in human cell lines (HEK, THP-1). Pooled clones expressing a HiBit-GPR19 fusion protein exhibited fluorescence when incubated with the cell-impermeable LgBit subunit and luciferase substrate, indicating cell-surface expression. A rapid decline following addition of 2 mM adropin is consistent with ligand-induced internalization of GPR19. In a single clone exhibiting moderate levels of GPR19, dose-dependent suppression of cAMP production with the addition of adropin was observed ( $EC_{50} = 8.9$  nM). This is consistent with published data suggesting that adropin activate a GPCR coupling to inhibitory G protein signaling pathways. Concentration response studies using N-acetylated was positive but C-amidated adropin analogs yielded a negative response. Labelling at the amino terminal end may therefore be possible to help collect information on the mechanism of interaction between GPR19 and adropin. These results represent the first step to provide a better understanding of the ligand-receptor interaction contributing to effector recruitment.

**Support/Funding Information:** Saint Louis University President Research Fund.

# Investigation of MMR Vaccination Rates and its Relationship with Measles, Mumps, and Rubella Outbreaks in California

Brianna Negrete McGinley<sup>1</sup> and Prashant Sakharkar<sup>1</sup>

<sup>1</sup>Roosevelt University

Abstract ID 23246

Poster Board 431

**Background:** There have been growing concerns of measles outbreaks in the United States. In 2019, more than 1200 cases of measles were reported in the US, the highest annual number since 1992. Eighty-nine percent of measles patients were unvaccinated or had an unknown vaccination status. The potential resurgence of measles could be due to the declining vaccine coverage as a result of vaccine hesitancy and an ever-growing number of anti-vaccination movements. Vaccine hesitancy negatively affects vaccine coverage and therefore the herd immunity conferred unto non-immune individuals. A recent data suggests that a 5% drop in MMR vaccination coverage leads to a threefold increase in measles cases per year. This is equivalent to \$2.1 million in cost to the public sector thus constituting a significant economic burden to the US healthcare system. The measles, mumps, and rubella (MMR) vaccine is an important vaccination among children. Any drop in the MMR vaccination rates most likely to increase the risk of measles, mumps and rubella outbreaks in population.

**Objectives:** The aim of this study was to examine the MMR vaccination rates among Kindergarteners and its relationship with measles, mumps and rubella outbreaks in population of California.

**Methods:** Publicly available data on MMR vaccination rates among Kindergartens in California between 2015 and 2019 were obtained from the Center for Disease Control and prevention (CDC). Whereas publicly available data on measles, mumps and rubella cases were obtained from California Department of Public Health and other published reports. Changes in incidence rates were assessed by time-trend analysis. The rates of MMR vaccination rates were compared between 2015 to 2019. MMR vaccination rates were also compared with measles, mumps, rubella outbreaks using correlational analysis. A p-value of <0.05 was considered statistically significant.

**Results:** Over a five-year period, vaccination rates among Kindergarteners ranged between 92.6% to 96.5%. The median MMR vaccination rate was 96.5%. A total of 259 cases of measles, 810 of mumps and seven cases of rubella were observed over five-year period. The median number of cases was 24 and 140 for measles and mumps, respectively, and zero for rubella. The MMR vaccination rates were dropped from 2015 to 2019 (96.5% vs. 92.6%,  $p < 0.05$ ). Similarly, the rates (cases/100,000) of outbreaks were increased for measles (0.18 vs. 0.32,  $p < 0.05$ ), mumps (0.08 vs. 0.89,  $p < 0.05$ ) and rubella (0.0 vs. 0.01,  $p < 0.05$ ) from 2015 to 2019. MMR vaccination rates correlated with measles, mumps and rubella ( $r = -0.90, 0.70, 0.67$ ) outbreaks respectively but were not statistically significant except for measles. No significant trends were observed for disease outbreaks.

**Conclusions:** Decline in MMR vaccination rates and increase in mumps, measles and rubella outbreaks is a major public health concern. Increase in MMR vaccination, improved disease surveillance and rapid outbreak containment are essential in curbing the measles, mumps, rubella outbreaks in California and in the US and it deserves serious attention of policy makers, public health experts and society at large.

# Asparagine depletion by the antileukemic agent PEGylated asparaginase induces hepatic stellate cell activation and fibrosis

Yin Zhu,<sup>1</sup> Keito Hoshitsuki, and Christian Fernandez

*Univ of Pittsburgh School of Pharmacy*

**Abstract ID 15650**

**Poster Board 451**

**Background:** One of the leading therapies for acute lymphoblastic leukemia (ALL) is the chemotherapeutic agent PEGylated asparaginase (PEG-ASNase). However, PEG-ASNase therapy is avoided in adults due to the high risk of liver injury, which presents clinically as elevated hepatic transaminases, bilirubin levels, and fatty liver. In our previous studies, we developed a murine model of PEG-ASNase-induced fatty liver that recapitulates clinical liver injury observations. We demonstrated, using this model, that PEG-ASNase-induced liver injury is associated with the activation of adipose triglyceride lipase (ATGL), which leads to adipocyte lipolysis, free fatty acid (FFA) mobilization, and fatty liver. However, whether the fatty liver induced by PEG-ASNase treatment progresses to advanced liver injury such as to hepatic stellate cell (HSC) activation and hepatic fibrosis is unknown.

**Hypothesis:** PEG-ASNase treatment activates HSCs and induces hepatic fibrosis.

**Methods:** Nine-week-old wild-type C57BL/6 mice received a 1,500 IU/kg single dose of PEG-ASNase or vehicle control intraperitoneally. Blood and liver samples were collected five days after administration. Alpha-SMA immunochemistry and Sirius Red staining were performed to assess the expression of the fibrogenic marker and collagen deposition, respectively. LX-2 (human HSC line) and isolated primary murine HSCs were treated with 1IU/mL of PEG-ASNase, and the mRNA and protein levels of the liver fibrosis markers (a-SMA, TGF- $\beta$ , COL1A1, and COL1A2) were assessed.

**Results:** We show that PEG-ASNase treatment was associated with increased immunostaining of a-SMA and collagen deposition in the liver, suggesting that PEG-ASNase activates HSCs. Consistent with our *in vivo* findings, PEG-ASNase treatment induced the protein expression of a-SMA and the mRNA expression of liver fibrosis marker genes, a-SMA, TGF- $\beta$ , COL1A1, and COL1A2 in LX2 cells and primary murine HSCs. Similar to our previous findings using adipocytes, we found that PEG-ASNase treatment induced the mRNA and protein expressions of ATGL, supporting that PEG-ASNase-induced HSC lipolysis may be associated with HSC activation and the development of liver fibrosis.

**Conclusion:** Our results support that PEG-ASNase therapy induces HSC activation and hepatic fibrosis. We hypothesize that PEG-ASNase therapy leads to ATGL-induced-HSC lipolysis, retinol release, and thereby HSC activation.

**Support/Funding Information:** National Institutes of Health grants CA216815 and TL1TR001858 (USA), the Pittsburgh Liver Research Center, and American Foundation for Pharmaceutical Education (USA), and the University of Pittsburgh School of Pharmacy (USA).

# Brazilian Green Propolis-Based Nanostructured System and its use in diabetic rats of *Staphylococcus aureus* resistant to methicillin (MRSA)-infected wounds

Fernando P. Beserra,<sup>1</sup> Marcos V. de Sa Ferreira,<sup>2</sup> Mariana Conceição,<sup>2</sup> Débora M. Rodrigues,<sup>1</sup> Stéfani T. Alves Dantas,<sup>2</sup> Vera L. Moraes Rall,<sup>2</sup> Priscyla D. Marcato Gaspar,<sup>1</sup> Jairo K. Bastos,<sup>1</sup> and Cláudia H. Pellizzon<sup>2</sup>

<sup>1</sup>School of Pharmaceutical Sciences of Ribeirão Preto, University of São Paulo; and <sup>2</sup>Institute of Biosciences, São Paulo State University

Abstract ID 56910

Poster Board 452

Diabetes Mellitus is a chronic disease that affects millions of people and causes severe metabolic changes. The difficulty in wound healing is one of its main complications, which can be explained by the continuous inflammatory process and the high rate of oxidative stress, and when associated with infection by *Staphylococcus aureus* resistant to methicillin (MRSA), causes an aggravation in the patient that results in a high number of limb amputations. Therapy with the use of antibiotics is costly for low-income people, and the search for new therapeutic treatments, mainly based on natural products of plant origin, has become a potential alternative to treat these wounds. In search of natural therapeutic alternatives to this comorbidity, Propolis has become a promising alternative since it is a source capable of producing high concentrations of Artepillin C and has anti-inflammatory and antibacterial properties. However, its direct use in topical formulations may be restricted due to its unfavorable physicochemical properties. Thus, we hypothesize that the encapsulation of these compounds in nanostructured systems is a suitable instrument to overcome these limitations. A nanoemulsion containing green propolis extract (NE-PV) was developed and its healing effects evaluated in *in vivo* experimental models. Initially, the physicochemical properties and the cytotoxic potential of this nanoemulsion in HaCat cells were analyzed. For animal tests, hyperglycemic male *Wistar* rats were used, randomly divided into 7 groups (n=7). The wounds were made with a 2 cm<sup>2</sup> punch in the dorsal region of the rodents, after which bacterial strains (*S. aureus* - USA 300) were inoculated into the lesions. After 48 hours, the first swab was collected to confirm the infection. The lesions were treated twice a day, for 10 days, and on the 11<sup>th</sup> day, euthanasia was performed, and samples were collected for analysis. The results showed that the nanoemulsion had a globular, spheroid and globular shape, with a size of 250nm, a polydispersion index below 0.3 and a negative zeta potential, while the cell viability test showed an IC<sub>50</sub> of 51.85 µg/mL. Regarding the *in vivo* tests, the analysis of wound closure showed that the groups treated with Mupirocin, Hydrogel containing NE-PV 6% and PV 6% achieved a high percentage of retraction significantly better than the group with untreated infected wounds. The CFU/mL determination showed a significant reduction in bacterial infection in the groups treated with Mupirocin and Hydrogel containing NE-PV 6% when compared to the “wound with infection and no treatment” group. These findings indicate that this nanostructured system showed good physicochemical stability and that the Hydrogel containing NE-PV 6% topically applied to the wounds for 10 days was able to accelerate wound healing in hyperglycemic conditions, as well as decrease bacterial infection, may be useful as a treatment for chronic wounds in diabetic patients.

**Funding source:** This work was supported by São Paulo Research Foundation (FAPESP) – Grant numbers #2019/14496-4, #2017/04138-8 and 2021/11550-8

# A Novel Charged Sodium-Channel Blocker, Ntx-1175, Is Effective In Reducing Acute Visceral Hypersensitivity In Vivo

Ehsan Noor-Mohammadi,<sup>1</sup> Casey LIGON,<sup>1</sup> Beverley Greenwood-Van Meerveld,<sup>2</sup> Nan Zheng,<sup>3</sup> Bridget Bridget Cole,<sup>3</sup> Jim Ellis,<sup>3</sup> and Anthony Johnson<sup>4</sup>

<sup>1</sup>University of Oklahoma HSC; <sup>2</sup>Oklahoma Univ Health Science Ctr; <sup>3</sup>Nocion Therapeutics; and <sup>4</sup>VA Health Care System

Abstract ID 21618

Poster Board 453

**Background:** Chronic abdominal pain is a hallmark feature of irritable bowel syndrome (IBS), a disorder of gut-brain communication with no observable tissue damage. In patients with IBS, chronic abdominal pain is the result of visceral hypersensitivity due to visceral afferent nerve sensitization. We have previously demonstrated that an enema of dilute (0.6% v/v) acetic acid (AA) provides a model of acute colonic hypersensitivity to distension. Sensory nerves can be selectively inhibited by charged sodium channel blockers (CSCBs) such as NTX-1175 through gaining access to nociceptors through large pore channels (e.g., Transient Receptor Potential (TRP)V1, TRPA1) that are open due to ongoing pain and inflammation. The goal of the current study was to evaluate the effect of the novel CSCB NTX-1175 in a rodent model of colonic hypersensitivity in male rats.

**Methods:** Thirty adult male Sprague Dawley rats were randomly assigned to saline enema/vehicle intracolonic (i.c.), AA enema/vehicle enema, or AA enema/NTX-1175 (i.c.) at 10, 25, or 50 mg/kg. For each rat, the saline or AA enema was administered before the drug/vehicle dosing. Sixty-minutes after the dosing, colonic sensitivity was quantified as the number of abdominal contractions, to graded pressures (0, 20, 40, 60 mmHg) of isobaric colorectal distension (CRD). At euthanasia, plasma and colonic tissue were collected for pK analysis. Data was presented as mean  $\pm$  standard error of the mean. Two-factor repeated measure ANOVA with Bonferroni post-hoc test or unpaired t-tests were used for analysis, n=6/group.

**Results:** We first verified that the AA model induced colonic hypersensitivity as measured by increased abdominal contractions compared to the saline enema controls (40 mmHg: AA=24.8 $\pm$ 1.2 vs. saline=11.7 $\pm$ 1.2, p<0.01; 60 mmHg: AA=30.7 $\pm$ 2.4 vs. saline=15.7 $\pm$ 1.3, p<0.01). Intracolonic administration of NTX-1175 provided a dose-responsive effect with significant attenuation of AA-induced colonic hypersensitivity at the highest dose tested (40 mmHg: 10 mg/kg=22.2 $\pm$ 0.9, p>0.05; 25 mg/kg=19.7 $\pm$ 2.3, p>0.05; 50 mg/kg=13.5 $\pm$ 1.3, p<0.01; 60 mmHg: 10 mg/kg=26.8 $\pm$ 1.3, p>0.05; 25 mg/kg=24.3 $\pm$ 2.5, p>0.05; 50 mg/kg=19.0 $\pm$ 1.4, p<0.05). At 50 mg/kg i.c., there was significantly more NTX-1175 in the colon than the plasma (83,700 $\pm$ 33,000 ng/g tissue vs. 11.5 $\pm$ 1.2 ng/ml plasma, p<0.01).

**Summary and Conclusions:** In a rat model colonic hypersensitivity, treatment with the novel CSCB NTX-1175 delivered directly into to the colon normalized colonic sensitivity in a dose-dependent manner. This is the first report of using a CSCB therapy to attenuate visceral pain, providing proof of concept rationale for the treatment of disorders such as IBS.

Funding provided by Nocion Therapeutics

# Renoprotective Effects of Empagliflozin Against Experimentally Induced Renal Fibrosis In Vitro

Sarah Bayne,<sup>1</sup> and Shankar Munusamy<sup>2</sup>

<sup>1</sup>Drake Univ; and <sup>2</sup>Drake Univ College of Pharmacy and Health Sciences

Abstract ID 21668

Poster Board 454

**Background:** Chronic kidney disease (CKD) is a progressive disease characterized by gradual loss of kidney function over time. Diabetes, hypertension, and obesity are the leading risk factors for developing CKD. Fibrosis is regarded as the final common pathway leading to CKD due to the irreversible damage it causes to the nephrons. Sodium-glucose co-transporter 2 (SGLT-2) inhibitors (Dapagliflozin and Canagliflozin) have been shown to be renoprotective in type 2 diabetes patients. However, the renoprotective mechanisms of the SGLT-2 inhibitors are unclear. Our study investigated whether empagliflozin (an SGLT-2 inhibitor) treatment inhibits fibrosis induced by transforming growth factor- $\beta$  (TGF- $\beta$ ) and profibrotic signaling in rat renal proximal tubular cells (NRK-52E).

**Methods:** NRK-52E cells were cultured and treated with TGF- $\beta$  with or without empagliflozin for 48 hours. The expression of fibrosis marker - vimentin, autophagy marker - LC3II, and TGF- $\beta$ -mediated profibrotic signaling marker - SMAD 2 - were measured by western blotting.

**Results:** TGF- $\beta$  treatment (at 5 ng/mL) for 48 hours induced fibrosis and activated autophagy signaling in renal proximal tubular cells. Specifically, 48 h TGF- $\beta$  treatment at 5 ng/mL induced the expression of Vimentin by 1.57-fold and LC3II by 2.6-fold and increased the phosphorylation of SMAD 2 by 3.49-fold compared to vehicle-treated cells. Co-treatment with empagliflozin (100 and 500 nM) reduced the expression of the fibrotic markers (vimentin), autophagy marker (LC3II), and TGF- $\beta$ -mediated phosphorylation of SMAD-2 in renal proximal tubular cells.

**Conclusions:** Our findings indicate that TGF- $\beta$ -mediated induction of fibrosis, autophagy, and profibrotic signaling in renal proximal tubular cells could be attenuated by empagliflozin treatment. Further studies are required to understand the molecular mechanisms that underpin the antifibrotic effects of empagliflozin against TGF- $\beta$ -induced renal fibrosis.

**Keywords:** Chronic Kidney Disease; Fibrosis; SGLT2 inhibitors; Empagliflozin

**Support or Funding Information:** This study was supported by Drake University's intramural funds (Harris Research Endowment, Kresge Endowment, and Provost fund) and Drake Undergraduate Science Collaborative Institute (DUSCI) - Summer Undergraduate Research Fellowship.

# Safety Evaluations of Rapamycin Perfluorocarbon Nanoparticles in Ovarian Tumor Bearing Mice

Adam Mitchell,<sup>1</sup> Qingyu Zhou,<sup>2</sup> Antonina Akk,<sup>3</sup> John Harding,<sup>3</sup> Luke E. Springer,<sup>3</sup> Joseph P. Gaut,<sup>3</sup> Ping Fan,<sup>4</sup> Ivan Spasojevic,<sup>4</sup> Christine T. Pham,<sup>3</sup> Samuel Wickline,<sup>5</sup> Daniel Rauch,<sup>6</sup> Katherine Fuh,<sup>7</sup> and Hua Pan<sup>6</sup>

<sup>1</sup>Washington Univ School of Medicine in St. Louis; <sup>2</sup>Univ of South Florida College of Pharmacy; <sup>3</sup>Washington University School of Medicine in St. Louis; <sup>4</sup>Duke University School of Medicine; <sup>5</sup>Morsani College of Medicine; <sup>6</sup>Washington University School of Medicine; and <sup>7</sup>University of California San Francisco School of Medicine

Abstract ID 50713

Poster Board 455

In the US, ovarian cancer is the 2<sup>nd</sup> most common gynecologic cancer of the female reproductive system and claims more lives than any other gynecologic cancer. Cisplatin is used as part of the first-line of treatment for ovarian cancer and has demonstrated better therapeutic outcomes than carboplatin. Independent reports indicated that about 40% of ovarian cancer patients developed acute kidney injury (AKI) after cytoreductive surgery and cisplatin-based hyperthermic intraperitoneal chemotherapy. Although efforts to protect kidney function from cisplatin induced toxicity were initiated in the 1970's, current clinical managements remain as supportive measures, such as hydration and/or magnesium replacement. Our recent studies demonstrated the benefits of rapamycin perfluorocarbon nanoparticles (PFC NP) in mitigating cisplatin induced AKI and favorable safety profiles in normal mice. Here, we report the safety evaluations of rapamycin PFC NP in ovarian tumor bearing mice. Fourteen Athymic nu/nu mice received a subcutaneous implantation of 1 million OVCAR-8-eGFP cells. Two weeks after the implantation, palpable tumors were observed, and the mice were treated with either rapamycin PFC NP or saline administered intravenously twice a week for two weeks. Seventy-two hours post last treatment, mice were euthanized for blood testing and histopathological evaluations. The results demonstrated that rapamycin PFC NP treatment reduced the tumor burden (8±3 mg) by 89% compared with the control (72±22 mg) (p=0.012). The immunofluorescent evaluation on tumors illustrated that tumors from the control group exhibited a well-established blood vessel network from the peripheral to the core, which did not exist in the tumors from rapamycin PFC NP treated mice. Consistent with our previous report, the rapamycin PFC NP treatment (Rx) didn't impair the kidney function (BUN: 26.11±1.86 vs 22.67±1.67 mg/dL; Creatinine: 0.20±0.03 vs 0.26±0.03 mg/dL; control vs Rx), liver function (Total protein: 5.18±0.10 vs 5.48±0.19 g/dL; AST: 142.70±20.03 vs 150.56±14.00 U/L; ALT: 38.60±1.68 vs 46.44±1.99 U/L; ALP: 95.20±7.93 vs 100.33±4.68 U/L; control vs Rx), nor affect blood glucose (177.89±10.48 vs 186.22±8.17 mg/dL; control vs Rx) and blood electrolytes (Sodium: 153.67±0.76 vs 153.86±0.34 mmol/L; Potassium: 3.77±0.10 vs 3.54±0.07 mmol/L; Chloride: 113.00±1.00 vs 112.00±0.82 mmol/L; control vs Rx). Moreover, the rapamycin PFC NP treatment didn't alter the total number of splenocytes (28.43±4.27 x10<sup>6</sup> vs 30.57±5.37 x10<sup>6</sup>; control vs Rx) or splenocyte subpopulations (B cells: 22.24±3.32 x10<sup>6</sup> vs 23.70±4.76 x10<sup>6</sup>; PMN: 3.41±0.77 x10<sup>6</sup> vs 3.20±0.39 x10<sup>6</sup>; Monocytes: 2.38±0.61 x10<sup>6</sup> vs 3.78±0.86 x10<sup>6</sup>; control vs Rx). All the results were reported as mean±SEM. In conclusion, our results suggested that rapamycin PFC NP treatment didn't alter normal vital organ function nor normal immune system but inhibited ovarian tumor progress partially due to preventing tumoral blood vessel establishment. These observations suggested that rapamycin administered in PFC NP format is effective against ovarian cancer in a preclinical model without exhibiting significant toxic effects.

The work is supported by NIH, R01DK125322.

Supported by NIH, R01DK125322



# Diagnostic and predictive value of circulating microRNAs and their regulation of BDNF signaling pathway in stroke patients

Mikolaj Marszalek,<sup>1</sup> Disha Keshwani,<sup>2</sup> Ceren Eyileten,<sup>3</sup> Zofia Wicik,<sup>2</sup> Anna Nowak,<sup>2</sup> Salvatore de. Rosa,<sup>4</sup> Dagmara Mirowska-Guzel,<sup>2</sup> Anna Czlonkowska,<sup>2</sup> Guillaume Paré,<sup>5</sup> and Marek Postula<sup>2</sup>

<sup>1</sup>Medical Univ of Warsaw; <sup>2</sup>Medical University of Warsaw; <sup>3</sup>Med Univ of Warsaw; <sup>4</sup>Magna Græcia University; and <sup>5</sup>McMaster University Michael DeGroote Centre for Learning & Discovery

Abstract ID 13936

Poster Board 456

**Aim:** We aimed to identify and validate circulating miRNAs, modulated in ischemic stroke (IS) patients in order to distinguish the most specific as biomarkers to facilitate diagnosis and prognosis.

**Method:** Two microarray miRNA profilings were done and validated by RT-qPCR to explore (i) diagnostic miRNAs (29 acute IS patients vs 30 controls), and (ii) predictive miRNAs (24 patients with single stroke vs 24 patients with multiple stroke or TIA-NAVIGATE-ESUS cohort (ClinicalTrials.gov, NCT02313909). Stat: TAC software, R using Signal information, FDR correction, logistic reg, Mann-Whitney, t-test and calculated AUC using ROCp R.

**Results:** Microarray data identified 404 differentially expressed (DE) probes. 146 up- and 258 downregulated. Target prediction of those miRNAs showed 67 up- and 125 downregulated miRNAs mapped by multiMir R package (fig1a). Targets of upregulated top miRNAs were most associated with BDNF, IL-2 signaling pathway, FSH regulation of apoptosis, Axon guidance and TGF-beta regulation of EC matrix. Downregulated miRNAs were most associated with Axon guidance, Neuronal system and Signaling by NGF. Targets of up/down regulated top miRNAs most associated with CVD-related terms are presented in fig1b. ANKRD52, AGO1 were targeted by all types of DE miRNAs. Most susceptible to regulation by up-regulated miRNAs: ANKRD12 and HIF1A and down-regulated miRNAs: GNAI2 and GRIN1 (fig1c).

**1. Diagnostic analysis:** miR-18a-5p was higher in IS patients both at day1 and day7 compared to control ( $p=0.001$ ,  $p=0.009$ , res). MiR-199a-5p was higher in acute IS, and stayed upregulated at day7 ( $p<0.001$ ,  $p=0.002$ , res). MiR-4467 was lower in the IS patients at day1 compared to control ( $p<0.001$ ). MiR-3135b was downregulated in IS patients at day1 and day7 compared to control ( $p<0.001$ ,  $p<0.001$ , res). ROC curve showed diagnostic value for all studied miRNAs for acute stage of IS ( $p<0.01$ ), see fig1d).

**2. Predictive analysis:** MiR-4786 (AUC=0.88; $p=0.008$ ), miR-1288 (AUC=0.93; $p=0.027$ ), miR-548ar-3p (AUC=0.85; $p=0.009$ ), Let-7e-5p (AUC=0.52; $p=0.005$ ) and miR-125a-5p (AUC=0.52; $p=0.008$ ) were upregulated, whereas miR-4676 (AUC=0.91; $p=0.003$ ) was downregulated, in patients with multiple stroke and/or TIA compared to single stroke in second microarray analysis (fig2a). qPCR validation results confirmed the microarray results for all studied miRNAs ( $p<0.0001$ ), which showed predictive value for risk of second stroke and/or TIA in ROC analysis ( $p<0.0001$ -fig2b/c). Enrichment analysis: IL-2, lipid metabolism, BDNF/MAPK signaling pathway, Intellectual Disability and Alzheimer's Disease are significantly related to stroke (fig2d).

**Conclusions:** None of the identified miRNAs were studied in stroke before. All studied miRNAs have diagnostic value for acute IS. Moreover, our results show predictive significance for the risk of a second stroke. Found miRNAs and pathways have thus potential diagnostic, prognostic and therapeutic utility in neurovascular diseases.

M.P. was supported financially as part of the research grant 'OPUS' from National Science Center, Poland (grant number 2018/31/B/NZ7/01137), and M.M and D.K. were supported by NN from the National Science Center, Poland (MEiN/2022/DIR/3261).



# Building Undergraduate Professional Identity and Persistence in the Pharmaceutical Sciences through Inquiry-Team-Based Lab Courses

Nicholas Denton,<sup>1</sup> and Amy Kulesza<sup>2</sup>

<sup>1</sup>Ohio State Univ; and <sup>2</sup>The Ohio State University

Abstract ID 16397

Poster Board 188

**Hypothesis:** One of the strongest predictors of student persistence in the pharmaceutical sciences is the formation of a professional identity as a pharmacologist. However, underrepresented 1st generation and minoritized students face additional challenges of opportunity gaps and identity threat that prevents them from having the socialization to the authentic pharmacologist experiences that are vital for developing a pharmacologist professional identity. While laboratory courses are often the formative experiences for undergraduates' identity formation, traditionally designed lab courses often don't explicitly socialize students to authentic inquiry-based pharmacologist experiences nor provide the psychological safety necessary for underrepresented students to fully engage in team-based learning. The research team hypothesizes that professional identity formation may be promoted in undergraduate students by implementing an authentic inquiry-team-based learning (ITBL) STEM laboratory course design.

**Methods:** The pharmaceutical sciences laboratory course was redesigned with inquiry-team-based principals of authentic student discovery, explicit team roles, psychologically safe engagement, and reflection on individual responsibilities to the research team. Undergraduate juniors and seniors enrolled in the ITBL-based pharmaceutical science lab course or an otherwise comparative traditionally-designed biology lab course were compared for traits predictive of persistence in the sciences using the experimentally validated Persistence in the Sciences (PITS) survey and an open-ended question asking them to recount a moment that validated or questioned their science identity. Univariate analyses and a codebook validated for initial interrater reliability based on Cohen's Kappa determined the effect of ITBL STEM lab course design on factors that may impact underrepresented students' indicators of professional identity formation.

**Results:** Students taking an ITBL-based pharmaceutical sciences lab course demonstrated an improved sense of professional identity compared to students in the traditionally designed biology lab. With exception of non-white males, ITBL lab students demonstrated significantly higher subsection PITS scores in Project Ownership-Emotion while white students had higher Project Ownership-Content and non-white female students reported higher Science Identity. Interestingly, both first-generation and continuous generation students demonstrated enhanced Project Ownership-Content and Project Ownership-Emotion, but only continuous generation students demonstrated enhanced Science Identity and Networking in the ITBL lab. Students cited multiple mechanisms such as validating science identity through gaining confidence in individualistic laboratory performance, collaborating through learning barriers and fostering confidence and societal impact in a future career in pharmacy.

**Conclusion:** The pharmaceutical sciences ITBL lab offered a collaborative, growth-promoting environment with experiments that are authentic to perspective pharmacologists, which resulted in students reporting higher persistence in the sciences scores indicative of feeling like a pharmacologist such as project ownership content/emotion, science identity, and networking across various student demographics.

# Demystifying the Concept of “Spare Receptors” in Pharmacology Education Through Novel Didactic Approaches

Jorge Iniguez-Lluhi

*Univ of Michigan*

Abstract ID 23348

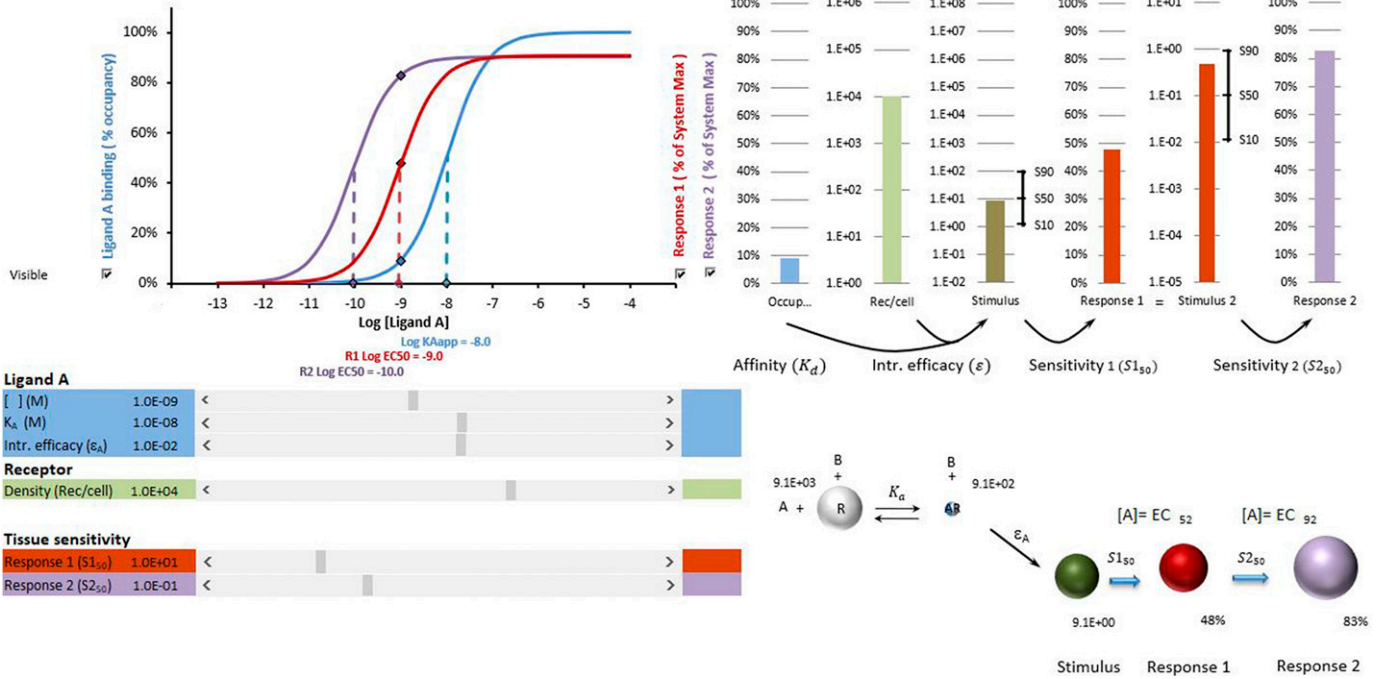
Poster Board 189

A major goal of pharmacology education is to provide learners with a solid understanding of the factors that drive the relationship between administered dose and both therapeutic and undesirable effects. Among the most challenging pharmacodynamic concepts to convey is the idea of “receptor reserve” or “spare receptors”. This concept is difficult to define and explain, even for seasoned pharmacologists. It is often introduced using an example: If the number of receptors in a system is reduced, and an agonist can still generate a maximal response, this means that there were “spare receptors” or that there was “receptor reserve”. This operational definition, however, describes only an extreme condition that puts receptor number as the only relevant parameter and obscures the key underlying agonist, and system properties that give rise to this important behavior.

As part of my involvement in pharmacology instruction at undergraduate, graduate, and professional levels, I have found that concept of receptor reserve can be introduced effectively as part of a comprehensive pharmacodynamic framework complemented with illustrative analogies and simulations. This didactic framework is based on a generalization of the classical Furchgott model of agonism, and leverages a **Versatile Simulation** tool for effective didactic illustration of **Pharmacodynamic** concepts (**VesPha**) that I have created. In this framework, the system mounts a response based on its sensitivity to the stimulus generated by occupied receptors. The stimulus, in turn, is proportional to the number of occupied receptors and their intrinsic efficacy, that is, the amount of stimulus each occupied receptor generates. The number of occupied receptors, in turn is driven by the concentration and affinity of the agonist and the total number of receptors.

At its core, receptor reserve can be viewed as conditions where a significant response can be generated by agonist occupancy of a relatively low fraction of available receptors, that is, when the  $IC_{50}$  is significantly lower than the  $K_d$ . In the context of the above framework, it is clear that receptor reserve is not simply a consequence of receptor number but depends critically on the intrinsic efficacy (a property of the drug-receptor complex) and the sensitivity of the system to the stimulus generated by the receptors, (a property of the system). The influence of each of these parameters on receptor reserve can be easily illustrated by dynamic simulations in **VesPha**. Using this tool, it is easy to demonstrate how the response to a ligand with higher intrinsic efficacy can display higher receptor reserve than one with a lower intrinsic efficacy in the same system despite a constant receptor number. Similarly, it is possible to illustrate how response to a particular agonist can display higher receptor reserve in a system that has higher sensitivity than another, even if the number of receptors is the same in both. It is also easy to illustrate how signal amplification contributes to receptor reserve, i.e., how, for the same agonist and system, receptor reserve increases as responses further down the amplification cascade are measured.

In conclusion, providing a self-consistent framework for pharmacodynamics and appropriate tools to illustrate it, is an effective way for learners to master fundamental concepts and demystify terms that are otherwise challenging to grasp.



VeSPha simulation illustrating receptor reserve.

# Strategies Used to Improve Quality of Multiple-Choice Questions: A Systematic Review

Tanvirul Hye,<sup>1</sup> and Monzurul Roni<sup>2</sup>

<sup>1</sup>Oakland University William Beaumont School of Medicine; and <sup>2</sup>The Univ of Illinois College of Medicine

Abstract ID 20956

Poster Board 190

**Introduction:** Multiple-choice questions (MCQ) are highly efficient for testing knowledge and they can be reliably used to assess a large cohort in the shortest possible time. However, good quality MCQs are relatively difficult to write and MCQs are subject to technical flaws such as redundant distractors and cueing the correct answers. Item flaws reduce the validity of the MCQ exam. Therefore, many health professions schools employ various quality control processes to remove these flaws. Although the literature describes various approaches to improve MCQ quality, there needs to be integrated research demonstrating their effectiveness and efficiency. This systematic review aims to accumulate evidence of different methods to improve the quality of MCQs in medical schools. Firstly, the review compares the effectiveness of various approaches to enhance the quality of MCQ. Secondly, the study explored how the quality of MCQ is quantitatively measured. Thirdly, the review examined the efficiency of different quality improvement approaches.

**Methods:** We adopted the population, intervention, comparison, and outcomes (PICO) as a search strategy tool. We searched PubMed, Embase, and Web of Science databases. Studies published between 2002-2022 were retrieved and screened by two independent investigators using inclusion and exclusion criteria. Articles focused on strategies to improve MCQ quality, targeting basic and clinical science in undergraduate and graduate medical schools were reviewed. The investigators independently extracted the following data from the articles: type of participants, sample size, study design, methods used to assess MCQ quality, data analysis methods, and outcomes.

**Results:** We identified 1143 articles from a primary search of the databases. Twenty-one studies from 9 different countries met the review criteria. Faculty training workshops (11 studies), committee/peer reviews (8 studies), or a combination of both (2 studies) approaches were used to improve MCQ quality. Despite wide methodological variations, most studies (95%) demonstrated that these processes were effective in significantly improving the measures of quality in MCQ exams. The quality improvement was measured by psychometric analysis, quality scores, Bloom's cognitive level, and distractor efficiency. None of the studies reported the efficiency of these quality improvement processes.

**Conclusion:** The reviewed studies indicated that faculty training or committee/peer review has a positive effect on the quality of MCQ exams. Considering the extensive use of MCQs in health professions schools, any of these quality assurance interventions should be adopted by educational institutions. Further research with more robust designs is required to examine the efficiency of these processes and to establish a standardized vetting process for MCQ exams.

# Monitoring metacognition and well-being in a medical pharmacology course: the role of information technologies

Ricardo Pena Silva,<sup>1</sup> Juanita Velasco Castro,<sup>1</sup> Christos Matsingos,<sup>2</sup> and Sandra Jaramillo Rincon<sup>1</sup>

<sup>1</sup>Universidad de los Andes; and <sup>2</sup>Queen Mary University Of London

Abstract ID 13618

Poster Board 191

**Introduction:** Metacognition is one of the most important thinking skills in any area of knowledge. This skill is particularly important in areas such as medicine or pharmacology, where health professionals must make complex decisions when providing care to patients or communities. There is little literature on how to promote, assess, and track metacognition in health sciences students. This self-reflection is especially important after the COVID-19 pandemic, which changed learning and teaching systems for several cohorts of students.

Journaling is an effective strategy for self-assessing our actions, mapping out plans, prioritizing tasks, and managing stress and anxiety. Student response systems facilitate the capture of information on student behaviors and knowledge in and out of the classroom. The objective of this study is to evaluate the usefulness of student diaries and student response systems as a strategy to improve productivity, planning, study methods, and mental health of students in a medical pharmacology course.

**Methods:** Over 2 years, since 2021, our medical pharmacology course has formally implemented weekly journaling as part of course activities. At the beginning of the semester students contribute to review and adapt a list of questions about physical and mental health care, meeting goals and commitments, study methods, perception of learning and teamwork. Each week students choose and thoughtfully respond to 4-5 questions from the list in a private forum on the institution's LMS. At the end of the semester students answer a short survey that evaluates their perception of the usefulness of the journals. In addition, during the two semesters of 2022 we are testing the effectiveness of a Student Response System, as a tool to collect information on study strategies, well-being and mental health in medical students.

**Results:** We have collected responses from 143 students, who reported that keeping a journal was helpful in improving their physical and mental health (63%), organizing their homework and assignments (75%), achieving their goals (89%), reflecting on their role as a person (83%) or student (90%). Of the available categories, the topic that students most liked to write about was "taking care of their physical and mental health" (64% of responses). Students felt that writing about their goals and commitments (92%), and about their study method and assignments (83%), helped them to better organize their time. Although 78% of students reported that they liked to reflect on teamwork, only 58% felt that the journals helped them improve the way they worked with colleagues.

**Conclusions:** Students rated the journals positively as a planning tool in their academic tasks and for maintaining their mental health, giving an overall rating of 7.97/10. We are currently analyzing Data Science tools to curate data collected through Student Response Systems to generate a dashboard that facilitates tracking student progress and well-being during an academic semester, and throughout their programs.

**Support/Funding Information:** FAPA grant to Ricardo Pena from the School of Medicine and the Vicepresidency for Research at Universidad de los Andes

# Can Virtual Reality Improve Pharmacology Education in Medical Students?

Monzurul Roni,<sup>1</sup> Kevin Kim,<sup>1</sup> Nicholas Xie,<sup>1</sup> Leslie Hammersmith,<sup>1</sup> and Yerko Berrocal<sup>2</sup>

<sup>1</sup>University of Illinois College of Medicine; and <sup>2</sup>Alice L. Walton School of Medicine

Abstract ID 14902

Poster Board 192

**Background:** Virtual reality (VR) is a powerful tool that allows participants to learn by exploring and manipulating an immersive 3D environment. In recent years, VR technology has successfully been applied in some areas of health professional education, including anatomy and clinical skills. The 3D immersive visualization in VR can potentially be applied to learn complex pharmacology topics. Despite its potential, the application and effectiveness of VR technology in pharmacology education are mainly unknown. The present study aims to investigate the effectiveness of VR technology in learning complex pharmacological concepts.

**Methods:** A prospective mixed methods design was used for this study. Undergraduate medical students at the University of Illinois College of Medicine evaluated a VR learning module on cardiovascular drugs affecting the autonomic nervous system. The 3D assets and visualizations for the VR module were developed by the Jump simulation center. The participants (n=20) were briefed on the operation of the HTC Vive headset and the virtual interface (Enduvo) before the intervention. The pharmacology knowledge was assessed using a pre- and post-intervention test. The students also participated in a post-intervention survey of 10 items (5-point Likert scale) and an open-ended question on learner satisfaction, ease of use, perceived usefulness, quality of visual elements, intention to use, and comfort level regarding the VR experience.

**Results:** The participants scored significantly higher in the post-intervention test than in the pre-intervention test ( $p < 0.05$ , paired t-test). The post-intervention survey demonstrated high internal reliability (Cronbach's alpha  $> 0.8$ ). Most of the participants agreed that they were satisfied with the VR module (90%), the VR was easy to use (90%), and their time was efficiently used (90%). A minority of participants thought they would have preferred a traditional learning format (15%), and some participants felt VR caused feelings of discomfort (20%). The majority of the comments regarding the VR module were positive.

**Conclusions:** Our data suggest that VR-based learning improves pharmacology knowledge in medical students, and most undergraduate medical students are receptive to this innovative learning tool. Therefore, immersive VR technology has the potential to make pharmacology education deeply engaging by providing 3D visualization of complex drug actions. Further studies are needed to compare the effectiveness of VR-based learning with traditional passive learning approaches in pharmacology education.

**Support/Funding Information:** Dean's Award for Innovative Medical Student Education (UICOMP) and OSF Healthcare Foundation.



# Pharmacology Education, Osteopathic Principles Integration, Osteopathic Manipulation Treatment relations: Osteopathic Graduating Seniors' Perception

Khalil Eldeeb

*Campbell Univ School of Osteopathic Medicine (CUSOM)*

**Abstract ID 55284**

**Poster Board 193**

Pharmacology education in the preclinical years of medical school focuses on different drug classes and their uses, side effects, and contraindications to provide the base for clinical applications. In osteopathic medical schools, students are additionally introduced to osteopathic principles that focus on the body's capability of self-regulation, self-healing, and health maintenance. They also get appropriate training on osteopathic manipulation treatment (OMT) as an additional tool to help their future patients. The relationship between osteopathic medical students' perception and evaluation of pharmacology education, integration of osteopathic principles in the course work, and OMT training has not been thoroughly studied. This study analyzed the self-reported perception and evaluation of graduating seniors in osteopathic medical schools in the United States for their first two years of medical education between the 2012/2013 and 2020/2021 academic years. Descriptive statistics and correlations were analyzed using SPSS version 26.0, and statistical inferences were considered significant whenever  $P \leq 0.05$ .

A statistically significant positive correlation was found between the percentage of students who agreed that osteopathic principles were adequately integrated into coursework and the percentage of students who reported the perception of time devoted to pharmacology instruction as excessive ( $r=0.737^*$ ,  $p=0.023$ ). A statistically significant negative correlation was founded between the percentage of students who agreed that an appropriate amount of training was provided in OMT and the percentage of students who reported a perception of time devoted to pharmacology instruction as excessive ( $r=-0.735^*$ ,  $p=0.024$ ) or appropriate and ( $r=-0.894^{**}$ ,  $p=0.001$ ). On the other hand, a statistically significant positive correlation was founded between the percentage of students who agreed that an appropriate amount of training was provided in OMT and the percentage of students who reported a perception of time devoted to pharmacology instruction as inadequate ( $r=0.883^{**}$ ,  $p=0.002$ ).

While pharmacology and OMT are excellent tools for osteopathic physicians in their practice guided by osteopathic principles, the current correlations in students' perception and evaluation may support the calls for better integrations in preclinical years curriculum and more detailed studies to improve the osteopathic medical student learning experiences.

# Embedding Diversity and Equity Conversations in Cardiovascular Pharmacology: Teaching Arrhythmia Management from A Diversity Context

Ashim Malhotra

California Northstate Univ Coll of Pharmacy

Abstract ID 28562

Poster Board 194

**Background and Objectives:** Foundational and pharmaceutical sciences are an integral part of health professions education. Ever since the publication of the seminal 1910 Flexner Report, foundational sciences are placed early in the medical education curriculum to maximize learners' ability to apply these principles in the evaluation and management of diseases. This "traditional" approach contextualizes clinical decision-making in a foundational sciences reference frame and has been extended to other health professions education programs such as pharmacy education. However, the integration of foundational sciences with clinical application remains difficult to achieve and measure. To bridge this gap, we designed, implemented and assessed an Integrated Cardiovascular Simulation (ICS), placing it in the Second Professional Year (P2) of our 4-year Pharm.D. curriculum. ICS engaged P2 learners to begin to connect the pharmacotherapeutic management of congestive heart failure (CHF) and arrhythmia emphasizing the pharmacological basis of clinical decision-making while incorporating select elements related to empathy, cultural competencies such as a linguistic barrier, patient history taking, and communication strategies such as the "SBAR" technique.

**Methods:** ICS employed Case-Based Learning principles and focused on congestive heart failure (CHF) with preexisting arrhythmias as comorbidity. A Laerdal SimMan 3G manikin was programmed to present CHF symptoms. P2 student teams were assessed on accurate identification of both symptoms and the underlying pathophysiology. ICS was staged through ER presentation (phase 1), admission to the ICU (phase 2), and hospital stay and discharge (phase 3). Laboratory values were integrated during phase 2, while the manikin presented atrial and ventricular fibrillation, Torsades de Pointes, and asystole, allowing students to learn rhythm identification. Additionally, students practiced the SBAR communication technique and patient counseling skills, and recommended therapy, elaborating MOA and adverse effects. ICS was assessed through pre- and post-session quizzes and perception data.

**Results:** Respondents indicated that ICS helped them learn: 1) arrhythmia pathophysiology (85%), 2) EKG interpretation of arrhythmias (89%), 3) adverse effects of antiarrhythmic medications (93%), 4) clinical decision making (92%), and 5) communication skills between team members (85%). Ninety-one percent felt that ICS made the content more clinically relevant than lecture, while student perception of their interaction with the simulated patient was rated at 74%. Student performance improved on a post-test (80.2%) compared to the pre-test (66.9%), with an increase in symptom and arrhythmia pattern recognition (41.2% and 36.7% increase in the post-test).

**Conclusion:** High-fidelity ICS is a novel tool to achieve and assess the integration of foundational and clinical knowledge.

# Design and Delivery of Small Group Pharmacology Exercises Facilitated Synchronously to Multiple Groups

Jennelle Richardson

*Indiana Univ School of M*

**Abstract ID 15865**

**Poster Board 391**

As pharmacology curricula have transitioned from lecture to active learning in small group, new challenges have arisen including ensuring appropriate student preparation and facilitating multiple small groups simultaneously with a limited number of session facilitators. Through continuous quality improvement and seeking student and faculty feedback, we have developed a structure for small group exercises that introduces, reinforces, and connects pharmacological concepts and drug classes.

The small group sessions are designed on two premises: that the value of the small group comes from the discussion within the groups among the students and that the facilitator's role is simply to reinforce and expand after that discussion. Student preparation is essential for successful discussions. In order to increase the likelihood of students completing pre-work, we design pre-work that is targeted specifically to that session. The pre-work generally takes the form of a short pre-recorded video accompanied by slides but may also include quick-check questions to help guide and reinforce content. We have found that students prefer recordings to assigned readings and that they prefer a targeted review video rather than referring them back to a topic covered in a prior course.

The session begins with "warm-up" questions that are answered with polling software by each student and discussed with the entire class. The session facilitator is able to quickly clarify any concepts that are unclear before the students start on the session exercises. The warm-up questions also allow for students to enter into the small group discussion having refreshed drugs and concepts that are fundamental to the session and whose understanding is necessary for application in the cases and questions.

In our pharmacology sessions it is common to have a single facilitator for 36 groups of students across 4 classrooms. This presents three specific challenges: ensuring full discussions rather than a race to answer, helping groups that get stuck, and identifying the areas that need further explanation. The depth of discussion often varies across the groups and can be gauged by spot checking groups and by reviewing answers that each group is required to submit. These answers can be used to adjust the questions in the following year and occasionally can result in multiple choice questions that are designed from the incorrect answers submitted. To decrease the time that groups are stuck and not making progress, we add "stuck questions". These are guiding questions that reflect the way a facilitator would steer a group back on track. Because each group is submitting answers in real time, the facilitator has the opportunity to review the answers and identify areas where there is confusion. During the full-class case review, the facilitator can clarify discrepant answers, expand on the information in the case, and connect concepts across sessions and courses.

Students are generally satisfied with the design and delivery of these sessions. In session and end-of-course evaluations, students often identify pharmacology small groups as a best practice. At the end of the pre-clerkship phase, 84% of students rated their pharmacology education as good/excellent. On the AAMC Graduation Questionnaire, 89% of students rated their pharmacology preparation for clinical clerkships as good/excellent. Observations from facilitators are that students are actively engaged with their groups and that the sessions are effective.

# Contributions of 15 ASPET DPE Members to the International Collaborative Core Concepts Project in Pharmacology Education: Reflections and Opportunities for ASPET

A. Laurel Gorman,<sup>1</sup> Mark Hernandez,<sup>2</sup> Kelly Karpa,<sup>3</sup> Carolina Restini,<sup>4</sup>  
Fabiana Caetano Crowley,<sup>5</sup> Joseph Goldfarb,<sup>6</sup> Clarie Guilding,<sup>7</sup> and Paul White<sup>8</sup>

<sup>1</sup>Univ of Central Florida - College of Medicine; <sup>2</sup>Alabama College of Osteopathic Medicine; <sup>3</sup>East Tennessee State University Quillen College of Medicine; <sup>4</sup>Michigan State Univ; <sup>5</sup>Western Univ; <sup>6</sup>Icahn School of Medicine at Mount Sinai; <sup>7</sup>Newcastle University; and <sup>8</sup>Monash University

Abstract ID 20585

Poster Board 392

**Introduction:** For pharmacology educators worldwide it can be challenging to curate the vast amount of pharmacology information that exists. Recently it was recognized that pharmacology, unlike other disciplines, lacks core concepts. Core concepts are big ideas that are essential to understand and practice a discipline, the mastery of which results in enduring understanding and ability to address novel problems across that discipline. Therefore, between 2021 and 2022, 15 ASPET Division of Pharmacology Education (DPE) members participated in a collaborative effort led by a team of international leaders in pharmacology education to develop the Core Concepts for Pharmacology Education. The goal of this abstract is to share the process and camaraderie that resulted from this global project.

**Methods:** A forum on ASPET Connect and an officer on the ASPET DPE Executive Committee (EC) recruited ASPET members interested in participating in an international expert group to develop, in two sequential phases (Fig. 1), worldwide pharmacology education core concepts. During an exploratory phase, global research project leaders from the United Kingdom, Australia, and United States (including an officer from the ASPET DPE EC) utilized a large-scale survey approach. Working asynchronously, using Excel, core concepts were generated by soliciting key pharmacology terms provided by several hundred expert educators and combining those with terms identified through text mining key pharmacology textbooks. During a refinement phase with the aid of Google Docs, participants revised and offered feedback to support or oppose potential core concepts and engage in dialogue. Virtual meetings via Zoom, often duplicate ones to accommodate participants in different time zones, further facilitated the process and collaboration. In July 2022, participants were able to meet in person, with other members of the team joining remotely to finalize the core concepts and develop consensus about their definitions. A manuscript was drafted and circulated to project members.

**Results:** The Pharmacology Education Core Concepts project was successfully executed with video meetings and other collaboration tools such as Google Docs, the cloud and email, to develop a consensus on definitions based on the expert input from over 200 pharmacology educators across the globe. Using the Delphi method and analysis by a research team consisting of leaders from international professional pharmacology education organizations, including ASPET, 25 core concepts were developed. This project demonstrated that participants from different countries can effectively collaborate. Those involved, after establishing core concepts, went on to generate sub-concepts and definitions.

**Conclusions:** Collaborative international efforts can be expensive, time consuming, and travel can be logistically challenging with limited input. The successful Core Concept project represents effective use of virtual technology to promote global collaboration. The strategy developed and disseminated products will aid pharmacology educators worldwide as they design and/or curate pharmacology information to provide the essential foundational pharmacology content for their students. This process serves as an efficient model, with a low carbon footprint, for future global collaborations with a lower cost.

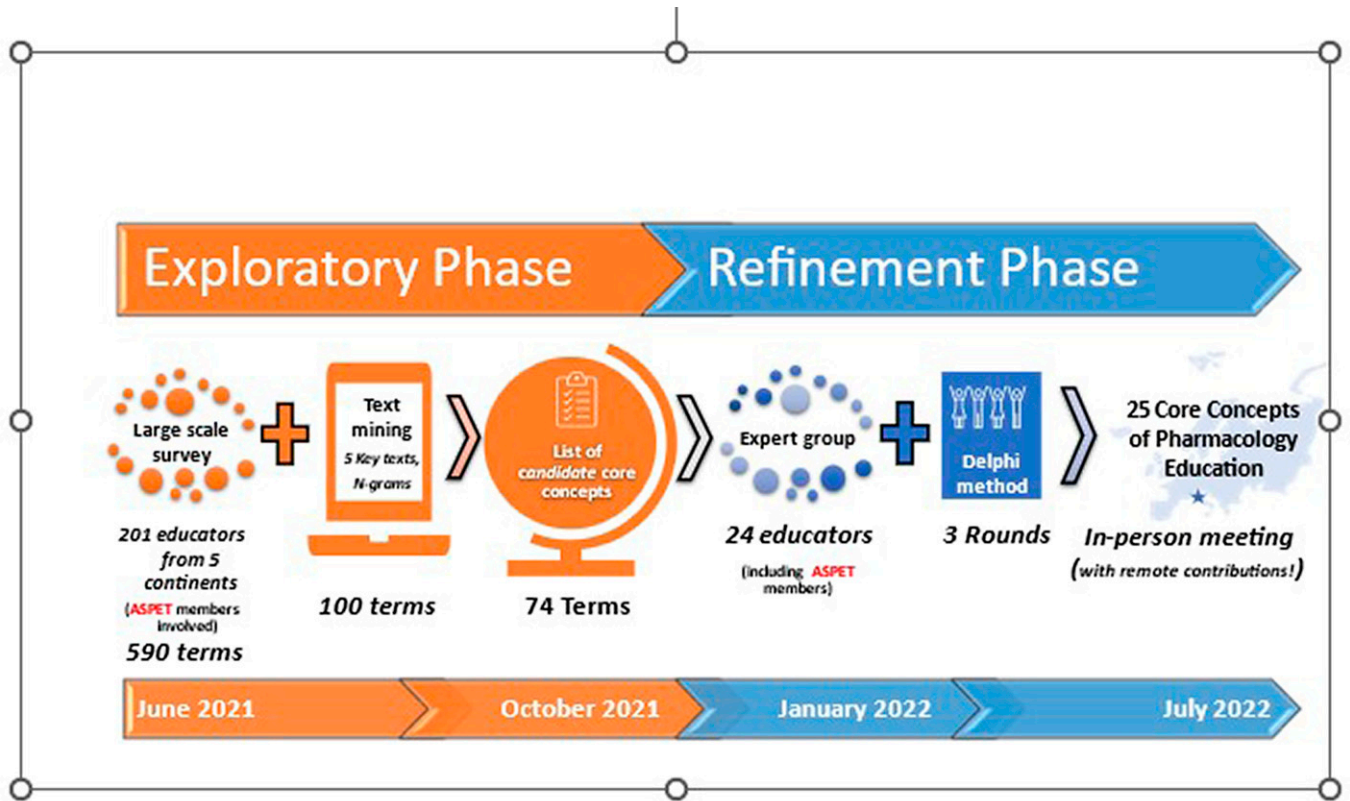


Fig 1: Global Pharmacology Education Core Concepts Process

# Our Approach to Updating the Cardio System Pharmacology Knowledge Objectives

Mark Hernandez,<sup>1</sup> Youssef Soliman,<sup>2</sup> Andy C. Chen,<sup>3</sup> Joe B. Blumer,<sup>4</sup> and Kelly Karpa<sup>5</sup>

<sup>1</sup>Alabama Coll of Osteopathic Medicine; <sup>2</sup>Geisinger Commonwealth School of Medicine; <sup>3</sup>Ohio University Heritage College of Osteopathic Medicine; <sup>4</sup>Medical University of South Carolina; and <sup>5</sup>East Tennessee State University Quillen College of Medicine

Abstract ID 13913

Poster Board 393

**Introduction:** In medicine, pharmacology content introduced during pre-clerkship years must align with best practices and guidelines taught in the clinical years of training. Due to the large volume of content students must master during pre-clerkship training, learners often rely on board preparation resources, which may contain errors. Furthermore, the rapidly changing landscape of new drug approvals and practice guidelines requires frequent updates to pharmacology curricula. These issues prompted an update to the Pharmacology Knowledge Objectives (KO) last published in 2012, which have traditionally served as a standard content guide for educators. The purpose of this abstract is to present our approach in reviewing and updating the KO for the Cardiovascular System.

**Methods:** During the ASPET annual meeting in Philadelphia in 2022, the Division of Pharmacology Education sponsored a session detailing plans to update the KO, which in the past had been updated by the American Association of Pharmacology Chairs (AMSPC). A call for ASPET members was made to participate in the process and committees were formed. The Cardiovascular System Committee discussed the intent of the KO and best practices for the update. A shared Google document was used for timely updates and commentaries, and weekly meetings via Zoom were used to facilitate dialogue. A 3rd year medical student who completed the required medical licensing examination and clerkship rotations was invited to provide input from a medical student perspective.

**Results:** A numbering system with subheadings was proposed with a process of referencing KO from other organ systems. Objectives were revised to be more concise, with a focus on using terminology that is more specific and accurate. Action verbs were updated to target higher order cognitive processes of learning. Where appropriate in the clinical pharmacology section, a reference on most recent recommendations by the American College of Cardiology guidelines were included.

**Conclusions:** Since last published in 2012, drug discontinuation and/or removal from the market and new drug approval with novel mechanisms of action led to updated practice guideline for the management of hypertension (2017), hyperlipidemias (2018), and heart failure (2022). New classifications were also proposed for antiarrhythmic drugs (2018). Pharmacology textbooks lag in describing new therapies and treatments. Leading electronic resource tools often do not provide specific information related to basic science content. The process for updating the KO was a learning experience for all involved. Pharmacology educators are encouraged to use the KO when developing new curricula and even provide the KO to learners to guide their self-directed study. Likely in 2023, additional updates to the Cardiovascular System KO will be needed as the field is constantly evolving.

# Diversity, Equity, and Inclusive Course Design in Pharmacology Education: Strategies, Opportunities and Lessons Learned

Katerina Venderova

*Kaiser Permanente Bernard J. Tyson School of Medicine*

**Abstract ID 56827**

**Poster Board 394**

**Aim:** Medicine and medical education continue to struggle with persistent health disparities and inequitable learning opportunities and outcomes. The aim of our work was to develop learning objectives, activities, instructional materials, and assessments that implement core principles of inclusive course design to teach basic and clinical pharmacology in our new undergraduate medical curriculum. Approach: At KPSOM, basic and clinical pharmacology is mainly taught in five Integrated Science courses that utilize case-based learning (CBL) approach and that span across the first 3 years of the curriculum. Here are examples of strategies we have implemented to support achievement of our aims: 1. Variety of strategies to present information (video with script, textbook, activities, discussion, peer teaching, panel discussion, simulation, peer-teaching). 2. Variety of assessment methods to demonstrate competency: multiple-choice questions, objective structured clinical examination, small group participation, open ended questions, written report, oral presentation). 3. Creating space for students to share personal experiences. 4. Equal representation of diverse communities in clinical vignettes, without stereotyping. 5. Including pictures of relevant clinical presentations in patients with different skin tones (for example for cyanosis or skin conditions). 6. Addressing and correcting dated or inappropriate language or medical terminology in study materials. 7. Avoiding using ethnicity or race as a proxy for inter-individual genetic variations that, for example, affect response to a drug. 8. Discussing how and why individual characteristics, such as age, sex, body composition, pregnancy, can affect response to a drug. 9. Highlighting why and how one's background, identity, or circumstances (such as socioeconomic status, age, geography, language, national origin, race, gender, gender identity, sexual orientation, disability status, mental health challenges) may profoundly impact how they are treated and their treatment outcomes. 10. Emphasizing the need for clinical trials and other research to include a diverse and representative pool of subjects. 11. Recognizing health inequities and data gaps, and the impact of dominant power structures and biases in generating and perpetuating them. 12. Recognizing and celebrating diversity in pharmacology. Results: The inaugural curriculum launched in July 2020 with the first cohort of 50 students and we are currently completing curriculum development for our third-year students. Overall, the feedback from our students and faculty indicates increased student engagement and satisfaction with the inclusive learning experience. Some of the challenges included need for more faculty development, and increased demands on time to develop the sessions. Conclusion: Pharmacology is typically perceived by students as challenging, highlighting the importance of providing inclusive and equitable learning experience for all learners. We have successfully implemented several strategies for inclusive course design and teaching of pharmacology in a new medical curriculum. Serving as a bridge between biomedical and clinical sciences, pharmacology provides many opportunities to integrate topics of diversity, equity, and inclusion and to foster a holistic view of the patient. This ultimately helps tackle systemic barriers, address the health inequities, and improve care for marginalized populations.

# The Pharmacology Knowledge Objectives (KOs)-Current Status

Robert Theobald,<sup>1</sup> and Joe B. Blumer<sup>2</sup>

<sup>1</sup>*AT Still Univ of Health Sciences; and* <sup>2</sup>*Medical Univ of South Carolina*

**Abstract ID 26669**

**Poster Board 395**

The Pharmacology Knowledge Objectives (KOs) are a compilation of concepts and content originally developed to guide faculty members in the education of medical students in the mid-1980s by the Association of Medical School Pharmacology Chairs (AMSPC), and to guide the development of core pharmacology content and suggested contact hours for undergraduate medical student education. They provided guidance towards a standardized knowledge base for content decisions. The KOs were maintained by AMSPC, with the last iteration occurring in 2012.

The need for such guidance seems apparent when one considers the variety of curricula in medical education today. To provide some consistency in content and concepts for undergraduate medical students, and perhaps other healthcare students, seems an important goal. To bring the KOs up to date, AMSPC and ASPET's Division for Pharmacology Education (DPE) combined to update them, with the DPE providing oversight of updates and future maintenance. AMSPC and DPE formed working groups chaired by content experts with committee members from numerous institutions. Peer review was minimal since each committee was comprised of content experts who currently teach in each area. Co-editors reviewed the documents for formatting, grammar, and spelling, plus any clarification needed. Important drugs in each class were listed along with content recommendations for faculty consideration with suggestions of relevant physiology and pathophysiology, pharmacodynamics, pharmacokinetics, and pharmacogenomics. Faculty can modify suggestions to meet the needs of their individual students and/or the culture of their institution.

The final document contains over 170 pages of guidance in fifteen major areas of pharmacology for undergraduate medical education. It has been compiled and reviewed by content experts who are pharmacology educators in universities and medical schools around the country, providing their expertise to help all faculty who request assistance. The current edition of the Knowledge Objectives in Pharmacology, 2022, is maintained on the ASPET/DPE and the AMSPC websites and is available to all. The KOs may also benefit international medical education faculty and curriculum development.

In conclusion, this document is a concept and content document that contains prototypical and representative drugs in each drug class. The Knowledge Objectives have served the discipline of pharmacology well for almost 4 decades. They provide a guide for consistency in pharmacology education of undergraduate medical students. The update, and the relationship between AMSPC and ASPET/DPE will allow a timely maintenance of the KOs to the benefit of medical students, faculty, and the public, enhancing the consistency and quality of undergraduate medical education, and hopefully, clinical practice. They may find use in the international educational community.



# The Notable Integration of Clinically Relevant Pharmacology in Problem-Based Learning Cases

Tawna Mangosh

Case Western Reserve Univ

**Abstract ID 23747**

**Poster Board 396**

At Case Western Reserve University, self-directed learning serves as the cornerstone of medical education. To ensure students are trained for their future careers as life-long learners, first- and second-year medical students engage in Problem-based Learning (PBL) to cultivate their skills. Despite the current inclusion of pharmacology throughout the PBL curriculum, student satisfaction as it relates to their pharmacology education continues to fall short of faculty expectations. Efforts must be made to develop innovative learning opportunities to foster self-directed pharmacology learning and improve student satisfaction and exam performance in this area. The purpose of this study is to determine if the introduction of pharmacology learning objectives and novel video resources for each PBL case improves student satisfaction and learning outcomes related to pharmacology education.

New learning objectives are being mapped to pharmacology resource videos created by our faculty via the Notability application. Videos address pathophysiology, drug mechanisms, and important pharmacologic considerations relevant to each existing PBL case. Using Notability, these teaching resources can be repurposed by the students to practice recalling and applying their knowledge. Students are being asked to rate their satisfaction with these learning opportunities at the conclusion of each course and provide comments for qualitative analysis. In the future, pharmacology-related summative assessments will be examined and compared to cohorts who did not receive the pharmacology learning objectives or video resources. Additionally, student perception ratings of clinical preparedness regarding pharmacology education on the AAMC Graduation Questionnaire will be compared with previous years upon graduation of the first cohort with this intervention.

Data collection is ongoing but initial student feedback is encouraging. Student satisfaction data has been collected for one major curricular block of the pre-clerkship phase. Of the students (n=105) that rated the educational effectiveness of the pharmacology resource videos, over 95% of students indicated the videos were either effective, very effective, or extremely effective. Notably over 70% of students indicated the videos were extremely effective. Additionally, student comments were classified as either positive or negative and thematic comment analysis revealed six themes. Most comments were positive and aligned with the themes of excitement and appreciation, effective explanation of complex concepts, curricular alignment of content, quality visual resource, and clinically relevant pharmacology focus. The limited number of negative comments aligned with the themes of technology barriers and curricular alignment of content. To complement these findings, satisfaction ratings and exam performance from subsequent curricular blocks are being collected and analyzed.

The integration of pharmacology learning objectives and the development of Notability-based pharmacology resources received an overwhelmingly positive response. Moving forward, these resources will continue to help guide student's self-directed learning thereby improving student satisfaction and learning outcomes in their pharmacology education.

# ASPET Academy of Pharmacology Educators: Twelve Years of Pharmacology Educators' Recognition

Khalil Eldeeb

*Campbell Univ School of Osteopathic Medicine (CUSOM)*

**Abstract ID 56816**

**Poster Board 397**

American Society for Pharmacology and Experimental Therapeutics (ASPET) launched the academy of pharmacology educators in 2010 to distinguish individuals who exemplarily contributed to pharmacology education. In their detailed applications, applicants show evidence of ASPET's active membership, scholarship in pharmacology education, involvement in life-long learning, professional service, and others. However, there is limited data about the program outcomes. This study examined the diversity among the ASPET academy of pharmacology educators' fellows over the last twelve years.

This study reviewed the academy fellows between 2010-2022 profiles. We utilized data published on the ASPET website and other public websites to gather the fellows' demographic, geographic distribution, terminal degree, and academic rank information.

Between 2010-2022, the ASPET academy of pharmacology educators program inducted 28 fellows (64% were males). Thirty-two percent (32%) of the fellows are earlier DPE Pharmacology Educator Awards recipients. Terminal degrees distribution among the fellows was Ph.D. (75%), M.D. (7%), M.D./Ph.D. (11%), and PharmD/Ph.D. (7%). Geographically, the Fellows were in North America (92%), Asia (4%), and Australia (4%). Most fellows (91.7%) work in the U.S.A., mainly in the southeastern and midwest states (76.9%). The fellow's affiliations included allopathic Medical schools (57%), Pharmacy schools (21%), Osteopathic Medical schools (14%), Nursing schools (4%), and Dentistry schools (4%). The fellow's academic ranks included Professor (46%), Associate Professor (39%), and Assistant Professor (14%).

Academy of Pharmacology Educators fellows is a diverse group of pharmacology educators. Future studies will evaluate the impact of the academy membership on the fellow's teaching, scholarship, academic promotion, and leadership activities.

# Identifying Students' Causal Mechanistic Reasoning (CMR) in Medical Pharmacology

Rosalyn Bloch,<sup>1</sup> Carolina Restini,<sup>1</sup> Nathan Bautista,<sup>2</sup> and Keenan Noyes<sup>3</sup>

<sup>1</sup>Michigan State Univ; <sup>2</sup>Michigan State University College of Osteopathic Medicine; and <sup>3</sup>University of Nebraska-Lincoln

Abstract ID 18675

Poster Board 593

**Background:** Many medical students struggle with the overload of information in pharmacology and lack knowledge of foundational pharmacology principles compared to pharmacy students. Education research states that when students use epistemic heuristics such as causal mechanistic reasoning, they can better construct precise inferences and are more likely to make strong predictions on new phenomena than those who learn using recall and memorization methods.

**Hypothesis:** students using CMR to understand pharmacologic pathways can develop predictive insights regarding currently taught pharmacologic agents and novel ones they will approach in the clinic

The study **AIMED** to: investigate how students respond to a prompt designed to elicit causal mechanistic reasoning about the adverse effect of an adrenergic antagonist and Na<sup>+</sup>-glucose-like type-2 transporter inhibitor; analyze the extent to which students use CMR to explain pharmacological phenomena.

**Methods:** short-answer responses were collected from 100-200 2<sup>nd</sup>-year osteopathic medical students enrolled at a large mid-western university (IRB approval: 7350). Demographic information was collected; personal information was de-identified. Students were asked about: pharmacology education/background, undergrad major, research or job experience, and clinical experience and to rank their study materials and methods. We are analyzing connections between this information and students' use of CMR, with particular attention to students' pharmacology background and study methods. **Causal mechanistic approach:** a coding scheme was developed to explore the sophistication responses in a problem scaffolded to elicit medical pharmacology knowledge. Based on data from a smaller subset of responses, two independent researchers coded the answers to establish inter-rater reliability (IRR), calculated via Cohen's kappa values to collect qualitative and quantitative data. The qualitative data of the binned responses were analyzed for independence via the Pearson Chi-square test and their level of CMR via the Chi-square test.

**Results:** 25% of the students could provide a fully causal mechanistic account of the phenomenon. Still, 50% of the students could provide at least some part of the CMR model in their explanation. No significant relationship ( $p=0.17$ ) was found when comparing the pharmacology background (*None, Moderate, or Strong*) with whether they correctly predicted the phenomenon. Similarly, no significant association ( $p=0.2$ ) was found when comparing their primary study resource (*Active, Passive, or Memorization*) with whether they correctly predicted the phenomenon.

**Conclusion:** Students primarily use recall for pharmacologic information, particularly with identifying drugs' adverse effects, rather than using a CMR model. Students using recall methods are less likely to integrate their knowledge regarding pharmacological phenomena and make robust predictions about novel treatments. While there is no significant association between the correctness of the students' prediction and their pharmacology background or methods of studying, there is a significant relationship between their prediction correctness and their engagement in CMR.

**Perspectives:** Collectively, our data's evidence supports that using a more integrative, pathway-based pharmacology curriculum would allow students to use CMR when engaging with agents/drugs pharmacological pathways.

**Support Info:** MSUCOM Dep Pharm & Tox

# Addressing Healthcare Inequities Through The Medical Pharmacology Curriculum

Jennelle Richardson

*Indiana Univ School of M*

**Abstract ID 27490**

**Poster Board 594**

Healthcare inequities have become more of a focus in medical education in the last few years as we explore the impact of social, cultural, financial, and systemic factors on patient care. Barriers occur at the individual level as well as organizational and policy levels. We have recently added context to race-based and race-conscious treatment recommendations as well as information regarding treatment access to our pharmacology content.

We have included healthcare equity information impacting treatment in a number of pharmacology sessions. We do teach race-based treatment recommendations, but we provide context regarding both the strength of the underlying evidence along with presenting potential factors that may underlie differences in effectiveness among different populations. We explicitly discuss the limitations of using race as a proxy for population variations while also acknowledging that different populations face inherent health inequities. For example, when discussing the use of hydralazine/isosorbide dinitrate in Black patients, we discuss factors that impact racial disparities in heart failure. As we discuss options for monotherapy antihypertensive treatments, we include discussions of social, financial, and genetic factors. During our presentation on ethanol metabolism, we include information on variants of aldehyde dehydrogenase in certain ethnic groups and how those variants are associated with increased esophageal cancer risk. We talk about Medicaid coverage for direct-acting antiviral treatments for hepatitis C and state restrictions that negatively impact underserved populations. We discuss CYP2D6 isoforms across different populations and the impact on codeine metabolism. We continue to identify topics that impact healthcare equity. We want to avoid over-treating lower-risk patients in a particular population and missing risks in vulnerable patients who share contributing factors but are not included in a specific identified high-risk population.

As part of our focus on diversity, equity, and inclusion, we recognize that word-choice matters, and we are intentional in the language that we use. However, we also recognize that older language is not always updated and that students are often more attuned to this than faculty. We have recently begun including a question regarding DEI on a feedback form available for every session so that students can anonymously identify potential issues in content or delivery. We also enable a notes function in our exam software so that students can point out concerns with wording of exam questions. This has helped us respond in real time to concerns and has enabled students to be part of the process of improvement. Our overall strategy to addressing DEI in the pharmacology curriculum is a patient-centered approach that recognizes the impact of various factors on different populations.

# Successful Integration of Pharmacology Instruction From Day One of Medical School

Sandeep Bansal, Thomas Yorio, and Kelly Pagidas

*Anne Burnett Marion School of Medicine at TCU*

**Abstract ID 23564**

**Poster Board 595**

**Aim:** Pharmacology instruction has traditionally been presented during the second year of medical school training. Our innovative curriculum integrates pharmacology instruction from the beginning of preclinical year 1. We report our findings on student performance on customized, standardized testing with such an early adoption.

**Methods:** In our medical school's integrated, organ systems-based and active learning curriculum, Phase 1 covers basic science content tightly integrated within clinical contexts. As such, pharmacology is integrated beginning week one, within weekly problem-based learning cases, team-based learning sessions, as well as during their Phase 1 longitudinally integrated clerkships. We analyzed performance on pharmacology content covered during the first three months of preclinical training. The pharmacology topics covered during this period were pharmacokinetics, pharmacodynamics, principles of chemotherapy (anticancer, antimicrobials), anti-inflammatory agents, and immunotherapy.

Students are assessed by summative exams using the customized National Board of Medical Examiners (NBME) exams. Item analysis report is obtained using the NBME Customized Assessment Software. On the item analysis summary report, the NBME describes the performance of students outside of the school administering the test as "source." The source majorly includes students who have taken pharmacology in the second year of the curriculum as opposed to our students who are in year one.

**Results:** Twenty-six exam items represented pharmacology content covered over three months in the faculty-generated customized NBME exams. Our students' (n=57) performance level on these exam items was similar to the source average. Average difficulty level (p-value) of the pharmacology items on the administered customized NBME exams was 0.78 compared to the source's mean difficulty level of 0.81. Anecdotally, student feedback was positive. Students appreciated learning principles of pharmacology from week one of their medical training.

**Conclusion:** Item analysis of pharmacology questions on the summative exams shows that our students' performance is comparable to the "source." Level of performance on pharmacology items on tests that are normally taken by medical students upon completion of basic science curriculum has provided evidence that it is worthy to expose medical students to pharmacology content from day one of preclinical training. Early integration of pharmacology instruction appears to promote understanding of pharmacotherapeutic principles that students continue to build on as they progress through remaining curriculum content. Our pharmacology curriculum design and lessons learned from its successful implementation can be useful in informing other medical schools and educators attempting to integrate pharmacology throughout an innovative medical curriculum.

# Student perceptions of scholarly scientific writing in pharmacology: student generation of collaborative rubrics to score literature reviews in social pharmacology

Hanna Wetzel,<sup>1</sup> Terri Enslein,<sup>1</sup> and Edward Kosack<sup>1</sup>

<sup>1</sup>Xavier University

Abstract ID 15695

Poster Board 596

Scientific scholarly writing is an important skill in pharmacology and other fields in science. Despite a strong focus on writing in many courses, faculty and students have disparate expectations related to scholarly writing. Exploration of student expectations may lead to more effective teaching strategies in the area of scientific scholarly writing in pharmacology. Herein, we present a classroom exercise where students were asked to write a rubric that would be used to score a summative assessment (worth 20% of their grade) in an undergraduate pharmacology class. This was done in a 300-level undergraduate course titled "Foundations of Pharmacology". The course is targeted for upper-division biology and chemistry undergraduates. It is a writing intensive course that counts towards the university wide core curriculum as a writing flag. In this course, students are introduced to the basics of pharmacokinetics/pharmacodynamics, systems pharmacology, and drug development. Their final assignment is to explore Social Pharmacology by choosing a drug that has been impacted by societal factors, develop a thesis statement, and write a literature review supporting their thesis. They complete a series of scaffolded assignments including submission of a thesis statement, a synthesis grid of their citations, and peer review. Before beginning any work on their papers, students spend a 50-minute class period in pre-established groups writing the rubric that will be used to score their final product. They are provided with a list of elements that may represent good writing (ideas, organization, voice, word choice, sentence fluency, conventions, and presentation), then asked to define what effectively demonstrating these elements would look like, and what weight they give to each element (if any). Students weighed "ideas" heavier than any other category (42 ±26%), followed by "organization" (13±13%), "voice" (12±12%), "conventions (11±6%)", "word choice" (10±10%), "presentation" (7±8%), and "sentence fluency" (5±4%) (n=5 groups, 23 students). One group gave 20% to elements not listed. For comparison, we mapped our established departmental writing rubric to these elements. This rubric gave 25% weight to ideas, and the remaining elements were given 12.5% weights respectively. While there is a slight difference in what students and faculty perceive as important in scholarly writing, this demonstrates that students can be given ownership over these expectations without compromising pedagogy. There was also disparity between student groups, for example the weight assigned to "ideas" ranged from 12.5-70%. Students reported improvements in their scientific writing ability their end of semester course evaluations. Lastly, this is an example of how an undergraduate pharmacology course can be incorporated into the core curriculum of a university which will increase the reach of the class and expose more undergraduates to the field of pharmacology.

This work was supported by the Xavier University Center for Teaching Excellence through a Faculty Learning Community.

# Longitudinal Impact of Mnemonics Use on Pharmacy Students' Exam Performance and Perceptions of Knowledge Retention and Clinical Application

Shankar Munusamy,<sup>1</sup> Carrie Koenigsfeld,<sup>1</sup> and Ron Torry<sup>2</sup>

<sup>1</sup>Drake University College of Pharmacy and Health Sciences; and <sup>2</sup>Drake University College of Pharmacy & Health Sciences

Abstract ID 21983

Poster Board 597

**Background:** Health professions students attending pharmacology courses often feel overwhelmed with learning and remembering essential facts about medications, i.e., knowledge acquisition and retention. Moreover, applying pharmacological knowledge to clinical settings demands significant amounts of the student's working memory (i.e., a high cognitive load). Mnemonics (memory aids) are shown to reduce cognitive load and facilitate learning and knowledge retention among students. Our study assessed the longitudinal impact of mnemonics' use in a Pharmacology course offered to second-year pharmacy students on students' perceptions of knowledge acquisition, retention, and clinical application in correlation to their exam performance.

**Methods:** Eighteen mnemonics were developed and used in a course covering endocrine and autonomic pharmacology topics. The study was conducted in two student cohorts in the 2020-21 and 2021-22 academic years. A non-anonymous survey (survey 1) was administered after each exam to collect students' self-reported use of mnemonics on exam questions. At the end of the semester, on an anonymous survey (survey 2), students rated the impact of mnemonics' use on their knowledge retention, clinical application, critical thinking, reduction in learning anxiety, and increased confidence while answering questions on exams. To assess retention, an anonymous follow-up survey (survey 3) was administered to the same student cohorts at the end of the Therapeutics-I course five months later.

**Results:** Analysis of survey 1 findings (response rate: 55% in 2020-21; 65% in 2021-22) revealed that mnemonics use significantly improved students' exam performance (99.4% correct with vs. 87.3% correct without mnemonics in the 2020-21 cohort and 94.6% correct with vs. 84.7% correct without mnemonics in the 2021-22 cohort;  $p < .0001$ ). Survey 2 findings revealed that students consistently agreed that mnemonics' use improved their knowledge retention (98.2% in 2020-21 and 97.6% in 2021-22) and clinical application (98.2% in 2020-21 and 97.6% in 2021-22). Similarly, students agreed that mnemonics helped them think critically while answering exam questions (89.3% in 2020-21 and 87.8% in 2021-22), reported higher confidence during test-taking (96.4% in 2020-21 and 90.2% in 2021-22), and reduced learning anxiety (80.4% in 2020-21 and 61.0% in 2021-22). Furthermore, the longitudinal survey 3 findings were consistent with survey 2; most students agreed that mnemonics' use improved their knowledge retention (71.4% in 2020-21 and 66.7% in 2021-22), clinical application (76.2% in 2020-21 and 66.7% in 2021-22), critical thinking (64.3% in 2020-21 and 63.3% in 2021-22), confidence during test taking (66.7% in 2020-21 and 56.7% in 2021-22), and reduced learning anxiety (64.3% in 2020-21 and 60.0% in 2021-22).

**Conclusions:** Our findings indicate that 1) mnemonics' use improves students' exam performance and 2) mnemonics are perceived positively by students to facilitate their knowledge acquisition (by reducing learning anxiety), improve knowledge retention, application, critical thinking, and increase confidence while test-taking. When used intentionally, mnemonics could serve as an effective tool to promote student learning and long-term knowledge retention and application.

# Development and Implementation of Equitable and Inclusive Teaching Practices in Pharmacology

Elizabeth S. Yeh

*Indiana Univ School of Medicine*

**Abstract ID 16603**

**Poster Board 598**

In biomedical research, there exists a demographic gap in success from individuals from diverse backgrounds. Policy changes are currently being implemented in an effort to support diversity and create an environment of inclusion for students and trainees from historically underrepresented groups. Evidence shows that inclusive and equitable teaching practices positively inspire success in science educational areas and positively impacts career success. Faculty serve a critical role and have a responsibility to serve as examples of change in science learning environments. Trainees have the ability to provide valuable input to shape their learning environment. Through trainee interviews, a problem was identified that there was a gap in the learning environment. Educating trainees in professional and career development was lacking. Upon receiving this feedback, the objective as educators and mentors was to improve equity and inclusion for trainees by providing them with stage appropriate tools for professional development. This presentation aims to provide an overview of practices that were implemented to create a culture of mutual respect and inclusion to support pharmacology and toxicology graduate program trainee development and success. The implementation of these practices was based on the diversity of the trainee population, trainee feedback, areas of need identified by department leadership, and input from the faculty. The approach used was to implement workshops into the curriculum that directly addressed professionalism and career development. The goal of these strategies is to create a set of teaching practices that focuses on diversity, equity, and inclusive practices that foster scientific learning and post-graduate career success. Moving forward, data obtained from these studies will be used to intentionally design curriculum, improve mentoring quality, and cultivate equity-based tools to reach diverse groups of trainees to promote success through inclusion. The opportunity to address this gap has resulted in an observational hypothesis building study aimed to improve education for biomedical trainee outcomes.



# Evaluation of Diversity and Bias Topics in a Medical School Pain & Opioid Analgesic Curriculum

A. Laurel Gorman,<sup>1</sup> and Danny Kim<sup>2</sup>

<sup>1</sup>Univ of Central Florida - College of Medicine; and <sup>2</sup>UCF College of Medicine

Abstract ID 20961

Poster Board 599

**Introduction:** Despite national directives to improve pain, opioid, and analgesic pharmacology healthcare education to manage pain without promoting addiction, deficiencies persist in healthcare curricula in integrating educational activities with diverse patients. Given biases and misconceptions related to pain and analgesia hamper effective pain management and harm outcomes, improvements in medical education at all levels are essential. The purpose of this abstract is to present data from our undergraduate medical curriculum evaluating medical student misconceptions, biases, and perceptions on the effectiveness of integration of diversity topics into their opioid/analgesic education. Our goal in analyzing outcomes is to inform curriculum improvement in pharmacology/therapeutics education at our institution and others.

**Methods:** A Likert survey (anchored where 5=strongly agree to 1=strongly disagree) was developed with themes of Biases/misconceptions on pain/analgesia (B-M) and Educational activities in diverse populations (Ed-Dp). Three medical student cohorts were invited to participate: E-M2: N=34 emerging second-year (M2); E-M3: N=27 emerging clerkship; E-M4: N=26 emerging fourth-year. Anti-inflammatory analgesics were covered in medical school year one (M1) while opioids, antidepressants, anticonvulsants, drugs of abuse, substance use disorder, and pain diagnosis/management were all covered toward the end of M2 and integrated throughout M3. E-M2 served as a baseline (novice cohort) for comparison given their limited exposure to structured analgesic content.

**Results:** Mean Likert scores were used in statistical comparisons; % were reported for descriptive purposes. For B-M, 94%(E-M2), 89%(E-M3), 85%(E-M4) recognized poor pain management increases suicide risk; E-M2 (94%) were more likely to identify biases in minority pain treatment than E-M3 (70%) or E-M4 (81%); Gender biases were evident: 29%(E-M2), 46%(E-M3), 42%(E-M4) misbelieved that females exaggerate pain more than males; Age-related misconceptions/biases were evident in all cohorts for geriatric patients. E-M2 scored lower than E-M3 and E-M4 in non-opioid analgesic pharmacology knowledge (E-M2 vs E-M3 or E-M4,  $p < 0.01$  by Student's t-test of mean Likert scores). For (Ed-Dp), E-M3 (69%) and E-M4 (61%) rated general opioids/analgesia diversity significantly higher ( $p < 0.001$ ) than E-M2 (4%). All cohorts perceived education in geriatric pain and prescribing biases were insufficient.

**Conclusions:** Students perceived M2/M3 curricula were successful in general analgesic/opioid pharmacology education and better in comparison with M1 but about 40% of E-M3 and E-M4 felt it was insufficient in addressing diversity and biases. Most cohorts understood the need for effective pain management and identified concerns with poor pain management and opioid prescribing in underrepresented minorities. However, large percentages in all cohorts demonstrated gender biases and age biases which negatively impact pain management in these groups. Most perceived that more education in diverse patients was essential and many noted insufficient experiences with geriatric cases. Thus, our data support our previous data showing insufficient diversity in substance use disorders education and confirm national findings that much improvement is needed in integrating biases and diverse patient experiences into opioid/analgesia pharmacology, and pain management curricula.

# Integration and Alignment of Pharmacological Principles and Agents in a Preclinical Problem-Based Learning Curriculum Through a Web-Based Interface

Megan Amber Lim,<sup>1</sup> Lisan Smith,<sup>2</sup> Max Ledersnaider,<sup>3</sup> Diamond Coleman,<sup>3</sup> Noah Nigh,<sup>3</sup> Christopher Pecenka,<sup>3</sup> and Noelle Kwan<sup>4</sup>

<sup>1</sup>Carle Illinois College of Medicine - UIUC; <sup>2</sup>Carle Illinois Coll of Med; <sup>3</sup>Carle Illinois College of Medicine; and <sup>4</sup>Carle Foundation Hospital

**Abstract ID 24184**

**Poster Board 600**

In line with the majority of modern medical schools curricula, the Carle Illinois College of Medicine (CIMED) utilizes a preclinical curriculum organized by organ system [1]. At the core of the CIMED preclinical curriculum is the use of a problem-based learning (PBL) pedagogy. PBL is the primary mode of delivering key basic science, clinical science, engineering, and professional learning objectives through the context of a clinical case scenario. Additional related course content is supplemented through a mixture of lectures, flipped classroom, and team-based learning (TBL) approaches. While providing clear benefit by contextualizing the interplay between core concepts such as physiology, anatomy, biochemistry, and pathology, these approaches have revealed that teaching foundational concepts in pharmacology remains a challenge according to student feedback.

The aim of this project is to develop an interactive web interface aligned with the CIMED preclinical curriculum to address the challenge of teaching and incorporating pharmacological concepts while enhancing student learning and understanding of therapeutic agents. The interface design focuses on a few core principles, namely: 1) high yield information aligned with CIMED PBL content, 2) clinical relevance, 3) easy navigation, and 4) an ability to be used as an assessment tool. Specifically, this interface blends organ system-based indications, probable diagnoses, and relevant drug classes to create a unique concept-map. This visualization highlights the variety of major drug indications in each organ system, incorporates the structure of pharmacological agents to aid student learning and memory of drug classes, and elaborates on the breadth of pharmacological agent classes that are used as treatments. Given that CIMED's preclinical curriculum requires that students participate in case-based learning and have an introduction to clinical practice weekly during their first year, it's imperative that students conceptualize key pharmacologic concepts, e.g. interactions, mechanism of action, and adverse effects as many drugs are not always confined to a single organ-system or patient comorbidities. Using concept mapping will allow the students to formulate meaningful connections between drug classes and their uses versus memorizing individual drugs in isolation which will better equip them to develop treatment plans in clinical settings. This presentation demonstrates the first phase of the CIMED preclinical Pharmacology web interface construction focused on the first organ system CIMED first year medical students encounter, the cardiovascular system. The cardiovascular specific web interface will serve as the model for the construction of the web interface. Additionally, a component to provide a formative assessment of students' competency by allowing them to construct their concept maps and occlude portions of existing maps for self-assessment is planned. In conclusion, this web interface will be used as a modality to standardize pharmacology instruction across various organ blocks in order to promote cohesivity despite having different course directors throughout the pre-clinical phase.

## References:

[1] <https://www.ncbi.nlm.nih.gov/pmc/articles/PMC6140046/>

# A Cutaneous Nitrogen Mustard Murine Injury Model to Study the Pathophysiology of its Long-term Effects

Andrew Roney,<sup>1</sup> Dinesh Goswami,<sup>2</sup> Ebenezar Okoyeocha,<sup>1</sup> Steve Lundback,<sup>1</sup> Holly Wright,<sup>1</sup> Omid Madadgar,<sup>2</sup> Ellen Kim,<sup>2</sup> Jared M. Brown,<sup>3</sup> and Neera Tewari-Singh<sup>2</sup>

<sup>1</sup>Michigan State University; <sup>2</sup>Michigan State Univ; and <sup>3</sup>University of Colorado Denver

Abstract ID 23809

Poster Board 19

Vesicating agents cause skin injury with blisters upon cutaneous exposure and this can lead to secondary infections as well as systemic toxicity. These acute consequences can further lead to long-term skin effects including long-lasting lesions, necrosis, wounding, hyperpigmentation and scarring of the skin. Sulfur mustard (SM) has been the most widely used chemical weapon and it remains a concern for use in warfare and terrorist activities. We currently lack effective therapies for either the acute or long-term effects of SM. Development of therapies has become an urgent need as SM exposure is thought to be a contributing factor in Gulf War Illness, a syndrome experienced by many War veterans, and remains a potent chemical arsenal. In this study, we aimed to develop a nitrogen mustard (NM, a structural analog of SM) induced long-term skin injury model in C57BL/6 mice, which will enable future studies to explore underlying mechanisms of SM toxicity and to test potential therapies.

Male C57BL/6 mice were topically exposed to either 0.5 mg or 1.0 mg NM in 100 mL of acetone. Pictures were taken at various timepoints over a 3-month period and skin lesions were scored. Mice were sacrificed and skin tissue collected at various timepoints after NM-exposure. Skin samples were fixed, sectioned, and stained for histological analyses.

NM exposure caused skin lesions including erythema, edema, and necrosis in mice at both the exposure doses. In the 1 mg exposure group, erythema and edema were seen at 24 hours and worsened by day 3 post-exposure, at which point erythema plateaued while edema peaked at 5 days and declined by 7 days after exposure. In the 0.5 mg exposure group, erythema and edema were seen at 24 hours and worsened at day 3, with erythema disappearing by 2 weeks post-exposure and edema decreasing but remaining apparent throughout the study period. Necrosis was first seen at 3 days after exposure in both the groups, peaking at day 5 and then declining at day 7 post-exposure in the 1 mg group, while increasing slightly and remaining apparent throughout the study period of 3 months for the 0.5 mg group. Microvesications and scabs first appeared at 24 hours, worsened at 2 weeks, and mostly disappeared by 3 months post NM-exposure. Hyperkeratosis, epidermal thickness and scabbing were observed in both the exposure groups; however, scabbing and inflammatory response was more severe in 1.0 mg exposure group. Further analyses will be carried to characterize skin injury, such as changes in pigmentation, hair regrowth, wound size, and burns.

Overall, these results indicate that 0.5 mg NM can be used for further histologic and mechanistic studies in this mouse model to establish useful biomarkers that can assist to explore potential therapies for long-term mustard effects.

# Impairing Cytochrome P450-mediated metabolism aggravates the hepatotoxicity of serotonin and norepinephrine reuptake inhibitor duloxetine

Feng Li,<sup>1</sup> Xuan Qin,<sup>2</sup> John M. Hakenjos,<sup>1</sup> Kevin Mackenzie,<sup>1</sup> and Lei Guo<sup>3</sup>

<sup>1</sup>Baylor College of Medicine; <sup>2</sup>Baylor College of Med; and <sup>3</sup>U.S. Food and Drug Administration

Abstract ID 24646

Poster Board 20

Duloxetine (DLX), a dual serotonin and norepinephrine reuptake inhibitor for the treatment of major depressive disorder, is mainly metabolized by CYP1A2 and CYP2D6 in human. Despite DLX has a good tolerance for most patients, the cases with serious liver injury have been reported. Here, we investigated the roles of P450-mediated metabolism in the DLX hepatotoxicity *in vitro* and *in vivo*. We found that DLX is less toxic to CYP1A2- or CYP2D6-overexpressed HepG2 cells compared to their counterpart HepG2 cells transduced with empty vector, indicating that P450-mediated metabolism attenuates DLX cytotoxicity to HepG2. The CYP1A2 ( $\alpha$ -naphthoflavone and fluvoxamine) or CYP2D6 inhibitors (paroxetine, fluoxetine, and quinidine) significantly enhanced the toxicity of DLX to human primary hepatocytes. In Cyp1a2-knockout (Cyp1a2-KO) and *counterpart* wild-type (WT) mice, 50 mg/kg or 100 mg/kg (p.o.) of DLX for consecutive 5 days did not significantly increase the plasma ALT and AST levels compared with the vehicle group in both WT and Cyp1a2-KO mice, suggesting that Cyp1a2 is not a fundamental contributor to DLX detoxification at least in mice. However, DLX and a mouse Cyp2d inhibitor propranolol in both WT and Cyp1a2-KO mice lead to severe liver injury. The ALT levels increased for 2.9- and 8.7-fold in 50 mg/kg and 100 mg/kg groups, respectively in WT mice co-treated with propranolol. Similar increased folds of ALT were also observed in Cyp1a2-KO mice. H&E staining of mouse livers also confirmed the liver toxicity, presented as cell necrosis, in 100 mg/kg group in both WT and Cyp1a2-KO mice with the co-treatment of Cyp2d inhibitor.

In summary, our findings suggests that impairing P450-mediated metabolism exacerbates DLX hepatotoxicity *in vitro* and *in vivo*. Further studies are warranted to verify the roles of CYP1A2 and CYP2D6 in DLX liver toxicity using liver humanized mice and their inhibitors.

This work was supported by the NIDDK (R01DK121970) and NICHD (R61/33HD099995) to Dr. Feng Li. Feng Li was also partially supported by the NICHD (P01 HD087157, R01HD110038) to Dr. Martin M. Matzuk.

# The HMGB1/MAPKs/Nrf2 Signaling Arbitrates Hepatoprotection Conferred by Celecoxib in Preeclamptic Weaning Rats

Mahmoud El-Mas,<sup>1</sup> Salwa A. Abuissa,<sup>2</sup> Reem H. Elhamammy,<sup>3</sup> Nevine M. El-Deeb,<sup>4</sup> and Sherien A. Abdelhady<sup>5</sup>

<sup>1</sup>College of Medicine, Kuwait University, Kuwait; Faculty of Pharmacy, Alexandria University, Egypt; <sup>2</sup>Faculty of pharmacy-Alexandria Univ-Egypt; <sup>3</sup>Faculty of Pharmacy, Alexandria University; <sup>4</sup>Faculty of Medicine, Alexandria University; and <sup>5</sup>Faculty of Pharmacy, Pharos University in Alexandria

Abstract ID 14468

Poster Board 21

Preeclampsia (PE) is often associated with multiple organ damage that remains noticeable long beyond gestation. Here, we tested the hypotheses that antenatal therapy with nonsteroidal antiinflammatory drugs (NSAIDs), namely celecoxib, diclofenac, or naproxen, refashions liver damage induced by PE in weaning rats and that the high mobility group box 1 (HMGB1) and downstream inflammatory and oxidative effectors modulate this interaction. PE was induced by pharmacologic nitric oxide deprivation during the last week of gestation (N<sup>ω</sup>-nitro-L-arginine methyl ester, L-NAME, 50 mg/kg/day, via oral gavage). Compared with control rats, weaning PE rats (3 weeks post-labor) revealed substantial rises in serum transaminases together with clear histopathological signs of hepatic cytoplasmic changes, portal inflammation, and central vein dilation. While gestational NSAIDs reversed the elevated transaminases, they had no effects (celecoxib, naproxen) or even worsened (diclofenac) the structural damage. Molecularly, celecoxib was the most effective NSAID in: (i) reversing PE-evoked upregulation of hepatic gene expression of proinflammatory HMGB1 and concomitant increments and decrements in EMAPK<sub>ERK</sub> and MAPK<sub>p38</sub> abundance, respectively, and (ii) elevating and suppressing serum interleukin-10 and TNF- $\alpha$ , respectively. Amendments caused by PE in protein expression of the antioxidant transcription factor Nrf2 (decreases) and its negative modulator Keap-1 (increases) were also notably ameliorated by celecoxib. Alternatively, rises in serum IL-1 $\beta$  and shifts in macrophage polarization towards an inflammatory phenotype caused by PE were comparably diminished by all NSAIDs. Together, the data disclose an advantageous therapeutic potential for gestational celecoxib over diclofenac or naproxen in controlling hepatic dysfunction and HMGB1-interrelated inflammatory and oxidative sequels of PE.

# Effect of Vitamin E on Doxorubicin and Paclitaxel Induced Memory Impairments in Male Rats

Ahmad AlTarifi,<sup>1</sup> Kareem Sawali,<sup>2</sup> Karem Alzoubi,<sup>2</sup> Tareq Saleh,<sup>3</sup> Omar Khabour,<sup>2</sup> and Malik Abu Alrub<sup>2</sup>

<sup>1</sup>Jordan Univ of Sci & Tech; <sup>2</sup>Jordan University of Science and Technology; and <sup>3</sup>The Hashemite University

Abstract ID 22614

Poster Board 22

Cancer continues to represent a major contributor to morbidity and mortality worldwide. Despite the efficacy of conventional chemotherapy in abrogating tumor growth, these agents can also impact normal tissue, resulting in multiple treatment-limiting adverse effects. In addition to causing peripheral neuronal dysfunction, chemotherapy can also affect the function of central nervous system (CNS), causing significant cognitive dysfunction, difficulties with memory, thinking clearly, and increased anxiety. These heterogeneous group of central abnormalities are often described as post-chemotherapy-induced cognitive dysfunction, “chemofog”, or more commonly, “chemobrain”. Unfortunately, an exact pathophysiology and effective treatment for chemobrain are both lacking. Thus, this study aimed to investigate the short- and long-term effects of doxorubicin (DOX) and paclitaxel (PAC) on learning and memory in rats using radial arm water maze (RAWM). Also, we evaluated the possible beneficial effect of Vitamin E (as antioxidant vitamin) on DOX- and PAC-induced cognitive impairment. Adult male rats were injected with 4 doses of 2 mg/kg/week DOX (or its vehicle) or 2 mg/kg PAC (or its vehicles) every other day intraperitoneally. Vitamin E or its vehicle was co-administered with these drugs in other groups to study its antioxidative effects in the brain. Using radial arm water maze, each rat was assessed for learning and memory performance through two sets of six trials separated by a 5-minute rest period. These 12 trials were followed by a 30-minute trial (13<sup>th</sup> trial) to evaluate short-term memory and two long-term memory trials after 5 and 24 hours (14<sup>th</sup> + 15<sup>th</sup> trials). At the end of the treatment period and behavioral tests, all animals were decapitated, and the brain was promptly dissected, and hippocampal tissue was extracted for chemical analysis. TBARS and BDNF levels were measured using Enzyme-Linked Immunosorbent Assay (ELISA). Our results showed that there is no deficit in learning or long-term memory in both DOX and PAC groups compared to the control group. However, rats in the DOX or the PAC groups made significantly more errors in all short-term memory trials (trials after 30 minutes) than the other groups. This effect was improved in groups where Vit. E was co-administered with either DOX or PAC. PAC (but not DOX) was able to induce hippocampal lipid peroxidation as indicated by increasing the levels of standard biomarker thiobarbituric acid reactive substances (TBARS). Interestingly, the co-administration of Vit. E resulted in the reversal of PAC-induced hippocampal oxidative stress. Moreover, both DOX and PAC exposure reduced BDNF expression in the hippocampus, which was overcome by the co-administration of Vit. E. Our results indicate a potential role of Vit. E in mitigating short-term memory impairment in rats exposed to chemotherapy, possibly due to the reduction in hippocampal oxidative stress and neurodegeneration.

**Support/Funding Information:** Deanship of Research, Jordan University of Science and Technology (Grant number 2021/109)

# Evaluation of the Time- and Dose-Dependent Toxicity of Sunitinib Using a 3-D Human Hepatic Spheroid Model

Shalon L. Harvey,<sup>1</sup> Jessica L. Beers,<sup>1</sup> and Klarissa D. Jackson<sup>1</sup>

<sup>1</sup>UNC Eshelman School of Pharmacy

**Abstract ID 24159**

**Poster Board 23**

Sunitinib is a tyrosine kinase inhibitor (TKI) used to treat cancers such as imatinib-resistant gastrointestinal stromal tumors. This TKI has been associated with hepatotoxicity in some patients taking the drug, and numerous studies have been conducted in order to test the mechanisms of hepatotoxicity associated with sunitinib. The goal of this study was to evaluate the time- and dose-dependent toxicity of sunitinib using a 3-D human hepatic spheroid model. Cryopreserved human hepatocytes from a single donor were plated in a 384-well plate and allowed to form spheroids over 6 days in culture. After spheroid formation, cells were treated with varying concentrations of sunitinib (0, 0.2, 1, 2, 10, and 50  $\mu$ M) and acetaminophen (APAP, 0, 0.1, 0.5, 1, 5, 10 mM) as a positive control. Cells were dosed every 2-3 days over the 21-day experiment period. Cell viability and function were assessed by measuring ATP release and urea production using the CellTiter-Glo 3D Cell Viability assay and the QuantiChrom Urea Assay Kit, respectively. Assays were conducted on days 7, 14, and 21 after the initial day of plating (day 0). The results from the ATP and urea assays on days 14 and 21, when normalized to solvent control, showed an overall dose-dependent reduction in ATP and urea levels in spheroids treated with sunitinib and APAP. We believe these data indicate that 3-D hepatic spheroid models can be used to observe the hepatotoxic effects of sunitinib, at least through the observation of ATP levels and urea production. Future studies will focus on optimizing additional assays, such as the GSH-Glo™ Glutathione Assay, to determine the mechanisms of sunitinib-induced toxicity in the 3-D hepatic spheroid model.

This research is supported in part by the National Institutes of Health National Institute of General Medical Sciences [Grant R35GM143044] and by the University Cancer Research Fund of the University of North Carolina at Chapel Hill. Research reported in this abstract is solely the responsibility of the authors and does not necessarily represent the official views of the National Institutes of Health or the University of North Carolina at Chapel Hill.

# Arsenic trioxide impairs primary human NK cell responses against influenza A virus

Allison P. Boss,<sup>1</sup> Robert Freeborn,<sup>2</sup> Yining Jin,<sup>2</sup> Luca Kaiser,<sup>1</sup> Elizabeth Gardner,<sup>1</sup> and Cheryl E. Rockwell<sup>2</sup>

<sup>1</sup>Michigan State University; and <sup>2</sup>Michigan State Univ

**Abstract ID 20848**

**Poster Board 24**

Arsenic is a naturally occurring contaminant that is commonly found in water supplies. Chronic exposure to arsenic has been associated with multisystem disease, including respiratory diseases such as viral infections. Arsenic is known to regulate immune cell activity and has been shown to alter NK cell frequency and function. However, our knowledge on effects of arsenic on NK cell response to influenza remains limited. The following study aims to identify the effects of arsenic trioxide on NK cell activation and function against influenza A virus in primary human immune cells. Primary human peripheral blood mononuclear cells were treated with environmentally-relevant concentrations of arsenic trioxide prior to an influenza A virus challenge. Flow cytometric analysis of NK cells showed arsenic trioxide significantly decreased NK cell viability. Additionally, NK cell activation markers, CD69 and NKp46, were reduced with increasing concentrations of arsenic. Consistently, the production of NK cell effector mediators, including IFN $\gamma$ , granzyme B and perforin, were significantly impaired with treatment of arsenic trioxide. Overall, these data suggest that environmentally relevant concentrations of arsenic trioxide impaired NK cell responses to influenza A virus, which could negatively impact NK cell-mediated host defense. Furthermore, this study suggests that coculture of primary human NK cells with virally-infected cells is a useful model that can be used to assess the impact of chemicals on the effector function of human NK cells. This study was supported by the NIH R01 ES024966 and R21 ES033830.



# Multi-Walled Carbon Nanotubes Stimulate Arachidonate 5-Lipoxygenase-dependent M1 polarization of Macrophages to Promote Proinflammatory Response *in vitro*

Chol Seung Lim,<sup>1</sup> Michael Kashon,<sup>2</sup> Dale Porter,<sup>2</sup> and Qiang Ma<sup>2</sup>

<sup>1</sup>NIOSH, CDC; and <sup>2</sup>NIOSH

Abstract ID 53140

Poster Board 25

Polarization of the macrophages regulates the acute inflammation and its resolution in a time-dependent manner. Multi-walled carbon nanotubes (MWCNTs) induce the polarization of M1 and M2 macrophages in mouse lungs. The molecular and cellular pathways leading to the macrophage polarization induced by MWCNTs are incompletely understood. Here we examined the molecular mechanism by which MWCNTs induce M1 polarization using *in vitro* assays and the murine macrophage cell line, J774A.1. Carbon black (CB, Printex90) was used as an amorphous, carbon-based particle control. Treatment of macrophages with MWCNTs (Mitsui-7), but not CB, increased the expression of arachidonate 5-lipoxygenase (Alox5) mRNA and protein in a concentration- and time-dependent manner. MWCNTs, but not CB, induced the expression of CD68, a M1 cell surface marker, and the expression and activity of inducible nitric oxide synthase, a M1 intracellular marker, indicating M1 polarization. Induction of CD206, a M2 marker, was not observed, indicating polarization to M2 macrophages was not induced. Consistent with polarization to M1 macrophages, MWCNTs induced the production of the proinflammatory cytokines tumor necrosis factor- $\alpha$  and interleukin-1 $\beta$ , and the proinflammatory lipid-mediators leukotriene B4 (LTB4) and prostaglandin E2 (PGE2). Moreover, the cell-free media from MWCNT-polarized macrophages induced the migration of neutrophilic cells (differentiated from HL-60). MWCNT-induced chemotaxis was blocked by inhibition of leukotriene A4 hydrolase or the LTB4 receptor, but not cyclooxygenase 2, revealing LTB4 as a major mediator of neutrophilic chemotaxis from MWCNT-polarized macrophages. Knockdown of Alox5 using specific small hairpin-RNA suppressed MWCNT-induced M1 polarization, LTB4 secretion, and migration of neutrophils, revealing a critical role of Alox5. Taken together, these findings demonstrate that MWCNTs induce the polarization of M1 macrophages *in vitro* and that induction of Alox5 is an important mechanism by which MWCNTs promote proinflammatory responses by boosting M1 polarization and production of proinflammatory lipid mediators.

This work was supported by a grant (#9390HTN) from the Nanotechnology Research Center, National Institute for Occupational Safety and Health, Centers for Disease Control and Prevention.

# The Influence of Arsenic on Selenium Uptake by Red Blood Cell Anion Exchanger 1/*SLC4A1* Variants

Serena Li,<sup>1</sup> Kamran Shekh,<sup>2</sup> Naomi M. Potter,<sup>2</sup> Emmanuelle Cordat,<sup>2</sup> and Elaine M. Leslie<sup>1</sup>

<sup>1</sup>Univ of Alberta; and <sup>2</sup>University of Alberta

Abstract ID 20267

Poster Board 26

Chronic exposure to arsenic (As), a human carcinogen, is a global health concern affecting millions of people across the world; it can cause lung, skin, and bladder cancers and is associated with kidney and liver tumours, cardiovascular disease, and diabetes. In many regions, removal is economically unfeasible, and toxicity prevention and treatment strategies are greatly needed. Arsenic and the essential element selenium (Se) exhibit mutual protection via the formation of the seleno-bis (S-glutathionyl) arsinium ion  $[(GS)_2Asse]^-$  in red blood cells (RBCs), resulting in As and Se sequestration from other tissues in the body. As a result, dietary Se supplementation has been proposed as a potential solution to As toxicity. The RBC anion exchanger 1 (AE1/*SLC4A1*) is a chloride/bicarbonate ( $Cl^-/HCO_3^-$ ) exchanger which also transports selenite ( $HSeO_3^-$ ). The AE1 gene, *SLC4A1*, is highly variable and over 25 variants are linked to common hereditary human diseases including RBC disorders. The mutants have been well characterized for cellular localization and  $Cl^-/HCO_3^-$  exchange activity, but not for  $HSeO_3^-$  uptake. Our overall hypothesis is that differences in As and Se transport pathways in RBCs could influence how well individuals exposed to As will respond to Se supplementation as a means of preventing As-induced carcinogenicity and other diseases. We selected five naturally occurring AE1 variants, well-characterized for  $Cl^-/HCO_3^-$  exchange: the inactive Southeast Asian Ovalocytosis (SAO) deletion (AE1- $\Delta$ Ala400-Ala408), the endoplasmic reticulum-retained AE1-Arg760Gln, reduced anion exchange mutants AE1-Leu687-Pro and -His734Arg, and the hyperactive AE1-Pro868Leu. We hypothesized that  $HSeO_3^-$  transport by these variants would be proportional to established  $Cl^-/HCO_3^-$  transport. WT- and variant-AE1 were expressed in human embryonic kidney (HEK) 293 cells. AE1-wild-type (WT) transfected HEK293 cells demonstrated uptake of  $HSeO_3^-$  with similar kinetic parameters to RBCs, supporting AE1 as the main RBC uptake transporter of  $HSeO_3^-$  and validating the use of HEK293 cells as a model.  $HSeO_3^-$  uptake by HEK293 cells expressing empty vector (EV), AE1-SAO, -Leu687Pro, -His734Arg, -Arg760Gln, and -Pro868Leu, was 0.28, 0.55, 0.69, 0.37, 0.34, and 1.92-fold WT, respectively. We also hypothesized that Se accumulation would increase As retention proportionally, and vice versa. With arsenite,  $HSeO_3^-$  uptake by HEK293-EV, AE1-SAO, -Leu687Pro, -His734Arg, -Arg760Gln, and -Pro868Leu, was 0.33, 0.71, 0.77, 0.48, 0.43, and 1.97-fold WT, respectively. The low  $HSeO_3^-$  ( $\pm$  arsenite) accumulation for SAO, His734Arg, and Arg760Gln and high accumulation for Pro868Leu mutants were expected. However, the Leu687Pro mutant unexpectedly retained  $HSeO_3^-$  uptake at levels similar to WT-AE1. These data could have implications for the use of Se supplementation in human treatment for As exposure; exposed individuals expressing variants that increase Se accumulation in RBCs will likely benefit more from Se supplementation than those with reduced  $HSeO_3^-$  transport.

# Interrogating Environmental Contaminant Activity Against the Druggable GPCRome: A High Throughput Approach to Assess Interaction and Pathology

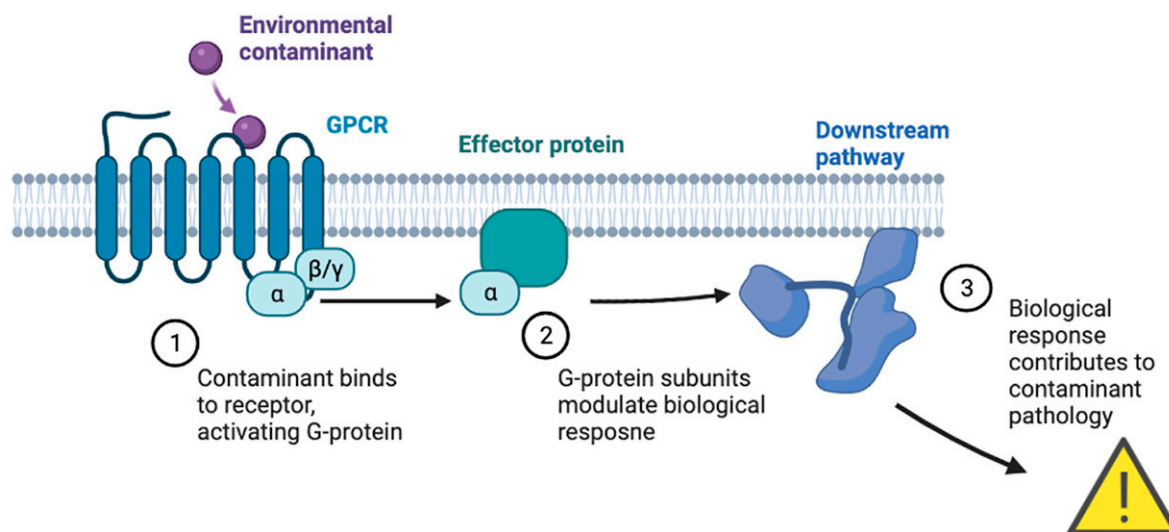
Joshua Wilkinson<sup>1</sup> and Dave Roman<sup>1</sup>

<sup>1</sup>Univ of Iowa

Abstract ID 28830

Poster Board 56

From intentional production and unintended byproducts of industrialization, large amounts of anthropogenic chemicals have been produced and amassed in the environment. These environmental contaminants can disrupt physiological equilibria and cause diverse harm to human health, such as developmental disorders, immunological-mediated diseases, and neurological pathologies. Past literature and emerging data show that certain environmental contaminants can activate specific GPCRs. However, studies focus on specific contaminant-receptor pairs in detail, leaving the vast majority of the GPCR landscape unexplored. As GPCRs act as signaling nodes in many physiological processes, we hypothesized that interrogating the activity of a contaminant against the GPCRome could be used to assess biological impact while simultaneously providing insight into potential mechanisms of pathology. This work applies traditional pharmacology and drug discovery practices toward toxicology efforts. Utilizing the open-source platform (PRESTO-Tango), we developed a screening methodology capable of investigating the activity of contaminants against 314 non-olfactory GPCRs amenable to high-throughput. From our initial screen of eight compounds, we identified several interactions between polychlorinated biphenyls (PCBs) and GPCRs, including both characterized and orphan receptors. Most interesting are the relationships uncovered between specific PCB congeners (PCB95 and PCB52) and receptor isoforms involved in sphingosine-1-phosphate and melatonin signaling pathways (S1PR4 and MTb). To our knowledge, this is the first report of these interactions, highlighting the utility of our approach to quickly assess the biological impact and pathology of a contaminant at the receptor level. Additionally, while detailed pharmacological experiments are underway, these findings could potentially support the involvement of sphingosine and melatonin signaling interplay in pathologies beyond the contaminant(s) alone.



# Induction of Thioredoxin-Interacting Protein and Role in NLRP3 Activation by Carbon Nanotubes in Macrophages

Qiang Ma,<sup>1</sup> Chol Seung Lim,<sup>2</sup> Fatimah Matakah,<sup>3</sup> Dale Porter,<sup>3</sup> and Mackenzie Buck<sup>3</sup>

<sup>1</sup>NIOSH/CDC; <sup>2</sup>NIOSH, CDC; and <sup>3</sup>CDC/NIOSH

Abstract ID 53145

Poster Board 57

The NLRP3 (NOD-like receptor family pyrin domain containing 3) inflammasome is an intracellular supramolecular complex that plays an important role in particle sensing and initiation of inflammatory responses to inhaled particles, including nanoparticles, in the lung. The mechanism by which NLRP3 is activated by carbon nanotubes remains unclear. The thioredoxin-interacting protein (TXNIP) is a multi-functional protein of the alpha-arrestin family implicated in redox regulation, glucose uptake, cell proliferation, and activation of NLRP3. Using an *in vitro* model, we investigated the regulation of TXNIP expression in macrophages and explored its role in NLRP3 activation by multi-walled carbon nanotubes (MWCNTs, Mitsui-7). We show that expression of TXNIP in murine macrophages (J774A.1, ATCC) is dependent on the concentration of glucose in the culture media. Expression of TXNIP is barely detectable in unstimulated cells in glucose-free media. Glucose stimulated the expression of TXNIP mRNA and protein in a concentration and time-dependent manner. Treatment of macrophages with MWCNTs stimulated the expression of TXNIP at mRNA and protein levels compared to vehicle control. MWCNTs also induced the interaction and colocalization between TXNIP and NLRP3, and the activation of NLRP3 as assessed by speck formation, caspase 1 activation, and IL-1beta production. Taken together, these findings indicate that TXNIP is a glucose-dependent regulatory protein and is induced in MWCNT-activated macrophages where it may modulate proinflammatory responses through NLRP3-mediated, caspase 1-dependent production of IL-1beta and other proinflammatory mediators.

This study was supported by a grant (#9390HTN) from the Nanotechnology Research Center, National Institute for Occupational Safety and Health, Centers for Disease Control and Prevention.

# Investigation of hepatotoxicity of structurally diverse pyrrolizidine alkaloids in zebrafish model

Yueyang Pan,<sup>1</sup> Jiang MA,<sup>2</sup> and Ge Lin<sup>1</sup>

<sup>1</sup>The Chinese University of Hong Kong; and <sup>2</sup>Guangdong Pharmaceutical University

**Abstract ID 53680**

**Poster Board 58**

Pyrrolizidine alkaloids (PAs) are hepatotoxic phytotoxins distributed in over 6000 plant species worldwide and pose a potential threat to human health via exposure to PA-contaminated foods and herbal medicines/supplements. PA-induced hepatotoxicity is due to metabolic activation in the liver to generate toxic metabolites, and significantly different hepatotoxic potencies have been demonstrated with structurally diverse PAs. Therefore, understanding of hepatotoxic potencies of different PAs is the prerequisite for establishing an appropriate risk assessment of PA exposure. In the present study, we used zebrafish model for evaluating hepatotoxic potency of 9 different PAs, because the zebrafish model can mimic the physiological processes, in particular the hepatic metabolism, in the body. At 6 hours after oral administration, individual PAs exhibited distinct structure-dependent hepatotoxic potencies in zebrafish, evidenced by a series of biochemical and histological detrimental changes in the liver. The assessed hepatotoxic potency order was determined to be lasiocarpine ~ retrorsine > monocrotaline > riddelliine > clivorine > heliotrine > retrorsine N-oxide ~ riddelliine N-oxide >>> platyphylline. In addition, compared to the control group, varied up- or down-regulated mRNA expressions in different PA treatment groups indicated that inflammation, apoptosis, and steatosis in the liver were all involved in PA-induced hepatotoxicity. Our findings demonstrated that zebrafish is a capable model for screening the hepatotoxicity and ranking the toxic potencies of different PAs, and the results obtained would assist the establishment of a more appropriate regulation for risk assessment of PA exposure.

This study was supported by Research Grant Council of Hong Kong SAR (GRF Grant No. 14106120) and CUHK Direct Grant (Grant No. 4054656)

# Molecular Investigation of the Ameliorative Potentials of *Cymbopogon citratus* Leaves Extract in Carbon tetrachloride- Induced Hepatotoxicity in rats

Olorunfemi Molehin,<sup>1</sup> Olusola O. Elekofehinti,<sup>2</sup> Ajibade O. Oyeyemi,<sup>1</sup> and Oluwabukola O. Olubaju<sup>1</sup>

<sup>1</sup>Ekiti State University, Ado-Ekiti; and <sup>2</sup>Federal University of Technology Akure

Abstract ID 14418

Poster Board 59

*Cymbopogon citratus* (*C. citratus*) is a green leafy vegetable used in traditional practices for the treatment of various diseases, such as hepatotoxicity, inflammation, rheumatism etc. The aim of this study is to evaluate the hepatoprotective potential of aqueous extract of *C. citratus* leaf extract on carbon tetrachloride (CCl<sub>4</sub>) - induced hepatotoxicity in rats thus putting scientific validation on the numerous medicinal relevance of the plant. Thirty Male wister rats were randomly separated into six groups each containing five rats. Hepatotoxicity was induced in rats by the administration of CCl<sub>4</sub> (at 40 mg/kg). Group 1 served as control (distilled water). Group 2 served as the negative control (40 mg/kg of CCl<sub>4</sub> and distilled water). Groups 3, 4 and 5 were administered 40 mg/kg of CCl<sub>4</sub> and treated with 100 mg/kg, 200 mg/kg, 300 mg/kg *C. citratus* extract twice daily. Group 6 was administered 40 mg/kg of CCl<sub>4</sub> treated with 100 mg/kg silymarin (the standard drug) twice daily for seven days. Animals were sacrificed by cervical dislocation and liver tissues were harvested for molecular studies. The mRNA expression of Heme oxygenase (HO-1), Cytochrome P<sub>450</sub> (CYP2D3, CYP3AF), Janus Kinase 2 (JAK2), Caspase 3 and Heat Shock Protein 70 (HSP70) were determined in the liver tissues by RT-PCR. Significant down regulation ( $p < 0.05$ ) of the CYP2D3, CYP3AF, JAK2, Caspase 3, HSP 70 gene were observed in groups treated with *C. citratus* when compared with the negative control, however HO-1 gene was also upregulated significantly ( $p < 0.05$ ) upon treatment with *C. Citratus*. This study depicts that the aqueous extract of *C. citratus* has hepatoprotective effect on carbon tetrachloride-induced hepatic injury.

# Ginsenoside Rc from *Panax ginseng* Ameliorates Palmitate-induced UB/OC-2 Cochlear Cell Injury

Nicholas N. Gill,<sup>1</sup> Presley Dowker-Key,<sup>1</sup> Katelin Hubbard,<sup>1</sup> Brynn Voy,<sup>1</sup> Jay N. Whelan,<sup>1</sup> Mark Hedrick,<sup>2</sup> and Ahmed Bettaieb<sup>1</sup>

<sup>1</sup>University of Tennessee; and <sup>2</sup>University of Tennessee Health Science Center

Abstract ID 14554

Poster Board 60

It is estimated that by 2050 nearly 2.5 billion people are projected to have some degree of hearing loss and at least 700 million will require hearing rehabilitation. Hearing loss can be classified into three groups: sensorineural, conductive, and mixed. Sensorineural hearing loss (SNHL) arises from the inability of the inner ear to convert fluid waves into neural electric signals because of injury to cochlear hair cells resulting in hair cell death. In addition, systemic chronic inflammation implicated in other pathologies may exacerbate cell death leading to SNHL. Phytochemicals have emerged as a possible solution because of the growing evidence of their anti-inflammatory, antioxidant, and anti-apoptotic properties. Ginseng and its bioactive molecules, ginsenosides, exhibit effects that suppress pro-inflammatory signaling, reactive oxygen species (ROS) generation, and protect against apoptosis. In the current study, we investigated the effects of ginsenoside Rc (G-Rc) on UB/OC-2 primary murine sensory hair cell survival and homeostasis in response to palmitate-induced injury. We demonstrated that at a human equivalent dose G-Rc promoted UB/OC-2 cell survival and cell cycle progression. Additionally, G-Rc enhanced the differentiation of UB/OC-2 cells into functional sensory hair cells. Importantly, G-Rc alleviated inflammation, oxidative stress, ER stress, and apoptosis induced by palmitate. The current study offers novel insights into the effects of G-Rc as a potential adjuvant for SNHL and warrants further studies elucidating the molecular mechanisms mediating the beneficial effects of G-Rc on cochlear hair cells.

# The Homemade Russian Drug Krokodil: Is it Good or Evil?

Emanuele Alves

Virginia Commonwealth Univ

Abstract ID 23123

Poster Board 61

“Krokodil” is the street name for the injectable mixture used as a cheap substitute for heroin. The main psychoactive compound in krokodil is desomorphine. Krokodil is usually prepared at home by the users themselves in a harsh uncontrolled reaction that starts with codeine tablets, alkali solutions, organic solvent, acidified water, iodine, and red phosphorus, all of which are easily available in retail outlets, such as supermarkets, and drugstores. The resulting product is a light brown liquid that is called krokodil. Due to its peculiar manufacturing procedure, the krokodil solution produces a large and complex mixture of different substances. The goal of this work was to understand the chemistry behind the krokodil synthesis by assessing the chemical profile of the resulting mixture using different analytical techniques. A reaction mechanism was proposed, and its toxicity and the possible clinical applications of the products formed during krokodil preparation were discussed. A street-like synthesis was performed in the laboratory and an analytical GC-MS methodology for the detection of desomorphine and codeine was developed and validated. This method allowed the confirmation of the successful synthetic methodology that mimicked the synthesis performed by users. The chemical complexity of the krokodil mixture was studied by reverse-phase high-pressure liquid chromatography coupled to a photodiode array detector (RP-HPLC-DAD) and by liquid chromatography coupled to high-resolution mass spectrometry (LC-ESI-IT-Orbitrap-MS).

The validated GC/MS method for the quantification of codeine and desomorphine proved to be selective. The regression analysis for the analytes was linear in the range of 0.62–10  $\mu\text{g/mL}$  with correlation coefficients  $> 0.99$ . The coefficients of variation did not exceed 15%, the acceptance criteria according to the EMA Guideline. The lowest limit of detection and quantification for desomorphine and codeine were  $0.150 \pm 0.002 \mu\text{g/mL}$  and  $0.170 \pm 0.02 \mu\text{g/mL}$ , respectively. Considering codeine as the only morphinan precursor and the reaction conditions for the krokodil synthesis, a theoretical chemical set of 95 possible morphinans in krokodil was defined. The exact mass approach was applied, and the defined morphinan mass fragmentations patterns were used as a targeted identification approach. The proposed 95 morphinans were searched using the full scan chromatogram and findings were validated by mass fragmentation of the correspondent precursor ions. Following this effort, a total of 42 morphinans were detected within the krokodil samples.

Due to its homemade nature, krokodil contains a great variety of substances and by-products formed during the reaction. This work highlights the presence of different morphinans formed during the krokodil synthesis. Most of these compounds share the morphine core and some of the pharmacophore sites, which makes them interesting candidates for further clinical and pharmacological studies aiming for possible applications for the treatment of opioid abuse, pain, and several other disorders.



# Nrf2-dependent and independent effects of tBHQ on dendritic cell function

Saamera Awali,<sup>1</sup> Yining Jin,<sup>1</sup> and Cheryl E. Rockwell<sup>1</sup>

<sup>1</sup>Michigan State University

Abstract ID 13818

Poster Board 62

Dendritic cells (DCs) are professional antigen presenting cells that initiate both the innate and adaptive immune responses upon detecting antigen. Through antigen processing, DCs can activate naïve T cells by presenting antigenic peptides on MHC class II molecules. Previous research from our lab demonstrated that *tert*-butylhydroquinone (tBHQ), a potent activator of nuclear factor erythroid 2-related factor (Nrf2) and a widely used food additive, blunts the expression of CD107a, fas ligand and CD44, which are markers of activation and effector function, on CD8+ T cells. This suggests that tBHQ impedes CD8 T cell activation and effector function, but the mechanism for this is unclear. Since DCs bridge the innate and adaptive immune systems and play an important role in T cell activation, we hypothesize that exposure to tBHQ in dendritic cells inhibits expression of MHC class II and other co-stimulatory molecules involved in T cell activation and effector functions in a Nrf2-dependent manner. In our current *in vitro* study, isolated DCs and unfractionated splenocytes were collected from spleens of female wildtype or Nrf2 <sup>-/-</sup> C57BL/6 mice. The cells were activated by Influenza A Virus (IAV) in the presence or absence of tBHQ for 24 hours, after which the expression of markers for DC maturation, activation, and T cell priming was measured. tBHQ treatment led to a significant decrease in DC maturation marked by a decrease in MHCII expression. In addition, tBHQ significantly suppressed DC activation, as evidenced by a decrease in CD80 and CD86 expression, which occurred in a Nrf2-dependent manner. Likewise, tBHQ also reduced secretion of IL-6 and IL-12 by IAV-activated dendritic cells, whereas TNF $\alpha$  secretion was not affected. Overall, our data suggest that tBHQ inhibits the expression of MHC class II and other co-stimulatory molecules expressed by activated DCs with the decrease in CD80 and CD86 occurring in a Nrf2-dependent manner. Furthermore, the tBHQ-mediated impairment of dendritic cell activation and maturation may account in part for the suppression of T cell activation by tBHQ. (This study was supported by NIH R01 ES024966 and R21 ES033830).

# Elucidating the Role of Inducible Nitric Oxide Synthase in E-cigarette Toxicity using Precision Cut Lung Slices

Melissa Kudlak,<sup>1</sup> Julia Herbert,<sup>2</sup> Alyssa Bellomo,<sup>2</sup> Andrew Gow,<sup>2</sup> Jeffrey D. Laskin,<sup>3</sup> and Debra L. Laskin<sup>2</sup>

<sup>1</sup>Rutgers, Ernest Mario School of Pharmacy; <sup>2</sup>Rutgers, Ernest Mario School of Pharmacy; and <sup>3</sup>Rutgers, The State University of New Jersey

**Abstract ID 15208**

**Poster Board 219**

Although e-cigarette (e-cig) use has continuously increased, little is known about its acute toxicity. Using the ex vivo Precision Cut Lung Slice (PCLS) model we previously showed that menthol-flavored e-cig condensate exposure increases mitochondrial dysfunction and oxidative stress while decreasing lung function. Inducible nitric oxide synthase (iNOS) is a key enzyme mediating nitric oxide production in macrophages; it is also known to drive proinflammatory signaling. In the present study, we analyzed the role of NO in e-cig toxicity. E-cig condensates were collected by aerosolizing e-liquids containing vehicle, nicotine only, and nicotine+menthol. Condensate exposure doses were normalized to glycerol content. For PCLS preparation, iNOS<sup>-/-</sup> and WT mice were euthanized, tracheotomized, and the lungs filled with agarose. Lung lobes were isolated and 300  $\mu$ m thickness PCLS prepared using a Krumdieck Tissue Slicer. After 24 hr incubation at 37°C, PCLS were treated with vehicle, nicotine, or nicotine+menthol condensates at concentrations of 10 mM to 150 mM, and ciliary beat frequency (CBF) was recorded using video-microscopy. Acute cytotoxicity was measured using a lactate dehydrogenase (LDH) assay. Exposure of PCLS to nicotine+menthol condensate caused a decrease in CBF and an increase in acute cytotoxicity in both WT and iNOS<sup>-/-</sup> mice. In iNOS<sup>-/-</sup> mice, CBF was significantly reduced at doses of 25 mM and 50 mM nicotine+menthol, whereas the same doses did not affect CBF in PCLS from WT mice. Similarly, acute cytotoxicity in PCLS from iNOS<sup>-/-</sup> mice was more pronounced at 100 mM and 150 mM in comparison to WT, indicating higher susceptibility to e-cig toxicity when iNOS is absent. Nicotine only and vehicle had no effect on ciliary function or cytotoxicity in both WT and iNOS<sup>-/-</sup> PCLS. These data suggest that the presence of iNOS has a protective role in e-cig toxicity by reducing the toxic effects on ciliary function and pulmonary cells. Further studies will investigate the effects of iNOS depletion in PCLS on oxidative stress, airway contractility, and nitrite/nitrate metabolism and will thus contribute to elucidating the mechanism behind e-cig toxicity in the lung.

**Support/Funding Information:** NIHES005022

# Arsenic Hepatic Sinusoidal Export is Stimulated by Methylselenocysteine and Mediated by Multidrug Resistance Protein 4 (MRP4/ABCC4)

Elaine M. Leslie,<sup>1</sup> Janet R. Zhou,<sup>1</sup> and Gurnit Kaur<sup>1</sup>

<sup>1</sup>University of Alberta

Abstract ID 53785

Poster Board 220

Arsenic causes lung, skin, and bladder cancer in humans. It is estimated that 92-220 million people worldwide are exposed to arsenic at levels exceeding the World Health Organization guideline (10 µg/L) through contaminated drinking water. In animal models, arsenic and selenium are mutually protective via the formation and biliary excretion of the seleno-bis (S-glutathionyl) arsinium ion [(GS)<sub>2</sub>SeAs]<sup>+</sup>. There have been selenium supplementation trials in arsenic endemic areas, but the influence of selenium on human hepatic handling of arsenic is not fully understood. Previously, we reported that sinusoidal efflux of arsenic was stimulated by methylselenocysteine (MeSeCys). The multidrug resistance protein 4 (MRP4/ABCC4) is localized to the sinusoidal surface of human hepatocytes and is thought to transport arsenic into sinusoidal blood for urinary elimination. We sought to characterize arsenic sinusoidal efflux in the presence of MeSeCys in human HepaRG cells, a surrogate for primary human hepatocytes. Sinusoidal efflux of arsenic was measured from parental and ABCC4 knockdown HepaRG cells after treatment with <sup>73</sup>As-arsenite (1 µM, 100 nCi) ± MeSeCys (1 µM) under various conditions using B-CLEAR® technology. A dose-dependent increase of arsenic sinusoidal efflux was observed with increasing concentrations of MeSeCys. Arsenic sinusoidal efflux was inhibited by a glutathione synthesis inhibitor, the general MRP inhibitor MK571, the more specific MRP4 inhibitor ceefourin-1, as well as at 4°C. ABCC4 knockdown in HepaRG cells resulted in a significant decrease of basal, and a complete loss of MeSeCys-stimulated arsenic efflux, relative to non-target knockdown cell controls. These data suggest that arsenic sinusoidal efflux is stimulated by MeSeCys and this process is MRP4-mediated. Overall, this work provides foundational knowledge for selenium supplementation trials.

Funded by Canadian Institutes of Health Research PJT-159547.

# Effects of 3,3'-Dichlorobiphenyl (PCB-11) on the expression of CYP2A, 2B, and 2F enzymes in the liver and brain of CYP2A6-humanized, CYP2B6-humanized, or wild-type mice

Weiguo Han,<sup>1</sup> Weizhu Yang,<sup>1</sup> Xueshu li,<sup>2</sup> Lehmler Hans-Joachim,<sup>2</sup> Qing-Yu Zhang,<sup>3</sup> Pamela Lein,<sup>4</sup> and Xinxin Ding<sup>5</sup>

<sup>1</sup>University of Arizona; <sup>2</sup>The University of Iowa; <sup>3</sup>College of Pharmacy, Univ of Arizona; <sup>4</sup>Univ of California - Davis; and <sup>5</sup>Univ of Arizona College of Pharmacy

Abstract ID 28389

Poster Board 221

Polychlorinated biphenyls (PCBs) are ubiquitous environmental pollutants that have been linked to adverse human health effects. Human exposure to PCBs occurs via dermal absorption, inhalation, and oral ingestion. Legacy PCBs are widely accepted developmental neurotoxicants that cause cognitive deficits. Cytochrome P450 enzymes metabolize PCBs to hydroxylated metabolites (OH-PCBs), some of which are more toxic than their parent compounds. PCB 11, a lower chlorinated (LC)-PCB, is one of the major PCB congeners detected in contemporary human serum samples. The aim of this study is to test whether PCB 11 exposure induces the expression of P450 enzymes in the liver and the brain that may be involved in its PCB metabolism. The effects of PCB 11 on human CYP2A6 and CYP2B6 expression were studied using CYP2A6-humanized and CYP2B6-humanized mice, respectively, which are on a *Cyp2abfgs*-null background. The effects of PCB 11 on mouse CYP2A5, CYP2B10, and CYP2F2 expression were also examined in wild-type C57BL/6 mice. Mice were exposed to PCB 11 (500  $\mu$ mol/kg b.w.) or peanut oil (vehicle control) via oral gavage. CYP expression at the mRNA and protein levels was examined 24 h after exposure, using qRT-PCR and western blot analysis, respectively. The results indicated that CYP2A6 expression was not induced by PCB 11 in the CYP2A6-humanized mouse model; in contrast, in the CYP2B6-humanized mouse model, PCB 11 increased CYP2B6 mRNA and protein levels in the liver by  $\sim$ 11 and  $\sim$ 2 times, respectively, but had no effect on CYP2B6 (mRNA) expression in the brain. In wild-type mice, PCB 11 induced hepatic CYP2A5 and CYP2B10, but not CYP2F2, and brain CYP2B10, but not CYP2A5, mRNA levels in female mice only. These results provide the basis for identifying potential PCB 11 exposure-induced changes in hepatic and brain PCB11 metabolism and OH-PCB metabolite levels and the relationship of these changes to neurotoxic outcomes following developmental exposures to PCB 11.

supported in part by NIH grant ES014901

# Sacubitril/Valsartan Alleviates Type 2 Diabetes-Induced NAFLD Through Modulation of Oxidative Stress, Inflammation and Apoptosis

Salim Al-Rejaie,<sup>1</sup> Mohammed M. Ahmed,<sup>2</sup> and Mohamed Mohany<sup>2</sup>

<sup>1</sup>King Saud Univ; and <sup>2</sup>King Saud University

Abstract ID 14539

Poster Board 222

The frequency of nonalcoholic fatty liver disease (NAFLD) in people with type 2 diabetes (T2D) is rising quickly worldwide. There may be a positive impact of LCZ696 on liver disease. Therefore, the goal of the current study was to explore LCZ696's therapeutic potential and underlying mechanism in T2D-induced NAFLD. In this study, a high-fat diet (HFD) and a single dose of streptozotocin (STZ, 30 mg/kg body weight) were given to rats to create a T2D model. T2D animals received valsartan or LCZ696 orally for eight weeks. The liver enzymes (AST and ALT), lipid profile, cytokines, nuclear factor kappa B (NF- $\kappa$ B), oxidative stress, caspase-3 activity, Bax expression, and caspase-3 expression were all significantly increased in HFD/STZ rats while IL-10, antioxidant markers, and Bcl-2 expression were significantly decreased. HFD/STZ rats also had hyperglycemia and impaired insulin secretion. When given to diabetic rats, LCZ696 decreased the levels of glucose, AST, ALT and lipid profile in the serum. Additionally, ELISA findings showed that diabetic rats treated with LCZ696 showed decreased levels of pro-inflammatory (IL-1, TNF-, and IL-6) and increased levels of anti-inflammatory (IL-10) cytokine. In addition, NF- $\kappa$ B and caspase-3 activity were shown to be significantly reduced. Diabetic rats treated with LCZ696 showed clear improvements in GSH content and other antioxidant enzyme levels, in addition to a considerable reduction in TBARS levels, at the level of hepatic tissue homogenate. Additionally, LCZ696 increased the expression of the Bcl-2 protein while suppressing the expression of the Bax and cleaved caspase-3 proteins. These biochemical findings were strengthened and considerably supported by improvements in histological alterations in liver tissues. In conclusion, LCZ696 reduced NAFLD through various mechanisms such as apoptosis and inflammation inhibition.

# Comparison of Mustard and Urticant Vesicating Agents' Induced Cutaneous Lesions in Wild Type and Mast Cell Deficient Mice

Dinesh Goswami,<sup>1</sup> Andrew Roney,<sup>2</sup> Omid Madadgar,<sup>1</sup> Satyendra K. Singh,<sup>1</sup> Steve Lundback,<sup>2</sup> Jared M. Brown,<sup>3</sup> and Neera Tewari-Singh<sup>1</sup>

<sup>1</sup>Michigan State Univ; <sup>2</sup>Michigan State University; and <sup>3</sup>University of Colorado Anschutz Medical Campus

Abstract ID 25825

Poster Board 223

Cutaneous exposure to mustards [Sulfur mustard (SM) and Nitrogen mustard (NM)] and urticant (Phosgene Oxime, CX) vesicating chemical threat agents' is known to cause devastating injuries that include skin erythema, edema and necrosis, and systemic toxic effects. The symptoms of CX-exposure appear instantaneously with skin blanching and urticaria while SM and NM-induced lesions appear a few hours after the exposure. The mechanisms underlying the injury from these agents is not fully known and there are no effective approved therapies to alleviate the injury. Our previous studies have shown that NM and CX-exposure causes significant increase in mast cell degranulation suggesting their role in vesicant injury. To further analyze the effect of mast cell activation in NM- and CX-induced clinical injury parameters, we compared the toxicity of these agents in wild type (WT; C57BL/6) and mast cell deficient (MCD; B6.Cg-KitW-sh/HNihJaeBsmJ) mice. Mice were exposed to NM (0.5mg NM/100 $\mu$ L of acetone) or CX (10  $\mu$ L CX for 0.5 or 1.0 min using two 12 mm vapor caps) on the dorsal skin. CX exposures were carried out at MRIGlobal (Kansas City, MO). Clinical assessments including body weight, skin bi-fold thickness, and scoring for erythema, edema, and necrosis were carried out. Mice were sacrificed at different time points (24 h and/or 14 Day) post-exposure, and skin and other tissues were harvested for analyses. NM and CX-exposures led to significant increases in mast cell degranulation in the skin of the WT mice. The increase in mast cell degranulation was more robust and instant upon CX-exposure compared to NM. Increased mast cell degranulation was accompanied with increases in mast-cell associated protease, tryptase in the skin of the WT mice upon NM and CX-exposure. MCD mice showed improved survival upon NM-exposure compared to WT mice. MCD mice also fared better in terms of NM-induced body weight-loss and increase in skin-bi-fold thickness compared to WT mice. MCD mice also exhibited reduced erythema, edema, and decreased wound size compared to WT mice. In case of CX-exposure, MCD mice also showed reduced erythema (at 2 h, and 24h post-exposure), and edema (at 2h post CX-exposure) compared to WT mice. MCD mice also had reduced necrosis compared to WT mice at day 3 post CX-exposure. Together, our results show that MCD mice developed less severe clinical lesions compared to WT mice upon cutaneous exposure to both NM and CX, suggesting the role of mast cells in the skin injury. A more robust increase in mast cell degranulation and urticaria like symptoms upon CX-exposure suggest that mast cells could play a more crucial role in CX-induced skin injury; however, this remains to be investigated. Further histopathological and molecular analyses are being carried out to delineate the role of mast cells in vesicant injury and to identify the underlying molecular pathways.

**Support/Funding Information:** Department of Defense (W81XWH-18-1-0169) and Countermeasures Against Chemical Threats (CounterACT) Program, Office of the Director National Institutes of Health (NIH OD) and the National Institute of Arthritis and Musculoskeletal and Skin Diseases (NIAMS) [Grant Numbers R21 AR073544 and U01 AR075470].

---

# Damage to Olfactory Organs of Adult Zebrafish Induced by Diesel Particulate Matter

Su Jeong Song

*Korea Institute of Oriental Medicine*

**Abstract ID 53636**

**Poster Board 224**

Particulate matter (PM) as environmental hazard are associated with various risk of human health. The olfactory system is directly exposed to PM; thus, the effect of PM on olfactory function must be investigated. In this study, we propose a zebrafish olfactory model to evaluate the effects of exposure to diesel particulate matter (DPM). The DPM was named the name Korean diesel particulate matter (KDP20). KDP20 contained heavy metals and polycyclic aromatic hydrocarbons (PAHs). KDP20 exposed olfactory organs exhibited damaged cilia and epithelium. Olfactory dysfunction was confirmed using an odor-mediated behavior test. Further, the olfactory damage was analyzed using alcian blue and anti-calretinin staining. KDP20 exposed olfactory organs exhibited histological damages, such as increased goblet cells, decreased cell density, and calretinin level. Quantitative real-time polymerase chain reaction (qRT-PCR) revealed that PAHs exposure related genes (*AHR2* and *CYP1A*) were upregulated. Reactive oxidation stress (ROS) (*CAT*) and inflammation (*IL-1B*) related genes were upregulated. Further, olfactory sensory neurons (OSNs) related genes (*OMP* and *S100*) were downregulated. In conclusion, KDP20 exposure induced dysfunction of the olfactory system. Additionally, zebrafish olfactory system exhibited a regenerative capacity with recovery conditions. Thus, this model may be used in future investigating PM-related diseases.

**Support/Funding Information:** KSN1823222

# The Nrf2 activator tBHQ promotes OVA-Elicited Food Allergy in Mice

Yining Jin,<sup>1</sup> Allison P. Boss,<sup>1</sup> Caitlin Wilson,<sup>2</sup> and Cheryl E. Rockwell<sup>2</sup>

<sup>1</sup>Michigan State University; and <sup>2</sup>Michigan State University

Abstract ID 24335

Poster Board 225

There has been a steady rise in the prevalence of food allergy for the past couple of decades for reasons that are not completely understood. While previous studies from our lab demonstrated that a food antioxidant present in many processed foods, *tert*-butylhydroquinone (tBHQ), promotes the development of allergy in mice, our current experiment focuses on the dose response of tBHQ in the mice chow. Mice were fed AIN-93G with 0.0014% tBHQ (standard), 0.0007% tBHQ (50% of the standard), and 0.00028% tBHQ (20% of the standard) or control diet. Mice were exposed to OVA once every week for 4 weeks during the sensitization phase. Sensitization to OVA was assessed by the rise in OVA-specific IgE. Upon oral challenge, mice were monitored for hypothermia shock response (HSR) and the degranulation of mast cells. Sensitization with OVA elicited a more robust OVA-specific IgE antibody response in mice on the tBHQ diet with high concentration. Likewise, in response to OVA challenge, a greater drop in rectal temperature was observed in the mice on the high concentration of tBHQ diet post-challenge compared to control animals. In addition, because tBHQ is a robust activator of the transcription factor Nrf2 in immune cells, we aimed to determine the role of Nrf2 in these tBHQ-mediated effects. Therefore, we performed a PCR array on splenocytes from SCID mice (immune-deficient mice) who received either wild-type CD4 T cells or Nrf2-knockout CD4 T cells and were sensitized to OVA. We found that the Th2-related genes were downregulated, but Tregs and Th1-related genes were upregulated in mice that received Nrf2-null CD4 T cells. Taken together, these data suggest that exposure to tBHQ through diet promotes OVA sensitization and exacerbates anaphylactic response to OVA challenge in a mouse model of food allergy. This effect is tBHQ dose-dependent and dependent on the transcription factor Nrf2.



# Hepatocyte Senescence is Initiated through a Klf6-p21 Mechanism which mediates the Production of Cxcl14, a Novel Prognostic Biomarker of Acute Liver Failure

David Umbaugh,<sup>1</sup> Nga Nguyen,<sup>2</sup> Giselle Sanchez Guerrero,<sup>2</sup> Cecilia Villanueva,<sup>1</sup> Bruno Hagenbuch,<sup>3</sup> Anup Ramachandran,<sup>2</sup> and Hartmut Jaeschke<sup>4</sup>

<sup>1</sup>Univ of Kansas Med Ctr; <sup>2</sup>Uni of Kansas Med Ctr; <sup>3</sup>Univ of Kansas Medical Ctr; and <sup>4</sup>Univ of Kansas Medical Center

Abstract ID 29424

Poster Board 226

**Background:** Acute liver failure (ALF) is characterized by hepatic encephalopathy, coagulopathy, peripheral vasodilation and organ failure. The majority of all ALF cases in the United States and UK are due to acetaminophen (APAP) overdose. An extensive body of work has elucidated the molecular mechanisms of hepatocyte necrosis during APAP overdose, but detailed mechanisms involved in the development of ALF have been largely unexplored. Previous work demonstrated that a severe overdose of APAP (600 mg/kg) results in prolonged injury, impaired regeneration and sustained inhibition of cell cycle progression mediated through p21. Cell senescence is a cell fate resulting in cell cycle arrest predominantly controlled by p16 or p21 dependent pathways. Some senescent cells acquire a senescent associated secretory phenotype (SASP) which consists of bioactive signals that can influence the microenvironment. Why some senescent cells develop a SASP, and others do not remains elusive, however the specific molecular program governing senescence is thought to vary depending on cell type and inducing factors. Klf6 is induced during senescence, promotes p21 expression, and when overexpressed decreases proliferation in hepatocellular carcinoma.

**Aim:** We hypothesized that senescent hepatocytes acquire a SASP that directly impedes liver recovery, mediated through the induction of a Klf6-p21 axis, which ultimately drives ALF.

**Approach and Results:** Initial bioinformatic analysis of flow-sorted perinecrotic hepatocytes after a moderate overdose of APAP (300 mg/kg) revealed that these hepatocytes express both Klf6, p21 and Cxcl14 (a SASP constituent). Further, we fractionated hepatocytes and non-parenchymal cells and confirmed that hepatocytes are the primary source of Cxcl14. In both male and female mice, we found a dose-dependent induction of Klf6/p21 and persistent circulating levels of Cxcl14 in the plasma. In parallel experiments, we targeted either the senescent hepatocytes with the senolytic drugs, dasatinib and quercetin, or the SASP constituent Cxcl14 with a neutralizing antibody. We found that targeting Cxcl14 greatly reduced APAP-induced liver injury while targeting the senescent hepatocyte failed to influence liver injury. Experiments analyzing human APAP overdose livers confirmed that Klf6-p21-Cxcl14 axis is upregulated compared to healthy controls. To confirm the link between Klf6, p21 and Cxcl14, we utilized the CRISPRa HepG2 system where we transcriptionally activated Klf6 which strongly induced p21 and Cxcl14 expression. Klf6 is a redox-responsive protein and we have previously demonstrated that APAP-induced inhibition of complex III is an initiating event in the APAP toxicity cascade. Therefore, we conducted further experiments *in vitro* inhibiting complex III with Antimycin A which resulted in increased Klf6 and p21 expression.

**Conclusions:** Collectively, our data suggests that sustained oxidative stress after a severe APAP overdose leads to continued elevation in Klf6 which promotes p21-mediated hepatocyte senescence and the production of Cxcl14. Importantly, we find that human plasma levels of Cxcl14 can accurately predict patient survival, as it gradually declines in surviving APAP overdose patients but remains consistently elevated in non-surviving APAP overdose patients. This data confirms that the sustained induction of hepatocyte senescence and SASP initiation are critical mechanistic events leading to ALF in human patients.

# Eugenol Protects Against Diclofenac-Induced Hepatocellular Injury in an In Vitro Mouse Model

Jaiden Martin,<sup>1</sup> Brendan D. Stamper,<sup>2</sup> and Jon Taylor<sup>2</sup>

<sup>1</sup>Pacific Univ; and <sup>2</sup>Pacific University

Abstract ID 14907

Poster Board 257

**Background:** Eugenol is a simple and widely available hydrocarbon derivative primarily found in cloves, as well as other natural sources like cinnamon and nutmeg. Its phenolic structure suggests that eugenol has the ability to exhibit antioxidant activity. The literature also suggests that eugenol may possess anti-inflammatory properties. The goal of this project was to investigate whether eugenol was capable of protecting against diclofenac-induced hepatocellular injury. Diclofenac, a non-steroidal anti-inflammatory drug (NSAID) has been reported to elevate serum aminotransferase levels, and in some cases may cause serious liver injury.

**Methods:** The toxicity of eugenol and diclofenac were measured by determining a median lethal dose (LC50) in an in vitro mouse liver model (TAMH; transforming growth factor- $\alpha$  transgenic mouse hepatocytes). LC50 values were determined using probit regression analysis in the SPSS statistical tool package. TAMH cells were then exposed to a low (non-toxic) dose of eugenol (0.05 mg/mL) for varying pretreatment times before being exposed to a toxic dose of diclofenac (0.70 mg/mL) over a 24-hour period. Cell viabilities were measured following each eugenol/diclofenac treatment condition using a resazurin-based assay.

**Results:** The LC50 values for eugenol and diclofenac were experimentally determined to be 0.14 and 0.57 mg/mL, respectively. An increase in cell viability (cytoprotective effect against diclofenac-induced toxicity) was directly correlated to eugenol pretreatment time. In fact, a five-day eugenol pretreatment resulted in an approximate 3-fold increase in the LC50 of diclofenac alone.

**Conclusions:** Relatively long-term eugenol exposure displayed hepatoprotective properties against diclofenac-induced injury. These findings suggest that eugenol may have utility as a dietary supplement capable of protecting the liver against toxic insult. In addition, eugenol might even improve therapeutic outcomes while simultaneously lowering the toxicity risk if combined with diclofenac. Future work is underway to not only explore mechanisms associated with eugenol's cytoprotective ability against diclofenac-induced toxicity, but also to investigate a potentially synergistic relationship between eugenol and diclofenac related to cyclooxygenase (COX) inhibition.

**Funding Information:** This work was supported by the Pacific University Research Incentive Grant Program and an ASPET Summer Undergraduate Research Fellow (SURF) Institutional Award.

# Determination of methylphenethylamine and Its Metabolites in Whole Blood of Rats Using MMSPE and UPLC-qTOF-MS

Ahmad M. Alamir,<sup>1</sup> James Watterson,<sup>2</sup> and Ibraheem Attafi<sup>1</sup>

<sup>1</sup>Jazan Health Affairs, Ministry of Health; and <sup>2</sup>Laurentian University

Abstract ID 22744

Poster Board 258

$\beta$ -methylphenethylamine (BMPEA) is a positional isomer of amphetamine that is used for doping and weight loss. The purpose of this study was to determine BMPEA concentrations and investigate its metabolic pathway in rats. Twelve adult male Sprague-Dawley rats were randomly assigned to four groups (n = 3 each): a control group that received no BMPEA; a low-dose group that received 10 mg/kg of BMPEA (i.p.); and two high-dose groups that received 30 mg/kg of BMPEA (i.p.). Within 20 minutes, the rats in the low-dose and one of the two high-dose groups were euthanized by CO<sub>2</sub> asphyxiation. The other high-dose group was euthanized by CO<sub>2</sub> asphyxiation 90 minutes post-injection. Perimortem blood samples were collected in sodium fluoride vacutainer tubes from the rat heart (cardiac puncture).

In this study, the validated UPLC-qTOF-MS analytical method using MMSPE extraction method was used to determine BMPEA concentrations and identify its metabolite in rat cardiac blood. The highest determined concentration of BMPEA was 899 ng/mL in a high-dose group sample, whereas the lowest determined concentration was 22 ng/mL in a high delayed dose group sample. All determined concentrations were within the validated working range of the assay (20-1,000 ng/mL). The high delayed-dose samples (collected 90 min post-injection) showed a sharp decline in the concentration levels of BMPEA (31 ng/mL  $\pm$  9 ng/mL) when compared to the high-dose samples (collected within 20 min of injection), which showed very high concentration levels of BMPEA (869 ng/mL  $\pm$  29 ng/mL). This finding demonstrated that BMPEA has a short half-life of elimination from the rat blood. More research is needed to precisely estimate the half-life of BMPEA.

This study was demonstrated that the validated UPLC-qTOF-MS analytical method was able to differentiate between BMPEA and amphetamine at the level of baseline and metabolite. The study's analytical method was able to distinguish between the positional isomers BMPEA and amphetamine by separating them at the baseline level and identifying their metabolite. There was a newly discovered BMPEA metabolite, which was identified as 1-amino-2-phenylpropan-2-ol. The discovery of the BMPEA metabolite was accomplished through comparison with drug-free samples. The fragmentation pattern of this proposed metabolite was obtained utilizing the MS E acquisition mode of qTOF-MS.

The study utilized UPLC-qTOF-MS to determine BMPEA concentrations and identified its metabolite in rat cardiac blood. It was capable of distinguishing between BMPEA and amphetamine at the baseline and metabolite levels and can be used in forensic laboratories to precisely identify them in doping and criminal investigations. 1-amino-2-phenylpropan-2-ol, a novel BMPEA metabolite, was discovered.

# Generation and Characterization of a Serum Albumin-Humanized Mouse Model For Biomarker Discovery

Xiangmeng Wu,<sup>1</sup> Weiguo Han,<sup>1</sup> Weizhu Yang,<sup>1</sup> Robert J. Turesky,<sup>2</sup> Laura Van Winkle,<sup>3</sup> Qing-Yu Zhang,<sup>1</sup> and Xinxin Ding<sup>1</sup>

<sup>1</sup>R. Ken Coit College of Pharmacy, University of Arizona; <sup>2</sup>University of Minnesota; and <sup>3</sup>Univ of California Davis

**Abstract ID 26143**

**Poster Board 259**

Human serum albumin (SA) is the most abundant protein in blood, typically at 30–50 mg/ml and is a commonly used serum protein for studying human exposure to xenobiotic compounds. A human SA transgenic mouse model was previously reported (PMC4868631), in which the endogenous mouse SA predominates and competes with the transgenic human SA for adduction with reactive xenobiotic metabolites. The aim of this study was to establish, via crossbreeding with a SA-null mouse, and characterize a SA-humanized mouse model, where only human, but not mouse, SA is expressed. Immunoblot analyses indicated that the level of human SA protein in the serum of the SA-humanized mouse was increased by six times, compared to that in the original SA-transgenic mouse. The genomic site of the SA transgene, determined by the optical genome mapping approach, was localized to mouse chromosome 14, between two marker positions at 56977284 bp and 57029068 bp. The genome mapping data for the humanized mouse enabled the design of a new genotyping protocol that can distinguish between hemizygous and homozygous SA-humanized mice. Homozygous SA-humanized mice were then studied for the ability of human SA to react with metabolites of naphthalene (NA) *in vivo*. NA is a ubiquitous environmental pollutant and a possible human carcinogen that contributes to tumor formation in the respiratory tract of rodents. The proximal reactive metabolite of NA, naphthalene-1,2-oxide (NAO), can form adducts with cysteine thiols, leading to depletion of cellular glutathione (GSH) and covalent modification of proteins. Adducts of a human SA-specific peptide (LQQCPF) with NAO were synthesized and used as standards for identification and quantification of adducted peptides in human SA isolated from the plasma of NA-exposed mice. Adult mice were exposed to NA by a single intraperitoneal injection at 200 mg/kg or 3 once-daily episodes of inhalation exposure at 20 ppm. Plasma was obtained at various times after NA injection for adduct analysis using liquid chromatograph-tandem mass spectrometry. The human SA-NAO adduct, detected as LQQCPF-NAO adduct following proteolytic digestion of serum proteins, was detected in mice exposed to NA through either routes. Of interest, the human SA-NAO adduct had a half-life of 74 hours in the exposed mice, which is much longer than that of the more abundant NA-glutathione adducts. These data illustrate the utility of the SA-humanized mouse model for biomarker discovery. (Supported in part by NIH grant ES020867)

**Support/Funding Information:** NIH grant ES020867

# Differential Induction of Microsomal and Soluble Epoxide Hydrolases by Arsenic in Drinking Water

Hui Li,<sup>1</sup> Xiaoyu Fan,<sup>2</sup> Shuang Yang,<sup>1</sup> Xinxin Ding,<sup>3</sup> Donna Zhang,<sup>1</sup> and Qing-Yu Zhang<sup>4</sup>

<sup>1</sup>the University of Arizona; <sup>2</sup>Univ of Arizona; <sup>3</sup>Univ of Arizona College of Pharmacy; and <sup>4</sup>College of Pharmacy, Univ of Arizona

Abstract ID 21455

Poster Board 260

Arsenic is naturally found worldwide. Consumption of arsenic-contaminated water has been associated with increased risks of multiple adverse health outcomes in humans. Our aim is to identify gene expression changes that may be mechanistically linked to arsenic's adverse effects. The current study is focused on the small intestinal epithelial cells, which is the main site of absorption of ingested arsenic and is understudied for exposure-related changes. C57BL/6 mice were treated with sodium arsenite in drinking water at 25 ppm for 28 days. Preliminary global gene expression analysis of the small intestine revealed an induction by the arsenite exposure of the microsomal epoxide hydrolase (mEH or Ephx1), an enzyme with a major role in converting xenobiotic epoxides to less reactive diols. Subsequent studies confirmed mEH induction at both mRNA and protein levels. Interestingly, the arsenite exposure induced the expression of mEH, but not the soluble epoxide hydrolase (sEH), which is known to prefer endogenous epoxides. Within the small intestine, mEH gene expression was induced only in the proximal, but not distal, part. The induction of mEH was accompanied by increases in microsomal enzymatic activity toward a model mEH substrate, *cis*-stilbene oxide. These data suggest that mEH, but not sEH, may be more relevant to the adverse effects of arsenic exposure. Our finding also points to the need to assess *in vivo* functional consequences of mEH induction in intestinal epithelial cells on the metabolism and toxicity of xenobiotic epoxides in arsenic exposed mice and humans. Ongoing studies are examining mEH induction by arsenic in other organs. (Supported by the Superfund Research Program, P42 ES004940-32)

# Evaluation of Immunomodulators as Therapeutic Treatments for Sulfur Mustard-Induced Ocular Injury

Ki H. Ma,<sup>1</sup> Bailey T. Chalmers,<sup>1</sup> and Albert L. Ruff<sup>1</sup>

<sup>1</sup>*U.S. Army Medical Research Institute of Chemical Defense*

**Abstract ID 54458**

**Poster Board 261**

This work was conducted in an effort to develop medical countermeasures to treat exposure to toxicants that can be utilized in mass casualty scenarios. The cornea and other ocular surface tissues are particularly susceptible to chemical exposures such as sulfur mustard (SM), and long-term prognosis can be poor due to delayed complications, including persistent corneal epithelial defects, dry eye, corneal opacification, and corneal neovascularization. Such long-term complications can lead to permanent discomfort and vision deficits or blindness despite the best current treatment regimens.

SM modifies basement membranes as an alkylating agent. The structures, once alkylated, may potentially be recognized as foreign by the immune cells. For example, laser debridement of a skin SM burn in a pig model resulted in superior healing, presumably because it cleared the alkylated basement membrane. Studies showed persistent inflammation affecting the cornea and anterior segment and elevated levels of inflammatory cytokines such as IL-1 $\beta$ , IL-6, TNF- $\alpha$ , and IL-8 after SM ocular exposure in animal models. The current study is to evaluate therapeutic efficacies of immunosuppressants and other immunomodulators in a mouse model of SM vapor-induced ocular injury. We have tested FDA-approved immunosuppressants mycophenolate mofetil (MMF) and tacrolimus, which have been extensively used in organ transplantation and some inflammatory, autoimmune diseases, including uveitis. MMF especially showed its effectiveness in a mouse model of corneal graft. Other immunomodulators in our analysis included IL-1 receptor antagonist (IL-1 Ra) and granulocyte colony-stimulating factor (G-CSF). Others have showed that IL-1 Ra significantly inhibited the development of autoimmune uveitis and improved ocular surface integrity of autoimmune-mediated aqueous-deficient dry eye in mouse models, and that G-CSF greatly improved ocular injuries in a rat corneal alkali burn model.

To our surprise the treatment with MMF significantly exacerbated injury progression, including corneal neovascularization, suggesting that some immune responses after ocular exposure are required for regulation of SM-induced corneal injury. In addition, SM-induced ocular injury may need agent-specific treatments based on findings that immune modulators with doses effective in other corneal injury models did not produce desirable outcomes. Findings of our study would help better understand the pathology of SM-induced ocular injury and dissect therapeutic targets.

# Exposure to DDX in Mice Reveals Impaired Energy Expenditure May be Mediated by DNA Methylation Changes

Juliann A. Jugan,<sup>1</sup> Sarah Elmore,<sup>1</sup> Kyle Jackson,<sup>1</sup> Annalise vonderEmbse,<sup>1</sup> Scott Tiscione,<sup>1</sup> and Michele A. La Merrill<sup>1</sup>

<sup>1</sup>University of California, Davis

Abstract ID 29773

Poster Board 262

Persistent pollutants dichlorodiphenyltrichloroethane (DDT) and dichlorodiphenyldichloroethylene (DDE) have been associated with obesity across human and rodent studies. Current research suggests the impairment of thermogenesis in brown adipose tissue plays a significant role in the decreased energy expenditure and increased adiposity of exposed individuals. We hypothesized that mice perinatally exposed to DDT or DDE would exhibit impaired thermogenesis mediated by changes in DNA methylation. At 9 weeks, exposed offspring exhibited a lower rectal temperature than age-matched controls (DDE  $p < 0.05$ , DDT  $p < 0.01$ ), which continued into adulthood (DDT  $p < .001$ ). Brown adipose tissue was isolated from mice at postnatal day 12 and 20 weeks for reduced representation bisulfite sequencing and RNA sequencing. 49 KEGG pathways were differentially methylated following DDT or DDE exposure ( $p < 0.05$ ). Of the 11 pathways enriched across more than one treatment, age, or nucleic acid; most notable were ovarian steroidogenesis, oxidative phosphorylation, mTOR signaling, and thermogenesis. Brown adipocytes were exposed to DDT or DDE over early differentiation and used to validate *in vivo* results. Preliminary results show increased expression of ribosomal subunit *18s* in adipocytes exposed to DDE ( $p < 0.05$ ), suggesting a dysregulation of protein synthesis. Adipocytes exposed to DDE also exhibited a trend in decreased mitochondrial DNA copy number and increased expression of ATPase subunit *g*, *Atp5mg*, ( $p < 0.05$ ) consistent with the enrichment direction in the oxidative phosphorylation pathway for both DNA methylation and RNA expression. These preliminary data are consistent with published findings describing impaired mitochondrial function following DDE exposure and may provide insight into the mechanisms behind thermogenic impairment.

This research was supported by the National Institute of Environmental Health Sciences [R01 ES024946 and T32 ES007059]

# Gallic acid modifies EGFR phosphorylation in rat with hepatic preneoplasia

Lourdes Rodriguez-Fragoso,<sup>1</sup> Erick Ayala-Calvillo,<sup>2</sup> and Felipe Rodríguez-López<sup>3</sup>

<sup>1</sup>Univ Autonoma Del Estado de Morelos; <sup>2</sup>Universidad Autónoma del Estado de Morelos; and <sup>3</sup>Universidad Autonoma del Estado de Morelos

Abstract ID 17052

Poster Board 263

Our aim was to study the effect of gallic acid on EGFR phosphorylation on liver rats with preneoplastic lesion induced by administration of diethylnitrosamine (DEN) and carbon tetrachloride (CCl<sub>4</sub>).

For this study, we used male Wistar rats which were randomly divided into four groups: (1) Control (50 mL) of water; (2) Gallic acid (50 mg/kg) per v.o. daily for 8 weeks; (3) Preneoplastic liver lesion induced by administration of unique dose of Diethylnitrosamine i.p. (200 mg/kg body weight) and then treated two weeks later with a single dose of CCl<sub>4</sub> (4 mL/kg) diluted in mineral oil (1:1), i.p. during 8 weeks; and (4) Rats receiving both carcinogens and gallic acid simultaneously as described above. Rats were sacrificed and liver tissue was collected for analyzing EGFR expression and tyrosine phosphorylation pY1068. For identification of total EGFR and pY1068 EGFR, a western blot and immunohistochemical analysis were carried out. We performed histological examination of liver tissue using H&E staining as well as an immunohistochemical analysis for PCNA. All procedures were approved by the Institutional Animal Care and Use Committee of the Veterinary Medical School at the National Autonomous University of Mexico. The experiments were conducted in accordance with the principles set forth in the Care and Use of Laboratory Animals Guide. Our study revealed, scattering preneoplastic lesions through liver parenchyma, such as focal coagulative necrotic changes, presence of bi-nucleated nucleus and focal fatty changes in animals receiving carcinogens. Total EGFR and tyrosine phosphorylation at pY1068 EGFR were significantly increased in animals developing preneoplastic lesions (2.5-fold and 10-fold, respectively) as compared to control group ( $p < 0.05$ ). Those findings were associated with a significant increase in PCNA expression (12-fold) ( $p < 0.05$ ). Interestingly, our result showed that gallic acid reduced EGFR expression and phosphorylation at pY1068 EGFR in animals developing preneoplastic lesions. A significant reduction in total EGFR (2.5-fold) and tyrosine phosphorylation at pY1068 EGFR (7.5-fold) were found as compared with preneoplasia group ( $p < 0.05$ ). The reduction in EGFR expression and phosphorylation was associated with a reduction in PCNA expression. A reduction of preneoplastic lesions and an improvement in liver tissue was also observed.

In conclusion, gallic acid might influence in EGFR cell signaling pathway in the liver during developing of preneoplastic lesion, reducing cell proliferation and improving liver architecture. Further studies are needed to evaluate the potential usefulness of gallic acid as a promising hepatoprotective agent.



# Mitragynine Pretreatment Prevents Morphine-Induced Respiratory Depression

Julio D. Zuarth Gonzalez,<sup>1</sup> Alexandria K. Ragsdale,<sup>1</sup> Sushobhan Mukhopadhyay,<sup>2</sup>  
Christopher R. McCurdy,<sup>2</sup> Lance McMahon,<sup>1</sup> and Jenny L. Wilkerson<sup>1</sup>

<sup>1</sup>Texas Tech University Health Sciences Center; and <sup>2</sup>University of Florida

Abstract ID 26122

Poster Board 264

**Objectives:** Kratom (*Mitragynine speciosa*), a natural product from southeast Asia, has become a popular self-treatment trend for pain and opioid use disorder (OUD) and users claim great success. Considering the current opioid epidemic, kratom is being studied as a potential OUD pharmacotherapy. Given that respiratory depression is a major cause of mortality due to opioid overdose, a great need exists to determine kratom-related respiratory effects alone and in the presence of opioids. For the current study we examined the effects of mitragynine, the most abundant alkaloid in kratom, in a rat model of intravenous (i.v.) administered morphine-induced respiratory depression.

**Methods:** Adult male and female Sprague Dawley rats arrived pre-implanted with a jugular catheter. Experiments were conducted using a within-subjects experimental design over 8 weeks and each session lasted 3 hours. During a 3-hour session, respiratory parameters including respiratory frequency, tidal volume, and minute ventilation were measured using whole body plesmography in freely moving animals. A 3-hour session was comprised of a 1-hour acclimation, followed by a 20-minute baseline. The first i.v. infusion was delivered at the end of the baseline and the second i.v. infusion was delivered 5 minutes later. After the second infusion the above-mentioned respiratory parameters were continuously monitored for 110 minutes. A 7-day drug washout period between sessions was utilized, and sessions were counterbalanced with no more than 2 animals of the same sex receiving the same condition on the same day. In all experiments a solution consisting of 0.9% saline, tween, polyethylene, and propylene glycol served as vehicle for mitragynine, morphine was dissolved in 0.9% saline.

**Results:** Saline + vehicle had no effect on the respiratory parameters measured. Morphine (32 mg/kg, i.v.) followed by vehicle injection produced robust respiratory depression as indicated by decreased frequency, tidal volume, and minute ventilation for the duration of the study. Mitragynine (10 mg/kg, i.v.) followed by vehicle injection significantly increased respiratory frequency and minute ventilation but did not alter tidal volume. When morphine (32 mg/kg, i.v.) was delivered before mitragynine (10 mg/kg, i.v.) no significant differences were observed in respiratory frequency, tidal volume, or minute ventilation compared to the morphine + vehicle administration results. However, when mitragynine (10 mg/kg, i.v.) was delivered first, 5 minutes prior to morphine (32 mg/kg, i.v.) mitragynine prevented opioid induced respiratory depression, as indicated by decreased frequency, tidal volume, and minute ventilation.

**Conclusions:** Intravenously administered morphine produced robust respiratory depression symptoms, whereas at the dose studied here, mitragynine did not. When given after morphine, mitragynine failed to alter morphine-induced respiratory depression symptoms. However, when given before morphine, mitragynine prevented morphine-induced respiratory depression. These findings have important implications in opioid use disorder and opioid overdose medication development.

Supported by National Institute on Drug Abuse grants DA25267 and DA048353.

# Evaluating the role of rodent macrophage immunometabolism in response to endotoxin

Rachel Sun,<sup>1</sup> Jaclynn Andres,<sup>1</sup> Jordan Lee,<sup>2</sup> Kinal Vayas,<sup>1</sup> Changjiang Guo,<sup>1</sup> Andrew Gow,<sup>1</sup> and Debra L. Laskin<sup>1</sup>

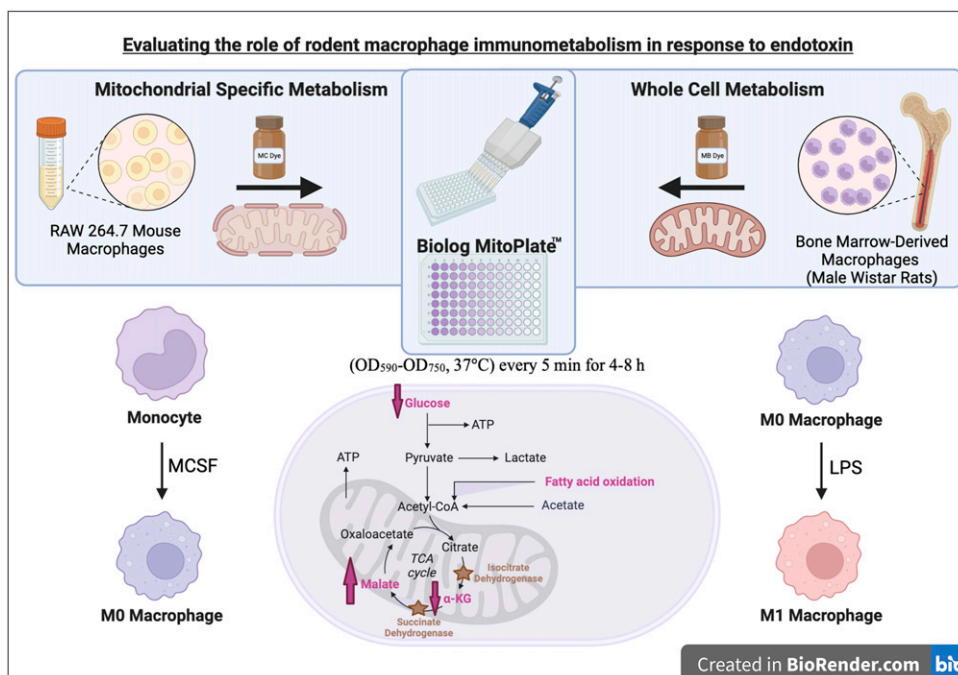
<sup>1</sup>Rutgers Univ; and <sup>2</sup>Rutgers, The State Univ of New Jersey

Abstract ID 18793

Poster Board 418

Cellular metabolism has emerged as a key regulator of macrophage activation towards a proinflammatory M1 or a proresolution M2 phenotype. Previous studies have demonstrated that M1 macrophages upregulate glycolysis for rapid ATP production, while M2 macrophages are dependent on mitochondrial respiration. One mechanism by which metabolism is regulated is by breaking the citric acid cycle (CAC) at points, such as succinate dehydrogenase. Evaluating the balance between metabolic pathways and macrophage activation is essential for elucidating the role of macrophages in tissue injury. Such analysis has required the use of expensive metabolomics, however, here we used the Biolog MitoPlate™ mitochondrial functional assay to assess macrophage immunometabolism by evaluating their substrate preference and respiration. RAW 264.7 mouse macrophages, cultured in Dulbecco's modified Eagle's medium (DMEM) with LPS (10 ng/mL) or DMEM control and bone marrow-derived macrophages (BMDMs) collected from male Wistar rats, cultured with macrophage-colony stimulating factor (MCSF, days 0, 3, and 6; 20 ng/mL/day) and LPS (day 6; 0, 10, 100 ng/mL) for 18-24 h were used. To assess mitochondrial specific metabolism, cells were permeabilized with saponin and treated with Redox MC Dye in Biolog Mitochondrial Assay Solution (BMAS). For whole cell metabolism, cells were treated with MB Dye in RPMI. Dye reduction, an indicator of substrate utilization, was measured spectrophotometrically ( $OD_{590}-OD_{750}$ , 37°C) every 5 min for 4-8 h. Cellular permeabilization was required to assess mitochondrial usage of malate,  $\alpha$ -ketoglutarate, or citrate metabolism. LPS treatment of RAW cells and BMDM resulted in increased reliance on malate, indicating a break in CAC at succinate dehydrogenase. Similar effects were observed at the whole cell level. Overall these data confirm breaks in CAC at isocitrate dehydrogenase and succinate dehydrogenase. These data demonstrate that the MitoPlate™ is effective to evaluate specific steps in the CAC that may be modified by toxicants.

Supported by NIH Grants AR055073, 5R25ES020721, and ES005022.



Biolog Mitoplate™ allows measurement of mitochondria-specific metabolism and whole cell metabolism. In mitochondria of RAW264.7 cells and BMDMs, LPS promotes mitochondrial malate consumption and reduces  $\alpha$ KG and glucose metabolism, indicating critical breaks in the citric acid cycle.

# Damage to Intestinal Barrier of Zebrafish Larvae by Polystyrene Nanoplastics exposure

Hyejin Lee

*Korea Institute of Oriental Medicine (KIOM), University of Science & Technology (UST)*

**Abstract ID 54777**

**Poster Board 419**

Plastic, one of the most pervasive materials on the earth, is exposed to humans daily in real life. According to WORLD WIDE FUND FOR NATURE (WWF), an average human could ingest approximately 5 grams of plastic weekly. But its impact on human health remains poorly understood. Over 90 percent of plastic is exposed in drinking water. Polystyrene (PS) is one of the common materials of plastic and is used for take-out cups and lunch boxes. But toxicity studies of exposure by ingestion of PS are poorly understood. In this study, we reported intestinal damage by ingestion of PS in the zebrafish larvae model.

We exposed 4 dpf(days post fertilization) zebrafish larvae to 10 – 300 ppm of the PS NPs for 48 h. First of all, we identified the morphology of the PS NPs before and after exposure with scanning electron microscope (SEM). We performed Fourier-transform infrared spectroscopy (FT-IR) analysis to confirm the alteration of the chemical structure of PS NPs. Also, we elicited the damage of the intestinal barrier via hematoxylin and Eosin (H&E) and alcian blue (AB) staining of the zebrafish intestinal tissue. The increased intestinal permeability was identified with the biochemical assay, diamine oxidase (DAO) assay. Also, quantitative real-time polymerase chain reaction(qRT-PCR) results show a decreased level of gene expression related to the tight junction (*OCLN*, *CLDN-1*, *ICAM-1*, *ZO-1*).

In conclusion, exposure to PS NPs damage the zebrafish larval intestinal barrier. Thus, these results can contribute studies of the toxicity of PS NPs on real life.

**Support/Funding Information:** KSN20223302

# Assessing the Impact of Benzalkonium Chlorides on Gut Microbiome and Liver Metabolism

Vanessa A. Lopez,<sup>1</sup> Joe Jongpyo Lim,<sup>1</sup> Ryan Seguin,<sup>1</sup> Joseph L. Dempsey,<sup>1</sup>  
Gabby C. Kunzman,<sup>2</sup> Julia Yue Cui,<sup>1</sup> and Libin Xu<sup>1</sup>

<sup>1</sup>Univ of Washington; and <sup>2</sup>University of Washington

Abstract ID 29280

Poster Board 420

Benzalkonium chlorides (BACs) are widely used disinfectants in a variety of consumer and food-processing settings, and the ongoing COVID-19 pandemic has increased the use of BACs. The prevalence of BACs in our daily environment raises the concern that regularly recurring BAC exposure could disrupt the gastrointestinal microbiota, thus interfering with the beneficial functions microbes provide to host health. Gut microbiota is known to be important for the expression of hepatic CYPs. We recently reported that BACs are metabolized by cytochrome P450s (CYPs) in the liver. Our preliminary data supports biliary excretion from the liver to the intestine being the major route of elimination for BACs and their metabolites. Thus, we hypothesize that exposure to BACs can alter the gut microbiome diversity and composition, which will lead to alterations in bile acid homeostasis, sterol biosynthesis, and xenobiotic metabolism in the liver. In this study, we exposed male and female mice to C12- and C16-BACs at 120 mg /g/day for one week via oral dosing. Intestinal content from cecum was collected and 16S rRNA sequencing was carried out on the isolated bacterial DNA. We found that treatment with either C12- or C16-BACs led to decreased alpha diversity and differential composition of gut bacteria, notably, the complete elimination of the actinobacteria phylum. Additionally, through a targeted bile acid quantitation analysis, we have found decreases in secondary bile acids in BAC treated mice. This finding is supported by decreases in bacteria known to metabolize primary bile acids into secondary bile acids, such as the families of Ruminococcaceae and Lachnospiraceae. Furthermore, targeted sterolomics analysis of liver extracts revealed that BACs caused decreased sterol abundance, including decreased cholesterol and lanosterol. Additionally, RNA sequencing analysis on RNA isolated from the livers of all groups found differential gene expression changes in relevant genes. Specifically, C16-BAC treatment in the female cohort led to upregulation of *Hmgcr*, a gene that encodes the rate-limiting enzyme in cholesterol synthesis. C16-BAC treatment in the male cohort led to upregulation of *Cyp4a10*, *Cyp4f13*, *Cyp2j6* and *Cyp2c38* genes, all encoding for hepatic lipid and xenobiotic metabolism. Lastly, UPLC-MS/MS analysis of intestinal sections and livers of BAC treated mice demonstrated the absorption and metabolism of BACs. Both parent compounds were detected in the liver along with their major Phase-I metabolites: the  $\omega$ -OH, ( $\omega$ -1)-OH, ( $\omega$ -1)-ketone, and  $\omega$ -COOH metabolites. Together, these data signify the potential impact BAC exposure may have on human health through disturbance of the gut microbiome and gut-liver interactions.

# Mitochondrial Modulation of Amplified Preconditioning Influences of Remote Ischemia Plus Erythropoietin Against Skeletal Ischemia/Reperfusion Injury in Rats

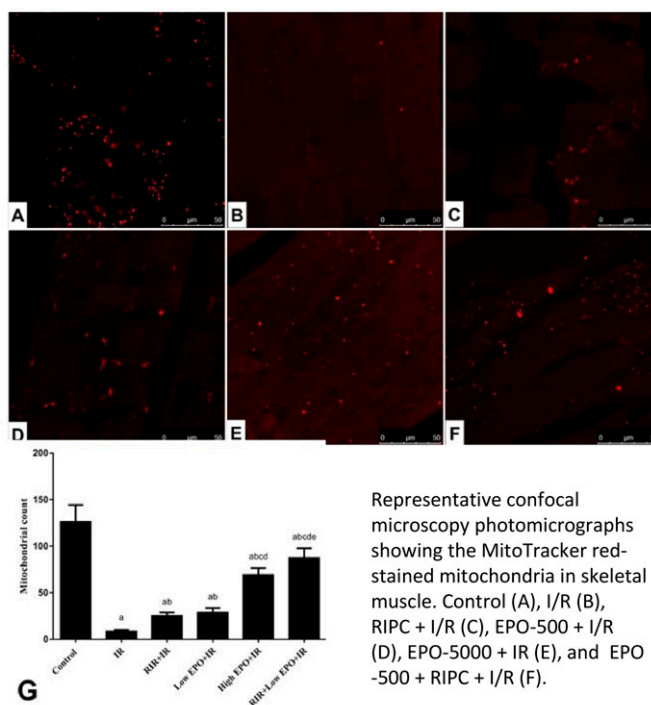
Mahmoud El-Mas,<sup>1</sup> Mennatallah A. Ali,<sup>2</sup> Nahed H. El-Sokkary,<sup>3</sup> Samar S. Elblehi,<sup>4</sup> and Asmaa A. Khalifa<sup>2</sup>

<sup>1</sup>College of Medicine, Kuwait Univ, Kuwait; Faculty of Pharmacy, Alexandria Univ, Egypt; <sup>2</sup>Faculty of Pharmacy, Pharos University in Alexandria; <sup>3</sup>Faculty of Medicine, Alexandria University; and <sup>4</sup>Faculty of Veterinary Medicine, Alexandria University

Abstract ID 18929

Poster Board 421

Skeletal muscle ischemia and reperfusion (S-I/R) is frequently associated with aggravated inflammatory response and tissue injury that could be relieved by interventions like remote ischemic preconditioning (RIPC) or the hormonal growth factor erythropoietin (EPO). Here, we tested the hypotheses that (i) the simultaneous exposure to a low dose of EPO boosts the protection conferred by RIPC against S-I/R injury, and (ii) this privileged EPO/RIPC effect is prompted by mitochondrial and extra-mitochondrial machineries. The effects of RIPC, EPO (500 or 5000 IU/kg), or combined RIPC/EPO-500 regimen on S-I/R injury induced by right hindlimb 3-hr ischemia for followed by 3-hr reperfusion were investigated. RIPC was induced by 3 brief consecutive I/R cycles (10-min ischemia and 10-min reperfusion each) of the contralateral hindlimb. S-I/R injury was verified by the (i) rise in serum lactate dehydrogenase, pyruvate, and creatine kinase, (ii) histopathological signs of sarcoplasm vacuolations, segmental necrosis, and inflammatory cells infiltration, and (iii) increments and decrements in electromyographic amplitude and duration, respectively. These defects were partially ameliorated by RIPC or by EPO in a dose-related fashion. Further, greater repairs of functional/structural anomalies of S-I/R were seen in rats pre-exposed to the combined RIPC/EPO-500 intervention. The latter therapy also caused more effective preservation of the number of MitoTracker red-stained mitochondria assessed by confocal microscopy and suppression of mitochondrial DNA damage and indices of oxidative stress and apoptosis like cardiolipin, succinate dehydrogenase, citrate synthase, and cytochrome c. Additionally the combined RIPC/EPO therapy was more influential than individual treatments in ameliorating rises in muscular myeloperoxidase and nitric oxide metabolites and preventing excessive calcium accumulation and glycogen consumption. Overall, the dual RIPC/EPO therapy additively mends mitochondrial dysfunction and interrelated skeletal structural and functional deficits induced by S-I/R injury. The use of relatively low EPO doses might serve to minimize adverse effects often encountered with the clinical use of the hormone



# Beta-Catenin Mediates PKM2's Role in LPS-induced Renal Injury

Katelin Hubbard,<sup>1</sup> Mohammed Alquraishi,<sup>1</sup> Samah Chahed,<sup>1</sup> Dina Alani,<sup>1</sup> Dexter Puckett,<sup>1</sup> Presley Dowker-Key,<sup>2</sup> Yi Zhao,<sup>1</sup> Ji Yeon Kim,<sup>1</sup> Laurentia Nodit,<sup>3</sup> Huma Fatima,<sup>4</sup> Dallas Donohoe,<sup>1</sup> Brynn Voy,<sup>1</sup> Jay N. Whelan,<sup>1</sup> Winyoo Chohanadisai,<sup>5</sup> and Ahmed Bettaieb<sup>2</sup>

<sup>1</sup>University of Tennessee Knoxville; <sup>2</sup>Univ of Tennessee, Knoxville; <sup>3</sup>University of Tennessee Medical Center; <sup>4</sup>University of Alabama at Birmingham; and <sup>5</sup>Department of Nutrition, Oklahoma State University

**Abstract ID 23750**

**Poster Board 422**

Acute Kidney Injury (AKI) is a serious health concern that may lead to alterations in the function and morphology of the kidney glomerulus and a significant decline in renal function. Recent research into the metabolic alterations associated with AKI within glomerular epithelial cells (podocytes) revealed significant dysregulations to glucose metabolism and related enzymes, specifically pyruvate kinase M2 (PKM2). However, the role of PKM2 in the pathogenesis of AKI remains to be elucidated. In the current study, we employed Cre-loxP technology to explore the effects of PKM2-specific deletion in podocytes on the activity of pivotal signaling pathways central to the pathophysiology of AKI. Lipopolysaccharide (LPS)-induced AKI was used as the experimental model. We demonstrate that mice with specific PKM2 ablation in podocytes exhibited a significant reduction in LPS-induced protein excretion and alterations to blood serum albumin and urea nitrogen levels. Quantitative immunohistochemical analysis revealed that PKM2 deficiency was also protective against LPS-induced renal injury. These effects were concomitant with a reduction in LPS-induced expression of pro-inflammatory cytokines, local induction of inflammation, endoplasmic reticulum stress, and apoptosis. At the molecular level, the beneficial effects of PKM2 on LPS-induced podocytes injury were mediated, at least in part, through a reduction in  $\beta$ -catenin activity and enhancement of autophagy. Reconstitution of PKM2- knockdown podocytes abrogated the protective effects of PKM2 deficiency. Taken together, our findings highlight a pivotal role for PKM2 in podocyte response to stress and demonstrates that targeting PKM2 in podocytes may be of therapeutic potential in the prevention and treatment of AKI.

# Common Pathways in Human Proximal Tubular Cells Altered by Exposures to Diverse Environmental Agents and Nephrotoxic Therapeutic Drugs

Lawrence Lash,<sup>1</sup> Patricia Mathieu,<sup>2</sup> Rita Rosati,<sup>3</sup> Paul Stemmer,<sup>4</sup> Xin Hu,<sup>5</sup> and Dean P. Jones<sup>5</sup>

<sup>1</sup>Wayne State Univ School of Medicine; <sup>2</sup>Wayne State University School of Medicine; <sup>3</sup>Wayne State University; <sup>4</sup>Wayne State Univ; and <sup>5</sup>Emory University School of Medicine

Abstract ID 15061

Poster Board 423

Primary cultures of human proximal tubular (hPT) cells were used as the model system to test the hypothesis that exposure to low, physiologically relevant concentrations of diverse chemical agents causes release of proteins, lipids and metabolites into the extracellular space that correlate with specific exposures and cytotoxicity. hPT cells were incubated with two environmental contaminants [S-(1,2-dichlorovinyl)-L-cysteine (DCVC) and HgCl<sub>2</sub>] or three clinically used drugs whose efficacy is dose-limited by nephrotoxicity [cisplatin (CDDP), polymyxin B (PmxB), and tenofovir disoproxil fumarate (TDF)]. Using quantitative mass spectrometry and isobaric tags, several proteins were found to be increased in the extracellular media of hPT cells incubated with these chemicals. Both time- and concentration-dependent effects on protein abundance were noted, including several cytoskeletal proteins and multiple mitochondrial proteins. Using high resolution mass spectrometry coupled with ultrahigh performance liquid chromatography, effects of the diverse exposures on low-molecular-weight metabolites were studied showing time- and concentration-dependent perturbations in several common pathways, including amino acid metabolism, fatty acid metabolism, and carnitine shuttle pathways. Importantly, most of the changes in proteome or metabolome were caused by exposure concentrations that produce modest or no detectable cytotoxicity, as determined by release of Kidney Injury Molecule-1 (KIM-1) or neutrophil gelatinase-associated lipocalin (NGAL) from exposed hPT cells. These findings further support the overall hypothesis and identify multiple candidate biomarkers and altered biochemical pathways associated with early exposure to diverse nephrotoxicants.

Supported by NIEHS Grant 1-R01-ES031584.

# The Kratom-Derived Alkaloid Mitragynine Upregulates the Cortisol Steroidogenic Pathway In a Human Adrenocortical Cell Line

Phillip Kopf,<sup>1</sup> and Walter Prozialeck<sup>1</sup>

<sup>1</sup>Midwestern Univ

Abstract ID 52920

Poster Board 424

Kratom is a tropical evergreen tree indigenous to Southeast Asia whose leaves and decoctions have long been used in traditional folk medicine for the relief of pain and enhancement of vitality. In recent years kratom use has increased in the United States, where an estimated 10-15 million people use the herb for the self-management of pain and opioid withdrawal. Kratom leaves contain over 40 active alkaloids. Previous studies in our laboratory demonstrated that mitragynine was the only kratom alkaloid that enhanced cortisol secretion in a human adrenocortical cell line. To further investigate the molecular mechanism by which mitragynine enhances cortisol secretion, we examined the effect of mitragynine on the expression of the steroidogenic enzymes and cofactors involved in cortisol production. HAC15 cells were exposed to vehicle or mitragynine (10  $\mu$ M). After 72 h, mRNA expression of the following steroidogenic enzymes, cofactors, and receptors was examined: CYP11A1, HSD3B2, CYP21A2, CYP11B1, StAR, FDXR, FDX1, and MC2R. While mRNA expression was upregulated for all of these steroidogenic factors, CYP11B1 was induced to the greatest extent (fold change: vehicle,  $1.0 \pm 0.2$ ; 10  $\mu$ M mitragynine,  $18.4 \pm 1.5$ ;  $n=6$ ). Analysis of protein levels of these steroidogenic factors is underway. These data indicate that mitragynine enhances cortisol secretion *in vitro* via upregulation of the cortisol synthesis enzymatic pathway. This mechanism may contribute to anti-inflammatory and analgesic actions of kratom *in vivo*. Additional studies are currently being done to determine what receptor is mediating this stimulation of the cortisol pathway.



# Effects of the E-liquid Flavoring Agents Vanillin and Ethyl Vanillin in Human Proximal Tubule Epithelial Cells

Ashley Cox,<sup>1</sup> Kathleen Brown,<sup>2</sup> and Monica Valentovic<sup>1</sup>

<sup>1</sup>Marshall Univ School of Medicine; and <sup>2</sup>Marshall Univ

Abstract ID 21988

Poster Board 425

E-cigarette usage and vaping have become increasingly popular over recent years, especially among teenagers and young adults. There are thousands of e-liquid flavors on the market, but the effects of inhaling e-liquid flavorings have not been well-characterized systemically. The lung remains the major focus of research, but some research shows that organs such as the kidney may be affected by e-liquid flavoring inhalation. The aldehydes vanillin (VAN) and ethyl vanillin (ETH VAN) are two popular flavoring ingredients found in e-liquids. The aim of this study is to evaluate VAN and ETH VAN cytotoxicity in renal proximal tubular epithelial cells. All studies were conducted using human renal proximal tubular cells (HK-2). Cells were obtained from ATCC and cultured according to vendor specifications. HK-2 cells were plated, equilibrated for 48 h, and treated with 0 (200 proof ethanol) or 100-1000 uM VAN or ETH VAN for 24 or 48 h. Viability was quantitated using the MTT assay and conversion to formazan. Cell Countess was performed to evaluate trypan blue exclusion and cell membrane leakage. Western blot analysis probed for oxidative stress as 4-hydroxynonenal (4-HNE) adducted proteins. Cell stress was evaluated as protein expression of: LC3B-I, LC3B-II, and caspase-3. Mitochondrial function was evaluated using an Agilent XFp Seahorse analyzer. Results were obtained from at least 4 independent experiments using different cell passages. Statistical differences between groups were analyzed using One-Way ANOVA followed by post hoc Tukey test at a 95% confidence interval. VAN and ETH VAN were not cytotoxic relative to control based on MTT assay after 24 h exposure, and ETH VAN showed an elevated conversion to formazan at 24 h. At 48 h, VAN treatment showed significantly decreased ( $p < 0.05$ ) conversion to formazan at 1000 uM concentration when compared to control. ETH VAN showed significantly decreased ( $p < 0.05$ ) conversion to formazan at 1000 uM concentration when compared to control and 100-500 uM treatment groups at 48 h. Countess trypan blue exclusion assay showed no significant difference between groups at all concentrations at 24 or 48 h. No significant 4-HNE adduction of proteins was observed for either VAN or ETH VAN at any concentration when compared to control. Autophagy was evaluated as the ratio of LC3B-II to LC3B-I. The ratio of LC3B-II to LC3B-I was not significantly different for either VAN or ETH VAN, but an increasing trend in ratio was observed. Apoptosis probing showed no significant increase in cleaved caspase-3 for either VAN or ETH VAN, however an increasing trend was observed for ETH VAN. Seahorse analyzer assay of mitochondrial oxygen consumption rate (OCR) showed that basal respiration significantly increased ( $p < 0.05$ ) at 1000 uM VAN 24 h when compared to control and the 100 uM concentration. ATP production was significantly increased ( $p < 0.05$ ) between 100 uM and 1000 uM concentrations for VAN 24 h. Basal respiration, non-mitochondrial respiration, maximal respiration, and proton (H<sup>+</sup>) leak all significantly increased ( $p < 0.05$ ) at 1000 uM ETH VAN 24 h when compared to control and the 100 uM concentration. Spare respiratory capacity significantly increased ( $p < 0.05$ ) between the control and 1000 uM ETH VAN 24 h group. These findings indicate that VAN and ETH VAN exposure induce changes within the mitochondria based on Seahorse assay and 48 h MTT assay. Further studies are needed in order to characterize specific changes within the mitochondria for these flavoring agents.

Supported by NIH Grant P20GM103424; AC supported by WV NASA Graduate Research Fellowship.

# Cutaneous Exposures to Nitrogen Mustard in C57BL/6 Mice Cause Hematologic Toxicity that could lead to Acute and Long-term Effects

Ellen Kim,<sup>1</sup> Dinesh Goswami,<sup>1</sup> Andrew Roney,<sup>1</sup> Ebenezar Okoyeocha,<sup>1</sup> Steve Lundback,<sup>1</sup> Dawn Kuszynski,<sup>1</sup> Adam Lauver,<sup>1</sup> and Neera Tewari-Singh<sup>1</sup>

<sup>1</sup>*Department of Pharmacology and Toxicology, College of Osteopathic Medicine, Michigan State University*

**Abstract ID 27457**

**Poster Board 457**

Mustard vesicating agents, sulfur mustard [SM; bis(2-chloroethyl) sulfide] and nitrogen mustard [NM; bis(2-chloroethyl) methylamine (HN<sub>2</sub>)], are powerful vesicating and alkylating agents that cause severe skin toxicity, and systemic toxicity upon penetration and absorption through the skin. Currently, there are no approved or effective therapies to treat SM- and NM-induced acute, systemic, and long-term toxicity. SM and NM attack rapidly dividing cells such as the hematological cells, and previous studies from acute exposures have shown that mustard agents cause toxic effects to the bone marrow. Specifically, initial leukocytosis followed by leukopenia has been reported in victims of SM-exposure. The hematologic effects of mustard exposure are not fully characterized and investigating these effects can further our understanding of the mechanisms of mustard vesicant-induced systemic toxicity and long-term injuries. In this study, we investigated the hematologic changes in male C57BL/6 mice after a single topical NM-exposure [0.5 mg or 1.0 mg of NM in 100  $\mu$ L of acetone or acetone alone (control)]. Mice were sacrificed at 1-, 7-, 14-, and 28-day post NM-exposure, and blood was collected and analyzed using the IDEXX ProCyte Dx Hematology Analyzer. NM-exposure caused transient toxic effects to the bone marrow. 0.5 mg and 1.0 mg NM-exposures caused a significant decrease in RBC's and hemoglobin at 1-, 7-, and 28-day post NM-exposure. Both doses of NM-exposure also caused a decrease in reticulocytes. Recovery was seen by 14- and 28-day post 0.5 mg NM-exposure. Similarly, lymphopenia and eosinopenia was observed after exposure to both doses of NM and recovery was observed by 28-day post 0.5 mg NM-exposure. Increases in monocytes and neutrophils were observed post 0.5 mg and 1.0 mg NM-exposures. Overall, our results indicate that cutaneous NM-exposure led to hematologic toxicity which could be involved in NM-induced injury including acute inflammatory responses and long-term illnesses. Furthermore, our findings corroborate some of the symptoms (bone marrow depression, immune suppression, infection, and toxicity) observed in veterans of real-world SM exposures. Further investigations are being carried out to fully characterize the hematologic toxicity and related mechanisms to identify effective countermeasures against mustard vesicant-induced injuries, especially the long-term effects, and mortality.

# Pyrrolizidine alkaloids induced obstructive pulmonary disease more than pulmonary vascular diseases

Zijing Song,<sup>1</sup> Yisheng He,<sup>2</sup> and Ge Lin<sup>2</sup>

<sup>1</sup>The Chinese Univ of Hong Kong; and <sup>2</sup>The Chinese University of Hong Kong

**Abstract ID 53998**

**Poster Board 458**

Pyrrolizidine alkaloids (PAs) are widely distributed natural toxins. Aside from their extensively-studied hepatotoxicity, our previous report demonstrated that pneumotoxicity was commonly induced by retronecine and otonecine types PAs. Monocrotaline (MCT) as a widely used agent to induce pulmonary arterial hypertension has been frequently investigated for its toxicity on pulmonary vessels. Besides vascular damage, PA-induced airway damage is poorly defined. Here we aimed to systematically investigate PA-induced chronic obstructive pulmonary disease.

In the present study, rats were orally administered with a single dose of MCT (0.2 mmol/kg) and sacrificed 4 weeks after exposure. Histological examinations including various staining techniques were applied to evaluate the pathological changes in airways and alveoli induced by MCT. The results revealed that, apart from pulmonary vascular pathology, MCT also induced alveolar inflammation (lymphocytes, neutrophils, and macrophages accumulation and infiltration into alveolar space), alveolar damage (alveolar type II pneumocyte hyperplasia, emphysema, and edema), and airway remodelling (goblet cell metaplasia, and loss of adherens ad-junction) in rats.

In conclusion, we present the first systematical characterization of MCT-induced obstructive lung diseases in rats, which is initiated by endothelial damage with inflammatory responses as a crucial mediator. Our findings have both clinical and public health implications. Till now, PA poisoning cases in humans are almost manifested by liver injury, mostly due to the ingestion of PA-contaminated grains or PA-containing herbal medicines. Considering that, i) different PAs commonly induce pulmonary toxicity, and ii) humans are frequently exposed to PAs via ingestion of PA-containing herbal medicines or PA-contaminated foods, it is extrapolated that PA exposure might serve as a contributor to human obstructive lung disease incidence, and further investigations are warranted.

[The present study was supported by General Research Fund (Project Nos. 14160817, 14107719 and 14106318) from Research Grants Council of Hong Kong Special Administrative Region and Direct Grant (Project No. 4054656) from The Chinese University of Hong Kong.]

# Molecular Mechanisms of Hippocampal Neurotoxicity Across Three Generations of Brominated Flame Retardants

Naomi Kramer,<sup>1</sup> Brian Cummings,<sup>2</sup> and John Wagner<sup>3</sup>

<sup>1</sup>Univ of Georgia; <sup>2</sup>Wayne State University; and <sup>3</sup>University of Georgia

Abstract ID 28060

Poster Board 459

Brominated Flame Retardants (BFRs) are ubiquitously utilized to reduce flammability in a wide range of household products including carpets, upholstery, and paints. While useful chemicals, BFRs also migrate from their products into the environment. This has resulted in continuous, population-level exposure that has been correlated to impaired learning and memory. To determine the effects of different BFR generations on hippocampal cells, HT-22 cells were exposed to tetrabromobisphenol-A (TBBPA), hexabromocyclododecane (HBCD), or 2,2',4,4'-tetrabromodiphenyl ether (BDE-47) (current, phasing out, and phased out BFRs, respectively). Cell viability analysis was assessed by MTT staining, as well as nuclear morphology after 48 hr of exposure. HBCD exposure resulted in lower IC<sub>50</sub> values in HT-22 cells (15 mM IC<sub>50</sub>), as compared to TBBPA (70 mM) and BDE-47 (60 mM). HT-22 cellular and nuclear morphology suggested the presence of apoptosis after exposure to the IC<sub>50</sub> for each BFR after both 24 and 48 hr exposure. To understand the mechanisms of toxicity, cell cycle and cell death were evaluated. Each BFR induced cell cycle alterations with increasing exposure time. Upon 24 hr exposure, HBCD (50 or 100 mM) induced significant S-phase arrest which was maintained upon 48 hr exposure. However, only upon 48 hr exposure did BDE-47 (50 and 100 mM) and TBBPA (100 mM) induce significant S-phase arrest. Annexin-PI staining verified a time and concentration-dependent neurotoxic effect, as evidenced by an increase in annexin V staining in cells, indicating the presence of apoptotic cell death. Both 24 and 48 hr exposure to HBCD (50 or 100 mM) or BDE-47 (100 mM) induced significant increases in apoptosis, although 100 mM TBBPA only induced apoptosis and necrosis after 48 hr. Further evaluation of the mechanisms of toxicity indicates that p53 and p21 may play a central role in the onset of cell cycle arrest and apoptosis. RNA-Sequencing was performed to understand the molecular mechanisms underlying flame retardant neurotoxicity. These data demonstrate that BFRs can induce chemical-dependent toxicity in neural cells *in vitro*; however, additional study will be necessary to determine if BFR-induced neural cytotoxicity would adversely affect learning and memory *in vivo*.

# Examining the Nephrotoxicity Induced by Benzalkonium Chlorides in 2D and 3D-Cultured Human Proximal Tubule Epithelial Cells

Marie Brzoska,<sup>1</sup> Ryan Seguin,<sup>1</sup> Jade Yang,<sup>1</sup> Edward J. Kelly,<sup>2</sup> and Libin Xu<sup>2</sup>

<sup>1</sup>University of Washington; and <sup>2</sup>Univ of Washington

Abstract ID 16894

Poster Board 460

Benzalkonium chlorides (BACs) are widely used antimicrobials in a variety of consumer products and settings, including disinfectants, medical products, and food-processing industry. Though initially recognized as safe, the FDA has called for additional safety data on BAC use in consumer products. Their toxicity becomes especially important during the COVID-19 pandemic due to the increased use of BAC-containing disinfectant products. BAC exposure in rats led to their accumulation primarily in the kidney (42-fold higher than blood); in contrast, accumulation did not occur in the liver, likely due to efficient metabolism of BACs by hepatic cytochromes P450 (CYPs), mainly CYP4F isoforms and CYP2D6. Thus, we hypothesized that BAC-metabolizing capacity determines the extent of the buildup of BACs in the kidney and subsequent kidney injury. Human kidney and liver microsomes were incubated with 1  $\mu$ M C12-BAC over 8 time points between 0 and 64 minutes, and LC-MS analysis showed C12-BAC was consumed much slower in the kidney microsomes than the liver microsomes, with the half-lives being 50 and 2.5 min, respectively. We then used cell viability assays to investigate the nephrotoxicity of C10-, C12-, C14- and C16-BAC and their  $\omega$ -OH metabolites ranging from 0–40  $\mu$ M over 48 hours in 2D-cultured human proximal tubule epithelial cells (PTECs). In general, the parent compounds displayed much larger cytotoxicity (at least 7-17-fold) than their  $\omega$ -OH metabolites, suggesting BAC metabolism by CYPs detoxifies BACs. EC<sub>50</sub> for C12-BAC is approximately 3  $\mu$ M while the EC<sub>50</sub> for the C14- and C16-BACs is around 1  $\mu$ M. The EC<sub>50</sub> value for C10-BAC was not captured in the concentration range examined. BAC-metabolizing CYP4F11 and CYP4F12 are expressed in the kidney, but administration of a CYP4F inhibitor, HET0016, to inhibit the metabolism of BACs did not significantly increase the cytotoxicity of parent BACs, suggesting that BAC metabolism by the kidney is not sufficient to detoxify them. We then examined the nephrotoxicity of BACs using a kidney-on-a-chip microphysiological system (MPS), in which the microenvironment of the chip mimics the functional characteristics of human proximal tubules. We found that 1  $\mu$ M of C14-BAC exerts potent toxicity to human PTECs in the kidney MPS system, compared to the untreated channel. However, kidney injury molecule 1 (KIM-1) displayed no difference between the C14-BAC and untreated channels, suggesting an alternative cell death mechanism by BACs. To summarize, our data suggest that the kidney has smaller BAC-metabolizing capacities than the liver and that BACs can potentially cause nephrotoxicity in humans.

Supported by grants from the National Institutes of Health, USA (NIH grant T32GM007750 and R01ES031927)

# Perturbation of Space-Time Gene Expression of the Liver Lobule by 2,3,7,8-Tetrachlorodibenzo-p-dioxin

Daniel Marri,<sup>1</sup> Omar Kana,<sup>2</sup> Rance Nault,<sup>2</sup> Giovan Cholico,<sup>2</sup> Timothy Zacharewski,<sup>2</sup> and Sudin Bhattacharya<sup>2</sup>

<sup>1</sup>Michigan State University, Department of Biomedical Engineering; and <sup>2</sup>Michigan State University

Abstract ID 28030

Poster Board 461

The mammalian liver is spatially structured into functional sub-units called lobules composed primarily of hepatocytes, the parenchymal liver cell type. Hepatocytes lie along an axis of a lobule and can be sub-categorized into those more proximal to either the central vein or the portal vein. Gene expression and resulting metabolic functions vary spatially along the portal to central axis of the liver lobule. Additionally, the liver lobule is subject to temporal gene regulation via circadian rhythm. The interaction between hepatic lobule zonation and the rhythmicity of the circadian clock has been termed the “space-time logic” of gene expression in the liver. 2,3,7,8-Tetrachlorodibenzo-p-dioxin (TCDD) is a persistent environmental toxicant that disrupts hepatic zonal expression and temporal gene expression in the liver lobule. However, it remains unclear how the different axes of rhythmicity and zonation interact and change with respect to TCDD perturbation. To elucidate the transcriptional impact TCDD treatment plays in disrupting hepatocyte rhythmicity and zonation, we used hepatic single-nuclei RNA-seq data from male C57BL/6 mice. Mice were housed in a room with a 12:12 light:dark cycle, gavaged with a single dose of 30  $\mu$ g/kg TCDD (or sesame oil vehicle) at time-point 0, after which the livers were collected and snap frozen at timepoints 2, 4, 8, 12, 18, or 24 hours. Gene expression profiles from previous studies were used to estimate zonation within liver hepatocytes. Genes were classified based on the effects of TCDD, zonation, temporal regulation, or a combination of these variables using a mixed-nonlinear effect model. We found that more genes are regulated by zonation independently than by rhythmicity and TCDD alone. Additionally, more genes were regulated by a combination of TCDD and zonation than by a combination of TCDD and rhythmicity. We performed pathway analysis on the class of genes regulated by a combination of zonation, rhythmicity and TCDD identifying genes involved in the glucuronidation pathway (e.g., Ugt1a10, Ugt2b34) and the leptin-insulin pathway (e.g., Socs2, Socs3). Collectively, these results suggest TCDD interacts with the spatial and temporal regulation of genes in the liver lobule.

This project is funded by R01ES029541 and the SRP P42ES004911.

# Development of an Extraction Method for the analysis of Synthetic Opioids in Bone Samples using the Bead Ruptor

Kala N. Babb,<sup>1</sup> David J. Cohen,<sup>1</sup> and Emanuele Alves<sup>2</sup>

<sup>1</sup>Virginia Commonwealth University; and <sup>2</sup>Virginia Commonwealth Univ

Abstract ID 23216

Poster Board 462

Synthetic opioids have been the leading cause of overdose deaths in recent years. Many of these deaths are attributed to novel synthetic opioids (NSO). Detecting NSOs in toxicological matrices can prove difficult due to their high potencies leading to low concentrations in the body and a general lack of literature on these substances. In the case of extreme decomposition or significant scavenging, the only toxicological matrix that may be available in bone tissue. In these instances, establishing blood:bone drug concentration correlation is important to help determine the cause of death. To achieve this, correlation studies of animal models are necessary, and a careful choice of a suitable animal model is required. Rabbits, as opposed to rodents, are the most appropriate choice, due to their exhibition of spontaneous cortical bone remodeling that is not present in rodents. Previous research has not yet been able to establish such a correlation using rodents, leading to studies with a new choice of animal model for appropriate correlation data. The aim of this work is to develop a fast and suitable method for the extraction of synthetic opioids from bone samples. This method will be applied to establish blood:bone drug correlation using rabbits as the chosen animal model. The method homogenizes bone samples and extracts the analyte simultaneously utilizing the Bead Ruptor. For the development of the extraction protocol commercial drug-free rabbit bone samples that were fortified with the following synthetic opioid standards: fentanyl, norfentanyl, bucinnazine, and AP-238 in a concentration range from 1 to 1000 ng/g of bone. Fentanyl-d5 and norfentanyl-d5 were included as internal standards. For the fortification process, bones were spiked with 25  $\mu$ L of the analytes solution and left drying naturally. 500 mg of fortified bone samples were homogenized in 4 mL methanol using the Omni International Bead Ruptor Elite. The homogenized samples were centrifuged, and the supernatant was collected. The supernatants were filtered through a 0.45  $\mu$ m syringe filter and then diluted to 15 mL with pH 10 deionized water to prepare for SPE, where a 3 cc flangeless Oasis MCX cartridge was utilized. After loading, the samples were first washed with 2 mL 0.1 M HCl, followed by a 2% formic acid in methanol solution. The analytes were eluted with a 5% ammonium hydroxide in methanol solution, which was evaporated and reconstituted with 50  $\mu$ L ethyl acetate for GC-MS analysis. A GC-MS method was developed and validated to identify and quantify the selected NSOs. Calibration curves were prepared using the standard addition method. Yields for all analytes varied from 29% to 89%, with norfentanyl having the lowest yield and bucinnazine having the highest. The use of the Bead Ruptor for the extraction during the homogenization process showed to be efficient with less time and cost spent, when compared to the traditional methods for bone analysis that consist of drying the samples, gridding them, and letting them soak in solvent for 24 hours. The GC-MS method showed sufficient linearity for all analytes at a linear range of 1-1000 ng/g with  $R^2 > 0.9984$  for all analytes. Both bias and precision were less than 20% for all analytes. The developed extraction and GC-MS methods were capable of extracting, detecting, and quantitating the target opioids. Once animal experiments begin, these methods can be applied to the bone samples obtained from the rabbits for the determination of the blood:bone correlation of synthetic opioids.

This work was supported by the VCU Quest Fund 2022.

# Maternal Electronic Cigarette Exposure Induces Inflammation, Oxidative Stress and Alters Mitochondrial Function in Postnatal Brain

Sabrina Rahman Archie,<sup>1</sup> Ali Sifat,<sup>2</sup> David Mara,<sup>2</sup> Yong Zhang,<sup>2</sup> and Tom Abbruscato<sup>3</sup>

<sup>1</sup>Texas Tech Univ Hlth Sci Ctr; <sup>2</sup>Texas Tech University Health Sciences Center; and <sup>3</sup>Texas Tech Univ HSC Sch of Pharm

Abstract ID 22490

Poster Board 463

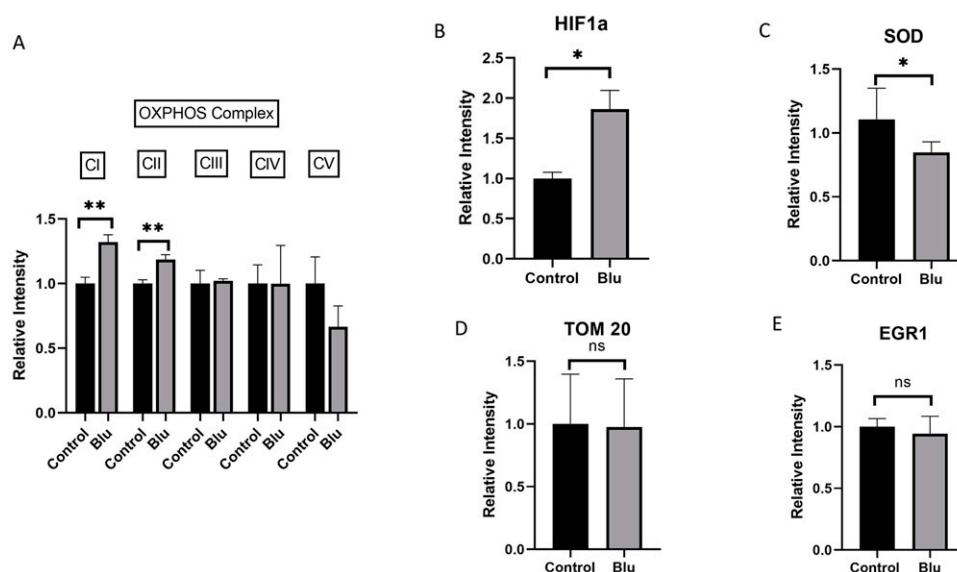
**Purpose:** Electronic nicotine delivery systems (ENDS), also commonly known as cigarettes (e-Cig) are often considered as a safer alternative to tobacco smoke and therefore have become extremely popular among all age groups and sex. Around 15% of pregnant women are now using e-Cigs in the US which keeps increasing at an alarming rate. Harmful effects of tobacco smoking during pregnancy are well documented for both pregnant and postnatal health, however a lack of preclinical and clinical studies exist to evaluate the long-term effects of prenatal e-Cig exposure on postnatal health. In our previous study, we have observed disruption of blood-brain barrier integrity and deteriorated motor, learning and memory function in prenatally e-Cig exposed offspring. In this study, we have evaluated the consequences of maternal e-Cig use on postnatal neuro-inflammation, oxidative stress, hypoxia and mitochondrial function at different age including evaluation of both male and female offspring.

**Method:** In our study, pregnant CD1 mice (E5) were exposed to e-Cig vapor (2.4% nicotine) till postnatal day (PD) 7. Body and brain weight were measured at PD7, PD23, PD45 and PD90. Immunobead assay was performed to measure the level of pro-inflammatory cytokines at PD7, PD23, PD45 and PD90. The expression level of oxidative phosphorylation or OXPHOS Complex (I, II, III, IV and V), hypoxia inducible factor (HIF-1 $\alpha$ ), antioxidant glutathione (GSH), mitochondrial protein TOM20, Manganese superoxide dismutase (MnSOD), EGRI and NRF2 were analyzed in offspring brain using western blot at PD7 and PD23.

**Results:** Significantly reduced brain to body weight ratio was observed at PD7 in prenatally e-Cig exposed offspring. Significantly increased expression of OXPHOS complexes and HIF-1 $\alpha$  and reduced expression of MnSOD, GSH and NRF2 were observed in prenatally e-Cig exposed offspring compared to control ( $P < 0.05$ ). However, no difference was observed in expression level of TOM20 and EGRI. Additionally, prenatally e-Cig exposed offspring had higher level of pro-inflammatory cytokines (IL-6, TNF- $\alpha$ ) at PD7, PD45 and PD90 ( $P < 0.05$ ).

**Conclusions:** Our findings suggest that prenatal e-Cig exposure induces neuroinflammation and oxidative stress on neonatal brain by increasing cytokines level, oxidative stress and disrupting mitochondrial function which may alter fetal brain immune function and mitochondrial activity that make such offspring more vulnerable to brain insults. Currently, we are evaluating mitochondrial activity in primary neuron from prenatally e-Cig exposed offspring.

**Support:** NIH R01DA049737 and R01DA02912.



Impact of maternal electronic cigarette use on postnatal brain A) Oxidative Phosphorylation (B) HIF-1 $\alpha$  (C) SOD (D) TOM20 and (E) EGR1. Prenatally e-cig exposed offspring showed higher level of OXPHOS complex I and II, HIF-1 $\alpha$  and lower level of SOD at PD7 (n=6),  $P < 0.05$ .